MICROBIAL LOOP : ITS SIGNIFICANCE IN OCEANIC PRODUCTIVITY AND GLOBAL CHANGE

F. Azam, L. B. Fandino, H.-P. Grossart and R. A. Long
Scripps Institution of Oceanography, University of California, San Diego, La Jolla, California, USA

Abstract
This paper discusses the need to integrate the microbial loop into models of pelagic ecosystems functioning. We emphasize the role of the microbial loop in ecosystem response to stress. An hypothesis is examined that small scale structure of the organic matter field can create hot spots of microbial activity. Microbial activity and interactions at such microscale features have important implications for the fundamental issues of nutrient and metal cycling and food web structure and dynamics. These ideas could provide mechanistic insights for modeling marine ecosystems subject to stresses such as eutrophication and pollution.

Key-words : bacteria, organic matter, pollution, eutrophication, models

"*... men are still under the strong influence of the medieval concept of an endless ocean*". Ward and Dubos, [1]

Society wants oceanographers to predict how human activities will affect the health of the ocean. But the "health of the ocean" is not a well defined concept. Broadly, it has been thought of in terms of maintenance of ecosystem homeostasis. In practice, the focus has been on studying the consequences of specific and localized human-induced perturbation such as pollutant or nutrient discharges into coastal waters. Generally, the emphasis has not been so much to predict the effects but to ameliorate present and obvious ecological damage. For example, we are asked to monitor and suggest ways to control eutrophication, contamination of edible fish by harmful chemicals and microbes or declines of local fishery. Clearly, the goal should be to predict, before-hand, the consequences of altering the ocean's chemistry and biology, but we lack sufficient knowledge of ecosystem structure and functioning to make reliable predictions. Ecosystem management at present amounts to trial and error because of our lack of understanding of underlying mechanisms.

This approach is untenable as concerns global change, due to the probable scale of the problem. Human-induced alteration of atmospheric chemistry can profoundly change the structure and functioning of the entire global ecosystem, with significant implications for human environment. This raises a number of urgent questions. What role will the ocean's biota play in various global change scenarios? Will it help purify the atmosphere of the greenhouse gases? Can we safely manipulate the ocean's biota to cause it to absorb additional carbon dioxide? Will global warming adversely affect marine fisheries and biodiversity? Will global change affect the aesthetic attributes of the oceans and their beaches? We do not know the answers to these questions. We do know, however, that trial and error is not a prudent option. We must acquire the ability to *predict* how the ocean's ecosystem will respond to global change. Ideally, one would want to develop a framework which enables one to predict the outcomes of global as well as local ecosystem perturbations. This will require elucidating the mechanistic bases of ecosystem functioning and response to stress.

A unifying theme is how biological forces determine the fate and spatial-temporal patterns of distribution of organic matter. This framework enables one to conceptually integrate the fate of organic matter from all sources, for example whether derived from *in situ* photosynthesis or from river or sewage outfalls. Also, one can develop an integrative approach for conceptualizing the response of the biota to variations in organic matter inputs. For example, eutrophication-enhanced organic matter production and increased photosynthesis due to global change could both be treated within the same framework. Pollutants introduced into the sea tend to associate with the biota and organic matter. Their pathways of transformation and transfer could also be studied within the general context of the consequences of the interactions of the biota with organic matter.

The microbial loop is a major biological force in oceanic carbon flux.

Our views of the ocean's biota as well as organic matter have changed dramatically. For the first hundred years of oceanography it was believed that the grazing food chain was mainly responsible for organic matter dynamics. Microbial abundances were considered too small to warrant their inclusion into ecosystem models. As a result, models of fisheries, productivity, nutrient recycling and pollutant transfer pathways were exclusively conceptualized in the context of the grazing food chain [2] and this trend has not ceased [3]. Older methods had failed to detect most microorganisms and their metabolism. Modern studies have established that bacteria account for a major fraction of the oceanic biomass and particulate carbon pool [4, 5] and use about one-half of the photosynthetically produced organic matter [6]. Bacterial use of dissolved organic matter (DOM) thus mediates large-scale organic matter fluxes through the pathway: DOM -> Bacteria -> Protozoa (or viruses) (the microbial loop [7]. Indeed, marine bacteria use about one-quarter of the total carbon fixed on earth. Organic matter flux into bacteria is highly variable and this could affect flux partitioning between major pathways: microbial loop, sinking and grazing food chain. We proposed that variability is due to bacterial interaction with a patchy organic matter field ([8] and below).

Organic matter is a continuum which creates microbial hot spots.

Recent discoveries are changing our view of the organic matter with which bacteria interact. The distinction between particulate organic matter (POM) and DOM is being replaced by the idea of an organic matter continuum — a gel-like matrix of polymers, replete with colloids and criss-crossed by "transparent" polymer strings, sheets and bundles, few to 100s of μm [9, 10, 11, 12] — the oceanic "dark matter" [13]. Chin *et al.* [14] used several physical techniques to demonstrate that the sea is a thin gel. The traditional particles, including living organisms would be encountered by bacteria as "hot spots" in the gel. The critical questions with respect to bacteria-organic matter interaction are: Do bacteria "care" about the structure of organic matter field in their microenvironments? Do they respond to the patchiness of the distribution of organic matter? It had been assumed that bacteria solely depend on DOM released from the grazing food chain [15]. However, recent studies show that bacteria do exhibit behavior towards organic matter [16, 17]. Five to 60% of bacteria in coastal assemblages were motile and could congregate in response to organic matter. Thus, bacteria do respond to the patchy structure of the organic matter field creating hot spots of abundance and activity.

Action of bacteria on patchy organic matter has microscale as well as ocean-basin-scale biogeochemical consequences.

A main adaptation for bacteria-organic matter interaction in pelagic bacteria is the expression of diverse ectohydrolytic enzymes (protease, glucosidase, phosphatase, lipase, nuclease [18, 19]). Cell-specific activities vary [20], so, shifts in species composition [21, 22] change the hydrolytic enzyme activities which pelagic bacteria exert on the organic matter field. Since bacteria attack the organic matter field, including living organisms, to generate DOM, they profoundly alter the behavior of organic matter (even when their own carbon demand is low; "modification interactions" [13]). Consequently, bacteria can influence all carbon flux pathways, not only DOM -> Bacteria. For instance, they can inhibit diatom aggregation by hydrolyzing diatom surface mucus [23], decreasing the downward flux of organic matter while increasing the intensity and the duration of the phytoplankton bloom. They can also solubilize marine snow, releasing most of the liberated DOM [24] – all these are small scale interactions with ocean-basin-scale consequences for carbon flux and energy transfer. Pollutants and radionuclides associated with

BENTHIC-PELAGIC BIODIVERSITY COUPLING

Ferdinando Bœro

Dipartimento di Biologia, Stazione di Biologia Marina, Università di Lecce, 73100 Lecce, Italy

Abstract

Coastal plankton dynamics is the driving machine of marine systems and its functioning depends on the availability of both nutrients and propagules. The incorporation of pelagic matter (either living or not) in the benthos and its resuspension to fuel the plankton, either as nutrients or as planktonic larvae (when entering in benthic organisms to be used for reproduction), are the recognised core of benthic-pelagic coupling. A complementary concept is the so called "supply-vertical ecology", stressing the importance of the bottomward flux of resting stages produced by coastal plankters from which active stages will be injected in the water column. In this framework, the nutrients that will sustain planktonic production come from both benthic resuspension (*e. g.* upwellings) and terrestrial run-offs, whereas propagules come from reproduction of active specimens leading either to immediately viable specimens, *i. e.* larvae that will grow into members of plankton (holoplankton) or of benthos and nekton (meroplankton), or from resting stages provided by benthic cyst banks. Resting stages accumulate in enormous quantities in coastal sounds, lagoons and harbours, forming veritable reserves of biodiversity. Marine canyons are at the other end of a spectrum of environments going from the littoral to the deep sea, and resting stages of both phyto- and zooplankters are being found in the millions in the sediments depositing in these widespread submarine valleys, probably to be re-shooted coastwards by the localised, canyon-driven upwellings. Benthic-pelagic coupling, thus, occurs through an almost unstudied life-cycle pathway, running parallel to both the food-web and the biogeochemical ones. If life cycles received far too little recognition in benthic-pelagic coupling, this is largely due to our ignorance of essential components of biodiversity expression such as larvae, resting stages and asexual propagules. A life-cycle oriented perception of biodiversity, highlighting the importance of intraspecific fluxes (life cycles) in benthic-pelagic coupling, is needed to complete a model of ecosystem functioning so far privileging interspecific (food webs) and extraspecific (biogeochemical cycles) fluxes. A new key to the understanding of the functioning of coastal ecosystems (a vital component of the Mediterranean and of all other seas and oceans) is now available, to challenge well established concepts and provide further insights in marine ecology.

Key-words: Plankton, Life cycles, Benthic-pelagic coupling

What is biodiversity?

Biodiversity is now a buzz word whose meaning ranges from the genetic diversity within species, to the number of species in a biotope (intended as a simple list of names), to the links among the living components of an ecosystem. The concept of biodiversity, thus, covers all aspects of biology and so, meaning almost everything, ends up meaning almost nothing. With the new concern on biodiversity, however, biologists are trying to gain more scientific respect for their discipline, showing the relevance of all its facets. This attitude stems from the widespread success of physico-chemical approaches, usually attracting more attention and resources than the biological ones within the framework of the wide scale study of the environment. It is paradoxical (and both ridiculous and tragic), furthermore, that biology becomes "attractive" again when dealing with extraterrestrial living beings. And non-biologists use the remote possibility of extra-terrestrial life to get enormous funding, leaving the exploration of terrestrial life at an almost amateurish level, due to fund shortage (1).

Coming back on Earth, and to the biological-abiological approach to the study of the environment, it appears logical, in fact, that it is not enough to, let's say, measure temperature and discover that it is rising (or falling). If this would not affect life at all, it would be almost meaningless for us. If a correlation exists between this change (better if on a global scale) and changes in genetic expression, species spectra and community organisation, the whole issue becomes more relevant to our perception of the change. Of course it is easier to measure the global temperature from a satellite than to transfer the study to bio-diversity, but the quality of the information is much higher when having this second type of information.

The "classical" study of biodiversity starts with the inventory of the many ways life expresses itself. This exploration started from the very beginning of culture, due to the extreme interest that we have in the organisms around us. Our species cannot survive by itself, we interact with other organisms, using them as food, as source of materials, as amusement aids. And they use us too, we still are the "food" of many parasites and micro-organisms. It is easy to understand that our species would not survive much if it would remain alone on the planet.

In spite of the overwhelming importance of other living beings, our scientific interest in them is fading since several decades. This is due to the entry of new disciplines in the hit-parade of science, but it is also linked to sociological and psychological attitudes. We have removed most wild creatures from our everyday landscapes, we have even removed from our sight the creatures we use for our everyday purposes. We do not like to see the slaughter of a cow or of a pig, so we pretend that these things do not happen. We are happy to see wild creatures on a TV screen or in a museum/aquarium, maybe when we are on vacation. But when we are "serious", there is no space for wild-life. To our common perception, an engineer who builds cars is surely more important to society than a zoologist who studies jellyfish. This attitude has been reinforced by the way zoologists and botanists work. They have a good time, and this is not serious. They like what they do as a job: they have the luck of having had the possibility of transforming their hobby into their job. This is seen with some sort of diffidence even by other scientists, who have to perform standardised experiments, often for innumerable times. These people, unfortunately, are right. Science evolves, and what was the right thing to do one hundred years ago can't be right nowadays. To go around the world, collect specimens, put them in jars and give them a name, arriving to have a nice collection of organisms, is still OK, but cannot be considered the avant-garde of research. It was so at the time of Aristotle, at the time of Linnaeus, even at the time of Darwin, but can't be so today, even though May's fundamental question (How many species are there on Earth?) (2) is very far from being answered. Deep sea environments, as hydrothermal vents recently showed us, are far from being fully known and understood, so we have still to "explore" many parts of the Earth. And also the explored ones still have many surprises, as shown by the diversity of the interstitial fauna, or of symbiotic communities.

In spite of this, however, when knowing that it is possible to read the code of a creature and modify it, making a brand new type of creature, or copy it, producing innumerable replicas of the original creature, it is obvious that those who make the inventory have a lower status, in terms of scientific prominence.

In one of his last editorials for Nature, the former director of one the two most influential scientific journals made a lapidary statement: life is chemistry (3). What I will try to argue is that there is more than chemistry in life, and that, for instance, a full appreciation of bio-diversity can lead to revolutionary concepts, widening our understanding of essential aspects of the functioning of the biosphere. To develop my arguments, I will choose one of the most important areas of the planet, the coastal zone, and I will try to show that our understanding of how it works is biased by the lack of consideration of the diversity of biological patterns and processes occurring in it.

Benthic-pelagic coupling

a - Extraspecific cycles (biogeochemical cycles)

The study of marine systems has been divided into two main approaches, one centred on the water column (the pelagic domain) and one centred on the sea bottom (the benthic domain). The tools and the concepts utilised to understand these two systems have been different. The pervading reductionist approach to science produced more and more specialised researchers, focusing on restricted topics. Syntheses were made mainly in textbooks, so that it is obvious that benthic organisms produce planktonic larvae and feed on plankton, as it is obvious that the things that fall on the bottom can be resuspended. But

GEODYNAMICS OF THE EASTERN MEDITERRANEAN SEA

S.J. Lallemant*, N. Chamot-Rooke, X. Le Pichon and D. Le Meur
Laboratoire de Géologie, Ecole Normale Supérieure, 24 rue Lhomond, 75231 Paris Cedex 05

Abstract

As a response to the rapid convergence between the African plate and the Aegea-Anatolia block, an accretionary complex (the Mediterranean Ridge) has grown in the Eastern Mediterranean basins by offscraping the upper sedimentary sequences of the downgoing plate. The boundary between this prism and its rigid backstop does not coincide with the so-called "Hellenic trenches" as previously stated. The rigid backstop instead occupies nearly one third of the surface of the Mediterranean Ridge system. The backstop might represent a seaward extension of the Hellenic nappes system. Incipient collision between this backstop and the Lybian margin results in internal deformation of the backstop and some lateral escape of the prism both westward to the West and eastward to the East. Fluid migration from deep origin causes mud diapirism and brine seeping by leaching the Messinian evaporites.

Key Words : Deep sea trench, Active margins, Tectonics, Mediterranean ridge

Introduction

Our knowledge of the active processes in the Eastern Mediterranean basins has greatly improved during the last decade, mostly because a great number of oceanographic research cruises have been conducted by european scientists. Among those, our group has been leading or co-leading five cruises. In this paper, we present a synthesis on the Eastern Mediterranean Sea mainly based on our experience but including results of other groups as well.

1) Plate kinematics : new insights from space geodesy

It has been noticed since the early days of the Plate Tectonics that the large scale motions of the plates resulted in a slow convergence between African and Eurasian plates during the Cenozoic times (1 cm/y in a S-N direction presently), is responsible for the building of the mountain chains bordering the Mediterranean Sea (*e.g.* [1]). The Aegean Arc is by far the most seismically active part of the Mediterranean due to the subduction of the African plate beneath the Aegean Arc system (*e.g.* [2]) nicely depicted by seismic velocity tomographic images [3]. However, the question whether crustal motions were related to a continuum of plastic deformation [4] or rigid rotations of platelets [5] remained unsolved until recently. Le Pichon and Angelier [6] have proposed however a rigid-type kinematic scheme for the relative motion between Africa and the Aegean Arc based on the focal mechanisms of the subduction earthquakes. The major breakthrough came from the space geodesy techniques allowing to get the motion not only at the plate boundaries but inside the plates. Le Pichon *et al.* [7], based on S.L.R. data, proposed that the deformation can be described by a rigid rotation of an Anatolian block (most part of Turkey and Southern Greece) with respect to stable Eurasia around a eulerian pole located near the Nile cone. This hypothesis has been recently confirmed by Oral *et al.* [8] or Reilinger *et al.* [9], using a dense array of more than 50 G.P.S. stations spread over the same area (Figure 1). Combined with the Eurasia/Africa, this predicts a convergence of about 4 cm/y in a NO2O°E direction along the Hellenic trenches, direction compatible with the slip vectors of the subduction earthquakes [10]. We further investigate the consequences of this subduction on the recent evolution of the Eastern Mediterranean Basin.

2) The Mediterranean Ridge : an accretionary prism related to the Aegean subduction zone

Most of the Eastern Mediterranean Sea is occupied by the Mediterranean Ridge (Figure 2), a broad submerged mountain chain (length about 1500 km, average width 200 km and average height above the abyssal plains of 1.5 km). After ruling out the hypothesis of a mid-oceanic spreading center, a compressional origin for the Ridge has been widely accepted. However, whether the compressional deformation involved the crust [11] or was restricted to accreted sedimentary sequences [12, 13] was still debated until recently.

In order to precise the internal structure of the Mediterranean Ridge, our group carried out a refraction study of the area in 1988 using two french research vessels (R.V. *Jean Charcot* and R.V. *Le Noroît*) in a E.S.P. (Expanded Spread Profile) experiment. As a main result of this cruise, we showed that the Eastern Mediterranean deep basins (Ionian Basin, Syrte abyssal plain and Herodotus basin) are most probably remnants of oceanic lithosphere [14]. We also showed that the velocity structures and thus the density distributions were in good agreement

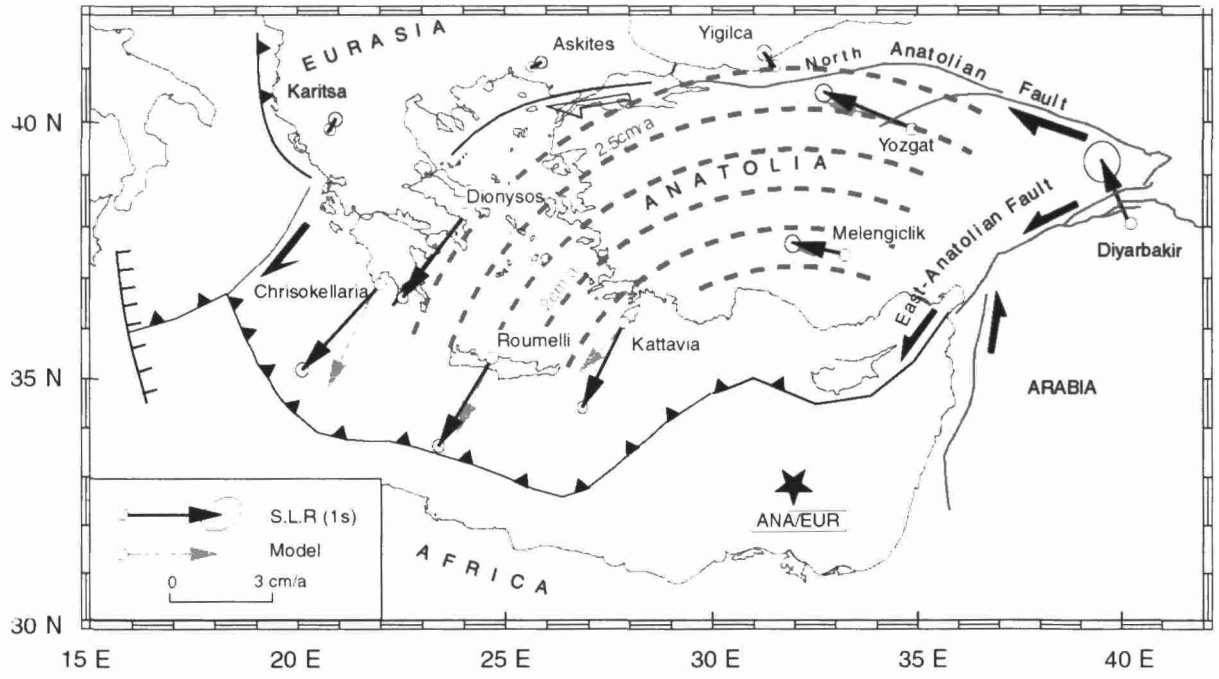

Figure 1. Plate kinematic scheme of the Anatolian platelet based on space geodesy results (from [7] modified).

THE GREAT EASTERN MEDITERRANEAN DEEP-WATER TRANSIENT

Wolfgang Roether* and Birgit Klein
Institut für Umweltphysik, Univ. Bremen, Postfach 330440, 28344 Bremen, Germany

Abstract
Around 1990 large volumes of Aegean Sea overflow began to be deposited in the near-bottom waters around the Cretan Arc. The resulting, transient situation contrasts with a quasi-steady state situation prevailing previously in which the depth range below about 1200 m depth was dominated by waters of Adratic origin. In the course of the transient the distribution of all properties changed drastically through the entire Eastern Mediterranean. The salinity of the outflow through the Sicily Channel was lowered and nutrient concentrations in the upper waters were raised. In this communication we provide a description of the changes, address the causes and the initiation of the transient and name certain of its implications. The transient represents a unique oceanographic event which warrants detailed studies also in the future.

key-words: deep waters, circulation, Eastern Mediterranean

Introduction

The textbook descriptions of the Mediterranean thermohaline circulation, which go back to the work of Wüst [1] and Lacombe and Tschernia [2], among others, depict it as a rather static anti-estuarine system (the so-called Mediterranean conveyor belt). The conveyor consists of Atlantic surface water entering through the Strait of Gibraltar, above outflowing high-salinity Mediterranean water (exchange flow on the order of 1 Sverdrup, or 106 m^3/s [3]), driven by a high net evaporation that increases the salinity, and hence the density, of the Mediterranean waters. A predominant water mass is the Levantine Intermediate Water (LIW) generated southeast of the island of Rhodes in the Levantine Sea, which forms a subsurface salinity-maximum layer that seemingly carries the bulk of the subsurface westward return flow. The textbooks also name the principal formation areas of the deep waters, *i. e.* the Gulf of Lions for the Western Mediterranean and the South Adriatic for the Eastern Mediterranean, while the role of the Aegean Sea remained controversial. This sea, quite like the Adriatic, is a marginal sea with a rather continental environment to the north of the Eastern Mediterranean proper, so that also here dense waters are generated [4]. More recent work revealed a slow, rather steady salinity and temperature increase in the Mediterranean subsurface waters. This drift is due to a changing fresh-water budget, for example by the cutoff of the Nile discharge [5], but left the principal thermohaline structure unaffected. Furthermore it was found that the deep waters have an active part in the subsurface return flow of the conveyor [6].

A big step forward was achieved through new, coordinated Mediterranean observation programs. For the Eastern Mediterranean a prominent one is POEM (Physical Oceanography of the Eastern Mediterranean [7], later on renamed POEM-BC, *i. e.* POEM including biology and chemistry [8]). Furthermore the Mediterranean programs of the European Union (EU-MAST) were developed, which lately have made up the bulk of the physical and biogeochemical work in the whole Mediterranean Sea. A specific new result is a determination of the formation rate of deep water of Adriatic origin of about 0.3 Sverdrup [9] from observations during a cruise of the German F/S *Meteor* in the summer of 1987. This rate is equivalent to an Eastern Mediterranean deep water residence time of approximately 120 years, and means that the renewal is equivalent to as much as about 30% of the conveyor belt flow. Furthermore the role of the Aegean Sea was clarified. The *Meteor* data proved that outflow from the Aegean through the straits of the Cretan Arc formed an intermediate-depth layer (termed Cretan Intermediate Water, CIW). CIW was found to be most prominent in the eastern Ionian Sea and south of Crete where it is centered in about 700 m [10, 11], thus replenishing what has often been called the "transition layer" between the LIW and the deep waters.

Although in 1987 the deep waters of the Eastern Mediterranean appeared to represent a well defined system near to a steady state, it was evident that the static stability between these waters and the Adriatic waters filling the Eastern Mediterranean from the bottom up to about 1200 m was a rather marginal one. In the years following there were indications that the situation was perhaps changing [12, 13], including surprising observations such as a reversed temperature gradient in the upper few meters of sediment in a region west of Crete [14]. During about the same period there was moreover a paradigm change in the physical oceanographic community towards questioning a view of the ocean circulation as a system that was basically stable [15].

A further Eastern Mediterranean cruise of F/S *Meteor* (successor of the previous ship of the same name) in January 1995, organized in connection with both the EU-MAST program and POEM-BC, was begun with the aim to investigate the situation as found in 1987 in more detail, but alerted by the findings mentioned. It came as a big surprise that the deep waters of the Eastern Mediterranean had in fact changed fundamentally, in that a large volume of Aegean outflow waters had entered the bottom and deep waters of the Eastern Mediterranean lifting the water column of the entire sea by several hundred meters within just a few years [16]. The nature of the change, its causes, and some implications are adressed in the following, primarily on the basis of observations of the two *Meteor* cruises mentioned.

Nature of the changes

Figures 1 and 2 compare the distributions of salinity and CFC-12 for the two surveys on a section along the entire Eastern Medi-

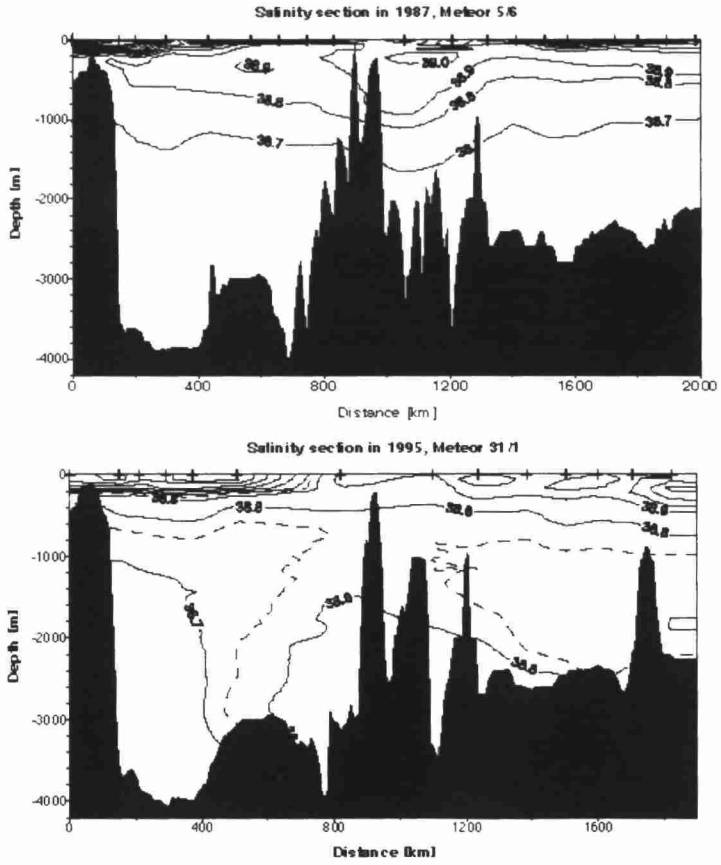

Fig. 1: Salinity isolines (psu) 1987 (Fig. 1a, upper panel) and 1995 (fig. 1b, lower panel) on sections along the entire Eastern Mediterranean as indicated in Fig. 3.

OBSERVATIONAL REQUIREMENTS FOR VALIDATION OF MARINE ECOSYSTEM MODELS IN THE MEDITERRANEAN

Job W. Baretta* and Hanneke (J.G.) Baretta-Bekker

Ecological Modelling Centre, joint department of the Danish Hydraulic Institute and VKI, Agern Allé 5, DK-2970 Hørsholm, Denmark.

Abstract

To test, verify and improve marine ecosystem models, data sets of key variables are necessary. Such data sets ideally should reflect the state of the system in terms of trophic status, productivity, nutrient cycling and oxygen dynamics. The data sets available presently for (sub-regions of) the Mediterranean generally are far removed from this ideal, because they contain only information on concentrations or density/abundance, but not on rates-of-change, nor on the spatial variability of the variables. An observational strategy to acquire internally consistent data sets of key variables, comprising physical, biological as well as chemical variables is suggested, with a rationale for the choice of variables.

Key-words: models, geochemical cycles, Adriatic Sea, eutrophication, oxygen

Introduction

Simulation models of ecological processes have slowly become established tools for integrating and testing our understanding of the different components of marine ecosystems. The first models were dealing with parts of ecosystems, often seen as steady state systems [1, 2, 3] and sometimes as dynamical systems [4, 5]. From the end of the 70's on, complex dynamical models began to appear, describing complete estuarine and marine ecosystems, including pelagic and benthic processes as well as advection and dispersion processes [6 - 9]. Apart from a mathematical description of the biogeochemical processes and a physical model to describe the water transports, data are needed to run a model. This paper sketches the requirements and the availability of data sets necessary for models of the Mediterranean Sea in general and of the Adriatic Sea in particular, as well as some recommendations for observational strategies.

ERSEM

ERSEM is a comprehensive ecosystem model which dynamically simulates the cycling of organic carbon, oxygen and the macro-nutrients N, P and Si over the seasonal cycle. The model consists of an interlinked set of modules, describing the biological and chemical processes in the stratified or non-stratified water column and in the benthic system, as forced by light and temperature. The model domain is subdivided into smaller units, which are called boxes or grid cells, depending on their size. Physical transport between the boxes or grid cells is included by either driving the model with the aggregated output of physical circulation and dispersion models in the form of a time series of daily advective and diffusive exchange coefficients across all box boundaries or by directly forcing the biological model with a hydrodynamical model. In all the different spatial set-ups the biology in each of the boxes or grid cells is exactly the same.

The ERSEM model has been implemented in different regional seas and in different spatial set-ups, *e.g.* in the North Sea in a 15-box set-up and a 130-box set-up as well as a 1D-vertically resolved column model of a mooring site [10]. In the first two set-ups the transport model consists of daily exchange coefficients between the boxes calculated from a fine-scale hydrodynamical model [11], while the last set-up is coupled to a entrainment/detrainment model [12], forced with a meteorological high-frequency data set. In [13] and in the papers published in two special issues of the (Netherlands) *Journal of Sea Research* [9-11, 12-28] a full description of the biological modules has been given.

Data needs

Apart from the physical set-up (bathymetry) the model needs initial values for all state variables before it can be run. Then, during a run it needs time series for the forcing functions and the boundary conditions for the entire duration of the model run. Last but not least, after the model run, independent data are needed data to calibrate and/or verify the model results.

The initial values for those state variables not available from observations are obtained by running the model for a number of years repeating the same forcing and boundary conditions for each year until the model reaches a repeating cycle, so-called perpetual-year forcing. The forcing functions, as water temperature, irradiance, and the boundary conditions for all transported state variables have to be extracted from measurements. Calibration/verification data in the form of concentrations and fluxes are necessary to calibrate the model and to draw conclusions as to how well or badly the model reproduces the biogeochemistry of the modelled system.

ERSEM in the Adriatic Sea

For the Adriatic Sea ERSEM has been coupled to 1D and to 3D versions of the Princeton Ocean Model, a general circulation model described in [29]. A 1D-vertically resolved water column model has been constructed by [30]. This model has been applied to three different sites in the Adriatic Sea representing the northern, the central and the southern Adriatic Sea, with depths of 30, 150 and 1000 m, respectively.

The 3D model uses an idealised Adriatic Basin as described in [31]. It is constituted by a rectangular basin, without open boundaries, with approximately the same size and geographical position as the real Adriatic Sea. The basin has a minimum depth in the North of 50 m, sloping towards a maximum depth of 500 m in the south. The grid used in this model set-up has a horizontal resolution of ~25 km and 10 sigma layers in the vertical. As forcing functions climatological data of wind-stress, heat flux and river runoff have been used.

Data availability and use

For the Adriatic Sea the following data sets are available:

- May data, a data set of monthly climatology, compiled by May [32] and used for the atmospheric surface forcing.
- ATOS, the Adriatic Temperature, Oxygen and Salinity data set, reported by Artegiani *et al.* [33, 34], used to initialise the temperature and salinity fields.
- ABCD, the Adriatic BiogeoChemical Data set [35], used for verification of the model. The number of casts containing nutrient and chlorophyll-a data ranges from 1353 for nitrite and nitrate down to 611 for Chl-a. Even at the coarse spatial scale (~25 km) of the POM 3D/ERSEM set-up in the Adriatic, the observational coverage is such that it has not been possible to extract climatological monthly means at this spatial resolution. Instead, it has been necessary to aggregate the data into a seasonal climatology (winter, spring, summer, autumn) for much larger sub-regions of the Adriatic [31]. This necessitates aggregating the model results to a much coarser spatial resolution in order to compare them directly to the available data. The requirement here clearly is for finding more synoptic data sets. This has partly been accomplished by extracting information from the
- CZCS, the Coastal Zone Colour Scanner data set held by ISPRA [31], containing chlorophyll-a data.

Implications of model results and data

In the Adriatic, the results of the 1D model show remarkable similarities and differences between the northern, the central and the southern study sites. At all three sites the seasonal cycles show a well-mixed period during winter with relatively cold water and a stratified summer period when vertical mixing is weak, decoupling the euphotic zone from regenerated nutrients. Benthic-pelagic coupling plays a significant role in nutrient recycling, weakening with increasing depth from north to south.

Although the 3D model was primarily developed to test the coupling of the physical model with the biogeochemical modules, the results do show the North-South trophic gradient with the northern part of the basin being the most productive by river-borne nutrients inputs and by the recycled nutrients from the benthic system. The south with smaller river inputs and a more distant benthic-pelagic coupling is a less productive system. The model correctly predicts the occurrence of a winter phytoplankton maximum in the northern sub-basin, confirmed by the CZCS chlorophyll data, and it reproduces observed regional differences in nutrient distributions over the whole

DIATOM BLOOMS AND PLANKTONIC PRODUCTION IN THE NW MEDITERRANEAN

Marta Estrada
Institut de Ciencies del Mar, P. Joan de Borbo, s/n, 08039 Barcelona, Spain

Summary
This contribution discusses the occurrence of diatom proliferations in western Mediterranean waters, with emphasis on the stratification period, and considers the composition of the planktonic food web of the NW Mediterranean within a general framework. The data are based on studies carried out in the Catalano-Balearic sea by the Pelagic Ecology Group of the ICM, largely as part of MTP-MAST projects.

Key-words : diatoms, primary production, food webs, Western Mediterranean

When globally considered, the Mediterranean can be characterized as an oligotrophic sea. The negative estuarine circulation in the strait of Gibraltar and Sicily appears to be one of the major causes of the proggressive decrease of nutrient concentrations in Mediterranean deep waters, along a gradient going from the Atlantic, through the straits of Gibraltar, to the eastern part of the basin. In addition, the Mediterranean lacks extensive upwelling regions comparable to those of the major oceans.

However, the Mediterranean planktonic production is not as low as could be expected from the manifest nutrient scarcity. This so-called "paradox of the Mediterranean" (1) can be extended to the consideration of living resources. The Mediterranean seems to produce more exploitable fish than can be predicted by simple usual models (2).

There are several possible explanations for this paradox. One is that the Mediterranean is far from being uniformly oligotrophic and presents a number of hydrographic features which contribute to increase its potential fertility, specially in its western basin (3). Another is the episodic character of many fertilisation events (including atmospheric inputs), which may have eluded observation. In addition, it could be that food chains in oligotrophic systems function in a more efficient manner than in eutrophic ones (4, 5).

The production of living resources in a pelagic area is related to the amount of new production and the structure and function of the planktonic food web. As a simplification it is usual to consider two extreme types of trophic pathways, the herbivorous (or "classical") trophic chain, with transfer from nano-microphytoplankton to metazoan zooplankton and other trophic levels, and the microbial food web, based on small phytoplankton, in which a large part of the synthesised organic matter cycles through bacteria, small flagellates and protozoan predators. The general oligotrophy of the Mediterranean and the dominance of stratification during much of the year favour an important role of the microbial food web. Another particular feature of the Mediterranean planktonic food web is the possibility of phosphate limitation of both heterotrophic bacteria and autotrophic plankton.

Recent technological developments including epifluorescence microscopy and cytofluorometry have helped in the study of the distribution of the smaller components of the plankton, from heterotrophic bacteria to autotrophic prokariotes and picoeukariotes. These organisms, as parts of the microbial food web, may account for a large part of the total carbon flux in oligotrophic situations. However, when considering exportable biogenic carbon fluxes, it is important to ascertain the contribution of the larger components of the phytoplankton. Among them, diatoms tend to show the faster response after fertilisation events and represent major contributors to new production and to export of biogenic C, as pointed out by studies of sediment trap samples.

This contribution attempts to consider 1) the conditions of appearance of diatom proliferations in western Mediterranean waters, with emphasis on the stratification period, and 2) to evaluate macroscopic characteristics of the composition of the NW Mediterranean food web within a general framework. The study will be based on data from surveys carried out in the Catalano-Balearic sea by the Pelagic Ecology Group of the ICM, largely as part of MTP-MAST projects (6).

The alternance of mixing and stratification periods confers strong seasonal variability to the magnitude of phytoplankton biomass in the Mediterranean. Diatoms are characteristic of the seasonal phytoplankton maxima which occur typically in autumn and late winter or early spring. These blooms are associated with the breakdown of the thermocline in late autumn, which facilitates input of nutrients into the upper layers, and with the stabilization of the water column in late winter-early spring. However, the occurrence of phytoplankton blooms is not limited to the autumn and winter seasonal maxima. During the stratification period, patches of high diatom concentration occur in the deep chlorophyll maximum (DCM), in frontal areas and in other ergoclines. Multivariate analyses show that these high phytoplankton biomass patches are dominated by a few diatom genera (Chaetoceros, Pseudo-nitzschia, Thalassiosira). However, not all relatively large diatoms are associated with high production conditions. Some diatom genera, like Rhizosolenia (with or without symbiotic cyanobacteria) may be found in the nutrient limited upper water layers. The localized character of the diatom patches found at the DCM and the other ergoclines suggests that they are the result of episodic fertilization events, probably related to phenomena like internal wave breaking or instabilities at fronts. The intermittent nature of such events makes it difficult to collect evidence of their effects on other trophic levels. However, there are examples of DCM diatom blooms accompanied by dense populations of mesozooplankton and high phaeophytin concentrations, presumably as a result of grazing activity. In the Catalan front, the presence of diatom populations of relatively large size (>5 m) has been associated with enhanced mesozooplankton production.

Current hypotheses suggest that the relative contribution of heterotrophs to total planktonic biomass decreases with increasing phytoplankton biomass and primary production (4, 5). Thus, oligotrophic marine areas would be characterized by a higher ratio of heterotrophic to autotrophic biomass than more eutrophic regions. The studies of the pelagic Ecology Group of the ICM indicate that this is indeed the case in the NW Mediterranean ecosystem. Theses differences in ecosystem structure could have important implications concerning the potential production of renewable resources in oligotrophic marine areas.

References

1 - Sournia A.-1975. La production primaire planctonique en Méditerranée. Essai de mise à jour. *Bulletin de l'Etude en Commun de la Méditerranée*, 5:1-128.
2 - Estrada M.-1996. Pimary production in the northwestern Mediterranean. *Sci. Mar.*, 60 (suppl.2):55-64.
3 - Salat J.-1996. Review of hydrographic environmental factors that may influence anchovy habitats in northwestern Mediterranean. *Sci. Mar.*, 60(suppl.2):21-32.
4 - Alcaraz M., M. Estrada, J. Flos and F. Fraga-1985. Particulate organic carbon and nitrogen and plankton biomass in oligotrophic and upwelling systems. In C. Bas, R. Margalef, P. Rubies (eds). Simposio internacional sobre las areas de afloramiento mas importantes del Oeste Africano. CSIC, Barcelona:435-438.
5 - Gasol J.M., P.A. del Giorgio and C.M. Duarte. (In press). Biomass distribution in marine planktonic communities. *Limnol. Oceanogr.*
6 - Estrada M. and Pelagic Ecology Group of the ICM.-1997. The pelagic ecosystem of the Catalano-Balearic sea during the stratification period. Poster, Conference on Progress in Oceanography of the Mediterranean sea, Rome, 17-19 November 1997.

MULTIDISCIPLINARY DATA SETS AND MODELLING STUDIES

Jordi Font

Institut de Ciències del Mar CSIC, P. Joan de Borbó s/n, 08039, Barcelona, Spain

Abstract

Different spatial and temporal scales interact in the Mediterranean dynamics. An efficient interaction between adequate observations and modelling is needed to improve the present understanding of this dynamics. The scales of several biological processes are not the same than the scales of the different hydrodynamic processes that can influence them, and the corresponding sampling methods or strategies appear sometimes to be incompatible. The present development of new sensors and instruments, together with coherent approaches and strategies in the study of the Mediterranean system, will progressively generate consistent multidisciplinary data sets, as a first step to the construction of realistic ecological models.

Key -words: Mesoscale phenomena, Models, Sampling methods

Sampling the Mediterranean

The Mediterranean, as any oceanic system, has a lot of spatial and temporal scales interacting on its dynamics. Mesoscale plays a significant role in driving or modifying the general circulation of the different Mediterranean water masses, and in forcing biogeochemical fluxes. In most of subbasins the mean currents are weak and mesoscale features can be more energetic. An extreme example of this is the Algerian basin, where the circulation variability is much more linked to strong mesoscale events than to seasonal or longer scale forcings. Remote sensing has been a key tool in shifting our image of the Mediterranean circulation from the traditional "smoothed" patterns computed by Ovchinnikov (1) to a more complex system with frontal currents and intense mesoscale activity, as the one first proposed by Millot (2) in 1987.

Taking into account that the Rossby radius of deformation in the Mediterranean is of the order of 15-20 km, it is obvious that a good description of its dynamics requires a much higher spatial resolution for in situ sampling than it was done in the past, and than it is done in the open oceans. This strategy was closely faced by the different experimental efforts done from the early eighties, as the joint international actions POEM(3) and WMCE (4), and later PRIMO (5). And also by the numerical modelling activities, that had to progressively reduce their mesh dimensions, and also substitute the traditional climatological forcings by more realistic data analysis. During the first phase of MTP we have seen several examples of fruitful interactions between observational and numerical modelling approaches to the understanding of different Mediterranean phenomena, as EUROMODEL and MERMAIDS projects (6, 7). The experimental results are continuously raising questions about the functioning of the system that require a precise modelling to be answered. And models show features that could be checked or require inputs that can only come from dedicated observations. An adaptation in the two different "languages" is needed to improve this exchange of information, for example by arranging similar procedures for the presentation of both kinds of results, as can be sections across channels or time series in specific locations.

In spite of this, not always a full agreement is achieved when comparing both kinds of results. One should in principle think that the mistake comes from the modelling side: unresolved phenomena, inadequate parameterisation of any process, inappropriate boundary conditions ... Although problems can also come from the sampling, or the analysis or interpretation of its results, for example those coming from a lack of synopticity in the measurements. Recently, several examples exist of accurate control of the sampling strategy by real-time remote sensing, or of a precise checking of the data interpretation, by running synopticity tests besides objective analysis of the significance of the different spatial scales.

Modelling the ecosystem

When leaving the physical dynamics and looking at a more complex aspects of the Mediterranean system, as biogeochemical or ecological, the problem of *in situ* sampling, data analysis and modelling appears to increase its difficulty. Of course a major problem is modelisation itself, that is when trying to express the several relationships between the different parts of the system into mathematical formulae, able to be numerically integrated. Even one of the apparently more simple aspects, the hydrodynamical advection and diffusion of passive particles in any marine environment, is not always an easy job. But let's only concentrate on the problems of measuring, that is how to obtain adequate interdisciplinary data sets for modelling, and forget for the moment how models will work with these data.

The scales of several biological processes are not the same than the scales of the different hydrodynamic processes that can influence or even determine them. In addition to this, the sampling methods or strategies in biology are sometimes (let's say most of the times) incompatible with the sampling of the hydrodynamic parameters unavoidably linked to them. Is this an unsolvable problem? Or just a result of traditional methods that come from times when nobody was worried about this, or the available technology did not allow a different approach? Can we really build multidisciplinary sets where all the data are comparable and, for example, physical and biological information can be used to help each other in increasing the understanding of the different dynamical processes?.

To sample the Mediterranean mesoscale structures we have now instuments that measure the physical parameters (CTD, ADCP, underway water pumping to deck sensors...) at a quite reasonable high speed. Although this is not so simple, as can be seen when performing synopticity tests or examining time series of satellite imagery in highly energetic areas. In fact, sampling a moderately large area (say 100 x 100 km^2) from an oceanographic vessel, even in the Mediterranean where everything is quite small, strictly poses a problem of mixing spatial with temporal variability, that not always has a satisfactory solution.

Some of the approaches traditionally used to study the marine ecosystem should be changed if one expects to understand which is the real dynamics. To keep the vessel in a theoretically fixed point for 24 or 48 h to sample any biological cycle can be completely nonsense if the environmental hydrodynamic conditions (three-dimensional) are not measured accordingly: who can discriminate whether observed changes are due to the studied process or to modifications of the physical dynamics? However, some questions will never be answered if one is not able to sample the system not only with the adequate spatial and time resolution, but also by discriminating for example the effect of diel cycles. In summary, the obtention of a multidisciplinary data set useful to validate, or to feed, an ecological model is most of occasions a hard task.

Another major problem has also to be mentioned. While most of physical variables are measured world-wide under very well defined standards (*i.e.* sensors in commercial probes that can be strictly calibrated and give final physical values after brief computations), this is not the case with a lot of chemical, and especially biological variables. In these fields the obtained data values can strongly depend on methods or protocols, and full calibration is not always a feasible task. Hard work has to be done with quality control and inter-comparison procedures to ensure a really confident use of data coming from different sources. This, together with extra handling problems dealing with supports and formats, is the reason why most of operative oceanographic data bases only contain standard CTD profiles and similar information.

At present several instruments have been developed, and others are under development, to push the biogeochemical information collection close to the approach of in situ electronical sensors: light cells, flow cytometers, fluorimeters, chemical sensors ... Of course the technology is far from being operative for large ranges of variables, but this approach, completed with surface information obtained by

ROLE OF ULTRAVIOLET RADIATION IN THE MEDITERRANEAN SEA: INTERACTION BETWEEN MIXING PROCESSES, PHOTOCHEMISTRY AND MICROBIAL ACTIVITY

Gerhard J. Herndl [1*], Jesus M. Arrieta [1], Ingrid Obernosterer [1], Bettina Reitner [2]

[1] Department of Biological Oceanography, Netherlands Institute for Sea Research, P.O. Box 59, 1790 AB Den Burg, The Netherlands
[2] Institute of Zoology, University of Vienna, Althanstr. 14, A-1090 Vienna, Austria

Abstract

Ultraviolet (UV, 280-400 nm) radiation penetrates deeper into the water column than previously assumed and acts on dissolved organic matter (DOM) as well as on planktonic organisms. Evidence is presented that originally labile DOM is becoming more refractory upon UV exposure while refractoy DOM becomes more labile. The development of a pronounced diurnal thermocline leads to a prolonged exposure of DOM and microorganisms entrappped in the upermost water layer to UV radiation. Only, when the diurnal thermocline breaks up in the late afternoon, the upper water column is mixed again and the photolytically cleaved DOM is made available to bacterioplankton.

Key-words: Plankton, bacteria, pelagic, surface waters, global change

Introduction

More than 2 decades ago, our view on the carbon and energy flow through marine ecosystems was challenged by the finding that bacterioplankton are much more abundant than perviously thought [1] and that they are responsible for the major part of the respiratory activity in the water column [2]. The notion that bacterioplankton growth is roughly in the same order of magnitude as phytoplankton primary production [3, 4] and that they are efficently grazed by protists [5, 6] placed them into the center of a microbial food web [7, 8]. In this "microbial loop" [7] carbon and energy is efficiently recycled and competes with the metazoan food web for the available organic material [9, 10]. Currently, molecular approaches are applied to decipher the bacterioplankton species distribution over time and space in order to better understand the interactions within the bacterioplankton communities [11-14]. To date there is no doubt about the significance of bacterioplankton within the planktonic communities. In oligotrophic environments, bacterioplankton dominate over phytoplankton biomass even in the euphotic zone and represent the largest living surface in the sea [15, 16].

The discovery of a major ozone hole over Antarctica and its spreading to mid-latitudes during the austral spring [17, 18] stimulated research on the role of the accompanied increase in ultraviolet-B (UVB, 280-320 nm wavelength) radiation reaching the Earth's surface [19]. This research originally focused on Antarctic systems since major fishery resources are located there; the initial scietific question centered around the extent the productivity of these Antarctic systems might be influenced by the increased UVB radiation [19-22]. UVB increases, however, not only in the near-polar region of the southern hemisphere but is on the increase also in mid-latitudes of the northern hemisphere [23]. Thus, the increase in UVB radiation might also have an effect on temperate marine ecosystems. At northern temperate latitudes, ozone levels in the early 1990's were about 10-15% lower than that estimated in the late 1970's, when compared on an annual basis [24]. Translated into DNA damaging weighted biological radiation, these ozone reductions amount to a nearly 10.5% increase in damaging dose, or an average of about 0.75% per year for the last 14 years [25]. The change in stratospheric ozone, however, has little effect on the flux of incoming UVA (320-400 nm) radiation or photosynthetic active radiation (PAR, 400-700 nm). Thus, changes in stratospheric ozone alters the spectral balance between UVB: UVA:PAR. As outlined in detail below, these changes in the spectral balance have a severe impact on the recovery of organisms from UV stress.

The Mediterranean Sea and particularly the Adriatic Sea is heavily exploited by fishery and, moreover, an economically important region where millions of tourists spent their vacation every summer. Thus, possible alterations in the food web and the carbon flow through theses systems due to altered UVB radiation regimes might have a profound influence on the sustainable use of the Mediterranean Sea in general and the Adriatic in particular.

In this contribution we will first pinpoint the major role of UV radiation on the dissolved organic matter (DOM) pool which is one of the largest organic carbon reservoirs of the biosphere [26]. Then we discuss the impact of UV radiation on the living biota, in particular, the bacterioplankton as the principal consumers of the DOM pool and, finally provide a synthesis of the possible interactions between the DOM and bacterioplankton as influenced by UV radiation. Possible scenarios are then drawn on the impact of increasing UVB radiation on the carbon flux through the pelagic food web in the Mediterranean and the Adriatic Sea.

The radiation regime and its impact to the stability of the water column.

As shown in Fig. 1, even short wavelength UV radiation (305 and 320 nm) penetrates to considerable depth in the coastal Northern Adriatic Sea. In open oligotrophic environments such as the tropical Atlantic, the 10 % radiation level of the 320 nm wavelength is at about 25 m, while the 10 % radiation level of the 340 nm and 380 nm wavelengths is at 35 m and 60 m depth, respectively (Obernosterer, unpubl. data). This radiation, particularly in the UV range, has an direct impact on the DOM and the biota in these layers as outlined in greater detail below. However, also longer wavelength radiation (> 700 nm) influences the upper water column by introducing heat over a diurnal cycle (Fig. 2). During the night, surface cooling and convection result in a nearly well-mixed boundary layer with a small unstable surface layer [27]. Solar heating leads to rapid shoaling of the boundary layer and the formation of a diurnal thermocline (Fig. 2). Following sunset, surface cooling erodes the stratification and deepens the boundary layer again (Fig. 2). Diffusivities are large during the night-time with peak values exceeding 300 $cm^2\ s^{-1}$ [27]. Daytime diffusivities are more than one order of magnitude lower due to the shallow boundary layer and reduction in the turbulent velocity scale under stable forcing [27]. Thus, the long wavelength spectrum (> 700 nm) of the solar radiation establishes a diurnal thermocline in the upper water layer creating a surface layer where DOM and non-motile plantonic microorganisms are trapped over almost the entire period of sunshine. In the open oligotrophic ocean, this layer of reduced turbulent mixing extends from the air-surface interface to about 15-20 m depth (Obernosterer, unpubl. data). The shorter wavelength spectrum of the solar radiation (300 to 400 nm) acts on the DOM and the biota entrapped in this layer.

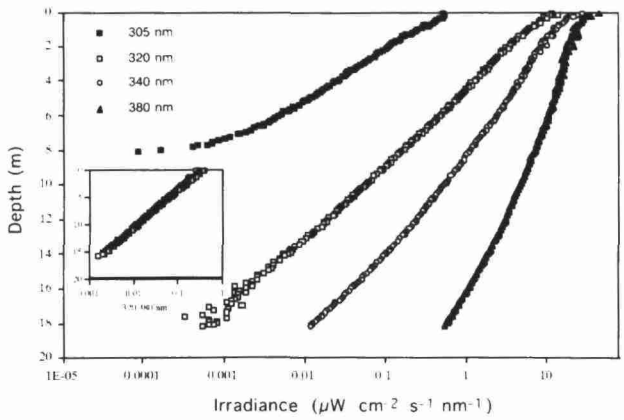

Fig. 1. Penetration of UV radiation of different wavelengths into the water column of the Northern Adriatic Sea measured on a cloudless day (16 July 96) at local noon. The inset shows the development of the ratio between 320 : 380 nm with depth. While the 320 nm wavelength represents the damaging wavelength range the 380 nm stands for the wavelength range used for inducing photoenzymatic repair. The ratio varies from 0 to 15 m depth over 3 orders of magnitude.

STEADY STATE MODELS OF THE MICROBIAL FOOD WEB. A USEFUL TOOL IN EXPLORATION AND MANAGEMENT OF MEDITERRANEAN SURFACE WATERS ?

T. Frede Thingstad

Department of Microbiology, University of Bergen, Jahnebk. 5, N-5020 Bergen, Norway

Abstract

Characteristic time scales for division of micro-organisms are potentially short compared to those of larger animals and those of water exchange processes. An approximate description may therefore be obtained assuming steady state within the microbial part of the food web. Particular properties of the Mediterranean ecosystem (P-limitation of both phytoplankton and heterotrophic bacteria, relatively high levels of silicate), makes the mathematical solutions particularly simple. If such descriptions can be verified experimentally, fairly elaborate representations of the microbial food web could be included in large scale ecosystem models without excessibe demands for computing power.

Key-words : geochemical cycles, models, food webs, bacteria.

Why model the microbial food web ?

Basic research

The latest two decades has brought us a lot of knowledge on individual trophic interactions in the microbial food web, but few tools to link this knowledge into a unifying concept of food web and how its structure and function is regulated. We therefore still need models to explore how the system of unicellular phytoplankton, protozoa, bacteria, and viruses really works.

Applications

The microbial food web is the system that transforms dissolved substances into particulate form and small particles into larger ones, eventually producing food for organisms large enough to be of commercial value. This system links the ocean's uptake of atmospheric CO_2 to the downwards transport of organic matter and it links the C-cycle to those of N, P, and Si, as well as all other elements that are natural components of microbial biomass. As the organic-C:N:P:Si ratio is highly variable with the source of runoff-water and its contamination with farmland drainage or urban sewage, the fate and effect of such discharges is closely linked to the mechanisms regulating structure and function in the microbial food web. Since most of the particle surface area is associated with the smallest particles, while sinking particles are large, the fate and effect of surface-active pollutants originating from industrial waste, transport of crude oil or anti-fouling ship paints, will also be associated with functions of the microbial food web. As in any ecosystem, the success of any microbe in the pelagic ecosystem depends on a successful strategy for obtaining a share in the flux of energy and matter through the food web. Diversity and food web functioning are thus just two aspects of the same reality, and have ultimately to be understood from the same description of the food web. To get a description of the integrated type needed to approach such problems, there seems to be few alternatives to some kind of mathematical model of the microbial food web.

How to model the microbial food web

Most mathematical models of the microbial food web are based on sets of coupled differential equations linking the rate of change in one microbial population to its trophic neighbours in the food web. Such models have, however, at least two problems.

- It is difficult to get a good insight into how assumptions concerning interactions and parameter values influence the model's behaviour.
- Due to rapid dynamics, numerical solutions may require the use of short time steps. Combining such models with 3-D models of physical oceanography may therefore require excessive computing power ?

We have proposed a different approach where either parts of (1), or the whole microbial complex (Fig. 1) is assumed to be in internal equilibrium. When this assumption is used, the whole state of the microbial part of the food web can be solved from the set of algebraic equations formed by the equilibrium conditions :

$$\text{Growth} = \sum \text{Losses}$$

for each functional group of micro-organisms, and the mass balance requirement that :

$$N_t = N + \sum N_i$$

where Nt is the total concentration of limiting element in the microbial community, N is concentration in the pool of free mineral nutrients, and N_i is the concentration in functional group i of micro-organisms (*e.g.* P in bacteria biomass).

In the Mediterranean, bacterial, as well as phytoplankton growth rate have been suggested to be P-limited (2, 3). In the case where there is a surplus of silicate, this means that all osmotrophs in the microbial food web in Fig. 1 are limited by the same mineral nutrient. In this case the solution to the steady state equations become particularly simple. Using this simple solution as a reference, the significance of observations such as the bacterial P-limitation and the dominance of bacterial over phytoplankton biomass in the eastern Mediterranean (4) will be discussed.

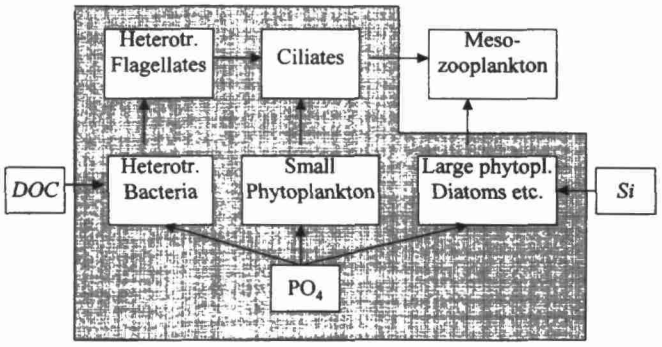

Figure 1. Schematic diagram indicating the microbial part of the food web inside the shaded area. The approach suggested is to assume steady state inside the microbial complex. This steady state can then be found as a function of the total nutrient content in the microbial part of the food web, and the mesozooplankton biomass. In more complex models where changes in the zooplankton population and in the total nutrient content is obtained from differential equations, the state of microbial food web may be derived from solving a set of algebraic equations. These equations will be particularly simple when there is an excess of both DOC and silicate.

In the simplest case, the algebraic solutions contain only the total nutrient content, the mesozooplankton biomass, and the water exchange rate as independent variables. In the ideal case, this approach therefore delivers an algebraic microbial 'module' that can be inserted into larger models. If the larger model describe loss terms, reproduction, and migration of zooplankton by differential equations, the algebraic module may in principle produce zooplankton food availability as well as the whole state of the microbial food web (bacterial biomass, bacterial consumption of organic-C, phytoplankton size-distribution, etc.).

Further research aimed at validation of this approach, and at defining the conditions under which it is applicable, is needed.

References

1- Thingstad T.F., Havskum H., Kaas H., Lefevre D., Nielsen T.G., Riemann B. and Williams P.J.Le.B. Bacteria-protist interactions and organic matter degradation under P-limited conditions. Comparison between an enclosure experiment and a simple model. *Limnol. Oceanogr.* (submitted)

2- Thingstad T.F., Zweifel U.L. and Rassoulzadegan F. Indications P-limitation for both phytoplankton and heterotrophic bacteria in NW Mediterranean summer surface waters. *Limnol. Oceanogr.* In press.

3- Zohary T. and Robarts R.D. Experimental study of microbial P-limitation in the eastern Mediterranean. *Limnology and Oceanography.* In press.

4- Van Wambeke F., Christaki U., Bianchi M., Psarra S. and Tselepides A. Heterotrophic bacterial production in the Aegean Sea. *Progress in Oceanogr.* In press.

GEOCHEMICAL INDICATORS OF RIVERINE INFLUENCES ON TROPHIC GRADIENTS IN THE NORTHERN MEDITERRANEAN SEA

N. B. Price [1], P. Giordani [2], V. Balboni [2], D. E. Hammond [3], S. Miserocchi [2], A. Malaguti [4], S. Mowbray [1] and T. Brand [1]

[1] University of Edinburgh, Department of Geology and Geophysics, King's Buildings, West Mains Road, Edinburgh EH9 3JW, U.K.
[2] Istituto per la Geologia Marina, CNR, Via Gobetti 101, 40129 Bologna, Italy
[3] Department of Earth Science, University of Southern California, Los Angeles, USA
[4] ENEA AMB CAT FRAL, Via Don Fiammeli 2, 40128 Bologna, Italy

Abstract

Studies of sediment and suspended particulate matter (SPM) have been made on the western Adriatic shelf, the northwestern Mediterranean margin and the Aegean Sea, to identify and geochemically characterise trophic gradients influenced either by river nutrient inputs or where production is controlled by vertical circulation, as in pelagic environments. Gradients in west Adriatic shelf sediments calculated as rain rates of C_{org}, Si_{bio} as well as rates of oxygen consumption show a well defined southward gradient. SPM studies of C_{org}, P_{org} and Si_{bio} in the three areas identify standing crop : these show a general decrease southwards although certain pelagic areas can also show high values. These elements by themselves cannot be used to discriminate between environments either influenced or not influenced by riverine nutrient inputs. To do this requires information on two indicator elements, Al and Mn. The former broadly relates to river discharge and bottom sediment resuspension. Mn on shelves is also river derived but is redox cycled depending on the rain rate of organic matter.

Key-words : Primary production, continental margin, particulates

The Mediterranean Sea is characterised by oligotrophism that increases from west to east. However, several areas, particularly at its northern margin and especially the Gulf of Lions, the western Adriatic and Northern Aegean Seas show moderate to high levels of primary productivity and chlorophyll concentrations such that there is also a north to south gradient of increasing oligotrophy. This latter trend to a significant extent is induced by nutrient discharges from the coastal zone, particularly from the rivers Rhone and Po and others entering the north Aegean. This paper is an attempt to explore the effect of increased biological productivity on the composition and concentrations of elements in suspended particulate matter (SPM) from these three areas, as well as identifying particulate elements that enable discrimination between primary produced by riverine discharge and that produced within the pelagic environment.

Given that there is likely to be considerable seasonal and interannual variation in SPM element concentration, a study has also been made on the compositional trends of biogeochemical elements in the surficial sediments of one of these areas, the western Adriatic shelf, in order to relate them to the distributionsof SPM elements in the overlying waters.

Materials for study

During the MTP-I project (1993 - 1996) selected stations, mostly representing transects crossing the shelf and upper slope within the Gulf of Lions and western Adriatic, have been sampled at different seasons. These investigations were constituent parts of the EUROMARGE - NB, EUROMARGE - AS and OTRANTO projects.

Within the Adriatic, 5-6 transects normal to the coast as well as spot stations have been sampled on its western shelf (mostly between 20-70 m), from the River Po outfall to south of Pescara during two contrasting seasons. The results can be used to assess the southward dispersal of riverine discharge and the effect this has on trophic systems within the western limb of the Adriatic cyclonic gyre. Discharge of SPM through the Strait of Otranto has been studied from a transect across the strait sampled at two contrasting seasons, August 1993 and November 1994. Such a data set for the Adriatic provides a means of assessing the southward gradient of oligotrophy from an area of comparatively high productivity in the north. Coupled to this, box cores have been sampled at eight stations, many of which underlie the SPM transects. Two of these stations, however, are located in the mid- and southern Adriatic basins, and essentially represent an end member of the trophic gradient within the Adriatic.

In the northwestern Mediterranean, SPM was sampled seasonally, as depth profiles (8-10 depths) on transects normal to the coast off Marseilles and Banyuls-sur mer, as well as a transect intersecting the Balearic Islands. Given an easterly flow of upper waters in the Gulf of Lions, only the transect off Banyuls-sur-mer is directly influenced by the Rhone discharge and its SPM composition should reflect this.

In the Aegean the composition of SPM in its northern waters relates to a complicated water mass structure as well as to river discharges from northern rivers in Greece, and the influx of Black Sea waters via the Dardanelles. In contrast, water from the Cretan Sea, taken on a transect at approximately 36°N during the PELAGOS 1994 and MATER 1997 projects, is isolated from direct sources of riverine influence. Here the terrigenous, biogenic and authigenic constituents within the SPM relate to mechanisms associated with a pelagic environment, and can be regarded as an end member of the Mediterranean trophic gradient.

Results

Sediments

Depth integrated values of primary production estimates in the Adriatic for two contrasting seasons (Fig. 1) show highest values in April, but there is only a general decrease southwards to Station 5. The correlation between primary production and potential limiting factors (nutrients, chlorophyll-a, PAR) suggests that PAR is the main controlling factor for production on a yearly time scale, as has been observed at Station 2 (off Cesenatico). At northern stations, production can be higher in autumn and spring where smaller light availability is compensated by higher riverine nutrient supply. At the southern stations (*e.g.* Station 5) PAR is the likely controlling factor over the year.

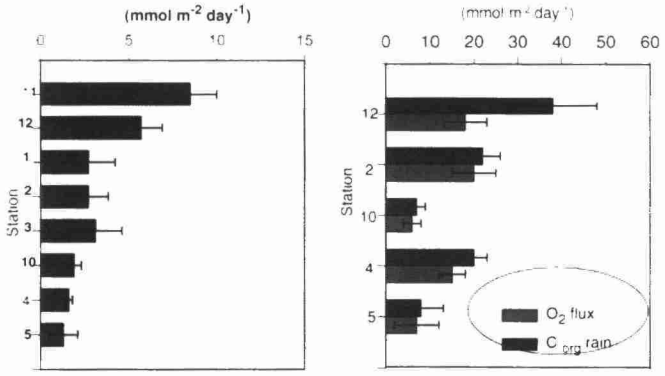

Fig. 1. Calculated oxygen consumption fluxes (left) and Si and Corg rain rates (right) of west Adriatic shelf sediments from north (top) to south (bottom).

Surficial sediments have been analysed for sediment accumulation rates (^{210}Pb), on-deck oxygen penetration depth, C_{org} (C/N atomic ratios) and biogenic SiO_2 concentrations. The relative magnitude of these depends on the combined effects of processes in the water (terrestrial atmospheric input, biological productivity, hydrodynamics) and in the sediments (water exchange reactions, benthic biological activity, organic respiration). Their distributions are important in indicating the gradient of the trophic activity in the overlying waters. In this context a station contrast occurs between the five northern stations (11-3) and the middle shelf (4) and middle and southern basins (10 and 5). Sediment accumulation rates (SAR) show a well defined southward decrease commensurate with dispersal of a major

CARTOGRAPHIE DE LA MEDITERRANEE ORIENTALE : CONTRIBUTION FRANÇAISE

Benoît Loubrieu* et Catherine Satra
DRO/GM Ifremer Brest, B.P. 70 - 29280 Plouzané, France

Résumé
Plusieurs laboratoires français de recherche ont dirigé des campagnes dont les objectifs majeurs sont la cartographie bathymétrique et l'imagerie acoustique de la ride méditerranéenne en Méditerranée orientale. Le département Géosciences Marines de l'Ifremer a participé activement aux traitements des données de ces campagnes : les résultats associent deux types d'information, bathymétrie et imagerie, essentiels et complémentaires pour la connaissance des fonds marins et les études scientifiques aux échelles locales ou régionales. Nous avons envisagé de systématiser les traitements déjà réalisés à la suite des différentes campagnes dans le but de produire une compilation des données de bathymétrie et d'imagerie des campagnes des navires de L'IFREMER sur la ride méditerranéenne. La question est posée de l'intégration de cette compilation à des travaux déjà réalisés ou en cours par d'autres groupes au plan international.

Mots-clés : Bathymetry, Geomorphology, Acoustics, Eastern Mediterranean

Au cours de plusieurs campagnes océanographiques, les navires de l'Ifremer ont réalisé, pour le compte de laboratoires français, une reconnaissance cartographique en Méditerranée Orientale (figure 1), avec parmi la panoplie d'outils mis en oeuvre, les sondeurs multifaisceaux et les sonars latéraux. Les campagnes du N/O *L'Atalante* concernées sont les missions Heralis (juillet 92, chef de mission J.P. Foucher, IFREMER), Médée (juillet 95, chefs de mission N. Chamot-Rooke et X. Le Pichon, ENS Paris), PrismedII (programmée en février 98, chef de mission J. Mascle, Observatoire de Villefranche-sur-Mer), auxquelles s'ajoutent la mission Jason du N/O *Suroît* (mai 94, chefs de mission J.P. Foucher, IFREMER, et S. Lallemand, ENS Paris) et les campagnes et transits du N/O *Jean Charcot*, dont Heat (septembre 78, chef de mission X. Le Pichon, Université de Paris VI) et Escarmed (janvier 80, chef de mission Y. Morel, IFREMER).

Le groupe Cartographie/Traitement de données du département Géosciences Marines de l'Ifremer, en association avec les laboratoires français demandeurs de ces campagnes, a contribué activement aux traitements des données EM12D, Seabeam et SAR acquises au cours de ces missions. Les équipements de cartographie mis en oeuvre permettent la production de documents de bathymétrie et d'imagerie à des échelles locales à régionales. Selon les caractéristiques de chaque équipement, et également selon les conditions d'acquisition qui influent sur la qualité des données (type de positionnement, état de la mer, ...) [1], les échelles cartographiques escomptées sont le 1/20000ème et 1/50000ème pour l'imagerie SAR (Système Acoustique Remorqué de l'IFREMER), le 1/100000ème et 1/250000ème pour le sondeur multifaisceaux Simrad Em12D et le 1/250000ème pour le sondeur Seabeam du N/O *Jean Charcot*.

Dans le but de fournir des documents cartographiques aussi complets que possible, les traitements déjà réalisés à l'issue de chacune des campagnes peuvent être systématisés et conduire à la réalisation d'une compilation numérique des données de bathymétrie et d'imagerie. L'objectif est d'intégrer et d'homogénéiser l'ensemble des données.

De manière à respecter les caractéristiques des données, en particulier le détail d'information apporté par chaque outil d'acquisition, la compilation est "multi-échelle" : chaque type de données est classifié et s'intègre à l'échelle cartographique avec

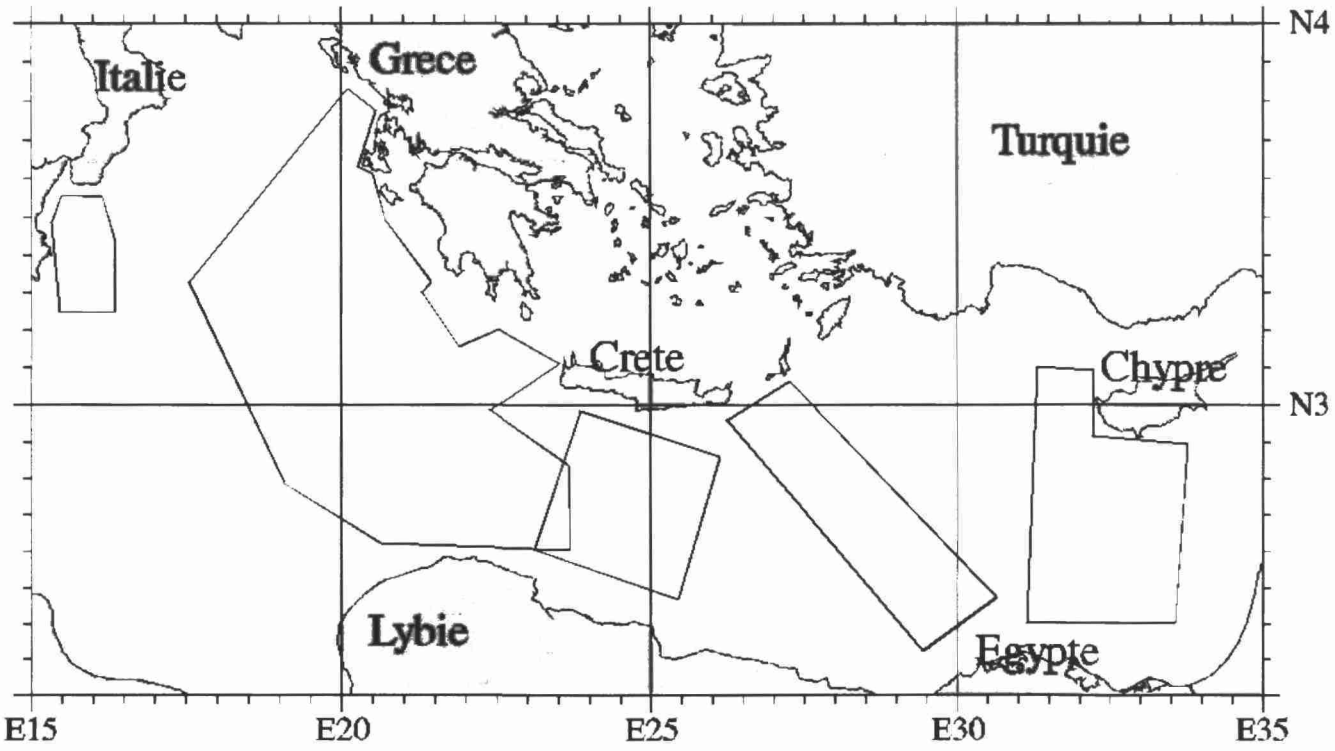

Figure 1 : Zone des levés multifaisceaux en Méditerranée Orientale effectués lors des campagnes océanographiques françaises.

MAPPING THE ANAXIMANDER MOUNTAINS WITH EM12D SWATH MAPPING

J.M. Woodside

Geomarine Centre, Free University, De Boelelaan 1085, 1081 HV Amsterdam, The Netherlands

Key-words : swath mapping, Mediterranean Ridge

The Dutch ANAXIPROBE Project to determine the origin and evolution of the Anaximander Mountains in the eastern Mediterranean was based on five days of Simrad EM12D swath mapping. This type of surveying, carried out at a rate of about 20 km^2 per hour, at the depths found in this area (about 2000 m), provides not only highly accurate bathymetric data but also acoustic backscatter information related to the type of sedimentary cover as well as the morphology and fine scale relief of the seafloor. Rudimentary sedimentology is a development from such mapping to be expected in the near future. With the addition of seismic reflection profiles, gravity and magnetic anomalies, and low frequency echo-sounder profiles along the same lines, the survey data set is a rich and detailed source of information which is both daunting in its vast size and demanding in the level of analysis which it warrants.

The data from this 1995 survey aboard the French research vessel *L'Atalante* were used for detailed follow-up work in 1996 aboard the Russian research vessel *Gelendzhik*. The high backscatter data in areas of steep bathymetry indicated slopes where it might be possible either to sample hard rock outcrops or coarse talus from the exposed bedrock. High backscatter from circular targets with low relief (about 50 to 200 m relief and diameters of 500 m to 2 km) was inferred to be caused by mud breccia erupted at mud volcanoes, and therefore potential sources of rock samples from basement rocks at depth. The high backscatter had been shown previously (1) to be caused by volume scatterers in the upper metre or so of seafloor sediments (*i.e.* bedrock clasts in the mud breccia typical of mud volcanoes). Sampling of these targets successfully confirmed the basic assumption of mud volcano deposits; and the sampling programme successfully confirmed the hypothesis that the Anaximander Mountains are a continuation of the Tauride geology of southwestern Turkey, as reported elsewhere in this congress. Detailed deep tow sidescan sonar and subbottom profiler data from the follow-up survey clarified many of the swath mapping results, allowed the sampling targets to be determined with greater precision, and indicated the presence of gassy sediments in large parts of the survey area, but did not change the general expectations issuing from the original survey.

The combination of detailed bathymetry and backscatter "'imagery" is a powerful tool in neotectonic studies such as this. Subtle neotectonic deformations of the seafloor are visible to such swath mapping methods while they may remain invisible or at best ambiguous in the more traditional surveying methods (using, for example, single profiles of even high resolution subbottom profilers). The human eye (and computer methods) can resolve linear features related to seafloor structures and sedimentary deformation as well as small changes in backscatter strength related to changes in sedimentary facies, when these patterns are reinforced within the large volume of data. (For example, although a single pixel of data related to the crossing of a deep sea telephone cable would normally not be noticed, when the single pixel is accompanied by many such pixels the eye is easily able to correlate the pixels as a linear feature; this is the benefit of accurate and repetitive data forming broad swaths.)

The ANAXIPROBE EM12D swath mapping data in combination with similar EM12D data from the 1998 PRISMED-II expedition in adjacent areas show neotectonic deformation which must be explained in any interpretation. It is clear that there are important northeast-southwest trends across the area which are probably related to the Strabo Trench/Pliny Trench trends forming the transpressional plate boundary along the eastern Hellenic Arc. These cross-cutting trends cause offsets in the general northwest-southeast orientation of the eastern Anaximander Mountains and the Florence Rise. The northeast-southwest trends are clearly related to a direction of compression across the mountains also because there is a clearly imaged fold belt in the Antalya Basin which appears to have been created by the northeastward movement of the Anaximander Mountains into the Antalya Basin.

Acknowledgements

The swath mapping carried out during project ANAXIPROBE was financed by the Netherlands Geosciences Foundation (Stichting GOA) under project number 750.195.02. The cooperation within this research of colleagues from France, Russia, and Turkey is also gratefully acknowledged.

References

(1) Volgin, A.V., and Woodside, J.M., 1996, Sidescan soar images of mud volcanoes from the Mediterranean Ridge: possible causes of variations in backscatter intensity. *Marine Geology*, 132:39-53.

PRISMED II CRUISE IN EASTERN MEDITERRANEAN SEA MAIN RESULTS (28 JAN - 28 FEB 1998)

Jean Mascle*
and the PRISMED II Scientific Party
Observatoire Oceanologique de Villefranche - UMR 6526, Geosciences Azur, B.P. 48, 06235 Villefranche-sur-mer, Cedex, France

Key-words : sawth mapping, Eastern Mediterranean

During PRISMED II cruise (conducted on board the R/V *L'Atalante* by UMR CNRS Géoscience Azur, Villefranche-sur-Mer) four main sectors of the eastern Mediterranean basin were surveyed in great detail. The objectives were to study both the characteristics of the recent to present deformations and the sedimentary processes acting in this narrow Mesozoic basin still separating the African Continental Margin from the southern border of the Anatolian-Aegean Microplate and Europe.

EM12 Dual survey (bathymetry and acoustic imagery) at 100 % recovery, together with geophysical profiling (serial 6-channel continuous seismic reflection, 3,5 kHz echo-soundings, magnetic and gravimetric data) were continuously recorded on board the R.V. *l'Atalante*.

This strategy was considered as the best to better map, understand and finally interprete, at a regional scale, the morphological, structural and sedimentary characteristics of this area involved in incipient continental collision between African Plate and European Plate in the Aegean sector. In the near future (some Ma), this region will give rise to a mountain belt system.

The successively surveyed four main zones were:

- (1) a broad domain of the Mediterranean Ridge (250 km in length, 200 km in width), **between the south of Crete and Libyan Margin**. There, data (especially the acoustic imagery) clearly demonstrate the presence of different structural domains, characterized by numerous tectonic features (thrusts, folds, normal faults, strike-slip faults), reflecting the coexistence of sub-surface ductile deformations, and deep brittle fracturing. Numerous mud volcanoes, localized in two main distinct belts, were also described.
- (2) a wide elongated area (450 km in length, 100 km in width), **between the south-east margin of Crete and the Nile Deep-Sea Fan**. In this sector, deformation of the Mediterranean prism shows, in front of the Nile Delta, broad asymmetrical folds bordering a northern internal domain where large flows of probably highly fluid material (under-compacted mud ?) were observed. The Nile Delta shows, in this sector, an important network of meandering channels distributing the Nile sedimentary input to the abyssal plain, even locally almost directly to the present-day compression front.
- (3) two contiguous zones were also surveyed, respectively **west and south of Cyprus island.** The first zone (Florence sector) illustrates the transpression type structural connection, between the Mediterranean Ridge and the active subduction/collision south of Cyprus. In the second area, a detailed study of the Eratosthenes Sea Mount was performed. This sea mount, which consists of a fragment of the African craton colliding with Cyprus, is intensively cut by normal and strike-slip faulting, and its contact with the Cyprus Margin shows intense compressional deformations.
- (4) At last, a broad sector of the **Nile Deep-Sea Fan** was also surveyed at the end of the cruise. Towards the east, growth pattern indicates the halokinetic influence of underlying Messinian salt layers, and active tectonism, most probably of transtensional type related to the Suez rift system. Active tectonism also clearly controlled the distribution of numerous salt diapirs. Offshore Port Saïd, the fan is affected by huge submarine mass-flows, that are controlled by both deep active tectonics and by upflow of underlying Messinian strata.

During this cruise, more than 13,000 km of geophysical profiles and about 200,000 km^2 (more than 1/3 of the surface of France) of EM12 data (bathymetry and acoustic imagery) were collected in the Eastern Mediterranean, thanks to the particularly high tech geophysical and computer equipments of the R/V *L'Atalante*.

PRISMED II Scientific Party : BELLAICHE Gilbert, BENKHELIL Jean, BUFFET Georges, CHAMOT-ROOKE Nicolas, CHAUMILLON Eric, DROZ Laurence, ERGUN Mustafa, FOUCHER Jean-Paul, GAULLIER Virginie, GRIBOULARD Roger, HUGUEN Caroline, JOHN Alastair, KOPF Achim, LAMARCHE Geoffroy, LEVY Ronit, LIMONOV Anatoly, LOUBRIEU Benoît, MART Yossi, METAYER Bernadette, SHAKED Yonathan, VOLKONSKAIA Anna, WOODSIDE John, ZITTER Tiphaine.

MUD VOLCANOES ON THE MEDITERRANEAN RIDGE SEAFLOOR MAPPED BY SWATH BATHYMETRY AND ACOUSTIC IMAGERY: PRELIMINARY RESULTS FROM THE MEDEE AND PRISMED II CRUISES.

J.P. Foucher [1*], J. Mascle [2], N. Chamot-Rooke [3], B. Loubrieu [1], C. Satra [1], V. Motti [4]
and the shipboard scientific parties of the MEDEE and PRISMED II cruises

1 Département Géosciences Marines, Ifremer, BP70, 29280 Plouzané cedex, France
2 Geosciences Azur, BP48, 06230 Villefranche sur Mer, France
3 Laboratoire de Géologie, ENS, 24 rue Lhomond, 75231 Paris cedex 05, France
4 Université Bretagne Occidentale, 6 avenue Le Gorgeu, 29287 Brest cedex, France

Abstract

Bathymetry and acoustic imagery data of the MEDEE (1995) and PRISMED II (1998) cruises bring further insights into the distribution and properties of mud volcanoes on the Mediterranean Ridge Accretionary Prism. An inner belt of mud volcanoes is traced on the summit and inner flank of the ridge, throughout its western and central parts, between longitudes 20°30'E and 25°30'E. This inner belt includes the Pan di Zucchero, Prometheus 1 and 2, Olimpi, and United Nations mud dome fields. Mud volcanoes of this inner belt have grown in an area of maximum contraction of the prism against the rigid backstop. A distinct line of small mounds, tentatively interpreted as a second belt of mud volcanoes, is traced over a distance of 70 km, on the outer flank of the central part of the Mediterranean Ridge. In contrast to the mud domes of the inner belt, mounds of the outer belt do not exhibit a high backscatter, thus suggesting different properties of the erupted muds.

Keywords: Mud volcanoes, bathymetry, swath mapping, Mediterranean Ridge

One major acoustic feature of the Mediterranean Ridge seafloor, in the Eastern Mediterranean Sea, is the occurence of sharply defined patches of high reflectivity. These patches, with subcircular or elongated shapes and lateral dimensions of several hundred meters to a few kilometers, were first observed during four cruises of the RRS *Discovery* (1971, 1973, 1977, 1979) by means of 6.5 kHz GLORIA long-range sidescan sonar (1). Further highbackscattering patches were discovered south of Crete in 1993 during Leg-2 of the Third Training Through Research cruise of R/V *Gelendzhik* by means of both 9.5 kHz OKEAN and 30 kHz MAK-1M (2,3). A multibeam bathymetric survey during *Meteor* Cruise 25/4 in 1993 by means of the Hydrosweep echosounding system supplemented the sidescan sonar records in the latter area (4). Additional sidescan sonar records during the Fifth and Sixth Training Through Research cruises of R/V *Professor Logachev* in 1995 (5) and R/V *Gelendzhik* in 1996 (6) detected several new highbackscattering patches in the Eastern Mediterranean Sea. Recently, two cruises of L'Atalante operating an EM12-D echosounding system, MEDEE in 1995 and PRISMED II in 1998, have produced bathymetric maps and seafloor acoustic images of broad areas of the Mediterranean Ridge, thus providing for the first time with a ridge-scale view of the areal distribution and associated morphological characteristics of highbackscattering patches in those surveyed areas.

Proposed interpretations (1) of the high backscattering patches on the Mediterranean Ridge include outcrops of hard rocks (such as Messinian evaporites), fold crests, debris flow deposits, mud volcanoes or mud diapirs. The presence of mud breccia at or near the seafloor is one simple explanation for the highbackscattering of mud volcanoes in the Eastern Mediterranean Sea (2, 7). A combination of bathymetric data and seafloor acoustic images from the MEDEE and PRISMED II cruises clearly shows that a large number of highbackscattering patches on the Mediterranean Ridge are associated with conical or elongated mounds, often several tens of meters high. Also, areas of highbackscatter are not strictly limited to those areas covered by the mounds but extend into seafloor depressions at their base. Our current interpretation of most of the high-backscattering patches on the Mediterranean Ridge is that they express the presence of mud volcanoes and mud breccia flows.

The high backscattering patches define a belt, approximately 30 km wide, of mud volcanoes at the prism-backstop boundary. This belt is traced throughout the western and central parts of the ridge, approximately from 20°30'E to 25°30'E. It includes the Pan di Zucchero, Prometheus 1 and 2, Olimpi and United Nations Rise mud volcano fields. Mud volcanism along this belt appears to be controlled by the ridge deformation in relation with the Africa-Aegea convergence. In the westernmost part (Prometheus 1), mud volcanoes follow a linear transpressive structure interpreted as the result of a dextral shear that partly accomodates the obliquity of the Africa motion with respect to the backstop. In the Pan di Zucchero area, the eastward escape motion of the prism produces a wide senestral shear band associated with N110°E to N150°E en-echelon folds along which mud volcanoes have grown. Further east, the Olimpi and United Nations Rise fields are associated with intensive deformation ahead of two backstop promontories.

A second belt of mounds, which we suggest are also mud volcanoes, was discovered during the PRISMED II cruise. This second belt (outer belt) is traced over 70 km in the central part of the Mediterranean Ridge, south of the Olimpi mud volcano field. The mounds of this second belt are located at a constant distance, approximately 40 km, from the front of the prism. They are of smaller lateral dimensions. They do not exhibit the high backscattering characteristics of most of the mud volcanoes of the first belt (inner belt), presumably because the erupted materials are different.

The PRISMED II data brings further information on the Olimpi mud dome field (8). The Olimpi field, sensu stricto, contains 9 principal mud domes over an area of approximately 20 km by 15 km. The Napoli, Milano, Bergamo, and Hilo domes are the prominent ones, with diameters between 1 and 4 km and elevations between 40 and 80 meters above the mean seafloor level (8, 4, 3). Napoli, the largest dome, has a flat top and a 100 deep circular moat at its base. Napoli and Hilo exhibit a low backscatter in strong contrast with Milano, Bergamo and Monza which exhibit a high backscatter (3). The PRISMED II data shows that areas of high backscatter for these three domes form a single elongated patch , extending 1-2 km onto the seafloor away from their flanks in all directions. The low backscatter of Napoli and Hilo suggests a different nature of the subseafloor, possibly the presence of a larger amount of gas (9). Not all the parts of Napoli are acoustically characterized by a low backscatter: its very axial part is a spot of high backscatter. The PRISMEDII data also suggest the presence to the north of Napoli of a broad, shallow furrow, over 20 km long, along which fluid muds or brines, erupted from the dome, could have flowed to the Pline trough.

References:

1. Fusi N., Kenyon N.H., 1996. Distribution of mud diapirism and other geological structures from long-range sidescan sonar (GLORIA) data, in the Eastern Mediterranean Sea. *Mar. Geol.*, 132 : 21-38.
2. Volgin A.V., Woodside, J.M., 1996. Sidescan sonar images of mud volcanoes from the Mediterranean Ridge: possible causes of variations in backscatter intensity. *Mar. Geol.*, 132 : 39-53.
3. Galindo-Zaldivar J., Nieto L., Woodside J.M., 1996. Structural features of mud volcanoes and the fold system of the Mediterranean Ridge, south of Crete. *Mar. Geol.*, 132 : 95-112.
4. Hieke W., Cita M.B., Mirabile G.L., Negri A., Werner F., 1996. The summit area (Antaeus/Pan di Zucchero) of the Mediterranean Ridge: a mud diapir belt ? *Mar. Geol.*, 132 : 113-129.
5. Ivanov, M.K., Limonov, A.F., Cronin, B.T. eds, 1996. Mud volcanism and fluid venting in the eastern part of the Mediterranean Ridge. Unesco Rep. *Mar. Sci.*, 68 , 126 pp.
6. Woodside, J.M., Ivanov, M.K., Limonov, A.F. eds, 1997. Neotectonics and fluid flow through seafloor sediments in the Eastern Mediterranean and Black Seas. Part 1: Eastern Mediterranean Sea. UNESCO/IOC Techn. Ser., 48 , 128 pp.
7. Almendinguer, R., Guillon, L., 1997. A model for acoustical backscatter from mud volcano breccia. In : Abstract volume, Gas and fluids in marine sediments Conference, Amsterdam, January 27-29, 1997 : 34.
8. Camerlenghi, A., Cita, M.B., Della Vedova, B., Fusi, N., Mirabile, L., Pellis, G., 1995. Geophysical evidence of mud diapirism on the Mediterranean Ridge Accretionary Complex. *Mar. Geophys. Res.*, 17 : 115-141.
9. Robertson, A., Ocean Drilling Program Leg 160 Scientific Party, 1996. Mud volcanism on the Mediterranean Ridge: Initial results of Ocean Drilling Program Leg 160. *Geology*, 24, 3 : 239-242.

MORPHOLOGIE ET STRUCTURE DE LA RIDE MÉDITERRANÉENNE AU SUD DE LA CRÈTE D'APRÈS LES DONNÉES DE LA CAMPAGNE PRISMED II

Huguen C., Mascle J.*, et l'équipe scientifique embarquée
UMR Géosciences Azur, BP 48, 06235 Villefranche-sur-Mer Cedex, France

Abstract
We briefly present and discuss a set of geophysical data which has recently been recorded across a large area of the Mediterranean Ridge south of Crete. The preliminary interpretation of these data allows to indicate that, in this area, the Mediterranean Ridge consists of a thick wedge of sediments submitted to different types of brittle and ductile tectonics. We believe that the overall structure reflects the effect of incipient ongoing continental collision.

Mots clés : Mud volcanoes, swath mapping, Mediterranean Ridge

La campagne PRISMED II, qui s'est déroulée du 28/01 au 28/02 1998 a bord du NO *Atalante*, a permis l'acquisition en continu d'une grande quantité de données géophysiques. Le premier des grands domaines étudiés au cours de cette campagne représente une surface d'environ 50000 km^2 s'étendant entre les marges continentales de la Libye au sud et de la Crète au Nord. Cette zone recouvre un vaste domaine de la Ride Méditerranéenne. Nous présentons ici les premiers résultats concernant la morphologie et la structure de cette région sur la base des données de bathymétrie multifaisceaux, d'imagerie acoustique (réflectivité), et de sismique réflexion rapide (6 traces), enregistrées le long de 14 profils de direction N10, d'environ 120 milles de long. L'analyse préliminaire de ces données a permis de distinguer plusieurs grands domaines offrant des caractéristiques morphologiques et structurales bien distinctes. Ce sont du Sud vers le Nord : la marge continentale libyenne, la Ride Méditerranéenne au sein de laquelle se distinguent plusieurs unités, enfin, la marge Crétoise.

La marge libyenne présente, aux environs de 24°E, un changement de direction également souligné par une morphologie de détail et des structures internes différentes. La région occidentale (1500 à 2000m de profondeur) ne montre que peu de traces de remobilisations sédimentaires de surface, mais est affectée par une tectonique cassante récente soulignée par des failles relativement rectilignes de direction N80. Au delà de 24°E, la marge s'approfondit plus rapidement et comporte un grand nombre de canyons très accusés. A ce niveau, la sismique indique une séquence sédimentaire épaisse sous laquelle se distinguent des horizons profonds, souvent discontinus et décalés par de nombreux petits accidents distensifs. Dans ce secteur, la base de la pente continentale et la transition avec la Ride Méditerranéenne sont de morphologies très variables. Vers l'Ouest existe un contact direct entre la marge libyenne et la Ride Méditerranéenne, alors que vers l'Est, les deux ensembles sont séparés par une série de bassins sédimentés de taille et de profondeur variables (entre 2800m à 3400m de profondeur).

Au contact avec la marge libyenne, le front de la Ride Méditerranéenne se présente sous la forme d'un escarpement sédimentaire et possède une géométrie et une structure très variables; cette variabilité résulte à la fois d'un contrôle par la morphologie de la marge et vraisemblablement par la quantité des sédiments impliqués dans l'accrétion tectonique. Vers l'Ouest, le front de déformation s'exprime par plusieurs chevauchements superposés moulant le promontoire de la marge et dont la déformation évoque un phénomène de poinçonnement. Vers L'Est, le front de déformation se caractérise par un système de plis dissymétriques dont l'amplitude et la longueur d'onde s'accroissent progressivement en réponse à une quantité plus importante de sédiments impliqués (proximité du delta du Nil), et à la présence probable d'évaporites messiniennes. Au plan de la réflectivité, le front de déformation se caractérise par une réponse relativement inhomogène du fait de son intense déformation de surface. L'imagerie acoustique permet de distinguer un réseau de failles subrectilignes, d'orientations N130 et N40. Ces fractures sont également décelables sur la sismique, où elles affectent clairement les sédiments profonds de la couverture de la marge. Au nord de cette région, s'observe un domaine de réflectivité beaucoup plus faible et régulière, correspondant à une région plus plane caractérisée par une très faible déformation de surface. Dans cette zone, la bathymétrie et la réflectivité acoustique mettent en évidence la présence d'une ceinture de petits volcans de boue apparemment alignés selon une direction N120. Ces structures sont de dimensions modestes et ne montrent pas de coulées boueuses importantes. Au delà, vers le Nord, la déformation de surface de la Ride Méditerranéenne s'accroît, montrant des directions dominantes N0 à N130. On remarque en particulier une direction subméridienne très bien soulignée par la bathymétrie. Cette dernière matérialiserait une grande zone à valeur décrochante le long de laquelle se sont mis en place plusieurs gros volcans de boue avec de nombreuses coulées superposées. Le phénomène de volcanisme boueux s'observe également au niveau de la Zone Olympie et de la ride dite des Nations Unies, déjà été décrites dans la littérature. Cependant, ces volcans apparaissent installés préférentiellement face à des excroissances qui pourraient appartenir au butoir continental crétois.

La marge crétoise serait ainsi divisée en deux grandes régions. Une première, située à une profondeur moyenne de 2700m est en contact direct avec la Ride Méditerranéenne et se caractérise par une réflectivité très faible et une topographie peu accentuée. Une seconde séparée de la précédente par le système des fosses de Pline, constitué de dépressions profondes (3000 à 4000m de profondeur), est intensément découpée par des accidents à caractère distensif.

Au niveau de la Ride Méditerranéenne l'ensemble des données recueillies permet de mettre en évidence la coexistence de plusieurs types de déformation affectant la pile sédimentaire du prisme d'accrétion. Ainsi on observe, au sein de l'édifice, à la fois les effets d'une structuration profonde (crustale?) aboutissant à un découpage en grand du soubassement de la Ride (suivant des directions subméridiennes), un réseau de fractures qui découpent (ou remobilisent) les ensembles sédimentaires profonds de la marge Africaine passant en subduction et ,finalement, une déformation souple de surface et de subsurface. L'analyse ultérieure de détail de l'ensemble des données acquises devrait permettre de bien illustrer et discuter les caractères structuraux d'un domaine que nous pensons être représentatif d'un début de collision entre la marge africaine et la bordure égéenne.

DEFORMATION OF THE FLORENCE RISE, EASTERN MEDITERRANEAN, FROM EM12D SWATH MAPPING DATA

J.M. Woodside [1*], J. Mascle [2]
and shipboard scientists from the PRISMED II Expedition

[1] Centre for Marine Earth Sciences, Free University, De Boelelaan 1085, 1081 HV Amsterdam, The Netherlands
[2] Observatoire Oceanologique de Villefranche - UMR 6526, Geosciences Azur, B.P. 48, 06235 Villefranche-sur-mer Cedex, France

Key-words : Tectonics, swath mapping, Mediterranean Ridge

The Florence Rise was mapped in detail with Simrad EM12D swath mapping and a suite of geophysical methods (high speed seismic reflection profiling, 3.5 kHz echo sounding, gravity and magnetic measurements) during the French PRISMED II Expedition in February 1998. These data have been merged with similar data over the Anaximander Mountains, the northwesterly continuation of the Florence Rise structural trend, from the Dutch ANAXIPROBE expedition in 1995.

The Florence Rise is a gentle seafloor rise extending west from Cyprus to the Anaximander Mountains. It is an arcuate section of the Cyprus arc which runs from northern Syria through Cyprus to the Lycian promontory of southwestern Turkey. Because the Cyprus Arc has been considered to be a zone of late stage subduction of the thinned northern margin of northern Africa, the Florence Rise was thought to play the role of accretionary prism. The problem was that there is relatively low seismicity, no volcanism, no trench, and not much typical accretionary prism relief along the Florence Rise. The Antalya Basin to the north of the rise is a northward deepening and tilting sedimentary basin which existed already in late Miocene and therefore collected Messinian evaporites including massive halite. The Florence Rise, according to DSDP drilling results and other previous studies has only very thin evaporites (mainly gypsum) and thus was already a positive bathymetric feature in the late Miocene.

The swath mapping imagery from the Florence Rise region displays even subtle seafloor lineations and other evidence of neotectonic deformation, and the bathymetry shows the seafloor in unprecedented detail. The principal lineations do not provide an arcuate definition of the Florence Rise as might be expected; rather, there are cross- cutting features which are inferred to be strike-slip fault traces, with a general trend of about 065° to 075°. These cut obliquely across the roughly 116° trend of the rise in the area surveyed. The same east-northeast trends are most strikingly developed in the vicinity of the Eratosthenes Seamount to the south of Cyprus where they are also inferred to be faults.

Taking the Florence Rise and the eastern Anaximander Mountains to be tectonically and possibly structurally related, the entire arc from Cyprus to Turkey appears to be made up of about 5 or so more or less straight segments with slightly different trends and separated by faults or zones of discontinuity. Immediately west of Cyprus, the trends of the feature are roughly east-west despite two or three east-northeast to west-southwest oblique cross-cutting faults. West of about 32°E the trend shifts to about 116°, then west from near 31°E to about 145°, changing to 155° and then 165° in the Anaximander Mountains where the cross-cutting faults break the continuity of the structure.

If, as seems sensible to assume, the Florence Rise was formed originally as a result of subduction, then this has probably stopped or slowed substantially, and the tectonic situation altered. This may be a result of difficulties with the subduction of Eratosthenes Seamount under Cyprus. In any case, the Florence Rise is undergoing segmentation by the system of east-northeast to west-southwest faults, and the different segments are probably behaving independently. This is most evident where the eastern Anaximander Mountains segment is moving east-northeastward against the sediments of the Antalya Basin which have formed an arcuate fold belt as a result. The intensity of the compressional deformation here is probably responsible for the elevation of the eastern Anaximander Mountains which lie perpendicular to the inferred direction of compression. Closer to Cyprus the compression is more oblique and therefore causes less spectacular deformation, although this segment of the Florence Rise contains the uplifted block which was drilled during DSDP Leg 13.

One of the cross-cutting faults in the eastern Anaximander Mountains has caused a sinistral offset in the relief of the mountains, and gas vents and mud volcanoes are found along it. The mud and gas eruptions are believed to result from the release of pressure by penetration of the faults to a zone of overpressure (possibly a result of overthrusting) beneath or within the mountains. Analysis of the rocks brought up in the eruptions indicates that they are part of the Antalya Nappes Complex of southwestern Turkey. This suggests in turn that the deformation and relief of the eastern Anaximander Mountains is in part a result of fundamental geological differences with the eastern part of the Florence Rise. The swath mapping also suggests the presence of mud volcanoes on and just to the south of the eastern branch of the Florence Rise (high backscatter spots of circular positive relief), possibly also associated with faulting.

In summary, preliminary analysis of the swath mapping data in the few months since the PRISMED II campaign, along with the adjacent ANAXIPROBE data, suggests that the Florence Rise and eastern Anaximander Mountains are not part of a subduction system but form a zone of deformation related to the westward movement (escape) of the Anatolian plate and relative east-northeast to west-southwest convergence between the Anatolian plate and the African plate. The relative pole of rotation for this convergence is not likely to be too far to the south, which implies that the associated deformation is relatively slow.

CARACTÈRES MORPHOSTRUCTURAUX ET IMAGERIE DE LA DÉFORMATION DE L'ARC DE CHYPRE ET DU MONT ERATOSTHÈNES D'APRÈS LES RÉSULTATS DE CAMPAGNE PRISMED II

Jean Benkhelil [1], Jean Mascle [2], Yossi Mart [3*] et l'équipe scientifique embarquée

[1] URA-CNRS n°715, Laboratoire de Sédimentologie et Géochimie Marines, Université de Perpignan, 66860 Perpignan, France
[2] UMR Géosciences Azur, BP n°48, 06230 Villefranche-sur-Mer, France
[3] Centre for Marine Studies, Haifa University, Haifa 31905, Israel

Abstract

The Eratosthenes seamount and surroundings have been surveyed during the PRISMED II cruise, and from the swath bathymetry, acoustic imagery and seismics several zones have been individualized according to their morphostructural characteristics. A southern zone includes part of the Nile Deep Sea Fan crosscut by a N150E trending fault zone. The Eratosthenes seamount is affected by E-W trending normal faults while its northern slope is subjected to compression along a depression dominated by the Cyprus margin. Deformation of recent sediments along the foot of the Cyprus margin is related with thrusting which passes northeastwards to transcurrent faulting.

Mots clés : swath mapping, seismics, Levantine Sea

Le mont Eratosthènes est un vaste relief sous-marin de nature continentale situé entre Chypre et la marge africaine. Il a été interprété comme étant un bloc détaché de la marge africaine au début du Tertiaire (1), actuellement entrant en collision contre l'arc de Chypre (2). Au cours de la campagne PRISMED II (14/02 au 01/03/98), une couverture bathymétrique, imagerie acoustique, des profils de sismique réflexion, sondeur 3.5 kHZ complété par des levés gravimétriques et magnétiques, ont été réalisés sur une zone allant du pied de la marge Chypriote au delta profond du Nil. L'analyse préliminaire de cet ensemble de données permet de distinguer plusieurs domaines aux caractéristiques sédimentaires et structurales bien différenciées.

Le domaine méridional comporte une couverture sédimentaire caractérisée par 3 ensembles majeurs : un ensemble superficiel attribué au Plio-Quaternaire clairement relié au delta du Nil; son épaisseur varie considérablement (0.5 à 2 std) de part et d'autre du méridien E32°40. Sous cet ensemble une séquence à faciès sismique transparent est attribuée au Messinien, constitué d'évaporites dont l'épaisseur (0.5 std) de l'orde de 1 km diminue vers le Nord jusqu'à disparaître totalement au pied du mont Eratosthènes vers N33°10'. Un ensemble inférieur souligné à son toit par quelques forts réflecteurs correspond aux séries pré-messiniennes; il contient en profondeur de forts réflecteurs subhorizontaux.

La bathymétrie et l'imagerie acoustique de cette région permettent de distinguer : un domaine oriental à morphologie régulière s'approfondissant progressivement vers le nord et un domaine occidental accidenté par des rides orientées selon deux directions majeures N150°E et N10° délimitant des domaines à faible relief. L'examen des profils sismiques montre des domaines à fort remplissage plio-quaternaire bordés par des accidents injectés de matériel évaporitique.

La partie centrale du domaine étudié est occupée par le mont Eratosthènes ; ce dernier est recouvert par une mince pellicule de sédiments récents reposant sur un ensemble attribué au Crétacé/Tertiaire inférieur (1) peu ou pas déformé. La bathymétrie et l'imagerie acoustique illustre un relief de forme subcirculaire comportant un sommet plat légèrement basculé vers le Nord, bordé par des pentes à déclivités inégales, la pente septentrionale étant plus raide que la pente méridionale. Le mont est accidenté par des directions morphologiques orientées N80E qui correspondent en fait à un découpage en horsts et grabens dont l'activité actuelle est attestée par la déformation des dépôts les plus récents. On reconnaît cette direction sur la marge méridionale où elle semble être affectée par les accidents de la zone de déformation orientée au N150E.

Au Nord du mont Eratosthènes, une large dépression à fond sub-plan est bordée par des escarpements correspondant à la marge de Chypre. Les séquences acoustiques décelables sous le mont Eratosthènes plongent régulièrement vers le nord et sont recouvertes au sein de cette fosse par un ensemble qui s'épaissit contre des accidents actifs à composante inverse décelables en base de la marge chypriote. Vers le Nord-Est, ces accidents se prolongent par une zone à composante décrochante comportant des structures en fleur. Le pied de la marge chypriote se caractérise par un bourrelet de sédiments récents intensément déformés par le chevauchement de la marge sur le bloc Eratosthènes. Vers le Nord-Ouest ce dernier est entaillé par un escarpement arqué très abrupt contre lequel vient se mouler un système de plis localisé à l'extrémité du domaine de la ride de Florence.

L'analyse morphostructurale de la région du mont Eratosthènes montre que cette dernière correspond à un carrefour tectonique où se rencontrent plusieurs structures soumis à des régimes différents. Son secteur méridional est recouvert par l'extrémité du Deep Sea Fan du Nil et recoupé par des structures distensives transverses constituant le prolongement du rift de Suez. Leur activité en transtension est attestée par une sédimentation importante de sédiments récents et par de très nets décalages sénestres décelables le long d'accidents N150°E. Le mont Eratosthènes lui-même correspond à un bloc rigide surélevé qui est actuellement soumis à une extension N-S dans sa partie centrale, et à un début de compression à son contact avec la base de la marge chypriote sous laquelle il plonge.

Références

(1) Mart Y., Robertson A. H. F., Woodside J. M. and ODP Shipboard Science Party. 1997. Cretaceous tectonic setting of Eratosthenes Seamount in the eastern Mediterranean Neotethys : initial results of ODP Leg 160, C. R Acad. Sc. Paris, 324 (IIa), 127-134.

(2) Robertson A. H. F., Kidd R. B., Ivanov M. K., Limonov A. F., Woodside J. M., Galindo-Zaldivar J., Nieto L. and the Scientific Party of the 1993 'TTR-3' Cruise. 1995. Eratosthenes Seamount: collisional processes in the eastermost Mediterranean in relation to the Plio-Quaternary uplift of southern Cyprus, *Terra Nova*, 7, 254-264.

LE DEEP-SEA FAN DU NIL : RÉSULTATS PRÉLIMINAIRES DE LA CAMPAGNE PRISMED II DU N.O. *L'ATALANTE*

G. Bellaiche [1*], J. Mascle [1], L. Droz[2], V. Gaullier [3], Y. Mart [4]
et l'équipe scientifique embarquée.

[1] Observatoire Océanologique, GeoscienceAzur, 06230 Villefranche sur mer, France
[2] Université de Bretagne Occ., Brest, France
[3] Université de Perpignan, LGSM, Perpignan, France
[4] Recanati Center for Marine studies, Haifa, Israel

Abstract

Up to now, the Nile Cone, despite of its size, remains poorly known due to unsuited exploring methods which could not allow to clearly identify specific features commonly described in most deep-sea fans. In february 1998, PRISMED II cruise of the R/V *Atalante* allowed to survey the Nile Cone, thanks to swath multibeam bathymetric profiles, acoustic imagery (with Simrad EM 12 dual), high resolution seismic profiling. Three main structural and sedimentary provinces are identified. A detailed networks of sinuous distributary channels and channel structures are well evidenced. Associated features such as growth-faults , debris-flows layers etc. are present.

Mots clés : Swath mapping, sediments, Nile delta

Introduction

Malgré ses dimensions importantes — il s'agit du plus grand deep-sea fan de Méditerranée après celui du Rhône — le cône du Nil était jusqu'à présent très mal connu, en dépit d'études assez nombreuses. En particulier cela provenait du fait que les méthodes utilisées étaient inadaptées. La morphologie de cet appareil sédimentaire n'était connue qu'à partir de sondages classiques à faisceaux larges et il n'a jamais été possible de délimiter avec netteté les différentes provinces physiographiques, ou d'identifier les réseaux de chenaux de distribution. Au point de vue structural, les techniques de sismique pénétrantes utilisées jusqu'à présent, visaient surtout à mettre en évidence les réflecteurs profonds; elles étaient de ce fait incapables de révéler la structure sédimentaire détaillée du deep-sea-fan.

La campagne PRISMED II, réalisée à bord du N.O *l'Atalante* en Méditerranée orientale, a eu en partie pour objet l'exploration du deep-sea fan du Nil. Cette exploration s'est faite par des méthodes de bathymétrie et d'imagerie au sondeur multifaisceaux Simrad EM 12, au sondeur 3,5 kHz et par sismique haute résolution.

Résultats

Cette campagne a montré que le deep-sea fan du Nil comportait trois provinces sédimentaires et structurales très contrastées.

Province occidentale

Dans ce domaine, la bathymétrie Simrad, mais surtout l'imagerie, mettent en évidence, pour la première fois les chenaux d'alimentation du deep-sea fan du Nil. Ces derniers, très nombreux, sont de très grande longueur (près de 200 km), et sont affectés de méandres très resserrés évoquant ceux d'autres deep-sea fans comme l'Amazone, le Rhône ou le Zaïre. Ces chenaux apparaissent avec plus ou moins de netteté. Certains sont manifestement assez anciens et sont très estompés, d'autres, surtout dans le secteur Ouest, sont plus récents.

Un autre caractère de cette zone occidentale est la présence, dans le secteur amont, de phénomènes d'instabilité sédimentaire comme en témoignent les très nombreuses failles de croissance, que les profils sismiques mettent nettement en évidence. Ces failles synsédimentaires actives prennent appui sur les dômes salifères ou viennent s'ancrer profondément dans la couche de sel sous-jacente, d'âge probablement messinien. Le rejet vertical des failles peut atteindre 200 mètres, et localement, à leur contact, l'épaisseur des sédiments atteint 2 secondes t.d. En aval, la couverture sédimentaire s'épaissit uniformément et, on peut mettre en évidence, au sein de la sédimentation turbiditique du Nil, des couches interstratifiées ou superficielles de matériaux représentant probablement des débris flow. Ceux-ci se caractérisent par des faciès chaotiques et peuvent atteindre jusqu'à 0,7 seconde d'épaisseur. Leur extension géographique apparaît considérable.

Enfin dans le secteur le plus distal de cette province, les glissements s'estompent et les sédiments turbiditiques du cône, très épais, sont soumis, à proximité du front de la Ride Méditerranéenne, à un début de déformation compressive donnant naissance à des plis.

Province centrale

Cette région est surtout marquée par de nombreuses failles de croissance de 100 à 150 m de dénivellation, qui s'étendent sur un front de près de 200 km de large. En aval, les débris flows se manifestent en imagerie Simrad par des tons clairs. Il n'est pas possible cependant de savoir si de telles réflectivités sont dues réellement à la nature lithologique des sédiments remaniés, ou aux irrégularités du relief, les sédiments remaniés occupant des cuvettes faiblement déprimées.

Malgré cette déstabilisation généralisée, on arrive à suivre des tronçons de chenaux profonds, qui présentent toujours des cours très sinueux.

Dans la partie ouest de ce secteur central, il est possible de reconnaître la structure des chenaux, en corps acoustiques de forme lenticulaire et de mettre en évidence des phénomènes de migration vers l'Ouest, ce qui confirme les observations faites dans la province précédente.

Province orientale

L'imagerie acoustique révèle nettement un important contraste entre la région précédente et ce domaine oriental. La transition se fait de façon très franche, par l'intermédiaire d'un important accident de direction NW-SE, suivi sur au moins cent kilomètres. Cette région orientale recèle d'autres accidents de même orientation, et en particulier un accident qui semble commander la bordure sud-ouest du Mont Eratosthènes.

Toute cette région orientale, est fortement accidentée. Transversalement aux accidents NW-SE, il existe une série de grabens qui apparaissent injectés par des diapirs de sel, la couche de sel étant dans ce secteur omniprésente et très proche de la surface.

On observe encore un certain nombre de chenaux profonds du Nil. Certains d'entre eux ne semblent pas avoir été affectés par la tectonique active de ce domaine et peuvent être suivis sur de grandes distances (une centaine de kilomètres) en présentant toujours de spectaculaires sinuosités. Mais la plupart apparaissent très disloqués avec un cours nettement contrôlé par les gabens. Ils pourraient avoir participé à la dissolution de l'ensemble salifère et il n'est pas exclu que, localement, des lacs de saumures existent.

La carte bathymétrique au sondeur multifaisceaux illustre parfaitement cette tectonique active interprétée en termes de décrochements sénestres distensifs, ainsi que son interaction avec la série salifère et la sédimentation du cône du Nil.

TIME SERIES OF WATER PRESSURE AND BOTTOM TEMPERATURE IN A MARINE SHALLOW WATER HYDROTHERMAL VENT OF MILOS ISLAND (AEGEAN VOLCANIC ARC): PRELIMINARY RESULTS

Stefano Aliani [1]*, Luca Amici [1], P.R. Dando [2], Roberto Meloni [1]

[1] Stazione Oceanografica CNR. Forte S.Teresa, Pozzuolo di Lerici, 19036 La Spezia Italy
[2] School of Ocean Science, University of Wales-Bangor, Menai Bridge, Anglesey LL59 5EY UK

Abstract

Time series of measurements of water pressure and temperature were obtained from submarine hydrothermal vents off Milos Island (Aegean Sea). The presence of diurnal and semidiurnal frequencies of tidal origin were found in the temperature. The influence of water pressure on vent temperature is evident and the presence of other unknown and unpredictable factors superimposing tide during some periods is shown.

Key-words : thermal vents, sea level, temperature, time series, Aegean sea

Introduction

The venting of hot fluids from the seafloor is best known from the mid-ocean ridges. Many sites, however, are also known from shallow waters, especially along volcanic arcs, where the venting can have a marked influence on coastal waters (1, 2, 3, 4, 5, 6). Venting in shallow water produces large volumes of free gas (gasohydrothermal vents), both because of the lower solubility of the gases at low pressure, degassing of the subducted crust under the volcanic arcs and the breakdown of sedimented marine carbonates at high temperature. In shallow water much of this gas (largely carbon dioxide) is released directly to the atmosphere making flux calculations difficult.

Time series of venting periodicities are required in order to calculate long term fluxes from short term flow measurements. Temperature is the main parameter measured in long term studies due to its ease of measurement and to the sensor stability in corrosive environments. Knowledge of the variations in water temperature is important both in determining the distribution of vent biota (7, 8) and in following the dilution of hydrothermal water with seawater (9).

Temperature time series at deep vents have shown diurnal and semidiurnal frequencies which have been explained in terms of tidal cycles (10, 11). Short term time series relating venting periodicity to tidal changes have also been reported at Santorini (12) and Milos (13) in the Aegean Sea and Capo Palinuro in the Tyrrhenian Sea (14).

In this study, standard spectral analysis is used to investigate whether the temperature changes at a shallow hydrothermal vent off Milos (Fig.1) can be explained by tidal fluctuations.

Sea level in the Northeast Mediterranean basin was studied by Lascaratos & Gacic (15) and Yüce & Alpair (16) but the only measurements of sea level on Milos available at present are from Tsimplis and Vlahakis (17) that compared level data from a sea level meter positioned in the island of Siros with meteorological data from Milos, assuming that distance between two islands was not very far. Previous studies on hydrothermal activity in Milos were performed by Dando *et al.* (5), Fitzsimons *et al.* (13) but long term data of temperatures were not reported and start was not synchronised with sea level meters.

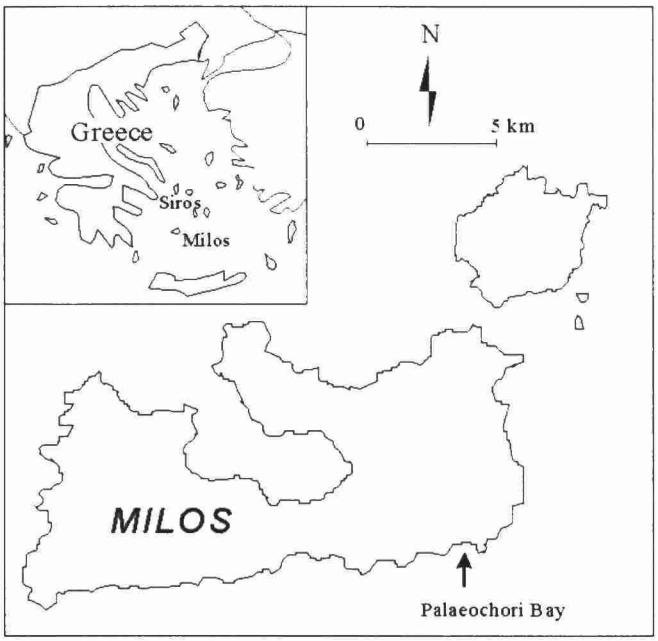

Fig. 1. Milos Island and the Aegean Sea.

Methods

Pressure data was collected from 28 June to 19 September 1996 using Aanderaa WLR7 depth gauges positioned on the sea bed in Paleochori Bay (Milos Island). This was compared to temperature data collected during the same period by a Venco Minilog temperature logger. The pressure sensors were calibrated and checked in the factory, a sampling interval of 30 minutes was used for all instruments. The temperature logger was placed at 5 cm sediment depth close to a vent outlet in 7 m water depth off Paleochori, Milos.

Time series were synchronised and spectral analysis was performed by Fast Fourier transformation on the sea level and temperature data sets. The average and trend were deleted from the series and power spectra were calculated by the autocovariance method. The software was developed from IMSL libraries of the VMS system.

Results

The bottom pressure oscillations were small in amplitude with a maximum of 1636.86 hPa and a minimum 1612.48; mean 1623.39, standard deviation 4.013 hPa. The plot of bottom pressure against time is shown in Fig. 2. The components of atmospheric pressure were not separated from the water pressure because they both contribute to the value of the bottom pressure and the contribution of every external pressure forcing was therefore included.

The plot of temperature vs time (Fig. 2) showed some large changes from a maximum temperature of 86.45 °C to a minimum of 24.06 °C with two large decreases in temperature. The reason of these fluctuations is still unknown but we can reject a lost of calibration because sensors worked well during post deployment checks. Such abrupt temperature falls could be caused by removal of overlaying sand, but no marked change in sensor burial depth was noted in logger retrieval. The pressure data did not show changes corresponding to the abrupt drops in temperature.

The time series were separated into three main periods (A,B,C) according to the temperature. Periods A and B presented similar trends (standard deviation 1.66 and 2.04). A greater variability in temperature was found during period C (standard deviation 4.5).

A comparison of the daily data of pressure and temperature from June 29 to July 1 (with no filtration and a sampling interval of 30 minutes) clearly indicated that a maximum in pressure corresponded to a minimum in vent temperature (Fig. 3).

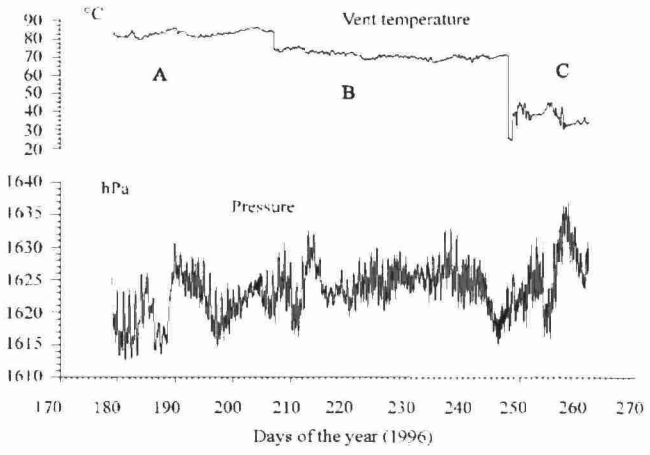

Fig. 2 : Plot of pressure and temperature. Three distinct periods are evidenced in the temperature series.

PLIOCENE SAPROPELS FROM THE EASTERN MEDITERRANEAN BASIN (LEG 160, HOLES 969E, 967C AND 966D) : IMPLICATIONS OF SEDIMENTOLOGICAL DATA

Sung-Ho Bae & Marie-Madeleine Blanc-Valleron *

SHB & MMBV: Laboratoire de Géologie, Muséum national d'Histoire naturelle, 43 rue Buffon, 75005 Paris, France

Abstract

Pliocene sapropels located just below the last common occurrence (LCO) of *Discoaster tamalis* can be correlated across the Eastern Mediterranean Basin, from Sicily to Cyprus. The deposition of these sapropels is mainly related to climatic control but sedimentation patterns show that local factors such as bathymetry and post-depositional processes may play an important role. Total organic values (TOC) can be very high. Organic matter (OM) is mainly amorphous and corresponds to high marine productivity, at least pro-parte from marine planktonic diatoms that are preserved within some sapropels.

Key-words : Mineralogy, Organic matter, Diatoms

Introduction

Middle Pliocene sediments from Sicily and Calabria (Italy) show periodical variations of the $CaCO_3$ content classically related to climatic control [1, 2, 3]. Sediments of the same age were recovered in the Eastern Mediterranean, during ODP-Leg 160, with numerous organic-rich layers (sapropels). We analysed a bundle of sapropels, along a transect from the South of Crete to the South of Cyprus in order to investigate the relative influence of the climate and of local factors such as bathymetry, post-depositional processes, etc. Hole 969E is located South of Crete, on the Mediterranean ridge (2201 m water depth), whereas the two other holes are located in the Eratosthenes Seamount (ESM) region : one toward the northern edge of the ESM plateau (Hole 966D, 926 m water depth), the other (Hole 967C, 2553 m water depth) on the lower northern slope of the northern flank of the ESM (fig.1).

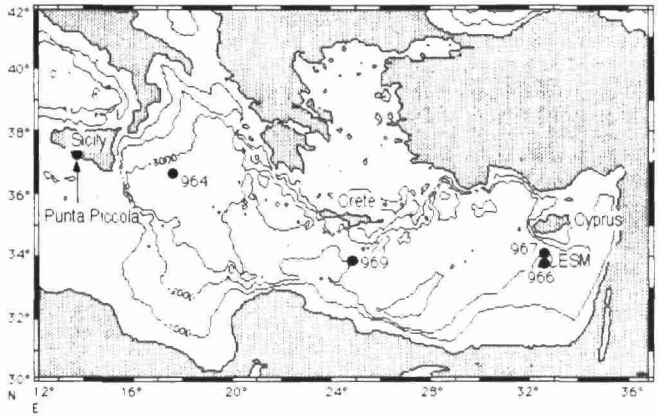

Fig. 1 - Location map.

Methods

The studied cycles were selected from preliminary biostratigraphic data acquired on board the Joides Resolution [4, 5, 6]. The stratigraphic correlations were refined by comparing the holes series with the classical succession of Punta Piccola (Sicily), using the abundance curves of *Discoaster tamalis* [7, 8, 9]. Mineralogical (carbonatometry, X-Ray diffraction, smear-slides, SEM & TEM) and geochemical studies (Rock-Eval pyrolysis) were also performed.

Results

Correlations, using *D. tamalis* curves and other sedimentological data, show that the sapropels studied correspond to the basis of Hilgen cycles numbered 102 to 110 in the Punta Piccola section of Sicily ([2] & fig. 2). Previous studies of the Sicily sections [1, 2, 3] showed that cycles 102 to 108 are controlled by earth-precession (# 22-kyr periodicity), whereas cycles 109 to 111 are influenced by obliquity (# 41-kyr periodicity) ([1] & Tab. 1). In the Ionian Basin (Hole 964A) and on the Mediterranean Ridge (Hole 969E), the control is similar (fig. 2). But, further east, in the ESM region, two sapropels are present in the inferred obliquity-controlled cycles 109 and 110, showing the influence of the precessional signal from Hilgen cycle 102 to 110.

Calcium carbonate, mainly corresponding to the calcareous nannoplankton, represents the most important mineralogical phase of the series. South of Crete (Hole 969E) carbonate values show large cyclic variations (fig. 3) as in the Ionian Basin (Hole 964A) [9]: they vary between 0 and 20 % in the sapropels and around 60 % elsewhere. In the ESM region, carbonate cycles are less differentiated, well developed in cycles 106 to 108 of Hole 967C, but absent or poorly marked in Hole 966D (located on top the ESM) where sapropels contain less organic-matter (OM) and are more bioturbated : bioturbation is inferred to disturb the OM and carbonate signals.

Table 1 : Time estimation of studied sapropels (from [1]); age refers to the mid-points of the sapropels.

Hilgen cycle number	Sapropel age (Ma)	time (Ka) between 2 sapropels
111	2.828	36
110	2.871	43
109	2.900	29
108	2.921	21
107	2.943	22
106	2.965	22
105	2.989	24

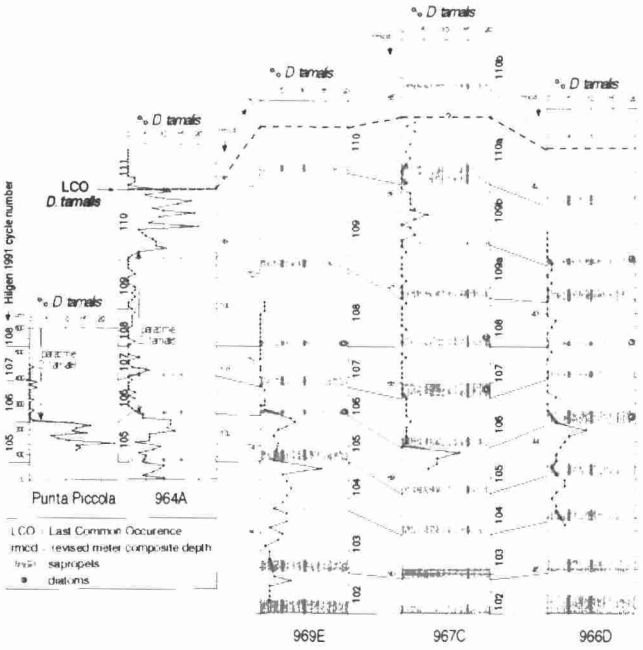

Fig. 2 - Correlation between cycles across the eastern Mediterranean, from Punta Piccola (Sicily) and Hole 964A [9] to Holes 969E, 967C, and 966D, using the fluctuation abundance curves of *D. tamalis*.

Total Organic Carbon values (TOC), in the studied sapropels can be very high (fig. 3), especially in the deep-water settings : up to 30 % in Hole 969E, 12 % in Hole 967C and 5 % in Hole 966D. The Hydrogen Index values (HI) and the HI/Tmax diagram (fig. 4) indicate a partial oxidation of the primary marine (type II) OM and/or an admixture with OM of terrigenous provenance. A general trend of co-variation between HI and TOC (fig. 5), and biomarkers data [10] show the importance of

LE VOLCANISME LITTORAL D'ALGERIE: NOUVELLES DONNEES CHRONOLOGIQUES ET GEOCHIMIQUES

Ouardia Belanteur [1], Amina Louni-Hacini [1], Hervé Bellon [2], Joseph Cotten [2], Alain Coutelle [2*], Serge Fourcade [3], René Maury [2], M'Hamed Megartsi [1], Aziouz Ouabadi [1] et Belkacem Semroud [1]

[1] Institut des Sciences de la Terre, USTHB, BP n°32, Bab Ez Zouar, El Alia, Alger, Algérie
[2] Département des Sciences de la Terre, UMR 6538, UBO, BP n°809, 29285 Brest Cedex, France
[3] Géosciences, Universite de Rennes 1, Campus de Beaulieu, 35042 Rennes Cedex, France

Résumé

Des travaux récents sur le magmatisme littoral algérien ont permis d'apporter des précisions significatives sur la chronologie de la mise en place des masses éruptives, leurs caractères géochimiques et leur signification dans la tectogenèse alpine. Une partie de ce magmatisme semble provenir de la fusion partielle d'un manteau à signature géochimique "orogénique" mais cette hypothèse est très difficile à inclure dans le contexte alpin qui ne fournit ni le temps, ni l'espace, ni la quantité de croûte océanique nécéssaires. Ce magmatisme témoignerait donc, soit de l'existence d'un processus original d'"océanisation" d'un manteau continental, soit de la reviviscence d'une contamination très ancienne.

Mots-clés : tectonics, volcanology, Western Mediterranean

Les principaux traits de l'évolution tectonique, sédimentaire et magmatique néogène de l'Algérie

La chaîne alpine d'Algérie du Nord s'édifie au Miocène en trois phases tectoniques principales, datées du Burdigalien "moyen" (vers 19 Ma), du Langhien "inférieur" (vers 16 Ma) et du Tortonien "supérieur" (vers 8 Ma). Ces crises ont une durée géologiquement brève, nettement inférieure à la microfaunizone qui les définit (1).

L'importance de chacune de ces phases varie selon les lieux.

La phase burdigalienne est la phase majeure, puisqu'elle voit la disparition définitive de la paléogéographie alpine et, en particulier du sillon des flyschs internes alpins dont aucune série ne dépasse le Burdigalien. La phase langhienne reprend le matériel précédemment tectonisé et étend l'aire de la mobilisation alpine vers des zones plus externes, relativement épargnées par la tectonique burdigalienne: la région sud-tellienne, les Baléares, la Murcie. La phase tortonienne ne se marque, dans le Tell, que par la formation d'un chevauchement d'ampleur déca-kilométrique qui s'étend de Bedjaïa à Cherchell en passant par le flanc sud du Djurdjura. Plus à l'ouest, dans le Rif et en Andalousie, jusqu'au Campo de Gibraltar, cette phase est géométriquement la plus importante. Ceci est dû à une remobilisation du matériel tectonisé lors des phases burdigaliennes et langhiennes, qui serré en N-S par le rapprochement Ibérie-Afrique, trouve un "échappement latéral" en glissant de l'est vers l'ouest, vers l'Atlantique dans le sillon marin développé sur la suture Ibérie-Afrique. Il est à noter qu'une même "exagération gravitaire" s'observe à l'est, vers la mer Ionienne, sur la suture Apulie-Afrique. D'autres déformations surviendront par la suite, mais leur importance reste comparativement faible, même si certains réajustements gravitaires peuvent, localement, faire illusion.

Cette dynamique est associée à un volcanisme, discret, mais toujours présent dans les périodes qui encadrent les crises tectoniques. Ainsi, peu avant l'expulsion des nappes, à la limite Aquitanien-Burdigalien, un volcanisme explosif acide a répandu, sur l'ensemble de l'orogène qui nous intéresse, une nappe de cendres d'une dizaine de mètres d'épaisseur en moyenne, d'une remarquable homogénéité de faciès, actuellement dispersée de Gènes à Gibraltar.

Après le paroxysme burdigalien (zone à *Globigerinoides altiaperturus/dissimilis*, zone N5-6 de Blow) des distensions se produisent, qui déterminent la formation de bassins sédimentaires et l'apparition d'un magmatisme particulier. Au Nord de ce qui sera le Tell, des séries discordantes se déposent sur les nappes et, plus au Sud, un vaste sillon est-ouest se creuse constituant l'avant-fosse sud-tellienne. A Dellys, les plus anciens témoins du "volcanisme littoral d'Afrique du Nord" apparaissent sous la forme de brèches hyaloclastiques et d'une coulée basaltique prismée.

Nous proposons de désigner l'intervalle de temps qui s'étend entre la phase burdigalienne et la phase langhienne par le terme de "Dellysien", emprunté aux anciens auteurs car, d'abord, il s'agit de la même série, et, ensuite, il correspond au même concept: celui de terrains pris entre deux phases tectoniques. Les attributions d'âge proposées par A. Pomel et E. Ficheur ne sont plus tout-à-fait les nôtres, mais il ne s'agit pas ici de faire oeuvre de stratigraphie formelle. La tectonique langhienne clôt cette première période post-paroxystique.

Vient ensuite une tranche de temps plus longue qui s'étend du Langhien (zone à *Praeorbulina glomerosa*, zone N8 de Blow) jusqu'au Tortonien inférieur. En Algérie, c'est le moment de la mise en place de la majorité des appareils plutoniques et volcaniques miocènes. Suivant la démarche précédente on peut dénommer "Cartennien" cet intervalle (de Cartenae, nom de la ville de Tenes dans l'antiquité).

Les charriages du Tortonien supérieur (zone à *Globorotalia acostaensis*, zone N16 de Blow) ferment l'intervalle cartennien et inaugurent une nouvelle et dernière subdivision qui s'étend jusqu'à nos jours et qui comprend la fin du Tortonien, le Messinien et le Quaternaire. Mal caractérisés à l'est d'Alger, ces terrains sont, par contre, bien développés en Oranie tant sous la forme de séries sédimentaires que d'épanchements volcaniques. Le terme de "Sahélien" proposé par Pomel, malgré toutes les réserves stratigraphiques que cette dénomination a pu appeler, correspond assez bien à ce qu'il représente pour nous et peut servir à désigner cette dernière période post-tectonique.

Le magmatisme miocène

Pendant longtemps, les phases majeures alpines ayant été placées dans l'Eocène, ce magmatisme a été considéré comme franchement post-tectonique. Les travaux modernes ont confirmé que le magmatisme littoral est effectivement lié aux distensions post-phases tectoniques, mais, dans la mesure où il y a plusieurs phases tectoniques, la question n'est plus aussi simple et il est apparu nécessaire, en préalable à sa réinterprétation dynamique, de resituer ce magmatisme dans un cadre chronologique, tectonique et paléogéographique alpin à jour et assuré. C'est pour cela que de nouvelles études ont été entreprises, dans l'Est-Algérois et l'Oranais, en des lieux où le contexte tectonique pouvait être considéré comme bien connu.

Dans l'Est-Algérois (2), le magmatisme miocène comprend les coulées et intrusions magmatiques de Dellys et du Cap Djinet, le massif granodioritique de Thenia et les coulées et brèches de nuées ardentes dacitiques et rhyolitiques de Zemmouri El Bahri et d'El Kerma. Dans de nombreux cas, l'âge isotopique de ces roches (méthode ^{40}K-^{40}Ar) a pu être comparé à la datation par microfaunes. La mise en place de ce matériel paraît s'être effectuée au cours de trois épisodes situés vers 19, 16-15 et 14-12 Ma. Ces roches calco-alcalines à calco-alcalines potassiques sont riches en éléments incompatibles avec des anomalies négatives en niobium. Les magmas acides déduits présentent une signature crustale très marquée ($^{87}Sr/^{86}Sr_i$ = 0,7082 à 0,7155; $\delta^{18}O$ = +9 à +13 ‰), attribuable, comme les variations du rapport La/Nb, à une contamination par la croûte supérieure.

De tels magmas pourraient dériver d'une source mantellique métasomatisée au cours d'un épisode de subduction, que le contexte tectonique oblige à situer avant le Miocéne, vers le Sénonien-Paléocène, sans d'ailleurs que des preuves définitives de son existence aient été fournies. Dans le cadre de la paléogéographie alpine, la localisation possible de cette subduction probable paraît cependant trop éloignée et son ampleur trop modeste pour expliquer la contamination mantellique est-algéroise.

Tectoniquement, les basaltes de Dellys (datés à 19,7 Ma +/- 1 et 18,6 Ma +/- 0,8) font partie de l'intervalle dellysien, toutes les autres manifestations éruptives s'inscrivent dans l'intervalle carténnien. Toutes ces formations sont donc déracinées, et même doublement pour les basaltes de Dellys, qui ont eu à subir deux phases de charriage.

En Oranie (3), le volcanisme se caractérise par l'existence de deux lignées. La première, localisée en bordure de mer, dans le Sahel d'Oran et dans le massif des M'Sirda, est composée de laves acides, d'affinité calco-alcaline à shoshonitique. La seconde, regroupée en Moyenne Tafna, comprend surtout des basaltes alcalins.

EXTENSION DES APPORTS SÉDIMENTAIRES DU VAR (PROVENCE, FRANCE MÉRIDIONALE) AU LARGE DE LA CORSE: INDICATIONS FOURNIES PAR L'ÉTUDE DES ZIRCONS.

Gilbert Bellaiche [1]* et Jean-Pierre Pupin [2]

[1] Observ.Océanologique.Univ. P. et M. Curie, Lab. de Géodynamique sous-marine, CNRS Géoazur, Villefranche-sur-Mer, France
[2] ZIRC, Lab. de Pétrologie-Minéralogie, Univ. de Nice, parc Valrose, 06108 Nice Cédex 2 France

Abstract

Extent of the Var river deposits off western Corsica: evidence from zircons analysis. The main areas of terrigenous sedimentation recorded off the Corsica island by morphological and geophysical methods, have been sampled. The collected sediments have been studied by the means of zircon typology, in view of identifying the turbiditic sources. It appears that recent sandy turbidites originating from the Alpes-Maritimes and channeled through the Var deep-sea channel, are deposited as far as the northern part of the western margin of Corsica. We conclude that in this area, the zircon crystals came from the aluminous migmatitic rocks of Provence. Southward from this area, the deposits seem to be supplied by the erosion of the calc-alkaline rhyolitic and granitic rocks of western Corsica.

Mots-clés : Western Mediterranean. Erosion. Sediment transport. Acoustics. Mineralogy.

Introduction

La campagne MeseaII-Mesim entreprise en 1991 à bord du N/O *Atalante* avait permis de réaliser des explorations d'ordre essentiellement morphologique et géophysique des marges corses. Sur ces bases, des hypothèses avaient été émises sur l'origine géographique des corps sédimentaires s'étendant au large de cette île (1, 2). Il avait en particulier été suggéré qu'une partie des sédiments composant ces formations pouvait provenir de la Côte d'Azur. Ces hypothèses viennent d'être directement testées par des prélèvements de sédiments sur lesquels a été appliquée la méthode des zircons (3).

Rappelons que des études sédimentologiques antérieures (4) avaient déjà pu montrer, grâce aux minéraux lourds, que les turbidites terrigènes prélevées dans la plaine abyssale ligure, entre la Provence et la Corse, provenaient d'apports à partir du Var. Mais aucun apport d'origine provençale n'avait jusqu'à présent été mis en évidence dans les environnements insulaires.

L'analyse des zircons : une méthode adaptée au problème posé

Le zircon constitue un excellent traceur de l'origine des sédiments. Il est connu pour être un minéral très résistant, peu altérable par les agents physico-chimiques. Il possède nombre de caractères qui permettent de préciser les conditions de genèse des roches hôtes (état des formes cristallines, morphologie et couleur des cristaux, caractéristiques des groupements cristallins etc.) (3, 5). Une typologie fondée sur le développement relatif des faces cristallographiques prismatiques et pyramidales apporte de précieux renseignements sur la pétrogenèse, notamment la température et le chimisme du milieu de cristallisation (6).

Dans le cadre de cette étude, le choix du zircon comme traceur se justifiait particulièrement car les roches éruptives drainées en Provence et en Corse sont riches en zircons et dérivent de magmas constrastés ou à évolution différente. Rappelons que le Var et ses affluents drainent notamment le massif de l'Argentéra-Mercantour, composé principalement de migmatites et de granite calco-alcalin intrusif (7) et le dôme permo-triasique du Barrot, où des grès conglomératiques à galets de rhyolites alcalines affleurent. Pour la Corse, le bassin versant occidental comporte principalement le premier cycle magmatique calco-alcalin hercynien granitique et rhyolitique (8, 9), et le second cycle alcalin permien également granitique et rhyolitique (9, 10), tous deux analysés par les zircons. Dans l'ensemble de ce secteur corse, les migmatites sont quasiment absentes. D'autre part les effets thermiques du métamorphisme alpin ont affecté les seuls zircons de l'Argentéra-Mercantour, tandis que ceux de la Corse occidentale ont été épargnés. Ces effets se traduisent par une coloration violette des cristaux après réchauffement (11).

Les méthodes utilisées

Les prélèvements ont été réalisés au cours de la campagne "Corsed 1" du N/O *Téthys* II (fig. 1). Leur profondeur s'échelonnait entre 2380 m et 2780 m, et leur localisation a été assurée de façon précise au moyen du système de navigation GPS (Global Positioning System). Grâce à l'utilisation d'un carottier-benne d'un mètre de long et à large section (40x40 cm), les sédiments recueillis sont très représentatifs des dépôts superficiels.

Il s'agit de sédiments à dominance pélitique, mais renfermant, sous quelques centimètres de boue hémipélagique beige-clair à ptéropodes et foraminifères (Holocène), des passées de turbidites terrigènes riches en sablons et sable fin. Les études minéralogiques ont été réalisées sur ces turbidites, après concentration des minéraux lourds dans la fraction 50-160 μm.

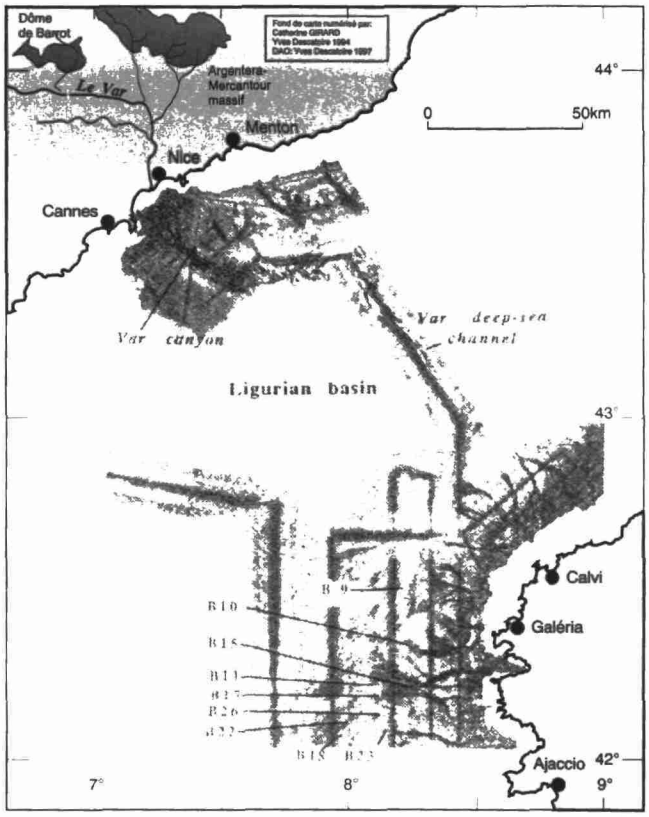

Figure 1: Carte de l'imagerie Simrad montrant les épandages turbiditiques au large de la Corse occidentale et la localisation des prélèvements de sédiments.

Résultats et interprétation

Dans le diagramme typologique (fig.1 et fig. 2), les zircons des échantillons prélevés montrent deux groupements principaux qui impliquent une double provenance:

(1) Zircons provenant des Alpes-Maritimes

Les zircons de la carotte B9, prélevée au sein d'un faciès turbiditique sableux bien diffusant attribué aux épandages varois (1), présentent la couleur violette caractéristique du réchauffement alpin, ce qui écarte une origine à partir de la Corse occidentale. La majorité de ces zircons sont en tous points semblables à ceux des gneiss migmatitiques du Mercantour, très rarement automorphes, sans excroissances, avec des indices A et T généralement faibles (327<A<-364 et 420 <T<461). Ils présentent fréquemment des coeurs hérités reliques de fusion anatectique. Les zircons dominants montrent encore parfois la face (112), témoin d'un milieu de cristallisation hyperalumineux avec développement de silicates d'alumine (cordiérite et/ou disthène).

A côté de ces types dominants existent:

(a) quelques cristaux peu automorphes, à indices A et T plus élevés, dérivés d'orthogneiss comme il en existe dans le socle de l'Argentéra-Mercantour.

LIPID BIOMARKERS AS INDICATORS OF THE ORGANIC MATTER SOURCES IN EASTERN MEDITERRANEAN SAPROPELS

Ioanna Bouloubassi

Département de Géologie et Océanographie, Université Bordeaux I, URA CNRS 197, avenue des Facultés, 33405 Talence cedex, France
Lab. de Physique et Chimie Marines, Université P. et M. Curie, URA CNRS 2076, Case 134, 4, place Jussieu, 75252 Paris, France

Abstract

A series of Pleistocene-Pliocene sapropels from ODP Site 969, located on the Mediterranean Ridge, were investigated for their extractable lipid components. The organic carbon contents in sapropels of Pleistocene age showed a typical range of values, up to 7.4%, whereas the Pliocene sapropels were extraordinary organic-carbon rich with values reaching 32.2%. The molecular composition of extractable lipids was dominated by alkyl diols and ketols, alkenones and sterols with less important amounts of n-alkanes and n-alcohols. The molecular data indicate that organic matter in sapropels is predominantly derived from marine algal sources. Nevertheless, the distribution of terrestrial lipids indicates a significant rise of land-derived influx during sapropel formation. Additionally, stanol/stenol ratios suggest that anoxic conditions prevailed during the formation of highly organic-rich sapropels.

Key-words : geochemistry, deep sea sediments, carbon

Introduction

One of the focus of the ODP Leg 160 was upon the origin and paleoceanographic significance of Mediterranean sapropels [1]. These are dark-colored layers rich in organic carbon which occur in young (less than 5 millions year) sequences, intercalated with oxidized, organic-carbon-poor hemipelagic sediments. Their deposition is thought to occur as a response to major climatic, hydrological and biogeochemical changes. Since their first discovery in the 60's, the Mediterranean sapropels (mainly those of late Pleistocene to Holocene age) have received much attention, and several hypotheses on their origin and significance have been proposed.

According to one hypothesis sapropels are the result of the establishment of anoxia in the Mediterranean bottom waters which leads to enhanced organic carbon preservation. This hypothesis was strongly supported by isotopic anomalies observed in sapropels [2] and by faunal studies indicating a stable density stratification of the water column [3]. Increased fresh-water inputs would have provoked this stratification and such inputs have been considered to originate either from floods of the Nile river [4] or from increased precipitation in the northern borderlands of the eastern Mediterranean [5].

An alternative hypothesis postulates that enhanced marine productivity and concurrent increased rise of the organic carbon flux to the seafloor would be responsible for the formation of sapropels [6]. Anoxic conditions alone could not have been responsible for the accumulation of organic carbon reaching values of 20%. The formation of such organic rich layers requires that primary productivity exceeds 500 gC/cm^2/yr, a value in the range of those encountered in modern upwelling systems. The postulated increase in productivity is thought to be triggered by riverine nutrient supply [7]. Other authors have argued that the very high organic carbon contents observed in several sapropels reflect both increased export production and decreased oxygen advection in deep waters. Whatever mechanism exerted the primary control on the formation of sapropels (basin-wide anoxia or increased export productivity) its operation appears to be triggered by an external forcing, since the occurrence of sapropels closely correlates with minima in the Earth's orbital precession cycle [8].

Bulk organic geochemical characteristics of sapropels

ODP Site 969 is located on the Mediterranean Ridge (33°50.40'N and 24°53.06'E) at 2200 m of water depth. Over 80 sapropel beds recovered from the lower Pliocene through Holocene section occurring in distinct bundles and separated by intervals of oxidized, yellowish brown sediment.

The upper group of sapropel beds comprises the typical Holocene-upper Pleistocene sequence with S1, S3, S4, S5, S6, and S7 all present, showing organic carbon contents up to 7%. In the uppermost Pliocene to lower Pleistocene sequence, sapropels have maximum organic carbon content of 17.6% with a more usual range of 2% to 10% [9]. Two distinctive groups of predominantly black sapropel beds occurred in a gray colored interval of middle Pliocene age. These sapropels are extraordinary organic-carbon rich with a maximum of 30.5% which, to our knowledge, is the highest organic carbon content ever measured in a Mediterranean sapropel.

Corg/N ratios for almost all sapropels exceeded the value of 12 with an average of 17 and a maximum of 23. The surprisingly high values of Corg/N ratios could suggest a predominance of terrestrial organic matter which however is not in accordance with the indications provided by the Rock Eval parameters [9]. These high Corg/N ratios in the sapropels are tentatively interpreted as representing an effective removal of nitrogen compounds from the marine organic matter during diagenesis; however, it cannot be ruled out that the primary marine organic matter was already poor in nitrogen-bearing constituents.

Results of Rock-Eval pyrolysis showed hydrogen indices for many samples to exceed 300 mg hc/g Corg, with a maximum value slightly above 450 mg hc/g Corg [9]. The hydrogen index values indicate partial oxidation of the primary marine organic matter and/or an admixture of terrigenous organic matter. Consistent with the relationship between organic matter type and elemental composition, oxygen indices show an opposite trend to the hydrogen indices. A general tendency for higher hydrogen indices with increasing content of organic matter is observed. Sulfur contents were high in all sapropels, especially for those of middle Pliocene age, where a maximum of 13.2% was encountered, and their downhole profile roughly paralleled that of organic carbon.

This paper deals with the study of major extractable (free) lipid constituents in selected Pleistocene and Pliocene sapropels. The data are used to assess the origin of the organic matter (marine *versus* terrestrial) as well as the dominant specific biological sources.

Experimental

Two types of sapropel samples have been examined here. First, a series of samples taken from Pleistocene sapropels S5, S6 and S7. Second, a series of closely spaced samples from within two middle Pliocene sapropel layers and in sediments above and below these layers. These middle Pliocene sapropels are located just below the last common occurrence (LCO) of *Discoaster tamalis*. The detailed experimental methodology has been reported in detail elsewhere [10]. Lipids were solvent extracted and separated by flash chromatography on silica gel. Non-aromatic hydrocarbons and long chain alkenones were analyzed directly by gas chromatography whereas hydroxyl-bearing compounds were firstly derivatized to their trimethylsilyl ethers. Structural confirmations were obtained by Gas chromatography-Mass spectrometry and quantitation was done using internal standard methods.

Lipid composition and origin

- ***n-Alkanes:*** The series of n-alkanes ranged from n-C15 to n-C37 and their distributions are dominated by long chain homologues. Total concentrations were from 5.03 to 11.4 µg/g in Pleistocene sapropels and higher, up to 38.20 µg/g , in Pliocene ones, while they remained low, less than 1 µg/g d.w., in non-sapropel sediments. The predominant long chain n-alkanes showed a strong odd-over-even chain length predominance, which is characteristic of terrestrial higher plants and can be thus used to trace inputs of terrigenous organic matter. Consequently the n-alkane series indicate a significant terrigenous contribution to the organic matter [10].

- ***n-Alcohols:*** n-alkan-1-ols ranged from C16 to C32 and were dominated by components higher than C20. Their concentrations vary from 4.46 to 16.84 µg/g in Pleistocene sapropels, and from 4.54 to 70.43 µg/g in Pliocene ones. Levels were very low in non-sapropel samples. The n-alcohol composition is characteristic of terrigenous higher plants inputs.

- ***diols, ketols:*** Long chain alkyl diols and ketols were among the most abundant lipid constituents identified in sapropels [10]. Their concentrations varied from 4.8 to 103.4 µg/g in Pleistocene sapropels and

ÉVOLUTION VOLCANO-TECTONIQUE DE L'ETNA (SICILE) : NOUVELLES DONNÉES DE GÉOLOGIE MARINE ET TERRESTRE

Bousquet J.C. [1*], Gabbianelli G. [2], Lanzafame G. [3], Sartori R. [2]

[1] Laboratoire de Tectonophysique, URA 1764, U.S.T.L., Montpellier, France
[2] Dipartimento di Scienze della Terra, Università di Bologna, Italie
[3] Istituto Internazionale di Vulcanologia, C.N.R., Catania, Italie

Résumé

La région de l'Etna, sur le bord externe de la chaîne apenninico-maghrebine, était encore affectée par une tectonique de raccourcissement pendant les premières phases du volcanisme etnéen; actuellement, elle est soumise à des épisodes successifs de compression N-S, dans un régime de distension NW-SE. La synthèse des données terrestres et de géologie marine permet de tracer un schéma de l'évolution volcano-tectonique, pendant laquelle s'est effectuée le passage entre deux régimes de contraintes, et de mettre en évidence le rôle fondamental joué dans cette évolution par le système de failles éoliano-maltais.

Mots-clés : tectonics, volcanology, Western Mediterranean

Tectonique

Dans la région de l'Etna (Fig. 1), des épisodes de compression N-S ont eu lieu avant et durant la construction du volcan, jusqu'à nos jours. Les compressions continuent à affecter le secteur, en se substituant momentanément au champ de contraintes dominant et distensif (1, 2, 3). A l'échelle régionale, la compression N-S peut être rattachée aux dernières phases compressives de la chaîne apenninico-maghrébine, qui suivent le blocage et la fin de la tectonique tangentielle (Pléistocène inférieur-moyen). Sur l'Etna et en Sicile orientale, la distention est clairement visible grâce au système de faille éolien-maltais (4), qui, depuis les monts de Medina (Mer Ionienne méridionale; Fig. 1) se développe vers le NNW, au moins sur une distance de 350 km : le long de l'escarpement de Malte, puis au travers du bord oriental de l'Etna et les monts Péloritains, jusqu'aux îles Eoliennes, dans le sud de la mer Tyrrhénienne. Sur l'Etna, dans les monts Péloritains et dans le sud de la Mer Tyrrhénienne les failles NNW-SSE ont un fonctionnement en faille normale avec une composante décrochante dextre. Sur le versant ionien de l'Etna (Fig. 1), elles coupent des coulées et des dépôts volcanoclastiques récents et actuels, et leur évidence morphologique est souvent spectaculaire.

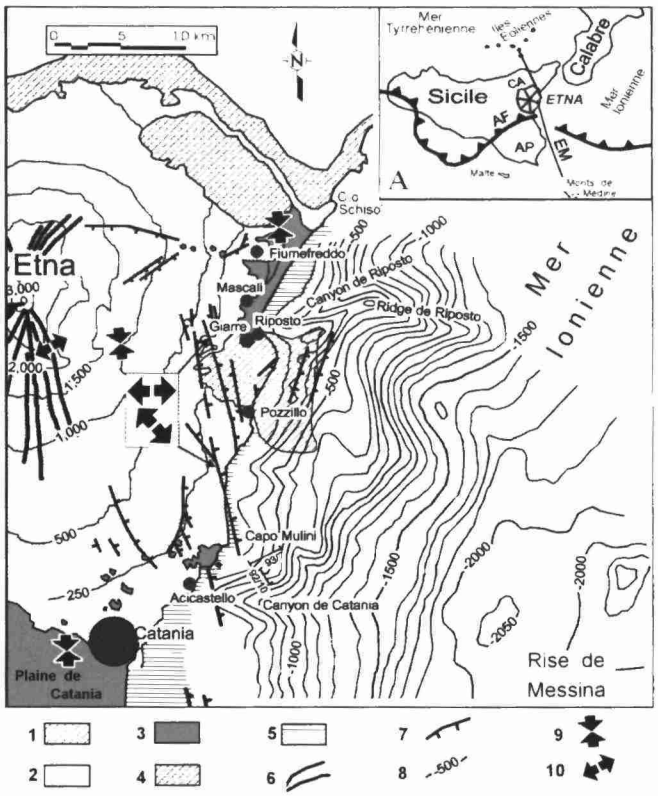

Fig. 1 - Schéma tectonique et morphologie sous-marine de la région de l'Etna: 1) dépôts volcanoclastiques du "Chiancone" (18-5 ka); 2) roches volcaniques de l'Etna (<600 ka); 3) sédiments quaternaires de l'avant fosse; 4) chaîne apenninico-maghrebine; 5) plate forme continentale (18 ka); 6) fractures éruptives; 7) failles; 8) isobathes; 9, 10) directions de compression (9) et d'extension (10) calculées avec des stries de mouvement sur des plans de failles. Encadré A: CA = chaîne apenninico-maghrebine; AF = avant fosse; AP = avant pays; EM = système de failles éoliano-maltais.

La région de l'Etna, comme toute la Sicile orientale, subit un soulèvement rapide. Celui-ci est prouvé par des faits aussi bien géologiques qu'historiques (5, 6, 7, 8). En faisant référence à des témoignages recueillis sur des constructions anciennes, originairement au niveau de la mer, sur les variations de la nappe phréatique le long de la côte et grâce aux reproductions de paysages au pied de l'Etna, ce secteur aurait été soulevé de 1,5 à 2 mètres en l'espace de trois siècles.

Géologie marine

Les relevés de géologie marine ont été effectués par le navire océanographique *Urania* du C.N.R., dans la zone comprise entre le Capo Schisò et Catania (Fig. 1), jusqu'à une profondeur d'environ 2.000 m. On a exécuté des profils électro-acoustiques (échosondeur, sub-bottom profiler 3,5 kHz) et sismiques à haute résolution (Sparkarray 4.5-8 kj), accompagnés de dragages et de carottages. La zone étudiée comprend un escarpement continental, accidenté et complexe, qui a une inclinaison de 4 à 6°, avec une largeur pouvant atteindre 17 km, et qui se termine à une profondeur de 1.800 à 2.000 m. Au-delà, après une nette rupture de pente, commencent les fonds plus ou moins plats, qui constituent les parties les plus internes de la rise de Messine. Le raccord entre l'escarpement et les zones émergées se fait par une plate-forme continentale, qui se suit de façon presque continue, parallèlement à la côte. Le début de l'escarpement est à une profondeur qui varie avec régularité (Fig. 1) : depuis Pozzilo, où il est le moins profond (60- 80 m), il descend graduellement vers le nord (110-120 m à Riposto; 130-150 m à Fiumefreddo) et vers le sud (90-95 m à Capo Mulini; 100 m à Acicastello et 120- 130 à sud de Catania). Les enregistrements sismiques mettent en évidence que sur toute la plate-forme, au-dessus d'une nette surface de discordance, une couverture détritique de faible épaisseur se développe (Fig. 2). Sur la base de ces caractéristiques, de la position stratigraphique et des corrélations avec des situations similaires sur les marges méditerranéennes voisines (9), la discordance et les dépôts sus-jacents sont rattachés aux processus d'érosion et de dépôts associés à la dernière oscillation glacio-eustatique du niveau marin. Cette oscillation a fait enregistrer un abaissement moyen de 120 m dans le Pléistocène (minimum niveau marin à 18 ka); pendant l'Holocène (derniers 10 ka) on est revenu à des conditions proches de l'actuel, avec un haut niveau marin et une phase de dépôt.

Dans leur ensemble, à l'est de la plate-forme continentale, la bathymétrie des fonds etnéens est dominée au nord, par une dorsale marquée et par la dépression contiguë qui la borde au nord (ride et canyon de Riposto); une deuxième dépression évidente, le canyon de Catania, caractérise la partie la plus méridionale de la zone étudiée. La ride de Riposto est bien nette déjà sur la plate-forme et se prolonge ensuite au delà de -1.500 m, avec une orientation E-W. Dans la zone de raccord à la terre ferme, il présente une faible couverture de lave avec de dépôts détritiques grossiers et de concrétions calcaires d'origine organique. Plus au large, il est constitué par une épaisse séquence, peu déformée (tectonique distensive), de la boue, correspondant à la sédimentation actuelle, reposant sur des argiles plastiques vert-bleu à faune du Pléistocène supérieur (A.M. Borsetti, com. pers). Cette séquence est superposée à un "substratum acoustique", toujours de type détritique mais visiblement déformé par une tectonique avec raccourcissement, qui pourrait représenter le prolongement en mer des unités allochtones de la chaîne apenninico-maghrebine, qui affleurent sur la terre ferme en correspondance de la dorsale (8).

A SAPROPELIC SEDIMENT UNIT FROM THE SOUTHERN MARMARA SHELF

M. N. Çagatay [1]*, O. Algan [1], C. J. Eastoe [2], M. Sakinc [3], L. Egesel [4], N. Balkis [1], D. Ongan [1], H. Caner [1]

[1] Institute of Marine Sciences and Management, University of Istanbul, Vefa, 34470, Ystanbul, Turkey
[2] Department of Geosciences, University of Arizona, USA
[3] Mining Faculty, Istanbul Technical University, Turkey
[4] Marmara Research Centre, Tübitak, Gebze, Turkey

Abstract

A sapropelic unit, having an age of 4.7 - 3.4 ^{14}C ky, was identified in the Holocene sediments on the southern shelf of the Marmara Sea. It is a 10-35 cm-thick, phosphorescent green, plastic, clayey hemipelagic mud horizon, located at depths ranging 1-2.35 mbsf. The increase in organic carbon (up to 2.5 %) and biogenic carbonate (8-12% $CaCO_3$), together with a rich planktonic foraminiferal fauna, indicates increased organic productivity and warm surface waters during the deposition of the sapropelic layer. The benthonic foraminiferal fauna indicates reduced oxygen levels in bottomwaters during the deposition. Deposition of this sapropelic layer was initiated by a large input of terrestrial organic matter and fresh water under a relatively warm and wet climate. The fresh water probably caused a strong water stratification, which in turn together with the high organic matter input, resulted in reduced oxygen levels in the bottomwaters.

Key-words : sapropel, Sea of Marmara

Sapropel/sapropelic layers are found from the Black Sea and Mediterranean Sea which range in age from 7.000-3.000 to 400.000 - 6.300 y BP, respectively (1, 2, 3, 4). The youngest Mediterranean sapropel (S1) was deposited between 8.3 and 6.3 ^{14}C ky BP (5, 6, 7). There is no previous report on the sapropelic sediments from the Marmara Sea which is a transitional basin between the Black Sea and Mediterranean. The sapropelic layer found in this study is dated at 4.7-3.4 ^{14}C ky BP, and thus younger than the latest Mediterranean sapropel, but overlaps the age of the Black Sea sapropel.

The sediment cores from sites 1, 2, 4, 6, 13, and 22, (Fig. 1) from the the southern Marmara shelf consist mainly of various tints of brown, gray and green, texturally homogeneous, hemipelagic, plastic, clayey muds (Fig. 2). The sapropelic layer is typically a phosphorescent green, plastic, clayey mud horizon, which contain the highest organic carbon and the total carbonate values.

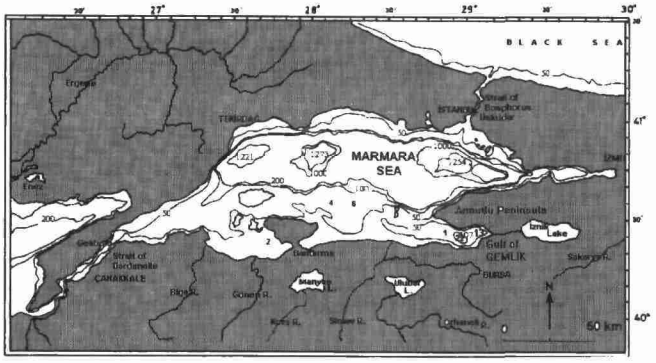

Fig. 1 : The locations of gravity core sites.

The carbonate and C_{org} contents of the core samples vary between 8-13 % $CaCO_3$ and between 0.2-2.1%, respectively (Fig. 3). The organic carbon values are relatively higher in cores 6, 4 and 2, compared to those in cores from the eastern part of the shelf. The thickness of sapropelic layer is about 35 cm in the cores from the Gemlik Bay and 50 cm in cores 4 and 6. The total-carbonate profiles show a good match with the organic carbon profiles along the cores, suggesting that the carbonate fraction is mainly of biogenic origin. The enrichment of biogenic carbonate in the sapropelic layer suggests increased organic productivity during their deposition.

The high organic productivity is supported by a rich planktonic foraminiferal fauna during the sapropelic sediment deposition (Fig. 4). The planktonic assemblage (mainly, Globogerinidae and Goborotalidae, including *Globigerina calida* Parker, *Globigerina rubra* d'Orbigny, *Globigerina ruber* d'Orbigny and *Orbiluna universa* d'Orbigny) in the sapropelic layer and the layer immediately below points to a warm climate during deposition. The planktonic forams decrease in abundance towards the upper levels and start to increase again both in diversity and abundance in the top 20 cm of the cores. Similar to the planktonic one, the benthic foraminiferal assemblage, becomes more diversified and abundant in the top 20 cm part of the cores, with the appearance of new species. The benthic foraminiferal assemblage include Brazilinidae, Cassudilinidae, Nonionidae,

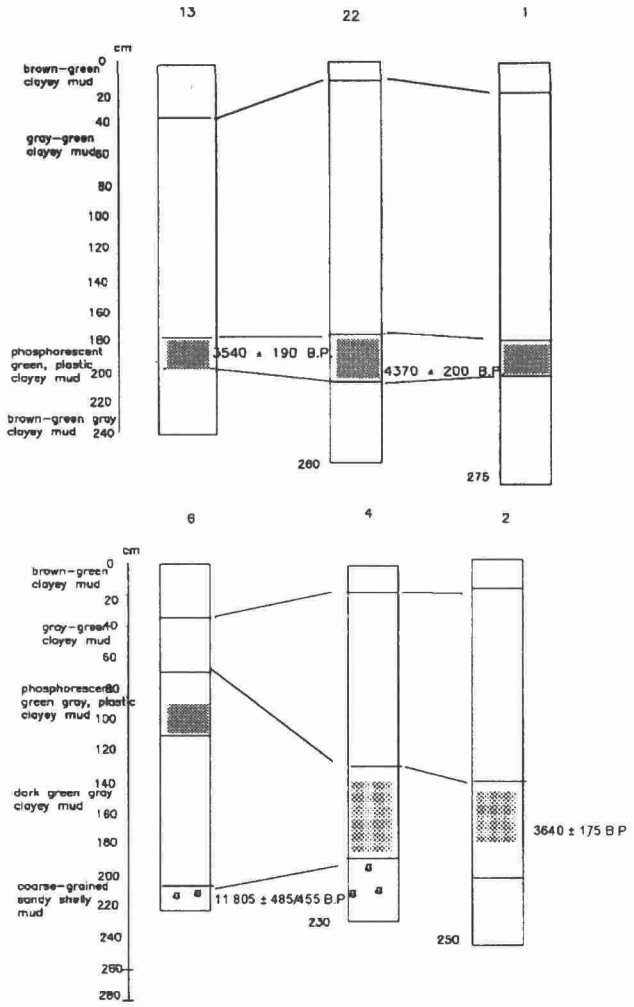

Fig. 2 : Lithological description of the studied cores.

Chilostomellidae, Uvigerinadae, and Milliolidae in the lower levels of the cores, including the sapropelic layer (Fig. 4). Although the presence of benthonic forams, in general, implies well oxygenated water, in these levels, the abundant presence of particular benthic forams, such as Brazilinidae together with Cassidulinidae, indicates reduced oxygen levels in bottomwaters during deposition. The decrease in the abundance of both the benthic and planktonic forams between 40-70 cm bsf. show high fresh or brackish water input during this interval.

The Marmara Sea, being on the waterway between the Mediterranean and the Black Sea, was a lake separated from its neighbouring seas during the last glaciation. The connection with the Mediterranean was established with the inflow of the Mediterranean

GEOPHYSICAL DATA OF THE BLACK SEA MUD VOLCANOES

Çifçi G. [1], Krylov O.V. [2] and Ergün M.[1*]

[1] Dokuz Eylül University, Eng.Faculty, Depart. of Geophysics, Bornova/Izmir, 35100, Turkey
[2] Moscow State University, Geological Faculty, Moscow, 119899, Russia

Abstract

Mud volcanoes exist in the deep eastern Western Black Sea sub-basin within rather limited areal distribution. Morphological and structural characteristics of the Black Sea mud volcanoes were investigated during several Unesco-ESF "Training-Through-Research (Floating University)" cruises (1991-1996). These mud volcanoes were formed usually under an extensional regime with high terrigenous input. They generally have mushroom or cone-like shape and rise 20-150 m above the surroundings, relatively flat seafloor. In sonar records they are indicated with strong backscatters. All seismic sections across them show bending down reflectors towards the feeder channel(s) and bright spots between 400 and 600 ms (TWTT) below the seafloor.

Key-words : mud volcanoes, seismics, Black Sea

Introduction

Black Sea is one of the largest enclosed marine seas occupying an area of 432000 km^2 and having depths greater than 2 km. It is clear that the Caspian-Black Sea region is, at present, tectonically active (1). The very recent subsidence characterize not only the abyssal Black Sea, but also a series of more-or-less elongated basins extending westward to Italy. The mechanism of immense subsidence has given way to the deposition of thick sedimentary sequence reaching up to 14-15 km. From detailed seismic investigations (2, 3), the lower part of the southern Black Sea basin generally preserves the extensive tectonics associated with the rift processes, whereas the Middle upper margin is affected by compressive tectonics accompanied by overthrusts.

Mud volcano features (Fig. 1) were observed in the abyssal plain of the Mid-Black Sea Basin towards the southern and southeastern margins of Crimea (4, 5). Mud volcanoes and diapirs have been studied by the Russian scientists and the institutions over a long period in the Black Sea and the Sea of Azov. Mud volcanoes were discovered in the deep Black Sea during the joint geological/geophysical in 1988 cruise (5). Besides these large volcanoes, some others were mentioned by Ivanov *et al.* (6). The distribution of the mud volcanoes is given in Fig. 1. The works of Konyuhov *et al.* (7), Kruglyakova *et al.* (8) and Limonov *et al.* (9) have shaded more light into the knowledge about the geological, geophysical and geochemical aspects of these features.

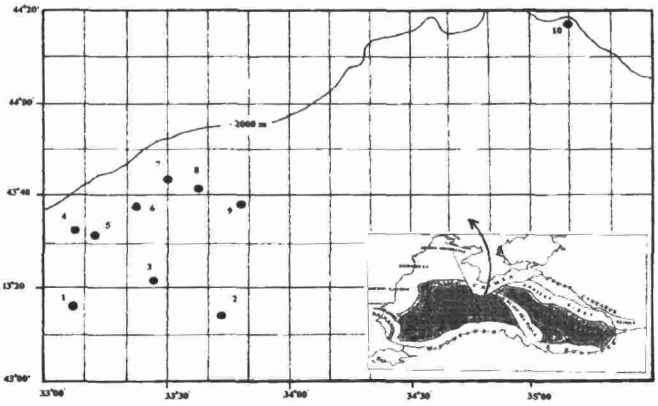

Fig. 1: Distribution of the large mud volcanoes in the deep Black Sea basin: 1-TREDMAR, 2 Kovalevskiy, 3-Vassoevitch, 4-MSU, 5-Yuzmorgeologiya, 6-Malyshev, 7-Kornev, 8 Stakhov, 9-Goncharov, 10-Kazakov.

The second leg of the Sixth Unesco/Tredmar Training-Through-Research Floating University (TTR-6) cruise was carried out in the Sorokhin trough area during July-August 1996 on board the R/V *Gelendzhik* that belongs to the Russian Federation. The following data were collected in the Sorokhin trough near the Crimean continental slope and the deep Black Sea Basin: (i) Multibeam swath mapping (as well as reflectivity) with the SIMRAD EM 12S; (ii) Single channel high resolution seismic data; (iii) Data of the deeptow combined system of side-scan-sonar and subbottom profiler (MAK-1); (iv) Sampling with gravity corer.

Swath bathymetric (SIMRAD EM 12S) surveys were carried out in the area in 1996 during the TTR-6 cruise at the first time. In the context of this paper, some information shall be given for the mud volcano features in the deeper abyssal plain of the Black Sea and to describe the seafloor features related to the mud volcanoes and identify their origin with respect to the neotectonic processes.

Data collection systems and the technical details

Swath Bathymetry

During the expedition of TTR-6, a SIMRAD EM 12S low frequency (13 KHz) multibeam echosounder was used to make both high resolution bathymetric and reflectivity maps of the seafloor. The basic model of the echosounder EM 12S, which has an angular coverage sector of 120°.

Seismic System

A single channel seismic system was used during the works. The seismic source is comprised of 3 liters air-gun source (Pulse-5 system) at the working pressure of 130 atmospheres. The streamer is composed by 100 m of active section towed behind the vessel by 500 m of distance. The data were recorded by an IBM PC based seismic station for duration of 3000 msec.

Marine acoustic deep-tow system (MAK-1)

The MAK-1 system is designed by Yuzmorgeologiya Co. (Russian Federation) to obtain acoustic images of both the seafloor surface (side scan sonar) and subbottom sediments (subbottom profiler). This system makes it possible to obtain acoustic images of the seafloor surface with the sidescan sonar system for a swath of up to 1500 m per side in long range (LR) mode (30 kHz) and up to 500 m per side in high resolution (HR) mode (100 kHz). The subbottom profiler works at 6 kHz frequency. This system has to be operated at low speeds of 1 to 2 knots.

Results of the bathymetry, sonar and seismic data

Three parallel swath bathymetric profiles with a SW-NE strike were made in the deep Black Sea basin within the coordinates of 43°31 N and 33°01 E; 43°51 N and 33°30 E; 43°42 N and 33°39 E; 43°23 N and 33°10 E. The whole area is almost flat, except the isolated mud volcano cones (Fig. 2). There is a gradual increase of seafloor relief towards to the NE. Water depths decrease from 2190 m down to 2060 m here. Therefore there is only 130 m difference for about 70 km. This means the approximate gradient of 0.002 m/km.

Five large mud volcanoes which were known before, were reconfirmed as the Moscow State University (MSU), Yuzhmorgeologiya, Malyshev, Kornev and Gocharov (5, 6, 9, 10). The main geomorphological features for these mud volcanoes are summarized in Table (1). The largest mud volcanoes are the Yuzhmorgeologiya and Malyshev ones by height and size. The diameters of the bases and the heights of these volcanoes are about 4 km and 110 m respectively with slope gradients of approximately 7°. The Goncharov mud volcano is the smallest but with the sharpest gradient which was calculated to be about 11°.

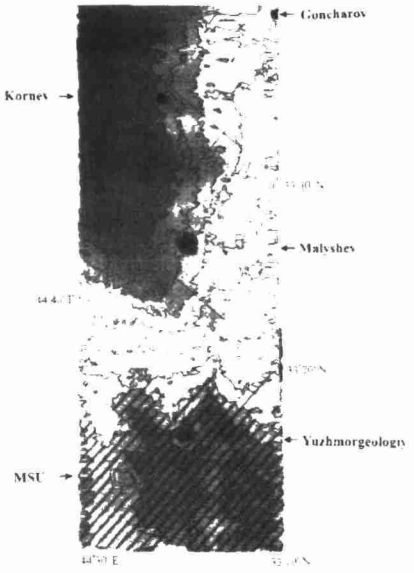

Fig. 2: The bathymetric map of the deep Black Sea prepared from the SIMRAD EM12S data (TTR-6, R/V *Gelendzhik*, 1996).

THE ALBORAN SEA BASIN: NEW INSIGHTS FROM ODP DRILLING AND GEOPHYSICAL DATA

Menchu Comas* and Juan I. Soto

Instituto Andaluz de Ciencias de la Tierra (CSIC and University of Granada), Campus Fuentenueva, 18002 Granada, Spain

Abstract

Geophysical data combined with the study of basement rocks and sedimentary cover drilled in the Alboran Sea basin at Ocean Drilling Program Leg 161 sites provide constrains on extensional and contractional tectonics during basin evolution. Site 976 confirms the presence of continental crust and the NS continuity of the stretched Alboran Domain of the Betic-Rif orogen beneath the Alboran Sea basin. Main results are consistent with an early-to-middle Miocene rapid exhumation and associate heating of the basement by late tectonic extension and lithosphere stretching; thus constraining geodynamic genetic models to favor lithospheric delamination.

Key-words : Alboran Sea, Tectonics, Basin Formation

Introduction

The continental crust deformation and lithospheric behavior in extensional basins developed in collisional settings is a long-standing problem in Mediterranean tectonics. The Alboran Basin has been attributed to crustal thinning processes developed from early Miocene onwards within the Eurasia-African plate convergence setting, and the Alboran Sea (Fig. 1) is an ideal target in the Mediterranean to study these extensional processes. A prime objective for Ocean Drilling Program Leg 161- The Western Mediterranean was to sample de crust beneath the Alboran Sea basin (Fig. 1), particularly in regard to: a) the origin of extensional basins developed on former collisional orogens, b) the dynamics of the extension on collisional ridges resulting in basins surrounded by arc-shaped orogenic belts, and d) actual or sub-actual contractional processes (1). Leg 161 was successful in achieving this aims and the Alboran Sea drilling results have immediate applications in establishing geodynamic models on the origin and evolution of Mediterranean-type backarc basins.

Fig. 1.- Bathymetric map of the Alboran Sea showing ODP Leg 161 Sites, DSDP Site 121, and commercial boreholes (Alb-A1, And-A1, G1 and EJ). Insert map: location of the Alboran Sea between the Betic and Rif Cordilleras. ACH= Alboran Channel. AI= Alboran Island. AR= Alboran Ridge. CHB= Chella Bank. DB= Djibouti Bank, and XB= Xauen Bank. Contour lines every 200 m.

Geological and geophysical constraints

The Alboran Sea basin lies behind an arc-shaped orogenic belt formed by the Betic (Southern Spain) and Rif (Morocco) Chains. The roughly N-S Neogene convergence between the Eurasian and African plates at the westernmost Mediterranean has resulted in a region of distributed deformation which encompass the Betic, Rif, and Tell Cordilleras, linked across the Gibraltar Arc, and the basins beneath the Alboran and South Balearic Seas. (Fig. 1, inset map).

Geophysical data indicate the continental crust thins from 38 km in the Betic Chain to about 15-20 km beneath the central Alboran Sea (2, and references therein). Heat flow data suggest an eastward decrease in lithospheric thickness from 60-90 km in the West Alboran Basin to about 35-40 km and concurrent crustal thinning from 14-16 km to 10-12 km in the transition from the East Alboran Basin to the South Balearic Sea (3). There is no witness for the existence of Cenozoic oceanic lithosphere at the Betic-Rif-Alboran region. Multichannel deep seismic data, however, suggest the presence of oceanic crust east of 1° W meridian in the South Balearic basin (4).

A more than 6 km-thick lower Miocene (Burdigalian) to Pleistocene sedimentary sequence occurs in the West Alboran Basin; however, in the central Alboran Sea, and South and East Alboran basins the sedimentary cover is thinner (less than 3.5 km). No direct sample information exists about specific ages of pre-Messinian sediments in the East and South Alboran basins. Several intra-mountain depressions (Fig. 2) and corridors within the Betic and Rif Chains (currently known as Betic or Rifean "Neogene Basins") contain Miocene marine sediments similar to those that fill the Alboran Sea basin, which indicates that during the Miocene the Alboran Basin spread out N-S beyond the present limits of the Mediterranean Sea.

The basement of the Alboran Basin, cropping-out inland, is formed primarily of metamorphic complexes belonging to the Alboran Crustal Domain (the internal complexes of both the Betic and Rif Chains) composed of a syn- and post-metamorphic pre-Miocene polyphase thrust-stack that includes three nappe complexes: the Nevado-Filabride, Alpujarride, and Malaguide (Fig. 2).

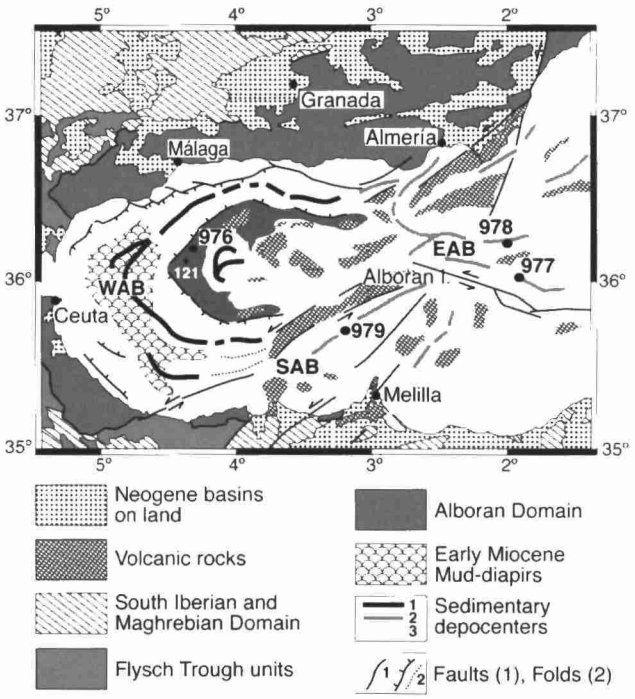

Fig. 2.-. Geologic map of the Alboran Sea basin showing the location of main sedimentary depocenters, DSDP site 121, and ODP Leg 161 Sites. Neogene Betic Basins onshore Iberia and Africa are indicated. Sedimentary depocenters in the Alboran Sea: 1= Depocenters consisting of lower Miocene to Pleistocene deposits; 2= Depocenters consisting mainly of middle Miocene to Pleistocene deposits; 3= Depocenters consisting of Messinian/Pliocene to Pleistocene deposits. EAB= Eastern Alboran Basin, SAB= Southern Alboran Basin, WAB= Western Alboran Basin.

The Alboran Basin was structured by superimposed extensional and contractional tectonics. In the outcropping Alboran Domain, large-scale extensional detachments are superimposed on the continental collisional structures. Rifting and progressive exhumation of the Alboran Domain took place from at least the early Miocene to the early Tortonian, while thrusting in the peripheral arc which surrounds the basin occurred (5, 6, and references therein). A prominent middle to early-late Miocene rifting (from about 16 Ma to 11-10 Ma) is identified in the seismic record of the West Alboran Basin (4, 7, 8). Patterns of middle Miocene extension, as well as areal distribution of metamorphic basement units and sedimentary sequences are consistent with a WSW directed extensional detachment system to produce crustal thinning. According offshore and onshore data the West Alboran Basin is located on the hanging wall of a major crustal detachment. Generalized early Miocene and late-Serravallian-to- early Tortonian magmatism, as well as notable mud diapirism in the West Alboran Basin, have likely resulted from these extensional processes (Fig. 2). This rifting, which is connected to large-scale extension detach-

PALAEO-ENVIRONMENTAL CHANGES LEADING TO THE PARTIAL OR COMPLETE REMOVAL OF EASTERN MEDITERRANEAN SAPROPELS

G. J. De Lange [1*], P. Van Santvoort [1], H. Passier [1], C. Langereis [1], M. Dekkers [1], J. Thomson [2], C. Corselli [3], and A. Michard [4]

[1] Dept. Geochemistry, Institute for Earth Sciences, Utrecht University, Budapestlaan 4, 3584 CD Utrecht, The Netherlands
[2] Southampton Oceanography Centre, Southampton, United Kingdom
[3] Dipt. Scienze della Terra, Univ. Milano, Italy
[4] Géosciences de l'Environnement, Aix-en-Provence, France

Abstract

The occurrence of distinct organic-rich intervals (sapropels) in the eastern Mediterranean appears to be cyclic and to be associated with the Monsoonal / Insolation Index. A postdepositional downward migrating oxidation front may result in the partial or complete removal of a sapropel unit. Using the Ba/C.org relationship established for eastern Mediterranean sediments, the initial C.org content of sapropel units may be determined. The distribution of Ba and some trace elements on the one hand, and of the paleomagnetic parameters NRM/ARM on the other hand, appear to be accurate recorders of the initial occurrence of distinct organic-rich units, even if now invisible.

Key-words : sapropel, deep sea processes, geochemistry, paleoceanography, eastern Mediterranean

Understanding the mechanisms of sapropel formation and sapropel preservation is not only necessary for an improved reconstruction of palaeoenvironmental conditions in the E. Mediterranean, but may also assist in understanding the present-day situation and possible future developements. The Corg-rich marine sediments, sapropels, may be regarded as modern analogues for Corg-rich black shales. In addition, there are similar uncertainties on the conditions and environments under which black shales and sapropels are formed and preserved. In the deep marine environment, the Corg content preserved in a sediment is primarily a balance between the input flux of organic matter and its oxidation by bottom water O2. Most marine sediments have Corg contents in the range 0.2 - 2%. The E. Mediterranean sedimentary record therefore comprises an intercalation of unusually Corg-rich sediments (the sapropels) within Corg-poor sediments (*e.g.* 1), caused by repeated fluctuations through time in either or both the Corg flux from surface ocean export production and bottom water O2 levels.

Interpretations of the environmental conditions leading to sapropel formation are based on the sedimentology, micropalaeontology and geochemistry of the dark-coloured layers and the cream/brownish sediments above and below them. Generalised sequences of sapropel formation, based on examination and interpretation of a large number of sapropel units and the sediments enclosing them, have been presented (*e.g.* 2,3). The interval of dark colour associated with a sapropel is often somewhat thicker than that defined by the >2% Corg definition (4). Three sharp colour changes are generally associated with the most recent sapropel S1: the upper and lower limits of the dark Corg-rich sapropel layer itself, (typically 6-8 cm thick in the central basin), and at the base of the grey "proto-sapropel" layer of variable thickness which underlies the sapropel layer. A few cm above the S1, a dark-brown interval of 2-3 cm thickness is usually found, having a diffuse often mottled upper boundary and a relatively abrupt colour transition at the lower boundary. This colour is characteristic of Mn oxyhydroxide enrichments. In the interval from the dark-brown layer to the visible upper S1 boundary, an increasingly red-brownish colour usually appears (*e.g.* 5,6,7).

For a full understanding of the observations described above, the Ba / C.org relationship found for sediment trap samples and sediments at various sites is important (*e.g.* 8). Although mobilization of barite-Ba is possible during severe anoxic conditions, this does not seem to have influenced the Ba profile around the eastern Mediterranean S1 sapropel (*e.g.* 6,7,9). Using barite-Ba as a paleo- productivity indicator, enhanced fluxes hence accumulation rates of Organic carbon to the seafloor must have occurred from aproximately 9 - 5 ky BP, in uncorrected 14-C years (Fig. 1). The perfect correlation of the C.org calculated from the C.org / Ba relation, in the visible S1 interval, as well as the complete lack of such correlation in the interval between the darkbrown layer and the visible S1 layer are remarkable. It seems, therefore, that S1 deposition extended from 9 - 5 ky BP but that the organic carbon for the upper part has been removed. Such removal processes have been known to occur for the upper parts of organic-rich distal turbidites deposited in the Madeira Abyssal Plain (10,11,12,13).

At the end of S1 deposition, high organic carbon accumulation rates were followed by low organic carbon fluxes. As a consequence, only part of the oxygen diffusing from the bottomwater into the topmost sediment was, and is, consumed by the oxidation of the reactive organic matter. Subsequently, the remaining oxygen continues to diffuse into the sediment, leading to an oxidizing front slowly moving downward into the S1 sediments, degrading via microbial processes most of the organic matter on its way. Depending on the post-S1 organic carbon accumulation rates, the sediment accumulation rates, the organic carbon content and thickness of the S1 sediments, this oxidation front may have resulted in the removal of organic matter in part or even in all of the S1 sediment interval. As a consequence, the age found for the lower S1 boundary is relatively constant at approximately 9 ky BP, whereas that for the uper boundary usually varies between 6 and 8 ky BP (*e.g.* 14).

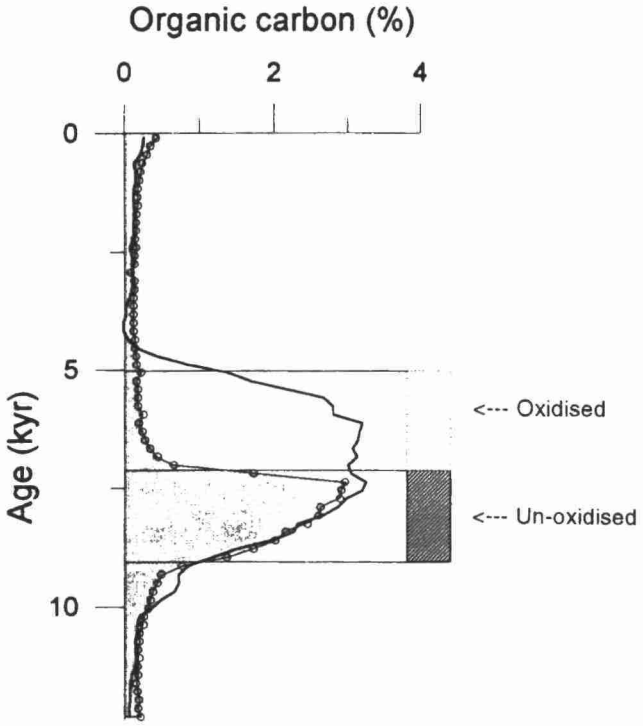

Fig. 1. Organic carbon content from the top 30 cm of sediments typical for the eastern Mediterranean. Organic carbon content calculated from C.org/Ba relationship (solid line; see text), and observed (open symbols) have been indicated. The dark-brown interval occurs at approx. 5 kyr.

During such downward oxidation process certain trace elements are relocated in a characteristic sequence, which allows the recognition of paleo-sapropel occurrences even after the (nearly) total removal of their visible evidence, *i.e.* organic carbon. Even if some mobilization of barite-Ba has occurred, it seems not to have moved far away from the sediment interval of its initial deposition. This is probably due to the rather local and limited time of sulphate reduction during formation of each sapropel (Fig. 2; 15,16). In the case of remobilized barite-Ba, it is not possible to determine C.org accumulation rates directly from the Ba content of the samples. Only after assigning the total Ba content to the associated initial sapropel interval, the extent of which is detemined from trace element characteristics, it is possible to assess an average organic carbon accumulation rate for that sapropel interval.

In this way Ba appears to be a reliable indicator for (initial) sapropel deposition in eastern Mediterranean sediments. In addition, some trace elements, and in particular paleomagnetic parameters such as NRM/ARM appear to be additional and accurate recorders for the initial occurrence of

RECENT WARMING OF DEEP SEA SEDIMENTS IN THE EASTERN MEDITERRANEAN

Della Vedova B. [1]*, Pellis G. [1], Camerlenghi A. [2], Foucher J.P. [3] and Harmegnies F. [3]

[1] Dipartimento di Ingegneria Navale, del Mare e per l'Ambiente, Università di Trieste, Via Valerio 10, I-34127 Trieste, Italy
[2] Osservatorio Geofisico Sperimentale, P.O. Box 2011 I-34016, Trieste, Italy
[3] IFREMER, Centre de Brest, B.P. 70, F-29280 Plouzanè Cedex, France

Abstract

Marine geothermal data, collected in 1993 and 1994 during three cruises of the MEDRIFF project along a 300 km SW-NE oriented transect traversing the Mediterranean Ridge accretionary complex, are used to deduce recent changes in bottom water temperatures in the Eastern Mediterranean. About 130 temperature profiles in the sediments showed decreasing temperatures from the seafloor down to 3 to 6 meters depth, indicating transient temperature regimes. Modelling the conductive heat propagation into the sediments suggests a warm deep water intrusion that started to propagate from the Hellenic Trench in summer 1992 and reached the Mediterranean Ridge crest in late 1992-early 1993.

Key-words : Ionian Sea, deep waters, deep sea sediments, temperature, global change

Introduction

We present a novel application of heat flow (HF) measurements in deep sea sediments to reconstruct temporal changes in the bottom water hydrography. We use temperature profiles in the sediment, integrated by CTD profiles in the water column, to document the recent intrusion of dense and warm water masses in the deep Eastern Mediterranean [1,2]. The data, collected from September 1993 to May 1994, record the variability of the thermal structure of the deep water masses and indicate transient thermal regimes, at week, month and interannual time-scales [3]. A regional transect (Fig.1) of closely spaced HF measurements was performed during three oceanographic cruises within the MEDRIFF project (An Integrated Investigation of the Fluid-Flow Regime of the Mediterranean Ridge). The purpose was to identify areas of anomalous HF that could be interpreted as possible sites for fluid outflow from the Mediterranean Ridge (MR) accretionary complex [4]. Instead, a completely different scenario was encountered: temperature profiles in the sediments showed strong negative thermal gradients just below the seafloor, with temperature minima at depths ranging between 3 and 6 m below sea-bottom [5]. Moreover, the temperature profiles in sediments had modified in the few months of time elapsed between cruises.

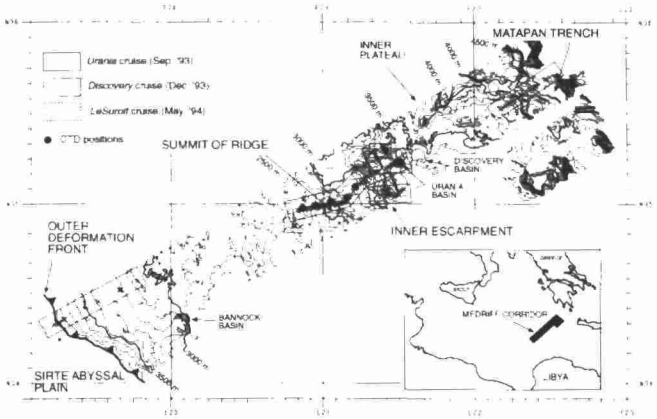

Fig.1. Simplified multibeam bathymetry of the MEDRIFF survey corridor in the eastern Mediterranean, showing the major features of the morphology of the ridge and the CTD and HF measurements collected during the MEDRIFF cruises.

MEDRIFF data set

During the *Urania* cruise (Sept. 1993), 80 HF measurements were acquired in the NE portion of the MEDRIFF corridor (Fig. 1), from the Matapan Trench (nearly 4600 m water depth) to the MR crest (about 2400 m water depth). The upper 5-6 m of sediment were found colder than the overlying bottom-water (Fig. 2), with temperature profiles mostly upward convex or with highly variable temperature gradients, including zero gradient. Seventeen other HF acquisitions, collected on the ridge crest during the *Discovery* cruise (Dec. 1993 - Jan. 1994), confirmed the anomalous thermal structure of the sea-bottom sediments.

During the *Le Suroit* cruise (May 1994), seventeen HF measurements were performed at the SW end of the corridor, on the outer deformation front of the MR. In this area, temperature profiles in sediments are normal, with values increasing with depth.

Seven CTD profiles from sea surface to seafloor, collected along the MR transect from the crestal area to the Inner Plateau (Fig. 1), show the highest values of temperature and salinity, below 1800 m, at the sea bottom. This means that the deep waters of the investigated area are warmer and denser than the overlying seawater.

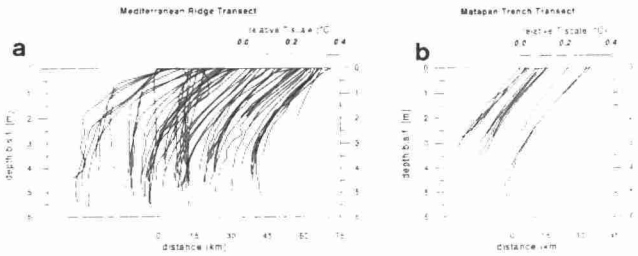

Fig.2 - Temperature distribution in the few upper meters of sediment along the MR transect (a) and Matapan Trench transect (b), collected during the Urania cruise. The location of each measurement along the transect is given by the position of the temperature profile at zero depth.

2-D thermal distribution in sediments and bottom-water

The 2-D distribution of potential temperature in shallow sediments of the MEDRIFF Corridor closely matches that in bottom-water (Fig. 3). The lowest bottom-water temperatures are on the Ridge crestal area (13.4 °C), whereas a progressive increase occurs toward NE, with 13.75 °C on the Inner Plateau and an estimated temperature of 13.95 °C in the deep Matapan Trench. As in the water column, the lowest sediment temperature are found on the crestal area (minima < 13.4 °C and thermal gradients close to zero).

Moving toward NE, temperature gradients in the sediments show increasing negative values, with minimum temperature observed deeper and deeper. In the Matapan Trench, thermal gradients are strongly negative and the minimum temperature is predicted at about 6 m depth or more. The thermal structure of the sediments clearly indicates unsteady-state heat transfer between the water column and the seafloor sediment. We propose that an increase of bottom-water temperature is transferring heat conductively into the seafloor.

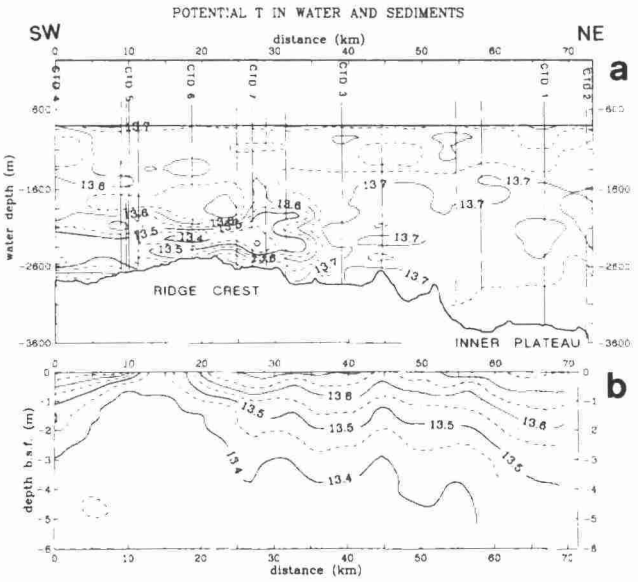

Fig.3 - Composite vertical section showing the contoured potential temperature (°C) distribution with depth in the water mass (a) and in the upper few meters of sediment (b) from the MR crestal area to the Inner Plateau (central three-segment profile in Fig. 1). CTD profiles and intercalibrated HF probe thermistor data were used in the seawater and thermistor data only, in the sediment.

TECTONIC IMPLICATIONS OF BOUGUER AND MAGNETIC ANOMALY MODELS IN THE EVOLUTION OF THE CENTRAL ALBORAN SEA

J. Galindo-Zaldivar [1], F. Gonzalez-Lodeiro [1], A. Jabaloy [1*], A. Maldonado [2] and A.A. Schreider [3]

[1] Departamento de Geodinamica, Universidad de Granada, 18071-Granada, Spain
[2] Instituto Andaluz de Ciencias de la Tierra (C.S.I.C - Universidad de Granada), 18071-Granada, Spain
[3] P.P. Shirshov Institute of Oceanology, Russian Academy of Sciences, 23, Krasikova, 117218 Moscow, Russia

Abstract

Largest magnetic anomalies in central Alboran Sea are related to ENE-WSW elongated bodies of basic igneous rocks located along the Alboran Channel. Bouguer anomaly models show that minimum crustal thicknesses are reached in this area and along the arched western Alboran basin. These two axes of crustal thinning were probably active during the Oligocene - Early Miocene. The western Alboran basin axis is subparallel to the Gibraltar Arc and its origin may be related to the origin of the arc. The ENE-WSW trending Alboran Channel axis may represent the western end of the Algerian-Balearic basin rift.

Key-words : crust structure, Alboran Sea

Introduction

The Alboran Sea developed above the Internal Zones of Betics and Rif. The thickest depositional sequences of the sea are located at the western Alboran Basin (1), and begin in Late Aquitanian (1). Deep seismic refraction profiles (2, 3) indicate that Alboran Sea has a thinned continental crust that thickens towards the Betics and Rif. The low P and S spread velocities (3) and high regional heat flow (4), suggest that an anomalous mantle exists below the sea (4). Gravimetric studies confirm this deep structure for the Alboran Sea (5, 6, 7). Magnetometric studies, however, are scarce (8, 9, 10). The objective of this work is to determine the geometry of the bodies responsible for the largest gravimetric and magnetic anomalies. Gravimetric and magnetic data have been compiled, reinterpreted, and 2D profile models have been developed for these anomalies.

Magnetometry

The largest dipoles have N70°E elongation and are located in the central Alboran Sea (Fig. 1). Another N45°E elongated anomaly occurs in the NE Alboran Sea, where acid and intermediate volcanic rocks crop out onshore. The most important isometric anomalies coincide with peridotite outcrops, to the W of the sea.

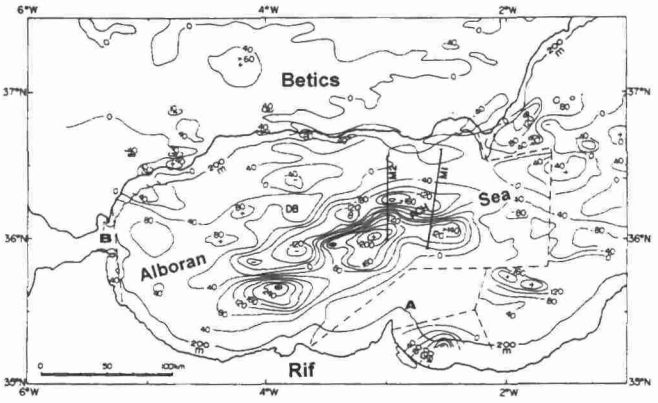

Fig. 1. Total field magnetic anomaly map of the Alboran Sea (nT). Based on the marine magnetometric data (9 and 10) and aeromagnetic data (8 and 15). A: area with complex local aeromagnetic anomalies; B: Gibraltar Strait area not included in this study. ACH, Alboran Channel. DB, Djibouti Bank.

The 2D magnetic models (Fig. 2) cut the anomaly bands in the central Alboran Sea and are located along seismic profiles (1, 10). Tops of magnetic bodies coincide with the top of acoustic basement. Normal polarity of dipoles suggests that remanent magnetism oblique to induced one may be of very low intensity. In the models, we consider equivalent magnetic susceptibilities that include the effects of induced and parallel remanent magnetism. The models indicate that the main body producing the intense magnetic anomalies in the central Alboran Sea (polygon 5, profile M1; polygons 5 and 7, profile M2) is more than 90 km long, trends N70°E- N80°E and is probably located below the Alboran Channel. Westward, another body, subparallel to the previous one, although displaced southward, is found.

Gravimetry

The most intense negative Bouguer anomaly approximately coincides with the western Alboran basin and is concave (Fig. 3). A N70°E elongated positive anomaly follows the Alboran Channel (Fig. 3).

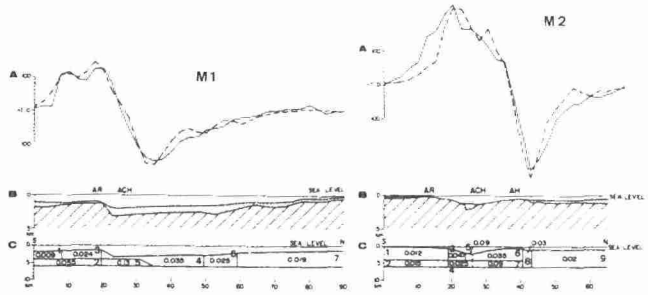

Fig. 2. 2D magnetic models elongated in a N70°E trend. A, observed total field magnetic profile (continuous line) and model profile (dashed line); B, simplified geological cross-section. Dotted area: sediments; dashed area: basement. Vertical exaggeration 1:2; C: magnetic models; large numbers: anomalous bodies; small numbers: equivalent magnetic susceptibilities (IS). Total field intensity: 43000 nT; inclination: 51°N; declination: 5°W.

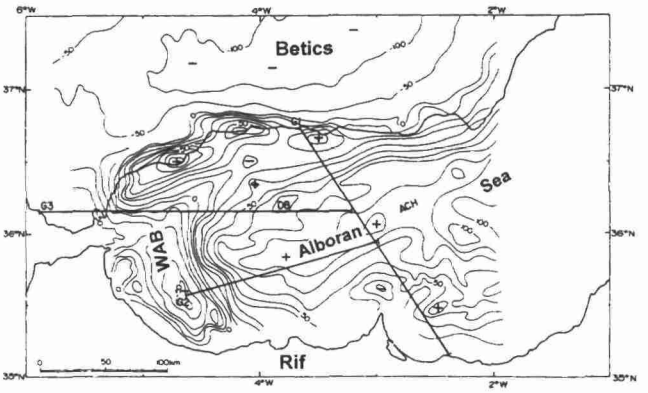

Fig. 3. Bouguer Anomaly map of the Alboran Sea (mGal). Based on Casas and Carbo (5). WAB, western Alboran basin.

Furthermore, there exist other isometric local maxima, as the located in the Djibouti Bank. The 2D gravimetric models along three profiles (Figs. 3, 4) are based on the results of the deep seismic refraction profiles (2, 3, 11), seismic reflection and borehole data (12).

Discussion and conclusions

The positive Bouguer anomaly along the Alboran Channel (profile G1, Fig.4) may have originated by the crustal thinning mainly in the deep and intermediate zones of the crust. The N70°E trend of the anomaly indicates that the thinning is oblique to the present-day boundaries of this sea, and extends toward the Algerian-Balearic basin, floored by oceanic crust (8). The crustal thickness variation is more gradual towards Africa than towards Spain, where the Moho may dip more than 60°N (6). The most intense magnetic anomalies of the Alboran Sea also are located along this gravimetric maximum (Figs. 1 and 3), and are probably related to bodies of basic igneous rocks. These data suggest that in the Alboran Channel there exists an asymmetrical axis of crustal thinning, where basic igneous rocks are intruded. Radiometric ages of basic volcanic rocks of Alboran Island are comprised between 25 and 18 m.y. (13).

CONTRIBUTION À L'ÉTUDE DE L'ENVIRONNEMENT SÉDIMENTAIRE AU QUATERNAIRE TERMINAL EN MER D'ALBORAN : APPORT MICROPALÉONTOLOGIQUE

F.Z. Hassouni [1]*, B. El Moumni [2], A. Ammar [1], B. Alonso [3] et A. Monaco [4]

[1] Univ. Mohamed V, Fac. Sci., Dépt. de Géologie, Rabat, Maroc
[2] Univ. Abdelmalek Essaadi, F.S.T., Dépt. de Géologie, B.P. 416 Tanger, Maroc
[3] CSIC, Institut de Ciencias del Mar, Passeing Joan de borbo, S/n- 08039, Barcelona, Espagne
[4] Univ. de Perpignan, L.S.G.M., C.N.R.S. (URA 715), 52, Av. de villeneuve, 66860 Perpignan, France

Résumé

Ce travail s'appuie sur l'analyse de sédiments prélevés par carottages en mer d'Alboran. Il se focalise sur l'étude des espèces des foraminifères planctoniques thermosensibles, qui par corrélation avec les datations absolues nous ont permis (i) d'établir une chronostratigraphie des dépôts, (ii) de les replacer dans le cadre des variations climatiques récentes, et (iii) de mettre en évidence deux types majeurs d'assemblages fauniques séparés par une période de transition au cours du Quaternaire terminal. Cette évolution se fait dans un contexte environnemental particulier, caractérisé par la proximité des continents et par l'importance des échanges hydrologiques entre l'Atlantique et la Méditerranée.

Key-words : foraminifera, pelagic, paleoceanography, Alboran Sea

Introduction

Le présent travail entre dans le cadre d'une étude pluridisciplinaire (sédimentologique, minéralogique, micropaléontologique et géochimique) sur l'environnement de la marge marocaine méditerranéenne et le bassin d'Alboran (1, 2, 3, 4, 5, 6). Il se fixe comme objectif principal l'étude des mécanismes hydrosédimentaires dans une zone de forts échanges : (i) échanges hydrologiques à travers le détroit de Gibraltar, (ii) échanges continent-océan à travers les marges méridionale (marocaine) et septentrionale (espagnole) de la mer d'Alboran. Ce qui est recherché à travers l'étude de l'accumulation sédimentaire, c'est l'évolution de ces mécanismes au cours des variations glacio-eustatiques et climatiques récentes (Quaternaire terminal).

Situation et environnement de la zone d'étude

La mer d'Alboran (fig. 1) forme l'extrémité Ouest de la Méditerranée occidentale, enclavée au sein de l'orogène bético-rifain. Elle constitue un bassin de dimension modeste et de physiographie particulièrement tourmentée, résultant d'une évolution structurale complexe (1, 3, 7). Trois secteurs y sont distingués : occidental, central et oriental.

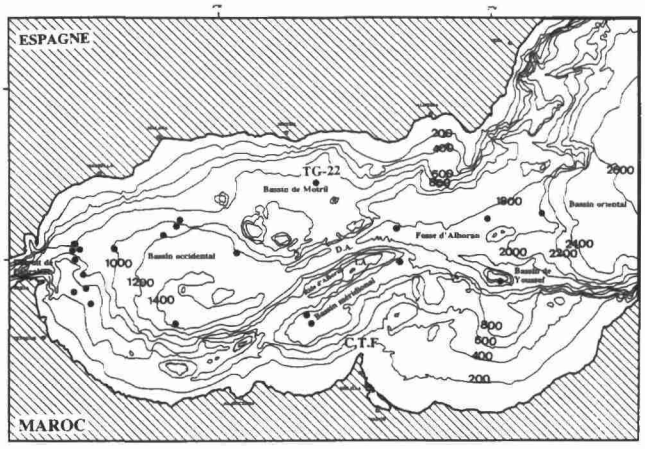

Fig.1 : Situation de la zone d'étude, (•) situation des carottes, TG-22 : Carotte présentée dans ce travail. D.A : Détroit d'Alboran, I.A : Ile d'Alboran, C.T.F : Cap des Trois Fourches.

(i) - Le secteur occidental comporte le bassin le plus large (et le plus étudié) qui est le bassin Ouest-Alboran.
(ii) - Le secteur central possède une morphologie complexe dominée par la ride d'Alboran qui s'intercale entre des zones profondes. Ce secteur est formé du Sud vers le Nord par le bassin méridional, le détroit d'Alboran et le bassin de Motril.
(iii) - Le secteur oriental comprend la fosse d'Alboran, le bassin oriental et le bassin de Youssef (8).

Sur le plan hydrodynamique, la circulation des masses d'eaux superficielles d'origine atlantique se fait en permanence d'Ouest vers l'Est, selon un schéma de deux gyres anticycloniques de part et d'autre du Cap des Trois Fourches (9). Ce schéma de circulation est prépondérant (9) mais il subit des variations importantes au cours de l'année avec la disparition de l'un des deux gyres (10). De type cyclonique, la circulation des eaux profondes d'origine méditerranéenne est fortement conditionnée par la topographie du fond (11). Ces eaux longent les parties profondes de la marge marocaine en direction du détroit de Gibraltar (11).

Matériels et méthodes

Le matériel étudié dans ce travail consiste en 22 carottes de type Kullenberg, prélevées lors de la campagne océanographique "Strakhov" (octobre 1993) en collaboration avec l'institut des Sciences de la Mer de Barcelone (Espagne). Ces carottes ont fait l'objet d'une étude sédimentologique détaillée. La minéralogie des argiles (< 2 µm) est réalisée par diffractométrie aux Rayons X à partir des dépôts orientés. Les carottes à caractère hémipélagique ont été sélectionnées pour une étude micropaléontologique par détermination et comptage des espèces de foraminifères planctoniques thermosensibles. Cette étude couplée avec les résultats des datations absolues au ^{14}C a permis d'établir la chronologie des dépôts et d'estimer localement les taux de sédimentation.

Résultats et discussions

Sur l'ensemble des résultats obtenus, la carotte TG-22 (longueur totale : 280 cm), située dans le bassin de Motril (fig.1) dans une zone à upwelling et de forte productivité (12), a été choisie comme carotte type pour être présentée dans ce travail. Sa situation, son caractère hémipélagique et l'évolution verticale nette des associations des espèces de foraminifères planctoniques au cours du Pléistocène supérieur et l'Holocène sont trois critères en faveur de ce choix. Cette carotte est constituée de vase argilo-silteuse, hémipélagique de couleur beige, entre 0 et 3 cm, puis grise, entre 3 et 240 cm avec des taches noires entre 110 et 240 cm. Elle passe ensuite à une couleur verte vers la base de la carotte (de 240 à 280 cm). La médiane évolue selon un gradient décroissant de la base (2 µm) vers le sommet (1 µm). Les taux de carbonates du sédiment total sont en moyenne de 28%. La fraction sableuse (<10%) est à composition biogénique largement dominante constituée essentiellemnt de tests de foraminifères planctoniques bien conservés et montre des pelotes fécales entre 0 et 60 cm. Le cortège des minéraux argileux est dominé par l'illite (37% en moyenne). La chlorite et la kaolinite constituent respectivement 24% et 25%. La smectite a des taux qui ne dépassent pas 16%.

Sur le plan micropaléontologique, le groupement des espèces de foraminifères en associations caractérisant les différents types de climat a fait l'objet de nombreuses discussions (13, 14). Dans ce travail nous considérons que les espèces *Globigerinoides ruber* (forme alba et rosea) forment l'association subtropicale et caractérisent un climat chaud. L'espèce *Globorotalia inflata*, indique un climat transitionnel à tendance chaude et l'espèce *Globigerina bulloides* est à tendance plutôt froide. Les espèces *Neogloboquadrina pachyderma* (dextre et senestre) et *Globorotalia quinqueloba* forment l'association des espèces subarctiques et caractérisent un climat froid.

Pour la carotte TG-22 (fig. 2), deux biozones principales y sont distinguées : (i) entre 0 et 200 cm : biozone marquée par l'abondance de l'espèce transitionnelle *G. inflata* à tendance chaude dont les pourcentages évoluent selon un gradient décroissant entre le sommet de la carotte (82%) et 160 cm (13%). Cependant l'espèce subarctique *N. pachyderma* inexistante ou très faiblement représentée vers le sommet constitue 51% de l'assemblage faunique à 160 cm. Les espèces subtropicales ou "d'eaux chaudes" marquent une augmentation vers 80 cm et leur fréquence est maximale à 200 cm (28%). (ii) entre 200 et 280 cm se rencontre une biozone caractérisée par la dominance de *N. pachyderma* (entre 50 et 66%). L'espèce *G. bulloides*, à tendance froide, faiblement représentée dans la zone précédante, montre une évolution croissante entre 220 cm (9%) et la base de la carotte (32% à 280 cm). Toutefois, les espèces subtropicales ont une fréquence très faible voir même nulle vers la base de la carotte.

L'assemblage faunique du premier tronçon de la carotte TG-22 (ente 0 et 200 cm) peut être attribué à l'Holocène. La distinction entre l'Holocène supérieur (H2 : de 0 à 7000 ans B.P.) et l'Holocène inférieur (H1 : de 7000

THE CRUST OF THE IONIAN ABYSSAL PLAIN - OLD OCEANIC ?

Werner Hieke [1]*, Hans B. Hirschleber [2], G. Ali Dehghani [2]

[1] Technische Universität München, Lehrstuhl für Geologie, Lichtenbergstr. 4, 85747 Garching, Germany
[2] Universität Hamburg, Institut für Geophysik, Bundesstr. 55, 20146 Hamburg, Germany

Abstract

New observations from the Ionian Abyssal Plain give arguments for a thinned continental crust underneath. They support the idea that the abyssal plain is not a relic of the Jurassic Tethys ocean but part of the Adria promontory of the African plate.

Key-words : crust structure, Ionian Sea

The nature of the crust beneath the Ionian Abyssal Plain (IAP) is contested at all times. Base of the controverse interpretations are seismic observations and models as well as plate tectonic reconstructions made to explain the mountain building processes of the Alps-Apennines-Hellenides system. The spectrum of interpretations includes: oceanic and thinned continental crust, thicknesses of the igneous crust between 5 and 50 km, ages of the crust between Lower Jurassic and Miocene.

A synopsis of the published interpretations of the crust beneath the IAP is given by Hieke and Dehghani [1].

The controversy can be simplified to the extreme questions:

- Is the IAP underlain by an old oceanic crust as a relic of the Tethys or by a young, thinned continental crust ?
- Is Adria a microplate separated completely from the African plate since Jurassic time or is Adria only a promontory of the African plate even with a fragile connection to the main part ?

The published data and observations allow to find support for various scenarios. Thus, the data are obviously not as definite as necessary for a clear interpretation. New observations made during the campaigns MEDRAC (cruise *Valdivia* 120, 1992) and MEDRAC II (cruise *Meteor* 25/4, 1993) may help to clarify the contested situation.

The southeastern corner of the IAP is traversed by a narrow, SW-NE trending subbottom structure (Victor Hensen Structure = VHStr). There, pre-Messinian non-volcanic rocks rise to higher stratigraphic levels and culminate in the Victor Hensen Seahill (VHS). In the southwestern prolongation of the VHS, this structure also rises above the seafloor, building the Victor Hensen Seahill 2 (VHS-2) within the Medina Ridge Glacis. Northeast of the VHS, the VHStr obviously influences the relief of the deepest part of the Mediterranean Ridge flank where the isobath trend changes from the usual S-N to a SW-NE orientation (Fig. 1).

The reported elements of the VHStr are separated from each other and shifted in a left-lateral sense. Following this sense, VHStr can be connected with the eastern finger of the Medina Ridge. A reflection seismic profile crossing the latter shows a structural situation which is almost identical with those of the VHS and the VHS-2. Therefore, the complete chain from the eastern finger to the SW-NE trending isobaths on the Mediterranean Ridge flank is considered as a particular structure with a minimum length of 270 km (Medina-Victor Hensen Structure = MVHStr). Recent or subrecent vertical movements are documented along this structure.

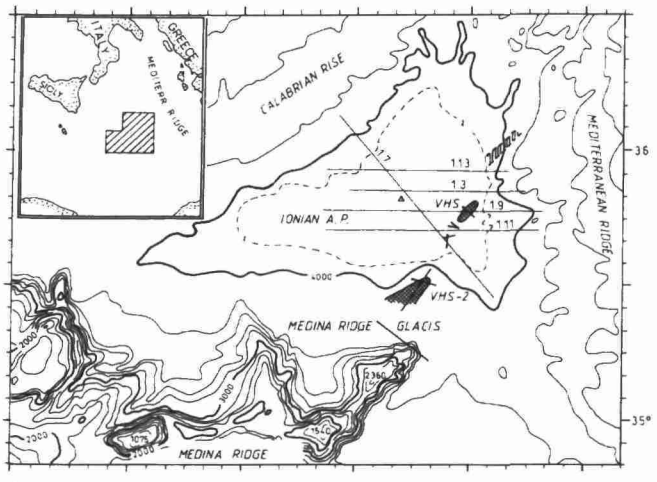

Fig. 1: Bathymetric map of the central Ionian Sea (IBCM). Isobaths in meter. Dashed line: Contour of the Ionian Abyssal Plain. Crosshatched: VHS and VHS-2. Hatched: Area of SW-NE trending isobaths. Unnumbered short lines: bottom and subbottom records of VHStr. Numbered lines: reflection seismic records (MEDRAC). Triangle: DSDP Site 374.

The area of the VHStr is characterized by a strong positive Bouguer gravity anomaly. In contrast, the pattern of the residual magnetic anomalies is not easy to correlate with the VHStr. The eastern finger of the Medina Ridge is not conspicuous in the Bouguer gravity but characterized by positive magnetic anomalies. Details are published by Hieke and Dehghani [1].

The MVHStr is the most spectacular one in the plain but not the only one. It is accompanied in the northwest by a similar structure of less extent (Nathalie Structure = NStr). The existence of more structures is not yet evidenced.

VHStr and NStr are prominent elements in a tectonic pattern which dominates the main part of the subbottom of the IAP (recorded along tracks 1.13, 1.3, 1.9, 1.11 and 1.7 in Fig. 1): Tilted sequences of parallel reflectors beneath the Messinian evaporites as shown in Fig. 2 (as an example). Tilted blocks are characteristic features originating during rifting of continental crust. The tilted units have a SW-NE orientation similar to those of the VHStr and the NStr which may represent extreme horsts (more details will be published by Hieke *et al.*) [2].

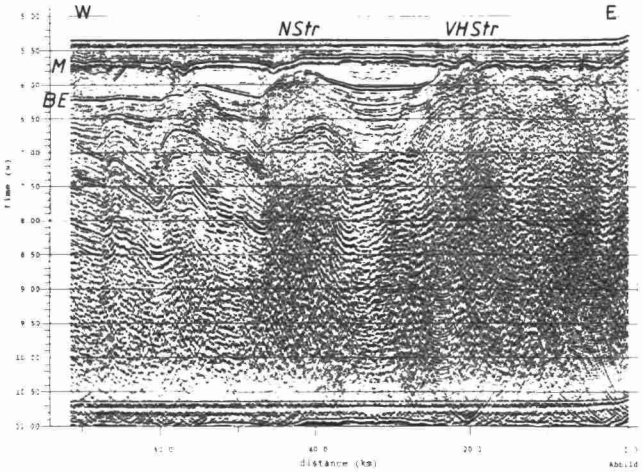

Fig. 2: Multichannel seismic line 1.11. M = Reflector M (top of evaporites). BE = Base of evaporites.

The Medina Ridge is accepted generally as an area underlain by continental crust. From our observations we conclude the following concerning the nature of the crust underneath the IAP:

- The 270 km long and only a few kilometers wide MVHStr comprises the eastern finger of the Medina Ridge (continental crust) as well as those parts passing the abyssal plain (oceanic or thinned continental crust). This is a powerful argument for the same kind of crust beneath the Medina Ridge and the Ionian Abyssal Plain - namely a continental one though in different stages of thinning.
- The tilted units underneath the abyssal plain support strongly the idea of a thinned continental crust.
- The age of the wedge-like syn-rift sediments (just pre-Messinian) suggests a maximum activity of the rifting processes during Miocene times. Dislocations of the M Reflector (top of the evaporites) as well

THE IMPACT OF SEDIMENT OXYGEN-CONTENT, CHEMICAL AND PHYSICAL WATER COLUMN PROPERTIES ON THE LIVING STANDING STOCKS OF BENTHIC FORAMINIFERA IN THE SE LEVANTINE BASIN (OFF THE ISRAELI COAST)

Jannink N.T. [1,2*], Herut [3] B., Almogi-Labin [4] A. and Van der Zwaan G.J. [1,2]

[1] Institute of Earth Sciences, Budapestlaan 4, 3584 CD Utrecht, The Netherlands
[2] Dept. of Ecology, Toernooiveld 1, 6525 ED Nijmegen, The Netherlands
[3] Israel Oceanographic & Limnological Research, National Institute of Oceanography, Haifa 31080, Israel
[4] Geological Survey of Israel, 30 Malke Yisrael St., Jerusalem, 95501, Israel

Abstract

Standing stocks of living benthic foraminifera, and oxygen contents in the sediment were studied in the SE Levantine Basin off the Israeli coast. Box cores, CTD-profiles, nutrients and chlorophyll-a concentrations were taken, every two months during a two-year period, along a depth transect (40-700 m). Here, we discuss the data obtained at our 40 m station during the first year (June '96 - February '97). Standing stocks as well as the benthic foraminiferal species distribution patterns in the 0-1 cm sediment layer show strong variation throughout the seasons. Over that period also oxygen penetration depth varied considerably. Analysis of the results indicate that the seasonal variation in the benthic foraminifera assemblage and the fluctuations in standing stock, do not seem to be induced by primary production fluctuations, but probably are due to variation in oxygen penetration in the sediment column.

Key-words : Foraminifera, Levantine Basin, nutrients, oxygen

Introduction

The Levantine Basin, off the Israeli coast, is an area where deep pycno- and nutriclines, in combination with an extremely deep photic zone, create a highly stable benthic environment. The extremely low phosphate and nitrate concentrations lead to ultra-oligotrophic conditions during most of the year (1, 2, 3). Such conditions are ideal to study the ecology, microhabitat-structure and population dynamics of benthic foraminifera, since the relatively stable oligotrophic conditions imply that physical and chemical factors regulating benthic foraminiferal distribution have minor effects on the population, certainly if compared to highly unstable environments, as for instance the northern Adriatic Sea, where population dynamics are presumed to be driven by seasonality and large fluctuations in food supply.

Material and methods

To establish population time series and patterns of microhabitat occupation, box cores were taken during a period of 2 years on board of the R/V *Shikmona*. Along a depth transect from 40 to 700 m, 9 permanent stations (Fig. 1) were sampled on a two-monthly basis. In each of the stations continuous profiles of temperature, salinity and oxygen were measured with a Sea-Bird electronics CTD. Water samples for the measurement of nutrients (nitrate, nitrite, ammonia, o-phosphate, silicic acid and chlorophyll-a (chl-a)) were collected with Niskin bottles mounted on a General Oceanic Rosette. Water samples for chl-a analyses were filtered at sea using glass fiber filters after pre-filtration through 60 µm sieve. Chl-a was determined using the procedure developed by Holm-Hansen *et al.* (4). Nutrients were determined in the laboratory using a segmented flow technicon Autoanalyser II system by the methods described by Krom *et al.* (2). The box cores were subsampled and subsequently sliced into 0.5 cm or 1 cm slices and stored in a Rose Bengal-ethanol solution. Rose Bengal stained benthic foraminifera from the 63-150 µm and the 150-595 µm size fractions were picked and counted. The oxygen content in the box core sediments was measured immediately upon arrival on board, with oxygen needle-electrodes attached to a micromanipulator.

This study focuses on the benthic foraminiferal assemblages (63-595 µm) occurring at Station 1 (40 m) during the period June 1996 - February 1997.

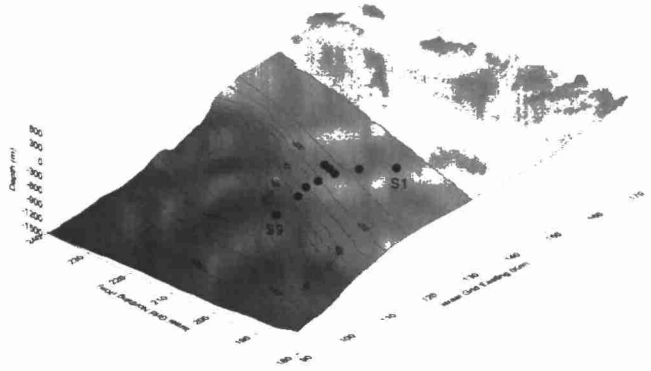

Fig. 1: Positions of the 9 permanent sampling stations (S1-S9).

Results and discussion

Chemical and physical structure of the water column

The nine stations cover the complete range from the Levantine surface water, through the Atlantic water mass, the Levantine intermediate water mass and down to the Deep water mass. Surface water temperatures show high seasonal variations and ranges between 18.2°C during winter and 28.4°C during summer. Generally, during winter the water column is well mixed in the upper 50 m and becomes stratified during the remainder of the year, with a upper mixed layer of about 25 m thickness bounded below by a sharp halocline and thermocline.

The concentrations of o-PO_4 in surface waters is close or below the detection limit (0.01 µM) increasing to 0.27 µM in deep waters. Nitrate concentration show a similar trend with values between detection limit and 4.94 µM. Chlorophyll-a concentrations were between 0.003 and 0.339 µg/l, similar to chl-a concentrations of the open sea in the Levantine basin (3, 5). Generally the distribution profile of chl-a concentrations show a deep chlorophyll maximum (DCM) between 80-120 m water depth. The DCM is associated with maximum oxygen concentrations. The depth integrative values of chl-a were found to be seasonally depended with values ranging between 10 and 30 mg m^{-2} in the upper 120 m (Fig. 2) and between 28 and 39 mg m^{-2} in the upper 400 m.

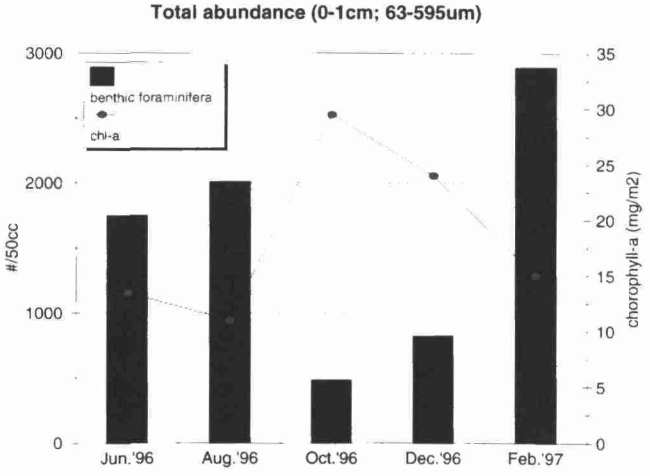

Fig. 2:Chorophyll-a (mg/m2) and standings stocks (numbers/50cc).

Benthic foraminifera

The faunal distribution patterns in the 0-1 cm sediment layer of Station 1 (40 m) display strong variation throughout the season. Surprisingly, the numbers of benthic foraminifera per 50cc (Fig. 2) in the oligotrophic Levantine Basin are considerably higher than the numbers of benthic foraminifera (per 50cc) in the highly eutrophic northern Adriatic Sea (6). Standing stocks do not seem to respond to primary productivity changes: no clear correlation is visible with chlorophyll-a profiles. One reason for this lack of correlation could be a phase shift, *i.e.* that the benthic associations show a retarded response to primary productivity. However, a time lag of the observed magnitude (4 months) does not seem feasible for the shallow water environment where sampling took place. Gooday (7) found

ARAGONITE SEDIMENTATION IN A RESTRICTED MARINE ENVIRONMENT (MLJET LAKES, ADRIATIC SEA)

Mladen Juracic [1*], Ivan Sondi [2], Ognjen Milat [3] & Ivan Gusic [1]

[1] Department of Geology, Faculty of Science, University of Zagreb, Zvonimirova 8, 10000 Zagreb, Croatia
[2] Center for Marine Research, "Ruder Boskovic" Institute, Bijenicka 54, 10000 Zagreb, Croatia
[3] Institute of Physics, Bijenicka 46, 10000 Zagreb, Croatia

ABSTRACT

Unusual sedimentation of aragonite mud in the Malo and Veliko jezero on Mljet island is discussed. Earlier investigations (1) already suggested that aragonite mud ("drewit") was being deposited in Malo Jezero. However, Seibold (2) denied the existence of aragonite. Here we present results that unequivocally confirm the existence of aragonite needles in suspended matter and in the Lake sediments. The origin of aragonite needles is discussed.

Key-words : lagoons, particulates, sediments, coastal waters

Introduction

Veliko and Malo Jezero (the Mljet Lakes) are located on the western part of Mljet Island (Adriatic Sea) (Fig. 1). Due to its scenic beauty, ecological peculiarities, and environmental values this western part of the island was proclaimed a National Park in 1960. Veliko and Malo Jezero (Large and Small Lake = Mljet Lakes) are semi-enclosed depressions connected with the open sea by a narrow, shallow channel. The "lakes" are typical karst depressions (a dolina and an uvala), which were formed under subaerial exposure and are now submerged due to Holocene sea-level rise (3). Being connected with the sea, they have saline water and therefore are not true lakes. Due to their depth (46 and 29 m respectively) they can hardly be termed lagoons because lagoons are often defined as shallow semi-enclosed water bodies (4), "having depths that seldom exceed a couple of meters" (5).

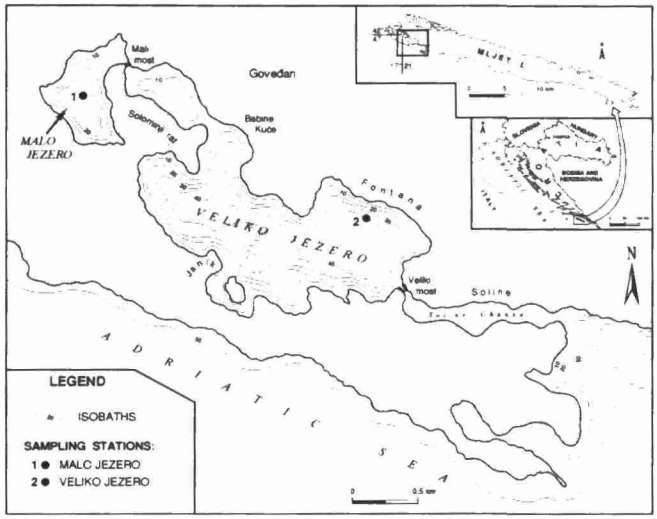

Figure 1. Map of the Mljet Island, Croatia, showing the study area and sampling stations

Water exchange with the open marine waters is only at the surface layer through very shallow and narrow straits. The water exchange is driven by tidal currents, but is insufficient for aeration of deeper water layers (6). This latter situation, coupled with a weak wind influence favours water stratification and give rise to temporary stagnant conditions with anoxia in deeper parts of the "lakes", especially in Malo Jezero (7). Hydrographic data indicate that the surface of the lakes may reach temperatures over 27°C and salinity over 38 ‰ during summer (7). Therefore the Mljet Lakes are restricted environments not only in spatial sense, but also in the sense of stress-producing environmental factors (8). Within the broader frame of investigation of sedimentation in the Mljet Lakes, the aim of this paper is to clarify the long lasting dilemma on aragonite sedimentation in "lakes".

Sampling and methods

Sediment cores up to 80 cm long were collected by scuba diving in Mljet Lakes (Fig. 1) in May 1995. On the same locations suspended matter samples were collected from the surface (0,5 m) by filtration of 2 litres of water through 0.45 μm Millipore filters. Sediment cores and suspended matter samples were frozen within 4 hours, and transported frozen to the laboratory. After freeze-drying in the laboratory, adequate subsamples were used for analysis.

Gross mineral composition was analysed by powder X-ray diffraction analysis (Philips, mod. PW 1050). Suspended matter and sediment-particle gross morphology was analysed on scanning electronic microscope (SEM) micrographs (Philips, SEM 515), whereas detailed investigation of crystal structure and morphology of particles was performed by using electronic microscope Philips EM 400T (operating at 100kV) in transmission imaging mode (magnification: 3.000 - 30.000 times), and in diffraction mode (with goniometer tilt: ± 60°). Selected-area diffraction patterns from individual grains were taken with the spot size 1 μm and the smallest diffraction aperture (30 μ), giving the size of the selected area (about 1 μ at the specimen plane). Carbonate content was determined volumetrically by measuring CO^2 evolved by dissolving a 0.5 g dry sample in 15 % HCl.

Results

Preliminary investigation of suspended matter and surface sediment samples from Malo Jezero by SEM and powder X-ray diffraction analysis revealed a high carbonate mineral content with prevalence of aragonite, and lower incidence of calcite, Mg-calcite (2 mol. % of $MgCO_3$) and dolomite (total carbonate content in surface sediment sample was 72 weight %) (9). SEM micrographs reveal the prevalence of needle-like particles in surface-sediment samples from Malo Jezero (Fig. 2). Combining these two results it can be assumed that these are aragonite needles. In order to clarify and support this assumption, additional transmission electron microscopy and diffraction analysis (TEM&ED) on selected samples were performed. The most dominant morphology was confirmed to be elongated particles with a needle-like shape and particle sizes ranging from 0.1 to 1 mm in thickness and 1 to 10 μm in length (Fig. 3). Crystalline features of these particles were confirmed by electronic diffraction.

Polycristalline ring pattern obtained from clusters (Fig 3. c) revealed the presence of abundant aragonite and some calcite. Spot patterns of properly oriented grains with needle-like morphology (as in fig. 3a) could be unambiguously indexed on the basis of aragonite orthorom-

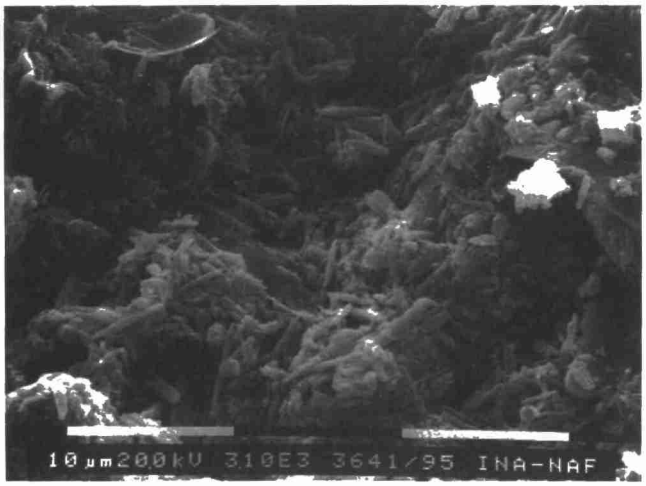

Figure 2. SEM micrograph of recent surface sediment from Malo Jezero showing prevalence of needle-like particles.

GEOCHEMISTRY AND MINERAL ASSEMBLAGES OF THE MEDITERRANEAN EVAPORITE DEPOSITS : THE TUZLA ROCK - SALT DEPOSIT IN BOSNIA - HERCEGOVINA

Goran Kniewald [1,2]*, Vladimir Bermanec [3] and Darko Tibljas [3]

[1] Center for Marine and Environmental Research, Rudjer Boskovic Institute, POB 1016, 10001 Zagreb, Croatia
[2] Institute of Applied Physical Chemistry (ICG-7), Department for the Chemistry and Dynamics of the Geosphere, Research Center Juelich (KFA), 52425 Juelich, Germany
[3] Department of Mineralogy and Petrology, Faculty of Sciences, University of Zagreb, Horvatovac bb, 10000 Zagreb, Croatia

Abstract

The evaporitic deposit of the Tuzla salt basin in Bosnia-Hercegovina is treated in terms of the regional Mediterranean evaporite formations. The geological and tectonic processes leading to the breakup of the Tethyan ocean during the middle and upper Miocene have caused a sequence of dessication and marine transgression periods which have resulted in the formation of extensive evaporite deposits along the continental margins of the Paratethyan and Mediterranean Seas. The lithofacial, mineralogical and geochemical characteristics of the Tuzla evaporite series show a similar pattern with the Gessoso-Solifera Messinian series in Sicily and set the requisite framework for a complex investigation of the depositional environments of Mediterranean evaporites.

Key-words : basin formation, diapirs, evaporites, geochemistry, mineralogy

Introduction

Evaporites in the Mediterranean region occur in a variety of environmental settings. Depositional environments range from coastal intertidal and supratidal zones (sebkhas), small coastal or atoll-type lagoons, deeper marine basins and sub-sealevel basins with marine inflow, to non-marine interior freshwater and saline lakes. The paleogeographic and tectonic settings include continental margins and shelves, interior cratonic basins and rifted continental slopes. The passage from one evaporitic sub-environment to another is often not obvious, as in the case of the carbonate deposits or sedimentary facies in less dynamic regions. The inherent diversity of the evaporitic series is further complicated by diagenetic processes. Moreover, some of the products of late diagenesis exhibit outward similarities to textures actually developed during sedimentation, including early diagenetic features which developed from and may be superposed on any characteristic facies of the depositional environment.

Mediterranean evaporites older than Tertiary age are comparatively rare. This appears to be a consequence of Miocene plate tectonic activity which created regions of relatively restricted marine sedimentation - the Mediterranean and the Paratethyan Seas, which evolved from the Tethyan ocean. Rapid changes in marine depositional environments seem to have occurred in the Mediterranean region during the middle Miocene. Following a peak in marine sedimentation during the early Badenian, there was widespread dessication in the Carpathian foredeep and eastern intramontane basins followed by a number of short marine transgressions. This event, decribed as the "middle Miocene salinity crisis", was caused by the closing of the marine seaway to the Indo-Pacific oceans and gave rise to the brackish water beds of the Karagangian stage of the eastern Paratethys and Mediterranean Seas (1). The subsequent and far-reaching transgression flooded the entire area of the central and eastern Paratethys during the late Badenian stage and covered the evaporitic series with radiolarian and pteropod marls, with a wide variety of lateral equivalent facies depending on the geological and stratigraphic setting of the small local basins which formed after the breakdown of the Paratethys intracontinental sea.

The origin of Mediterranean evaporites should also be assessed in view of the formation and occurrence of seafloor brines. A recent study reports brines from the Discovery basin in the eastern Mediterranean which have the highest salinity ever found in the marine environment (2). These brines, formed by dissolution of bischofite ($MgCl_2.6H_2O$), give the first clear evidence for bischofite formation during the the Miocene salinity crisis, when the eastern Mediterranean evaporated near to dryness.

The Tuzla evaporite series

The salt deposit of Tuzla is located in the north-eastern part of Bosnia-Hercegovina and is the largest rock salt reservoir in the Balkan peninsula, with estimated reserves of ca. 170 million tons of salt. The essentially stratified salt-dome type deposit is of mid-Miocene age and consists of a sedimentary sequence of banded halite and anhydrite. Despite the rather well investigated geological setting of the area, the depositional environment in which these evaporites formed is still uncertain. Early investigations of the Tuzla salt basin indicate that halite crystallization has occurred cyclically –several times, as the basin became shallower during the Styrian orogenetic phase (3). Anhydrous and hydrated salts were deposited on tertiary dolomites and marls. The geochemistry of coexisting brines and their saturation states imply that the formation environment may be interpreted in terms of the mixing-zone model, rather than as an end-member marine or salt lake deposits (4,5). On the other hand, the close relationship of the evaporite series with the associated dolomitic limestones as well as evidence of progressive dolomitization, may reflect their possible formation under evaporative, non-evaporative or seepage-reflux conditions (6). The described framework shows some similarities with the depositional environment of the Messinian deposits of Sicily which may serve as a sedimentary model for the extensive Messinian evaporite deposits throughout the Mediterranean basin (7).

The mineral assemblage and trace element distribution

The mineral association of the Tuzla rock-salt series consists of halite, thenardite and anhydrite. The $a(H_2O)$ indicator couple is thenardite-mirabilite. Several accessory minerals, including northupite, are present in varying amounts. The assemblage, as well as possible lithotype indicator minerals have been studied in detail (4,8).

An earlier investigation into the thermodynamics of northupite precipitation from brines percolating the halite strata (10) using the equilibrium computer code SOLMINEQ.88 showed that the major ion composition of the saline waters are consistent with either primary (formed by seawater evaporation) or secondary brines (formed by dissolution of evaporites). However, trace element concentrations can be used to differentiate between the two brine types since Li, Br and B do not form evaporite minerals during seawater evaporation.

In the paragenesis, a new mineral - named tuzlaite to honour the occurrence - with a pentaborate sheet structure has been discovered in the marls laterally equivalent to the evaporites (9). The conditions of its formations and thermodynamic stability are still unclear, but there are indications that diagenetic changes could have affected the nucleation kinetics of the normal succession of borate minerals in the sequence, resulting in the precipitation of tuzlaite.

Another highly interesting feature of the host rock, especially the lateral equivalents of the evaporite series is the content and distribution of microelements in these sediments. A preliminary instrumental neutron activation analysis (INAA) study of marls and the tuzlaite mineral indicate that several transition group metals (Fe, Cr, Ni) are related to sulfides present in the marls as pyrite. These are a consequence of the syn- and postdiagenetic conditions of low redox potential which is often associated with seepage reflux. Strontium shows an interesting distribution pattern both in tuzlaite and the proximal and distant marls. Strontium replaces calcium in the tuzlaite structure and has Kd values of about 2 compared to those of the proximal marl rock and of about 5 for the distant marls, indicating probable Sr absorption from the parent marl series.

Elements of the lanthanide series (REE's) also display significant interrelationships, both in the tuzlaite mineral and the host rock. The crystal structure of tuzlaite strongly influences the concentration and distribution of individual lanthanide elments, so that REE concentrations in the marls are up to a hundred times greater than in the tuzlaite. This mineral displays a peculiar negative Eu and Yb anomaly and a positive Tb anomaly, contrary to the marls which have no pronounced anomalies. The distribution of REE's in the proximal marls shows the same overall pattern as in the distant northupite-containing marl

THE STRUCTURE OF THE SEDIMENTARY COVER AND ACTIVE FLUID VENTING IN THE SOROKIN TROUGH (NORTHERN BLACK SEA)

A.F. Limonov [1], M.K. Ivanov [1], E.V. Kozlova [1], Tj. C. E. van Weering [2], L. B. Meisner [3], J. M. Woodside [4]*

[1] Faculty of Geology, Moscow State University, Moscow, Russia
[2] NIOZ, Texel, The Netherlands
[3] Okeangeofizika, Gelendzhik, Russia
[4] Free University, Amsterdam, The Netherlands

Abstract

The structural trends of clay diapiric ridges and folds in the Sorokin Trough south of the Crimea radically differs from those earlier assumed. The diapirs and folds are interpreted as being the result of a lateral tectonic compression. New geological-geophysical data obtained in the trough provide much evidence for active hydrocarbon fluid flux through the seafloor, including mud volcanoes, different seismic and acoustic anomalies, gas hydrate accumulation, etc.

Key-words : tectonics, diapirs, mud volcanoes, Black Sea

Introduction

In summer 1996, during leg 2 of the 6 th UNESCO-IOC Training-through-Research Cruise of the Russian R/V *Gelendzhik*, geological-geophysical investigations were carried out in the Sorokin Trough south of the Crimea. The methods applied included seismic profiling with a 3 litre air-gun, Simrad EM-12S multibeam echosounder swath-mapping, deep-towed survey with the MAK-1 sidescan sonar equipped with a subbottom profiler, and bottom sampling with a large diameter gravity corer. The seismic profiles were run in the direction approximately parallel to the Sorokin Trough trend and spaced closely enough (4.5 km apart on the average) allowing us to make a confident correlation between the structural features. The MAK-1 lines were placed between the seismic ones, and thus the surficial and shallow subbottom acoustic data complemented the deeper seismic information. The bottom sampling was based on the preliminary sidescan sonar and profiler data interpretation, providing a real ground-truthing.

Geological setting

The Sorokin Trough is located on the Crimean continental margin, at waterdepths of 800 - 2100 m (Fig. 1). The trough, about 150 by 50 km in size, is considered as the Crimean fore-deep [1]. It is filled with the more than 5 km thick clayey Maikopian Formation (Oligocene-Lower Miocene), overlain by Middle Miocene to Quaternary sediments, totally 3-4 km thick [2]. The Quaternary sediments largely belong to the paleo-Don/paleo-Kuban fan accumulation that covers the entire northeastern part of the Black Sea floor. The northern flank of the trough is a steep, faulted escarpment of the Triassic-Jurassic basement of the Crimean Mountains, and to the south it is bordered by the Cretaceous-Eocene Tetyaev Rise and Shatskii Ridge, on the top of which the thickness of the Maikopian Formation decreases by 1-2 km.

Since the first seismic investigation in the trough in the 1970s it was widely accepted that the Maikopian Formation forms several zones of clay diapirs aligned in accordance with the general trend of the trough. However, any details of the trough structure remained unknown.

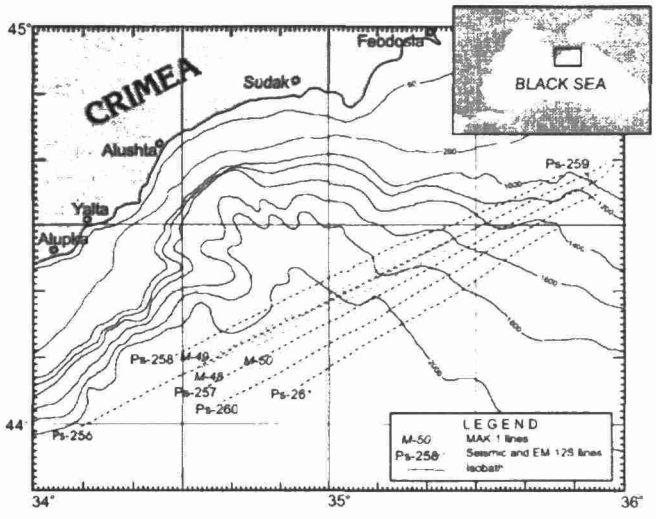

Fig. 1. Location map of seismic, multibeam echosounder, and sidescan sonar lines in the Sorokin Trough.

The data analysis

Two seismic members can be distinguished in the seismic sections. The upper one is identified as Quaternary hemipelagic and turbiditic sediments [2]. Its observed thickness varies between 100 and 1300 ms TWTT (90-1200 m). This member appears as acoustically layered, with some acoustically transparent units, each 70-80 m thick, whose abundance and thickness increase northeastward. The peculiar feature of the upper seismic member is well-defined, negative polarity bright-spot acoustic anomalies at different subbottom depths : from 230 to 800 m. The tectonic disturbance of the upper member is completely determined by the dislocation in the lower one. The latter can be dated by the Pliocene to the upper part of the Maikopian Formation [2]. It is generally acoustically semitransparent or transparent and is disturbed by numerous folds and faults. The boundary between the lower and the upper members sometimes is difficult to pin-point in the seismic profiles.

The seismic profiles show that the deformation in the lower seismic member has a complex pattern. Both diapiric structures and fault-related folds were observed in it within the study area (Fig. 2). They are grouped in 9 linear zones, 6 of them (southwestern) clearly being of diapiric origin, and other 3 zones (northeastern) representing faulted folds. The Maikopian Formation is deeply buried in the northeastern part of the study area and is not seen in our seismic profiles, hence it is not excluded that the faulted folds could develop above clay diapirs. Each diapiric zone consists of 1 to 4 diapiric ridges. In turn, some of these ridges produce individual diapirs or mud volcanoes that rise from their tops and slopes. Three diapiric zones are characterized by mud volcanoes. On the MAK-1 sonographs and the seafloor reflectivity map, totally 16 mud volcanoes were distinguished, all of them at waterdepths of 1600-2100 m. They vary in morphology form regular cone-shaped structures, through "mud pies" and collapsed features, to fissure eruptions of the mud breccia. The average sea bottom diameter of the mud volcanoes is about 800 m. Their craters are poorly expressed. The fissure eruptions are related to a system of parallel faults oriented in a sublatitudinal direction. Some pockmarks were observed in the high-resolution sonographs as well.

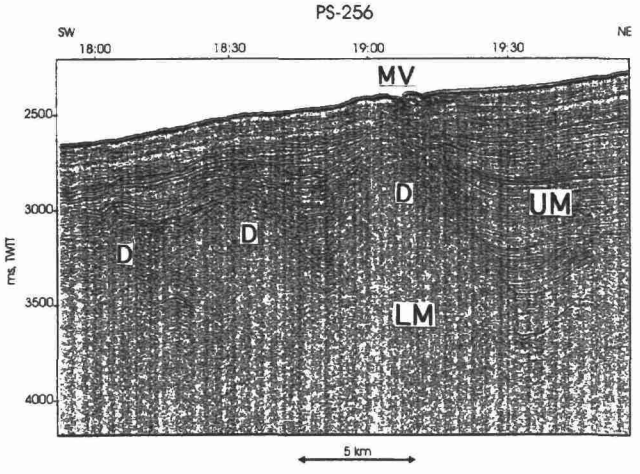

Fig. 2. Part of seismic profile PS-256. UM - upper seismic member, LM - lower seismic member, D - clay diapir, MV - mud volcano.

EVOLUTION OF THE GULF OF CADIZ MARGIN INFLUENCED BY THE MEDITERRANEAN ALPINE BELTS

Andrés Maldonado [1*], C. Hans Nelson [2], Jesús Rodero [1] and Luis Somoza [3]

[1] Instituto Andaluz de Ciencias de la Tierra, C.S.I.C./Universidad de Granada, Facultad de Ciencias, 18002 Granada, Spain
[2] U.S. Geological Survey, 345 Middlefield Road, Mail Stoop 999, Menlo Park, CA 94025, U.S.A.
[3] Instituto Tecnológico Geominero de España, Rios Rosas, 23, 28003 Madrid, Spain

Abstract

The initial Mesozoic and Early Cenozoic evolution of the Gulf of Cadiz margin was characterized by passive style, which controlled development of extensional structures and carbonate platforms. Subsequent ocean-spreading in the North Atlantic induced extensional tectonics, which deformed synsedimentary Cretaceous deposits. The African-Eurasian plate boundary experienced transpression during Tertiary and the Mesozoic basins floored by oceanic crust underwent subduction. An olistostrome was emplaced during Tortonian as results of the westward motion of the Alboran Domain. The closing of the Betic and Rif seaways in Messinian and the subsequent opening of the Strait of Gibraltar controlled the recent evolution.

Key-words : tectonics, Western Mediterranean, seismic, stratigraphy, continental margin

Introduction

This study of the Gulf of Cadiz summarizes the evolution of the Iberian continental margin from its Mesozoic inception until the present day. The main objective is to provide an integrated view of the growth patterns and factors that controlled the evolution of the margin through time. The Cadiz margin developed near the boundary between the two major Eurasian and African plates under the control of a complex tectonic evolution (Fig. 1). It is located also in an area largely influenced by the closing and opening of straits, which acted as major gateways between the Atlantic Ocean and the marginal, semi-enclosed Mediterranean Sea (1, 2).

Evolution of the Cadiz margin

The Gulf of Cadiz straddles the boundary between the African and Iberian plates and it is intersected in the eastern area by the orogenic Gibraltar Arc (Fig. 1). It occupies a key location for understanding the development of the central North Atlantic and the Alpine belts of the Mediterranean The evolution of this area was influenced by the successive phases in the opening of the North Atlantic, the closure of the Tethys ocean and the opening of the western Mediterranean basins (1, 3).

Triassic to Early Cretaceous rifting and Mesozoic passive margins

The breakup of Pangea in Triassic time and the subsequent rifting formed the southern margins of Iberia and northern Africa. The initial stages in the evolution of these margins are characterized by a passive style linked to the development of the Tethys and Central-North Atlantic domains. Later during the Early Mesozoic, the Azores-Gibraltar Fracture Zone constituted a major transcurrent boundary where the Central Atlantic ridge ended and which caused extension into the Tethys area along deep oceanic basins (3). The Late Jurassic and Early Cretaceous progressive rifting of the Central Atlantic resulted in a major sinistral translation between Africa and Laurasia plus spreading in the Tethys. Very active rifting in the Gulf of Cadiz occurred during the Kimmeridgian-Tithonian times (143-155 Ma), and the Valangian-Barremian times (118-143 Ma), while the northern pasive margin of Iberia was occupied by extensive carbonate platforms (1, 4).

A wide spread unconformity recorded in the Gulf of Cadiz before Early Aptian time (anomaly M0, 118 Ma) indicates a compressional event. The southern margin of Iberia was probably affected during this time by a transpressional regime. Active sea-floor spreading in the North Atlantic since anomaly M0 favored further spreading and transcurrent motions between Iberia and Africa. During this Late Jurassic and Early Cretaceous evolution, half graben structures were developed in the Gulf of Cadiz, which were subsequently filled with carbonate slope facies and submarine fans. (Fig. 1)

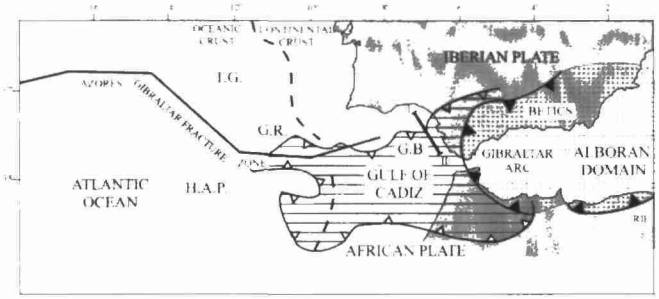

Fig. 1.- Geographic chart showing the regional tectonic setting of the study area and distribution of the present major lithospheric structures. Legend: G.B., Guadalquivir Bank G.R., Gorringe Bank; H.A.P., Horseshoe Abyssal Plain; T.G., Tagus Abyssal Plain; Open triangle, olistostrome front: Bold triangle; Alboran domain thrust front. Explanation in the text. (Modified from 1). Profile I-II in Fig. 2.

Late Cretaceous to Early Tertiary intraplate evolution

From about the time of Late Albian (110 Ma) to the Late Eocene (41 Ma) Iberia moved as part of the African plate (3). This intraplate evolution was characterized by the development of generally thin depositional sequences, which draped the structural highs and grabens of the basement (1). These deposits are characterized, however, by significant facies and thickness variations and many parts of the margin underwent extensive erosion.

Late Eocene to Early Miocene active margin

During Late Eocene to Early Miocene (41-24 Ma) Iberia became again an independent plate (3). The relative motion between the Iberian and African plates in the Gulf of Cadiz was small between anomalies 18-13, but since then a significant amount of shortening occurred in the area. The tectonic evolution was characterized by an increase of the subsidence rate and graben development (1). The Lower Oligocene deposits are very reduced or absent, which reflected the compresional regime along the AGFZ. Extensive areas of erosion show uplifted blocks developed during the generalized compressional regime. Middle-Late Oligocene carbonate platforms onlaped the Cretaceous and Early Tertiary highs, while a high-energy, carbonate platform linked the Central Atlantic and Mediterranean basins through the north African Rif and south Iberia Betic seaway corridors. Thick turbidite deposits of the "Campo de Gibraltar" flysch, were also developed during this time interval in deep troughs between the Iberian and African margins and the forearc of the westward thrusting Alboran Domain (1).

Miocene foredeep basins of the Gulf of Cadiz

The northward drift of Africa caused the progressive closure of the Tethys basins and the rapid westward migration of the Gibraltar Arc front towards the Gulf of Cadiz area (5, 6). The existence of closely juxtaposed regions of compression and extension between Iberia and Africa is attributed to the westwards progression of the Gibraltar Arc mountain front over a subducting thinned Tethys crust (Maldonado et al., this issue). The Gulf of Cadiz was part of the extensive area of deformation located along the transcurrent fault system between Africa and Iberia, while wrench zones within conjugate fault systems induced the development of subsiding, roughly oriented WSW-ENE basins (1).

An autochtonus calcareous margin developed along southern Iberia, while an allochtonous terrigenous margin was located around the morphological highs of the Betic Cordillera (Figs. 1, 2). Between these two margins, deep basins and straits connected the Atlantic and Mediterranean basins forming the Betic corridor (6). In addition, the westward migration of the Gibraltar thrust front into the flysch trough during the Burdigalian led to the formation of an accretionary forearc which collided with the passive margins of southern Iberia and northern Africa (1, 5). The progression of the mountain front continued into the Middle Miocene when the olistostrome of the Gulf of Cadiz is emplaced. Rapid increase of basement subsidence rates in the Gulf of Cadiz during Early Tortonian may have favored the foredeep basin formation and the emplacement of the olistostrome (1).

Late Miocene closing and opening of straits

The generalized compressional regime during the Late Tortonian and Messinian time in the southern Iberian margin induced relative sea level lowering and together with a global low eustatic sea level resulted in the closure of the Betic and Rif straits (5). This stress field facilitated, however, transcurrent movements and extension in an east-west to ESE-WNW direction. At the end of the Messinian and during the Early Pliocene, the stress field changed to a more roughly north-south oriented direction and pull-apart basins were developed under a transtensional regime, which induced the reopening of the connection between the Atlantic and the Mediterranean through the Strait of Gibraltar. The Gulf of Cadiz was affected by significant foredeep subsidence with the development of deep depositional basins trending NE-SW (1).

ACTIVE FAULTS IN THE COASTAL ZONE OF ISRAEL

Yossi Mart
Leon Recanati Center of Marine Studies, University of Haifa, Haifa 31905, Israel

Abstract
Historical reports describe fatal earthquakes that hit the coastal cities of the southern Levant and many of these tremors are not linked to the Dead Sea rift. Geological and archaeological evidence for these earthquakes are ambiguous, because the coastal plain has been cultivated for millennia, and it is difficult to differentiate between products of active faulting and artifacts. High-resolution seismic surveys in the shallow continental shelf show evidence for small faults that offset Pleistocene calcareous sandstone. Off Caesarea, central Israel, geophysical data show a fault that displaces Herodian breakwaters, setting the age of neotectonic activity to less than 2,000 years.

Key-words: continental shelf, tectonics, Levantine Sea

Introduction

Historical documents, some dating back 2,500 years, repeatedly describe catastrophic earthquakes and tsunamis (Appendix I) that inflicted fatal casualties and heavy damages to the coastal cities of the southern Levant (1-6). Any attempt to estimate the real number of casualties and the true rate of damage of a natural disaster from surviving literary accounts should be carried out with great caution. Ancient writers commonly used stock phrases and descriptions in their accounts of the events. In the absence of other information, however, such texts are useful, but should never be considered definitive. Archaeological data, when available, can provide more reliable indicators, especially where they confirm historic documentation. Bearing these reservations in mind, it seems that numerous tremors affected the coasts of the southern Levant in historic times, in addition to the earthquakes that hit the Dead Sea Rift and its environs. The historic records also report on damages caused by tsunamis, but the tectonic significance of such damages undoubtedly ambiguous, because the tsunamis could have originated either along the Levant margin, or in the Anatolian or Hellenic margins.

Geological setting

The present research tried to find out whether the historical records could be supported by geophysical data. The coastal plain of the southern Levant has been cultivated for millennia, and most straight lineament in the rocks there are suspect of being artifacts (7). Therefore we searched for lineaments and elongated cliffs in submarine outcrops of Pleistocene calcareous sandstone in the proximal continental shelf. Indeed, indications for neotectonic activity have already been encountered along the shallow continental shelf of central Israel, off Caesarea and off Atlit, and other sites are yet to be explored. Series of small escarpments, attributed to faulting, were encountered in both places, trending predominantly N-S, and downthrowing their western flank (Figs. 1, 2). Faults of this series occur also along rocky segments of the shoreline in places. Additional faults, trending NE-SW were encountered off Caesarea, and a series trending NW-SE was traced off Atlit. These findings suggest the local characteristic of the NW and NE trending faults, and the regional distinction o the N-S trending ones. Most faults are associated with straight and elongated escarpments, so that they can be considered neotectonic, and had the escarpments been arcuate, a geotechnical process, such as slump or landslide, would have been suggested (6, 8). Since all the faults discerned in the shallow continental shelf offset calcareous sandstone of Pleistocene age, they can be considered active. However, most of the N-S trending faults seemed to outcrop at the sea-floor, whereas many of the NW trending faults seem covered by sediments, and their Holocene activity is dubious.

Complex series of archaeological, geological, and geophysical data

pertaining faulting and earthquakes was encountered off Caesarea. The ancient harbor of Caesarea presents apparently ambivalent structural evidence for neotectonic activity. Caesarea was built in 20-10 BC by King Herod the Great, who named the new city after his mentor, Augustus. The city was built from scratch, and was famous for its outstanding civic installations, such its sophisticated water supply system, its harbor, which was second only to that of Alexandria, and its theater, stadium, temple, and other amenities required in a Roman metropolis. The large Herodian breakwaters , which extended some 400 m seawards, are presently submerged 5-8 m below sealevel, whereas other contemporary coastal and harbor installations remain at sealevel. The submerged marine constructions prompted some to suggest faulting along the coast in Caesarea (9, 10), while the stability of coastal constructions led others to suggest structural stability (11, 12).

In the course of the present study, high resolution seismic reflection profiles were carried out in the shallow continental shelf. These profiles encountered a series of coast-parallel faults that displace both the Pleistocene calcareous sandstone, which crops out along the coastal zone, as well as the submerged Herodian breakwaters. The faults show

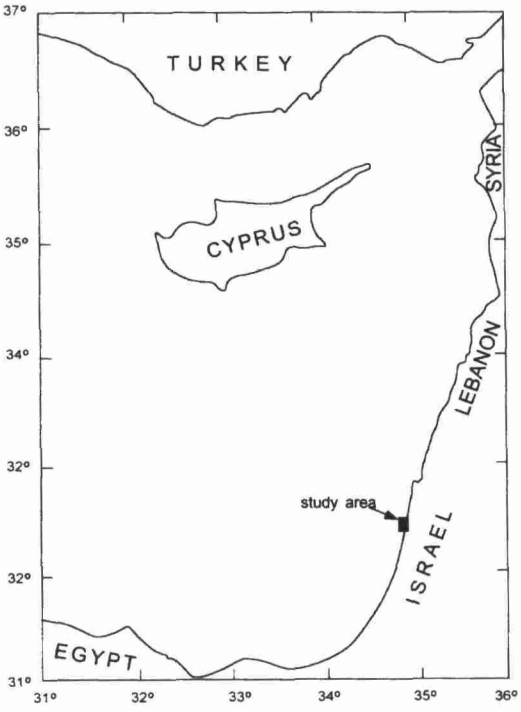

Fig. 1. The eastern Mediterranean and the study area.

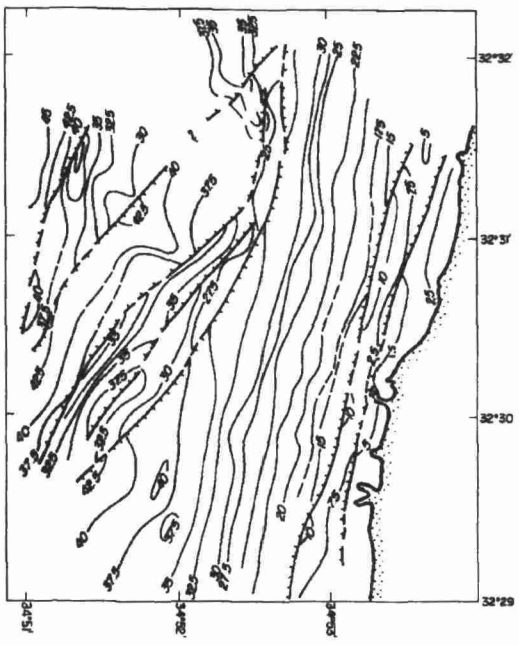

Fig. 2. Structural map of the upper surface of the Late Pleistocene calcareous sandstone off Caesarea in central Israel. See Fig. 1 for location.

RECENT EVOLUTION OF THE BEACHES OF THE GULF OF LERICI (LA SPEZIA, ITALY)

Meloni R. [1], Cavallo C. [2], Corradi N. [2]*, Ferretti O. [3], Francioli G. [2]

[1] CNR ISDGM, Stazione Oceanografica, La Spezia, Italy
[2] Dipartimento di Scienze della Terra, Università di Genova, Italy
[3] ENEA Centro Ricerche Ambiente Marino, La Spezia, Italy

Abstract

The aim of this work is to verify the impact of the new pier of Lerici harbour on the nearby beaches. During the summer '90 and '96, bathymetric and beach profiles were executed and compared. Sea bottom and beach sample sediments were also collected to determine textural characters. The results show a seaward movement of the isobaths with the increase of the sedimentary material. Erosional processes, in addition, do not seem relevant on the nearby beaches.

Key-words : Thyrrenian Sea, bathymetry, coastal management, shoreline evolution, sediments

Introduction

In this paper we show the results of the analysis carried out on the beaches of the Comune di Lerici, wich was part of a periodical research project run by the research centre ENEA in the structure of S. Teresa. This project had the aim of evaluating the changes of the coastline caused by different constructions along the seafront. In particular the lenghtening of the pier in Lerici which was built in 1950 and lenghtened by about 60 metres at the end of the 1980's, was investigated.

The study was focused in the morphological, sedimentological and textural characteristics of the beaches and the sea bed. It was conducted using topographic and bathimetric surveys and about 60 samples of sediment from the shore and the sea bottom.

Characteristics and general conditions of the coast

The coastal area examined is situated on the eastern promontory of the Gulf of La Spezia and is bounded by the Punta di S. Teresa in the NW and the promontory of Maralunga in the SE (Fig.1). The area is mainly a high coast characterised by small pebbly pocket beaches (1). Along the coastline there are also some parallel defense structures, at Venere beach, which has more than once in the past almost been completely eroded away especially after the construcion of the pier at S. Terenzo and the Lido groins, which trapping the sediment, prevent the redistribution in the adjacent beaches. The area has been generally developed in the urban but especially touristic field. In the gulf there are two small harbours: at S. Terenzo for mooring small touristic boats and at Lerici for both tourist and fishing boats as well as commercial boats travelling between the islands of the Gulf of La Spezia.

Analysis of the variations in the shoreline

The comparison between variations in the morphology of the shore during the period from 1973 to 1996, was carried out using two different procedures. Comparisons of aerial photographs to reconstruct the last twenty years and topographic measures taken directly from the beach to compare the current shape to that observed in 1990.

From the morphological and morphometrical studies it was seen that the beaches can be subdivided, either by the geomorfological characteristics or the results of the textural analysis, into two groups. The first group consists of the beaches known as "pocket" the Baia Blu, Marinella and Colombo and the second group the beaches of S. Terenzo, Venere and the Lido (Fig.1). All of the beaches belonging to the second group show a progressive advancement in the shoreline. The advancement of the beaches of Venere and S. Terenzo is recorded as having started in 1973 while for the Lido there was first a regression before the advancement.

Marine hydrology and wave dynamics

Inside the Gulf of Lerici the current moves in anti-clockwise direction in accordance with the general movement of the water mass which come

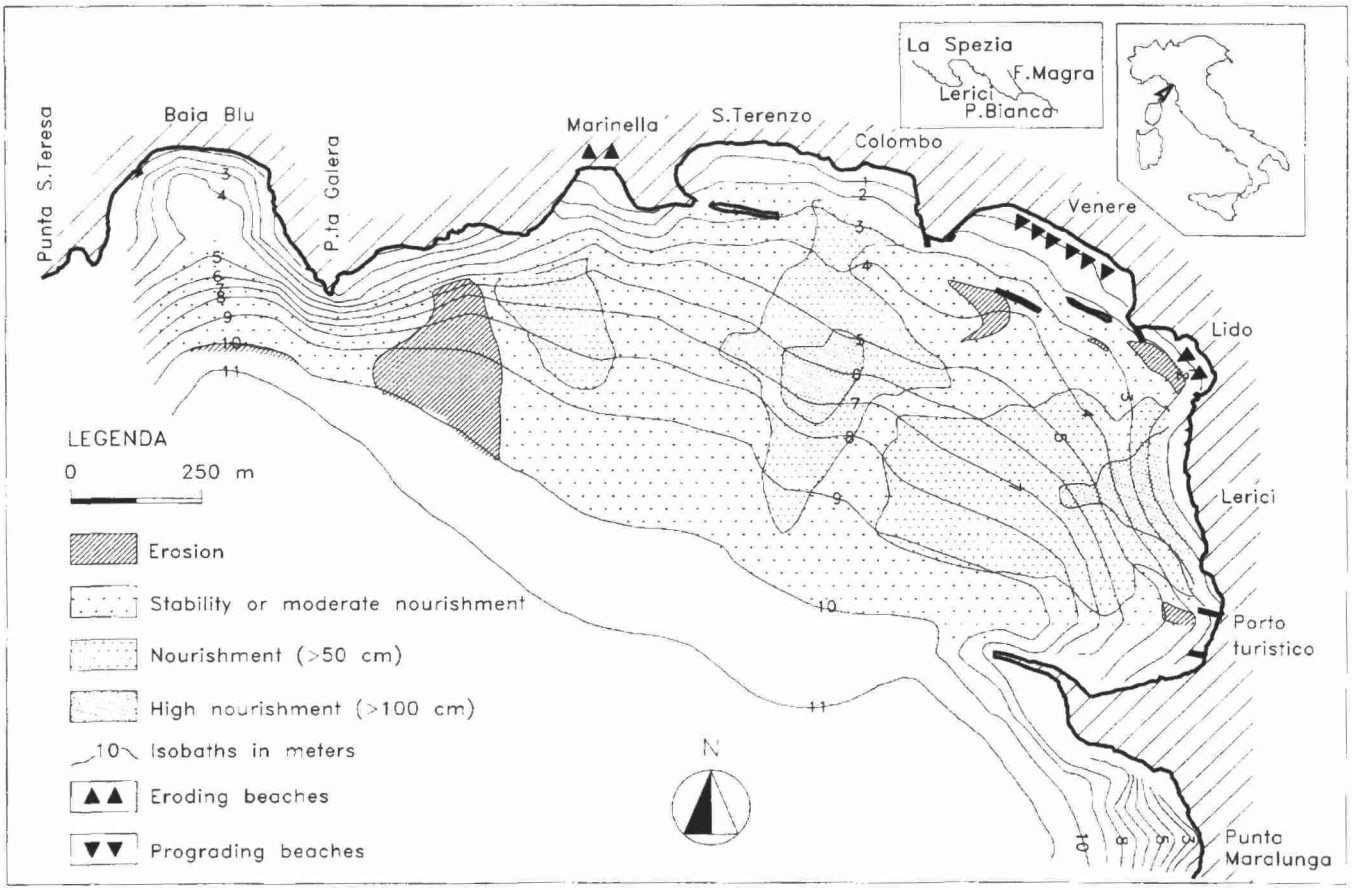

Fig.1 - Map of recent evolutive trends of the Gulf of Lerici (1991/1996).

VOLCANOGENIC - SEDIMENTARY DEPOSITS ON THE SLOPES OF THE TYRRHENIAN SEA SUBMARINE VOLCANOES AS AN EVIDENCE OF EXPLOSIVE VOLCANISM

V.N. Moskalenko*, K.M. Shimkus

Southern Branch of Institute of Oceanology named by P.P.Shirshov of Russia Academy of Sciences , 353470, Gelendzhik, Russia.

Abstract

Complex geological - geophysical research of Tyrrhenian sea underwater volcanoes has been performed during 16-th expedition of R/V *Akademik Mstislav Keldysh* (1988). Stratified siesmic layers consisting of volcanic-sedimentary rocks, formed due to explosive volcanism, have been for the first time discovered on slopes of submarine volcanoes during seismic single channel profiling. Certain geological evidences have been received during underwater geological survey, performed from submersible manned apparatus "Mir".

Key-words : deep sea basins, seismic, stratification, volcanology

Stratified siesmic layer distribution.

Vavilov, Magnaghi and Marsili underwater volcanoes are usually considered as a lava flow's cones (1,3). In 16-th expedition of R/V *Akademik Mstislav Keldysh* a lot of geological information, proving the wide spreading of basalt lavas in structures of all mentioned volcanoes, has been collected. Furthermore, for the first time we have received data of participation of volcanogenic - sedimentary complexes in their structures. The evidences are seismic sections with stratified structure, crossing the mountain slopes (1).

Vavilov volcano is the biggest submarine mountain in the central part of Tyrrhenian sea deep-water basin, its height is 2.9 km, the top is at the depth of 0.7 km (fig 1). It is asymmetric by geomorphological and tectonic structure: its western slope is steep (up to 26.5 degree.), and the eastern slope is gentle with numerous tectonic steps. Lava flows are discovered everywhere on western slope and on northern and southern ends of this submeridionally stretched volcano. On the seismic section of western slope there is steeply inclined stratified formation with thickness from 80 to 150 ms. Photo / video shooting has revealed a number of tectonic ledges, where the stratified formations, related to lavas, has been found. By the character of bedding some of them could be considered as tuff-lavas, lava-breccia. Stratified structures on this slope are found during dives of French apparatus "Siana" (2).

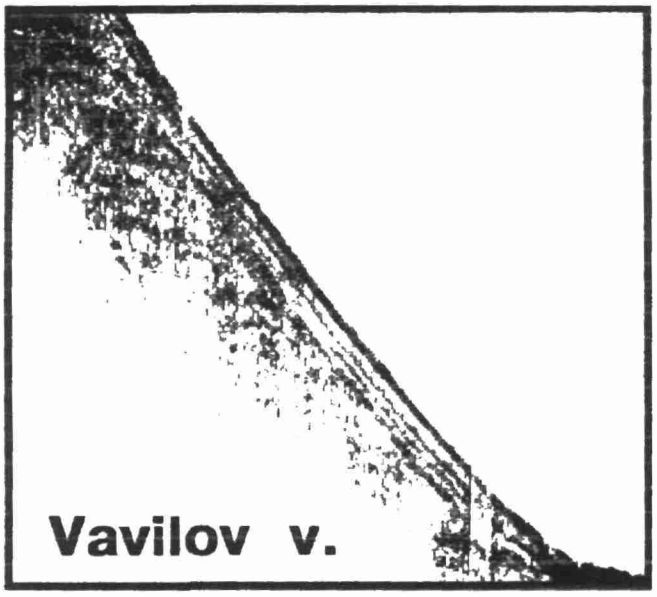

Figure 1.

Magnaghi. Several stratified siesmic layers were revealed on Magnaghi underwater volcano with top on 1465 - 1600m, located on west from Vavilov mountain. The upper siesmic layer is monitored not everywhere. It is spreaded on north - eastern slope and elevation adjacent to Magnaghi. Its small fragments are marked out in southern part of mountain. On western slope, on the part, which transits to the adjacent elevation, the upper stratified siesmic layer is presented by three consecutively overlapping formations, each of them ended at different distance from the top.

On the southern slope this siesmic layer is divided into steps, located at different hypsometric levels and is exposed on tectonic ledges in its whole thickness that equals 300 - 500 m (fig. 2). On almost vertical ledges the visual monitoring, photo and video shooting had discovered thick lava flows partially overlaid with stratified, obviously volcanogenic - sedimentary formations.

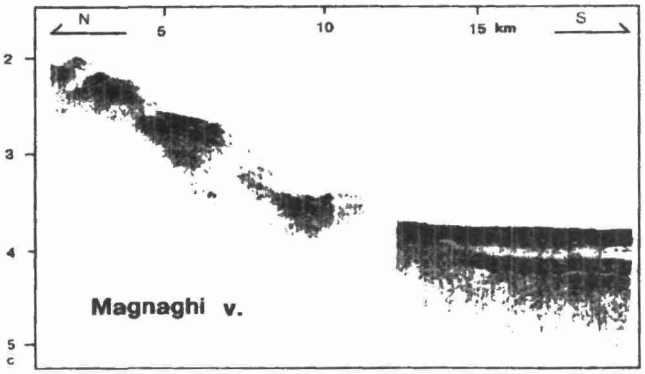

Figure 2.

Marsili volcano is located in south - eastern part of deep-water basin, and, like the others, is stretched in submeridional direction. Its width is twice bigger than Vavilov volcano. Its height is 2700 m, and its tops are at depths 500-800 m. Lava flows are exposed, mainly, on northern and southern ends of volcano, in the areas of young tectonic activity. The stratified formation is revealed on seismic sections crossing upper and middle parts of slope (fig.3). Its thickness increases downhill from 50 to 100 ms. On some parts of slope it is underlaid with lava formations, creating very uneven surface. In the bottom part of north - eastern slope the thickness of stratificated formation is 200 - 250 ms, it is smaller in upper part of western slope.

During underwater survey performed from "Mir" apparatus, the stratified formation has been photographed and video recorded in one

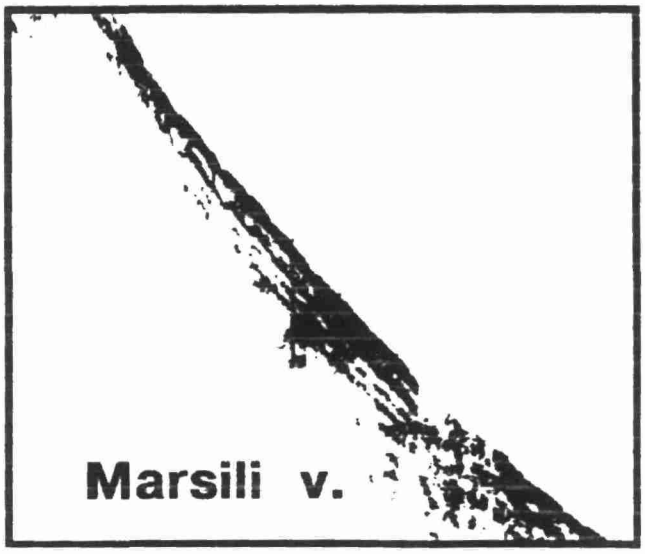

Figure 3.

GRAVITY AND MAGNETIC DATA OF THE ANAXIMANDER MOUNTAINS

E.Z. Oral [1], M. Ergun [1]* and J.M. Woodside [2]

[1] Dokuz Eylül University, Izmir, Turkey
[2] Free University, Amsterdam, The Netherlands

Abstract

The Anaximander Mountains lie at the junction between the Hellenic Arc and the Cyprus Arc where the Mediterranean Ridge meets the Florence Rise. Results from the ANAXIPROBE project indicate that these mountains are a southward-rifted and foundered continuation of the southwestern Turkish Tauride mountains to the north. The mountains are separated by faults and are undergoing independent movements and deformations. Free air gravity anomalies indicate a crustal discontinuity running directly through the middle of the mountains. Free-air gravity anomalies decrease towards the Rhodes basin (northwest), the Finike basin (north) and the south side at the eastern mountains. These are partly correlable with water depths. The Rhodes Abyssal Plain has a depth of approximately 4000 m and a Bouguer gravity high of nearly 180 mGal. On the other hand, the Anaximander Mountains are marked by a gravity low only 0 to 20 mGal. It seems however, that changing sediment thicknesses and density alone can not explain the rapid change in gravity. In addition crustal thickening and a change from continental to oceanic type crust must be involved. The magnetic data of the region are rather patchy thus suggesting a complex block structure.

Key-words : crust structure, tectonics, Mediterranean Ridge

Introduction

The Anaximander Mountains lie at the junction between the Hellenic Arc and the Cyprus Arc where the Mediterranean Ridge meets the Florence Rise. The three principal mountains in the complex rise from depths of around 2000 to 2500 m to peaks at about 700 m (Western Mountain), 900 m (Southern Mountain), and 1200 m (Eastern Mountain). However surrounding depths can reach more than 4000 m to the west (Rhodes Basin) and 3000 m to the north (Finike Basin). Each mountain in the group has a different shape the others: Anaximenes is a curved ridge of moderately dipping (about 250) sedimentary strata, Anaximander is a north tilted (at about 40) tabular block, and Anaxagoras comprises a broken NW-SE ridge on a broader plateau of rough relief (1).

The boundary between the African and Eurasian plates is delineated by the Hellenic arc and Pliny-Strabo trench to the west and the Cyprus arc to the east. The complex geomorphology of the Mediterranean Ridge and Florence Rise around the Anaximander Mountains makes it difficult to distinguish true neotectonic deformation resulting from the regional plate interactions from local effects which may be caused by karstic processes, mud diapirism, or halokinesis (2). The mountains are separated by faults and are undergoing independent movement and deformation. They are caught up in the relative northeastward movement of the African plate with respect to the Aegean and Anatolian microplates, resulting on the one hand in transpression along the Pliny trench and the extension of this transform boundary into southwestern Turkey and, on the other hand, in the compression of the Mediterranean Ridge against the Florence Rise (3).

In order to determine the origin of the Anaximander Mountains and the current neotectonic deformations, three marine geophysical expeditions were carried out in the region within the framework of UNESCO/TREDMAR "Training-Through-Research (TTR)" program and the ANAXIPROBE Project during 1991, 1995 and 1996.

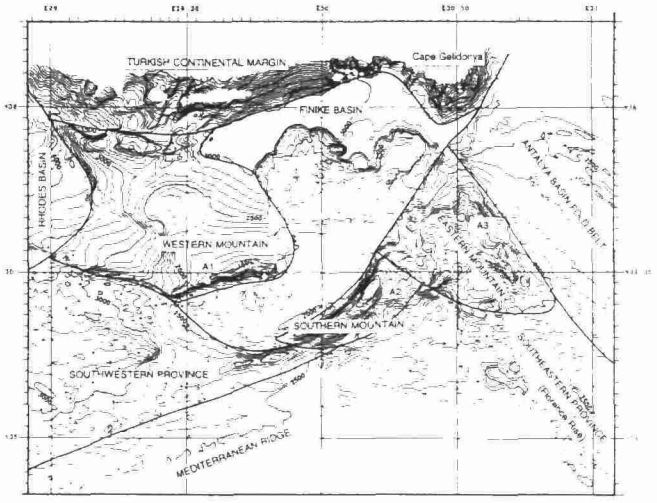

Fig.1: Bathymetry of the Anaximander Mountains and the different geographical regions (1).

The gravity measurements during the ANAXIPROBE Project cruise of 1995, were made by the gyro-stabilised marine gravimeter KSS 30 designed by Bodenseework Geosystem which has three main subsystems : (I) GSS 30 gravity sensor subsystem; (ii) KT 30 stabilisation subsystem; (iii) data handling subsystem. All the necessary corrections were operated on the raw data in the office of IFREMER in Brest in the same way as for the magnetic data. The magnetic data were collected by a M-244 Recording Proton Precession Magnetometer from Barringer. The sensitiviy of the magnetometer was 0.1 nT and towed 250-300 m behind the ship.

Results and discussion

Multibeam bathymetric data indicate five different morphological provinces in the Anaximander Mountains area, which are as follows : (i) the steep margin of southern Turkey with canyons, slumps, and cross-slope faulting; (ii) the consistent western mountain with a relative flat but northward dipping northern slope and steep southern escarpment; (iii) the relatively flat areas of the Finike Basin and the region between the western and the southern mountains; (iv) the rough and irregular eastern mountains; and (v) the irregular low relief of the region southwest of the mountains. A large tongue of sediment seems to extend over the Finike basin between the western and southern mountains. The impression is that the southern mountain is being pushed northward and squeezing the sediments lying between it and the western mountain outward to the north. The northern edge of the tongue of sediments has almost semicircular lobes with, in some cases there are spots of high reflectivity near their centres. Differential tectonic movements are thought to be responsible for both the elevations of the Anaximander Mountains and for the subsidence of the Finike and Antalya basins to the north and northeast of the Anaximander Mountains, respectively (2). Both the Antalya and Finike basins appear to have been tilted northeast and northwest, respectively, effects which seem to be connected with the development of the Hellenic Arc in the case of the Finike basin and with the development of the Cyprus Arc in the case of the Antalya basin.

Gravity results (free-air and Bouguer gravity anomaly maps are given by Figs. 2 and 3) indicate that there is a major crustal disconti-

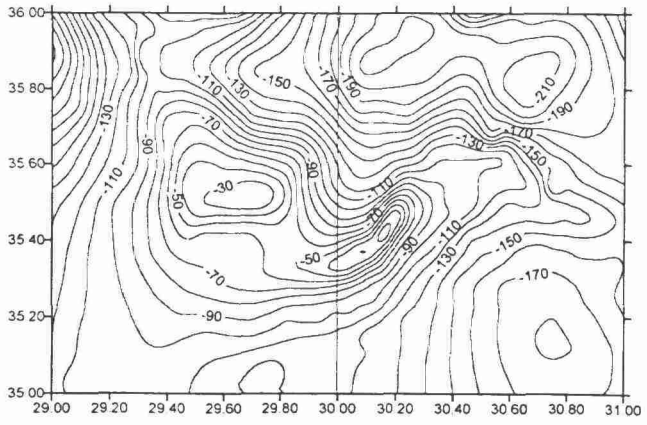

Fig.2: Free-air gravity anomaly maps of the Anaximander Mountains.

SHORT PERIOD VARIABILITY OF THE CLAY MINERAL SUSPENDED SUPPLY OF A MICROTIDAL ALGERIAN ESTUARY.

Henri Pauc
L.S.G.M., URA715, University of Perpignan, France

Abstract
The variability of the clay mineral supply at the mouth of a small microtidal Algerian estuary is studied from time series of repeated annual cycles. The annual cycle of the Mazafran river was divided into six dynamic stages which govern the variability of the mineral content of the suspended material. The coarse minerals such as illite or quartz and/or dense as calcite are more present during the strongest dynamic phases (floods). The small minerals as smectite overfloat in the suspension during low dynamic phases, whereas the large ones settle rapidly. Kaolinite follows the decreasing hydrodynamics. This pattern could be applied to other small Mediterranean rivers.

Key-words : Algerian basin, estuaries, river input, mineralogy

Introduction

The Mazafran river estuary lies thirty kilometers west of Algiers (Algeria). It flows on the North-Algerian margin into the western Mediterranean Sea. During an annual hydrological cycle, the clay mineral content varies largely in the estuary of the Mazafran river although its drainage basin is of a small size (about 1850 km^2). The riverine dynamics of the Mazafran river is highly influenced by the semi-arid characteristic of the Mediterranean climate of its drainage basin. Due to its microtidal environment a salt wedge appears at the beginning of the low waters and disappears with the first flood (1).

The strategy of the present work is a weekly sampling of the suspended material carried out during several years at the river mouth. River dynamics was studied and the nature and quantity of its suspended supply were examined to understand the variability of the clay mineral composition in a microtidal Mediterranean estuary.

The phases of the annual cycle of the Mazafran river

The annual cycle has two seasons : the flood season, typically from November-December to March-April, and the low water season from spring to autumn. Their respective duration is highly variable from one year to the other (2).

The dynamic phases of the annual cycle of the Mazafran river were defined by the suspended matter characteristics (concentration, particulate organic carbon percent -POC%-, microflora) and related to the mean daily freshwater discharge. The flow phases have been divided into five stages numbered from I to V (fig. 1). During the rising flood (stage I), suspended matter concentration increases drastically from $mg.l^{-1}$ to several $g.l^{-1}$. Its organic content (POC%) lowers strongly from low waters values (>10%) to a few percent. The flood peak (stage II) is the most dynamic period : suspended matter concentration is the highest (to 25 $g.l^{-1}$ in the Mazafran river waters), and the POC% is the lowest (0.4%). When flood lowers (stage III), the discharge and the suspended load decrease respectively to <10 $m^3.s^{-1}$ and about 500 $mg.l^{-1}$. At the same time POC% increases quickly to 10%. An interflood stage (stage IV) occurs sometimes between the peaks of repeating floods. The interflood dynamics is rather high in spite of the low discharge and low suspended load (10 $mg.l^{-1}$). The organic content is relatively high (POC%>10%). Small floods (stage V) take place either during spring (May to June) or during autumn (October to December). Though discharge increases weakly (1 or 2 to 10 $m^3.s^{-1}$), its environmental impact is important, especially in autumn, because nutrients are supplied. The suspended load increases weakly (to 100 $mg.l^{-1}$) and POC% varies largely. It decreases from more than 30% to a few % at the peak of the flood and comes back to 20% a few days later.

During low waters, five others stages were defined (fig. 2) : the beginning of low waters (stage VI), summer low waters (June and July, stage VII), the long low waters stage in autumn (stage VIII), the optional very long low waters stage which can last to winter (IX), and at least the end of low waters (X). The transitory phase of low waters building (state XI) is always well marked. During these periods, the freshwater discharge is about zero, the particulate load is very low and its content is mainly biogenic and organic.

During the low water phases, the suspended matter has a low content in minerals because the particulate transport is not competent enough. Hence, clay mineral analysis is possible only during the rising (I), peak (II) and lowering (III) of flood, interflood (IV), small floods (V) and a set of indiscriminate low waters stages (VI).

Clay mineral content and its variability

During the annual cycle, the mineral content vary widely over short periods of time. Each dynamic phase is characterized by the mean values of mineral fractions.

Figure 3 shows the variations of the global mineral composition, expressed by the relative percent of total clay, calcite, quartz and other minerals characterized by diffractometry. The highest percentage of clays is observed during the stages of small floods (74%) and during the peaks of floods (69%). The lowest one is found during low waters (49%) which has to be explained. The amount of detritic minerals (sum of quartz and feldspars versus clay materials and calcite) follows an opposite variation with a minimum during floods (20%) and small floods (21%) and a maximum during low waters (41%). The quartz percentage of the detritic minerals is always high. It has two maxima during high (98%) and small floods (94%) and a low minimum during low waters (75%). Calcite presents two maxima, the first one at flood peak (9%) and the second other during low waters (9%) and it is minimum during small floods (3.5%).

Figure 4 shows the nature and the variability of the clay mineral content. Illite is often dominant and always high (about 34%). It is maximum during small floods (58%) and minimum during the rising flood stage (27%). Kaolinite is well represented during rising and flood peak (31%) and then decreases regularly during the others less dynamic stages to 14% only during low waters. Chlorite is more concentrated by low waters (22%) and also during flood rising (19%) but less during peak and small floods (12%). Smectite is well repre-

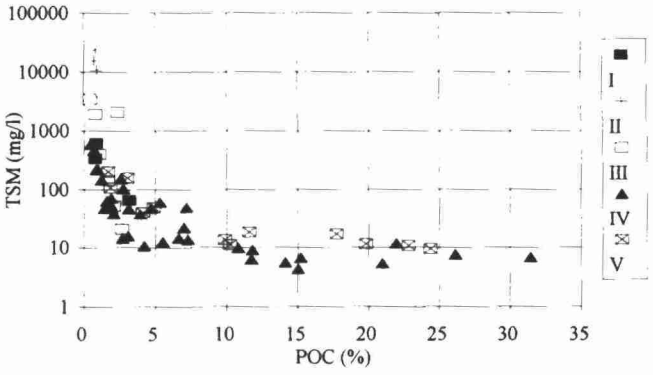

Figure 1 : suspended material characteristics during the various stages of the annual cycle in the Mazafran river estuary : flowing stages. (stages I to V, see text).

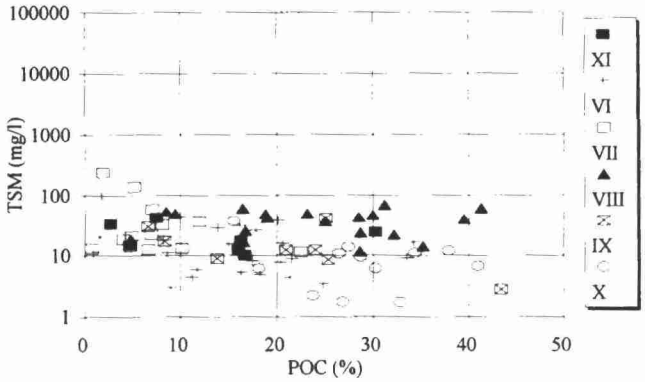

Figure 2 : suspended material characteristics during the various stages of the annual cycle in the Mazafran river estuary : low waters stages. (stages VI to XI, see text).

SEDIMENTARY PROCESSES CONTROLLED BY THE MEDITERRANEAN OUTFLOW AND ATLANTIC INFLOW CURRENTS IN THE GULF OF CADIZ CONTINENTAL MARGIN

Rodero J. [1], Maldonado A. [1]*, Nelson C.H. [2] and Lobo, F. [3]

[1] Instituto Andaluz de Ciencias de la Tierra, C.S.I.C./Univ. Granada, 18071 Granada, Spain
[2] U.S. Geological Survey, Menlo Park, CA 94025, USA
[3] Facultad de Ciencias del Mar, Univ. Cádiz. 11510 Cádiz, Spain

Abstract

The Late Quaternary pattern of sedimentary facies on the Spanish Gulf of Cadiz continental shelf results from an interaction between a number of controlling factors that are dominated by the Atlantic inflow currents flowing southeastward across the Cadiz shelf toward the Strait of Gibraltar. This currents generate depositional processes which develop large prodeltaic bodies prograding southeasternwards. The slope processes, in contrast, are dominated by the Mediterranean outflow flowing under 300 m northwesternwards. Variations in the current speed gives way to the existence of different sedimentary processes on the continental slope. The southeastmost region is characterized by erosive processes as a consequence of an increased current speed northwards. The depositional processes generate, however, large contourite sediment bodies in the areas protected of the current by the diapiric ridges. These depositional processes take place in the southern region of the Gulf of Cadiz.

Key-words : sedimentation, Strait of Gibraltar

Introduction

Recent studies have demostrated that echograms recorded on high-frequency precision provide a valuable tool for the study of near-bottom sedimentation processes in the Gulf of Cadiz continental margin (1; 2; 3). However, these studies are orientated toward a study of the continental shelf or continental slope as a independent sedimentary environments. This paper focuses on the Atlantic surface water effects on the entire Spanish continental shelf and integrates new data with the Mediterranean outflow effects on the Spanish continental slope area in the southeastern Gulf of Cadiz.

Methods

A total of 3.400 km of tracklines of high-resolution 3.5 kHz, Geopulse, and single channel 20-40 cu. in. airguns seismics profiles, taken in the GC-86-1 and G-86-1 seismic surveys, have been analyzed (fig. 1) (4; 5). In addition, 700 subbottom including dredges, rock cores and gravity cores were taken from the Gulf of Cadiz continental shelf and slope, at water depth ranging from 15 to 959 m. Grain-size analyses were conducted with the SEDIGRAPH 5000D (<63 microns), and by sieving (>63 microns). The sand fraction composition was studied with the binocular microscope.

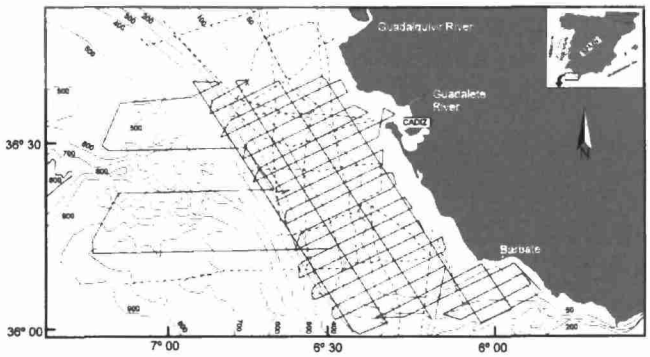

1.- Area of study and simplified bathymetry. Map showing 3.5 Khz, Geopulse and single-channel airgun tracklines. Continuous line: G-86-1; Dashed line: GC-86-1.

Oceanographic setting

The Gulf of Cadiz is located west of Strait of Gibraltar forming a reentrant of the eastern Atlantic Ocean (fig.1). Above 300 m water depth there is a strong southeastward inflow of North Atlantic Surficial Water (NASW- hereafter called Atlantic inflow) that intensifies toward the Strait of Gibraltar (6; 7). Atlantic surface current flows eastward to southeastward over the Gulf of Cadiz continental shelf (fig.2). Extensive sand dune fields across the entire southeastern end of the shelf indicate that current speeds accelerate significantly toward Strait of Gibraltar (8). Between 300-1200 m water depth there is a significant development of bottom-current deposits with bedforms because the deep Mediterranean Outflow Water (MOW-hereafter called Mediterranean outflow) shears northwestward from Gibraltar along the Cadiz continental slope as the Mediterranean undercurrent (9; 10). Because of density differences with respect to the surrounding Atlantic water, the warm and dense (>12° C; salinity (36.2%) Mediterranean

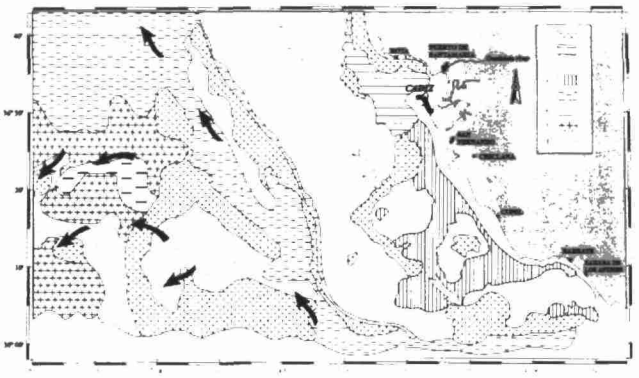

2.- Maps with the distribution of the currents and sedimentary proceses in the Gulf of Cadiz, showing the Atlantic inflow current (white arrows) and the Mediterranean outflow (black arrows) modified from (10, 7). Sedimentary processes: 1, erosive; 2, litoral; 3, fluvio-deltaic; 4, Atlantic inflow processes; 5, slope depositional processes; 6, gravitatory; 7, mixed processes; 8, Mediterranean outflow processes.

outflow progressively sinks as it flows northwestward at varying depths between 300 and 1800 m as an independent stream, the geostrophic Mediterranean undercurrent (fig.2)(7; 11). The Mediterranean undercurrent maintains contact with the seafloor up to 1000 m water depth on the eastern region of the Gulf of Cadiz and approximately to 1400 m depth on the western side of our study area (10; 12).

Maximum undercurrent speeds are 80 cm/s in the eastern part of our study area (10; 7) but decrease to 75-40 cm/s on the central slope (13). Current ribbons splay southwestward through the valleys producing faster channelized bottom-current flows downslope that average 80 cm/s in a region where the contour-parallel currents of the Mediterranean outflow average only 40 cm/s (13; 14). Along the western Cadiz slope, current speed decreases to 10-20 cm/s and speed in channels declines to 25 cm/s (15). Current speeds at the southern fringes are considerably slower than inmediately upslope because the Mediterranean outflow has higher speed cores there (7). Previous studies recognize the variability of current speed east to west, upslope to downslope and valley to intervalley areas in the patterns of bedforms observed on the Cadiz continental slope (4; 10; 11).

Distribution of sedimentary processes

Previous studies show the existence of three main sectors in the study area of the Gulf of Cadiz. The southwestern sector contains dune field and outcrops of acoustic basement (8). Recent deposits of the northwestern area is characterized by the existence of an extensive prodeltaic body developed from the Guadalquivir river. Between these regions there is a transition zone with intermediate characterics (5).

A series of sedimentary processes have been established for each physiographic region of the continental margin (fig. 3). The shelf is dominated in the northern area by fluvio-deltaic depositional processes, affected by the Atlantic mass water crossing the shelf northwest-southeastwards. Large prograding bodies are developed by terrigenous fine-grained materials derived from river inflow in the Gulf of

GEOCHEMICAL CHARACTERIZATION OF HG-CONTAMINATED SEDIMENTS OF THE "PIALASSA BAIONA" (RAVENNA LAGOON, ITALY)

Francesca Sangiorgi *, Rosita Setti, Giovanni Gabbianelli & Claudio Trombini

Corso di Laurea in Scienze Ambientali, University of Bologna, Via Tombesi Dall'Ova 55, 48100 Ravenna, Italy

Abstract

The "Pialassa Baiona" is a transitional, heavily mercury polluted area connected to the Ravenna harbour and the North Adriatic Sea (Italy). The aim of this work has been to characterize sediments collected in the southern part of the area, called Chiaro del Pontazzo, from a geochemical point of view to understand which of the detected parameters (organic matter, S, particle-size) is mainly related to mercury. For this purpose, sediment cores, nepheloid layer samples and surficial sediments have been collected and analized. Benthic nepheloid layer (a fine-grained, thin, surface sediment layer) seems to be able to bind high quantity of contaminants.

Key-words : Interfaces, lagoons, mercury, sediments, Adriatic Sea

Introduction

The origin of the Ravenna lagoon goes back to the first decades of 18th century, due to sandy bars deposition by long-shore currents. Up to 60's, an internal, artificial, dendritic channels system acted to avoid harbour landfill. After this period, the area lost its function and sea sedimentary contribution became nearly void.

At present, the "Pialassa Baiona" is a brackish marsh placed in the north-eastern part of Ravenna (Italy); it consists of small, shallow ponds and deeper artificial channels connected to the North Adriatic Sea through the Candiano Channel (Ravenna harbour). This area also receives fresh waters from inland through some drainage channels (Fig.1).

Generally, inside ponds, there is a 30-100 cm pelitic material layer, over sandy sediments (1), whose deposition is promoted by an almost complete water standstill (both in flood and in ebb tide) (2).

During the period 1957-1977 high quantities of mercury (about 100-200 t) were carried in this area coming from an industrial discharge channel (Via Cupa) which inflows in the southern part of the lagoon. For this reason our research is focused on sediments collected in the southern pond (Chiaro del Pontazzo) which are particularly mercury polluted (3, 4, 5).

Previous investigations (4, 6, 7, 8) found high levels of mercury (up to160 µg/g, dry weight) in surface sediments even if a burial of the toxic element had been supposed on the basis of a crude estimation of sediment accumulation rate (on average about 2.6 cm/y).

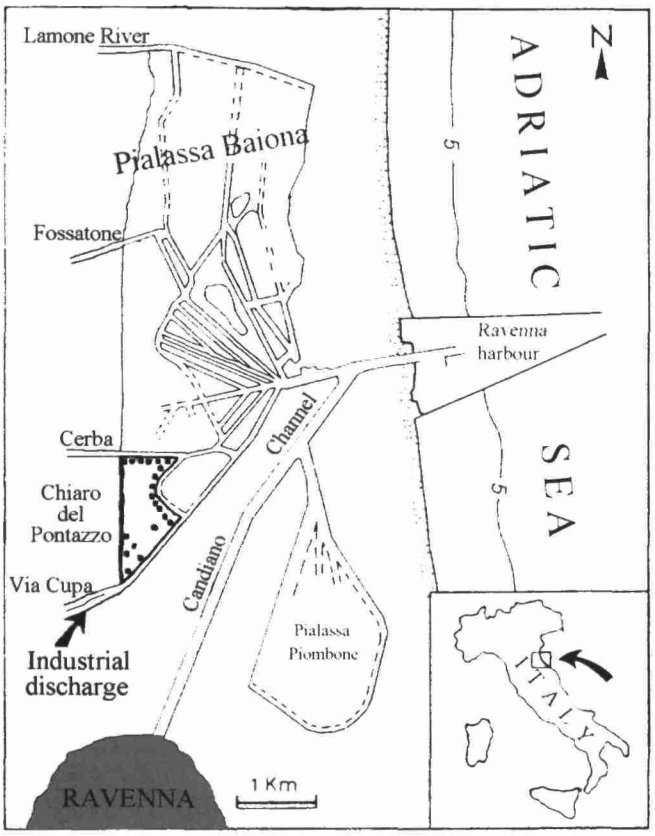

Fig. 1 - Ravenna lagoons. Study area and location of samples.

Results

For this research we collected 21 sediment cores, 9 surficial sediments and, in particular, 16 benthic nepheloid layer samples (Fig.1). The latter are very important due to the scarcity of studies concerning this particular layer.

Nepheloid layer is a muddy, generally thin (few mm) and easily movable layer placed under water column, close to sediment-water interface. It is a reactive zone crossed by both vertical and horizontal fluxes before entering sediment reserve (9).

Total mercury concentration (10) in nepheloid layers ranges from 1.96 to 40.28 µg/g (d.w. sediment); nevertheless, only 6 of 16 samples have Hg values lower than 10 µg/g (d.w.). It can be pointed out that the unique sandy sample shows the lowest mercury concentration. Other nepheloid layer samples have a pelitic lithology and higher Hg values.

A concentration of methylmercury (11), which is the most bio-available and dangerous kind of Hg for food webs, was also detected in 5 nepheloid layer samples. All samples show methylmercury concentrations lower than method detection limit (0.005 µg/g).

A comparison between total mercury concentration in nepheloid layers and in their corresponding surficial sediment samples (2-3 cm deep) (Fig. 2) shows that in 4 of 9 cases mercury values are much higher in nepheloid layers than in surficial sediments. In other 3 samples mercury concentration is always higher in nepheloid layers, but the difference between the two kinds of sediment is not so stressed.

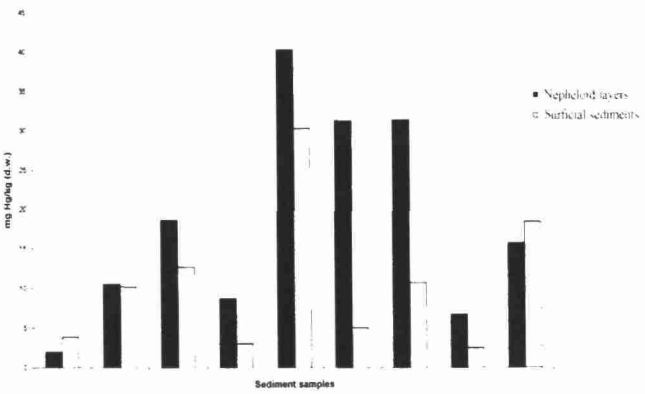

Fig. 2 - Mercury concentration (µg/g, d.w.) in nepheloid layers and in their corresponding surficial sediment samples.

The 21 sediment cores were also analized for a qualitative lithology. This study shows that, along Chiaro del Pontazzo northern boundary, cores have a sandy surficial layer (30-80 cm thick) which is indicative of a probable decortication due to frequent anthropic actions. In the eastern side of the area surficial core sediments are fine-grained with aboundant organic matter.

9 sediment cores were analized for total mercury, methylmercury, organic matter and sulphur (10). Total mercury concentration results (Fig. 3) show that high quantity of this toxic element are concentrated in the first 30-40 cm; in particular, one core, at a depth of 5-10 cm, shows a mercury concentration of 95.63 µg/g (d.w.).

GEOLOGICAL STRUCTURE AND BOTTOM SEDIMENTS OF THE SEAMOUNTS IN THE TYRRHENIAN SEA

K.M. Shimkus [1]*, E.M. Emelyanov [2], V.S. Yastrebov [3]

[1] Southern Branch P.P.Shirshov Institute of Oceanology, Golubaya buchta, 353470 Gelendzhik, Russia
[2] Atlantic Branch P.P.Shirshov Institute of Oceanology, str.Myra 1, 236000 Kaliningrad, Russia
[3] P.P.Shirshov Institute of Oceanology, str. Krasikova 23, 117218 Moscow, Russia

Abstract

Geological structure and recent evolution of tectonically different types of seamount spreaded in the Tyrrhenian basin discussed on the data of complex geological-geophysical investigations conducted by some Russian expeditions. Modern and Late Quaternary sedimentation on the seamounts including ore formation as a result of hydrothermal activity are also described.

Key-words: metals, stratigraphy, tectonics, sediments, Tyrrhenian Sea

Introduction

The structure and geological evolution of the submarine mounts in the Tyrrhenian Sea is fraught with many uncertainties till now although they have been studied almost half a century [1-5]. In the course of the 7th and 12th cruises of the r/v *Vityaz* (1984,1986), the 4th and 10th cruises of the r/v *Rift* (1984, 1988) and 16 th cruise of r/v *Akademik Mstislav Keldysh* (1988), an underwater geological survey of five seamounts (Verchelli, Baroni, Magnaghi, Marsili, Vavilov) was carried out with the help of inhabited submersible apparatus, such as "Argus", "Mir-1", "Mir-2" and towed submerged apparatus. Visual observation, continous video- and sidescan survey, undersea photography, sampling with the help of manipulator and small drilling sets installed on the submersibles were done. The mount tops and near-top areas but also the slopes down the base (Magnaghi, Vavilov), *i.e.* down the depth of 3300 m (Fig. 1) were investigated. Samples of bottom sediments and rocks were thoroughly studied in the laboratory. Data on composition and stratigraphy of bottom deposits and on petrography of bedrocks were obtained.

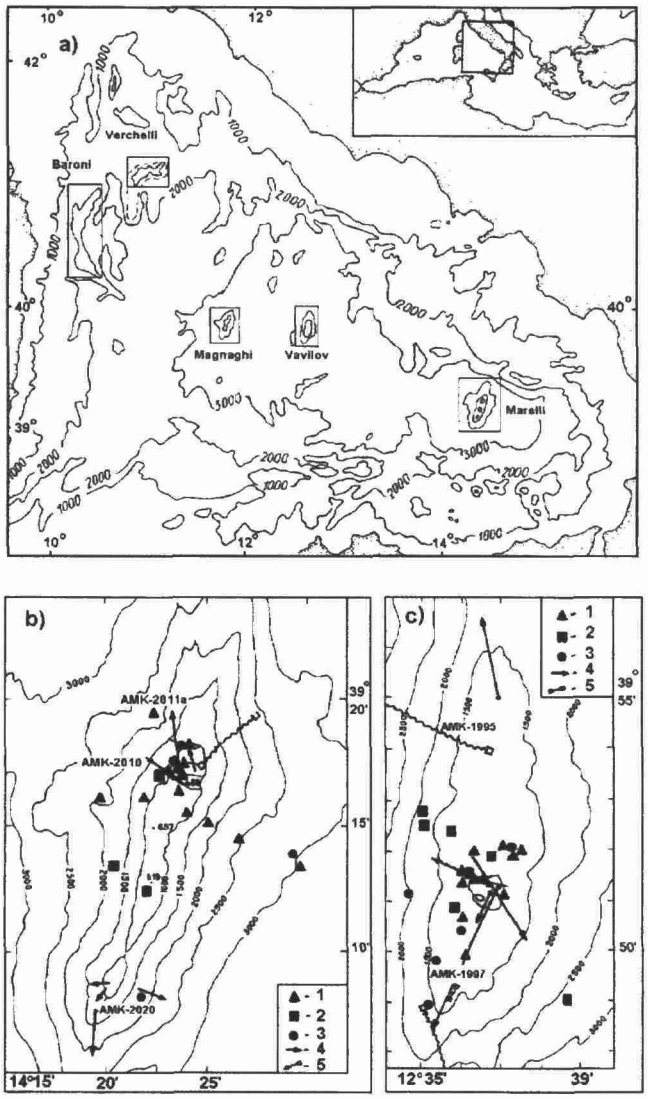

Fig. 1 : Geological studies of the seamounts in the Tyrrhenian Sea a) polygons, b) smt. Marsali, c) smt. Vavilov. 1 - grab sampling, 2 - dredging, 3 - gravity coring, 4 - route of towed submersible aparatus, 5 - route of manned submersibles "Mir-1" and "Mir-2".

Mount structure and their recent evolution

Baroni and Verchelli mounts are tectonically elevated horst type blocks made of a basement with continental crust rocks, stretched in submeridional direction. Their slopes are complicated by numerous faults and tectonic steps.

The lower part of the Verchelli mount consists of Palaeozoic metamorphic rocks. They are intruded by a granite batholith which composes the middle part of the mount and its domed top. The batholith is complicated by intrusions of pegmatite-aplites of Tortonian age. Most probably, a deep denudation of them occured in subaerial conditions, beginning from the time of Messinian regression. In Pliocene-Quaternary this island underwent an irregular sinking which was marked by several belts of corals and series of bench-like steps on the mount slopes [6]. Ancient coastlines are marked by surf wave niches in rock granite outcrops. The central part of the Baroni mount's is formed by an ophiolite rock complex, outcropping on land in the Ligurian Alps [4]. Outcrops of olivine basalts were found in the mount centre, and on the Quirra mount, located to the south. Dark rock outcrops are widely spread on the mount slopes (depth is 232 and 446-458 m). Cores drilled out in one outcrop by submersible "Argus" brought breccias and conglomerates made of olivine basalts clasts. Submarine volcanoes (Magnaghi, Vavilov, Marsili) are situated on the submeridional fractures which cross the basaltic basement of the deep Tyrrhenian basin. Their cones were built up by basaltic lava flows in several stages preceeded by repeated rupturing of volcanic structures by submeridional faulting. Faults can be traced by the presence of steps and benches on seamount slopes and tops. Morphologically they resemble as "swallow tail" (Fig. 1b c). These areas are the most barest ones. Just here numerous pillow and tubular lava covers were found, that allow to trace zones with the largest volcanic activity. The top area of the Magnaghi mount is covered mainly with loose sediments and does not show tectonic activity.

The top area of the Vavilov mount is more bare of sediments. Near the southern top only a small volcanic cone resembling "hayrick" and made of tubular lavas was found. Crater-like holes composed by pillow and tubular lavas were also found. They are slightly powdered with sediments. Most parts of the Vavilov mount are covered with Late Quaternary sediments, separate lumps or lava flows outcrop ping under them. All this testifies to the damping of volcanic activity in Late Quaternary period. Lithified foraminifera-coccolithic muds of Early-Quaternary age covering lavas in the lower part of the Vavilov mount slope (Fig. 2b) indicate that formation of

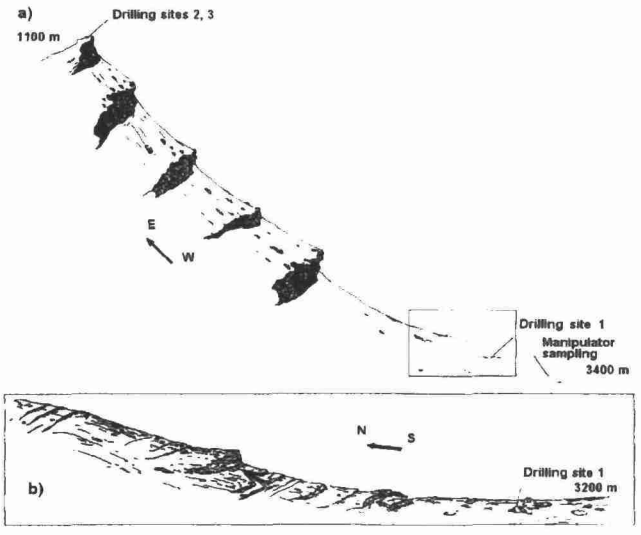

Fig. 2 : Outcrops of basaltic lava flows along recent faults heading N-E (a) and that ones of Early Quaternary marlstones (b), on the western slope of the Vavilov mount - geological sketch compiled on visual observations during dive of manned submersible "Mir-1" (route AMK-1995, depth is 1100-3400 m).

CENTENNIAL EVOLUTION OF A RECURVED SPIT : A CASE STUDY FROM THE SPIT OF THE GORO LAGOON, PO DELTA (ITALY)

U. Simeoni [1], P. Ciavola [1], G. Fontolan [2]*, E. Mazzini [1] & U. Tessari [1]

[1] Dipartimento di Scienze Geologiche e Paleontologiche, Università di Ferrara Corso E. I d'Este 32, 44100, Ferrara, Italy
[2] Dipartimento di Scienze Geologiche, Ambientali e Marine, Università di Trieste Via E. Weiss 2, 34127, Trieste, Italy

Abstract

The evolution of the Scanno di Goro, a spit delimiting the Goro Lagoon in the southern Po Delta, during the last 100 years is described. The main evolutionary phases and mechanisms were identified by comparing historical maps, aerial photography and field mapping. The study found out that in the last 50 years the spit grew in length despite the sedimentary deficit that affected the nearby Po di Goro. It is forecasted that this process will continue in the future.

Key-words : Shoreline evolution, geomorphology, coastal processes, Po Delta

Introduction

The Goro Lagoon is part of the Po Delta and its historical evolution is strictly connected with the development of the main delta complex. The Po River has an average yearly water discharge of 1441 m^3/sec (calculated over the period 1980-1992) and in its delta areas is branched into five main channels (Fig. 1): Po di Maistra, Po di Pila, Po di Tolle, Po di Gnocca and Po di Goro. The Goro Lagoon is found southwards of this last river branch.

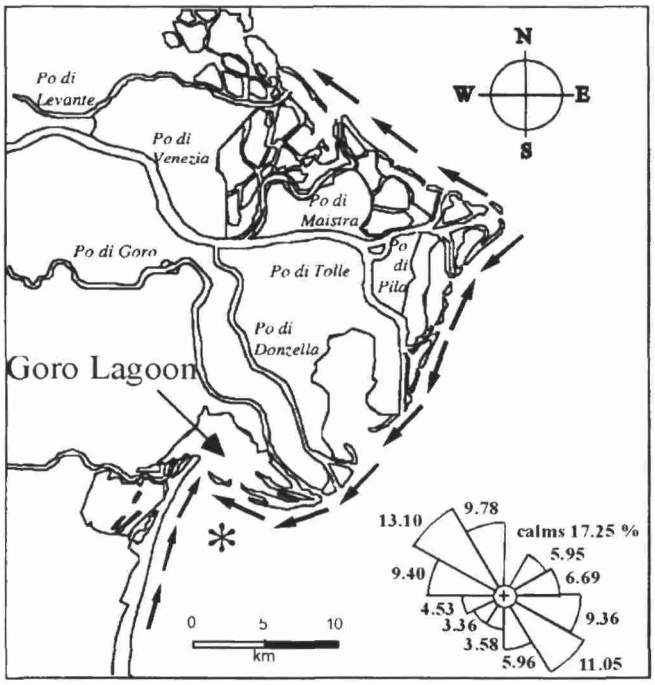

Fig. 1. Index map of the Po Delta, directional distributions of waves (referred to the point marked by the asterisk) and patterns of longshore drift.

Studies on the development of the delta found that historical reconstructions are difficult because of the variable quality of data and due to the dynamic environment together with man-made effects. Cartographic sources and previous studies indicate a continuos growth of the delta plain until the 1940s that was followed by an erosive trend [1, 2] triggered by a reduction in the sediment load of the Po River, caused by man activities such as engineering works and quarrying of river beds [3, 4]. The consequence of these events is that the delta is now controlled by wave action [5] and not by river discharge as indicated previously [6, 7].

Evolution of the Goro Lagoon

The lagoon covers a surface of 2000 hectares, it has an average depth of about one metre and a maximum tidal range of 120 cm is observed during the largest spring tides. Its geomorphology is complex, since the present landscape results from the overlapping between morphologies of medieval age and more recent ones, particularly the man-made interventions of the last fifty years. The area is affected by natural subsidence, exacerbated by anthropogenic activities. The rate of downward ground movement is considerable: recent studies [8] calculated a rate of 1.63-3.61 cm/year for the period 1984-1993.

Due to the sheltering effect of the delta itself (Fig. 1), the coastline is exposed to waves coming from a direction between 60°N and 120°N (75% of occurrences) with small heights (68% of occurrences have an height smaller than 0.5 m). Longshore drift is mainly controlled by the predominance of waves with a direction between E and SE.

Sedimentary inputs are provided mainly by the load of the Po di Goro and to a smaller extent by the other river branches southward of the Po di Pila. The lagoon has acted as a natural sediment sink throughout the present century, even in the period of sedimentary crisis of the Po (1960s-1980s), presenting a net positive sediment budget. Between 1984 and 1993 about 8 x 10^6 m^3 of sediment have been deposited on the sea bed in front of the Goro Spit (area marked by the asterisk in fig. 1). Estimates of net longshore drift along the spit [8] indicate a progressive decrease from the mouth of the Po di Goro towards the lagoon's inlet: transport varies from 120 x 10^3 m^3/year at the river mouth to 46 x 10^3 m^3/year at the spit's end. Estimates of northward drift along the coast at the southern boarder of the Sacca are between 27 and 30 x 10^3 m^3/year.

Evolution of the Goro spit

The spit has always been an element of control on the physical, biological and sedimentary environments of the lagoon. Cartographic sources prove that the spit formed between the end of the 19th century and the beginning of the present one (Fig. 2). Until the 1930s a group of spits and linear islands was stretching from the Po di Goro towards the NW for about 3.5 km, at a position further inland than the present one. A series of small islands was present at the spit's end (Fig. 3), producing a system with a total length of about 6 km. On the inner side of the system a large sandy island, 2.5 km in length and 200 m wide, was present. Part of this system is still visible at the present time in the eastern part of the lagoon, despite having been reduced in extension because submerged due to the subsidence and/or eroded.

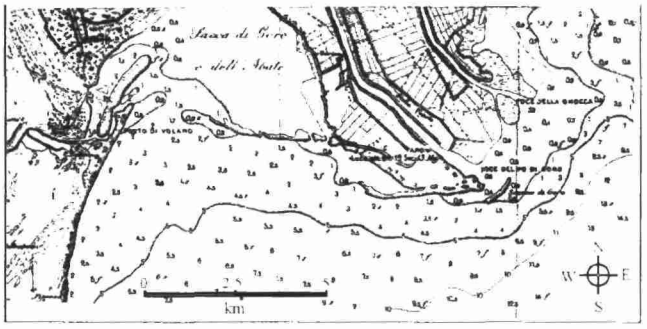

Fig. 2. Hydrographic chart of 1905.

The spit in its present configuration starts to take shape in the 1940s, whilst the old one was eroded and submerged, developing in a W-NW direction and rotating anticlockwise with reference to the previous one. In 1950 the spit was already 5 km long, growing other 1.7 km in the following 14 years, but between 1964 and 1971 its growth stopped and it became 500 m shorter (Fig. 3). In the 1970s there is a new phase of accretion and by 1977 the peninsula is already 7.8 km long.

It is interesting to notice that in the period 1954-1977 the mouth of the Po di Goro started to be eroded, due to a decrease in river sand input, despite the fact that the spit grows for 3 km, hinting that for many years the main input for the spit's sediment budget came from

COMPOSITION OF HYDROCARBON GASES, ORGANIC MATTER, AND AUTHIGENIC MINERALS FROM SEABED SEDIMENTS, UNITED NATIONS RISE, EASTERN MEDITERRANEAN RIDGE

Alina Stadnitskaia* and Irina Belenkaia

UNESCO/MSU Centre for Marine Geosciences, Faculty of Geology, Moscow State University, Vorobjevy Gory, 119899, Moscow, Russia

Abstract

The United Nations Rise is the newly discovered in the Eastern Mediterranean Ridge area of mud volcanism and gas venting. Two recent and several dormant mud volcanoes were found within the Rise [1]. This paper presents the geochemical study results which outline general regularities in distribution of hydrocarbon gas and organic matter (OM), and also determine their role in autigenic mineral assemblage forming. The detailed study of the cores taken from fault zone and mud volcanoes allowed for revealing the connection of hydrocarbon gas and OM with inflow from deep sources. Abundance of high-Mg calcite and dolomite in all these cores is also evident for that.

Key-words : mud volcanoes, geochemistry, Mediterranean Ridge

Introduction

This work is based on the materials obtained in 1995 on 5th UNESCO-IOC Training-Through-Research Cruise of R/V *Professor Logachev*. During this cruise, a large new area of mud volcanism and gas venting was discovered and named the United Nations Rise. Two recent mud volcanoes (Dublin and Stoke-on-Trent) were found at the southern boundary of the Rise (southern boundary of the Deformation Front), and several dormant mud volcanoes were observed onward the Deformation Front [1]. During the cruise, a comprehensive geological and geophysical investigation was carried out. It included single channel seismic profiling, swath survey with a long-range and a deep-towed sidescan sonars, as well as bottom sampling with gravity corers and a TV-controlled grab-sampler. A system of underwater navigation for the precise positioning of the outboard devices was in use. The ship navigation was fulfilled with the GPS NAVSTAR and an underwater navigation was based on the Sigma-1001 hydroacoustic system [2].

Methods

The routine analysis of the gas phase in sediments was executed on the ship board (176 samples from 20 cores). The standard methods of sampling, degassing of sampled sediments and chromatographic analysis were applied. The degassing was accomplished according to the Head-space analysis [2]. Afterwards, the collected samples were studied in Moscow State University, in Shirshov Institute of Oceanology, and in Mendeleev Institute of Geochemistry and Analytic Chemistry, Russian Academia of Science. Bottom sediments were investigated by the following set of methods: fluorescent analysis (107 samples from 10 cores); determination of total organic carbon (TOC) content (86 samples from 10 cores); solvent extraction by chloroform (36 samples from 6 cores); gas-liquid chromatography (15 samples from 5 cores); isotopic analysis $\delta^{13}C(CH_4)$ (2 samples from 2 cores) [3]; microscopic study in thin sections of the authigenic minerals (23 samples from 13 cores); powder test by X-ray method with Co-target in the limited interval of the Bragg angles (25.04Θ-55.04Θ) (23 samples from 13 cores); isotopic analysis of $\delta^{13}C(CaCO_3)$ and $\delta^{18}O(CaCO_3)$ on the Varian-MAT-230 (4 samples from 3 cores).

Results and discussion

The results of the complex geochemical analyses allowed for choosing 4 most representative cores taken from zones of different environments: Core 166G located far from gas seeps and recovered normal undisturbed pelagic sediments (was used as a reference); Core 169G located close to a fault observed on the long-range sonograph; Cores 172G and 178 G taken from the Dublin and Stoke-on-Trent mud volcanoes [2] (fig. 1).

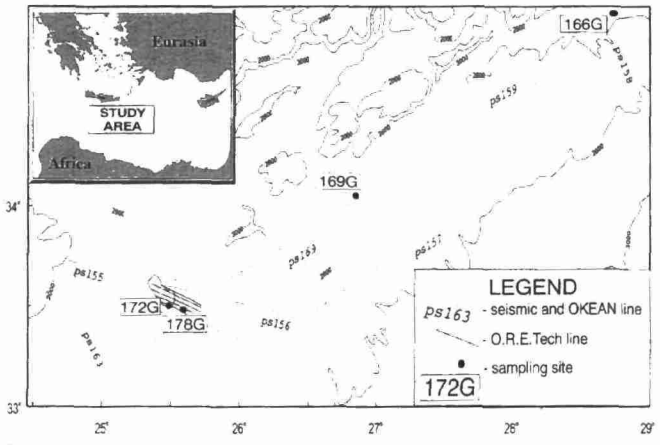

Fig.1 : Location map

Gas measurements show that the reference core generally has a very low level of gas concentrations ($0.1x10^{-4}$ - $38x10^{-4}$ ml/l) [3]. TOC content in the core varies from 0.04% till 6.06%. The main peaks of hydrocarbon gases and TOC associate with sapropel layers S1 and S5, which might be caused by good sorption capacity and higher content of organic matter (OM) normal for sapropels. Methane and TOC contents relates to each other and are almost completely controlled by lithology (fig. 2). Thus, taking into account the process of anaerobic destruction of OM in sediments, which results in methane formation, one may assume that methane there has been formed *in situ*. The extractable organic matter (EOM) composition shows that the EOM from the reference core is immature, with predominance of matter of marine genesis, partially biodegraded. The observed predominance of wax and asphaltenes among the bitumoids is also normal for recent sediments. In opposite, cores taken from the active zones are characterized by higher concentrations of hydrocarbon gases and unusual composition of EOM.

In Core 169G (fault zone), concentrations of hydrocarbon gases are 10000 times higher then in Core 166G (fig. 3). The methane concentrations increase with the depth up to 4 ml/l at 4 m, while saturated hydrocarbons predominate over those unsaturated and iC_4 predominates over nC_4. Core 178G (Stok-on-Trent mud volcano) is characterized by methane concentrations of $11.4x10^{-4}$ - $217x10^{-4}$ ml/l, with significant content of its homologues and almost complete absence of unsaturated hydrocarbon gases (fig. 4). Isotopic composition of methane δ13C from this core is about -55‰. The composition of hydrocarbon gases is similar to that for gas from the fault zone (169G) [3]. All this might indicate mixed nature of methane from the Stoke-on-Trent mud volcano (178G). In Core 172G (Dublin mud volcano), concentrations of methane vary from $7.7x10^{-4}$ ml/l to $10x10^{-4}$ ml/l increasing with the depth.

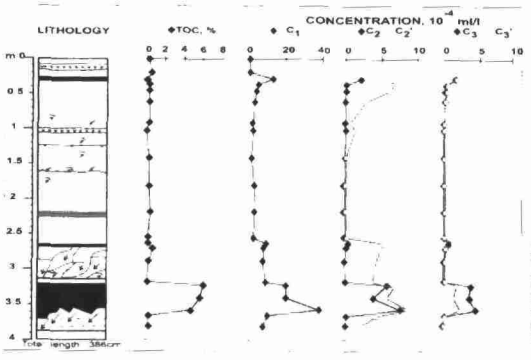

Fig.2 Distribution of hydrocarbon gases and TOC along Core 166G

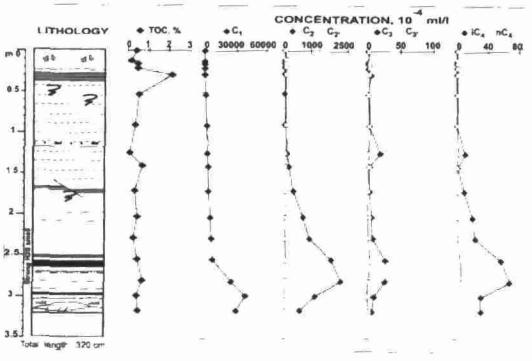

Fig.3 Distribution of hydrocarbon gases and TOC along Core 169G

CHEMICAL CHARACTERISTICS OF A SUBMARINE HYDROTHERMAL SYSTEM OFFSHORE KOS ISLAND, ON THE HELLENIC VOLCANIC ARC

S.P. Varnavas*, D. Panagiotaras, and P.S. Megalovasilis
University of Patras, Department of Geology, 26100 Patras, Greece

Abstract

A submarine hydrothermal system offshore Kos is described in terms of its geomorphological setting, temperature, pH, conductivity and the compositional variability of the hydrothermal waters. Fine yellow to brown colour hydrothermal precipitates accumulate around the hydrothermal springs forming a thin film on the surface of the seafloor. Temperature increases in hydrothermal springs relative to the ambient bottom water. The hydrothermal water at the main hydrothermal field is of low pH, and of lower conductivity and dissolved oxygen relative to the ambient bottom water. Ca and F increase distinctly in the hydrothermal springs relative to the ambient water, while Mg decreases in the hydrothermal springs relative to the ambient bottom water. The hydro- thermal water discharging on the beach is enriched in Ca and F, while it contains lower amounts of Mg relative to the submarine hydrothermal spring.

Key-words: Chemical Analysis, pH, Oxygen, Hellenic Arc

Introduction

Submarine hydrothermal systems occurring along the mid-ocean ridge system were extensively investigated during the last few decades. The compositional variability of hydrothermal waters and sediments was determined and the hydrothermal processes involved in their formation were deduced in a variety of hydrothermal environments. However, our knowledge on island arc submarine hydrothermal systems is relatively limited. Although the Santorini hydrothermal field is known for some time only a few other submarine hydrothermal fields were described from the Hellenic Volcanic Arc (Figure 1), such as the Kephalos Bay, Kos, and Yali [1], the Milos hydrothermal fields [2,3] and recently a hydrothermal field offshore Methana Peninsula [4].

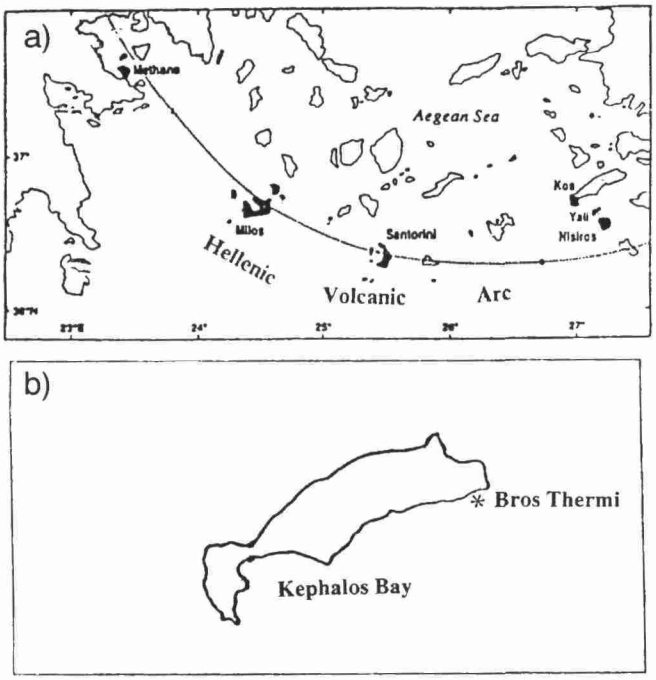

Figure 1 : a) Map showing the location of Kos island in the Hellenic Volcanic Island Arc and b) Location of the hydrothermal field in Bros Thermi.

Considering the existing petrological and tectonic variability along the Hellenic Volcanic Arc the detailed description of new hydrothermal systems is of great importance, because they will allow the deduction of the specific hydrothermal processes occurring in the whole Arc. In this work a submarine hydrothermal field is described offshore Kos, the location of which is shown in Figure 1.

For the morphological description of the hydrothermal field scuba diving was undertaken. The visual observations made and the pictures taken by scuba diving revealed that in the area investigated three major hydrothermal fields occur. One hydrothermal field propagates along a 15 m line of NE-SW direction, starting at 40 m from the coast. A second hydrothermal site occurs on the same line but nearer to the coast. These two areas constitute the zone A. The third hydrothermal site appears as a circular zone of 1.5 m diameter occurring west of the first area at 30 m from the coast described as zone B (Figure 2). Hydrothermal precipitates varying in colour from brown to yellow are very characteristic of the seafloor around the submarine hydrothermal vents.

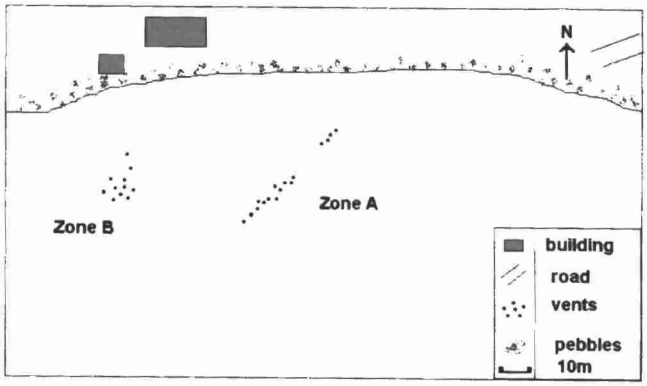

Figure 2 : Sketch map of the hydrothermal field Bros Thermi Kos, Greece.

Methodology

Vent waters were carried immediately after collection to the field laboratory. After filtration through pre-weighted dry 0.45μm pore size membrane filters, samples were put into plastic acid-cleaned containers and were acidified to pH=2 . After the appropriate dilution with de-ionised water of the filtered hydrothermal waters, samples were analysed applying Flame Atomic Absorption Spectrometry for Ca, Mg and Sr. Working standards were prepared from "1000 mg/l Ready to use" Merck stock solutions. To avoid contamination problems all glassware and labware were immersed in 10% HNO3 for 72 hours and rinsed thoroughly with de-ionised water while results checked both with reagent blank and sample blank while precision was checked with replicate analyses. Spectroscopic techniques, carried out with the operation of a PERKIN ELMER 2100 Atomic Absorption Spectrometer equipped with a deuterium-arc correction. Fluoride was determined operating Ion 85 Analyser Radiometer Copenhagen, a potentiometric apparatus [5].

Oxygen concentrations were obtained with the Rosemount Delta 4010 Oxygen digital analyser immediately upon collection, applying the conditions described by the manufacturer. Conductivity and pH measurements were taken with pH-meter (temperature compensated), and Conductivity-meter LF95 of WTW both instruments were calibrated prior analysis.

Water sampling

Hydrothermal water sampling was carried out by SCUBA diving using inverted funnels placed over the seeps, connected with 2 plastic bags, while timing the collection of gas and water [3]. Sampling of this type results in more condense samples due to the isolation of the vent spots from the penetration of the ambient seawater into the sampler while the first bag was used to flush out the seawater from the funnel. The water depth varied from 2.50m to 5.50m. The hydrothermal field has been divided in zones A (east) and B (west), on the basis of the differences in location and appearance of the venting sites (Figure 2).

THE TECTONIC INTERACTION BETWEEN THE CYPRUS AND HELLENIC ARCS AT THE ANAXIMANDER MOUNTAINS COMPLEX

J.M. Woodside [1*], A.F. Limonov [2], J.-F Dumont [3], M.K. Ivanov [2], and Shipboard Scientific Parties of ANAXIPROBE and the Training Through Research Programme

[1] Geomarine Centre, Free University, De Boelelaan 1085, 1081 HV Amsterdam, The Netherlands
[2] UNESCO-MSU Centre for Marine Geosciences, Faculty of Geology, Moscow State University, Vorobjevy Gory, Moscow 119899, Russia
[3] ORSTOM, Observatoire Océanographique de Villefranche-sur-Mer, Géosciences Azur (EP 125), 06230 Villefranche-sur-Mer, France

Abstract

The Anaximander Mountains Complex is formed by southward-rifted and foundered blocks of the Tauride mountains. They are currently undergoing neotectonic deformation in the collision zone between the African and Anatolian/Aegean plates. As a result, two of the mountains are being underthrust, tilting them both to the north; and the southern one is pushing the eastern one eastward, creating a large fold-belt in the sediments of the Antalya Basin, raising up and tilting the eastern mountain eastward, and bending the southern one.

Key-words : active margins, geophysics, seismic, tectonics, Cyprus Arc

The Anaximander Mountains (fig. 1) lie just south of southwestern Turkey, near the intersection of the Cyprus and Hellenic Arcs and roughly midway between Cyprus and Rhodes. They are geologically a part of the southwestern Turkish Taurides but are currently tectonically a part of the African plate undergoing collision with the Anatolian-Aegean domain within the African-Eurasian collision zone. The eastern part of the mountains belongs to the Antalya Nappes Complex; and the western part belongs to the Bey Daglari - Susuz Dag province. The connection was established though examination of samples from all parts of the Anaximander Mountains and the faulted southern margin of Turkey, and comparison with the known geology of the land area (as part of the Dutch ANAXIPROBE Project and the international Training Through Research Programme).

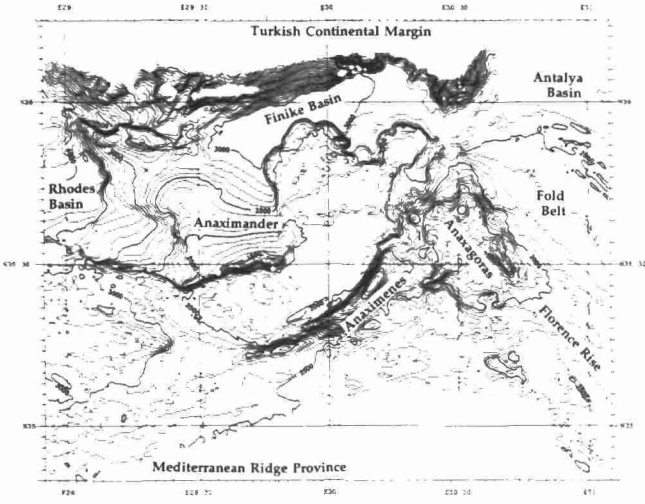

Figure 1. Generalized Simrad EM-12D bathymetric map of the Anaximander Mountains Complex with a contour interval of 100 m. The three principal mountains are indicated by name: Anaximander, Anaximenes, and Anaxagoras.

Rifting of the mountains began probably in Middle Miocene as a part of the rifting in western Turkey and the Aegean. The actual foundering of the mountains did not result in submergence below sea-level until Late Miocene, and had not developed to the point that significant layers of Messinian evaporites were deposited on them. Messinian evaporites are well-developed in the Antalya Basin to the east as well as to the south. On the other hand, Pliocene-Pleistocene sediments are present over most of the area in varying thickness, to over 2 s two-way travel time (TWTT), indicating deposition on a surface having substantial relief (fig. 2); and northward dipping reflectors in the Finike Basin provide evidence of the gradual development of that basin during the post-Miocene period. Differences in the present vertical configuration of the post-Miocene sediments attest to the significant vertical displacements which have taken place, up to at least 1500 m (*e.g.* fig. 2).

The configuration of the western (Anaximander) and southern (Anaximenes) mountains in the complex is simpler than that of the eastern mountain (Anaxagoras). Seismic lines across Anaximander Mountain show north-dipping (at about 4°) Pliocene-Pleistocene sediments disconformably overlying a basement which appears to dip to the west on the west part of the mountain, but may actually be anticlinal under Anaximander, with east dipping basement strata to the east. This is consistent also with the general anticlinal structure of the Susuz Dag - Bey Daglari directly to the north. The Pliocene-Pleistocene sediments on Anaximander are thinnest in the central part of the mountain (north side of figure 2) and thicken to the north to over 2 s TWTT and to the south to about 2 s TWTT (fig. 2). To the southeast, Anaximenes Mountain does not appear to have a significant cover of Pliocene-Pleistocene sediments, but it is difficult to tell from the seismic profiles because of the steep (about 25°) northwest dip of the basement sedimentary rocks. The large tilt of Anaximenes, and the lesser tilt of Anaximander are both caused probably by underthrusting of Anaximander by Anaximenes and Anaximenes by the Mediterranean Ridge from the south. Northeast-southwest compression of Anaximenes has given it a curved (concave to the northwest) shape in plan view.

Anaxagoras Mountain appears to be continuous with the Florence Rise to the southeast as well as with the Antalya Nappes Complex to the north. It is distinct from the other two mountains in the complex not only in morphology and structure but also because of a significant lithospheric discontinuity between Anaximenes and Anaxagoras, indicated by a sharp northeastward decrease in the Bouguer gravity field by 150 mGal over a distance of about 70 km, with a maximum gradient of about 4 mGal/km. The increased relief of the Florence Rise, a gentle seafloor bulge forming the western branch of the Cyprus Arc, where it merges with Anaxagoras Mountain, probably relates to the compressional deformation caused by the northeastward movement of Anaximenes Mountain. The curvature of Anaximenes can be seen as a consequence of this compression. To the northeast of Anaxagoras can be seen a large fold belt which coincides with, and is inferred to result

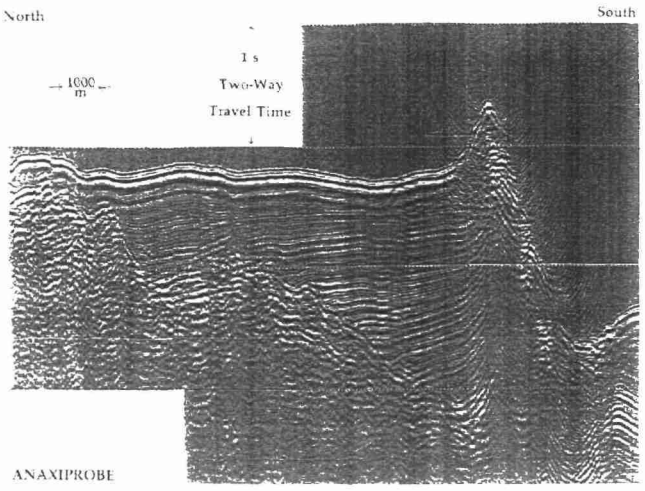

Figure 2 : Seismic line running almost north-south across the southern escarpment of Anaximander Mountain at roughly 29°30'E (see fig. 1). Post-Miocene marine sediments onlap Miocene Susuz Dag rocks. Vertical displacement at the escarpment took place after most of the post-Miocene sediments had been deposited in a basinal setting. (Processing by Anna Volkonskaya, Serguei Bouriak, Roman Almendinguer, and Valery Gaynanov of MSU).

GEOGRAPHICAL PROVINCES OF THE MEDITERRANEAN SEA FROM THE SURFACE COLOUR AND TEMPERATURE HISTORICAL RECORD

Vittorio Barale *, Isabella Zin and Carlos Villacastin
Space Applications Institute, Marine Environment Unit
Joint Research Center of the European Commission
Ispra (VA), Italy

Abstract
Sea surface colour and temperature images, derived from time series of CZCS (1978-1986) and AVHRR (1982-1991) data, have been used to assess the main features of the Mediterranean basin. The data were processed to apply sensor calibration, to correct for atmospheric contamination, and to estimate chlorophyll-like pigment concentration and surface temperature. Long-term composites derived from the images show differences between western and eastern sub-basins, inshore and offshore domains, northern and southern coastal areas. Continental runoff and wind-driven mixing, geo-morphology and meteorology of basin margins, appear to influence water dynamics and bio-geo-chemistry.

Key-words : Remote Sensing, Biogeography, Hydrography, Mesoscale Phenomena

Remote Sensing (RS) techniques provide the means to investigate environmental processes at the scale of entire marine basins. Optical and thermal RS data are of considerable interest for the Mediterranean Sea, due the combination of low cloudiness, predominance of waters optically dominated by plankton alone (dissolved organics and suspended sediments render the surface colour field more difficult to interpret) and marked thermoaline density gradients. The compilation of historical time series of RS data on the Mediterranean Sea - primarily Coastal Zone Color Scanner (CZCS) and Advanced Very High Resolution Radiometer (AVHRR) - has pointed out, for the first time, the space/time heterogeneity of surface parameters derived from optical and thermal indices [1, 2]. The variability observed in the satellite data record points at specific geographical provinces, where a relationship seems to exists between such indices and the climatic features of the region.

Sea surface colour and temperature images give complementary views of the Mediterranean water bodies. Historical time series of CZCS (1978-1986) and AVHRR (1982-1991) data have been used to derive composite images of the entire basin. The raw data (2465 CZCS and 9396 AVHRR original images) were processed to apply sensor calibration algorithms, to correct for atmospheric contamination, and to derive chlorophyll-like pigment concentration and surface temperature [3, 4]. Single images were generated for each available day, co-registered using the same geographic equal-area projection and resolution, and then averaged pixel by pixel, to compute monthly and annual composites. The composites cover an area of 4000 x 2000 km^2, with a 1 km pixel size, and retain only persistent features of the surface colour and temperature fields. Given the pixel by pixel correspondence of the long-term composites, a new multi-band image could be constructed, for the annual and monthly intervals, in which the colour and temperature histogram-matched images constituted two different bands. An unsupervised classification was performed, using spectral distance to assign each pixel to a cluster, and highlight the patterns inherent in the data.

Marked differences appear in both the pigment and the temperature mean annual composites (Figure 1) between western and eastern sub-basins, inshore and offshore domains, as well as northern and southern near-coastal areas. The western basin is characterized by higher pigment concentrations and lower temperatures than the eastern basin - where the Aegean Sea represents a notable exception. Contrary to common geographic subdivisions, this qualifies the Adriatic Sea - and the northern Aegean, up to a point - as one of the western sub-basins, at least as far as the pigment and temperature fields are concerned. The classification of Mediterranean waters (see also Figure 1) suggests that the transition between the western and the eastern regimes corresponds with the line of straits going from the Sicily Channel, to the Strait of Messina and the Strait of Otranto - and perhaps the central Aegean. The classification of western sub-basins seems to be dominated by the stronger pigment signal, while that of the eastern sub-basins by the more pronounced temperature signal.

A single class groups together all of the plumes due to the main rivers entering the Mediterranean Sea, *i.e.* the Ebro, Rhone, Po, and Nile. The same class also includes the areas influenced by river discharges and coastal runoff along the Italian coast in the Thyrrenian Sea, along both the Italian and Albanian coastlines in the Adriatic Sea, along the northern shores of the Aegean Sea and the Marmara Sea. Another area included is the shallow bank off southern Tunisia, where however the enhanced pigment signal is due to other factors than runoff and/or mixing, *i.e.* to direct bottom reflection through the clear waters (coupled to a distinct temperature signature, colder in winter and warmer in summer).

A second, broader class appears to account for most of the near-coastal areas of the Mediterranean. The southern coastal areas do have different characteristics, but this may be simply due to the fact that along the African coastline, in the eastern basin in particular, the data are somewhat altered by signal contamination due to the notorious CZCS sensor ringing in the downscan direction, after imaging a bright

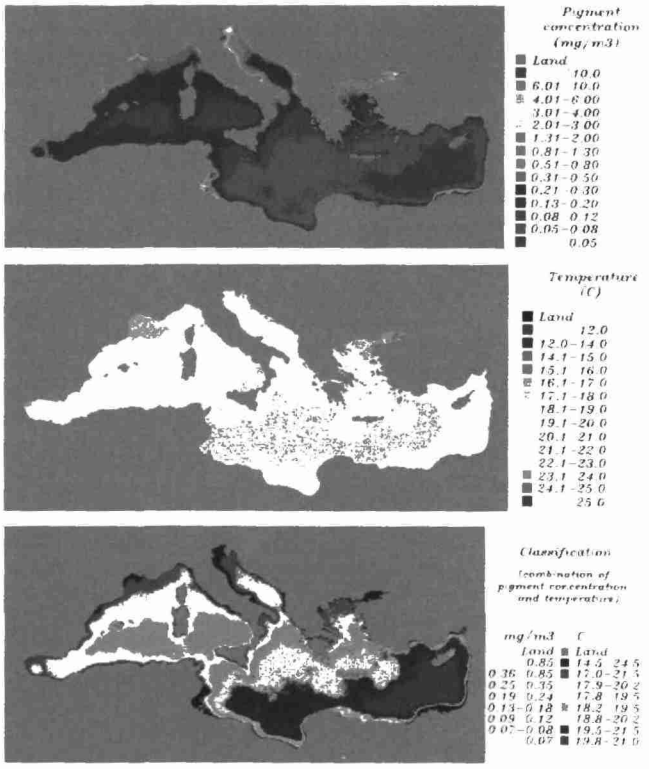

Figure 1 : Upper plate: annual mean of chlorophyll-like pigment concentration derived from the CZCS (1978-1986) data set; the colour coding represents mg/m^3. Middle plate: sea surface temperature derived from the AVHRR (1982-1991) data set; the colour coding represents °C. Lower plate: unsupervised classification of the Mediterranean Sea surface characteristics derived from a combination of the annual pigment and temperature images; the arbitrary color coding highlights the 8 different classes obtained. **See color figure in p. 214.**

THE EFFECT OF PHYSICAL FORCINGS ON THE NUTRIENTS GRADIENTS IN THE MEDITERRANEAN SEA: A NUMERICAL APPROACH

A. Crise* and G. Crispi
Osservatorio Geofisico Sperimentale, P.O. Box 2011 34016 Trieste, Italy

Abstract
The oligotrophic regime of the Mediterranean, although widely accepted, remains, as yet, inadequately resolved in its space and time variability. Here a numerical approach is presented to evaluate the relevance of ocean dynamics on nutrient distributions. A three-dimensional hydrodynamical ecological model was developed to understand the roles of the subbasin-scale upper ocean features as well as lateral advective and diffusive processes, in this context. The model is able to reproduce the large scale zonal and meridional trophic gradients while the phytoplankton standing crop, as estimated by model and confirmed by CZCS data, exhibits the same large scale features. In particular, Ekman pumping seems to be related to the meridional gradient while subbasin cyclonic structures contribute to the perturbation of the general trophic conditions.

Key-words : Nutrients, geochemical cycles, open sea, ocean colours

Introduction

The general oligotrophic regime of the Mediterranean is explained by the inverse estuarine circulation with a net loss for nitrate at Gibraltar Strait ranging from 1.25 Mtons/year [1, 2] to 3.11 Mtons/year [3, 2], which seems to be only partially compensated by terrestrial inputs sources. This general picture needs to be refined in order to explain the east-west and north-south trophic gradients, which are present, on average, both in the surface layer and at depth.

This paper is focused on modelling these gradients in terms of interactions between general circulation processes and the biogeochemical fluxes, assuming that the first trophic level dynamics is nitrogen limited. The proposed nitrogen model explicitly includes the biogeochemical interactions that alter its form, in particular, autotrophic production and remineralisation via bacterial activity. In the following presentation, we will outline the model, and discuss the results proposing a dynamical explanation of the Mediterranean trophic gradients.

The model

The three-dimensional formulation is needed in order to appraise the influence of horizontal transport, of upwelling/downwelling processes and of vertical mixing on the nutrient distribution and cycling, and eventually on phytoplankton standing crop. For the sake of simplicity, the model complexity was held at a minimum, describing only the first trophic level with a trophodynamic scheme based on nitrate, phytoplankton and detritus (NPD) exploiting the advection/diffusion/reaction biological equations as presented in Civitarese *et al.* [4], enhanced with a cloudiness dependent irradiance submodel.

The coupling between physical and trophic dynamics is obtained through the advective terms and temperature dependencies present in the biological equations which are synchronously calculated with the dynamical fields. The hydrodynamics is simulated with a 31 level 1/4 degree MOM-like hydrodynamical model with "perpetual year" NMC wind forcings developed as in Roussenov *et al.* [5]. The MOM-NPD model has been described in detail in Crise *et al.* [6] together with a model sensitivity analysis to the trophic parametrization. The timestep was 2400 s and the biological runs typically lasted not less than three years after five years of spin-up for the hydrodynamics. The initial conditions for the NPD submodel were-basin wide laterally homogeneous profiles for phytoplankton and detritus (assumed initially as null) and averaged values calculated from experimental data for different subbasins (Alboran, Algero-Provençal, Ionian, Aegean, Levantine).

At Gibraltar, biological tracers were allowed to be exchanged with an academic ocean outside the Mediterranean, where climatological profiles of nitrate, phytoplankton and detritus are considered as constant over time.

Results

The model estimates of nitrate fluxes at Gibraltar Strait are in good agreement with literature data, ensuring proper conditions at the western boundary (a loss of 2.5 Mton/year predicted by model). The climatological distribution of the meridionally integrated nutrients as obtained by 24 months averaging exhibits a pronounced east-west gradient induced by the different physical and physically driven processes in the two basins, (fig. 1.a) with superimposed the average values derived from the data set shown in fig. 2. The maximum in the Alboran Sea can be ascribed to the biological impact, also relevant at basin scale, where the autotrophic activity is able to rapidly incorporate the inorganic nitrogen entering through the Gibraltar Strait.

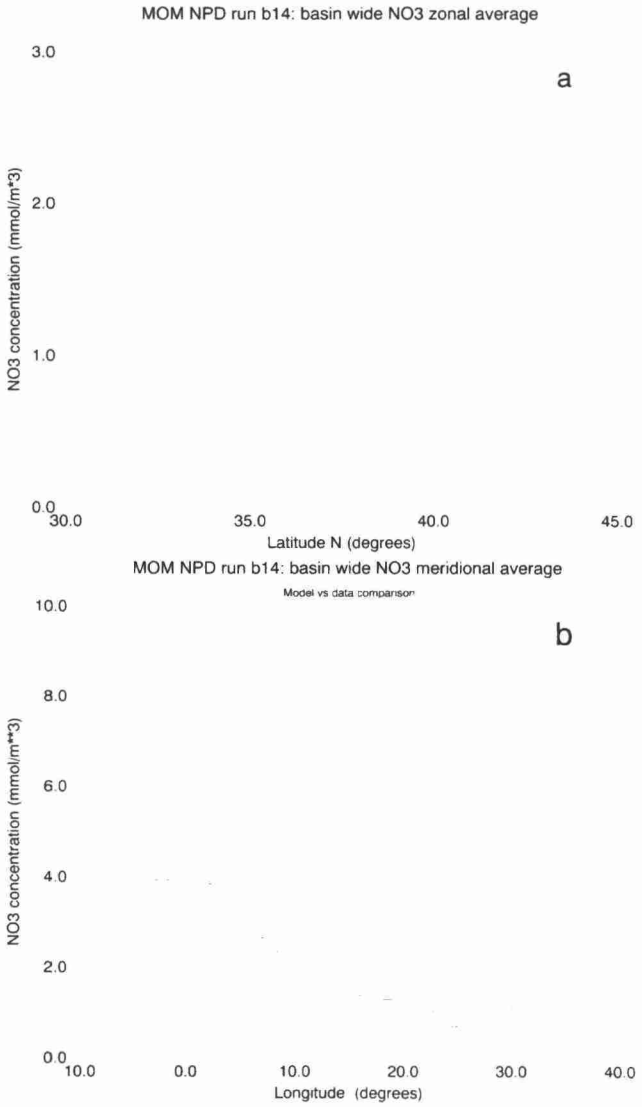

Figure 1 : Two year average of zonal (a) and meridional (b) means in the first 140 m layer: DIN (white dot) and experimental reference meridional averages expressed in mmol/m**3.

VARIATIONS IN TIME AND SPACE SCALES IN THE PHYSICAL AND BIOLOGICAL CHARACTER OF THE MEDITERRANEAN SEA

Paul E. La Violette *[1] and Robert Arnone [2]

[1] Gulf Weather Corporation, Stennis Space Center, Ms 39529 601 688 3397, USA.
[2] Naval Research Laboratory, Stennis Space Center, Ms 39529 601 688 5268, USA

ABSTRACT

The combination of satellite and in situ data form a powerful tool to use in the study of the Mediterranean Sea at varying scales of time and space. Whereas a great deal of information may be inferred from in situ data alone, the coupling of satellite with the in situ data provides a more accurate picture of what actually takes place before, during and after a series of in situ measurements. With the satellite's ability to provide broad spatial displays of surface data, the in situ measurements are no longer isolated points on the sea surface; one can see them in relation to their broader dynamic surroundings. In sample studies, we demonstrate that satellite data can be usable in such combinations not only in the single high resolution image format, but as long series of high resolution imagery, as long-term composites and finally, as graphs of long-term (multi-year) data. Recent data indicate that conditions in the Mediterranean are changing. We feel that marine studies using combinations of long-term (decades) *in situ* and satellite data are one of the most powerful tools available to provide both a baseline of comparison as well as a timeline monitor of the ongoing changes. We realize that while what we describe here is a doable methodology, there is a basic problem in the poor accessibility of satellite data to the average marine scientist. We feel that this is a critical problem that the CIESM should address.

Key-words : coastal processes, remote sensing

Introduction

Data collection by a ship at sea has long been the most accurate method of deriving information about the Mediterranean. In a span of several hours, a ship at an ocean station, using sophisticated data collection instruments can obtain detailed biological/physical data from the surface to the ocean bottom. Upon completing the station, the ship can move to another station and obtain similar data. This process repeated over a number of stations results in a powerful data set. From such data sets, marine science analysts have for years derived their view of what the Mediterranean is like. Very often these views have been presented as horizontal (*e.g.*, see Figure 1) and vertical slices of the Mediterranean showing the spatial distribution of the parameter(s) of interest to the analyst. Physical oceanographers use such views to derive the Sea's dynamic structure; biologists, to derive the distribution of organisms; and modelers, to derive the mechanisms that force the various parameters to become so displayed.

This is the classical methodology of oceanography that has been in use since the *Challenger*. It is the principal methodology in use today and undoubtedly will be so for years to come. There are, however, certain limitations to this method of data collection. Limitations that we, as marine scientists, too often do not consider in our final analysis of the data. That is, that the ship data is limited in both space and time.

Space

We often forget that the data collected at an ocean station is a collection of the actual conditions that were present at a particular point in the ocean and no place else. We often infer that the station conditions are representative of a broader area and, if there is no other data source, this inference is justified. However, we must not forget that the data is >from that station only and may be completely different from conditions just a few kilometers away from the ship. Even if a series of stations is made, there can be problems. If the studied phenomena is poorly sampled (due to either the spatial or temporal distribution of stations) then the data is worse than useless, it may well present a set of conditions that another more apropos station distribution might show to be completely different.

Time

Quite often, we try to overcome this difficulty by tighter station spacing. However, an ocean station takes time to occupy. And, once the data collection at a station is completed, it takes time to go to the next station. The new station also takes time, and the movement to the next station will again take time. If the parameter being studied is part of a dynamic ocean process, then the number of stations that can be occupied during any campaign is limited by the temporal variability of the process. It may well happen that, despite the best of plans, we cannot derive as accurate a picture of the process from the data as we would like.

Space and time

We must consider that the phenomena or event indicated by the data represents the period of the data collection. Conditions may change in several days, weeks, or even months that are starkly different from the conditions for the time the data set were collected. Seasonal and interannual changes must also be taken into account.

In this discussion, we will look at the problem as that of dealing with varying scales of space and time. We will show that any *in situ* data collection is normally limited by its spatial and temporal coverage. We will also show that this coverage needs to be expanded from immediate area and time scales to basin and short (days and weeks), long (seasons and interannually), and longer (decades) scales. To fully understand the evolution of physical, biological, optical, and or chemical processes in the Mediterranean Sea, one must use satellite and *in situ* data and models in a the integrated matrix of different scales of space and time.

As a critical part of this discussion, we will demonstrate how *in situ* sampling can be optimized using satellite data in conjunction with the *in situ* data collection. Although combined satellite - ship data analyses are fairly common in the marine science analyses published today, quite often these involve only one or two satellite images. We will show that a more intensive utilization of satellite data is needed to properly understand Mediterranean conditions.

The short term data

Figure 1 may be used as an example of the limitations of ship data isolated in space and time. This figure, part of a treatise on a multi-ship campaign in the Alboran Sea by Lanoix (1), shows a large gyre occupied the entire western Alboran during the period of a multi-ship campaign in 1964. The analysis also shows that no gyre was present in the eastern Alboran.

Lanoix's was an excellent treatise on the data he had available at the time. His study presented a gross picture of the circulation that set the stage for multiple platform operations in the sea for many years after its publication (*e.g.*, Donde Va?) (2). In 1964, the time of the multi-ship campaigns, satellite data were not available and any depiction of the circulation of the Alboran Sea could only be derived from ship data. The 1964 investigators of the Alboran had an idea of the spatial and temporal complexity of the Alboran circulation; hence, their choice of the multi-ship approach. The resulting data was what Lanoix used for his study and his final analysis reflects the limitations of the data collection methodology of the period.

In Figure 2, La Violette and Lacombe show daily satellite data of the same region, but for a different year (3). In the figure, we see that the shape of the gyre varied during the several days of satellite imagery. This variability is not disclosed by the multiple-ship analysis of Lanoix. Indeed, in the numerous studies of the Alboran since the Lanoix study, an Alboran gyre the size depicted in his analysis has never been found. Although a gyre-type circulation does exist in the Alboran, it is often found to consist of two gyres; a Western and an Eastern Alboran Gyre. In a study by Heburn and La Violette (4), both

MODELING OF THE NEAR-COASTAL UPWELLING IN THE SHELF ZONE OF THE CRIMEA AND ITS INFLUENCE ON DYNAMIC OF THE OXYGEN-HYDROGEN SULPHIDE INTERFACE

Natalya M. Stashchuk*, Vasiliy I. Vlasenko, Vitaliy A. Ivanov
Marine Hydrophysical Institute, the National Academy of Sciences, Sevastopol, Ukraine

Abstract
An hydrodynamic model was used to study upwelling event caused by wind in the Black Sea. It was conceived to study the influence of water dynamics on oxygen and hydrogen sulphide distributions in the shelf zone of Crimea. A chemical reaction between these dissolved gases was taken into account. During upwelling event upward fluxes of cold bottom water were accompanied by displacement and penetration of the hydrogen sulphide into the near-surface layers enriched by oxygen and the extensive coexistence zone of oxygen and hydrogen sulphide formed over the shelf break. The extended area with small oxygen concentration remained after the end of chemical reactions between hydrogen sulphide and oxygen as a "trace" of upwelling event.

Key-words: Black sea, Anoxia, Waves, Models

Introduction

The Black Sea, as all inland seas, has a very specific hydrological and hydrochemical structure of waters. Due to the existence of the cold intermediate layer (CIL) with temperature lower than 8°C at 50-80 m, the Black Sea acts as an unique basin. The oxygen penetration depth do not exceed 80-100 m in central areas and 180-200 m in offshore ones. So 99% part of the Black Sea contains hydrogen sulphide and is not suitable for biological forms and communities living.The presence of oxic and anoxic zones designate the fact that investigation of space-temporal characteristics of oxygen and hydrogen sulphide distributions and their interactions is one of the central questions. If the time scale of the oceanic near-coastal upwelling is of the about weeks, a day wind forcing is sufficient for development of upwelling in the Black Sea due to the shallow thermocline and steep bottom topography. This experimental fact was often observed and confirmed. The lifting of the near-bottom cold water was accompanied by uprising of passive admixture together with dissolved gases. What is happening in upwelling areas is an important question of the up-to-date ecology.

Methodology

Coastal upwelling regions are typical areas where both advection and mixing play an important role in the water movement and transformation. So, we used a complete system of Reynolds hydrodynamic equations with non-linear terms, as well as terms responsible for turbulent exchange. The model and numerical scheme were described in Vlasenko *et al.* [1] in detail. Briefly, the full system of equations reduced to the equations for eddy and stream function. Two kinds of variables substitutes were realised. The first one concerned the transformation of an irregular calculation domain to a rectangular one, the second exaggerated the numerical grid in the layers with sharp density gradients. These manipulations resulted in a high accuracy of calculations.

Results

It is likely that the hydrogen sulphide may penetrate to the oxygen layers during deep water uprising. As it was shown [2], the minimum time of oxygen and hydrogen sulphide interaction is nearly 6 hours in the coexistence zone. Because we are concerned with processes of more than a one-day duration, diffusion - advection equations for hydrogen sulphide and oxygen with chemical reaction between them were also added for investigation of influence of upwelling events on distributions of O_2 and H_2S in the Crimean coastal zone.

The model domain was a vertical plane ranging from the sea surface to the bottom and from the coast to 200 km offshore. The depth varied from 20 m on the shelf to 2000 m in the deep part at a distance of 40 km. Typically (for the Black Sea) short wind forcing (approximately one day) and following relaxation processes of hydrophysical and hydrochemical fields were considered. At the first stage of evolution of the near-coastal upwelling, it has all features inherent to the oceanic ones [3]: the development of an alongshore Stocks drift in the upper layer due to the wind stress, excitement of cross-shore circulation by the action of the Coriolis force and formation of vertical advective cells on the shelf and a thermohaline front moving seaward.

The first interesting finding from this studies is the consideration of upwelling relaxation. After the cessation of wind forcing, an evolution of the thermochaline fields continued without any external influence. So, two types of movements were formed on the shelf and in the open part of the sea. The diagram of cross-shelf circulation during the upwelling relaxation is represented in Fig. 1. A quasi-stable dissipating vertical advective cell was formed on the shelf. Its dimension coincided with the first baroclinic Rossby radius of deformation. At the open part of the sea the following types of motions were established :

- the horizontal subinertial oscillations with current and countercurrent in upper and lower layers;
- the thermohaline front moving shoreward;
- the presence of cold water during days near the shore;
- progressive internal waves, generated at the frontal side of the moving density (thermocline) front. In the transition zone, these internal waves were divided to reflected waves and waves passed on the shelf;
- vertical subinertial oscillations over the continental slope in the transition zone.

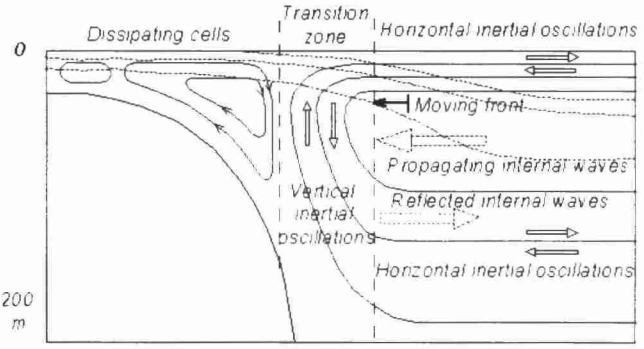

Fig. 1. Schematic diagram for upper 200 m of cross-shelf motions during upwelling relaxation. Solid lines are stream function, dashed lines are isopicnals.

Due to the different values of the local vorticity of along shore currents and different horizontal density gradients in various points of the tested area the period of subinertial oscillations changes from the inertial one (Tin = 17h) near the bottom out of the shelf up to 22 hours at the free surface in the shelf break area.

The possibility of excitement of vertical subinertial oscillations during relaxation of a near-coastal upwelling is confirmed by *in situ* data, collected in the coastal zone. Figure 2 represents the vertical displacements of the thermocline measured over the shelf-break (isobath of 100m) in the shelf zone. Measurements of thermocline dynamics were conducted by distributed sensors of temperature [4] during upwelling event in summer, 1993. It is clearly seen from Fig. 2 that during first stages of upwelling (13.06- 14.06), the thermocline was lifted by the wind forcing. After the cessation of the wind action it returned to its initial position. This return was not monotonous and took place on the background of vertical oscillations. The period of these oscillations (T = 17.9h) was not equal to the inertial one (Tin = 17.0 h) and was shift to the red part of spectrum. These results first of all confirmed the existence of the model predicted subinertial vertical oscillations in the transition zone (see Fig. 1) during process of upwelling relaxation and show also the red frequency shift.

WATER MASSES AND SEASONAL HYDROGRAPHIC CONDITIONS IN THE SARDINIA-SICILY-TUNISIA REGION

M. Astraldi*, G.P. Gasparini and S. Sparnocchia

Istituto per lo studio dell'Oceanografia Fisica-CNR, Forte S. Teresa, 19036 Pozzuolo di Lerici (SP), Italy

Abstract

Several hydrographic cruises and long term current measurements carried out in the Sardinia-Sicily-Tunisia region as a part of different EU projects allowed us to significantly improve the knowledge on the water masses flowing into this region and their time variability. The observation of the different water types indicates that the mass exchanges between the two principal sub-basins of the Mediterranean are more complex than previously known. The analysis of the seasonal characteristics of the Modified Atlantic Water (MAW) and the Levantine Intermediate Water (LIW) clearly indicates that they are subject to significant seasonal changes.

Key-words: Hydrography, Sicilian Channel

Introduction

The area between Sardinia, Sicily and Tunisia is a key region for the comprehension of the exchanges between the Eastern and Western Mediterranean basins. It is bounded by three of the most important straits and passages in the Mediterranean: the Sicily Strait to the East, the Sardinia Channel to the West and the Sicily-Sardinia passage to the North. The Sicily Channel, about 140 km wide at the surface, reduces its extension below 200 m with two narrow passages 450 and 325 m deep, respectively. The Sardinia Channel is a zonally oriented passage connecting the Algerian and the Tyrrhenian basins, with a sill depth of about 1900 m. Finally, the Sicily-Sardinia section forms the southern boundary of the Tyrrhenian characterized by two main passages, of which the deepest one tightly connected with the Sardinia Channel. Previous studies (1,2) pointed out the complexity of the processes in the region and the role of the bottom topography in sustaining them, and provided a first estimation of the involved fluxes. The main knowledge about the water masses crossing this region mostly concerns the MAW and the LIW. MAW enters the area from the Algerian Basin and principally flows towards the Sicily Channel and the Tyrrhenian Sea. After having recirculated inside this basin, part of this vein exits again from the Sicily-Sardinia section, while another part outflows from the Corsica Channel. LIW reaches the region trough the Sicily Channel. From it, it flows towards the Tyrrhenian Sea following the same fate as the MAW: most of it outflows again from the Sicily-Sardinia section and only a small part from the Corsica Channel. Concerning the Deep Water, the few available information, indicate the importance of the exchanges between the Algerian and the Tyrrhenian Basins (3). It can be said, however, that, until very recently, most of the knowledge was derived from oceanographic campaigns covering only partially the considered area.

Starting from November 1993 a new experiment was initiated as a part of the MTP1 of the EU. It was mostly based on a seasonal intensive hydrological investigation of the whole region (seven cruises for the period 1993-97) and on direct long term current measurements in the Sicily Strait and the Sicily-Sardinia section. The achieved results permitted to verify the presence and patterns of different water types, some of them not identified before (4,5). In addition, the collected data show that MAW and LIW are subject to a clear seasonal signal. In the following we will describe the principal characteristics of water masses present in the area and some aspects connected with their seasonal variability.

The water types in the Sicily-Sardinia-Tunisia region

The analysis of the hydrographic characteristics along the Sicily Channel indicate that:

a) At the Sicily Strait the MAW is always present with two veins. While the most evident of them is along the Tunisian coast, the other is in correspondence of the southeastern Sicilian Shelf.

b) The Levantine flow is divided by the central ridge enhancing from the Strait of Sicily and constrained in the two resulting channels which induce different dynamic properties in each of the two veins.

c) The Levantine flow is actually composed of two water types: the one known as LIW (T=13.85, S=38.75), and another one colder and denser which always flows close to the bottom of the Tunisian side of the Strait. The latter was identified as a transitional Eastern Mediterranean Deep Water (tEMDW) (T=13.65, S=38.73), resulting from a mixing between LIW and EMDW (5).

d) Both the MAW and LIW display a significant seasonal variability while crossing the Sicily Channel.

The hydrographic data along the Sardinia Channel, besides displaying the inflow/outflow of MAW and the outflow of LIW, indicate that two other water masses enter the considered region (Fig.1):

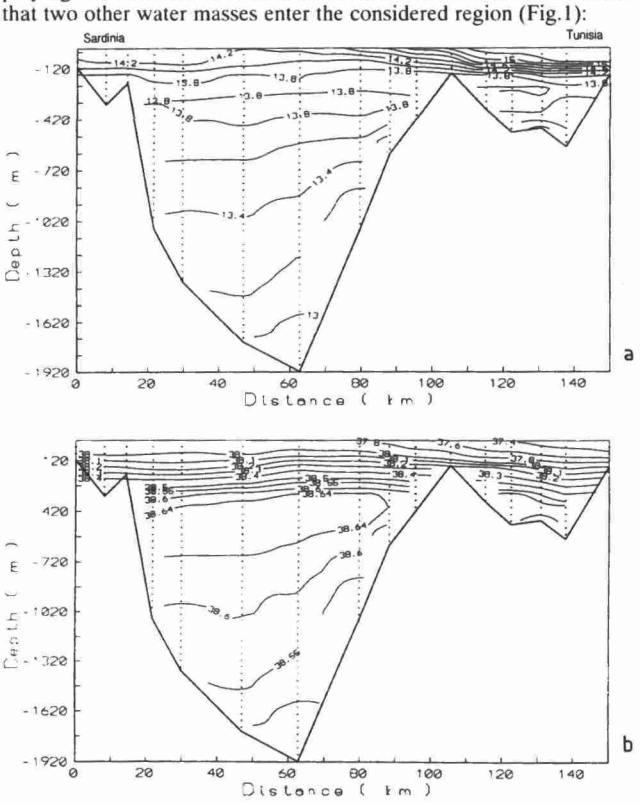

Figure 1 : Sardinia-Tunisia cross-section. (a) Temperature distribution and (b) Salinity distribution during January 1997.

1) one at the bottom of the deepest part of the Channel. The hydrographic characteristics (T=12.80, S=38.44), and the Oxygen values higher than the upper layers, indicate it as a Western Mediterranean Deep Water (WMDW). After having recirculated in the Western Mediterranean, a significant part of WMDW crosses the Sardinia Channel and flows into the Tyrrhenian;

2) the other has the characteristics of the Intermediate Water present the Western Mediterranean (T=13.10, S=38.50). This means that a significant part of LIW flowing in the Western Mediterranean, instead of outflowing from the Strait of Gibraltar, follows the African slope and crosses the Sardinia Channel from where it enters the Tyrrhenian Sea at about 800 m of depth.

After having recirculated in the Tyrrhenian, where they are subject to intense mixing processes that significantly change their original properties, both these waters exit from the basin along the Sardinia slope of the Sicily-Sardinia section.

The seasonal variability of MAW and LIW.

The analysis of hydrographic data all over the region, allowed to verify if the seasonal variability evidenced by the current measurements at the Sicily Strait can even be observed in the hydrographic pattern within the area. Concerning the seasonal signature in the

RESULTS OF THE FIRST MEDITERRANEAN MODELS EVALUATION EXPERIMENT MEDMEX
E.U. Concerted Action (MAS2-CT94-0107)

J.-M. Beckers [1] and MEDMEX partners

[1] Research Associate, National Fund for Scientific Research, University of Liège, GHER, Sart-Tilman B5, B-4000 Liège, Belgium

Abstract

The present paper will summarize the results of the first MEDMEX experiment, in which 5 general circulation models were applied to simulate the seasonal cycle in the Mediterranean. The intercomparison was designed so as to impose identical resolutions and forcing functions on the models, aiming at eliminating interpretation problems due to different forcings. The models participating in the intercomparison are two versions of the MOM model, the GHER model, OPA and POM model, whose results are compared.

Key-words: circulation models

Setup of the coarse resolution experiment

Individual descriptions of the models applied to the Mediterranean can be found in the report, but the implementation caracteristics for the intercomparison are given in figure 1.

The first MEDMEX modelling experiment was set up to study the behaviour of the models when forced by the classical perpetual year approach, repeating each year the atmospheric data of a monthly averaged atmosphere, including sea surface relaxation of temperature and salinity towards climatological monthly means. The participating models were set up as indicated in figures 1 and described in [1]. Horizontal resolution was identical in all models (1/4) and 31 vertical degrees of freedom were allowed.

	GHER	LODYC CETIIS OPA	IMGA-CNR MOM	UA POM	UIB MOM
Grid	C	C	B	C	B
Advection	TVD	Centered in Time and space	Centered in time and space	Centered	Centered in time and space
Turbulence	k	k	constant vertical diffusion at 0.3 cm^2/s for tracers and 10 cm^2/s for momentum	k, l (Mellor-Yamada)	constant vertical diffusion at 1 cm^2/s for tracers and for momentum
Pressure treatment	free surface, mode splitting	rigid lid, streamfunction formulation	rigid lid, streamfunction formulation	free surface, mode splitting	rigid lid, streamfunction formulation
Horizontal diffusion	Laplacian in model coordinates 300 m^2/s for u 90 m^2/s for T,S	Bi-Laplacian in model coordinates A_M=8 10^{10} m^4/s for u A_M=8 10^{10} m^4/s for T,S	Bi-Laplacian in model coordinates A_M=5 10^{10} m^4/s for u A_M=2 10^{10} m^4/s for T,S	Smagorinsky formulation, with c_{Smag}=0.20	Laplacian in model coordinates 6000 m^2/s for u 100 m^2/s for T,S Now 400 m^2/s for u 400 m^2/s for T,S
Time stepping	One time step method: barotropic 60 s baroclinic 3600 s	baroclinic 3600 s	Mixed centered finite difference and Euler: 1200 s	Leapfrog method barotropic 40s baroclinic 4320s	Leapfrog method baroclinic 10000s

Figure 1 : Model specifications

Data preparation and modelling experiment setup

For the purpose of the perpetual year run, the ECMWF wind stress data were averaged to obtain monthly mean wind stress values, as explained in the first MEDMEX report [1]. The sea surface fields of temperature and salinity were taken from the MED4 data base described in [2] and found on the WWW http://modb.oce.ulg.ac.be/. Similarly, initial conditions and boundary conditions for the Atlantic box were taken from this data base. The whole modelling setup and data set is accessible through http://modb.oce.ulg.ac.be/MEDMEX

Model Results

Here we will only give a flavour of the results which were obtained during the intercomparison by showing circulation pattern and some globale analysis of drift trends. Results were obtained by simulating 15 years of the perpetual forcing. A first feature is that the horizontal variability is very different when comparing one model to the others: UIB and CETIIS show the lowest variability of the five models. IMGA and UA have high variability of which UA has a lower signal. This general trend is readily observed on most horizontal sections and can be attributed to the horizontal diffusion coefficients and numerical diffusion of the advection scheme. Generally all models reproduce the main large scale features of the surface circulation, with differences in local representations: For exemple:

• the UIB model produces no Alboran gyre, neither does the other MOM or POM, while CETIIS and GHER produce small Alboran gyres ;

• all models are showing an Algerian current detached to the north, but in the GHER model this feature is always very strong and a recirculation is seen at the African coast ;

• each model shows a westward flow in the Ligurian basin, with a northern current which is partly formed by the flow through the Corsican channel ;

• Gulf of Syrthe: All models produce an anticylone except UIB ;

• IMGA presents a big cyclone in the southern Ionian. CETIIS an UIB produce a weaker cyclone, whereas UA and GHER also show a cyclonic gyre but with some meanders and some additional small scale anticyclones. These smaller gyres are probably controlled by horizontal diffusion, since a run by IMGA with lower diffusion also produced these features, while a run of GHER with higher diffusion eliminated them.

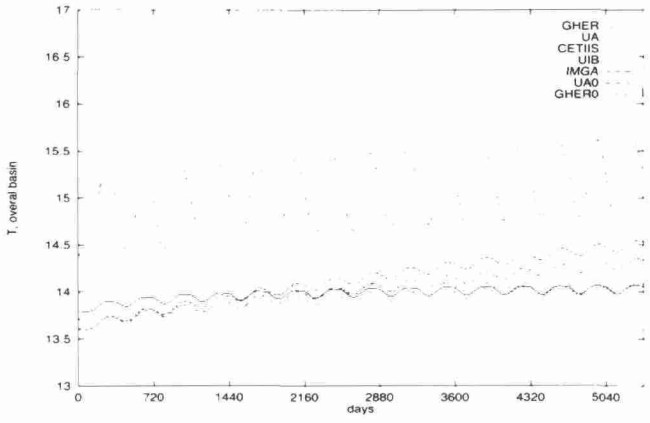

Figure 2: Average temperature

• the Southern Adriatic cyclonic circulation is present in all models.

• the Rhode gyre is present and bifurcation east and west of Cyprus is represented in all models.

• the Antalia anticyclone is represented by GHER and UA very well, in the other modeis only weakly.

Though the large scale circulation patterns and even some strait transports are similar, the hydrographic structure in the models showed some drift tendencies, due to the monthly averaged forcing, inadequate to form correct water masses. These drifts, though unphysical, can nevertheless be compared and we show as an exemple some volume transports, basin averaged temperatures and diagnosed air-sea interactions.

Conclusion after the first experiment

Forcing with monthly mean averages and a low relaxation is surely not appropriate to form correctly the water masses in the Gulf of Lions and the Levantine basin . This deficency of the modelling setup limits of course the physical realism of the simulation results, but at least the model drifts and beaviours are simular. To eliminate drifts, more complex air-sea interactions are needed and hopefully, the results obtained by using daily air-sea fluxes rather then monthly averaged wind-stress and relaxation fields will be available at the conference. At the time being, current conclusions can be summarised as follows:

• Models give similar response concerning Strait transports and their seasonal cycle, general heat budgets, salt budgets and drifts, overall circulation in surface and deep layers and spectra of the time evolution of diagnosed fluxes of salt and heat at the air-sea interface (due to the relaxation towards linearly time-interpolated SST and SSS data) ;

TURBULENT STRUCTURE FUNCTIONS IN GEOPHYSICAL FLOWS

O. Ben Mahjoub*, J. M. Redondo and R. Alami

Dept. Fisica Aplicada, (*Estadistica) Universitat Politècnica de Catalunya, Campus Nord B5, 08034 Barcelona, Spain

Abstract

In geophysical flows, there are many instances, where turbulence is originated locally, such as in surface wave breaking at the surfzone or by internal wave breaking in the lee of a mountain. The use of velocity structure functions and their moments may give an indication of the spatial and time delay from the source of turbulence. The variation of the structure functions and the scaling exponents in decaying non-homogeneous turbulence flows produced by a grid is investigated by means of sonic velocimeter SONTEK3-D. In the analysis we invoke the concept of the Extended Self Similarity (ESS) and find that there are changes in the structure functions related to the intermittency.

Keywords: Turbulence

Introduction

In recent years, new interest has emerged concerning the scaling properietes of turbulence flows. They are reflected in the scale invariance of Navier-Stokes equations, both in two dimensions (2D) and three dimensions (3D).The statistical behaviour of two-dimensional and three-dimensional fully developed turbulence at large and small scales has been investigated as shown by Sreenivasan [1]. A common way to approach this problem is through the velocity structure functions. Usually the scaling properties of moments of velocity differences at the scale r $S_p(r)$ are investigated using the following definition:

$$S_p(r) = \left\langle |V(x+r) - V(x)|^p \right\rangle = \left\langle |\delta V(r)|^p \right\rangle \quad (1).$$

where $\langle ....\rangle$ stands for ensemble average and the V is the velocity component parallel to r. At high Reynold number, $Re = U_o L/\nu$ the structure function $S_p(r)$ satisfies the relationship :

$$S_p(r) \propto r^{\zeta p} \quad (2).$$

For turbulence within the inertial subrange $L > r >> \eta$ where the L is the integral scale, $\eta = (\nu^3/\varepsilon)^{1/4}$ is the Kolmogorov scale,

$\varepsilon = 15\nu\left\langle \left|\frac{dv}{dx}\right|^2 \right\rangle$ is the mean energy dissipation rate, ν is the fluid kinematic viscosity and U_o is the mean velocity of the flow [2,3].

In general, one can define the scaling exponents $\zeta(p)$ of the structure functions $S_p(r)$ in the inertial range by the relation (2), or its equivalent scaling expression : $\langle V(L)^p\rangle = \langle L^{\zeta p}\langle \epsilon(L)\rangle^{\zeta p}$. Kolmogorov's 1941 theory (K41)[4], predicts that the statistical properties of $\delta v(r)$ depend only on ε and r, it then follows by dimensional analysis that $\zeta(p) = \frac{p}{3}$, but in recent years many experimental and numerical simulations at very high Re [1], have shown that Kolmogorov scaling is violated in the the inertial range. Therefore, scaling exponents $\zeta(p)$ are a nonlinear function of p [5].

From a practical point of view, the inertial range is defined by the range of scales where the third-order structure function S_3 follows the K41 law:

$$S_3 = -\frac{4}{5}\varepsilon r \quad (3).$$

The larger the Reynolds number, the broader the inertial range but for low to moderate Reynolds numbers accessible to direct numerical resolution, this range is often very narrow.

Extended Self-Similarity (ESS)

The Extended Self-Similarity is a property of the velocity structure functions of homogeneous and isotropic turbulence. It was recognized by Benzi *et al.* [2], that the moments of any order may be plotted as a function of another order, then the scaling is much more pronounced and there seems to be self-similarity for a larger range of scales:

$$S_n \approx S_m(r)^{\zeta(m,n)} \quad (4).$$

where $\zeta(m,n) = \frac{\zeta(n)}{\zeta(m)}$. In the other words, the ratio of two scaling exponents remains constant for a wider range of scales than when taken separately, the reason for this behaviour is still not clear. As was show in [6,7], the ESS scaling comprises not only the inertial range, but reaches as far down as few Kolmogorov scales η.

We have taken advantage of this property to compute scaling exponents $\zeta(m,n)$ with higher accuracy than by spectral methods even at relatively moderate Reynolds numbers. Another important feature of ESS that we exploit in this paper, is that providing information in terms of the relative scaling exponents $\zeta(m,n)$, is universal in geophysical flows, in the sense that they remain valid also in 2D case [8]. But this kind of universality, observed in different flows, disappears if the system is influenced by the presence of strong shear as shown in experiments in wakes behind a cylinder [9] and in boundary layer turbulence [10].

In our study we use $m = 3$ and $\zeta(m) = 1$ derived exactly by Kolmogorov equation, so we determine the scaling of the modulus of any structure function with respect to the modulus of the third order structure function using the following expression :

$$\left\langle |\delta V(r)|^n \right\rangle = A_n \left\langle |\delta V(r)|^3 \right\rangle^{\zeta(n)} \quad (5).$$

where $\delta V(r) = V(x+r) - V(x)$, and $\zeta(n)$ the scaling exponents of the order n. With the resolution of our data, we were able to study the structure functions up to 6th order.

The experimental apparatus

We study the structure functions and their scaling exponents in decaying non-homogeneous turbulence produced by a grid as a model of geophysical turbulence decaying as we move away from the source of the turbulence. The turbulent velocity fluctuations in an open water flume are measured with an ultrasonic velocimeter SONTEK3-D, (Vx,Vy,Vz). The flume has a test section with a length of 1 m, base cross-section, 0.15 m, and height, 0.3 m. The grid used had a mesh of 0.008 m with a corresponding bar size of 0.002 m and a solidity ratio of 0.34 and was placed 0.06 m downstream of the flow inlet. The mean velocity ranged between 0.04 - 0.3 (m/s). The sampling volume of the sonic velocimeter SONTEK3-D was about 5.10^{-9} m^3 measured at a distance of 0.005 m to 0.008 m from the sensor tips. The sampling frequency was 25Hz. Velocity time series were recorded at a number of control points in the wake of the grid, all of them were centered on the axis of simetry of the tank, at the following downstream distances from the grid : X = 0.105 m, 0.155 m, 0.205 m, 0.255 m, 0.305 m, 0.355 m, 0.405 m and 0.455 m, each time series, with practically constant average mean velocity, in our experiment consisted of around 4000 samples. The velocity time series were transformed from time to spatial domain, this was accomplished by means of Taylor's hypothesis in order to evaluate the structure functions defined in (1). It has to be noted that in presence of large coherent structures Taylor's hypothesis is known to give inaccurate results [11].

Experimental results

The Reynolds number $Re = \frac{u_{mean} L}{\nu}$ was found to vary with the downstream distance from the grid. Its dependence on $\frac{X}{M}$, where X is the distance from the grid and M is the mesh of the grid, is $Re = 630\left(\frac{X}{M}\right)^{-1.27}$ between Re = 11000 and Re = 71000.

The dependence of the structure functions $S_p(r)$ with p = 2,3,4,5,6 on the separation distance r normalized with respect to the Kolmogorov length scale η is shown in Fig.1, for the downstream distance X = 40.5 cm. The structure functions $S_p(r)$ are recovered from the time series by means of the standard Taylor's hypothesis [3], as mentioned above, due to the moderate to low Reynolds numbers in our experiment one can hardly find a range where the spectrum slope remains constant so in principle we can not determine the scaling exponents with the required accuracy. For calculating the scaling exponents for such flows, similar to those encountered in the ocean and the atmosphere, we use Extended self-similarity (ESS), and the structure functions $S_p(r)$ are plotted against $S3=\langle|(V(x+r)-V(x))|3\rangle$. It has also been verified, following Benzi *et al.* [6], that for our data the behaviour $S3=\langle|(V(x+r)-V(x))|3\rangle$ scales in a similar way as: $s_3=|\langle(V(x+r)-V(x))^3\rangle|$. This possible difference due to the use of the absolute value of the velocity signals has centered the reservations on ESS by Streenivasan [1].

We checked the relationship $\frac{S_3}{s_3}$ for different distances from downstream from the grid for our 3D moderate Reynold turbulent flow, as shown in Fig. 2. We show in Fig. 3, the structure functions of order p up to 6th order *versus* $\frac{r}{\eta}$. The data is the same as shown in fig.1 for values $\frac{r}{\eta} > 100$, with $\eta = 0.008$ m, there the scaling exponents could not be determined with the required accuracy but from the representation in Fig. 3 we can observe a much better scaling.

It was found [10] that changes of the limits of the ESS range could influence the values of the scaling exponents, providing the main source of error, it is then necessary to determine the limit of the scaling range, and avoid using the fits outside the inertial subrange, so we define a uniform criteria for the determination of the lower and the upper bounds of the ESS range.We can take the lower bound equal to a certain multiple of the Kolmogorov scale η.

CIRCULATION VARIABILITY IN THE CHANNEL OF SARDINIA OBSERVED FROM IN SITU AND ALTIMETRIC DATA

Catherine Bouzinac [1], Jordi Font [1*], Claude Millot [2], and Jorge Vazquez [3]

[1] Institut de Ciencies del Mar, CSIC, P. Joan de Borbó, 08039 Barcelona, Spain
[2] Laboratoire d'Océanographie et de Biogéochimie, COM-CNRS, BP 330, 83507 La Seyne sur Mer, France
[3] Jet Propulsion Laboratory, California Institute of Technology, Pasadena, USA

Abstract

The channel of Sardinia is one of the less known areas of the Western Mediterranean sea and the circulation paths of the different water masses in this wide passage are still debated. *In situ* data from the PRIMO-1 experiment and merged TOPEX/Poseidon plus ERS-1 altimetric maps have been used to verify hypotheses about the possible migration of deep mesoscale eddies from Algeria to Sardinia and their effect on the circulation. Current meters were deployed on the Sardinian slope, Tunisian slope and central part of the channel from November 1993 to October 1994. No seasonal variations have been clearly detected, but the mesoscale variability is large in the western part of the channel and has a deep signature. A CEOF analysis of the Sea Level Anomaly maps (derived from altimetric data) has been used to see the correlation of the different dynamical features of the observed variability.

Key-words: mesoscale phenomena, currents, straits and channels, remote sensing, western Mediterranean

Introduction

The Algerian basin is characterized by a large mesoscale turbulence and acts as a buffer zone which partially disconnects the flux coming in at Gibraltar from the flux going out in the channel of Sardinia (1,2). The channel of Sardinia is the passage between the Algerian basin, on the west side, and the Tyrrhenian basin and the channel of Sicily on the east side, limited by the Sardinia island and the northern Tunisian coast. The sill is at about 2000 m near 9°E. Four different water masses have been identified by previous studies in the area: the Modified Atlantic Water (MAW), the Levantine Intermediate Water (LIW), the Tyrrhenian Deep Water (TDW) and the Western Mediterranean Deep Water (WMDW), but the circulation paths of these water masses in this wide passage are still debated. Recent XBT data (3) confirm that anticyclonic eddies, generated by instability of the Algerian current, are advected toward the channel and, before reaching it, they deviate northward and westward following the deep bathymetry. They can strongly interact with the current and influence the circulation in the channel at different depths.

In this presentation we summarize the results of two recent papers on the circulation variability in this region, one based on *in situ* measurements (4) and the other on satellite altimetry (5).

As part of the PRIMO-1 experiment, hydrological data were collected with a CTD probe at 13 stations along a cross section of the channel near 8.9°E (Fig. 1) in November 1993. Deployment and recovery of current meters was done in several times between November 1993 and October 1994 at four different points called N, O, S and E (Fig. 1). During the first deployment period a lot of instruments were lost due to a material failure, and as a consequence the recorded data were only partial: N (100 m - 8 months, 300-8, 1000-11, 2000-11), O (200-5, 2700-5), S (450-5, 1000-1, 2500-6), E (1800-6).

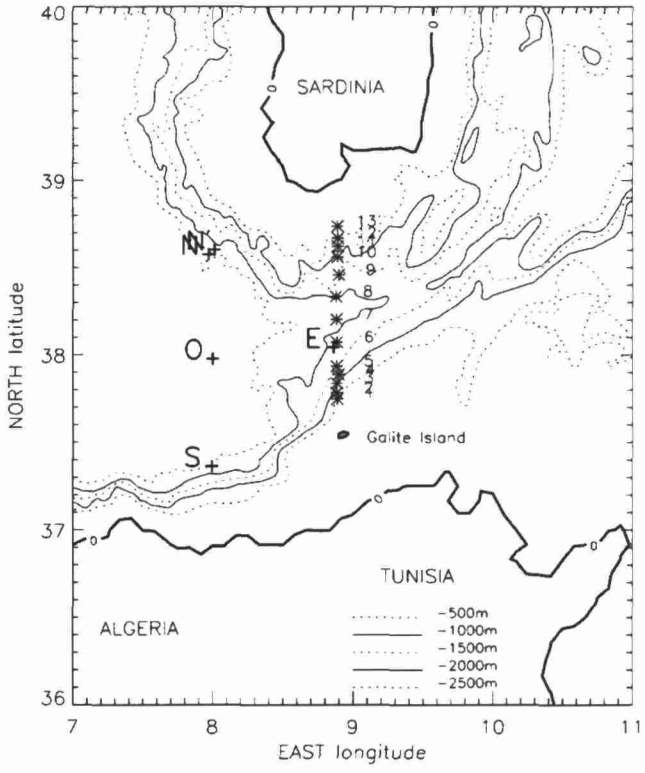

Figure 1: Location of the 13 CTD casts (*) in November 1993 and the 4 mooring points (+) of PRIMO-1 in the channel of Sardinia.

The TOPEX/Poseidon and ERS-1 altimeters provide complementary space and time sampling of the oceanic circulation. The data of both satellites have been merged on a common period, from October 1992 to December 1993, by CLS Toulouse (6). The lack of knowledge of the geoid impedes the use of the absolute heights of the sea level. So, the Sea Level Anomalies (SLA) relative to the annual mean have been calculated, and gridded every 10 days with a spatial resolution of 0.2° using an objective analysis scheme. For the present study, the data in the area of 0-15°E and 35-40°N have been extracted, to focus on the MAW flow until its entry in the eastern Mediterranean sea. The resulting 44 maps that are regular in time and space have been used to perform a Complex Empirical Orthogonal Functions (CEOF) analysis in order to extract the information on the variability of spatially correlated signals.

Results : *in situ* data

The in November 1993 hydrological section presents the low salinity MAW flowing eastward at the surface on the Tunisian slope (Fig. 2, left). This situation could correspond to an unperturbed alongslope vein crossing the channel of Sardinia in its path to the Tyrrhenian Sea and strait of Sicily, according to the classical schemes for the western Mediterranean surface layer circulation. Unfortunately, no current meter record was obtained within the surface layer in this southern part to account for the time evolution of the current. A secondary salinity minimum found in the northern part of the CTD section, together with westward geostrophic velocities (Fig.2, right), indicate that old MAW is re-introduced in the Algero-Provençal basin along the continental slope of Sardinia, after having circulated in the Tyrrhenian sea. Below it, a temperature minimum at 100-150 m identifies another water mass also flowing in the same direction, well separated from the vein of subsurface Winter Intermediate Water (WIW) circulating eastwards at the same depth in the southern half of the channel.

The current meter mooring situated on the Sardinian slope in the western opening of the channel shows an intense and very variable circulation at 100 m, while below the surface layer the motion is predominantly along the slope, although also affected by significant mesoscale variability. In spite of the low correlation between the records at 100 and 300 m, an Empirical Orthogonal Function analysis has shown that more than 90% of the variability at both levels can be explained by one single statistical mode. This means that the flow can be strongly perturbed by mesoscale events at least in the whole surface and subsurface layers. The stick diagrams show that in most occasions these events have an anticyclonic nature. Following the lag in the correlation between the records in the center and the north of the channel, they are usually propagating northwards with intense southward currents. These could be associated with the eastern edge of anticyclonic eddies being detached from the Algerian current region maybe due to topographic constraints. In the centre of the channel, no clear geostrophic motion (Fig. 2) is associated with the intermediate layer LIW core (250-400 m), so that the "coming from" or the "going to" of this water mass cannot be specified. Nevertheless, the important mesoscale activity that prevails in the surface layer could have a considerable influence on the intermediate circulation. Anticyclonic eddies, as described by Benzohra *et al.* (7), can reach the channel with a deep conical extension and can strongly interact with the surrounding superficial and intermediate waters. At the intermediate layer the currents recorded near the slopes at the western opening of the channel (S 450 m and N 300 m) indicate a cir-

LONG TERM VARIABILITY OF THE MEDITERRANEAN LARGE SCALE CIRCULATION

Jean-Michel Brankart * and Nadia Pinardi

Istituto per lo studio delle Metodologie Geofisiche Ambientali, CNR, Via P. Gobetti, 101, I - 40129 Bologna, Italy

Abstract

It is now well established that the Mediterranean Sea general circulation exhibits a strong interannual variability, appreciably affected by seasonal influence, and notably dependent on decadal and interdecadal changes. The purpose of this contribution is to show that existing long term global data sets contain sufficient information to diagnose a significative part of this signal. In particular, an analysis of SST interannual anomalies over the gulf of Lions is presented, revealing a clear signature of 2, 3 and 6 years periodicities in that region.

Key-words : circulation models

The Mediterranean Sea general circulation has been found recently to be strongly dependent on the time variability of the forcing at the air-sea interface (1). In various part of the basin, observations clearly indicate that currents can be very different form season to season and from year to year. Water masses formation rates are found to vary interannually and water mass properties can evolve on much longer time scales.

The outstanding coupled seasonal and interannual signal stands out from many observation. In particular, the Winter season shows the greatest water mass formation interannual variability due to the strong air-sea coupling at the level of momentum, heat and water fluxes. The Summer season shows instead the largest interannual variability in the current regimes, anticyclonic versus cyclonic surface flow field, temperature of the mixed layer.

Even sub-basin scale gyres can change or disappear from year to year. For example, the Shikmona gyre was not present from 1979 to 1982 but became persistent ever since or with occasional disappearances (2, 3) ; the Iera-Petra gyre, not previously mentioned in the Levantine basin circulation, has been the largest sea surface height anomaly from 1992 to 1994, as revealed by satellite dynamic topography (4).

Decadal or interdecadal changes are recorded by strait transports and by the recently discovered change in the Eastern Mediterranean abyssal circulation (5). The latter occured during the first pentade of the nineties, perhaps due to a combination of decadal salinity changes and interannual variability of the atmospheric forcing over the Levantine and Aegean sea regions.

Despite of all those observational evidences, theories explaining seasonal-interannual-decadal changes in the Mediterranean Sea general circulation and its associated water mass properties have not been formulated for the whole interacting system. Seasonal and interannual variability has only been interpreted as a response of the basin to the atmospheric forcing variability at the corresponding time scales (6, 7). In particular, wind forcing was found to be responsible for more than 70 % of the basin current kinetic energy ; its changes in magnitude and direction can cause very rapid changes in circulation structures (8).

Numerical simulations show already that anomalous amplitude of the winter wind stress curl can induce changes susceptible to modify the regular occurence of the seasonal cycle in the basin (1).

But observation suggest that other sources of energy should be searched for. It seems for instance quite difficult to explain such radical changes in sub-basin scale gyres (especially in the Eastern Mediterranean) without invoking additional mechanisms, such as internal non-linear energy redistribution / dissipation or topography trapping. However, initial results from numerical simulations suggest that the internal variability due to nonlinear processes can be small with respect to the interannual signal directly forced by atmospheric forcing. Theoretical investigation should continue to investigate the possibility of topographic interactions as directly responsible for the persistence of anomalous features in the basin.

However, a general conclusion that comes out from that observational as well as theoretical picture, is the necessity of a global approach across the time scales (from seasonal to decadal) and over the whole basin. Indeed, due to the strong coupling between the different processes involved, there is a need for a comprehensive and coherent study of atmospheric forcing and hydrographic parameters together with long term numerical modelling. The purpose of this contribution is to show that long term global data sets contain an interannual variability signal as well as numerical simulations.

As surface atmospheric data, we use the COADS fluxes (9), extending from 1946 to 1993. Theses fluxes are used to force a general circulation model implemented on the Mediterranean (1), with an horizontal resolution of a quarter of a degree and 31 vertical levels. On the other hand, the MODB and MEDATLAS hydrographic data bases provide an adequate interannual data coverage for about the same period. It is indeed possible to show that, using the final MODB monthly climatological cycle (10) as reference, we can obtain a relevant estimation of the interannual temperature signal for this full period, nearly everywhere in the basin. This remarkable property comes from the very long horizontal correlation length that we can use to analyse temporally the interannual anomalies.

As an example, we present here (fig. 1) the interannual SST signal objectively analysed from the MODB data, in the Gulf of Lions area, using a 45 days correlation time scale. The solution obtained, sampled every month, extends from 1950 to 1990. A spectral analysis of this time serie (fig. 2) reveals three powerful periodic components emerging from the noise, at the 6, 3 and 2 years time period (respectively 1/6, 2/6 and 3/6 years^{-1} frequencies). Let us also note that the peaks observable at the frequencies 0 years^{-1} (annual climatic mean) as well as at 1 years^{-1} (with all harmonics, seasonal cycle anomaly) represents a correction that this time analysis would suggest to the background climatology that we have used (that did not care of the year to year repartition of the data).

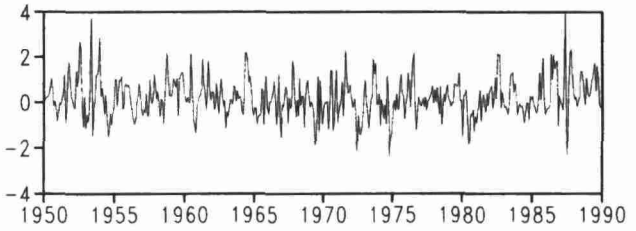

Figure 1 : SST interannual anomaly in the gulf of Lions area, objectively analysed from the MODB data, using a 45 days correlation function. The solution, sampled every month, extends on 40 years from 1950 to 1990. It is expressed in Celsius degrees.

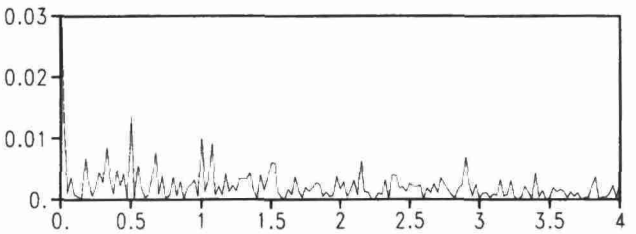

Figure 2 : Power spectrum (computed by FFT) of the time serie represented on figure 1. Frequencies are in years-1. The 2, 3 and 6 years periods are clearly emerging.

Figure 3 compares the reconstructed signal for the window of period ranging from 2 to 10 years (dashed line) to the 6 years periodic signal reconstructed from the three main frequencies (continuous line). (The latter was reconstructed for a spectrum computed for the last 36 years, in order for the main frequencies to correspond exactly to the spectrum discretisation values). Except for the 1964 to 1972 period where a 3 years signal seems to come up, this figure shows that this time window (2 to 10 years) is strongly dominated by the 3 frequencies mentionned before. We should consequently be able to track back those periodicities in the atmosphere, especially in the North Atlantic Oscillation which governs the Western Mediterranean

DYNAMICS OF A MID-ADRIATIC COASTAL AREA. FIRST EXPERIMENTAL RESULTS OBTAINED IN THE FRAMEWORK OF PRISMA-2 PROJECT

G. Budillon*, M. Moretti, E. Sansone, G. Spezie

Istituto di Meteorologia e Oceanografia. Istituto Universitario Navale.
Via Acton 38, 80133 Napoli. Italy

Abstract

The Adriatic Sea coastal area offshore Ancona (Italy) has been intensively investigate in the framework of the Italian national PRISMA-2 project. Hydrological and current meter data collected during the first summer leg (July-September 1996) have been analyzed; preliminary results show typical synoptic dynamics resulting from the combination of the thermohaline field with the atmospheric forcing. We computed the alongshore transport by means of the geostrophic method adjusted with current meter data; the results show an average southeast transport in the surface warmer layer of about $55*10^3$ m^3/s. This coastal flow carry on also the fresh waters originated from the dilution of the river outflow in the northern Adriatic Sea. This fresh water transport estimation is about $2*10^3$ m^3/s. These measurements were made at the beginning of September 1996 with very favorable meteorological conditions, therefore we can suppose our estimation not affected by external forcing as the wind stress.

Key-words : Adriatic Sea, coastal waters, water transport

Introduction

Recently the Italian coastal areas of the Adriatic Sea have been intensively investigated in the framework of the Italian national PRISMA-2 research program that is a multidisciplinary study focused on the physical and biochemical processes which determine the fate and the distribution of all the pollutants discharged in the Adriatic Sea.

The general circulation of the Adriatic Sea, as derived by several experimental and modeling studies, shows a seasonal and annual dependent cyclonic characteristic. Typically the surface circulation in the southern and middle Adriatic Sea consists of a smooth flow encircling cyclonically the entire basin, while during the winter the general circulation consists of several cyclonic gyres (1, 2, 3).

The cyclonic circulation of the Adriatic Sea is intensified in the central coastal region, about at latitude 43.5° N, where the local bathymetry shows a strong inclination over a wide longhsore area (4).

The flow along the Italian coastlines is also characterized by the presence of fresh waters coming from the river discharges and transporting substances as pollutants and nutrients. Furthermore coastal waters offshore Ancona, as literature reports on the basis of some hydrological surveys, show a strong seasonal variability of the physical and bio-chemical parameters depending on river discharges.

Sampling

During the summer 1996 synoptic surveys (3÷4 days each) were carried out, at interval of about one week, along the coastal zone offshore Ancona, performing hydrological casts along transects perpendicular to the coast and to the expected flow (see figure 1). These transects have been extended to include the coastal waters, the frontal area and the "open sea". The position of frontal system was detected on the basis of synoptic surface measurements collecting continuously temperature and salinity (conductivity) data during a fast survey previously carried out. During the summer, the presence of the front was revealed mainly by the strong changes in salinity values more than in temperature.

Simultaneously current meter time series were collected by three moored instruments positioned in two locations of the studied area (figure 1).

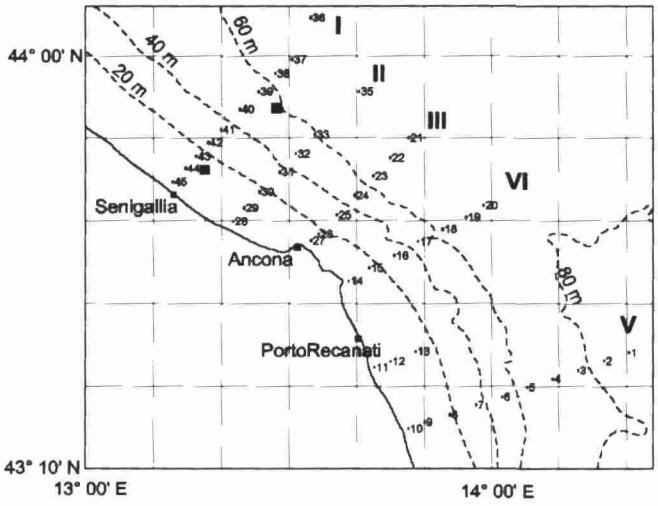

Figure 1 : Hydrological casts and mooring positions. Isobath are show every 20 meters.

Discussion

Typically the vertical structure of the water column (as shown in figure 2) exhibits the presence of a coastal low salinity zone with the minimum close to the surface. The solar heating, especially in this period, affects the surface layer with a well developed thermocline. Below it two water masses may be identified mainly on the basis of their salinity values. Maximum salinity values highlight the influence of the Modified Levantine Intermediate Water (MLIW) in the eastern (right) flank of the section, while close to the bottom, in the western continental slope, relatively low salinity and temperature values are mostly indicative of waters originated in the Northern Adriatic Sea during the winter season [5].

From these hydrological and current meter data we calculated the alongshore transports in this area. The results reported in the table are concerning with the data collected during the survey of 2-4 September 1996. These measurements have been made at the end of a period in which the meteorological conditions were favorable and consequently we can suppose these values representative of a state not affected by the atmospheric forcing (wind stress).

Transport values have been obtained on the basis of the classical geostrophic method imposing the zero reference level, on first step, at the base of the thermocline (at about 10-20 meters depth, see figure 2). Subsequently the data have been adjusted using the low-pass filtered current meter time series recorded in two different sites (figure 3).

Results

In table 1 we reported the transports, obtained along five sections performed from Senigallia to Porto Recanati (figure 1), computed for the two alongshore directions.

Table 1 : Transport estimations calculated from hydrological and current meter data collected during 2-4 September 1996.

Section number	Transport of "marine" water m^3/s		Transport of fresh water m^3/s	
	SE	NW	SE	NW
I	62670 (83%)	12483 (17%)	2998 (99%)	38 (1%)
II	54893 (77%)	6803 (23%)	1924 (98%)	36 (2%)
III	37304 (73%)	13459 (27%)	1428 (92%)	130 (8%)
IV	54745 (80%)	13456 (20%)	1975 (97%)	57 (3%)
V	66132 (77%)	19218 (23%)	2024 (90%)	234 (10%)
Mean	55154 (78%)	13084 (22%)	2070 (95%)	99 (5%)

Obviously, along the southern-east direction we found larger transports (78%) which are bordered in the coastal flow of warmer water over the thermocline.

The concentration of the fresh water was calculated by the:

$$C = \frac{\bar{S} - S}{\bar{S}}$$

where $\bar{S}$ is the salinity of the local MLIW and S the salinity of the southeastern flow; integrating over all the transect we obtained the "fresh" transport reported on table along the sections of figure 1. It is clear, from figures 2 and 4, that the low salinity values are close to the coast and, obviously, over the thermocline therefore these fresh waters are carried out in the warmer coastal layer.

The mean transport of about 2000 m^3/s obtained for the fresh water is consistent with the total fresh inflow of all rivers discharged in the northern Adriatic Sea (that is about twice of the Po river one) [6].

Some changes of the calculated transports in the different sections (particularly between the first and the others) can be due by the distinct geo-

BUOYANCY FLUXES IN THE AEGEAN SEA

P.G. Drakopoulos [1*], S. Poulos [2], A. Lascaratos [3]

[1] Department of Environment, Institute of Marine Biology of Crete, PO Box 2214, 71003, Iraklio Crete, Greece
[2] National Centre for Marine Research, Hellenikon 166 04, Athens, Greece
[3] Laboratory of Meteorology, Department of Applied Physics, University of Athens, Panepistimioupolis, Build. PHYS-V Athens, 15784 Greece

Abstract

Recent observations have shown that outflowing Aegean waters have replaced about 20% of the deep and bottom waters of the eastern Mediterranean basin. This indicates changes in the hydrology of water masses in the Aegean Sea and the corresponding thermohaline circulation. In this work we estimate the driving mechanism of the thermohaline circulation, the buoyancy fluxes using 45 years of COADS data. The long term buoyancy loss is estimated to be about $5x10^{-6}$ kg m^{-1} s^{-3}. However for certain periods lasting a few years the flux reverses sign and there is buoyancy gain . The reversal of sign is expected to lead in changes of the thermohaline circulation in the basin.

Key-words: air-sea interactions, river input, hydrology, Aegean Sea

Introduction

The Aegean Sea constitutes the northeasterly part of the eastern Mediterranean Sea located northward to the island of Crete . It covers an area of approximately $1.8x10^{11}$ m^2 containing a water volume of some $7.4x10^{13}$ m^3 [1]. The basin has a complex topographical structure with irregular bathymetry (water depths >2,000 m). At its northeastern end, the Aegean Sea exchanges flows with the Black Sea through the Sea of Marmara and the Dardanelles. To the south, the Aegean Sea communicates with the open (eastern) Mediterranean Sea through the Cretan Straits.

Recent developments in the understanding of deep water formation in the eastern Mediterranean Sea have shown that a water mass (Cretan Deep Water (CDW)), originating in the southern Aegean Sea, exits through the Cretan Straits; it sinks there in the deep layers of the adjacent SE Ionian and NW Levantine Seas [2]. Furthermore, Aegean Sea water has replaced about 20% of the deep and bottom waters of the eastern Mediterranean basin [3]; it was believed previously that the only source of such waters was the Adriatic Sea. This influx has induced changes in the overall characteristics and upward displacement of older waters of the Eastern Mediterranean and is caused by an increasing salinity and thermohaline circulation pattern changes in the Aegean Sea waters.

The present investigation examines, against this background, the water budget, the freshwater balance and the buoyancy fluxes in the Aegean Sea, as this is implied by heat budget calculations, freshwater inputs, and horizontal advection of sea water masses (*i.e.* Dardanelles Strait exchanges).

Water Budget

The water balance (W) of the Aegean Sea is descibed by the relationship:

$$W = P+R+E+B\pm C$$

where, P is the amount of precipitation, R is the river runoff, E the evaporation, B is the inflow from the Black Sea and C is the exchange of fluxes between the Aegean and the open (eastern) Mediterranean Sea.

Precipitation

Annual precipitation over the Aegean Sea varies generally between 400 and 700 mm per annum [4], with a mean annual relative humidity of between 65% and 75%. Observed levels of precipitation, representing mean monthly precipitation levels based upon daily average measurements from 10 coastal meteorological stations over a 16 year period (1975-1990), were between 372 mm (Athens) and 672 mm (Rhodes), with an overall mean value of some 495 mm yr^{-1}

River inputs

The Aegean Sea receives the freshwater outflows from various Greek and Turkish rivers discharging along its coastline. The main Greek rivers (Axios, Aliakmon, Gallikos, Pinios, Sperchios, Evros, Strimon and Nestos) provide some $19x10^9$ m^3 of freshwater whilst the smaller Turkish rivers (K. Menderes, Bakir, Gediz, Kuguk Menderes, and Bujuk Menderes) discharge some $5.1x10^9$ m^3 [5]. The previous referred discharge levels represent only part of the river catchment area (60-90%) as the location of the gauge stations do not coincide with the river mouths. In addition to the riverine supply, a substantial water inflow is attrributed to the sewage outfall of the numerous cities located adjacent to the coastlines; for example, Athens discharges some $0.22x10^9$ m^3 yr^{-1} of waste [6]. Hence, the total amount of freshwater water inputs (R) to the Aegean Sea is expected to reach as much as $25x10^9$ m^3 yr^{-1}, when the inputs of the numerous small ephemeral rivers and torrents are incorporated into the total water discharge of the main river systems.

Evaporation

The evaporation rate is derived by evaluating empirical bulk formulae. Here we adopt the estimation of Poulos *et al.* [5] which is based upon the calculation of the overall heat budget of the Mediterranean Sea, on the basis of monthly observations averaged for a long period (1945-1990); the source of data was the COADS (Comprehensive Ocean Atmospheric Data Set [7]). The estimated value is -104 Wm^{-2} which corresponds to an evaporation rate of 1.3 myr^{-1} .

Black Sea Waters.

The Aegean Sea receives the colder and less saline Black Sea Water (B) though the Dardanelles Strait, where a two-layer stratification and opposing flow circulation has been established, on the basis of density differences between the Aegean and Black Sea waters [8]. Furthermore, the two different water masses are separated by a pycnocline, at an average depth of 25 m. The upper layer is occupied by the less saline (S=29.6 psu) Black Sea Waters (B) and the lower layer by the more saline (S=38.9 psu) Aegean Sea Waters [9]. The surface layer in the Dardanelles flows towards the Aegean Sea, at velocities ranging between 50 and 200 cm s^{-1} wlile the bottom layer moves in the opposite direction, towards the Sea of Marmara, with velocities ranging from 20 to 40 cm s^{-1} [10]. Thus, Umluata [9] have calculated that some 1257 km^3 of colder and fresher water outflows annually into the Aegean Sea whilst, at the same time, 957 km^3 of the more saline Aegean Sea Water enters the Sea of Marmara through the Dardanelles Strait. The former implies a net annual water inflow to the Aegean Sea equal with 300 km^3.

The annual mean components comprising the water balance of the Aegean Sea are presented on Table 1.

Table 1 : The main components of the annual water balance of the Aegean Sea.

	(m yr^{-1})
Precipitation (P)	+0.5
Evaporation (E)	-1.3
River Runoff (R)	+0.1
Black Sea Water (B)	+1.7
Water balance (W):	+1.0

The annual amount of evaporation (E) over the region exceeds the sum of precipitation (P) and river runoff (R). However, if the net Black Sea Water inflow (B) is considered, then the water balance of the Aegean Sea is positive (*i.e.* P+R+B-E>0) indicating net outflow through the Cretan Straits.

Estimation of Fresh Water Balance

The amount of equivalent fresh water input from the Black Sea V_f is given by:

$$V_f = \left[V_b \frac{V_a + V_b}{V_a + V_b} - 1 \right]$$

where V_b is the outflow from the Black Sea with salinity S_b and V_a is the volume of the Aegean with mean salinity S_a. The salinity of the Black Sea outflow is ~29.6 psu and the mean salinity of the Aegean ~38.9 psu. Assuming the net volume transport through the Dardanelles

INTERANNUAL SEA LEVEL VARIABILITY IN THE MEDITERRANEAN SEA AND ITS RELATION TO LOCAL METEOROLOGICAL FACTORS

P.G. Drakopoulos [1*] and A. Lascaratos [2]

[1] Department of Environment, Institute of Marine Biology of Crete, PO Box 2214, Iraklio Crete, 71003 Greece
[2] Laboratory of Meteorology, Department of Applied Physics, University of Athens, Panepistimioupolis, Build. PHYS-V Athens, 15784 Greece

Abstract

The response of the sea level in the Mediterranean to local meteorological forcing for time scales larger than the seasonal is examined. Multiple regression has indicated that the average sea level response to local air pressure is ~-0.8 cm/mb (15% of variability), and decreases toward the Eastern Mediterranean with no significant frequency dependence. The response to local wind stress is responsible for no more than 2% of the sea level variance and for most stations maximum response is in a cross shore direction. The annual cycle has amplitude ~5 cm (25% of variance) and peaks in October. According to these findings, almost 60% of variance cannot be explained by local meteorology.

Key-words: air-sea interactions, wind, time series

Introduction

The interpretation of sea level changes and variability is a complex task involving consideration of many factors. Sea level records comprise both mean sea level variability and adjacent land vertical movements. The former is a superposition of many different forcing factors operating at different time scales. For scales larger than the annual, the interpretation becomes rather difficult since the forcing is not always direct but a result of numerous positive and negative feedbacks between the atmosphere and the ocean. This variability (interannual and interdecadal) can be significant in certain parts of the world ocean hiding secular sea level changes. Due to the almost closed nature of the Mediterranean basin, climatic changes are expected to leave stronger footprints on the sea level records. Previous work in the Aegean, Ionian and Adriatic Seas [1, 2, 3] have shown that in fact this is the case in Eastern Mediterranean where sea level changes at interannual time scales can easily exceed 15 cm. In this work, we examine the effect of local meteorological factors on sea level variability, for scales ranging from seasonal to interannual and for the entire Mediterranean. Where possible, the interpretation is both qualitative and quantitative.

Data and methods

For sea level data, the PSMSL database for the Mediterranean was employed. In addition, for the Aegean and Ionian Seas, the PSMSL time series were updated with recent data obtained from the Hellenic Navy Hydrographic Service. Only the Revised Local Reference (RLR) records were analyzed since these time series have the monthly means reduced to a common datum making use of the tide gauge benchmark datum history and thus are suitable for time series analysis. A total of 76 RLR time series were analyzed, some of them going back to 1880 and some as recent as 1991. Unfortunately, with the exception of the Port Said record, the series came from the northern coasts of the Mediterranean Sea and only for comparison purposes some metric series from Israel and Africa were also examined. Records from the Black Sea and from the adjacent Atlantic Ocean were also incorporated in the analysis in order to address the spatial extend of the observed variability.

For atmospheric parameters, the COADS global marine database was employed. This database has been collected primarily from ships of opportunity and has an overlap with the temporal range of the sea level records. The data are summarized for each month of each year of the analysis period, in 2°x2° in latitude and longitude boxes. The following parameters which are included in this database were used: Sea level pressure (P), eastward and northward components of wind (u,v), scalar wind (w), eastward and northward components of wind stress (<uw>, <vw>,brackets denote monthly mean). Prior to processing, the time series were checked for spurious spikes. For multiple regression analysis, common overlap blocks between sea level and meteorological forcing were composed. For other analyses where filtering was needed in order to remove the seasonal cycle, gaps were filled prior to filtering based on seasonal means and then a 23 point low-pass triangular filter was applied. For the COADS data set one further step had to be taken. Kaufeld [4] has shown that the algorithm used to convert Beaufort scale to wind speed underestimates wind strength by a factor of about 1.4 depending on the wind speed. This introduces an artificial trend in the data because after 1960 anemometers started coming into use. Parameters having wind as an integral component were corrected in a way similar to Garrett *et al.* [5]. All the examined stations, their locations and the number of overlap PSMSL-COADS monthly data are tabulated in Table 1.

The response to local atmospheric forcing was studied by means of multiple regression in the time domain, using a model similar to that described by Thompson [6]. More specifically, the model used is:

$$h(t) = a_1 P(t) + a_x \tau_x(t) + a_y \tau_y(t) + a_{12}\cos(\omega_{12} t + \theta_{12}) + a_6 \cos(\omega_6 t + \theta_6)$$

where t denotes time (monthly values), h sea level, P air pressure, τ_x eastward wind stress component, and τ_y northward wind stress component. The frequency ω_{12} is that of the annual cycle and ω_6 of the semi-annual. The coefficients a and θ are to be determined by the regression analysis. The sine and cosine terms have been introduced in order to account for seasonal variability other than that present in the pressure and wind stress time series (*i.e.* steric). It should be noted here, that if the assumption of a sinusoidal response of the sea level to the wind stress is assumed, then the coefficients a_x and a_y can be replaced by $a_w=(a_x^2+a_y^2)^{1/2}$, and $\theta_w=\tan^{-1}(a_y/a_x)$. Then a_w represents amplitude of the response, and θ_w the direction of maximum response.

Results

The regression results are tabulated in Table 2 and can be summarized as follows: The response a_p of sea level to air pressure was found to be responsible for about 13% of the variance. For most of the stations was not exactly isostatic, *i.e.* -1.0 cm per mbar. It ranges from 0.0 to -1.8 cm/mb with a mean of -0.8 and a standard deviation of 0.4. Although the distribution of the response parameters is normal, there exists a correlation with longitude significant at $p<.05$. As we move eastward, a_p becomes for most of the stations smaller (less negative). Moreover no correlation was found between latitude and a_p and number of data points of each time series.

The local wind stress was responsible for about 2.5% of the total sea-level variance. Most of stations had a cross-shore maximum response to sea-level. As was the case with pressure, also the response to wind stress was significantly correlated to the longitude, and has a tendency to become weaker towards Eastern Mediterranean.

For the time series that were long enough, multiple regression was also performed in the frequency domain. However we found no significant variation of the response to pressure and wind as a function of the forcing frequency. Also it should be noted that the small amount of variance accounted for by the inverse barometer effect is not unique to the Mediterranean. Similar results have been reported for stations on the west coast of North America [7]. For the seasonal cycle, the average amplitude of the annual signal was about 5 cm and had a phase of ~295 degrees, which corresponds to maximum amplitude during late October. The amplitude exhibited substantial spatial variability resulting mainly from the long term circulation patterns; similar behavior has been observed from TOPEX/POSEIDON altimetry [8]. The semi-annual component of the seasonal cycle had an average amplitude of 2 cm and phase of ~250 degrees (early September). The variance explained by the seasonal cycle was almost 16% of the total (14% annual, 2% semi-annual). The a_{12} amplitude was correlated with longitude, while a_6 was correlated with latitude. In addition, the semi-annual phase was anti-correlated with longitude and correlated with latitude.

Although the variability of the sea-level records increases towards the eastern Mediterranean, the explained variance is higher in West Mediterranean, indicating that the former is more vulnerable to variability originating from other factors such as interannual steric fluctuations and possible vertical land movements (*e.g.* [9]). Concluding, only 31% of the variance was explained by the multiple regression procedure, and 69% of the total variance, most of it at interannual time scales.

Finally, linear trends were calculated for the longer SL records prior and after regression (on residual time series). For these records there exist enough meteorological data in order to avoid aliasing. No significant changes were noted, indicating lack of linear trends present in the meteorological forcing data.

Conclusions

In brief, from this study the following can be concluded: The average sea level response to local air pressure is ~-0.8 cm/mb (15% of variability), and decreases toward the Eastern Mediterranean. There is no significant frequency dependence. The response to local wind stress is responsible for no more than 2% of the sea level variance. For most stations maximum response is in a cross shore direction. The annual cycle has amplitude ~5 cm (25% of variance) and peaks in October. According to these findings, almost 60% of variance cannot be explained by local meteorology. Linear trends were not significantly modified by the exclusion of local meteorology. Most of the interannual variability in atmospheric and oceanic parameters is in phase in both subbasins.

References

1. Manzzarella A. and A. Palumbo, 1985: Long-Period variations of mean sea level in the Mediterranean Area, *Bollettino di Oceanologia Teorica ed Applicata*, 6:253-259.
2. Lascaratos A.and P.G. Drakopoulos, 1993: Interannual sea level variability in the Aegean an Ionian Seas, final report for EEC reserch contract EPOC-CT90-0015.
3. Drakopoulos P.G. and A. Lascaratos, 1993. Interannual variability of the sea level in Eastern Mediterranean, fifth international conference on natural and man-made hazards, 98-99.
4. Kaufeld, L., 1981. The development of a new Beaufort equivalent scale, *Meteor. Rundsch.*, 34: 17-23.
5. Garrett C., R. Outerbridge, K. Thompson, 1993. Interannual variability in Mediterranean heat and buoyancy fluxes, *J. Climate*, 6: 900-910.
6. Thompson K.R., 1986. North Atlantic sea-level and circulation, *Geophys. J. R. astr. Soc.*, 87: 15-32.
7. Chelton D.B. and R.E. Davis, 1982. Monthly mean sea level variability along the west coast of North America, *J. Phys. Oceanogr.*, 12: 757-784.
8. Larnicol G., P.Y. Le Traon, N. Ayoub, P. De Mey, 1995: Mean sea level and surface circulation variability of the Mediterranean Sea from 2 years of TOPEX/POSEIDON altimetry, *J. Geophys. Res.*, 100: 25163-25177.
9. Milliman J.D., 1992. Sea level response to climate change and tectonics in the Mediterranean Sea, in Climatic Change and the Mediterranean, edited by L. Jeftic, J.D. Milliman and G. Sestini UNEP, 45-57.

DOUBLE-DIFFUSION PROCESSES AND LIW CHARACTERISTICS IN THE ALBORAN SEA

M.V. Emelianov*, E. García-Ladona, J. Font
Instituto de Ciencias del Mar, CSIC, P. Joan de Borbo, s/n, 08039 Barcelona, Spain

Abstract
The interaction of warm and salty Levantine Intermediate Water (LIW) with colder and fresher environmental water masses in the Alboran basin (western Mediterranean) creates favourable conditions for small-scale mixing processes. The present analysis is based on the 134 CTD profiles gathered in the Alboran Sea during the Spanish expedition "FE-92" in autumn 1992. The values of the Turner angle calculated for the layers above, below and inside the LIW core, showed the predominance of a diffusive regime on the upper limit of LIW, and a salt fingering on its lower limit in few cases in the western part of the region. The analysis of the spatial distribution of small-scale processes activity, calculated using several statistical properties of the termohaline profiles allows to distinguish the areas of predominance of dia- or isopycnal regime in the small-scale mixing processes. The spatial distribution of diapycnal processes in the upper layer of LIW qualitatively correlates with the vertical velocity distribution, associated with mesoscale features of circulation, as diagnosed by other authors through a primitive equation model with mesoscale resolution.

Key-words: Temperature, salinity, vertical profile, Alboran Sea

Introduction

The mixing processes of LIW occur at different scales in space and time. At small scale, inhomogeneities in the thermohaline profiles account for the occurrence of complex turbulent processes (1). Double-difussion instabilities are one of the characteristic small-scale processes arising from the contrast between warm and salty LIW and colder and fresher environmental water. The presence of small-scale mixing processes manifests in the different forms of fine structure inhomogeneities on the temperature and salinity profiles. These processes are usually divided into two main classes: diapycnal and isopycnal. Diapycnal processes lead, as a rule, to the creation of thermohaline step profiles, whereas isopycnal advection leads to the formation of thermohaline intrusions (2,3). In this manner the shape of thermohaline inhomogeneities in a CTD profile contain information about the processes that formed them. The analysis of the spatial distributions of parameters, calculated from statistical characteristics of fine structure peculiarities in CTD profiles, allows us to determine the type of small-scale processes (dia- oisopycnal) present and detect the areas of their activity in the Alboran Sea.

Materials and methods

To analyse the intensity of the small-scale processes, and how they affect the LIW thermohaline characteristics in the Alboran Sea, 134 CTD profiles from the "FE-92" Spanish cruise in September-October 1992 were analysed.

For the small-scale mixing processes analysis the range of depths was choosen taking into account the typical vertical gradients of temperature and salinity. In this manner three characteristic layers of LIW were determined:
A - the upper layer with positive temperature and salinity gradients;
B - the LIW core with quasi homogeneous distributions of temperature and salinity;
C - the lower layer with negative gradients of temperature and salinity (Fig.1).

To estimate the double-diffusive activity, the Turner angle (Tu) was calculated for each layer with a vertical step of 7 meters:
$Tu = arctg\ (R_\rho) + 45°$,
where $R_\rho = (\alpha dT/dz)/(\beta dS/dz)$ is the density relationship and $\alpha = -(1/\rho)d\rho/dT$, $\beta = (1/\rho)d\rho/dS$ are the thermal expansion and haline contraction coefficients, respectively (4).

The analysis of statistical characteristics of the finestructure inhomogeneities in the thermohaline profiles is based on Pingree's results (5) who showed that:
- for finestructure inhomogeneities resulting from isopycnal advection (isopycnal regime) $\alpha T'/\beta S' = 1$, where T' and S' are the temperature and salinity inhomogeneity, respectively;
- for finestructure inhomogeneities resulting from vertical mixing (diapycnal regime) $\alpha T'/\beta S' = R\rho$.

The finestructure inhomogeneities obtained by separating the original CTD profile into mean and pulsating components by HF filtering, form a cloud of points on the $/\beta S', \alpha T'/$ - plane. This cloud of points has a determined inclination angle φ_p (Pingree angle) to the $\beta S'$-axis. By evaluating the proximity of $tg\varphi_p$ to $tg\varphi_i = 1$ (isopycnal regime) or $tg\varphi_d = R\rho$ (diapycnal regime) we can determine the degree of isopycnicity or diapycnicity of finestructure inhomogeneities. The parameter $\gamma = (tg\varphi_p - tg\varphi_i)/(tg\varphi_d - tg\varphi_i)$ ranges from 0 to 1; when $0<\gamma<0.5$, finestructure temperature and salinity fluctuations are mainly formed by isopycnal processes, and when $0.5<g<1.0$ by diapycnal ones (6,7).

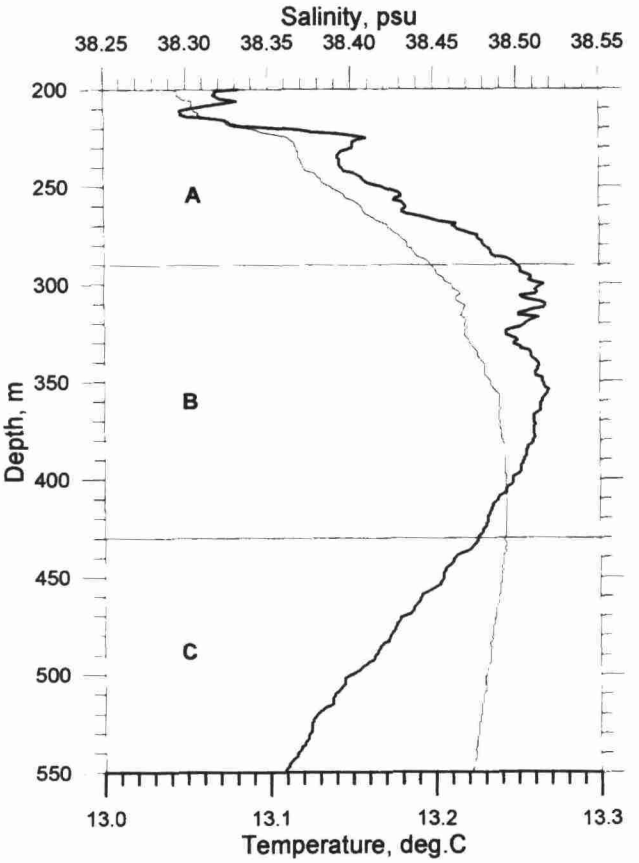

Figure 1: The characteristic layers determined in the temperature and salinity profiles of LIW.

The statistical characteristics of fine structure inhomogeneities were calculated for vertical scales (λ) in the range $5 < \lambda < 50$ m (8). Using the CTD data, the dependencies of γ and the mean square deviations of temperature T_{rms} and salinity S_{rms} as functions of the vertical scale λ, were calculated. The intensity of diapycnal (Id_T, Id_S) and isopycnal (Ii_T, Ii_S) processes in the temperature and salinity fields, respectively, was determined by a combined analysis of the dependency of γ vs λ and of the mean square deviations of T_{rms} and S_{rms} vs λ (Fig.2).

In Fig.2 the point D of the curve γ vs λ corresponds to the change of the diapycnal regime to the isopycnal one. The corresponding values in the curves T_{rms} vs λ (point D1) and S_{rms} vs λ (point D2) characterize the intensity of diapycnal processes in the temperature (Id_T) and salinity (Id_S) fields, respectively. In the same figure the point E of the curve γ vs λ corresponds to its stable regime (the weak deviation of the curve from the stable regime lies in the range of CTD sensors sensibility). The corresponding values in the curves T_{rms} vs λ (point E1) and S_{rms} vs λ (point E2) characterize the intensity of diapycnal processes in the temperature (Ii_T) and salinity (Ii_S) fields, respectively.

ALGERS'96 CRUISE, OCTOBER 1996: AN INTERDISCIPLINARY STUDY OF A MESOSCALE INSTABILITY OF THE ALGERIAN CURRENT (WESTERN MEDITERRANEAN SEA)

Jordi Font* and the ALGERS'96 Group
Institut de Ciències del Mar CSIC, Barcelona; Laboratoire d'Océanographie et de Biogéochimie COM-CNRS, La Seyne; Universitat de Barcelona; Universitat Autònoma de Barcelona; Universitat de les Illes Balears, Palma de Mallorca;
DCN Ingénierie Sud LSM, Ministère de la Défense, Toulon; Instituto Español de Oceanografía, Palma de Mallorca.

Abstract

ALGERS'96 was the first MATER (MAST 3 Mediterranean Targeted Project MTP II) campaign in the Algerian basin, carried out on board the Spanish R/V *Hesperides* in October 1996. A mesoscale meander of the Algerian current, developed near 1°E, was exhaustively sampled: ADCP, CTD and XCTD/XBT profiles and transects, multibeam echosounding, dissolved oxygen, nutrients, chlorophyll, suspended particulate matter, primary production, bacterial abundance and radioactive tracers, together with satellite-tracked surface drifters and real-time remote sensing. The detailed analysis of all this interdisciplinary data set is giving, for the first time, a three-dimensional characterisation of the phenomenon and allows gaining some important answers on the coupling of physical and biological dynamics in the Algerian basin.

Key-words: Algerian basin, circulation, density, fronts, primary production

Algerian current instabilities

Downstream from the Alboran Sea, the Modified Atlantic Water incoming into the Mediterranean forms a well defined flow along the African slope: the Algerian current. Due to complex hydrodynamical processes, baroclinic instability mainly, this alongslope current develops meanders as soon as 0°-1°E, creating an upwelling cell and an anticyclonic eddy inside (1). Sometimes a cyclonic circulation also develops, but it is superficial and short-lived: it will decay within few days. Only anticyclonic eddies are observed to grow up to 50-100 km in diameter, while translating eastwards along the slope at a few km/day. Large open sea anticyclonic eddies (100-200 km diameter), that are probably later stages of the coastal ones, can be quasi-motionless while still energetic for months. These mesoscale phenomena play a major role in the configuration of the general circulation and the distribution of the biogeochemical parameters and hence, of the ecosystems, in the Algerian basin (see a summary in 2).

ALGER'S 96 cruise

MATER (MAss Transfer and Ecosystem Response) is the second phase of the European Union Marine Science and Technology programme Mediterranean Targeted Project (MTP-II). The interdisciplinary study of the Algerian basin mesoscale instabilities is one of the MATER tasks, and ALGERS'96 on board the Spanish R.V. *Hespérides* was the first one in a series of oceanographic campaigns to be carried out in the region.

The main objective of the cruise was to exhaustively sample the three-dimensional structure of a mesoscale instability of the Algerian current from the dynamical, geochemical and biological points of view. An official authorization for the *Hespérides* to work in the Algerian waters was a unique opportunity to completely sample this alongslope current. From October 15 (Málaga) to October 21 (Cartagena), 1996, a series of sections perpendicular to the alongslope current upstream (A), in the middle (B, C, D) and downstream (E) of the instability, were performed from the outer boundary of the area influenced by the recent Modified Atlantic Water, to near the coast. The measurements included ADCP, CTD and XBT/XCTD profiles, multibeam echosounding (38, 120, 200 kHz), and underway surface analysis (T, S, fluorescence, meteorology). Water samples were taken at 22 depths for determination of dissolved oxygen, nitrite, nitrate, phosphate, aliphatic and aromatic hydrocarbons, total chlorophyll, pigment speciation, bacterial abundance, primary productivity, suspended particulate matter, and radioactive tracers (^{210}Pb, ^{210}Po, ^{226}Ra, ^{239}Pu, ^{247}Pu, ^{137}Cs, ^{90}Sr). Eighteen surface drifting buoys equipped with an ARGOS transmitter were released upstream of the instability in the core of the current (along section A), and across the cyclonic part of the meander (along section B). All of them had a 10-m long WOCE standard drogue.

Prior to and during the campaign, the region was monitored by satellite remote sensing. NOAA/AVHRR infrared images are well-known to be adequate in identifying coastal and offshore eddies in the Algerian basin (3). By the end of September, a mesoscale meander of the Algerian current was developed near 1°E. It was then continuously tracked with a portable NOAA/AVHRR satellite receiving station installed on board the *Hespérides* which acquired four passes a day. It appeared on images like an usual instability associating a coastal anticyclonic eddy with a well-marked secondary cyclonic circulation (offshore) (fig. 1). It was decided that this was the phenomenon to investigate, and daily updating the location of the main thermal gradients and hence the position of the boundaries of the evolving instability provided an efficient and detailed guidance of the *in situ* sampling.

First results

Figure 1 shows the location of several CTD stations, as well as the initial trajectories of the surface drifters, plotted on a satellite infrared image. The cyclonic and anticyclonic motions are clearly correlated with the surface thermal structures, although the latter are rapidly evolving: the trajectories at the end of the period indicate a growth and eastward displacement of the anticyclonic eddy, as well as a NW enlargement of the cyclonic one.

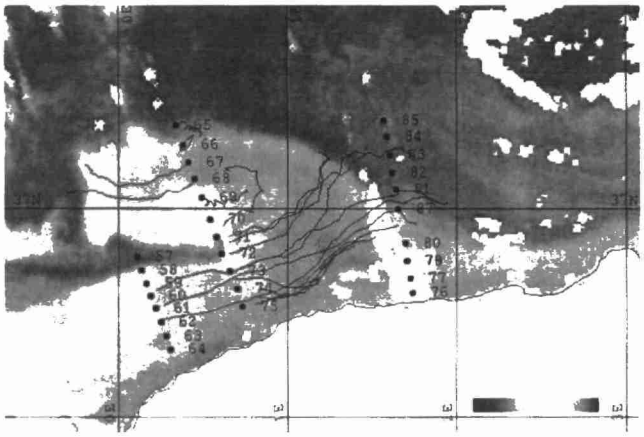

Figure 1. NOAA/AVHRR Sea Surface Temperature image of 16 October with location of CTD stations on sections A, B and D, and satellite-derived trajectories for the 18 surface drifters until 21 October.

The analysed vertical profiles of the hydrological data clearly depict the structure corresponding to the undisturbed yet alongslope current (section A), the offshore cyclonic eddy (northern part of section B, fig. 2) and the coastal anticyclonic eddy with the Algerian current displaced offshore around it (section D). The distribution of the maxima of chlorophyll in section B across the cyclonic eddy and coastal current (fig. 3) is correlated with the areas of strong velocity shear, i. e. on the current's edge (st. 73) and on the cyclonic eddy's edge (st. 71-70 and 67-66). Similar maxima

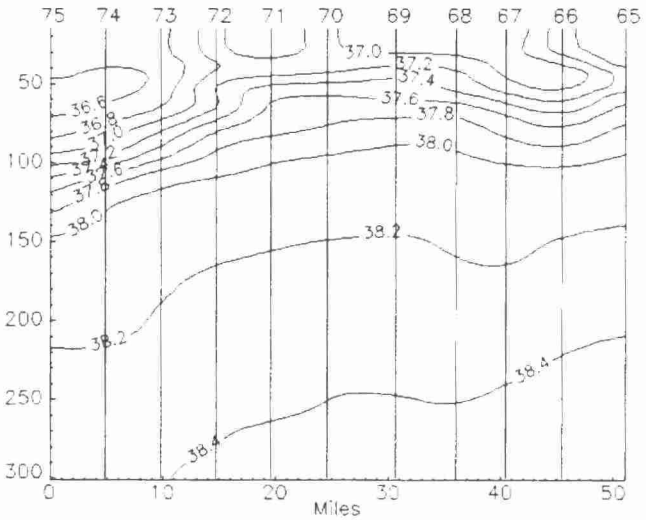

Figure 2. Salinity (in the surface and subsurface layers) along section B on 18 October. The sloping of the isohalines shows the presence of the Algerian current near the coast (left) and the cyclonic eddy centered on stations 70-68.

ADVECTION OF ANTICYCLONIC EDDIES ACROSS THE BLANES CANYON, NW MEDITERRANEAN

M.A. García*, P.A. Arnau and A. Sánchez-Arcilla

Laboratori d'Enginyeria Marítima, E.T.S. d'Enginyers de Camins, Canals i Ports,
Universitat Politècnica de Catalunya, c/Jordi Girona, 1-3, mòdul D1. 08034 Barcelona, Spain

Abstract

Time series observations of temperature were carried out at several mooring locations in the Blanes canyon area during summer 1993. The temperature records reveal the southward advection of mesoscale anticyclonic eddies at a mean speed of 5-10 cm/s. These eddies are also evidenced by collateral AVHRR imagery and trajectories of Lagrangian drifters. Research is in progress to understand the genesis of these mesoscale features, which have very important effects on the shelf circulation. It is suggested that both the alongslope advection of light water from the gulf of Lions and the morphology of the Creus-Palamós-Blanes canyon system may play a crucial role in eddy generation.

Key-words : Circulation, mesoscale phenomena, remote sensing, time series, Western Mediterranean

Introduction

In the framework of a study of the mean circulation in the northern Catalan shelf, R/V *Hespérides* performed a high-resolution oceanographic survey of the Blanes canyon area in June 1993 (see figure 1). The cruise included the acquisition of CTD and ADCP data and the release (and further Argos-tracking) of Lagrangian LCD drifters upstream of the Blanes canyon. Rojas *et al.* [1] reported the mesoscale circulation patterns observed during the cruise, and Olivar *et al.* [2] and Granata *et al.* [3] discussed the influence of the mean flow on the distribution of larval fish species and on the fluxes of particulate matter. In the upper layer, a mesoscale anticyclonic vortex was observed in association to a low salinity core advected by the Liguro-Provençal-Catalan or Northern Current into the Blanes canyon. The surface circulation pattern was interpreted by Rojas *et al.* [1] as the result of geostrophic adjustment.

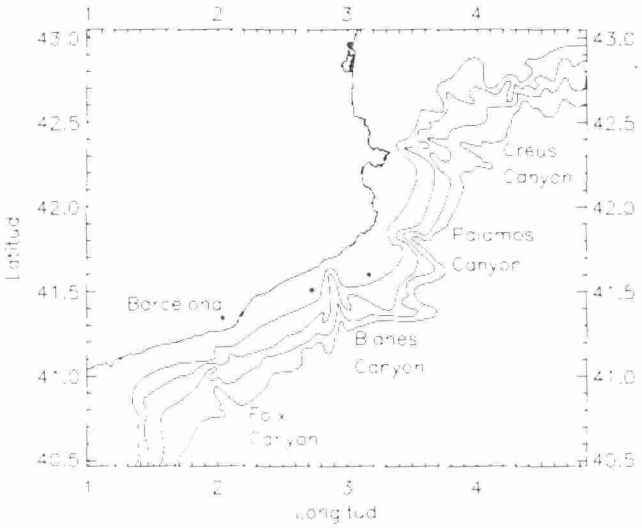

Figure 1 : Location of the Blanes canyon off the Catalan coast and location of the "upstream" and the "downstream" moorings described in the text.

3-month series of current and temperature data were recorded by means of several moorings deployed at the end of the hydrographic survey. In particular, two moorings containing one single RCM-7 current meter at 70 m depth were deployed respectively upstream and downstream of the canyon on bottom depths of 140 m. The current meters happened to remain just below the pycnocline and recorded very low flow velocities (the current data time series are not shown here), but their temperature records exhibited very interesting features.

Results and discussion

Figure 2 displays the time series of temperature measured at 70 m on the upstream and the downstream moorings. A number of strong temperature signals can be easily traced in both records, in particular several transient temperature increases by 0.5°C to 1.0°C. The duration of each of these warm events is of the order of 10 days, and the interval between two consecutive events in a record is about 20 days. The coherence between the two temperature records is high, and the phase lag between both time series is around 9 days. On the basis of the post-cruise trajectories of our Lagrangian LCD drifters and of collateral AVHRR imagery covering the time series observation period, we conclude that those temperature signals were caused by mesoscale anticyclonic eddies advected southwestwards across the Blanes canyon producing transient depression of the isotherms. According to our interpretation of the temperature records, the eddies were advected by the Northern Current at a mean speed of 5-10 cm/s.

Figure 3 shows the SST field derived from an AVHRR image of the study area acquired on 24th June, 1993 -*i.e.* during the first temperature "jump" recorded on the upstream mooring-. The geometry of the cool water tongue advected alongslope from the gulf of Lions reveals an anticyclonic circulation pattern on the shelf northeast of the Blanes canyon. Furthermore, the trajectory of drifter

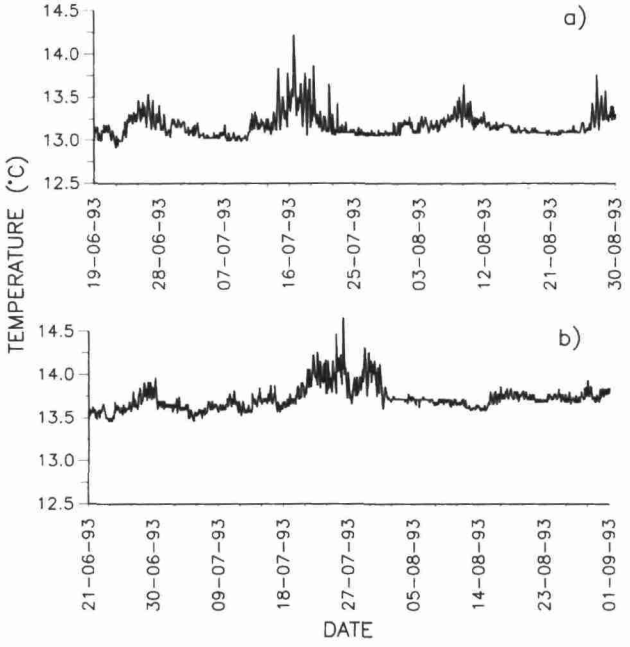

Figure 2 : Time series of temperature measured upstream (a) and downstream (b) of the Blanes canyon at 70 m in summer 1993.

#5 (it is one of the five drifters launched during the *Hespérides* cruise) between 22nd and 28th June suggests that the shelf stretch extending between the Blanes and the Palamós canyons was occupied by an anticyclonic eddy at the time when the first positive temperature anomaly was observed on the upstream mooring. The diameter of this eddy could be about 30 nautical miles according to the trajectory of the drifter. Figure 4 displays the distribution of SST on 28th June, *i.e.* when the first positive temperature anomaly was observed at the downstream mooring, and the quasi-contemporary trajectory of drifter #2. Both figures evidence that the shelf circulation was anticyclonic southwest of the Blanes canyon, which again supports our interpretation of the warm events in the temperature records as the signature of anticyclonic eddies. In fact, the trajectory of drifter #2 suggests that there were possibly two different length scales of anticyclonic motion downstream of the Blanes canyon, one of about 12 nautical miles related to a cool (and fresh) core "detached" from the leading edge of the tongue of gulf of Lions water southwest of the downstream mooring site, and another larger one of about 30 nautical miles.

The previous observations sustain our ideas about the fact that the warm events in the temperature records were related to anticyclonic eddies causing depression of the isotherms. However, the thesis that these eddies are advected across the Blanes canyon deserves further explanation. A closer inspection of figure 4 reveals that the anticyclonic circulation pattern southwest of the Blanes canyon coincided in time with the presence of an anticyclonic eddy on the shelf stretch extending between the Blanes and the Palamós canyons (which is possibly the same structure observed in the 24th June image), but we have no evidence to affirm that the first anomaly of the downstream temperature record was caused by the advection of a previous anticyclonic eddy across the Blanes canyon. Despite this, we do have other indications that such advection occurs. Figure 5 shows the SST field of 8th July and the trajectory of drifter #1 from 28th June to 14th July. The SST image shows the cool tongue of gulf of Lions water invading the shelf stretch between the Blanes and the Palamós canyons in relationship to southward flow on the shelf, which suggest that the anticyclonic eddy observed in both the 24th and 28th June images was not there on 8th July. On the other hand, if the drifter tracks shown in figures 3 and 5 are compared, it is noticed that the northeastern limb of the anticyclonic eddy migrated more

MONITORING OF THE FLOW OF ATLANTIC WATER AND ITS PROPERTIES IN THE EASTERN SECTION OF THE STRAIT OF GIBRALTAR. SUBINERTIAL VARIABILITY.

Jesus García Lafuente [1*], Juan M. Vargas [1] Francisco Plaza [1], Manuel Vargas [1], Tarek Sarhan [1] and Natalio Cano [2]

[1] Departamento de Física Aplicada II, Universidad de Málaga, Spain

[2] Centro Oceanográfico de Málaga, Instituto Español de Oceanografía, Spain

Abstract

Data acquired in the northern part of the Strait of Gibraltar during a pilot study previous to CANIGO-MAST Project have been analysed in order to provide estimates of some local properties of the inflow and their time variability in the subinertial (meteorological) frequency band. Local exchange, which is not represented by a simple two-layer model, is modulated by zonal winds in the Strait. An interesting result is that local inflow and outflow have a tendency to oscillate in-phase, thus smoothing out the oscilations of the net local flow. Another result is that this net local flow is not always directed toward the Mediterranean.

Key-words : Sea level, water transport, wind, air-sea interactions

Introduction

The importance that the Strait of Gibraltar has with regard to the general circulation and ventilation of the Mediterranean Sea is quite obvious: it represents the only connection with the open ocean. Around $3 \cdot 10^{13}$ m^3 of "fresh" Atlantic water come through it into the Mediterranean every year (somewhat less than 1% of its total volume). This water is transformed into "salty" Mediterranean water that flows out as an undercurrent. The overall exchange results in a net inflow to compensate for the net evaporation that takes place in the Mediterranean basin.

While this general point of view is of interest for climatic and/or other long term studies of the properties of the Mediterranean (residence time of the water, interannual variability), it is not sufficient for more detailed studies of its circulation on shorter time-scales. This is particularly true for surface circulation in its westernmost basin, the Alboran Sea. The knowledge of other properties of the Atlantic inflow like the relative vorticity, the incoming angle or the current intensity (in addition to water transport) and their time variability are of the greatest interest to this kind of studies.

One objective of CANIGO MAST Project is the monitoring of the exchange through the Strait at the eastern section to provide estimations of these properties. From October 95 to May 96 and previously to the start of the Project, a pilot study was carried out to check new acoustic methods of estimating the horizontally integrated transport. As a part of the experiment, a mooring line with five conventional currentmeters was deployed at site "N" (see figure 1). The results obtained from the processing of this information are presented below.

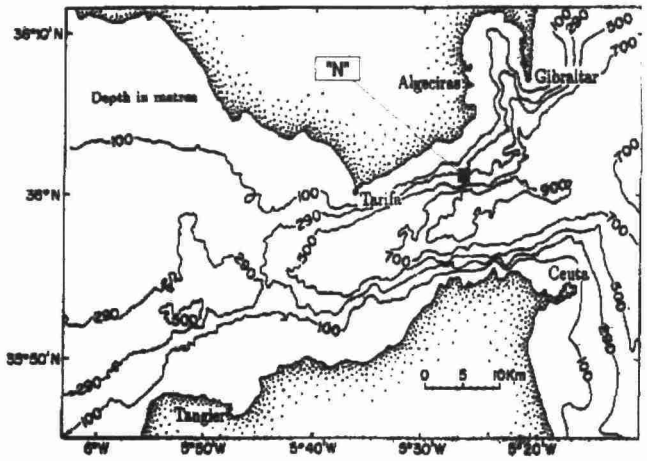

Figure 1 : Map of the Strait showing the mooring's location.

Data and data processing

The mooring line was deployed on the 24th of October 1995 and recovered on the 8th of May 1996 with a short servicing on the 23rd-24th of February. Site "N" was at 36° 02.3N, 5° 23.8W and nominal depths of the instruments were 30, 60, 110, 240 and 400m in 450 m water depth. All instruments were equipped with conductivity and pressure cells so that time series of salinity and depth in addition to velocity and temperature are available. Sea level data from Ceuta (Instituto Español de Oceanografía Data Base) Gibraltar (British Oceanographic Data Centre) and local atmospheric pressure and wind velocity (Instituto Meteorológico Nacional, Spain) were also gathered to investigate cross-strait geostrophy and atmospheric forcing.

Sea level and meteorological variables were filtered out with a gaussian filter with cut-off frequency of 4 cpd to remove tidal variability. Oceanographic data were harder to process: salinity series had trends due to biological contamination of conductivity cells and were corrected. Another problem occuring in this area is the periodic sinking of instruments due to tidal currents. As a result, data collected by a given instrument are not taken at a given depth (this is why instruments were equipped with pressure sensors). Standard filtering techniques are inadvisable and some kind of daily average has been performed instead. Daily means have been filtered with a gaussian filter of the same cut-off frequency as the series above mentioned to compare both types of observations. Further details can be seen in Garcia Lafuente *et al.* [1].

Results and discussion

Vertical structure of the flow. Figure 2 shows time variability and depth structure of the along-strait component of velocity (labelled contours) and salinity (shadowed areas). The local depth of zero along-strait velocity, which separates inflow and outflow, is around 100 - 125 m except for a ten-days period at the beginning when it was considerably deeper. Salinity at this depth is higher than 37.5 (in Practical Salinity Scale Units). This isohaline is sometimes taken as the interface between Atlantic and Mediterranean waters. If so, we must conclude that Mediterranean water recirculates toward the Mediterranean by the northern part of the Strait. However, salinity distribution shows that a two-layer description of the flow at this location is not adequate. A three layer model with an "Atlantic" layer of S<37, a "mixed" layer of 37<S<38 and a deep "Mediterranean" layer of S>38 as that put forward by Bryden *et al.* [2] provides a better picture. In this three-layer structure, the mixed layer flows mainly toward the Mediterranean, in agreement with the description of Bray *et al.* [3] who presented a more elaborated three-layer model.

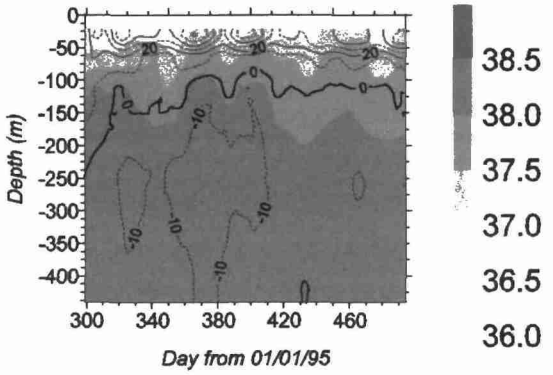

Figure 2 : Depth structure and time variability of along-strait velocity and salinity.

Cross-strait geostrophy. An issue of importance is to check to what extent cross-strait geostrophy keeps validity. The solid thick line of figure 3A represents the along-strait velocity measured by the uppermost instrument (a velocity representative of the ten-meter thick bin from 30 to 40 m). Dashed line is the velocity predicted by the formulae $u=(g/f)(\Delta\xi/\Delta y)$ (1) which is a horizontally averaged version of the actual cross-strait geostrophic relationship with $\Delta\xi$ the sea level difference (Ceuta minus Gibraltar) of two sites separated a distance Δy (21 km). The prediction is shifted toward high values due to the lack of accurate levelling between both shores. This is better shown in the lineal fit of figure 3B which gives a non-zero independent term, contrary to what equation (1) states (it can be written as $\Delta\xi = (f\Delta y/g)u = 0.183u$ for $\Delta y = 21$km). It provides however a very good estimation of the coefficient of u. Taking into account the independent term of the fitting in the prediction, the thin solid line of figure 3A is obtained, which compares well with observations, despite of equation (1) is a horizontally averaged estimate of u while the observations are local values. The lagged correlation of figure 3C gives a highvalue for the correlation coefficient, slightly shifted toward positive lags, what means that u leads sea level slope.

Local transport

The vertical structure of velocities of figure 2 has been used to estimate flows per unit length perpendicular to the strait at site "N", what we call local flows and transports. Their units are m^2/s and are defined as $\int u\,dz$, where u is the low-passed along-strait velocity. Limits of the integral are the depth of u = 0 and the surface for inflow and the sea floor and the depth of u = 0 for outflow. Thin solid, dashed and thick solid lines of figure 4 represent local inflow, outflow and net flow respectively. There are two noteworthy features: first, that net transport is not always directed toward the Mediterranean and secondly, that inflow and outflow behave symmetrically, that is, both increase and decrease simultaneously.

EXPERIMENTAL AND NUMERICAL INVESTIGATION OF EDDY EXCHANGE COEFFICIENTS IN THE SURFACE LAYER OF THE MIDDLE ADRIATIC SEA

B. Grbec, M. Bone, G. Beg Paklar and V. Dadic
Institute of Oceanography and Fisheries, P.O.Box 500, 21000 Split, Croatia

Abstract
Vertical eddy exchange coefficients in the surface layer in the middle Adriatic Sea were studied using boundary conditions for the heat and salt fluxes and one dimensional modeling. Results for experimental data are in concordance with those obtained from the model.

Key-words: turbulence, models, Adriatic Sea

Scope and methods

The main scope of this work was to study vertical eddy exchange in the surface layer of the middle Adriatic using boundary conditions for heat and salt fluxes and one dimensional modeling. The results brought up vertical eddy exchange coefficients for the surface layer.

Data from the period January 1961 to December 1980 were used for calculating vertical exchange coefficients on the seasonal scale. Data were collected on the regular monthly or seasonal basis at oceanographic stations of the transect Split-Gargano (Fig. 1). Measurements were done mostly once a month (only exceptionally few times) but on different dates. Data were analyzed on an annual time scale, so that the data set extended from t=1 to t=365 days. Only the data with the same number of measurements for standard oceanographic depths (0, 10, 20, 30, 50, 75 and 100 m) at stations 8,9,10,11,12 and 13 (Fig.1.) were used, while the data from the depths below 100m were rare, and were not considered. On the basis of the monthly mean values of bulk variables, heat and water fluxes were calculated for meteorological station Hvar.

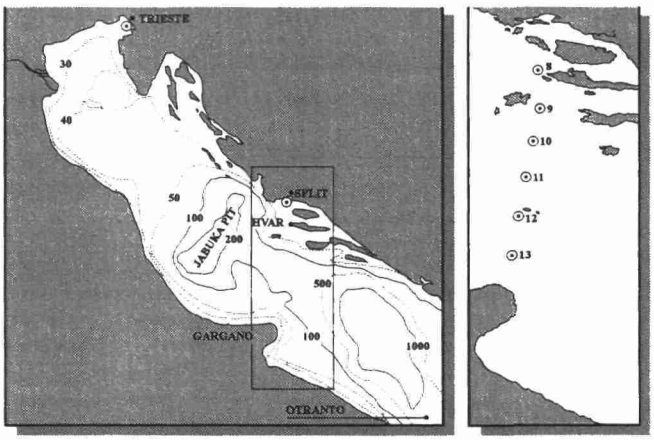

Figure 1. The transect Split-Gargano in the middle Adriatic Sea.

The situation on the 5th August 1972, when measurements were performed every six hour was used for numerical experiment. Experimental area includes station 9 on the transcect Split-Gargano. Both temperature and salinity at standard oceanographic depths were measured as well as the bulk variables. Hourly mean sum of incoming solar radiation was taken from the Split station (1).

Eddy exchanges coefficient obtained from climatological data

Using boundary conditions in finite difference form and climatological mean values for heat and water fluxes, and temperature and salinity for surface and at 10 m depth, it was possible to determine vertical eddy exchange coefficients in the surface layer: K_T and K_S.

To smooth seasonal variability, introduced using data from different years and different stations, the function of the form:

$$Y(t) = A_0 + A_1 \sin(\frac{2\pi}{T} t + \varphi_1) + A_2 \sin(\frac{4\pi}{T} t + \varphi_2), \qquad 1$$

was least-square fitted to temperature data as well as to climatological heat values. It was not possible to approximate salinity data by a harmonic function (2), so salinity means were determined averaging between months.

Eddy exchange coefficients obtained from 1D model

It is supposed that the surface layer turbulence mainly depends on the wind forcing. The divergence and vorticity of the wind induced currents in the open middle Adriatic are small (3). The wind induced currents in this case may be described with the one-dimensional model. Only the vertical mixing and the Coriolis force should be included in the model. The defined boundary conditions at sea surface describing air-sea interaction will be the governing factors in the model. The simplest method to describe air-sea interaction using the measured meteorological data is the bulk method. It is important to split this problem from a general three-dimensional model to obtain the clear idea how the boundary equations and the closure model work for the vertical exchange.

The Mellor and Yamada (4; 5) Level II closure model was taken for the closure. The Nihoul form (6) for the turbulent length scale including surface and bottom boundary layers is used. The bulk method is applied (7;8) to obtain surface boundary conditions for the heat exchange. Short wave radiation attenuation coefficients are introduced according Jerlov (9) for the optical water type IB. The trapezoidal scheme (10) is used for the Coriolis term and turbulent exchange of momentum is obtained from the implicit scheme (11). The scheme for the temperature and salinity continuity equations is the implicit scheme, the same as for the turbulent exchange of momentum.

Results

Coefficients of vertical turbulent exchange in the surface layer were first determined for both heat and salt. Surface boundary conditions were applied and climatological means were taken for heat and water flux. Function (1) was fitted to the data of heat flux and sea temperatures at 0 and 10 m. Vertical heat and salt gradients were determined from the difference between the surface and 10 m depth. Correlation coefficient between the vertical heat gradient and heat flux is 0.91 (significant at the 0.001 level). It allowed us to determine vertical exchange coefficient for heat using the least square method. Seasonal course of the vertical heat exchange coefficient is shown in Fig.2. The value obtained by the least square method is:

$K_T = (3.05 \pm 0.09) \cdot 10^{-4}\ m^2\ s^{-1}$

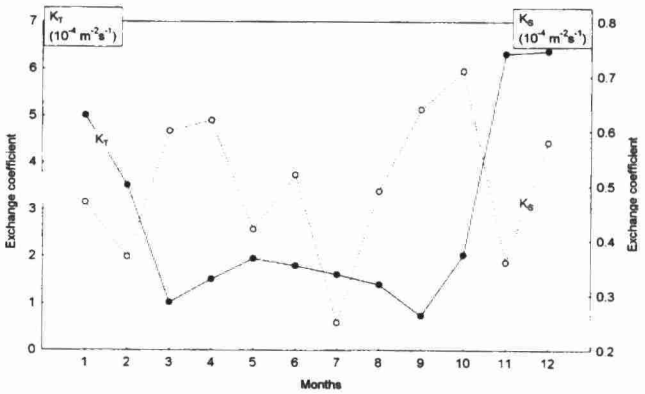

Figure 2. Monthly mean values of eddy exchange coefficients for heat and salt for the surface layer.

Salinity in the surface layer during the heating season is proportional to the differences P-E, while in autumn and winter salinity and P-E are opposed in phase. Earlier investigation (12) proved that north Italian rivers, especially the Po River, influenced waters of the Jabuka Pit. When the thermocline is well developed, lighter north Italian waters reside in the surface layer and are transported by the SE current to the Split-Gargano transect (13). They cause decrease of salinity in the surface layer. As a consequence of ice melting, the largest Po runoff is observed in May which coincides with salinity spring minimum at the transect (14; 15). Less saline water resides at the surface, since the mixing is prevented by the fully developed thermocline and it seems that the influence from the Po River inflow could be observed. For this reason, vertical coefficient of salt exchange for the surface layer is determined using different relations throughout the year, as indicated in the schema:

$$E - P = \begin{cases} E - P & \textit{September - April} \\ E - (P + R) & \textit{May - August} \end{cases}$$

where R denotes the quotient between the Po river inflow and the Adriatic shelf area. Taking the Po river into account, correlation coefficient between

INTERANNUAL SALINITY FLUCTUATIONS IN THE MIDDLE ADRIATIC SEA

B. Grbec , M. Morovic [1], M. Zore-Armanda [1] and N. Leder [2]

[1] Institute of Oceanography and Fisheries, P.O.Box 500, 21000 Split, Croatia
[2] State Hydrographic Institute, 21000 Split, Croatia

Abstract

In order to explain interannual salinity fluctuations the data series for the open middle Adriatic were subjects to the principal component analysis. Results were compared to the meteorological factors leading to the conclusion that salinity fluctuations in the surface layer were correlated with the water flux while the intermediate layer responded to the pressure gradient between the northern and the southern Adriatic. To describe the advection mechanism additional attention was payed to the pressure field, analysing frequency of cyclones and anticyclones over the larger area (from 70W-40E and 20N-80N).

Key-words: salinity, Adriatic Sea

Introduction

The transect Split-Gargano laying over the Palagruža Sill in the middle Adriatic is a region with a strong temporal variability of thermohaline structure as being exposed to the influences both from the northern and the southern Adriatic. The dynamics on the investigated transect is controlled also by the topographic constraint on the Palagruža Sill (1). In winter, in the northern Adriatic, very cold dense water is formed, which sinks to deep layers of the Jabuka Pit, and is advected across the Palagruža Sill (2). The transect area is also under the influence of saltier water advected from the southern Adriatic. The most important feature of the Mediterranean waters advected into the Adriatic (in the intermediate layer) is their high salinity (3). This high salinity is a property of the Levantine Basin, which has one of the highest salinities of the world ocean (>39 psu) (4). Intensification of the inflow of Mediterranean water, called "ingression" (5), result in transient increase in salinity in the middle Adriatic. Since the temperature of the Levantine intermediate water (LIW) is higher than that of the Adriatic water, "ingressions" are observed in the temperature as well (3). The most important factor enhancing the water exchange between the two basins is the horizontal pressure gradient over the eastern Mediterranean (2;6). The location of the Iceland cyclone and the Siberian anticyclone centers were found responsible for this pressure gradient (7). It was observed that such changes could be related to the pressure conditions of a wide area of the north Atlantic and Europe.

Therefore, interannual salinity changes in the whole water column in the middle Adriatic depend on the three different processes: advection from the north Adriatic, advection from the south Adriatic (and/or Mediterranean) and atmospheric input. The principal goal of this paper is to analyse long-term salinity changes in order to distinguish layers influenced by different processes.

Materials and methods

Data used in this work span the time interval from January 1961 to December 1980 (8) and were collected on the regular monthly basis at oceanographic station Stončica.

For the analysis of a wide area pressure conditions, mean monthly surface maps (9) from 1956-1981 were analysed. In the region between 70°W-40°E and from 20°N-80°N spatial grid was defined of 10^0 x 10^0 gridpoint distance. Spreading of local minimum and maximum of surface pressure centers were determined within such grid and their frequency counted from each monthly map in each year.

The evaporation rates were calculated for the station Hvar (Fig. 1), for the same period (1961-1980), on the basis of the monthly mean meteorological data (10). Air pressure data were taken from Trieste and Palagruza station.

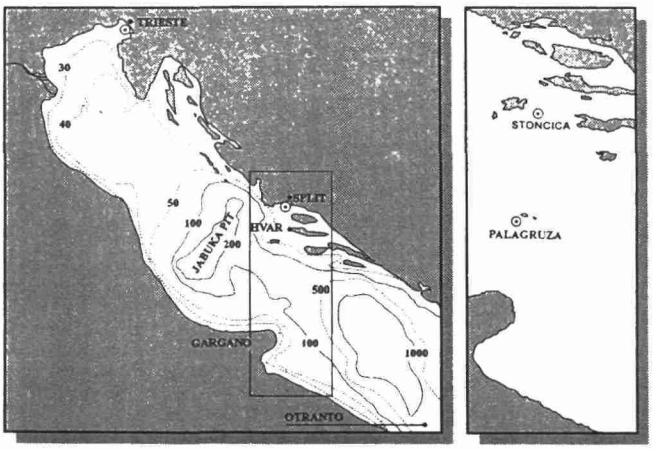

Figure 1.The transect Split-Gargano in the middle Adriatic Sea.

Salinity time series were subject to the correlation matrix based principal component analysis (PCA) (11). Eigenvalues and eigenvectors were determined, applying the varimax rotation. The significance of principal components were tested with Rule N (11), using Monte Carlo simulation of the random matrix of the same size as the original data matrix.

Results and discussion

PCA was applied to the salinity data from Stončica station at seven available depths (0, 10, 20, 30, 50, 75 and 100m). Eigenvalues and factor matrix of component loadings were determined for the first two components.

On the basis of distribution of PC loadings it was possible to distinguish two layers whose variability contribute with different amount to the total variability in the salinity field. First principal component (87.2%) has significant loadings for layers 30-100m. Second principal component (9.2%) has significant loadings in the surface layer down to 20m (Fig. 2). According to its properties, the layer from 30m to the bottom belongs to the intermediate layer at Stonèica station. Salinity fluctuations in these two layers were explained comparing PC scores to atmospheric fluctuations. Significant correlation coefficient (0.31) was found between PC2 (surface layer) of the salinity field and E-P, with three months lag.

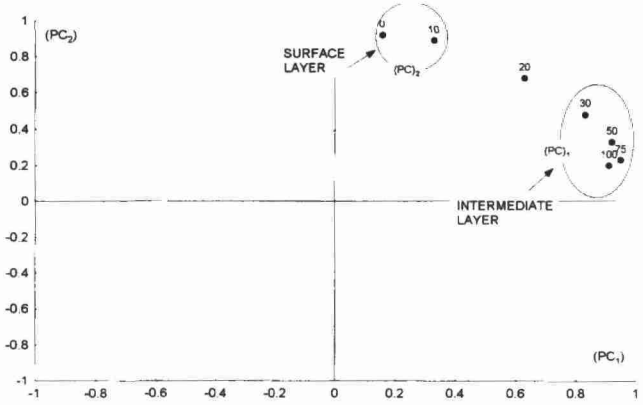

Figure 2. Distributions of PC loadings in the salinity field

Intermediate layer is influenced by the inflow from the Mediterranean whose higher salinity causes increased salinity in the middle Adriatic. As already known (7), the mechanism of exchange between the Adriatic and the Mediterranean can be explained by the horizontal pressure gradient between the northern and the southern Adriatic (pressure differences between Trieste and Palagruza). In the years with higher pressure differences, higher salinity in the intermediate layer of the middle Adriatic can be expected. A higher pressure gradient does not always correspond to higher salinity, due to various influences. Comparing the horizontal pressure gradient with salinity fluctuations in the intermediate layer (Fig.3) two characteristic periods are evident. In the period 1961-1970 salinity fluctuations are not accompanied by pressure gradient fluctuations. In this period their correlation was not significant because salinity in the Mediterranean was mainly increased due to the Assuan damm construction. It caused the fresh water input decrease from 41 to 11 km^3 $year^{-1}$ (12) which reflected upon higher salinity of the eastern Mediterranean. In the period 1973-1980, salinity fluctuations seem to respond to pressure gradient fluctuations and the correlation coefficient between them was 0.55 (significant at the 0.001 level). Besides by higher salinity, the LIW can be also detected in the intermediate layer of the middle Adriatic by higher temperature, so that the Mediterranean influence can also be seen through temperature. Like salinity fluctuations, temperature fluctuations also show two characteristic periods. In the second period, from 1973-1980 temperature fluctuations

WESTERN BLACK SEA CURRENTS BY THE SHIP AND SATELLITE DATA

Yuri P. Ilyin [1*], Vitali A. Ivanov [1], Evgeni M. Lemeshko [1], Sukru Besiktepe [2], Emin Ozsoy [2], Halil I. Sur [2]

[1] Marine Hydrophysical Institute (MHI) of the Ukrainian National Academy of Sci., Sevastopol, Ukraine
[2] Institute of Marine Sciences (IMS) of the Middle East Technical University, Erdemli, Turkey

Abstract

In spring-time of 1993,94 both CTD, ADCP and satellite infrared measurements were carried out in the framework of CoMSBlack international program. Geostrophic flow field, ADCP current vectors and thermal structures at the sea surface displayed good agreement. Satellite data essentially assist in the interpretation of ADCP currents data and explain several peculiarities in vectors distribution as manifestations of meso-scale dynamic features. The results reflect the effect of the Black Sea flow field transformation from winter type to summer one. These seasonal changes are superimposed over the strong inter-annual variability of the water dynamics.

Key-words: Circulation, Hydrography, Mesoscale phenomena, Remote sensing

Introduction

In spring time of 1993,94, both CTD, ADCP and satellite infrared measurements were carried out in the framework of CoMSBlack and NATO TU-Black Sea international programs to study the water circulation and bio-chemical processes in the western Black Sea. The aim of this paper is to present some results concerning the integration of different kinds of information (satellite images, measured currents and geostrophic flow fields) for the description of water circulation within the upper 100m layer of the sea, including the meso-scale dynamical features. The same approach is often used for other regional studies (*e.g.*, [1]) , but there was no opportunity before to obtain more or less full set of quasi-synchronous high-quality data covering the most part of the Black Sea. General structure of the Black Sea surface water circulation has been recently described on the base of geostrophic currents calculations and qualitative analysis of satellite images [2]. The cyclonic meandering Rim Current (RC) follows along the continental slope around the sea. The flow field between the RC and shelf break consists of meso-scale anticyclonic eddies to the right of meandering jet. Some of them are quasipermanent and other meso-scale features are unstable and variable on a short-time scale (*e.g.*, upwellings and cold jets, mushroom-like structures, RC instabilities) [3]. Seasonal (spring) changes in external forcing (wind weakening, surface layer heating and riverine runoff) lead to the current pattern transformation towards the less intensive and more meandering Rim Current. Sometimes the systems of meso-scale eddies are observed instead of continuous jet stream.

Data and methods

CTD data obtained during international experiments in the framework of CoMSBlack and TU-Black Sea programs (2-27 April, 1993 and 25 April - 14 May, 1994) were used for geostrophic circulation calculations. Observational stations grid had a spacing no more than 10 n.miles along meridian and 20 n.miles along parallel. Within the frontal and dynamically complex regions, stations have been sampled more frequently (steps were 2.5- 5 miles). Resulting grid covered deep-water, slope and shelf areas (in 1993, exception was the Bulgarian economic zone). The maps of geostrophic current vectors as well as the dynamical topography were produced. Dynamic heights were interpolated by means of Kriging procedure on the regular grid spaced by 0.20° in longitude and 0.12° in latitude, then geostrophic current components were revealed on the same grid from the horizontal gradients of dynamic heights. Also, CDT data were used to estimate the density of available potential energy (APE) distribution through the displacement of isopycnal surfaces regarding to their average levels for each survey.

ADCP current measurements were performed on board of R/V Bilim within the areas of CTD surveys, but without the Ukrainian economic zone in 1994. Data processing procedures were used for the ADCP information, such as: computing of absolute currents by means of the precise navigation data; error control and median filtration; statistical analysis for each level; producing of horizontal vector maps and vertical sections of currents. In present paper the vectors at 10 m level were analysed together with the satellite thermal images as the nearest to the sea surface valid ADCP data. Some statistical parameters for the 10 m depth are presented in Table 1. They give the first impression about general currents intensity and variability in the subsurface layer for the both surveys. Next steps of the data analysis were: (i) qualitative comparison of the vector current patterns with CTDderived dynamical topography and (ii) estimation of correlation between ADCP-measured and geostrophic velocities. The second procedure based on the data set for those points of dynamical topography regular grid where the ADCP measurements were made. Measured current components were obtained as the mean values for all ADCP-vectors within the half-step limits around the geostrophic vector nodes. Figure 1 presents the maps of dynamical topography calculated referring to the 500 m level, where the mean ADCP vectors used for the correlation calculations are shown as well. Finally, these current vectors were also used for the density of kinetic energy (KE) estimation. Table 2 presents the correlation coefficients derived for the different levels within the upper 100 m layer of the sea and Table 3 contains the results of basin-averaged APE and KE calculations for the same levels as well as the integrated values for 10-100 m layer.

Satellite images obtained from NOAA AVHRR in HRPT mode on MHI receiving station are used in the present work. Software developed in MHI is used for the pre-processing, geographical positioning and geometrical transformation of images to the rectangular projection maps. Second stage of processing gives the digital radiation temperature maps for the infrared channel 4.

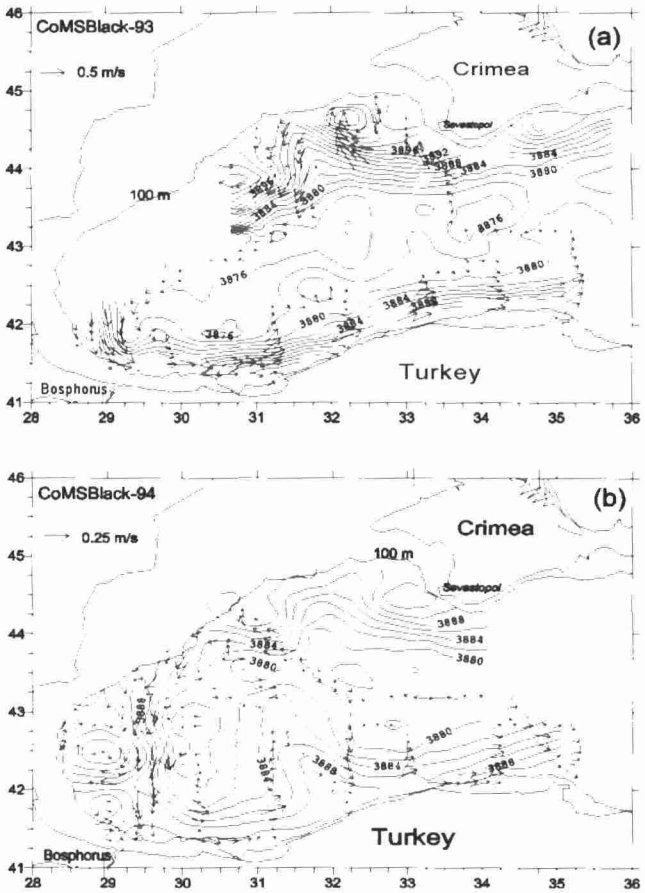

Figure 1. Dynamical topography (dyn/cm) and ADCP current vectors on the depth 30 m in April 1993 (a) and May 1994 (b).

Their spatial resolution is 1' along meridian and 1.5' along parallel, and radiation temperature resolution is 0.1°C. Finally, shoreline, shelf boundary and ADCP measured current vectors were superimposed on the images.

Surface layerwater circulation and mesoscale features

Sea surface dynamical topography map for April 1993 demonstrates all of the main large and meso-scale peculiarities described earlier, such as, meandering jet of the RC, series of quasi stationary anticyclonic eddies to the right of it, cyclonic gyres in the central part (see Fig. 1a). Large-scale structures coinciding to the RC jet to the west of the Crimean peninsula and along the Turkish coast are well distinguished by the ADCP vectors having maximal velocities. Respectively weak flows on the north-west shelf (10-15cm/s), and in central regions of the sea (20-25cm/s) are observed. ADCP data reflect the complex meso-scale current picture. This makes them more preferable for the comparison with high resolution satellite thermal images, especially in higher spatial variability zones (RC's meanders and frontal regions of eddies). The comparison of current vector distributions at the 6 - 20 m levels allows to infer the vertical homogeneity of upper layer circulation and thus is a good base for the interpretation of sea surface satellite imagery.

Considering the distribution of ADCP current vectors and thermal patterns together, we can note a good agreement between the measured flows and thermal structures at the sea surface in April 19, 1993 for those areas where the ship tracks passed. The velocity maxima coincide with the temperature gradient locations of the RC and the vector directions correspond to the satellite

FLOW PHENOMENA IN THE NORTH AEGEAN SEA DERIVED FROM SATELLITE DATA

L. Jönsson [1] and G. Zodiatis [2*]

[1] Department of Water Resources Engineering, University of Lund, Sweden
[2] Laboratory of Physical Oceanography, Department of Fisheries, Nicosia, Cyprus

Abstract

The spreading pattern of Black Sea Water into the North Aegean Sea was studied using NOAA-AVHRR, thermal data obtained during one year, 1995-1996. A strong, seasonal variability of the spreading pattern was revealed in agreement with the wellknown physiodynamical structure of the NAS. Moreover extensive upwelling appeared to take place off the Asia Minor coast during summer/autumn 1995. Finally the Maximum Cross Correlation method was applied in selected occasions in order to derive surface advective velocity vectors.

Key-words: Aegean Sea, remote sensing, circulation

Introduction

The Black Sea is connected to the North Aegean Sea via the straits of Bosphorus and the Dardanelles respectively and the Sea of Marmara. There is a significant surface layer flow from the Black Sea to the North Aegean Sea and a subsurface, slow intrusion of Levantine water from the North Aegean Sea to the Black Sea. The discharge pattern of the Black Sea Water origin (BSW) into the surface layer of the North Aegean Sea (NAS) is important to understand due to several environmental problems related to the dispersion of pollutants from various sources in the Black Sea towards the Mediterranean. Therefore, the knowledge of the hydrodynamic properties of the North Aegean Sea and especially the transport and spreading patterns of BSW is essential for assessing the fate of pollutants, especially in case of accidental release. Satellite data can provide important, qualitative information on circulation patterns and also a potential to quantify surface advective velocity fields.

The surface water temperatures and temperature differences were used as a tracer to identify different water masses and water movements based on:
a) a qualitative description of the main hydrodynamic features of NAS, with emphasis on the discharge pattern of the BSW, analysed by a large number of NOAA-AVHRR data collected during one year, between 1995-1996
b) application of the Maximum Cross Correlation Method (MCC) to obtain quantitative information on surface advective velocities using sequences of NOAA-AVHRR data.

Satellite data for circulation studies and image processing

An alternative method to study the spreading pattern of BSW in the North Aegean Sea is the use of satellite thermal data related to the surface water temperature. The BSW, which is characterized by low salinity and low density, is well stratified in the surface layer of the North Aegean Sea. Consequently the BSW has a lower density and will remain in the surface waters of the North Aegean Sea even after intense mixing processes. Moreover, the BSW is much colder than the surrounding waters - a difference of up to 3-5°C. Thus surface water temperature could be utilized as a "tracer" for the transport and spreading of the BSW. A very limited study, based on only four NOAA scenes, has been reported earlier (1). However, no comparison was made with known flow patterns and no applications of the MCC method was reported.

For this study NOAA-AVHRR data was obtained from the NOAA receiving station at the Department of Physical Geography, University of Lund, Sweden during one year - March 1995 - March 1996. A total of about 50 scenes were analyzed, representing all the months of the studied period.

Maximum cross correlation method

The image processing technique of the Maximum Cross Correlation method (MCC) was utilized in order to determine surface advective velocity vectors. This technique provides the potential to derive surface velocity fields using sequences of NOAA images, separated by a certain time interval - say of the order of 24 h. The MCC is basically a statistical method to determine the displacement of small surface water temperature patterns during a given time interval - on the basis of known time and distance an average velocity is calculated in a straightforward way. A more detailed description of the MCC method is given in the literature, see for instance (2, 3).

The trace of BSW in the NAS

Approximately 50 NOAA-AVHRR scenes representing the period March 1995 - March 1996 were analyzed as to the spreading pattern of BSW in the North Aegean Sea. Due to the limited space available in this paper only two scenes - one typical summer situation and one typical winter situation can be shown (for a more comprehensive description, see (4).

The first scene, Fig 1, refers to a summer situation, 95-07-31, 0552 GMT, N-12, ch4 with a grey-scale coding comprising three digital levels for each grey-scale tone - see bottom of Fig 1. Dark areas correspond to cold water and bright to warmer water. One could notice vast areas of cold water south of the entrance of the Dardanelles most probably linked to upwelling. There is also a very distinct thermal front south of the islands of Imvros and Limnos separating the cold water in the Chios basin and the somewhat warmer water north of it. Outflow can be distinguished between the front and the island of Imvros as a surface water with temperatures between the upwelled water and the surface water of the Athos basin. There is also a distinct feature showing upwelled water being transported south of both the islands of Imvros and Limnos and then northwards to the west of Limnos towards the island of Thasos.

The second scene, Fig 2, refers to a winter situation, 96-01-18, 1652 GMT, SST, N-12. The surface water temperature is grey-scale coded with 0.5°C for each grey-scale tone - see bottom of Fig 2. A dark tone is cold water and a bright tone is somewhat warmer water. The coldest surface water occurs in a limited area just at the entrance of the Dardanelles. There is a flow from the Dardanelles westwards to the south of Imvros after which transport turns to the northwest between Imvros and Limnos approaching the northern Greek coast east of Thasos. Most parts of the Athos basin surface waters will thus be covered with relatively cold water. There is a very sharp thermal front between the outflow structure near the entrance and the Athos basin water north of it with a temperature difference of near 4.0°C. There is also a sharp boundary towards the south, however not as distinct as the northern one and with a temperature difference of about 2.7°C. There is no upwelling off the Asia Minor coast.

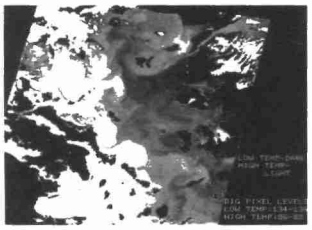

Figure 1.North Aegean Sea. 95-07-31, 0552 GMT, ch4, 8 LSB, N-12. Grey-scale code: three digital levels for each tone. Dark is coldest, bright is warmest

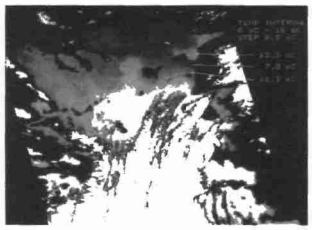

Figure 2.North Aegean Sea. 96-01-18, 1652 GMT, SST, N-12. Grey-scale code: 0.5°C for each tone. Temperature is about 7.3°C at the entrance (dark) of the Dardanelles and about 12.8°C just south (bright) of the entrance

The qualitative studies of the 50 NOAA-AVHRR scenes obtained during one year, between 1995-1996 in the NAS, are summarized as follows:
- at most occasions the BSW outflow from the Dardanelles is distinguished due to its low surface water temperature compared to the surrounding surface water temperatures of the NAS. Temperature differences of more than 4°C have been observed between the BSW and the surrounding NAS surface water. The outflow can be traced at least to the island of Imvros and passed it more or less as a jetlike structure with strong temperature gradients - *i.e.* a distinct boundary - towards the surrounding NAS surface water. At a number of occasions a distinct, colder surface flow with limited lateral extent can be traced from the entrance of the Dardanelles westwards and then heading to the northwest between the islands of Imvros and Limnos all the way to the coast of northern Greece.
- the surface waters of the Dardanelles and its entrance area are colder as compared to regions further off the entrance area for the period Oct/Nov up to May approximately. For the rest of the year the temperature structure is more complex most probably due to an interaction between the outflow and the upwelling phenomena off the Asia Minor coast. Thus there is often a situation during summer when the temperature appears to decrease along the outflow axis, at least up to a certain point.
- upwelling was observed over extensive areas off the Asia Minor coast south of the entrance region of the Dardanelles for all the scenes but one during the months July, August, September, October (altogether ether 18 scenes). During the months November, December, January, February, March, April, May no upwelling was observed except at one occasion (altogether 17 scenes). June and October appeared to be transition months with a more or less equal distribution of upwelling and no upwelling (altogether 12 scenes). Thus there is a strong seasonal component in the upwelling phenomenon which is in agreement with other observations. The cause of the upwelling is thus stated to be strong northeasterly winds (Etesian winds) during summer.
- there is a seasonal pattern as to the spreading pattern of the BSW outflow. On a monthly basis the observations were as follows:

Jan-March: Distinct discharge between Imvros and Limnos and then heading to the northwest. At one occasion the outflow seems to turn northwards along the Asia Minor coast immediately after discharge into the NAS.
April: Discharge reaches the southern part of Imvros and then heads northwest
May: Distinct discharge between Imvros and Limnos after which it is heading to the northwest. The outflow can be traced far away - all the way to the coast of northern Greece and even further.
June: Relatively distinct or distinct discharge between Imvros and Limnos and then heading to the northwest.

BOX MODELING STUDIES OF THE MEDITERRANEAN THERMOHALINE CIRCULATION

Gerassimos Korres and Alex Lascaratos*

University of Athens, Department of Applied Physics, Laboratory of Meteorology, University Campus, Build. PHYS-V, Athens 157-84, Greece

Abstract

A 6 x 4 and a 2 x 2 simple box models are used to study the stability of the thermohaline cells of the Mediterranean basin under mixed boundary conditions and stochastic fluctuations of the freshwater flux superimposed. Results indicate that under present - day conditions the two cells connected with the deep waters production within the basin are sensible to freshwater flux fluctuations and can undergo weakening while the main thermohaline cell of the basin remains stable. By modifying the external conditions applied and making them comparable to those prevailing during the last sapropel formation event in the basin (8 kyrs B.P.) we find that the main cell can switch between two different states.

Key-words: circulation, models

Introduction

Mediterranean present - day circulation involves the production of at least two deep and intermediate water types by surface heat and water fluxes forcing [1]. To these water types there are distinct thermohaline cells associated with, possibly sensitive to external (*i.e.* atmospheric) conditions changes and to the internal dynamics of the basin as well.

The main thermohaline cell of the Mediterranean basin is linked to the eastward path of surface waters of Atlantic origin (AW), their transformation into intermediate waters (LIW) taking place in the Eastern Levantine basin and their subsequent westward return route all the way to the Gibraltar Strait.

Two additional cells are related to the deep water formation processes occurring inside the basin in geographically separate areas namely the Lions Gyre and the Adriatic region.

It is well known by now that the thermohaline circulation in the ocean is set by the interplay between thermal and saline fluxes. High temperatures in the equatorial regions versus low surface temperatures in the polar regions favour sinking at the poles and upwelling at the equator. This thermal cell is opposed by the distribution of precipitation and runoff which induces low salinities at high latitudes and thus favours a reverse meridional circulation. In the Mediterranean however, judging on the present - day distribution of temperature and salinity along the longitudinal direction, the main cell seems to be driven by the salinity east-west gradient while the temperature increase to the east can potentially oppose it. Thus there is an open question related to the existence of other possible states (weak or reversed east - west thermohaline circulation due to thermal effects) within the basin. Another important issue is related to the stability of the two "secondary" cells involving the deep waters formation processes in the Western (WMED) and Eastern (EMED) basin respectively.

The box modeling approach

A first approach to the issues stated in the previous section is accomplished through a box modeling study of the Mediterranean dynamical system.

In the 6 x 4 box model developed, the main body of the Mediterranean basin is divided into three subsystems namely the Western Mediterranean the Ionian and the Levantine basins while three additional subsystems stand for the deep and intermediate waters formation areas (Lions Gyre - Adriatic and Rhodes Gyre regions respectively). Each of the six subsystems consists of four distinct boxes in vertical, allowing for the representation of surface, intermediate and deep waters of the basin. Volume of all different boxes is considered to be fixed.

Within the model individual boxes are connected by horizontal/vertical advection and mixing. In particular horizontal advection of properties is parameterized as being proportional to the hydrostatic pressure gradient while convective overturn is treated as a vertical diffusion process.

Within each box water properties are well mixed and the density is calculated using a linear state equation. Forcing is in the form of a Rayleigh boundary condition for temperature and a flux boundary condition for salinity. Restoring the sea surface temperature to prescribed values is a good approximation for the actual coupling of SST and surface heat flux. On the other hand the use of restoring boundary condition on the salinity has no physical justification. Temperature at the surface boxes is relaxed to prescribed climatological values with a time constant equal to 5 days. Temperature and E-P flux values used to drive the model to a steady state are shown in fig. 1. Although the model by construction is not representing the full dynamics of the system, a quite fair representation of the basin's T-S characteristics is attained at the steady state.

A possible way to study the existence of different states of the Mediterranean dynamical system is by adding a stochastic (white noise in time) component to the E-P flux used to drive the model to the steady state. This procedure has been already used by Mikolajewicz and Maier-Reimer [2] in their global ocean model and by Cessi [3] in a simple Stommel type box model [4].

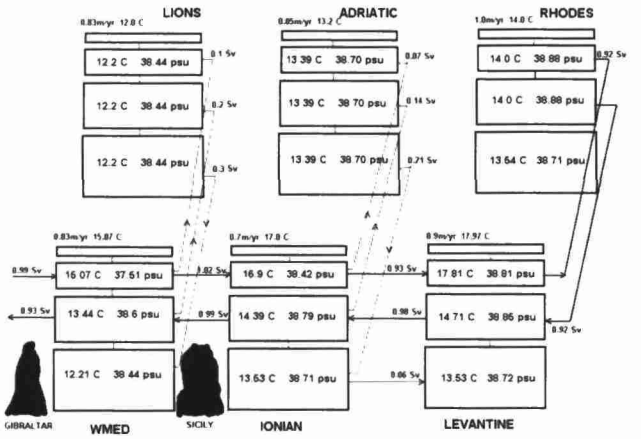

Figure 1: Steady state reached by the 6 x 4 box model under mixed boundary conditions. Arrows indicate direction of transport between the boxes.

Stochastic forcing is randomly picked from a Gaussian distribution with a standard deviation equal to 0.5m/yr and zero mean. In fig. 2 we show the basin mean temperature time series for a 50000 years integration of the model in the case where the stochastic component is applied with a period of one year. The system after a certain period reaches a state which involves a weakened deep waters formation cell in the WMED. This reflects in the increased (~14°C) basin mean temperature attained. The system exhibits also additional peaks of variability due to the weakening of the EMED deep waters formation cell which comes into play. The duration of these peaks approximately equals to 500 years and their excitation is connected to the frequency of the stochastic forcing application. In this experiment the main thermohaline cell of the basin is never perturbed even if the standard deviation of the stochastic component is highly increased. The same holds also in the case where the frequency of the stochastic forcing application is changed.

To study the behavior of the main cell alone, we develop a simple 2 x 2 box model with a longitudinal length scale L = 4000 km and a typical width of 350 km. Upper boxes (with a depth of 150 m) stand for the fresh waters of Atlantic origin (AW) while lower boxes represent the saltier intermediate waters of the basin (LIW) with a depth of 350 m. Advection is parameterized as being proportional to the density difference between the boxes. Apart from mixing associated with advection and overturning, there is no other type of mixing between boxes in the model. With the above configuration and a volume transport at Gibraltar of ~1 Sv the advective time scale of the cell is approximately equal to 22.5 years. The forcing is still in the form of a Rayleigh boundary condition for temperature and a flux boundary condition for salinity. The conservation equations for temperature and salinity for each of the four boxes are:

$$V_1\dot{T}_1 = \gamma V_1(T_1^* - T_1) + \begin{cases} U_m T_m & U_m > 0 \\ U_m T_1 & U_m < 0 \end{cases} - \begin{cases} U_1 T_1 & U_1 > 0 \\ U_1 T_2 & U_1 < 0 \end{cases} + \begin{cases} W_1 T_4 & W_1 > 0 \\ W_1 T_1 & W_1 < 0 \end{cases} + \kappa(T_4 - T_1)$$

$$V_2\dot{T}_2 = \gamma V_2(T_2^* - T_2) + \begin{cases} U_1 T_1 & U_1 > 0 \\ U_1 T_2 & U_1 < 0 \end{cases} + \begin{cases} W_2 T_3 & W_2 > 0 \\ W_2 T_2 & W_2 < 0 \end{cases} + \kappa(T_3 - T_2)$$

$$V_3\dot{T}_3 = \begin{cases} U_2 T_4 & U_2 > 0 \\ U_2 T_3 & U_2 < 0 \end{cases} - \begin{cases} W_2 T_3 & W_2 > 0 \\ W_2 T_2 & W_2 < 0 \end{cases} + \kappa(T_2 - T_3)$$

$$V_4\dot{T}_4 = \begin{cases} U_e T_e & U_e > 0 \\ U_e T_4 & U_e < 0 \end{cases} - \begin{cases} U_2 T_4 & U_2 > 0 \\ U_2 T_3 & U_2 < 0 \end{cases} - \begin{cases} W_1 T_4 & W_1 > 0 \\ W_1 T_1 & W_1 < 0 \end{cases} + \kappa(T_1 - T_4)$$

$$V_1\dot{S}_1 = \begin{cases} U_m S_m & U_m > 0 \\ U_m S_1 & U_m < 0 \end{cases} - \begin{cases} U_1 S_1 & U_1 > 0 \\ U_1 S_2 & U_1 < 0 \end{cases} + \begin{cases} W_1 S_4 & W_1 > 0 \\ W_1 S_1 & W_1 < 0 \end{cases} + \kappa(S_4 - S_1)$$

SUBTIDAL WATER FLOW ACROSS THE STRAIT OF OTRANTO DURING WINTER, SUMMER AND AUTUMN PERIODS

Vedrana Kovacevic [1*], Miroslav Gacic [2] and Pierre Marie Poulain [3]

[1] Osservatorio Geofisico Sperimentale, Trieste, Italy
[2] Osservatorio Geofisico Sperimentale, Trieste, Italy
[3] Naval Postgraduate School, Monterey, CA, USA

Abstract

The subtidal flow across the Strait of Otranto during the three periods (winter, summer, and autumn) is investigated on the basis of direct current measurements. It is shown that in winter and autumn the greatest portion of the flow variance is associated with the intense fluctuations of the outflow along the western shelf and of the inflow in the upper layers along the eastern flank of the strait. These fluctuations are mostly driven by the local north-south winds. The flow fluctuations in the remaining zones are of much lesser importance. In summer when the wind forcing is less enhanced, the barotropic flow fluctuations, intensified in the bottom layers, and confined to the western slope and central regions, are evidenced. They are connected with the outflowing Adriatic Deep Water over the Otranto Sill. The forcing for these fluctuations has not yet been identified.

Key-words: currents, time series, wind, Adriatic Sea

Introduction

The Strait of Otranto is about 80 km wide passage, with a maximum sill depth of about 800 m, through which the Adriatic Sea communicates with the adjacent Ionian Sea. The water masses of different origin take part in the circulation across the strait: relatively warm and saline Ionian Surface and Levantine Intermediate Waters (ISW and LIW, respectively) inflow into the Adriatic along the eastern portion of the strait; the Adriatic delivers its fresh surface waters along the western shore, while the dense Adriatic Deep Water (ADW) contributes to the bottom waters of the Eastern Mediterranean (see [1] for the review). A subtidal flow in this paper is discussed on the basis of a recently conducted direct current measurement experiment.

Experiment design

During 1994 and 1995 six currentmeter moorings were deployed along the southernmost transversal section in the Strait of Otranto (Fig. 1), in the framework of the MAST-Otranto Project and Otranto Gap Experiment. Current flow was monitored by autonomous classical currentmeters and by the Acoustic Doppler Current Profiler. Raw data sampled at 10 and 20 minutes time step were transformed into mean hourly current speed and direction time series at each location in the three layers. Nominal depths are 50 and 300 m below the sea surface for the surface and intermediate layers, respectively, and a few tens of metres above the sea floor for the bottom layer.

Results and discussion

The mean circulation confirms general cyclonic shear of the flow across the strait. Due to the strait morphology the flow is polarized in the north-south direction, especially along both eastern and western boundaries, and in the deepest zones of the strait. Over the shallow western continental shelf the mean flow is southward (mean speed is about 17 and 6 cm/s in the surface and bottom layers, respectively), and is associated with the coastal, density driven outflow from Adriatic [2]. Along the eastern side, the surface and intermediate flows are northward, with mean speed of about 18 cm/s and 4 cm/s, respectively, and are associated with the inflow from the Ionian Sea. In the surface and mid-depths in the central region of the strait the mean flow is less polarized and less intense than along the boundaries. There it is influenced by the frequent passages of the mesoscale eddies in the shear zone between the prevalent outflow to the west and inflow to the east [3]. In the central bottom layer the mean flow is southward and more intense (4-5 cm/s) than above, and is associated with the ADW outflow into the Ionian.

At almost all measurement sites a substantial variability occurs, both in the tidal and subtidal frequency range. In order to study the subtidal flow fluctuations across the strait, mean hourly north current components, perpendicular to the mouth of the strait, were filtered using a digital symmetric filter [4]. The subtidal flow was examined in the three time intervals during which a relatively good spatial coverage with current data permitted a determination of the flow structure across the strait. These periods are identified roughly as winter (December 1994 - January 1995), summer (May - August 1995), and autumn (September - November 1995) seasons.

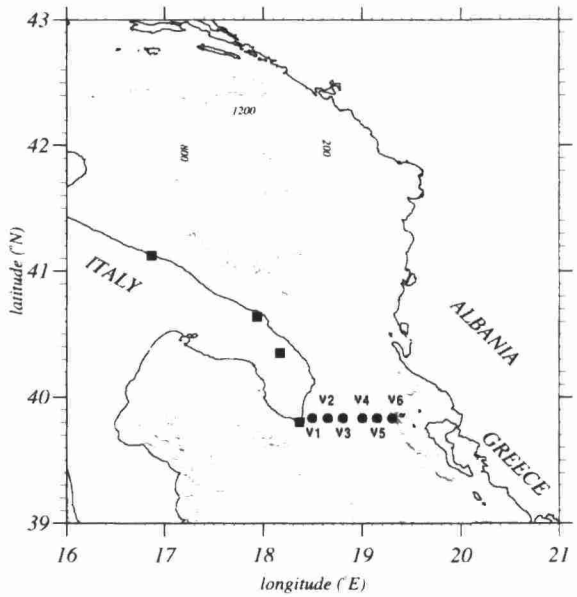

Figure 1 - Bathymetric chart with depth contours each 200 m. The currentmeter stations along the southernmost section in the Strait of Otranto (M1, M2, M3, M4, M5, and M6), are denoted by solid circles. Wind is measured at the locations indicated by a solid box.

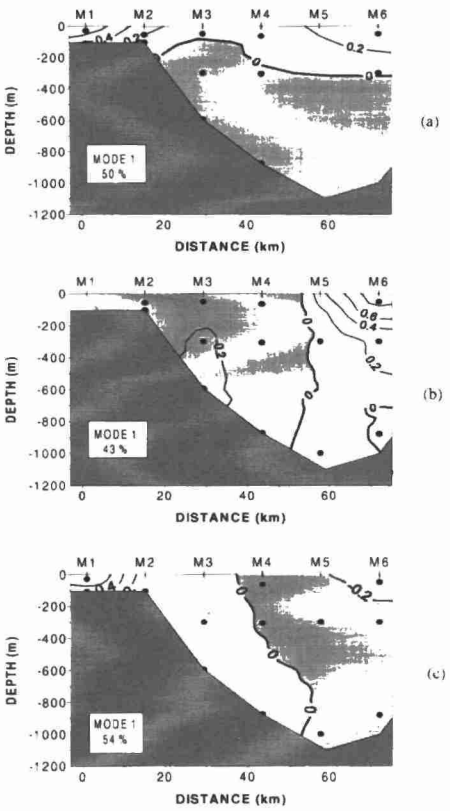

Figure 2 - Spatial patterns of the first vertical EOF modes: (a) in winter (December 3, 1994 - January 29, 1995), (b) in summer (May 17 - August 25, 1995), and in autumn (September 10 - November 18, 1995). The percentages given show the contribution of each mode to the total variance of the flow. The dots mark the data points used in the analysis. The shaded area represents negative mode values.

THE GEOSTROPHIC CIRCULATION AND CURRENT STRUCTURE IN THE EASTERN MEDITERRANEAN BETWEEN THE SYRIAN COAST AND CYPRUS ISLAND IN WINTER AND SUMMER SEASONS

V.G. Krivosheya [1*], V.B. Titov [1], I.M. Ovchinnikov [1], L.V. Moskalenko [1], V.G.Yakubenko [1], F. Abousamra [2], I. Aboucora [2], C. Bouras [2]

[1] Southern Branch of P .P. Shirshov Institute of Oceanology, Gelendzhik-7, 353 470, Russia
[2] Higher Institute of Applied Sciences and Technology, Damascus, Syria

Abstract

The geostrophic circulation and the structure of currents have been examined on the basis of quasi-synchronous hydrophysical surveys and current measurements on 7 mooring carried out in this area for the first time in February 1992 and October 1993.

Key-words: Levantine Sea, Deep Waters

In spite of a long history of the Mediterranean Sea oceanographic research, the north-eastern Levantine Basin between the Syrian coast and the Cyprus island (we suggest to call it "Lattakia Strait") was the least studied one till recently. From 1 to 14 hydrological stations in one-degree square can be numbered there (1, 2, 3, 4). Later, large investigations were fulfilled in the Levantine Basin within the POEM Project (5, 6, 7), but only few stations were carried out in Lattakia Strait. There were no current measurements at all performed at a modern technical and methodological standard.

Two expeditions of the P.P. Shirshov Institute of Oceanology, Russian Academy of Sciences, and Higher Institute of Applied Sciences and Technology of Syria in winter 1992 and autumn 1993 have made the greatest contribution into oceanographic research of Lattakia Strait. The first expedition (the 24th Cruise of the R/V *Vityaz*, February 6 - March 16, 1992) has performed two hydrophysical surveys down to the bottom with the help of performant instruments (107 STD stations 10 miles apart and simultaneously 7 mooring buoy stations (MBS) during 20 days; Fig. 1) (8). The second expedition (the 27th cruise of the R/V *Vityaz*, September 26 - November 17, 1993) has also performed two similar surveys (110 STD stations 10 miles apart and current measurements at 7 MBS for 24 days) (9). The main results of these investigations are given hereafter.

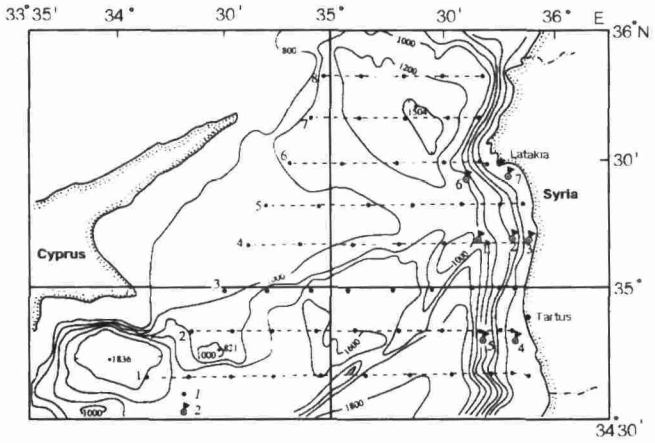

Fig. 1. The bottom topography and the location of hydrophysical stations (1) and mooring buoy stations (2). (1-8 : number of the latitudinal hydrophysical sections).

Maps of geostrophic currents are calculated for the two surveys (Fig. 2). The current field is an intensively meandering northward flow with a number of eddies on its edges, *i.e.* cyclonic eddies on the left and anticyclonic ones on the right. Three cyclonic and one anticyclonic eddies were observed during the first survey (Fig. 2a). Two cyclonic eddies were in the southern part of the area (34°50'N) and the third one was in the north (only a part of it was covered). Cyclonic eddies southward of 35°N are, apparently, a part of the Lattakia cyclonic eddy (5, 6). The anticyclonic eddy was situated between the flow and the Syrian coast (35°15'N). Eastward of the anticyclone near the shore there is a slightly marked secondary cyclonic eddy.

According to the second survey data the dynamic picture was quite different. This survey was done east of 35°E. An anticyclonic eddy, stretching in the meridional direction, was found at the place occupying by a cyclonic eddy during the first survey (Fig. 2b). On the north the southern part of a second anticyclone might be signed. In the central part of this area, a cyclonic eddy was encountered.

When comparing the location of the characteristic eddy centres, it can be concluded on the basis of the first and second survey data that the whole dynamic system has seemingly shifted to the north in the direction of the general flow for 40-50 miles, with a mean velocity of 2.5-3 miles per day. The wave length of the meander is about 40-45 miles.

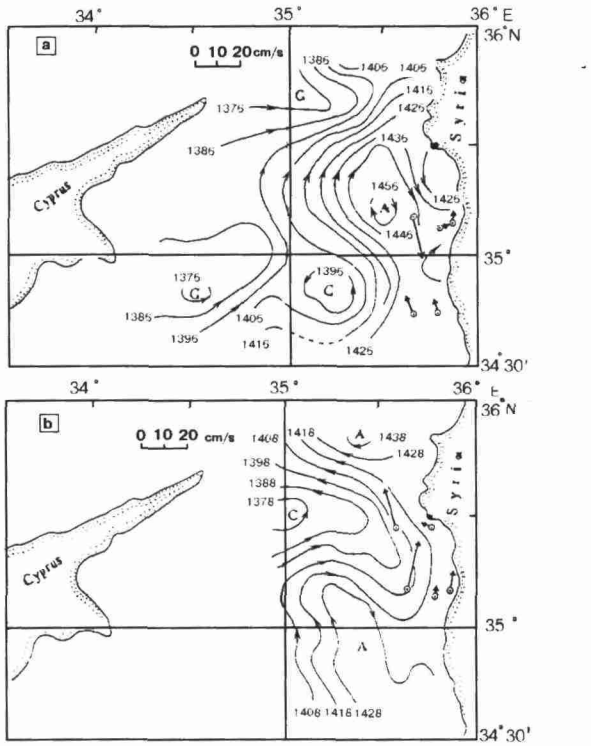

Fig. 2. Dynamical topography maps of the sea surface relative to reference level of 800 dbar according to the data (a) of the first survey (15.02-22.02.92) and (b) of the second survey (05.03-08.03.92). (A - anticyclone, C - cyclone. The arrows show mean currents from moored instruments).

The above mentioned character of the geostrophic circulation and its large-scale elements (meanders, eddies) are observed within the whole water column, as confirmed by currents measurements : water flow is running in one direction from the surface down to the bottom. Changes of current velocity and direction happen simultaneously at all levels (Fig. 3). Such peculiarities of the current field are typical of eddies and meanders whose vertical structure is quasi-homogeneous in winter. Homogeneity of winter hydrological structure is characterized by vertical gradients whose maximum values are :

$$\frac{dT}{dz} = -0.0104°C/m, \quad \frac{dS}{dz} = 0.0018/m, \quad \frac{d\sigma}{dz}dz = 0.0007/m$$

(depth is 325-350 m). Above and below this layer, vertical gradients were close to zero (10). A joint analysis of wind and currents showed that the changes in the current field depend on the spatial shift of meanders and eddies and are not connected with local winds (Fig. 3) (8).

Thus, in winter a flow to the north crosses the Lattakia Strait from its surface down to the bottom. This current is, probably, a part of the Mid-Levantine Jet, which divides into three streams near the Cyprus Island. One of them swerves to the left (to the south-west of Cyprus) and enters the Cyprus eddy, the second turns to the south and flows into the Shikmora Gyre (7, 11, 12), and the third one returns to the north to the Lattakia Strait (4). This stream carries Modified Atlantic Water (MAW), Levantine Intermediate Water (LIW) and a part of Deep Water (DW) to the Cilicia Basin. According to the data of two hydrophysical surveys in October 1993 the maps of dynamical topography were calculated for levels 0, 100, 250 and 500 m relative to a reference level of 800 dbars. The field of geostrophic currents was characterized by an intensive space-time variability.

ADRIATIC SEA TIDES IN THE ERA OF SATELLITE ALTIMETRY

Milivoj Kuzmic [1] and Carl Wagner [2]

[1] Rudjer Boskovic Institute, CMER, Zagreb, Croatia
[2] NOAA, National Ocean Service, Silver Spring, U.S.A.

Abstract

This study addresses the question of how well some recent model solutions fit the established image of the Adriatic Sea tides. To that end harmonic constants for 33 stations have been compiled and compared to the same output from a purely hydrodynamic (HD) model, and two models incorporating satellite altimetry on a global scale. The comparison shows that the pure HD model produces better agreement with the perimeter gauges. The two global models, despite inherent disadvantages, apparently can produce Adriatic results generally in accord with the pure HD solution and the gauge data, except at anomalous locations largely on the east Adriatic side.

Key-words: tides, models, remote sensing, Adriatic Sea

Introduction

Satellite altimetry has reached such a level of precision that it allows direct evaluation of marine tides, but also demands accuracy for the tidal correction to avoid the contamination of other parts of the oceanographic signal. The marginal shallow seas provide both the need for predicting a rapidly changing and spatially complex tidal environment, and a challenge to researchers to show the utility of altimetry and/or altimetry-adjusted models.

Although the Mediterranean Sea is not known for pronounced tides, in some of its parts shallow topography contributes to harmonic amplitudes of appreciable magnitude. Such is the case of the Adriatic Sea, an elongated basin spanning more than 800 km between the Strait of Otranto, and the Gulf of Trieste (Fig. 1). Common understanding of the Adriatic tides, developed earlier in this century (1) and reinforced in more recent works (2,5), pictures a basin co-oscillating with the Ionian Sea with only minor correction arising from the direct action of the tide generating potential.

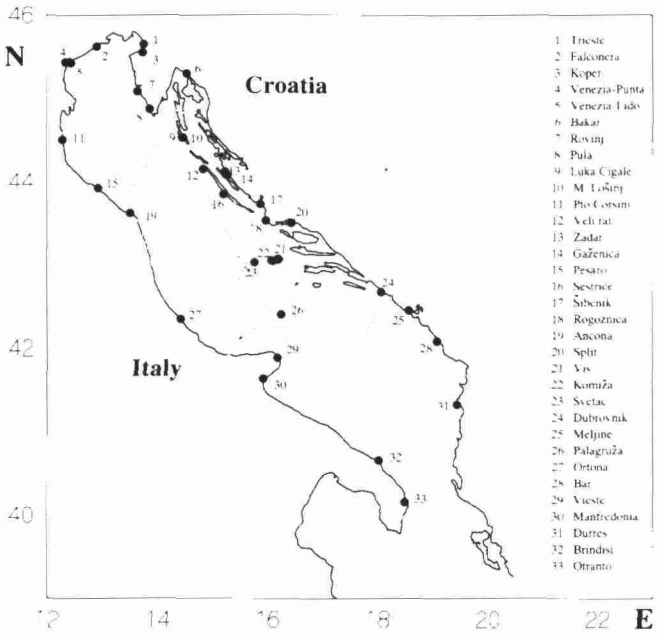

Figure 1. Location and names of the Adriatic tidal gauge stations and Topex/Poseidon track segments.

In this study we aim to assess how well some recent tidal models fit the established image, and to glean how successful altimetry can be in extracting a relatively weak tidal signal over a narrow basin with complex topography.

Gauge data and mathematical models

We have compiled harmonic constants from the available literature for 33 Adriatic coastal and island gauge stations as depicted in Fig 1. These empirical data have been compared to the same output generated by 3 tidal models, one purely hydrodynamic while the other two include Topex/Poseidon (T/P) altimetry on a global scale, but seek to accomodate the tidal complexities of the Mediterranean Sea in different ways.

The POL model (2) is a high resolution (1/12 x 1/12 degrees), nonlinear, two-dimensional, pure HD model of the Mediterranean Sea forced only by the equilibrium tide inside and the actual tides at the Strait of Gibraltar. The CSR3.0 model (3) is a global tidal solution referenced to the high resolution Grenoble HD model (4) in which long wavelength accruacy is sought by fitting altimeter residuals from this and a Mediterranean (5) model to tide harmonics through a response formalism, and broadly smoothing the resulting corrections. In the FES95.2 model (3) improvement on global scale is sought through statistical assimilation of a pure altimetric solution (CSR2.0) into the same global reference HD model (4). In the Mediterranean however, FES95.2 is completed by adding the same local gauge-constrained HD model (5) resampled on a coarser grid. All models compute at least the 4 major constituents we have considered in the present study (M2, S2, K1, and O1).

Results and conclusions

Two parameters are used to aid the comparisons. One is the magnitude of the vectorial difference (distance d) between observed (o) and modeled (m) harmonic constants (H, G - phase lag relative to Greenwich) calculated as:

$$d = \sqrt{(H_o \cos G_o - H_m \cos G_m)^2 + (H_o \sin G_o - H_m \sin G_m)^2} \qquad (1)$$

and the other is the classic Form number:

$$F = (K1 + O1)/(M2 + S2) \qquad (2)$$

While the gauge values provide a useful test generally, the comparisons with particular gauges which have site problems may not be representative. Thus the larger distances to some gauges do not necessarily imply an inferior model. One should also bear in mind that binning and smoothing applied in CSR3.0 or coarse resampling in FES95.2 inevitably distort their solutions, particularly at the margins where the gauges are located. The hope for CSR3.0 has been that the altimeter data in the mid-basin would provide some positive effect, while FES95.2 results should gauge the penalty for subsampling. Some of the observed behavior with respect to the gauges is captured in Fig 2.

Comparing model performance in two parts of the basin we note that all experience difficulties in the shallower northern part. An example is a pronounced discrepancy at Trieste, the most studied station with particularly reliable constituent estimates. We note in passing that station 4 inside the Venice Lagoon is understandably beyond the reach of the three models. Judging the ability to predict the overall diurnal and semi-diurnal tide behavior, we find problems for all models along the island-rich eastern Adriatic coast, and along both coasts close to the amphidromic center. There, the solutions are particularly vulnerable to numerical noise, and the distances can reach or surpass the M2 amplitude.

Comparing the pure HD (POL) with the 2 global model solutions we find that the two ways of accomodating the Mediterranean tides produce solutions that depart from POL in a similar fashion. This clearly testifies to their common hydrodynamical background in the Mediterranean (5) and to the ineffectiveness of the small and broad altimetric adjustment. Preliminary analysis of solutions along Adriatic T/P tracks (not shown) suggests there are similar deviations of both global model solutions from POL in the open areas of the sea as well, with somewhat better CSR3.0 performance. A notable exception is Ancona station where CSR3.0 and FES95.2 largely differ in predicting diurnal and semi-diurnal waves as well as their ratio (see Table I). It is worth noting that Ancona is one of the five gauge stations (and the only one in Adriatic) providing empirical constraint to the model on

THE SURFACE CIRCULATION AROUND CRETE INFERRED FROM SATELLITE, DRIFTER BUOYS, AXBTS DATA AND A PHYSICAL MODEL

Paul E. La Violette [1]*, James A. Price [2], Robert Mosher [2] and N. E. Kotsovinos [3]
[1] Gulf Weather Corporation, Stennis Space Center, Ms 39529 601 688 3397, USA
[2] Naval Oceanographic Office, Stennis Space Center, MS 39529 601 6885268, USA
[3] Democritos University of Thrace, Gr 67100 Xanthi, Greece

Abstract

The long term (1987 through 1997) surface circulation around Crete is described using drifter buoy trajectories, AXBTs, satellite thermal imagery and altimetry data. The long term data is provided by weekly satellite images and altimetry data augmented by the three-month trajectories of four satellite-tracked drifter buoys. These buoys were air-dropped into prominent frontal features and eddies around Crete that had been noted as a result of a pre-drop two-year study of satellite thermal imagery. Permanent changes that appear to have occurred after late 1995 in one of the more prominent of the eddy features are discussed and a physical model is presented to show its possible relation to the surrounding circulation.

Keywords: Remote Sensing, Circulation, Cretan Sea

Introduction

A brief report on the surface circulation around Crete as inferred from satellite imagery and drifter buoy trajectories was presented by Price *et al.* (1) at the CIESM meeting in Perpignan, France in October 1990 (Fig. 1). The report concentrated on the three-month trajectories of four satellite-tracked drifter buoys (2) air-dropped on 25 February 1990 into prominent frontal features and eddies around Crete that had been noted as a result of a two-year study of satellite thermal imagery. Price *et al.* discussed in particular several prominent thermal features that were noted in the study of the satellite imagery and that appeared to control the trajectories of the buoys. The 1990 report indicated that the region contained permanent cyclonic and anticyclonic sub-basin scale gyres that were fed and interconnected by jet-like currents. Although the features appeared to be permanent (within the two-year time scale of the report), they showed wide temporal variation, displaying broad shifts in the location of their centers as well considerable deformations in their boundaries.

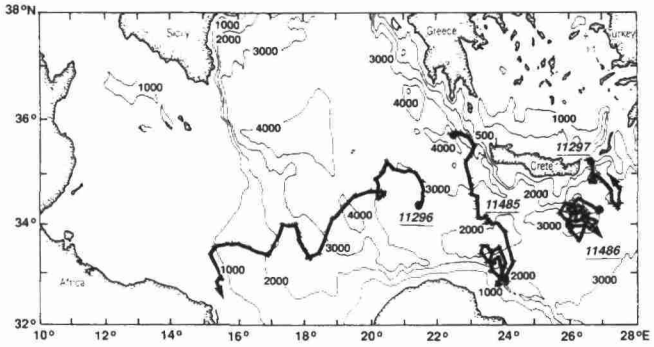

Figure 1 : Vertical distribution of a cross-transect current component for winter. Transect location is shown in the insert map.

In this report we will 1) discuss in more detail the trajectories of the buoys and their relation to the satellite-derived thermal field; 2) update the persistence of these eddies using a broader temporal base of satellite imagery and altimeter data (1987 through 1997), and airborne expendable bathythermograph data; 3) show that although one of the most prominent of the eddies were generally present to late 1995, it has since disappeared; 4) use a physical model to show the possible ramifications of this change in the local circulation in relation to the regional circulation.

There is a difficulty in using single buoy drops in characterizing a region's circulation in that some anomalous perturbation may influence the drift in away that does not describe the general regional movement. Our examination of the co-incident thermal satellite imagery has helped alleviate that problem and we believe the trajectories, as a whole, represent pertinentcirculation features.

The pre-fall 1995 circulation

The preliminary study of satellite imagery by Price *et al.* indicated that a large cool band of surface water flowing out from the Aegean Sea constitutes much of the surface water mass found in the area to the west and east of Crete. For lack of a previous reference to this current feature, Price *et al.* termed this the Aegean Sea Outflow. The buoy deployment in their report was designed to study this outflow and help in determining its relationship with the general Cretan circulation, especially the strong and variable eddy-field found south of Crete. In this part of our study, we will present an expanded description of the trajectories. Although temporally short (90 days), the description will show the general regional circulation as it was prior to the fall of 1995. Data details such as the daily imagery or buoy thermal and wind data are not presented due to space constrains. Instead the

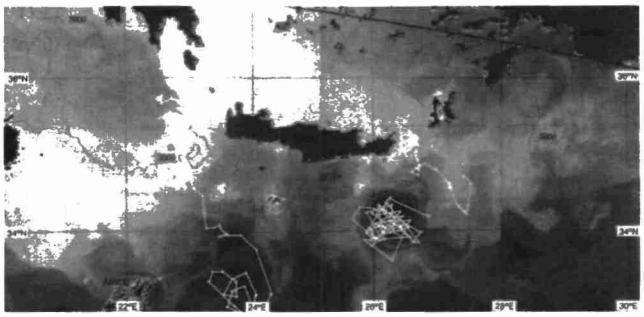

Figure 2. **See color figure p. 215.**

following will summarize comparisons of the buoy trajectories (Figs 1 and 2) with simultaneous satellite thermal imagery, and the regional bathymetry, wind conditions as reported by the individual buoys and the regional winds. Note that the single-day image in Figure 2 was chosen to best depict the overall circulation during the three-month buoy deployment. Altogether, 62 cloud-free images were examined during the three month period. It is important to note that the day-to-day depiction of the thermal field by these 62 images varied considerably during the three months (this will be presented in Dubrovnik). In the buoy discussions that follow, the remarks are based on specific segments in the trajectories in direct comparison with the satellite images for the periods of those segments.

The Eastern Mediterranean East-West Frontal (Buoy 11296). Figures 1 and 2 shows that Buoy 11296 traveled in a general southeast direction after leaving its initial drop point southeast of Crete. The buoy drifted at speeds between 20 and 56 cm/sec. The thermal imagery showed that weak anti-cyclonic eddies inhabiting the Afro-Sicilian Basin and that the highly variable circulation associated with these features were effecting the track of the buoy. Although the buoy followed the deep isobaths of this gradually slopped region on occasion (e.g., see the initial track of the buoy), it just as often crossed the isobaths of the gradual sloped area. Once the buoy crossed 15°E, it turned south, following the Libyan coast until it ceased transmitting on 26 April.

The Pelops Gyre (Buoy 11485). Buoy 11485 was dropped just southwest of a warm anticyclonic permanent eddy located northwest of Crete that had been noted in all of the two years of satellite imagery - Robinson *et al.* (3) termed the feature, the Pelops Gyre, and this terminology is used here. Thedrift of the buoy was influenced by this eddy for a short period, moving at 25 cm/sec along its eastern side before becoming entrained in a flow indicated by the daily imagery to have initiated in the Aegean Sea. Typical speeds in this flow were slower:15 cm/sec. Upon crossing 34°N, the buoy became entrained in a large jet associated with a warm eddy lying north of Libya and speeded up to 46 cm/sec. The buoy became trapped by this warm eddy, moving deep into its interior drifting at 15 cm/sec along its outerwall and 35 cm/sec nearer the core. The buoys last transmission was also on 26 April.

The Cretan - Ierapetra Eddy (Buoy 11486). Of especial interest was the drifter entrapped for 50 days in a well defined semi-permanent eddy located at the southeastern end of Crete which Price et al. termed the Cretan Eddy.This eddy was also noted in the POEM ship data (3 and 4) and termed the Ierapetra Gyre. To avoid confusion, we will term the eddy the Cretan -Ierapetra Eddy. Price *et al.* thought it odd that the buoy remained entrained in the eddy for such a long period (approximately 60 days), despite at times coming quite close to the thermal rim (as detailed in the overlays of the driftertrack on simultaneous AVHRR imagery). The data shows the buoy making a complete loop within the eddy every five

THE USE OF VISIBLE AVHRR NOAA SENSORS IN COASTAL AND ESTUARINE STUDIES AREAS OF THE MEDITERRANEAN SEA

Paul E. La Violette [1]* and Robert Arnone[2]

[1] Gulf Weather Corporation, Stennis Space Center, Ms 39529 601 688 3397, USA

[2] Naval Research Laboratory, Stennis Space Center, MS 39529 601 688 5268, USA

Abstract

The delay in the launch of SeaWiFs has reduced the scope of turbidity and ocean energetic studies in the ocean's coastal and estuarine areas. SeaWiFs is now up and follow-on ocean color sensors (*e. g.*, MODIS, MERIS and Landsat ETM+) will soon be in orbit. This study explores the use of an interim algorithm made up of the visible channels of the NOAA AVHRR in these type studies. This study shows an unexpected dividend in that the AVHRR visible data will continue to be useful in coastal studies even after the availability of data from the new ocean color systems.

Key words : Remote Sensing, ocean color, coastal processes

Introduction

Knowing the optical variability of coastal and estuary regions is important toward understanding these regions' physical / biological processes. High concentrations of suspended sediments (from river discharges and bottom re suspension) and colored dissolved organic matter are responsible for the strong coloration of the waters in these regions. The optical signal from these sediment / biological mixes can be used alone or in combination with the thermal signal to define turbulent mixing areas, areas of strong biological activities and to trace circulation patterns. here are a number of satellite sensors that may be used to monitor these processes as well as the coastal environment in general. Those having a long proven history for such use, are two "workhorses" of remote sensing, the visible and thermal infrared sensors (for examples of their use in the Mediterranean, 1, 2, 3, 4). Although the thermal sensors have, provided a long and relatively uninterrupted data stream that may , be used to provide long-term statistical analyses of the coastal regions, the visible data steam has been relatively short; mostly limited to that provided by the Coastal Zone Color Scanner (CZCS) during the period late 1978 through mid 1986. At the time of this writing, a new ocean color sensor, SeaWiFs, has been placed in orbit after a series of prolonged delays. This sensor should shortly be providing ocean color (visible) data to the oceanographic community. (Although not available at this time, examples of the SeaWiFs data related to the Mediterranean will be presented at the CIESM meeting in Dubrovnik). SeaWiFs data will be different from that of the Coastal Zone Color Scanner (CZCS) in that the new sensor's data can be adjusted to provide high reflectance information of the shallow regions of the coastal regime. CZCS data of highly turbid regions have problems due to the red and green channels being saturated. In addition to SeaWiFs, other satellites (*e.g.* MODIS, MERIS) will be orbited in the near future that will carry sensors with ocean color data collecting capabilities that will work in the coastal environment. Thus, by the turn of the century, new data will be available. Used en suite, the repeat looks provided by this assemblage, will be highly useful in the quick-changing coastal shallows. The time spent waiting for the launch of SeaWiFs was not wasted. The easily accessed, easily processed NOAA AVHRR data has been shown to be of use in the shallow water coastal environment. This began with an algorithm developed by Stumpf (5) to derive the distribution and characteristics of highly turbid coastal regions using the NOAA AVHRR two comparatively wide (+100mm) visible channels (640 and 850 mm). Gould and Arnone (6) have modified the Stumpf algorithm to relate, remotely-sensed reflectance data to the beam attenuation coefficient at 660 mm (*i. e.*, c660), a frequently measured oceanographic parameter. Despite the extensive spectral limitations of AVHRR visible channels in comparison to those of CZCS and SeaWiFs, the use of the AVHRR data for marine research has several very practical advantages:

- AVHRR ocean color data are available now for coastal research. In this regard, the NOAA polar orbit and direct readout are ideal. NOAA 14 sees the Mediterranean shortly after local noon each day, an ideal time for ocean color research. In addition, AVHRR data can be received directly at sea and thus, can be used to control *in situ* data collection as well as be part of the post-campaign analysis.
- Unlike Nimbus 7 or Sea Star color sensors, each NOAA satellite contains identical AVHRR sensors. There has been at least one NOAA satellites in orbit since the mid 70's. When NOAA 14 reaches the end of it's operational life, a NOAA satellite with an identical AVHRR sensor will be launched. Two decades of AVHRR ocean color data are now available as a data base.
- AVHRR visible and thermal data are co-registered. Each AVHRR channel shows the same earth scene. Coincident CZCS thermal/visible coverage was available for only a short period. No thermal channel is to be on SeaWiFs. The AVHRR ability to provide temporal and spatial coincident thermal/visible data offers unique marine study opportunities.

The AVHRR algorithms have been used in a number of far ranging studies that have shown the NOAA AVHRR to be a valuable data source in the monitoring of coastal areas (*e. g.*, 7, 8, 9). An interesting aspect of these studies was to show that AVHRR data can define wind- and tidal current-induced changes in shallow waters (>5 meters). Thus, in a fashion not previously realized, the AVHRR visible and thermal data were found to be usable in small scale study of lagoons and estuaries. The data sets thus derived may be used as single images or as groups of sequential images or, as will be shown here, as statistical sets. In recent years, ocean studies utilizing both graphs and composite images of long-term satellite data have begun to emerge as methods of showing the ocean's seasonal and interannual variability (*e.g.* 10, 11). While not as spatially detailed as the instantaneous views of the high resolution daily satellite imagery, these compositing studies have provided information useful in unraveling details in the ocean's long-term variability and better defining the forces that cause this variability. This methodology has now been applied to the shallow water environment using the AVHRR visible and thermal data. When TIROS-k is launched late this year, its improved AVHRR sensor will be added to the suite of sensors available to work the shallows. So, after years of successful exploitation in the open and deep ocean, satellite remote sensing visible data (starting with AVHRR, and, as they come available, SeaWiFs, MODIS, MERIS and Landsat ETM+) are slowly coming into their own as standard tools to study and monitor the shallow water environment.

Due to the limitations of these proceedings, the examples of the AVHRR work will be limited to Figures 1 and 2. In the presentation at Dubrovnik, this paper will provide examples of the use of the c660 algorithm to 1) trace estuarine discharge and coastal flow structure and 2) provide long-term (seasonal) shallow water optical information in the coastal waters. It will show that even after the spectrally more definitive SeaWiFs et al., data become available, the dependability and easy accessibility (in reception and computer manipulation) of the AVHRR data will continue to make it a major instrument in coastal color studies. This dependability is (*i. e.*, the long term continuity of the NOAA AVHRR series) is especially emphasized in the short life span of the Japanese OCTS sensor

Examples of the C660 technique in the Mediterranean

The Gulf of Venice (Fig. 1). As stated earlier, studies of shallow water (>5 meters) lagoons and estuaries show that AVHRR data can define wind- and tidal current-induced changes. Thus, in a fashion not previously realized, the AVHRR visible and thermal data were found to be usable in studying day-to-day changes in these comparatively small regions. Note the thermal field at this time of year is relatively flat and the visible data contain the most information. The Po River Outflow (Figure 2). Unlike the other areas within the Adriatic, the area of the Po Delta always displays a strong thermal field due to the differential temperature of the river water in comparison to the Gulf waters. The coincident c660 / thermal imagery are quite similar in their general pattern characteristics, although close examination will show significant differences that reflect the involvement of different processes. The Po River outflow varies seasonally and year-to-year. Thus, there are seasons / years in which the river outflow drastically changes the composition of nearby waters and conversely, there are seasons/years when such changes are minimal. These seasonal/interannual changes can be monitored using AVHRR visible and thermal data

Conclusions

This paper demonstrates that coastal optical research can be conducted using the comparatively easily accessible NOAA AVHRR data. The following are our preliminary conclusions.

1. The algorithm of the coastal volume scattering coefficient, c660, derived from NOAA AVHRR visible channel data is effective in the study of highly turbid marine areas; in many cases marine features are revealed in the AVHRR visible data that are poorly defined by AVHRR thermal data.
2. The c660 algorithm is an excellent tracer of flow patterns and coastal water masses during seasons when sea surface temperature values are essentially homogeneous (late-spring, summer and early fall). During other seasons, a combination of the c660 algorithm and thermal images can be highly successful in studying coastal optics and dynamics.
3. The c660 algorithm is useful in studying high suspended sediment loads associated with nearshore discharge plumes and resuspensions with significant remote sensing reflectance. However, it cannot be used to resolve optical values or marine features in waters having low turbidity concentrations or reflectance. Thus, the c660 algorithm is ineffective in coastal regions with low turbidity.

WIND-DRIVEN CURRENTS IN THE CHANNEL AREA: AN EXAMPLE OF THE CHANNELS ZADARSKI KANAL AND PASMANSKI KANAL (EAST ADRIATIC COAST)

Nenad Leder [1*], Gordana Beg Paklar [2], Zvonko Gržetić [1], Ante Smirčić [1] and Ivica Vilibić [1]

[1] State Hydrographic Institute, Zrinsko Frankopanska 161, 21000 Split, Croatia

[2] Institute of Oceanography and Fisheries, Šetalište I. Mestrovica 63, 21000 Split, Croatia

Abstract

The paper deals with the response of the channel area to the different wind forcings. For that purpose current measurements were performed in the channels Zadarski kanal and Pašmanski kanal. Basic statistic, spectral and system analysis and low-pass filter have been applied on the data, and the results have been verified by numerical model. The interesting results are eddies appearing at the wider entrance of the channel Zadarski kanal, both detected from the data and achieved by the model.

Key-words: Adriatic Sea, circulation models, straits and channels

Introduction

The region of the channels Pašmanski kanal and Zadarski kanal, which embraces the eastern coast of the Adriatic Sea (Fig. 1), is a typical enclosed channel area of limited dimensions. The southeastern part of the channel (Pašmanski kanal) is narrower (about 2 km) and shallower, with the depths from 10 to 25 metres, as distinguished from its northwestern part (Zadarski kanal). The depths of the channel Zadarski kanal reach 50 metres at the mouth, and width is more significant (about 7 km at the mouth). An important factor are the small islands and shoals (8-10 m) inside Pašmanski kanal, as they considerably reduce the horizontal section of the channel and in this way influence circulation.

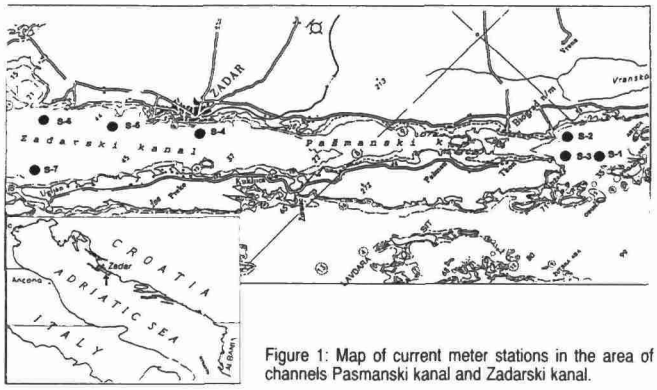

Figure 1: Map of current meter stations in the area of channels Pasmanski kanal and Zadarski kanal.

Data and methods

Current measurements were done at the stations S-1 to S-7 (Fig. 1) from 28 June to 21 July and from 24 August to 17 September 1994. Current direction and speed were being measured using AANDERAA RCM4S and RCM7 current meters in the surface layer (3-5 metres) and bottom layer (4-5 metres above the sea bottom), with a sampling interval of 5 and 10 minutes. Positions of current meters were selected so as to describe properly the marginal processes and the circulation inside the basin.

Characteristics of the circulation system were being investigated analyzing the time series of hourly and daily current vectors, progressive vector diagrams and current roses. In order to investigate the influence of wind on circulation in such an enclosed channel area, the wind data obtained from the meteorological station Šibenik were used. This was the nearest meteorological station at which wind measurements were carried out. Current and wind vectors were divided into components, vertical to the coast and parallel with it, and passed through a low-pass filter. Spectral and system analyses, according to Jenkins and Watts (1) were applied as well.

Experimental results of current measurements were used for verification of the results obtained from application of a three-dimensional numerical hydrodynamic model (2). The model is based on the equations for momentum of mesoscale marine hydrodynamics with Boussinesq and hydrostatic approximations. For horizontal diffusion the Joseph-Sendner approximation (3) is used, while vertical diffusion is defined from the turbulent energy equation with second-order closure (4). Sea surface boundary is forced by wind, while the bottom boundary condition is calculated from the logarithmic bottom profile (5). At the solid boundary no-slip conditions are used, and no divergence at open boundaries. The numerical scheme for the model is space-centered with semi-staggered grid, and time integration is performed using forward-backwards scheme.

Results

Weather conditions during the experiment were influenced by high-pressure circulation, occasionally disturbed by slow and rather weak low-pressure systems. Several times from 20 August to 17 September, stable and warm weather was disrupted by cyclonic disturbances, particularly after 2 September. The entire measurement period was characterized by frequent calms, so that even the typical summer Etesian (northwest wind) was not recorded.

In the first part of the experiment, circulation in the researched sea area was a typical channel, two-layer circulation of SE-NW direction, because of the stable weather conditions. In the surface layer, circulation of SE direction was prevailing, while in the bottom layer occurred a counter-current of lower intensity. The data analysis shows the prevailing low-frequency circulations with several day periods, on which are superposed tidal oscillations. Current polarization is less manifested at the stations S-6 and S-7 due to the channel width and influence of the circulation from the neighbouring sea areas.

In the second part of the experiment, the current field is more extended in the channel direction, with higher speeds at all stations, due to an intensified cyclonic activity above the researched area. Low-frequency oscillations are better manifested, with periods of cyclonic disturbances (Fig. 2), while stability of the current flow is disrupted by a frequent change of inflowing and outflowing current direction.

The comparison between wind and currents (Fig. 3) shows a great correlation between surface currents and wind during strong wind. In such weather conditions circulation can be described as a two-layer model with wind driven currents in the surface layer and counter-currents in the bottom layer.

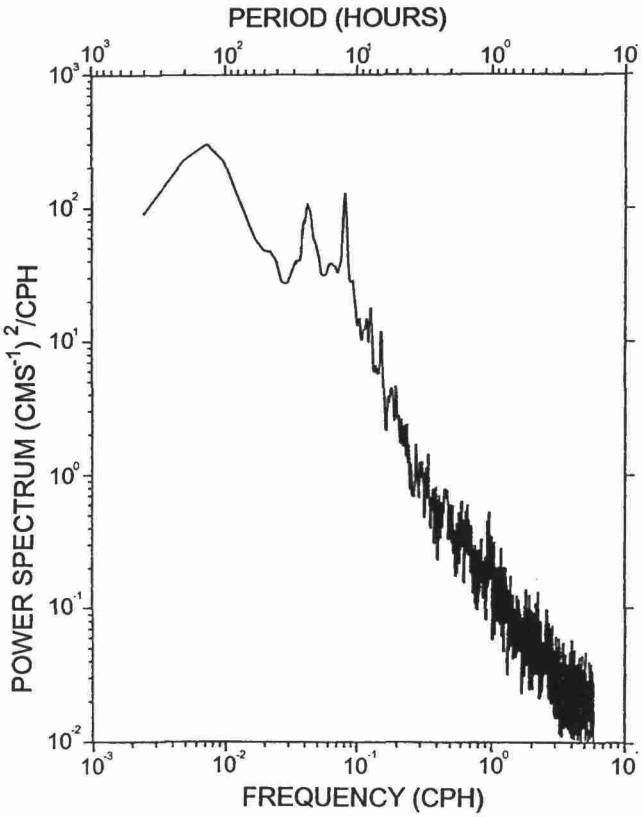

Figure 2: Total power spectrum of surface currents measured at the station S-1 from 24 August to 19 September 1994.

HYDROLOGY AND ASSOCIATED SPM DISTRIBUTION OVER THE NORTHERN MARGIN OF THE ISLAND OF CRETE

V. Lykousis, V. Zervakis*, S. Poulos, D. Georgopoulos and G. Chronis
National Centre for Marine Research, Aghios Kosmas, 16604 Hellinikon, Greece

Abstract

The circulation over the continental margin of Crete in 1994-1995 was dictated by a mesoscale eddy dipole system, inducing a shoreward flow at the study area. Light transmission was correlated to SPM concentrations ranging between 1.5 mg/l and 0.2 mg/l. The highest SPM concentrations were found close to the sea-bed over the shelf-break and upper slope (mostly terrigenous), and in the upper water column offshore (mostly biogenic). The offshore SPM distribution is governed by the general circulation pattern. The bottom nepheloid layer (BNL) over the shelf-brake and upper-slope region may be attributed to seismicity, bottom currents, internal waves and trawling.

Key-words: particulates, Cretan Sea, Coastal Processes, Continental Margin

Introduction

The present investigation was performed within the framework of the CINCS (Pelagic-benthic Coupling IN the oligotrophic Cretan Sea) experiment, aiming to study the coupling of biogeochemical fluxes over the southern margin of the Cretan Sea, the largest and deepest (2500 m deep) basin of the Aegean Sea (Fig.1). The Cretan Sea exchanges water with the N. Aegean Sea through various passages of the Cyclades Plateau, and with the eastern Mediterranean Sea through the Cretan straits. In particular, the area under investigation extends from the narrow continental shelf of Crete through the steep (3°-4°) continental slope to the deeper than 1700 m basin.

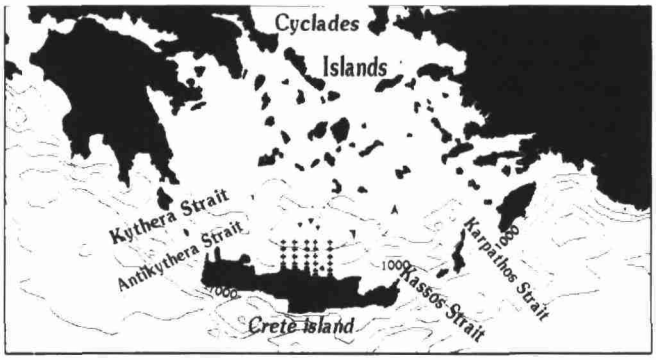

Figure 1. The geographical ambience and bathymetry (isobath every 1000 m) of the Cretan Sea. The dominant mesoscale circulation is shown, as well as the CINCS station network.

The major hydrodynamic features of the Cretan Sea have been described in the past by various investigators (1, 2, 3). A more recent picture has emerged through the POEM (4) and PELAGOS (5) programs; an interesting feature since 1992 is the presence of a semi-permanent mesoscale eddy dipole consisting of an anticyclone in the western Cretan Sea, and a cyclone in the eastern part.

CTD casts accompanied by nephelometric measurements have been widely used for the study of suspended particulate matter (SPM) in Mediterranean continental margins (off the mouth of major rivers): the Gulf of Lions (6), the R. Ebro (Spain) continental shelf (7) and the Thermaikos Gulf (NW Aegean Sea) (8, 9).

Data collection and methodology

A hydrographic network of 35 stations was laid over the Cretan slope, extending from the inner shelf to the deep basin (Fig. 1). The stations were distributed on a square grid of five meridional sections (code-named A-D from south to north) and seven zonal sections (code-named 1-7 from west to east). CTD and light transmission measurements (with a 10-cm path transmissometer) were used to provide "snapshots" of the distribution of the various water masses and the associated SPM on a seasonal basis (5/1994, 11/1994, 2/1995, 5/1995 and 9/1995). For the measurement of SPM, water samples (4 to 8 liters) were collected using Niskin bottles from depths where low light transmission was observed. The samples were immediately filtered through pre-weighted Nuclepore membrane filters filters (47mm diameter, 0.4mm pore size). Samples from selected depths were used to relate the observed (%) light transmission with SPM in mg l^{-1}; the correlation was fairly good ($0.77<R<0.98$) during the various sampling periods.

Water masses and circulation

The various water masses identifiable in figure 2 are present in the Cretan Sea throughout the CINCS experiment. The surface water (SW), with characteristics determined mainly by air-sea interactions, is generally distinguished by its high salinity and temperature. Often, and depending on the degree of suface mixing, low salinity water of North Atlantic origin, the Modified Atlantic Water (MAW) is traceable as a very thin subsurface layer, from 15 to 50 dbar. A salinity maximum below 50 dbar denotes a layer of the locally formed Cretan Intermediate Water (CIW), similar in characteristics with the Levantine Intermediate Water (LIW) but still warmer and slightly saltier. In the deeper layers, the so-called Transition Mediterranean Water (TMW) can be identified by the low salinity (S~38.9 psu) of its core, the latter lying between 300-400 dbar. The deep and bottom layers are occupied by the very dense Cretan Deep Water (CDW).

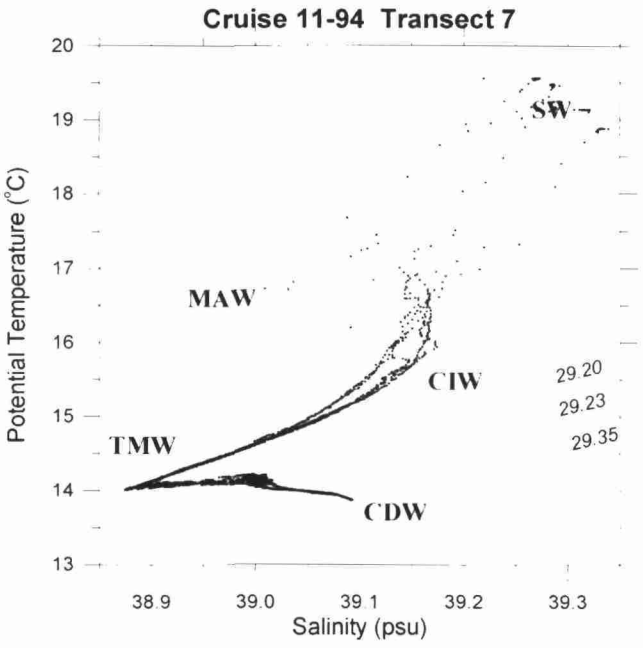

Figure 2. θ/S diagram from all the stations of the deepest zonal transect during the CINCS-II cruise, identifying the various water masses present.

As mentioned above, the PELAGOS project has revealed the dominance of a mesoscale eddy dipole over the central Cretan Sea throughout 1994-1995. The dipole consisted of a cyclone over the eastern-central Cretan Sea and an anticyclone over the western-central part. As the CINCS observations certified (Fig. 3), these eddies induced a southward flow at the northern boundary of the sampling area towards Crete. The local signature of the eddy dipole is identifiable through the upward slope of the isopycnals towards the east. Throughout most of the sampling period, the CINCS region remained between the southern extensions of the two eddies, thus the northern boundary experienced only southward flow. However, during winter 1995, the cyclone shrunk in size and increased in intensity, moving the local signature of its centre by about 20 km to the west. Then, the southward flow became stronger, and a northwest flow is observed exiting the CINCS sampling area at its northeastern corner.

ESTIMATION OF THE AMPLITUDE OF THE SEASONAL VARIATIONS AT TWO KEY SITES OF THE MEDITERRANEAN FROM THE MEDATLAS CLIMATOLOGY

Catherine Maillard [1*], Efstahios Balopoulos [2], Michèle Fichaut [1], Maria Jesus Garcia [3], Didier Jourdan [4]

[1] IFREMER/SISMER, Centre de Brest, 29280 Plouzané, France
[2] NCMR/HNODC, Hellinikon 16604, Athens, Greece
[3] Instituto Español de Oceanografia, c/ Corazon de Maria 8, 28002 Madrid, Spain
[4] EPSHOM/CMO, rue du Chatellier, 29200 Brest, France

Abstract

This paper gives new estimates of the seasonal variations in two key sites of the western and eastern basins of the Mediterranean : the Gulf of Lions deep water formation region and the Rhodes gyre. The quantification of the permanent climatological signal is important to estimate further mesoscale phenomena. This study is based on a new base created in the frame of the MEDATLAS project, which released and qualified several thousand of new temperature and salinity profiles.

Key-words : temperature, salinity, G.I.S.

Introduction and description of the data set

It is known that the Mediterranean has a renewal time shorter than the Atlantic ocean and is submitted to a higher seasonal and meso-scale variability. Whether the seasonal variations or the mesoscale variability is the dominant process has been debated in the past (1). From more recent experiments like PRIMO (2) and POEM (3), it seems that both processes interfere. It is therefore important for any study, observational or numerical, to be able to quantify properly the amplitude of the climatological mean and seasonal signals. This was one of the objectives of the MEDATLAS project. Preliminary results are presented in this study in two key sites of the western and eastern basins of the Mediterranean : the Gulf of Lions deep water formation region and the Rhodes gyre. Before discussing the first result, a brief overview of the database will be presented.

The MAST MEDATLAS supporting initiative, is related to the international GODAR (Global Ocean Data Archaelogy and Rescue) programme, to safeguard, qualify and disseminate data dispersed in the scientific laboratories. It was initiated by a consortium of several Mediterranean Data Centres including the Hellenic Data Centre (Greece), the IEO Data Centre (Spain), the EPSHOM/CMO (French Navy), IFREMER/SISMER (France) the co-ordinating centre and the ICES (Denmark) supervised the Quality control (QC) procedures. In this frame, almost all of the French, Spanish, Italian and Hellenic laboratories and Hydrographic Services, the MODB database (4) and the IOC/IODE data centre network including the World Data Centre A (5) and the ICES have been contacted by the project partners to archive the data collected since the beginning of the century, and not yet released in the public domain. The database released with the digitised atlas (6) represents now the most complete available dataset, which after elimination of duplicates, amounts to :

Data Type	Cruises	Profiles
ctd	275	15 778
bottle :	1 239	33 976
thermistor	3	29
xbt	292	75 009
mbt	369	81 464

In addition to these data, classified data not yet available to users, have been used for the climatological computations. They consist in about 1000 recent scientific CTD profiles, and 12 603 MBT + 49 183 XBT from the navies.

The yearly distribution of the data per data type shows a continuous sampling from the middle forties to nowadays, with a progressive substitution of MBT by XBT since the seventies, and the appearance of the CTD in 1975. As it can been seen on the two diagrams of Fig. 1 a and b, the time distribution is large enough to avoid bias in the computation.

The monthly distribution of the data shows that there is fewer data during winter time (December, January and February) and that the maximum number of profiles is collected during May, however the number of observation remain important all the year long. In space, data are sparser to the East and South, but regions like the Gulf of Lions and the Rhodes regions have been relatively well investigated for several decades, recently during the PRIMO and POEM experiments.

The profiles have been checked for quality by using a common protocol (7), based on the IOC and MAST recommendations (8). It consists in series of objective automatic checks followed by subjective visual checks for :
1. date and location of the stations ;
2. observations (including broad range checks and comparison with previous climatologies (LEVITUS and MODB).
As a result, a quality flag is added on each numerical value. The data points which appeared correct got a flag=1.

Climatological Analysis

To implement the objective analysis, the bottle and CTD profiles have been interpolated at 28 standard levels from 0 to 4000 m, with the Reiniger and Ross method (9), taking into account only the data points flagged to 1 (correct elements). A further gross validation has then been performed on the interpolated data, which rejected less than 1% of them.

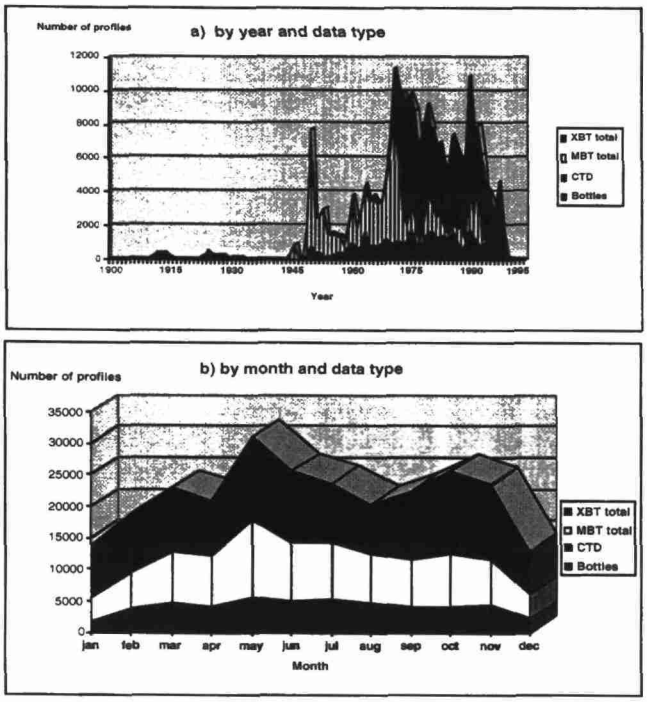

Figure 1 - Time distribution of the profiles

The kriging as discussed in (10), requires to set up numerous parameters prior to the computation, and after sensitivity studies, the adopted values were :
• average mesh size of the irregular adaptive grid : 40-km
• minimum radius inside which at least one observation is requested : 80 km
• maximum radius beyond which observations can not be used : 160 km.
• time resolution according to the data availability on the vertical : monthly from the surface down to 300 depth, seasonally between 400 and 800 m, annually below.

The computed climatological parameters are :
1 - Neural meshing for optimising the grid of calculation according to the data distribution and, to a less extend, to computation criteria.
2 - Neighbourhood search procedure to ensure temporal representativity
3 - Optimal interpolation of mean temperature and salinity, error estimates, variability

For practical use and mapping of the results, the values are afterwards reinterpolated on a regular grid, in such a way that the nodes of the adapted grid coincide with the regular grid and by using a linear combination of the estimated values at the 4 closest adapted nodes. The results include neuronal (irregular) grid and regular reinterpolated (205x73 elements) of average values, errors and other statistical estimates.

Compared climatological variations in the Western and Eastern basins

Seasonal variations are detectable down to 800 m, but the Western basin and Eastern basin present different characteristics. One aspect is that more meso-scale features appears with shorter space scale in the Eastern basin. The temperature distribution at 100 m (Fig. 2, a) February and b) August) show a smoothed however complex general pattern of the water masses. The Gulf of Lions cyclonic circulation and the Rhodes gyre appear as quasi-permanent features.

TIDAL DYNAMICS IN THE GULF OF TRIESTE - NORTHERN ADRIATIC

Vlado Malacic [1] and Dino Viezzoli [2*]

[1] National Institute of Biology, Marine Station Piran, 6330 Piran, Slovenia
[2] Osservatorio Geofisico Sperimentale, P.O. Box 2011, 340160 Opicina, Trieste, Italy

Abstract

Detailed analyses using numerical modelling of Northern Adriatic Sea examined the tidal dynamics in the Gulf of Trieste during two different tidal regimes. Within the Gulf of Trieste, double tidal ellipses are described by rotating transport velocities moving in a clockwise sense. The southern part of the gulf has elongated ellipses oriented along the gulf axis, while in the northern part the ellipses are broader (smaller eccentricity).

Key-words: Currents, Models, Coastal Waters, Adriatic Sea

Introduction

Seven tidal components (four semidiurnal, three diurnal) have a significant contribution to the tidal sea-surface elevation (SSE) in the Adriatic Sea (1). Mediterranean tides are strongest in the northern part of the Adriatic Sea (the Gulf of Trieste). This is with the exception of straits however, where throughflows amplify the tides. Numerical simulations previously made of the tidal dynamics of the small (12 miles x 15.6 miles), semi-enclosed, shallow (depth 20 m) gulf mainly dealt with analysis of the leading M2 tidal component (2, and 3). In (4) the dynamics of the gulf was numericaly simulated with imposed winds of steady direction, where the SSE's were taken from mareographic records. All these models adapted SSE and transport velocity boundary conditions at the gulf's entrance (more than 12 miles long). In order to achieve better understanding of the boundary conditions, the models should have simulated the tidal dynamics of the entire northern Adriatic basin.

The model

The aim of the numerical model was to evaluate the tidal transport of water mass within the Gulf of Trieste during two different tidal situations: one on 8 September 1994 in the south when the tidal rage was of about 100 cm in the port of Trieste and only the semidiurnal components were prevalent, and the other on 15 June 1995 near the Isonzo River mouth (north) when both the semidiurnal and the diurnal constituents were important. On 15 June 1995, the tidal range of the SSE over the gulf was smaller (by about 50%) than the range during 8 September 1994. The numerical model of tides had to simulate the dynamics of all seven major tidal components (M2, S2, N2, K2, K1, O1, and P1). To avoid the open-boundary problem along the western opening of the gulf, a 2D model of tidal dynamics to the entire northern Adriatic area was applied - an area expanding northward of the boundary line connecting two mareographic stations: Pesaro in Italy and Pula in Croatia (5). The tidal dynamics was numerically simulated using the 2D TRIM model (6). This is a non-linear, semi-implicit model which is unconditionally stable. The staggered-grid depth integrated model has a space resolution of 0.3 miles which is sufficient for Lagrangian tracking of "depth-averaged" particles, and for local SSE and Eulerian velocity studies. Values of amplitude and phase, for each of the seven tidal components in the cells along the open-boundary line, were found from a polynomial least-square fit, using points of intersection of co-range and co-tidal lines with the open boundary line (68 miles in length). The co-range and co-tidal isolines were obtained from tidal charts (7). The parameter of implicitness (8) and the depth dependent Chezy-Manning coefficient were adjusted for the port of Trieste, in a way such that the difference between the model and mareographic values of amplitude and phase of the M2 tidal constituent was at a minimum. Adjustments ceased once the difference in amplitude was below 1 cm, and the difference in phase was less than 2° (the M2 component in Trieste has an amplitude of 26.6 cm, and phase g = 277°). Further calibration procedures were performed, which involved modification of the initial least-square fit of SSE along the open boundary line, for each of the seven tidal constituents. This was necessary in order to obtain satisfactory matching of the model and mareographic constants, at the four ports situated along the northern Adriatic coast (Rovinj, Trieste, Malamocco (Venice), and Porto Corsini). The results obtained for the Gulf of Trieste were therefore of reasonable accuracy.

Results

Plots of model SSE values in the port of Trieste against values predicted from tidal tables (9), are shown in Fig. 1. In order that transient effects were unimportant, the model was run fourteen days prior to the days of interest. Since the model simulation of SSE in the port of Trieste was sufficiently accurate, it was believed that the model transport velocities would be representative enough. For each time step in the model, the Lagrangian velocity was calculated using the space interpolation method on the Eulerian velocity components (6). Both transport velocities for the two different tidal regimes are presented in Figs. 2 and 3, respectively. As the 24 hour period of transport velocity evolution is too short, it was analysed using the trigonometric least-square fit composed of just two harmonics: the diurnal and semi-diurnal (full lines in Figs. 2 and 3). The tips of the transport velocities describe double ellipses and move in a clockwise sense. The least-square fit composed of just two trigonometric terms agrees well with the transport velocities of the 2D model, which include the seven

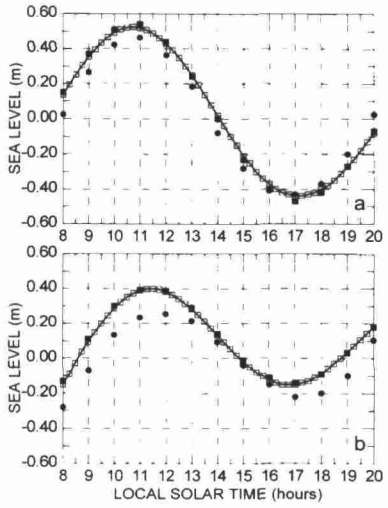

Figure 1 : Sea-surface elevation (SSE) at the port of Trieste (northern Adriatic) during: a) 8 September 1994, b) 15 June 1995. Full rectangles are elevations taken from tidal tables, composed of seven (major) tidal constituents. Empty rectangles are the values of SSE from the 2D model of the northern Adriatic. Circles represent mareographic measurements in the port of Trieste, subtracted by a mean SSE of the displayed period.

tidal constituents. The Eulerian and Lagrangian, semidiurnal and diurnal ellipse parameters show that, in the southern part of the gulf the tidal motion is very elongated and aligned with the coastline. The semidiurnal component of transport velocity, with an amplitude 11.5 cm/s, is of an order of magnitude greater than the amplitude of the diurnal component. In the northern part of the gulf - a few miles southward from the Isonzo river mouth, the semidiurnal tidal component is less elongated, with a speed ranging between 1-4.6 cm/s. The diurnal component is even more circular with a maximum value of 1 cm/s.

The numerically obtained Eulerian tidal transport velocity (Fig. 3 top) is similar to the pseudoellipse of the Eulerian tidal velocity deduced from mooring measurements, at a depth of six meters during the winter period of 1984 (10). The time series of the Eulerian transport velocity and of the SSE show that, in the southern part of the gulf (8 September 1994) where the depth is around 20 m, the velocity minimum lags behind the local SSE maximum by about 0.5 hours. Surprisingly, this lag is not detectable in the northern part (15 June 1995) where the depth of the water column is about 16 m. However, the starting position of Lagrangian particle of June 15 1995 was much closer to the cotidal line - ending in the port of Trieste, than the starting point of the particle of 8 September 1994. This indicates that the velocity and SSE fields over the gulf are related to fields over the rest of the northern Adriatic Sea.

Finally, although this paper deals mainly with the tide in the Gulf of Trieste it is useful to compare our results for the Northern Adriatic Sea as a whole with results obtained by other authors in the same area. Earlier numerical studies in the Northern Adriatic have concentrated either on the K1 and M2 tidal constituents (11) or on the M2 constituent only (12). The reported results for these constituents are in good agreement with ours despite the lower grid resolution (7.5 km) adopted in those models. Furthermore, our calibration procedure was more severe: the value of the M2 amplitude reported by (11) differed from observed values at Trieste by about 20 % whereas in (12), a comparison of the model results with observed constants for SSE was neglected. Our calibration procedure minimized the error to 2.3 % and 1.3° for the amplitude and phase on the M2 tidal constituent, respectively. The errors in the case of the other six constituents were similar.

References

1 - Defant A., 1961. Physical Oceanography. Pergamon Press, Oxford. 2: 1-729.
2 - Michelato A., 1973. Studio Sulle Correnti di Marea del Golfo di Trieste Mediante il Metodo Idrodinamico-Numerico B. Sc. thesis, University of Trieste: 1-94.
3 - Longo R., Raicich F., Mosetti, R., 1990. A numerical model of transport and diffusion of radionuclides in the Gulf of Trieste. *Boll. Oceanol. Teor. Appl.* 8: 13-24.
4 - Rajar R., (etina M., 1991. Modelling of tidal and wind-induced currents and dispersion in the Northern Adriatic. *Acta Adriat.* 32: 785-812.
5 - Malacic V., Viezzoli D., 1997. Numerical analysis of tidal dynamics of the Northern Adriatic Sea: submitted.

THE EASTERN MEDITERRANEAN IN THE 80'S AND IN THE 90'S: THE BIG TRANSITION EMERGED FROM THE POEM-BC OBSERVATIONAL EVIDENCE

Paola Malanotte-Rizzoli [1], Beniamino Manca [2*], Maurizio Ribera d'Alcala [3], Alexander Theocharis [4]

[1] Department of Earth, Atmospheric and Planetary Sciences, Massachusetts Institute of Technology, Cambridge, MA 02139 U.S.A.
[2] Osservatorio Geofisico Sperimentale, P.O.Box 2011, 34016 Opicina-Trieste, Italy
[3] Stazione Zoologica ôA. Dohrnö, Villa Comunale I, 80121 Napoli, Italy
[4] National Centre for Marine Research, Aghios Kosmas, Hellinikon 16604, Athens, Greece

Abstract

The thermohaline circulation of the Eastern Mediterranean underwent a dramatic change between 1987 and 1995. In 1987 the "engine" of the Eastern Mediterranean "conveyor belt" was the convective cell of the Southern Adriatic, while in 1995 the active convective region moved to the Aegean Sea. This change actually started as early as 1991. The phenomenological evidence of the POEM programme shows that in 1987 the source of Levantine Intermediate Water (LIW) mass was the Levantine basin and the bottom water mass was formed in the Southern Adriatic. In 1991 all the intermediate/deep water masses on the horizons sq = 29.00 to 29.18 kg/m^3 were formed inside the Aegean sea, from which they spread out into the entire Eastern Mediterranean through the Cretan Arc Straits.

Key-words: circulation, deep waters, hydrology, Eastern Mediterranean

In the last decade the Eastern Mediterranean has been the object of the multinational collaborative programme P.O.E.M. (Physical Oceanography of the Eastern Mediterranean) sponsored by UNESCO, IOC and CIESM. Under this programme a series of general hydrographic surveys was carried out by the R/V of Greece-Israel-Italy and Turkey in the period 1985-1987, culminating in POEM-AS87 in which the German R/V *Meteor* covered the entire Eastern Mediterranean with a basin-wide station network. In 1987 the regular CTD surveys were implemented by a transient-tracer survey (1). The observational dataset collected in these surveys was intercalibrated, pooled and distributed to all the participating scientists in a series of UNESCO sponsored workshops. The joint analyses and interpretation led first to a group paper summarizing the new findings that included extended modeling results (2); second a special issue of Deep-Sea Research was devoted to this POEM-Phase 1 research (3). Recently, the entire POEM-Phase 1 dataset has been revisited for the Ionian sea with an in-depth complete reanalysis that has led to important new findings (4). These include the first detailed definition of the upper thermocline circulation in the Ionian sea, with the discovery of the strong Mid-Ionian Jet (MIJ) crossing the basin interior in north/south direction and then becoming the Mid-Mediterranean Jet (MMJ); and the first definition of the pathways of the intermediate LIW and of the Eastern Mediterranean Deep Water (EMDW).

In 1990 POEM evolved into POEM-BC (Biology and Chemistry) a fully interdisciplinary programme, with the major overall objective of establishing the phenomenology of the 90's for the chemical and biological parameters together with a reassessment of the phenomenology of the physical properties, contrasted to that of the 80's, (POEM-Phase 1). The first interdisciplinary multi-ship general survey of the entire basin was carried out in October 1991, POEM-BC-O91, followed by a more restricted survey in April 1992 (the Ionian basin only) and a final basin-wide survey by the R/V *Meteor* in January 1995, with a second transient tracer network of stations. This was part of the LIWEX experiment aimed to investigate the successive phases of the LIW formation and concentrated in the Northern Levantine region of the Rhodes gyre during the successive months, February through April 1995. The analysis of the *Meteor* cruise, including the transient tracer observations revealed a very important, dramatic change in the deep thermohaline circulation, the Eastern Mediterranean "conveyor belt". Specifically, in 1987 the driving engine of the deep, closed thermohaline cell was the Southern Adriatic, where deep convection leads to the formation of the Adriatic Deep Water (ADW) that exits from the Otranto Straits, becomes EMDW and spreads throughout the eastern Levantine in the bottom layer. General upwelling to the intermediate transitional layer (below 1,000 m) provides the return pathways to the Southern Adriatic closing the cell (1). In winter 1995 the situation was completely different: the engine of the deep thermohaline circulation was now the Aegean sea, with deep, denser water masses exiting from the Cretan Arc Straits, spreading throughout the entire basin and pushing to the west, while simultaneously lifting, the less dense EMDW of southern Adriatic origin (5).

We present here the first observational evidence that this dramatic change in the Eastern Mediterranean circulation actually started in 1991 and involved not only the deep water mass pathways but the intermediate ones as well, specifically the LIW origin and pathways. This evidence is based on the first joint analysis of the POEM-BC-O91 general survey. This analysis revealed first that the upper thermocline circulation (upper ~250 dbar) was actually extremely similar in the 80's and 90's. Most important the MIJ, emanating from the Atlantic Ionian Stream (AIS) entering the Sicily Straits, is quite strong, crossing the Ionian interior from North to South and surrounding a general anticyclonic region in the Southwestern Ionian both in the 80's and 90's. Recent results based on drifter observations confirm the persistence of the MIJ from the 80's throughout 1995-96 (Poulain, personal communication).

On the other hand, a dramatic change is observed from 1987 to 1991 in all the intermediate and deep water mass pathways. In 1987 the LIW was formed in the proper Levantine basin, entered the Cretan

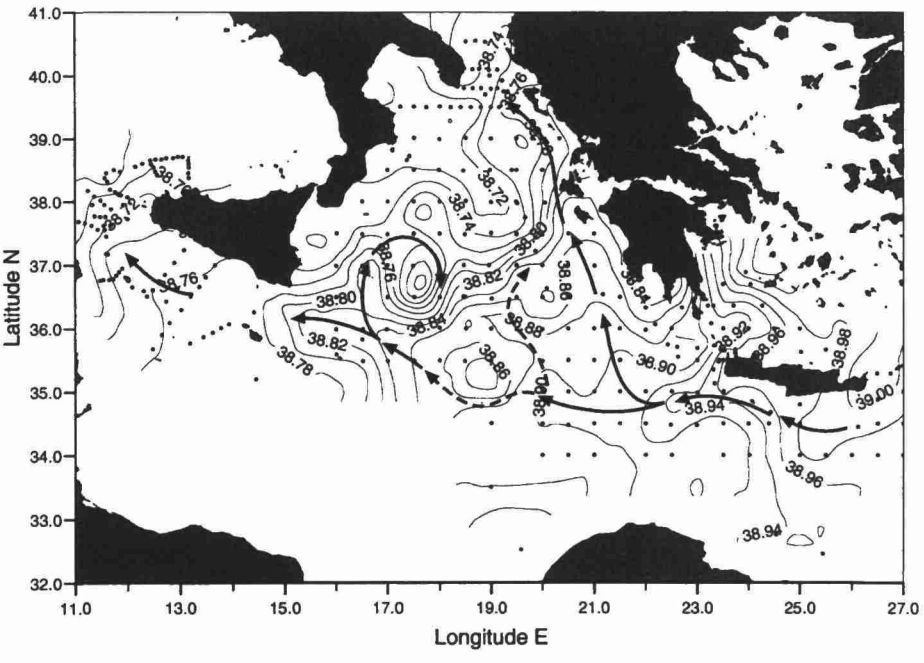

Cruise POEM-AS87: Salinity at density=29.05 kg/m3

Figure 1 - Distribution of salinity at the 29.05 kg·m^{-3} isopycnal horizon during August-September 1987 survey.

DENSE WATER FORMATION AND CIRCULATION IN THE SOUTHERN ADRIATIC SEA DURING WINTER 1996

Beniamino Manca [1*], Davide Bregant [2]

[1] Osservatorio Geofisico Sperimentale, P.O.Box 2011, 34016 Opicina-Trieste, Italy
[2] CNR, Istituto Sperimentale Talassografico, V.le Romolo Gessi 2, 34123 Trieste, Italy

Abstract

The South Adriatic has been indicated by many authors as a possible site of dense water formation. Experimental evidence of an open-ocean deep convection event has been documented by Ovchinnikov *et al.* (1). New evidence for such a process was observed during winter 1996. A very deep mixed water column and a baroclinic cyclonic circulation provided the necessary preconditioning. A strong northerly wind episode contributed to the cooling of surface high density waters ($\gamma_\theta \cong 29.15$ kg/m^3) upwelled from the deep layer, while a deepening of the oxygen rich water column from 300 down to 600 m was observed at a horizontal scale of a few tens of nautical miles after 8 days.

Key-words: Deep Waters, Hydrology, Open Sea, Water Convection, Adriatic Sea

Introduction

The Adriatic Sea is the primary source of the deep water mass for the entire Eastern Mediterranean (2). Even though results from a recent hydrographic survey show that the influx of Aegean water has replaced 20% of Eastern Mediterranean Deep Waters (3), the Adriatic Deep Water (ADW) still exits through the Otranto Strait and spreads into the deep layer of the Ionian interior (4). The role of the Southern Adriatic as a possible site of deep water formation has been pointed out by many authors, although experimental evidence for open-ocean deep convection events is poorly documented in historical data. Ovchinnikov *et al.* (1), from a few coarse spatially distributed hydrological data collected during mid-February and early April 1977 found only the initial and concluding stages of convection. Later on, during the March 1982 expedition, the energetic mixing and sinking phase of dense water formation after favourable weather conditions was documented.

The aim of the present work is to describe and discuss recent evidence of deep water formation in the Southern Adriatic observed during winter 1996. Cooling of saline surface water caused by a strong wind together with an intensification of cyclonic movement provided suitable conditions for deep water formation.

Plan of Measurements

During the winter 1996 cruise, carried out in the framework of the PRISMA (Programma di Ricerca e Sperimentazione del Mare Adriatico) collaborative Italian research program, the Southern Adriatic Sea was visited from 17 to 28 February. The hydrological station network (Fig. 1) was designed with the aim of investigating the transport of major water masses crossing the transects in Pelagosa sill (about 200 m depth) and Otranto Strait (about 800 m depth). The large topographic depression inside this region, down to about 1200 m depth, was investigated as well. Synoptic shipboard measurements included CTD casts, using a Seabird SBE 911 plus equipped with oxygen sensor, in combination with a Rosette water sampler to collect samples for salinity calibration and oxygen determinations following the Winkler method. The CTD data were checked and calibrated according to the standard procedures, and subsequently averaged over 1 dbar pressure intervals.

Results and Discussion

Objective analyses of temperature and salinity at surface (Fig. 2a and b) show that relatively cold (θ<13.4°C), high salinity (S>38.60) waters were found in the middle of Southern Adriatic basin. This area was occupied by a large multi-lobe cyclonic gyre marked at the surface by the 29.15 kg/m^3 isopycnal (not shown). Some elongations toward the north shelf break area and close to the eastern coast are indicative of isolated patches where vertical mixing events may occur at horizontal space scales of a few tens of nautical miles. The presence of a strong thermohaline frontal zone separates the light coastal water, which flows southward along the western Italian coastline, from the open-seawater limiting the area of vertical

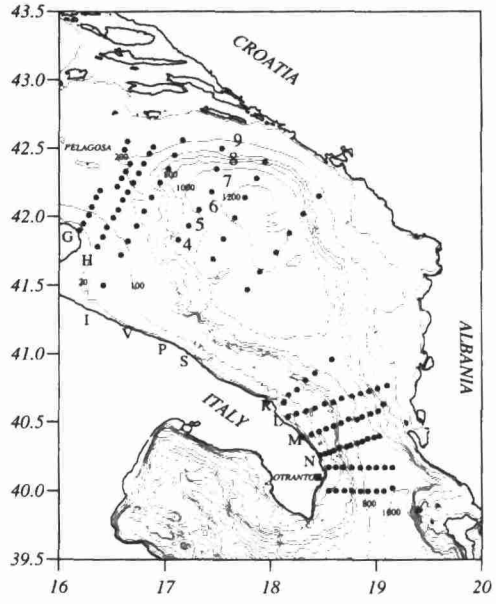

Figure 1- Location of hydrological stations (dots) superimposed on batymetry (depth in meters). The letters along the Italian coast denote the transverse sections. The numbers of stations mentioned in the text are indicated.

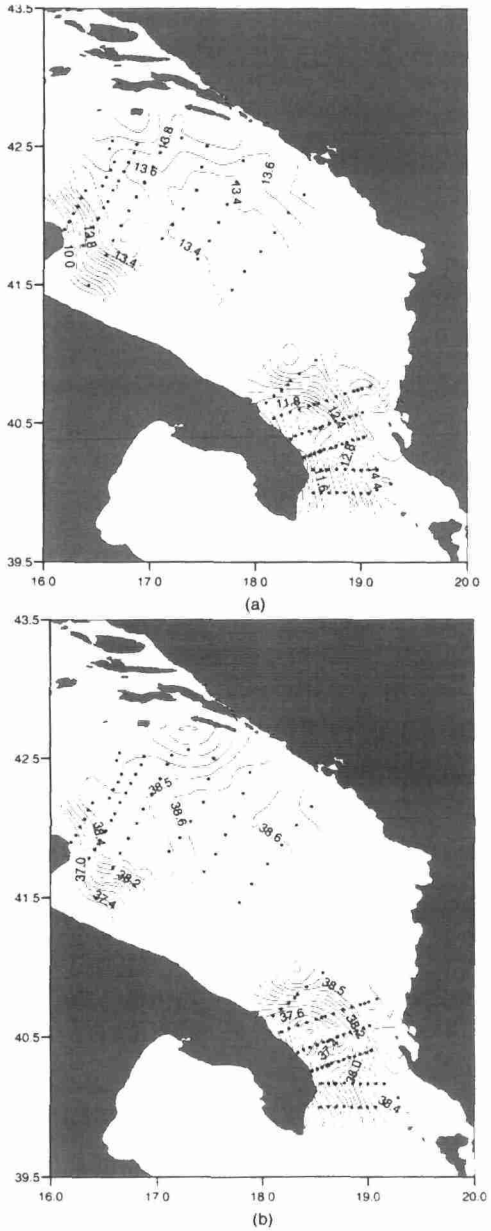

Figure 2 - Objective analysis of temperature(a) and salinity(b) at surface. The positions of stations used in the map are indicated by dots.

INTERANNUAL VARIABILITY OF LIW FORMATION : A HIGH RESOLUTION NUMERICAL STUDY

Kostas Nittis and Alex Lascaratos*

University of Athens, Department of Applied Physics, Lab of Meteorology, University Campus, Build. PHYS-V, Athens 157-84, Greece

Abstract

We study the interannual variability of LIW formation using an eddy resolving numerical model of the Levantine basin, forced by realistic atmospheric data from selected typical years. The strong interannual variability of winter heat loss modulates the characteristics of the formation process and the properties of the new water mass. During mild winters the formation rate can be significantly reduced compared to climatology. During severe winters the formation rate is not increased considerably but, instead, we observe simultaneous deep and intermediate water formation in the area. These experiments also revealed the significant role of extreme cooling events associated with the passage of storms over the basin.

Key-words : Intermediate waters, Levantine Sea, Air-sea interactions, Models

Introduction

Intermediate and deep convection processes at different locations of the Mediterranean sea are responsible for the formation of the various water masses of the basin. Among them and probably the most characteristic, is the Levantine Intermediate Water (LIW), the saline and warm water mass that occupies the intermediate layers of the basin (200-500m). Its is formed in the Levantine basin during winter-time cooling and evaporation. From its formation site, it spreads throughout the whole basin and exits through the straits of Gibraltar, being the main contributor to the Mediterranean outflow into the Atlantic ocean.

A wide range of "core" LIW temperature and salinity values can be found in the bibliography for the Levantine basin; minimum and maximum values reported are 14.5-16.4oC and 38.85-39.15 for T and S respectively [1]. This wide range of LIW core values is a first indication of the significant interannual variability of LIW characteristics. The second strong indication, comes from the different locations that have been reported in the past as possible LIW formation sites. Most observations indicate that the Rhodes cyclonic gyre, a permanent feature of the Eastern Mediterranean general circulation [2], is the formation site of LIW. There are, nevertheless, observations of intermediate water formation in the whole north Levantine [3], in the south Levantine [4] or in the SE Aegean sea

We describe results of numerical experiments that simulate the formation of LIW under different meteorological conditions. We apply the numerical model used in the past for the study of LIW formation under mean climatological conditions [5]. Those experiments proved that under such conditions, the Rhodes cyclonic gyre is the unique site of LIW formation. The duration of the event is typically 2 months (February-March) and the estimated annual formation rate 1.2 Sv. In the new experiments, we force the model by real 12hours atmospheric data from selected winter periods, instead of the monthly mean climatological forcing previously used. In these way, two new important factors are introduced : the interannual variability of atmospheric forcing and the effect of synoptic time scale events.

The Numerical Model

The numerical model we use is based on the Princeton Ocean Model (POM), a 3-D primitive equation ocean model widely used for both open ocean and coastal sea studies [6]. It is a free surface model that uses sigma coordinates in the vertical and a time splitting technique to calculate the 2-D and 3-D equations with different time step. The Mellor-Yamada scheme is used for computation of vertical mixing coefficients while horizontal diffusivities are calculated according to the Smagorinsky formula.

The model is applied in the Levantine using a 5.5x5.5 km eddy resolving grid. The same grid was capable to reproduce transient baroclinic eddies (20-50 km) associated with the instability of the rim current in the Rhodes gyre [5]. In the vertical, 30 sigma levels with logarithmic distribution in the top are used. Radiation boundary conditions are used along the western boundary of the domain that is considered to be open. The MED2 data base [7] is used for model initialization and for the T-S profiles updated seasonaly along the open boundary.

The surface boundary conditions are the fluxes of heat, fresh water and momentum. All of them are computed at each time step using the model's SST and atmospheric parameters from the 1980-1988 12hr NMC analysis (wind speed, air temperature and relative humidity). The cloud cover C is taken from the COADS 2x2 monthly mean data set for the same period, while precipitation is derived from monthly climatology.

For the interactive computation of surface fluxes we use the formulation developed in the framework of MERMAIDS [5] choosing a combination that gives realistic annual mean heat and water budgets for the Mediterranean and the Levantine : the formula of May for long wave back radiation, the formula of Kondo for sensible and latent heat and the formulation of Rosati & Miyakoda for solar radiation.

The Numerical Experiments

The scope of our numerical experiments was to study the formation of LIW under different winter conditions. We, therefore, decided to select from the 9 years period of available NMC data four winters with different characteristics. Our selection was based on the mean air temperature over the Levantine that can characterize each winter as "typical", "mild" or "severe". Each numerical experiment is a 5 months integration of the model during the cooling period of each year, *i.e.* from November to end of March starting from the same initial state, and using the same open boundary conditions; this means that we do not attempt to simulate the exact formation conditions or general circulation features of each specific year but to study the effect of different atmospheric forcing on the formation of LIW.

In figure 1 we present the five months long time series of total heat flux for the four numerical integrations. In all four cases, the variability of the surface buoyancy loss is composed by two time scales : the low frequency seasonal cooling and heating and the high frequency episodes associated with strong synoptic scale atmospheric events. The low frequency signal introduces in all cases an increasing buoyancy loss from November until mid January when we have the period of maximum cooling. The trend is then reversed and by the end of March we observe slightly positive heat budget that marks the beginning of the warming period for the sea.

On top of this common for all years low frequency variability, we have a number of short time scale events with variable intensity and duration. Most of them are related to the passage of atmospheric depressions over the area. The low air temperatures and strong winds associated with these systems increase the latent (mainly) and sensible heat loss to the atmosphere. Particularly effective are the north winds that follow these systems, since they bring over the sea very dry and cold air masses of Arctic origin. During these events, the heat loss can be as high as 500-600 W/m^2 which means 3-4 times above the typical value. Depending on its duration, the total amount of buoyancy lost during a single event can be equivalent to the heat loss during a whole month (*e.g.* events of January 1987).

Based on the mean heat loss during the 5 months of the experiments we can characterize the four winters as "mild" (1984 - 108 W/m^2), "typical" (1985 - 125 W/m^2, 1986 - 140 W/m^2) and "severe" (1987-171 W/m^2). The total budget of each winter is usually controlled by the characteristics of the short time scale events. The winter of 1987 is characterized as a very

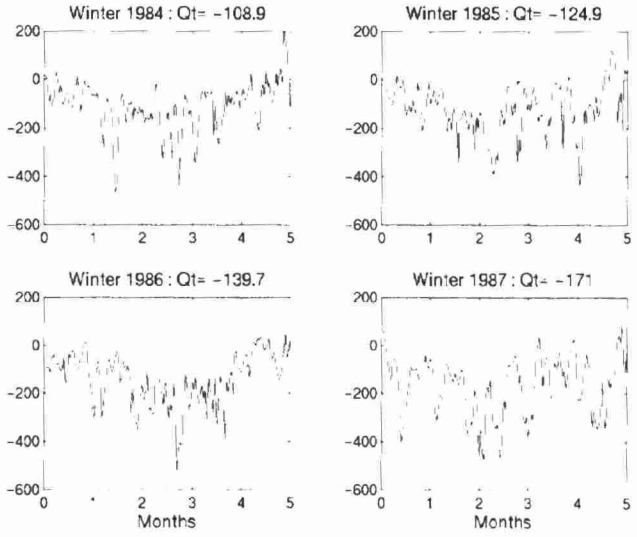

Figure 1 : Time series (November-March) of total heat flux (Q_{total})

THE OMEGA PROJECT: OBSERVATIONS AND MODELLING OF EDDY SCALE GEOSTROPHIC AND AGEOSTROPHIC CIRCULATION

The OMEGA group: Dept. Fisica, Universitat de les Illes Balears, Spain; Southampton Oceanography Center, UK; Institut de Ciències del Mar (CSIC), Spain; GHER, Université de Liège, Belgium; Università di Pisa, Italia; Dept. de Ecología, Universidad de Málaga, Spain; LODYC, Université Paris VI - CNRS, France.

Abstract

The OMEGA project is an interdisciplinary physically based initiative aimed to provide the scientific community with a new tool for computation of vertical velocity from routine CTD and ADCP data. The field studies were completed during October (BIO *Hespérides*) and December (RRS *Discovery*) 1996. Preliminary analysis of the data show the existence of significant variability at scales of the order of the internal Rossby radius and also indirect evidences of vertical motions. The data are being analyzed and used to compute the associated three-dimensional circulation through methods and models of different complexity.

Key-words: mesoscale phenomena, fronts, surface waters, Alboran Sea

Introduction

OMEGA, a research project of the European Union MAST programme, has three main objectives: to determine the three-dimensional ageostrophic circulation at mesoscale (10-100 km) fronts and eddies and quantitatively estimate the vertical velocity, to evaluate the impact of the ageostrophic vertical motion on the biogeochemical properties in the upper 400 m, and to provide the scientific community with a standardised tool for the computation of vertical motions from routine CTD and ADCP data.

The results of high resolution modelling of frontogenesis (1) showed that vertical velocities up to 100 m/day could be expected at Rossby deformation radius scale meanders due to frontal baroclinic instability. Several studies by members of the OMEGA group (2, 3) have diagnosed high vertical velocities in frontal eddies, also in the Alboran Sea (4). Other authors have recently investigated this phenomena (5, 6). Vertical motion couples the deep ocean with the near surface layers, providing an enhanced transport route for heat, nutrients and biomass. The distribution of primary production patchiness is driven by mesoscale physics (7, 8). At these scales, successful research requires interdisciplinary observational strategies.

OMEGA is a comprehensive proposal combining an observational strategy of remote sensing and *in situ* high resolution physical, chemical, biological and meteorological measurement with a numerical modelling/data assimilation strategy to quantify the errors involved in the diagnostic analysis of the observational data, and make prognostic simulations of mesoscale features. Mesoscale eddies are ubiquitous in the ocean and the conclusions from OMEGA will be relevant to all ocean regions.

OMEGA Cruises

The OMEGA experimental work concentrates on two specific frontal zones of the western Mediterranean: the northern edge of the western gyre in the Alboran Sea and the Almeria-Oran front. Both are regions of strong vertical shear and intense mesoscale circulation, and are usualy identified by strong gradients in satellite infrared imagery (fig. 1). Two cruises were carried out during autumn 1996: in October the Spanish BIO *Hésperides* sampled the western Alboran gyre (OMEGA-1) and in December the UK RRS *Discovery*, the Almeria-Oran frontal region (OMEGA-2). In both cruises, data obtained in 3-4 consecutive samplings of the same area included Seasoar (undulating CTD + optical sensors), ADCP, fluorescence, multibeam acoustic backscatter, nutrients, flow-cytometry, etc., in conjunction with differential and 3D GPS navigation, as well as meteorological information. The deployment of neutrally buoyant Lagrangian floats in OMEGA-1, at the depth where maximum vertical motion was expected (100 m), provides direct estimates of the vertical velocity. The floats, able to record vertical water motion, were tracked by 6 acoustic receivers previously moored in the area, and recovered 50 days after the deployment.

During OMEGA-2 some ship tracks (fig. 2) were aligned along ERS-2 and Topex-Poseidon satellite tracks so that the combination of altimeter data and in situ SeaSoar and ADCP vertical profiling can be used to derive the along track geoid. Knowledge of the geoid will allow long term monitoring of the cross-track surface geostrophic currents and their temporal variations over the lifetime of the ERS satellites.

An aircraft made meteorological and radiometric measurements during this second cruise.

Determination of mesoscale circulation

The different sensors and sampling methodologies used during the OMEGA cruises have highlighted the presence of active frontal zones in both study areas. Preliminary analysis of the data show the existence of significant variability at scales of the order of the internal Rossby Radius and also indirect evidences of vertical motions.

The combined *in situ* and remotely sensed datasets have enabled a detailed description of the surface water types, the fronts that separate them, the bio-optical properties, and the associated changes around the time of the cruises. Shipborne measurements indicate that the surface signatures visible from remote sensed data are indicative of circulation to a depth of more than one hundred metres. The results of the merging and interpretation of such a comprehensive dataset show the potential and capabilities of the combined satellite/*in situ* approach in rendering a picture of the relationship between the physics of frontal zones and bio-optical variability at the mesoscale with an unprecedented degree of accuracy. Particular attention is given to the relationship of the observed biological variability to the 3-D circulation at the front and to assessing the influence of sub-surface patchiness in the interpretation of ocean colour data from satellites.

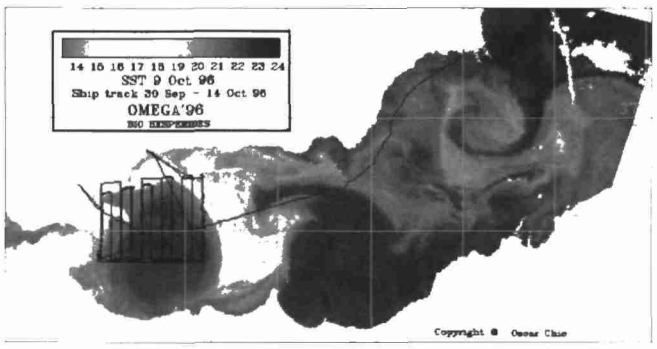

Figure 1: The western Alboran gyre (left) and Almeria-Oran front (right) observed in a NOAA/AVHRR infrared image recorded on board the BIO *Hespérides* on 9 October 1996, with the ship tracks for OMEGA-1 cruise overlaid.

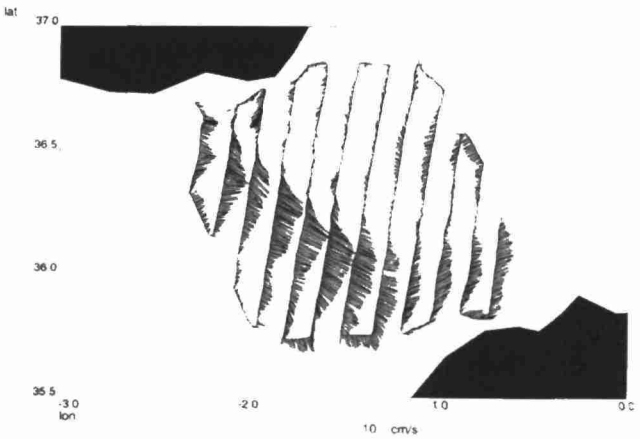

Figure 2: The Almeria-Oran frontal jet at 46 m depth, as measured by combining ADCP profiles and precise navigation data recorded on board the RRS *Discovery* in December 1996. Two of the parallel ship tracks coincide with ERS-2 altimeter groundtracks

TRANSVERSE CIRCULATION AND WATER EXCHANGE BETWEEN SURFACE AND DEEP WATERS OF THE BLACK SEA

Ovchinnikov I.M. *, V.B. Titov, V.G. Krivosheya

The Southern Branch of the P.P.Shirshov Institute of Oceanology of the Russian Academy of Sciences, Gelendzhik, Russia

Abstract

In this work all the components of the transverse circulation of the Black Sea waters with allowance for the climatic factor during the last 130 years are briefly discussed.

Key-words : Air-sea interactions, water convection, intermediate waters, Black Sea

The studies of hydrophysical processes in the Black Sea during the last 10 -15 years allowed to get a series of new fundamental results. As it was established by the numerous experimental data, the most active processes of water exchange between the surface and deep waters which determine the vertical structure of hydrological and hydrochemical fields, the ecological condition of waters and their bioproductivity, take place in the central deep part of the sea and in the nearshore zone (in the continental slope area) in winter.

Dynamic processes in the central part of the sea

The vertical exchange between the surface and deep waters is the most intensive in winter in the centres of the large-scale quasi-stationary cyclonic gyres (eastern and western). As the result of intensification of winter water circulation, an active kinematic rising of rather clean deep waters, saturated with hydrogen sulphide and biogens, to the pycnocline dome takes place here. In this case the constant pycnocline which is a boundary between the surface and deep waters, is rising in the centres of the cyclonic gyres in the form of a dome to the depth of 25-30 m (Fig.1a,b). [1,2].

In the period of autumn-winter cooling, the thin layer (25-30 m) of the surface waters over the pycnocline dome (in the centres of cyclonic gyres) which has the minimal heat content, cools down quicker than in the other regions. Its salinity is increased due to intensive evaporation, and its water density grows that leads to vertical winter convection down to the pycnocline dome (Fig.1a,b).

At the same time in the pycnocline layer which separates the surface and deep waters, internal waves (inertial and others) with the amplitudes from 10 to 12 m are developed. They destabilize the pycnocline and favour the interexchange between the surface and deep waters (Fig.2) [3]. As a result of such interaction between the cold surface waters and the deep waters of high salinity the cold intermediate waters (CIW) with the density of 15.0 are formed on the pycnocline dome. Slipping down its slope they spread to the periphery of the cyclonic gyres. Flowing under the less cold surface waters they form the cold intermediate layer (CIL) with the volume of about 21 000 km^3.

In such a way the kinematic rising of the deep waters from below, the convective mixing (sinking) of the surface waters from above and the internal waves at their boundary (within the pycnocline) are the major factors of winter interaction between the surface and deep waters in the centres of the Black Sea cyclonic gyres. As a result of such interaction the following important processes take place here.

a) The complete oxidation of hydrogen sulphide in the rising deep waters with oxygen from the surface waters which are sinking under the influence of the internal waves into the pycnocline layer.

b) The possible redox-zone formation as the result of dynamic (turbulent) interaction of the surface and deep waters at the boundary of their division under the action of the internal waves.

c) The replenishment and renewal of the surface waters at the expense of more clean deep waters (3 000 km^3/year) and the improvement of ecological condition in the upper sea level.

d) The formation or partial renewal of the cold intermediate layer (CIL) (21 000 km^3) and its distribution within the subsurface layer all over the deep sea area.

e) The enrichment of the surface waters (primarily the CIL) with biogenous elements from the deep waters (nitrates, phosphates etc.) and the increasing of the upper layer productivity in the open part of the Black Sea.

f) The active rising of the deep waters in the middle of cyclonic gyres in winter (3 000 km^3) could result in the sea level rising by more than 9 meters. But the absence of such a catastrophic rising is an evidence of the active transverse water circulation in the Black Sea.

g) The conservation of the balance of heat, salts and mass in the water exchange between the oxygen and hydrogen sulphide zones, the maintaining of the constant depth of the hydrogen sulphide zone upper boundary in the mean perennial aspect.

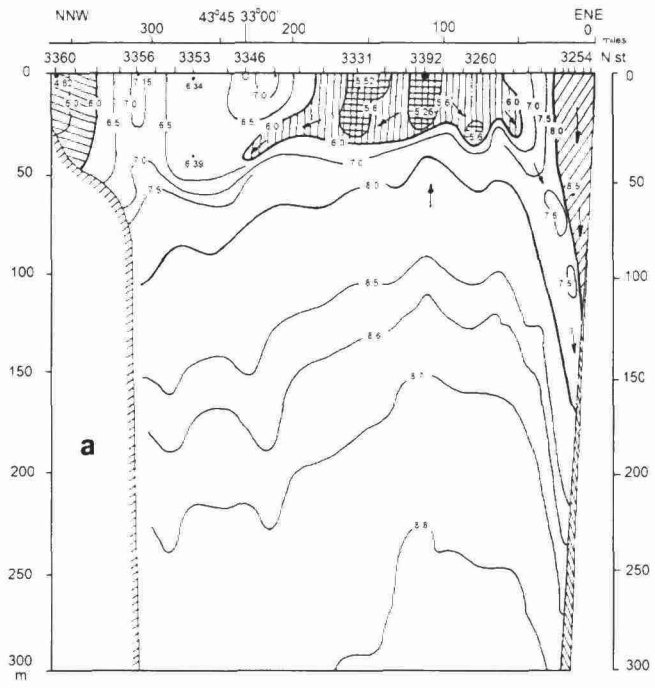

Fig.1a. Distribution of water temperature along the section directed from Odessa to SSE, across the middle of the north-western shelf, towards the supposed centre of the western cyclonic gyre (St.3346: 43°45'N; 33°00'E), and then to ENE, across the centre of the eastern cyclonic gyre, towards Novorossiysk. (According to the data of the 21-st cruise on board the r/v *Vityaz* in winter and spring 1991: 09.02-06.03.91).

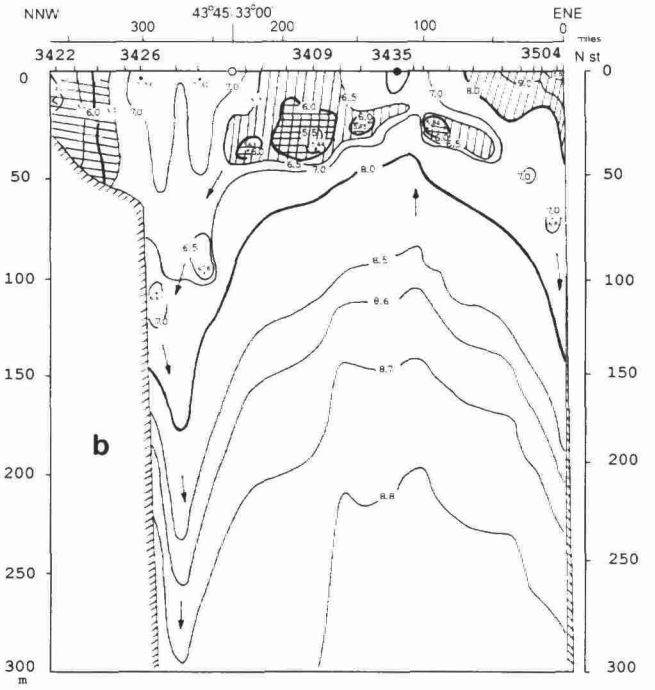

Fig.1b. Distribution of water temperature along the section directed from Odessa to SSE, across the middle of the north-western shelf, towards the supposed centre of the western cyclonic gyre (St.3346: 43°45'N; 33°00'E), and then to ENE, across the centre of the eastern cyclonic gyre, towards Novorossiysk. (According to the data of the 21-st cruise on board the r/v *Vityaz* in winter and spring 1991: 10.03-09.04.91).

RESPONSE OF THE ADRIATIC SEA-LEVEL SLOPE TO THE AIR-PRESSURE GRADIENT AND WIND FORCING AT SUBSYNOPTIC FREQUENCIES

Miroslava Pasaric* and Mirko Orlic

Andrija Mohorovicic Geophysical Institute, Faculty of Science, University of Zagreb, Horvatovac bb, 10000 Zagreb, Croatia

Abstract

Low-frequency variability (0.01 cpd < f < 0.1 cpd) of air pressure, wind and sea level is examined through long time series originating from three locations along the east Adriatic coast. Wind has substantial energy at subsynoptic frequencies, and could be related to the same atmospheric formations as air pressure. Response of sea-level slope to the atmospheric forcing is spatially variable. In the southern, deeper-sea region the sea-level slope is fully explained by isostatic adjustment to air-pressure gradient, whereas over the shelf it is considerably affected by the action of wind. Due to errors in determining wind stress a biased estimate of response to air pressure is obtained.

Key-words: Adriatic sea, air-sea interactions

Introduction

Subsynoptic oscillations (0.01 cpd < f < 0.1 cpd) of air pressure at sea surface are related to passage of planetary atmospheric waves. Empirical analyses carried out in the Adriatic (1, 2) and throughout the Mediterranean (3, 4, 5) show that at these time scales (i) sea level is highly coherent with the air pressure and (ii) adjustment of sea level by far surpasses the isostatic value of -1cm/mbar. It was concluded (5) that the overshoot cannot be accounted for by the direct action of wind. However, theoretical models (6, 7) predicted isostatic response to the air pressure alone. It is the aim of this paper to reexamine the action of wind which acts on sea level at planetary time scales, coherently with the air pressure.

Data

Seven and a half years (September, 1983 - April, 1991) of hourly sea-level data, recorded at three tide gauge stations along the east Adriatic coast (Bakar, Split and Dubrovnik), are used together with sea-surface air pressure and wind from nearest meteorological stations (Figure 1); meteorological data of somewhat shorter length are obtained at some of the stations.

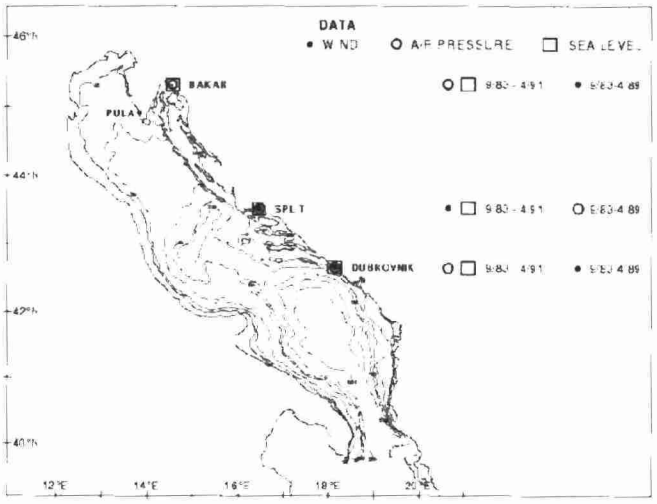

Figure 1. Map of the Adriatic showing the position of the tide gauge and meteorological stations. Also shown are periods over which the data were obtained.

Atmospheric forcing

All the time series exhibit a pronounced seasonal modulation of amplitudes. Seasonal energy spectra show that at all time scales energy is greater in winter than in summer. Furthermore, at subsynoptic frequencies there is a substantial amount of energy not only in air pressure and sea level but also in wind, the long-shore component being much more energetic than the cross-shore component. A very high coherence of the long-shore wind with difference of air pressure along the basin indicates that subsynoptic wind and air pressure could be related to the same atmospheric formations, namely to planetary atmospheric waves.

The seasonal variability of energy suggests that in the empirical analysis only the winter data be used; synoptic and higher frequency variability was smoothed out by low-pass filtering at ten days.

Response of sea level

Response of the Adriatic to forcing by slowly varying air pressure and the related winds is analysed through a one-dimensional model:

$$\Delta\zeta = A\cdot\Delta p_a + B\cdot\int_{x_1}^{x_2}\frac{\tau_{sx}}{H}\,dx + Residual.$$

which relates difference of sea level between two tide-gauge stations $\Delta\zeta$ to air pressure difference Δp_a and to integral between the two stations of long-shore wind stress τ_{sx} over depth of water column H. Thus one requires knowledge of wind stress along the whole distance; because of large-scale nature of subsynoptic processes in evaluating the integral it has been assumed that spatially homogeneous wind is acting over the open sea of flat bottom.

The response parameters A and B are determined in time domain through multivariate linear regression. The corresponding model in frequency domain is approached through two-input spectral analysis.

Analysis in time domain

Prior to examining the combined effect of air pressure and wind forcing, the response to air pressure alone is examined. Table 1 summarizes results of uni- and bivariate multiple regression, obtained for different pairs of stations. The analysis between the far points, namely between Bakar and Dubrovnik, yields a much stronger-than-isostatic response of sea level to forcing by air pressure alone. When the action of wind is considered (wind stress at Split taken as representative for the region), the overshoot is considerably reduced but still not fully accounted for. Since greater part of the Adriatic between Bakar and Split is occupied by shelf in contrast to the much deeper southerly part between Split and Dubrovnik, spatial variability of response is examined. The analysis over the shelf gives similar results, yet if the 95% confidence limits are taken into account, with the inclusion of wind stress (mean of Pula and Split) the response is brought near the isostatic value. Results obtained for the deeper sea region are quite different. Here the response to forcing by air pressure alone is isostatic. However when wind stress (mean of Split and Dubrovnik) is introduced into the analysis, the stress being highly coherent with air- pressure gradient, response to air pressure is reduced to a very low, physically unacceptable value. As for the response of sea-level slope to wind stress integral, analysis for the shelf gives estimate B that is surprisingly close to the theoretical value of $1\cdot10^{-4}$ m/(Nm^{-2}).

Analysis in frequency domain

Results of spectral analysis are very similar. Over the shelf (Figure 2), the single input analysis gives high coherence, phase equal to π and

Table 1. Results of one- and two-input linear regression, obtained for different pairs of stations. Here R is correlation coefficient, A and B are linear regression parameters, R_{12} and R_{mult} are correlation coefficient between the two inputs and multiple correlation coefficient. The 95% confidence limits, obtained by the Monte Carlo Method, are given in brackets. In $f(\tau)$, τ_{hom} is spatially homogeneous wind stress. Asterisk denotes results obtained from six 128-day winter intervals; otherwise eight intervals are used.

	single input		two inputs			
FORCING / PAIR	$\Delta p_a = p_{a_2} - p_{a_1}$		$\Delta p_a = p_{a_2} - p_{a_1}$		$f(\tau) = \tau_{hom}\cdot\frac{L}{H}$	
	R	A (cm/mbar)	R_{12}	R_{mult}	A (cm/mbar)	B cm/(10^{2}Nm^{-2}))
BAKAR-DUBROVNIK	-0.91 (-0.94, -0.87)	-1.70 (-1.81, -1.58)	-0.81 (-0.86, -0.76)	0.92 (0.89, 0.95)	-1.32 (-1.52, -1.12)	0.61 (0.37 0.87)
*BAKAR-SPLIT	-0.75 (-0.85, -0.65)	-1.71 (-1.98, -1.42)	-0.57 (-0.67, -0.47)	0.79 (0.70, 0.88)	-1.33 (-1.65, -1.01)	1.17 (0.73, 1.62)
*SPLIT-DUBROVNIK	-0.66 (-0.78, -0.53)	-0.91 (-1.09, -0.73)	-0.80 (-0.85, -0.72)	0.74 (0.66, 0.83)	-0.31 (-0.65, 0.04)	3.39 (1.94, 4.86)

ON THE ESTIMATION OF WIND STRESS FROM MEAN WIND TIME SERIES

Zoran Pasaric*[1], Mirko Orlic [2]

[1] Center for Marine Research, Rudjer Boskovic Institute, Bijenièka 54, 10000 Zagreb, Croatia

[2] Andrija Mohorovicic Geophysical Institute, Faculty of Science, University of Zagreb, Horvatovac bb, 10000 Zagreb, Croatia

Abstract

The relationship between smoothed wind stress calculated from hourly wind data and the wind stress calculated from smoothed winds is found to be linear, to a high degree (correlation coefficient squared greater than 0.85). A method of estimation of smoothed stress based on linear regression is proposed and successfully tested on 8 years of hourly winds measured at an Adriatic meteorological station.

Key-words: Adriatic Sea, wind

Introduction

Wind blowing over the sea surface is known to be an important forcing agent influencing sea water dynamics. In fact, it is the wind stress, and not wind itself, that acts directly on the sea. This action is manifested at various time scales. Thus, on synoptic time scale (~1-10 days) one finds numerous storm surge and related studies. Subsynoptic (~10 day -1 month) variability also attracted some attention, especially regarding sea-level variations (*e.g.* [1, 2, 3]). The monthly and even longer variability is important for analysis of interannual sea-level fluctuations (*e.g.* [4]). Hence, one often needs sufficiently long time series of averaged wind stress.

The wind stress is commonly calculated through the bulk formula: $\tau = \rho C_D |\mathbf{u}| \cdot \mathbf{u}$

where ρ is air density, C_D is dimensionless drug coefficient and **u** is horizontal, averaged (over typically 1 hour period) wind speed vector at some reference height (usually 10 m above the sea surface). It has long been recognized that in order to calculate averaged stress, the bulk formula should be applied to the original hourly, or at least daily, wind values prior to averaging (see [5]). Application of the formula to the already smoothed wind results in significant underestimation of the mean stress. The underestimation is negligible for 1-day averaging and increases by a factor of 2 or 3 for longer periods. Obviously, due to the nonlinear nature of the bulk formula, high-frequency variability of the original wind cannot be ignored. Thus, two wind stresses may be distinguished: Averaged Stress calculated from original Wind (ASW or averaged stress) and the Stress calculated from Averaged Wind (SAW or stress from averaged wind). The first stress, although exact (up to the bulk formula), requires the knowledge of finely sampled time history that is not always available. On the other hand, the second stress is easily obtainable and physically desirable but is wrong as the estimator of the true stress.

It is the purpose of this work to examine more closely, theoretically and practically, the relationship between the two stresses. It is shown that, to a high degree, this relation is linear. Furthermore, it is found that fluctuations, i.e. deviations from the overall mean of the ASW, can be fairly well estimated from the fluctuations of SAW and knowledge of the overall mean and variance of the original wind. On the contrary, the overall mean of the ASW can not be estimated in this way. The above mentioned linearity is found also in a previous paper [6], regarding the calculation of mean bottom stress in the presence of tidal current.

In Section 2 wind is modeled as a two-dimensional, Gaussian process and theoretical results are obtained. The non-Gaussian case is briefly discussed in Section 3 where the results are tested on 8 years of hourly wind data recorded at Split, Croatia. Fairly good agreement is found.

Theory

Let the wind time history be represented by a two-dimensional Gaussian process (u(t), v(t)). For simplicity, as well as uncertainty in the form of C_D, the stress is calculated from bulk formula with constant C_D and ρ. Then, without loss of generality, ρC_D is replaced by 1. Other forms, proposed in literature (see [7] for a review), can be treated as well.

Let us introduce some conventions. The time variable is omitted. The two components of wind as well as of various stresses are denoted by u and v, appropriately indexed. In the same way, mean values are denoted by m and standard deviations by σ. The two basic operations, *i.e.* averaging and calculation of stress, are denoted by subscripts A and S, respectively. For example, u_S is u component of stress calculated from original wind, while $v_{AS} = (v_A)_S$ is v component of stress calculated from averaged wind; m_u is mean value of u component of original wind, while σ_{uA} is standard deviation of averaged u component of original wind. Finally, for any variable u with mean value m, the centered variable is denoted by u', *i.e.* u'=u-m.

Thus, the wind vector (u,v) is supposed to possess bivariate, normal probability density function (PDF).

$$p(u,v) = \frac{1}{2\pi\sigma_u\sigma_v}\exp\left\{\frac{(u-m_u)^2}{\sigma_U^2}+\frac{(v-m_v)^2}{\sigma_v^2}\right\}.$$

Apparently, the variables u and v are uncorrelated, which can always be achieved by appropriate rotation of the coordinate axes (the simplest case of principal component transformtion, see *e.g.* [8]). In the sequel, the discussion is restricted to u component only. The main (computational) step is to examine linear relationship between the wind component u and corresponding stress $u_s = \sqrt{u^2+v^2}\cdot u$. Thus, we may write :

$$u'_S = u_S - m_{uS} = a_u \cdot u' + \varepsilon_u, \qquad (1)$$

where the slope a_u is determined by minimizing variance of the error term ε_u. At this point, for simplicity of exposition, it is assumed that the mean values of both components are zero, *i.e.* $m_u = m_v = 0$. For convenience, two cases are distinguished: case (1) if the ratio σ_v^2/σ_u^2 is ≤1, and case (2) otherwise. Correlation coefficient squared between u_S' and u' is calculated, by numerical integration, as a function of σ_v^2/σ_u^2 in case (1) (curve no. 1 on Fig. 1), and as a function of σ_u^2/σ_v^2 in case (2) (curve no. 2 on Fig. 1). It is always remarkably high, *i.e.* greater than 0.8, except in case (2) for $\sigma_u^2 << \sigma_v^2$, when it decreases to 0.61. In the later case, the wind is highly polarized and, probably, may be considered as a scalar. The slope a_u is given by

$$a_u = \sigma_u\, g_1(\sigma_v^2/\sigma_u^2), \quad \text{in case (1)}, \qquad a_u = \sigma_v\, g_2(\sigma_u^2/\sigma_v^2), \quad \text{in case (2)}, \qquad (2)$$

where the functions g_1 and g_2 are plotted on Fig. 1 (curves no. 3 and 4 respectively). Now, let us consider averaged wind u_A and corresponding SAW u_{AS}. The vector (u_A, v_A) is again bivariate normal. The components u_A and v_A are approximately uncorrelated having original mean values m_u and m_v, but lower variances $\sigma_{uA}^2 < \sigma_u^2$ and $\sigma_{vA}^2 < \sigma_v^2$. Hence, u_A and u_{AS} are again highly correlated, and we may write :

$$u'_{AS} = u_{uA} \cdot u'_A + \delta, \qquad (3)$$

where the slope a_{uA} is obtained from (2) by changing σ_u to σ_{uA} and σ_v to σ_{vA}.

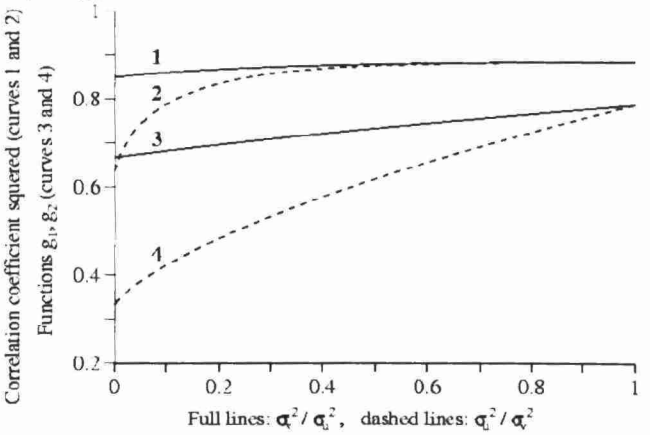

Figure 1. Results based on normal PDF. The correlation coefficient squared between u wind component and corresponding stress u_S (curves 1 and 2). The functions g_1 and g_2 entering formula (2) for the slope (curves 3 and 4).

TIME FLOW VARIABILITY IN THE BALEARIC CHANNELS AND ITS RELEVANCE TO THE WESTERN MEDITERRANEAN CIRCULATION

J.M. Pinot [1], J.L. Lopez-Jurado [2*], M.Riera [1], J. Jansa [2], J. Font [3], J. Tintore [1]

[1] Institut Mediterrani d'Estudis Avancats (CSIC-UIB), Palma de Mallorca, Spain
[2] Centro Oceanografico de Baleares (IEO), Palma de Mallorca, Spain
[3] Institut de Ciencies del Mar (CSIC), Barcelona, Spain

Abstract

The "CANALES 96" field experiment was carried out during March-July, 1996, to investigate the time variability of the water exchanges through the Balearic channels (Western Mediterranean). Four instrumented moorings were deployed and monthly hydrographic surveys were carried out. The main result is that ocean properties are characterized by energetic mesoscale events due to cold eddies of Winter Intermediate Water (WIW, T<13°C). Eddies aggregation can even lead to the sporadic appearance of a large anticyclonic WIW gyre to the north of the Ibiza channel which drastically modifies the water exchange dynamics through the channels, therefore affecting the northward spreading of Modified Atlantic Waters and the southward flow of Mediterranean Waters. Simulations with a numerical model are also carried out to help understanding *in situ* observations.

Key-words: Balear Sea, Straits and Channels, Hydrography, Monitoring

Introduction

For several years now, the Balearic Sea has been considered as a key transition basin between the northern Gulf of Lions and the southern Algerian basin in the Western Mediterranean. The Balearic Sea communicates with the Algerian basin through the Balearic channels: the Ibiza channel between Ibiza and the Spanish peninsula, and the Mallorca channel between Mallorca and Ibiza. The idea that the Balearic channels concentrate the meridional fluxes between the (thermo)dynamically well contrasted northern and southern Mediterranean leading to an energetic seasonal adjustement between the southward spreading of Mediterranean Water (MW) cooled in the north and the northward spreading of lighter Modified Atlantic Water (MAW) from the south was reinforced by recent satellite [1] and large scale modelling [2] studies. *In situ* high resolution surveys also highlighted that the circulation in this basin is characterized by a high mesoscale activity that substantially distorts the mean circulation pattern of along-slope currents [3]. More recent studies emphasized the role played by the Balearic channels in controlling the meridional mass transport and fluxes of heat, salt and other properties, hence showing its relevance to the general circulation of the Western Mediterranean [4, 5]. Satellite and *in situ* observations in the Balearic channels also suggested complex interactions between surface and subsurface mesoscale eddies and channel topography, with strong effects on the mean seasonal exchange dynamics through the Ibiza channel [6]. All these previous studies were extremely useful for defining the spatial characteristics of the circulation in the Balearic Sea but missed the time evolution of the flow.

The INTERMESO group, composed by oceanographers from the Institut Mediterrani d'Estudis Avancats, Centro Oceanografico de Baleares and Institut de Ciencies del Mar, carried out a unique field experiment during 1996-97 to investigate the annual cycle of the ocean circulation in the Balearic channels. The experiment was mostly oriented towards determining the nature and the time scales of circulation variability. The data presented here were collected during the "CANALES 96" field experiment, March-July, 1996, and relied on two major efforts: 1) The deployment of 4 instrumented mooring lines to continuously monitor currents and water properties and resolve the time variability at subinertial frequencies and 2) Repeated hydrographic surveys every month to sample the water mass structure and help assess flux seasonal variability. All CTD casts reached the bottom and moorings were designed to record the current and water properties for each layer of the water column. Additional data of sea surface temperature from NOAA satellite imagery were obtained and used to interpret *in situ* measurements. Also numerical modelling experiments were carried out to help in the understanding of observed phenomena. Crucial data were thus obtained for the first time, for a broad range of ocean processes in the Balearic Sea which appear to be fully relevant for the general circulation of the Western Mediterranean.

Design of the experiment and instruments used

The typical pattern of the mean circulation in the Balearic Sea is shown in Figure 1 which also highlights the question of the flow interaction in the channels. Triangular shape hydrographic surveys to be repeated every month were designed for each channel (Figure 1). Four days were needed every month to sample both channels (37 stations in total).

Four sub-surface moorings were also deployed to continuously monitor the fluxes and physical properties of ocean waters flowing through the channels at particular locations, over the 900 m isobath (Figure 1). The four moorings included a total of 12 mechanical current meters (vector average) and 2 thermistor strings (10 thermistors each).

During all cruises a SBE-25 CTD probe was used for hydrographic measurements. A critical point in this kind of study dealing with hydrographic climatology is the correct calibration of the sensors which should allow sensible comparison between all cruise data sets. The SBE-25 probe was calibrated in situ during the May cruise, half way between March and July using another SBE-25 probe which had been calibrated a few days prior to the cruise in OSI laboratory (Southampton, UK). Temperature and salinity data were obtained for all cruises on the basis of this particular calibration. Temperature and conductivity sensors of moored instruments were also calibrated using the closest CTD profiles performed in their vicinity at the time of the cruises.

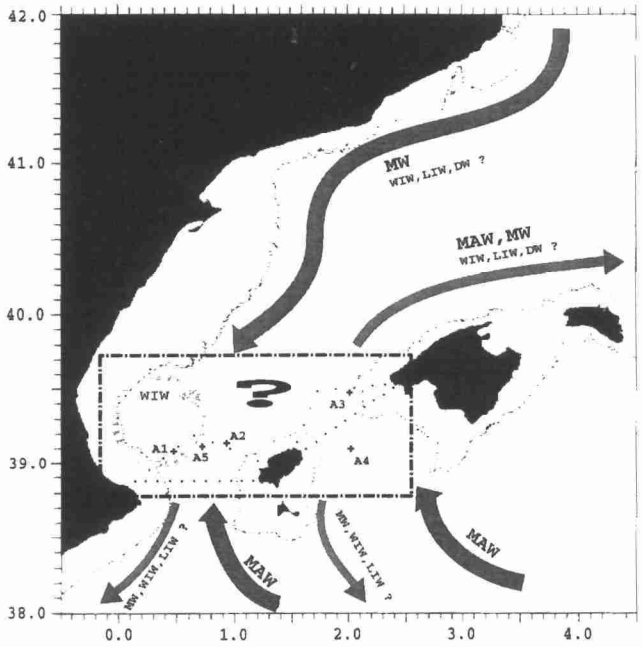

Figure 1: Classical picture of the main inflow patterns into the Balearic Sea (dark grey solid arrows). Surface Mediterranean Water (MW), Winter Intermediate Water (WIW), Levantine Intermediate Water (LIW) and Western Mediterranean Deep Water (DW) are assumed to enter the basin along the continental slope from the northern Gulf of Lions. Modified Atlantic Water (MAW) flows into the Balearic Sea from the southern Algerian basin. Light grey solid arrows sketch likely outflows resulting from water exchange dynamics through the channels where complex high frequency subinertial flow interactions are expected to occur. The WIW eddy recurrent in spring-summer to the north of the Ibiza channel is represented by a dotted arrow. Crosses indicate A1 to A5 mooring locations for long-term monitoring of the water fluxes and dots represent hydrographic stations repeated every month from March to July, 1996.

Overview of hydrographic data analyses

The hydrographic data set obtained from the March (late winter) to July (early summer) surveys, 1996, give snapshots of the circulation occurring in the Balearic Channels during the transition period from winter to summer with information on the structure, dynamics and transport of the water masses. The analyses were based on plotting distributions of temperature, salinity, density, dynamic height and geostrophic velocity. Dynamic height was computed with a reference at 600 m. For shallow profiles located over the slope, the closest offshore station was extrapolated. A general result that can be derived from the analysis of properties distributions is that two signals are superimposed: a mean, smooth seasonal month-to-month variability at climatological scale which modulates an energetic signal due to mesoscale eddies transiting through the channels.

The March survey evidences thermal homogeneity of the water column resulting from winter convective processes. The circulation in the different

LAGRANGIAN MEASUREMENTS OF SURFACE CIRCULATION IN THE ADRIATIC AND IONIAN SEAS BETWEEN NOVEMBER 1994 AND MARCH 1997

by Pierre-Marie Poulain

Naval Postgraduate School, Monterey, CA 93943, USA

Abstract

The near-surface circulation of the Adriatic and Ionian Seas is explored using Lagrangian drifting buoy measurements obtained between November 1994 and March 1997. The drifter trajectories reveal the complex and highly variable structure of the surface currents. The main pathways of the surface waters are defined and the major persistent surface circulation features are described. The seasonal variability of the surface currents is studied in the sea areas with maximum drifter data density, namely, in the Sicily Straits, the Northern Ionian, the Otranto Straits and the Southern Adriatic.

Key-words: Circulation, Surface Waters, Eastern Mediterranean

Introduction

The advent of efficient worldwide satellite tracking and telemetry systems in the late 1970's marked the beginning of Lagrangian measurements of ocean currents (and other parameters such as temperature and salinity) using expandable freely drifting buoy systems. Because of the direct wind/wave effects on their top elements (*e.g.*, the transmission antenna and other instruments) emerging at the sea surface, surface drifters do not follow the surface currents exactly. The downwind drifter movement with respect to the sea water, or slippage, can become substantial in high seas. Slippage problems were particularly important for the early drifter experiments (*e.g.*, the FGGE drifters in the Antarctic Circumpolar Circulation). They provided the impetus for the design of various buoy systems that provide maximum adherence to the sea water. Designs such as the CODE, the TRISTAR and the WOCE/TOGA SVP (holey sock) were developed in the 1980's. Calibration experiments [1] revealed that their relative slip with respect to the water only amounts to a fraction of one percent of the surface wind speed.

Drifter data in the Mediterranean Sea

Deployments of satellite-tracked drifters (with good water-following capabilities) in the Mediterranean started in the late 1980's as part of regional scientific surveys and operational military operations. Seeding continued into the 1990's when dedicated basin-wide drifter programs were conducted in the Ionian and in the Adriatic [2]. Most of these data sets have been quality controlled and combined in a common data base. The drifter data were processed to obtain low-pass filtered (36 hour cut-off) series of position (latitude and longitude), velocity (zonal and meridional components) and other ancillary parameters such as sea surface temperature at regular 6 hour intervals. The data of 112 modified CODE drifters extending within the first meter of water [2] and 6 WOCE/TOGA SVP drifters drogued to 15 m [1] for the time period between November 1994 and March 1997 are considered in this paper. Their low-pass filtered trajectories are depicted in Fig.1. The complexity of the sub-tidal surface currents patterns is striking. The tortuous drifter trajectories are the result of both spatial and temporal variability. Besides the strong mesoscale signal, in form of eddy, meander and filament patterns, significant seasonal variability is included in this Lagrangian drifter data.

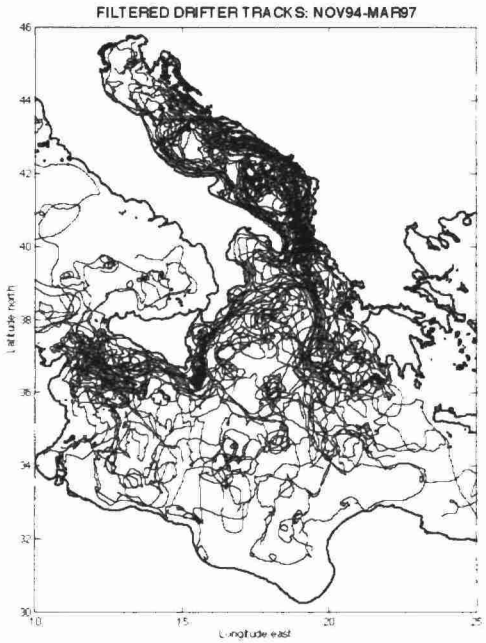

Fig. 1. Composite diagram of the low-pass filtered surface drifter trajectories in the Adriatic and Ionian Seas from November 1994 to March 1997. Arrows are only plotted in the bins sampled by the drifters.

Drifter trajectories

The composite "spaghetti" diagram of the low-pass filtered trajectories (Fig. 1.) in the Adriatic and Ionian Seas discloses some of their well-known persistent circulation features, such as the Atlantic Ionian Stream in the Sicily Straits and the northwestern Ionian, and the basin-scale cyclonic circulation gyre in the Adriatic. The Atlantic Ionian Stream is evident as a swift current flowing southeastward in the Sicily Straits, passing through the Malta Channel and extending into the northwestern Ionian where the mean circulation is mostly anticyclonic. South of this strong current, the Modified Atlantic Water flows southeastward and mostly recirculates on the Tunisian shelf, hence contributing very little to the mean inflow into the Ionian. Upon leaving the shelf east of Malta, Modified Atlantic Water bifurcates into a northward main swift branch and slower eastward and southward components. Recirculating cyclonic gyres are evident between the Sicilian coast and the strong northward branch. In the Adriatic, the classical basin-wide mean cyclonic circulation [3] with northwestward (southeastward) currents on the eastern (western) side, actually composed of two sub-basin cyclonic, circulatory patterns around the two main topographic deeps of the Adriatic, is confirmed by the drifter measurements.

The drifters reveal a novel structure of the Ionian surface circulation in which the Modified Atlantic Water appears to transit eastward in three different ways (Fig. 1): (1) As a strong anticyclonic mean loop current in the northern part of the basin extending into a concentrated southward-flowing limb west of Greece. This meridional jet in the northeast Ionian is in good agreement with circulation maps derived from hydrographic observations in the late 1980's [4]. Further south, drifters either move to the southeast and eventually get caught in the Pelops anticyclonic gyre southwest of the Peloponese Peninsula, or meander to the south towards Libya; (2) in the form of weak and chaotic currents in the central Ionian; and (3) as a relatively swift coastal circulation off the African continent, known as the African Current. The anticyclonic circulation pattern in the northern Ionian extends as far north as about 39°N where a confluence zone appears between the Modified Atlantic Water and the Adriatic Surface Water outflowing through the Otranto Straits. The latter water joins the main anticyclonic circulation either directly or after a cyclonic loop in the Gulf of Taranto.

Mean Circulation Maps and Seasonal Variability

The seasonal variability of the surface circulation was studied in areas of the Mediterranean Sea where the number of drifter observations is relatively large and well distributed over the seasons, i.e., in the Straits of Sicily, the Northern Ionian, the Otranto Straits and the Southern Adriatic. In order to map the mean surface circulation, the low-pass filtered drifter velocities were averaged in bins of 0.25° latitude by 0.25° longitude for each season. The mean circulation maps for winter, spring, summer and fall are presented in Figs. 2a,b,c,d, respectively. Arrows represent the mean velocities in bins sampled by the drifters. The deployment strategy adopted and the Lagrangian nature of the drifters combined to produce different non-uniform data coverages for the four seasons. Note that the southwest Adriatic and the northern Ionian have very few observations in spring.

In the Sicily Straits, the inflow of Modified Atlantic Water seems to be maximum in summer and minimum in winter in good agreement with geostrophic estimates reported in the literature [5]. In spring, summer and fall, most drifters proceeded eastward through the Malta Channel and upon leaving the Malta Shelf separated into three branches, the northernmost one corresponding to fast northward-northeastward currents following the sharp Ionian shelf break and forming a mean anticyclonic gyre in the Northern Ionian. This anticyclonic sense of rotation also persisted into winter, in some contradiction with hydrographic observations [6] and computer simulations that indicate alternate anticyclonic and cyclonic patterns in summer and winter, respectively. In winter, the drifters deployed upstream in the Sicily Straits tended to avoid the Malta Channel route and

DRIFTER AND SATELLITE THERMAL OBSERVATIONS OF THE ALGERIAN CURRENT IN AUTUMN AND WINTER 1996-97

José Salas [1*], Emilio Garcia-Ladona [1], Jordi Font [1], and Claude Millot [2]

Instituto de Ciencias del Mar, CSIC, Barcelona, Spain

Laboratoire d'Océanographie et de Biogéochimie, Centre d'Océanologie de Marseille, CNRS, La Seyne, France

Abstract

During autumn and winter 1996-97 surface floats observations and satellite sea surface temperature (SST) images of the Algerian Current were collected to study the evolution of mesoscale instabilities. The growth of an instability event and its evolution to a coastal anticyclonic eddy was observed between 0°-4°E. During several months the floats drifted to the east and some of them were trapped in an open sea eddy detaching from the coast.

Key-words: mesoscale phenomena, circulation experiments, remote sensing, Algerian basin

Introduction

The Algerian Current (hereafter, AC) is a component of the Modified Atlantic Water (MAW) circuit in the Mediterranean Sea. Several regional studies have been made, including observational campaigns, laboratory experiments and numerical models to explain the dynamics of instabilities of the AC, their evolution into anticyclonic eddies and their detaching from the coast [1].

The AC begins from the Almeria-Oran jet near 1°W, and then it flows along the Algerian coast [4, 5]. Between 0° and 1°E, the AC is seen to be affected by instability processes, mainly of baroclinic nature, which begin as an undulation of the stream and evolve into paired eddies (fig. 1a). Usually, the cyclonic part of the instability tends to vanish in a few days, while the anticyclonic one may persist as an eddy that strongly interacts with the main flow. This eddy propagates downstream at a few km/day with diameters ranging between 30 km and 100 km. Long time-series of satellite images account for lifetimes of several months at least [6,7,8].

Very few *in situ* data are available in the Algerian basin. Combining satellite-tracked surface drifters and series of SST maps is very useful to analyze the evolution of such eddies. The MATER/ALGERS experiment based on such a methodology was initiated in autumn 1996, in order to describe and quantify the dynamics of such events.

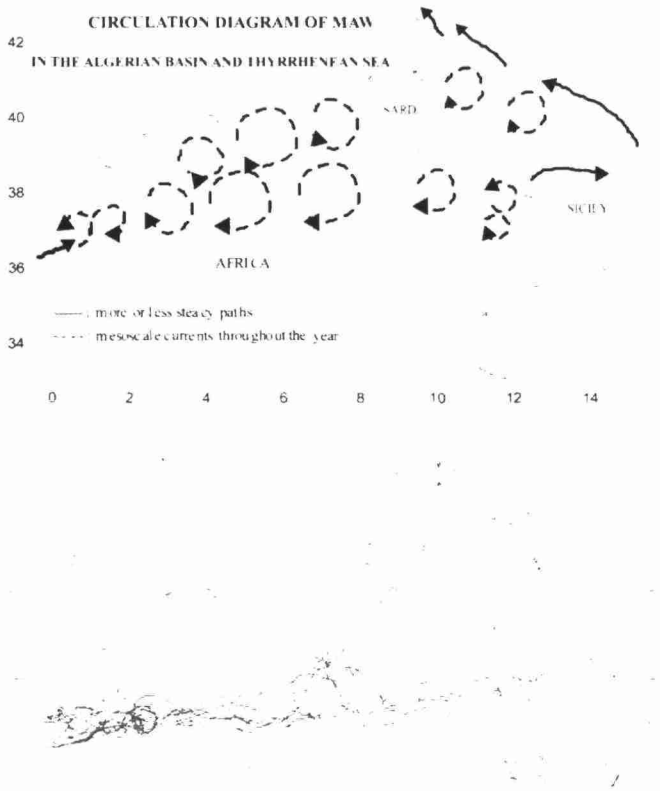

Figure 1. (a) Circulation of the water of Atlantic origin (from Millot, 1987). (b) Trajectories of the 18 drifters during their whole lifetime.

Data-set

The ALGERS'96 cruise on board the Spanish R/V *Hespérides* covered part of the Algerian coast, where a meander was observed near 1°E a few days prior to the cruise with satellite infrared imagery (fig. 2a). Near 0°, upstream of this event, on October 17, 3 surface drifters were launched 9 km apart in the core of the AC. On October 18, near 1°E, 15 drifters were launched 5 km apart across the cyclonic part of the meander (fig. 2). Each drifter was attached to a long sock (WOCE standard drogue) centered at 10m. The drifters were ARGOS-positioned 6-8 times per day, and they operated from several days to several months (fig.1b).

For the period October 1996 - January 1997, SST maps were obtained from daily composites of NOAA Advanced Very High Resolution Radiometer (AVHRR) images, using the GISIS (Graphical Interface to the Intelligent Satellite Data Information System) Internet facility

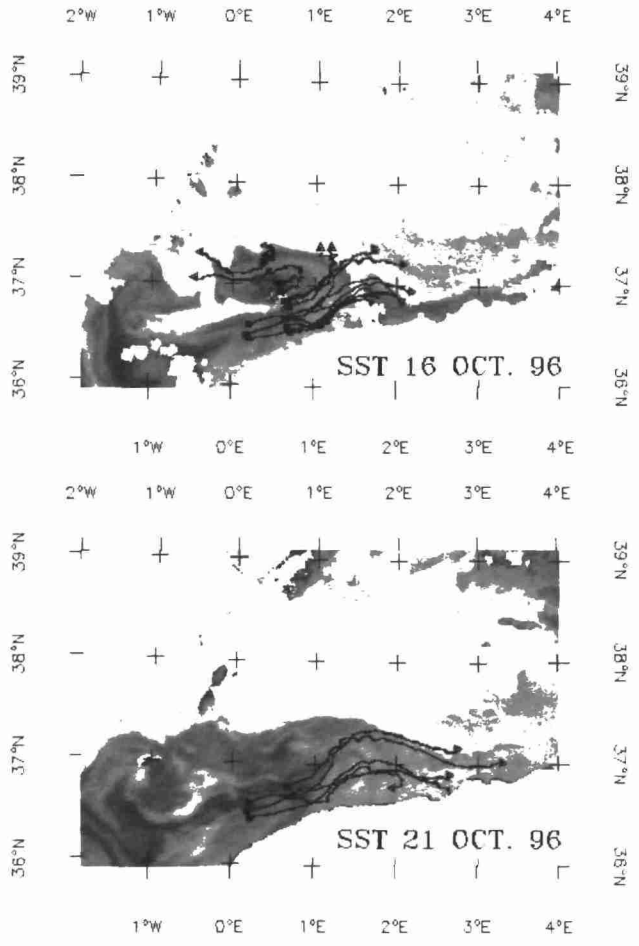

Figure 2. (a) NOAA/AVHRR SST image of October 16, showing the meander, the deployment locations of the ARGOS drifters, and their trajectories in the first five days (17-22 October 1996). (b) NOAA/AVHRR SST image of October 21 with superimposed drifter tracks during eight days, that evidenced the wave-like shape of the meander.

AN EVALUATION OF BULK FORMULAE FOR ESTIMATING RADIATION BUDGET COMPONENTS OVER THE WESTERN MEDITERRANEAN SEA

Maria Elisabetta Schiano [1*], Mireno Borghini [1], Franco Belardinelli [2], Costante Luttazzi [2], Livio Tagliacozzo [2]

[1] Istituto per lo Studio dell'Oceanografia Fisica-CNR Forte S.Teresa, 19036 Pozzuolo di Lerici (SP), Italy,

[2] Istituto di Fisica dell'Atmosfera-CNR, Area della Ricerca di Tor Vergata, Via del Fosso del Cavaliere, 00133 Roma, Italy

Abstract

Direct measurements of longwave radiation flux, incident solar radiation and meteorological parameters at sea were carried out in the Western Mediterranean Sea during different seasons in the years 1989-1997. The data collected were used to perform validation tests on the most widely used radiative empirical equations. Some results are reported.

Key-words: Western Mediterranean, Heat budget

Precise evaluation of the radiation budget at the sea surface is essential for world climate research as well as for the improvement of the marine circulation models. In spite of its importance, there is no network of radiation measurements over the oceans. Several radiative transfer models have been developed to compute this flux , but the data required as input are generally lacking over the ocean. Satellite measurements are attractive, but the most difficult problem is the validation of the techniques to extract the geophysical data from the remote sensing signals. Routine ship meteorological observations are the only overwater data available having a fairly good spatial and temporal resolution. As a consequence, in order to estimate this term of the air-sea energy balance, modelers and climatologists have favoured an empirical approach using only surface weather observations: air temperature, humidity, barometric pressure, water temperature and visual cloud cover. Many formulae of this type have been proposed and employed during the years but only few tests have been done to assess their applicability over the whole ocean and the results obtained are often contradictory. Thus, there is now no single universally accepted bulk scheme. The principal reason of the observed discrepancies between predictions and measurements and between the predictions obtained by different formulae is that the empirical equations as well as their numerical coefficients are determined by fitting some parameters which are highly variable both in space and in time. Therefore the data set used to achieve the fit becomes crucial. Many formula have been obtained from data sets collected over the land. When marine observations have been used, the data were too few and limited to allow a generalisation. As a consequence, the results of the validation tests of the different bulk formulae may be highly variable depending on the resemblance between the data set used to derive the formula and the data set employed in the comparison. Since the use of an incorrect bulk formula can produce considerable mistakes in the output of climatic and dynamic models and can even lead to inverting the estimated direction of the net heat flux, a careful examination of these expressions is necessary. The tests are especially required over the Mediterranean Sea, where air-sea energy exchanges play a fundamental role in the dynamics and climatology of the region. Additionally, the validation of empirical equations for the Mediterranean Sea must be performed *ad hoc* the atmospheric and marine features of this semiclosed basin being different from those of the open oceans.

Direct measurements of solar radiation, atmospheric radiation, sea surface temperature and meteorological parameters were carried out on board of the R/V *Minerva* and R/V *Urania* of the Italian National Research Council (Consiglio Nazionale delle Ricerche) during 13 cruises in the Western Mediterranean Sea in the years 1989-1997.

The period and the working area of each cruise are listed in Table 1, while a detailed description of the instrumental setup and of the methodology used to elaborate the data is given in Schiano *et al.* (1).

Table 1 : Period and working area of the 13 cruises.

1	Sept. 28 to Oct. 7, 1989	North Tyrrhenian Sea
2	Feb. 17-22, 1990	North Tyrrhenian Sea
3	Nov. 10-19, 1990	Ligurian Sea
4	April 20 to May 5, 1991	Ligurian Sea
5	Oct. 24 to Nov 8, 1991	South Tyrrhenian Sea
6	April 21 to May 5, 1992	South Tyrrhenian Sea
7	August 12-30,1992	Balearic Sea
8	Feb. 27 to march 15, 1993	South Tyrrhenian Sea
9	Nov. 4-22, 1993	Sicilian Channel
10	May 17-29, 1994	Sicilian Channel
11	Oct. 10-20, 1994	Sicilian Channel
12	July 4-30, 1995	Western Mediterranean Sea and Sicilian Channel
13	Jan 10-30, 1997	Sicilian Channel

These measurements have supplied the more large experimental radiation data set over this basin.

Part of this data set was used to carry out a first comparison between experimental measurements and the predictions obtained by the most widely used radiative bulk formulae.

Eight formulae for estimating the net longwave flux at sea were checked using the data collected from 1989 to 1992. This earlier test shows that the measured flux is systematically underestimated by about 30 Wm^{-2} (2). The bias was ascribed to the bad parameterization of the water vapour effect. and an alternative empirical formula was derived from these data.

The data from 1989 to 1994 were used to check the empirical formula proposed by Reed (3) for estimating the solar radiation at sea (4). The results reveal that the computed solar radiation is overestimated under clear sky conditions and underestimated for cloudy sky. The disagreement of clear sky predictions was ascribed to a regional misevaluation of both aerosols and water vapour attenuation that could be corrected by a simple adjustment of the numerical coefficients. The inadequacy of the cloud cover index was indicated to explain the discrepancy of the estimates under cloudy sky.

The enlargement of the data set allows a better analysis of the parametrizations for both the radiative terms. In particular, since the longwave radiation flux formulae require hourly values as input, the data set used to perform this analysis changes from 1335 to 2779 points, while the one employed for the test on the solar radiation formula, in which only mean daily values are included, changes from 88 to 126 observations.

The data increase is not sufficient to significantly improve the results given by Schiano (4), but the new data strengthen the main conclusions of that work. Figure 1 shows the measured daily values of solar radiation compared with the predictions obtained by Reed's formula (3) and by the same formula computed using the adjusted coefficients. The agreement between computed and measured solar radiationis is good using the formula in both original and revised configuration.

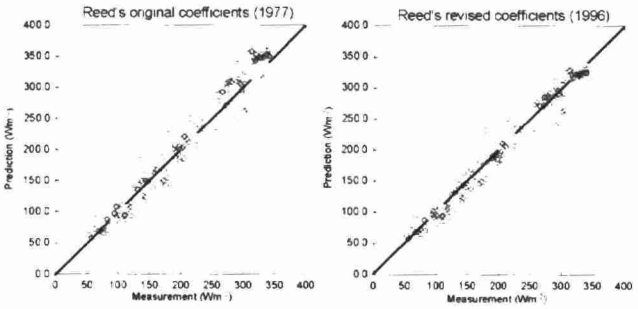

Figure 1 : Reed's predictions *versus* measurements. Original and revised formula.

More than 90% of the differences between predictions and measurements are within 10% of the measured value. The agreement is noteworthy, taking into account the coarseness of the formula and the experimental errors, that, due to the difficulties in making this type of measurements on board, cannot be completely left out. The new comparison demonstrates that the correction of the numerical coefficients for the water vapour attenuation is necessary for improving the predictions under clear sky, though, in order to select the numerical coefficients, the threshold value of water vapour density should be better definite. The disagreement between predictions and measurements under cloudy sky confirms that the cloud cover index is too much coarse to represent the cloud effects on the solar radiation transmission. The differences between measured and computed solar radiation under cloudy sky show a light dependence on the water vapour density, but the data are still too few for this analysis.

The nine formulae used for computing the longwave radiation flux are given in Table 2.

The validation of the formula by Bignami *et al.* (2) is achieved by using only the data obtained during the last six cruises (Figure 2).

Examining the whole data set, the new comparison confirms that the early seven tested empirical equations underestimate the longwave net flux, while the formula by Bignami *et al.* (2), *ad hoc* developed for the

EVOLUTION OF OXYGEN AND NUTRIENTS DEEP CIRCULATION THROUGH THE STRAITS OF THE CRETAN ARC: IMPACT ON THE DEEP LAYERS OF THE EASTERN MEDITERRANEAN SEA

E. Souvermezoglou*, E. Krasakopoulou
National Centre for Marine Research (NCMR), A. Kosmas, Hellinikon 16604, Greece

Abstract
The intensive research during the past decade, revealed important changes in the deep and bottom layers of the Eastern Mediterranean. The increase of oxygen and the corresponding decrease of nutrient content in the deep and bottom layers of this sea, observed after 1987 is mainly due to the increased outflow of the Cretan Deep Water (CDW). This water outflows towards the Levantine and Ionian Seas through the deeper straits of the Cretan Arc and displaces upwards the old Eastern Mediterranean Deep Water of Adriatic origin .

Key-words: deep waters, oxygen, nutrients, Eastern Mediterranean

Introduction

The Cretan Sea occupies the southern and larger basin of the Aegean Sea. It communicates with the SE Ionian Sea through the straits of Elafonissos (sill depth: 200m, width: 11 km), Kithira (sill depth: 160m, width: 33 km) and Antikithira (sill depth: 700m, width: 31 km) and with the Levantine Sea through the straits of Rhodes (sill depth: 350m, width: 17 km), Karpathos (sill depth: 850m, width: 43 km) and Kassos (sill depth: 1000m, width: 67 km).

The Cretan Sea and the straits of the Cretan Arc have been sampled several times since March 1986 in the framework of the multinational research programme for the exploration of the Eastern Mediterranean, POEM-I (1985-1990), POEM-II-EPICS (1991-continued). The survey consisted of an extensive grid of stations shown in the Figure 1.

The general remarks for the distribution of oxygen and nutrients in the Cretan Sea, can be summarised to the relative decrease of nutrients and to the corresponding rise of oxygen concentrations in the intermediate and deep waters of this sea with regard to the Eastern Mediterranean for all the periods (summer-winter) of observation [1].

The deep layers of the Cretan Sea are occupied by the Cretan Deep Water (CDW) which outflows through the Straits of the Cretan Arc and after 1987 affects the structure and the characteristics of the water column in large areas outside the Cretan Sea [2] [3]. The increase of the oxygen content of the deep and bottom waters of the Eastern Mediterranean by about 0.3 ml/l, observed during the last few years, is mainly due to the increased outflow of the Cretan Deep Water (CDW) towards the Levantine and Ionian Seas through the straits of the Cretan Arc [4]. This water displaces upwards the old Eastern Mediterranean Deep Water of Adriatic origin.

Among the straits of the Cretan Arc three straits with sill depths deeper than 700 metres, namely Antikythira, Kassos and Karpathos, play an important role for the deep circulation between the Cretan Sea and the Eastern Mediterranean. In the present paper we follow the deep circulation of oxygen and nutrients, from 1987 to 1992, through the Antikythira and Kassos straits.

Antikythira Strait

Exchanges between the Cretan Sea and the Ionian Sea through Antikythira Strait in late winter and in late summer 1987 show a supply of nutrients in the Cretan Sea between 200 and 800 decibars [5]. The inflowing water originates from depths 500-1000 metres in the Ionian Sea; the maximum nitrate, phosphate, silicate and the minimum oxygen concentrations in late summer 1987 (3.5 μM, 0.17 μM, 4.6 μM and 4.8 ml/l, respectively) are found at about 500 m in the Antikythira Strait (Figure 2).

In the near bottom layer (below 400 dbars) an outflow of the oxygen rich-nutrient poor CDW towards the Ionian Sea is observed (Figure 2). During the late winter and late summer 1987 cruises, this saline and warm deep water with low nutrient and high oxygen content is detected in form of patches to the west of the Cretan Arc at a depth of 900 m [6]. Our results showed that this intermittent outflow of CDW towards the Ionian Sea can not affect the concentrations of the chemical parameters in the deep layers of the Eastern Mediterranean. During 1987, the deep layer below 1000 metres is rather homogeneous, with oxygen about 4.2 ml/l and nitrates higher than 5.0 μM (Figure 7).

The distribution of oxygen along the Antikythira Strait in autumn 1991 (Figure 3) shows that the outflow of CDW towards the Ionian Sea, occurs below 200 m down to the sill depth. On the same figure, the important

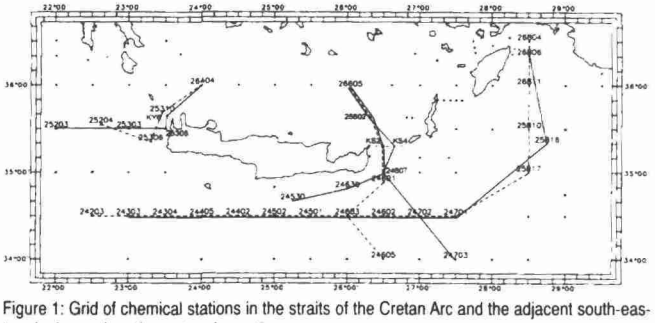

Figure 1: Grid of chemical stations in the straits of the Cretan Arc and the adjacent south-eastern Ionian and north-western Levantine seas.

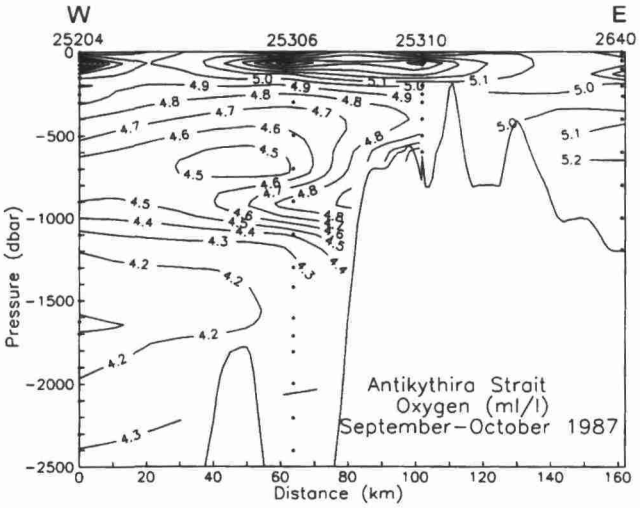

Figure 2: Vertical distribution of oxygen (ml/l) along the Antikythira Strait in late summer 1987.

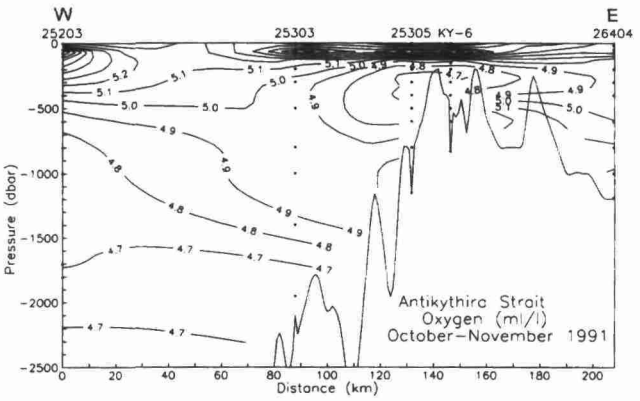

Figure 3: Vertical distribution of oxygen (ml/l) along the Antikythira Strait in autumn 1991.

increase of oxygen (about 0.5 ml/l) observed in the deep and bottom layers in the Ionian Sea, to the west of the Antikythira strait, led us to suppose that an important outflow of CDW towards the Ionian took place after 1987. The corresponding decrease of nutrients is about 1 μM for both nitrates and silicates. The intrusion of CDW has modified considerably the distribution of all properties in the Eastern Mediterranean affecting a large area around the island of Crete.

Kassos Strait

The distribution of oxygen and nitrates along a transect through the Kassos Strait in late summer 1987 (Figure 4) shows that the oxygen and nitrates concentrations below 1000 metres in the Cretan and the NW Levantine seas are considerably different. In the Cretan Sea below 1000 m the oxygen is higher than 5.2 ml/l while the nitrates are lower than 1.6 μM; considerably lower oxygen concentrations (O_2 ~ 4.1 ml/l) and higher nitrates concentrations (NO_3 ~ 5.2 μM) are found in the NW Levantine Sea indicating a very weak Aegean influence in the deep layers (>1500m) of the NW Levantine Sea during this period. The current meter measurements performed in the area during the same period [7] confirm our observations.

The important CDW outflow after 1987 is manifested in autumn 1991 by the important augmentation (~ 0.4 ml/l) of oxygen (Figure 5) and diminution of nutrients concentration in the layer below 800 metres in the NW Levantine Sea, in the viscinity of the strait.

Further increase of oxygen and decrease of nutrients concentrations in the deep layers of the NW Levantine Sea were observed during the late

ESTIMATIONS OF ERRORS ORIGINATING FROM THE ASSUMPTION THAT A SINGLE MEASUREMENT REPRESENTS THE MONTHLY MEAN OF TEMPERATURE AND SALINITY IN THE NORTHEASTERN ADRIATIC

Nastjenjka Supic* and Danilo Degobbis

Centre for Marine Research, Ruder Boskovic Institute, G. Paliaga 5, 52210 Rovinj, Croatia

Abstract

Errors originating from the assumption that a single measurement represents the monthly mean of temperature and salinity in surface and bottom layers have been estimated on the basis of weekly measurements in the periods 1929-1933 and 1937-1943 at station A1 off Rovinj in the northeastern Adriatic. The errors were high in April-July and in September/October and low during winter, ranging between 0.6°C-3.1°C (surface temperature), 0.7°C-2.2°C (bottom temperature), 0.2-2.5 (surface salinity) and 0.2-0.5 (bottom salinity).

Key-words: Adriatic sea, temperature, salinity.

Oceanographic data in the northeastern Adriatic have mostly been collected monthly to seasonally. The properties of the region are highly variable under the influence of air-sea interactions and dilution processes, mainly due to the Po River discharges. To study mechanisms of long-term changes of these properties, it is therefore essential to estimate the magnitude of the errors made by the assumption that a single measurement within a month represents the monthly mean of temperature or salinity.

To estimate this error we used a historical data set collected weekly in the periods 1929-1933 and 1937-1943 (Figure 1) at station A1 (45°04.0' N 13°37.0' E; 32 m depth), located in the northeastern Adriatic 1 Nm off Rovinj (western Istria, Croatia). As the temperature was measured by a reversing Richter's thermometer and salinity estimated after the Mohr and Knudsen's method (1) we expect the accuracy of measurements to be within the range of ±0.1°C and ±0.05. The mean value of a parameter (surface temperature, surface salinity, bottom temperature, bottom salinity) for i-th month and n-th year of the two intervals (P_{in}) was computed from k ($3 \le k \le 9$) monthly observations (P_{oin}; o=1,..,k):

$$P_{in} = \frac{1}{k}\sum_{o=k}^{o=k} P_{oin}$$

From the random choice of one between k values of P_{oin}, P_{in}' was defined and the absolute differences D_{in} were computed:

$D_{in} = /P_{in} - P'_{in}/$

The error in assessing monthly mean of a parameter from a single measurement for i-th month (E_{Pi}) was taken to be the highest one among n values of D_{in} (Figure 2).

The error for temperature ranged between 0.6°C (February) and 3.1°C (June) at the surface and between 0.7°C (February) and 2.2°C (December) in the bottom layer, while for salinity it varied between 0.2 (February) and 2.5 (July) at the surface and between 0.2 (February, July, August) and 0.5 (May, June, October, December) near the bottom. Seasonal cycles of the error for both parameters were similar (Figure 3): while the errors were higher in April-July and in September/October, minimal values occurred in February. The annual variations of the error can be related to seasonal cycles of temperature and salinity in the investigated area (Figure 4) obtained on the basis of monthly to seasonaly sampling in the period 1966-1992 at a location close to A1 (2).

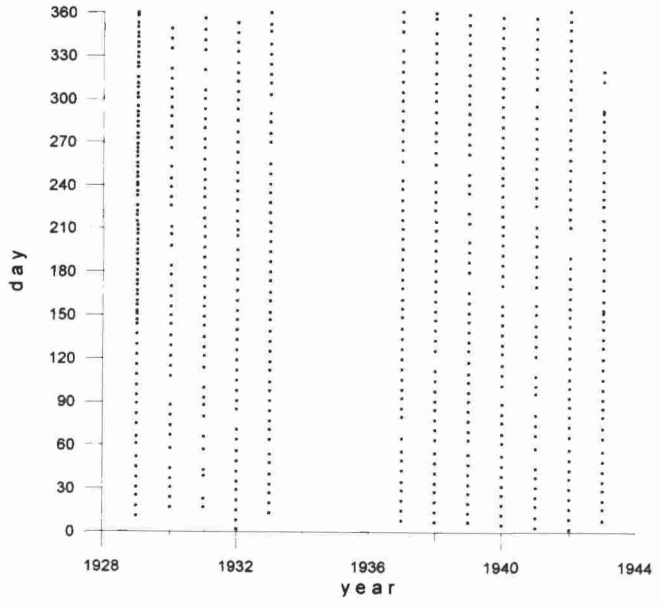

Figure 1. Frequency of measurements of temperature and salinity in the period 1929-1943 at station A1 (45°04.8' N 13°37.0' E; 32 m depth). First day of a year coresponds to January 1.

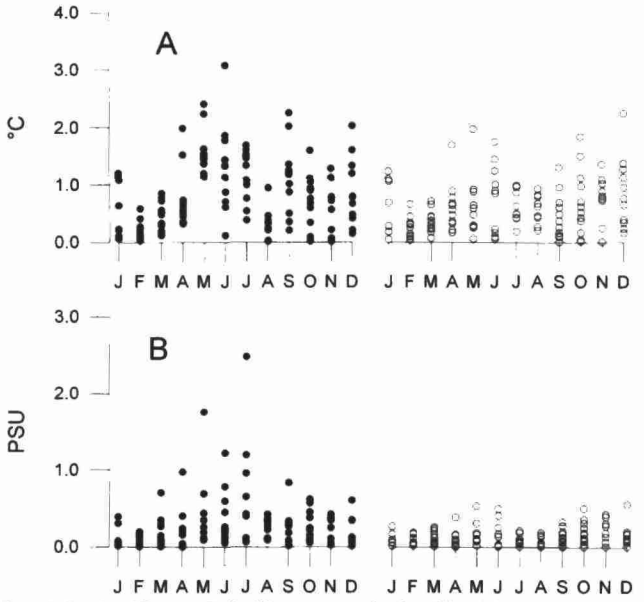

Figure 2. Absolute differences D_{in} for (A) temperature of surface (filled circles) and bottom layer (empty circles) and (B) salinity of surface (filled circles) and bottom layer (empty circles) of the station A1 (45°04.8' N 13°37.0' E; 32 m depth).

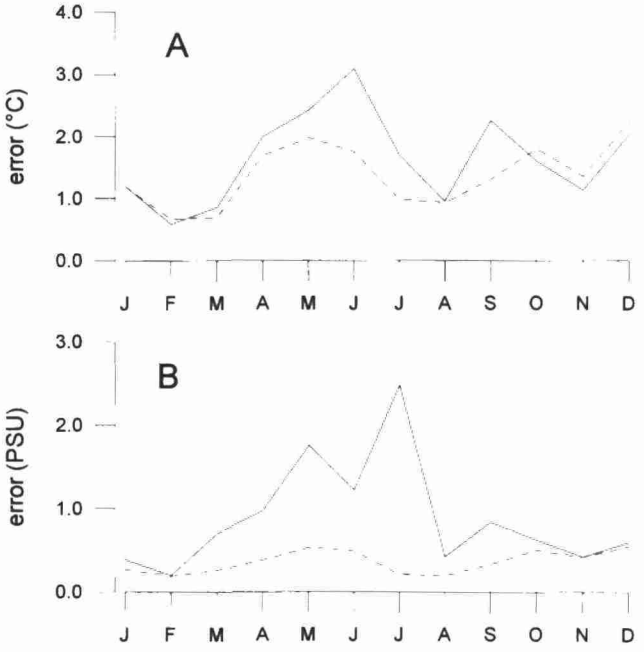

Figure 3. Seasonal variations of error estimates of monthly means for (A) temperature in the surface (solid line) and bottom layer (dashed line) and (B) salinity in the surface (solid line) and bottom layer (dashed line) in the northeastern Adriatic (45°04.8' N 13°37.0' E; 32 m depth).

THE EVOLUTION OF THE AEGEAN WATER'S INFLUENCE IN THE DEEP THERMOHALINE CIRCULATION OF THE EASTERN MEDITERRANEAN (1986-1995)

A. Theocharis*, E. Papageorgiou, H. Kontoyannis, K. Nittis and E. Balopoulos
National Centre for Marine Research (NCMR), A. Kosmas, Hellinikon 16604, Greece

Abstract

The significant changes of the Cretan Sea (S. Aegean) water mass characteristics during the last 8-9 years have considerably influenced the deep thermohaline circulation of the Eastern Mediterranean. Observations indicate that this change evolved in two phases. The first phase (1987-1991) is characterized by a pronounced increase of salinity (more than 0.1), while the second (1992-1995) by a dramatic drop of the deep waters' temperature (0.4°C). Both changes resulted in an increase of the Cretan deep waters' density of almost 0.2 and in a massive outflow of these waters towards the deep parts of the Eastern Mediterranean. This major climatic shift seems to be related to important meteorological anomalies in the area.

Key-words: Cretan Sea, Straits and Channels, water transport, Deep Waters

Introduction

The Adriatic sea has been historically considered as the main contributor to the Eastern Mediterranean deep waters [1]. Until the beginning of this decade, the horizontally homogeneous temperature and salinity values at deep layers have indicated an almost perfectly repeating cycle in both water mass characteristics and formation rates. The Aegean Sea has also been reported as a possible secondary source of intermediate and deep waters [2] but its contribution has been considered rather sporadic. The relatively warmer and more saline waters of the Cretan Sea (S. Aegean), were usually observed [2, 3] outside the Cretan Arc, just below the Levantine Intermediate Water (LIW) and above the Eastern Mediterranean Deep Water (EMDW) of Adriatic origin loosing rather quickly their characteristics due to mixing. Since the beginning of this decade, a number of observations indicate a major change in this picture of the Eastern Mediterranean deep thermohaline circulation: the deepest parts of the basin have been filled by denser and young waters with modified characteristics (warm and saline) outflowing from the Aegean Sea. The older deep waters of the basin, together with the newly formed dense waters of the Adriatic Sea, which still contributes to the deep waters, are lifted up several hundreds of meters, enriching with nutrients the intermediate depths of the basin [4].

The Cretan basin, the largest in volume and deepest basin of the Aegean Sea, communicates with the Levantine and the Ionian seas through the six "Cretan Arc" straits. The Antikithira Strait to the West (sill depth 700 m), and the Kassos & Karpathos Straits to the East of Crete (sill depths 1000 and 850 m respectively) are the most important for the deep water exchanges. The Rhodes strait is relatively narrow and shallow (250 m deep) but quite important for the upper layer exchanges between the Aegean and the Levantine Seas.

We present hydrological observations from the period 1986-1995 that describe the evolution of this climatic "shift" and the modification of the Cretan water mass characteristics which, as will be seen, occurred in two phases (1987-1991 & 1992-1995). The currentmeter data show the corresponding variability of deep water mass exchanges through the straits. The preliminary analysis of the meteorological conditions over the south Aegean gives some first indications for the mechanisms responsible for this transient.

Data analysis and results

We use hydrological and currentmeter data collected in the framework of the Greek national project "Open Sea Oceanography", the international project POEM "Physical Oceanography of Eastern Mediterranean" and the EU funded international research project PELAGOS/MTP-1. During the period 1986-1995 16 cruises were carried out in the south Aegean and the surrounding seas (E. Ionian and NW Levantine). The hydrological data were collected with a "SeaBird Electronics" CTD profiler on board the R/V Aegaeo. During the same period, currentmeter data were collected at the straits of the Cretan Arc: one array (P1) was deployed in the strait of Rhodes, two in the Karpathos strait (P2 east, P3 west), two more in the Kassos Strait (P4 east, P5 west) and one array in the Antikithira strait (P6). All deep current-meters were deployed within a depth range of 50 to 300m from the bottom. For each period, deep transports were computed at each strait and the data were compared with the hydrological structure of the area in order to estimate water mass exchanges through the straits.

The meteorological data (air temperature and precipitation) were collected by the National Meteorological Service at 9 stations of south Aegean islands for the period 1984-1995. The time series of precipitation clearly marks the extended period of dryness that lasted for more than 6 years (1988-1993). During this period we had a 40% decrease of the precipitation over the south Aegean compared to the period 1984-1987 (25 instead of 42 cm/yr). A second anomaly in these time series is related to the significant drop (DT > 2°C) in winter mean temperature during 1992 that has been attributed to the atmospheric dust from the Pinatubo eruption in 1991 [5]. The corresponding buoyancy loss caused deep overturning and mixing of the entire water column in the Cretan Sea.

The evolution of Cretan water mass properties

The typical hydrological structure in the Cretan Sea during the period 1986-1989 was composed by two water masses with T/S properties similar to the Levantine Intermediate Water (LIW). In the upper layers (50-400m) we meet the Cretan Intermediate Water (CIW) slightly colder (~14.5-15.5 °C) and saltier (S~38.95-39.10) and hence denser (σ_θ ~29.15) than the LIW. In the deeper layers (below 600m) we meet slightly colder (θ~13.9-14.2°C) and fresher (38.85-38.95) water with maximum density of 29.20 near the bottom. This means that the stratification was, in general, weak during this period and the water mass properties rather uniform but quite different from those of the Eastern Mediterranean at respective depths.

In March 1987 we first observe σ_θ > 29.2 below 1000m in the western Cretan Sea while in March 1989 we also observe these densities in the eastern deep basins. During 1989 we must have a significant formation rate since the 29.2 isopycnal was raised from 2000 to 1000m between March and September. In the same period we first observe dense water of Cretan origin outside the Straits at depths 700-1600m with σ_θ ~29.17-29.18. The increase of density was continued for the following years and during the first period was mainly attributed to increased salinity. During the period 1989-1992 we had an almost 0.1 increase of the salinity (fig 1) and a small

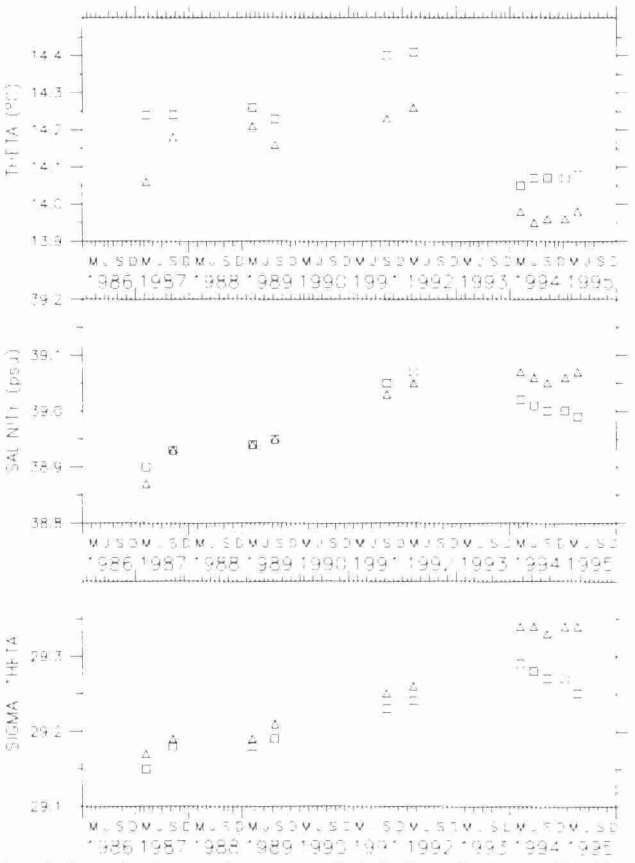

Figure 1: Time series of mean water mass properties in the Cretan Sea (squares: 600-1000m averages, triangles: 1000-2500m averages)

BASIN-WIDE USE OF A SHIP-MOUNTED ADCP GIVES A NEW PICTURE OF THE ADRIATIC SEA CIRCULATION

Ursella L., E. Accerboni, M. Gacic* and R. Mosetti
Osservatorio Geofisico Sperimentale, Trieste, Italy

Abstract
The analysis of the data obtained from a basin-wide ship-mounted ADCP survey in the Adriatic Sea shows the existence of the M2 amphidromic point in the Middle Adriatic area. The steady current field confirm the existence of the large scale cyclonic meander with two smaller cyclonic gyres situated over the two major topographic features (South Adriatic and Middle Adriatic Pits). The stratified season is characterized by a strong vertical shear, while from summer to winter (from stratified to homogeneous water column) the horizontal circulation scales change only to a smaller extent.

Key-words: acoustics, currents, tides, vertical profile, Adriatic Sea

Introduction

Adriatic Sea general circulation is characterized by an elongated basin-wide cyclonic gyre with several sub-basin scale cyclonic structures embedded in it (1) and located above the most prominent topographic features of the basin (Jabuka Pit, South Adriatic Pit). Longitudinal fluxes play an important role in determining the horizontal distribution and exchange of properties between various Adriatic sub-basins. Italian national project PRISMA1 was aimed at determining water and mass fluxes at selected transects separating different Adriatic sub-basins. Thus, long-term Eulerian current measurements in parallel with continuous one-year long ship-borne ADCP basin-wide survey were carried out within the framework of the project. Seasonal multidisciplinary cruises were also carried out in order to determine spatial distribution of various biological and chemical parameters together with the mass field structure. In this paper we present and discuss basin-wide tidal current field structure, vertical distribution of the residual current field in various transects as well as the differences between the current field structure in the stratified and unstratified conditions.

Experiment design

The experimental activities within the PRISMA 1 project with a basin-wide coverage of Eulerian and ship-borne ADCP measurements were carried out in the period from 15 May 1995 until 28 February 1996. Current measurements were focused on four areas that delimit three Adriatic major topographic features (North Adriatic shelf area, Mid-Adriatic - Jabuka Pit and South Adriatic Pit). Eulerian current measurements were carried out to complement ADCP data but due to the intensive fishery activity in the area heavy instrument losses were encountered. The ADCP survey of the four zones was done during multiple subsequent passages of cross-isobath transects of the length of about 100 km, thus an average time needed to cover a single transect was less than 10 hours. In order to have a basin-wide coverage, but at the same time in similar stratification conditions, all the ADCP data collected during the period May-September were treated as an unique data set. Since the period in question is characterized by a vertically stratified water column, it will be called "summer". On the other hand, data collected from October 1995 through February 1996 were analyzed separately as they belong to the period when the water column in the Adriatic is vertically mixed and it will be called in the rest of the paper "winter".

Results and discussion

Tidal and other high-frequency variability that have time scales comparable to the time needed for the ship to cover a single transect, can contaminate the basin-wide residual or steady current signal. First, the importance of various tidal components was estimated carrying out spectral analysis of the available Eulerian time-series. Then, tidal oscillations were eliminated from the data set using a method developed by Candela (2). As it was mentioned earlier, summer and winter were analyzed separately and it occurred that during the stratified season tidal phase changes appreciably with depth which suggests the importance of the baroclinic tides. On the other hand, during winter the tidal phase pattern does not vary a lot in the vertical. In both cases, however, the amphidromic point of the M2 component in the current field was clearly present. As predicted by numerical and analytical models (3), its position should be 1/4 wave length (in this case about 300 km) southeast of the sea surface elevation amphidromic point. In fact data analysis shows a minimum in the M2 tidal amplitude east of Dubrovnik in the centre of the basin and a corresponding jump in the phase of about 180 degrees.

Tidal components were thus estimated at each level separately during summer and, from the vertically averaged current field, during winter. The obtained tidal parameters were then used to remove tides from each transect separately and the detided current field was divided into the steady and residual parts. Residual current field in this paper is defined as the signal remaining after the removal of the tidal and steady current components. In general the steady current component is weaker than the residual one.

The summer horizontal distributions of a steady current component show clearly a swift coastal current along the western shelf. The more we go to deeper layers, the more important becomes the influence of topography. Thus, the cyclonic curvature of streamlines above the two Adriatic pits becomes more evident. Another interesting feature is the occurrence of an important offshore current component in deeper layers near the Italian coast in the Middle Adriatic area. In intermediate layers an important longshore component is evident in that area. A possible explanation can be found in an upwelling-related transversal circulation. In fact analyzing characteristics of the climatological wind field, one notices in summer the prevalence of the northwesterly winds producing upwelling along the Croatian coast and downwelling along the Italian one. Associated to that, a closed transversal circulation cell should appear. From our ADCP data only the deeper branch of the cell was evident since the instrument is "blind" in the first ten meters. In fact, from the climatological SST data it was documented that the eastern coastal area was colder than the western shelf area only in the summer (4) providing another evidence for the possible existence of upwelling phenomena.

Differences between stratified season and a part of the year when the water column is vertically mixed, are clearly evident also in the structure of the horizontal and vertical shear of the residual current field. During the winter season analyzing cross-shore transects, one can see that the residual current field is characterized by a strong and vertically constant horizontal shear (Fig. 1). Structures are thus vertically homogeneous having scales of the order of the water depth. Their horizontal scales are of the order of ten kilometers. On the other hand, during the stratified season apart from the horizontal shear, in the residual current field strong vertical shear occurs with the appearance of countercurrents in various layers. The horizontal scale, however, remains the same. The change in the vertical current field structure is evidenced from the Eulerian current measurements where we note the current field variability at two levels being out-of-phase in the stratified season, while in homogeneous density conditions the two time-series show clear in-phase behavior. The ADCP survey enabled us also to define in more details spatial and temporal scales of the longshore coastal current at the Italian shelf. In fact it was noticed that the longshore current has at a transect south of the Po delta, a cross-shore scale of the order of ten kilometers and that it is strongly time-dependent in function of the river Po pulses. With the low discharge rates the longshore current is rather weak while within few days after the Po river discharge pulses, strong longshore current is generated (Fig. 2) as evidenced at the transect located about 50 km downstream of the Po River mouth.

References

1 - Orlic, M., M. Gacic and P.E. La Violette, 1992: The currents and circulation of the Adriatic Sea. *Oceanol. Acta*, 15, 2.
2 - Candela, J., R.C. Beardslay and R. Limeburner, 1992: Separation of tidal and subtidal currents in ship-mounted Acoustic Doppler Current Profiler observations. *J. Geoph. Res.*, 97, C1, 769-788.
3 - Lozano, J., J. Candela, 1995: The M2 tide in the Mediterranean Sea: dynamic analysis and data assimilation. *Oceanol. Acta*, 18, 4.

IS THERE A CONNECTION BETWEEN THE FLUCTUATIONS OF THE NORTH ATLANTIC OSCILLATION AND THE INTERANNUAL VARIABILITY OF THE CIRCULATION IN THE NW MEDITERRANEAN ?

S. Vignudelli, G.P. Gasparini, E. Lazzoni, M.E. Schiano and M. Astraldi *
CNR - Istituto per lo Studio dell'Oceanografia Fisica, La Spezia, Italy

Abstract
A possible connection between the climatic fluctuations associated with the North Atlantic Oscillation (NAO) and the interannual variability of the water transport through the Corsica Channel is investigated. The latter has been considered an indicator of the changes of the large scale circulation in the NW Mediterranean. The data sets used here cover most of a decade since 1985. Over this period, NAO index tends towards increasing positive values. Similarly, the winter (December through March) air temperature and vapor pressure over the basin show a positive tendency while the total transport through the Corsica Channel undergoes a progressive and substantial decrease. A clear reversal of this tendency involving all the considered parameters, occurs at the end of the data period. These preliminary results seem to indicate that a prolonged period of anomalous atmospheric patterns over the North Atlantic can produce changes in the local atmospheric conditions which determine the strong interannual variability of the NW Mediterranean circulation.

Key-words: air-sea interactions, currents, gulf of Lions, water transport

Introduction

The motivation for the present study comes from a renewed attention to the climatic role of the Mediterranean region within the general climatic questions pertinent to the large scale atmospheric circulation (1). Different processes affect the climate patterns of the two basins of the Mediterranean (2); the western part has been found to be significantly influenced by the fluctuations of North Atlantic climate, especially in winter. The North Atlantic Oscillation (NAO) is the dominant mode of climate variability in the North Atlantic-European region. Its state reflects changes in the strength and orientation of the surface Atlantic westerlies across the North Atlantic as well as the temperatures on both sides of this ocean (3). A NAO index, defined by Hurrell (3), exhibits a seasonal evolution being most fully developed during the colder season, and alternatively weaken every 6-10 years. A significant feature is that the highest values have occurred since 1980 and the persistence of the positive phase (4) is unprecedented in the past years. According to Hurrell (3), concurrent conditions over most of Europe and the Mediterranean are anomalously mild.

The circulation of the water masses has been recognized to be an important component of the climatic scenario. In the Northern part of the Western Mediterranean Sea (Figure 1), many oceanographic observations (5) have provided evidence of distinct seasonality in the basin wide response indicated by an intensification of processes during winter season and a strong year-to-year variability that can be correlated with local climatic fluctuations. Among all the involved processes, the exchange of the water masses through the Corsica Channel between the Northern Basin and the Tyrrhenian Sea appears to be most significant. Using a three-year moored current time series, Astraldi and Gasparini (6) found that the water transport towards the Northern Basin increases significantly during winter and that this feature undergoes a significant interannual decrease in response to an improvement of the atmospheric-climatic conditions over the basin. Due to the effect that this current has on the general circulation of the NW Mediterranean, a substantial change in the winter conditions of the whole basin must exist.

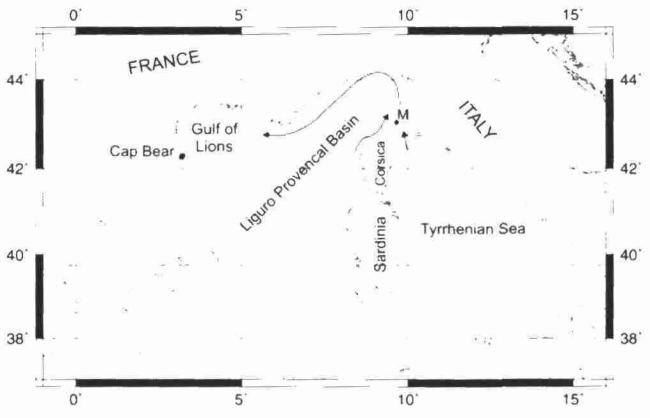

Figure 1: Survey area and mean current paths. M indicates the position of the mooring in the Corsica Channel.

The transport estimates in the Corsica Channel provide us with a clear signal of the marine environment representative of the large scale circulation processes and sensitive to the atmospheric events affecting the northern part of the Mediterranean. Since current velocities in the Corsica Channel continue to be monitored, the resulting longer time series can aid in the identification of the atmospheric parameters directly responsible of the basin wide winter variability and, through them, to verify if a connection can be established with the large scale atmospheric processes. In this framework a preliminary comparison of some primary variables, playing a key role in explaining the previous linkage, is carried out.

Data and methods

Current velocities were measured at four levels near the sill of the Corsica Channel (see Figure 1 for location), in 450m of water, from December 1985 to March 1996, with a two-year interruption in 1989-1990. The total transport through the channel was computed using these observed speeds and the cross-sections are approximately centered at each current meter level. The resulting time series, obtained from on going current mooring, is the most complete and long-term current data set in the Western Mediterranean Sea.

Observations of wind velocities and direction as well as air temperature and vapor pressure, provided by the French weather station at Cap Bear, were used. Due to its location, this station is a suitable place for the evaluation of weather conditions in the NW Mediterranean (7).

Three-hour observations of the atmospheric and oceanographic parameters were used to estimate mean winter (December through March) evolution over the considered years.

The winter (December through March) index of NAO was computed using the difference of the normalized sea level pressures at Lisbon (Portugal) and Stykkisholmur (Iceland). The sea level pressure anomalies were normalized by dividing each seasonal pressure by the long-term (1864-1893) standard deviation.

Preliminary results and future plans

Calculation of the winter total transport through the Corsica Channel is shown in Figure 2a. Consistent with the results of Astraldi and Gasparini (6), a progressive and substantial decrease in water transport is estimated throughout the whole period, which leads in 1995 to a transport about 70% less than that estimated at the beginning of the observation period. It is interesting to note that during winter 1996 the transport suddenly increases reversing the trend initiated in 1986.

Concurrent winter air temperature (Figure 2b) and vapor pressure (Figure 2c) measurements at Cap Bear indicate a tendency towards a progressive improvement of the weather conditions over the basin. Under these persistent conditions exchange processes at the air-sea interface are expected to decrease. It should be noted that an inversion of this tendency is seen by these parameters in the final year. In contrast, the wind speed (Figure 2d) does not exhibit any specific trend.

Confirming the previous indications (6), the comparison of these time series clearly indicates that the air-sea heat fluxes at the basin interface, rather than the direct wind stress, are to be considered the major forcing of the winter transport through the Corsica Channel. The

SURFACE SEICHES AND INTERNAL KELVIN WAVES OBSERVED OFF ZADAR (EAST ADRIATIC)

Ivica Vilibic [1*], Mirko Orlic [2], Ante Smircic [1] and Nenad Leder [1]

[1] State Hydrographic Institute, Zrinsko Frankopanska 161, 21000 Split, Croatia
[2] Andrija Mohorovicic Geophysical Institute, Faculty of Science,
University of Zagreb, Horvatovac bb, 10000 Zagreb, Croatia

Abstract

Surface seiches and internal Kelvin waves are documented by the data collected in the Zadar and Pasman Channels during summer 1994, and are reproduced using analytic and numeric models. Energy loss at the head of the basin is allowed by imposing radiation condition there, while nodal line is enforced at the basin mouth. Surface seiches are found to be excited by a strong meteorological disturbance which occurred in late summer 1994, whereas internal Kelvin waves could be related to a meteorological perturbation which preceded deployment of the instruments.

Key-words: Adriatic Sea, straits and channels, air-sea interactions, models

Introduction

Surface seiches of the Adriatic Sea have been widely examined since the beginning of this century (1). A major part of the work concentrated on standing waves of the whole Adriatic Sea (2), but coastal seiches also attracted some interest (3). Much less effort went into investigation of internal waves, both progressive and standing, which occur in the Adriatic coastal area. In one of the rare studies of such phenomena internal Kelvin waves have been experimentally detected in the Vir Sea (4). In this work both surface seiches and internal Kelvin waves will be explored on the basis of temperature, salinity, current and sea level data collected in the Zadar and Pasman Channels (Middle Adriatic) during summer 1994. Moreover, empirical findings will be interpreted using simple analytical and numerical models.

Results

Current and temperature time series have been collected between 28 June and 21 July and between 24 August and 18 September 1994 at seven stations (S-1 to S-7) and depths of 3 to 5 m from the sea surface and 4 to 5 m above the bottom. Vertical profiles of temperature and salinity were recorded on four occasions, while moorings were deployed and recovered, at 7 transects comprising 29 stations. Sea level were permanently registered at the Zadar tide-gauge station. The basin and experimental setting is illustrated in Fig. 1.

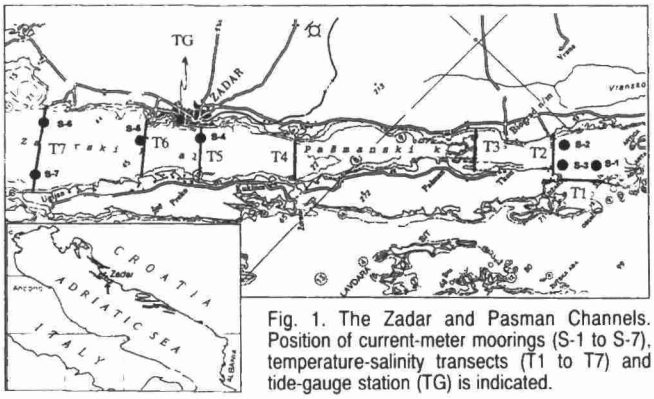

Fig. 1. The Zadar and Pasman Channels. Position of current-meter moorings (S-1 to S-7), temperature-salinity transects (T1 to T7) and tide-gauge station (TG) is indicated.

On 25 August 1994 a well-developed synoptic system coupled with mesoscale thunderstorms passed over the region causing strong surface seiches with sea level amplitude of about 20 cm and maximum current amplitude of cca 15 cm/s. All current-meter records northwest from the basin constriction, i.e. from transect T3 (7-9 m deep, 1.5 km wide) registered the seiches, which swiftly decayed after both the first and the second storm (*e.g.* data collected at station S-4, Fig. 2). The period determined by spectral analysis of measured currents and sea level series is about 2.1 hours. At the same time the records at stations S-1 to S-3 contained no oscillations of this period. So, the 2.1-seiche appeared in the channel area northwestward from the basin constriction. The seiche has been reproduced using simple one-dimensional rectangular basin model. Governing equations are shallow-water equations, with nodal line imposed at the basin mouth (x=0), and radiation condition applied at the head of the basin (x=L) in order to allow for the energy loss through the constriction area. Results of this model are plotted in Fig. 3. Furthermore, one-dimensional Defant-type model, which allows for the variable basin topography, has been applied on the Zadar and Pasman Channels. The theoretical results obtained for the amplitude of the first mode (Fig. 4) agree with empirical findings.

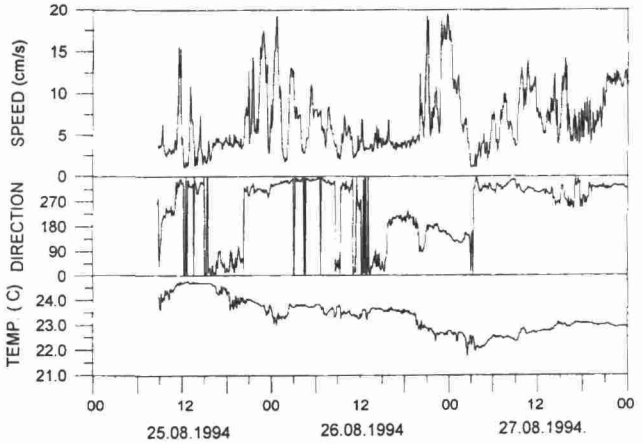

Fig. 2: Record of current speed and direction, and sea temperature at the surface layer of station S-4 during the disturbance 25-27 August 1994.

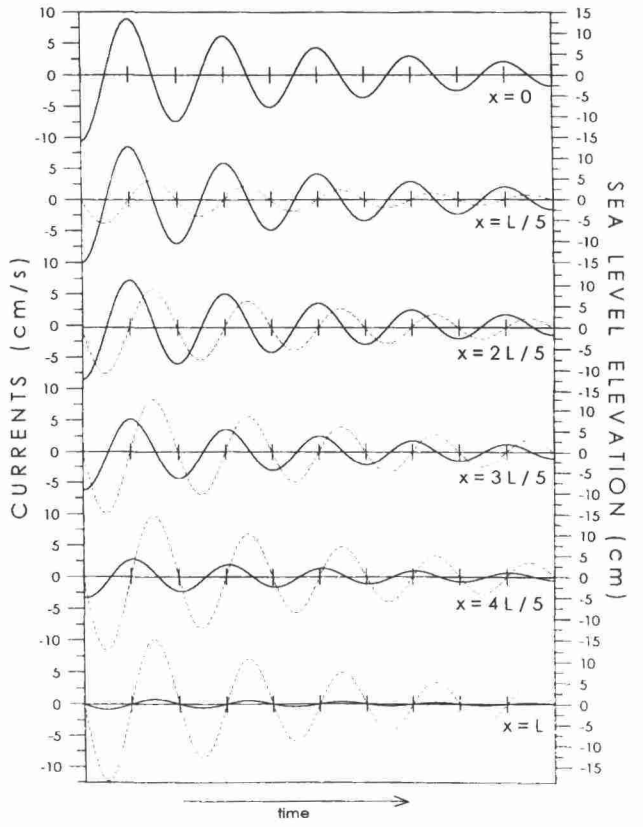

Fig. 3: Modelled sea level (thin) and current (thick) time series in the idealized rectangular basin. Here, one-dimensional barotropic model with radiation condition at the head (x=L) and imposed nodal line at the mouth (x=0) is used. Theoretical value of the period equals 2.1 hours.

SOME ASPECTS OF BAROCLINIC WAVE MOTIONS IN THE IZMIR BAY AND THEIR CONNECTION WITH AEGEAN SEA DYNAMICS

Vasiliy I. Vlasenko [1*], Natalya M. Stashchuk [1], Alexander S. Kuznetsov [1], Vitaliy A. Ivanov [1], Orhan Uslu [2]

[1] Marine Hydrophysical Institute, Sevastopol, Ukraine

[2] Erdem Sayin Institute of Marine Sciences and Technology, Izmir, Turkey

Abstract

Results of experimental investigations of baroclinic wave motions in the Izmir Bay is considered. It was found that low-frequency oscillations with periods 1-2 days are concentrated basically in the upper near-surface layer. They are connected with the dynamics of vortical formations constantly occurring in the Aegean Sea in the adjacent to the Izmir Bay areas. These eddies come into contact with the outer liquid boundary of the bay and initiate water exchange between the Izmir Bay and the Aegean Sea. Internal wave motions with periods from semidiurnal to inertial occur basically in the near-bottom layer of waveguide.

Key-words: Eastern Mediterranean, circulation, mesoscale phenomena, tides

Introduction

The ecosystem of the Izmir Bay is exposed to powerful antropogenic impact, which leads to its global changes [1,2]. At the same time, the processes responsible for the self-cleaning of the Izmir Bay waters have not been sufficiently studied. Active dynamical processes taking place in the Izmir Bay facilitate the reconstruction of the initial properties of marine environment. Barotropic and especially baroclinic oscillations contribute to the water mixing processes and ventilation of bottom water masses.

The bottom relief, occurrence of mean currents, tidal activity, seiches, upwelling motions - all these phenomena create conditions of the effective generation of both barotropic and baroclinic oscillations in the bay. Further progress in the understanding of the basic mechanisms responsible for generation and transformation of baroclinic oscillations, their influencing upon all dynamical processes taking place in the bay was achieved via conducting field experiments focusing on the study of a wide spectrum of variability of the hydrophysical fields using different methods.

Methods of investigation

Experimental investigations of the dynamics of background currents and their variability within the range of inertial gravity internal waves (hereafter IW) were conducted during the autumn of 1994 expedition of R/V *Piri Reis*. The main goal of these investigations was to carry out a study of the baroclinic oscillations occurring in the Izmir Bay, to determine their space-time characteristics, the mechanisms of generation of IW in various parts of the Izmir Bay. These investigations included the mapping of the areas exhibiting a large degree of intensification of short-period internal waves, the determination of their interaction with the bottom relief, and correlation with other hydrological processes taking place in the bay and adjacent areas of the Aegean Sea.

Six tested sites were chosen for conducting the investigations (Fig.1). The space temporal characteristics of vertical velocities and vertical deviations of thermocline caused by IW in test area 1, 2 and 5 were determined by means of the Gradient-Distributed Gauges of Temperature (hereafter GDGT) deploy from board of R/V *Piri Reis* (drifts D1, D2 and D3 in Fig.1). The GDGT covered the layer of thermocline, being intended for conducting long-term measurements of fluctuations of the integral temperature of a thermocline. For a range of short-period internal gravity waves, a special technique [3] permitted to define the orbital velocity's vertical component, using these data, and the vertical displacement of the fluid layer caused by IW. The space-time variability of the currents structure and IW vertical velocities in the areas 3, 4 and 6 was studied by means of moorings (M1, M2 and M3 in Fig.1). Current meters were deployed above and below thermocline. For determining the IW vertical velocity component and pycnocline's vertical wave oscillations due to IW, GDGT were set up at the moorings. The length of the current time series was equal to approximately two weeks.

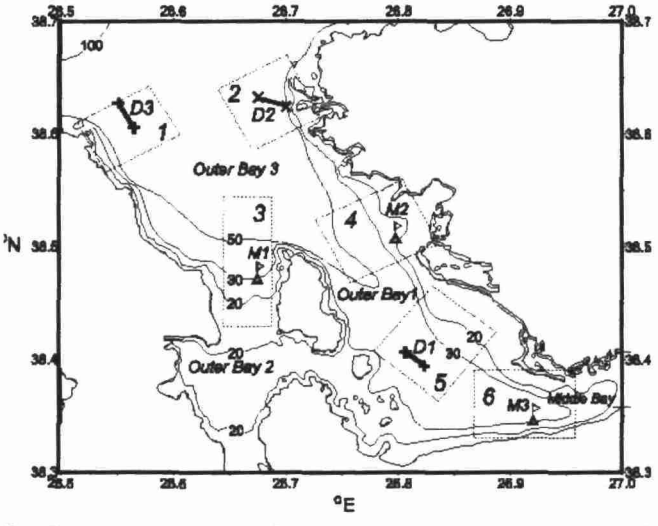

Fig.1. Bottom topography of the Izmir Bay and tested areas. (M 1-3 - moorings, D 1-3 - drift stations of R/V *Piri Reis*).

Analysis of *in situ* data

The analysis of *in situ* data have shown that the oscillations of the water masses with periods being in excess of 24 hours are concentrated basically in the upper near-surface layer (see spectra in Fig.2) and have the form of horizontal movements of fluid. The energy of such oscillations in the near-bottom layers is several times (and at the moorings 1,2 almost by an order) less than in the upper ones. The nature of these oscillations is, apparently, connected with the dynamics of vertical formations constantly occurring in the Aegean Sea within the triangle: Cape Kraburun - Lesbos island - Chandarly Bay (Fig.3). The periods of development and evolution of the eddies are equal to approximately 1-2 days. These eddies constantly come into contact with the outer liquid boundary of the bay and initiate water exchange between the Izmir Bay and the Aegean Sea in the upper layer of water. The assumption that the low-frequency fluctuations in the bay are produced externally is supported by the fact that as one moves away from the liquid boundary toward the Middle Bay (see Fig.1), the influence of these oscillations decreases (the difference in the levels of spectra of the near-bottom and near-surface layers diminishes, see Fig.2).

Horizontal mesoscale baroclinic motions with periods from semi-diurnal to inertial under the conditions of summertime stratification (the fluid is warmed and mixed up over the entire water column, and the pycnocline is located near the bottom), occur basically in the near-bottom layer of waveguide where the frequency of waves is lesser than the buoyancy frequency. The spectral level of horizontal oscillations in the frequency band from tidal to inertial at the nearbottom depth levels was several times larger than the counter part value in the near-surface one (Fig.2). The maximal vertical wave disturbances are concentrated slightly above the pycnocline in the intermediate layer. This probes how important it is to take into

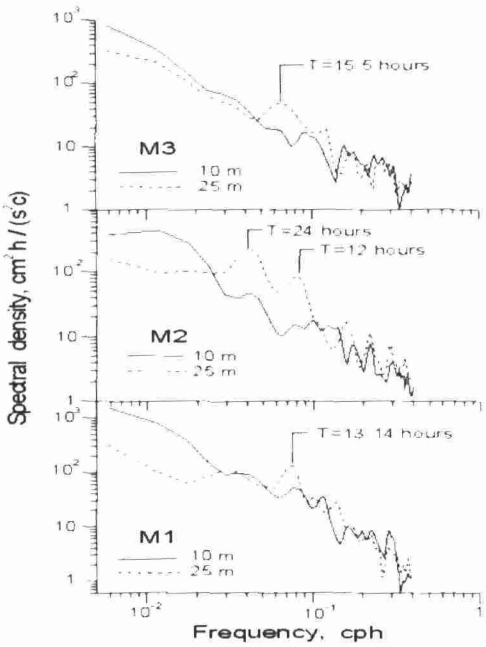

Fig.2. The energy spectra of current oscillations at the tepths of 10 and 25m at moorings M 1-3.

A REVIEW OF THE CIRCULATION IN THE CYPRUS BASIN, EASTERN MEDITERRANEAN LEVANTINE BASIN

G. Zodiatis [1*], A. Demetropoulos [1] and A. J. Theodorou [2]

[1] Laboratory of Physical Oceanography, Fisheries Department, Nicosia, Cyprus
[2] Laboratory of Oceanography, University of Thessaly, Volos, Greece

Abstract

The circulation of the Levantine Basin is reviewed on the basis of new oceanographic CTD data obtained during the last four cruises of the CYBO (Cyprus Basin Oceanography) project, between 1995-1997. The data analysis reveals the existence of some new, permanent as well as semi-permanent, mesoscale dynamic features in the Cyprus Basin, part of Levantine Basin in the Eastern Mediterranean, that can modify the flow pattern of the mid-Mediterranean jet in the region. Moreover, the Cyprus Basin is identified as an area of LIW formation. The interaction between the two Cyprus eddies, an anticyclonic eddy and another cyclonic one, contributes to the deeping of the newly formed LIW.

Key-words: mesoscale phenomena, currents, water transport, open sea, Levantine Sea

Introduction

The general circulation pattern derived from the flow investigations of the Eastern Mediterranean Sea during the late 1980s and the early 1990s, shows the existence of a meandering flow associated with several mesoscale eddies. The latter play an important role in the establishement of the general circulation and the hydrological structure of the water masses (1, 2). The circulation pattern of the Eastern Mediterranean Sea is dominated by the mid-Mediterranean jet, the cyclonic flow activity of the Rhodos gyre in the northwestern part of the region, and the two anticyclonic gyres: the Mersa Matruch and the Shikmona, to the south and southeast respectively. The latter two gyres encampass the Cyprus anticyclonic eddy (3). Generally, the mid-Mediterranean jet is meandering eastward between these three dominant flow features. To the southwest of Cyprus this flow jet bifurcates to the north. Moreover, the knowledge of smaller mesoscale eddies, as for instance, the cyclonic eddy in the Lattakia Basin (4), is crucial to the understanding of the regional circulation at the easternmost physiographic boundary of the Mediterranean, especially regarding the flow path of the mid-Mediterranean jet.

Nevertheless, until recently there were areas influenced by the mid-Mediterranean jet, like the Cyprus Basin and the Hecataeus Ridge, which were very poorly investigated. In order to fill the gaps in the oceanographic knowledge of the sea area south of Cyprus the CYBO- (Cyprus Basin Oceanography) project, a several year Cyprus National Oceanographic Programme, based on Physical Oceanographic studies, has been implemented by the Laboratory of Physical Oceanography, Fisheries Department (Center for Marine Research in Cyprus).

Results and discussion

Within the framework of the CYBO project four seasonal hydrographic cruises were carried out in the Levantine Basin between: 22 September-15 October 1995, 6-13 May 1996, 21-30 October 1996 and 6-13 May 1997. The cruises were aimed at obtaining reliable CTD measurements from a grid of more than 80 CTD stations in the deep waters of the open and the near coastal sea areas of the Cyprus Basin, an area of about 150x100 nm (Fig. 1).

The review of the circulation in the Cyprus Basin provides valuable information for the open and near coastal flow paths and their significant seasonal variabilities (Fig.2). The circulation of the water masses in the area is characterized by some well known oceanographic flow features such as the mid-Mediterranean jet and the Cyprus anticyclonic eddy.

In addition, new flow features have emerged in the Cyprus Basin from the recent CYBO's data set analysis. The definition of the circulation reveals in detail, the existence of the permanent Cyprus Basin Cyclonic eddy. This eddy with horizontal dimensions between 25 and 50 km undergoes significant seasonal changes in shape, size and intensity under the strong dynamic influence of the neighbouring flow features. The centre of the eddy was defined as an area of a well developed thermohaline dome owing to the winter mixing processes (Fig. 3). The latter contribute to the sinking along isopycnals of dense (saline) surface water initially down to 200m, thereby forming a water with a LIW singnature. Furthermore, the neighbouring strong hydrophysical depression of the Cyprus anticyclonic eddy contributes to the deepening of this saline waters down to 450 m depth.

The CTD data analysis from the four CYBO surveys, showed that the mid-Mediterranean jet during its eastward flow bifurcates twice to the south of Cyprus. At first, this current to the southwest of Cyprus bifur-

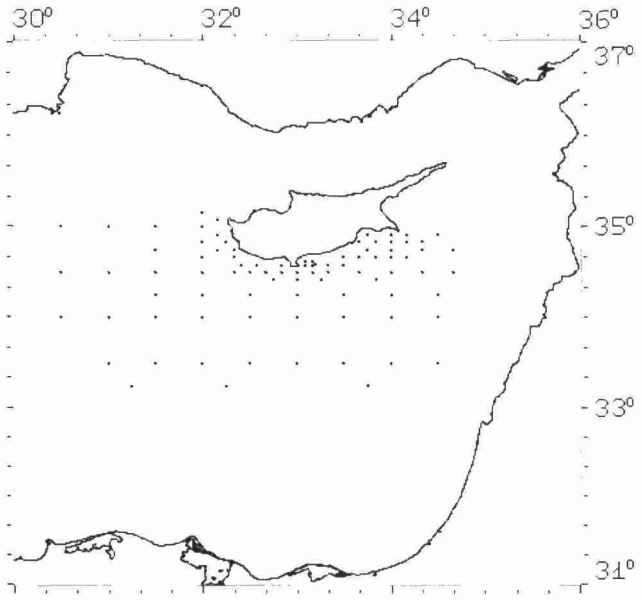

Figure 1 : CTD stations for CYBO project (1995-1997).

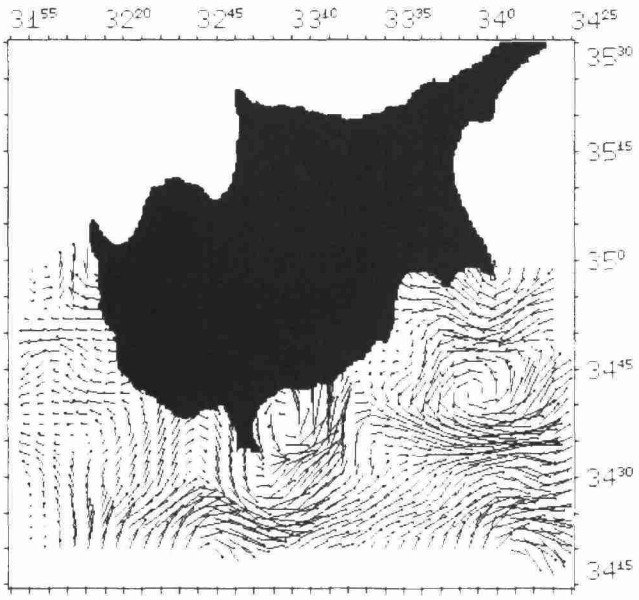

Figure 2a : Surface density currents, CYBO-1.

DISTRIBUTION PATTERNS OF MONOSACCHARIDES AND POLYSACCHARIDES IN THE NORTHERN ADRIATIC

Marijan Ahel*, Senka Terzic and Ivana Jelicic

Centre for Marine and Environmental Research, Ruder Boskovic Institute, Zagreb, Croatia

Abstract

Distribution of carbohydrates (CHO) was studied in the northern Adriatic during major phytoplankton blooms from October 1993 to September 1994. Total carbohydrates (TCHO) and monosaccharides (MCHO) were determined directly, using the MBTH-method, while the concentration of polysaccharides (PCHO) was calculated as their difference. Phytoplankton biomass was characterised by determining chlorophyll and carotenoid pigments using an HPLC technique. The TCHO concentration varied from 70 μg C/l to 1300 μg C/l with significantly enhanced values in the surface layer. Carbohydrates were found mainly in the form of PCHO (up to 92% of TCHO), and their spatial distribution suggested a link to the crop and physiological status of phytoplankton.

Key-words: organic matter, phytoplankton, pigments, Adriatic Sea

Introduction

Carbohydrates (CHO) represent one of the most important pools of organic matter in the sea. Recent studies by Pakulski and Benner [1] showed that carbohydrates comprised 21 (±7%) of DOC in surface waters of the world oceans. The importance of carbohydrates in estuarine and coastal waters is expected to be even greater, however, there are only few reports dealing with the CHO distribution in such ecosystems [2]. Large temporal and spatial variations of carbohydrates were observed along the salinity gradients in a small estuary [2] with maximum concentrations (up to 1080 μg C/l) during periods of enhanced phytoplankton activity. Studies performed in the North Sea [3] showed that large amounts of carbohydrates were released into seawater towards the end of a diatom bloom. A considerable percentage of the released CHO was in the combined form. Moreover, it was suggested that diatoms could have been an important source of carbohydrates that eventually led to hypertrophic formation of gelatinous aggregates observed in the northern Adriatic [4]. However, very little is known about their occurrence and distribution of in the northern Adriatic, especially about their relationship with phytoplankton. A weak but statistically significant correlation between the number of diatom cells and concentration of the total carbohydrates was noticed in a preliminary study which was conducted in the northern Adriatic during 1992 [5]. Moreover, enhanced concentrations of particulate carbohydrates (>100 μg/l) were found in the period characterised by macroaggregate formation, while in normal situations their contribution to the total particulate organic carbon was below 10% [6]. The aim of this paper was to determine concentration levels and spatial distribution of TCHO, MCHO and PCHO in the northern Adriatic during major phytoplankton blooms.

Experimental part

Study area and sampling. The northern Adriatic is a shallow semi-enclosed basin (maximum depth of 35 m) which receives large freshwater inputs from the Po River and other north Italian rivers. Samples for the carbohydrate and pigment analyses were collected at several stations along the Po River mouth-Rovinj transect (Fig. 1) which is generally accepted as representative of eutrophication gradients the northern Adriatic, especially during summer stratification [7]. Sampling was performed in the period from October 1993 to September 1994 from the research vessel *Vila Velebita* at 5-6 depths (0, 5, 10, 20, 30 m and near bottom) using 5 l Niskin bottles.

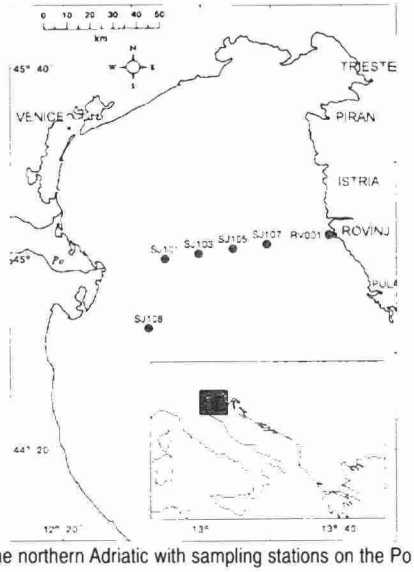

Fig. 1. Map of the northern Adriatic with sampling stations on the Po River mouth-Rovinj transect.

Determination of carbohydrates. Dissolved and particulate CHO were determined in nonfiltered seawater samples using the MBTH method. Determination of MCHO followed the original procedure by Burney and Sieburth [8], while TCHO were determined after HCl hydrolysis, using a method modified from Senior and Chevollot [2]. Concentration of PCHO was determined as the difference between the concentrations of TCHO and MCHO. Samples were analysed in duplicate and quantification was performed using glucose as a standard. The reproducibility of the carbohydrate determination was < 5% for the higher concentration range (> 200 μg C/l) and < 12% for the lowest concentrations. The limit of detection was 30 μg C/l. All concentrations are expressed in glucose carbon equivalents by multiplying the weight glucose equivalents by 0.4, because glucose is 40% carbon by weight.

Determination of biomarker pigments and break-down products of chlorophyll a. Chlorophylls and carotenoids were determined using a reversed-phase HPLC method [9]. Qualitative identification and quantitative determination of individual pigments was performed as described elsewhere [10]. The reproducibility of pigment determination was around 5%, while the detection limits varied from 1-5 ng/l, depending on the pigment extinction coefficients at 440 nm.

Results and discussion

Distribution of TCHO in the water column of the northern Adriatic is illustrated in Fig. 2. Two stations, representing western (SJ108) and eastern (SJ107) parts of the basin (Fig. 1), show rather different distri-

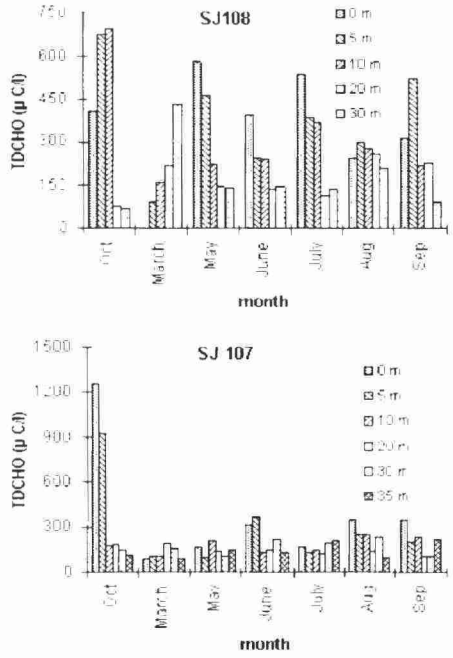

Fig. 2. Distribution of the total carbohydrates (TCHO) in the water column of the northern Adriatic during the major phytoplankton blooms in the period from October 1993 to September 1994.

HORIZONTAL AND VERTICAL DISTRIBUTION OF HEAVY METALS IN SEDIMENTS FROM THERMAIKOS GULF

Anagnostou Ch.*, Kaberi H. and A. Karageorgis
National Centre for Marine Research, Agios Kosmas, 16604 Elliniko, Athens

Abstract
The area under investigation is the inner part of Thermaikos Gulf which is comprised of Thessaloniki Bay and Thessaloniki Gulf. For several years this marine region has been accepting domestic and industrial discharges of Thessaloniki, thereby loading the ecosystem with several pollutants. A set of surface sediments and core samples from Thessaloniki Bay and Thessaloniki Gulf have been analysed for sedimentological properties, heavy metals and organic load. All analyses revealed that Thessaloniki Bay is the most polluted area of the inner gulf. The color of the polluted surface sediments was dark gray to black and the concentrations for Zn, Cu, Pb, Cd and the organic carbon content were higher than in the outer Thessaloniki Gulf. An examination of the vertical distribution for the same metals and organic load showed a significant increase of pollutants towards the upper layer of the sediment column forming a "polluted layer". The extent of this layer was calculated at about 25 km^2 and its volume at approximately $4.42x10^6$ m^3.

Keywords: pollution, metals, sediments, Aegean Sea

Introduction

The area under investigation includes the bay and the gulf of Thessaloniki, both of which comprise the inner Thermaikos Gulf. The southern border of the area is defined by the present outfall of the Axios river and the cape Megalo Emvolo (Fig. 1). Thessaloniki Bay, which extends northward of the line defined by the old outfall of Axios river (Paliomana) and Cape Mikro Emvolo, is a shallow embayment with a maximum depth of 19 m. The gulf of Thessaloniki is a wider marine area with a maximum depth of 29 m. The major characteristic of both areas is the very shallow zone across the western coast, which is a result of the Axios river sediment supply. In the last few decades the domestic and industrial wastes of Thessaloniki were totally discharged in the marine area under investigation. This anthropogenic influence caused certain changes of the seabed properties and also ecosystem disturbance.

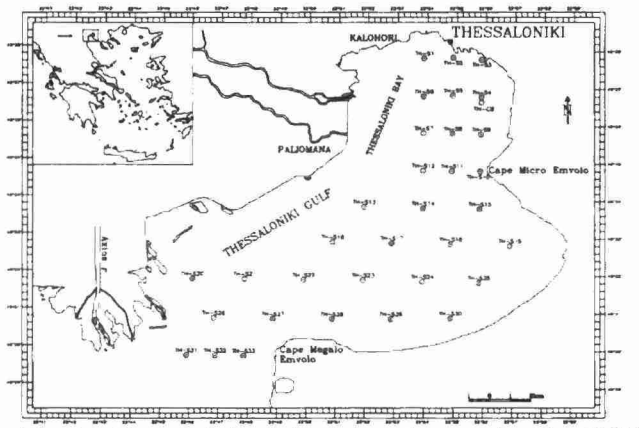

Fig. 1. Location of the area under investigation. Surface sediment sampling stations TH-S1 / TH-S33 and core station TH-C8.

The aim of this study is to describe the present situation of the seabed, to determine the horizontal and the vertical distribution of the anthropogenic polluted layer and, finally, to obtain data on the organic load and heavy metal content of this layer.

Materials and methods

Sediment sampling in the bay and the gulf of Thessaloniki was carried out during three cruises of R/V *Aegaeo* in 1995 (Fig. 1). Thirty three surface samples were collected with a McIntyre grab. In addition nine gravity cores were collected. In order to estimate the extent and the thickness of the polluted layer, 154 cores were taken using a square cross section stainless steel corer especially designed for this purpose [1]. The samples were analyzed for grain size (Sedigraph Micromeritics 5100), mineralogy (XRay-Diffractometer Rigaku D/Max B) and carbonate content [2], and for the heavy metals Zn, Cu, Ni, Cr, Pb, Cd, Fe, Mn and Al (Atomic Absorption Spectrophotometer Varian SpectrAA) and organic carbon content [3] in the Ø < 63mm fraction. For the total dilution of the sediments, the samples were successively attacked with concentrated nitric acid, hydrofluoric acid, *aqua regia* and perchloric acid in teflon bombs [4]. The analytical procedure was tested by analysing simultaneously the reference sediment SD-M-2/TM IAEA - Monaco, No 182.

Results

The sediments of the seafloor and the seabed of the bay and the gulf of Thessaloniki are homogeneous in terms of their grain size properties and are represented mainly by mud, sandy mud and sandy clay. This sedimentary facies is characteristic of the deltaic system of the area, showing relatively high sedimentation rates.

The input of domestic and industrial discharges in the area has affected the sedimentation processes. The continuous accumulation of anthropogenic by-products on the seafloor is still disturbing the sediment composition in terms of the organic load and metal content. The increase of the organic load in the sediments, which is caused by oxygen depletion at the sediment-water interface, gives them their characteristic gray black to black color. According to this feature, the extent and the thickness of the so called "polluted layer" was mapped. Figure 2 illustrates that the polluted area is the Thessaloniki Bay extending from the Cape Mikro Emvolo to the port establishments and the Kalohori inlet.

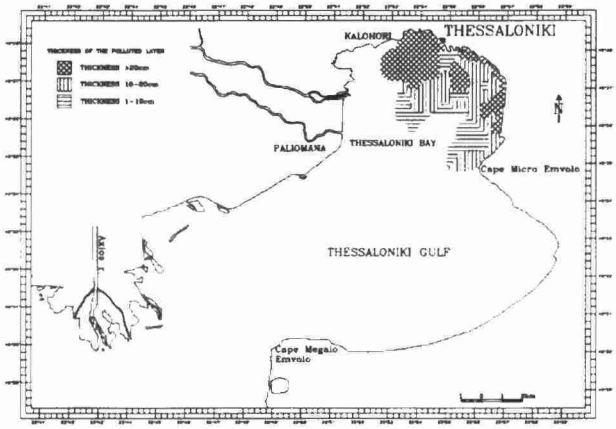

Fig. 2. Extent and thickness of the "polluted layer".

The thickness of the anthropogenic "polluted layer" varies between 1 cm in the south part of the bay, and 65 cm near the oil transport settlements of Kalohori inlet. The seafloor area covered by the "polluted layer" was calculated to be about 25 km^2 and its volume $4.42x10^6$ m^3. The dark colored "polluted layer", which is usually poor in benthic organisms and sometimes azoic, lies above deposits rich in coral skeletons of the genus *Cladocora* and other benthic organisms [1]. These deposits are evidence of the natural unpolluted environmental conditions which dominated in the area in the near past. Furthermore, this sub-surface layer can be used as an indicator of ecosystem remediation when the anthropogenic inputs are reduced or cease.

Table 1. Summary statistics for Thermaikos Bay and Thermaikos Gulf geochemical analyses.

	Zn	Cu	Ni	Cr	Pb	Cd	Mn	Fe	Al	Corg
			ppm						%	
Thermaikos Bay (n=12)										
Average	296	79	95	221	64	1,33	826	4,78	9,26	2,30
Minimum	193	57	76	196	46	0,55	535	3,33	8,09	1,69
Maximum	549	162	115	265	113	4,59	1322	5,54	15,61	3,39
Thermaikos Gulf (n=21)										
Average	158	43	106	190	41	0,44	1039	4,86	8,15	1,45
Minimum	105	35	93	151	30	0,19	557	3,71	6,47	0,94
Maximum	194	49	117	214	47	1,36	1515	6,29	9,09	2,05

ETUDE DES NIVEAUX DE CONTAMINATION CHIMIQUE EN MEDITERRANEE BASEE SUR L'UTILISATION DE STATIONS ARTIFICIELLES DE MOULES

Bruno Andral [1*], Jean-Yves Stanisiere [1], Didier Sauzade [1], Yves Henocque [1], Hervé Thebault [2], Pierre Boissery [3]

[1] IFREMER, Laboratoire Côtier de Toulon, BP 330, 83507 La Seyne sur Mer Cedex

[2] Institut de Protection et de Sécurité Nucléaire (IPSN), Laboratoire d'Etude Radioécologique, 83507 La Seyne sur Mer Cedex

[3] Agence de l'Eau Rhône-Méditerranée-Corse, Délégation de Marseille, 34 Rue Forbin, 13002 Marseille

Résumé

Quatre-vingt quatre stations ont été mouillées le long des 1800 km de côtes de la façade méditerranéenne française, pour mettre en stabulation des échantillons de moules et mesurer les niveaux de contamination chimique dans leurs chairs. Cette étude pilote, menée conjointement par l'Ifremer, l'Agence de l'Eau Rhône-Méditerranée-Corse (RMC) et l'Institut de Protection et de Sûreté Nucléaire (IPSN), a fourni localement et régionalement des données nouvelles relatives à la qualité du milieu littoral méditerranéen. Elle a permis de confronter la technique d'implantations artificielles et celle s'appuyant sur l'emploi de populations naturelles, pour utiliser les coquillages comme biointégrateurs de la contamination chimique du milieu marin.

Mots-clés : bivalves, pollution, bioindicators, aquaculture, Western Mediterranean

Introduction

Le Schéma Directeur d'Aménagement et de Gestion des Eaux (SDAGE), élaboré par l'Agence de l'Eau RMC dans le cadre de la loi sur l'Eau de 1992 (1), définit l'espace littoral comme une double frange terrestre (bassin versant de proximité) et marine (soumise aux apports telluriques), découpée en cinquante zones homogènes ou unités de gestion cohérentes quant à leur exploitation, protection et restauration (2).

Le Réseau Littoral Méditerranéen (RLM) a été conçu pour faciliter, à travers ces cadres territoriaux, la collecte d'indicateurs de la qualité de l'environnement. Ces informations synthétisées et spatialisées doivent permettre d'orienter la politique de lutte contre les pollutions et de protection du milieu et des usages. Un de ses objectifs est d'évaluer, les niveaux de contamination chimique dans le champ soumis à l'action cumulée des apports du bassin versant affectant chaque zone homogène. Dans cet espace, appelé champ moyen, les niveaux de micropolluants ne sont plus imputables à un apport identifié ou à son panache de dilution. La mesure directe des contaminants dans l'eau faisant appel à des techniques analytiques sophistiquées et coûteuses, il est difficile de mettre en oeuvre cette technique le long d'un important linéaire côtier. Par ailleurs, la variabilité du milieu littoral ne confère que peu de signification à une mesure ponctuelle.

Afin d'utiliser les moules comme biointégrateurs de contaminants, des stations artificielles ont été implantées le long des 1800 kilomètres de côtes de la façade méditerranéenne française, les gisements naturels ne permettant pas de couvrir toutes les zones homogènes définies par le SDAGE. Après un séjour de plusieurs mois dans l'eau, les moules accumulent les micropolluants jusqu'à atteindre un équilibre avec le milieu, atténuant les fluctuations rapides des concentrations en micropolluants (3).

Matériel et méthode

Mouillages

84 stations expérimentales ont été mouillées, 20 en milieu lagunaire, 64 dans la zone marine, pour renseigner chacune des 50 zones homogènes. En mer ouverte, les stations ont été disposées sur la ligne bathymétrique des 30 mètres, pour les côtes à forte pente, et sur la ligne bathymétrique des 20 mètres pour les côtes sableuses. Les distances à la côte variaient de 200 à 10 000 mètres. Le mouillage est composé de deux ensembles soutenant chacun un échantillon de moules dans une poche conchylicole en plastique alimentaire relié à un lest de 30 kg posé sur le fond. Chaque poche est maintenue dans la colonne d'eau au moyen d'un flotteur de 7 litres. La liaison des deux ensembles est réalisée au niveau des lests. La profondeur de stabulation est comprise entre 10 et 15 m. En lagune, le mouillage est composé d'une table en acier galvaanisé où repose à 0,5 m du fond, une poche conchylicole contenant l'échantillon de moules. Les relargages éventuels de contaminants par l'ensemble de ces dispositifs ont été considérés comme négligeables compte-tenu de la durée d'immersion et de la position des poches dans la colonne d'eau.

Echantillonnage

Deux tonnes de moules (*Mytilus galloprovencialis*) élevées en filières ont été utilisées : 10 kg par échantillon en mer ouverte, 3 kg en lagune. Les tailles étaient comprises entre 30 et 60 mm (moyenne 42 mm), ce qui correspond à des individus de 18 mois environ. En complément des analyses chimiques, des mesures de radioéléments ont été réalisées sur 37 stations de mer ouverte par l'Institut de Protection et de Sureté Nucléaire (IPSN). La durée d'immersion a été de 5 mois (février-juillet 1996). Sur site, les moules étaient lavées à l'eau de mer, dégrappées, triées et calibrées. Des lots de 3 kilogrammes étaient stockés en glacière réfrigérée, puis préparés selon les procédures du Réseau National d'Observation de la qualité des eaux (RNO) (4).

Analyse des contaminants

Les analyses chimiques ont été réalisées selon les protocoles du RNO. Plomb, Cadmium, Cuivre, Zinc : spectrométrie d'absorption atomique four ou flamme. Mercure : fluorescence atomique après formation des vapeurs froides en présence de chlorure stanneux. Chrome, Nickel : spectrométrie d'absorption atomique four graphite. Arsenic : technique des hydrures. Dichlorodiphenyltrichloroéthane (DDT +DDD+DDE), Hexachlorocyclohexane (γHCH, αHCH), Polychlorobiphényles [CB28, CB31, CB35, CB52, CB101, CB118, CB138, CB153, CB180] (PCB) : chromatographie capillaire en phase gazeuse couplée à un détecteur à capture d'électrons. Hydrocarbures Polycycliques Aromatiques [Benzo (b) fluoranthène, Benzo (k) fluoranthène, Benzo (a) pyrène, Benzo (ghi) pérylène, Indéno (1,2,3-cd) pyrène, Fluoranthène] (HAP) : chromatographie haute performance couplée à un détecteur à fluorescence.

Résultats

Récupération des mouillages

Le mouillage en mer ne disposant pas en général de repère de surface, pour éviter les dégradations, la localisation s'est faite par l'utilisation combiné du GPS, d'un sonar panoramique et d'un sondeur vertical. La récupération des échantillons sur les mouillages a été réalisée en plongée. Le pourcentage de récupération a été de 80%. Les stations où les mouillages ont été perdus se localisaient dans les zones à fond sableux où l'activité de pêche au chalut est importante (principalement à l'Ouest du bassin). Toutes les stations lagunaires ont été récupérées, 60% seulement ont été exploitées en raison de fortes mortalités (envasement, biosalissures, variations de salinité).

Caractéristiques des échantillons

Les tailles étaient comprises entre 40 et 69 mm (moyenne 50,4 mm), les moules du golfe du Lion ayant les tailles maximales. Sur les échantillons destinés à l'analyse des radioéléments (5), l'IPSN a déterminé un indice de condition basé sur le rapport poids sec de chair / poids sec de coquille (6). Cet indice est représentatif de la quantité de métabolites de réserve accumulées par les moules. Sa distribution (Fig. 1) et

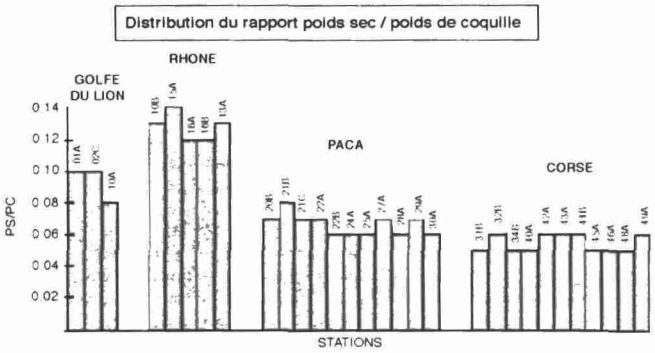

Fig. 1. Distribution des valeurs de l'indice de condition poids sec de chair /poids de coquille sur les stations en mer ouverte. PS: poids sec de chair; PC: poids sec de coquille, 21 B : code station.

EVALUATION OF METAL POLLUTION IN THE COASTAL SEDIMENTS OF LESVOS ISLAND, AEGEAN SEA

Michael O. Angelidis* and Maria Aloupi

Department of Environmental Studies, University of the Aegean, 17 Karadoni Str., 81100 Mytilene, Greece

Abstract

The concentrations of the metals Cd, Cu, Fe, Pb and Zn, which were determined in the sediments of the coastal area of Mytilene, Lesvos island, Greece, were normalised to Al in order to compensate for the granulometric and mineralogical variations of the associated material, and metal enrichment factors were calculated. This normalisation of the metal data set revealed that Cd, Cu and Zn (and to a lesser degree Pb) were enriched in the sediments of the harbour area, but no metal enrichment was found in the sediments of the coastal area outside the harbour. Normalisation to Al is shown to be a valuable tool in assessing the degree of metal contamination in coastal sediments.

Key words : metals,sediments, pollution, Aegean Sea

Introduction

The marine environment within the vicinity of cities along the Mediterranean coastline is the final receiver of effluents (usually untreated) generated in the greater urban area. The impact of these pollutants in the coastal environment depends on the discharged pollution load and the local hydrodynamic conditions, *i.e.*, the dispersion/dilution potential of the receiving marine body [1]. Although the impact of urban effluents on marine sediments in the coastal zone of the Aegean Sea islands has been well documented [2, 3], the magnitude of this impact cannot be easily assessed because of the large granulometric and mineralogical variability of the sediments. In these areas, the metal content of the sediments is affected by land-derived detrital metals, non-detrital metals (biogenous, authigenic, hydrothermal, diagenetic) as well as metals transported in the runoff from neighbouring urban/industrial areas. In order to be able to evaluate the importance of metal contamination of marine sediments from urban sources, metal data have to be re-examined with the use (among others) of different normalisation methods [4, 5]. In the present study the metal concentrations in the coastal sediments of Mytilene were normalised to the conservative element Al and Enrichment Factors (EFs) were calculated for comparing the degree of enhancement of metal pollution in the study area.

The study area is the coastal zone near the city of Mytilene in the eastern part of of Lesvos island (Fig. 1). The only major source of anthropogenic metals in the area is the city effluents which are discharged untreated into the sea through sewage outfalls located along the urban coastline. No significant industrial activity exists in the area.

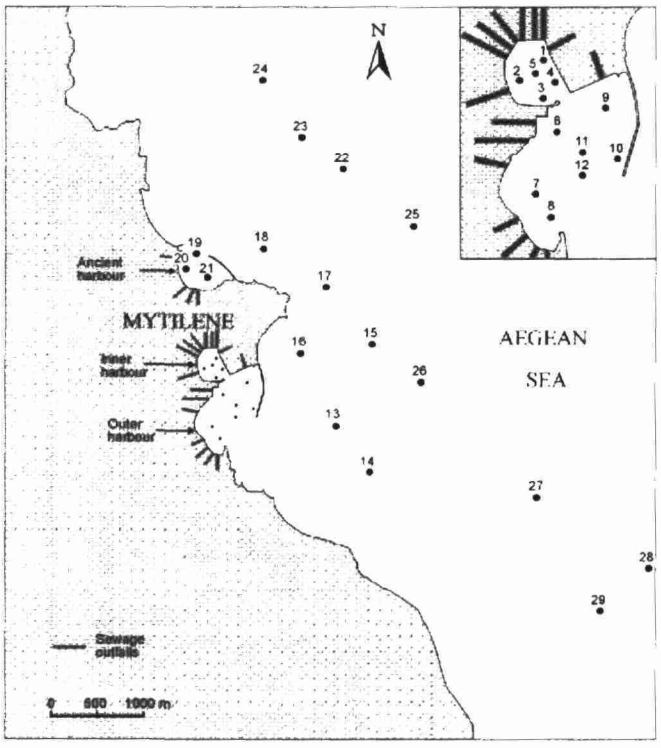

Fig. 1. Sampling stations in the coastal zone of Mytilene. Magnified insert shows the sample stations in the harbour area.

Methodology

Surface sediment samples were collected from 28 stations from the harbour and the wider coastal area of Mytilene (Fig.1). Grain size distribution was measured by wet sieving and the following fractions were determined: silt+clay (< 63 μm), sand (1 mm > x > 63 μm) and gravel (> 1 mm). The methods for the determination of organic carbon, carbonate and metal concentrations in the < 1 mm fraction are given elsewhere [6]. The quality assurance of the analytical results was controlled with the use of a Reference Material certified by NRCC (BCSS-1 marine sediment).

Normalisation to a conservative element

The term "conservative element" is used for elements of natural origin which are structurally combined to one or more of the major fine-grained trace metal carriers. Normalisation of metal levels aims to reduce the natural effect of grain size on trace metal distribution, to identify the predominant metal carriers and to estimate the extent of contamination [7]. Aluminium has been widely used as a conservative element for normalisation of metal data for marine sediments, because it is a major constituent of fine-grained aluminosilicates with which the bulk of trace metals are associated.

In non-contaminated sediments the Metal/Al ratio should be relatively constant, because it is assumed that a linear positive correlation exists between the concentration of the metal and that of Al. Since human activities normally add anthropogenic metals but not Al to the marine environment, it is assumed that contaminated sediments will present higher Metal/Al ratios. Using these ratios it is possible to calculate an "Enrichment Factor" (EF) of a metal in the sediment by dividing the Metal/Al ratio of a sample by the Metal/Al ratio of a non-contaminated sediment sample from a pristine area.

Results and discussion

The concentrations of metals in the coastal sediments of Mytilene are presented in Table 1, along with the grain size distribution (on a gravel free basis), the organic carbon content and the carbonate content of the samples. Although it is obvious that the higher metal concentrations were found in the harbour sediments, the spatial extent of metal contamination is not clear. In order to evaluate the degree of metal contamination in the area, the metal concentrations were normalised to Al. Such a normalisation is possible because in this data set a positive linear relationship exists between the concentrations of metals and the concentrations of Al and also, a positive linear relationship exists between the Al concentration and the percentage of the fine-grained material in the samples [6].

The normalised data were used to calculate the EFs for metals in the different stations by dividing the Metal/Al ratio of each station by the Metal/Al ratio of a non-contaminated reference area (Table 2). For the calculation of EFs the mean of the normalised concentrations from the 6 most remote stations of the area (stations 22, 23, 25, 27, 28 and 29) was used as a reference concentration. The mean normalised values of the non-contaminated reference area were: Cd/Al = 0.015 ± 0.005, Cu/Al = 2.64 ± 1.08, Fe/Al = 0.376 ± 0.10, Pb/Al = 8.48 ± 1.54, Zn/Al = 8.86 ± 3.37.

The calculated EFs revealed that the sediments of the harbour of Mytilene (stations 1-8 and 10-12) can be considered as polluted with Cd, Cu and Zn, because the EFs for these metals were higher than 2 (Cd pollution was recorded only at stations 1-8). Elevated Cu and Zn EFs were also found in sediments from the northern harbour of Mytilene (stations 19, 21). The value of 2 for EF as a pollution threshold has been defined arbitrarily. This value is considered appropriate

NATURAL RADIONUCLIDES IN RECENT MARINE SEDIMENTS OF THE ADRIATIC SEA

D. Barisic [1*], A. Vertacnik [1], S. Lulic [1], G. Mihelcic [1], I. Sondi [1], M. Juracic [2], E. Prohic [2] and R. Crmaric [3]

[1] Centre for Marine Research - Department Zagreb, Ruder Boskovic Institute, P.O.Box 1016, Bijenicka 54, 10001 Zagreb, Croatia
[2] Department of Geology, Faculty of Science, University of Zagreb, Kralja Zvonimira 8, 10000 Zagreb, Croatia
[3] State Hydrografic Institute, Geophysical Department, 10000 Zagreb, Croatia

Abstract

Adriatic sea sediment cores were sampled during a series of cruises by box corer. The activities of ^{40}K, ^{228}Ra, ^{226}Ra and ^{238}U were determined by gamma-spectrometry. Activities of these naturally-occurring radionuclides are generally high in pelitic sediments, whereas the lowest concentrations correspond to sands and silts which are mainly spread along the Croatian coast. ^{226}Ra distribution generally follows the distribution of uranium, and ^{40}K and ^{228}Ra distributions are strongly influenced and governed by grain size distribution whichwhich is, in fact, the clay mineral content of these sediments. Radionuclide concentrations are generally lower in sediments with higher carbonate content.

Key-words: radioactivity, sedimentation, geochemistry, Adriatic Sea

Introduction

The content of naturally occurring radionuclides in different types of recent Adriatic sediments in Croatian territorial waters has not yet been studied. The purpose of this study was to give the very first insight into the spatial distribution of natural radionuclides in Adriatic sea sediments. The shallowness of continental shelf and solid discharges from Po and other Italian and Croatian rivers have a strong influence on the grain size distribution and sedimentation rate. The Po River carries siliceous material from igneous and metamorphic rocks, and to a lesser extent, detritial carbonates from central and western parts of the Alps and from central Apennines. Erosion of the red soil (terra rossa) and the biogenic destruction of calcareous shells provide the material which has settled along the Croatian coast. Biogenic carbonates are produced throughout the area, but they are important sediment constituents only in areas where the input of terrigenous matter is negligible.

Due to the longshore current and wave transport, a narrow littoral belt of coarser and finer sand above the wave base is formed, spreading along the western and north-western Adriatic coast. The pelitic material continues north-eastward until the Adriatic drift current prevails and changes its direction to the south. Because of that, pelitic material has settled in a belt below the wave base parallel to the Italian coast [1]. In the offshore direction (where minor quantities of fine-grained material settle) pelites are mixed with older sands by means of bioturbation and resuspension, resulting in sediments characterised by a wide range of grain size: from clayey silt to silty sand [2, 3]. Part of the north central Adriatic shelf is covered with relict sands deposited as shore sands during the Holocene transgression. Similar deficiency of clastic material input prevail along the Croatian coast. There are no large rivers draining these terrains, and the relatively small quantities of material that the eastern Adriatic rivers carry (Mirna, Rasa, Zrmanja, Krka) are deposited in their estuaries [2, 4]. Cetina and Neretva rivers carry significant quantities of material, but due to the semi-enclosed nature of the sea, recent sedimentation of terrigenous material is restricted to relatively small deltaic (Neretva) or estuarine (Cetina) sedimentation areas. The central Adriatic is a shelf edge covered mostly by mud. In this part the sedimentary supplyis both longitudinal and lateral, and the distribution of the material is governed by marine agents [3, 5].

Sampling and methods

Cores of open Adriatic bottom sediments were sampled by box corer during the ASCOP 16 cruise in summer 1990. Cores were taken along seven different transects between the borders of Croatian and Italian territorial waters in the northern and central Adriatic Sea (Fig. 1). The sediments along the Croatian coast between Rijeka and Dubrovnik were taken by drop or vibro corer during summer and autumn 1993. Drop corer was used for collecting samples in sedimentation areas of the Cetina and Neretva river mouths in autumn 1994.

After sampling, the sediments were frozen at -18°C and kept until further use. Before the analyses, the samples were thawed at room temperature and dried at 106°C to the constant weight. Two core sections of open Adriatic and the Po River prodeltaic sediments were analysed: 0-3 cm and 12-15 cm. Only surface sections (mainly the first 20 or 30 cm) of cores taken along Croatian coast were analysed. Cores

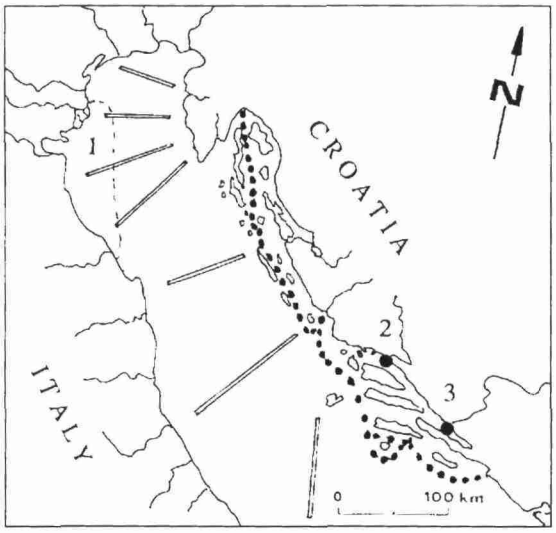

Fig. 1. Sketch-map of studied area. **1** - the Po River prodeltaic area; **2** - the Cetina River estuarine area; **3** - the Neretva River prodeltaic area; double lines - profiles between Croatian and Italian territorial waters; dot line - profile between Rijeka and Dubrovnik

taken in the Cetina and Neretva sedimentation areas were divided into 2 or 3 sections (*circa* 50 cm each) before analyses. Samples were granulometrically characterised by wet sieving, using ASTM standard sieves for fractions >32 μm, and by Coulter Counter (Model TA II) for fractions <32 μm. Dried soil samples were placed in the counting vessels of known geometry, sealed and stored at least for 4 weeks to allow ingrowth of gaseous ^{222}Rn. At the end of the ingrowth period, the samples were counted on a HPGe detector connected to a 4096 channel analyser. The detector system was calibrated using standards supplied by Amersham International, while precision and accuracy were checked by parallel measurement of IAEA-306 and IAEA-314 standards. Spectra were recorded for 80,000 seconds. Recorded spectra were processed on PC using GENIE PC software.

Resultats and discussion

The measured activitie ranges of ^{40}K, ^{228}Ra, ^{226}Ra and ^{238}U, as well as the mean values for different sedimentation areas in the Adriatic sea are presented in Table 1. Cores taken along transects between the Italian and Croatian coast (open Adriatic) were divided into three groups (sands, sands and pelites, pelites) and these results are also showenalso. The activities of measured natural-occurring radionuclides are higher in pelitic sediments. The lowest concentrations of naturally occurring radionuclides corresponded to the sand and silts which are mainly spread along the Croatian coast. However, the activity of ^{238}U in bottom sediments of open Adriatic sea progressively increases toward the open sea (from Croatian to Italian territorial waters). It seems that relatively elevated uranium activities in recent marine sediments are the consequence of terrigenous influences, *i.e.* deposition of material carried by rivers. This is evident in cases of the sedimentation areas of the Po and Neretva rivers which partly carry

SEASONAL AND SPATIAL VARIATION OF CU, CR, NI AND PB CONCENTRATIONS IN *MYTILUS GALLOPROVINCIALIS* OF SARONIKOS GULF, GREECE

F. Bei, V.A. Catsiki and E. Strogyloudi*

National Center for Marine Research. AG. Kosmas, Helliniko 16604, Greece.

Abstract

Accumulation of Cu, Cr, Ni and Pb by the mussel *Mytilus galloprovincialis* was studied seasonally at four stations in Saronikos gulf (Aegean sea, Greece). All metals showed a significant seasonal variation with the maximum mean values occurring in winter. The observed pattern was mainly related to the biological cycle of the mussels and only secondarily to environmental parameters. Concerning the spatial distribution of metal concentrations in mussels, higher values were detected at station 2 close to the central sewage outfall than those at station 4 located further away from the source of contamination.

Keywords: metals, bivalves, Aegean sea

Introduction

In marine ecosystems, heavy metals occur in the water mass, suspended particles, sediment and biota. The use of biological indicators to monitor environmental contamination by trace metals has many advantages over the measurement of metals in water or sediment samples, since their content of pollutants is proportional to the biologically available concentration of pollutants harmful to marine life and it represents a time integrated image of the bioavailability of a pollutant which is not affected by short term fluctuations in sea water (1). The common mussel, *Mytilus galloprovincialis*, is considered to be a sentinel organism in monitoring both acute and chronic environmental pollution (2). This work deals with Cu, Ni, Cr and Pb concentrations in mussels from Saronikos gulf (Aegean sea, Greece), and has been carried out within the framework of MED-POL Monitoring Programme.

Methodology

During 1995, samples of mussel (*Mytilus galloprovincialis*) of about 5 cm length were collected seasonally from four coastal locations by scuba diving (Fig. 1). Immediately after collection, the shell was cleaned and 6 pooled samples from each station were made from the soft parts of 6 to 12 individuals which had been carefully rinsed with abundant distilled water in order to eliminate sediment and other impurities.

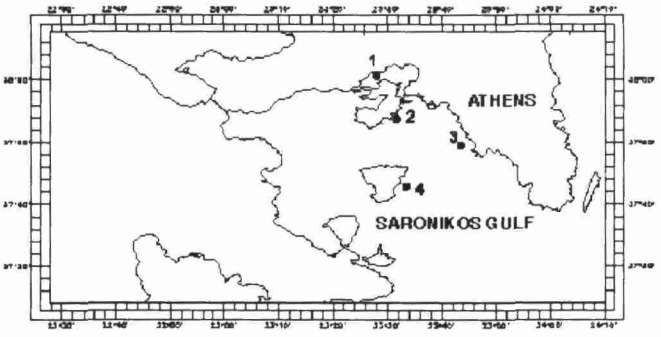

Fig. 1. Sampling stations in Saronikos Gulf.

The analysis of samples included lyophilisation, homogenisation and digestion with HNO_3 (proanalysis, MERCK) under pressure at 100°C for 12 hours. The determination of metals was performed by atomic absorption spectrophotometry with flame using a VARIAN SPECTR AA 20 Plus spectrophotometer. The quality control of the analytical methodology was carried out by analysing the reference material of BCR No 279 (*Ulva lactuca*). The data, after log transformation {log(x+1)}, were statistically treated by two-way ANOVA, in order to estimate if there are any differences among the sampling stations as well as between the different seasons (3).

Results

In total 90 samples of mussels were analysed. The mean concentrations of Cu, Cr, Ni and Pb, expressed in μg/g dry weight in the soft tissues of mussels, are summarized in Table 1. Mean values ranged from 2.62 to 15.94 for Cu, 0,80 to 27.57 for Cr, 1.61 to 12.14 for Ni and 2.09 to 11.02 for Pb. The highest concentrations for Cu and Cr were observed at station 2, for Ni at station 3 while Pb was maximum at station 1. It is important to mention that station 4 displayed the lowest concentrations for all metals.

Table 1. Mean metal concentrations in mussels from different areas of the Saronikos gulf during 1995 (in μg/g dry weight).

Station	Cu	Cr	Ni	Pb
1	7,99 ± 1.76	2,90(1.43	4,99 ± 1.09	6,14 ± 1.33
2	8,27 ± 2.37	9,32 ± 9.00	5,11 ± 2.00	5,95 ± 1.77
3	7,24 ± 3.60	3,83 ± 1.89	5,93 ± 3.81	5,90 ± 2.29
4	4,68 ± 1.57	2,55 ± 1.44	3,90 ± 1.20	4,69 ± 1.96

Seasonal mean concentrations (avg), standard deviation (sd), minimum (min) and maximum (max) values are presented in Table 2. Concerning the temporal variation in metal levels, we observe that it presents common patterns in the 4 localities where mussels were collected.

Table 2. Seasonal metal concentrations in *M. galloprovincialis* (μg/g dry weight) of Saronikos gulf (b: summer, c: autumn, d: winter).

		Cu				Cr			
Station	Season	avg	std	min	max	avg	std	min	max
	b	6,39	1,69	3,26	8,55	1,68	0,29	1,30	2,11
1	c	8,11	1,16	5,75	9,47	3,69	1,65	1,93	7,19
	d	9,47	0,58	8,55	10,15	3,32	1,02	2,07	5,28
	b	6,70	0,73	5,77	7,83	3,01	1,27	1,52	5,95
2	c	6,74	1,02	4,91	8,73	3,44	1,91	0,00	6,69
	d	11,38	0,93	10,22	13,13	21,51	3,84	17,73	27,57
	b	4,15	0,85	3,52	6,30	2,17	0,65	1,03	2,89
3	c	11,55	2,47	7,53	15,94	5,40	1,60	2,17	7,36
	d	6,95	0,84	5,92	7,87	4,81	1,12	2,92	5,73
	b	3,21	0,52	2,62	4,18	1,82	0,61	0,80	2,84
4	c	4,51	0,63	3,34	5,47	1,93	0,55	1,22	2,91
	d	6,88	0,57	6,15	7,78	4,37	1,48	3,01	7,20

		Ni				Pb			
Station	Season	avg	std	min	max	avg	std	min	max
	b	4,42	1,50	1,97	6,56	5,46	1,77	3,63	8,80
1	c	5,53	0,42	5,07	6,31	6,33	0,70	5,34	7,31
	d	5,02	0,71	4,10	6,15	6,62	1,00	4,33	7,76
	b	3,25	0,67	2,24	4,43	4,36	1,04	2,46	6,18
2	c	4,84	0,72	3,90	6,32	5,80	0,96	4,63	7,64
	d	7,23	1,73	5,54	11,49	7,70	1,34	4,85	9,68
	b	2,37	0,39	1,61	2,83	3,65	0,54	2,69	4,48
3	c	10,89	1,21	8,46	12,14	8,07	1,56	5,84	10,77
	d	5,61	0,50	5,10	12,14	7,14	0,86	5,77	8,10
	b	3,01	0,49	1,96	3,72	4,15	0,71	3,07	5,38
4	c	3,52	0,49	2,48	4,12	3,70	1,15	2,09	5,24
	d	5,52	0,80	4,36	6,58	6,74	2,41	2,81	11,02

Regarding the differences between stations and seasons, a statistically significant difference at the 95% level for the metal concentrations in mussels, for all stations and seasons, is apparent from the data in Table 3. Concerning the seasonal variation, an effect of the sampling season is recorded since mussels present higher values during the cold period of the year ($P < 0.05$). The variation in seasonal average concentration of metals in mussels from the four coastal areas of Saronikos gulf is presented in Figure 2.

Discussion

In this work the overall metal concentrations in mussels from Saronikos gulf are similar to those reported for other Mediterranean areas (4).

CR AND NI CONTENT IN SEDIMENTS FROM KASTELA BAY, ADRIATIC SEA, CROATIA

D. Bogner [1], M. Juracic [2] and A. Baric [1]

[1] Institute of Oceanography and Fisheries, Split, Croatia
[2] Department of Geology, Faculty of Science, University of Zagreb, Croatia

Abstract

Six sediment samples from the Kastela Bay and 6 samples of land rocks east of the bay were taken in order to evaluate the possible contamination of the sediments by Cr and Ni. The level of these metals in both the marine sediments and land (flysch) rocks indicate that they are, in large part, of lithogenous origin. The elevated concentrations are associated more with fine-grained sediments.

Key-words: metals, Adriatic Sea

Introduction

Some studies on the concentration of Cr and Ni in marine sediments have demonstrated their geological origin, but in some polluted areas they may have anthropogenic origin as well (1). Measurement of trace metal concentrations in parent rock can substantially help to determine the anthropogenic influence on concentrations of these metals in sediments (2). The work presented here was undertaken to asses the possible contamination of the Kastela bay by Cr and Ni.

The Kastela Bay is a semi-enclosed basin located on the eastern Adriatic coast (Fig.1). The wider area of bay is densely populated and industrially developed. The bay is also heavily contaminated by untreated domestic and partially treated industrial waste waters (3). Therefore, distributions of organic matter and carbonates in the bay sediment samples were also determined in this survey.

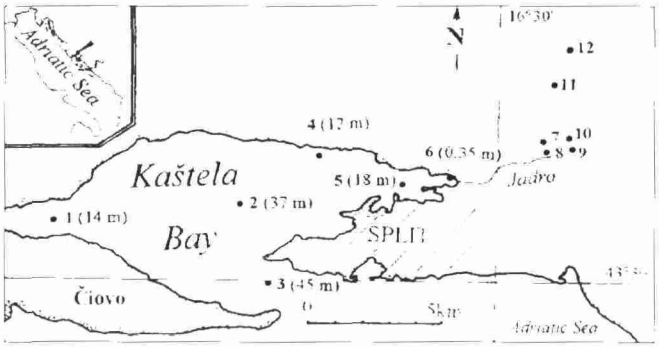

Fig. 1. Map of the study area and sampling locations. Depth in meters are given in parantheses next ot each station.

Material and methods

The sediment samples were collected using a plastic gravity corer in March 1994 at 5 stations in the Kastela Bay (Fig. 1). At the station 6, in shallow water, a sediment sample was taken by a manually operated corer in May 1995. On land and in the drainage area, samples of parent rocks were collected in March 1995 at 6 locations (locations 7-12 shown in Fig. 1).

Immediately after sampling, sediment samples were frozen. Before analysis the sediments were defrosted at room temperature, sliced into 1 cm thick subsamples, dried at 60°C, and left to cool at room temperature. The granulometric composition of sediment was determined by sieving (> 63 μm) and areometring (Casagrande < 63 μm) of 4 cm (2 cm for Station 6) thick subsamples. Samples of the dry sediments and parent rocks were digested with a mixture of HF, HNO_3 and $HClO_4$ (4). The organic matter content was determined as a weight loss on ignition after H_2O_2 treatment and ignition at 450°C for 6 h (5). Carbonate content was determined as weight loss after treatment with 4M HCl (6). Cr and Ni concentrations were measured by the graphite-furnace atomic-absorption spectrophotometry (GFAAS) method using a Perkin-Elmer 1100 B instrument. The accuracy of the analytical procedure used was repeatedly checked by analysing samples of reference sediment standards (marine sediments SD-M-2/TM and SRM 1646 estuarine sediments) (Table 1).

Results

The results of granulometric analysis, carbonates and organic matter content of the sediment samples are listed in Table 2, while the level and distribution of Cr and Ni along the sediment cores are presented graphically in Figures 2 and 3, respectively. The characteristics of the parent rock are presented in Table 3. At the shallower stations (1, 4 and 6), the sediment was composed mainly of fine sand and silt.

Table 1. Cr and Ni concentration (mean ± standard deviation) for U.S. Natural Bureau of Standards (NBS) estuarine sediment (SRM 1646) and (median) for marine sediments (SD-M-2/TM).

Metal	Certified values (mg/kg)	This study (mg/kg)
Cr (SRM 1646)	73±3	88
Cr (SD-M-2/TM)	72.2	98.5
Ni (SD-M-2/TM)	56.1	51.6

Table 2. Granulometric characteristics of sediment samples (stations 1-6) and organic matter content.

Station /depth	Core length (cm)	Carbonates %	Organic matter %	Clay %	Mz (μm)	Sediment type Shepard (7)
1/14 m						
	0-4	54.3	5.3	1	113	silty sand
	4-8	59.2	4.9	4	123.8	sandy silt
	8-12	55.3	4.4	5	121.7	sandy silt
2/37 m						
	0-4	45	8.8	16	22.8	silt
	4-8	44.5	8.2	16	21.4	silt
	8-12	39.6	8.4	29	11.3	clayey silt
	12-16	37.4	7.6	15	24	silt
	16-20	39.9	7.7	10	29.7	silt
	20-24	44.5	7.2	9	25.8	silt
	24-27	42.1	6.9	6	24.3	silt
3/45 m						
	0-4	45.7	6	17	20.5	silt
	4-8	48.6	6.2	17	18.1	silt
	8-12	45.4	5.2	19	16.5	silt
	12-16	47.2	5	16	20.6	silt
	16-20	46.7	5.3	16	17.3	silt
4/12 m						
	0-4	46.5	9.2		93.1	sandy silt
	4-8	46.6	6.6		75.9	silty sand
	8-12	48.5	5.7	9	30.8	silt
	12-16	47.9	5.7	8	32.3	silt
	16-20	49.6	5.6	3	37.8	silt
5/18 m						
	0-4	50	8.8	3	37.3	silt
	4-8	49.2	8.1	7	30.9	silt
	8-12	51.8	8.0	10	28	silt
	12-16	50.4	7.4	6	24.6	silt
6/0.35 m						
	0-2	61.7	2.7		78.1	silty sand
	2-4	63	2.6		75.3	silty sand
	4-6	59.4	2.2		74.4	silty sand
	6-8	60	2.1		71.2	silty sand
	8-12	59.1	2.1		74.7	silty sand

The average particle size (Mz = 30.8 - 123.8 μm) corresponded to silt -fine sand. On the other hand, the sediment samples taken from the deeper stations (2, 3 and 5) were mainly silt (Mz = 11.3 - 37.3 μm).

The organic matter varied from 2.1 to 9.2% (Table 2). The lowest content was in the sandy sediment from station 6 facing the river Jadro (Figure 1), while the highest amount was found at stations 2 and 5 area with the highest phythoplankton density (10). Station 5 is located nearby outlets discharging urban and industrial waste waters containing high organic matter concentrations (3). The carbonate content was very high, both in the parent rocks and marine sediments particularly those at stations 1 and 6. It varied from 39% in marl to 99.9% in limestone, while in marine sediments it ranged from 37.4 to 63% (Table 2).

Chromium and Ni in marine sediments (Figs. 2 and 3) were considerably higher than in the parent rocks samples taken at the locations 9, 11 and 12 (limestones), while the other parent rocks samples taken at the locations 7, 8 and 10 (marl) had similar Cr and Ni concentrations

DISTRIBUTION OF TOTAL BETA RADIOACTIVITY, SR-90 AND CS-137 CONTENT IN THE ROMANIAN AND NW BLACK SEA SECTOR BETWEEN 1994-1995

Alexandru S. Bologa*, Vasile Patrascu, Elvira Cuingioglu
Romanian Marine Research Institute, Mamaia 300, 8700 Constantza 3, Romania

Abstract

Total beta radioactivity and Sr-90 in abiotic (sediment, sea water) and biotic components (seaweeds, molluscs, fish) of the Romanian Black Sea coast between the Danube mouth and the southern limit (Mangalia), and from the shoreline up to 60 nautical miles offshore were continuously monitored during 1994 and 1995. Highest Sr-90 concentrations were found in sediments (8.6 Bq/Kg dry) and in the green seaweed *Bryopsis plumosa* (12.1 Bq/Kg f.w.). The results of radiometric research on bottom sediments collected from the north-western sector of the Black Sea in July-August 1995 showed values of total beta radioactivity between minimum detectable limits (< 20 1) and 818 Bq/Kg dry, and Cs-137 contents between 2 and 201 Bq/Kg dry.

Key-words: Radioactivity, radionuclides, monitoring, Black Sea

After the Chernobyl nuclear accident, the Black Sea due to its geographical location was contaminated by radionuclides originating from atmospheric fall-out and through riverine input [1]. A network of stations has been used for the characterization of marine radioactivity in the Romanian Black Sea sector between 1994 and 1995 (Fig.1).

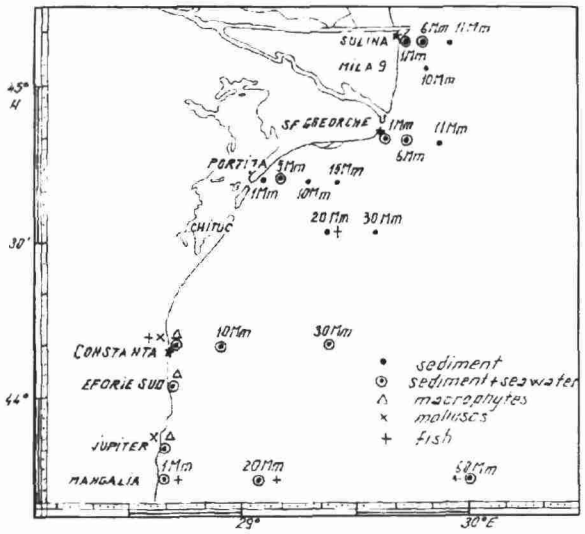

Fig. 1. Station network along the Romanian Black Sea coast.

Material and methods

Emerged and submerged sediments, seawater, common macrophytes, molluscs and fish were measured in the Romanian Black Sea sector for total beta radioactivity (K-40 reference) and Sr-90 in accordance with contemporary techniques [2] using specific low level radiometric equipment. The distribution of both parameters was computed as average values by stations (for sediments and seawater) and by species for marine biota for the two years considered. The International Programme "Investigations between the Danube River and the northwestern Black Sea/EROS 2000" [1] provided bottom sediment samples during the second cruise of R/V *Professor Vodyanitskyi* in July-August 1995. The cruise covered the Crimean coastal waters, the mouths of the Danube, Dniester, Dnieper rivers and the Romanian shelf and offshore areas. Among current monitoring activities for marine radioactivity [3,4,5,6,7], total beta and Cs-137 measurements for 26 sediment samples from the NW Black Sea sector were also made. The main instruments used in the radioanalyses of samples have included NIM instruments, NE 102A detector (total beta), and HPGe detector (10% relative efficiency and 2 keV resolution at 1333 keV) and ORTEC-NORLAND 5500 multichannel analyser for gamma spectrometric determinations. Gamma analyses were based on measurements of a minimum of 40000 sec. The results have a confidence interval of 68%.

Results and discussion

The fluctuations in the dynamics of sediment **total** beta activity (Fig.2) are mostly a result of the hydrological factors typical for the area, the dispersion and diffusion processes in the water mass [8], and the sizes and density of the particles which are deposited. Consequently, in many cases at the greatest depth investigated, the beta activity is more intense than near the river sources,

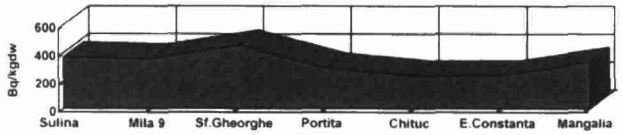

Fig. 2. Mean total beta radioactivity of sublerged sediments along the Romanian Black Sea coast during 1994-1995.

The total beta activity of eight species of macrophytes (green, red), three species of molluscs and seven species of edible marine fish (benthic and pelagic) typical of the Romanian littoral was measured (Fig. 3). In the NW Black Sea the total beta values ranged between < 20 1 and 818 Bq/Kg dry. Significant results (Fig. 4) were registered at the Dnieper mouth (stations 6, 7), Danube mouth (stations 18, 19, 20), Portita (station 22) and on the shelf (stations 13, 14, 15). In front of the Dniester mouth, only the minimum detectable levels were registered in shallow waters (less than 25 m depth). Significant natural contributions were registered in offshore stations at depths exceeding 100 m (stations 2, 3, 26).

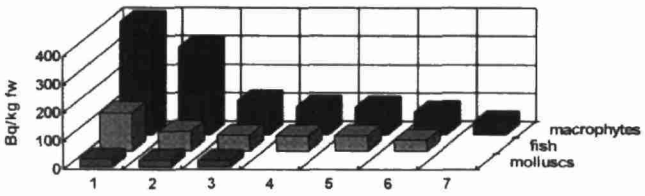

Fig. 3. Mean total beta radioactivity of biota along the Romanian Black Sea coast during 1994-1995.

Macrophytes : *1 - Bryopsis plumosa; 2 - Enteromorpha intestinalis; 3- Cladophora sericea; 4- Enteromorpha linza; 5- Ceramium rubrum; 6- Uvaria oxysperma; 7- Ceramium eleganfs.* **Molluscs** : *1-Rapan tomasiana; 2- Mya arenaria; 3- Mytilus galloprovincialis.* **Fish**: *1- Platichthys flesus lusus; 2- Engraulis encrasicolus ponticus; 3- Gobius melanostomus; 4- Sprattus sprattus phalericus; 5- Atherina mochon pontica; 6- Merlangus merlangus euxinus.*

The variability of Sr-90 content in sediments from the Romanian marine sector (Fig. 5) generally follows dynamics similarly to those of total beta activity. The average values of Sr-90 for the macrophytes decrease similarly to those of total beta activity. For marine fish the highest content was found in benthic species (Fig. 6). The results were in good agreement with other data both for the Black Sea [9] and the Baltic Sea [10].

The rather long period since the Chernobyl accident has enabled marine processes to influence the Cs-137 concentrations on the shelf (stations 14, 15) and in offshore river mouth areas (station 5). Nevertheless, the lowest Sr-90 concentrations (5.5-18.5 Bq/Kg dry) were noted at the Dniester mouth (stations 9,10,11) and in deep waters (stations 2, 3, 26, 28). The higest Cs-137 concentrations are frequently found at depth of 20-40 m (stations 6, 17, 22, 15) [7]. Local peculiarities can lead to exceptions at shallower depths (station 14) or in deeper waters (station 16). Where the depth exceeds 100 m (stations 3, 26, 28), the frequency of low values increases and is constant in deep waters (station 2). The stratification of water masses can prevent Cs-137 from interacting with the deep bottom [7]. A small difference was found at station 2 between the Cs-137 concentrations in the surface and deep bottom layers (6-4 Bq/Kg dry); this fact indicates the existence of relatively constant conditions in the deep sea. At depths

ETUDE DE LA VARIABILITÉ DES TENEURS EN MÉTAUX LOURDS CHEZ LA MOULE *MYTILUS GALLOPROVINCIALIS* (LMK) D'UN MILIEU LAGUNAIRE : LE LAC MELLAH (EL-KALA/ALGÉRIE)

B. Boudjellal* , W. Refes, N. Eddalia, F. Ounadi, S. Benchikh, M. Azzouz

ISMAL., laboratoire de pollution marine. BP. 54, Sidi-Fredj / Staouéli, Gouvernorat du Grand - Alger, Algérie

Résumé

Six métaux lourds (zinc, cuivre, manganèse, plomb, cadmium et mercure) ont été sélectionnés pour évaluer le degré de contamination d'un mollusque (*Mytilus galloprovincialis*), provenant d'un milieu lagunaire saumâtre situé à l'est de la côte algérienne : le lac Mellah (El-Kala). Les concentrations en ces métaux ont été déterminées par spectrophotométrie d'absorption atomique sur différents lots de moules. Les causes et la variabilité des concentrations mesurées sont discutées. A la lumière des résultats obtenus, il ressort que le niveau de pollution par les métaux lourds de cette lagune ne présente pas de caractères excessifs.

Mots-clés : metals, Mollusca, lagoons, pollution, Algerian basin

Introduction

Au cours d'un suivi mensuel allant de mai 1993 à mai 1994, la moule *Mytilus galloprovincialis* (Lmk) a été choisie pour diagnostiquer l'état de contamination par les métaux traces d'un milieu lagunaire. Sa résistance à la pollution, sa très large répartition géographique et son pouvoir important de concentration des polluants font de cet organisme un bon indicateur du niveau de pollution (1). Ce travail a été réalisé dans un site lagunaire saumâtre, le lac Mellah. Celui-ci est le siège d'une importante activité de pêche (mulets, soles, loups, anguilles), et d'essais de conchyliculture (moules, palourdes). Un contrôle sur les variations des concentrations en métaux traces chez *Mytilus galloprovincialis* (Lmk) a été entrepris, conformément à la recommandation du PNUE (Programme des Nations Unies pour l'Environnement) et du programme "MUSSEL WATCH" (2).

Site d'étude

Le lac Mellah est un lac côtier situé à l'est de l'Algérie dans la région d'El-Kala (36°53'50" N, 8°19'30" E); de forme ovoïde, il occupe une superficie de 865 hectares. Il s'étend du nord au sud sur une longueur de 5 km et une largeur est-ouest de 2,6 km. Sa profondeur est généralement faible et atteint un maximum d'environ 6 m dans sa partie centrale. Il est relié à la mer par un chenal de 900 m de long et 20 à 40 m de large (Fig. 1). Ce chenal est le siège d'échanges importants entre les deux milieux. Ces échanges influent intensément sur le renouvellement des eaux du lac, et sont en partie responsables de son caractère saumâtre (30 p.s.u.) (3). La lagune subit aussi l'influence simultanée de trois oueds : oued El Rekeibet, oued El Mellah et oued El Aroug ; ce dernier est relié au lac par l'intermédiaire d'un marécage. L'influence de ces oueds qui traversent des zones cultivées se traduit par des apports telluriques et hydriques importants, surtout en période hivernale.

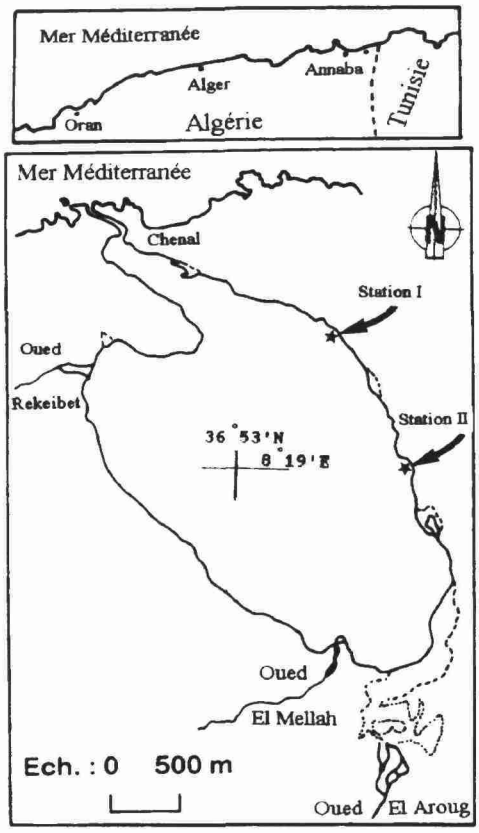

Fig. 1 : Situation géographique du lac Mellah et localisation des stations.

Echantillonage et méthodologie

Les échantillons de moules ont été récoltés au niveau de deux stations (Fig. 1) : la station I est située au sein d'un herbier à *Ruppia maritima* à 0.55 m de profondeur. La station II, au sud de la station I et plus abritée que cette dernière, est située dans un champ de roseaux servant de substrat aux moules (0.65 m de profondeur). Les prélèvements ont été étalés sur cycle annuel (de mai 1993 à mai 1994) avec un pas d'échantillonnage mensuel. Les moules recueillies dans ces deux stations ont été réparties en classes de taille (entre 3 et 6 cm).

Dans chaque station, une cinquantaine d'individus a été récoltée. Les échantillons sont débarrassés de leurs coquilles, lyophilisés et micro-pulvérisés (4), puis minéralisés à l'aide d'acide nitrique ultrapur (70 %, RIDEL DEHAËN).

La validité des résultats obtenus a été testée par la mise en oeuvre d'exercices d'intercalibration sur des échantillons standards d'une matrice biologique fournis par l'AIEA (Agence Internationale de l'Energie Atomique) de Monaco, codés TUNA 351 et MA(F)-MED-86/TM. Les dosages sont réalisés d'après les méthodes de UNEP (5) par un spectrophotomètre d'absorption atomique PERKIN ELMER 2380, équipé d'un four à graphite HGA500, une flamme air/acétylène et un système d'hydrures MHS 10.

Résultats et discussion

L'examen des concentrations en métaux essentiels (zinc, cuivre et manganèse) chez la moule *Mytilus galloprovincialis* dans le lac Mellah montre une différence entre les deux stations, en fonction des classes de taille et de la période d'échantillonnage (Tableaux 1 et 2).

Tableau 1. Teneurs moyennes des métaux lourds mesurées chez *Mytilus galloprovincialis* dans deux stations du lac Mellah (exprimées en μg/g de poids sec).

	Zn			Cu			Mn			Pb			Cd			Hg		
	L_1	L_2	L_3	L_1	L_2	L_3	L_1	L_2	L_3	L_1	L_2	L_3	L_1	L_2	L_3	L_1	L_2	L_3
STATION I																		
M	70.9	65.0	58.3	5.21	4.73	4.33	17.1	14.9	12.5	1.32	1.08	0.9	0.46	0.38	0.48	0.06	0.05	0.04
SD	10.9	8.74	2.6	2.55	2.46	2.18	6.1	6.1	4.0	0.34	0.25	0.27	0.16	0.13	0.18	0.015	0.02	0.015
M_T		66.1			4.76			14.9			1.02			0.37			0.045	
SD		11.6			2.33			5.6			0.33			0.15			0.018	
STATION II																		
M	61.5	54.6	50.0	5.12	4.69	4.05	13.6	12.5	10.4	1.05	0.81	0.63	0.36	0.33	0.35	0.05	0.04	0.03
SD	9.0	10.5	9.9	2.83	2.13	2.37	4.7	4.5	3.7	0.29	0.33	0.26	0.16	0.15	0.15	0.02	0.015	0.01
M_T		55.4			4.62			12.2			0.83			0.34			0.042	
SD		10.7			2.43			4.5			0.33			0.15			0.018	
M_G		**60.7**			**4.69**			**13.5**			**0.97**			**0.36**			**0.044**	
SD		**12.4**			**2.37**			**5.2**			**0.36**			**0.15**			**0.017**	

L (taille de coquille) : L_1 (3 - 4 cm). L_2 (4 - 5 cm). L_3 (5 - 6 cm).
M (moyenne). MT (Moyenne Totale).
MG (Moyenne générale). SD (Ecart-type).

Le zinc présente les concentrations les plus élevées par rapport aux autres métaux. Les écarts importants enregistrés entre les différentes périodes de prélèvement témoignent bien de l'existence de sources localisées, dues essentiellement à l'activité agricole (6). Les légères variations observées pour le cuivre sont liées à l'activité métabolique

SEASONAL VARIABILITY OF NUTRIENT AND CHLOROPHYLL A CONCENTRATIONS IN THE KARSTIC COASTAL LAKE VELIKO JEZERO (MLJET ISLAND, ADRIATIC SEA)

Marina Caric*, Nenad Jasprica

Institute of Oceanography and Fisheries, Laboratory of Plankton Ecology, P.O.Box 39, HR-20001 Dubrovnik, Croatia

Abstract

Vertical and seasonal distribution of nutrients and chlorophyll a (Chl a) were analyzed in relation to thermohaline conditions in a coastal karstic lake on the south-eastern Adriatic island of Mljet during 1987 and 1988. The water column through most of the year was thermally or saline stratified. Haline stratification was greatly influenced by the rainfall regime and freshwater input through underground springs. Trapped saline water of relatively high salinity was found in the deeper layers. Most of the nutrients did not exhibit a statistically significant difference between different seasons in the relation to the entire water column. The lowest nutrient concentrations were found in the layer above the pycnocline and the highest in the layer below it. Veliko jezero is an ecosystem characterized by separate water types in vertical profile during all the seasons.

Key-words: hydrography, vertical profile, stratification, Adriatic Sea

Introduction

The south-eastern Adriatic island of Mljet, with its dense forest vegetation and two picturesque coastal lakes, Veliko jezero and Malo jezero, has been proclaimed a national park in 1960 (Fig.1). The lakes were filled by the Holocene ingression of the Adriatic Sea during the Atlantic period ca. 5000 years BC. Paleohydrology of these lakes seems to be a suitable instrument for the reconstruction of climatic changes in the Mediterranean (1). Both lakes are highly isolated from each other and from the sea by narrow passages and shallow (1 respectively 2 m deep) sills. Veliko jezero is 2.5 km long, up to 1 km wide, with a maximal depth of 46 m and a volume of 0.036 km^3. The coastal line is 9.2 km long. Occasional subsurface decreases in salinity are caused by the so-called "vruljas"-subsurface springs, which are a characteristic karst phenomenon. The aim of this paper is to determine seasonal variability of nutrient and Chl a concentrations in relation to the hydrodynamic properties of the water column.

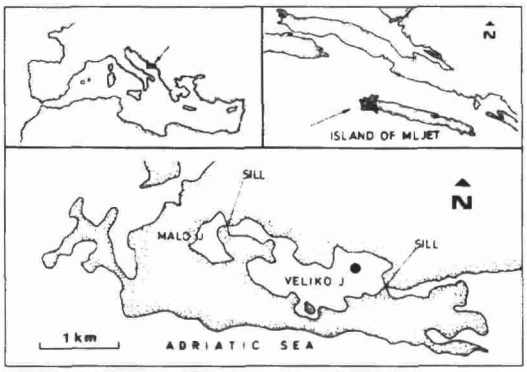

Fig. 1. Location of the Vrbovacka station in Veliko jezero (Mljet lakes).

Materials and methods

Water samples for the analyses of the nutrients and Chl *a* were collected at the Vrbovacka station (46 m max. depth) in the deepest basin of Veliko jezero. Four sampling cruises were carried out in December 1987, March, June and August 1988. The samples were taken by Niskin bottles every five meters from the surface to the bottom, except in the pycnocline where the samples were taken at every two meters. The nutrients and Chl *a* concentrations were determined by standard oceanographic methods (2, 3). Salinity and oxygen were measured using standard titration methods. Temperature was measured using inverted thermometers. Data were subjected to analysis of variance (ANOVA) and SNK-multiple range test (4).

Results and conclusion

This is the first report of Chl *a* concentration data for Veliko jezero. Thermohaline properties, oxygen saturation and Chl *a* concentration in the water column are presented in Fig. 2. Vertical distribution of the nutrient salts is presented in Fig. 3. In December 1987, the surface layer (from 0 to 10 meters) was relatively homogenous for most of the sampled parameters. Temperature was 12.8°C and salinity ranged from 37.41 to 37.59 psu. A temperature increase started at 13 meters depth to reach a maximum increase of 2.5° C between the 15 and 27 meters. At 13 meters depth salinity increased to 38.12 psu. Variation in density followed the temperature and salinity variations.

In the layer of increased temperature, an interesting distribution pattern of nutrient concentration was observed. The highest concentrations of reactive phosphorus and ammonia were recorded at 10 meters depth, namely, in the layer above the temperature increase. NO_3 with unusually high values within the increased temperature layer formed three peaks: at 13 m (50.4 μmol dm^{-3}), at 15 m (49.18 μmol dm^{-3}) and at 24 m (24.02 μmol dm^{-3}). In the drainage area dominated by pine forests, it is possible

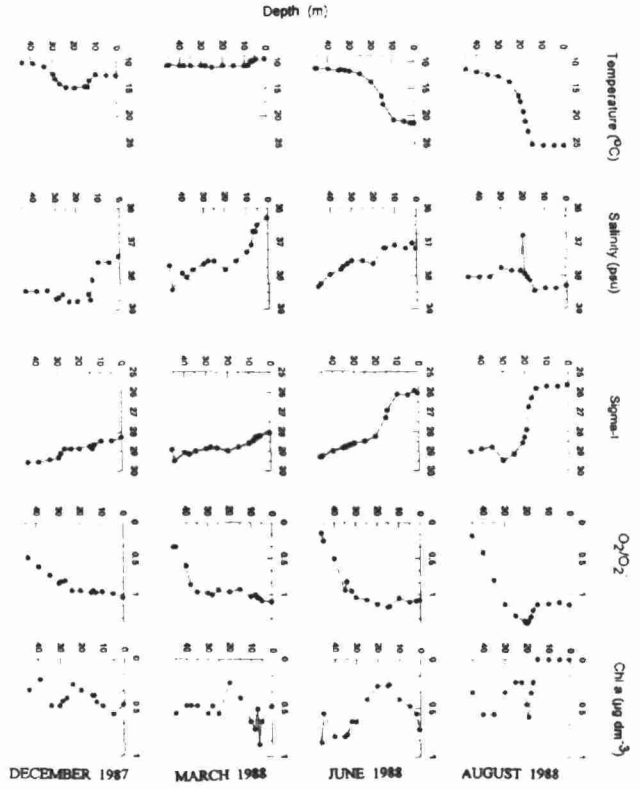

Fig. 2. Vertical distribution of temperature, salinity, density, oxygen saturation and chlorophyll *a* concentrations at Vrbovacka station.

that the amount of humic substances entering the water of Veliko jezero can be considerable. It seems that humic substances were utilized by bacteria both as a carbon and nitrogen source, and that nitrogen was incorporated in bacteria and later regenerated as inorganic nitrogen due to the activity of bacterial grazers and other grazers of higher tropic levels (5, 6). This is presumably the reason for the high NO_3 concentration levels which will be the topic of our future research.

Chl *a* has two maxima within the water column: the first maximum was recorded from the surface to 10 meters depth, and the second between 27 and 35 meters. The highest nitrite concentrations were concurrent with those recorded for Chl *a*. The dissolution of biogenic silica caused the increased reactive silicate concentrations registered at 27 meters and in the layer between 30 meters depth and the bottom. The results of the investigated parameters confirmed the existence of dynamic processes along the lines of contact as well as in the layer of the increased temperature. The increased temperature in between the 13 and 27 meter depths may probably be ascribed to a number of factors: the remnant summer temperatures after the winter cooling of the surface layer; suspended particles which absorb more intensively the energy coming from the sun than the water molecules, and to an intensified bakterioplankton activity (7).

The inverse temperature stratification was recorded to 10 meters in March. The warming of the sea in June and especially in August leads to the increase in the surface layer temperature and the formation of a sharp thermocline between 15 and 20 meters depth. Surface salinity values differed in March and June 1988 (*e.g.*, March 36.29-37.56; June 37.19-37.65), but not

INHERENT VARIABILITY IN METAL CONTENT OF *PATELLA ASPERA* (LMCK)

V.A. Catsiki*, F. Bei and E. Strogyloudi
National Centre for Marine Research. A.Kosmas, Hellinikon 16604, Greece

Abstract

The present work adresses inherent variability in metal concentration in organisms, a major cause of metal fluctuations in the gastropod *Patella aspera*. This phenomenon was studied under different environmental conditions in the Saronikos Gulf. The results were used for the calculation of the minimum number of replicates of *P. aspera* samples that are needed to give a representative metal concentration in *P. aspera* population.

Key-words : metals, gastropods, bio-accumulation, Aegean Sea

Introduction

The variability in metal concentrations of marine organisms depends on many factors, either environmental (concentration of metals in sea water, temperature, salinity, dissolved oxygen, hydrology of the area, etc.) (1, 2), or purely biological (species, sex, age, reproduction stage, etc.) (2). Part of the variability that has not been attributed to the above factors is reported in literature as "inherent variability" (3, 4). Sometimes it is so important that it exceeds 100%. We encounter this phenomenon very often and it seems to be more frequent and stronger in contaminated areas (5). Because inherent variability is a factor influencing the estimation of the average concentration of metals in samples collected from a specified area, the determination of the optimal number of replicates is of major importance (6, 7). The present work aims to study the phenomenon of metal variability in the gastropod *Patella aspera* which is considered as a good pollution bioindicator (8, 9). This species which is primarily herbivorous lives on the coastal rocks and is cosmopolitan and abundant in Greek waters. At the same time this study aims to define the minimum number of specimens (replicates) needed to be collected to obtain metal concentrations representative of the population.

Methodology

In order to study the phenomenon of metal variability under different environmental conditions, four coastal localities (stations) along the north-east coast of the Saronikos Gulf were chosen for the sample collection. From each location 30 specimens of similar size (2.5 to 3 cm diameter) were collected and transported within an hour to the laboratory. There the soft parts were removed with a PVC knife, rinsed abundantly with distilled water and placed into PVC Petri dishes. Each individual was treated and analysed as a separate sample. Consequently the samples were lyophilised, homogenised in a porcelain mortar and digested with HNO_3 under pressure at 120°C for 12 hours.

The metals copper (Cu), nickel (Ni), chromium (Cr) and zinc (Zn) were determined by atomic absorption spectrophotometry using a VARIAN AA157 device. The above analytical methodology was tested by analysing the N°279 (*Ulva lactuca*) reference material of BCR. The results of this test are given in Table 1.

Table 1. Control of the analytical methodology

Metal	certified value	value found
Cu	51.2 + 1.9	46.49+1.35
Cr	26.0	22.39+1.49
Ni	40.0	44.22+1.32
Zn	313+8	269.4+4.6

The variability of metal bioaccumulation was studied graphically and by regression analysis and one way ANOVA after log-transformation of the results.

Results and discussion

The results of the chemical analysis (as average and ranges) expressed in μg/g dry weight are given in Table 2. Generally the levels of chromium and nickel in the present study are similar to published values while those for zinc are lower and that of copper higher (10-14). It is interesting to mention that the spatial distribution of metal bioaccumulation in limpets was statistically different ($P < 0.005$) in the four sampling localities. But in all localities, the bioaccumulation showed a high degree of variation that in some cases reached 80% (Table 2). This is mainly attributed to inherent variability in individual metal content since the specimens were of similar size and the regression analysis between metal content and diameter did not reveal any relationship ($P > 0.05$). In an attempt to show how this variability influenced

Table 2. Average concentrations of metals in *P. aspera* (in μg/g dry weight) and variability (coefficient of variation-%).

Station		Cu	Ni	Cr	Zn
1	AVG(SD	11.30 ± 1.97	9.96 ± 2.31	1.78 ± 1.12	44.47 ± 4.01
	range	7.24-17.24	5.70-15.13	0.40-4.67	37.76-55.57
	c%	17.40	23.24	62.84	9.02
2	AVG ± SD	9.48 ± 2.01	23.05 ± 6.91	8.42 ± 6.71	65.75 ± 14.06
	range	5.63-15.30	10.08-44.57	0.40-30.06	30.63-96.83
	c%	21.18	29.96	79.76	21.38
3	AVG ± SD	11.01 ± 2.16	30.36 ± 12.10	14.16 ± 6.27	59.57 ± 6.96
	range	6.48-15.63	5.50-53.74	3.50-36.21	45.36-76.19
	c%	19.59	39.87	44.28	11.68
4	AVG ± SD	11.20 ± 1.97	19.06 ± 5.02	6.63 ± 4.37	60.12 ± 8.89
	range	7.70-14.72	10.59-30..39	0.88-17.97	42.72-87.29
	c%	17.55	26.33	65.95	14.79

the accuracy of the estimated average value of metals in the populations of *P. aspera*, we calculated (for each sampling station) the mean concentration of metals using a consecutively increasing number of samples (from 2 to 30). The results of these calculations are presented graphically in Figure 1. It is obvious that the left portion of the graphs – where the number of samples is low – shows a significant fluctuation and the calculated mean differs from that derived from 30 samples. It is also evident that it differs from the real mean concentration ($\bar{i}$) of the population. The phenomenon is especially marked for all metals in curves for station 2 and for copper and nickel in the curve for station 3. The optimal number of samples of limpets for bioaccumulation studies can be graphically determined from Figure 1: from the point where the curve becomes quite stable (15). In this case, it seems that 8 to 12 individual samples of limpets are sufficient for an accurate population estimate. In fact, the average of 8 to 12 values matches closely with those calculated from 30 samples (Table 3, Fig. 1).

Table 3. Summary statistics for bioaccumulation of metals in *P. aspera* depending on the number of samples/individuals (N) per sampling location.

Station		Cu		Ni		Cr		Zn	
	N	AVG	S. D	AVG	S. D	AVG	S. D	AVG	S. D
1	2	12.54	1.82	11.23	3.13	1.68	0.11	45.99	3.65
	12	11.25	1.72	9.70	2.16	1.45	0.81	44.11	3.34
	30	11.30	1.97	9.96	2.31	1.78	1.12	44.47	4.01
2	2	7.61	1.98	18.16	3.16	2.63	0.50	45.16	14.54
	12	9.91	2.36	24.32	6.89	8.21	7.31	62.64	15.42
	30	9.48	2.01	23.05	6.91	8.42	6.71	65.75	14.06
3	2	10.86	0.15	24.10	6.26	11.54	2.62	56.32	3.25
	12	11.09	1.58	24.28	14.42	14.79	7.94	60.59	4.95
	30	11.01	2.16	30.36	12.10	14.16	6.27	59.57	6.96
4	2	10.96	0.48	19.46	1.50	3.54	0.82	62.87	12.24
	12	11.05	1.44	17.50	3.43	5.49	2.54	61.20	10.97
	30	11.20	1.97	19.06	5.02	6.63	4.37	60.12	8.89

Alternatively to the graphical estimation is the mathematical estimate using the variance and the mean value from preliminary data and the acceptable error in the determination of the mean (15, 16). Using this method and with a 10% error, a variable number of samples is needed depending on the metal (Table 4). For Cu, Ni, and Zn, it seems that 8 to 12 samples are sufficient, while for Cr which displays a higher variability, the optimal number increases dramatically. However Puel *et al.* (6) have estimated a larger sample size (20 replicates) in order that an average concentration can be computed with a 5% error.

DEVELOPMENT OF ANOXIA IN THE SMALL COASTAL SEA LAKE, ROGOZNICA LAKE (EASTERN ADRIATIC COAST)

Ciglenecki* I. [1], Kodba Z. [1], Vilicic D. [2], Caric M. [3], and Cosovic B. [1]

[1] Rudjer Boskovic Institute, Center for Marine Research, Bijenicka 54, 10001 Zagreb, Croatia
[2] Faculty of Science & Mathematics, Dpt. of Botany, Roosewelтov trg 6, 10001 Zagreb, Croatia
[3] Institute of Oceanography and Fisheries, Laboratory of Plankton Ecology, 20001 Dubrovnik, Croatia

Abstract

Variations of temperature, salinity and concentration of dissolved oxygen, as well as vertical distribution of dissolved organic matter (DOC), surface active substances (SAS), phytoplankton, nutrients (NH_4^+, NO_3^-, NO_2^-, PO_4^{3-}, SiO_4^{4-}) and reduced sulfur compounds in the small, intensely eutrophicated, 15 m deep sea-lake, Rogoznica Lake, have been investigated during different seasons in 1996. Anoxic conditions in the lake and high concentrations of sulfur compounds (up to 10^{-4} M, mainly in the form of sulfide) were detected below 12 m depth during periods of stable stratification. Also, at the same time below 10 m depth, relatively high concentrations of organic matter (SAS up to 0.3 mg dm^{-3} equiv. Triton-X-100, DOC up to 0.22 mM), SiO_4^{4-} (up to 112 μM) and PO_4^{3-} (up to 1.9 μM) were detected, indicating the start of more pronounced remineralization. The stratification and mixing of lake water in 1996 were greatly influenced by rainfall as shown from decreased salinity in deeper waters. During the spring 1996 high phytoplankton activity over the entire water column and extremely high production of oxygen (oxygen saturation up to 300%) probably prevented the expected development of anoxia from occurring.

Key-words: anoxia, phytoplankton, Adriatic Sea

Introduction

Rogoznica Lake is a small, intensely eutrophicated sea-lake situated on the eastern coast of the Adriatic Sea (Fig.1). The lake is surrounded with sheer cliffs (4 - 23 m high) and has an area of about 5300 m^2 and the maximum depth of 15 m. Rogoznica Lake is a very interesting area for the study of biogeochemical processes owing to permanent stratification [1]. Vertical mixing occurs during winter when cold, oxygen-rich water from the surface sinks downwards. Despite of permanent water exchange between Rogoznica Lake and the surrounding sea through the porous karst [2], anoxic conditions are established in deeper layers of the lake, probably due to remineralization of organic matter produced in periods of intensive primary production. During thermohaline stratification, the surface water is well oxygenated while the layer below 9 m depth is anoxic [3, 4]. Anoxic deep water is rich in sulfur (up to 900 μM), especially sulfides and elemental sulfur [3]. The distribution of iodine species was found to be strongly influenced by the occurrence of anoxic conditions in the lake [4]. Phytoplankton was composed of a relatively small number of species which were mostly distributed above 10 m depth. The heterotrophic dinoflagellate *Hermesinum adriaticum* is mostly found near the oxic/anoxic interface of Rogoznica Lake [5].

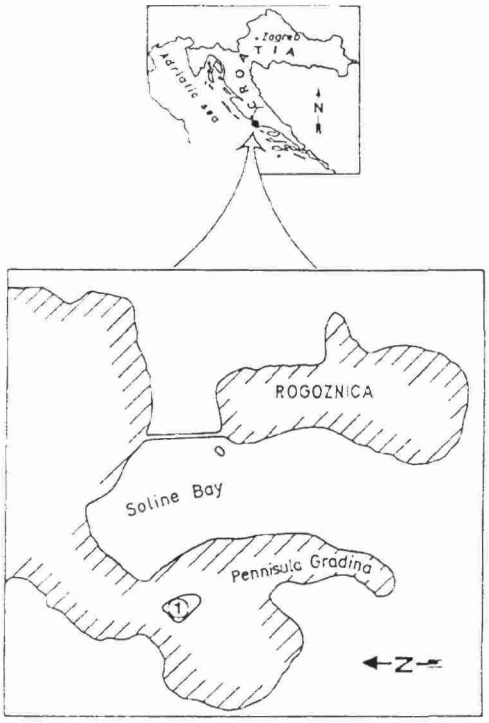

Fig. 1. Geographical position of the Rogoznica Lake.

This study describes the development of anoxic conditions, as well as the seasonal vertical distribution of dissolved organic matter, surface active substances (SAS), phytoplankton cell-density, nutrients and sulfur compounds in Rogoznica Lake during 1996.

Experimental

Electroanalytical methods of a.c.- and linear sweep voltammetry were used for the determination and speciation of sulfur compounds (sulfide, polysulfide, elemental sulfur, thiosulfate, organic sulfur) in the lake water [6-9]. The determination of each of these sulfur species is based on the intereaction between sulfur and the mercury electrode. Analytical determination of elemental sulfur, sulfide and polysulfide was based on acidification of the sample and elimination of sulfide with purging by nitrogen [3-9].

Electrochemical determination of $S_2O_3^{2-}$ is based on the cathodic stripping of formed $Hg(S_2O_3)_2^{2-}$ during the negative scan from 0 to -1 V vs.Ag/AgCl [9]. The appearance of voltammetric peaks of HS- and $S_2O_3^{2-}$ on the different potentials enables their determination in the mixtures. Rogoznica Lake samples were collected with Niskin bottles with over pressurized N_2. All samples were immediately measured unfiltered within 24 h to prevent biotic and abiotic processes which can change the content and speciation of sulfur species. Samples with very high concentrations of sulfur (up to $1 \cdot 10^{-6}$ M) were measured either by dilution with 0.5 M NaCl or by changing the measurement conditions (accumulation time).

Oxygen content was determined by the standard Winkler method. The content of surface active organic matter (SAS) was determined by a.c. voltammetry (out of phase mode and expressed as equiv. to Triton-X-100) [10] and DOC measurements were performed using a Shimadzu TOC-500 Analyzer which includes a high temperature oxidation system.

Phytoplankton cell counts were obtained by the inverted microscope method according to Utermöhl [11]. Nutrients were determined by standard oceanographic methods outlined by Strickland and Parsons [12]. Temperature and salinity were measured *in situ* with a Hg-thermometer and refractometer (Atago, Japan).

Results and discussion

During the study anoxic conditions with high concentrations of sulfur compounds (up to 10^{-4} M, mainly in the form of sulfide) were detected only below 12 m depth during the summer months as the result of increased stratification of the water column in spring. Besides the strong stratification, high phytoplankton activity (diatom bloom, 10 million cells/dm^{-3}) with extremely high production of oxygen (oxygen saturation up to 300%) and organic matter (SAS up to 0.3 mg dm^{-3}) was detected in the entire water column (0-12 m) during the spring months. After the spring, the diatom bloom decreased and remineralization of organic matter and development of anoxia with more pronounced production of reduced sulfur compounds and amonia, as well as higher values of DOC, phosphate and silicate were observed below 10 m depth (Fig. 2 A-F). In comparison to the situation in Rogoznica Lake recorded during 1994 and in April 1995, when the boundary between oxic and anoxic sulfur rich water (concentration of

ANNUAL FLUXES OF NITROGEN AND PHOSPHORUS THROUGH THE STRAIT OF OTRANTO (EASTERN MEDITERRANEAN)

G. Civitarese [1*], M. Gacic [2], A. Vetrano [3], A. Boldrin [4], S. Rabitti [4]

[1] CNR-Istituto Talassografico, Trieste,Italy
[2] Osservatorio Geofisico Sperimentale, Trieste, Italy
[3] North Carolina State University, Raleigh, NC, USA
[4] CNR-Istituto di Biologia del Mare, Venezia, Italy

Abstract

Annual rates of nutrient fluxes through the Strait of Otranto are assessed. The Adriatic Sea exports nitrate and phosphate but imports dissolved and particulate organic matter. Total nutrient fluxes are almost balanced. This suggests that the mineralization takes place in the southern Adriatic, and that the highly eutrophic northern Adriatic area has little influence on the rest of the basin.

Key-words: nutrients, Adriatic Sea

Introduction

The Strait of Otranto forms a 75 km wide, and up to 800 m deep connection between the Adriatic and Ionian seas (Fig. 1). The study of its dynamics and biogeochemistry is crucial for estimating budgets and long term changes in the Eastern Mediterranean. A series of seasonal cruises and Eulerian current measurements in the Otranto Strait were carried out to study the biogeochemical characteristics of the strait and to estimate the exchange of water, dissolved nutrients and particulate matter between the Adriatic and the Ionian Sea.

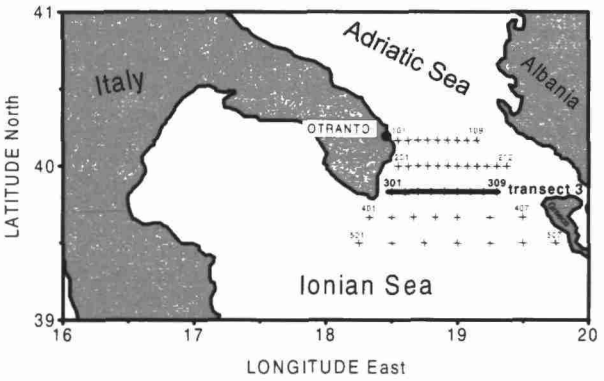

Fig. 1. Study area and station locations.

Fluxes computation

The grid of stations occupied during six seasonal cruises (OTR1-February 94, OTR2-May 94, OTR3-August 94, OTR4-November 94, OTR5-February 95, OTR6-May 95) is presented in Fig. 1. The current data span variable time intervals ranging from 53 days (station 308 at surface) to 597 days (station 304 at intermediate level). Mean current values were calculated by averaging all available time-series at each measurement location (for details on the experimental design, see [1]). The averaged current field was then interpolated over a regular grid (Fig. 2), and the fluxes of water across the strait calculated.

The same interpolation procedure was applied to the annual averaged chemical concentrations (Fig. 2), obtained by using the experimental data on nitrate, phosphate, and particulate nitrogen from seasonal OTR3, OTR4, OTR5 and OTR6 cruises along transect 3, the same transect where current meter moorings were deployed. Due to the low seasonal variability of the distribution patterns over the major portion of the water column except for the surface layer, the use of annual averages does not introduce any significant error into the flux computations. The resulting current and chemical concentration data interpolated to the same regular grid were then multiplied to estimate the material fluxes.

Results and Discussion

Vertical distribution (Fig. 2) of the longitudinal current component shows a cyclonic shear over the entire water column with a maximum inflow/outflow in the surface layer. Another local maximum occurs in the bottom layer associated with the Adriatic Deep Water (ADW) outflow. Dissolved nutrient distributions (Fig. 2) show depleted surface layer (0-50 m), separated from the rest of the water column by a nutricline centered at about 100 m depth. The slight decrease of nitrate and phosphate in the bottom layer is associated with the ADW. In contrast, particulate matter displays maximum concentrations in the surface layer while the rest of the water column (below 300 m depth) is very poor in particulate nitrogen.

Annual flux computations (Fig. 3) show a net loss from the Adriatic of nitrate (29,500 x 10^6 moles y^{-1}) and phosphate (950 x 10^6 moles y^{-1}), representing 26% and 21% of the total export, respectively. Particulate nitrogen (PN) exhibits a net gain of 2,170 x 106 10^6 moles y^{-1} respectively, representing about 30% of the total import (see Table I for explanation). There is also an almost perfectly balanced water exchange as would be expected.

A more detailed analysis of the contributions of the various layers to the exchange is reported in Figure 3. The loss in the layer between 200 m depth and the bottom is responsible for the net annual nutrient export from the Adriatic. On the other hand, for the particulate matter, the most active layers in terms of the transport are the uppermost (from the surface down to 200 m). PN flux computations result in a net positive imbalance (particulate matter gain for the Adriatic by exchange through the Strait of Otranto). This was unexpected because it is known that the western part of the strait, occupied by waters of Adriatic origin, is richer in particulate matter than the eastern sector [2]. We must, however, take into account that the transport is the result of the combined action of water transport and mass distribution. Considering the annual average fluxes of water (Fig. 3), it is evident that the layer from 0 to 200 meters shows a net positive imbalance, giving rise to the corresponding net positive transport of particulates. On the other hand, the higher water flux out of the Adriatic in the layer from 200 meters down to the bottom cannot compensate for the imbalance of particu-

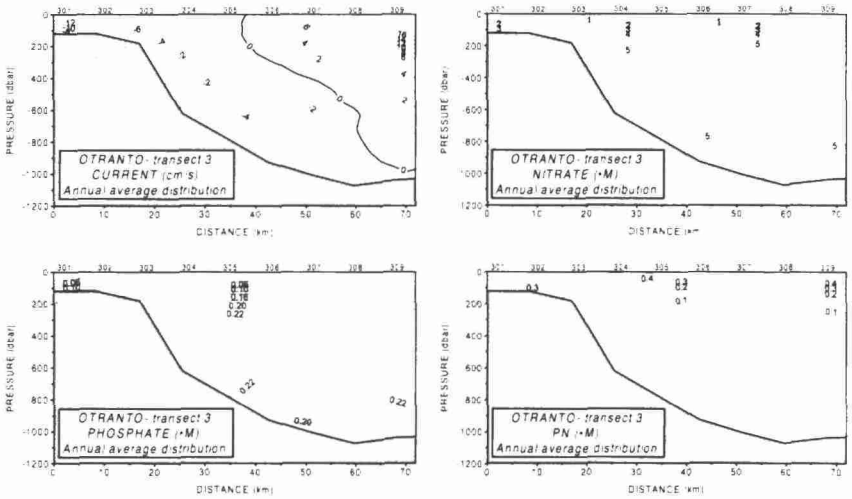

Fig. 2. Annual average vertical distribution of the north current component and biogeochemical compounds.

A COMPARATIVE STUDY ON THE METALLOTHIONEIN CONTENT OF SIX MARINE BENTHIC ORGANISMS

Efthimia Cotou [1], Vassilios Roussis [2]*, Theodora Rapti [2] and Constantine Vagias [2]

[1] National Centre for Marine Research, Agios Cosmas, Hellinikon 16604, Athens, Greece

[2] University of Athens, Department of Pharmacy, Division of Pharmacognosy, Panepistimiopolis Zografou, 157 71, Athens, Greece

Abstract

The levels of the metallothionein content of five bivalves and one ascidian collected from two different sites ion the central Greek coast were determined spectrophotometrically using Ellman's reagent. The marine organisms used in this study can be found in quite diverse environments. The studied specimens were collected from the same areas and had been exposed to the same pollution levels. The results of this preliminary study showed that all investigated bivalves expressed very similar concentrations of metallothioneins. The ascidian showed lower levels of metallothioneins but still within the same order of magnitude.

Key-words: bivalves, metals, Aegean Sea

Introduction

The last decades great scientific efforts have been devoted towards the assessment of the bioavailability of metals in the aquatic ecosystems and the development of methods for the determination of their environmental impact [1,2].

Studies have shown that water and sediment analyses cannot be used to predict or assess environmental impact. It is known that benthic invertebrates are capable of accumulating metals at concentrations many thousand times greater than those present in the surrounding water and therefore can be used for determinations of the accumulation of metals in animals from polluted sites. Based on these facts the concept of "indicator organisms" for filter feeding bivalves, on suspended particulate metals was formulated [3, 4, 5, 6].

Metallothioneins are metal complexes of the sulfur rich protein, thionein and can be found in a wide array of marine organisms. Metallothioneins are complexes of small proteins with a molecular size ranging between 6.000 and 7.000 Daltons. MTs consist of 60-62 amino acids and contain 20 cysteine residues which do not form disulfide bridges. So far, four different charge isoforms of MTs have been identified and it has been suggested that the role of MT is to protect the organisms against the toxic effects of certain metals. The induction of MT synthesis was first demonstrated with high doses of cadmium and it was shown that once the synthesis of MTs is initiated, the producer organism can withstand higher levels of Cd^{2+}. Most of the studies on MT have been done in relation to cadmium, since it is one of the most toxic metals. Other essential trace metals such as Cu and Zn were proven capable to complex with MTs as well.

The major consideration towards the "bioindicators" approach, for the assessment of environmental impact, is the selection of the most suitable organism that could be used globally for the "biomonitoring". Several marine invertebrates, including commonly occurring species such as worms, molluscs (including clams, mussels, oysters and scallops) and crustaceans possess specialized mechanisms for immobilizing and accumulating excess metals in specific organs, cell types or in specific metallothioneins [7, 8, 9, 10].

Extensive work has been done on the metal uptake by oysters (*Crassostrea* or *Ostrea* spp) for the reason that oysters rather than mussels are found in most areas of the eastern coast of the USA. It is known that oysters possess a metallothionein of 75 amino acids with 21 cysteine residues the synthesis of which is induced upon exposure of the oyster to cadmium. The difficulty with these organisms is the occurrence of naturally high metal levels, metal displacement reactions and competition between sequestration mechanisms [11].

One of the organisms that combines the majority of the selection criteria is *Mytilus galloprovincialis* (Lamarck). This mussel species is quite common in most of the Mediterranean coastal areas. Even though *M. galloprovincialis* is a common bivalve in the Mediterranean basin there are still many areas that it cannot be found. The habitat of the *M. galloprovicialis* is the littoral and sublittoral zone and is very infrequently found at depths greater than 5 meters. The scope of this study is to determine the MT levels in some of the common bivalves and mussels found around the coasts of Greece and correlate those with the values obtained from the respective assays employing *M. galloprovincialis*.

Methods and materials

In order to find organisms that could provide supplementary data to those obtained from *M. galloprovincialis*, in the framework of an environmental assessment programme, five of the most common marine benthic organisms were investigated. The other studied organisms were: *Chlamys varia* (Linnaeus), *Cerastoderma edule* (Linnaeus), *Venus verrucosa* (Linnaeus), *Mactra corallina* (Linnaeus) and *Phallusia mammilata* (Cuvier). These organisms can be found in a wide array of habitats and depths (2-140 meters). Some of them grow on rock formations and others are burrowing in sand, gravel or mud. *C. edule* can tolerate salinities between 3,4% and 4,0% [12]. The specimens used in our studies were hand collected by scuba divers and were brought alive to the laboratory for the determination of MTs. The collection sites were the Gulf of Elefsis (Neraki) and the Gulf of Chalkis (Chalia). Care was taken to use individuals of the same size, since size roughly represents the age of the organisms. The specimens were found no more than 100 meters apart from each other. All species were identically treated in order to minimize experimental errors.

The bivalves were dissected and the digestive glands were removed and homogenized. In the case of *Phallusia mammilata* only part of the digestive track of the ascidian was used for the assays. The experimental protocol applied was the spectrophotometric assay suggested by Prof Viarego [1] for the determination of MTs in *M. galloprovincialis*. The small size proteins were isolated from the homogenized tissue, through a series of precipitations and resolubilizatios and were allowed to react with DTNB (5,5-dithiobis-2-nitrobenzoic acid). The colored solutions were then analyzed photometrically and based on the values of standard solutions; the absorbancies were correlated to concentrations of MTs (μg of MT/gr of tissue).

Results and discussion

Between 4 and 7 samples from every organism were assayed and the average of the values along with the standard deviation is shown in the following table.

Table 1: Concentration of metalothioneins (μg/ g of tissue) in selected organisms

organism	Average Concentration	Standard Deviation
Mytilus galloprovincialis	175.869	27.435
Chlamys varia	264.041	38.765
Cerastoderma edule	198.207	4.828
Venus verrucosa	172.401	13.854
Mactra corallina	240.484	20.553
Phallusia mammilata	101.670	12.263

It is clear from the above data that the concentrations of MTs in all investigated organisms are comparable. *C. varia* and *M. corallina* exhibited the highest and *P. mammilata* the lowest levels of MTs. It is worth noting that *C. edule*, among all organisms investigated showed the smallest individual variation in the concentration of MTs.

In order to confirm that the highest levels of MTs are found in the digestive track of the organisms, the gills and the digestive gland from a set of *C. edule* were dissected and separately analyzed (Table 2).

Table 2: Comparison of the metallothionein levels in different tissue types of the same organism.

Tissue	Average Concentration	Standard Deviation
Digestive gland	198.207	4.828
Gills	120.394	5.053

LIPID COMPOSITION OF SUSPENDED AND SINKING PARTICLES COLLECTED BY SEDIMENT TRAPS IN THE GULF OF TRIESTE DURING JUNE 1995

Derieux S. [1*], Saliot A. [1], Fillaux J. [1], Cauwet G. [2] and Wassmann P. [3]

[1] Laboratoire de Physique et Chimie Marines de l'Université Pierre et Marie Curie, Observatoire des Sciences de l'Univers, URA CNRS 2076; Tour 24, 4 Place Jussieu, 75252 Paris Cedex 05, France

[2] Groupement de Recherche Interactions Continent-Océan, Obs. Océanologique CNRS, Lab. Arago, F- 66650 Banyuls/mer, France

[3] Norwegian College of Fishery Science, University of Tromsø, 9037 Tromsø, Norway

Abstract

Organic carbon and lipid class composition were determined for suspended and rapidly sinking particles in June 1995 in the Gulf of Trieste, Adriatic Sea. Analyses of lipids were carried out by chromarod thin-layer chromatography with flame ionization detection in order to give insight into stuctural components of biomembranes from living organisms, metabolic energy reserves and compounds originating from the breakdown of glycerides in dying cells and detritus. Lipids/organic carbon ratio and lipid class distribution patterns showed large variations between the two types of investigated particles. Lipid composition of suspended and sinking particles suggested that trap material did not reflect an aggregation of small-size suspended particles at this time of year.

Key-words : carbon, particle flux , Adriatic Sea

Introduction

The coupling between production of matter in the upper ocean layers and accumulation in sediments is mainly related to fast-sinking particles such as aggregates and fecal pellets. The efficiency of this coupling is highly significant for the flux of organic matter to sediments. The organic matter flux, identified as part of the biological pump for CO_2 in the ocean, represents a primary potential source of energy for the deep pelagic and benthic food webs (1-3). Among various compounds lipids, although representing a minor fraction of the total analysable organic carbon, play a key role because of their energetic value which has often been recognized for pelagic and benthic organisms. In the framework of the Paloma programme (Production and Accumulation of Labile Organic Matter in the Adriatic), one of our objectives was to give insight into processes of formation of fast sinking particles and into knowledge of lipids associated with the flux of organic matter in the water column. Thus, a chemical study of various types of particulate material was performed in the Gulf of Trieste in Summer 1995 (see Fig. 1). We present here data dealing with: 1) a comparison of lipids associated with surface suspended particles collected by filtration of seawater, and fast sinking particles collected by drifting sediment traps; 2) an estimation of fluxes of various lipid classes throughout the water column.

Material and methods

All samples were collected from the semi-enclosed, shallow Gulf of Trieste in the Northern part of the Adriatic Sea (Fig. 1). The Gulf of Trieste has a surface area of about 600 km^2 and a maximum depth of 25 m. The most important source of freshwater along with allochthonous nitrogen is the Isonzo River, with high interannual variability in discharge and consequent phytoplankton blooms (4).

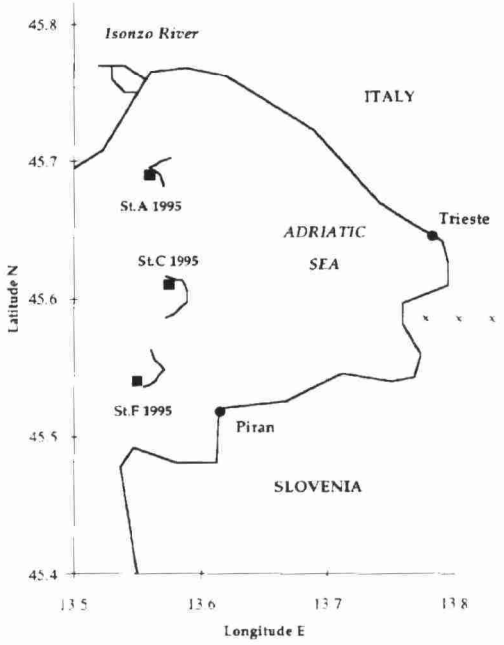

Fig. 1 : The Gulf of Trieste. Location map of sampling sites and trajectories of the drifting sediments traps (June 1995).

Double, gimballed cylindrical sediment traps, 573 mm high, 72 mm wide, equipped with a vane, were deployed in a drifting mode in June 1995 at 5 and 9 m (trajectory around station A), at 5 and 12 m (trajectory around station C) and 5, 9, 12 and 16 m (trajectory around station F), (Fig. 1). Drifting time was about 12 hours. Prior to deployment, traps were filled with seawater from the actual sampling depth to avoid contamination from surface water without addition of any preservative. Upon retrieval of the drifter, the content of each couple of traps was collected and thouroughly mixed before subsampling. Organic carbon and inventory of biological material (phyto- and micro-zooplankton and fecal pellets) were also determined on sediment trap material (5).

Simultaneously to the trap deployment, CTD profiles were recorded along the trajectory of the drifting traps, water samples were taken at several depths for analyses of nutrients, POC and PON (6), and large volume water samples were collected respecting ultra-clean conditions by *in situ* pumping (20 l) and filtered on board through 0.7 μm pore size Whatman GF/F filters to obtain suspended particles for further lipid analyses.

Lipids were extracted by the one phase solvent mixture methanol-water-chloroform procedure (7). Total lipid extracts were analysed for lipid classes by thin layer chromatography with the flame ionization detection (TLC-FID) Iatroscan technique which is sensitive and quantitative for each lipid class with internal calibration (8).

Results

The drifting trajectories are given in Figure 1. During June 1995, which was characterized by heavy rain fall previous to the experiment and consequent massive discharges from the Isonzo River, the traps were deployed three times in the plume close to the river mouth (A), in the centre of the gulf (C) and close to the coast of Slovenia (F).

Temperature decreased steadily from the surface (21-25°C) to the bottom (13-15°C). The vertical profiles of salinity reflected the discharge of Isonzo River. Closest to the river mouth (A), salinity increased sharply from about 21 to 34 from the surface to 3 m depth. In the centre of the gulf (C) salinity increased from about 23 (in surface) to 33 (at 10 m). In the south (F), salinity was higher and the increase was smaller, 31 (in surface) to 37 (at 10 m).

Phosphate concentration was low (0.01 to 0.14 mM). Ammonia ranged between 0.1 to about 2.5 μM (usually lower than 0.5 μM in the upper 10 m) and increased in the lower part of the water column. Nitrate concentrations were low in the bottom water, ranging from 0.4 to about 1.4 μM and increased towards the surface. Concentrations > 100 μM were recorded in the river plume 6. Silicate varied between 0.4 and more than 30 μM in the surface layer.

Concentrations of particulate organic carbon (POC) and lipids of suspended particles were highly variable during the sampling cruise. POC varied from 207 μg/l at 1 m at station C, up to 628 μg/l at station A (at 1 m), whereas lipid concentrations varied from 32.6 μg/l at station A (at 10 m), up to 139 μg/l at station A in surface water. Thus the percentage of organic carbon associated with lipids varied in the range 14.3 - 37.2, with an average of 25.5 (n = 10).

HEAVY METAL CONCENTRATIONS IN SOME MOLLUSCS AND IN SURFICIAL SEDIMENTS FROM IZMIR BAY / TÜRKEY

Özdemir Egemen*, Ugur Sunlu, Asly Kaymakçi

Ege University, Faculty of Water Products 35440 Yskele- Urla-Izmir, Turkiye

Abstract

Izmir bay has been affected by industrial and heavy metal pollution from the surrounding facilities and domestic effluent from the city. Concentrations of heavy metals (Pb, Cd, Cu, Zn, Ni) have been determined in the common edible molluscs *Mytilus galloprovincialis* (L. 1758), *Cerastoderma glaucum* (B. 1789) and *Tapes decussatus* (L. 1758) collected from different regions of Izmir Bay along with bottom sediment samples from their environment. Samples were analysed seasonally from May 1994 to February 1995. The levels of heavy metals in *M. galloprovincialis* L. 1758 ranged between 0.04-1.12 μg Cd/gr wet weight, 0.58-1.82 μg Pb/gr wet weight, 9.55-58.50 μg Zn/gr wet weight, 0.32-3.25 μg Cu/gr wet weight and 0.30-3.25μg Ni/gr wet weight. Corresponding ranges were 0.08-0.20 μg Cd/gr w.w., 0.20-2.85 μg Pb/gr w.w., 10.70-22.10 μg Zn/gr w.w., 0.80-3.48 μg Cu/gr w.w., 0.80-2.35μg Ni/gr wet weight in *T. decussatus* and 0.08-0.51 μg Cd/gr w.w., 0.72-2.15 μg Pb/gr w.w., 8.70-20.55 μg Zn/gr w.w., 0.60-5.58μg Cu/gr w.w., 5.18-9.21μg Ni/gr w. w. in *C. glaucum*. Concentrations of heavy metals in surficial sediments varied between 1.60-3.70 μg Cd/gr dry weight, 24.10-54.50μg Pb/gr d.w., 11.00-68.20 μg Zn/gr d.w., 7.50-28.50 μg Cu/gr d.w. and 29.00-110.00 μg Ni/gr d.w.

Key-words: Pollution, bio-accumulation, Aegean Sea

Introduction

More than 3 million people live near Izmir which is located at the western end of Anatolia. Parallel to the population growth, there has been a rapid increase in fisheries, industrial and commercial activities. The domestic and industrial wastes of this densely populated settlement enter the Bay water. The untreated waste waters of Izmir city, consisting of factory discharges (leather, textiles, food, detergents, beverages, chemical etc.) and sewage, are released directly into the Bay through 128 canals and 10 streams. All these wastes dumped into the sea could have an adverse effect both on the marine organisms and the water quality; hence, Izmir Bay has become an important focal point for potential marine pollution in Türkiye. The main sources of pollution are organic substances, suspended matter, hydrocarbons, heavy metals and pathogenic microorganisms.These contaminants reach the Bay in many ways such as domestic and industrial wastes (50%), rainfall (15%), rivers and streams (10%), agricultural pesticides and fertilisers (10%), erosion (8%), Bay activities and traffic (4%) and other sources (3%) (1).The aim of this study was to investigate the present status of the distribution of heavy metals in economically important molluscs and their environment, *i.e* bottom sediments and compare these results with other coastal areas of Türkey and the Mediterranean Sea.

Study area

Izmir Bay, situated in the western coast of the Aegean Sea, lies between 38° 20'-38° 42' N latitude and 29° 25'-27° 10' E longitude. From the topographic and hydrografic point of view, it is divided into the inner, middle and outher bay regions (2) (Fig. 1). The inner bay is connected to the middle and outer bay by a narrow channel. The length of the coast is 55 km and the width varies between 2.5-6.4 km. The area of the bay is roughly 65.5 km^2 and the volume of the sea water 636.6 x 10^6 m^3. The average depth of bay is about 20-25 m. The inner bay which is shallower reaches a maximum depth of about 12-15 m., whereas the middle and the outer bay which is deeper reaches a maximum depth of 70 m. (Fig. 2).

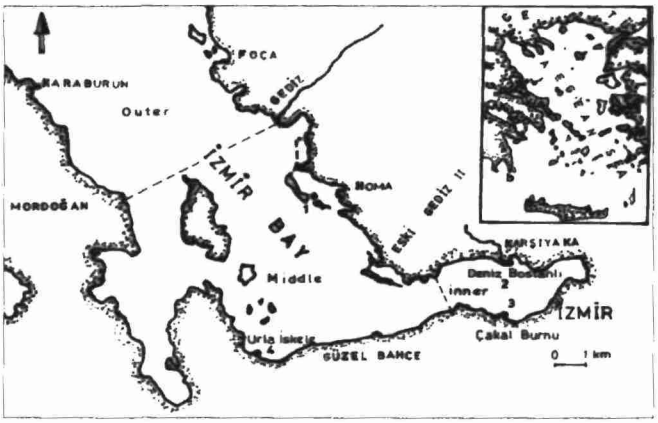

Fig. 1. Map of sampling locations. (2)

Materials and methods

This study was carried out at two stations of the inner bay and two stations in the middle bay as indicated in Fig 1. Samples were analysed seasonally from May 1994 to February 1995. Edible molluscs and surficial sediment samples were collected from these stations at the same time. *Mytilus galloprovincialis* (Mediterranean mussel), *Tapes decussatus* (Surf clam) and *Cerastoderma glaucum* (Cockle) were collected by hand and transported daily to the laboratory. These samples were kept in a deep freeze (-21°C) until analysis and were prepared according to international standard methods (3). The composite samples of molluscs were weighed and digested with conc. HNO_3 : $HClO_4$ (5:1) (extra pure Merck) under reflux and filtered. Sediments were collected seasonally with a "Orange peel" grab of capacity 4,5 l. then stored in plastic bags at -21°C. Each sediment sample oven dried at 60°C for 24 h and then sieved using a mesh. From the dried sediment samples,. an aliquot of 1g (<160 μ) was oxidized with 10 ml., conc. HCl:HNO_3 (3:1) (extra pure Merck) under reflux at 120°C for h and then filtered through Whatman 40 filter paper. All samples were diluted with bidistilled water and analysed (4). Metal samples were analysed by atomic absorption spectrophotometery using a 2380 Perkin-Elmer (AAS). Metals were determined by direct aspiration using an air acetylene flame. Intercalibration homogenate samples (MA-A-2, SP-M-1, from the IAEA, Monaco Laboratory) were used as a quality control for the analytical methodology.

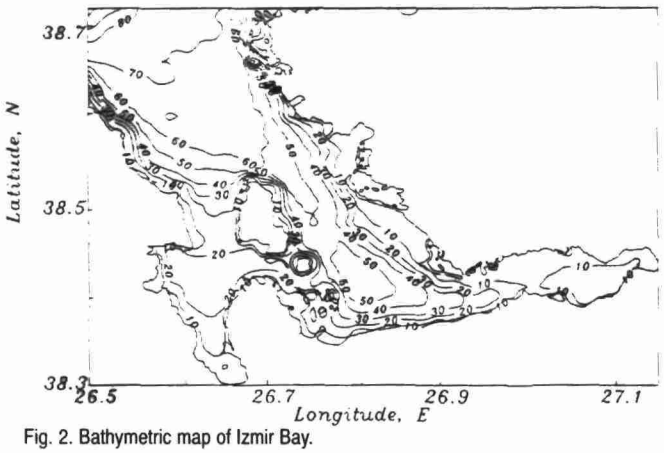

Fig. 2. Bathymetric map of Izmir Bay.

Results

Molluscs. The concentrations of some heavy metals (Pb, Cd, Cu, Zn, Ni) in the tissues of the afore mentioned species were determined separetely from different regions of Izmir Bay. Minimum, maximum and mean levels of these metals in the various species are given in Table I. It is evident from the table that there are differences in the metal concentrations according to the species and localities. Heavy metal concentrations in *M. galloprovincialis* are slightly higher than in *C. glaucum* and *T. decussatus*. The sites of Deniz Bostanlysy [2] and Çakalburnu [3] are in the inner bay, Homa [1] and Urla Iskele [4] are in the middle bay. The outer bay is less contaminated than the inner and middle parts of the bay. According to our results, levels of heavy metals in all mollusc species from the inner and middle parts of the bay are higher than in the outer bay. *M. galloprovincialis* seems to be much better adapted to the environmental conditions of contaminated bay waters than the other molluscs (5).

Sediments. Table II presents the minimum, maximum and mean values obtained from analyzing the superficial sediments of Izmir bay. According to the results obtained (40 samples), surface sediments from the study area show heavy metal concentrations similar to those reported for other polluted Mediterranean regions (Table IV). Levels of contamination by heavy metals in the inner bay is more important due to the factories, harbour activities and domestical discharges, but a clear decrease upon leaving this zone is also noted.

ELECTROCHEMICAL CHARACTERIZATION OF CADMIUM-BINDING PROPERTIES OF METALLOTHIONEIN

Marijana Erk* and Biserka Raspor

Ruder Boskovic Institute, Center for Marine Research Zagreb, P.O.Box 1016, 10001 Zagreb, Croatia

Abstract

A voltammetric study on the binding properties of the metallothionein (MT) for cadmium ions was performed. The capacity of metallothionein to complex cadmium and the stability constants of cadmium-thionein complex have been determined from the direct titration of MT with cadmium ions in model seawater medium at pH 7.9. At this pH the formation of the Cd-T complex has been followed measuring the specific anodic signal height of the complex. The apparent concentration stability constants of Cd-T complex, $K'=(7.6\pm0.2)\cdot10^8$ $dm^3\ mol^{-1}$, in 0.59 M NaCl, pH=7.9, 25°C, have been evaluated from the experimental data using three different procedures.

Key-words: cadmium, electrochemistry

Introduction

Metallotioneins (MTs) are low molar mass (6000 to 7000 for the protein of mammalian origin) metal-binding proteins known to occur in all animal phyla as well as in fungi, in some plants and cyanobacteria (1). The protein was designated as "metallothionein" on account of its exceptionally high metal and sulphur content (2). SH-groups involved in the metal coordination are considered essential to the structure and the function of the protein. MTs induced in the hepatic tissues are specific molecular biomarkers of the exposure of vertebrate and invertebrate species to metals (3,4). They can be induced by and bind the essential metals copper and zinc, and toxic metals such as cadmium, mercury and silver. MTs of mammalian origin are characterized in detail regarding their biological and physico-chemical features, the binding sites, stoichiometry and geometry of metal complexes (1). To the mammalian protein 7 atoms of Cd(II) are bound per MT molecule (Cd7-MT), and metal is tetrahedrally coordinated in two isolated domains with stoichiometries of M_4S_{11} and M_3S_9 (5).

The induction of MTs in *Mytilus* sp. has been determined in both laboratory and field studies (6-10). In contrast to the mammalian type of MTs, the mussel type of MTs is insufficiently characterized. It has recently been published (11) that the mussel MTs consist of seven isoforms and exhibit more similarity to the vertebrate MTs than to those of non-molluscan invertebrates. Isoforms of mussel MTs exhibit homology to the mammalian class I MTs. Therefore, a preliminary study on cadmium binding properties of commercially available well defined MTs of mammalian origin has been performed in order to evaluate the experimental conditions and the procedure suitable for subsequently studying cadmium binding properties of MTs isolated from the *Mytilus* sp. which are insufficiently characterized (12, 13). The purpose of providing complexing data on this specific inducible type of protein with Cd^{2+} is to gain a better understanding of the biological role of MTs during metabolism and detoxification of cadmium ions.

Experimental

A simple model seawater medium, *i.e.* 0.59 M NaCl solution was used in order to reduce the competitive reactions with Cd^{2+} as would occur in a complex medium of genuine seawater (14). The pH of model seawater was kept at pH 7.9 with the borate buffer. When needed, the model seawater was acidified to pH<2 with the destiled HNO_3. The standard Cd^{2+} solution (1.000±0.002 g/l) was prepared from the Titrisol solution (Merck, Germany), which contains $CdCl_2$. Metallothionein (MT I+II rabbit liver M7641) was produced by Sigma (USA). All solutions were prepared with Milli-Q water.

The voltammetric technique has been applied due to its sensitivity and selectivity in determining metal content and various chemical forms. The measurements were carried out with a μAutolab instrument (Eco Chemie, The Netherlands). Voltammetric measurements were performed under potentiostatic control with a three-electrode system consisting of a Metrohm 290E hanging mercury drop electrode (HMDE) as a working electrode, a platinum wire as a counter-electrode and a reference Ag/AgCl-saturated KCl electrode, which was connected to the cell by a salt bridge filled with 0.59 M NaCl (suprapure, Merck) in a 20 ml Metrohm-type polarographic cell. Measurement parameters set up for differential pulse anodic stripping voltammetry (DPASV) were the following: deposition potential -0.9 V vs. the potential of reference electrode, deposition time 120 s, resting time 30 s, pulse amplitude 25 mV, pulse duration 57 ms, scan rate 5 mV/s and clock time 0.5 s. All measurements were performed at constant temperature of (25.0±0.5)°C.

Results

Titrations of MT Sigma M7641 have been carried out with a standard $CdCl_2$ solution at pH=7.9 and pH<2 in a well defined electrolyte (0.59 M NaCl). At pH=7.9 two distinct anodic signals which represent two types of cadmium species (12, 13) are observed on the voltammograms. One type corresponds to the cadmium-thionein complex (Cd-T - where T denotes the apoprotein molecule), with the peak potential at -0.67 V vs. Ag/AgCl reference electrode (Fig. 1).

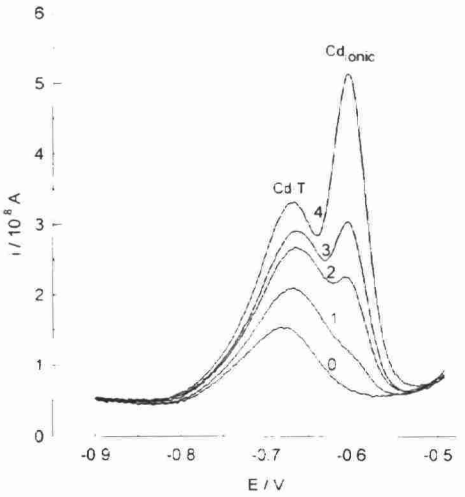

Fig. 1. Current-potential curves of $3.2\cdot10^{-8}$ M MT in 0.59 M NaCl at pH=7.9 (curve 0). Concentration of added $CdCl_2$ was the following: $7.10\cdot10^{-9}$ M Cd(II) (curve 1); $1.06\cdot10^{-8}$ M Cd(II) (curve 2); $1.42\cdot10^{-8}$ M Cd(II) (curve 3); $2.48\cdot10^{-8}$ M Cd(II) (curve 4). Two types of Cd(II) species are denoted as Cd-T complex (where T denotes the apoprotein molecule) and Cd_{ionic}.

The other one corresponds to the Cd_{ionic} (comprising hydrated Cd^{2+} ions and Cd(II)-chloro complexes), with the peak potential at -0.60 V vs. Ag/AgCl reference electrode (Fig. 1). The formation of the Cd-T complex has been directly followed at pH=7.9 measuring the anodic signal height of the Cd-T complex. Concentrations of Cd-T complex and Cd_{ionic} were calculated according to the slope of the calibration straight-line for cadmium under three different conditions:

(I) at pH=7.9 without the addition of MT;

(II) at pH<2 without the addition of MT;

(III) at pH<2 with the addition of $3.2\cdot10^{-8}$ M MT.

After the addition of MT at pH<2 only one signal of Cd(II) is visible at -0.60 V vs. Ag/AgCl, which corresponds to the ionic Cd(II) form (Fig. 2).

According to Ruzic (15), plotting $[M]_{ionic}/(M_T\text{-}[M]_{ionic})$ vs. $[M]_{ionic}$, a straight line should be obtained if one type of complex is predominant (MT is the total metal concentration and $[M]_{ionic}$ is the concentration of the labile metal species). From the slope the metal-

MODELING THE BIOACCUMULATION OF TRACE METALS IN MARINE HERBIVORES

Nicholas S. Fisher [1]*, Wen-Xiong Wang [1], and Samuel N. Luoma [2]

[1] Marine Sciences Research Center, State University of New York, Stony Brook, NY 11794-5000 USA
[2] Water Resources Division, US Geological Survey, Menlo Park, CA 94025 USA

Abstract

We show that bioenergetic-based kinetic models can effectively be used to predict metal concentrations and delineate metal uptake pathways in marine herbivorous animals. Radiotracer experiments have been performed to determine key parameters of metal influx and efflux from diverse sources. These parameters were incorporated into kinetic models to understand the accumulation of cadmium, silver, selenium, cobalt, chromium, and zinc in marine copepods and bivalve molluscs. Sensitivity analyses underscore the importance of determining the assimilation efficiency of ingested metal as a first-order parameter which regulates the bioaccumulation of these metals in animals.

Key-words : metals, bivalves, copepoda, models, bio-accumulation

Modeling approach

The metal content of an animal is a function of the uptake of the metal from the dissolved phase, metal uptake from ingested food, and retention of the metal in the animal, and can be described by the following first-order equation [1, 2]:

$$dC/dt = (\alpha_w * FR * C_w) + (AE * IR * C_f) - (k_e+g) * C \quad (1)$$

where, C is the metal concentration (μg g^{-1}) in the organism at time t (d), α_w is the metal absorption efficiency from the dissolved phase, FR is the animal filtration rate (L g^{-1} d^{-1}), C_w is the metal concentration in the dissolved phase (μg L^{-1}), AE is the metal assimilation efficiency from ingested food, IR is the ingestion rate (mg g^{-1} d^{-1}), C_f is the metal concentration in the food (μg mg^{-1}), k_e is the metal efflux rate constant (d^{-1}), and g is the growth rate constant (d^{-1}). Under steady state conditions, this equation becomes:

$$Css = \frac{(\alpha_w * FR * C_w) + (AE * IR * C_f)}{(k_e + g)} \quad (2)$$

Metal influx rate from the dissolved phase can be expressed as:

$$I^w = \alpha_w * FR * C_w = k_u * C_w \quad (3)$$

where I_w is the experimentally determined influx rate from the dissolved phase (μg g^{-1} d^{-1}), and ku is the dissolved uptake rate constant (L g^{-1} d^{-1}), which is equal to α_w * FR. If metal efflux rate constants are different following uptake from the dissolved and food sources, Eq. 2 can then be expressed as:

$$C_{ss} = \frac{(k_u * C_w)}{(k_{ew} + g)} + \frac{(AE * IR * C_f)}{(k_{ef} + g)} \quad (4)$$

where k_{ew} is the efflux rate constant for metal obtained from the dissolved phase (d^{-1}) and kef is the efflux rate constant for metal obtained from ingested food (d^{-1}).

Review of parameters

Recent experimental progress in applying gamma-emitting radiotracer techniques to quantifying the assimilation of ingested metals and the absorption of dissolved metals in marine animals has resulted in a large data set for key parameters useful in the modeling of contaminant concentrations in aquatic organisms. Numerical values of the parameters in Eq. 4 for a variety of metals in marine bivalve molluscs and calanoid copepods have been compiled [2-9]. Table 1 summarizes representative values for k_u, k_{ew}, k_{ef}, and AE for diverse metals in the mussel *Mytilus edulis*. Table 2 summarizes values for these parameters in the calanoid copepod *Temora longicornis*.

AEs of trace elements in marine mussels depended greatly on the quantity and quality of food that the mussels ingested. For example, Ag AEs varied by a factor of 9 (4 *vs* 34%) when mussels ingested the prasinophyte Tetraselmis maculata and the dinoflagellate *Alexandrium tamarense*. Cr(VI) AEs also varied by a factor of 10 when mussels ingested diatoms and dinoflagellates [5]. For other metals, AEs generally varied by a factor of 3-6 depending on the particle type provided to the mussels [3]. Recent evidence suggests that several factors, including mussel digestive physiology (gut passage time, partitioning of extracellular and intracellular digestion), phytoplankton physiology (trace element cytoplasmic distribution in algal cells), and metal chemical behavior (metal desorption within the acidic environment of mussel gut), can all contribute to varying trace element assimilation in mussels [7]. The effect of each process on metal assimilation is also metal-specific. For Se, the cytoplasmic distribution within algal cells appears to be the sole determinant of Se assimilation in mussels, where a 1:1 relationship between Se assimilation in mussels and Se distribution in algal cytoplasm has been noted [2,4]. For Cd, metal desorption within the acidic gut environment influences its assimilation in mussels [4].

Table 1. Kinetic parameters for metal behavior in the mussel *Mytilus edulis*. Parameters presented are the mean uptake rate constant, k_u (L g^{-1} d^{-1}), of metal from the dissolved phase; mean absorption efficiency, α_w (%), of metal from the dissolved phase; mean efflux rate constant, kew (d^{-1}), of metal following 6 d uptake from the dissolved phase; mean efflux rate constant, k_{ef} (d^{-1}), of metal following 7 d uptake from diatom food; and assimilation efficiency, AE (%), of ingested metal. AE values are for seven different algal foods. Details are given elsewhere [2, 3, 5].

Metal	k_u (L g^{-1} d^{-1})	α_w (%)	k_{ew} (d^{-1})	k_{ef} (d^{-1})	AE (%)
Ag	1.794	1.533	0.019	0.034	4-34
Am	0.398	0.340	0.019	0.020	1-6
Cd	0.365	0.312	0.011	0.014	11-40
Co	0.124	0.106	0.018	0.010	20-43
Cr(III)	0.034	0.029	0.012	0.010	0.2-1.3
Cr(VI)	0.100	0.085	0.011	nd	1-10
Se	0.035	0.030	0.026	0.022	15-72
Zn	1.044	0.892	0.020	0.015	16-48

Table 2. Kinetic parameters for metal behavior in the copepod *Temora longicornis*. Parameters presented are the mean uptake rate constant, k_u (L g^{-1} d^{-1}), of metal from the dissolved phase; mean efflux rate constant, k_{ew} (d^{-1}), of metal following 2 d uptake from the dissolved phase; mean efflux rate constant, k_{ef} (d^{-1}), of metal following 2 d uptake from diatom food; and assimilation efficiency, AE (%), of ingested metal. From Wang *et al.* [12].

Metal	k_u (L g^{-1} d^{-1})	k_{ew} (d^{-1})	k_{ef} (d^{-1})	AE (%)
Ag	10.42	0.173	0.294	8 - 20
Cd	0.694	0.108	0.297	33 - 53
Co	0.606	0.122	0.281	14 - 20
Se	0.024	0.155	0.155	50 - 60
Zn	3.294	0.108	0.079	52 - 64

In contrast to marine mussels, metal assimilation in marine copepods is relatively independent of food quality and quantity [6]. Food concentration within a range of 16-800 μg C L^{-1} has little influence on the AEs of Cd, Co, and Se. AEs of Am and Zn are highest at low food concentration (16-56 μg C L^{-1}) but remain relatively constant when the food concentration exceeds 160 μg C L^{-1}. Different phytoplankton diets also have no major effect on metal assimilation in copepods. In these herbivores, the cytoplasmic distribution of metals is critical in affecting metal assimilation [9,10], where a 1:1 relationship between trace element AE and distribution in algal cytoplasm suggests a "liquid" digestive strategy. Because of the relatively rapid gut passage of food particles in copepods (gut passage time generally is less than 0.5 h [11]), gut passage time does not directly determine metal assimilation. Recent studies have also demonstrated that the time to complete digestion andassimilation of metals from ingested food particles in marine copepods (ca. 10 h) is much longer than the gut passage time [12]. In marine mussels, the time to complete digestion and assimilation (ca. 3 d) is also much longer than the metal gut passage time (1-2 d [3]).

For both copepods and mussels, dissolved uptake rate constants are highest for metals that bind preferentially with protein ligands and are ranked in the order of Ag>Zn>Cd>Co>Cr>Se. Using the metabolic blocker N-ethylmaleimide to specifically inhibit the sulfhydryl group of ligands, Wang and Fisher [13] found that uptake of dissolved Ag, Zn and Cd is significantly inhibited, indicating that transport of these metals is primarily governed by a protein ligand (*e.g.*, facilitated transport process). The degree of inhibition by this blocker was highest for Ag, followed by Zn and Cd, consistent with the order of dissolved uptake rate constants. In contrast to these metals, influx of Co is not inhibited by N-ethylmaleimide, indicating that its transport is primarily a passive diffusive process. Se may be taken up through an anionic channel analogous to a sulfate or phosphate channel. It also appears that Ag, Zn and Cd can be transported through the calcium channel [13].

According to Eq. 3, the dissolved uptake rate constant can be controlled by an animal's filtration activity and metal absorption efficiency from the dissolved phase. It is not known whether filtration rate and absorption efficiency are independent parameters such that absorption efficiency is independent of filtration activity. The change of uptake rate of dissolved Co and

BIOACCUMULATION AND BIOMARKER RESPONSES TO ORGANOCHLORINES, POLYCYCLIC AROMATIC HYDROCARBONS AND TRACE METALS IN ADRIATIC SEA FISH FAUNA

S. Focardi*, M.C. Fossi, C. Leonzio, S. Aurigi, S. Casini, I. Corsi, S. Corsolini, F. Monaci, J.C. Sanchez-Hernandez

Dipartimento di Biologia Ambientale, Università di Siena, Via delle Cerchia, 3, 53100 Siena, Italy

Abstract

The primary aim of our study was set up the current knowledge of the environmental quality and the state of health of a great impacted basin, such as the Adriatic Sea, by an evaluation of the "state of chemical stress" of its fish communities. Bioaccumulation of trace metals (Hg, Pb, Cd, Zn, Cu, Fe) and of persistent contaminants such as polychlorobyphenyls (PCBs), dichlorodiphenyltrichloro-ethan (DDT), hexachlorobenzene (HCB), polycyclic aromatic hydrocarbons (PAHs) were investigated in liver samples of three fish species : *Merluccius merluccius, Sprattus sprattus* and *Sardina pilchardus* were collected in three different sites of north Adriatic Sea. A suite of biochemical biomarkers such as the induction of 7-ethoxyresorufin-O-deethylase (EROD), benzo(a)pyrene monooxygenase (BPMO) activities and metabolic intermediates (porphyrins associated with haem synthesis) were measured in the liver of fish samples in order to determine their environmental exposure to xenobiotic compounds. Preliminary results are : trace metal levels were higher in sprat than in whiting; levels of organochlorines and polycyclic aromatic hydrocarbons compounds were higher in whiting than in sprat and pilchard. These results were compared with biomarker responses on CYT. P-4501A activities were detected both in whiting and pilchard but absent in sprat. The highest EROD activity was recorded in whiting and BPMO activity in pilchard.

Key-words: Adriatic Sea, bio-indicators, chlorinated hydrocarbons, metals, PAH.

Introduction

The specific aim of this research was to investigate environmental quality and the health status of this basin by evaluating the state of chemical stress of its fish communities. The Adriatic Sea has been the subject of attention because of the periodic occurrence of degenerative phenomena, due partly to its structural and oceanographic characteristics and to human impact. Evaluation of the effects of pollution on marine communities is essential to safeguard the marine environment.

The objective of the present study was to assess the presence of contaminants of different types (trace metals, PCBs, DDT, HCB and PAHs) and their impact and/or toxic effects on specimens of certain fish communities regarded as being a target. This evaluation was done by a biomonitoring programme based on residue analysis of these contaminants and on the assessment of CYT. P4501A activity, determined by 7-ethoxyresorufin-O-deethylase (EROD) and benzo(a)pyrene monooxygenase (BPMO) assays, which is commonly used as a biochemical biomarker of exposure. A biomarker is "a change induced by a contaminant in a biochemical or cellular component of a process, structure or function that can be measured in a biological system" (1). The specificity and sensitivity of biomarker responses combined with data on accumulation levels could make it possible to determine dose-effect relationships for compounds present in the environment, in this case the Adriatic Sea. These contaminants are known to induce detoxification systems and may therefore be responsible for a toxic effect in organisms (2). Comparison of tissue concentrations of these compounds, levels of enzyme induction of CYT P-4501A activity and accumulation of metabolites in these fish could confirm that given environmental concentrations of these contaminants cause changes in biological functions and, in severe cases, damage to organisms and communities (3).

Materials and Methods

The first stage of our biomonitoring programme was carried out at three sites in the northern Adriatic Sea : 51 near the Lagoon of Venice, 50 further north at the limits of territorial waters, and 156 off the coast of Venetum (Fig. 1). Specimens of *Merluccius merluccius* and *Sprattus sprattus* were captured in December 1996 in site 50 and site 51 and stored on ice and frozen at -20°C on reaching the laboratory. Some specimens of both species were dissected on the spot and their livers placed in liquid nitrogen and stored at -80°C in the laboratory. Specimens of *Sardina pilchardus* were captured in March 1997 in site 156 and placed whole in liquid nitrogen. The following analyses were performed on individual liver samples of all species: trace elements (Hg, Cd, Pb, Zn, Fe, Cu) by plasma emission spectrometry according to the method of Broekaert (4) and mercury by flow injection mercury system by the method of Stoeppler and Backhaus (5). Blanks and standard reference materials (SRM n°1566a "oyster tissue" supply by U.S. Department of Commerce National Bureau of Standards Gaithersburg, USA) were analysed in each batch of samples.

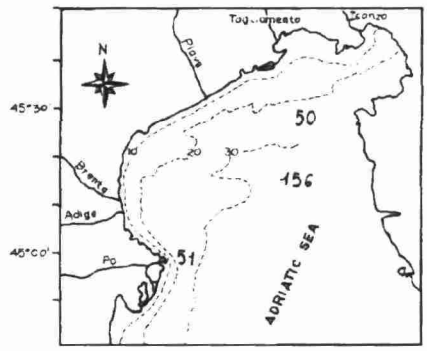

Fig. 1. Map of North Adriatic Sea with the locations of the sampling sites.

Total and coplanar PCBs, HCB, DDT were extracted and cleaned up from individual liver samples by the method of alkaline-alcohol digestion (6). Analysis was performed with a Perkin-Elmer Autosystem model gas chromatography equipped with Ni^{63} electron capture detector and type SBP-5 (Supelco) bonded-phase, fused silica capillary columns. Pure reference standard solution (Aroclor 1260 for total PCBs supply by Supelco Inc., PCB coplanars non-*ortho* substituted as PCB-77, PCB-126, PCB-169 supply by Dr. Ehrenstorfer GmbH, DDT and HCB supply by Supelco Inc.) were used for determination, quantification and evaluation of total PCBs, coplanars non-*ortho* substituted PCBs, DDT and HCB. Mixtures of specific isomers (PCB-77; PCB-126; PCB-169) were used for calibration, recovery evaluation and confirmation of non-*ortho* coplanar PCB congeners.

Polycyclic aromatic hydrocarbons (PAHs) were extracted and separated by the method of alkaline-alcohol digestion with KOH/MeOH (1:4 v/v) for the extraction and n-hexane for separation. Toluene eluates were reserved for PAHs determination using an HPLC/fluorescence and GC/MS. Pure reference standard solution for total PAHs were supplied by Supelco.

Biochemical analysis on CYT. P4501A activity (induction of benzo-(a)pyrene monooxygenase and 7-ethoxyresorufin O-deethylase activities) were performed previous isolation of microsomal fraction. Microsomal EROD activity was measured by spectrofluorimetric assay using the original method of Burke and Mayer (7) by kinetic measurement at 30°C using a Perkin Elmer LS50B spectrofluorimeter (Ex 544 nm, Em 584 nm). The amount of resorufin produced was calculated from a calibration curve of standard resorufin (Pierce) in the range 0.01-5μM range. BPMO activity was measured by the method of Kurelec *et al.* (8). The protein content of microsomal samples was evaluated following the Bio-Rad assay, using serum albumin for the standard calibration curve.

Metabolic intermediates (liver porphyrins) were extracted by the method of the Matteis and Lim (9). The method of Grandchamp *et al.* (10) was used for quantitative determination of porphyrins with reference standard of porphyrin products (supply by Logan, Utah, USA). This fluorimetric procedure was used to determine the percentages and concentrations of uroporphyrin, coproporphyrin and protoporphyrin in a mixture of porphyrins in the nanomolar range. The porphyrin were measured using a Perkin Elmer LS 50B spectrofluorimeter.

Results and Discussion

Hg, Cd, Zn, Cu and Fe levels detected in liver samples of *M. merluccius* and *S. sprattus* are summarised in Figure 2 (also see Table 1). Lead levels in both species were below the instrumental detection limit and therefore

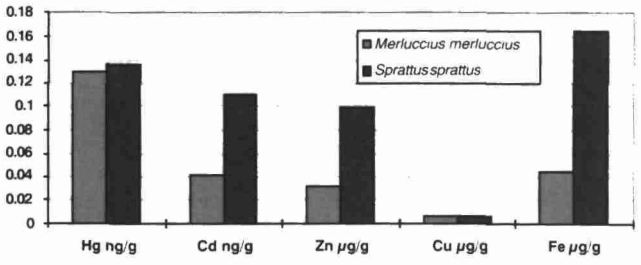

Fig. 2. Mean concentrations (ng/g and μg/g f.w.) of trace metals in the liver of *M. merluccius* and *S. sprattus*.

TRENDS IN CHLORINATED HYDROCARBONS AND HEAVY METALS IN SEDIMENTS OF VENETIAN CANALS

Fossato V.U., Campesan G.*, Dolci F., Stocco G.
Istituto di Biologia del Mare, CNR, Venezia, Italia

Abstract

Sediments of the Laguna Veneta (north-east Italy) sampled around the contaminated area between the industrial zone of Porto Marghera and the city of Venice were analysed for their chlorinated hydrocarbon (DDTs and PCBs) and heavy metal (Cd, Pb, Hg, Zn) content in 1985 and 1995. Comparison demonstrates the overall decline of total DDT, while PCBs, Cd, Pb, Hg and Zn appear to be almost unchanged during this 10 year period.

Key-words: chlorinated hydrocarbons, metals, sediments, Adriatic Sea

Introduction

The distribution of chemical pollutants in sediments of the Lagoon of Venice has been largely studied during the last years (1, 2). The emerging profile shows that the most contaminated area lies in the central part of the lagoon around the industrial zone of Porto Marghera and the city of Venice where the most still canals have mud bottoms ideal for accumulation and preservation of chemical pollutants. In 1985 a survey was carried out at twenty five stations distributed in this area to measure existing concentrations of chlorinated hydrocarbons and heavy metals in sediments (3, 4); ten years later the survey was repeated at eight selected stations with the aim of investigating the spatial and temporal trends for these contaminants. In this paper we describe the results from the latter survey.

Materials and methods

At each station, three samples of surface (top 10 cm) sediments were collected, combined, carefully homogenised and frozen at -20°C until analysis. Extraction of chlorinated hydrocarbons was accomplished by Soxhlet refluxing about 30 g of wet sediment for eight hours, firstly with acetonitrile then with n-hexane. CB-29 was added as internal standard for recovery determinations. Extracts were analysed by ECD gas chromatography (Carlo Erba FV 4160 with a SE-54 fused silica column, 30 m long x 0.32 mm i.d.) following partition into n-hexane, clean-up with sulphuric acid and fractionation on a silica gel microcolumn (3). Identity of the compounds was assumed from their retention times. Quantification was based on peak area measurement and comparison to responses of reference standards: pp'DDE, pp'DDD, pp'DDT, PCB Aroclor 1260 and CB congeners No. 29, 52, 101, 118, 138, 153, 180.

For heavy metal analysis, dissolution was accomplished by refluxing 5 g of dry sediment for 2 hour with HNO_3 (5); Hg was extracted with a mixture of HNO_3/H_2SO_4 (6). Instrumental determination was performed using a Perkin-Elmer mod. 372 atomic absorption spectrophotometer equipped with Deuterium Background Corrector. Cd, Pb and Zn were determined directly in an air-acetylene flame, while Hg was measured using cold vapour technique by reduction with $NaBH_4$. Organic carbon was determined by the chromate digestion method of FAO (7).

Quality control of the analytical results was based on repeated analyses of the lagoon sediment IAEA-357 and the standard estuarine sediment CRM 277 (BCR/EU) for organochlorine and heavy metals, respectively.

Results and discussion

The stations, plotted in Fig. 1, were selected as representative of a variety of hydrographic and pollution load conditions. Stations 2, 8, 11, 12 and 16 were located in the deepest canals (2-4 m depth) inside and around the city. These stations have a favourable exchange of waters due to tidal currents. Station 18 was fixed on the side of a ship channel (12 m deep) between Porto Marghera and Venice. Stations 23 and 24 were located in the shallow canals (about 1 m depth) interior of the city which receive raw municipal sewage and have limited water circulation.

Sedimentation rates are highly variable within the study area, due to the complex current patterns. Values between 0.23 and 0.41 cm y^{-1} were determined by radiometric analysis on a sediment core taken in the open lagoon near station 18 (8); however, in the most still canals in the interior of the city a sedimentation rate of 2-3 cm y^{-1} may be estimated on the basis of their depth variation over time.

Organic carbon values in sediments sampled in the years 1985 and 1995 are plotted together in Fig. 2 to permit direct spatial and temporal

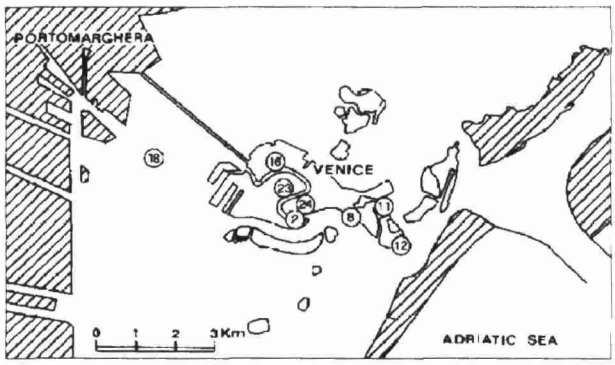

Fig. 1. Sampling stations in the Venice Lagoon.

comparisons: values range from 0.5% (Sta. 12) to 4.5% (Sta. 23) and are generally well correlated with pollutant content of the sediments, and weakly correlated with pelite (silt + clay; < 0.063 mm) content. Fine-grain size sediments of the most still canals near the inner city, rich in organic matter, are expected to have higher affinity for contaminants. This is evident when the concentrations are expressed on dry weight basis, while the differences between stations greatly diminish when basing the concentrations on organic carbon weight.

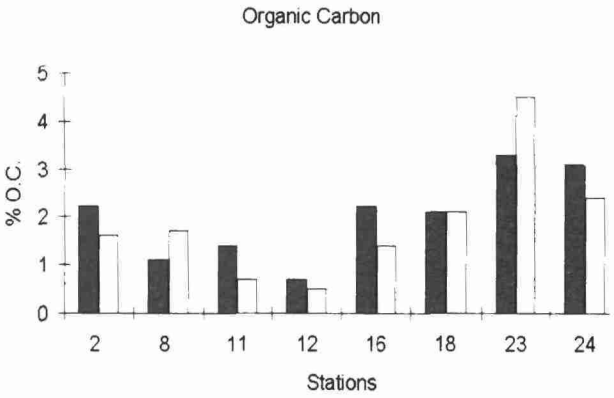

Fig. 2. Organic carbopn values (% dry wt.) in sediments sampled in the years 1985 (grey histograms) and 1995 (white histograms).

Distribution patterns are basically similar for total DDT (Fig. 3A) and total PCB (Fig. 3B) which may reflect a common biogeochemical pathway in the lagoon consistent with their low water solubilities and high affinity for organic matter ($r = 0.85$ $p < 0.01$). Our data demonstrate the overall decline of the magnitude of DDT residues in the sediments (Fig. 3) and the increase of the amount of the metabolites DDD and DDE versus the total amount of DDT (not shown). Results also indicate a more severe and persistent contamination by PCB in this area. For DDT and PCB it is likely that the greatest input occurred in the past, before the ban in the use of chlorinated pesticides and polychlorinated biphenyls. However, resuspension of sediment by wave action and transport of fine materials by tidal currents may be responsible of the increase of DDT and PCB in some less contaminated areas (Sta. 2 and 12).

GEOCHEMICAL CHARACTERISTICS OF THE SURFICIAL SEDIMENTS OF THE AEGEAN SEA

N. Friligos, A. Moriki*, E. Sklivagou, E. Krasakopoulou and I. Hatzianestis
National Centre for Marine Research, Aghios Kosmas 166 04, Athens, Greece

Abstract

Surface sediment samples were collected during an oceanographic cruise in October 1996 and analyzed in order to estimate grain size distribution and carbonate content, metal concentrations, organic carbon and organic nitrogen. The grain size parameters vary widely, while the carbonate content ranges between 18-81%. The results show an almost uniform distribution regarding concentrations of Pb, Cu and Cd, while Cr, Ni, Zn, Fe and Mn present maximum values which correlate well with each other. Total carbon ranges between 3-10%, organic carbon between 0.2-0.77% and nitrogen content between 0.008 and 0.056%. Both carbon and nitrogen are found in the natural concentration ranges. However, the C:N ratio in a few stations in the Northern Aegean varies from the value suggested in the literature.

Key-words: trace elements, sediments, Aegean Sea

Introduction

Trace element concentrations in marine sediments is a result of both natural and anthropogenic processes. Monitoring of trace metals can therefore contribute not only to the understanding of the geochemical history of a certain area, but in the identification of anthropogenic enrichment as well. However, most of the studies on heavy metal pollution in the eastern Mediterranean sediments have been conducted in coastal areas and embayments [1-3], whereas only a single study has been performed around the Cyclades islands [4]. Our study aims at identifying the sediment type, organic carbon and nitrogen content and metal distribution in surface sediments of the open Aegean Sea, which will serve as baseline information for future studies in the region.

Methodology

Surface sediment samples (0-3 cm) were collected with a Smith-McIntyre type grab sampler from 15 stations in the Aegean Sea at depths ranging from 45 to 814 m. The cruise took place in October 1996 and the sampling locations are shown in Figure 1.

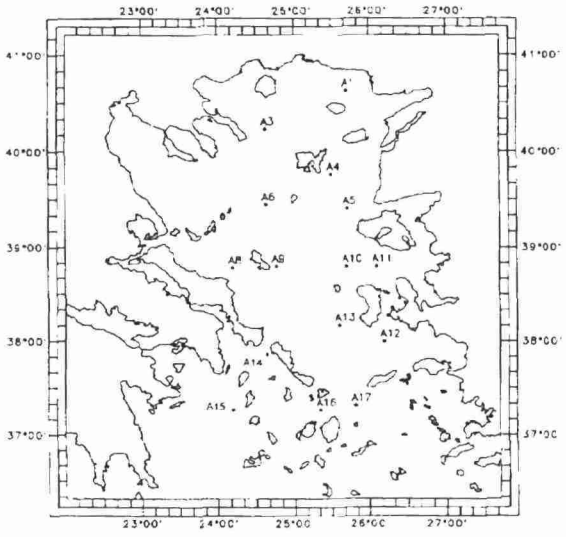

Fig. 1. Map with the 15 sampling locations in the Aegean Sea.

For trace metal analysis, about 20 g of undisturbed sediment was collected from the central part of the grab sample with a plastic tool and stored in a polyethylene bag. Grain size analysis was carried out by wet-seiving. The samples were dried at 60°C, the < 63 μm fraction was estimated, ground in an agate mortar and a portion was analyzed for silt-clay content by X-ray analysis with Sedigraph (Micromeritics 5100). Heavy metal analysis was performed after a complete digestion of the ground sample with subsequent addition of HNO_3, HF, aqua regia ($HCl:HNO_3$) and $HCLO_3$ [5, 6]. The final sample was analyzed for Pb, Cu, Zn, Ni, Cr, Mn and Fe by flame atomic absorption spectrometry on a Varian SpectrAA 20 Plus. Cd determinations were performed on a Perkin-Elmer 4100 spectrophotometer with a HGA 100 Graphite Furnace. A reference material (SD-M-2/TM IAEA Monaco, N° 182) of known concentrations was treated like the samples and analyzed in order to check the accuracy of the analyses.

Organic carbon, total carbon and nitrogen and carbonate content were determined in the bulk sample after oven drying the samples at 60°C and grinding in an agate mortar. The method is a modification of Nieuwenhuize *et al.* [7]. Splits of 10-15 mg of powdered homogenized samples were accurately weighed into silver cups. Organic carbon was determined after the removal of inorganic carbon by in situ acidification of samples with hydrochloric acid 1:1 and drying the samples at 60°C. Silver cups were pinched closed, compacted and formed into a ball. The balls were transferred to the autosampler of the Fisons Instruments CHN elemental analyzer type EA-1108. For total carbon analysis, carbon splits of 5-50 mg of dried samples were weighed into tin cups, sealed and analyzed without any pretreatment.

Results and discussion

Sampling locations, maximum water depth, geographical coordinates, carbonate content and sediment distribution are shown in Table 1. The grain size parameters fall among a wide range of values. Carbonate content follows the sand and total carbon distribution and presents the higher values at stations A8, A14, A16, A17 and A1.

Table 2 shows the concentrations of heavy metals in the surface sediments of the 15 stations. Pb and Cu were low among the stations and were similar to natural background values for the Mediterranean [8]. Zn concentrations were 72 mg/kg at station A7 and 140 mg/kg (the highest value) at station A1. The highest value of Ni was observed at

Table 1. Sampling locations, maximum depth, geographical coordinates and grain size parameters of sediments.

Station	Depth(m)	Longitude	Latitude	$CaCO_3$%	Sand. %	Silt. %	Clay. %
A1	45	25 42.00	40 38.00	65.46	70.56	12.71	16.73
A3	814	24 38.00	40 14.00	18.56	3.53	36.80	59.67
A4	93	25 30.00	39 46.00	22.00	85.00	10.52	4.48
A5	300	25 42.60	39 24.50	28.37	10.55	51.69	37.76
A6	358	24 38.30	39 26.90	35.84	23.23	39.00	37.80
A8	365	24 11.90	38 47.20	80.67	92.00	3.88	4.12
A9	254	24 46.00	38 48.00	53.55	45.36	32.90	21.74
A10	375	25 42.00	38 48.00	41.66	29.53	37.51	32.96
A11	284	26 06.00	38 48.00	36.78	15.85	51.31	32.84
A12	770	26 12.00	38 00.00	30.13	4.64	47.68	47.68
A13	427	25 36.00	38 10.50	71.35	70.22	16.85	12.93
A14	168	24 38.60	37 51.80	79.09	97.81	1.51	0.68
A15	476	24 12.00	37 16.00	57.59	18.38	47.34	34.28
A16	106	25 21.00	37 16.00	75.89	87.93	8.81	3.26
A17	325	25 48.80	37 19.00	68.53	68.23	19.32	12.45

Table 2. Heavy metal concentrations in the < 63 μm fraction of surface sediments from the Aegean Sea. Results are expressed in mg/kg, except for Fe in %.

Stations	Pb	Cu	Zn	Ni	Cr	Cd	Mn	Fe%
A1	30.11	33.68	140.34	76.29	85.91	0.17	419.00	3.94
A3	30.36	47.06	123.72	108.71	89.95	0.16	2205.00	3.96
A4	24.34	23.40	96.71	75.02	70.50	0.14	618.00	3.19
A5	27.65	34.45	103.84	106.66	71.41	0.15	2164.00	3.51
A6	26.02	33.66	93.94	100.27	68.32	0.16	2031.00	3.19
A8	29.34	41.87	105.48	151.02	100.02	0.22	1899.00	3.31
A9	23.86	28.92	81.40	127.91	118.60	0.15	1196.00	2.78
A10	24.26	33.60	90.38	133.80	92.71	0.13	2050.00	3.36
A11	26.42	30.95	94.55	130.09	92.05	0.15	1884.00	3.35
A12	25.38	38.72	99.63	216.51	129.58	0.16	1427.00	3.69
A13	26.21	37.47	86.63	153.98	83.13	0.18	1420.00	2.96
A14	23.75	24.63	82.53	84.80	78.46	0.20	579.00	2.47
A15	28.61	32.15	86.14	93.53	62.48	0.17	1190.00	2.27
A16	22.72	15.25	68.76	70.18	55.43	0.14	406.00	1.98
A17	25.02	28.62	71.90	125.58	63.14	0.16	1170.00	2.31

THE PATTERN OF AIR-SEA INTERACTION OVER THE MEDITERRANEAN SEA AND ITS EFFECT ON THE STABLE ISOTOPE COMPOSITION OF ATMOSPHERIC MOISTURE AND WATER MASSES OF THE EASTERN MEDITERRANEAN SEA

Joel R. Gat* and Aldo Shemesh

Department of Environmental Sciences and Energy Research, Weizmann Institute of Science, 76100 Rehovot, Israel

Abstract

The isotope composition of winter precipitation in the eastern Mediterranean Sea area suggests that the source of moisture is derived from evaporation under conditions of a large humidity gradient, such as occurs when cold (dry) continental air meets relatively warm sea waters. Direct measurement of the isotopic composition of atmospheric moisture, collected over the sea during January 1996 by the research vessel *Meteor*, confirmed this hypothesis. "d-excess" values of up to 33‰ were encountered close to the shores of the European continent south of the Adriatic Sea and Turkey, compared to values of d ~10‰ over the continent itself. The continuing trajectory of the continental air masses over the sea resulted in a moderation of this high d-excess, reaching values of close to d = 20‰ which are typical for the precipitation on the eastern shores of the Mediterranean and further downwind into the Middle East.

Key words: air-sea interactions, Eastern Mediterranean

It has been recognized that the isotope composition of atmospheric waters and, in particular, the d-excess value [defined as d ≡ δ(d) -8xδ(O-18) (1), where δ is the measure of the isotope composition expressed as the relative deviation from the standard SMOW (2) with δ(D) and δ(O-18) referring to the hydrogen and oxygen heavy isotopes, respectively] is established through the air-sea interaction at the source region of the atmospheric moisture (3). The Atlantic air masses, which give rise to precipitation throughout Europe and western North-Africa are characterized by d = 10‰ (4), close to the worldwide average (5). Winter precipitation in the Mediterranean region, on the other hand, shows a higher "d" value (6, 7). This excess has been explained by the special situation of cold and dry continental air masses which come into contact with a relatively warm sea, resulting in evaporation over a large humidity gradient accompanied by extreme isotope fractionation. From the geographic distribution of this parameter (Fig. 1), which is based on GNIP (Global Network of Isotopes in Precipitation), one infers this interaction to be most effective in the coastal regions on the leeward side of the European continent, especially in the Aegean Sea and along the Turkish coast (8). A year long survey of the isotopic composition of air moisture at Rehovot (Israel's coastal plain) showed this high deuterium excess to be a winter feature, especially marked in precipitating air masses (9).

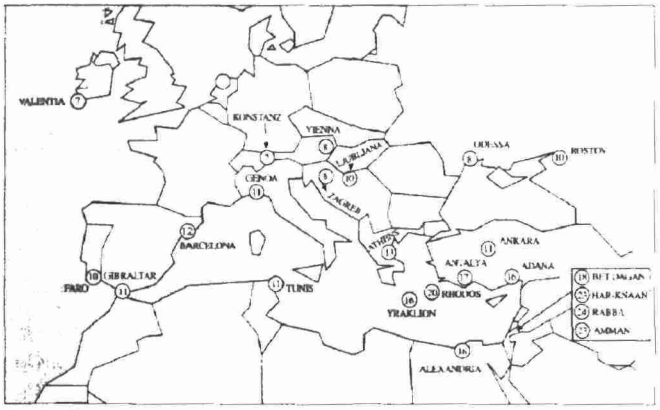

Fig. 1. The average d-excess values in winter precipitation in the Mediterranean Sea region, based on the IAEA (GNIP) data.

A recent set of water vapour samples obtained at mast height above the sea during the cruise of the research vessel *Meteor* in January 1996, confirmed this inferred pattern. As shown in Fig. 2, d-excess values of more than 30‰ were found in the Adriatic Sea and south of Turkey. Over the open sea, further from the coastline and where humidities increase, these high values are lowered indicating the moderating effect of continuing air-sea interaction. This pattern indeed parallels the buildup and dissipation of tritium values in the atmospheric moisture, reported in 1970 by Gat and Carmi (8). The d-excess over the eastern Mediterranean then attain lower values characteristic of Middle Eastern precipitation, namely close to d = 20‰.

A simple model of the vapour buildup over the sea as dry air from the continent picks up moisture is shown in Fig. 3. The advecting

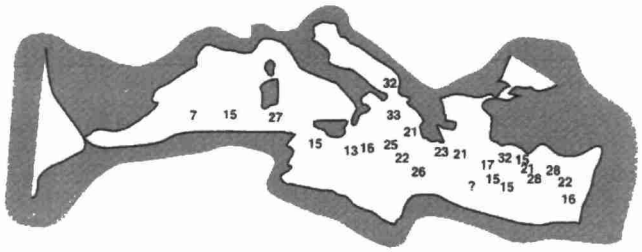

Fig. 2. The d-excess value in atmospheric moisture over the Mediterranean Sea, January 1969, from the *Meteor*-cruise vapour collection. Numbers shown are the values of the d-excess at the site of the vapour collection during the cruise.

continental air is characterized during winter by a low relative humidity (normalized relative to the saturated water pressure over the sea at SST), whose isotopic composition is depleted in the heavy isotopes O-18 and deuterium. Typical δ values of this moisture are $\delta(^{18}O)$ = -5‰ to -30‰ and d~10‰. As the air picks up evaporated vapour from the sea to form a blanket of modified (marine) vapour, the isotopic composition is also modified because of the extreme isotope separation which accompanies the evaporation process (which takes place over a large humidity gradient). The expected changes in the isotope composition of the marine air, resulting from the admixture of the evaporation flux into the advected air under conditions of increasing humidity, were calculated based on the Craig-Gordon evaporation model (10). The results, shown in Fig. 4, illustrate how the d-excess increases in the initial phases of the air-sea interaction, reaching a maximum value of about d = 40‰ at humidities around 35%. As humidity builds up further, the calculation shows the relaxation of these high d-excess values. The measured values show a pattern which is basically in accord with this simple model (for the case of the near-coastal sites, Fig. 4). However, in order to achieve a quantitative agreement with all the data, some refinement of the model will be necessary.

The extreme and intense air-sea interaction in the Mediterranean during winter affects not only the atmospheric moisture but also controls the isotope enrichment of the surface waters on the leeward-side of the continent. Under usual marine conditions the heavy water

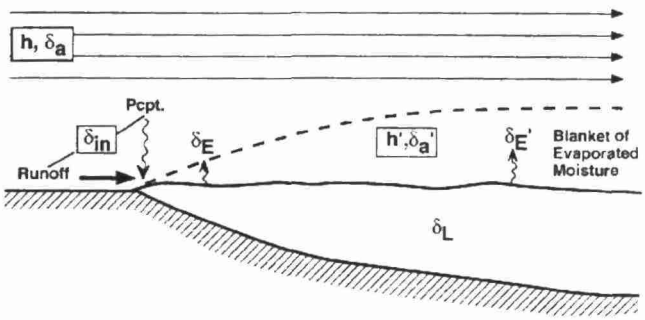

Fig. 3. Conceptual diagram of the buildup of a blanket of marine-derived moisture over the sea.

HYDROCARBONS IN SURFACE SEDIMENTS FROM THE NORTHERN AEGEAN SEA

J. Hatzianestis*, E. Sklivagou and N. Friligos
National Centre for Marine Research, Ag. Kosmas, 166 04 Hellinikon, Greece

Abstract
Aliphatic and polycyclic aromatic hydrocarbon (PAH) concentrations were determined in 15 superficial sediments collected from northern Aegean Sea, during 1996. The values found varied from 10.5 to 57.3 μg/g for total aliphatic hydrocarbons and from 31.0 to 176.3 ng/g for total PAH. Several diagnostic criteria used to identify the origin of the hydrocarbons indicated in most cases a major contribution of petroleum inputs.

Key-words: sediments, PAH, Aegean Sea

Introduction

In the last decades the development of sophisticated analytical techniques such as gas chromatography/mass spectrometry has enabled the identification of organic compounds which are present at very low concentrations and in complex mixtures in the marine environment. In this context, the analysis of the hydrocarbons has become an issue of major importance for marine research. The origin of hydrocarbons in sediments can be either natural or anthropogenic. Natural hydrocarbons derive mainly from terrestrial plants and marine algae, while the main sources of the man-made hydrocarbons are the various petroleum inputs into the ocean, the industrial discharges and the atmospheric fallout [1]. In this work, the study of aliphatic and aromatic hydrocarbons in surface sediments of northern Aegean Sea was performed. In fact, no other references concerning hydrocarbon contents in the sediments of this area are available in the literature. Therefore, this study provides baseline information for hydrocarbon distribution and origin in the sediments of Aegean Sea.

Experimental details

Surface sediment samples (the upper 2 cm) were collected from 15 stations in the northern Aegean during October 1996 using a Smith-McIntyre type grab sampler. The sampling locations are shown in Fig.1.

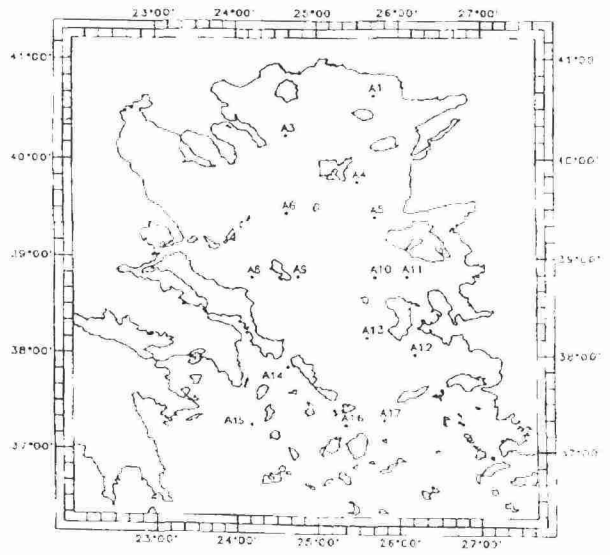

Fig. 1. The sampling locations of surface sediments from the northern Aegean Sea.

The analysis was performed according the methods suggested by IOC [2]. After oven drying at 40°C, the sediment samples were pulverized, spiked with internal standards (androstane and pyrene-D10) and extracted in a Soxhlet apparatus for 24 h with a mixture of dichloromethane-methanol 2:1. The extract was saponified with a methanolic solution of KOH and the hydrocarbons were extracted with hexane. The clean-up and fractionation step was performed by silica gel and alumina column chromatography and resulted in the collection of two hydrocarbon fractions. The first fraction contained the aliphatic compounds and the second the aromatic ones. The final determination was carried out by gas chromatography-mass spectrometry (Hewlett Packard 6890 GC-MS).

Results and discussion.

The results of the hydrocarbon analysis and some other compositional parameters are given in Table 1. The total hydrocarbon concentrations found ranged between 10.7 and 57.5 μg/g dry sediment (average 25.6 μg/g). The highest concentrations were observed at stations A1 and A3, while the lowest values occur at stations A10, A14, A15. These concentrations are generally higher than those reported in unpolluted Mediterranean open sea sediments (<10 μg/g) [3].

Table 1. Organic carbon content (Corg), concentrations of total hydrocarbons (THC), unresolved complex mixture (UCM), total aliphatic hydrocarbons (ALIPH), total n-alkanes (n-ALK) and polycyclic aromatic hydrocarbons (PAH), the ratio unresolved/resolved compounds (U/R), the carbon preference index (CPI) calculated from C23 to C34 and the ratio pristane/phytane (Pr/Ph) in the sediments of the Aegean Sea (See Fig. 1 for station location).

Stations	Depth (m)	Corg (%)	THC (μg/g)	UCM (μg/g)	ALIPH (μg/g)	n-ALK (μg/g)	PAH (ng/g)	U/R	CPI	Pr/Ph
A1	45	0.40	43.8	37.3	43.7	4.7	147.8	5.8	1.5	0.6
A3	814	0.75	57.5	45.3	57.3	8.6	159.8	3.7	1.9	0.8
A4	93	0.27	13.8	12.0	13.8	1.2	34.1	7.1	1.8	0.7
A5	300	0.75	32.3	26.2	32.2	4.3	155.7	4.4	2.5	0.9
A6	358	0.62	34.9	28.7	34.8	4.3	149.0	4.8	3.1	0.7
A8	365	0.30	33.5	27.1	33.4	4.2	145.2	4.3	1.7	0.8
A9	254	0.44	29.5	23.5	29.4	4.2	111.8	4.0	2.2	0.5
A10	375	0.56	10.7	7.6	10.6	2.3	176.3	2.6	4.5	1.0
A11	284	0.63	14.5	12.5	14.5	1.3	56.8	6.4	2.5	0.3
A12	770	0.78	20.0	15.8	19.9	3.2	118.7	3.7	2.4	0.6
A13	427	0.39	31.6	24.9	31.5	4.2	119.7	3.8	2.0	0.8
A14	168	0.22	12.1	10.5	12.1	1.1	30.9	6.9	1.5	0.5
A15	476	0.52	12.4	10.3	12.4	1.3	47.9	5.2	2.2	0.8
A16	106	0.40	13.7	11.4	13.7	1.4	43.0	5.1	1.9	0.9
A17	325	0.39	18.2	15.2	18.1	1.9	52.5	5.3	2.4	0.6

Aliphatic hydrocarbons. Total aliphatic hydrocarbon concentrations varied from 10.6 to 57.3 μg/g dry weight and accounted for the 98.4-99.8% of the total hydrocarbons. Fig. 2 shows their distribution in the study area. In all samples the gas chromatographic traces of the aliphatic fraction were characterized by two general features: resolved compounds and a unimodal hump corresponding to a mixture of unresolved compounds (UCM) with 15-34 carbon atoms (Fig. 3). The UCM is considered as an elaborate mixture of branched and cyclic hydrocarbons and it is generally well correlated with degraded or weathered petroleum residues [4,5]. In the sediments analyzed the UCM was always the major component representing 72.3-87.4% of the total aliphatics. The ratio unresolved/resolved compounds (U/R) is widely used to identify the origin of the hydrocarbons in marine sediments. Values U/R > 4 are considered as evidence of petroleum residues [6].

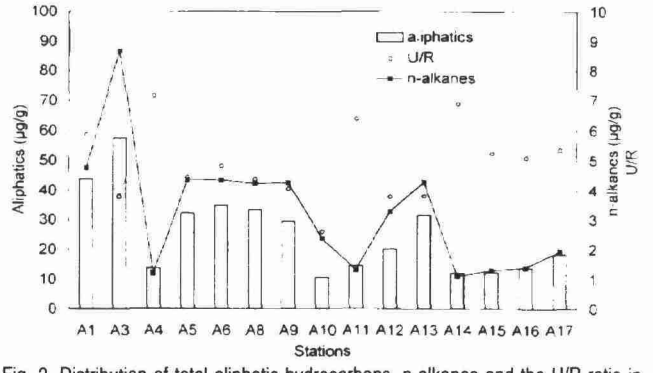

Fig. 2. Distribution of total aliphatic hydrocarbons, n-alkanes and the U/R ratio in the sediments of the Aegean Sea.

LONG-TERM CHANGES OF PHOSPHORUS AND NITROGEN COMPOUNDS IN THE NORTHERN ADRIATIC SEA

Ingrid Ivancic* and Danilo Degobbis
Institute Ruder Boskovic, Centre for Marine Research, Rovinj, Croatia

Abstract
This paper aims to synthesize 29 years of data on nutrient concentrations in the northern Adriatic (1966 to 1995). A significant long-term decrease in phosphorus concentrations was detected since the mid-1980's. From the beginning of the 1980's total inorganic nitrogen concentrations were usually higher than in the previous period. The observed changes could be related to changes of phosphorus and nitrogen concentrations in the Po River waters.

Key-words: phosphorus, nitrogen, Adriatic Sea

Introduction

Obtaining knowledge of long-term changes of nutrients is a basic step in verifying eutrophication trends in shallow marine ecosystems such as that in the northern Adriatic. Preliminary research suggests that this ecosystem is sensitive to the anthropogenic nutrient load (1). Consequently, changes of inputs may significantly affect the primary production of the region. The principal external source of nutrients in the region is the Po River (~75% of the total inputs; 1) the waters of wich markedly influence the composition and activity of the plankton community in the sea (2, 3).

Since 1966 the Center for Marine Research in Rovinj (CMR) has investigated various aspects of primary production, plant nutrient environment, and associated hydrography in the northern Adriatic. This extensive data set allows estimating the long-term "mechanism" controlling nutrient concentrations in this area.

Material and methods

Long-term changes of phosphorus and nitrogen were studied from a data set obtained in the period 1966-1995 at five stations along the Rovinj-Po River delta transect (Fig. 1). Measurements were performed monthly, or at least seasonally. A total of about 7000 data for phosphorus and nitrogen compounds were collected.

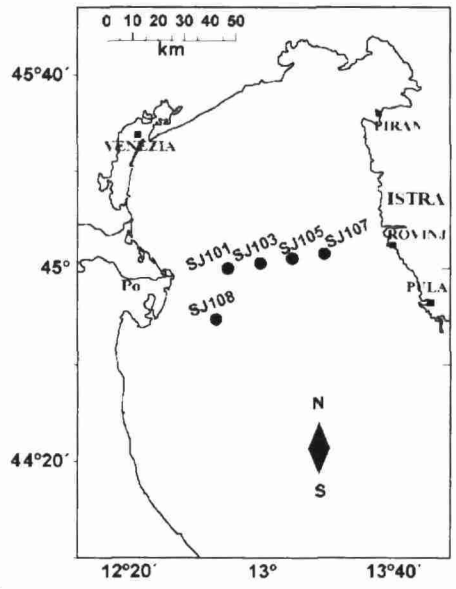

Fig. 1. Sampling stations in the northern Adriatic.

Water samples were collected with 5 l Niskin samplers from at least four depths (0, 10, 20 m and 2 m above the bottom). Nutrient analyses were performed aboard immediately after sample collection. Analyses were made by Beckman DU and Cecil CE 2040 spectrophotometers with methods widely used in oceanography (4)

Samples for total phosphorus were kept at -30°C for subsequent analyses ashore. Analyses were performed by chemical oxidation (before 1981) or UV-irradiation (after 1981) of samples (4). The results obtained for sea water samples using both methods were not different (5). Organic phosphorus was calculated as a difference between total phosphorus and orthophosphate values.

Data for the Po River discharge rate were kindly provided by Dr Alodi (Hydrological Office for the Po River in Parma), or originated from published sources (6). A total of 28000 data was collected.

Results and discussion

Based on the knowledge of seasonal cycles, data were grouped within five typical annual periods, each characterised by different prevailing hydrological (Po River discharge rates), oceanographic (stratification, circulation type) and biological (nutrient assimilation and regeneration) processes (7). During the period of July-August and December-January the Po River flow is minimal and, consequently, the data variability lower than in other periods. However, these two periods differ greatly. During summer the water column is highly stratified, and water exchange between the northern and central Adriatic is reduced compared to winter. During winter strong vertical mixing prevails. In this season the biological activity is minimal and assimilation and regeneration processes are approximately balanced. Contrary, during summer an active recycling of organic matter occurs in the upper water column, while in the bottom layer decomposition processes predominate.

The periods of February-April and September-November are characterised by higher variability, due to the increased freshwater input compared to winter and summer. However, these two periods are also substantially different. During February-April the stratification process starts. The weather conditions and imported nutrients favour phytoplankton blooms in the surface layer. An approximate equilibrium between assimilation and regeneration processes still persists through the remainder of the water column. In contrast, during September-November convective vertical mixing strongly reduces the water column stratification and brings into the upper layers nutrients regenerated in the deep waters. Regenerated nutrients, as well as "new" freshwater nutrients, stimulate phytoplankton blooms in the surface layer, while regeneration processes predominate in the bottom layer.

During May-June the freshwater input is maximal for the year, and the degree of stratification significantly increases. In the surface layer phytoplankton activity is maximal for the year, but regeneration processes start to occur in the bottom layer. Significant interannual concentration changes of phosphorus and nitrogen compounds in February-April and May-June, when the mean freshwater input is generally higher than in other seasons, can be related to the influence of the Po discharge. This influence combines both fluctuations of the discharge rate and nutrient concentration changes in the Po River waters. During February-April the freshwater input and orthophosphate (PO_4) and organic phosphorus concentrations in the sea were higher during the 1970's than in the 1980's (Fig. 2). Moreover, the most marked decrease of PO_4 and organic phosphorus concentrations in the sea was observed only since the mid-1980's, whereas the Po discharge rate during the 1980's did not change significantly (Fig. 2).

During May-June organic phosphorus concentrations in the surface layer were related to changes in the freshwater input (Fig. 3), but PO_4 concentrations were rather scattered. However, in the intermediate and bottom layers both organic phosphorus and PO_4 concentrations have decreased since the mid-1980's (Fig. 3).

Since the beginning of 1980's total inorganic nitrogen (TIN) concentrations in the surface layer were more frequently higher than previously and were independent of changes in the Po discharge rate (Figs. 2 and 3). In the intermediate and bottom layer TIN concentrations did not change significantly during the investigation period. The observed changes in phosphorus and nitrogen concentrations in the northern Adriatic may be related to composition changes of the Po

FLUX ATMOSPHERIQUES ET MARINS DE METAUX-TRACES EN MER LIGURE

Blandine Journel [1, 2*], Emmanuel Nicolas [1], Christophe Migon [1], Valérie Sandroni [1] et Jean-Pierre Béthoux [1]

[1] Laboratoire de Physique et Chimie Marines, Université Paris 6, CNRS INSU, BP 8, 06238 Villefranche-sur-mer Cedex, France
[2] CEREGE, URA 132, Europôle méditerranéen de l'Arbois, BP 80, 13545, Aix-en-Provence, Cedex 4, France

Résumé

Les flux atmosphériques totaux de Cd, Co, Cu, Ni, Pb et Zn sont mesurés sur le site côtier du Cap Ferrat (France), du printemps à l'automne 1993. En parallèle, les flux particulaires marins sont mesurés à 200 et 1000 m de profondeur, en Mer Ligure centrale. Le transfert des apports atmosphériques vers les eaux profondes se traduit par des flux d'importance décroissante de l'atmosphère vers la mer profonde (*i.e.*, pas ou peu de sources internes) et par une réponse marine dont l'intensité dépend de la saison, c'est-à-dire en fonction des variations de l'activité biologique.

Mots-clés : air-sea interactions, metals, particle flux, Ligurian Sea

Introduction

L'atmosphère est le vecteur principal de matière vers les zones océaniques (1-3). Ceci est particulièrement vrai en Méditerranée occidentale, bassin semi-fermé soumis à des influences anthropiques (4) et naturelles (apports de poussières sahariennes; 5, 6). De plus, cette mer présente un temps de réponse relativement court, de l'ordre de l'année, aux fluctuations des apports externes (7, 8). Les flux totaux de traces métalliques ont déjà été décrits pour la région ligure (9, 10). Cependant, il existe peu de données sur la concomitance des données atmosphériques et océaniques. Situé en Mer Ligure centrale, le site DYFAMED permet la mesure des flux océaniques à - 200 et - 1000 m. Protégé des apports advectifs par le courant liguro-provençal (11, 12) et couplé au site atmosphérique côtier du Cap Ferrat, le site DYFAMED permet une observation à long terme de la réponse marine aux perturbations environnementales. On peut ainsi étudier les processus de transferts des apports atmosphériques vers les couches marines profondes, c'est-à-dire essentiellement l'activité biologique (13-15), elle-même dépendante des conditions hydrologiques (stratification estivale des eaux) et climatiques (coups de vent, ensoleillement). Le présent travail, qui se définit comme une étude préliminaire dans ce domaine, a pour objectif de mettre en regard les flux atmosphériques et marins de Cd, Co, Cu, Ni, Pb et Zn, afin d'appréhender le devenir des apports atmosphériques, d'abord au-dessous de la couche euphotique (- 200 m), puis en eaux profondes (- 1000 m).

Méthodologie

Les échantillons atmosphériques ont été collectés au site côtier du Cap Ferrat (43°41'10" N, 7°19'30"E) en 1993. Les apports totaux ont été mesurés et répertoriés selon un pas de temps de 15 jours (10, 16) qui correspond au pas d'échantillonnage des trappes à particules. Les échantillons marins ont été prélevés au site DYFAMED, situé à 28 milles de la côte ligure française, sur la radiale Nice-Calvi. Des trappes à particules y sont mouillées à 200 et 1000 mètres de profondeur (17, 18). Les retombées atmosphériques totales ainsi que les échantillons de pièges à particules ont été dosés par voltampérométrie de redissolutions anodique et cathodique. Les limites de détection sont les suivantes : 1; 2; 20; 3; 2 et 20 ng l^{-1} pour Cd, Co, Cu, Ni, Pb et Zn respectivement. Les détails méthodologiques et analytiques ont déjà été publiés antérieurement (10, 18, 19).

Résultats et discussion

Les apports atmosphériques ont été collectés de mars à septembre 1993. Les échantillons marins sont disponibles de mai à novembre 1993. Bien qu'on ne dispose pas d'une année entière, les périodes considérées devraient permettre de mettre en parallèle les flux atmosphériques et marins au cours de saisons contrastées (printemps et été) au point de vue de la production biologique. En effet, les mécanismes de transfert des apports atmosphériques à travers la couche euphotique seront vraisemblablement conditionnés par le cycle saisonnier de l'activité biologique (20). Le flux de matière particulaire étant dûs essentiellement aux grosses particules biogéniques détritiques (18), l'activité biologique et la sédimentation régissent les transferts de matière dans la colonne d'eau. L'ensemble des données atmosphériques et marines est disponible dans des publications antérieures et les valeurs de flux atmosphériques ont été comparées à celles obtenues par d'autres auteurs dans différentes régions méditerranéennes (10, 16).

Le tableau 1 donne les valeurs moyennes des flux élémentaires atmosphériques, sous la couche euphotique (- 200 m) et en mer profonde (-1000 m). Pour tous les éléments, on observe un flux atmosphérique toujours supérieur au flux marin (Fa/Fm > 1), ce qui signifie que l'atmosphère enrichit le stock disponible dans les eaux de surface, du moins pour la période considérée. Le flux à 200 m est toujours supérieur (Cd, Ni, Pb, Zn) ou égal (Co, Cu) au flux profond à 1000 m. Ceci rend compte de l'efficacité de l'exportation de la matière vers les couches profondes. Les éléments transportés par l'atmosphère se déposent à la surface de la mer sous forme dissoute (dans les pluies) ou particulaire (dans les pluies et dans les retombées sèches). Cette dernière phase va elle-même se dissoudre pour une large part dans la couche superficielle (21, 22).

Tableau 1. Moyennes géométriques des flux atmosphériques (Fa) et marins (Fm), en 1993, exprimées en $\mu g\ m^{-2}\ j^{-1}$, et rapports des flux Fa/Fm. Les écarts-types, calculés à partir de moyennes arithmétiques, illustrent la variabilité des flux.

Flux Elémentaires		Atmosphérique	Marin (-200 m)	Marin (-1000 m)
Cd	moyenne	0,17±0,07	0,04±0,03	0,02±0,02
	Fa/Fm		4,6	10,1
Co	moyenne	0,28±0,36	0,14±0,14	0,13±0,25
	Fa/Fm		1,8	1,9
Cu	moyenne	5,77±4,2	1,7±1,65	1,32±1,48
	Fa/Fm		4,1	4,1
Ni	moyenne	3,1±2,02	1,28±0,91	0,86±1,5
	Fa/Fm		2,1	2,9
Pb	moyenne	6,72±5,1	2,09±1,94	0,65±0,96
	Fa/Fm		2,2	5,3
Zn	moyenne	173±157	11,3±7,9	4,5±6,1
	Fa/Fm		20,6	41,2

Cependant, les particules collectées dans les pièges proviennent aussi bien d'apports atmosphériques dissous (après assimilation par l'activité biologique) que particulaires. Le pas de temps de collecte des pièges étant de 15 jours, les processus de dissolution de la matière atmosphérique ne sont pas pris en compte. Par conséquent, le fractionnement dissous-particulaire des apports atmosphériques, quand ils pénètrent dans la couche de surface, n'intervient pas dans cette discussion.

Ensuite, le transfert du matériel atmosphérique vers les couches marines profondes résulte d'une série de processus complexes (adsorption/désorption et agrégation/désagrégation) résultant de l'activité biologique. Les échantillons de pièges sont le résultat de cette séquence, mais ces processus ne sont pas discernables.

La figure 1 met en parallèle les évolutions saisonnières des flux atmosphériques, marins sous-jacents à la couche euphotique (200 m) et marins profonds (1000 m) de Cd, Co, Cu, Ni, Pb et Zn.

Les flux atmosphériques présentent une variabilité saisonnière assez peu marquée par rapport aux concentrations élémentaires (9). Par conséquent, les valeurs maximales de flux correspondent d'autant plus manifestement à des périodes particulièrement intenses, à partir desquelles on pourra tenter d'identifier une réponse océanique.

Le flux de matière (DYFAMED, série temporelle, Miquel *et al.*, données non publiées) mesuré à 200 m décroît de 196 mg $m^2\ j^{-1}$ en mai à un minimum de 16 mg $m^2\ j^{-1}$ en juillet. Il oscille ensuite entre 30 et 65 mg $m^2\ j^{-1}$ entre les mois d'août et septembre pour atteindre un second maximum de 103 mg $m^2\ j^{-1}$ en octobre et décroître jusqu'à 22 mg $m^2\ j^{-1}$ en novembre. Ces fluctuations traduisent des variations des conditions hydrologiques et biologiques en surface. Le mois de mai marque la fin du bloom printanier. Les eaux de surface, en se réchauffant, se stratifient, ce qui empêche leur alimentation en sels nutritifs par les eaux profondes. Pendant la saison estivale, le renforcement de la stratification des eaux induit un épuisement progressif des ressources nutritives qui ralentit l'activité biologique et favorise le recyclage en surface, et enfin ralentit la chute des particules. Le second maximum du mois d'octobre peut s'expliquer par des conditions météorologiques susceptibles de relancer l'activité biologique par le mélange des couches marines euphotique et sous-jacente (coups de vent) ou par approvisionnement atmosphérique (pluies; 23). De fait, l'apport atmosphérique des mois de septembre et octobre 1993 se résume quasiment à des épisodes pluvieux, soit 171 et 185 mm respectivement (16).

Le flux de matière à 1000 m croît de 100 à 160 mg $m^2\ j^{-1}$ pendant le mois de mai. Il décroît jusqu'à 20 mg $m^2\ j^{-1}$ à la fin juin et se stabilise à cette valeur jusqu'au mois de septembre. On remarque que le flux maximum (à 200 et à 1000 m) correspond à une période de type mésotrophe (mois de mai).

ESTIMATION OF LEVELS OF 10 METALS IN THE PHANEROGAMS OF THE ANTIKYRA GULF (VIOTIA, GREECE)

Paraskevi Malea

Institute of Botany, School of Biology, University of Thessaloniki, Box 109, GR-54006 Thessaloniki, Greece

Abstract

Concentrations mainly of Fe, Cu, Cd, Pb, Ca and in some instances of Na and K in *Halophila stipulacea, Posidonia oceanica* and *Cymodocea nodosa* collected near an aluminium factory in Antikyra Gulf were generally higher than those measured in the same or different species of the genus or subfamily from other areas. The same trend was also noted in the environment (sediment, water) of the study area.

Key-words: metals, phanerogams, Aegean Sea

Introduction

The submerged and widespread (along Mediterranean coasts) angiosperms *P. oceanica, C. nodosa* and the lessepsian migrant *H. stipulacea* (1) are the three most abundant seagrasses along the Antikyra Gulf (Viotia, Greece). Very few studies on metal accumulation in these species have been carried out (see references of Tables 2, 3, 4); moreover less information is available on seasonal variation of metal concentrations in these species.

Antikyra Gulf is interesting because of the bauxatic composition of the substrate and the waste discharges from an aluminium factory. Bauxite substrate is composed, among other elements, of Al, Fe, Cu, Ca, K and Mg, whereas the solid wastes contain, apart from other metals, Al, Fe, Ca and Na. In addition to the above metals Zn, Cd and Pb which are very toxic and relatively available to plants were also selected in our study. The aim of this survey was to discern the bioaccumulation potential of ten metals in three phanerogams from the Antikyra Gulf (Viotia) as well as to compare their concentrations with those in sea plants from other geographic areas and to assess the possibility of using these bioindicators to discern the presence of metal pollution in the Gulf.

Materials and methods

Seasonal sampling (from December 1985 to October 1986) of the phanerogams *P. oceanica, C. nodosa, H. stipulacea* was carried out at 12 stations in Antikyra Gulf (Greece) where the factory "Aluminium of Greece" is located as well as at Itea which served as a control station (in control station *P. oceanica* samples were not found) (Fig. 1). Aluminium, Fe, Cu, Zn, Cd, Pb, Na, K, Ca and Mg concentrations in seagrasses, *C. nodosa, H. stipulacea* (the entire plant) and the leaves of *P. oceanica*, the sediment and the dissolved metals in seawater were measured by Atomic Absorption Spectrophotometry by flame (Perkin Elmer 403) or by graphite furnace (Perkin Elmer HGA 72) (*e.g.* 1, 2).

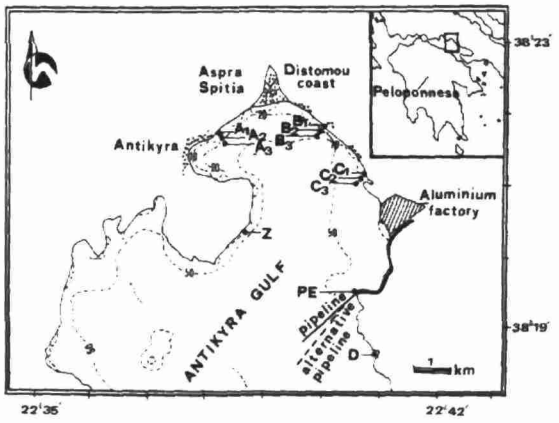

Fig.1. Sampling stations in the Gulf of Antikyra.

The accuracy of method was tested with standard reference material of Orchard leaves (N.B.S. no 1571); the results were within 10% for Fe, K, Na, Ca and Mg and 3% for Zn of NBS values, whereas for Cu, Cd and Pb the results were 6%, 20% and 2%, respectively, lower than the standard.

Results and discussion

Table 1 presents the mean (± standard error) and the range of the concentrations of 10 metals in the phanerogams *P. oceanica* leaves, *C. nodosa* and *H. stipulacea* from Antikyra Gulf. Comparison of the above concentrations (Table 1) with those observed in other populations of these species or other species of the same genus or subfamily, Posidonioideae (Table 2), Cymodoceoideae (Table 3) and Halophiloideae (Table 4), respectively, has shown the following:

Table 1. Mean value (x), range and standard error of the mean value (S.E.) of all concentrations (N) of each metal (μg g^{-1} d.w.) in *Halophila stipulacea, Cymodocea nodosa* and *Posidonia oceanica* from different samplings and from all stations of Antikyra Gulf.

	Halophila	*stipulacea*	*Cymodocea*	*nodosa*	*Posidonia*	*oceanica*
	X̄(±SE)	Range	X̄(±SE)	Range	X̄(±SE)	Range
Al	376(± 46)	52.0- 860	148(±22)	32.7-487	162(±46)	22.3- 793
Fe	850 (±106)	449- 2244	851(±102)	349 -2325	372(±32)	164 - 815
Cu	16.4(±6.4)	2.0-82.7	16.1(±5.9)	2.1- 98.3	18.0(±7.5)	2.8 -148
Zn	25.4(±4.2)	11.0-76.4	31.8(±2,3)	17.3- 50.5	43.4(±3.0)	27.1- 97.7
Cd	11.9(±5.3)	1.3-93.7	18.8(±4.7)	0.88-83.0	20.8(±3.0)	2.7 - 44.0
Pb	37.8(±7.7)	10.5-123	50.9(±14.8)	147- 297	39.5(±6.6)	10.5 - 123
Na	62596(±2410)	48457-87197	20557(±1073)	11845-28216	34275(±1028)	25736-44668
K	18023(± 563)	13149-21780	20421(±1248)	12318-36715	24320(±1433)	14167-36385
Ca	25365(±3491)	6235- 51343	25533(±4436)	3745-65018	13285(±1581)	4800-32275
Mg	11788(± 411)	9727- 16184	7565(± 318)	5191-10111	6791 (±112)	5940- 7974

1. Iron, Cu, Ca and Mg concentrations in *P. oceanica* at the study area (Table 1) are higher than corresponding concentrations in other species of the genus (7-13) (Table 2). Copper, Pb and Cd concentrations in *P. oceanica* fromAntikyra Gulf (Table 1) are higher than those of the same species from other areas (3-6) (Table 2) as well as mean concentrations in other phanerogams from "non-polluted" areas (14, 19, 20). Moreover, Pb and Cd concentrations exceed those in *P. australis* from an area characterized as "little or moderately polluted" by the above metals (10).

2. Exactly the same information was selected as concerns *C. nodosa*. Copper, Pb and Cd concentrations as well as the maximum Fe concentrations in *C. nodosa* from Antikyra Gulf (Table 1) are in general high (Table 3). More specifically, they exceed the corresponding values measured in the Gulf of Itea (control) (mean value ± SD: 2.8 ± 0.5 μg g^{-1}d.w. for Cu, 11.8 ± 1.0 for Pb, 13.7 ± 0.6 for Cd, 1644 ± 86 for Fe) and those observed in phanerogams from tropical, subtropical and intertidal "non-polluted" areas (14, 19, 20). However, Pb and Cd values in *C. nodosa* from the study area do not exceed those from a location highly polluted by these metals (10).

3. Cadmium, Pb, Na, K and Ca concentrations in *H. stipulacea* from Antikyra Gulf (Table 1) are higher than those in different species of the genus from other areas (see references in Table 4). It has also been observed that Cd and Pb concentrations are higher than those in the same species from Itea (control) (mean value ± SD: 4.3 ± 0.4 μg g^{-1} d.w. for Cd, 31.4 ± 4.0 for Pb) and Cd levels are greater than concentrations reported for the same species from the Red Sea (17).

Concerning Al, no information has been found on its concentrations in marine phanerogams from other geographic areas.

The generally high Fe, Cu, Ca, Pb and Cd concentrations in phanerogams from Antikyra Gulf are explained by their respectively high values in the sediment and seawater from the same area (21). Besides Fe, Cu and Ca constitute the main bauxite components of the area, whereas Fe and Ca also make up the main components of the sewage being discharged from the "Aluminium of Greece" factory. The differences derived from the above comparisons may also be attributed to interspecific and intraspecific variations, to differences in the age of plants and their collection time, as well as to differences in environmental factors (*e.g.* salinity, pH) that influence metal uptake.

VARIABILITY OF $^{13}C/^{12}C$ AND $^{15}N/^{14}N$ IN DIFFERENT MUSSEL TISSUES (*MYTILUS GALLOPROVINCIALIS*) : IMPLICATIONS FOR FOOD WEB STUDIES

Alenka Malej [1], Tadej Dolenec [2] & Sonja Lojen [3]*

[1] National Institute of Biology, Marine Station Piran, Slovenia
[2] University of Ljubljana, Faculty of Natural Sciences and Engineering, Dept. of Geology, Slovenia
[3] J. Stefan Institute, Department of Environmental Sciences, Slovenia

Abstract

Measurements of the stable isotope ratios of carbon and nitrogen were obtained for different mussel (*Mytilus galloprovincialis*) tissues from two locations in the Gulf of Trieste (Adriatic Sea). We found no significant differences in $\delta^{13}C$ and $\delta^{15}N$ between the two sites ($p > 0.5$) nor between two size classes ($p > 0.9$) of mussels. Differences were significant ($p < 0.05$) among different mussel tissues indicating that within the organism variability may be large enough to affect the conclusions drawn about trophic position of animals when based only on analysis of one particular tissue.

Key-words: bivalves, food webs, Adriatic Sea

Introduction

The use of stable isotope ratios as indicators of animal trophic position and food web relationships has become increasingly widespread, especially using combined measurements of $\delta^{13}C$ and $\delta^{15}N$ (1). The characteristic isotopic composition of each biogenic material depends on the isotopic ratios of diet (substrate), metabolic pathways and fractionating processes (2); consequently, stable isotope signatures of organisms may provide information of the trophic linkages within food webs (3). The stable isotopic ratios of C and N in consumers have been shown to reflect those assimilated with about 1-2 enrichment of ^{13}C and 3-4 enrichment of ^{15}N (4, 5). Generally, implicated organic matter pathways are based on bulk samples and/or the isotopic composition of whole animals and plants, despite variations within individuals and populations (6), and variability among different tissues (7). Moreover, significant spatial differences in isotopic compositions have been found within a few kilometres (8, 9).

In our previous studies we used C isotopic ratios to assess the food sources of the planktivore jellyfish *Pelagia noctiluca* in the northern Adriatic (10) and to elucidate the sources of sedimentary organic matter in the nearshore marine environment (11). The aim of the present study was: (1) to determine the C and N isotopic composition of the benthic filter feeding, mussel *Mytilus galloprovincialis*, (2) to determine mussel $\delta^{13}C$ and $\delta^{15}N$ at two different locations in order to assess spatial variations, and (3) to determine $\delta^{13}C$ and $\delta^{15}N$ of different mussel tissues in order to estimate how the selection of a particular tissue for isotopic analysis may affect the trophic positioning of animals.

Material and methods

Mussels (*Mytilus galloprovincialis*) were collected at two sites on the south-eastern coast of the Gulf of Trieste (Adriatic Sea), one in the bay of Piran (SEC) close to the Dragonja river outflow, and the second in the bay of Strunjan (STR) which is without significant freshwater input (Fig. 1). Sampling was carried out in June 1996 after the spring spawning period of mussels (12).

Individual mussels were pooled according to shell length in the two size classes: 40-60 mm and 60-90 mm, the former less than two years and the latter more than two years old (12). Different tissues (foot, gills, byssus, stomach) were carefully dissected for isotopic analysis. Stomachs were analysed together with their food content.

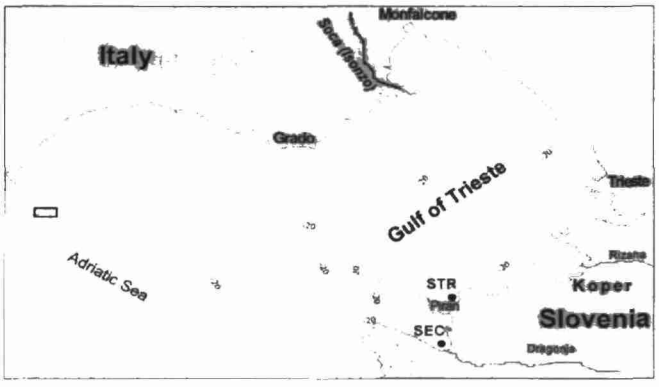

Fig. 1. Study area and sampling locations, sec and str.

To determine the stable isotope composition of nitrogen and carbon, freeze-dried samples of different tissues were ground and analysed using an Europa 20-20 Stable Isotope Analyser (Europa Scientific Ltd., UK) with an ANCA-NT preparation module for automatic combustion and separation of produced gases (13). Samples were treated with 1N HCl and washed with distilled water several times prior to measurement to eliminate residues of carbonates, which might be present in tissues in contact with the sediment. Stable isotope compositions of C and N were expressed as values in per mill deviation from a standard as follows:

$$\delta^{13}C \text{ or } \delta^{15}N = \delta^{13}C \text{ or } \delta^{15}N[‰] = \left(\frac{R_{sample}}{R_{standard}} - 1\right) x1000$$

where $R=^{13}C/^{12}C$ or $^{15}N/^{14}N$, respectively. PDB and atmospheric nitrogen were used as standards. Analytical error was 0.2 for both $\delta^{13}C$ and $\delta^{15}N$.

Results and Discussion

The $\delta^{13}C$ and $\delta^{15}N$ data obtained for mussels (*Mytilus galloprovincialis*) from both locations varied between - 22.63 and - 18.58‰, and between 4.18 and 5.69‰, respectively, with an overall mean for $\delta^{13}C$ of - 20.79 ± 1.21‰ (n = 46) and mean for $\delta^{15}N$ of 4.84 ± 0.44‰ (n = 46). These results are similar to or slightly lower than those reported for different benthic filter feeders in the literature (14, 4). The mean $\delta^{13}C$ of mussels (results from all analyses pooled) was around 2.5‰ higher than that of their presumed food - phytoplankton dominated suspended organic matter (- 23.3 ± 1.3‰; 11), consistent with the widespread recognition of C isotopic fractionation in consumers. Unfortunately, we have no data for $\delta^{15}N$ in suspended organic matter as source material.

When data for all tissue samples were combined, we did not find significant differences between the two sites ($p > 0.5$) in either $\delta^{13}C$ or $\delta^{15}N$, nor between the two size classes of mussels ($p > 0.9$). However, differences were significant ($p < 0.05$) among different mussel tissues (Tables 1, 2). The highest $\delta^{13}C$ or $\delta^{15}N$ was found for mussel byssus followed by gills, while other tissues contained less heavy isotopes of C and N.

Table 1. Mean $\delta^{13}C$ and $\delta^{15}N$ of different tissues at two sites (mean ± SD,‰, n=6)

	STR		SEC	
tissue	**$\delta^{13}C$**	**$\delta^{15}N$**	**$\delta^{13}C$**	**$\delta^{15}N$**
foot	- 22.0 ± 0.18	4.84 ± 0.23	-21.36 ± 0.86	4.75 ± 0.28
byssus	- 19.31 ± 0.88	5.17 ± 0.23	- 19.15 ± 0.74	5.16 ± 0.35
gills	- 20.49 ± 0.29	5.19 ± 0.31	- 20.33 ± 0.28	5.0 ± 0.42
stomach	- 22.0 ± 0.39	4.26 ± 0.07	- 21.4 ± 0.27	4.31 ± 0.16

Table 2. Results from multiple comparison test (Scheffe test) to detect differences between the $\delta^{13}C$ and $\delta^{15}N$ of different tissues (data for mussels from both sites pooled together, positioning of * denotes similarity and/or dissimilarity $\delta^{13}C$ and $\delta^{15}N$ of analyzed tissues)

	Homogeneous groups (95 % Confidence intervals)	
tissue	**$\delta^{13}C$**	**$\delta^{15}N$**
foot	*	*
stomach	*	*
gills	*	* *
byssus	*	*

DISTRIBUTION OF ORGANOLEAD COMPOUNDS IN THE ADRIATIC COASTAL MARINE ENVIRONMENT

Nevenka Mikac [1*], Marko Branica [1], Yun Wang [2] and Roy M. Harrison [2]

[1] Center for Marine and Environmental Research, Institute Rudjer Boskovic, Zagreb, Croatia
[2] School of Chemistry, University of Birmingham, Birmingham, United Kingdom

Abstract

The distribution of alkyllead compounds, originating from leaded gasoline, between different marine compartments was studied. The following concentration ranges of organic lead in samples collected in the eastern Adriatic coast during period 1994-1995 were obtained: water 7-7.8 ng/l, mussels 1-3.9 ng/g, fish 0.2-2.7 ng/g and sediment 0.04-0.42 ng/g. The percentage of organic lead was found to decrease going from water (2.7-16%) to mussels (0.3-1%), fish (0.4-1.6%) and sediments (0.0006-0.001%). Evidently, organolead compounds are not accumulated in sediment, but they could be accumulated from water into living organisms. Biomagnification in the marine food chain most probably does not take place. This study confirms the limited extent of organolead pollution in the Adriatic marine environment.

Key-words: lead, mollusca, Adriatic sea

Introduction

Organolead compounds are introduced into the environment by their use as an antiknock additive in gasoline. It is estimated that about 1% of lead in gasoline is emitted from vehicles in the form of tetra- and ionic alkyllead compounds (TAL and IAL). The presence of alkyllead compounds has been established in different kinds of environmental samples, mostly abiotic compartments such as air and rainwater, in which organolead compounds exist in appreciable concentrations (1). The fate of organolead compounds in aquatic organisms and especially in the marine environment is still not well known, although there is evidence that alkyllead is appreciably more toxic than inorganic lead. Our previous study has shown that alkyllead compounds are readily accumulated in sedentary organisms such as the mussel *Mytilus galloprovincialis* (2) which has been widely used as an indicator organism for heavy metal pollution in the marine environment. The aim of this work was to establish the distribution of alkyllead compounds introduced into the Adriatic marine environment from local sources (coastal gasoline stations and navigation) between different marine compartments, and to study in more detail the uptake of these compounds in the mussel *Mytilus galloprovincialis*.

Methods

Samples of subsurface seawater, surface microlayer, sediment, various fish species and the mussel *Mytilus galloprovincialis* were collected in July 1995 from the Sibenik area in the central part of the eastern Adriatic coast. Mussels and water samples were also collected in front of gasoline stations in the towns of Split (July 1995) and Rovinj (October 1994 and September 1995). Organolead compounds were extracted from water, sediment and biota (after tissue digestion by tetramethylammonium hydroxide) into hexane (TAL directly, IAL after complexation with carbamate), evaporated to smaller volume, cleaned by passing through a silica column and after propylation analysed by GC AAS (gas chromatography/atomic absorption spectrometry). Total lead was measured by DPASV (differential pulse anodic stripping voltammetry) after UV irradiation of unfiltered water samples or acid digestion in the case of sediments and organisms. Analytical methods are described in more detail elsewhere (3,4).

Results and discussion

Distribution between different compartments. Previous studies of the organolead distribution in the marine environment of the Adriatic sea have shown that gasoline stations represent a continuous source of organolead compounds as demonstrated by both contamination of seawater (4,5,6) and mussels (2). In July 1995 in addition to seawater and mussels, samples of microlayer, sediment and fish were also collected from Sibenik Bay, in order to see how organolead contamination is reflected in other marine compartments (Table 1).

Table I. Concentration ranges of organolead compounds and total lead in different marine compartments of Sibenik Bay in July 1995.

Sample type	Concentration range (ng/l for water or ng/g w.w. for solid samples)					
(number of data anlyzed)	Et_4Pb	Et_3Pb^+	Me_3Pb^+	Pb_{org}	Pb_{tot}	$\%Pb_{org}$
Water (20)	<0.5-1.1	1.0-2.9	2.0-4.9	4-7.8	132-220	2.7-4.3
Microlayer (5)	<1.0	<0.5-3.3	2.9-8.4	8.5-11.7	2700-3400	0.3-0.4
Sediment (5)	<0.2	<0.02-0.3	0.04-0.12	0.04-0.42	6800-44800	0.0006-0.001
Mussels (20)	<0.2-1.5	<0.2-1.4	1.0-1.2	1.0-3.9	210-530	0.3-1.0
Fish-muscle (10)*	<0.2-1.0	<0.2-1.3	0.2-0.5	0.2-2.7	20-112	0.4-1.6
Fish-intestine (5)	<0.2-1.2	<0.2-1.4	0.3-0.5	0.4-2.9	144-3400	0.04-0.1

* *Species of fish are given in Fig 2.*

A decrease of organolead concentration and percentage going from water to sediments (Table 1) indicates insignificant settling of organic lead into sediments. However, few times higher concentrations of ethyllead derivatives were observed in the imediate vicinity of the pollution source (gasoline station-GS, Fig. 1) in comparison with a 200 m distant location (center of the Bay-C, Fig. 1). The concentration of trimethyllead was lower and comparable at these two locations (Fig. 1). A low organolead percentage in sediment could be a consequence of decomposition (photolysis) of alkyllead compounds in the photic layer of the water column (1,7) or their elimination by accumulation into biota (1,2). Contrary to the organic lead, the distribution of total (inorganic) lead demonstrates that sediment represents a sink for inorganic lead (Table 1), an observation that is in agreement with a much higher affinity of inorganic lead for particulate matter than the organic form (5,8). The extent of such pollution is also limited, since the concentration of the total lead is an order of magnitude higher in front of the gasoline station (30-45 μg/g) than in the centre of the bay (6-8 μg/g).

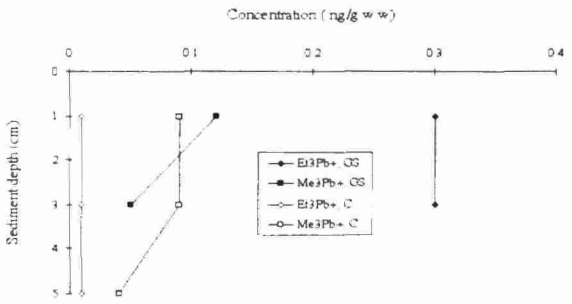

Fig. 1. Alkyllead coumpounds (triethyllead-Et_3Pb+; trimethyllead-Me_3b+) in sediments of Sibenik Bay (GS = gasoline station; C = center of the bay) in July 1995.

The concentration of lead species in mussels obtained in July 1995 are comparable with the levels obtained earlier in the same area (2). The previous study confirmed that such organisms could serve as a good indicator of the environmental organolead level (2). A similar organolead concentration is obtained in fish samples (Table 1), indicating that these compounds are not biomagnified in the marine food chain. Bioconcentration factors (BF) for organic lead are of the same order of magnitude for mussels (about 200-500) as fish muscle (50-300). A difference in the internal distribution of organic and the total lead in fish is evident, as organic lead is more equally distributed in the whole organism (Fig. 2), compared to the total lead which is accumulated primarily in the intestine (Table 1). The concentration of trimethyllead is less variable than those of ethyllead derivatives (Fig 2), similar to that found for the mussel *Mytilus galloprovincialis* from the eastern Adriatic (2). This seems to be a general trend in biological samples and could be related to either higher stability of methyl derivatives or their formation by biomethylation.

Uptake into mussels. In order to learn more about the uptake of organolead compounds into mussels, the tissue distribution of these compounds was determined in samples containing different organolead levels (Figs. 3 and 4). Samples collected from Sibenik and Split (SI/GS, ST/GS, Figs. 3a and 4 a,b) were within the concentration range of 0.1-10 ng/g, established as a common organolead level in mussels polluted by leaded gasoline (2). Samples collected from

PARTICULATE AND ORGANIC FLUXES IN A COASTAL HYDROTHERMAL AREA OFF MILOS, AEGEAN SEA

J.C. Miquel [1*], S.W. Fowler [1], J. La Rosa [1], S. Aliani [2] and R. Meloni [2]

[1] IAEA, Marine Environment Laboratory, B.P. 800, MC98012 Monaco

[2] Stazione Oceanografica - CNR, Forte S. Teresa, Pozzuolo di Lerici, 19123 La Spezia, Italy

Abstract

Two moorings were deployed from June to September 1996 along the SE Coast of Milos in an area known for its extensive area of geothermally active seabed. Moorings were fitted with current meters and sediment traps to measure particulate fluxes at 60 m over a bottom of 90 m depth. The vertical particulate fluxes were integrated over periods of 12 days. Surface currents were relatively high but at the trap depth rarely reached 5-10 cm s^{-1}. Vertical mass fluxes were extremely variable at both sites, ranging from 7 mg $m^{-2}d^{-1}$ to 5.9 g $m^{-2}d^{-1}$, with mean fluxes over one order of magnitude higher at the vent site, increasing to as much as 200 times higher during periods of maximum flux. Carbon and nitrogen fluxes showed a similar pattern whereas pigment fluxes had a completely different variability over time. The high POC fluxes measured were not related to phytoplankton biomass but were likely related to the export of organic material produced at the vent sites.

Key-words: thermal vents, particle flux, sediments, Aegean Sea

Introduction

The Aegean Sea is an area of high seismic activity (1) associated with important geothermal gas venting (2). The island of Milos, located on the Hellenic volcanic arc, is noted for extensive areas of submarine vent fields with some 35 km^2 of geothermally active seabed in shallow waters which vent large volumes of free gas as well as phosphate and manganese (3, 4). Venting typically consists of diffusive seepage of warm water and chemicals from fractures in the seabed. In close proximity to these vents, a vent ecosystem based upon thermophilous bacteria and chemosynthesis is normally present. Fluids from the vents, bacteria and particles produced in the vent ecosystem are advected by currents and create a plume that spreads laterally at a level of neutral buoyancy. The geochemical cycling and biological production based on chemosynthesis in these shallow hydrothermal vents is still largely unknown, particularly the importance of vents in the production and export of particulate organic material. The present communication reports the first results on vertical fluxes of material associated with these vent fields.

Material and Methods

In summer 1996 two moorings were deployed along the SE coast of Milos off Paleohori Bay in an area known for its numerous shallow water vent fields (site C, Fig. 1) and off Provatas Bay in an area presumed to be free of any major vent influence (site A, Fig. 1). Both moorings were located about 1 nautical mile offshore in a water column of 90 m depth, and were 3.5 nautical miles distant from one another. They included sediment traps (Technicap cylindro-conical model PPS3 with an opening of 1/8 m^2) for collection of particles and flocs sedimenting through a depth of 60 m, and current meters (Aanderaa RCM7, InterOcean S4 and RDI ADCP sentinel) located closer to the bottom (85 m) and the surface (12 m) in order to obtain three-dimensional current measurements. Current meters were calibrated at the factory prior to deployment and were set to sample every 30 minutes. Prior to deployment, the trap sampling cups were filled with a 2% buffered formaldehyde solution in filtered local sea water (0.22 μm) to prevent *in situ* microbial degradation and grazing by swimmers. Moorings were deployed on June 19 and recovered on September 25. At each site 8 trap samples covering 12 days each were obtained to study temporal changes on downward particulate fluxes over the 3 month-period.

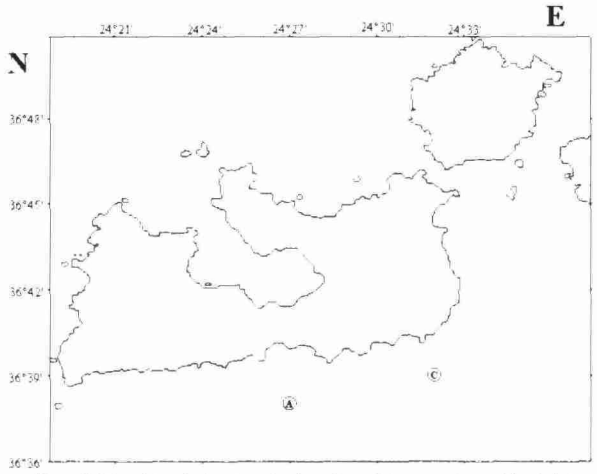

Fig. 1. Map of Milos island showing the location of the moorings. Site A is located off Provatas Bay (area without submarine geothermal vents) and site C is located in the vent zone off Paleohori Bay.

Trap samples were analyzed in the laboratory following standard methodologies (5). Swimmers were first separated by sieving through 1500 μm and 600 μm to remove larger species, and then the remainder was "hand-picked" under a dissecting microscope. Liquid subsamples of the trap material were taken for the analysis of pigments and particle composition. The remaining sample was desalted and freeze-dried for further analyses and estimation of mass flux. Carbon and nitrogen were analyzed by high temperature oxidation using a Heraeus CHN elemental analyzer. The organic carbon fraction was measured in samples treated with a one molar phosphoric acid solution for removal of carbonates (6). Chlorophyll a and phaeopigment were measured spectrophotometrically in 90% acetone extracts and quantified as Chl.a-equivalents using the equations of Lorenzen (7).

Results and Discussion

Currents in surface waters at both sites were strong and mainly directed towards the southwest. At the vent site they reached 50 cm s^{-1} and displayed some peaks oriented in a northerly direction. Current speed decreased rapidly with depth and, in the vicinity of the traps (60 m), they were generally less than 5 to 10 cm s^{-1} flowing in a southwesterly direction (Fig.2). Current speeds closer to the bottom were very low and at the vent site (C), they were often below the threshold of the RCM7 Aanderaa. Furthermore, the bottom currents at the vent site were oriented in a southwesterly direction, whereas at the control site (A) they formed a clockwise vortex shear. Therefore, despite strong surface currents, the traps were located in a relatively calm environment in terms of water mass transport.

At both sites mass fluxes were highly variable and, at least during some periods, quite high. Mean mass flux was one order of magnitude higher at the vent site than at the control station, however during the period of maximum sedimentation, the flux was over 200 times higher at the vent site (Fig. 3). Only during August were fluxes comparable at the two sites or higher at the control area. Total mass fluxes at the vent site were extremely variable ranging between 7 mg m^{-2} d^{-1} and 5.9 g m^{-2} d^{-1}. The range of mass flux at the control station was less, *i.e.* 11 to 1000 mg m^{-2} d^{-1}. During periods of low sedimentation, sinking particles at both sites were composed of plankton debris and marine snow, whereas large flocs of biogenic material and elongated ellipsoidal fecal pellets comprised the bulk of the particles during periods of maximum flux. POC and N fluxes presented similar trends over time and between stations indicating that there were two periods of pulsed sedimentation of organic material at the vent site and one period of much smaller magnitude at the control site. Maximum POC and N fluxes at the vent and control site were 1359 and 115 mg POC m^{-2} d^{-1}, and 238 and 21 mg N m^{-2} d^{-1}, respectively. The C and N content of the sedimenting particles was high and similar at both sites throughout the study except in September when concentrations sharply decreased and the C/N ratios increased, a consequence of a significant

NATURAL RADIOACTIVITY AND ^{137}CS IN SURFACE SEDIMENTS OF THE BAY OF ALGIERS, ALGERIA.

A. Noureddine [1]*, B. Baggoura [1], M. Boulahdid [2], K. Agouar [2], T. Aitabdelmalek [2]

[1] Lab. d'Environnement, Centre de Radioprotection et de Sûreté, 2 Bd F. Fanon, B.P. 399 Alger-Gare, Algérie
[2] Département de la Pollution Chimique, Institut des Sciences de la Mer et de l'Aménagement du Littoral, Villa n°4, Sidi-Fredj/plage ouest B.P. 54 Staoueli, DZ-42321 Tipaza, Algérie

Abstract

Samples of surface (0-15cm) marine sediments of different nature, namely sand, muddy sand and fine sand were collected in the Bay of Algiers during August 1993 using a Van Veen type grab. They were analysed directly by gamma spectrometry for uranium and thorium series radionuclides and ^{137}Cs. Samples analysed contained relatively high activities of natural radionuclides, 8-66, 7-41, and 127-447 Bqkg $^{-1}$ for uranium and thorium series and ^{40}K, respectively, and ^{137}Cs concentrations ranged from 0.5-6.9 Bq kg^{-1} dry weight. The concentrations of natural and artificial radionuclides in sediments appear to depend on the grain size composition of sediment samples.

Keys-words: radioactivity, sediments, Algerian Basin

Introduction

Different radioactive sources may contribute to the introduction of radioactivity into the marine environment. In addition to the artificial radioactivity, natural radionuclides can occur, by weathering and recycling of terrestrial minerals and rocks, in the sea floor (anthigenic rocks) and in sea water to give rise to ^{40}K, ^{87}Rb, uranium and thorium series [1]. Therefore within the framework of the radiological monitoring programme for the Algerian littoral, surface sediment samples were collected from the Bay of Algiers, located in the central part of the Algerian coast, and analysed to measure activity in Bq kg^{-1} dry weight of ^{137}Cs, ^{40}K, ^{238}U and ^{232}Th daughters.

Experimental

The semi-circular Bay of Algiers is delimited in the east by the "Cap Matifou" and in the west by the "Pointe Pescade" as shown in Figure 1 [2]. Surface sediment samples of about 2 kg were collected with a Van Veen type grab in 14 nearshore stations during August 1993 (see Fig. 1) at depths ranging from 10 m to 60 m. The samples were stored in plastic bottles, labelled, and brought to the laboratory to be oven dried at 100°C, crushed and homogenised for direct counting by gamma spectrometry. Radionuclide measurements were made on a GeLi detector of 20% relative efficiency and (FWHM) resolution of 1.8 keV at 1332 keV gamma-energy of ^{60}Co. The detection efficiency of GeLi was determined using an IAEA 500 cm^3 sealed Marinelli beaker filled with a solid material of density 1, and contaminated with a radioactive source of ^{152}Eu of 11655 Bq on 01/03/91. The concentrations of ^{40}K, ^{238}U and ^{232}Th daughters were measured using the gamma-ray of highest emission probability for each radionuclide. The beakers were put in contact with the top of the detector and counted for 57600 s, which is statistically enough to give reliable results. To enhance the credibility of our results, our laboratory took part in several intercomparison exercises organised by the IAEA laboratories (Monaco and Seibersdorf), the main samples analysed were IAEA-134/135/300/315/326/327. Our results were in agreement with those reported by the IAEA, particularly in the range (300-1700) keV, however, between (0-300) keV, corrections should be brought to improve the results.

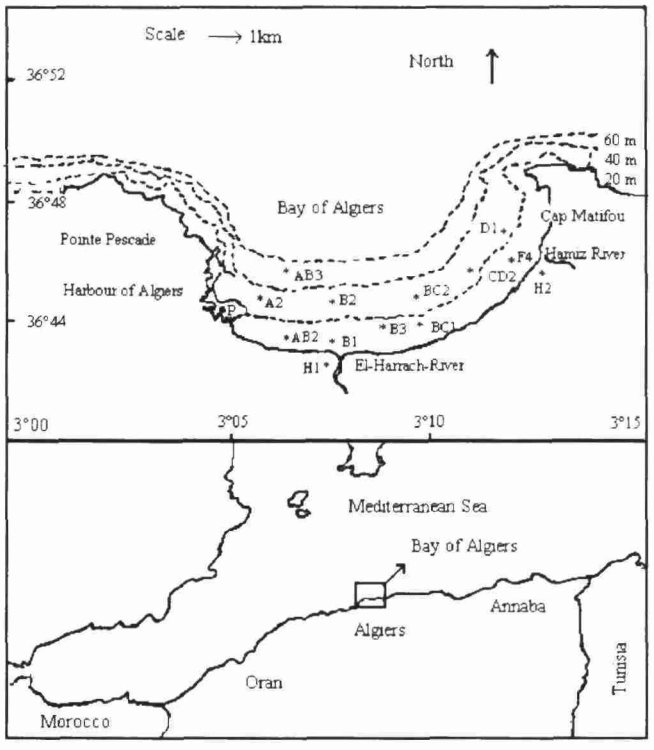

Figure 1. Sampling locations in the Bay of Algiers.

Results and discussion

Radionuclide concentrations in Bq kg^{-1} dry weight are given in Table 1. The description of sediment samples according to grain-size composition is given in Table 2. The sampling points H_1 and H_2 were located at the mouth of rivers and the others inside the Bay. The radioactivity at the sampling points H_1 and H_2, outside the Bay, is much lower than that inside the Bay. This is due to the grain size composition of sediments further offshore which is coarse sand at these stations. The range of concentrations of the main natural radionuclides recorded in the whole samples, ^{226}Ra and ^{40}K are 25 ± 3.4 - 66.5 ± 7.5 and 127 ±24.0-447± 49.0, Bq kg^{-1} dry weight, respectively. However, for artificial radioactivity, ^{137}Cs concentrations measured in the sediments depend on the grain size of the sample and ranged from the minimum detectable activity, 0.5 ± 0.2, Bq kg^{-1} dry weight, to 6.9 ± 0.9, Bq kg^{-1} dry weight. Activities of ^{137}Cs in Bq kg^{-1} dry weight recorded in this Bay are of the same order than those measured in the Bay of Ghazaouet [3], which range from 0.7 ±0.1 - 8.5 ± 1.9 but are much higher compared with those obtained for the Bay of Zemmouri 0.5 ± 0.1 - 1.5 ±0.2 Bq kg^{-1} dry weight [4]. The concentrations of natural and artificial radionuclides reported in this work were also compared with published values and found to be in the same order as those reported in the literature [5-7]. The origin of ^{137}Cs, appears to be most likely from nuclear weapons tests and the Chernobyl accident. This study enabled us to monitor the site, to determine the uptake of radio-

Table 1. Concentrations in Bq kg^{-1} dry weight of ^{137}Cs, ^{40}K, and ^{238}U and ^{232}Th daughters in surface sediments of the Bay of Algiers.

	Activity in Bq kg^{-1} dry weight						
Samp. point	^{226}Ra	^{214}Pb	^{214}Bi	^{228}Ac	^{212}Pb	^{40}K	^{137}Cs
A_2	40 ± 5	13 ± 1	14 ± 2	19 ± 2	32 ± 3	331 ± 37	7.0 ± 1
P	66 ± 8	20 ± 2	18 ± 2	29 ± 3	41 ± 4	447 ± 49	6.2 ± 0.7
AB_2	44 ± 5	18 ± 2	16 ± 2	25 ± 2	36 ± 4	388 ± 42	2.0 ± 0.3
AB_3	30 ± 4	15 ± 2	14 ± 2	21 ± 3	33 ± 3	353 ± 40	0.7 ± 0.3
B_1	46 ± 5	17 ± 2	16 ± 2	22 ± 3	35 ± 3	334 ± 37	1.5 ± 0.2
B_2	32 ± 4	14 ± 2	14 ± 2	18 ± 3	30 ± 3	302 ± 34	1.3 ± 0.4
B_3	53 ± 6	19 ± 2	17 ± 2	23 ± 3	34 ± 3	298 ± 34	1.4 ± 0.2
BC_1	43 ± 5	16 ± 2	15 ± 2	20 ± 3	33 ± 3	318 ± 36	1.1 ± 0.2
BC_2	49 ± 6	17 ± 2	16 ± 2	23 ± 3	37 ± 4	356 ± 39	1.1 ± 0.3
CD_2	33 ± 4	14 ± 2	16 ± 2	20 ± 3	34 ± 3	291 ± 34	1.1 ± 0.2
D_1	29 ± 4	9 ± 1	8 ± 1	7 ± 1	15 ± 2	191 ± 24	1.4 ± 0.2
F_4	47 ± 5	18 ± 2	17 ± 2	25 ± 3	37 ± 4	342 ± 38	0.6 ± 0.3
H_1	25 ± 3	11 ± 1	12 ± 2	14 ± 2	25 ± 2	285 ± 35	1.1 ± 0.2
H_2	25 ± 3	11 ± 1	11 ± 1	10 ± 2	21 ± 2	127 ± 24	< LD

REMINERALIZATION RATES OF ORGANIC CARBON IN THE SEDIMENTS IN THE GULF OF TRIESTE (N ADRIATIC)

Nives Ogrinc [1]*, Sonja Lojen [1] and Jadran Faganeli [2]

[1] Dept. Environmental Sciences, J. Stefan Institute, Jamova 39, 1000 Ljubljana, Slovenia
[2] Marine Biological Station, Fornace 41, 6330 Piran, Slovenia

Abstract

Remineralization rates of organic matter were calculated in high carbonate coastal marine sediments of the Gulf of Trieste, northern Adriatic, using a non-local exchange, vertical diffusion-reaction model of the dissolved inorganic carbon (DIC) depth profiles. It appears that there is a reactive portion of organic matter which is oxidized at the sediment water interface. Examination of the dissolved Ca^{2+} profiles indicated that there was significant production of acid which dissolved $CaCO_3$ in the sediment in winter and late spring. The calculated remineralization rates varied seasonally with the highest observed in September 1995. During this period the dissolution of $CaCO_3$ accounted for only 9% of DIC produced.

Key-words: carbon, sediments, Adriatic Sea

Introduction

Sediment biogeochemistry plays an active role in the regulation of carbon cycling in aquatic environments. Processes in sediments are coupled to the microbially-mediated degradation of organic matter deposited from the overlying water. The electron and mass balances in sediments are coupled to each other and are determined primarly by the microbial oxidation of organic matter. The concentration of dissolved inorganic carbon in marine sediment interstitial solution reflects the remineralization of organic carbon to CO_2 in marine sediments. In coastal environments other factors influencing the dissolved inorganic carbon (DIC) in pore water are dissolution or precipitation of carbonates, and mixing with dissolved inorganic carbon from the overlaying water column [1, 2]. In order to investigate the complex mechanisms that regulate the remineralization of organic carbon, pore water and solid profile measurements are made [3] and combined with benthic flux measurements [4, 5, 6], or laboratory experiments [4, 7]. Additionally, mathematical models may be used to provide quantitative estimates of the remineralization of organic carbon in sediments [8, 9]. Most commonly applied are stoichiometric models assuming that organic matter with Redfield stoichiometry (C:N:P = 106:16:1) is oxidized to CO_2 using O_2, NO_3^-, MnO_2, Fe_2O_3, SO_4^{2-}, CO_2 as electron acceptors. Changes in DIC with depth are predicted considering equilibrium with calcite, the stoichiometry of oxidation, the diffusion of solutes through pore water, and assumed rates of oxidation of organic matter [8, 9]. This approach has been useful in understanding processes in deep-sea sediments, but its application in nearshore sediments is more uncertain. The active benthic community in coastal sediments enhances solute transport through mixing and irrigation [1, 2].

In this paper the amount of organic carbon oxidized to CO_2 was estimated by applying a simple non-local - diffusion - reaction model to the DIC depth profiles. This study shows that in high carbonate surficial sediments of coastal marine environments, the degradation of organic carbon is the principal source of DIC in pore water during all seasons. However, the contribution of calcite dissolution should be taken into account, especially in the colder months when the rate of degradation of organic matter is slower.

Methods and site description

Site description. Sediment samples were collected in the central part of Gulf of Trieste in the northern Adriatic. The sampling site is at a depth of 21 m. Vertical temperature and salinity gradients in late summer often result in bottom water hypoxia (occasionally anoxia). The sediment is composed of silty sand with up to 80% carbonate. Carbonate minerals are mostly composed of low-magnesium calcite. The sediment contains approximately 0.7 wt % C of dry sediment as organic carbon. The composition of the sediment in profile is practically uniform. Sedimentation rates, based on ^{210}Pb distributions, are approx. 1-2 mm yr^{-1} in the central part of the gulf [10]. The surficial sediments are bioturbated mostly by polychaetes and bivalves.

Sampling methods. Sediment samples were taken in June and September in 1995 and in January 1996 by SCUBA divers inserting a plexiglass tube (6 cm i.d.) directly into the sediment (approx. 30 cm). Undisturbed sediment cores were transported immediately to the laboratory. In a N_2-filled glove bag, cores were cut into 1, 2 or 4 cm segments. Pore water was squeezed from the sediment under 0.4 MPa nitrogen through a 0.45 μm membrane filter. The pH electrode was inside the glove bag and pH was measured immediately after collecting the sample. Subsequent samples were collected for alkalinity, Ca^{2+}, Mg^{2+}, dissolved Fe and Mn, PO_4^{3-}, NO_3^-, NH_4^+ and SO_4^{2-}. Samples for metal analysis were acidified with ultrapure HNO_3. A portion of the sediment solid phase was freeze-dried and ground to a fine powder for analysis of organic C and total N.

Chemical analysis. Standard analytical methods were used. Alkalinity was determined by the Gran titration method; the precision of the analysis was ± 1% [11]. DIC was calculated from alkalinity, pH and salinity data using the apparent dissociation constants of Mehrbach *et al.* (using the fitting functions given by Dickson and Millero [12]), and the boric acid acidity constant of Lyman [12]. Concentrations of metal cations were determined by flame AAS. Phosphate, nitrate, ammonia, and sulphide were analyzed using standard colorimetrical methods [13]. Analysis of organic C and total N in sediment samples were performed using a Carlo Erba elemental analyzer (mod. EA 1108) after acidification with 1M HCl [14].

Results and discussion

The data collected in this study were used to calculate seasonal rates of mineralization of organic carbon to CO_2. The rate of oxidation of organic carbon was determined by modeling the seasonal profiles of DIC in the central part of the Gulf of Trieste. The major processes affecting the pore water concentration of DIC described in the model are diffusion, irrigation, oxidation of organic carbon and dissolution or precipitation of $CaCO_3$. Changes in the concentration of DIC by oxidation of organic matter or equilibration with $CaCO_3$ are described by the CO_2-production rate, Rc(z). Rc(z) is assumed to decrease exponentially with depth and in our model it is described by two exponential functions. This assumption was based on a study by Westrich and Berner [15], which showed that organic matter was composed of two reactive fractions of different reactivities, and a non-degradable fraction. Thus the functions describing Rc(z) are [1]:

$$Rc = R_0 \exp(-\beta_1 z) \qquad \text{from 0 to } z_b \qquad (1)$$

$$Rc = R_{zb} \exp[-\beta_2 (z-z_b)] \qquad \text{from } z_b \text{ to } \infty \qquad (2)$$

where R_0 is the production of DIC at the sediment-water interface, β_1 and β_2 are the so-called depth attenuation coefficients, and z_b is the depth at which the rapidly degradable material is exhausted and $R_{zb} = R_0 \exp(-\beta_1 z_b)$. The transport of DIC due to biological irrigation was described using the non-local source model of Emerson *et al.* [16]. Given the above assumptions, the equation defining the change of DIC with time and depth is:

$$\frac{\partial C}{\partial t} = D_{HCO_3} \left(\frac{\partial^2 C}{\partial z^2} \right) - \alpha (C_z - C_0) + Rc(z) \qquad (3)$$

In the equation C_z and C_0 [mM] are the concentration of DIC at the depth z and at the sediment-water interface at z=0, respectively, t is time [sec], D_{HCO_3} is the sediment diffusion coefficient for HCO_3^- corrected for temperature and tortuosity from the diffusion coefficient of Li and Gregory [17] [cm^2 sec^{-1}], and α is the irrigation parameter [sec^{-1}]. Eqn. (3) was solved assuming steady-state conditions, *i.e.* $\partial C/\partial t = 0$. To use the model to calculate Rc(z), the irrigation parameter, α must

RADIOACTIVITY OF BOTTOM SEDIMENTS SAMPLED IN 1996 FROM THE ROMANIAN SECTOR OF THE DANUBE RIVER

Ana I. Pantelica[1] and Iulia I. Georgescu [2*]

[1] Institute of Physics and Nuclear Engineering, PO Box MG-6, 76900 Bucharest, Romania
[2] University "Politehnica", Faculty of Industrial Chemistry, 1 Polizu Street, Bucharest, Romania

Abstract

Man-made and natural radioactivity of 23 bottom sediments sampled in spring 1996 along the Danube river from its entrance in Romania to the Black Sea and on the Black Sea coast was investigated by gamma-ray spectrometry. Specific activities of ^{134}Cs, ^{137}Cs, ^{226}Ra, ^{228}Ra and ^{40}K were determined. The highest natural and artificial radioactivity was found at Orsova upstream to the Portile de Fier (Iron Gates) dam and in the Black Sea off Razelm Lagoon at Gura Portita. A comparison of the radioactivity levels of Danube bottom sediments collected from the same sites over the last few years was made.

Key-words: radionuclides, Danube delta,

Introduction

The aim of this work was to investigate the presence of man-made and natural radionuclides of the U-Ra and Th families in the bottom sediments along the Danube river in Romania and on the Black Sea Romanian coast, during spring 1996. The sediment samples were collected by the National Institute of Meteorology and Hydrology, Bucharest from the principal cross-sections of the Danube river and from the same stations in the Black Sea which had been studied before 1977 by the Polytechnical Institute of Bucharest [1]. For radioecological purposes, the survey of the Danube river and Black Sea radioactivity was generally carried out during specific hydrological periods, *i.e.* in spring, summer and autumn seasons at high and relatively low flow rates, under conditions of high and low water dilution.

More recently, data on ^{134}Cs and ^{137}Cs radioactivity in sediments collected from the same areas during 1993, and on the ^{134}Cs, ^{137}Cs, ^{238}U, ^{232}Th and ^{40}K radioactivity in sediments collected in the summer and autumn of 1994 and 1995 from 20 and 21 locations, respectively, have been presented in previous papers [2, 3]. Twelve of the sediments collected during 1994 were analyzed for ^{210}Po radioactivity [4]. The annual averages of ^{137}Cs specific activities in sediments from some of these locations during 1986-1990 [5], and a ^{137}Cs vertical profile in some selected lake sediments of Danube Delta during 1994 [6, 7] have also been determined.

Experimental

The bottom sediment samples were collected from the principal cross sections along the Danube river, from the entrance in Romania to its mouths (delta included), and from the Romanian coast of the Black Sea, during spring 1996 (22 samples). An additional sample was collected at Cernavoda (km 300) from about 300 m along the Danube-Black Sea man-made channel in the vicinity of the CANDU Nuclear Power Plant.

The sediment samples of 1.5-2 kg each have been collected from depth of 0-15 cm using a stainless steel cup and then placed in plastic bags. Associated *in situ* hydrological measurements were made according to the procedures of the National Institute of Meteorology and Hydrology of Bucharest. Sediments were dried in an electric oven at 110°C and then homogenized in an agate mortar. About 100 g of each sample were enclosed in a standard polyethylene box (7.3 cm diameter) and kept inside for one month to permit ^{226}Ra (U-Ra radioactive family) to establish radioactive equilibrium with its decay products.

The gamma ray measurements were carried out by means of a high resolution, low background PC multichannel spectrometer, using a HPGe EG&G ORTEC detector of 30% efficiency and 2.1 keV resolution for the ^{60}Co 1332.5 keV line. As standards, the reference materials IAEA-135 (Radionuclides in Irish Sea sediment) and IAEA-306 (Radionuclides in Baltic Sea sediment) with certified radioactive concentrations were used. Counting times ranged between 14-24 hours.

Results and Discussion

Table 1 presents the ^{134}Cs, ^{137}Cs, ^{226}Ra, ^{228}Ra and ^{40}K specific activities (Bq/kg dry) in Romanian Danube and Black Sea coastal sediments. In this table, the sampling sites in the Danube delta start with Ceatal Sfantu Gheorghe (km 63), *i.e.* the split of the Danube into the Sulina and Sfantu Gheorghe branches; Stambulul Vechi (km 4) is located on the Chilia branch while Sulina (km 4.6) and Sfantu Gheorghe (km 8) are located on the Sulina and Sfantu Gheorghe branches, respectively; on the Black Sea coast the sampling sites are noted from north to south with (1), (2) and (3).

Table 1. Specific activity of the bottom sediments sampled in spring 1996 along the Danube river from the Romanian border to the Black Sea and on the Black Sea coast [Bq/kg dry].

Samplig site / Date	Distance* (km)	^{134}Cs	^{137}Cs	^{226}Ra	^{228}Ra	^{40}K
Bazias / 18.05.96	1072.4	–	11.7 ± 0.6	31.7 ± 1.2	32.0 ± 1.6	396 ± 14
Svinita / 19.05.96	995	1.0 ± 0.3	56.4 ± 2.2	43.0 ± 2.1	38.1 ± 1.9	501 ± 18
Orsova / 19.05.96	957	1.7 ± 0.2	79 ± 2.0	44.1 ± 2.2	41.6 ± 2.1	548 ± 17
Tiganasi / 21.05.96	889	–	6.1 ± 0.4	22.0 ± 1.1	16.7 ± 1.3	576 ± 17
Calafat / 21.05.96	787.9	–	2.4 ± 0.4	16.7 ± 0.8	16.5 ± 1.3	392 ± 14
Bechet (upstream) 22.05.96	709	–	1.4 ± 0.3	17.8 ± 0.8	13.7 ± 1.0	400 ± 12
Bechet (downstream) 22.05.96	678.7	–	1.7 ± 0.3	12.1 ± 0.7	12.4 ± 0.9	366 ± 10
Turnu Magurele / 23.05.96	596.3	–	0.8 ± 0.3	11.1 ± 0.7	11.1 ± 0.8	521 ± 15
Giurgiu / 25.05.96	493	–	0.8 ± 0.3	12.6 ± 1.1	12.7 ± 1.6	401 ± 11
Chiciu Calarasi / 27.05.96	379.6	–	0.9 ± 0.4	13.2 ± 1.1	12.4 ± 1.4	393 ± 9
Cernavoda (upstream) 27.05.96	303	–	1.4 ± 0.3	14.4 ± 0.9	14.9 ± 1.2	373 ± 9
Cernavoda (channel to Black Sea) 27.05.96	300	1.2 ± 0.3	34.6 ± 0.9	47.1 ± 2.1	47.0 ± 1.7	595 ± 15
Cernavoda (downstream) 27.05.96	297		1.0 ± 0.3	16.9 ± 0.8	15.8 ± 1.0	353 ± 10
Vadu Oii / 29.05.96	238	–	0.7 ± 0.3	16.9 ± 1.1	15.8 ± 1.2	392 ± 10
Braila / 05.06.96	167	–	0.3 ± 0.3	17.6 ± 1.1	19.3 ± 1.1	221 ± 13
Ceatal Izmail 07.06.96	80.9	–	0.5 ± 0.3	21.6 ± 1.0	18.0 ± 1.1	274 ± 8
Ceatal Sfantu Gheorghe 14.06.96	63	–	1.0 ± 0.3	17.6 ± 0.8	14.5 ± 1.0	326 ± 10
Sfantu Gheorghe / 14.06.96	8	–	0.3 ± 0.3	18.8 ± 0.9	11.0 ± 0.8	286 ± 9
Sulina / 11.06.96	4.6	–	0.8 ± 0.3	14.3 ± 0.8	12.8 ± 0.9	276 ± 8
Stambulul Vechi / 10.06.96	4	–	1.3 ± 0.3	43.7 ± 2.2	40.5 ± 2.5	305 ± 9
East Sulina / 27.04.96	(1)	0.6 ± 0.2	16.6 ± 0.7	24.1 ± 1.1	25.9 ± 1.6	504 ± 12
Gura Portita / 25.04.96	(2)	1.4 ± 0.2	86.1 ± 3.0	32.6 ± 1.6	35.8 ± 1.3	638 ± 17
East Constanta / 06.05.96	(3)		6.9 ± 0.5	28.7 ± 1.0	34.0 ± 1.2	389 ± 10

**) Distance between sampling site and the Danube mouths to the Black Sea: Sulina is considered "km 0", except for the sites placed on the Chilia and Sfantu Gheorghe branches.*
(1) In front of Sulina Port, 6.5 km offshore and 26.5 m depth in the Black Sea;
(2) In front of Razelm lagoon, south of the Danube delta, 13.7 km offshore and 21.0 m depth in the Black Sea;
(3) In front of Constanta, 8.6 km offshore and 31 m depth in the Black Sea.

In order to calculate the activities of ^{226}Ra and ^{228}Ra, the gamma peaks of 352 keV (^{214}Pb) and 609 keV (^{214}Bi) for ^{226}Ra, and 583 keV (^{208}Tl) and 911 keV (^{228}Ac) for ^{228}Ra were taken into consideration.

The following conclusions drawn from the data are summarized below:

1) In all samples analyzed, only the fission products ^{134}Cs ($T_{1/2}$ = 2.06y) and ^{137}Cs ($T_{1/2}$ = 30.17y) were identified as man-made radionuclides. ^{137}Cs was present in all the samples with specific activity levels between 0.5±0.3 and 86.1±3.0 Bq/kg dry, while ^{134}Cs was measured in the range of 0.6±0.2 to 1.7±0.2 Bq/kg dry only at 5 sampling stations where higher activities of ^{137}Cs were recored. The activity

SEASONAL VARIABILITY OF WATER COLUMN BIOGEOCHEMISTRY IN THREE COASTAL AREAS IN THE IONIAN AND AEGEAN SEAS

P. Pitta*, M. Tsapakis, S. Zivanovic and I. Karakassis

Institute of Marine Biology of Crete, PO Box 2214, Heraklion 71003, Greece

Abstract

The dynamics of phyto- and microzooplankton communities was investigated during July, November and April at three coastal stations in the Ionian and Aegean seas coupled with measurements of hydrographical and chemical parameters (nutrients, POC, PON). The values determined for most variables were among the lowest reported for such environments in the Mediterranean. In April nutrients, Chla, POC and PON showed maximal concentrations which resulted in an increase of the phyto- and zooplankton abundance (by a factor of 10) and species richness (by a factor of 2) in comparison to November. In April, diatoms dominated in the Ionian sites and dinoflagellates in the Aegean one, while the opposite was observed in November. The high abundance of ciliates and flagellates found at Sounion suggests the importance of the role of the microbial food web in this region.

Key-words: coastal waters, nutrients, plankton, organic matter, Eastern Mediterranean

Introduction

Coastal ecosystems contribute to the global carbon fixation an amount disproportionally higher than the area they occupy (1). In the oligotrophic Eastern Mediterranean Sea (2) this contrast between coastal and offshore ecosystems is even more pronounced and imposes the need for integrated investigation of the coastal marine ecosystems. Several studies have addressed aspects of the dynamics of phytoplankton and nutrients in eutrophic bays or polluted areas (3-7), while only limited information is available on the dynamics of undisturbed coastal ecosystems (8, 9). Three coastal areas in the Aegean and Ionian seas, were selected for the investigation of the seasonal variability in nutrient availability and the response of the phyto- and microzooplankton assemblages. Since none of these sites is influenced by urban wastes or any other evident anthropogenic activity, this study could be considered as a comparison between the Ionian and Aegean undisturbed coastal ecosystems.

Materials and methods

During three cruises in July, November 1995 and April 1996, sampling was performed from the R/V *Philia* at three coastal areas, two in the Ionian Sea (Cephalonia Bay and the eastern coast of Ithaki) and one in the Aegean Sea (Sounion). All stations were located at a distance of less than one km from the shore (at depths between 25 and 45 m) and none of them is influenced by urban waters or any other evident anthropogenic activity. Vertical profiles of salinity and temperature were measured by means of a SEABIRD-19 CTD. Current meters (AANDERAA CM-7) were deployed at the mean depth of each site. Water samples for plankton community analysis and measurements of nutrients (total inorganic N: TIN, PO_4, SiO_2), particulate organic carbon (POC), particulate organic nitrogen (PON) and chlorophyll *a* (Chl a) were taken with 5-litre Niskin bottles at depths of 1, 10, 20, 30 and 40 m. Plankton samples for microscopy were preserved with an acid Lugol solution. On board the ship, water from each sample was filtered onto Whatman GF/C filters. Both filters (for pigments and POC-PON analysis) and filtered water destined for nutrient analysis were stored at -18°C. Analyses for the concentrations of nutrient species were performed using standard chemical methods (10), chloroplastic pigments were determined fluorometrically (11) by means of a Turner 112 fluorometer, and POC-PON was analyzed with a Perkin-Elmer CHN elemental analyzer. Phyto- and microzooplankton were identified and counted with an inverted microscope (Olympus IX-70) using the Utermöhl technique (12).

One- and two-way analyses of variance as well as the Tukey test were used in order to detect significant differences among seasons and sites concerning the levels of nutrients, chlorophyll and POC-PON. Multivariate analysis on species-abundance data was performed using non-metric Multidimensional Scaling (MDS) (13). A transformation of log(x+1) as well as the Bray-Curtis similarity index were also used.

Results

A weak stratification appeared at Cephalonia during July and a more conspicuous one at Ithaki during the same period. At Sounion, the strong wind-driven currents induced a vertical mixed layer throughout the year. During November and April, the water column at all three sites appeared well mixed. In general, nitrate comprised approximately 65% of the total inorganic nitrogen, ammonia 25% and nitrite 10%. At all sites, total inorganic N (TIN) was minimal during July (Table 1). The station at Ithaki showed higher TIN concentrations in comparison to the other sites especially in April. Phosphate did not present a uniform distribution; Sounion displayed minimal phosphate concentrations in July, Ithaki during November and Cephalonia during April. All sites presented maximal concentrations of silicates during April, and minimal concentrations during July. According to a two factor (season and site) analysis of variance, significant differences were detected for silicates between April and July, for TIN between April and the two other seasons and for TIN between Ithaki and Sounion (post hoc comparisons in Table 2). One way analysis of variance for the concentrations of all nutrient species revealed no significant differences among depths ($p<0.05$) for any season or site.

Table 1. Concentrations of chlorophyll *a* ($\mu g\ l^{-1}$), nutrients ($\mu mol\ l^{-1}$) and POC, PON ($\mu g\ l^{-1}$) at the sites studied

Season	Site		TIN	PO_4	SiO_2	Chl a	POC	PON
July	Cephalonia	*av.*	0.66	0.06	0.74	0.27	218	17
		range	0.52-0.82	0.04-0.08	0.49-0.99	0.14-0.50	166-297	11-25
	Ithaki	*av.*	1.60	0.02	0.98	0.15	131	17
		range	0.50-5.35	0.01-0.04	0.36-2.72	0.10-0.24	111-142	13-19
	Sounion	*av.*	0.44	0.01	0.52	0.11	130	19
		range	0.35-0.51	0.01-0.02	0.43-0.60	0.10-0.13	94-179	13-29
October	Cephalonia	*av.*	1.39	0.07	1.39	0.38	120	22
		range	0.40-2.84	0.02-0.27	0.64-5.91	0.17-0.85	95-159	16-28
	Ithaki	*av.*	1.57	0.02	0.95	0.14	76	9
		range	0.51-3.57	0.01-0.07	0.48-1.76	0.03-0.20	56-97	7-11
	Sounion	*av.*	0.91	0.04	0.68	0.23	97	14
		range	0.15-2.26	0.03-0.09	0.45-1.04	0.19-0.28	74-136	11-19
April	Cephalonia	*av.*	0.95	0.03	1.26	0.50	277	29
		range	0.84-1.06	0.02-0.03	1.17-1.36	0.38-0.61	228-360	24-35
	Ithaki	*av.*	3.34	0.05	1.52	0.19	136	14
		range	1.58-5.91	0.02-0.11	1.09-2.15	0.12-0.23	74-208	10-18
	Sounion	*av.*	1.37	0.03	1.61	0.24	115	13
		range	0.94-2.56	0.01-0.06	1.25-1.90	0.15-0.35	83-178	8-17

Table 2. Results of two-way ANOVA for all the parameters sampled.

Variable	Source of variability	df	F	p		TUKEY post hoc test				
						July	Nov		Ceph	Ithaki
TIN	Season	2	8.95	0.000	Nov	ns		Ithaki	ns	
	Site	2	4.62	0.014	April	**	*	Sounion	ns	*
PO_4	Season	2	0.40	ns						
	Site	2	1.49	ns						
						July	Nov			
SiO2	Season	2	3.38	0.042	Nov	ns				
	Site	2	0.29	ns	April	*	ns			
Chla	Season	2	4.73	0.013		July	Nov		Ceph	Ithaki
	Site	2	14.73	0.000	Nov	ns		Ithaki	**	
					April	*	ns	Sounion	**	ns
						July	Nov		Ceph	Ithaki
POC	Season	2	27.99	0.000	Nov	**		Ithaki	**	
	Site	2	30.44	0.000	April	ns	**	Sounion	**	ns
						July	Nov		Ceph	Ithaki
PON	Season	2	4.67	0.014	Nov	ns		Ithaki	**	
	Site	2	24.29	0.000	April	ns	*èè	Sounion	**	ns

** p<0.05 ; ** p< 0.01; ns : non significant*

Chlorophyll *a* concentrations were maximal in April (Table 1) at the three sites (0.5 mg l^{-1} at Cephalonia, 0.19 mg $^{-1}$ at Ithaki, 0.24 mg l^{-1} at Sounion) and minimal during July (0.27 mg l^{-1} at Cephalonia, 0.15 mg l^{-1} at Ithaki, 0.11 mg l^{-1} at Sounion). During all seasons higher concentrations were noted at Cephalonia than at the other two sites (Table 1). These differences were significant according to the two factor analysis of variance (Table 2). One way analysis of variance for the concentrations of Chla revealed no significant differences among depths ($p<0.05$). Particulate organic carbon (POC) as well as particulate organic nitrogen (PON) concentrations were highest in April at all sites (77-359 mg C l^{-1}) while high values were also recorded in July. Among all sites, values were maximal at Cephalonia; these values

DETERMINATION AND REACTIVITY OF FOLIC ACID IN NATURAL WATERS

Marta Plavsic [1]*, Xiankun Lu [2] and C.M.G. van den Berg [3]

[1] Ruder Boskovic Institute, Center for Marine, and Environmental Research, PoBox 1016, 10001 Zagreb, Croatia
[2] Ocean University of Qingdao, Qingdao, China
[3] Oceanography Laboratories, University of Liverpool, Liverpool L693BX, UK

Abstract

Folic acid (FA) was determined in natural waters (Adriatic Sea water and Rogoznica Lake water) and in algal cultures by cathodic stripping voltammetry. The concentration of FA in seawater varies between 0.03 and 4.3 nML^{-1}. In Rogoznica Lake water (S = 30-38) the concentration of FA varies between 0.18 and 4 nML^{-1}. High concentration of FA (36 nML^{-1}) was determined in the Rogoznica Lake at the depth below 8 m during the period of anoxia. The influence of different types of organic matter (humic and fulvic acid, polysaccharide and protein), and sulfide ions on the determination of FA in natural waters was studied. The interfering effect of humic acid could be eliminated by passing the sample through Sep-Pak-C-18 cartridges. The experiments with algal cultures (*Dunalliela, Emiliania* and *Phaeodactylum*) have shown that folic acid could be a tentative nutrient.

Key-words: nutrients, organic matter, Adriatic sea

Introduction

Folic acid is the most common name, among several synonyms (vitamin Bc, vitamin M, biotin, folacin, foliamin, folsan, folvit), for a compound N-4-(2-amino-1,4-dihydro-4-oxo-6 pterydinyl) methyl aminobenzoyl L-glutamic acid. Folic acid is a vitamin that is required in the transfer of single carbon moieties, thus playing an important role in several metabolic pathways in mammals (1). FA is also produced by plants (green leaves, algae) and by microorganisms. Little is known about folic acid occurrence and distribution in natural waters, although its occurrence as a result of algal exudations or involuntary releases has been reported (2). Recently, a very sensitive electrochemical method of cathodic stripping voltammetry has been developed (3), which has enabled us to determine the relatively low concentrations of folic acid in natural waters (3, 4, 5). In this paper we report on the reactivity of FA in natural waters as well as the influence of several organic compounds and sulfide on its determination. The possible importance of FA as a nutrient for algae was evaluated from uptake experiments with cultured marine algae.

Experimental

Measurements of FA in seawater and lake water have been done on a PAR 174 A polarograph connected to a Metrohm HMDE (hanging mercury drop electrode) and μ-Autolab (ECO-CHEM) connected to a Metrohm VA 663. For capacitive current measurements a Metrohm E-506 instrument was used. Folic acid in natural water samples was determined according to a previously described procedure (3). Milli Q water (Millipore water purification system, USA) was used throughout the experiments. Monocultures of *Emiliania huxleyi, Dunalliela minuta* and *Phaeodactylum tricornutum* were grown in 250 F/2 medium in synthetic seawater to which 1 ml of algal culture was added, giving a starting concentration of $3x10^3$ cells mL^{-1}. Incubation was carried out in a temperature controlled incubator (Mercia scientific) with 24 h illumination at 15°C. Samples were filtered off through a GF/F glass fibre filters of 0.7 μm pore size.

Results and discussion

Voltammetric analyses of seawater samples from different parts of the Adriatic Sea revealed the presence of FA, variable with depth, throughout the year. The highest FA concentration was found in a surface seawater sample in May (Fig.1A) which could be a result of increased biological activity at that time. In summer months, the concentration of folic acid in surface waters decreased due to the sensitivity of folic acid to photo-decomposition. In deeper waters of the Adriatic sea a certain increase in FA concentration was observed. In the case of Rogoznica Lake (~14 m deep, salinity 30-38, anoxia below 8 m in certain periods of year) near Sibenik, which is connected with the Adriatic Sea, the concentration of FA in surface waters was relatively low (few nmoles L^{-1}) (Fig.1B). In deeper waters, especially in the anoxic water, the concentration of folic acid increased with its maximum at 11 m in April 1995 and at 12 m in May 1997. The maximum at 11 m depth in April 1995 coincided with the chlorophyll *a* maximum, and the combined concentration of sulfur and sulfide (6) as well as with the iodide maximum (7). The high FA concentrations in anoxic waters are probably derived from sinking, decomposing algae, which are not broken down by oxidative bacterial activity in the prevailing anoxic conditions. In Fig. 3 the cathodic stripping scans for water samples from Rogoznica Lake are presented. The presence of sulfur species did not mask the FA voltammetric peak in the sample. The interference of some organic compounds (humic acid, fulvic acid, Dextran T-500 and protein - egg albumin) with the FA determination was investigated (Fig. 3). Egg-albumin does not influence the determination of FA significantly. Dextran-T-500 influenced the determination of FA in a concentration range 2 mgL^{-1}. Humic and fulvic acids influenced the determination of FA even at low concentration ranges (1 mgL^{-1} of fulvic or humic acids). The influence of humic acid on the FA peak can be minimized by passing the seawater through a SEP-PAK-C-18 column at high flow rate (15 ml min^{-1}) and pH = 1.8. The determination of FA in the samples has been done with a standard addition method and it was estimated that there was no complexation reaction between HA and FA, only the sensitivity of the determination was changed (5).

Variation of the FA concentrations in the water column in the Atlantic Ocean (4) suggests localized FA production and uptake by microorganisms. The uptake of FA was studied in algal cultures of *Dunalliela, Emiliania* and *Phaeodactylum* to see if they derive an advantage from this uptake. Preliminary experiments showed that FA

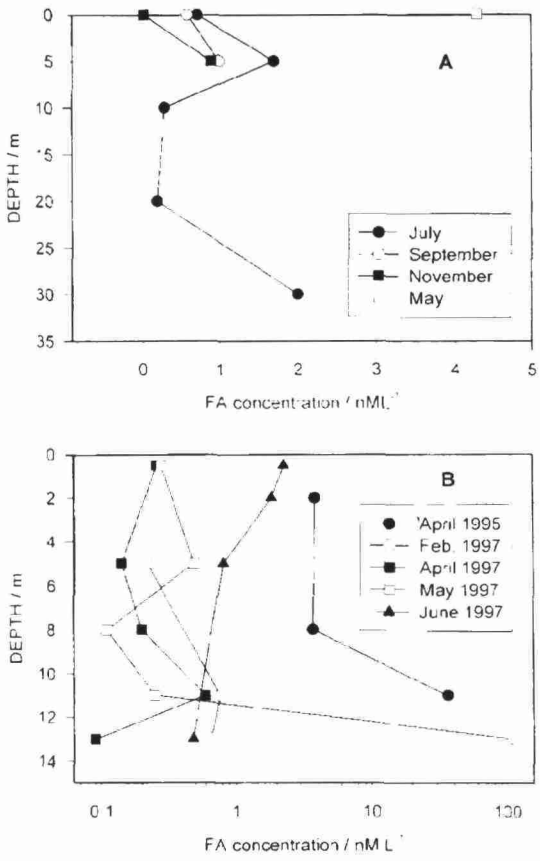

Fig. 1. Vertical profiles of FA for North Adriatic seawater samples for different months in 1994 (A) and for Rogoznica Lake water column(B).

COMPARATIVE STUDY OF HEAVY METAL RESIDUES IN SOME TISSUES OF THE FISH *GALEUS MELASTOMUS* CAUGHT ALONG THE ITALIAN AND ALBANIAN COASTS

M.M. Storelli*, E. Ceci, G.O. Marcotrigiano

Istituto di Chimica, Facoltà Medicina Veterinaria, Università di Bari, Strada Prov.le per Casamassima Km 3, 70010 Valenzano, Italia

Abstract

This work presents results obtained during an investigation on the levels of heavy metal residues (Hg, Cd, Pb and Cr) in various tissues (dorsal and ventral muscle, liver and skin) of Galeus melastomus specimens caught along Italian and Albanian coasts. Analytical results for 757 specimens have demonstrated a variable distribution of metals in these tissues with maximum levels of Pb, Cr, Cd in liver, and Hg in dorsal and ventral muscle. Furthermore, with respect to certain tissues, significant correlations between mercury concentration and fish weight have been observed.

Key-words: trace elements, pollution, monitoring, Adriatic Sea

Introduction

Investigations of metals in fish are an important aspect of environmental pollution control (1). The subject of this study was to screen the metal content of different-sized specimens of *Galeus melastomus* caught along Italian and Albanian coasts, and to compare the metal concentrations found in these fish from two different areas of the southern Adriatic Sea in order to determine the relative degree of contamination in these regions.

Materials and methods

During the period June-September 1996, along Italian and Albanian coasts (southern Adriatic Sea) 757 *Galeus melastomus* specimens were caught. Eleven pooled samples were obtained from the 501 specimens weighing between 20.8 and 387.8 g caught along Italian coast in three different areas (Vieste-Bari-Brindisi), while the remaining 256 specimens between 15.1 and 252.4 g, caught along Albanian coast, formed 5 pools. Dorsal and ventral muscle, liver and skin were taken from specimens of similar size. From single homogenized tissues, samples were also taken for analyses. The quantitative analysis of heavy metals was carried out by A.A. spectrophotometry (Perkin Elmer 5000) after organic matrix digestion with HNO_3-$HClO_4$ (8:3) for Pb, Cr, Cd, (2), and H_2SO_4-HNO_3 (1:1) for Hg (3). For Pb, Cr and Cd determination a graphite furnace (HGA-500 Perkin Elmer) with L'VOV platform was used. Mercury was determined by the cold vapour technique after reduction to Hg^0 with $SnCl_2$ using a A.V.A. Thermo Jarrel system connected to A.A. spectrophotometer. The analytical procedures were tested and controlled using certified Reference Material DORM-1 of the National Research Council of Canada.

Results and discussion

Table 1 shows minimum, maximum, and average values of metal concentrations (Hg, Cd, Pb and Cr) expressed in mg/Kg wet wt. in skin, liver, dorsal (D.M.) and ventral muscle (V.M.) of *G. melastomus* caught along Italian and Albanian coasts. Figure 1 presents mean concentrations of metals in the tissues of both Italian and Albanian samples.

For dorsal and ventral muscle, Hg concentration in specimens caught along Italian coast was higher than fish of Albanian origin while the average Hg level in skin was about the same in both. Concentrations in the liver of Italian specimens ranged from N.D.-0.66 mg/Kg wet wt.; in 36.4 % of these samples and in all liver samples of Albanian origin, Hg concentrations were below the instrumental detection limit. The highest Hg concentrations in Italian fish were found in dorsal muscle, followed by ventral muscle, skin and liver. Specimens of Albanian origin did not show remarkable differences in Hg concentrations in dorsal muscle, ventral muscle and skin. It is known that, normally, liver is the organ which shows the highest metal levels, Hg included, as demonstrated in previous studies involving different species of fish (4, 5). Nevertheless, Hg concentrations in liver lower than those in the muscle, as observed in this work, were also found by other authors in plaice (*Pleuronectes platessa*) (6) and in cod (*Gadhus morhua*) (7). Moreover, in a study of uptake and depuration of Hg in cod exposed to methylmercury, muscle had higher levels of Hg than in liver measured during the time of depletion (8). This unusual trend, could be ascribed to a greater total percentage of lipids in liver (22.72%-52.50) compared to that found in muscle (0.19%-0.80%) in the fish examined.

Tab. 1 - Min., max., mean values of metal residues (mg/Kg wet. wt. ± standard deviation) in different tissues.

Metals	Location	Dorsal Muscle	Ventral Muscle	Skin	Liver
Hg	S. Adriatic Sea (Italy)	0.14-3.39 0.97±0.96	0.18-2.05 0.82±0.62	0.18-0.76 0.44±0.22	N.D.-0.66 0.22±0.20
Pb	"	N.D.-0.45 0.20±0.11	N.D.-0.79 0.23±0.21	N.D.-0.45 0.22±0.10	N.D.-0.65 0.37±0.16
Cr	"	0.10-0.55 0.29±0.14	0.21-1.12 0.47±0.29	0.24-1.14 0.56±0.24	0.18-0.82 0.43±0.18
Cd	"	0.03-0.06 0.04±0.01	0.03-0.07 0.05±0.02	0.04-0.09 0.06±0.02	0.09-0.28 0.16±0.05
Hg	S. Adriatic Sea (Albania)	0.20-0.88 0.46±0.31	0.10-1.21 0.46±0.51	0.15-1.10 0.41±0.46	N.D.
Pb	"	N.D.-0.09 0.07±0.02	0.04-0.07 0.06±0.01	0.05-0.11 0.08±0.03	0.21-0.42 0.31±0.09
Cr	"	0.14-0.29 0.18±0.07	0.12-0.40 0.27±0.12	0.43-0.77 0.58±0.15	0.38-0.58 0.46±0.08
Cd	"	0.02-0.07 0.04±0.02	0.03-0.10 0.06±0.03	0.03-0.21 0.10±0.08	0.13-0.19 0.16±0.02

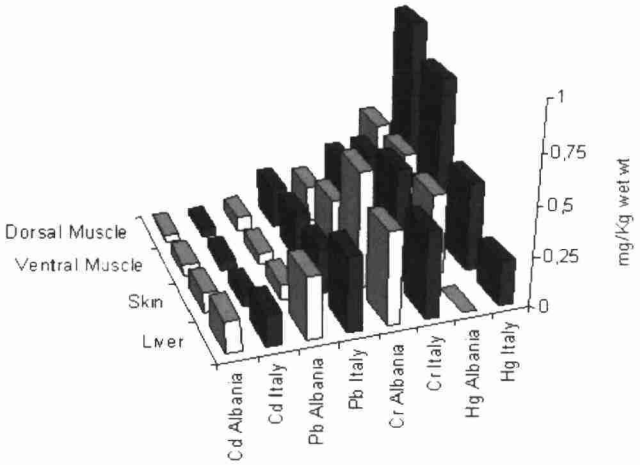

Fig. 1 - Mean concentrations of metal residues in different tissues of fish caught along Italian and Albanian coasts.

Grimas *et al.* (9) reports that it is not only levels of nonpolar substances that are correlated with the amount of fat in tissue, but also substances which are protein-bound. In some monitoring studies which examined heavy metals in cod liver, it has been observed that as the percentage of fat increases, the protein fraction decreases and with it the amount of protein-bound metals as well (9). Statistically positive correlations between concentration of Hg and weight of the specimens from Italy have been found in some tissues (D.M. $r = 0.89$, $P < 0.001$; V.M. $r = 0.91$, $P < 0.001$; Skin $r = 0.96$, $P < 0.001$) (Fig. 2) as previously observed by other authors for similar species (10, 11).

Our results for Hg in the muscle of *G. melastomus* were lower than those found in *Scyliorhinus canicula* (belonging to the same family), caught in the central Adriatic (aver. 0.45mg/kg wet wt.) (12) and northern Adriatic Sea (0.12-0.60 mg/Kg wet wt.) (13). In all analyzed tissues, Pb concentrations were higher ($P < 0.05$) in specimens of Italian origin compared to those of Albanian origin except for liver, in which average concentrations were the same. Among the Italian specimens sampled, significantly higher concentrations ($P < 0.05$) were found in liver, with respect to skin, ventral and dorsal muscle. A similar distribution was observed in samples caught along Albanian coast, where concentrations in liver ($P < 0.05$) were higher than those in other tissues. In 9% of dorsal and ventral muscle and skin samples from Italy, and in 25% of dorsal muscle samples from Albania, concentrations were below the instrumental detection limit. Pb values reported in the

COPPER AND NICKEL IN MARINE FISH FROM GREEK WATERS

E. Strogyloudi*, V.A. Catsiki, F. Bei

National Centre for Marine Research, Ag. Kosmas, Hellinikon, Athens 16604 Greece

Abstract

This study deals with the levels of Cu and Ni in flesh and gills of the demersal fish *Mullus barbatus*, collected during 1988 to 1995 from three different areas of the Aegean Sea (Greece). The concentrations of Cu and Ni in edible tissue are comparable to those from the literature. Gills have higher levels than flesh. No major differences in metal levels in fish between sampling sites were observed.

Key-words: metals, Aegean Sea

Introduction

At suitable concentrations some heavy metals are essential for enzymatic activity but they also form an important group of enzyme inhibitors when natural concentrations are exceeded (1). Consequently most heavy metals, whether essential or not, are potentially toxic to living organisms. Fish are widely used as sentinels of contamination in aquatic environments (2). Contaminant accumulation in various fish tissues is used as a measure of contaminant exposure and effects. According to the mechanisms of absorption, regulation, storage and excretion of trace metals, different tissues have different roles in these processes (3).

Methodology

Samples of similar sized fish *M. barbatus* (striped mullet) were collected twice a year (spring and autumn) from three different areas of the Aegean Sea. For the purposes of the MEDPOL programme, heavy metals have been regularly monitored in fish from Greek waters since 1988. The determination of heavy metals was made by digestion with nitric acid in teflon vessels under pressure. A Varian SPECTR AA 20 Plus Atomic Absorption Spectrophotometer was used (4). A total of 536 samples were analysed for Cu and Ni. The accuracy and precision of the analytical methodology was tested with the reference material of BCR N° 279 (*Ulva lactuca*).

Results and discussion

The results of metal analysis are given in Table 1. Figures 1 and 2 analytically present all concentrations fom every sample by tissue, station and year. Cu ranged between 0.28 and 20.56 ppm and Ni values varied from 0.08 to 52.68 ppm. It is noteworthy that, in most cases, fluctuation of the values is not high. It must be emphasised that fish are not exactly in the same metabolic state (different seasons and size), and due to their movement they do not necessarily integrate the same pollution (different areas and depth in the vertical water column). Heavy metal concentrations in fish are a function of both space (where they have been) and time (how long they were in each area), and the two effects cannot be separated. Generally the uptake, retention, toxicity and tolerance of metals by fish are governed by many environmental and biological factors (1).

Table 1. Metal concentrations (mean and range) in flesh and gills of striped mullet from the Aegean Sea during 1988 to 1995 (in μg/g dry weight)

stations	flesh	Cu	Ni	gills	Cu	Ni
Alexandroupoli	N=88	1.68±0.77 (0.68-3.75)	1.73±1.86 (0.08-14.12)	N=88	5.09±2.44 (0.4 -15.20)	6.40±4.89 (0.22-23.55)
Hios	N=90	1.63±0.80 (0.59-5.67)	1.72±1.31 (0.16-5.01)	N=90	4.26±1.75 (2.24-10.25)	7.75±8.57 (0.40-52.68)
Hania	N=90	1.96±0.99 (0.28-4.98)	1.72±1.06 (0.15--5.00)	N=90	4.96±2.51 (1.61-20.56)	6.15±4.67 (0.27-19.66)

Results showed that the two analysed tissues accumulate metals to different levels. The ratio of the metal concentrations in gills and flesh is greater than 1 (concentrations of metals in gills / concentrations of metals in flesh > 1) for Cu and Ni in all cases (stations and years). It is known that fish gills are a primary target for direct metal absorption from the external environment and thus serve as a major route for metal uptake by these species (5). On the other hand the lower metal concentration of flesh samples is partially due to the lower metabolic activity of this tissue in comparison with gills. Metal uptake by the gills does not involve direct and rapid transfer from the water to the blood, but rather an intermediate step for metal transport to the other tissues. Furthermore, flesh is the tissue most commonly chosen because of the implications it carries for human consumption and related health risks.

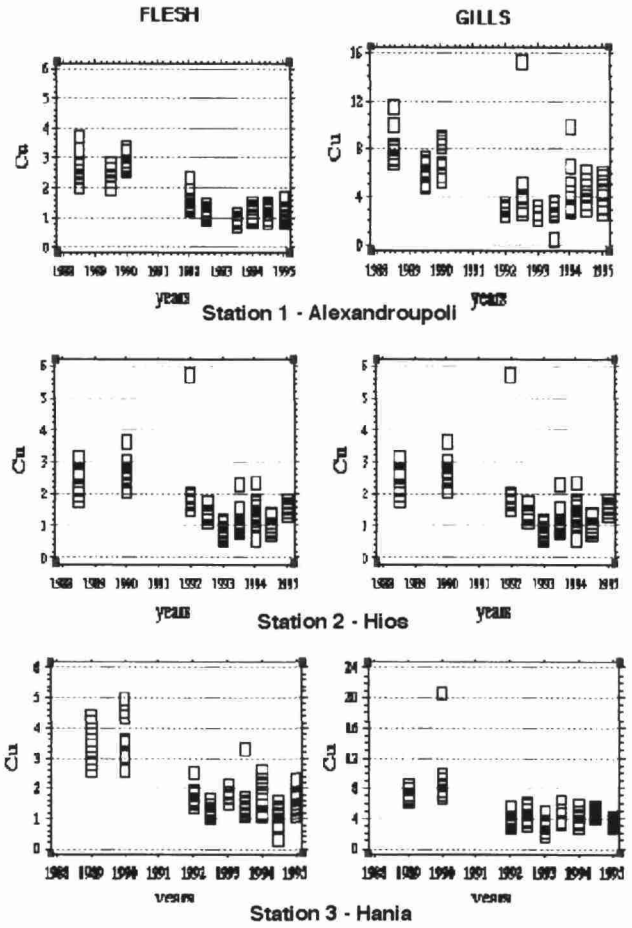

Fig. 1. Concentrations of Cu in flesh and gills of *M. barbatus* from Alexandroupoli, Hios and Hania. Every square corresponds to one individual sample

Temporal changes in the concentrations of Cu and Ni in the flesh and gills of demersal fish showed, in general, a low degree of variation. Both metals had similar trends at all stations. However during 1988 to 1990 Cu, and to the some extent Ni, appeared to be higher; however for the following years of the study stabilisation of the values was observed in all cases with the exception of some extreme values (Figs. 1 and 2). It is interesting to note that covariation of the concentrations of the metals did not follow any particular trend of increase or decrease during the latter years of the study. From our results it did not appear that concentrations of Cu and Ni follow any common pattern. This could be attributed to the fact that every metal probably originated from a different source. Furthermore, marine organisms, tend to accumulate heavy metals from the environment and are adapted to handle natural fluctuations by slight regulating changes in their bioavailability from water or food.

The distribution of the frequency of the determined concentrations is not symmetrical. For both metals, large numbers of the values in flesh were between 1 and 2 ppm (especially for Ni). In gills, values were not limited to a strictly defined range and the distribution of the frequency seems to be more normal. Although there is not a clear trend in metal concentration in the two tissues of the fish through the years,

THE GIRMED DATABASE PROJECT : PRESENT STATUS AND FUTURE PROSPECTS

Hervé Thebault [1*], Mireille Arnaud [1], Anne-Sylvie Pruchon[1], Dominique Calmet [2]

[1] Institut de Protection et de Sûreté Nucléaire (IPSN), Laboratoire d'Etudes Radioécologiques Continentales et de la Méditerranée. BP 330, 83507 La Seyne/mer Cedex, France

[2] Institut de Protection et de Sûreté Nucléaire, Laboratoire de Mesure de Radioactivité de l'Environnement. Bt 501, Bois des Rames, 91400 Orsay Cedex, France

Abstract

During the CIESM congress in 1988, the Marine Radioactivity Committee decided to launch a co-ordinated research program called Global Inventory of Radioactivity in the MEDiterranean Sea (GIRMED). It was then decided in 1990 to set up a database of radionuclide concentrations for the most representative Mediterranean marine indicators and for the time period preceding and following to the Chernobyl accident (1986-1992). The current status of the database is reported and the data volume and distribution are discussed. Recommendations for a further step in the GIRMED project, including user-friendly information access implementation, are proposed.

Keywords: radionuclides, Mediterranean Sea

Introduction

During the Congress of the International Commission for the Scientific Exploration of the Mediterranean Sea (CIESM) held in Athens in 1988, the Marine Radioactivity Committee decided to launch a co-ordinated research program called Global Inventory of Radioactivity in the MEDiterranean Sea (GIRMED) (1). Such a programme seems essential in the context of the Barcelona Convention in particular after the major event represented by the Chernobyl accident. The original main objectives of GIRMED were:

- intercalibration of sampling and measuring procedures from laboratories involved in monitoring networks of radionuclides in the marine environment at national scale,
- selection of bioindicators reflecting radioactivity levels in the Mediterranean Sea
- status reports on time trends and distribution of artificial radionuclides present in the sea water, sediments, and marine organisms,
- evaluation of partition coefficients of radionuclides between water, sediments and organisms,
- study of radionuclide transfer to human populations from the marine environment.

During the 1990 Marine Radioactivity Committee meeting in Perpignan (France), the GIRMED progress report pointed out that quality assurance of radionuclide measurements was achieved through the intercalibration exercises regularly organised by the International Atomic Energy Agency (IAEA) with the participating laboratories (2). In parallel, a complete inventory of existing land-based nuclear activities around the Mediterranean Sea (and the Black Sea) was set up, as potential sources of radionuclide releases to the marine environment (3). It was also decided during this meeting to set up a data base of radionuclide concentrations for the most representative and common Mediterranean marine indicators. The collection of data starts from 1st January 1986, showing the impact of Chernobyl fallout and the subsequent evolution of radioactivity in the selected indicators. The expected information might help to identify the main processes and areas of scientific interest, and to validate the indicators selected for the Mediterranean and the Black seas (4, 5). The 1992 progress report indicated qualitative distribution of data collected during the database constitution phase and proposed a further step concerning dose assessment to relevant populations from data on marine components in relation with the MARINA-MED project (6).

The aim of the present paper is then to report on the present status of the database, as the collection of data sets went on until 1995 (7), to show quantitatively the results gathered up to now (number, distribution, activities), to evaluate fulfilment of the initial GIRMED objectives, and to propose further evolution of the database content and access of end-users (including data producers).

Material and method

Following the GIRMED founding act in Athens, a questionnaire was sent by the CIESM Secretariat to all potential participating laboratories in the Mediterranean countries addressing staff composition, scientific experience and objectives in this topic, recent publications, current techniques, lab facilities and study area. From the replies, participating laboratories were invited to a round table (during the 1990 meeting in Perpignan) to present their national monitoring networks and methodological approaches. From this discussion, a first selection of potential indicators was suggested and a new questionnaire was sent out by the IAEA on behalf of the CIESM Marine Radioactivity Committee. It contained a data reporting form and a guideline document specifying for each sample type (sea water, sediment, suspended matter and biota) a full description of essential database fields to be filled in, with coding prescription, unit, and data format. For biota, a non restrictive list of bioindicators was proposed, including: *Posidonia oceanica, Padina pavonia, Mytilus sp.* and finfish.

The collected data were then directed to the IPSN Marine Radioecology Laboratory in Toulon as a support institution, validated for data coherence and integrity with the contributing laboratories and stored in a computer. The present database is implemented on a dedicated PC machine using Microsoft Access 2.0 software as a relational database management system (RDBMS).

Results and discussion

The first inquiry revealed that 15 laboratories, distributed among 8 Mediterranean countries could collaborate in the GIRMED project. Up to 1995, however, only 9 laboratories from 7 countries have actually participated in the constitution of the database by sending their results. Most of the data concern samples collected essentially in the coastal zone where the monitoring networks are regularly operated. The most abundant results are represented by sediments and molluscs samples and ^{137}Cs is the radionuclide most frequently reported in the database. Almost all these data are subsequent to the Chernobyl accident, so the missing baseline information make any estimate of the inventory of the Chernobyl fallout on a global scale uncertain. In addition, the spatial distribution of the sampling locations is quite patchy (Fig. 1), making aerial extrapolation to the whole Mediterranean to a difficult exercise. Reports on radionuclide concentrations measurements are missing, in particular from the eastern and southern countries, and are scarce from Italy, Spain, and Greece where monitoring and research activities are known to exist. From a review of published data, an inventory of ^{137}Cs and $^{239,240}Pu$ in the Mediterranean Sea was recently compiled (8), also highlighting the lack of measurements from the

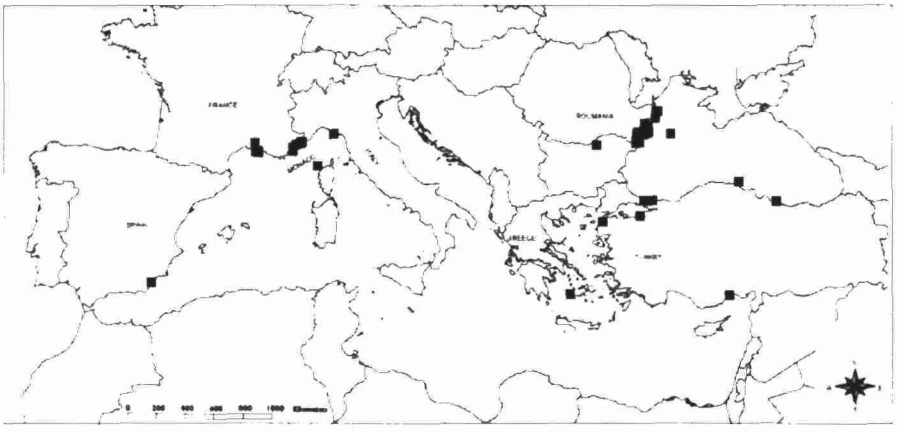

Fig. 1. Samples locations in the GIRMED database.

TRACE ELEMENTS AND RADIONUCLIDES IN SEDIMENTS AND BIOTA FROM THE KÜÇÜKÇEKMECE LAKE

S. Topcuoglu*, D. Kut, N. Esen, N. Güngör, E. Seddigh, R. Küçükcezzar
Çekmece Nuclear Research and Training Center, P.O. Box 55 Sefaköy, Istanbul, Turkey

Abstract

This paper reports concentrations of selected elements and radionuclides in sediments and biota from the Küçükçekmece Lake near Istanbul. Comparisons of the Cr concentrations in sediments with data reported for the Sediment Quality Guidelines of the Ontario Lake indicate that Küçükçekmece sediments are heavily contaminated. The Cr and Co values in macroalgae were higher than that of shrimp and fish species. The maximum and minimum activity levels of ^{137}Cs in sediments were 4.5 and 13.5 Bq/kg. The level of ^{137}Cs in macroalgae was 6 Bq/kg whereas in shrimp ^{137}Cs was not detectable. In contrast, ^{232}Th concentration in shrimp was higher than that of sediment and macroalgae.

Key-words : trace elements, radioactivity, sediments, Sea of Marmara

Introduction

The Küçükçekmece Lake (41°00 N-28°43 E) is a brackish water lagoon of 15.22 km^2 surface area and a maximum depth of 20 m. It is connected to the Marmara Sea via a narrow channel. The main fresh water supply comes from underground springs and several small streams.

The Çekmece Nuclear Research and Training Center was established near the lake and the drainage system of the Center is connected to lake. The lake water has been contaminated by trace elements and organic pollutants from a combination of industrial, agricultural and municipal activities. At the same time, this lake was greatly affected by atmospheric input of particulate matter originating from the sweepings of waste storage and use of fossil fuels in the region.

Some paper have been previously published concerning heavy metal, detergent and radioactivity levels observed in water samples of the lake (1-3). However, no data on trace elements and radioactivity levels in sediment and biota samples from the lake have yet been published in the scientific literature. On the other hand, several radioecological investigations have been carried out using lake species and radiotracers (4-6).

This paper reports data for the trace element (As, Se, Zn, Cr, Cs, Co, Sb, Ni, Sc, K, Ca, Fe) and radionuclide (^{238}U, ^{232}Th, ^{137}Cs, ^{40}K) levels in sediment and biota collected from the lake 1994.

Material and Methods

The sediment samples were collected from five stations of the lake by using of a Lenz Bottom sampler (Fig. 1). About 4 cm of the top of the sediment samples were dried at 85°C for 48 h, crushed and homogenized prior to the analyses. The biota samples were *Enteromorpha linza* (macroalgae), *Crangon vulgaris* (shrimp), *Proterorhinus marmoratus* (goby fish), *Syngnathus abaster* (pike fish). The samples were pooled and freeze-dried for several days to constant weight.

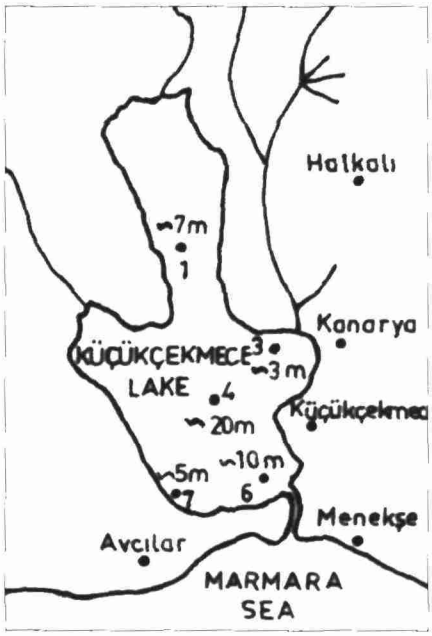

Fig.1. Sampling stations at the Küçükçekmece Lake.

Trace element analyses were carried out by an instrumental neutron activation technique. About 0.2 g. sediment and biota samples were placed in 1 cm^3 polyethylene tube and irradiated for 4 hours at the thermal neutron flux of about $2*10^{13} ncm^{-2} s^{-1}$ in the TR-2 Reactor of the Çekmece Nuclear Research and Training center. IAEA's CRM SL-1 was used as the standard. The gamma spectra of both samples and standards were measured using a Canberra S-85 4K MCA gamma-ray spectrometer. The detector was high purity Germanium (Ortec, GMX) and its resolution was 1.9 keV (at 1333 keV for ^{60}Co). Decay periods were 24 hours for short-lived and 3-4 weeks for long-lived isotopes. Counting times were varied between 3000 and 8000 sec.

The sample powders (about 100 g) were pressed by hand into special cups for gamma isotopic analyses. Determination of the radioactivity levels was similar to that previously described (7, 8).

Result and Discussion

The trace element contents of the sediments are shown in Table 1. The highest concentration of As, Zn, Cr and Co were detected at station 3 (Fig. 1), probably due to the municipal and factory waste discharged into the lake. The Co, Fe, Ni, Cs and As concentrations at station 7 were lower than the other stations. At the same time the Sc, K and Ca contents at station 7 were significantly different from levels at the other stations. It is suggested that these differences depend on sediment composition.

Table 1. Trace element concentrations in sediment samples (μg/g dry weight).

Station / Element	No.1	No.3	No.4	No.6	No.7
As	6.8±1.9	12.8±1.4	10.6±2.0	10.2±1.7	3.9±1.7
Se	<1.6	~1.4	<1.6	~1.0	<1.6
Zn	153±9	219±8	135±6	212±10	155±13
Cr	105±7	120±6	100±5	115±7	102±10
Cs	6.8±0.8	5.8±0.5	5.0±0.4	4.1±0.4	1.3±0.4
Co	13.7±0.6	15.0±0.4	11.4±0.4	11.8±0.4	5.1±0.3
Sb	1.4±0.2	1.5±0.2	1.3±0.1	1.5±0.2	~0.1
Ni	~40	70±26	67±16	72±29	<40
Sc	12.2±0.4	12.3±0.7	8.8±0.2	8.8±0.2	2.7±0.4
K,%	1.4±0.1	1.5±0.1	1.2±0.1	1.4±0.1	0.7±0.1
Ca,%	9.0±1.7	13.0±1.6	7.8±1.0	13.9±1.6	20.8±2.5
Fe,%	3.2±0.1	3.4±0.1	2.5±0.1	2.4±0.1	0.7±0.1

The Cr concentrations in Küçükçekmece Lake sediments were higher than those in sediments collected from the Black Sea and Bosphorus (9, 10). These concentrations in sediment indicated that they were heavily polluted and are approaching the "severe effect level" when compared with the Sediment Quality Guidelines of the Ontario Ministry (11). The Ni concentrations were also near the severe effect level at stations 3, 4 and 6. The trace element concentrations in the algae, shrimp and fish samples are given in Table 2. The Cr and Co values

BIOGEOCHEMICAL FLUXES ACROSS THE GULF OF LIONS : A COUPLED MODELING APPROACH

Marie-Hélène Tusseau-Vuillemin [1] and Laurent Mortier [2*]

[1] Institut de Biogéochimie Marine - Ecole Normale Supérieure, 1, rue Maurice Arnoux, 92120 Montrouge, France
[2] Ecole Nationale Supérieure des Techniques Avancées, 32, boulevard Victor, 75015 Paris, France

Abstract.
A thirteen compartment biogeochemical model has been coupled with a general circulation model so as to quantify the exchanges between the Gulf of Lions and the open Mediterranean. Quasi-equilibrium is obtained after one year of spin-up simulation, and model computations compare reasonably well with field data. Nitrate inputs from the Rhône river, the sediment and marine advection are compared. Regarding the open sea, the margin acts most of the time as a nitrate sink. During winter, however, it is shown to export nitrate toward the open sea through cascading of dense waters.

Key-words : nitrogen, circulation models, Gulf of Lions

Introduction

The Gulf of Lions is one of the major margins in the western Mediterranean (~20000 km^2) and forms a shallow receptacle for the most important Mediterranean river, the Rhône. The oligotrophic character of the Mediterranean sea is locally counterbalanced by continental inputs of nutrients (1), as shown by CZCS images that reveal a permanent higher productivity in the Gulf of Lions than in the adjacent area (2). Whether this river impact is confined to the coastal area or can extend offshore remains poorly understood and depends both on the biogeochemical functioning of the Gulf of Lions and on its exchanges with the open sea. In order to obtain some insight into the nitrate cycle from the Rhône river toward the open sea, we developed a coupled three-dimensional biological model of the Gulf of Lions.

Methodology

General circulation model. The hydrodynamics of the Gulf of Lions has been numerically simulated with a general circulation model covering the whole northwestern Mediterranean Sea (8.5°W-17°E x 34.8°N-44.8°N), whose results have been truncated to our area of interest (2.5°E-7°E x 41.5°N-43°N). This finite difference, primitive equation model has previously been described in (3, 4, 5). For this simulation, the horizontal grid mesh is 1/8° in longitude and 1/10° in latitude (*i.e.* ~11 km x 11 km). 31 vertical levels (z-coordinates) of increasing thickness are used (6 m at the surface, 140 m at the bottom). The bottom topography is based on the DBD5 atlas. This rather coarse resolution does not allow to describe mesoscale processes, but the northern current and the deep water formation are well simulated (5, 6).

Biological model. The biological model describes C, N and Si cycling through the pelagic food-web as represented by thirteen compartments. The model is described *in extenso* elsewhere (7 and 8). Emphasis has been given to the mechanisms describing photosynthesis and organic matter degradation (9, 10). The nitrate stock can be renewed only by mixing with the deeper layers, whereas ammonia is part of a complex remineralization loop involving bacteria, zooplankton and heterotrophic nanoflagellates. Detritic silica settles down and is progressively dissolved throughout the water column. The calibration of the biogeochemical model was achieved on a one-dimensional basis (7), with a one-year data set (twelve 200 m-profiles of temperature, salinity, NO_3, Si and chlorophyll) available from a fixed FRONTAL station (43°24'N, 07°52'E, Fig. 1) commonly used for 1D models (*e.g.* 11).

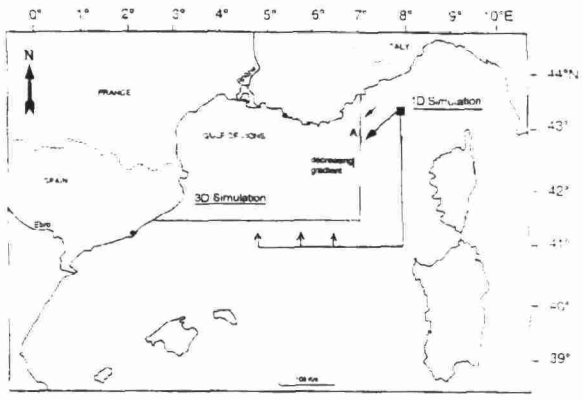

Fig. 1 : The simulation domain and a schematic description of the boundary conditions.

Three-dimensional model. The biological model has been carried in an off-line mode with a sub-sampling and an averaging every ten days of the velocity, temperature and salinity. The advective scheme is of FCT type, based on the antidiffusive correction algorithm (12). No explicit horizontal diffusion was included.

The thirteen biogeochemical equations ($\partial C/\partial t = -\{\partial(uC)/\partial x + \partial(vC)/\partial y + \partial(wC)/\partial z\} + D_X^H + D_X^V + (\text{Biol.evolution})$) are simultaneously solved using a fourth-order Runge-Kutta scheme (13) with a 1 hour time-step.

Initial conditions. Initial conditions have been obtained after a one year spin-up run leading to global stationality.

Boundary conditions. As eastern and southern boundary conditions, we used for all biogeochemical compartments the 1D simulation realized during the calibration phase at the eastern entrance of the Gulf of Lions (7, Fig. 1). In order to represent the well-known, dome-shaped structure of the Ligurian Sea divergence, we applied a south-north decreasing gradient to the boundary conditions, as estimated after the Prolig cruise's measurements (14). The exact formulation is given in (8).

As our model does not describe the early diagenesis in the sediments, we had to parametrize the nutrient fluxes at this interface. We take them into account by setting the concentrations of NO_3, NH_4 and Si equal to an observed value, in the bottom layer of the model and at each time-step. These values are spatially and temporally interpolated from a five cruise data set (EROS 2000 project).

The Rhône river has been coarsely described as a pinpoint source of nutrients (NO_3 and Si). The seasonal variations of the nutrient fluxes are described with a statistical model based on a twenty year time-series of data on discharges and nutrient concentrations (1). No non-point source of nutrient is considered. Finally, the atmospheric flux of nutrients was neglected at the scale of the Gulf of Lions, following (15)

Validity of the results. The biological model has been calibrated and thoroughly investigated apart from a three-dimensional simulation (7). The three-dimensional simulation has been compared in detail with available data and shown to provide satisfying results (8).

Discussion : Nitrate fluxes

The quasi equilibrium obtained for all the biogeochemical compartments (8) allows us to analyze the simulated fluxes on an annual scale. We consider here a "margin box", defined as the upper 200 m of the portion of the water column where depth is less than 500 m (Fig. 2, in white). We integrate the daily nitrate fluxes due to biological uptake by phytoplankton (Bio), sediment release (sed), Rhône river discharge (Rhône), vertical turbulent mixing (Mx), zonal (Z), meridional (M) and vertical advection (V) in the margin box. The annual budget of these fluxes is given in Table 1.

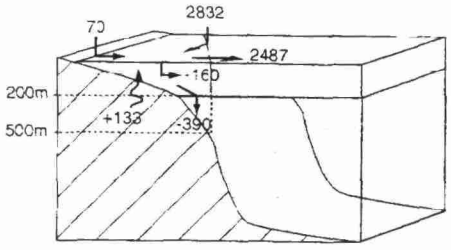

Fig. 2: Schematic description of the margin box (200 upper m where depth is less than 500m) and of the nitrate fluxes analyzed in the discussion.

Table 1 : Predicted integrated annual fluxes of nitrate (thousands of tons of N-NO_3) through the margin box (Fig. 1, in white). The last column (Total) displays the global annual budget for the margin box, which would be equal to zero if the model would be fully stationnary.

Bio	Sed	Rhône	Mx	Z	M	Z+M	V	Z+M+V	**Total**
-159	+133	+71	(+0.3)	+2832	-2487	+345	-390	-45	**(-0.1)**

Z and M are by far greater than the other fluxes, which underscores the predominance of horizontal transport in terms of mass balance. Z and M roughly compensate each other, Z being a positive flux entering the margin box at the eastern boundary, M being the negative flux going out at the southern boundary. Due to the non-divergence of the flow, the water trans

TRACE METAL ACCUMULATION IN THE SEDIMENT OF THE SUBMARINE CAVE "ZMAJEVO UHO" (SOLINE BAY, CROATIA)

I. Ujevic[1], D. Bogner [2] and A. Baric [2*]

[1] Faculty of Natural Science and Arts, Split, Croatia
[2] Institute of Oceanography and Fisheries, Split, Croatia

Abstract

A vertical profile in a sediment core from the submarine cave "Zmajevo uho" has been analysed for granulometric composition, organic matter, carbonate contents and trace metal concentrations (Cd, Pb, Cu, Zn and Ni). The carbonate content and granulometric composition are interrelated indicating that sediments from the cave having more carbonates are usually coarse grained. The concentrations of all trace metals decreased down the sediment core and showed good correlation with the organic matter content. The surface enrichment of Pb, Cu and Zn is an indication of anthropogenic influence to the sediment. The cave acts as a trap where a significant accumulation of different contaminants may occur.

Key-words : sediments, trace elements, Adriatic Sea

Introduction

The role of sediments has been recognised to be increasingly important in determining the distribution and fate of pollutants released into water bodies. Sediments can act as both a sink and source of pollution, and diagenetic reactions can remove or dissolve contaminants (such as trace metals) producing a concentration gradient at the sediment-water interface, the direction of which determines the water fluxes of contaminants. Therefore, the determination of trace metal concentrations in sediment is important in assessing the extent to which the marine environment is contaminated. The proportions of natural and anthropogenic trace metal levels in sediments are difficult to determine, since sediments can be deposited under a wide variety of environmental conditions. Trace metal distributions in cores of nearshore sediment may reflect the natural history of anthropogenic trace metal inputs [1].

The "Zmajevo uho" submarine cave is a karst phenomena located in the karstic region near Rogoznica, Soline Bay on the Adriatic sea (Figs. 1 and 2). Its entrance is located at a depth of 1.5 m and is less than 1 m in diameter. The total water depth is 29 m. Because of the location and size of the entrance, it is assumed that the cave has not suffered anthropogenic impact.

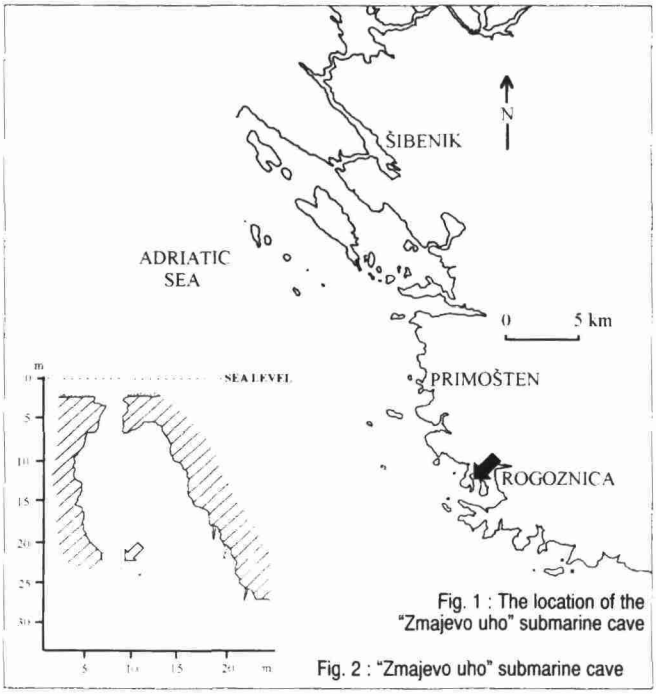

Fig. 1 : The location of the "Zmajevo uho" submarine cave

Fig. 2 : "Zmajevo uho" submarine cave

Methods

A sediment core (21 cm long) was sampled by a scuba diver using a plastic tube 3 cm in diameter. The sediment core was sliced into 2 cm long subsamples. Organic matter and carbonate contents as well as trace metal concentrations (Cd, Pb, Cu, Zn, and Ni) were determined in the subsamples. Granulometric composition of the sediment was determined by sieving and areometring (Casagrande). The organic matter content was determined as a weight loss by weighing the sample before and after H_2O_2 treatment followed by ignition at 450°C. The carbonate content was determined as weight loss after treatment with 4M HCl.

Trace metals were determined by the ET-AAS method using Perkin-Elmer 1100 B spectrophotometer. The accuracy of the analytical procedure was repeatedly checked by analysing samples of reference sediment standards (SRM 1646 estaurine sediment).

Results and discussion

Granulometric composition of the sediment core is shown in Table 1. The proportion of coarse particles (> 63 μm) increases with the sediment depth, while small particles (silt/clay grade) predominated in the upper layers of sediment. Upper sediment layers were sandy silt (1-12 cm), the middle layer was silty sand (13-20 cm) and the deepest was sand (21-24 cm).

Table 1. Granulometric composition of the sediment core (clay < 4 μm, silt 63-4 μm, sand > 63 μm).

1-12 cm	4.0 % clay	
	65.0 % silt	Sandy silt
	20.0 % sand	
13-16 cm	2.5 % clay	
	25.5 % silt	Silty sand
	48.0 % sand	
17-20 cm	1.0 % clay	
	17.0 % silt	Sand
	65.0 % sand	
21-24 cm	0.5 % clay	
	22.5 % silt	Sand
	66.0 % sand	

Carbonates (range 66.29-93.13%) were the main mineralogical component of the sediment core. Carbonate content increased with the sediment depth (Fig. 3) as the proportion of coarse particles increased. Organic matter content decreased with sediment depth as coarse particles and the carbonate content increased (Fig. 3). Linear regression between the organic matter and carbonate contents showed a significant negative correlation (Table 2).

The results obtained for the trace metal concentrations are illustrated in Figure 4. Increased surface concentrations (upper 10 cm) were observed for all the trace metals examined, especially Pb. Although the sediment originates from an area which is not considered to be polluted, the increased concentrations in the surface layer suggest some kind of contamination by these metals. While leaded gasoline would appear to be the main source of Pb, agricultural runoff may be an additional source of Cu, and domestic waste water a point source of Zn [3]. Nevertheless, the pathway in which these metals reached the cave is not clear. Namely, the entire area is karstic and the cave is very probably directly connected to ground waters. Therefore, there are two possible transport pathways for these trace metals: indirectly by sedimentation from the sea or directly by ground water.

The distribution of Pb, Cd, Cu, Ni and Zn in the sediment core is most likely controlled by the organic matter content. The trace metal concentrations in the core are correlated with the organic matter

THE INFLUENCE OF SOME NATURALLY OCCURRING MINERALS ON THE PRECIPITATION OF CALCIUM CARBONATE POLYMORPHS

Neda Vdovic* and Damir Kralj
Ruder Boskovic Institute, Bijenicka 54, HR-10000 Zagreb, Croatia

Abstract

In this work precipitation of calcium carbonates, initiated by the addition of suspended mineral particles (quartz, kaolinite or montmorillonite) was investigated. In the precipitation system the initial concentrations of calcium and carbonate species, as well as the ionic strength, were similar to those in seawater. In the model system, in which no mineral particles were added, vaterite was the only solid phase precipitated after an induction period of approximately two minutes. Quartz had no influence on the precipitation, while the addition of kaolinite to the system partially inhibited the precipitation process; the effect could probably be attributed to the organic matter desorbed from its surface. In contrast, the addition of calcium montmorillonite caused an instantaneous precipitation of calcite thus indicating montmorillonite to be a suitable substrate for the overgrowth of this polymorph.

Key-words: calcium

Introduction

Calcium carbonate exists in three polymorphic modifications: calcite, aragonite and vaterite. Calcite is thermodinamically stable, whereas vaterite is the least stable of these polymorphs at conditions on the earth's surface. Besides the major influence of the initial concentration of constituent ions, temperature and dissolved impurities on the formation of certain modification [1, 2], suspended mineral particles may also play an important role. Namely, when crystals are formed at moderate or low supersaturation, as is the case in calcium carbonate precipitation from natural water, the mechanism of their nucleation cannot be homogeneous because the work of forming the nuclei is too large. The nucleation process may be catalyzed by the presence of any solid surface (heteronuclei); in this case the similarity of crystal lattices of a substrate and growing phase is much more important than any chemical similarity. When the lattice mismatch, δ, defined as $\delta = |a-b|/a$, is less than *ca.* 0.02, the growth of nuclei on the substrate follows a specific orientation (a and b are the stress-free lattice parameters of the substrate and the overgrowing phase respectively). This special case of heterogeneous nucleation, epitaxy, requires the initial formation of an immobile monolayer of regular atomic patterns which serves as the embryo [3, 4]. In this paper the influence of suspended mineral particles on the precipitation of calcium carbonate polymorphs was investigated. Three types of naturally occurring minerals, quartz, kaolinite and montmorillonite, were used to inoculate the solution supersaturated with respect to all calcium carbonate polymorphs. The total concentrations of calcium and carbonate species, as well as the ionic strength, were similar to those found in seawater.

Experimental

The chemicals used, $CaCl_2$, Na_2CO_3, HCl, NaOH, NaCl and $MgCl_2$ were all analytically pure (Merck Darmstadt, Germany) while the solutions were made from triple-distilled water. Quartz, kaolinite and montmorillonite (Aldrich, USA) were used as they were, without any purification and the specific surface area of these minerals was determined by the B.E.T. method (Micromeritics Flowsorb II 2300, USA) using nitrogen. Samples of magnesium, calcium and sodium montmorillonite were prepared by soaking the natural montmorillonite (bentonite) in a solution of respective salt (c($MgCl_2$, $CaCl_2$ or NaCl) = 1 mol dm^{-3}). These samples were occasionally shaken and after three days were separated by centrifugation and thoroughly rinsed with water.

The experiments were started by pouring 100 cm^3 of 2.10^{-2} mol dm^{-3} $CaCl_2$ solution into the same volume of 4.10^{-3} mol dm^{-3} freshly prepared Na_2CO_3 solution. Both solutions were preadjusted to pH = 10 by means of NaOH or HCl, while the ionc strength (I = 0.5 mol dm^{-3}) was adjusted by adding NaCl. The mineral particles, kaolinite, montmorillonite or quartz, were added into the sodium carbonate solution before pH adjustment. The suspension was additionally homogenized by means of an ustrasonic bath. During the experiments, the temperature was kept constant (t = 25 ± 1°C) and the system was continuously stirred at a constant rate by means of a teflon-coated magnetic stirring bar. The propagation of reaction was followed by measuring pH of the solution. For that purpose a combined glass-calomel electrode (GK 2401 B) connected to a digital pH meter (ION 85) and a recorder (REC 80 Servograph with a REA 160 Titrigraph Module), all Radiometer, has been used. Commercial standard buffer solutions (Radiometer) were used to adjust the pH meter (pH 7.01 and 9.18 at 25°C) prior to the start of each experiment. Composition of the precipitate was determined by using a FT-IR spectroscopy (Perkin-Elmer FT-IR spectrophotmeter, Mo 2000). For this purpose, the suspensions were filtered through 0.22 μm membrane filter, the precipitate was dried at 105°C for one hour, the KBr pellet was prepared and then analyzed. The morphology of individual particles was observed by optical (Ortoplan photographic microscope, E. Leitz, Wetzlar) and scanning electron microscopy (Hitachi S 530). Calculations of solution composition were performed by means of a BASIC program on a personal computer [5].

Treatment of data

From the recorded pH data and the initial total concentrations of calcium chloride, $[Ca]_i$, sodium carbonate, $[CO_3]_i$, and sodium chloride, the concentrations and the corresponding activities of ten ionic species assumed to exist in the solution to a considerable extent (H^+, OH^-, CO_3^{2-}, HCO_3^-, $CaCO_3^0$, $CaHCO_3^+$, $NaCO_3^-$, Ca^{2+}, Na^+, Cl^-) were calculated by means of a BASIC program. The equilibrium constants, determining the protolytic and other equilibria, were taken from the paper of Plummer and Busenberg [6], while the activity coefficients, y_z, of the ionic species of the charge z were estimated by means of the Davies equation [7]. The amount of precipitate, [ppt], was found by subtractig the calculated total concentration of carbonate ions ($[CO_3]_{tot}$ = 2 $[CO_3^{2-}]$+$[HCO_3^-]$+$[CaHCO_3^+]$+$[NaCO_3^-]$) from the known initial total concentration of carbonate ($[CO_3]_i = 2.10^{-3}$ mol dm^{-3}) – in the precipitation system decribed, total initial concentration of calcium species is in excess in comparison to total concentration of carbonate species ($[Ca]_i = 1.0.10^{-2}$ mol dm^{-3}; $[CO_3]_i = 2.0.10^{-3}$ mol dm^{-3}); therefore, the maximum amount of calcium carbonate that could precipitate is determined by the concentration of carbonate. The program furthermore calculated the supersaturation given as saturation ratio, S, expressed as a square root of the activity quotient:

$$S = \sqrt{\frac{[Ca^{2+}]\cdot[CO_3^{2-}]\cdot\gamma_z^2}{K_S^0}}$$

where K_s^0 is the thermodynamic solubility product of calcite.

Results and Discussion

The initial total concentrations of calcium and carbonate species (c($CaCl_2$) = $1.0.10^{-2}$ mol dm^{-3}) and (c(Na_2CO_3) = $2.0.10^{-3}$ mol dm^{-3}) in the systems investigated in this work, as well as the concentration of NaCl (c(NaCl) = 0.5 mol dm^{-3}), were similar to those found in seawater. The initial supersaturation has been adjusted by the addition of different amounts of NaOH or HCl to calcium or carbonate solution. The artificial seawater was not used in these experiments, since it would contain significant amount of Mg^{2+} (c = 5.10^{-2} mol dm^{-3}). Namely, it is well known that, among the inorganic components dissolved in seawater, Mg^{2+} undoubtedly has a principle influence on the calcium carbonate precipitation [8]. Spontaneous precipitation of calcium carbonates from artificial seawater always results in formation of aragonite; the effect is so strong that aragonite precipitates even in the case when such solution is inoculated by vaterite or calcite [9]. By using a natural seawater, the system would become even more complex because of the presence of dissolved phosphates and organic constituents. In Figure 1 the progress curves (Fig.1a) and the corresponding desaturation curves (Fig. 1b) for unseeded precipitation of calcium carbonates in the systems having different initial supersaturations ($5.5 \leq Si \geq 8.5$) are shown. It can be seen that the onset of precipitation succeeded after a delay of a certain period of time (induction period) that varied between 2 and 20 minutes. In each system the final supersaturation is approximately 1.9 which corresponds to vaterite

GEOCHEMICAL FEATURES OF SURFACE SEDIMENTS ALONG THE IONIAN COASTS

Fanny Voutsinou-Taliadouri
National Centre for Marine Research, Aghios Kosmas, Hellenikon, Athens 166 04, Greece

Abstract

Surface sediment samples collected from five coastal areas of the Ionian Sea were analysed for grain composition, organic carbon and Fe, Cr, Ni, Mn, Zn, Co, Cu, Pb concentrations. Analysis of the data reveals that generally the Ionian surface sediments have not been affected by anthropogenic influences and contain naturally higher amounts of heavy metals when compared with Aegean Sea sediments.

Key-words : metals, sediments, Ionian Sea

Introduction

Marginal marine environments including estuaries, lagoons, bays, gulfs, etc., are especially sensitive to long- and short-term external factors. In particular, coastal areas are subject to diverse anthropogenic influences including industrial development, domestic wastes, maritime transport and agricultural activities. In addition, the effects of the weathering of nearby soils also have to be considered. For all these reasons sediment analyses of coastal areas play a very important role in the quality assessment of the marine environment as far as metal pollution is concerned. Coastal sediments are important hosts for pollutant heavy metals and as such should be included in routine environmental monitoring programmes, although they do not furnish quantitative data on the absolute degree of pollution. This is due to the fact that marine sediments naturally contain different quantities of metals, so "background values" cannot be as readily established as for other parameters. Therefore, the knowledge of heavy metal baseline concencentrations is required. The most reliable way for the selection of baseline material is to consider those sediments within the area under investigation for which the distribution pattern of the metals becomes far less distinct or disappears altogether. The aim of the present work is to assess the environmental state of the region under study, as far as the heavy metal pollution is concerned, in comparison with other Greek coastal areas.

The study area comprises the following regions of the Ionian Sea: The Kerkyra Strait, Amvrakikos Gulf, Messolonghi Lagoon, Patraikos Gulf and Navarino Bay (Fig. 1). The Kerkyra Passage is situated in the uppermost northeastern part of the Ionian Sea between Kerkyra Island and mainland Greece. It communicates with the Ionian Sea through two straits: 1 n.m. wide in the North, 6 n.m. in the South; max. width of the area 1 6 n.m. The depth contours generally follow the coastal lines, and maxima of around 70 m are attained in the central part of the region. The study area receives agricultural and industrial wastes brought by the Kalamas River (mean annual discharge: $1{,}619 \cdot 10^6$ m^3) and domestic and industrial wastes by a small torrent north of the city of Kerkyra (pop. approximately 40,000 and more than 80,000 tourists). The second study area comprises the Amvrakikos Gulf, a semi-enclosed embayment and a lagoonal complex consisting of three systems. The Gulf is connected with the Ionian Sea through Preveza Channel (sill depth 4 m; width 60 m; length 5 km). Water depths in the Amvrakikos Gulf are less than 60m, while in the adjacent lagoons they do not exceed 3 m. The Arachthos and Louros rivers (mean annual discharge of $2{,}202 \cdot 10^6$ m^3 and $609 \cdot 10^6$ m^3 respectively) discharge into the bay. These rivers receive the main load of the domestic (pop. around 100,000), agricultural and industrial wastes of the surrounding area. The third study area, Messolonghi Lagoon, consists of four lagoons, which do not communicate with one another and have depths from 0.2 m to 2.00 m (except in the Aitolikon lagoon, where the depth is around 25 m). The town of Messolonghi (pop. around 10,000) discharges its wastes in the Kleisova lagoon. The Patraikos Gulf, with depths not exceeding 110 m in the central part, receives mainly domestic and industrial effluents of the city of Patras (pop. around 100,000). Navarino Bay, a semi-enclosed embayment in the southwestern part of Peloponnesus with depths less than 50 m, receives some agricultural effluents from the nearby land.

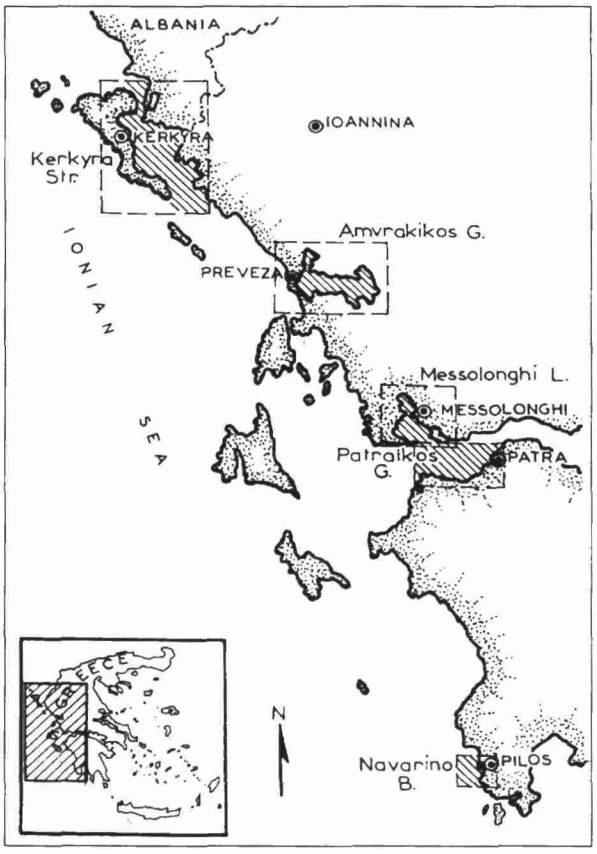

Fig.1. Sampling locations.

Methodology

Surface sediment samples taken from 193 stations located along the Ionian coasts during the period 1980-1991 were analysed for grain size, organic carbon and the trace metals Fe, Cr, Ni, Mn, Zn, Co, Cu and Pb. The samples were collected using a 0.1 m^2 van Veen grab. The grain size measurement was performed by a technique (1) modified from that of Buchanan (2). Organic carbon was obtained according to Gaudette *et al.* (3). For the trace element determination the leaching of sediment samples with cold dilute HCl, which affects only the non-residual part of the metals and gives the "anthropogenic fingerprints" for the bottom deposits, provides more data on the extend of heavy metal pollution compared to the total sediment analysis.

The trace metal analysis was carried out with the sediment fraction < 1 mm which was crushed in a mortar to <0.063 mm to reduce the influence of grain size on the analytical results. About 5 g of each representative sample were shaken for 16 h at room temperature with 75 ml of 2N HCl. The determination of the metal content of the leachates was performed on an AAS (4). The accuracy was checked by analysis of standard samples from the International Laboratory of Marine Radioactivity (IAEA) during international exercises (5). The values (μg/g) found and the certified ones were the following: Mn 0.85±0.07/ 0.88±0.06; Cu 4.30±0.30/ 4.50±0.30; Zn 35.20±0.30/ 37.00±3.00; Fe 66.20±1.20/ 57.00±3.00. The analyses, in triplicate, indicated the following average standard deviations and coefficient of variation: O.C. 0.032%, 0.9; Fe 0.85‰, 4.4; Mn 38 mg/kg, 5.0; Zn 4.19 mg/kg, 6.0; Cr 1mg/kg, 2; Ni 1 mg/kg, 1; Co 0.2 mg/kg, 2; Cu 0.1 mg/kg, 1; Pb 0.5 mg/kg, 2.5.

Results and Discussion

Table 1 depicts the granulometry, organic carbon content and heavy metal concentrations in the sediments. The granulometric analyses of the sediments showed that the greater part of the open sea regions of the areas studied is covered by fine sediment (silt or clay)

TRANSPORT AND BUDGET OF NUTRIENTS IN KASTELA BAY (ADRIATIC SEA)

Ilija Vukadin

Institute of Oceanography and Fisheries, Setaliste I. Mestrovica 63, 21000 Split, Croatia

Abstract

Kastela Bay is a semi-enclosed coastal bay in the middle Adriatic which acts as a dilution basin due to the fresh water, industrial and urban inflows. Nutrient content and basic hydrographic parameters were studied and discussed, as well as the effects of some other biological and geochemical processes on their concentrations. The following phenomena were studied: fresh water, waste water, and atmospheric input, water mass exchange between the Kastela Bay and the adjacent sea, and loss of nutrients through the sedimentation of organic matter. On the basis of the results obtained, Kastela Bay may be categorized as a very eutrophic area with its eastern part (Vranjic basin) suffering from an extremely high degree of eutrophication. During the last few years the Bay has shifted into the highest category of productivity (> 500 mg C m^{-2} a^{-1}) of sea water.

Key-words: nutrients, eutrophication, Adriatic Sea

Introduction

Calculation of the nutrient balance provides a basis for quantitative studies of the biogeochemical mechanisms in a particular aquatic environment.The nutrient balance for Kastela Bay was obtained from long-term studies carried out in this area by the Institute of Oceanography and Fisheries, (IOF) Split, and data from the literature. Balance calculations took into account a series of input and loss mechanisms of which some are particular for nutrients. Fresh water, waste water and atmospheric input, water mass exchange by transport between Kastela Bay and the adjacent sea, and loss of organic matter by sedimentation were studied.

The annual mean rate of nutrient recycling linked to biological processes (*e.g.* phytoplankton assimilation, regeneration through excretion of heterotrophic microorganisms and macrozooplankton) and sediment release were also estimated. A simplified conceptual model of nutrient cycling in the enclosed bays is outlined in Figure 1.

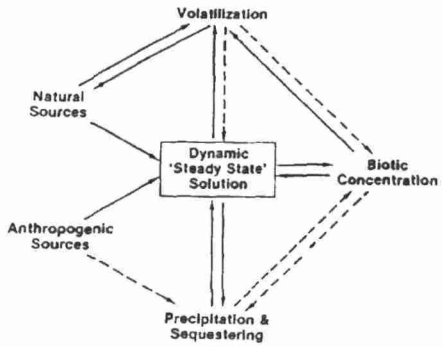

Fig. 1. A simplified model of nutrient cycling in the marine environment.

Study area

Since 1952 the IOF has been collecting oceanographic, nutrient and biological data from some stations in Kastela Bay, as well as an open sea station (Fig. 2). Cruise frequencies ranged from weekly (summer period) to monthly. In this paper the data for the period 1982-1995 has been used.Kastela Bay is 14.8 km long, about 6 km wide and 23 m deep on the average (Fig. 2). The Bay communicates with the adjacent sea through an inlet 1.8 km wide and 40 m depth. The small Jadro River which flows into the eastern part of the Bay (Vranjic basin) is the most important fresh water source with an annual average inflow of about 10 m^3 s^{-1}. The eastern part of the Bay also receives large quantities of untreated municipal and industrial effluents (104 x 10^6 m^3 a^{-1}). The Bay has a total area of 61 x 10^6 m^2 with a water volume of 1.4 x 10^9 m^3. Water exchange and changes in the current field are mostly induced by local winds related to the passing of mid-latitude cyclones over the area (2). The annual average precipitation of 1 m and the total rate of water over the Bay surface exceeds 61 x 10^6 m^3 a^{-1}. The local coastal drainage basin is approximately twice the area of the Bay (*i.e.* 122 x 10^6 m^2). Precipitation is also doubled there, *i.e.* 122 x 10^6 m^3 a^{-1}. The Bay is particularly threatened by organic matter and nutrient input which cause an extreme phytoplankton bloom each summer (3, 4). Anoxia in the bottom layer develops as the most frequent consequence. Furthermore, microbial pollution jeopardizes the Bay's eastern part and northern coast (5).

Results

For the nutrient balance calculations, water quantity and chemical component contents in the Bay were considered to be in a "steady

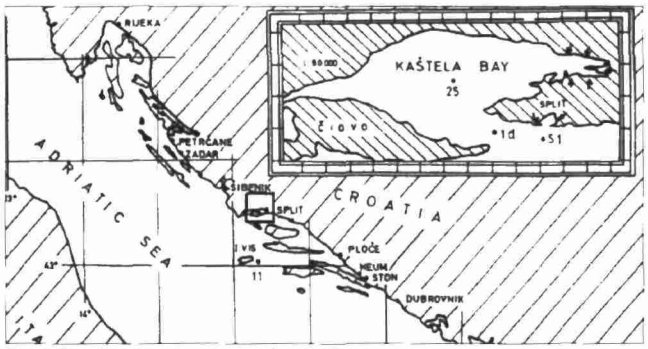

Fig. 2. Position of stations in the Kastela Bay.

state" that is, the supply of chemical substances and their removal through different physical and chemical processes were assumed to be equal. Water balance was calculated by a simple salinity balance calculation (6) : **Si * (Q+x) = So * x**

where S_i is the mean value of water salinity, which was 36.80 in Kastela Bay. S_0 is the mean salinity value (38.40) at the offshore station (I.Vis). Q is the annual mean input of fresh water into the Bay (Q= 474 x 10^6 m^3 a^{-1}). This value is the sum of rainfall, river discharge and losses by evaporation. The x value is the annual input of seawater from the open sea (x = 10902 x 10^6 m^3 a^{-1}) Residence time of sea water in the Bay was calculated to be as 0.12 years or 44 days. This is in good agreement with values obtained from current flushing time (30 days) (7). This calculation shows Kastela Bay to be a dilution area for the adjacent sea where the outgoing water mass exceeds the water input, (Q + x) = 11376 x 10^6 m^3 a^{-1}). Nutrient balance calculations for the Bay require knowledge of nutrient levels in the Bay and open sea water as well as in all the waters which enter the Bay from the mainland (Table 1 and 2). As shown in Table 1, nutrient concentrations decrease with distance from the source of nutrient input.

So, the highest values were recorded in the Bay, slightly lower values at the mouth of the Bay. The lowest values were recorded in front of the town port (S-1), even though this station is strongly affected by urban effluents carrying large quantities of nutrients, particularly phosphates (PO_4-P). Higher concentrations of NH_4-N at the open

Table 1. Ranges (R), mean nutrient concentrations (x), standard deviation (s) and data number (n) in Kastela Bay and offshore waters.

Stations		NH_4-N mmol m^{-3}	NO_2-N mmol m^{-3}	NO_3-N mmol m^{-3}	PO_4-P mmol m^{-3}	SiO_2-Si mmol m^{-3}
25	R	0.16-3.02	0.04-0.75	0.22-10.1	0.042-0.250	0.42-
	x	0.81	0.136	1.32	0.079	6.20 1.88
	s	0.43	0.05	0.34	0.014	0.48
	n	840	840	840	840	840
1d	R	0.24-1.48	0.03-0.35	0.29-13.6	0.042-0.115	0.36-5.70
	x	0.74	0.99	1.63	0.076	1.98
	s	0.39	0.03	0.45	0.024	0.23
	n	740	740	740	740	740
S-1	R	0.28-1.82	0.03-0.30	0.24-12.1	0.042-0.17	0.13-5.40
	x	0.68	0.09	1.00	0.103	1.81
	s	0.32	0.03	0.46	0.03	0.91
	n	388	388	388	388	388
11 I.Vis	R	0.36-1.98	0.04-0.12	0.60-0.91	0.04-0.20	0.53-7.53
	x	1.08	0.08	0.81	0.09	1.78
	s	0.39	0.02	0.34	0.01	0.21
	n	960	960	960	960	960

ENVIRONMENTAL GRADIENTS OF NUTRIENTS AND PHYSICAL-CHEMICAL PARAMETERS IN A MEDITERRANEAN COASTAL EMBAYMENT

T. Yiannakopoulou

Department of Civil Engineering, Democritus University of Thrace, Xanthi, 67100 Greece

Abstract

Temperature, salinity, pH, dissolved oxygen, Secchi depth, phosphates, ammonia and chlorophyll-a were studied for one year in Vistonis, a shallow, turbid, partially mixed coastal embayment in N. Greece. In summer, a salinity wedge of 4.5 ‰ reached the head of the estuary. pH values remained above 8.00 and the Secchi depth was below 1 m. In summer and late fall, anoxia was observed near the bottom. Phosphates remained below 20 mg/m^3 but, in the fall, bottom-derived phosphates resulted in a mean water concentration of about 100 mg/m^3. Ammonia remained below 360 mg/m^3, while in July it reached 1300 mg/m^3. The annual maximum of Chl-a (86 mg/m^3) in August was two orders of magnitude higher than the annual minimum (0.6 mg/m^3 in January).

Key-words: brackish water, salinity, nutrients, stratification, Aegean Sea

Introduction

Information on general patterns of nutrient cycles and phytoplankton dynamics in estuaries is relatively limited mainly because of the great diversity of estuarine types (ranging from large deep fjords to shallow tidal creeks) and of the extreme complexity of estuaries that have unique circulation, complex bathymetry and large horizontal and vertical gradients of properties [1]. Vistonis Estuary protected by the Ramsar International Convention on Wetlands of International Importance is part of a wetland system extending over the coast of Thrace (N.E. part of Greece). With the exception of one preliminary study [2] and some subsequent publications by the author [3-7], no other publications exist which describe the physical factors and nutrient status of this estuary. In this work, the general framework dealing with the physical factors, nutrients and chlorophyll-a and their complex environmental gradients is presented in order to understand this type of aquatic ecosystem in the Mediterranean region.

The Environmental setting

Vistonis is a bar-built, shallow (3 to 4 m maximum depth) estuary with a surface area of 45 Km^2. The only outlet to the sea is about 60 m wide and 4 m deep (Fig.1). The catchment area covers about 1355 Km^2; the mountain zone encompasses about 75% of the total drainage basin, the remaining 25% being low hills or plains. The mean annual rainwater reaching Vistonis, mainly in its northern and eastern regions, is about 403x106 m^3, 97% of which originates in the mountain area. The Kompsatos river contributes more than half of the total inflow, while the Kossynthos river and other smaller creeks contribute about 40%. The estuary has a total water volume of about 75x106 m^3, and the mean annual hydraulic residence time is about 38 days in winter and 467 days in summer.

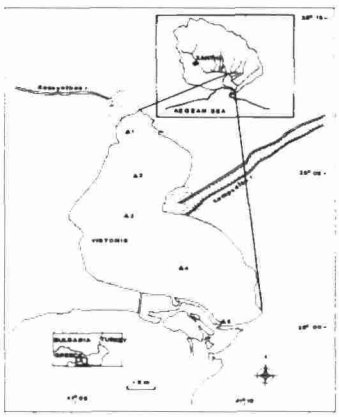

Figure 1: Vistonis estuary and catchment area. Triangle: sampling stations.

Materials and methods

During a one year period, samples were collected monthly from five sampling stations, with a Ruttner 0.5 l capacity sampler at 1 m intervals in the water column. Their distance from the mouth (Station 5) was 2.53 Km for St 4, 5.41 Km for St 3, 7.00 Km for St 2 and 8.76 Km for St 1 (Fig. 1). Temperature, salinity, dissolved oxygen, pH profiles and the Secchi depth were measured *in situ* with a YSI oxygen meter, a Hydrobios temperature-salinity bridge and a Consort pH meter. Samples were filtered through Millipore GF/F filters (nominal pore size μm) and the filters were immediately processed for Chlorophyll-a spectrophotometric determination [8]. The filtrates were transported in an ice chest to the laboratory where ammonia and phosphates were immediately determined [8, 9, 10].

Results

Mean monthly temperature ranged from 5.5°C in December to 26.1 °C in July. Vertical stratification of temperature was of minor importance. However, strong vertical, spatial and seasonal salinity differences were recorded due to a strong salinity gradient created by the intrusion of sea water (Figure 2). In January, a salinity wedge of over 2.0 ‰, almost reached the head at about 1 m depth creating over it a slight salinity gradient. In April, at the end of the wet season, almost holomictic conditions prevailed, while a well-mixed layer of only 0.9 ‰ remained near the mouth. In August, in the middle of the dry season, a salinity wedge of about 4.5 ‰ reached the head. However, vertical salinity differences away from the mouth were relatively small, since the shallow depth favored mixing of the layers. In October, salinity at the head reached the annual maximum (about 7 ‰). In October, the surface-to-bottom salinity differences from head to mouth were 0, 7.4, 8.2, 10.5, and 24.8 ‰, while the longitudinal salinity gradient at 3 m depth was 0.88 Km^{-1}.

In winter and spring the water column was well oxygenated down to the bottom (Fig. 3). In summer and late fall, however, the paucity of oxygen at the bottom created strong vertical gradients. In October, at the bottom of Stations 2 and 3, zero values of dissolved oxygen were recorded. Less than one mg/l oxygen values were also recorded at the bottom of station 3 in July, August and September.

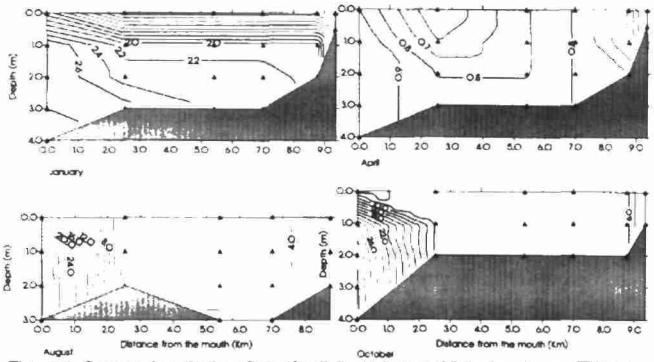

Figure 2: Seasonal vertical profiles of salinity (‰) along Vistonis estuary. (Triangle: Recorded values).

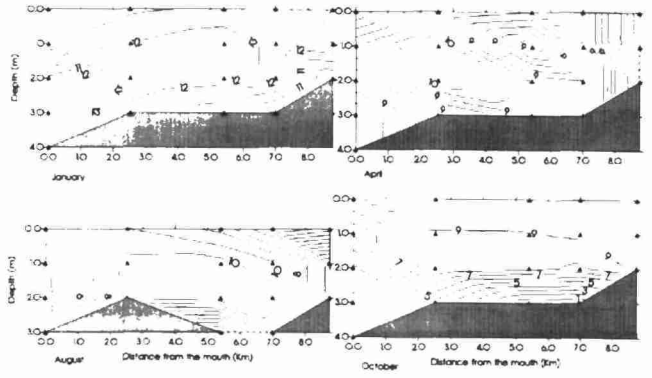

Figure 3: Seasonal vertical profiles of dissolved oxygen (mg/l) along Vistonis estuary. (Triangle: Recorded values).

APERÇU SUR LES CONDITIONS DE SURFACE D'UNE LAGUNE MEDITERRANEENNE (LAGUNE DE NADOR, MAROC)

Nasser Eddine Zine [1*] et Mohamed Menioui [2]

[1] Faculté des Sciences, B.P. 4010 Beni M'hammed, Meknès, Maroc
[2] Institut Scientifique, B.P. 703, Rabat-Agdal, Rabat, Maroc

Résumé

Cette étude sur la distribution spatiale des facteurs des eaux superficielles de la lagune de Nador a essentiellement permis de définir sa zonation hydrologique, de donner une situation de référence avant la mise en oeuvre du système de lagunage destiné à épurer les eaux usées de la ville de Nador. Il y a d'importants échanges entre l'enceinte lagunaire et la Méditerranée, et ce bassin lagunaire est constitué de quatre zones : le centre de la lagune, les deux extrêmités confinées NW et SE, et la bordure continentale. Cette dernière présente des signes d'engraissement organique lié à l'intensification des apports continentaux, bénéfique pour la conchyliculture.

Mots-clés: hydrology, lagoons, Western Mediterranean

Introduction

La lagune de Nador constitue l'unique enceinte lagunaire méditerranéenne du Maroc (entre les parallèles 35°7'N et 35°16'N et les méridiens 2°44'W et 2°80'W) et est, de plus, la plus grande de toutes les lagunes marocaines (115 km^2 de plan d'eau pour une profondeur ne dépassant pas 8,2 mètres). Elle communique avec la Méditerranée par l'intermédiaire d'une passe de 100 m environ de largeur et 3 m de profondeur; son débit moyen est de 86 m^3/h.De nombreux travaux y ont été consacrés, en particulier sur la malacofaune [1], la dynamique de population des bivalves [2], la biogéographie de la faune benthique [3], la biodiversité de la faune benthique [4], la géologie [5, 6], l'hydrobiologie et la sédimentologie [7, 8, 12], l'économie de pêche [9] et l'aquaculture [10], le confinement [10, 11]. Les prélèvements hebdomadaires (janvier 1987 à décembre 1987) des caractéristiques physico-chimiques (température, salinité, oxygène dissous, et pH), de la matière particulaire (matière en suspension, chlorophylle a et phéopigments) et des éléments nutritifs minéraux dissous (nitrites et silicium), ont été réalisés dans 36 stations reparties dans la lagune (Fig. 1). Les données traitées dans ce travail correspondent à des moyennes annuelles.

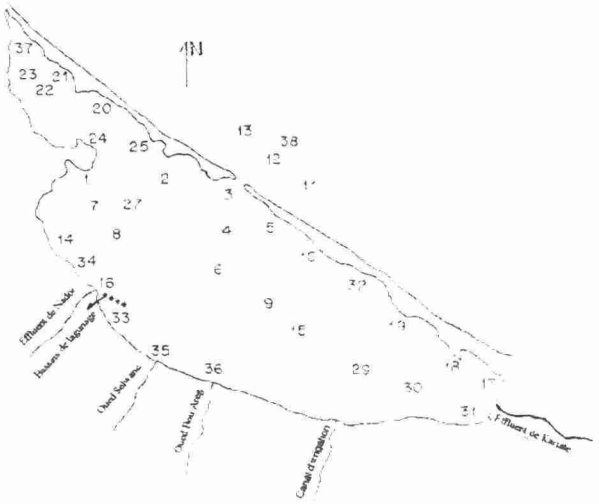

Fig. 1 : localisation des stations dans la lagune de Nador.

L'importance de cette analyse réside dans le fait qu'elle traduit un état de référence avant la mise en place en 1991 d'un système de lagunage à l'intérieur même de l'enceinte lagunaire pour l'épuration des eaux usées, ce qui, selon nos données encore inédites, a complètement changé les caractéristiques de ce milieu, l'un des plus important de la Méditerranée.

Résultats

Température. La température moyenne de surface à l'intérieur de la lagune est de 20,2 ± 0,19°C. Quatre stations ont des températures relativement plus fraîches (19,2 ± 0.023°C). Il s'agit des stations 11,12, 13 et 38, situées à l'extérieur de la lagune. Ce faible écart entre l'intérieur et l'extérieur de la lagune s'expliquerait par : - le bon fonctionnement de la passe; - le fait que la lagune est sous influence des eaux marines. Les températures moyennes minimale (janvier) et maximale (août) à l'intérieur de la lagune sont respectivement de 11,8 ± 1,96°C et 27,57 ± 0,31°C, contre 14,62 ± 0,095°C et 24,6 ± 0,081°C dans le milieu marin. Elles sont essentiellement enregistrées dans les zones peu profondes dont la bordure continentale et les extrémités NW et SE de la lagune. Dans une autre lagune méditerranéenne, la lagune de Karina en Turquie [13], les températures moyennes minimales et maximales sont obtenues pratiquement pendant les mêmes périodes (janvier et septembre), cependant avec des valeurs relativement plus faibles: respectivement 9,07°C et 22,34°C. Dans le système lagunaire de Koycegiz, toujours en Turquie [14], la température moyenne annuelle est de 19,56°C, très légèrement inférieure à celle trouvée à Nador. Dans le lac Mellah en Algérie [15], le cycle des températures fait ressortir deux grandes périodes : chaude de mai à août avec un maximum en juillet (29°C) et froide de septembre à avril avec un minimum en janvier (4,5°C).

Salinité. La salinité moyenne à l'intérieur de la lagune est de 36,97 ± 0,47‰, légèrement supérieure à celle de l'eau de mer (36,15 ± 0,038‰ en moyenne, dans la zone franchement marine). Ce paramètre permet de définir quatre zones à l'intérieur de la lagune : - les stations du centre de la lagune avec une moyenne de 37,03 ± 0,168 ‰; - les stations de la bordure continentale (14, 16, 33, 34, 35 et 36) dont la moyenne est de 36,17 ± 0,37‰, temporairement dessalées par les apports d'eaux douces (la plus faible valeur de la salinité est obtenue au mois de mars dans la station 36: 29,4‰) des trois principaux émissaires que sont l'effluent de Nador, l'oued Selouane, et l'oued Bou Areg (Fig. 1); - et les stations des deux extrémités NW (21, 22, 23 et 37) et SE de la lagune (17, 18 et 31), faiblement brassées par les courants de marées, dont les salinités moyennes sont respectivement : 37,57 ± 0,115‰ et 37,16 ± 0,08‰ (la valeur maximale de 40,2‰ est enregistrée au mois de septembre à la station 37 très confinée). Dans la lagune de Karina en Turquie, la salinité moyenne est de 38,01‰, [13] légèrement supérieure à celle obtenue à Nador. Pour le système lagunaire de Koycegiz en Turquie, la salinité minimale est de 2,34‰, la maximale de 12,35‰ pour une moyenne de 5,63‰ [14]. Dans le lac Mellah en Algérie, les salinités relevées mettent en évidence deux période halines: une période de salinité importante de mai à novembre avec un maximum de 33,25‰ en novembre qui coïncide avec la saison sèche et une période de faible salinité entre décembre et avril avec un minimum de 18,73‰ en janvier [15].

Oxygène dissous. Les concentrations moyennes de l'oxygène sont relativement stables (7,14 ± 0,28 mg/l), inférieures à celles des quatre stations situées à l'extérieur de la lagune (7,44 ± 0,042 mg/l). Les seuls prélèvements dont les concentrations sont inférieures à 7mg/l et qui paraissent montrer une carence en oxygène, certainement à cause d'une forte demande biologique, sont ceux situés sur la bordure continentale entre les stations 14 et 36 où les rejets domestiques sont permanents et auxquels s'ajoutent périodiquement des apports supplémentaires dus au lessivage des zones voisines. La teneur moyenne en oxygène y est de 6,74 ± 0,384 mg/l, ce qui correspond à un taux de saturation d'environ 86%, et peut descendre jusqu'à 3,6mg/l en période estivale. On assiste ainsi à un gradient décroissant du taux d'oxygène depuis les stations marines (7,44 mg/l) vers les deux extrémités confinées NW (7,11mg/l.) et SE (7,29mg/l) de la lagune, et vers les stations de la bordure continentale (6,74 mg/l). Dans le système lagunaire de Koycegiz en Turquie, la valeur minimale est de 7 mg/l et la maximale de 9,6 mg/l alors que la moyenne elle est de 8,35mg/l [14]. Sur la côte de la mer Adriatique en Croatie, la valeur moyenne du taux d'oxygène est bien plus faible qu'à Nador: 5,03 mg/l [16]. Quant au lac Mellah en Algérie [15], le taux d'oxygène y est important en période hivernale (14,6 mg/l en janvier), faible (4,38mg/l) en période estivale.

pH. L'évolution de ce paramètre montre qu'il n'y a pas de différences notables entre les pH à l'intérieur de l'enceinte lagunaire (8,41 ± 0,045) et l'extérieur (8,28 ± 0,012). A l'intérieur même de la lagune, il n'y a pas de différences majeures entre les pH des stations supposées polluées, situées sur la bordure continentale (8,37 ± 0,04) et celles situées à proximité de la passe qui sont sous l'influence des eaux marines (8,29 ± 0,01 en moyenne). C'est une valeur moyenne relativement plus élevée que celle obtenue dans la lagune de Karina en Turquie où le pH moyen est de 7,63 [13]. Dans le système lagunaire de Koycegiz toujours en Turquie [14], on signale que la valeur minimale du pH est de 7,22, alors que la valeur maximale est très proche de celle trouvée à Nador (8,28). Une valeur également très proche (8,2) été obtenue sur la côte de la mer Adriatique en Croatie [16].

AN ELECTROCHEMICAL APPROACH TO ORGANIC AGGREGATION

V. Zutic, N. Ivosevic*, S. Kovac and V. Svetlicic

Center for Marine and Environmental Research, Ruder Boskovic Institute, PO Box 1016, 10 001 Zagreb, Croatia

Abstract

At an electrode/seawater interface, surface-active organic molecules can be detected and characterized through their adsorption, while surface-active organic particles (≥ 1 μm) can be simultaneously detected and characterized through their attachment. Frequency of electrical attachment signals reflects the abundance of particles. Amplitude and shape of each attachment signal depends upon the reactivity and interfacial area of attachment (size) of a single particle. For a population of particles, potential of appearance of attachment signals serves to estimate the critical interfacial tension of attachment and energy of adhesion. We investigate attachment signals of single cells, of exopolymeric particles and aggregates formed in bacterial cultures and compare them with signals of surface active particles that are abundant (up to 10^5/ml) in Northern Adriatic. The electrochemical approach, although *a priori* lacking molecular specificity, has an advantage over other recently developed techniques in directly measuring interfacial properties of single particles that are critical for the onset of aggregation phenomena.

Key-words: electrochemistry, bacteria, adsorption, Adriatic Sea

Introduction

The complex interfacial processes responsible for aggregation can be decoupled using a model fluid interface, mercury electrode/seawater, where the interfacial energy and charge density are controlled by applied potential. Fast dropping mercury electrode (DME), among other surface attributes such as hydrophobicity and variable surface charge, mimics interfacial dynamics of natural fluid interfaces.

Adsorption of organic molecules at DME is manifested as a regular suppression of current of polarographic maxima in the potential range of adsorption, while adhesion of fluid particles (≥ 1 μm) yields pronounced current spikes - attachment signals. Average frequency of electrical attachment signals reflects the abundance of particles. Amplitude and shape of each attachment signal depends upon the reactivity and interfacial area of attachment (size) of a single particle. The critical potentials of appearance of attachment signals serve to estimate the energy of adhesion (1). We present typical attachment signals for single phytoplankton cells and for aggregated bacterial cells and compare them with signals of surface-active particles (SAP) that were identified in stratified Mediterranean estuaries (2-4) (up to 10^5/ml) and in the Northern Adriatic (5) that are closely related to transparent exopolymeric particles, identified more recently (6).

Experimental

Electrochemical measurements. The electrochemical technique used is chronoamperometry at the DME at potentials of streaming maximum of oxygen reduction (7-9). Laboratory experiments were performed in diluted seawater (1:5). The maximum contact time between a sample and mercury surface is 2 s. The potentials are referred to Ag/AgCl reference electrode.

Phytoplankton cells: naked microflagellate Isochrysis galbana was grown in seawater sterilized and enriched with F-2 nutrients in batch cultures. Cells were separated after 6 days of growth. Viability of cells was controlled in all stages of the experiment by microscopic observation of cell motility. Bacterial suspensions: marine bacteria isolated as attached (strains S3 and LHAT1) or free-living (strain BF2) in natural habitat (Scripps Pier 10,11) and filamentous bacteria *Saprospira grandis A* (12) were grown as batch monocultures. The cells were harvested after 3 days and separated from the growth medium. Marine snow: samples from Northern Adriatic were taken by scuba diver, at a depth of 16 m, in August 1994.

Results and discussion

The dropping mercury electrode is used here as a model interface to identify physico-chemical interactions in the interfacial process involving phytoplankton cells, marine bacteria and extracellular polymers. Amperometric curves were recorded at two characteristic potentials where the mercury surface is positively charged (E = -400 mV, σ = +3.8 μC/cm^2), negatively charged (E = -800 mV, σ = -6.5 μC/cm^2) and at E = -550 mV where the electrode is uncharged.

In Fig. 1 we compare attachment signals of North Adriatic surface-active aggregates contained in a marine snow sample with the signals of single phytplankton cells and aggregated bacteria. The model unicellular organism we used (*Isochrysis galbana*) is a marine nanoflagellate without cell wall. The cell size of 4-7 μm and flexibility of cell membrane are features of choice to obtain characteristic electrical signals for attachment of single cells. We selected yellow pigmented bacterium S3 related to *Cytophaga/Flavobacteria* (11) that are associated with particles and have surface dependent gliding motility.13 The cell dimensions were 1.4-4.0 μm in length and 0.4-0.6 μm in width. The cells appear mucoid in colonies, and in liquid medium they exist as a mixture of single cells and stable aggregates, up to 200 cells.

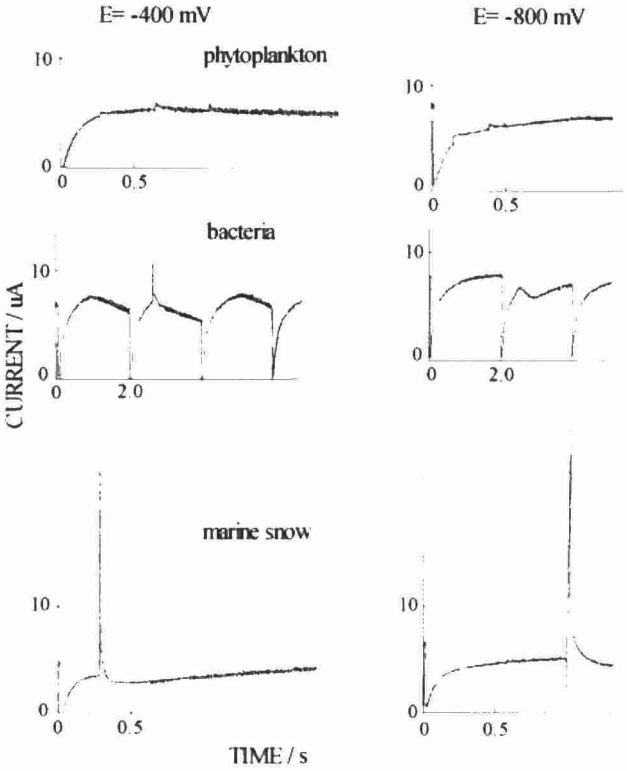

Fig. 1. Current-time curves of oxygen reduction in dispersion of phytoplankton cells, (*I. galbana*, 1.6x10^6/ml), aggregated bacterial cells (S3 strain, 5.4x10^8/ml) and samples of marine snow (N. Adriatic, 08/18/94, 16 m depth) recorded at potentials - 400m mV (positively charged electrode, +3.8 μC/cm^2) and at - 800 mV (negatively charged electrode, -6.5 μC/cm^2).

Surface-active particles (SAP) yield typical attachment signals that can be clearly distinguished from signals of single phytoplankton cells and aggregated bacteria. Signals of individual aggregates in the sample of marine snow recorded at two potentials (Fig. 1) show distinct features corresponding to a fast attachment and spreading (t~100ms). Note that the signal at -800 mV commences with a spike of the opposite sign corresponding to the displacement of the negative surface charge at the electrode/seawater interface by attachment and spreading of the aggregate. The surface charge displacement is direct evidence for the molecular contact between the aggregate and the mercury surface.

The effect of aggregation on the form of electrochemical attachment signals was studied in suspensions of bacteria that appear in different association state: single cells, single cells + clumps, and filaments.

DISTRIBUTION OF HG, CU, ZN, CD AND PB IN SURFACE SEDIMENTS FROM THE COASTAL REGION OF THE CENTRAL ADRIATIC

T. Zvonaric* and N. Odzak

Institute of Oceanography and Fisheries, P.O.Box 500, 21000 Split, Croatia

Abstract

Surveys of Hg, Cu, Zn and Cd concentrations in surface sediment began in 1983 at six main stations along the central Adriatic coast. The results of chemical and statistical analyses for 1983-1995 show that the highest concentrations of almost all the heavy metals examined are found in the naturally enclosed areas with marginal biodegradation abilities (Kastela, Sibenik, Gruz Bays), where some heavy metals have already accumulated in edible organisms (mussels, fish) in concentrations higher than the WHO recommended values for human consumption. Although these bays are still receiving uncontrolled quantities of different pollutants, it is encouraging that owing to the semi-enclosed nature of the bays, pollution by these metals has not yet reached the open sea.

Key-words: metals, pollution, sediments, Adriatic Sea

Introduction

Since the biogeochemical cycles of individual metals could not be studied in detail, the monitoring of sediment became the principal focus based on the assumption that the history and present state of ecosystem pollution could be identified in sediments. Even though the available data give a rather rough estimate, it is sufficient to determine the intensity and the extent of anthropogenic loads in individual areas.

Materials and methods

Sampling and analytical procedures. The sediment samples were collected using a plastic gravity corer. Immediately after sampling, surfacial sediment sample (5 cm top layer) was cut from the core tube and frozen until further treatment. Before analysis the samples were defrosted at room temperature, dried at 60°C and, after cooling to room temperature, ground in a mortar. The granulometric composition of sediment was determined by sieving (> 63 μm) and areometring (Casagrande < 63 μm). The organic matter content was determined as a weight loss after H_2O_2 treatment and heating at 450°C for 6 h.

Chemical analysis. For Cu, Zn, Cd and Pb determination, 0.1-0.2 g of dry sediments were placed in a Teflon vessel and digested with a mixture of hydrofluoric (HF), nitric (HNO_3) and perchloric ($HClO_4$) acid in a microwave oven [1]. The digested samples were cooled and diluted to 25 ml with milli-Q water. The concentrations of Cu, Zn, Cd and Pb were determined by the ET-AAS method using Perkin-Elmer 1100B, equipped with a HGA 700 Graphite furnace. Each sample was analyzed at least in duplicate. The accuracy and precision of the methods were evaluated on the basis of analysis of international standard reference materials (marine sediments SD-N-1/2/TM: SD-M-2/TM-IAEA, Monaco; SRM 1646-NBS) with each batch of samples.

Total mercury values were obtained by digestion of dry sediments with HNO_3 and H_2SO_4, reduction to Hg^0 by $SnCl_2$, and detection by cold vapour atomic absorption or fluorescence spectrophotometry (CV AAS/AFS). The accuracy of the results was also checked by the analyses of SRM IAEA 356, certified for mercury [2].

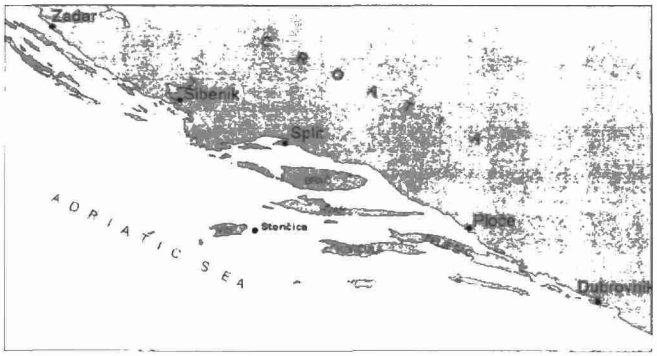

Fig. 1. Study area in the Central Adriatic.

Results and discussion

Granulometric characteristics of surface sediments from the study area, together with average percentage of organic metter, are presented in Table 1. According to the sand-silt-clay ratio [3], surface sediments (0-5 cm) in front of Zadar, Sibenik and Split were clayey silt, off Ploce and Dubrovnik sandy silt, and at the reference station Stoncica silty sand. Organic matter varied in the range from 3,65 to 8,95%. The results of the chemical analyses and statistical interpretation for the survey period (1983-1995) are given graphically and tabulated for each individual metal.

Table 1. Granulometric characteristics of sediment samples and organic matter content.

Stations	Bottom depth (m)	Sediment tipe [3]	Organic matter (%)
ZADAR	34	Clayey silt	6,97
SIBENIK	38	Clayey silt	8,84
SPLIT	34	Clayey silt	6,10
PLOCE	20	Sandy silt	7,38
DUBROVNIK	33	Sandy silt	8,95
STONCICA	103	Silty sand	3,65

Mercury (Hg). Mercury levels in sediment were considerably more than the background concentrations at almost all the stations, with the exception at Ploce and Zadar where the mercury level was slightly higher than at the reference station Stoncica (Fig. 2). Mercury content in sediment showed enhancement (positive regression coefficients b-Table 2) at almost all the stations (except in Split and Ploce). This was particularly pronounced at the stations close to Dubrovnik and Sibenik. Because Kastela Bay is rather enclosed, high mercury concentrations in its sediment (KZ_1, KZ_2) do not significantly affect mercury levels in sediment from Split, where the tendency for a decrease in mercury content was recorded.

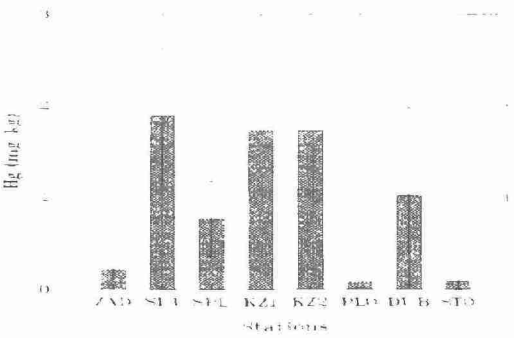

Fig. 2. Average mercury values in sediments from the study area for the study period.

Table 2. Trends of mercury level variation in sediment for the study period. N - number of sampling; b - regression coefficient.

	STATIONS							
Hg	ZADAR (ZAD)	SIBENIK (SIB)	SPLIT (SPL)	KASTELA BAY (KZ1)	(KZ2)	PLOCE (PLO)	DUBROVNIK (DUB)	STONCICA (STO)
N	10	10	10			9	10	6
b	0.013	0.072	-0.067			-0.008	0.132	0.016

Copper (Cu). Copper concentrations in sediment from Sibenik, Split and Dubrovnik stations differed considerably from the level in sediments from the reference station Stoncica (Fig. 3). However, copper level in sediment of Kastela Bay was lower than at the station off Split. It should be pointed out that a tendency for a reduction in copper content (Table 3) was recorded in the sediments of Split, Stoncica and Sibenik during the study period. This tendency was also noted at the central Kastela Bay station (KZ_2).

HIGH SPECIALIZED DETECTORS OF BIOACTIVE MOLECULES FROM MARINE ENVIRONMENT

A. Fontana, M.L. Ciavatta, M. Gavagnin and Guido Cimino *

Istituto per la Chimica di Molecole di Interesse Biologico (ICMIB) del CNR, Via Toiano 6, 80072, Arco Felice (Napoli), Italy

Abstract

The paper concerns the detection of bioactive marine products moving from their natural functions. This study is directed to sessile and slow moving organisms which, being apparently unprotected, use to be chemically armed. In particular, the main attention is focused on Mediterranean molluscs, such as opisthobranchs, which are able to feed specifically on sponges and algae, well known to be protected by chemicals against most of other marine predators. Following the sluggish track left from such invertebrates, chemists have isolated oustanding, chemically different molecules, usually involved in a number of ecological endowments. But is the utility of these compounds confined at such functions or may they be involved in more general processes? In other words, can the ecological role be only the first evidence to move interest in investigating, extensively, further bioactivities? This is the current challenge.

Key-words : porifera, algae, mollusca, natural products

How is it possible to find out bioactive molecules from natural sources? There are a few different strategies. Sometimes, by a random approach, compounds are first isolated and then submitted to a series of aimed tests, sometimes, by guided screening, bioassays are used to select natural products with specific activities. Both strategies demand a huge amount of work and only big, well organized groups have proved able to detect potentially feasible applications for human purposes. Fortunately, there is a third way that directly aims at selecting molecules which play a vital role in the organisms where they are contained. In the ecological approach, the expensive requirement of preliminary tests is replaced by field observations of the marine habitat. In fact, it is surprising how sessile organisms are able to survive in an environment where the competition for existence is extreme. Sponges, soft corals, bryozoans, algae have conquered, in spite of their apparent fragility, a lot of marine space. Analogously, other organisms, moving very slowly, seem to be completely unprotected against aggressive predators. This is the case of opisthobranchs which being molluscs without the mechanical protection of the shell, which is either reduced or completely absent, have elaborated a series of alternative defensive strategies including the use of chemicals (1-4). In this communication we will present several evidences in order to prove the ability of opisthobranchs to detect bioactive molecules from their preferred dietary sources, mainly sponges and algae. In our idea, the ecologically relevant properties of such compounds can be the starting point for further studies which, moving from the comprehension of their natural function and mechanisms of action, aim at finding out more general (pharmacological or technological) applications.

The subclass Opisthobranchia belongs to the class Gastropoda and is split in eight orders: Cephalaspidea, Anaspidea, Saccoglossa, Thecosomata, Gymno-somata, Notaspidea, Acochlidiacea, Nudibranchia (5). With a major reference to our studies, the present report summarizes the main results obtained on species belonging to the orders Sacoglossa and Nudibranchia. From an evolutionary point of view, the order Sacoglossa is highly intriguing for the presence of ancestral species, hardly protected by relic shell, together with evolute animals showing reduced or completely absent shell. On the contrary, all slugs of the order Nudibranchia are totally naked. The survival of the organisms of both orders depends on chemicals able to repel common marine predators. A relevant topic is to establish how the molluscs are able to procure their protective weapons.

Almost all saccoglossans are herbivores with a diet based mainly on green algae. The Mediterranean *Ascobulla fragilis* is an infaunal mollusc possessing a hard shell. The taxonomical collocation of *A. fragilis* between Cephalaspidea and Saccoglossa is matter of debate. Although its external feature shows strong likenesss with cephalaspideans, the mollusc is, analogously with other conchoid sacoglossans, closely associated with the rhizoid of the green alga *Caulerpa prolifera*. In fact, two conchoid molluscs, *Oxynoe olivacaea* and *Lobiger serradifalci*, live on the leaves of the same alga where they are well concealed by their green colour. All three molluscs are chemically protected by the algal metabolite caulerpenyne [**1**], but the defensive strategy of conchoid species appear much more sophisticated than that of *A. fragilis*. In fact, all these molluscs are able to increase the toxicity of 1 by transforming it into the more toxic oxytoxin-1 [**2**] and oxytoxin-2 [**3**] (6, 7). But, besides secreting toxic mucus, *O. olivacea* and *L. serradifalci* are able to autotomize part of their body. In particular, as molested, *Oxynoe* uses to lose the tail, whereas *Lobiger* sacrifices some dorso-lateral appendages, generally called cerata. Moreover, whereas oytoxin-2 is present only in the mucous secretion of the three molluscs, oxytoxin-1 is accumulated by *O. olivacea* and by *L. serradifalci* specifically in the autotomizable parts of their body. All these molluscs are highly specialized detectors of bioactive molecules. The partial structure of **1**, characterized by a dienolacetate, will be found in other algal metabolites sequestered by aconchoid saccoglossans belonging to the superfamily Elysioidea (8): the compound **4** sequestered by *Elysia translucens* from *Udotea petiolata*; the compound **5** by *Bosellia mimetica* from *Halimeda tuna;* the compound **6** by *Thuridilla hopei* from *Derbesia tenuissima. T. hopei* is, also, able to modify **6** to its dihydroderivative **7**. All these molecules exhibit a masked conjugated 1,4-dialdehyde which, probably is responsible of a series of biological properties (cytotoxic, antimicrobial and feeding-deterrent activity (9)). A strong parallelism was found studying a number of other sacoglossans from Caribbean Sea: *Ascobulla ulla, Oxynoe antillarum, Lobiger souverbiei, Elysia subornata, Elysia patina, Elysia tuca, Elysia nisbeti* (10).

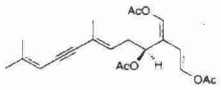

1

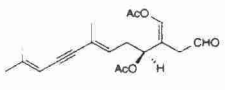

2

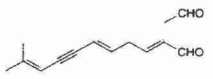

3

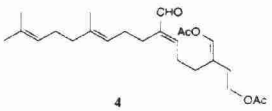

4

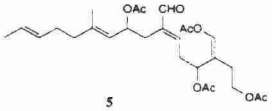

5

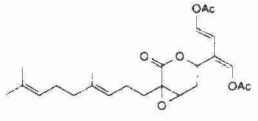

6

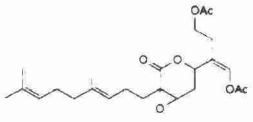

7

On the basis of the above evidence we have identified a first group of highly specialized detectors of bioactive molecules. But, moving to other saccoglossan species we observed (11, 12, 13) that these molluscs, from both Mediterranean and Caribbean Sea, are also able to construct *de novo* bioactive molecules completely absent in their algal diet. Generally, these compounds, some of which are summarized in Table 1, display a polypropionate skeleton containing a α - or γ-pyrone ring. They possess obvious deterrent properties against marine preda-

RECENT MARINE NITROGEN-CONTAINING METABOLITES

Yoel Kashman* and Amira Rudi
School of Chemistry, Tel Aviv University, Ramat Aviv 69978, Israel

Abstract
A large variety of nitrogen-containing marine natural products (M.N.P.s) were isolated from marine organisms, mainly sponges and tunicates. Many of these compounds possess interesting biological activities. A variety of M.N.P.s isolated by the Tel Aviv group from red Sea and Indo-Pacific organions are reported, including examples of the isolations, structure elucidations and details on their bioactivities.

Key-words: Tunicata, porifera, natural products

Nitrogen-containing secondary metabolites which were quite rare when the research of marine natural products (M.N.P.) began in the seventies, are now well known and a spectacular array of novel and unique compounds has been unveiled (1, 2). Many of these compounds possess useful biological or pharmaceutical properties. The most important of these compounds were obtained from sessile marine organisms such as sponges and ascidians and to a lesser extent soft corals, gorgonoins. Until recently, our research of M.N.P. concentrated primarily on Red Sea organisms. In the last few years, Indo-Pacific ocean organisms have been added to our research.

Nitrogen-containing M.N.P. may be divided into three groups : **a** acyclic and non-aromatic cyclic compounds, **b**. linear and cyclic peptides and depsipeptides and **c**. heterocyclic compounds.

This paper details nitrogen-containing M.N.P.s from Red Sea and Indo-Pacific ocean sponges, tunicates and soft corals, isolated and characterized by the Tel Aviv group over the last few years. All isolations of the M.N.P. described below were guided by NMR spectra and bioactivity tests in a variety of different systems. Each separation started with freeze-drying of the organisms followed by selective extractions, solvent partitions and chromotographies on Sephadex LH-20, silicagel and RP-18 columns. The structure elucidation of the purified compounds was achieved mainly by NMR and MS experiments and was assisted in certain cases by chemical transformation and X-ray diffraction analyses.

Examples of acyclic and non-aromatic cyclic N-containing M.N.P.s

Latrunculins (Fig. 1) are macrolides isolated from the Red Sea sponge *Latrunculia magnifica* (3). *In vivo*, they alter cell-shape, disrupt microfilament organization and inhibit the microfilament-mediated processes of fertilization and early development (4, 5). *In vitro*, latrunculin A was recently found to affect the polymerization of pure actin in a manner consistent with the formation of a 1:1 molar complex with G-actin. These *in vitro* effects, as well as previous indications that the latrunculins are more potent than the cytochalasins, suggest differences in the *in vivo* mode of action of the two classes of drugs (5). The latrunculin-induced changes are strikingly different from those induced by cytochalasin D. Latrunculins A and B were isolated from the sponge by a Sephadex LH-20 purification guided by ichthiotoxcity and their structures were determined by MS and various NMR experiments and confirmed (for latrunculin B methyl acetal) by X-ray diffraction analysis (3). Due to the potent interaction of the latrunculins with G-actin, they became a valuable tool in cell biology for the investigation of processes in which actin is involved. Most recently, latrunculin A, for example, was shown to be a very potent inhibitor of immunological phagocytosis by normal and activated macrophages (obtained from mice injected i.p. with LPS), as well as by polymorphonuclear leukocytes (6). This toxin blocks the interiorization of the immune complexes but does not interfere with their binding to the phagocyte (recognition phase); activated macrophages were more susceptible to this inhibition than normal macrophages and polymorphonuclear leukocytes.

A second example of category **a** are the *Erylus* metabolites. Fusetani, in his screening for IL-6 antagonists from Japanese marine invertebrates, has found the extract of the sponge *Erylus placenta* to be very potent (7). Interleukin-6 (IL-6) is a multifunctional cytokine which exhibits its function through binding with its specific receptor. Abnormal production of IL-6 causes development of an autoimmune state such as rheumatoid arthritis or inflammation, whereas it constitutive production results in disease states of HTLV-1 or HIV infections. Therefore, inhibitors of IL-6 may be of potential therapeutical importance. This activity was traced to a complex mixture of related metabolites from which the active erylusamines A-C were isolated (7). From another *Erylus* sp., namely *Erylus* cf. *Lendenfeldi*, collected from Dahlak archipelago, Eritrea, we have isolated three series of compounds (8). The first group, erylusamine TA, is closely related to erylusamines A-C, while the other two, erylusine and erylusidine differ not only in the sugar portion but also in the nitrogens containing long chain (Fig. 1).

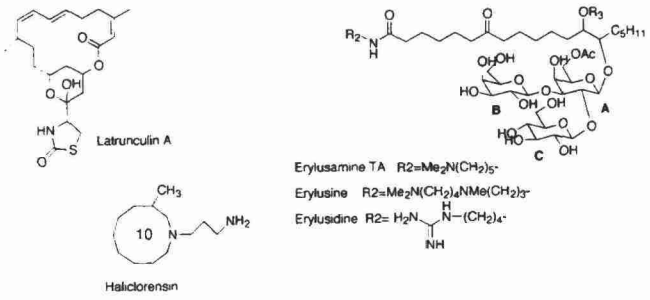

Figure 1.

The final example in this group is haliclorensin. A novel diamino alkaloid, isolated from the sponge Haliclona tulearensis and possessing an azacyclodecane ring (Fig. 1), which has been found to be cytotoxic against P388 mouse leukemia cells (IC_{50} = 0.1 μg/mL) (9). The structure of haliclorensin was established by HREIMS (*m/z* 212, $C_{13}H_{28}N_2$) and 1D and 2D NMR experiments.

Linear and cyclic peptides and depsipeptides

We isolated several linear and cyclic peptides from marine sponges (1, 10). Sponges are targets for extensive studies which seek to isolate new substances. Indeed, a large variety of new compounds have been isolated from this primitive source. Sponges are actually simple cell aggregates which are usually referred to as "the most underdeveloped multicellular animals". Therefore, sponges provide lodging for many macro organisms, bacteria, blue-green algae and dinoflagellates. Occasionally the weight of these guests reaches 50% of the biomass of the sponge. Hence, certain classes of compounds, isolated from sponges, are structurally identical or similar to those of microorganisms from other sources. As a result, similar (or the same) secondary metabolites can be isolated from completely different sponges. On the other hand, it is often impossible to re-isolate the same compounds from different collections of the same sponge (11). Sponge peptides are also suspected to be of microbial origin due to the presence of both D amino acids and other unusual amino acids, in addition to the L amino acids.

The sponge *Hemiasterella minor* (Kirkpatrick) (class, Demospongiae; order, Hadromerida; family, Hemiasterellidae), collected in Sodwana Bay, north of Durban, South Africa, was found to contain a variety of bioactive compounds (11). The major metabolite in four examined specimens was found, on the basis of its spectral data, to be the earlier reported (12) bioactive cyclic depsipeptide jaspamide (jasplkinolide) isolated from *Jaspis* sp. (order, Astrophoride (Choristida)) (0.2%, dry wt). Two of the sponge samples studied contained minute amounts of a second peptide, hemiasterlin and one specimen, a third

NEW ANTITUMOR AGENTS FROM BLUE-GREEN ALGAE: THE SEARCH CONTINUES

Richard E. Moore

Department of Chemistry, University of Hawaii, Honolulu, HI 96822, USA

Abstract

Over 2000 extracts of laboratory-cultured blue-green algae were screened for solid tumor and tumor selective cytotoxicity in the Corbett assay. Of the 0.8 % extracts that were solid tumor selective, the lipophilic extract of Nostoc sp. GSV224 was the most cytotoxic and one of the few extracts that were both solid tumor and tumor selective. Cryptophycin-1 was found to be the most active compound in this alga and in vivo studies indicated that it was active against a broad spectrum of solid tumors implanted in mice, including multiple-drug-resistance tumors. Several analogs of cryptophycin-1 have been prepared by total synthesis and one of them, cryptophycin-52, has been selected for human clinical trials. The search for other potentially useful antitumor agents from other extracts of laboratory-cultured and field-collected blue-green algae is continuing.

Key-words: cancer drugs, natural products, cyanophyta

In the mid 1970's my research group initiated an intensive program to screen extracts of blue-green algae (cyanobacteria) for antitumor activity (1). Over the 20 years that followed we found that 6-10% of the extracts of laboratory-cultured cyanophytes were cytotoxic against human tumor cell lines at <25 μg/mL (2, 3). An even greater percentage of extracts of field-collected cyanophytes showed comparable cytotoxicity (4). By the summer of 1988 we had accumulated a relatively large number of extracts of new blue-green algae and had isolated and identified many structurally-novel cytotoxins and cytotoxic fungicides. We needed a procedure to prioritize these leads for *in vivo* evaluation. In 1998 we began a collaboration with Drs. T. Corbett and F. Valeriote at Wayne State University (WSU) to screen pure cytotoxins and crude extracts for solid tumor and tumor selective cytotoxicity (5, 6).

Description of the Screening Procedure

Toward the goal of obtaining efficacious drugs for solid tumors, which account for most of the cancer deaths in the United States, Corbett *et al.* (7). had developed a rapid and relatively inexpensive disk-diffusion assay to find agents with greater cytotoxicity against solid tumors than leukemias. The assay was modeled after the disk diffusion assay that is commonly used in antifungal and antibacterial screens. The test sample, *e.g.* a crude extract or a pure compound, was applied to a 6 mm paper disk which was then placed on the surface of a soft agar plate containing the solid tumor and leukemia cell lines. Ideally what one wanted to visualize in this assay was the total elimination of the solid tumor cells from the plate, i.e. a zone of inhibition so large that it extended to the plate's periphery, and, concomitant with this, no zone of inhibition for the leukemia cells. For the test sample to be classified as minimally (marginally) solid tumor selective, the zone of inhibition for the solid tumor (Z_{ST}) had to be at least 7.5 mm (250 zone units) larger that the zone of inhibition for the leukemia (Z_L). A zone differential of this size (Z_{ST} - Z_L = ≥250) had been found to be of significance in predicting efficacy in mice. Initially the assay was performed by directly comparing the cytotoxicity of the test sample against the solid tumor and leukemia on the same plate. The morphologically different solid tumor and leukemia cells could be easily distinguished when the plate was examined under a microscope at the end of the assay run. Studies ultimately showed, however, that the same results could be obtained by carrying out the comparison of solid tumor and leukemia cytotoxicity on separate plates. The latter procedure is presently being used.

Each test sample is examined against five different cell types, viz. a murine leukemia (L1210 or P388), a drug-sensitive murine solid tumor (colon adenocarcinoma C38, pancreatic ductal adenocarcinoma P03 or mammary adenocarcinoma M16), a multidrug-resistant (MDR) murine solid tumor (mammary adenocarcinoma M17), a human solid tumor cell line (colon CX-1, HCT8, H116 or lung H125), and a normal cell (fibroblast L-929 or intestinal I18), in the Corbett assay. Based on zone differentials the test substance is categorized into one of five groups: (i) solid tumor selective when Z_{ST} - Z_L = ≥250, (ii) leukemia selective when Z_L - Z_{ST} = ≥250, (iii) tumor selective when Z_{ST} - Z_N or Z_L - Z_N = ≥250 (ZN is the zone of inhibition for a normal cell), (iv) equally active when Z_{ST} - Z_L = <250 and Z_{ST} or Z_L = ≥250, and (v) inactive when Z_{ST} and Z_L = <250.

The test samples that are found to be either solid tumor selective or tumor selective became candidates for *in vivo* trials in mice against appropriate, subcutaneously-implanted solid tumors of murine and human origin. Generally, the test samples are evaluated by intravenous (IV) injection. Highest priority for *in vivo* evaluation is given to test samples that are MDR solid tumor selective.

Leukemia selective or equally cytotoxic test samples are subsequently evaluated in a secondary *in vitro* assay (Valeriote Assay) to compare cytotoxicity against a tumor cell and the stem cell of hematopoietic tissue obtained from murine bone marrow (CFU-GM), a normal cell. Test samples which show a zone differential equal to or greater than 250 units in favor of the tumor cell are termed tumor selective and become candidates for *in vivo* evaluation.

Interestingly most of the antitumor compounds that we had found in the 1975-1985 period through *in vivo* screening tested positively in either the Corbett or Valeriote assays. Tubercidin, tolytoxin and the scytophycins exhibited solid tumor selective cytotoxicity in the Corbett assay, whereas aplysiatoxins, oscillatoxins and lyngbyatoxins displayed tumor selective cytotoxicity in the Valeriote assay. This evidence made us very confident that a relatively large pool of test samples could be effectively pruned and the most important leads would be found using these two assays.

In the five year period from 1989-1993, 82 pure cytotoxins, some of which were potent fungicides, and 2005 extracts were screened for solid tumor and tumor selective cytotoxicity at WSU (1). Ten of the cytotoxins (12%) and 16 of the extracts (0.8%) were identified as solid tumor selective in the Corbett assay. An additional 12 extracts (0.6%) were found to be tumor selective in the Valeriote assay.

Discovery of the Cryptophycins

Unfortunately none of the 10 solid tumor selective cytotoxins displayed significant *in vivo* activity. From one of the solid tumor selective cytotoxic extracts, however, viz. the lipophilic extract of *Nostoc* sp. GSV 224, we discovered a very important class of new antitumor agents, the cryptophycins.

Of the various cyanobacterial extracts examined through 1993, the lipophilic extract of *Nostoc* sp. GSV 224 was by far the most cytotoxic, showing MIC's of 0.24 ng/mL against KB and 6 ng/mL against LoVo. More importantly, the extract exhibited both solid tumor and tumor selective cytotoxicity in the Corbett assay. Bioassay-guided fractionation led to a fraction which was predominantly cryptophycin-1 (**C-1**) (see Chart 1), (8) a cyclic depsipeptide derived from a polyketide-type d-hydroxy acid (Unit A), an a-amino acid (Unit B), a b-amino acid (Unit C), and an a-hydroxy acid (Unit D) (Fig. 1). **C-1**, however, was a known antifungal agent that had been first isolated from *Nostoc* sp. ATCC 53789 by researchers at Merck and found to be very active against strains of *Cryptococcus* (9, 10). [*Cryptococcus neoformans* is an opportunistic fungus that infects immunodeficient patients suffering from AIDS and cancer.] Merck, however, had found **C-1** to be too toxic in animal trials for use as an antifungal agent and had lost interest in pursuing the lead further. In our hands, **C-1** showed potent cytotoxicity against human tumor cell lines at 10-20 pM, equal cytotoxicity against drug-sensitive and multidrug-resistant cell lines, (11) a vinblastine-like inhibitory activity against microtubule assembly, (11) and displayed good activity against a broad spectrum of drug-

THE SEARCH FOR BIOLOGICALLY ACTIVE, PARTICULARLY ANTIMALARIAL, MARINE NATURAL PRODUCTS.

Gabriele M. König and Anthony D. Wright*

Institute for Pharmaceutical Biology, Technical University of Braunschweig, Mendelssohnstrasse 1, D-38106 Braunschweig, Germany

Abstract

In the following paper some aspects of the current status of antimalarial agents with blood schizonticidal activity are given. Strategies employed for the discovery of new sources of antimalarials are outlined and the marine environment is proposed as a still unexploited resource, in terms of novel antimalarial agents or lead structures. A discussion of some of the authors' sponge derived in vitro antimalarial compounds serve as examples in the discussion of approaches suitable for the isolation and identification of active natural products. Some of our newest finds, which include a series of tri- and tetracyclic diterpene formamides, which are new natural products, some dibromopyrroles, and 4α-methyl-5α-cholest-8-en-3β-ol, are also reported.

Key-words : biotechnologies, antibiotics, natural products

Introduction

An estimated 1.5 x 10^9 people live in regions where malaria is endemic, and in excess of 2 million people die from it each year, the majority being under 5 years of age. The disease is caused by protozoan parasites, *Plasmodium* sp., which are transmitted by the female Anopheles mosquito. Of the four species of *Plasmodium* known to infect man (*P. falciparum*, *P. vivax*, *P. malariae*, and *P. ovale*), *P. falciparum*, responsible for the cerebral form of the disease, is by far the most dangerous.

Malaria is currently restricted to mainly economically poor, tropical and sub-tropical regions of the world, where people can ill afford to pay for the high technology facilities needed to do adequate research into these types of health problems. In the last two decades, malaria has regained its status as one of the foremost threats to the health and economic prosperity of the human race. The main reasons for this being, the emergence of drug resistant strains of *Plasmodium* and insecticide resistant mosquitoes, as well as a general apathy on the part of Western Governments, and their associated health-care organisations to acknowledge that malaria represents a real health problem, and to provide adequate funding for research into a disease that does not affect them directly.

It is hoped that in the not too distant future, funding for malaria research will come to reflect the severe threat that this disease represents to us as a world population, more so than is currently the case. If reports concerning global warming are to be believed, the regions of the globe that will become havens for this dreadful disease will increase markedly in the next century. Although there have been a number of serious attempts at the development of antimalarial vaccines, to date they have proven to be unsuccessful, even though a recent report suggests this may not be the case for much longer [1]. It is also clear, that irradication of the transmitting vector is difficult, hence, there will always be a need for new antimalarial agents, particularly those that may have a novel mode of action.

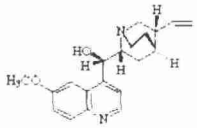

1 Quinine

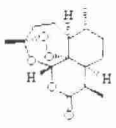

2 Artemisinin

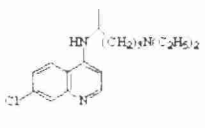

3 Chloroquine

Research into the discovery of new natural sources of potential antimalarial agents has been restricted mainly to terrestrial organisms, which have in the past yielded a number of natural agents effective in the treatment of malaria *e.g.*, quinine (**1** [2]) and artemisinin (qinghaosu) (**2** [3]), and as lead structures for the development of synthetic/semisynthetic antimalarial drugs (**3, 4, 6**). Researchers working with higher plants have been able to make use of local knowledge to aid in the selection of natural materials for pharmacological and chemical investigations, particularly in regions of the world where malaria is endemic and where folk remedies are used as a matter of course in the treatment of malaria. While this approach has worked in the past and is still successfully applied [4, 5], it is clear, however, that new sources of antimalarial agents are desperately needed. One of the still unexploited resources for antimalarial agents being the marine environment.

Life Cycle of the Malaria Parasite

Infected mosquitoes introduce sporozoites of *Plasmodia*, through their "bite", into the blood stream of the human host. Once infective forms of *Plasmodium* have entered the host, they quickly find their way to parenchymal cells of the liver, where they reproduce asexually to form merozoites. After an incubation period of 1-2 weeks the liver cells rupture releasing the merozoites back into the host's blood stream where they attach to and enter erythrocytes. Once in the red cells, the merozoites continue to reproduce asexually, eventually causing these cells to rupture, releasing more merozoites, which invade further erythrocytes. In the phase between being released from erythrocytes and reinvading, some of the merozoites differentiate into sexually reproducing gametocytes which can be ingested by the mosquito vector. The sexual forms reproduce both sexually and asexually to generate more gametocytes and sporozoites, hence completing the life cycle.

Current and Potential Antimalarial Agents (Blood Schizonticides) from Higher Plants

Traditionally, natural products play a major role in the treatment of malaria. In many malaria stricken regions of the world the local inhabitants still rely on remedies based on plant extracts, as they are either too poor or too far from medical facilities to enable them to utilise pharmaceutically proven antimalarial preparations. To use this local knowledge is certainly a very sound starting point for identifying plants and plant preparations which may prove efficacious in malaria treatment [6].

The efficacy of the extract of bark from various species of *Cinchona* trees, the active component of which is mainly quinine (**1**), in the treatment of malaria/intermittent fevers has been known in Peruvian Indian folklore for centuries [2]. The use of quinine was supplanted over the years by synthetic derivatives which had/have improved potency and selectivity *e.g.*, mefloquine (**4**) and chloroquine (**3**). Chloroquine itself has in the last ten years been found to be an inadequate treatment against certain strains of *Plasmodium* which have developed resistance to this drug, and in such cases quinine has been applied with good effect. The natural product quinine is today once again the drug of choice in cases of multi-drug resistant cerebral malaria. Another approach to overcome resistance has been to use other synthetic quinine based drugs *e.g.*, mefloquine (**4**), which, unfortunately, has already proven to be ineffective against some strains of Plasmodium, which have developed mefloquine resistance [7]. Thus, other drugs have been applied that are structurally different to the quinoline based ones, a recent example being halofantrine (**5**). The use of halofantrine is, however, restricted, since it has been shown to have some serious side effects [8]. In reality, no one drug represents an ideal treatment, and so, combinations of two or more drugs are often applied when drug resistance may be considered to be a problem.

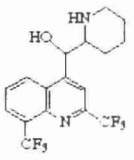

4 Mefloquine

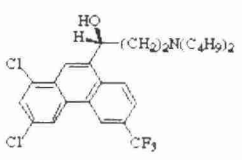

5 Halofantrine

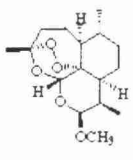

6 Artemether

VARIATIONS DES COMPOSÉS PHÉNOLIQUES CHEZ LA PHANÉROGAME MARINE *POSIDONIA OCEANICA*

Sylvia Agostini [1], Jean-Marie Desjobert [2], Gérard Pergent [1]*

[1] EqEL, Université de Corse, Faculté des Sciences, BP 52, 20250 Corte, France
[2] CEVAREN, Université de Corse, Faculté des Sciences, BP 52, 20250 Corte, France

Résumé

L'analyse des composés phénoliques a été réalisée dans des tissus foliaires de *Posidonia oceanica* par chromatographie liquide à haute performance (HPLC). Les échantillons, prélevés au printemps, correspondent à des stations présentant différentes conditions de milieu: surpâturage par des herbivores, rejets anthropiques, compétition inter- et intra-spécifique. 23 composés phénoliques ont été identifiés et dosés; l'acétosyringone et l'acide férulique présentent les plus fortes concentrations. La teneur en composés phénoliques varie en fonction (i) des tissus pris en compte (les concentrations les plus fortes se trouvent dans les jeunes feuilles) et (ii) des conditions de milieux (facteurs abiotiques et "stress").

Mots clés : Posidonia, physiology

Introduction

La présence de "cellules à tanins", spécialisées dans l'élaboration des composés phénoliques, a été mise en évidence chez de nombreuses phanérogames marines (1). Ces composés phénoliques semblent jouer un rôle au niveau de la protection de ces végétaux vis à vis des compétiteurs, des prédateurs ou des pathogènes (2). Ces observations rejoignent les études effectuées sur plusieurs plantes terrestres qui synthétisent et accumulent des composés phénoliques en réponse à un stress (3). Chez *Posidonia oceanica* (Linnaeus) Delile, phanérogame marine endémique de Méditerranée qui constitue de vastes herbiers, la présence de ces "cellules à tanins" a été vérifiée (4). Leur densité semble augmenter lorsque l'on se rapproche du rejet en mer d'un émissaire (5) ou lorsqu'il existe une forte compétition interspécifique (*e.g. Caulerpa taxifolia* in 6). Afin de vérifier s'il est possible d'utiliser la teneur en composés phénoliques pour évaluer le niveau de stress chez cette phanérogame, une quantification et une identification de ces composés sont réalisées dans les tissus foliaires dans des stations présentant différentes conditions de milieu : surpâturage par des herbivores, rejets anthropiques chimiques et organiques, compétition interspécifique avec l'algue *Caulerpa taxifolia* et compétition intra-spécifique (herbiers denses).

Matériel et méthodes

Cent faisceaux foliaires de *Posidonia oceanica* sont prélevés en scaphandre autonome dans cinq stations de Méditerranée occidentale, en mai 1996, à une profondeur de 10 m : **1- Tonnara** (Corse du Sud): station peu anthropisée où l'herbier présente une densité élevée (484 faisceaux par m^2); **2- Livourne** (Italie): station située à proximité d'un important rejet d'origine industrielle; **3- Nice-Cap Martin** (Alpes Maritimes): station où l'herbier présente une forte compétition vis à vis de l'algue tropicale *Caulerpa taxifolia*; **4- Marseille** (Bouches du Rhône : station caractérisée par une forte pression de broutage par les herbivores *Sarpa salpa* (Linnaeus, 1758) et *Paracentrotus lividus* (Lamarck, 1816); **5- Figari** (Corse du Sud) : station située à proximité d'installations aquacoles à l'origine d'importants rejets de matières organiques (alimentation, excrétion).

Avant d'être lyophilisés, les faisceaux foliaires de *Posidonia oceanica* sont séparés en trois groupes, en fonction de l'âge des feuilles et de la nature du tissu : (i) le limbe des feuilles intermédiaires, (ii) le limbe des feuilles adultes, (iii) le pétiole des feuilles adultes.

Le protocole d'extraction retenu est dérivé de celui appliqué à des végétaux terrestres modifié pour les phanérogames marines par Cuny *et al.* (7). La séparation et l'analyse des composés phénoliques sont réalisées par chromatographie liquide de partage à polarité de phase inversée, avec comme phase mobile utilisée un mélange eau/acide acétique/acétonitrile. La détection des composés phénoliques est réalisée par spectrométrie U.V. sur une longueur d'onde de 275 nm. L'identification de chaque composé phénolique se fait par comparaison de son temps de rétention avec les temps de rétention de produits de référence. Pour chaque extrait, le pourcentage des différents composés phénoliques présents est calculé, par rapport à l'aire des pics identifiés sur le chromatogramme. Le dosage des composés phénoliques est réalisé par étalonnage externe.

Résultats et discussion

Identification et teneurs des différents composés phénoliques

La quantité totale des composés phénoliques identifiés s'élève à plus de 53% des composés présents sur les chromatogrammes (tous tissus et sites confondus). Les 23 produits de référence ont été retrouvés dans nos échantillons (Fig. 1) dont l'acétosyringone (39.3%) et l'acide férulique (22.4%) qui représentent en moyenne plus de 61% de la teneur totale des composés phénoliques dosés.

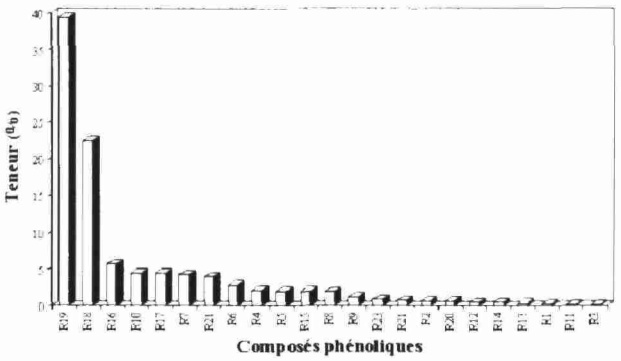

Fig.1 : Teneur moyenne des différents composés phénoliques identifiés par HPLC. **R1**: Phloroglucinol, **R2**: Pyrogallol, **R3**: Acide gallique, **R4**: Acide protocatéchique, **R5**: Pyrocatéchol, **R6**: Protochaldéhyde, **R7**: Acide hydroxy-4 benzoïque, **R8**: Phénol, **R9**: Hydroxy-4 benzaldéhyde, **R10**: Acide vanillique, **R11**: Acide caféique, **R12**: Acide syringique, **R13**: Hydroxy-4 acétophénone, **R14**: Vanilline, **R15**: Acide p coumarique, **R16**: Syringaldéhyde, **R17**: Acétovanillone, **R18**: Acide férulique, **R19**: Acétosyringone, **R20**: Acide benzoïque, **R21**: Acide sinapique, **R22**: Acide p anisique, **R23**: Acide cinnamique.

Sur les 27 composés phénoliques connus chez *Posidonia oceanica* (8, 4, 7) 21 ont été retrouvés et deux composés nouveaux ont été identifiés : le pyrogallol (0.6%) et l'hydroxy-4 acetophénone (1.1%). Le nombre de composés identifiés chez *Posidonia oceanica* est beaucoup plus élevé que pour les autres phanérogames marines de Méditerranée (8, 9, 10). Les études précédentes réalisées sur *Posidonia oceanica* font également apparaître une forte disparité dans la teneur respective des différents composés phénoliques, avec une forte concentration du couple acide férulique/acétosyringone, représentant 59% en moyenne (7). De même, ces auteurs notent une concentration en acide p-anisique forte en hiver (13%) et faible à la fin de l'été (0.3%); nos valeurs (printemps), sont intermédiaires, ce qui semble confirmer le caractère saisonnier de ce composé phénolique.

Plusieurs composés phénoliques ne sont pas présents dans tous les tissus et/ou dans tous les sites étudiés. C'est à Tonnara que le nombre de composés identifiés est le plus élevé (21 composés), et à Figari qu'il est le plus faible (17 composés). De même, c'est dans les limbes des feuilles intermédiaires que le nombre de composés phénoliques est le plus élevé, alors qu'il est minimum dans les limbes des feuilles adultes. Seuls le syringaldéhyde et l'acétovanillone sont présents à la fois dans les cinq sites et dans les trois tissus.

Variation des teneurs en composés phénoliques

La teneur totale en composés phénoliques (Fig. 2) varie de façon significative en fonction du tissu étudié ($p < 0.05$). C'est dans les limbes des feuilles intermédiaires que les teneurs moyennes relevées sont les plus importantes (45.4 ± 6.4 mg.g^{-1}) puis dans les limbes des feuilles adultes (32.0 ± 4.6 mg.g^{-1}) et enfin dans les pétioles de ces feuilles (16.8 ± 0.9 mg.g^{-1}). Cette répartition des composés phénoliques, en fonction des différents tissus de *Posidonia oceanica*, confirme les observations réalisées par Cariello et Zanetti (11) pour l'acide chicorique. La teneur en composés phénoliques varie également de façon significative en fonction du site étudié ($p<0.05$). Trois groupes

UTILISATION DE LA MICROSCOPIE CONFOCALE POUR L'ÉTUDE DES ENDOSYMBIOSES MARINES APPLICATION À L'ÉTUDE DE L'ANÉMONE DE MER MÉDITERRANÉENNE *ANEMONIA VIRIDIS*

Sylvie Bénazet-Tambutté et Denis Allemand*

Observatoire Océanologique Européen, Centre Scientifique de Monaco, MC-98000 Monaco

Résumé

Afin d'étudier les relations qui existent chez les Anthozoaires entre les cellules animales et leurs endosymbiotes intracellulaires photosynthétiques (Dinoflagellés), une méthode originale basée sur le fort pouvoir de discrimination spatiale qu'offre la microscopie confocale a été développée. L'approvisionnement en carbone inorganique nécessaire à la photosynthèse des Dinoflagellés est suivi par des mesures directes du pH intracellulaire. Les mesures de pH sont réalisées à l'aide de la sonde fluorescente carboxy SNARF-AM. Les résultats préliminaires obtenus montrent une hétérogénéité dans la distribution du pH, avec un gradient de pH décroissant du Dinoflagellé vers le cytoplasme animal.

Key-words : Cnidaria , Dinoflagellates, instruments and Techniques, physiology, symbiosis

L'endosymbiose est caractérisée par la présence, à l'intérieur d'un organisme appelé "hôte", d'un autre organisme appelé endosymbiote. Ce type de symbiose revêt une importance écologique et physiologique majeure. L'endosymbiose modifie en effet profondément l'écologie, la physiologie, le développement et le comportement des deux partenaires (1) et représente l'un des moteurs les plus puissants de l'évolution du monde vivant (2). Cependant, les relations symbiotiques et les interactions cellulaires qui existent entre les endosymbiotes phototrophes et leurs hôtes hétérotrophes restent encore énigmatiques sur de nombreux points.

La répartition géographique de l'endosymbiose établie entre les Cnidaires Anthozoaires et leurs zooxanthelles (Dinoflagellés phototrophes du genre *Symbiodinium*) s'étend des eaux tempérées (et donc de la Méditerranée) aux régions tropicales : dans les régions tempérées, l'hôte animal est principalement l'anémone de mer alors qu'en milieu tropical l'endosymbiose est également contractée avec les coraux constructeurs de récifs (3). Les zooxanthelles sont contenues à l'intérieur des cellules endodermiques de l'hôte. Elles sont isolées du cytoplasme par une membrane d'origine animale, la membrane périsymbiotique. Les zooxanthelles permettent aux cellules animales d'être autotrophes par rapport au carbone en leur procurant des produits issus de leur photosynthèse. Pour réaliser leur photosynthèse, les dinoflagellés symbiotiques ont besoin de gaz carbonique (CO_2). Cet approvisionnement pose cependant un double problème. En effet d'une part la source majeure de carbone inorganique en milieu marin est le bicarbonate et non le CO_2 (ce dernier représentant moins de 0,5% du carbone inorganique dissous), d'autre part les Dinoflagellés ne sont pas en contact direct avec l'eau de mer, mais séparés du milieu intérieur de l'animal (coelentéron) par la cellule endodermique dans laquelle le Dinoflagellé vit en symbiose et du milieu extérieur par une couche de cellules ectodermiques, une lame basale de collagène (mésoglée) et par une couche de cellules endodermiques.

Des travaux effectués à l'Observatoire Océanologique Européen (4-9) ont montré que les cellules hôtes animales développent des systèmes originaux d'absorption et de transport transépithéliaux de bicarbonate (de type échangeur Cl^-/HCO_3^- décrit primitivement dans les globules rouges de vertébrés) afin de fournir du CO_2 aux symbiotes photosynthétiques. Ces études ont été réalisées au niveau de l'organisme entier ou de tissus isolés. Afin de caractériser les systèmes de transport au niveau cellulaire, il était nécessaire d'utiliser les techniques de l'imagerie cellulaire. Le transport de carbone inorganique et le pH étant deux paramètres directement liés, nous avons choisi d'étudier les variations de pH intracellulaire comme étant le reflet de modifications (stimulation ou inhibition) du transport de carbone inorganique. La différence importante de volume existant entre l'endosymbiote et le cytoplasme de la cellule hôte (qui ne représente que quelques % en volume de la cellule endodermique) rendait aléatoire toute tentative de mesure du pH avec des isotopes. L'utilisation de sondes fluorescentes permettait en revanche une étude au niveau de cellules isolées. Cependant, les techniques classiques d'imagerie cellulaire ne permettaient pas une discrimination spatiale entre le cytoplasme animal et l'endosymbiote (Fig. 1).

Grâce à sa grande capacité de discrimination spatiale, le microscope confocal nous a permis de différencier la cellule animale endodermique de la cellule algale. Cet outil permet de se positionner précisément sur l'axe z et donc de choisir le plan de coupe à étudier (Fig. 2). De plus, l'effet confocal, c'est-à-dire l'élimination des contributions lumineuses situées hors du focus, permet d'obtenir un pouvoir résolutif important dans le trajet optique axial.

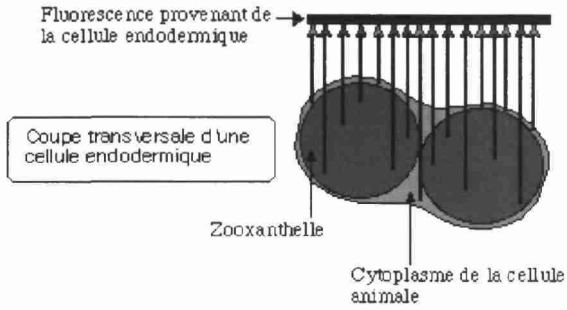

Fig. 1. Imagerie cellulaire classique. Il n'y a pas de discrimination entre la fluorescence émise par la zooxanthelle et par le cytoplasme de la cellule animale.

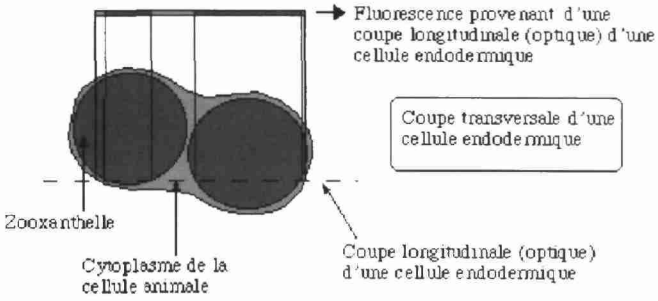

Fig. 2. Microscopie confocale. Il y a discrimination entre la fluorescence émise par la zooxanthelle et par le cytoplasme de la cellule animale.

L'étude est réalisée sur des cellules endodermiques extemporanément isolées de l'anémone de mer. Dix tentacules d'*Anemonia viridis* sont découpés transversalement et longitudinalement, puis sont rincés dans de l'EMC (NaCl 540 mM, KCl 9,5 mM, $NaHCO_3$ 2 mM, EGTA 25 mM, pH 8,2). Les cellules endodermiques sont dissociées de l'ectoderme dans l'EMC par grattage à l'aide d'une pince courbe. Les cellules endodermiques sont reprises dans 10 ml d'EMC et sont filtrées 4 fois dans une seringue équipée d'un filtre de 30 μm de diamètre de maille. Les cellules sont centrifugées à 950 g pendant 2 min à 20°C. Le culot est repris dans 2 ml d'eau de mer filtrée et l'ensemble est homogénéisé à la pipette. De l'agarose (type VII-A, low gelling temperature, Sigma) 1,8% est préparé à 37° dans de l'eau de mer filtrée, la solution est ensuite refroidie à 22°C. 366,5 μl de la préparation cellulaire sont déposés sur la lamelle d'une chambre de culture Lab Tek et sont mélangés à de 233,4 μl d'agarose 1,8% afin d'obtenir un gel final à 0,6%. La polymérisation a lieu à température ambiante sous atmosphère humide pendant 7 min. Le gel est recouvert d'1 ml d'eau de mer filtrée. A partir d'une solution mère de carboxy SNARF1-AM, 12 mM dans de l'eau ultrapure, du carboxy SNARF1-AM 12 μM est préparé dans de l'eau de mer filtrée. Une solution à 4% d'acide pluronique dans de l'eau distillée est chauffée et passée aux ultrasons. La solution de charge comprend 0,04% d'acide pluronique et 12 μM de carboxy SNARF1-AM dans de l'eau de mer. L'eau de mer baignant les cellules dans leur gel est remplacée par la solution de charge. La charge a lieu à l'obscurité pendant 30 min, à température ambiante. Les cellules dans le gel sont rincées dans de l'eau de mer filtrée et reprises

ANTI-XENOBIOTIC DEFENSE MECHANISMS AND ENVIRONMENTAL HEALTH

Bresler V.M.[1*], Fishelson L.[2] and Abelson A[1].

Institute for Nature Conservation Research[1] and Department of Zoology[2], George S. Wise Faculty of Life Sciences, Tel Aviv University

Abstract

This work proposes a new approach and methodology to studying and assessing the effect of pollutants on biota. Animals possess several anti-xenobiotic defense mechanisms, particularly a system of active transport of organic anions (SATOA) and a multixenobiotic resistance transporter (MXRtr), whose activity varies within specimens, populations, and species. These defense mechanisms can reduce pollutant damage to cellular functions, structures and metabolism. Comparative studies of these mechanisms, as well as determination of early signs of genotoxicity (one-strand DNA breaks, aneuploidy, micronuclei formation), and pathology, enable assessment of the health of various animals and can be used for reliable early warning monitoring.

Key-words: pathology, monitoring, ecotoxicology

Under contemporary ecological risk assessment there is a necessity for new and innovative scientific ideas and methods to study the biological and ecological effects of anthropogenic pollutants, from early cryptic primary and secondary responses to overt changes in environmental health and community structure. Conventional methods of ecological assessment of environmental stability and alterations in community structure are, in many cases, similar to post-mortem diagnostics in medicine. However, the use of an early warning monitoring system can reflect the more effective diagnostics of determining cryptic signs of disease, as used in prophylactic medicine. Such medicine uses a selected set of physiological, biochemical and morphological parameters which determine human health. An analogous set of parameters can be selected to determine the health of various animal species. For this purpose, it is crucial to monitor the primary and secondary responses of eukaryotic cells to various pollutants (on selected sites), especially the defensive and adaptive reactions and early pathological alterations in cellular metabolism, functions, genetic activity and cytopathology caused by pollutants. We propose a new approach to this type of monitoring, based on the following (1-5) :

- the selection of a set of reliable parameters which characterize the health of all eukaryotic organisms. Several such possible parameters and study methods are presented in Table 1;
- the selection and development of rapid and precise methods for examination of the selected parameters: specific fluorescent probes, markers, analogues, fluorogenic substrates and vital quantitative fluorescent microscopy, especially contact fluorescent microscopy. These enable the *in vivo* and *in vitro* study of metabolism, specific functions and chemical and structural organization at the molecular and subcellular levels, as well as a study of the pathomorphology of cells and organs (Table 1);
- a comparative study of the morphology, physiology, biochemistry, and ecological functions of various anti-xenobiotic defense mechanisms in individuals, populations and species.

In the present work, we offer examples of the interrelations between the activity of anti-xenobiotic defense mechanisms, especially transport systems for xenobiotic elimination, and early signs of genotoxicity and environmental pathology in selected marine and terrestrial species, such as protists, corals, bivalves, gastropods, fishes and turtles (1-7), collected from different sites along the Israeli coast of the Mediterranean Sea, the Red Sea and from the North Sea shore. The examined organisms revealed a number of general anti-xenobiotic defense mechanisms (Table 2). The studied benthic epiphytic community of protozoans also possesses extraorganismal anti-xenobiotic defense mechanisms such as a common mucous matrix, exoenzymes, and other released organic compounds. Two multisubstrate carrier-mediated transport systems for xenobiotic elimination were detected in the studied organisms: a) a system of active transport of organic anions (SATOA) (1-7) and b) a multi-xenobiotic resistance transporter (MXRtr) (5, 9, 10). SATOA eliminates a wide spectrum of organic anionic xenobiotics. Its fluorescent marker transport substrate is fluorescein, whose transport is competitively inhibited by other organic anions such as *p*-aminohippurate and probenecid. SATOA was described in some protozoa (foraminifera), in the Malpighian tubules of insects, in the "kidney" of molluscs and crustaceans, in gills of molluscs and fishes, and in the renal proximal tubules, liver trabecules and choroid plexus of vertebrates (1-7).

Table 1. Main parameters of environmental health and corresponding microfluorometrical methods for their determination.

PARAMETER	METHOD
Cell and tissue respiration: Metabolic state of mitochondria in living cells and tissues *in situ*	Microfluorometry of inherent blue and green fluorescence of NADH and FAD
DNA, RNA, proteins and lipids content and dynamics	Quantitative fluorescent cytochemistry
Enzyme activity in living cells *in situ* a. non-specific esterases, b. detoxifying enzymes, c. marker enzymes	Fluorogenic substrates, specific inhibitors and microfluorometry. Determination of main enzyme kinetic parameters: K_M, K, and V_{max}
Permeability of plasma membranes, epithelial layers and histohaematic barriers	Fluorescent markers of permeability and microfluorometry
Carrier-mediated transport systems for xenobiotic elimination: System of active transport of organic acids (SATOA) and multixenobiotic resistance (MXR) transporter	Fluorescent substrates, specific inhibitors and microfluorometry. Determination of main transport kinetic parameters: K_M, K, and V_{max}
Xenobiotic-binding proteins	Fluorescent analogs of ligands and microfluorometry
Intra- and extracellular depot for xenobiotic accumulation and storage	Fluorescent analogs of xenobiotics and microfluorometry
State of lysosomes and cell viability	Vital test with acridine orange or neutral red and mictofluorometry
Functional state of nuclear chromatin and cell cycle phases	Staining with acridine orange and microfluorometry at 530 and > 590 nm
Complete pathological and histopathological examination	Section and macroscopic examination. Organo-somatic indexes. Staining of tissue blocks and contact fluorescent and epi-microscopy
Cytogenetic examination	Functional activity of nuclear chromatin, one-stranded DNA break, aneuploidy, apoptosis, micronucleus test, anaphase chromosome aberrations

Table 2. Main general anti-xenobiotic defense mechanisms of eukaryotic organisms.

Mechanism	Functions
External diffusion barriers: membrane lipid bilayer, epithelial layers, additional structures (mucin, chitin, keratin, shells)	Impermeable for watersoluble compounds, decreased permeability for lipidsoluble compounds
Internal (histo-haematic) barriers	Protect brain, gonads and endocrine organs from all xenobiotics
Multisubstrate detoxifying enzymes mediated by cytochrome P450	Detoxify some polycyclic aromatic xenobiotics in all species
Enzymes conjugating xenobiotics	Make xenobiotics less toxic and more useful for transport systems
Peroxidases and nonspecific esterases	Protect from excess of oxygen, iodine and bromine, bind some xenobiotics
Multisubstrate carrier-mediated pumps for xenobiotics' elimination: MXRtr and SATOA	MXRtr eliminate lipophilic xenobiotics, SATOA eliminate watersoluble anionic xenobiotics
Extracellular xenobiotic-binding proteins: mucins, serum albumins etc	Bind xenobiotics and decrease their reactivity or eliminate them
Cellular metal-binding proteins	Bind and eliminate heavy metals
Intracellular compartments: lysosomes	Accumulate, store and eliminate some cationic xenobiotics
Extracellular structures/compartments: concretions, fat tissue etc	Accumulate and store xenobiotics

MXRtr eliminates various lipophilic cationic xenobiotics (Rhodamin B, ethidium bromide and Acridine Orange are its fluorescent marker substrates) and is inhibited by the specific blocker, Verapamil, or by its transport substrates. MXRtr was primarily discovered in drug-resistant cancer cells but has recently been described in some parasitic protozoa, sponges, worms and molluscs (5, 9, 10). Recently, we discovered and studied MXRts in marine foraminifera and ciliates, in the pseudogills and mantle of the gastropods *Patella coerulea* and *Cellana rotha*, in the gills and mantle of various bivalves, as well as in the gills of fish, and in the proximal tubules and liver of fish, amphibia (tadpoles) and turtles. Our observations show that the activity of these transport systems varies among different taxons and also varies among populations from different sites. For example, MXRtr and SATOA in the gills of *Patella coerulea* and its cotaxon *Cellana rotha* from polluted sites along the Mediterranean Sea and Red Sea in both cases showed higher activity than those in populations of the same species from clean sites. Increased activity of the MXR transporter was also detected in the gills and mantle of various bivalve molluscs from the polluted sites along the Mediterranean and Red Sea coasts, as

CYTOCHROME P450 MONOOXYGENASE SYSTEM AND GLUTATHIONE S- TRANSFERASE IN *MYTILUS GALLOPROVINCIALIS* AS BIOCHEMICAL MARKERS FOR POLLUTION MONITORING

J.A. Campillo [1], J. Benedicto [1]* and M. Cánovas [2]

[1] Instituto Español de Oceanografía, 30740 San Pedro del Pinatar, 30001 Murcia, Spain

[2] Dep.de Bioquímica y Biología Molecular B e Inmunología, Facultad de Química, Universisdad de Murcia, 30001 Murcia, Spain

Abstract

Wild mussels were collected from several locations along the Spanish Mediterranean coast with different pollution levels. Soft tissues were analyzed to identify the contents of PAHs, PCBs, HCB, lindane and DDTs. In the context of biological effects monitoring, the cytochrome P450 monooxygenase system components [benzo(a)pyrene hydroxylase (BaPH), NADPH cytochrome c reductase and cytochrome P450 content] and the glutathione S-transferase [GST] activity were determined within the digestive gland, and the biochemical responses related to the pollutant tissue levels. Results showed an increase of the cytochrome P450 content and the NADPH cytochrome c reductase activity related to the PAHs tissue concentration. However no differences were observed for BaPH and GST activities as a result of pollution exposure.

Key-words : pollution, bivalves, physiology

It is now well established that bivalves, particularly mussels, are a very usefull marine pollution indicator organism due to their sedentary habits, wide distribution and their general ability to bioaccumulate and concentrate most pollutants. The cytochrome P450 monooxygenase, or mixed function oxidase system (MFO), has been found in the digestive gland of the mussel *Mytilus edulis*. The existence of four cytochrome P450 gene families (CYP1A, 3A, 4A y 11A) is known [1]. This fact is in accordance to the capacity of the cytochrome P450, partially purified, to metabolize benzo(a)pyrene [2]. Furthermore, the digestive gland is also a particularly rich source of glutathione S-transferase enzymes, because of its role in detoxification process.

In this work we have been assessing the possibility of using MFO system [benzo(a)pyrene hydroxylase (BaPH), NADPH cytochrome c reductase and cytochrome P450 content], as well as the GST activity as biomarkers of pollution in *Mytilus galloprovincialis*.

In 1993 mussels of uniform size (4-5 cm) were sampled at different locations along the Spanish Mediterranean coast, which situation is in Figure 1. A subsample of a hundred mussels was stored at -20°C in order to analyse the nuclear aromatic hydrocarbons (PAHs), polychlorinated biphenyls (PCBs), hexachlorobenzene, lindane and DDTs levels. The PAHs and organochlorines were determined using the Albaiges *et al.* [3] and de Boer [4] methods, respectively.

Fig. 1. Sampling location along the Mediterranean Spanish coast.

Total protein concentration, cytochrome P450 content, and the BaPH, NADPH cytochrome c reductase and GST activities were measured by standard procedures as described below [5, 6, 7, 8, 9].

Results of the chemical analyses in the whole tissue of the samples of *M. galloprovincialis* are presented in Table 1. These analyses show fluctuations in the contents of PAHs, PCBs and the other chemical contaminants studied within different mussel populations.

The values of the components of the MFO system, as well as the GST activities from the digestive glands of the *M. galloprovincialis*, are shown in Table 2. The content of cytochrome P450 was higher in

Table 1. Levels of PAHs (g/g dry wt. of chrysene equivalents), PCBs, lindane, -hexachlorociclohexane (- HCH), hexachlorobenzene (HCB), DDT, DDD y DDE (ng/g dry).

Sampling site	HPAs	PCBs[1]	-HCH	HCB	Lindano	p,p'-DDE	p,p DDD	p,p'-DDT
Alicante	11,7	125,9	0,3	0,45	2,85	49,1	16,5	76,0
Castellón	6,0	62,9	0,9	0,20	0,50	18,8	6,0	15,9
Vallcarca	6,0	258,0	0,8	0,26	0,30	276,6	15,8	20,9
Salou	4,1	83,4	0,6	0,27	1,05	47,4	6,7	2,9
Benidorm	1,8	63,0	0,1	0,30	0,00	7,9	2,3	1,5
Cadaqués	1,7	33,6	0,3	0,25	0,56	15,8	13,1	4,7
Tortosa	1,4	81,8	0,6	0,15	1,30	44,4	25,8	20,9
El Portus	0,3	17,0	0,2	0,00	0,20	6,5	0,5	0,7
Cabo de la Nao	0,3	33,7	0,9	0,7	2,40	18,9	10,2	5,3

[1] *Sum of ten congeners (IUPAC Nos 31, 28, 52, 101, 118, 153, 105, 138, 156 and 180).*

Table 2. Responses of digestive gland microsomal MFO system components and the glutathione S-transferase enzymatic activity in *M. galloprovincialis*.

Sampling sites	Cytochrome P450[1]	NADPH cit. c[2] reductasa	BaPH[3]	GST[4]
Alicante	60,5 ± 1,4	23,0 ± 0,7	9,0 ± 2,5	114,6 ± 18,5
Castellón	61,0 ± 4,5	21,8 ± 2,3	6,6 ± 2,0	89,2 ± 22,1
Vallcarca	58,0 ± 4,2	22,2 ± 3,0	3,0 ± 0,8	120,9 ± 7,7
Salou	64,2 ± 3,5	29,4 ± 1,2	13,1 ± 0,5	124,9 ± 22,6
Benidorm	57,1 ± 2,5	24,0 ± 2,3	14,1 ± 1,2	145,1 ± 9,5
Cadaqués	56,9 ± 1,0	23,2 ± 1,2	27,1 ± 1,9	95,4 ± 7,8
Tortosa	50,9 ± 5,0	18,5 ± 1,0	8,0 ± 1,3	92,0 ± 8,9
El Portus	40,4 ± 3,7	18,6 ± 1,7	28,2 ± 4,4	116,8 ± 16,2
Cabo de la Nao	52,2 ± 3,6	12,3 ± 1,8	8,1 ± 1,0	132,1 ± 3,1

Values are means ± ESM (n = 4). Each sample is a pool of 8 digestive glands.
[1] pmol/mg microsomal protein.
[2] nmol/min.mg microsomal protein.
[3] arbitrary fluorescence units/min.mg microsomall.
[4] nmol/min mg cytosolic protein.

the sampling sites where greater pollution levels of PAHs were detected (Alicante, Castellón, Vallcarca and Salou). Furthermore, the cytochrome P450 content was strongly correlated to the log of the concentration of PAHs within the mussel tissues ($r = 0,78$, $P < 0,05$) (Fig. 2). However, there were no meaningful correlations between the content of cytochrome P450 and the rest of the analyzed pollutants.

On the other hand, the NADPH cytochrome c reductase activity seemed sensitive enough to the increase of PAHs (being the correlated coefficient respect to the logarithm of the PAHs concentrations $r = 0,69$, $P < 0,05$). These activity values were also correlated to the levels of cytochrome P450 ($r = 0,71$, $P < 0,05$).

An increase in the cytochrome P450 level and in the activity of NADPH cytochrome P450 reductase in the digestive gland microsomes of *M. galloprovincialis* occur after experimental exposure to planar molecules such as PAHs, 3-metylcholantrene, benzo(a)pyrene, and the PCB 3,3',4,4'-tetrachlorobiphenyl [10]. These results suggest that the increase of the cytochrome P450 content and the activity of the NADPH cytochrome c reductase detected in the present work, are induced by the exposure to PAHs. This fact is in accordance to the results of others field studies that demonstrate the usefulness of some of the biochemical parameters used in this work as biomarkers of pollution. For example, Porte *et al.* [11] observed in mussels from the Catalonian coast (Spain) an increase in the levels of cytochrome P450,

RAPID DETECTION OF *ESCHERICHIA COLI* IN COASTAL WATERS BY USE OF THE FLUOROGENIC SUBSTRATE 4-METHYLUMBELLIFERYL-β-D-GLUCURONIDE: PRELIMINARY RESULTS

Caruso G.*, Zaccone R., Crisafi E., Monticelli L.
Istituto Sperimentale Talassografico, C.N.R., Messina, Italy

Abstract
The application of an enzymatic assay using the 4-methylumbelliferyl-β-D-glucuronide (MUG) substrate for the spectrofluorometric determination of fecal pollution in marine environments is evaluated. Results of the analysis carried out on a total of 80 samples collected from nearshore areas show the presence of significative correlations between plate (m-FC medium) and microscopical (direct immunofluorescence, IF) counts and the enzymatic methods (r=0.807 and r=0.747 respectively for MUG-FC and MUG-IF). The advantages and the quantitative and qualitative limits to the use of this biochemical assay are discussed.

Key-words: bacteria, pollution, monitoring

Introduction

Pollution of marine coastal waters is mainly caused by the discharge of sewage effluents containing high densities of human pathogens. The need for water quality monitoring is of great importance for public health protection and environmental safeguarding. *Escherichia coli* is the indicator organism universally accepted by the Italian directive (DPR 470/82) which defines the suitability of marine waters for bathing purposes: on the basis of the research and quantitative enumeration of this coliform it is possible to evaluate the degree of fecal contamination of seawaters. The inadequacy of the conventional standard methods based on the membrane filtration technique has already been demonstrated, because of their long analysis and incubation times which prevent the application of immediate remedial measures. The development and optimization of rapid methodologies, such as immunofluorescence, for the detection of *E. coli*, is becoming more and more urgent and it has been the first aim of the studies carried out in our laboratory over the last years (1). Considerable attention has recently been paid to the use of fluorogenic methylumbelliferyl substrates for the specific research of fecal and total coliforms in marine wastewaters, food and drinking waters (2).

We report here the results of a rapid method for the spectrofluorometric detection of *E. coli* in marine waters based on the 4-methylumbelliferyl-β-D-glucuronide (MUG). The analysis has been carried out in the general framework of the C.N.R. Strategical Project "Monitoring of the marine pollution in the South of Italy" aimed at developing new techniques for the assessment of bacteriological contamination levels in nearshore waters surrounding the city of Messina.

Material and methods

The use of the 4-methylumbelliferyl-β-D-glucuronide (MUG) compound in liquid medium was first proposed by Berg and Fiksdal (3) and then by Muller-Niklas and Herndl (4), Fiksdal *et al.* (5). The technique relies on the determination of the β-D-glucuronidase activity present in fecal coliforms, which causes the substrate hydrolysis with release of the fluorescing 4-methylumbelliferone (MU). The increase in fluorescence is measured after incubation of the sample with appropriate aliquots of the substrate.

From August 1996 to March 1997, a total of 80 seawater samples were collected monthly from coastal stations located along the Ionian coast of the Straits of Messina, heavily polluted by urban effluent discharges. In some cases the sampling was carried out during two successive days, in coincidence with opposing tidal patterns (called "montante" and "scendente") in order to evaluate the possible occurrence of variations in water quality in relation to the current regime.

For the biochemical assay, sample volumes ranging from 50 to 500 ml, according to their turbidity, were filtered through a Nuclepore membrane (0.22 μm pore size); the filter was then homogenized in 50 ml of PBS pH 7.2. Aliquots of a 0.5 mM stock solution of the MUG substrate (Sigma) dissolved in MethylCellosolve (Sigma) were added to 10 ml sub-samples in order to obtain final concentrations of 10, 25, 50 and 100 μM. A blank was prepared by boiling each sample. Fluorescence was measured at 0 time and after 3 hours of incubation in a water bath at 37°C in a Hitachi 2000 spectrofluorometer set at 365 nm (excitation) and 440 nm (emission); before measurements, pH was adjusted to >10, by adding NaOH 0.1 M. The fluorescence increase was transformed into mg of MU released based on a calibration curve obtained with MU standard (Sigma) and expressed in terms of Vmax of substrate hydrolysis, per hour and per litre (6).

In addition, the density in fecal coliforms (FC) was evaluated through filtration of 100 ml of sample on a Nuclepore membrane (0.45 μm) incubated on m-FC medium (Difco)+1.2% agar for 24h at 44.5°C. On the same samples the direct immunofluorescence count (IF) was carried out according to the procedure described by Zaccone *et al.* (1).

The three methods were compared through correlations by linear regression and Pearson analyses.

Results

As far as the optimization of the assay is concerned, on the basis of the results obtained from preliminary trials performed with a pure culture of *E. coli* O-26 collection strain, we decided to use a pH of 10 and an incubation temperature of 37°C. In these conditions, MU was highly fluorogenic and the early detection of fluorescence was possible rather than at 44.5°C. In our study, the use of the 25 min procedure proposed by Fiksdal *et al.* (5) was insufficient to appreciate significative differences between the initial and final measurements; therefore, the period of incubation was extended up to 3 hours, the same time as that used for other esoenzyme assays (7).

Samples analyzed were characterized by generally high contamination levels, in the order of at least 10^2 FC/100 ml of water. Bacterial plate counts ranged from $9.1x10^1$ to $2.48x10^6$ CFU/100 ml of water, whereas immunofluorescence counts varied between $5x10^2$ and $4.64x10^5$ cells/100 ml. Enzymatic values detected were quite variable, comprised between 0.0013 and 67.75 μg MU l^{-1} h^{-1}. Both the bacterial numbers and the levels of enzymatic activity increased corresponding to the sites subjected to higher input of urban effluents. With regard to the samplings repeated over two successive days (37 samples in total), the highest concentrations were generally observed during the "montante" current coming from the Ionian basin (data not shown).

A good linear correlation was found between β-glucuronidase and FC (r= 0.807) values and MUG-IF values (r=0.747) by pooling all data obtained, as well as during almost all sampling periods (Table 1 and Fig. 1 a,b).

Table 1. Pearson's correlation coefficients calculated between enzymatic activity (Vmax) and plate (FC) and microscopical (IF) counts.

		Vmax versus:	
	Pair no.	FC	IF
August	4	0.999(**)	0,865
September	8	0.999(**)	0,619
October	9	0.702(*)	0.875(**)
November	11	0.662(*)	0,23
December	12	0.644(**)	0.682(**)
January	12	0.891(**)	0.927(**)
February	12	0.837(**)	0.738(**)
March	12	0.881(**)	0.672(**)
All samplings	80	0.807(**)	0.747(**)

(*) significant value at P<0.05
(**) significant value at P<0.01

Discussion

In previous research carried out in our laboratory, we evaluated the accuracy and selectivity of a solid medium incorporating MUG; however, the long time of incubation required (24 h) did not allow to suggest the use of this method for rapid environmental monitoring (8). The method proposed here allows to overcome time limitation. The

IMPORTANCE OF PHAGOTROPHIC PIGMENTED FLAGELLATES (MIXOTROPHS) IN THE OLIGOTROPHIC EASTERN MEDITERRANEAN, A FIRST APPROACH

Christaki U.[1*], Van Wambeke F. [2], Dolan J.R. [3], Bianchi M. [2], Rassoulzadegan F. [3]

[1] NCMR Aghios Kosmas, 16604 Hellinikon, Greece

[2] Microbiologie Marine, CNRS, UPR 223, Campus de Luminy, Case 907, 13288 Marseille, Cedex 9, France

[3] Station Zoologique, URA 2077 06234 Villefranche-sur-Mer, France

Abstract

The vertical distribution and abundance of mixotrophic nanoplankton (MNAN) was examined in the oligotrophic Cretan Sea (East Mediterranean) in the framework of MAST/MTP-II MATER. Fluorescently labelled bacteria and minicells were used to identify potential algal grazers. Mixotrophic algae biomass was almost as great as the biomass of typical heterotrophs and represented 27 ± 2% of the total nanoplanktonic biomass in the 0-100 m layer. Based on minimal estimates, 12 ± 8% of total number of chlorophyll containing organisms were found to be phagotrophic.

Key-words: Phytoplankton, bacteria, biomass, Eastern Mediterranean

Introduction

The ecological role of natural populations of mixotrophic flagellates (MNAN) is a new research field (1). Photosynthesis is presumably the primary energy source for these flagellates; phagotrophy is used to acquire nutrients in a particulate form when dissolved forms are scarce (2, 3, 4) and/or carbon, if photosynthesis is light limited (5, 6). The few existing data suggest a quite variable abundance and grazing activity of MNAN in aquatic environments (*e.g.* 4, 7, 8, 9). It would appear reasonable to assume that mixotrophy among phytoflagellates would be relatively more important in oligotrophic environments. However, to our knowledge, only one previous study has been conducted in an oligotrophic marine environment, the Sargasso sea (10). The present study was designed to obtain quantitative information on the nanoplanktonic mixotrophic algae (MNAN) in a pelagic oligotrophic ecosystem, the Eastern Mediterrean. For this we conducted *in situ* grazing experiments and quantified the relative contributions of apochlorotic nanoplankton (HNAN) and of chloroplast containing phototrophic (PNAN) and phagotrophic nanoplankton (MNAN) to the total nanoplanktonic flagellate population.

Materials and methods

This study was carried out from 6 to 9 March 1997 in the oligotrophic Cretan Sea (South Eastern Mediterranean), during the first cruise of the MATER programme, on the RV *Aigaio*. During the sampling period the water column was well mixed, with very low nitrate and phosphate concentrations and T 14.2°C. Four stations were sampled (South Aegean MATER stations, MSB 1, 2, 6 and 7, depth 1300-2000 m) water samples were collected in the euphotic zone at 5, 10, 30, 50, 75 and 100 m depths. To distinguish which of the chlorophyll containing nanoflagellates are potentially phagotrophs we added fluorescent food tracer particles: FLB (Fluorescent Labelled Bacteria) or fluorescently labelled minicells. The FLB (length 1.6-2.4 μm, ESD 0.8-1.0 μm), were prepared following the protocol of (11) the fluorescent mini-cells (0.65 μm diameter) were prepared following the protocol of (12). FLB and minicells were sonicated (1 min.) on-board before every experiment to obtain monodispersed prey items. The final concentration of the prey items in the experimental bottles was approximately half of the natural bacterial density. This concentration was high (usual additions do not exceed 5-15% of natural bacteria) and of course changed the total bacterial density in the sample, but when the final minicell or FLB density is less than 10^5 ml^{-1} it is difficult to detect tracer particle uptake by flagellates.

Acid-cleaned 150 ml glass bottles were filled with seawater from each depth in duplicate. Before inoculation with the fluorescent food tracers, bottles were left undisturbed for 1 hour in a thermoregulated water bath (14.2°C). After adding the FLB and minicells, subsamples were immediately withdrawn for T0 counts, and counts of bacteria, cyanobacteria, initial densities of tracer particles, and nanoplanktonic organisms. Samples were preserved with buffered formol (1% final concentration). Subsequent subsamples of 25 ml were removed from bottles after 30 and 60 min. Samples were filtered within the same day on black Nuclepore filters (0.2 μm for picoplankton counts and 0.8 μm for nanoplankton counts), stained with DAPI (13) and stored at -20°C until counting. All populations were enumerated using epifluorescence microscopy, autofluorescence was distinguished under blue (nanoflagellates, labelled bacteria) and green (cyanobacteria) light excitation.

Among the nanoplankton in the size range 2-20 μm we differentiated three functional groups: HNAN (apochlorotic cells, mainly flagellates), PNAN (chloroplast-containing nanoplanktonic protists) and MNAN (mixotrophic nanoflagellates, chloroplast containing nanoplanktonic protists with ability to ingest particles). The organisms were classified in different size categories using an ocular micrometer. Biovolume-carbon conversion factors were 250 fg C μm^{-3} for cyanobacteria (14), 220 fg C μm^{-3} for HNAN and PNAN (15). Bacterial abundance data were converted to biomass using 20 fg C cell^{-1} (16).

Because of the probability that not all MNAN were consuming bacteria at a given time in the samples, as well as the possibility of selection against fluorescent prey and the egestion during fixation we calculated "minimal" and "maximal" abundance of MNAN (Table 1). Minimal numbers were calculated based solely on "confirmed grazers" *i.e.*, cells with ingested food tracers; and maximal abundance were calculated based on the concentration of the mixotrophic morphotype, that is the abundances of cells with the same morphology as the "confirmed grazers". Morphotypes were distinguished by cell shape, the number and insertion of flagella, as well as chloroplast location, shape and number.

Table 1. Mean population abundances (±SD, n = 6 depths) in the 0-100 layer determined from water samples from 4 stations in the Cretan Sea (East Mediteraanean) during March 1997.

Station date	Bacterial abundance	Chroococcoid cyanobacteria	Total phototrophic nanoplankton (PNAN))	Total mixotrophic nanoplankton (MNAN)	Mixotrophic cells containing prey (HNAN	Heterotrophic nanoplankton
	10^5 ml^{-1}	10^5 ml^{-1}	10^3 ml^{-1}	10^3 ml^{-1}	10^3 ml^{-1}	10^3 ml^{-1}
2						
6 march	4.3±0.6	0.21±0.01	0.68±0.14	0.23±0.10	0.09±0.07	0.30±0.04
1						
7 marc	3.6±0.4	0.22±0.01	0.54±0.13	0.25±0.03	0.08±0.04	0.25±0.05
7						
8 march	3.7±0.4	0.19±0.01	0.64±0.15	0.23±0.05	0.05±0.01	0.38±0.2
6						
9 march	5.8±4.2	0.21±0.07	0.70±0.3	0.30±0.16	0.05±0.04	0.43±0.09

Results

The water column 0-100 m was nearly isothermal on the sampling dates (14.2°C). The vertical distribution of pico- and nanoplakton in the 4 profiles studied was almost homogenous in the 0-100 layer, only slightly decreasing under 75 m (Fig. 1). The biomass structure of the microbial community was represented by an "inverted pyramid" characteristic of oligotrophic waters, where bacterial biomass is greater

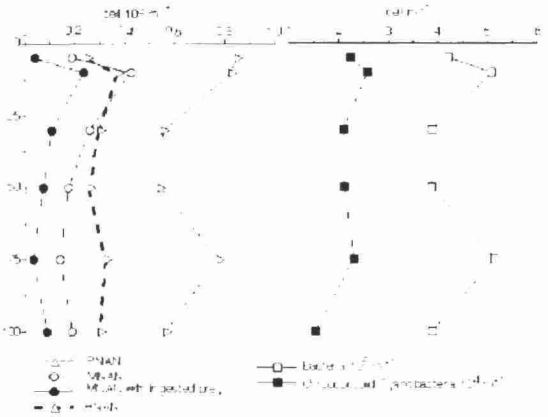

Fig. 1. Vertical distribution of nanoplanktonic organisms on 6 march 1997, station 2. Phototrophic (PNAN total number of cells containing chlorophyll), heterotrophic (HNAN), and Mixotrophic nanoplankton (MNAN). MNAN with ingested prey = confirmed grazers.

SEASONAL DISTRIBUTION OF INDICATOR BACTERIA IN SEAWATER FROM BOSPHORUS

Aysin Çotuk*, Ayten Kimiran
Istanbul University, Science Faculty, Biology Department, 34459, Istanbul, Türkiye

Abstract

In this study, enumeration of fecal coliforms in seawater from Bosphorus was performed since 1991 with two samplings per month. Beside this study, sulphite reducing *Clostridium perfringens*, fecal streptococci and total aerobic bacteria were detected in 1996. The results showed that there is direct relationship in the presence of all indicator bacteria at the same time. Total and fecal coliform numbers in the seawater samples were high (10^3 - 10^4 / 100 ml) as compared to the standard value. It seems that there is seasonal variation in indicator bacteria numbers. Especially, total coliform numbers in seawater were found very high in summer time. The number of total aerobic bacteria was found as 10^5 and 10^4 - 10^6 per ml-1 at 22°C and 37°C incubation temperatures, respectively.

Key-words : bacteria, sewage pollution, Bosphorus

Introduction

Microbiological pollution in seawater is a very common problem on almost all the coast of developing countries. Rumelikavagi region of Bosphorus (Fig. 1) is the main area where is mussels harvesting and heavily used for recreation, fishing during the all seasons. This place is also a coastal area with high average population density. Time to time, sewage is discharged directly or indirectly into the sea at various points along the coast. So, seawater in this area may become gradually contaminated with human pathogenic microorganisms (1, 2, 3, 4).

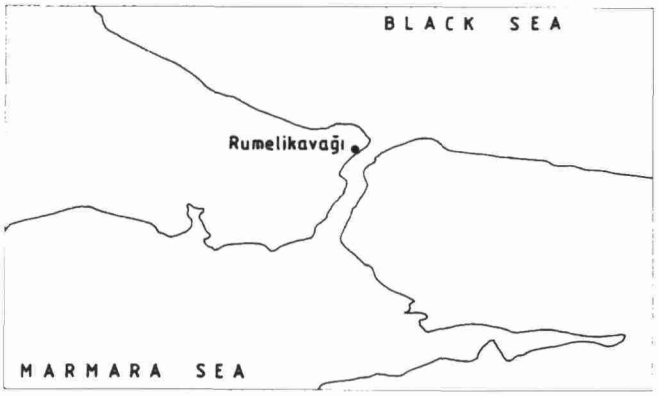

Fig. 1. Location of sampling site in Bosphorus.

Seawater must be examined to ensure that contaminating microorganisms are not present. It is known that there are great difficulties for detection and enumeration of pathogenic microorganism of seawater. For these reasons indicator organism have been used to evaluate water quality and potential health hazards associated with the consumption of contaminated mussels. A few microbiological studies have been carried out in seawater from Bosphorus (1, 5). In these studies, generally fecal coliform, *Escherichia coli* have been determined as indicator bacteria for fecal pollution for water quality surveys.

In this study, seawater samples were analyzed for the presence of total and fecal coliforms, fecal streptococci, sulphite reducing clostridia and total aerobic bacteria count to verify the extention of pollution in Rumelikavagi region of Bosphorus. Another purpose of this study was to find possible relationship among the indicator microorganisms of fecal pollution.

Materials and methods

Seawater samples were collected from Rumelikavagi region of Bosphorus where is the main area for mussel harvesting. Water collection was carried out in monthly samplings in accordance with the standard methods (6). During the samplings, the temperature of the seawater was regularly measured. Seawater samples were taken withing 15 m distance far from the shore and 2 m bottom of sea surface and analysed within 6 h after collection. Total aerobic bacteria were determined in triplicate according to standard procedures using Plate Count Agar (Difco) at 22°C for 72 ± 3 h and 37°C for 48 ± 3 h in aerobic condition (7).

Total coliform, fecal coliform, fecal streptococci and *Clostridium perfringens* numbers were quantified over 1 year period from January 1996 to January 1997 seasonally. Fecal coliform and total coliform concentration was determined by the Membrane Filtration Technique using Membrane Lauryl Sulphate Broth at 44.5°C for 48 ± 3 h and Endo -NKS (Sartorius) at 37°C for fecal coliform and total coliform, respectively (7, 8).

The analysis of fecal streptococci and *Clostridium perfringens* was carried out using Most Probable Number Techniques (7, 9). For quantitative analysis of fecal streptococci, Azide Dextrose Broth and Bile Aesculin Agar were used as isolation media. Differential Reinforced Clostridia Medium and Litmus Milk were used for determination of *Clostridium perfringens*. Seawater samples were heated at 75°C for 10min., so that only the *Clostridium* spores counted (7, 9).

Results and discussion

Seasonal variation of temperature in seawater of Bosphorus in 1991 and 1996 were given in Table 1. As can be seen the temperature of the seawater varies seasonally from 5°C to 22°C.

Results indicated that the mean fecal coliform counts, in spring and summer of 1991 and summer and autumn of 1996 were usually higher (10^3 - 10^4 per 100 ml) than standards established for seawater (Fig. 2).

Table 1. Seasonal variation of seawater temperatures in 1991 and 1996.

Seasons	Temperature °C ± SE 1991	1996
Winter[a]	5 ± 1.5	7.3 ± 2.3
Spring[b]	8.1 ± 2.0	10.3 ± 3.5
Summer[c]	20.1 ± 2.0	22 ± 2.0
Autumn[d]	15.1 ± 2.4	15.6 ± 1.4

a *: December - January - February,* ***b*** *: March - April - May,* ***c*** *: June - July - August,* ***d*** *: September - October - November. Each number is the mean of three values.*

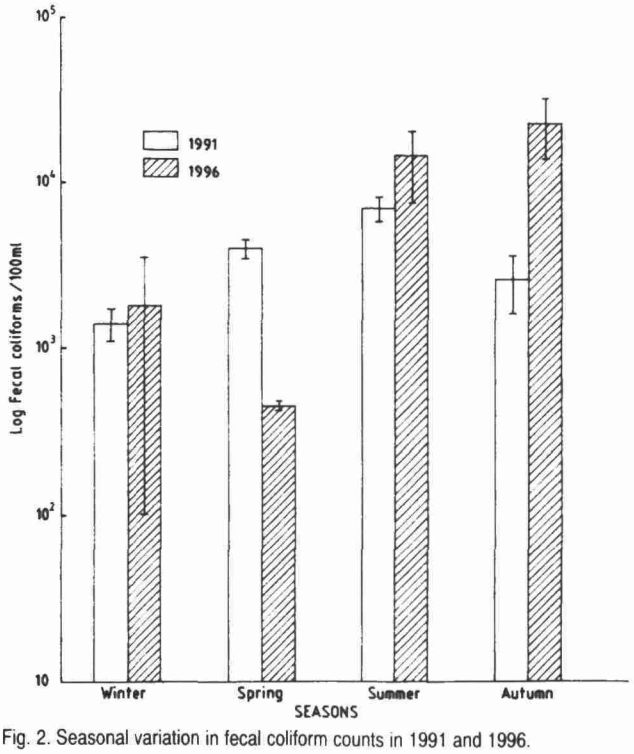

Fig. 2. Seasonal variation in fecal coliform counts in 1991 and 1996.

ISOLATION AND CHARACTERIZATION OF THERMOTOLERANT HYDROCARBON-UTILIZING BACTERIA FROM MARINE, SHALLOW HYDROTHERMAL VENTS

Gugliandolo C., Maugeri T.L.*, Costa F., Caccamo D.

Dipartimento di Biologia Animale ed Ecologia Marina, Università di Messina, Salita Sperone, 31, 98166 S. Agata (Messina), Italy

Abstract

In order to isolate hydrocarbon-utilizing microorganisms water samples were collected from shallow vents offshore the coasts of the Aeolian Islands (Southern Italy) and inoculated onto modified natural sea water (NSW) agar supplemented with emulsified crude oil (Arabian light, 5 gl^{-1}). Temperature and pH values recorded during sample collection and ranged from 30 to 95°C and from 5.2 to 6.4 respectively. Bacterial isolates were characterized by morphological, physiological and biochemical properties. Facultative anaerobic, spore-forming bacteria were identified at genus level as Bacillus spp. Strains able to grow on crude oil as sole source of carbon and energy were lipolytic on Tween 20 and 80 and exopolysaccharide producers.

Key-words: bacteria, thermal vents, petroleum, Tyrrhenian Sea

Introduction

The marine, shallow hydrothermal vents around the Aeolian Islands represent an easier accessible field than the deep-sea oceanic sites to studying unusual environments. Microbiological investigations in these sites have been shown the presence of mesophilic phototrophic, chemotrophic and heterotrophic bacteria [1, 2, 3, 4]. These sites allow the growth of thermophilic and thermotolerant microorganisms. Their enzymes display high activity and thermal stability.

A number of reports on the distribution of marine hydrocarbon-utilizing bacteria from temperate and tropical zones demonstrated the widespread presence of this activity in the marine environment [5, 6, 7, 8]. Moreover, Mills *et al*, (1978) [6] reported that all strains of oil-degrading bacteria were lipolytic, but the converse was not always true.

The hydrophobic nature of the outermost bacterial surface seems to be an important factor in the growth of microorganisms on insoluble substances, such as hydrocarbons, as well as in the adherence of bacteria to non-wettable plastic surface [9]. Many hydrocarbon-degrading microorganisms produce emulsifier, which enhance growth by increasing the available surface area and provide a mechanism for desorption [10].

The aim of this study is to investigate the ability of isolates from marine, shallow hydrothermal vents to degrade crude oil. The selection of strains was based on the presuntive correlation between the lipolytic and hydrocarbon clastic activity. Moreover, the hydrocarbon utilization was related to the exopolysaccharides production.

Materials and Methods

Study sites - The Aeolian Islands represent an arc of vulcanic origin where submarine hot waters and gases flow from sea-floor at various depths. The sites of the sampling stations in correspondence of the hydrothermal vents off the Aeolian Islands are depicted in Figure 1.

Samples collection - During an oceanographic cruise around the Aeolian Islands, venting water samples were collected by SCUBA-divers using sterile samplers. Temperature and pH values were immediately recorded by a multiparameter probe during samples collection.

Isolation of hydrocarbon utilizing bacteria - To isolate hydrocarbon-utilizing bacteria was used a mineral natural sea water (NSW) agarized [8] consisting of ammonium nitrate 1g, dipotassium hydrogen phosphate 0.2 g, ferric citrate 0.02 g, pH 7.8, dissolved in 800 ml sea water and 200 distilled water, agar 30 g, added with crude oil (Arabian light, 5 $g.l^{-1}$). Inoculated plates were incubated at 55°C for three days.

After isolation and purification 51 strains were checked for the following characteristics: growth at different temperatures (37, 55, 60, 65, 70 and 75°C), pH values (5.5, 6, 7, 8, 9) and NaCl contents (0, 2, 3, 5, 7, 10%). All strains were tested for Gram stain, spore-production, cellular morphology, and for the tests contained in the standardized and miniaturized API 20E and API 20NE systems. The strains were characterized at genus level according to the Bergey's Manual.

The lipolytic activity on Tween 20 and 80 was studied on Degryse *et al.* (1978) [11] medium (peptone 0.5%, NaCl 0.5%, $CaCl_2.H_2O$ 0.01%, agar 3%, pH 7). Incubation was carried out at optimal temperature of each isolate for three days.

Lipolytic strains were successively tested for their ability to grow into NSW medium supplemented with gasoline or kerosene at final concentration of 2%. Emulsion at the interface culture-hydrocarbons was visually observed and the bacterial growth was spectrophotometrically monitored. A pre-screening on exopolysaccharides production was based on i) the ability of each isolate to grow in the 162 mineral basal medium [11] with glucose or saccharose at a final concentration of 0.6%; ii) the ability to produce extracellular carbohydrate, demonstrated by staining technique proposed by Allison and Sutherland [12].

Results and discussion

Temperature and pH values recorded during sample collection and ranged from 30 to 95°C and from 5.2 to 6.4 respectively.

All strains were Gram-positive, spore-forming rods, moderately halophilic, facultative anaerobic and were distinct in thermophilic or thermotolerant according to their optimal values of growth. Mostly of the isolates were positive for gelatinase, esculine hydrolase, amilase, nitrato-reductase, oxidase and catalase tests; utilized glucose and saccharose. According to the Bergey's Manual, they were ascribed to the genus Bacillus.

Most (50) of the 51 isolates were lipolytic on Tween 20 and 80 media. Only 12 strains were able to utilize gasoline and kerosene as sole source of carbon and energy.

All of the hydrocarbon-utilizing isolates were positive for the pre-screening of exopolysaccharides production. Since many microbially derived surface-active compounds are known to be involved in the hydrocarbons degradation [13], the exopolysaccharides could mediate the attack to crude oil.

The recovery of thermotolerant hydrocarbon-utilizing microorganisms from shallow hydrothermal vents should allow to develop strategies for marine bioremediation. From an ecological point of view, the thermotolerance may be an useful tool to survive at the environmental variations that the hydrothermal habitat may offer.

References

1- Amend J., Inguaggiato S., Italiano F., Caccamo D., Gugliandolo C, Maugeri T.L., 1997. Microbial biomass and bacterial isolates from shallow hydrothermal vents. XII Int. Symp. on Environmental Biogeochemistry 21-26 September, Monopoli (Italy). Abstract book p. 222.

2- Gugliandolo C., Maugeri T.L., 1993. Chemolithotrophic sulfur-oxidizing bacteria from a marine shallow hydrothermal vent of Vulcano (Italy). *Geomicrobiol. J.*, 11: 109-120.

3- Gugliandolo C., Maugeri T.L., (in press) Temporal variations in heterotrophic mesophilic bacteria from a marine shallow hydrothermal vent off the island of Vulcano (Eolian Islands, Italy), Accepted by *Microbial Ecology*.

4- Maugeri T.L. Acosta Pomar M.L.C., Allegra A., Gugliandolo C., 1990. Microbial population of hydrothermal marine vent. Procs. Thermophily today Viterbo 7-9 may 1990, pp: 26-27.

INITIAL MONOLAYER FORMATION IN MARINE BIOFILMS

S. Kovac*, V. Zutic, V. Svetlicic

Center for Marine and Environmental Research, Ruder Boskovic Institute, PO Box 1016, 10 001 Zagreb, Croatia

Abstract

Studies of biofilm formation are essential for understanding and control of processes in natural aquatic systems and for industrial application. Experiments with expanding mercury electrode/seawater interface offer an approach to studies of initial monolayer in biofilm formation in seawater. Chronoamperometry of dissolved oxygen was used as a measuring technic. Dynamics of film formation is measured as a time which is necessary to reach a full coverage of the electrode by adsorption of dissolved biomolecules and/or adhesion of cells suspended in aqueous electrolyte solution. Phytoplankton organism *D. tertiolecta*, a free-living bacteria strain and hydrophobic *Acinetobacter* sp. were chosen as model organisms. Dextran and albumin were chosen as dissolved biomolecules, and triton T-X-100 as non-ionic detergent. We have demonstrated direct competition of adsorption of dissolved biomolecules and adhesion of cells in the initial monolayer formation at a freshly exposed surface and a high rate of such processes.

Key-words: bacteria, electrochemistry

Introduction

Zobell in 1943 alerted us to the importance of the attached microbial community in the sea, but until now it is not clear completely how cells sense surfaces nor the relative importance of biochemistry and physico-chemical interaction behind the mechanism of adhesion.

A biofilm consists of cells immobilized at a substratum and frequently embedded in an organic polymer matrix of microbial origin (1, 2). In marine environment marine biofilms cause loss of performance on ships, increase fuel consumption, and corrosion on a ship surface. It has been accepted generally that the first step in the formation of a biofilm on a clean surface is the adsorption of an organic layer onto the surface from the aqueous milieu (2). Adsorbed organic films affect adsorption of other dissolved compounds as well as microbial colonization and subsequent growth on surfaces (3). In mixed population (bacteria and diatoms) each organism had a chance to attached sequentially. In nature, both population, in theory, would have the opportunity to attach simultaneously (2).

Mixtures of dissolved molecules and suspended microbial cells are typical for natural aquatic environment such as seawater. The interaction between the various components in biofilm systems occurs via transport and interfacial transfer processes. For dissolved components it occurs via molecular diffusion and volumetric displacement (including cell motility) for particulate components (3). From applied and fundamental points of view, the transport step is important since insufficient transport can be the limiting factor in biofilm formation (4).

Methods and material

Adsorption of dissolved organic molecules and adhesion of phytoplankton cells at the mercury electrode/seawater interface, which we use as a model, results in coverage of the electrode with organic material that displaces counter ions and water molecules from the interface (Fig. 1). Chronoamperometry of dissolved oxygen at renewable mercury electrode (5, 6) is used as a measuring technique. The experiments were performed under conditions of maximum attraction at positively charged and hydrophobic interface, and enhanced transport to the interface by convective streaming.

Fig. 1. Schematic presentation of interaction of a cell and a biomolecule with positively charged mercury electrode in aqueous solution and the current-time transient (attachment signal).

Phytoplankton organism *Dunaliella tertiolecta* (8-10 μm) has been chosen as model organism because it forms stable suspensions, has fluid cell wall and adhesion of individual cells to the electrode results in well defined electrical attachment signals. Their duration is 0.06-0.2 s, and amplitudes 0.6-2.2 μA (Fig. 2.). Biomolecules dextran and albumin, and nonionic detergent Triton-X-100 were chosen as soluble molecules in concentration range 0.05-500 mg/l. Measurements were performed in seawater and in 0.1 M NaCl.

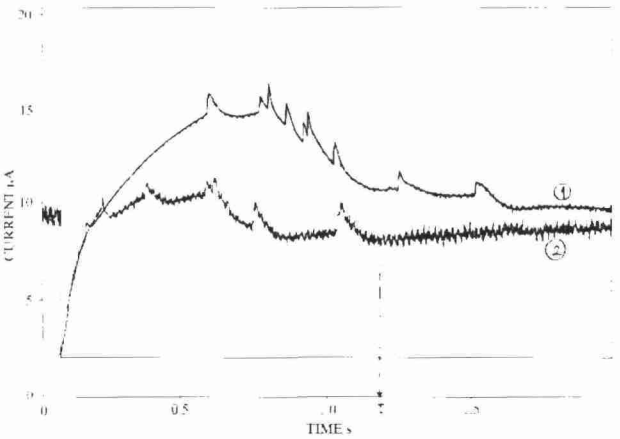

Fig. 2. Current-time curves of oxygen reduction in suspension of *D. tertiolecta* ($5x10^7$/l) alone (curve 1) and in mixture with 15 mg/l dextran sulphate M = 500.000 (curve 2) in 0.1 M NaCl at -400 mV. The spikes are attachment signals of individual cells.

Results and discussion

Dynamics of film formation is measured as a film formation time (τ) (Fig. 2.) which is necessary to reach a full monolayer coverage of the expanding mercury electrode in the time scale 10-2000 ms. Figure 3 shows dependence of film formation in presence of dissolved molecules (dextran sulphate M = 500.000), and in mixture with *D. tertiolecta* cells. Adsorption of dissolved dextran molecules causes a decrease of the current of streaming maximum of oxygen reduction, of attachment signals frequency of cells (Fig. 2.), and a film formation time (τ) (Fig. 3.).

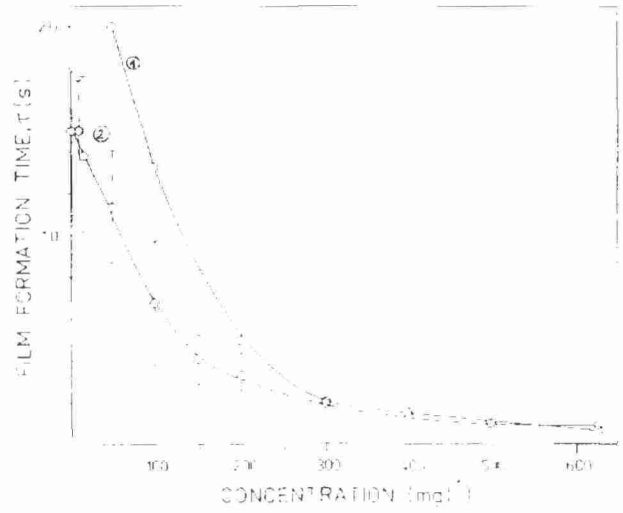

Fig. 3. Dependence of film formation time (τ) on concentration of dextran sulphate M = 500.000 alone (curve 1) and in a mixture with *D. tertiolecta* $5x10^7$/l (curve 2).

REGULATION OF BACTERIAL ABUNDANCE ALONG THE TROPHIC GRADIENT IN THE CENTRAL ADRIATIC

N. Krstulovic*, M. Solic and I. Marasovic
Institute of Oceanography and Fisheries, P.O.Box 500, Split, Croatia

Abstract

Bacterial and heterotrophic nanoflagellates (HNF) abundance, as well as bacterial production and chlorophyll *a* levels, were measured at five sites extending from the coastal zone toward the open Adriatic in the period from March to October 1995. The investigated areas were grouped into trophic categories according to concentrations of chlorophyll *a*. All investigated parameters increased along the trophic gradient, leading to eutrophy, but they did not increase at the same rate. Different increasing rates of individual parameters caused decreasing B/chl *a* and increasing B/HNF ratios with increasing trophy which might reflect the different structures of microbial food web. In the oligotrophic system bacterial abundance was more closely related to bacterial production and chl *a* than in the eutrophic system, suggesting stronger control of bacterial abundance by substrate supply. On the other hand, the coupling between bacteria and HNF and uncoupling between bacterial abundance and production in the eutrophic system, showed that the importance of bacteriovory increased in richer system.

Key-words: bacteria, biomass, Adriatic Sea

Introduction

Many authors have shown that bacterial abundance changes with trophic state in freshwater and marine systems (1, 2, 3). Within these systems, the trophic relationships are undoubtedly very complex and characterized by numerous feedbacks. There is a considerable empirical evidence of resource control of bacteria (bottom-up control) and of grazing control of bacteria (top-down control) (4). Large scale comparative studies demonstrate strong correlations between bacterial abundance and bacterial productivity and between bacteria and chlorophyll, suggesting significant resource regulation of bacteria (1, 5, 6). On the other hand, comparisons of the abundances of heterotrofic nanoflagellates (HNF) and bacteria imply that in some cases predatory control (top-down regulation) of bacteria may be of major importance in eutrophic environments (7, 8).

One way to determine whether regulation of the bacteria is by top-down or bottom-up control is to consider how bacterial abundance and growth rates change along a resource gradient. For this purpose, we evaluated the regulation of bacterial abundance by comparing the relationship between bacterial abundance and production, between bacteria and chl *a* and between bacteria and HNF along a range of trophic gradient in the Adriatic sea.

Material and methods

Samples for bacterial and HNF counts, chl *a*, and bacterial production were collected on monthly basis from March to October 1995 at a 5 stations (A - E) located from coastal zone toward the open Adriatic. Samples for counting were poured into sterile, acid washed, glass bottles, fixed with formalin (final conc. 2%), and processed in the laboratory within two days after collecting.

Chlorophyll *a* content was measured on a Turner 112 fluorometer after acetone extraction (9).

Enumeration of bacteria and heterotrophic nanoflagellates (HNF) were made by epifluorescence microscopy using the standard acridine orange direct counting technique (10) for bacteria, and proflavine staining technique, which enable distinguishing of heterotrophic from autotrophic cells, for HNF (11). For biovolume estimates, length and width of bacterial and HNF cells were measured with an eyepiece graticule (New Porton G12; Graticules, Ltd, UK). Biovolume was converted to carbon biomass assuming 0.220 pg C μm^3 for bacteria (12) and HNF (13).

Bacterial cell production was measured with the ^{3}H-thymidine incorporation technique (14). (Methyl- ^{3}H) thymidine was added in 10 ml samples at a final concentrations of 10 nM (specific activity 86 Ci $mmol^{-1}$; Amersham Ltd, UK). Triplicate samples and a formalin killed adsorption control (final conc. 0.5%) were incubated at *in situ* temperature in the dark for 1 h. The incubations were stopped with formalin (final conc. 0.5%). To each 10 ml sample and control an equal volume of ice-cold 10% (wt/vol) TCA was added and mixtures were kept on ice for 15 min. The TCA-insoluble fraction was collected by filtering the sample through a 25 mm 0.2 μm pore size cellulose nitrate filter. The filters were rinsed five times with 1 ml of ice-cold 5% (wt/vol) TCA. The filters were dried, placed in scintillation vials, dissolved in 10 ml Filter-count™ (Packard scintillation cocktail) and counted after 24 h storage in a scintillation counter (Packard Tricarb 2500 TR).

Results and discussion

The investigated areas were grouped into trophic categories according to concentrations of chl *a* and were arranged by increasing chl *a* concentrations (Fig. 1).

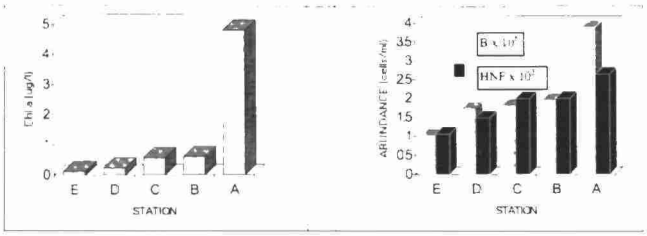

Fig. 1. Average concentrations of chl *a* and abundance of bacteria (B) and HNF at the investigated sites.

Chl *a* concentrations in the oligotrophic area (E site) ranged from 0.04 to 0.57 mg m^{-3} with a mean value of 0.126 ± 0.015 mg m^{-3} (SE), in the eutrophic area (A site) from 0.16 to 18.36 mg m-3 with a mean value of 4.8 ± 1.14 mg m^{-3}. Ratio of the average chl *a* concentrations in the oligotrophic system to that in eutrophic area was 1 : 34. In the mesotrophic area (B, C, D sites) chl *a* concentrations averaged 0.239 ± 0.04 mg m^{-3}, 0.572 ± 0.071 mg m^{-3} and 0.613 ± 0.51 mg m^{-3} at sites B, C and D respectively (Fig. 1).

Abundances of bacteria and HNF showed similar patterns along the trophic gradient as shown by chl *a* concentrations (Fig. 1), but the ratios of bacterial and HNF abundance in the oligotrophic system to those in the eutrophic systems was considerably lower than of chl *a*. Thus, a 34-fold increase in the chl *a* level was accompanied by only 4-fold increase in bacterial abundance and 2.5-fold increase in HNF abundance.

The coefficient of determination, which measure the degree of association between bacteria and phytoplankton (chl *a*) along a trophic gradient was $R^2 = 0.36$ ($p < 0.001$; $n = 35$). That is, 36% of the variability in bacterial abundance can be explained by concentration of chl *a*. However, in the oligotrophic system bacterial abundance was much more closely related to phytoplankton ($R^2 = 0.94$; $p < = 0.001$; n=7), than in the eutrophic system where R^2 was not statistically significant.

BB/chl *a* ratio also changed with trophic status. The ratio was extremely high in the oligotrophic system (10.5 ± 0.94) and decreased gradually toward the eutrophic site where BB/chl *a* ratio was only 0.8 ± 0.21 (Fig. 2). A striking result from this study is that in oligotrophic waters bacterial biomass exceeded phytoplankton biomass. We do not know what mechanisms are responsible for maintaining bacterial abundance at relatively high levels even in highly oligotrophic waters. This may be due to changes in the way algae and bacteria compete for nutrients in waters of differing trophic status. Curie (6) proposed that in very oligotrophic systems both bacterial and algal growth is P limited. Because bacteria are better competitors when orthophosphate is very scarce, bacteria obtain a larger share of the P, and increase in abundance relatively more rapidly than do algae. In richer systems, bacterial growth becomes simultaneously P and C limited. Algae then obtain greater portions of P, and algal abundance begins to increase

BACTERIAL COMMUNITIES FROM MARINE, SHALLOW HYDROTHERMAL VENTS OFF THE EOLIAN ISLANDS (ITALY)

Maugeri T.L.*, Gugliandolo C., Caccamo D.

Dipartimento di Biologia Animale ed Ecologia Marina, Università di Messina, Salita Sperone, 31, 98166 S. Agata (Messina) Italy

Abstract.

The marine shallow hydrothermal vents represents a more accessible field of study than the deep-sea oceanic sites. Bacterial communities living in the marine, shallow hydrothermal vents off the Eolian Islands have been studied in water and sediment samples. The microbial abundances in water samples from shallow vents, estimated by epifluorescence microscopy were in the order of 10^4- 10^6 cells·ml^{-1} similar to the lowest values observed at the Galapagos Rift. Microbial abundances in the sediment samples ranged from 10^6 to 10^8 cells·g^{-1}. The densities in phototrophic picoplankton, or picophytoplankton, ranged from 10^2 to 10^4 cells·ml^{-1} and were higher than temperate marine zones. Chemolithotrophic sulphur-oxidising bacteria varied in the order of 10^2 and 10^4 MPN·ml^{-1} and were more abundant in the sediment samples where they reached values of 10^7 MPN·g^{-1}.

Key-words: thermal vents, bacteria, Tyrrhenian sea

Introduction

Chemosynthetic production by marine bacteria is now known to support diverse thriving and unusual communities of living organisms in location such as deep-sea hydrothermal vents that were not to be expected a decade ago. With the discovery of deep-sea hydrothermal vents, numerous scientists attempt to isolate typical obligate chemolithotrophic sulphur bacteria. Aerobic chemosynthesis seems to be responsible for the bulk of productivity at deep-sea hydrothermal vents. In these sites, other than aerobic chemosynthesis anaerobic chemosynthesis, by sulphur- and sulphate-reducing as well as methanogenic bacteria, has also been reported. In addition, the presence of all types of bacterial metabolism has been demonstrated (1, 2).

The approach to shallow, marine hydrothermal vents is generally more complex because the presence of the sun-light represents the usual energy source for the phototrophic planktonic organisms. The marine shallow hydrothermal area off the Eolian Islands (Italy) represents a more accessible field of study regarding extreme environments than the deep-sea oceanic sites.

Since 1983, species belonging to the Archea dominion, both thermophilic, *Staphylothermus marinus* (3), *Archeoglobus fulgidus* (4), *Thermotoga* (Prieur, personal communication) and *ultrathermophilic Pyrodictium* (5) and *Pyrococcus furiosus* (6) have been isolated from the coastal area of Vulcano Island. Furthermore, a new species of *Thiobacillus, Th. prosperus*, has been recognised (7).

Materials and Methods

Bacterial communities living in the marine, shallow hydrothermal vents off the Eolian Islands have been studied in water and sediment samples collected from different sites by SCUBA-divers and temperatures were recorded immediately by a multiparameter probe during sample collection.

The microbial abundances from water and sediment samples were estimated by epifluorescence microscopy (8). The concentration of ATP (9) was used as an indirect measure of living microbial biomass in water samples. The densities in phototrophic picoplankton, or picophytoplankton were evaluated according to Gugliandolo and Acosta Pomar (10). The estimation of the chemolithotrophic sulphur-oxidising bacteria, able to grow on thiosulphate as the only energy source, was made in the S6A medium (11).

Thiosulphate-oxidizing strains were tested for morphological, cultural and biochemical characteristics. The viable counts in heterotrophic, mesophilic bacteria were evaluated onto Marine Agar 2216 (Difco) plates incubated at room temperature for 7 days. Heterotrophic isolates were tested for the biochemical characteristics of the API 20NE system. Heterotrophic, thermophilic bacterial numbers were evaluated in Marine Broth incubated at 60 and 75°C for 3-5 days.

Results and Discussion

A briefly description of the sampling sites is given in Table 1.

The microbial abundances in water samples from shallow vents, were in the order of 10^4- 10^6 cells·ml^{-1} similar to the lowest values observed at the Galapagos Rift (12, 13). The concentration of ATP was found to be two to four times higher than in the surface waters of the same region. Microbial abundances in the sediment samples ranged from 10^6 to 10^8 cells·g^{-1} (wet weight).

The densities in picophytoplankton, ranged from 10^2 to 10^4 cells·ml^{-1} and were higher than temperate marine zones. Yellow-orange autofluorescent prokaryotic organisms, ascribable to cyanobacteria, were more abundant than the red autofluorescent ones.

Table 1. Sampling sites at the Eolian Islands.

Station	Sample	Origin	Site	Temperature (T°C)	Depth (m)	pH
A	A1	Water	Vulcano - P.to Levante	25	0.3	5.3
	A2	Water	Vulcano - P.to Levante	25	0.3	5.2
	A3	Water	Vulcano - P.to Levante	25	0	5.2
S	S1	Sediment	Vulcano - P.to Levante	93	0	
	S2	Sediment	Vulcano - P.to Levante	75	0	
	S3	Sediment	Vulcano - P.to Levante	85	0	
B	B1	Water	Vulcano - P.to Levante	24	6	6.4
	B2	Water	Vulcano - P.to Levante	43	6	6.4
	B3	Water	Vulcano - P.to Levante	65	0.7	5.2
T	T1	Sediment	Vulcano - P.to Levante	24	6	
	T2	Sediment	Vulcano - P.to Levante	43	6	
	T3	Sediment	Vulcano - P.to Levante	65	0.7	
U1a	U1a	Water	Vulcano - P.to Levante	48	6.3	5.6
	U1aS	Sediment	Vulcano - P.to Levante	48	6.3	
U1b	U1b	Water	Vulcano - P.to Levante	44	5	6.76
U3	U3	Water	Vulcano - La Roya	49	3	6.03
	U3S	Sediment	Vulcano - La Roya	49	3	
U4	U4	Water	Vulcano - P.ta Conigliara	45	15	6.09
	U4S	Sediment	Vulcano - P.ta Conigliara	45	15	
U5	U5	Water	Lipari - Inzolfata	30	3.1	5.86
	U5S	Sediment	Lipari - Inzolfata	30	3.1	
U6	U6	Water	Panarea - Campo 7	54	18	5.36
U7	U7	Water	Panarea - La Calcara	95	19.8	5.1
	U7S	Sediment	Panarea - La Calcara	95	19.8	

The counts obtained for chemolithotrophic sulphur-oxidising bacteria varied in the order of 10^2 and 10^4 MPN·ml^{-1} and were more abundant in the sediment samples where they reached values of 10^7 MPN·g^{-1}. Numerical analysis based on 42 characteristics of the 25 sulphur-oxidising bacteria isolated from water and sediment samples off the Island of Vulcano produced three separate ecotypes of the:

i) obligate chemolithotrophs, assigned to a *Thiobacillus*-like organisms, present only in venting water samples;

ii) facultative chemolithotrophic bacteria, assigned to *Thiobacterium*-like bacteria, recorded in both water and sediment samples;

iii) heterotrophic sulphur oxidisers, assigned to *Pseudomonas*-like bacteria, present in sediment (11).

Filamentous forms that cover the substratum around the vents were recorded from the deepest hot sources (20 m depth) off the Island of Panarea. Microscopic examination of the whitish mat revealed *Thiothrix*-like bacteria containing sulphur inclusions as the dominant filamentous form in this microbial community (Fig. 1).

Viable counts in heterotrophic, mesophilic bacteria, ranged from 10^2 and 10^4 CFU·ml^{-1} from water and 10^3 to 10^5 CFU·g^{-1} from sediment samples. Almost all strains isolated were able to hydrolyse gelatine; the fermentative strains appeared to be very few, moreover the occurrence of nitrate to nitrite reducing bacteria does not exclude the possibility of a facultative anaerobic metabolism. Heterotrophic, thermophilic bacterial numbers were higher in the sediment than in the water samples. Strains of thermophilic bacterium *Thermus aquaticus*,

EVALUATION DE LA QUALITÉ MICROBIOLOGIQUE DE L'EAU DE MER DE LA PLAGE OUEST DE SIDI-FREDJ (ALGÉRIE)

H. Merabtine*, A. Merzoug, B. Bouali, C. Boukahel, S. Bouhank, N. Refes, H. Chaab

Institut des sciences de la mer et de l'aménagement du littoral, BP 54, plage Ouest Sidi-Fredj, W. Tipaza, Algérie

Résumé

Un programme de surveillance de la qualité microbiologique de l'eau de mer de la plage Ouest de Sidi-Fredj (Algérie) a été entrepris de juin 1992 à juin 1995. Les concentrations obtenus en germes fécaux ont été traitées par la méthode de distribution des probabilités lognormale. L'analyse de variances montre une différence entre les quatre années de suivi; le plus grand écart est noté pour l'année 1992. Comparativement aux normes algériennes et celles de l'OMS/PNUE (1983) relatives aux eaux récréatives, la plage Ouest est considérée comme acceptable pour la baignade avec des variations temporaires de sa qualité microbiologique (1<écart type<3).

Mots clés: sewage pollution, Algerian basin

Introduction

La qualité des eaux littorales algériennes est probablement un des concepts les plus ardus à définir, car l'idée même qu'on s'en fait est pour le moins subjective. Toutefois, les aspects de salubrité de l'eau de mer ont pris une importance croissante, traduite en Algérie par une législation réglementant les conditions sanitaires des eaux à caractère récréatif (1). Une surveillance de la qualité microbiologique de l'eau de mer de la plage Ouest de Sidi-Fredj, a été entreprise de juin 1992 à juin 1995. Ce site récréatif (Fig. 1), situé à 24 km à l'Ouest d'Alger, est l'une des stations balnéaires les plus fréquentées de la région.

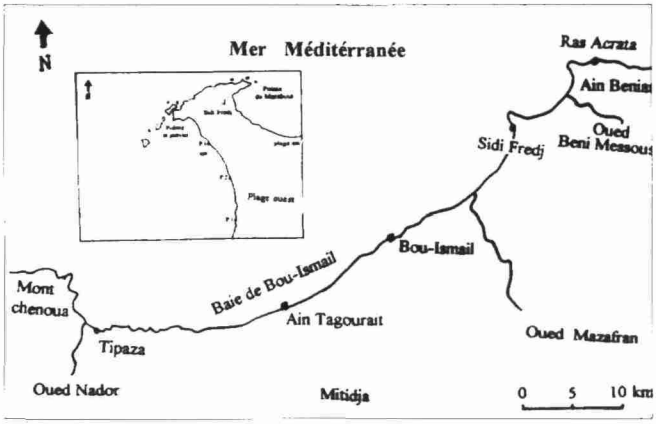

Fig. 1. Situation géographique de la plage Ouest de Sidi-Fred.j

L'évaluation de la contamination fécale est basée sur le dénombrement des coliformes totaux, coliformes fécaux et streptocoques fécaux, ainsi que la mesure des trois paramètres physico-chimiques (température, salinité et potentiel hydrogène).

Matériel et méthodes

Soixante-quinze (75) prélèvements ont été effectués, à raison d'un prélèvement par semaine pendant la période estivale et une fois par quinzaine le reste de l'année.

Les prélèvements, le transports et l'analyse des échantillons d'eau de mer ont été réalisés conformément aux directives applicables à la surveillance sanitaire de la qualité des eaux littorales (2). La méthode utilisée pour la recherche des germes tests de contamination fécale, est celle des séries de dilution en milieu liquide décrite par l'OMS/PNUE (2). Les données collectées sont traitées et comparées aux valeurs guides et impératives en germes fécaux. Cette comparaison est basée sur l'étude de la régression du logarithme des concentrations observées en fonction du logarithme naturel de la fréquence cumulée (3).

L'analyse de variance du niveau de contamination en fonction des années est réalisée par le test de Kruskal et Wallis et le test des rangs (4). Les valeurs expérimentales ont également été comparées aux normes algériennes parues au journal officiel N°46 le 14/07/1993 (Décret exécutif N°93-164).

Résultats et discussion

La variation saisonnière des germes fécaux montre leur prédominance en période estivale (Fig. 2). Des maxima sont également relevés en automne, résultant d'un apport supplémentaire en germes après lessivage des terrains avoisinants par les premières pluies.

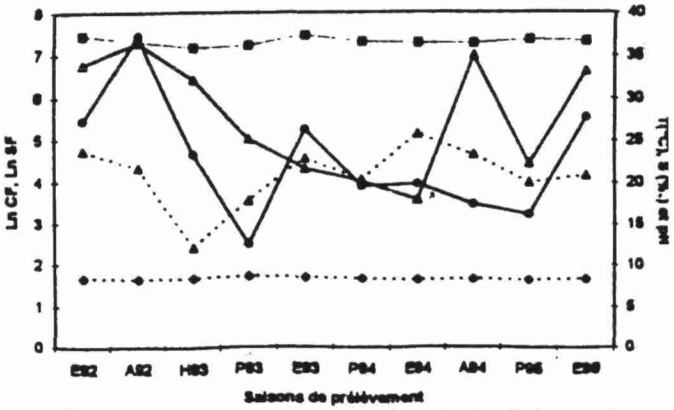

Fig. 2. Evolution des germes tests et des paramètres physico-chimiques en fonction des saisons.

Les paramètres physico chimiques (T°, pH, S‰) observés restent dans les limites des variations saisonnières. Les valeurs moyennes logarithmiques des coliformes fécaux (CF50) présentent une diminution pendant la période de suivie (tableau 1).

Une légère augmentation des teneurs est observée de 1994 à 1995, celle ci n'est pas significative étant donné le chevauchement de l'intervalle de confiance (Fig. 3).

Dans leur ensemble ces résultats sont supérieurs aux normes algériennes et aux valeurs guides proposées par l'OMS / PNUE (5). De même les valeurs impératives (CF90) confirme la contamination de l'eau de mer, les concentrations en coliformes fécaux obtenues dépassent les critères de salubrité, dans 90% des échantillons analysés (tableau 1).

Tableau 1. Résultats des teneurs en coliformes fécaux (CF) et streptocoques fécaux (SF), traités par la méthode de distribution lognormale.

Années	n	XX/ 100ml	S	IC
1992	24	CF50 = 1470 CF84 = 7132 CF90 = 8792	1.57	[762-2870]
	24	SF50 = 1451 SF84 = 9897 SF90 = 12836	1.92	[646-3264]
1993	15	CF50 = 245 CF84 = 683 CF90 = 783	1.03	[139-433]
	15	SF50 = 58 SF84 = 550 SF90 = 742	2.26	[17-203]
1994	15	CF50 = 135.63 CF84 = 794.94 CF90 = 943.88	1.71	[53-902]
	15	SF50 = 32.45 SF84 = 105.63 SF90 = 122.73	1.18	[17-62]
1995	21	CF50 = 188.67 CF84 = 749.94 CF90 = 934.48	1.38	[102-348]
	21	SF50 = 46 SF84 = 138.37 SF90 = 159.17	1.1	[29-75]

n = effectifs, XX = concentrations bact_riennes, S = écart type, IC = intervalle de confiance.

THE USE OF *ESCHERICHIA COLI* AS FOOD SOURCE FOR PROTOZOA IN EXCRETION EXPERIMENTS : PRELIMINARY RESULTS

Sílvia P. Pelegrí*, Urania Christaki, John Dolan & Fereidoun Rassoulzadegan
Laboratoire d'Océanographie Biologique et d'Ecologie du Plancton Marin, CNRS-URA 2077,
Station Zoologique BP 28, 06230 Villefranche-Sur-Mer, France

Abstract

Quantification of dissolved organic carbon (DOC) egestion rates of marine protozoa is hindered by the uptake of the egested DOC by marine bacteria. Here, we present a new method to measure DOC egestion rates of protozoa by replacing the marine bacteria by *Escherichia coli* as food source. *Escherichia coli* is an enterobacteria that becomes instantaneously inactive upon addition to seawater. Thus, *E. coli* will not take up or release any metabolic products in spite of being alive. Indeed, we found no uptake or release of DOC by *E. coli* in seawater. Also, *E. coli* appeared to be a good food source for a ciliate, *Strombidium sulcatum*, and a small flagellate isolated from NW Mediterranean waters.

Key-words: carbon, bacteria, predation

Introduction

Dissolved organic matter (DOM) represents a major fraction (> 95%) of total organic matter in the ocean and has important short and long term implications for plankton trophic interactions and oceanic biogeochemistry (1). However, little is known about the characterization, transformation and absolute concentration of DOM in seawater (2). Recently, it has been reported that dissolved organic carbon (DOC) integrating this DOM seemed to accumulate in high concentrations in upper and biologically active waters during stratification periods (3). This net production of DOC originates from in situ biological production. Direct active or passive exudation from phytoplankton, sloppy feeding and excretion from protozoan and metazoan grazers, and cell lysis from viral infection have been suggested as sources for this DOC production.

The degradability of this surface DOC pool has been studied intensely over the past years (4). Apparently 50% of it is refractory DOC while the other 50% is semi-labile and degradable over the time scale of months (5). To some degree, the recalcitrant DOC is imported from allochthonous sources, but it may also be the result of transformations of labile compounds originating from autochthonous primary production. Tranvik (6) reported that DOC produced by flagellates was digested slowly by the bacterial assemblage. He suggested that flagellate bacterivory could contribute to the transformation of labile organic matter into more refractory forms.

Theoretical calculations indicate that small flagellates could ingest 10^4 - 10^5 bacteria per ml per day (7). Assuming a carbon content of 20 fg C bacteria^{-1} (8), and 20% of the ingested bacteria eliminated as DOC (6), we calculate that small flagellates could release 0.04-0.4 mg C l^{-1} d^{-1}. The DOC accumulation reported for the surface layer in the Mediterranean during the stratified period, 200 mg C l^{-1} over 6 months (3), is equivalent to about 1 mg DOC l^{-1} d^{-1}. Approximately 4 to 40% of this DOC could be produced by the stock of small flagellates. In spite of the possible importance of protozoan excretion on DOC dynamics in surface waters, there is a lack of reliable data on assimilation efficiencies and egestion rates of protists (9, 10). Information on the assimilation efficiencies of protozoa feeding on natural prey is essentially non-existent. This is due to the difficult task of recovering egested materials and added complications derived from bacterial uptake of the produced DOC.

Due to the consumption of egested DOC by the bacterioplankton, the use of live bacteria represents a problem in obtaining reliable DOC data. In order to circumvent this obstacle, we have developed a new method consisting on using *Escherichia coli* as food source for the protozoa instead of marine bacteria. *Escherichia coli* is an enterobacteria that becomes instantaneously inactive upon addition to seawater. Thus, the bacteria will not take up or release any metabolic products. However, E. coli will remain alive as opposite to the often used heat-killed bacteria. The use of live bacteria will avoid heat-killing (at 60°C for 4 h) natural assemblages and therefore the denaturalization of organic compounds that may affect DOC egestion rates. Although of non marine origin, E. coli is a gram-negative bacteria like most marine assemblages. Another advantage of using E. coli in our experiments is the absence of metabolic products derived from bacterial activity.

Material and methods

Escherichia coli (strain HB10B) was grown on Luria-Bertani medium at 37°C and with vigorous shaking. The culture, which had reached ~ 1 unit optical density at 600 nm, was centrifuged in 15 ml centrifuge tubes at 9000 rpm during 10 min. The supernatant was rejected and substituted by 0.2 μm filtered and autoclaved seawater. Each centrifuge tube was sonicated for 1 min to detach bacteria from medium particles, and centrifuged again. This procedure was repeated 4 times.

Uptake or release of DOC by E. coli

Centrifuged *E. coli* were added to two 1 l Erlenmeyers containing 400 ml of 0.2 μm filtered and autoclaved seawater to a final concentration of ~ 7 x 10^6 *E. coli*/ml. To one of the erlenmeyers, sterile D-glucose was added to a final concentration of ~140 mM. Both Erlenmeyers were incubated at 37 °C and with vigorous shaking.

Dissolved organic carbon samples were taken initially, at 1 h intervals for 10 h, and 21 h after setup. These samples were filtered on 0.2 μm Gelman Supor filters, which had been previously acid-washed (10% HCl) and rinsed with distilled water. The filtration was carried out on a glass Millipore filtration unit which had been ignited at 500°C for 4 h. The first 5 ml of the filtrate was rejected and the last 10 ml collected on 20 ml ignited Pyrex tubes, acidified to pH 2 with 2 N HCl, and stored at 5°C until DOC analysis. All samples were analyzed within a week of collection. Dissolved organic carbon was determined by high-temperature catalytic oxidation. Samples were sparged with an artificial air mixture (AGA, France) containing ≤ 0.1 ppm CO, CO_2 or hydrocarbons, and measured on a Shimadzu TOC-5000 instrument equipped with a high sensitivity catalyst. Dissolved organic carbon concentrations were calculated with the instrument software and a 4- (no D-glucose addition samples) or 2-point (D-glucose added samples) standard calibration curve made with potassium biphthalate. The coefficient of variation of duplicate injections was always < 2%.

Samples for bacterial enumeration were taken initially, every 3 h for 10 h, and 21 h after setup. These samples were fixed with 0.2 μm filtered formalin (4% vol./vol. final concentration), DAPI stained (11), and counted on an epifluorescence microscope.

Adequacy of E. coli *as food source for protozoa*

A 3 μm flagellate isolated from Northwestern Mediterranean waters and a 30 μm ciliate, *Strombidium sulcatum*, were fed *E. coli*. Samples were taken for counting S. sulcatum (enumerated on an inverted microscope by Utermöhl's (12) counting technique), and the flagellate and bacteria (counted on an epifluorescence microscope as described above).

Results

Uptake or release of DOC by E. coli

During the 21 h of incubation, DOC values were 130 ± 6 μM and 141.5 ± 4.9 mM in the Erlenmeyers containing *E. coli* and incubated without and with D-glucose, respectively. No accumulation or consumption of DOC ($n = 12$, $p < 0.0001$) took place during the incubations (data not shown).

Bacterial numbers were 7.7 ± 0.5 x 106 E.coli/ml for the 21 h of incubation and for both D-glucose added and not added Erlenmeyers. No bacterial growth ($n = 5$, $p < 0.0001$) took place during the incubations (data not shown).

Adequacy of E. coli *as food source for protozoa*

Figures 1 and 2 show the growth curves for the small flagellate and *S. sulcatum*, respectively. As the number of protozoa increased, there

INTERACTIONS BETWEEN BACTERIA AND THEIR PROTOZOAN PREDATORS ON THE DIEL SCALE

Mladen Solic* and Nada Krstulovic
Institute of Oceanography and Fisheries, P.O.Box 500, 21000 Split, Croatia

Abstract.
Diel variations in bacterial and heterotrophic nanoflagellates (HNF) abundance, bacterial production as well as grazing on bacteria were studied in Kastela Bay (Adriatic Sea). Pronounced diel patterns of all studied parameters were established. Bacterial abundance and growth rate were higher during the day than during the night. Maxima were measured during afternoon and early evening, and minima during the second half of the night and early morning. On the other hand, abundance of HNF was higher at night than during the day. Grazing on bacteria peaked in the evening, but grazing exceeded bacterial production during dark period, therefore, bacterial biomass produced during the day was removed by grazing during the night.

Key-words: bacteria, predation, Adriatic Sea

Introduction

In contrast to seasonal changes in microbial activity, which would be expected to be strongly affected by physical parameters most notably temperature, diel changes are primarily a manifestation of the diel sunlight cycle. It is obvious that primary production should have a pronounced diel cycle with carbon fixation occurring only during daylight hours. Due to strong coupling between phytoplankton and bacteria, significant diel variations of bacterial activity have also been observed (1, 2). Therefore, diel variations of bacterivorous protozoa could also be expected due to diel variations of bacteria as their main source of food. Moreover, bacterivorous protozoa might be able to regulate their feeding rates as a result of changes in light intensity (3).

However, in comparison to a number of studies reporting diel variations of phytoplankton and bacteria, there are still few data which explain interactions between bacteria and their protozoan grazers on the diel scale.

Methods

Samples were collected at a station located in the enclosed, shallow basin Kastela Bay, mid Adriatic Sea (43°31'N, 16°22'E). Samples were collected using sterile, acid washed microbiological samplers, from 1 m depth, and were processed in the laboratory within 24 h after collecting. Samplings were performed at 3 h intervals from 12 to 17 September 1994. Enumeration of bacteria and heterotrophic nanoflagellates (HNF) were made by epifluorescence microscopy using the standard AODC technique (4) for bacteria, and proflavine staining technique (5) for HNF.

Bacterial cell production was measured with the ^{3}H-thymidine incorporation technique (6). (Methyl- ^{3}H) thymidine was added in 10 ml samples at a final concentrations of 10 nM (specific activity 86 Ci mmol^{-1}; Amersham Ltd, UK). Triplicate samples and a formalin killed adsorption control (final conc. 0.5%) were incubated at *in situ* temperature in the dark for 1 h. The incubations were stopped with formalin (final conc. 0.5%). To each 10 ml sample and control an equal volume of ice-cold 10% (wt/vol) TCA was added and mixtures were kept on ice for 15 min. The TCA-insoluble fraction was collected by filtering the sample through a 25 mm 0.2 μm pore size cellulose nitrate filter. The filters were rinsed five times with 1 ml of ice-cold 5% (wt/vol) TCA. The filters were dried, placed in scintillation vials, dissolved in 10 ml Filter-count™ (Packard scintillation cocktail) and counted after 24 h storage in a scintillation counter (Packard Tricarb 2500 TR).

Grazing on bacteria was estimated by the size fractionation technique (7, 8) using diffusion chambers with and without predators, as a difference in bacterial growth between ungrazed and grazed samples.

Results and discussion

Diel fluctuations of bacterial and HNF counts are shown in Figure 1. Bacterial abundance increased during afternoon and early evening, reaching maximal number at 18 h, and declined during night, reaching minimal number at midnight. Bacterial abundance at 18 h was nearly twice that at 24 h. On the contrary, abundance of HNF peaked during night and early morning, whereas low values were measured during daylight. Maximal values of HNF abundance were recorded between 3 h and 6 h in the morning, whereas minimal abundance was found at 12 h.

Diel variations of thymidine incorporation rate (TI) and specific thymidine incorporation rate (STI) or thymidine incorporation per bacterial cell are shown in Figure 2. TI peaked in the afternoon to early evening (between 15 h and 21 h), whereas minimal values were measured at night and early morning. STI showed nearly the same diel rhythm as TI suggesting that increase in bacterial production during daylight was not only because there were more bacteria, but, on average, each cell grew faster.

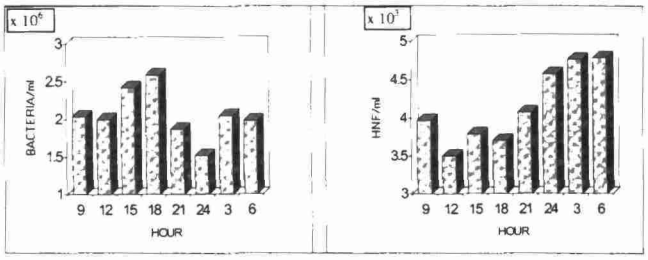

Fig. 1. Diel fluctuations of bacterial and HNF abundances.

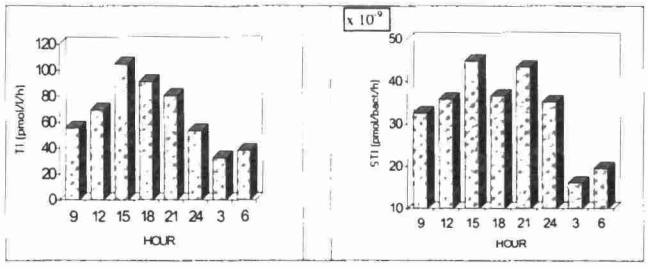

Fig. 2. Diel fluctuations of thymidine incorporation (TI) and specific thymidine incorporation (STI) rates.

The same diel pattern in bacterial production with maximal values during afternoon and early evening and minimal values during night and early morning have been reported for other marine environments (9, 10, 11). Higher bacterial production and abundance during the day than at night was also reported for the north Adriatic Sea (12), western Mediterranean Sea (13), southern California Bight (2) and Bothnian Sea (14). Diel variations in oxygen consumption and bacterial production indicated that bacteria were substrate limited during the night and early morning (11). This suggests that bacterial production may be supported by a small labile fraction of the total DOC pool which may be turned over remarkably fast (15, 16). However, other studies reported inconsistent or no diel variation in bacterial activities (1, 17, 18). The reason whether diel pattern in bacterial activities are observed or not could lie in the source of organic matter that supports bacterial growth. Thus, if phytoplankton are the predominant substrate source, diel variations in bacterial activities are expected. The higher abundance of HNF during the night, particularly during the second half of the night and early morning were in accordance with several studies in which HNF abundance increase occurred during the night (12, 19), during the night and early morning (13) and during the morning (2).

Grazing on bacteria also showed diel rhythm with maximal values between 18 h and 21 h, and minimal between 9 h and 12 h (Fig. 3). However, the average specific grazing rate on bacteria was higher during the dark period than during daylight (Tab. 1).

Production exceeded grazing during daylight, whereas grazing exceeded production during dark period (Fig. 3). Thus, positive net growth rates were recorded during daylight and negative during night (Table 1). Bacterial net production was near zero during the period from 15 h to 21 h, suggesting equilibrium between growth and grazing

SCALES OF TEMPORAL VARIABILITY OF GROUNDFISH LANDINGS IN NORTH-WESTERN MEDITERRANEAN

Y. Aldebert [1]*, P. Sanchez[2] and M Demestre[2]
[1] IFREMER, 1, rue Jean Vilar, 34200 Sete, France
[2] Instituto de Ciencias del Mar (CSIC), P. Joan de Borbo s/n, 08039 Barcelona, Spain.

Abstract
The paper deals with the question of interrelationships between the abundance of fishery resources and their exploitation. Three different types of variations could be identified from the analysis of groundfish landings in the Gulf of Lions and in the Catalan Sea. Various examples were used to illustrate the daily, seasonal and inter-annual variations of demersal resources and of fishing intensity.

Key-words : fisheries, Western Mediterranean

Introduction

Speaking of reciprocal relationships between the abundance of fishery resources and exploitation is quite a truism. The biology and ecological behaviour of fish constitute one of the main types of factors that can determine variations in the dynamics of fishing effort and in the strategies of fishing fleets (1). The influence of resources on fishing intensity is widely taken into account by fishery biologists, while the major question of marketing is often poorly considered.

The aim of the present paper is to introduce reflection on this theme and the results might be considered as preliminary. In order to furnish elements on this topic for further discussion, several actual cases of temporal variations in landings of demersal resources were analysed. These variations can be intra-annual (daily or seasonal) or inter-annual. They suggest various questions, the response to which is related to the different components of the exploitation. Some examples issued from data collected in the Catalan Sea and in the Gulf of Lions illustrate these three different types of variations. The possible causes and impact on fishing intensity and on dynamics of fishing fleets will be considered.

Material and methods

Data used for the estimation of daily variations were obtained from the daily catch statistics of the Barcelona auction market for January, March, August and November 1992. Monthly catch statistics of ten ports of the Catalan coast, from 1987 to 1993, have been used to illustrate the seasonal variations of *Sepia officinalis*. Concerning the Gulf of Lions, landing data were taken from the Sete auction market. This market was computerised in 1970. Therefore, a time series of 25 years landings is now available, this being mainly from the trawler fleet fishery.

Monospecific time series analyses (2) were based on monthly data available for the period. They allowed highlighting general trends, seasonal cycles and even pluriannual cycles in some case (3). Several procedures from the Statgraphics-Plus package were used. viz.

* The Seasonal Decomposition procedure performing a classic decomposition of a time series ; the multiplicative ratio-to-moving-average method was used, the computed seasonal index for each month being based on average ratios to the moving average.
* The Autocorrelation Function procedure, allowing to show pluriannual cycles in addition to seasonal patterns.

Results and discussion

Daily variations

The daily variations observed in landings may be due to various causes. The direct impact of meteorological conditions on the fishing fleet's dynamics and on their catches is well known : possible reduced accessibility of the fishing grounds (4) as well as modification in the behaviour of fish (including bottom fish). Market demand must also be of consequence on fishing activity. The example of daily landings of the red shrimp *Aristeus antennatus* (Fig. 1) shows a weekly periodicity with higher catches on Mondays and Fridays and lower catches during the middle days of the week (Wednesday-Thursday). This pattern occurs throughout the year, as can be observed in the four analysed months, representing the four seasons of the year.

Seasonal variations

Seasonal patterns can be observed in landings for many species. Different cases may be encountered corresponding to different biological behaviours :

Case 1. Recruitment to fishing grounds

The red mullet (*Mullus barbatus* and *M. surmuletus*) landings from trawl fleet on the Catalan coast and in the Gulf of Lions (Fig. 2) show a high autumnal peak, with a maximum in September and October respectively. This peak corresponds both to the arrival and to the concentration of new recruits (mainly *M. barbatus*) belonging to the 0 group in the coastal fishing grounds. Consequently, the fishing fleets move towards these fishing grounds looking for these recruits (5).

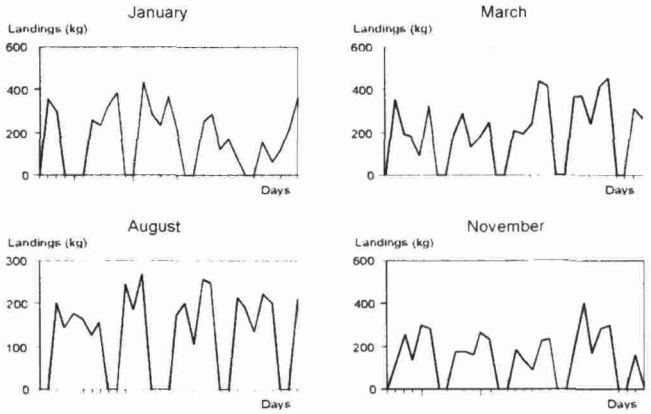

Fig. 1. Red shrimp *Aristeus antennatus* : daily landings of the Barcelona trawler fleet in 1992. (On X axis Sundays points are shown with continued broken vertical lines).

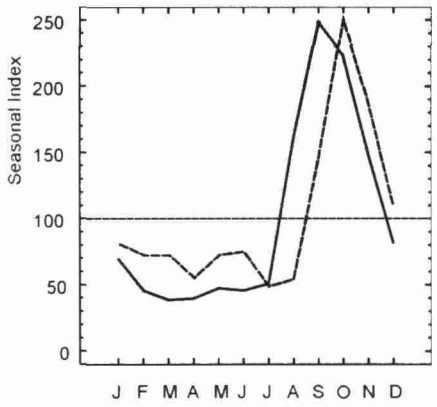

Fig. 2. Mean seasonal variations in landings of *Mullus* spp from trawler fleet. ——— = Catalan coast (1987-93). - - - - - - = Gulf of Lions (Sete, 1971-95).

Case 2. Seasonal trophic or spawning migrations

In the Gulf of Lions, the sea bass (*Dicentrarchus labrax*) moves during the period spring to autumn into lagoons to feed and in winter into the sea where reproduction takes place (6). Mean annual landings of the species at the Sete auction market reflect these migrations and show the seasonal availability of resources for the trawl fleet : the level of catches is seen to be higher from September to April (Fig. 3).

Case 3. Sequential fisheries

Various patterns of exploitation can be observed according to the concerned species. For cuttlefish *Sepia officinalis*, in the Catalan Sea, different seasonal peaks can be observed according to the different types of gear and depth in which they fished (Fig. 4). Cuttlefish is a shallow water species and trawlers can catch only a part of the population *i.e.*, mainly small and medium sized immature individuals. The small-scale fishery fleets take advantage of the spawning migrations to catch the large specimens in shallower waters (less than 25 m depth) when the mature animals move towards the coast (7).

A METHOD FOR THE AGE DETERMINATION OF TWO MEDITERRANEAN SCIAENIDS, *SCIAENA UMBRA* (LINNAEUS, 1758) AND *UMBRINA CIRROSA* (LINNAEUS, 1758).

E. Arneri*, S. Colella and G. Giannetti

Istituto di Ricerche sulla Pesca Marittima, Consiglio Nazionale delle Ricerche, Largo Fiera della Pesca, 60125 Ancona, Italy

Abstract

A method for the age determination of two Mediterranean sciaenids *S. umbra* and *U. cirrosa* by means of stained thin sections of the otoliths is described. The staining enhances the contrast between opaque (fast growth) and hyaline (slow growth) zones in the otolith sections. *S. umbra* up to 19 years of age are easily aged.

Key-words: Growth, Teleostei, Adriatic Sea

The family Sciaenidae is present with three genera, *Argyrosomus*, *Sciaena* and *Umbrina*, and five species in the Mediterranean Sea (1). *Sciaena umbra* and *Umbrina cirrosa* are rather common fishes along the coast of the Mediterranean sea: they generally inhabit inshore waters on rocky and sandy bottoms at depths ranging from the shoreline to about 100 m (1; 2, 3). They are locally important commercial fishes, in particular for small scale artisanal fisheries (4).

Age of fishes can be determined from different hard structures such as scales, vertebrae and otoliths. By far the otoliths (sagittae) are the most common and widespread hard structure used. Various otolith preparation techniques are available and their applicability depend on the specific characteristics of fish otolith. The large size and thickness of the otoliths in sciaenids make them difficult to age just by inspecting the whole otolith under reflected or transmitted light. The dense calcium carbonate deposition reduces light transmission, making very difficult to distinguish hyaline and opaque zones (5). Because it was impossible to examine the whole otolith also in Mediterranean sciaenids, different otolith preparation techniques (grinding, polishing, sectioning and staining) were tried in order to find the best method for age determination.

The specimens of *S. umbra* and *U. cirrosa* used for this study come all from the Central Adriatic and have been collected at IRPEM (Istituto di Ricerche sulla Pesca Marittima) during various scientific activities at sea such as artificial reef studies, inshore trawling studies and from landings of the commercial fishing fleet at the port of Ancona. Otoliths were removed, cleaned and stored dry. As preliminary trials of grinding and polishing the internal side of the otolith were unsuccessful, it was decided to prepare otolith sections. The right otolith was embedded in epoxy resin (6) using semi-rigid plastic moulds sprayed lightly with a silicone spray to facilitate subsequent extraction (7). The resin block was examined with a dissecting microscope at low magnification and the central area of the otolith containing the core was marked on the resin. This was done to achieve a careful positioning on the saw of the resin block for the cut. Transverse sections 0.7-0.8 mm thick were obtained by means of a low speed saw (Remet Micromet) equipped with two diamond blades separated by a metallic spacer. Otolith sections were then stained for about 20 minutes with the histological stain Neutral Red Solution (Sigma) which was prepared adding 1% of Sodium Chloride and acidified with 0.5% of acetic acid (R. Millner, pers. com.). Stained sections were rinsed in tap water, dried and then observed with a dissecting microscope at low magnification under reflected light. An alternating pattern of white and dark zones appears both in *S. umbra* (Fig. 1) and in *U. cirrosa* (Fig. 2). The dark zones corresponds to translucent zones in not stained sections and can therefore be considered as winter (slow growth) zones. Validation of annual deposition of the dark zone has been obtained for *S. umbra* in the Adriatic (Arneri, in preparation) and can be reasonably assumed for *U. cirrosa*. As these two sciaenids reproduce in spring and summer in Mediterranean (8) and the dark zone is laid down in winter thus one white and one dark zone can be considered as an annulus and age determined consequently by counting the number of dark zones on the section.

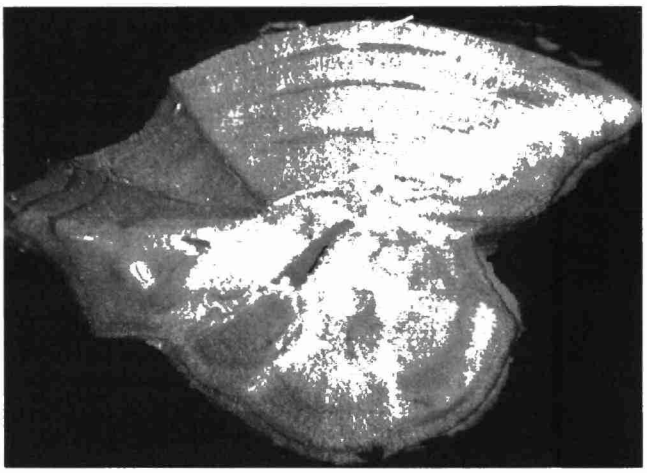

Fig 2 - Stained thin section of otolith of Umbrina cirrosa (total length 67 cm , weight 3200 g) aged 3 years old: arrows indicate winter zones (magnification 13x).

In Figs. 1 and 2 otolith sections of three years old *S. umbra* and *U. cirrosa* are shown. The otoliths of Sciaenids present an inner surface smooth and convex (top in Figs. 1 and 2) and an outer surface covered with large granules (9) which tend to cluster together with growth. False rings are seldom observed in both species and only in the first two years of life. In older individuals annuli are easy to detect toward the inner surface of the otolith (top of sections in Figs. 1, 2 and 3). The huge difference in size of the individuals certainly reflect a

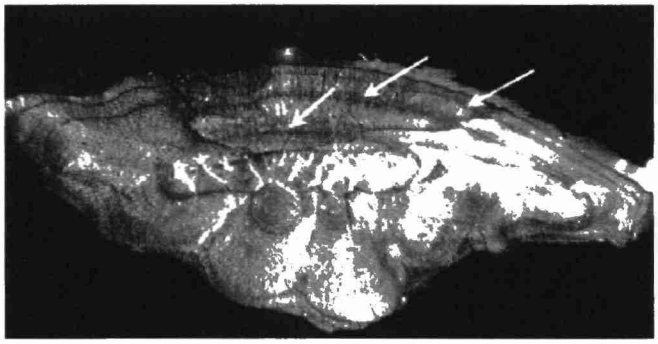

Fig 1.- Stained thin section of otolith of Sciaena umbra (total length 36.5 cm , weight 818 g) aged 3 years old: arrows indicate winter zones (magnification 13x).

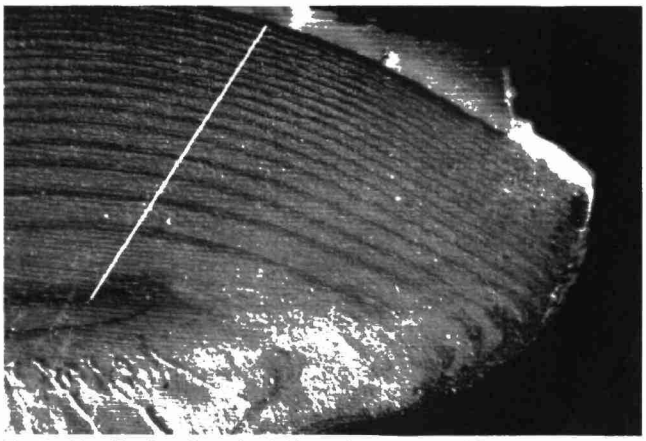

Fig. 3 - Magnification of a stained thin section of otolith of Sciaena umbra (total length 46.5 cm , weight 1612 g) aged 19 years old (magnification 20x). The white line shows the profile along which the light luminance has been measured by Image Video Analysis.

QUANTITATIVE ASSESSMENT OF INTERACTIONS BETWEEN SEISMIC SHOOTING ACTIVITIES AND SMALL PELAGIC FISH IN MIDDLE ADRIATIC SEA

Azzali Massimo [1], Rivas Giovanni [2*], Modica Alfonso [2], Panzeri Adelio [3]

[1] IRPEM-Istituto Ricerche sulla Pesca Marittima del CNR, Ancona, Italy
[2] CEOM-Centro Oceanologico Mediterraneo SCpA, Palermo, Italy
[3] AGIP SpA, Unità GEDA, S. Donato Milanese, Milano, Italy

Abstract

Present study describes the results of a quite large investigation carried out in Middle Adriatic sea during 1996. The study had the aim of assessing potential impact attributable to geophysical seismic prospection with air-gun on distribution and schooling behaviour of small pelagic fish. Results reported show a weak recoverable influence due to disturbance ; for a definitive statement further investigation is needed.

Key-words : acoustics, seismics, biomass, fishes, Adriatic sea

Introduction

In those marine areas where E&P activities are relevant, particular concern is given to the effects elicited by seismic shooting on marine fauna of commercial interest (1). In the Adriatic sea the activities of detection of the crust layers are important. AGIP promoted in 1995-96 a series of studies concerning the assessment of possible effects elicited by air-gun seismic shooting on fishable resources (2).

In particular the task of present study deals with the assessment (by acoustical methods) of the effects elicited by seismic prospection on geographical distribution, of biomass and schooling behaviour of small pelagic fish (*Sardina pilchardus* and *Engraulis encrasicolus*) rising up to 80% of the resource). These items were detected before, while and after the prospection performed by AGIP in the Adriatic sea during the period lasting from February 28th to March 10th 1996.

Material and methods

The study area lies inside the Pescara Basin (Middle Adriatic sea) and it is delimited between 42° and 43° and the depths of 30 and 100 m. The total area amounted to 200 nm^2. The area was sampled in 24 h in order to average the day-night fish behaviour. The surface was delimited by an outer "skeleton" and by an inner path. Sampling design foresaw the covering of outer part before and of the inner path after, in order to ensure a representative sample even if the weather conditions were bad. The total coverage arose to 162 nm^2 (80% of the total area). The values of the biomass occurring in the remainder 20% were interpolated according to "interpolation by numerical approximation" method (5). The same method allows the interpolation of the biomass surrounding the sampled area ; the total interpolated area reached nearly 290 nm^2. The bias about the assessment of the biomass varied about 14 and 25% and it can be attributed to the interpolation process.

The area was sampled as follows : two surveys were carried out before the seismic shooting ; two during profiling and one after the energization. Weather conditions did not allow the performance of the second survey to be carried out one week after profiling, which would have assessed the recovery period.

The echoes given by the pelagic fish were collected by EK-500 system, installed on the R/V *S. Lo Bianco*. The sample frequency generated by the "Split Beam" transducer (ES120-7 model) was equal to 120 kHz. Such a device is able to detect (ping per ping) both multiple echoes (mean volume density : SW) and the single echoes (target strength : TS) due to single specimens of pelagic fish. The TS evaluation enables to assess the size/species (or species groups) of those fish for which the theoretical TS values are available (previously measured in calibration assays). The mean biomass values were detected both on the whole water column and by layers (each layer equal to 10 m). In order to validate the interpretation of size/species data from the TS values, is important the collection of biological samples during the echosurvey (4).

In case of absence of single echoes (TS) the collection of biological samples is needed in order to assess the composition and distribution of the target species acoustically detected (4). The gear employed in present study was a low selectivity pelagic trawl net (stretched mesh 800 mm in the frontal part, 36 mm in the sack). The mouth of the net had a surface of 80 m^2 (6-8 m height, 12-13 m width). The position of the trawl net was regulated and constantly monitored by the ITI (Integrated Trawl Instrumentation System) system (SIMRAD). The information about the position of the net, with respect to the water column allowed the correlation between the biological samples and the echoes (acoustical samples). Each tow lasted 30 minutes at a 4 knots speed. The tows were splitted as follows : 9 were performed during the AGIP air-gun prospecting activities (while surveys), 6 were carried out during the two pre-surveys and 3 during the post survey. The all data collected during the 5 echosurveys were elaborated by software named Geographical Data Base System (GBDS) developed by I.R.PE.M. The elaboration of three kinds of different sets of data was performed :

1) horizontal distribution (biomass density referred to the whole water column, paths of the ship and catches) ;

2) vertical distribution (biomass densities inside selected depth layers);

3) time variations of the total biomass densities and of biomass in each layer.

The energy source used for the trials was formed by one air-gun array made-up by two subarrays consisting in 8 air-guns each developing a total volume equal to 1500 i^3 at 2000 psi, with an intensity of 240 dB//μPa. The interval between two shots was 15 sec.

The acoustical data in each echosurvey were splitted in 4 different depth layers :

1. the first layer includes the whole water column. In such a layer is contained all the pelagic biomass (fish long at least 5 cm). This dimension was established by the frequency employed and by the minimum value of TS chosen by the operator ;

2. the second layer goes from the surface to a depth of 10 m ;

3. the third layer reaches 10 m upon the bottom ;

4. the last was the intermediate layer and goes from 10 m upon the bottom as far as 10 m beneath the surface.

The absolute density and biomass were computed in two different ways :

* the first way is based on the computation of a mean TS of all pelagic species ;

* the second way is based on the classification of TS by species according the method of Split Beam, using the calibration data integrated with catch data.

Figures 1 and 2 show the trend of Total Pelagic Biomass and Pelagic Biomass by species, before, while and after the seismic survey.

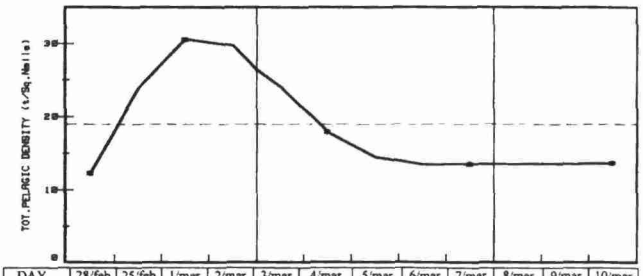

DAY	28/feb	25/feb	1/mar	2/mar	3/mar	4/mar	5/mar	6/mar	7/mar	8/mar	9/mar	10/mar
density t/SqNm	*12.1	24.5	*31.6	29.8	22.7	*15.7	12.9	13.2	*14.2	14	12.6	*10.7
tomass (t)	3085		9219			4665			4166			3153
Schooled %	26.7		47.6			14.2			29.9			31.4
Dispersed %	73.3		52.4			85.8			70.1			66.6
schools	245		667			137			321			266

Figure 1. Total pelagic biomass trend before, while and after the seismic survey.

EFFECT OF SOME ENVIRONMENTAL AND PHYSIOLOGICAL FACTORS ON THE BLOOD COUNT OF *MUGIL CAPITO* DURING THE BREEDING SEASON

Baghdadi H.H.[1], El-Gharabawy, M.M.[2], Zaki, M.I.[2] and El-Greisy Z.A[2]

[1] Institute of Graduate studies and Research, University of Alexandria, Egypt
[2] National Institute of Oceanography and Fisheries, Alexandria, Egypt

Abstract

The blood count was affected by the change in environmental factors. The number of red and white blood corpuscles of *Mugil capito* has been affected by environmental changes of the photoperiod, temperature and salinity. human chorionic gonadotropic hormone (HCG) also resulted in a change of the blood count. The increase of photoperiod resulted in a significant increase in the erythrocyte count and a significant decrease in the leucocyte count. Continuous darkness resulted in a decrease in both erythrocytes and leucocytes. High temperature resulted in an increase in both erythrocytic and leucocytic counts while the low temperature led to a decrease in erythrocytic count of *Mugil capito*. The increase in salinity was accompanied by a significant increase in the erythrocyte count and a decrease in the leucocyte count. The HCG injection resulted in increase in both erythrocyte and leucocyte counts.

Key words: fishes, physiology, cell, temperature, salinity

Introduction

Fish respond immediately even to small changes in their ambient environment. The impact of environmental variables on fish haematological parameters has been studied in many different species. The complete blood picture of *Tilapia zilli* and the effect of environmental and physiological factors on the blood cellular and non-cellular constituents of this economically important fish in Egypt have been investigated (1). Also, the influence of temperature and salinity on the erythrocyte count, leucocyte parameters and plasma constituents of juvenile milkfish, *Chanos chanos* from three different brackish water fish farms has been studied (2). The changes in leucocyte count in smoltifying 1- and 2- year old salmons and 2-year old sea trout, both at ambient water temperature and after acclimation to 10°C, in order to exclude the temperature dependent variation have been investigated (3).

Material and Methods

Fish samples

Grey mullet *Mugil capito* were transported from a fresh water fish farm in Barciek, Behaira Governorate of Egypt to the laboratory in suitable continuously aerated aquaria. (2 x 1.5 x 1.25 m) fiber glass aquaria. The fish were acclimated to the laboratory conditions for 7 days. All the experiments were undertaken during the same period (from mid October to late December), *i.e.* within the breeding season, before the natural resorption of the gonads which starts at January and February (4). Fish used were carefully selected to be healthy and more or less robust. Their body length ranged between 29.1 cm and 36 cm, and their body weight ranged between 280 and 390 g. the age of such population lies within the end of the second year class.

Experiments

1. Effect of photoperiod

Four aquaria beside the control were used in this experiment. All these aquaria were provided with 3.4% salinity water, as it was in the natural habitat "Barceik fish farm" to keep the same salinity. The average of the actual sunshine duration over Alexandria during this period is (6.5L+ 17.5D) as reported by Mosalam (5). So the control group received (6.5L+ 17.5D) during the experiment.

The four tanks which involved photoperiodicity experiment were arranged as follows:

	Tank (1)	Tank (2)	Tank (3)	Tank (4)
Photoperiod	6L+ 18D	18L + 6D	Continuous light (24L)	Continuous darkness (24D)
Temperature	17.5°C	17.5°C	17.5°C	17.5°C
Salinity	3.4%	3.4%	3.4%	3.4%

The illumination in this experiment was done by 3 lamps for each tank, the lamp was 100 watt, produced by Philips company. The tank which represented continuous darkness had a heavy black plastic glued top its sides and to so that absolute darkness was obtained.

2. Effect of temperature

The aquaria used in this experiment were placed directly in the front of windows of the laboratory and thus received identical amounts of day light. The aquaria were arranged as follows:

	Tank (1) : lower temperature	Tank (2) : higher temperature
Photoperiod	6.5L+ 17.5D	6.5L+ 17.5D
Temperature	15°C	20°C
Salinity	3.4%	3.4%

The tank with lower temperature (15°C), the temperature had been lowered by using ice bags. In the tank with higher temperature (20°C), the water temperature was thermostatically controlled by using electric heaters.

3. Effect of salinity change

Four aquarium beside the control were used in this experiment to determine the effect of salinity.

	Tank (1)	Tank (2)	Tank (3)	Tank (4)
Photoperiod	6.5L+ 17.5D	6.5L+ 17.5D	6.5L+ 17.5D	6.5L+ 17.5D
Temperature	17.5°C	17.5°C	17.5°C	17.5°C
Salinity	15%	25%	35%	38% (seawater)

4. effect of Human chorionic gonadotrophic hormone (HCG):

A group of male and female *Mugil capito* was injected three times with human chorionic gonadotropic hormone (HCG) intramuscularly, Each fish received 500 IU each week and thus 1500 IU during the three weeks.

Blood sampling

the blood was obtained from the caudal artery by a syringe previously washed with anticoagulant. In the present work, heparin 5000 IU/ml was used. A small drop of the blood directly from the fish was used to make a blood smear for differential white blood cells analysis.

Results and discussion

The blood composition does not only reflect the physiology of the animal in the normal state, but also reflects all changes which occur due to any stress. There are many stresses that induce physiological changes in the animal. These stresses may be internal or external. In the present investigation, the effect of some important environmental and physiological factors on some haematological parameters of *Mugil capito* has been shown during the breeding season.

The Red blood corpuscles (Erythrocytes)

From our results, it is clear that erythrocyte count of males always exceeds that of females during the period of study (breeding season). This observation confirms sexual differences in erythrocyte count. The red blood count among males is usually greater than in females in fish species. Sexual variation in the erythrocyte count of the mountain whitefish, *Prosopium williamsoni* was reported (6).

The present study also revealed that the number of RBCs tends to increase with increasing photoperiod, while continuous darkness (24D) cause a remarkable decrease in the erythrocyte count. The increase in erythrocyte count at long photoperiod and continuous illumination may be due to the increased feeding regime. It is evident that acclimation of *Mugil capito* to a high temperature (20°C) increases the red cell count to a considerable high value.While, the acclimation to a low temperature (15°C) led to a diminution of the erythrocyte count. The variations of environmental temperature affect the number of erythrocyte count in both high and low temperature conditions (7,1). These studies indicate that haematological variations may in some instances follow thermal acclimation.

The results obtained in the present work are in a good agreement with other authors for other species. An increase in erythrocytic count was observed during warm acclimation of trouts, *Salmo gairdneri* (7), the goldfish, *Carassius auratus* (8), the river shiner, *Notropis blennius* (9) and *Tilapia zilli* (1). The increase in erythrocyte count due to the elevation of water temperature may be due to increase of evaporation

THE SEASONAL POPULATION STRUCTURE AND VERTICAL DISTRIBUTION OF *SAGITTA DECIPIENS* FOWLER AND *SAGITTA LYRA* KROHN IN THE SOUTH ADRIATIC PIT

Mirna Batistic

Institute of Oceanography and Fisheries, Laboratory of Plankton Ecology, 20 001 Dubrovnik, Croatia

Abstract

On the basis of samples collected in South Adriatic Pit during five cruises, abundance and vertical distribution of *Sagitta decipiens* and *Sagitta lyra* and their developmental stages were investigated. A wide vertical distribution (from surface to 1000 m) was noted for both species. Moreover, in the layers below 100 m depth, these species made more than 90% of total chaetognaths. The bulk of the *S. lyra* population (mostly juveniles) was located in the upper 200 m, whereas S. decipiens was most numerous in the 100 to 300 m depth. Both species displayed an ontogenetic vertical distribution with the older stages occuring at greather depth.

Key words: Zooplankton, Chaetognatha, Adriatic Sea

Introduction

In the Adriatic Sea available literature on chaetognaths regards mostly species composition, their frequency and seasonal variation (1-5). Most of the literature data mainly refers to neritic areas of the Adriatic, devoid of oceanic species. Only sporadic specimens of *S. decipiens* and *S. lyra* may be found northward from the southern deep Adriatic in some seasons where they have been carried by the eastern Adriatic incoming current (3, 5). The vertical distribution of chaetognath species has not been well documented for the Adriatic Sea. Hure (6) has provided some general data for the south Adriatic in the upper 300 m. Detailed information on the vertical distribution of the different developmental stages of chaetognaths is completely lacking. The purpose of this study is to present the first data on seasonal abundance and vertical distribution of *S. decipiens* and *S. lyra* and their developmental stages in the open waters of the Southern Adriatic.

Materials and methods

Planctonic samples were collected at station P-1000 in South Adriatic Pit (Fig. 1) during five cruises: 20 April 1993; 16 September 1993; 25 November 1993; 26 February 1994 and 17 June 1994. The first and the last sampling dates samples were collected during night-time while on the other dates samples were taken in day light.

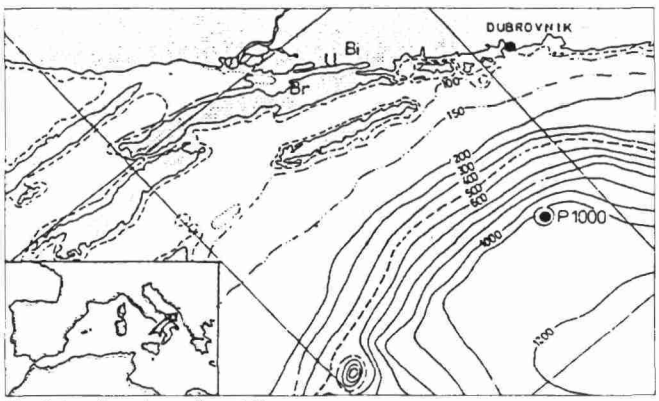

Fig. 1. Location of sampling station.

A total of 35 samples were collected with a Nansen opening-closing net (114 cm diameter, 380 cm length and mesh size of 250 (m) by vertical hauls in the following layers: 0-50, 50-100, 100-200, 200-300, 300-400, 400-600 and 600-1000 m. Salinity and temperature were determined using a CTD multisond (SEA Bird Electronics Inc., USA) at 0, 5, 10, 20, 50, 75, 100, 200 and 300 m.

Maturity stages of chaetognath species were classified using Thomson's (7) criteria as follows: the primitive germ cell of the gonads have not started to develop in Juvenile; the gonads are formed in Stage I; small ova are present in Stage II; some large ova appear in Stage III. Developmental stages in *S. decipiens* specimens with male characteristic were determined as follows: testes visible in Stage I; seminal vesicles present in Stage II, seminal vesicles fill in Stage III. The mean vertical position (weighted mean depth, WMD) of *S. decipiens* and *S. lyra* in the water column was determined using the method of Pearre

(8): $WMD = ((n_i \times d_i)/N$

where d*i* is the depth of sample i, n*i* is the number of individuals collected in sample i and N is the sum of all individuals collected in all samples at all depths. To determine differences in mean vertical position of the different developmental stages of each species, Kruskal-Wallis test was used.

Results and discussion

S. decipiens and *S. lyra* had a wide vertical distribution, from the surface down to 1000 m depth. Moreover, in the layers below 100 m depth, these species made more than 90% of total chaetognaths.

There exist a problem in terminology regarding *Sagitta decipiens* in the pertinent literatury hence the incongruity in terms of its distribution. Most authors treat *S. decipiens* and *S. sibogae* as one species. Tokioka (9) described a new species from the North Pacific, *S. neodecipiens*, closely related to *S. decipiens*. According to Pierrot-Bults (10) *S. neodecipiens* Tokioka 1959, is a junior synonym of *S. decipiens* Fowler 1905. *S. sibogae* Fowler 1906 is the valid name for the species usually incorrectly named *S. decipiens*.

S. decipiens was recorded below 50 m depth where temperature variations are small during all seasons (Fig.2, Table 1). Species was most abundant in the layers from 100 to 300 m which is in accordance with data provided by Hure (6). In the Eastern Mediterranean *S. decipiens* was found from 50 m to the deepest extent of sampling (500 m), mainly deeper than 100 m and caracterized as mesopelagic (11). Data from other parts of Mediterranean Sea are similar (12, 13, 14, 15). In the North Atlantic *S. decipiens* was most abundant in the layers from 500 to 800 m, while a single specimens are recorded down to 2000 m depth (16).

Table 1. Ranges of water temperature and salinity in the 0-300 m layer for the cruise dates.

Depth layers	April 93		Sept. 93		Nov. 93		Feb. 94		June 94	
(m)	T (°C)	S(‰)	T (°C)	S(‰)	T (°C)	S(‰)	T (°C)	S(‰))	T (°C)	S(‰)
0 - 50	13.2-14.9	38.45-38.60	14.4-22.5	38.55-38.67	14.4-16.4	37.87-38.60	12.7-13.0	37.95-38.24	13.6-20.3	38.00-38.52
50 -100	13.0-13.2	38.56-38.57	13.6-14.4	38.59-38.65	13.9-14.4	38.60-38.66	13.0-13.8	38.24-38.58	13.3-13.6	38.52-38.59
100 - 300	13.0-13.1	38.56-38.59	13.4-13.6	38.63-38.65	13.5-13.8	38.61-38.66	13.6	38.58-38.63	13.3-13.4	38.61-38.62

S. decipiens was absent from the upper 100 m layer in April and September. In the 100 - 200 layer, juveniles and Stage I individuals represented more than 95% of the total population. Adult specimens occurred in the 200 - 300 m layer, and dominated the population in the deeper layers (Fig. 2). In the layers where this species was most numerous (100 - 300 m), maximum values did not exceed 7.5 and 12 ind.10m-3 in April and September, respectively.

In November and February *S. decipiens* inhabited the 50 - 100 m layer (Fig. 2). The specimens may have been transported to the surface by upwelling since according to Vilicic *et al.* (17) the Southern Adriatic cyclonic gyre is strongest in winter and early spring. In addition to juveniles and Stage I individuals that dominated the layers down to 200 m, adult specimens (Stage III) participated by about 25% to total numbers. The abundance of adult specimens increased with depth (Fig. 2). During these periods, maximum numbers did not exceed 12 ind.$10m^{-3}$ in the 100 - 300 m layer. Vucetic (18) associates the abundance and vertical position of the *S. decipiens* in the Southern Adriatic with the inflow of the Mediterranean water, especially in winter. However, our results indicated that *S. decipiens* does not enter periodically in the Adriatic. On the contrary, individuals in all developmental stages were present permamently throughout the water column in the Southern Adriatic.

In June, *S. decipiens* was also not recorded in the 0 -100 m layer. A maximum of 14.3 ind.10m-3 was recorded in the 100 - 200 m layer where an important decrease in juveniles contribution (5% of the total)

DAYLIGHT *VS* NIGHT VARIATIONS IN THE RED SHRIMPS CATCHES OF THE STRAIT OF SICILY

Marco L. Bianchini [1], Lucio Di Stefano [2], Sergio Ragonese [3]*

[1] P.F. Raisa/CNR, National Research Council, Roma, Italy
[2] Istituto Istologia Embriologia, Università, Palermo, Italy
[3] Istituto Tecnologia Pesca e Pescato, CNR, Via L. Vaccara 61, 91026 Mazara del Vallo (TP), Italy

Abstract

The red shrimps, *Aristaeomorpha foliacea* and *Aristeus antennatus*, represent an important resource for the fisheries of the Strait of Sicily. According to fishermen, a night haul yields a smaller catch than during daylight, even if a greater proportion of large-size animals is caught. In order to check for any statistical difference between yields, sex-ratios and size frequency distributions, a few comparative night hauls were performed. In all cases the daylight catches, both in weight and number, resulted significantly higher than the night catches. The carapace length frequency distributions showed statistically significant differences, with the night catches trailing the daylight ones.

Key-words: Decapoda, Fisheries, Vertical migration, Sicilian Channel

Introduction

The red shrimps, *Aristaeomorpha foliacea* and the companion species *Aristeus antennatus* represent an important resource for the fisheries of the Mediterranean, in particular in the Strait of Sicily (Central Mediterranean Sea) [1].As in other places, Sicilian fishermen prefer to fish the red shrimp bottoms in daylight, and target the red shrimps at night (usually doing one prolonged haul) only if no alternatives, such as banks or epibathyal grounds, are around; in fact, according to the fishermen, a night haul yields a smaller catch than during daylight, even if a greater proportion of large-size animals is caught in comparison to the daylight hauls. A similar phenomenon has been studied for *Aristeus antennatus* [2, 3, 4], and is often qualitatively reported in literature for *Aristaeomorpha foliacea*; for the latter, it has been confirmed statistically, limited to the reduction in catches, for the population of the Australian slope [5].

In order to confirm these results and to check for any statistical difference between mean weights and length frequency distributions, a few comparative night hauls were performed within the framework of a study aimed at evaluating the selectivity of the commercial bottom trawl net used for the red shrimp fishery in the Strait of Sicily [6].

Material and methods

A total of 12 night hauls (by convention those started at or after 7 p.m.) were realized, 7 and 5 in Spring and Summer 1994 respectively, and compared with one (or more) corresponding daylight haul (same day, same area); the depth of trawling was in the 500-700 m range, the duration of each haul was 3 hours and, even if the gear had different configurations, the cod-ends were covered with 14-mm (side) mesh bag. The total captured red shrimps were sorted by species and sex; the catch was weighed, counted and expressed in kg/h or n/h; the carapace length was measured (to the nearest mm) in each specimen; sexes were thereafter combined. Since the capture of *Aristeus antennatus* was modest, only data on *Aristaeomorpha foliacea* were further analyzed.

Paired t-tests were used to compare the differences in the hourly yield (in weight) and catch (in number), and in the average weight; the differences in mean weight were analyzed also with a non-parametric Wilkinson's sign test. The length frequency distributions were converted to cumulative percentages and tested with the Kolmogorov-Smirnov method.

Results

The hourly capture (Table I) was very variable among the hauls but, in all cases (with the exception of the violet shrimp in hauls 50 *vs* 51), the daylight catches, both in weight (Fig. 1) and number (Fig 2), resulted consistently higher than the night catches.

In *Aristaeomorpha foliacea*, the overall mean differences were 219 *vs* 488 animals (ratio 0.45) and 5.2 kg/h *vs* 9.7 kg/h (ratio 0.53), for night and daylight respectively, and the probability of both t-tests was less than 0.001. For the violet shrimp the night yielded half the weight and number of the daylight hauls (Table I). As concerns the mean weight, in *Aristaeomorpha foliacea* the opposite trend was not as strong (Fig. 3); still, at a overall mean weight of 23.5 g in the night catch corresponded 19.8 g in daylight (ratio 1.19), with a probability for the t-test lower than 0.03 (the non-parametric sign test was only marginally significant, at 0.06). On the contrary, *Aristeus antennatus* did not show differences in size between daylight and night hauls.

The comparison of the carapace length frequency distributions also showed dramatic differences: in all the 11 sets the differences were statistically significant (Table II), with the night catches always

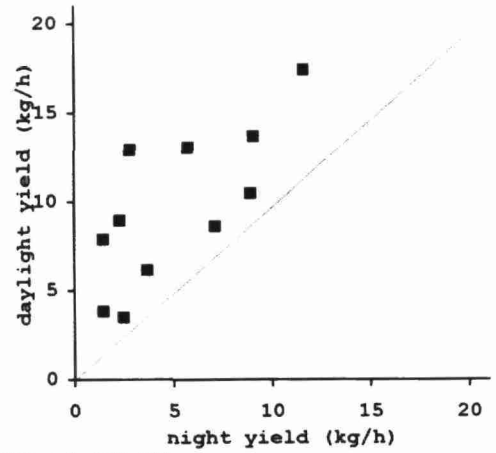

Fig. 1. Nigth *vs* daylight yields

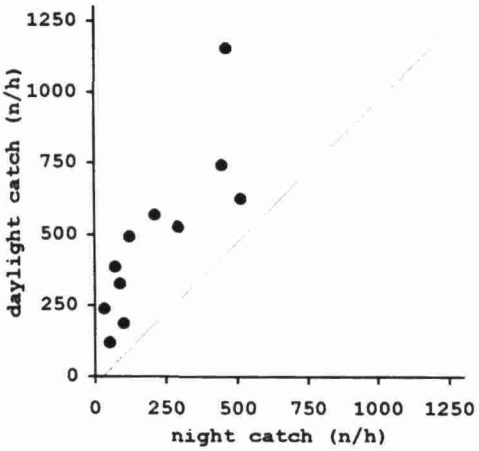

Fig. 2. Nigth *vs* daylight catches

but once trailing the daylight ones. Notwithstanding the smoothing due to the pooling, this behaviour was still visible in the combined data set (Fig. 4).

Discussion and conclusions

The common believing that red shrimps are caught more in daylight than during the night has been verified, for the seasons considered, at least; still, the values from this study are far from those (weight ratio night/daylight = 6.2%) reported by Rainer [5] for an Australian population of *Aristaeomorpha foliacea*.

Moreover, it appears that on average the captured animals are effectively larger in the night hauls; the length frequency distributions show that a relative "disappearance" from the catch of the smaller fraction is mainly responsible for this situation.

The red shrimps are not strictly benthic animals, and they normally inhabit the water layers close to the bottom being able to carry out horizontal and vertical displacements [4, 7].

ANNUAL VARIABILITY OF THE POPULATION DENSITY AND BIOVOLUME OF NON-LORICATE CILIATES IN THE KASTELA BAY

Natalia Bojanic
Institute for oceanography and fisheries, Split, Croatia

Abstract

This paper presents data on population density and biovolume of non-loricate ciliates on a station in the Kastela Bay in 1995 (20 m depth). Maxima of population density and biovolume were recorded during spring and autumn at the surface, with maxima in October (702±540 ind./ l), and September (17.34±28.43*10^6 μm^3/l respectively, while minima were recorded in February during the lowest temperatures.

Keywords: zooplankton, biomass, Adriatic Sea

Introduction

An important role in the conversion of the organic matter to the higher trophic levels in the sea belongs to bacterioplankton, protozooplankton and micrometazoa (1, 2, 3). Researches over the last two decades indicate that cca 50 % of phytoplankton cell constituents may simply bypass the traditional food chain and instead pass through a complex "microbial loop" of bacteria - flagellates - microzooplankton, which is important in rapid recycling of nutrients (4, 5, 6). The abundance of ciliates in the eutrophicated area increases with the increase of the phytomass and necromass (7, 8). Because of that, several studies on ciliates distribution in the water column, which is particularly influenced by some environmental factors (1) and predator - prey relationship were carried out (9). In the last ten years, microzooplankton researches along the eastern Adriatic coast has been intensified (8, 10, 11, 12), but data on non-loricate ciliates are sporadic. For that reason, one-year study of the density and the biovolume of the non-loricate ciliates population in the artificially eutrophicated Kastela Bay (13, 14) have been carried out for the first time.

Materials and methods

Investigations were performed at one station in Kastela Bay (43°31'N and 16°19.5'E) in 1995 (fig. 1). Samples were taken monthly (except in August and December), at 5 m intervals from surface to the bottom (20 m), with 1.7 l Nansen bottle. A 100 ml aliquot was analysed. Plankton was preserved in 2.5 % formaldehyde solution, buffered with $CaCO_3$. Samples volume was reduced by sedimentation and decanting to a volume suitable for microscopic analysis (20 ml) (10). Analysis was performed on "Olympus" IMT- 2 inverted microscope. 1/4 of the total sample was analysed in glass chamber (76-47-6 mm) at a magnification of 200 x, while dimensions were measured with an eyepiece micrometar at a 400 x magnification. Biovolume was determined by comparing the shape of the plasmatic body with the geometrical shape (15). Temperature was measured by a reversing thermometer and salinity using a induction salinometer (model RS 10).

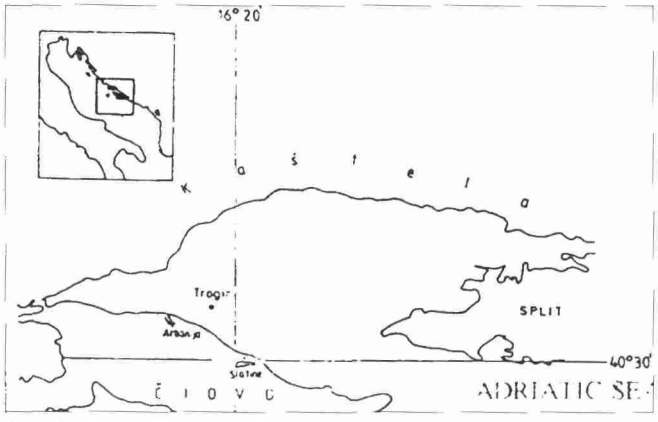

Fig. 1.Study area (The Kastela Bay).

Results

In the Kastela Bay microzooplankton community, non-loricate ciliates were present throughout the year (figs. 2 and 3), and the highest population density at the surface was recorded in September (1400 ind./l), with temperature of 21.71°C and 35.86 of salinity, while their average contribution to the total of protozoans was 80.76%. Lower densities were recorded in October at the surface and at 10 m depth where the average contribution to the total was 70.05%. Minimal population density of 40 ind./l for this group was recorded in February at 5 and 15 m depths, and in May at 20 m depth. During the year, density fluctuation at the surface was equal to 1311 ind./l, while at 15 m depth it was equal to 520 ind./l. As average 75.28% of the non-loricate ciliates abundance was found in the upper part of the water column (from the surface to 10 m depth). However, in July, the highest number of individuals was recorded at the bottom (914 ind./l). After the September mixing they arose at the surface. As the water column cooling, they sunk to 10 m depth, so that in November, only a slight difference between layers in population densities (120 ind./l) was found.

Values exceeding 10*10^6 μm^3/l of non-loricate ciliates biovolume were recorded in April, July, September and October. (Fig. 2) As for densities, two biovolume maxima were recorded, the first in April (12.17±10.00*10^6 μm3/l) and the second in September (17.34±11.09*10^6 μm^3/l, while the lowest average value was found in February (1.69±1.33*10^6 μm^3/l). Measured biovolume values ranged from 0.02*10^6 μm^3/l (recorded in May at 20 m depth) to 39.58*10^6 μm^3/l which was recorded at the same depth in July, with temperature of 14.59(C and 38.24 of salinity. Biovolume differences between surface and bottom were most evident in July (39.26*10^6 μm^3/l), while in February they were only 3.16*10^6 μm^3/l. Annual fluctuation of biovolume values varied from 6.03*10^6 μm^3/l at 15 m depth to 39.56*10^6

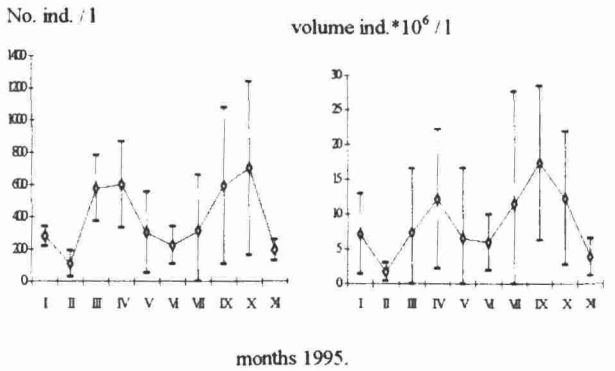

Fig. 2. The average population density and biovolume ($\mu m^3 l^{-1}$) of non-loricate ciliates at the station Trogir in 1995.

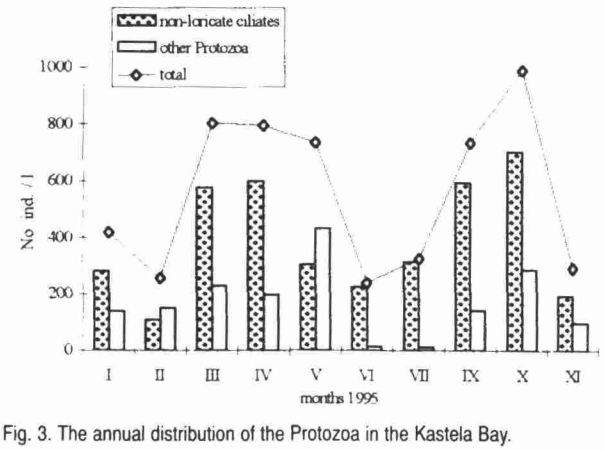

Fig. 3. The annual distribution of the Protozoa in the Kastela Bay.

LE MERLU DES CÔTES ALGÉRIENNES : IDENTIFICATION ET CROISSANCE

A. Bouaziz [1*], A. Bennoui [1], C. Maurin [2], F. Djabali [3]

[1] ISMAL B. P. 54 Sidi Fredj Staouali 42321, Tipaza, Algérie
[2] L'Aumandière, 85390 Bazoges en Pareds, France
[3] IFREMER Brest B. P. 70 29280, Plouzané, France

Résumé

L'augmentation, d'ouest en est, de la moyenne vertébrale et de l'indice Lcpl / Lp a permis de distinguer le merlu des côtes algériennes, qui ne semble pas effectuer de grandes migrations horizontales, de celui de l'Atlantique. En outre, l'analyse des fréquences de tailles montre que la longévité des femelles (9 ans) est nettement supérieure à celle des mâles (5 ans). Dans le bassin algérien, le merlu de la région centre de la côte algérienne croît de la même façon que celui de la mer Tyrrhénienne et moins vite que celui de la rive nord de la Méditerranée occidentale (îles Baléares et golfe du Lion).

Mots clés : Fishes, Demersal, Growth, Algerian Basin

Introduction

Afin d'infirmer ou de confirmer les observations faites (1, 2) à savoir, la validation de la sous-espèce méditerranéenne (*Merluccius merluccius mediterraneus* Cadenat, 1950), il a été jugé utile d'étudier les caractères métriques et numériques de ce poisson le long des côtes algériennes, du fait de leur importance dans la détermination des espèces, sous-espèces, races ou groupements. Dans la région centre de la côte algérienne comprise à l'est (3°10'E) et le mont Chenoua à l'ouest d'Alger (2°20'E), le merlu n'est plus aussi bien représenté que par le passé : un déclin des quantités de *Merluccius merluccius mediterraneus* (Cadenat, 1950) débarquées à Bouharoun, considéré comme l'un des plus grands ports de pêche en Algérie, a été constaté, et ce depuis une dizaine d'années : sa production annuelle a baissé de moitié depuis 1987 pour atteindre 31 128 Kg en 1993 (laboratoire halieutique de l'Institut des Sciences de la Mer et de l'Aménagement du Littoral - ISMAL, 1995). A cet effet, l'étude de la croissance a été entreprise par l'analyse des fréquences de tailles, dont les paramètres sont des éléments d'entrée essentiels dans les modèles de dynamique des populations.

Matériel et méthodes

En complément des données obtenues par le navire océanographique français (*Thallassa*) en juin 1982, des sorties mensuelles ont été réalisées à bord d'un chalutier professionnel en baie de Bou Ismail (de novembre 1987 à novembre 1988). Par ailleurs, ces observations ont été associées à celles du laboratoire halieutique de L'ISMAL recueillies entre 1987 et 1993 le long des côtes algériennes. La quasi totalité des apports provient du plateau continental entre 50 et 200 m. Pour l'étude des caractères métriques et numériques, des mensurations et des dénombrements ont été effectués (3), parmi lesquels seuls le rapport Lcpl/Lp (longueur de la tête/longueur de la nageoire pectorale) et le nombre de vertèbres, dont le comptage s'est effectué du condyle occipital exclu à lurostyle inclus, présentent un intérêt dans la détermination des sous-espèces et groupements raciaux (4). Enfin, le test de l'écart-réduit $|\varepsilon|_{Cal}$, donné ci-après, basé sur la comparaison de deux pentes (5) a été introduit afin de confirmer ou d'infirmer le type d'allométrie de la relation :

$$Wev. = aL^b ; \quad |\varepsilon|_{Cal.} = \frac{|P - P_0|}{S_{P_0}} ; \quad S^2_{P_0} = \frac{\left(\frac{Sy}{Sx}\right)^2 - P_0^2}{N-2}$$

P: pente théorique ; P_0 = pente calculée par la méthode des moindres carrés; S_{P0} = écat-type de la pente calculée, avec : Sy = écart-type des W_{ev}; Sx = écart-type de L_T; N = nombre des couples de valeurs (W_{ev}, L_T).

Suite aux recommandations de la première réunion du groupe de travail DYNPOP tenue à Tunis en 1994, la méthode des différences logarithmiques (6) et le programme Fishparm (7) ont été utilisés respectivement pour la détermination des groupes d'âges de la population et les paramètres de croissance linéaire de 3269 femelles de tailles comprises entre 6,5 et 66,5 cm et de 3254 mâles de longueurs moyennes allant de 6,5 à 46,5 cm regroupés en classes de tailles de 2 cm. Les jeunes individus à sexe indéterminé, dont la taille est inférieure à 11 cm, ont été comptabilisés avec les deux sexes afin d'avoir une meilleure estimation de l'âge des juvéniles.

Résultats

Caractères métrique et numérique

Indice Lcpl / Lp. Les résultats obtenus montrent une augmentation graduelle de cet indice d'ouest en est (l'écart-réduit $|\varepsilon|_{Cal} = 2.69$, $\alpha = 5\%$, entre Béni-Saf et Skikda), c'est-à-dire une légère diminution de la taille relative de la pectorale par rapport à celle de la tête, autrement dit une augmentation du caractère méditerranéen d'ouest en est (Table 1).

Table 1. Evolution de l'indice Lcpl / Lp par région. (R. P. = Résultats personnels)

Région	Béni-Saf (R.P.,1993) (35°18'N; 1°23'O)	Boulsmail (3) (36°38'N; 2°40'E)	Skikda (3) (36°52'N; 6°54'E)
Lcpl/Lp	1.78	1.82	1.86
Effectif	88	313	70
Précision (α=5%)	0.03	0.02	0.05

Nombre de vertèbres. Les résultats montrent une augmentation graduelle et significative de la moyenne vertébrale d'ouest en est (Table 2).

Table 2. Moyennes vertébrales par région et résultats du test de l'écart-réduit ($|\varepsilon|_{Cal}$) pour le merlu des côtes algériennes.

Région		Moyenne vertébrale	Intervalle de confiance (α= 5%)	$\lvert\varepsilon\rvert_{Cal}$ (α= 1%)	Effectif
Beni-Saf	1	51.16	0.13	2.64 (1/2)	124
Bou Ismail	2	51.36	0.07	2.88 (2/3)	505
Skikda	3	51.66	0.19	4.24 (1/3)	53

Age et croissance du merlu de la region centre de la côte algérienne. La méthode des différences logarithmiques (6) décompose l'échantillon en 9 cohortes femelles et 5 cohortes mâles (Table 3), à chacune d'elles correspond une taille (μ) et un écart-type (S). La première taille obtenue lui a été attribuée l'âge 1 (8).

Table 3. Clé âge-longueur obtenue par la méthode de Bhattacharya (1967) pour les merlus femelles et mâles de la région étudiée. h = pas (2cm).

Sexe	Age	1	2	3	4	5	6	7	8	9
	(F	15	22.8	30.1	37.1	43.2	47.4	51.6	57.1	57.8
Femelle	SF	2.42	2.62	5.67	2.84	1.16	2.03	2.27	2.38	3.42
	h/S.≤2.2	0.83	0.76	0.35	0.70	1.24	0.99	0.88	0.84	0.58
	(M	14.4	23.4	30.2	36.7	38.6				
Mâle	SM	2.16	2.60	2.16	2	2.16				
	h/S≤2.2	0.93	0.77	0.93	1	0.93				

Le calcul des paramètres de croissance linéaire de l'équation de Von Bertalanffy conduit aux expressions suivantes :

femelles : $L_t = 80.64\ (1\text{-}e^{-0.139(t+0.442)})$;

mâles : $L_t = 48.72\ (1\text{-}e^{-0.321(t+0.0749)})$.

Les équations de la relation taille-poids sont résumées dans la Table 4 :

Table 4. Equations de la relation taille-poids des merlus femelles et mâles de la région étudiée.

Sexe	Relation	Effectif	r	$\lvert\varepsilon\rvert_{Cal}$, α = 1%	Type d'allométrie
Femelle	$W_{ev} = 0.00655\ L^{2.99}$	200	0.9466	0.071	Isométrie
Mâle	$W_{ev} = 0.00443L^{3.11}$	133	0.9917	0.502	Isométrie

Enfin, la combinaison de l'équation de croissance linéaire de Von Bertalanffy et la relation taille poids aboutit à l'équation de croissance pondérale qui s'écrit :

REGIME ALIMENTAIRE DE *SPONDYLIOSOMA CANTHARUS, DIPLODUS PUNTAZZO* ET *D. VULGARIS* (TELEOSTEI, SPARIDAE) DANS LE GOLFE DE GABES, TUNISIE

Mohamed Nejmeddine Bradai [1], Mohamed Ghorbel [1]*, Othman Jarboui 1 et Abderrahmen Bouain [2]

[1] Institut National des Sciences et Technologie de la Mer, Centre de Sfax, B.P. 1035, 3018 Sfax, Tunisie
[2] Faculté de Sciences, 3038 Sfax, Tunisie

Résumé

Les trois espèces étudiées ont une prédilection pour les organismes benthiques des herbiers peu profondes. Toutefois, l'essentiel de leurs bols alimentaires varie beaucoup d'une espèce à l'autre. *Spondyliosoma cantharus* ingère de préférence les mollusques céphalopodes, les poissons et les crustacés. Le régime alimentaire de *Diplodus puntazzo* est basé principalement sur les végétaux et les spongiaires. Les proies préférentielles de *D. vulgaris* sont les mollusques bivalves et les crustacés.

Mots-clés : Teleostei, diet, Gulf of Gabès

La dorade grise *Spondyliosoma cantharus*, le sar à museau pointu *Diplodus puntazzo* et le sar à tête noire *D. vulgaris* sont capturés principalement par la pêche artisanale. Leurs débarquements sont irréguliers et relativement peu importants et coïncident essentiellement avec leurs périodes de reproduction.

Les études concernant le régime alimentaire sont, à notre connaissance, inexistantes dans la région du golfe de Gabès qui est considérée comme la première zone de pêche maritime en Tunisie.

Dans cette note, nous donnons la liste des proies contenues dans les estomacs et nous déterminons le coefficient de vacuité. L'aspect quantitatif des proies ingérées est abordé par le calcul de certains indices alimentaires.

Matériel et méthodes

Nous avons utilisé pour cette étude 467 individus de *S. cantharus* de longueur standard (LS) comprise entre 64 mm et 236 mm, 317 *D. puntazzo* entre 93 et 270 mm de LS et 523 *D. vulgaris* mesurant de 63 à 251 mm. Les proies des estomacs pleins ont été déterminées et pesées. Les estomacs vides ont été notés. Le régime alimentaire a été analysé par :

- le coefficient alimentaire (Q) proposé par Hureau (1). Cette méthode tient compte du nombre et de la masse des proies ingérées.

$$Q = Cn\% \times Cp\%$$

$$Cn\% = \frac{\text{Nombre d'individus de chaque item i}}{\text{Nombre total des proies}} \times 100$$

$$Cp\% = \frac{\text{Masse de l'item i}}{\text{Masse totale des proies}} \times 100$$

- la méthode de Geistdoerfer (2) qui tient en outre de l'indice de fréquence d'une proie (F) :

$$F = \frac{\text{Nombre d'estomacs contenant l'item i}}{\text{Nombre total d'estomacs pleins}} \times 100$$

Nous avons également déterminé le coefficient de vacuité moyen de Chaque espèce (Cv) :

$$Cv = \frac{\text{Nombre d'estomacs vides}}{\text{Nombre d'estomacs examinés}} \times 100$$

Résultats

Variations du coefficient de vacuité

Les coefficients de vacuité moyens de *Spondyliosoma cantharus*, *Diplodus puntazzo* et *D. vulgaris* sont respectivement de 61,46, 59,31 et 88,91. Ils sont élevés comme cela a été constaté d'ailleurs pour d'autres Sparidae (3 et 4). Nous pensons que le coefficient de vacuité est essentiellement le reflet de la méthode de pêche et de la durée d'exposition au marché; les filets sont en général posés le soir et relevés le matin et parfois même le lendemain, les animaux ont eu le temps de digérer.

Nature des contenus stomacaux

Nous avons identifié et regroupé par ensemble systématique 288 proies représentant au total 263,81 g chez *Spondyliosoma cantharus*, 193 proies (234,62 g) chez *Diplodus puntazzo* et 66 proies (33,41 g) chez la troisième espèce. Le nombre moyen des proies par estomac et leur masse moyenne sont respectivement de 1,60 et 0,92 g pour la première espèce, de 1,50 et 1,22 g pour la seconde et 1,14 et 0,51 g pour la dernière.

A partir du calcul du coefficient alimentaire Q et de l'indice de fréquence F (Tabl. 1), nous avons établi le classement des différentes proies (Tabl. 2). Nous avons établi également une liste exaustive des proies ingérées par les trois espèces (Tabl. 3).

Tableau 1. Valeurs des indices alimentaires; S.c.(1); D.d.(2); D.v.(3).

PROIES	Esp.	Cn%	Cp%	Q	F%
Spongiaires	2	27,98	39,89	1116,12	41,86
	3	01,52	00,80	01,22	01,72
Annélides	1	12,50	08,37	104,63	10,00
	2	01,55	00,35	0,548	02,33
	3	10,61	05,21	55,28	06,70
Mollusque	1	28,82	53,33	1536,97	45,00
	2	03,63	03,64	13,21	05,44
	3	33,33	32,42	1080,56	37,93
- Bivalves	1	02,43	02,45	05,95	03,89
	2	02,59	02,63	06,81	03,88
	3	22,73	22,18	504,15	25,86
-Gastéropodes	1	01,74	01,54	02,68	01,67
	2	00,52	00,26	00,14	00,78
	3	03,03	01,86	05,64	01,72
-Céphalopodes	1	25,69	48,83	1254,44	41,11
	2	00,52	00,65	0,39	00,78
	3	04,54	04,61	20,93	05,17
Crustacés	1	02,43	08,55	246,41	22,78
	2	05,70	10,18	58,03	08,53
	3	25,76	42,65	1098,66	27,59
Echinodermes	1	02,43	01,00	02,43	02,78
	2	04,15	06,78	28,14	06,20
	3	04,54	03,62	16,43	05,17
Ascidies	1	00,69	00,25	00,17	01,11
	2	07,25	14,78	107,16	10,85
	3	01,52	01,50	02,28	01,72
Poissons	1	12,15	20,81	252,84	19,44
	2	01,04	02,18	02,27	01,55
Végétaux	1	07,29	02,87	20,92	11,67
	2	41,97	66,65	2797,30	62,79
	3	01,52	00,27	00,41	01,72

Nous constatons que les deux méthodes donnent pratiquement les mêmes résultats pour les trois espèces. Pour *Spondyliosoma cantharus*, les mollusques et principalement les céphalopodes avec l'espèce *Sepia officinalis* (Q = 1028,06 ; F = 36,11) viennent en tête de liste des proies préférentielles. Les poissons et les crustacés sont également classés dans cette catégorie de proies. Toutefois, ces deux dernières proies et les Annélides sont des proies principales occasionnelles selon la méthode de Geistdoerfer (2). D'après la méthode de Hureau, les Annélides sont considérés avec les végétaux comme proies secondaires. Les échinodermes, les ascidies et les mollusques gastéropodes et bivalves sont des proies accessoires. Le régime alimentaire de la dorade grise est donc basé principalement sur les seiches *Sepia officinalis;* d'ailleurs les pêcheurs locaux appellent ces poissons "les mangeurs de seiche".

PRESENCE DE LA TORTUE LUTH *DERMOCHELYS CORIACEA* DANS LES EAUX TUNISIENNES

Mohamed Nejmeddine Bradai[1*] et Amor El Abed [2]

[1] INSTM, B.P.1035, 3018 Sfax, Tunisie

[2] INSTM, 28, rue du 2 mars 1934 , 2025 Salammbô, Tunisie

Résumé

Trente cinq observations de la tortue luth *Dermochelys coriacea* ont été enregistrées sur les côtes tunisiennes (captures accidentelles et échouages) dont 10 sont nouvelles. Ces observations ont concerné toutes les côtes tunisiennes et tous les mois de l'année avec un maximum de distribution pendant la période été-automne. Cette distribution serait en relation avec celle de la méduse *Rhizostoma pulmo*. Ces tortues adultes sont souvent accompagnées par le poisson pilote *Naucrates ductor*.

Mots clés : turtles, migration, gulf of Gabes

La tortue luth *Dermochelys coriacea*, espèce pélagique des eaux chaudes et tempérées des océans atlantique, indien et pacifique (1), se rencontre en petit nombre en Méditerranée. Le nombre des observations tend à diminuer considérablement de l'Ouest à l'Est de cette mer (2). Ce comportement est d'ailleurs commun à toute espèce atlantique s'introduisant en Méditerranée. D'après les mêmes auteurs, les tortues luth pénètrent en Méditerranée au printemps. Le maximum des observations est enregistré pendant la période été-automne surtout en Méditerranée occidentale et centrale. Vers le mois d'octobre commence la migration inverse vers l'Atlantique. Ce schéma migratoire est en relation étroite avec celui des courants atlantiques. Toutefois, il est à noter que beaucoup d'observations ne sont pas signalées et un effort doit être fait dans ce sens par chaque pays méditerranéen. Dans ce cadre, nous essayons de présenter et analyser les informations concernant ce reptile dans les eaux tunisiennes.

Le nombre total d'observations de la tortue luth dans les eaux tunisiennes s'élève actuellement à 35 dont 11 sont relativement anciennes, signalées de 1907 à 1965, 14 relativement récentes observées de 1978 à 1987 (Tableau 1) et 10 sont signalées pour la première fois dans ce travail et concernent la période 1990-96 (Tableau 2). Le nombre relatif d'observations est en nette augmentation d'une période à l'autre ce qui refléterait un effort de signalisation de plus en plus important. A cet effet, nous nous intéressons plus particulièrement aux données enregistrées depuis 1985 et dans la région du golfe de Gabès où nous avons concentré notre effort d'observation depuis cette date.

Tableau 1. Compilation des données bibliographiques concernant les observations des tortues luth *Dermochelys coriacea* dans les eaux tunisiennes.

AUTEURS	DATES	LIEU	SEXE	Lt (m)	OBSERVATIONS
(6)	1907	Golfe Tunis			
(7)	juin 1930	Sidi Daoud		2,00	
(7)	13/09/30	Gabès**		2,10	
(7)	17/05/33	Monastir	F	1,50	
(7)	27/05/33	Gabès**	F	1,95	
(7)	03/06/33	Sidi Daoud	M	1,80	
(8)	18/04/50	Sfax**	F	1,67	
(9)	jav. 1955	Sfax**			
(9)	fév. 1955	Sousse			
(9)	fév. 1955	Bizerte			
(10)	dec. 1965	Kélibia		1,80	Morte après 24 h dans les bassins de l'INSTOP
(11)	1978	Djerba**			Echouage
(4)	09/09/83	Golfe Tunis		1,40*	Filet trémail (25 m de prof.) *R.remora* sur la carapace
(4)	23/11/83	Hammamet		1,60*	dans une pélamidère par 6m de pof.
(4)	10/12/83	Kélibia	M	1,67*	Filet trémail
(12)	21/08/85	Djerba**	M		TSCL = 1,67 m
(12)	dec.85	Golfe Tunis			
(12)	dec.85	Golfe Tunis			
(12)	dec.85	Ghar melh			
(12)	août 86	Ksibet			
(12)	11/11/86	Sidi Raïs			
(12)	dec 87	Kélibia			
(12)	25/03/87	Djerba**		1,45*	Pêche côtière
(12)	avril 87	Monastir			
(12)	02/07/87	Skhira**		1,49*	Vivante ds filet trémail

* SCCL ; ** région du golfe de Gabès

Les tortues signalées sont essentiellement capturées accidentellement par les engins de pêche côtière tels que filets trémail et filets maillants dérivants par des faibles profondeurs. Deux tortues luth ont été capturées récemment par le chalut benthique. Les échouages sont peu fréquents. Depuis la fin des années 80, le lâcher en mer de ces animaux, protégés par la législation tunisienne, est devenu une pratique courante.

La longueur des tortues mentionnées dans la littérature est généralement mal définie. La longueur courbe standard de la carapace (SCCL) des 11 spécimens que nous avons pu observer et mesurer, varie de 1,29 m à 1,80 avec une moyenne de 1,52 m. Toutes les tortues observées sont adultes. La distribution des juvéniles de cette espèce est en effet largement inconnue (3).

Les tableaux 1 et 2 récapitulent toutes les informations disponibles concernant les 35 observations. D'après ces tableaux, nous constatons que la tortue luth est observée sur toutes les côtes tunisiennes et principalement à l'est et au sud du pays (golfe de Gabès), côtes qui coïncident avec le bassin oriental de la Méditerranée. Les observations ont été réparties tout au long de l'année avec un maximum pendant la période été-automne dans la région du golfe de Gabès et pour les données postérieures à 1985, constatation déjà faite pour toute la Méditerranée (2). Cette constatation serait en partie en relation avec l'apparition en cette période de la méduse *Rhizostoma pulmo* sur nos côtes. Cette méduse est en effet une proie préférentielle de la tortue luth (2).

Ces tortues marines sont des hôtes préférentiels pour deux espèces de rémora *Remora remora* et *Echeneis naucrates* qui adhèrent à leurs carapaces (4 et 3). Pour trois de nos récentes observations, nous avons constaté que la tortue luth est accompagnée par les poissons pilotes *Naucrates ductor*, poisson carangidé présentant une relation de commensalisme semi-obligatoire avec quelques grands poissons comme le requin pèlerin *Cethorhinus maximus* (5). Les deux tortues capturées au chalut le 10/11/94 et le 27/11/96 ont été accompagnées respectivement par 2 et 3 poissons de cette espèce mais la quantité qui a accompagné la tortue luth capturée à Kerkennah le 23/10/96 au filet maillant dérivant "Mernine" était spectaculaire ; 140 Kg dans les filets et environ 400 Kg pêchés dans le bassin du port El Kratten où la tortue a été tractée avant d'être relâchée.

Tableau 2. Nouvelles mentions de *Dermochelys coriacea* dans les eaux tunisiennes.

DATES	LIEU	SEXE	SCCL(m)	ENGIN	OBSERVATIONS
18/04/90	Ellouza**	F	1,50	Trémail	10-15 m de prof.; blessée
27/06/90	Boughrara**		1,80	P.côtière	
10/07/91	Ghannouch**		1,40		Echouée morte
12/11/91	Sidi Mansour**	M	1,60	F maillant dérivant	Prof. 6 m
10/11/94	Golfe de Gabès**			Chalut benthique	60 m de prof., avec 3 poissons pilotes
07/05/96	Sousse			P.côtière	
03/06/96	Skhira**		1,90*		
juillet 96	H.Chott				Echouage rapporté dans la presse
23/10/96	Kerkennah**		1,47	F maillant dérivant	Accompagnée par un banc de *N.ductor*
07/11/96	G. Gabès**	M	1,29	Chalut benthique	La tortue et 2 *N.ductor* ds filets

PLANKTONIC OSTRACODS OF THE SOUTH ADRIATIC BASIN

Igor Brautovic

Institute of Oceanography and Fisheries, Laboratory of Plankton Ecology, P.O. Box 39, HR - 20101 Dubrovnik, Croatia

Abstract

Planktonic ostracods of the South Adriatic basin were investigated by the m/b *Bios* at five fixed stations in five seasonal cruises from 20 April 1993 to 22 February 1995. Fifteen species have been registered: *Conchoecia spinirostris, C. porrecta adriatica, C. porrecta, C. magna, C. curta, C. procera, Archiconchoecia striata,* and for the first time in the Adriatic, *Conchoecia echinulata, C. microprocera, C. macroprocera, C. elegans, C. rotundata, C. spinifera, C. loricata and C. rhynchena*. The greatest number of them is present in winter period, and the highest total value of 8.05 specim./m^3 has been registered at the P - 300 station, in the 200 - 100 m layer.

Key-words: Adriatic Sea, zooplankton, vertical migration

Introduction

Planktonic ostracods in the Adriatic sea have not been sufficiently investigated so far. Claus (1) was the first one to note down the existence of planktonic ostracods in the North Adriatic. Not far away from Trieste he discovered the species *Conchoecia spinirostris*. In the investigating expedition Rudolf Virchow, Schweiger (2) found four species of ostracods: *C. spinirostris, C. procera, C. curta* and *Archiconchoecia striata*, and he concluded that their number was decreasing from the south to the north. In the Central Adriatic Gamulin (3, 4) registered *Archiconchoecia striata* and *C. spinirostris*. Besides these two species Hure (5, 6) found *C. claussi* G.O. Sars (= *C. curta* Lubbock), *C. magna* and *C. procera*. Gooday and Angel (7) described a new subspecies in the North Adriatic - *Conchoecia porrecta adriatica*.

In this work some preliminary data on the qualitative structure, abundance and distribution of planktonic ostracods in the South Adriatic basin are given.

Material and methods

Planktonic samples have been collected during five cruises at five fixed stations in the eastern part of the South Adriatic basin (Fig. 1) by the motor-boat *Bios* in the following periods: 20 - 21 April 1993; 16 - 17 September 1993; 26 - 27 February 1994; 17 - 18 June 1994; 21 - 22 February 1995. The stations are located at the following hydrographic co-ordinates:

P - 100: 42°38.5' N 18°02.0' E; P - 100A: 42°44.0' N 17°15.0' E;
P - 300: 42°27.0' N 17°53.0' E; P - 300A: 42° 32.0' N 17°29.0' E;
P - 1000: 42°44.0' N 17°15.0' E.

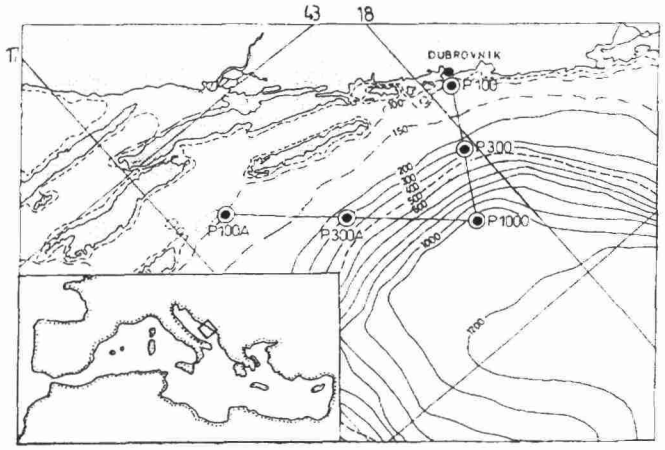

Fig. 1. Location of investigation stations.

For the collecting of samples a Nansen type net (diameter 114 cm, length 380 cm) with the mesh netting of 250 μm and equipped with a closing mechanism was used. The samples were collected by vertical hauls above the depths of 100, 300 and 1000 m, in the layers of 0 - 50, 50 - 100, 100 - 200, 200 - 300, 300 - 400, 400 - 600, and 600 - 1000 m.

As the samples were collected, several hydrological parameters - temperature, salinity, nutrition salts and dissolved oxygen - were also recorded. A total of 17.380 specimens of planktonic ostracods were isolated in night and daily series. The samples have been examined in the Laboratory of Plankton Ecology, using "Wild" and "Carl Zeiss" microscope. Species densities were expressed as number of specimens/100 m^3, except for *Archiconchoecia striata* (specimens/m^3).

Results and discussion

In the zooplanktonic sampled during the five cruises of the m/b *Bios*, a total of fifteen species of planktonic ostracods have been identified: *Conchoecia spinirostris, C. porrecta adriatica*, C. porrecta, *C. magna, C. curta, C. procera* and *Archiconchoecia striata* already registered before, as well as the species: *Conchoecia echinulata, C. microprocera, C. macroprocera, C. elegans, C. rotundata, C. spinifera, C. loricata* and *C. rhynchena*, which are mentioned for the first time for the Adriatic sea fauna.

All the species are always present only at the deepest station and going towards the coast the number of species is diminishing. At the shallow stations (Fig. 2.1. and 2.2.) ostracods are more numerous in deeper layer in all seasons. The most numerous one is *Archiconchoecia striata*, the smallest Adriatic ostracod with the highest value of 3.4 specim./m^3 in September 1993 at the P-100 A station, depth 100 - 50 m. It is also the maximal number of specimens of a particular species registered so far.

C. spinirostris is most abundant in 200 - 50 m depth. Maximal number was found in April 1993 at P-1000 station, depth 200-100 m: 52 females, 42 males and 284 juveniles. Beneath 300 m is rare, represented particularly with adult females and males, rarely juveniles.

C. porrecta adriatica according to Angel (7) makes up 78.42 % of the ostracod fauna of the North Adriatic. In South Adriatic it is rare. The maximal number of specimens was collected in February 1995 at P-300 station, depth 100-50 m: 14 females, 6 males and 8 juveniles.

C. porrecta is also rare. In depth 200 - 50 m there were single juvenile females A1, and some adult females. Only one male specimen was found.

C. magna is large and well recognizable ostracod. It lives in the depth between 200 and 100 meters. It was represented with 3-4 specimens, and numerous juveniles.

C. curta is most abundant in depth 200-50 m. Maximal number was found in February 1995 at P-300 A station, depth 100-50 m: 26 females, 34 males and 28 juveniles. According to Deevey (8), *C. curta* forms denser populations between 100 and 400 m. In Adriatic its median level is 145 m (6).

C. echinulata has a similar shape as *C. curta*, but it is smaller. This species has just 5 pegs on the e - seta of the first antenna, *C. curta* has 8. Only two adult females were found.

C. procera is more abundant species then the previous one. The biggest part of population exists on the depth 300-50 m. Between 600 and 300 m it is also possible to find, but deeper then 600 m it was noted very rare, only as singles. Maximal number was found in April 1993 at P-1000 station, depth 300-200 m: 18 males, 17 females and 29 juveniles.

C. microprocera is smaller then *C. procera*. Maximal number is found in depths 300-50 m, but can be found as single specimen in deeper layers till 1000 m. In February 1995 at P-1000 station, depth 100-50 m, 12 females, 10 males and 42 juveniles were found.

C. macroprocera is abundant in the depths 300-100 m. Maximal number was recorded in February 1994 at P-300 station, depth 200-100 m: 25 females, 50 males and 32 juveniles.Instead of Adriatic species: *C. microprocera* and *C. macroprocera* a new recording from Tyrrhenian and Ionian seas (9) shows existence of *C. procera procera* and *C. procera mediterranea*.

C. elegans, the main population is between 400 and 300 m depth. At shallow stations P-100 and P-100A was found at the bottom of the water column. Maximal number was recorded in February 1994 at P-300 station, depth 300- 200 m: 77 females, 31 males and 119

OBSERVATIONS ON THE BIOLOGY OF *GYMNAMMODYTES CICERELLUS* (RAF. 1810) FROM THE LIGURIAN SEA (NORTH-WESTERN MEDITERRANEAN)

Bussotti S.[1], Bavastrello G.[1], Guidetti P. [1]*, Repetto N.[2]

[1] Istituto di Anatomia Comparata dell'Università di Genova, Viale Benedetto XV 5, 16151 Genova, Italy
[2] R.S.T.A., Viale Brigate Liguria 105r, 16121 Genova, Italy

Abstract

A total of 3133 specimens (larvae and adults) of *Gymnammodytes cicerellus*, collected between June 1995 and June 1996 with nets off the western coast of the Ligurian Sea (North-Western Mediterranean), were analyzed. Total length and weight were measured in order to obtain size-frequency distributions and the size-weight relationship. The reproductive period, evaluated by the annual trend of the Gonadosomatic Index, was observed from December to March with a peak in February, when larvae and recruits occurred too. The sex ratio showed a prevalence of females.

Key-words: fishes, reproduction, spawning, recruitment, Ligurian Sea

Introduction

In the Mediterranean Sea the Ammodytidae family is represented by two species both belonging to the same genus, Gymnammodytes. Since few years ago, only *Gymnammodytes cicerellus* was known to be present in the mediterranean basin. Nevertheless, Sabatés *et al.* (1) collected for the first time larvae and adult specimens of *Gymnammodytes semisquamatus* off the Catalan coast (NW Mediterranean). The differences between the two species are based on morphological, meristic and pigmentation characteristics of larvae and adults (1, 2). *G. cicerellus*, which is characterized by a gregarious behaviour, is mainly distributed in the Mediterranean and Black seas, and along the coasts of Portugal, Marocco and Senegal (3, 4). A detailed morphological description of the species can be found in Tortonese (3) and Sabatés *et al.* (1). This species, whose reproductive biology is poorly known, represents a resource for a small-scale fishery in various areas of the Western Mediterranean (Ligurian: present work; Sicilian: 5, 6, Catalan: 7, French coasts: 8).

In this study we report data on various aspects of the biology of *G. cicerellus* in the Ligurian Sea in order to provide information for a rational exploitation of this fishery resource.

Materials and methods

Samples of *G. cicerellus* were collected at Noli (SV, Ligurian Sea: 44°13' N, 08°25' E; Fig. 1). A total of 8 samplings were carried out between June 1995 and June 1996 using a trawler with a mesh size at the cod-end of 3 mm. The collected specimens were immediately frozen and then processed in laboratory. The identification of larvae and adults was based on Sabatés *et al.* (1). Overall 3133 specimens were measured for total length (TL) and total weight. Gonad weight was also measured for a representative subsample and the gonadosomatic index was calculated (G.I.=gonad weight/ total weight x 100). Sex identification was made macroscopically, while, when the macroscopical observation was not clear, a solution of 0.1 M Toluidine Blue was employed. Thus, sex ratio was determined for all samples.

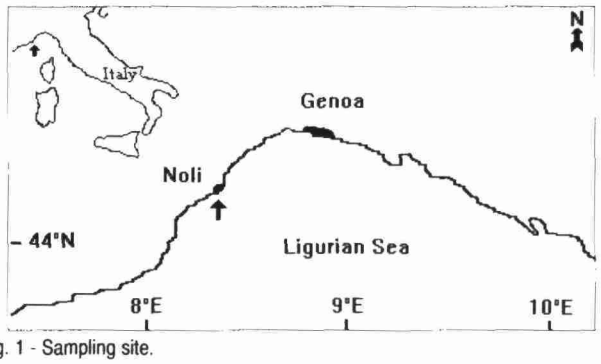

Fig. 1 - Sampling site.

Results

The length-frequency distribution is shown in Fig. 2. The different cohorts throughout the study period are easily identified. Total length ranged between 2 and 15 cm, although specimens longer than 12.5 cm were very scarce. In the catches of February and March 1996, two new cohorts occurred; probably, they must be considered as two subcohorts belonging to the same reproductive event. Young specimens appeared in February 1996 included larvae (mean length: 2.66 ± 0.31cm) and recruits (mean length: 4.95±0.20 cm). Compared to the successive year (Fig. 2), in the sample of June 1995, juveniles deriving from the reproductive season 1994-95 were not present.

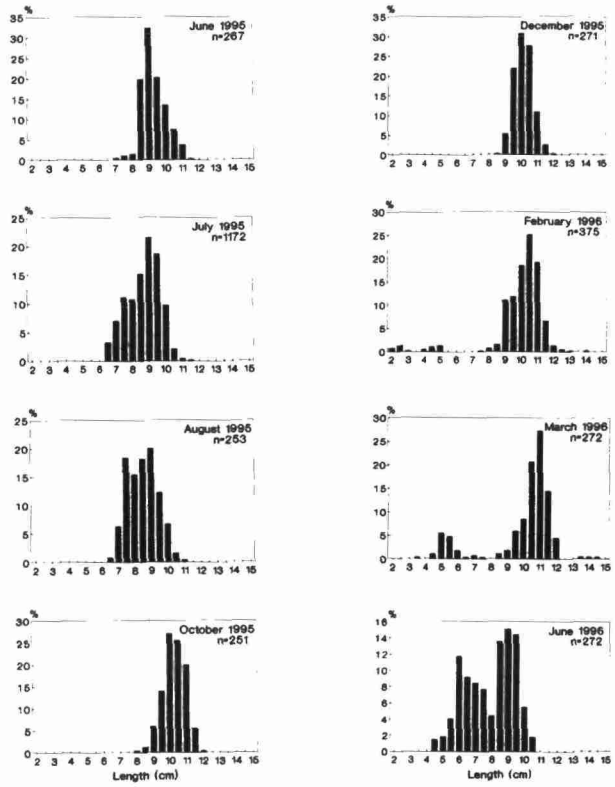

Fig. 2 - Length-frequency distributions of *Gymnammodytes cicerellus*.

Overall, 2211 specimens were used for the computation of the length-weight relationship. The resulting equation is: $W = 0.0022\ L^{3.075}$; $r = 0.97$, $P < 0.001$, where W = weight in grams, L = total length in cm, r = regression coefficient and P = significativity level (Fig. 3).

The cyclic trend of the G.I. (Fig. 4) showed that the reproductive period occurred approximately from December to March with a maximum spawning activity in February. Furthemore, females matured at a slightly smaller size (8.5 cm) than males (9 cm).

Based on the analyzed gonads, 46 males (6.8 %) and 111 females (16.4 %) were identified; this indicates that the bulk of specimens (522, 76.8 %) were undetermined (all individuals in the samples of June, July 1995 and June 1996). In any case, the overall sex ratio (males:females) was found to be 0.41, with a clear prevalence of females.

Five accessory species (*Pagrus pagrus, Pagellus acarne, Atherina sp., Mullus surmuletus, Sardina pilchardus*) were collected in July and August 1995 together with *G. cicerellus*, which represents the target species of this peculiar kind of fishery. All specimens resulted juveniles, but negligible in terms of number of individuals or percentage in weight, except for *Sardina pilchardus* in the sample of July.

IS THE LEATHERBACK (*DERMOCHELYS CORIACEA* VANDELLI, 1761) A PERMANENT SPECIES IN THE MEDITERRANEAN SEA ?

Juan A. Camiñas

Malaga Oceanographic Center, Spanish Institute for Oceanography, P. O. Box. 285; 29640 Fuengirola, Spain

Abstract

Dermochelys coriacea is a marine turtle that appears, according to the literature, in the Mediterranean Sea for many centuries. The authors agree on the non existence of reproduction in beaches of this Sea, although many specimens are present during the reproduction period within the Mediterranean. Leatherbacks can travel long distances, and tagging experiences register specimens from Guyana along the Atlantic European coast, mainly in France, Spain and Portugal. Migratory paths to this Atlantic border indicate the entry of the species into the Mediterranean Sea. New data of incidental fishing captures and strandings in the Western Mediterranean Sea indicate the importance of *Dermochelys coriacea* in the Mediterranean, where it is present all around the year. Western Mediterranean new data presented in this paper confirms the presence of the species near Gibraltar Strait mainly during the first and last months of the year and the presence in higher number at the Balearic Sea during summer and autumn. The presence of leatherback in Israel area is not so scarce as previously reported supporting the hypothesis of a distribution in the whole Mediterranean basin. The final proposal includes the change of the characterization of the species, usually rare or uncommon in the literature to a common or regular species in the Mediterranean Sea.

Key-words: turtles, conservation, biogeography, Mediterranean Sea

Introduction

According to most of the consulted authors, *Dermochelys coriacea* (Vandelli, 1761) is a marine turtle that does not normally reproduce in the Mediterranean Sea, though it could occasionally (1). Leatherback presence in these waters has been mainly referred to by the catches of some specific fishing gear (2-6) or by strandings produced in beaches, whether live or dead (7-12). The main Atlantic nesting areas of this species are concentrated in beaches of Central and South America, mainly in the French Guyana (13, 14). But also important are the beaches extending from Costa Rica to Colombia, including Trinidad and the Guyanas, in addition to various Caribbean islands (15). It is the marine turtle that presents the greatest distribution area (16). Tagged specimens of the French Guyana have reached as far off as the waters of Placentia Bay (Newfoundland, Canada) (17). Numerous leatherbacks of American origin arrive each year to the Eastern Atlantic coast (18), including France (19, 20, 21), Northwestern Spain (22-24), Portugal (25, 26) and the South Atlantic Spanish coast (27), making possible their entry into the Mediterranean Sea through the Gibraltar Strait. During the last years we have found numerous large-size dead leatherbacks along the South Atlantic coast of Spain, though none of the strandings had been tagged.

The presence of this species in the Mediterranean has been plagued with uncertainties, although in the last decades much new information has been gathered, and it has been observed in waters of nearly all the Mediterranean countries (**28**) including Spanish waters (29, 30), French ones (31), the Northeastern Adriatic (32) and the Eastern Mediterranean. *Dermochelys coriacea* is known from ancient times in the Mediterranean Sea (33), but due to its great size and non-commercial interest, it has not been recorded and sighted with frequency. This review on the status of the species into the Mediterranean indicates its presence in all the basins, although the authors indicate it as a rare turtle, uncommon or infrequent (34, 35). Likewise, it has been recorded frequently off the coasts of Israel (36).

Material and methods

In this document, new data is presented on fortuitous captures and strandings of leatherbacks in two distinct geographical areas of the Mediterranean: the Alborán and the Balearic Sea. To complete the discussion, I have used in addition some published data. Data from the coast of Israel (between 1956 and 1987) were compiled by Dr. S. Ashkenazi and other personnel from the Ecological Date Center of Israel Nature Reserve Authority (MAP, 1990 and pers. comm.). Also included in this paper is a citation of published data by Ben Tuvia and other two turtles included in a unpublished document that was sent to us by Dr. Ashkenazi ("Sea turtles from the Mediterranean and the Red Sea coast of Israel and Sinai").

Results

Western Mediterranean (Alboran Sea and Balearic Sea)

The leatherback turtles captured by the Spanish surface longline in the Western Mediterranean from 1985 are presented in Table I. Furthermore, they include data of 1 or 2 specimens (37); a specimen that was affected by an oil spill that expelled a small hook, cleaned and recovered by the Aula del Mar (Málaga), and another one that was captured in Sicily, (50 Km. from Palermo) sent to me by Prof. R. Sará from a local paper. Two were captured in the coast of Africa (south of the Alboran Sea): one was captured in Melilla (Sagarminaga, pers. com.), Spanish territory of the North of Africa, in November of 1989; the other one was captured in the Alhoceima proximity, next to the Moroccan locality to Melilla (Srour, pers. com.), in March of 1993. Two other turtles appeared in the newspapers of Alicante and Nerja (Málaga). The other data correspond to incidental captures of the Spanish longline fleet. Data corresponding to 1985 and 1986 has not been included in the previous paper. Leatherback that could be measured presented carapace length over 1,4 m. and mean weights superior to 200 Kg., though the weight, as well as the length, were estimated in some instances *de visu* by the fishermen or informers.

Table I. New *Dermochelys coriacea* data from Alborán Sea, Balear Sea and Sicily.

Nº	DATE	SITE/AREA	WEIGTH/LENGTH	OBSERVATIONS
1	10/85	South Ibiza	1200 kg.	
1	31/86	East of Mallorca	350-400	
1	9/86	Gulf of Valencia	/ 1.70 m.	
1	10/88	South of Alicante		
1	5/89	Gibraltar Strait		Gillnet. Alive
1	7/89	East. of Cartagena		Alive freed
1	9/89	South of Ibiza		Very big. Alive
1	10/89	Altea (Alicante)	/1.90 m.	Death (Newspaper)
1	11/89	Melilla (N. Africa)	250-300/1.4 m	Sagarminaga
1	11/89	South of Alicante		Alive. Freed
1	8/91	SE of Cartagena		Alive freed
1	1/92	Nerja (Málaga)	200/	Newspaper. Death
1	3/93	Alhoceima (Morocco)	200/1.50 m	A. Srour. ISPM
1	23/7/95	Gulf of Valencia		Vessel Roselló Blanquer
1	24/6/96	E. of Palermo	250-300/1.85	Gillnet. Alive (R. Sará.)
1	33/ 92	Málaga Bay	Freed Alive	Oil covered. Aula del Mar
1-2	7/8/92	Balear Sea	Alive	Aguilar, Mas & Pastor, 1992
1	18/9/93	Ebro river Delta	Dead	Pérez et al., 1994
1	5/6/93	Palma Bay	Dead	Pérez et al., 1994

If we group all the Table I data (with exception of the turtle captured in Sicily) and we distribute them by month, we will observe that in the western Mediterranean *D. coriacea* is present during every month of the year except February, April and December. The greatest number of observations corresponds to the months of September and October, with 3 turtles in each month.

If we analyzed the data in function of their geographical origin, separating the Alboran Sea and the Balearic Sea, observations in Alboran Sea are concentrated in the final and initial months of the year (winter and spring), while the data from the Balear Sea correspond with the summer and autumn months, indicating a certain geographical distribution in relation with the annual seasons. Previous data refer 17 leatherbacks from Gibraltar Strait to Alboran Sea during winter (9).

On the other hand, the geographic distribution indicates that the turtle strandings are grouped mainly South of the Ebro river Delta and in a marine area between the Balearic Islands and the Iberian Peninsula known as the Ibiza Channel, with an important surface current in a southern direction. The total surface Spanish long line fishing area includes waters much more to the east of the Balearic Islands.

Eastern Mediterranean Basins.

Among the four species of marine turtles in Israel (38), the leatherback is observed in counted occasions in the Mediterranean as well as in the Red Sea. Fourteen records from the coast of Israel (Table II), correspond to captures with nets or strandings between 1956 and 1987. Only one turtle was freed after capture by a long line; the others appeared dead, or we do not have information on what occurred with them. Some are in Museums of that country. The length of the carapace of the measured specimens varies between 138 and 175 centimeters, though we can not indicate what carapace measurement. The greatest incidence originate from the fishing nets.

All the leatherback were captured or appeared dead in the first months of the year. Information on strandings, captures or sightings during the last year period are non existent.

VERTICAL DISTRIBUTION AND MIGRATION OF FISH LARVAE DURING THE NIGHT IN THE N.W. AEGEAN SEA

E. Caragitsou*, A. Siapatis and C. Papaconstantinou
National Centre for Marine Research, Hellinikon, Greece

Abstract

The variability of fish larvae composition and abundance, caught with a 60-cm Bongo net, was determined after analysing data from ten hauls carried out at a station, during night and early morning, at two different depths (22 and 70 meters). The greatest aggregation of larvae was found at 09:30h-09:50h in both depths and the lowest at 03:00h in the 22-meter hauls and at 21:00h in the 70-meter hauls. From the 33 taxa, which have been identified, the six most numerous species *(Sardina pilchardus, Gymnammodytes cicerelus, Benthosema glaciale, Lampanyctus crocodilus, Myctophum punctatum* and *Maurolicus muelleri)* presented different temporal variability of larval abundance, while depth was also an important factor influencing such variation.

Keywords: ichthyoplankton, larvae, vertical profil, migration, Aegean Sea

Introduction

Very few icthyoplankton surveys have been conducted in Greek waters since the beginning of our century, when the Danish *Dana* and *Thor* expedition in the Mediterranean took place. (1, 2, 3). Till now, there have been very few attempts to study the abundance and distribution of many fish eggs and larvae and juveniles in the Aegean Sea. (4). The objective of the present work was to study the variability of fish larvae composition and abundance at a station, during night and early morning, at two different depths (22 and 70 meters), using a 60-cm Bongo net.

Materials and methods

At the 9th of February 1991 a station in N.W. Aegean Sea was selected for night and early morning sampling, on a three-hour basis. The depth of the station was 232 meters. Plankton hauls were made using a paired Bongo net with a mouth diameter of 60 cm and a mesh size of 0.500 mm. Every 3 hours, from 21:00h. to 09:50h, two different horizontal tows, one at depth of 22-m and the other at 70-m respectively, took place. Continuous recording and adjusting the haulling depth was made using a depth sensor of SCANMAR system S-400. A variety of opening and closing towed nets have been used recently to investigate the vertical distribution of icthyoplankton (5). The lack of opening and closing net has been compensated by increasing the hauling duration. The duration of each haul was 15 minutes, except the shooting and hauling time, which was rather short in relation to the total duration of the haul. Proportionally, the bulk of the organisms caught in each haul should have come from the selected depth with little contamination from layers above. Samples from each haul labeled, preserved in 4% neutralized formalin and stored in plastic vials for subsequent analysis in the laboratory. The time, the duration and the depth of each haul were recorded. The mean value of filtered water of all hauls was 602.24 m^3. Sunset on the 9th of February took place at 17:57h and sunrise at 07:22h, and the moon was two days old. From the ten hauls only the last two were made during daylight.

Results

A total of thirty-three taxa of fish larvae were identified. The numbers of larvae per 1000 m^3 filtered water of each taxon, as well as the times and the depths of the hauls are given in Table 1. More than 80% of the total abundance of larvae in each haul was composed of only 6-7 species. *Myctophidae* larvae made up the greatest part of the icthyoplankton community and were represented by eight species. The species *Benthosema glaciale, Lampanyctus crocodilus* and *Myctophum punctatum* were the most abundant species of this family. Another mesopelagic species, whose larvae exhibited great aggregation, was *Maurolicus muelleri*. Finally the species *Sardina pilchardus* and *Gymnammodytes cicerelus* displayed also high abundance.

The total abundance of all larval taxa collected during the night at two different depths is presented at Figure 1. At 22-m samples the maximum value was observed at 09:50h and the minimum value at 03:45h, while at 70-m samples the maximum value was observed at 09:30h and the minimum at 21:30h. At the samples of 22-m the greatest aggregation of sardine larvae (*Sardina pilchardus*) found at 21:00h and 09:50h (104,8 and 156,5 larvae per 1000 m^3 filtered water) and the lowest at 03:00h (19.8 larvae/1000 m^3 filtered water). In all 70-m samples the abundance of larvae did not show considerable variation (between 20 and 40 larvae/1000 m^3 filtered water).

The larvae of sand eel (*Gymnammodytes cicerelus*) were found at greater abundance at 22-m than at 70-m, from 21:00h to 21:30h. However between 03:00h and 03:50h the opposite occurred which probably indicates a night vertical migration from surface to deeper waters from 21:00 to -03:50h.

The larvae of *Benthosema glaciale* were found at significantly greater values at samples of 70-m than at samples of 22-m. Two peaks of high concentration of larvae were observed at 70-m samples, one at 00:50h (59.8 larvae/1000 m^3 filtered water) and another one at 09:00h (91 larvae/1000 m^3 filtered water).

The larvae of *Lampanyctus crocodilus* presented a simultaneous increment of abundance in both depths during the night and the greatest aggregation occurred early in the morning. It is possible that the larvae of this species, migrate from deeper to upper layers during the night.

The abundance of larvae of *Myctophum punctatum* exhibited the same temporal variation in the two different depths, except early in the morning, when at the 70-m sample we found a significant greater quantity of larvae than at the 27-m one.

Finally the larvae of *Maurolicus muelleri* presented a quite different abundant variation at two depths during the night. However, the greatest aggregation of larvae was found at 70-m samples.

The larvae of *Benthosema glaciale, Lampanyctus crocodilus, Myctophum punctatum* and *Maurolicus muelleri* were found in plankton in the Aegean Sea during the whole year. The larvae of *Sardina pilchardus* and *Gymnammodytes cicerelus* occurred in the plankton only in winter and spring (1).

The literature on the relationship between light intensity and vertical distributions of fish larvae seems confusing. Most species appear to migrate towards the surface at night (6, 7). According to Tanning (3) the great majority of the larvae of Myctophidae were found to the phaeplankton and the upper knephoplankton, and different vertical distributions of larvae were found between day/night hauls and also between winter/summer hauls. Russell (8) in his study of the vertical distribution of postlarvae in the Plymouth area, found that pilchard were much more numerous in the collections made at night when there might be more than thirty times as many as caught in the day-time.

A Kolmogorov-Smirnov Test (9) showed no significant differences in length frequency distributions for the six species by depth and time. Similarity of family compositions between hauls was determined by non-metric multi-dimensional scaling (MDS) (10) ordination, using logarithmic transformed pooled data from the replicates at each hauls, with Bray-Curtis similarity index (11). MDS separated haul B10 from

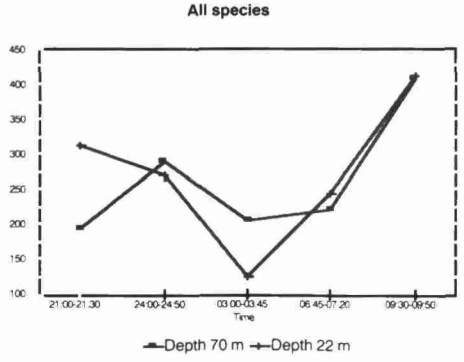

Fig. 1. Temporal variation of larval abundance at two depth.

DISCARDS OF THE WESTERN MEDITERRANEAN TRAWL FLEETS

A. Carbonell [1]*, P. Martin [2], S. de Ranieri [3] and WEDIS team [4]

[1] IEO-Centro Oceanográfico de Baleares, Moll de Ponent S/N, 07080 Palma de Mallorca, Spain
[2] DSUA University of Pisa, Via Volta, 656100 Pisa, Italy
[3] ICM-CSIC P. Joan de Borbo s/n, 08039 Barcelona, Spain
[4] Working team WEDIS of project-contract number 94/027 "Discards of the western Mediterranean trawl fleets" *

Abstract

We present a quantitative analysis of the composition (commercialized catch and corresponding discard) of trawl catches, in seven ports of the western Mediterranean. Discards are defined here as the fraction of the catch from the haul that is returned to the sea by the fishermen, because it does not have commercial value. A sampling programme on board commercial was performed from June 1995 to June 1996. The hauls were sampled for the collection of the total catch in weight, by species, for the commercial and discarded fractions separately. The factors of stratification considered were in all the ports, depth, with three strata, stratum A (<150 m), B (between 150-300 m) and C (>350 m), to which factor for two types of gear in the Porto Santo Stefano or two classes of vessel power in Vilanova were added. The results obtained have allowed to characterize the commercial and discards fractions. The discarded biomass always constituted an important fraction of the total catch. However, the discard of species with high commercial interest was very low or nil.

Key-words : fisheries, biomass, western Mediterranean

Introduction

In the fisheries management, some technical measures (1, 2) such as those of mesh regulation in order to reduce the catches of smaller sizes, are widely accepted (3). However, the effects and repercussions of the discards caused by fishing, such as, economic losses (losses of future catches), or ecological impacts (in terms of protection of resources and environment) remain largely unknown and constitute a problem faced by management, evaluation in the long term and regulation of fisheries in the whole world (4, 5) that is on the other hand necessary to approach. A recent review on the state of the discards at a world level, carried out by Alverson *et al.* (6), provisionally estimates global fish discards of around 27 million tonnes which gives an idea of the importance that such practices represent. This same study makes clear that there is a shortage of information on the Mediterranean. In the western Mediterranean the demersal fishery is one of the most important, as much for the volume of its catches (biomass) as for the economic value it attains. The trawl fishery shows the phenomena of commercial species discards. The present work is included in a research project financed by the European Community about the discards of the trawl fishery in the western Mediterranean (Study n°94/027). Discards are defined as that fraction of the catch from the haul that is returned to the sea because it does not have commercial value, which are fishes, crustaceans cephalops or other invertebrates such as equinoderms, gastropods, bivalves, sponges, etc., as well as the vegetal fraction (algae and phanerogams). The aim of this study is to show the differences observed in the practice of discards in seven ports of the western Mediterranean, considering two fractions in the total catch : commercialized and discarded.

Material and methods

Seven fishing ports were selected in the study area Porto Santo Stefano (Italy), Vilanova i la Geltru, Valencia, Santa Pola, Fuengirola, Palma and Alcudia (Spain). The sampling programme was carried out from June 1995 to June 1996, by observers on board commercial fishing vessel during normal fishing activity. In all areas three depth strata were defined as stratum A <150 m depth, stratum B between 151-350 m and stratum C >350 m deep. In Porto Santo Stefano the fleet was subdivided into two categories, identified as those vessels equipped with the traditional trawl nets and those working with wide opening ("French") trawl nets. In the port of Vilanova i la Geltru the fleet was subdivided into two categories depending on the power, less than 150 hp vessels and greater than 150 hp. The sampling unit was the haul. A total 458 hauls were samples.

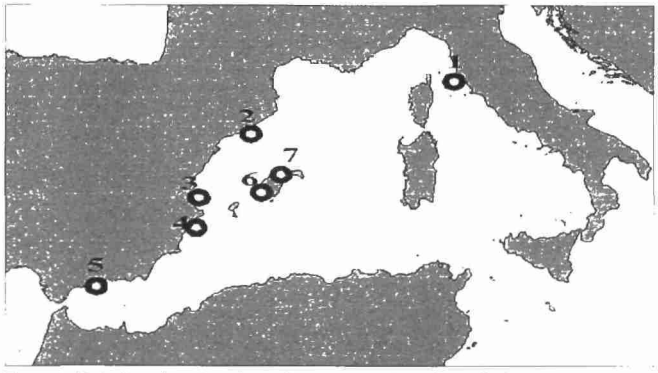

Figure 1. Study Area. Location of sampling ports : 1= Porto Santo Stefano, 2= Vilanova i la Geltru, 3= Valencia, 4= Santa Pola, 5= Fuengirola, 6= Palma, 7= Alcudia port.

For each haul, date, position, duration, depth and course were noted. The weight of the commercialised and discarded catch was estimated by species using dinamometers. The catch of the total, commercial and discarded fractions by haul was standardized to hourly yields (kg/h). The total mean annual yields of both fractions were obtained by an average of the standardized hourly yields, and its standard deviations. As well as were calculated the relative proportion of commercialised species and discarded species and discards to the total catch by each port, stratum, gear type or horse power of the boats.

Results

The sampling effort, 1463 fishing hours in total, was distributed as follows : 218 hauls in stratum A, 136 in stratum B, and 104 in C. A total of 609 species were identified. The most frequently represented groups were fish, with 239 species, molluscs with 137, and crustaceans with 101. The mean annual values of total catch and its standard deviation are shown in Table 1 by each port, stratum, and of the gear type or horse power of the vessels. Figures 2, 3 and 4 represent the relative proportion corresponding to the commercial and discard fractions.

Table 1. Mean annual hourly yields (kg/h) of the total catch and its standard deviation.

	Stratum A		Stratum B		Stratum C	
	Mean	STD	Mean	STD	Mean	STD
Fuengirola	61.78	21.60	39.91	9.95	29.62	11.85
Santa Pola	44.49	56.32	146.83	213.17	17.39	12.20
Valencia	49.14	24.32	91.57	66.30	36.38	19.58
Palma	179.56	148.21	104.29	122.16	23.59	12.63
Alcúdia	120.36	72.40	118.78	113.79	14.61	7.75
Pisa w.o.t.	37.28	22.84				
Pisa Traditional	26.32	6.56	39.16	20.19	23.49	12.96
Vilanova<150 hp	72.51	115.21	15.09	7.20	11.75	5.19
Vilanova>150 hp	50.01	29.05	134.61	162.51	25.87	13.14

Stratum A, the most coastal, was characterized by important catches of fish such as *Mullus barbatus, M. surmuletus, Merluccius merluccius*, and in minor quantities, among others, Sparidae, Trachinidae, Scorpaenidae, Triglidae, Soleidae, Scyliorhinidae and Rajidae species, and cephalopods such as *Octopus vulgaris* and *Eledone cirrhosa*. All of them have a large commercial importance and in general their discard is practically nil. In this stratum the discard showed two situations : in the ports of Palma and Alcudia the discard of invertebrates and flora was very much higher than for fish (up to 67% in Palma de Mallorca, due fundamentally to rhodophytic algaes), whereas in the other ports fish constituted the most important fraction of the discard, with some species such as *Boops boops* and *Sardina pilchardus* being important.

DAILY EGG PRODUCTION METHOD FOR SPAWNING BIOMASS ESTIMATES OF ANCHOVY IN THE SOUTH-WESTERN ADRIATIC DURING 1994

Nicola Casavola

Laboratorio Provinciale di Biologia Marina, Molo Pizzoli (Porto) 70123 Bari, Italy

Abstract

During the month of July 1994, an Egg Production Method Cruise was carried out with the purpose of evaluating the spawning biomass of the anchovy (*Engraulis encrasicolus* L.) along the Apulian coasts of the lower Adriatic. The area, covering a surface of 14,790 km^2, extends from Gargano to Otranto. The results of the egg production and of the biological parameters relative to the adult population, are compared to those of other Mediterranean areas. The D.E.P.M. applied in July 1994 estimated a spawning stock biomass of 8,129 metric tons (CV = 0.235) for the South-Western Adriatic anchovy population. The D.E.P.M. experimental research shows an anchovy biomass evaluation 7.3 times smaller than the one reckoned with the egg and larva method.

Key-words: Fishes, biomass, spawning, Adriatic Sea

Introduction

The spawning biomass is defined, in the Daily Egg Production Method (D.E.P.M.) (1), as the relationship between the daily egg production during the survey and the daily fecundity of the adult population. The biomass estimate is based on the following equation:

$$B = \frac{KPoAW}{RFS}$$

where B = the spawning biomass in metric tons, Po = the number of eggs per sampling unit (m^2 per day), A = total survey area (in m^2 per sampling units), W = average weight of mature females (grams), R = sex ratio (fraction of mature females by weight), F = batch fecundity (average number of eggs per mature female), S = fraction of mature females spawning per day, k = conversion factor from grams to metric tons. The daily egg production in the zone is based on the sampling of eggs at sea and on the temperature dependent model of the speed of egg development, while the parameters of the daily fecundity of the population are based on the capture of adult samples during the fishing campaign. The egg surveys and adult surveys are thus obtained as part of campaigns carried out at the same time during the peak of the spawning season.

This research applies for the first time the D.E.P.M. to the lower Adriatic *Engraulis encrasicolus* L., as part of the "small pelagic biological resources" programme financed by the Ministry of Agricultural, Food and Forestry Resources in this area. Two other methods have been employed in the evaluation of the biomass estimate for Clupeiforms in Apulian waters: the echo survey (2) from 1976 and the egg and larva method (3) since 1984. Until this year the D.E.P.M. had been applied for Mediterranean anchovy by Palomera and Pertierra (4) (North Eastern Spanish coast), Garcia *et al.*, (5), Garcia and Palomera (6) (North Western Mediterranean).

Material and Methods

The survey was carried out between 3 July and 3 August 1994, both during the day and at night, covering most of the reproductive zone in the eastern arc of the lower Adriatic. Both the egg surveys and adult surveys were carried out using chartered research ships equipped with midwater otter trawls. In order to catch more adult samples were additionally used commercial vessels equipped with flying midwater pair trawls and purse seine. The methodology used for the sampling and the elaboration of data in relation to the egg survey and adult survey has been described by Casavola (7), Casavola *et al.*, (8, 9, 10).

The samples of plankton were collected using a CalVET net (335 m mesh) in order to keep a continuity with samplings carried out in the previous years, when Bongo 60 with the same kind of mesh was used. The net was raised, where possible, from a depth of 100 metres, with coverage of 14,790 km^2 of the surface of the sea. In the area examined samples were taken at 88 stations (Fig. 1) situated at a distance of 7 NM, along 23 transects also at a distance of 7 NM, angled at 45°. These latter continued until, examining the plankton collected, anchovy eggs could be found and above all knowing, through many years' experience (since 1984) in the egg-larva method research, the limits of the spawning grounds. Temperature and salinity profiles were recorded at the same stations using the multi-parameter OCEAN SEVEN probe. The anchovy eggs (Fig. 2) were counted and subdivided in the laboratory by stage of embryonic growth. This classification was carried out taking into account the relationship between the length of egg development and the temperature of the water according to the model obtained by Regner (11) for the Adriatic anchovy. Then the stages of the anchovy eggs were regrouped manually into "spawning nights"

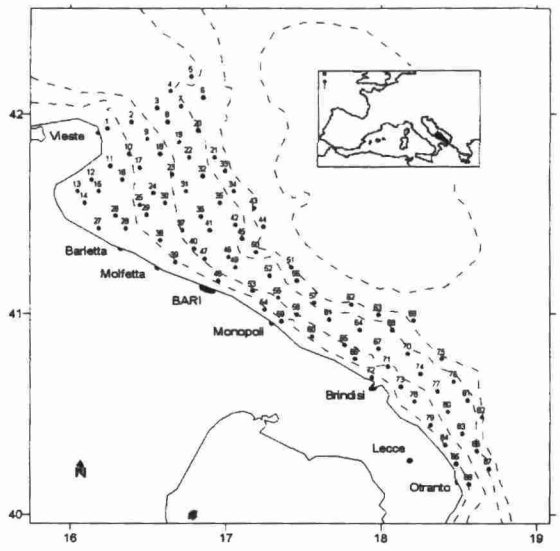

Fig. 1 - D.E.P.M. Engraulis encrasicolus egg survey.

and the ages of the eggs were recalculated on the basis of the time that passed after 24:00 (GMT) (the time of maximum spawning assigned by the authors) and the time of egg collection.

The whole zone investigated, with the understanding of the reduction of the variance, has been post-stratified, following the procedure employed by Picquelle and Stauffer (12), into two strata: stratum 0 (egg production = 0) and stratum 1 (positive stations). The elaboration of the data relative to the positive stratum, obtained using a weighted nonlinear least squares regression (13), has made it possible to define

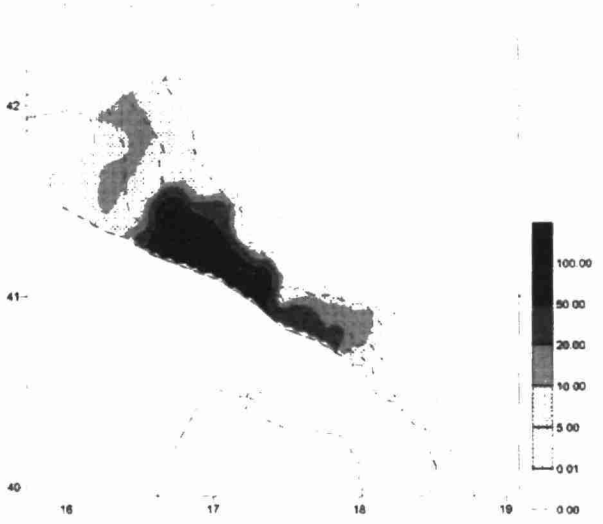

Fig. 2. Distribution and abundance of *Engraulis encrasicolus* eggs (No/m^2) during the July 1994 survey in the lower adriatic Sea.

DAILY EGG PRODUCTION METHOD FOR SPAWNING BIOMASS ESTIMATES OF SARDINE IN THE SOUTH-WESTERN ADRIATIC SEA

N. Casavola*, P. De Ruggieri, E. Rizzi, S. Lo Caputo

Laboratorio Provinciale di Biologia Marina, Molo Pizzoli (Porto) 70123 Bari, Italy

Abstract

In the month of November 1994, an Egg Production Method Cruise was carried out, aiming at the evaluation of the spawning biomass of the sardine (*Sardina pilchardus* Walb.) along the coasts of Apulia in the lower Adriatic. The results of the egg production and of the biological parameters relative to the adult population, are compared to those of other Mediterranean areas. The D.E.P.M. applied in November 1994 estimated a spawning stock biomass of 14,196 metric tons (CV = 0.144) for the South-Western Adriatic sardine population. The D.E.P.M. experimental research shows a sardine biomass evaluation 7.69 times smaller than the one reckoned with the egg and larva method.

Key-words: Fishes, biomass, spawning, Adriatic Sea

Introduction

So far two evaluation methods have been employed in the Apulian coasts to estimate the biomass of Clupeiforms: acoustic, or "echo-survey" campaigns, from 1976; "eggs and larvae", from 1984. In 1994, within the biological resources small pelagic fish program, the Ministry of Agriculture Food and Forest Resources recommended the introduction of the D.E.P.M. (1) to be followed side by side with the traditional methodology. The present research is the first applying the D.E.P.M. on *S. pilchardus* in the waters of the lower Adriatic. Before now the D.E.P.M. was applied on European sardine by Pérez *et al.*, (2) (North Atlantic Spanish coasts).

This methodology is based on the following model:

$$B = \frac{KP_oAW}{RFS}$$

where B = spawning biomass in metric tons, P_o = daily egg production (number of eggs per sampling unit, m^2 per day), A = total survey area (in m^2 per sampling units), W = average weight of mature females (grams), R = sex ratio (fraction of mature females by weight), F = batch fecundity (average number of eggs per spawning per mature female), S = fraction of mature females spawning per day, k = conversion factor from grams to metric tons. Egg surveys and adult surveys (3) were obtained as part of the campaigns carried out contemporaneously during the peak spawning season .

Material and methods

The survey was carried out from 4 to 29 November 1994, the period of the highest spawning intensity for *S. pilchardus*, covering three quarters of the reproduction area in the western zone of the lower Adriatic sea. Both the egg surveys and adult surveys were carried out using chartered research ships equipped with midwater otter trawls. In order to catch more adult samples were additionally used commercial vessels equipped with flying midwater pair trawls and purse seine. The sampling and data processing methods as regards the egg and adult campaigns have been described by Casavola and Rizzi (4) and Casavola *et al.*, (5, 6). The plankton samples were collected by means of a CALVET net (335 m mesh), raised vertically from a depth, when possible, of 100 m, covering a sea surface of 14,790 km^2. In the area surveyed samples were taken in 88 stations (Fig. 1) at a distance of 7 NM each, along 23 transects also at a distance of 7 NM, angled at 45°. These latter continued until, examining the plankton collected, sardine eggs could be found (Fig. 2), and above all knowing, on the basis of many years' experience (from 1984) in the egg-larva method research, the limits of the spawning grounds (7). The temperature and salinity profiles were recorded in the same stations by means of a multiparameter probe.

In the laboratory the eggs of *S. pilchardus* were counted and staged according to the degree of embryonic growth, as described by Gamulin and Hure (8); the eggs were classified according to age and to the relationship between the degree of egg development and water temperature. Then, using again manual procedures, the stages of sardine eggs in each station were grouped into "spawning nights" (5) and eggs' ages were recalculated on the basis of the time that passed between 20.00 (GMT) (highest spawning time assigned by the authors) and the eggs collecting time.

The whole area surveyed, with the purpose of reducing the variance, was post-stratified, following the Picquelle and Stauffer (9) procedures, into two strata: stratum 0 (egg production = 0) and stratum 1 (positive stations). The data processing referring to the positive stratum, obtained using a weighted nonlinear least squares regression

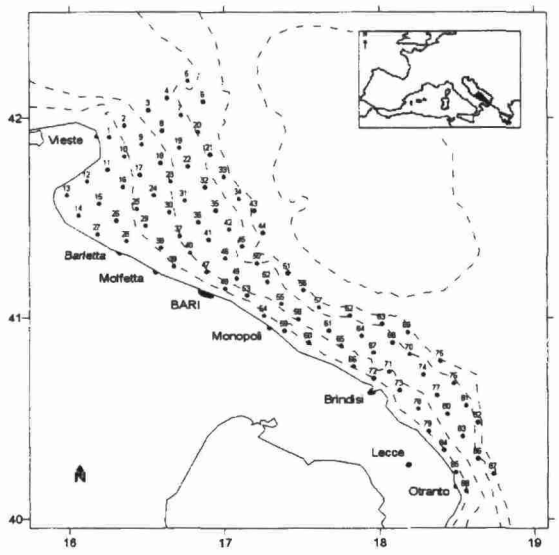

Fig. 1 - D.E.P.M. *Sardinia pilchardus* egg survey.

(10), allowed to define a mortality curve (Fig. 3), using the classic model $P_{(t)}=P_0 \times e^{-zt}$, where t = age in days measured as the time elapsed from spawning to the time of sampling, $P_{(t)}$ = number of eggs per m^2 in age category t, P_0 = daily egg production per sampling unit (m^2), z = daily rate of instantaneous mortality.

52 samplings were carried out on board the ships (Fig. 4), and only in 46 cases sardines could be caught. As the number of sampled individuals per trawls was not always the same, the parameters referring

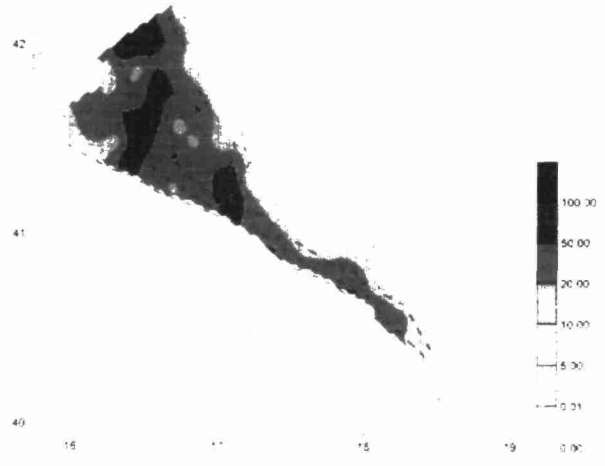

Fig. 2. Distribution and abundance of *Sardinia pilchardus* eggs (No/m^2) during the November 1994 survey in the lower adriatic Sea.

CYCLE REPRODUCTEUR ET RELATIONS TAILLE-POIDS CHEZ *SCIAENA UMBRA* LINNAEUS, 1758 DES COTES TUNISIENNES

Nadia Chakroun-Marzouk* et Mohamed-Hédi Ktari
Laboratoire de biologie animale, Faculté des Sciences de Tunis, 1060 Tunisie

Résumé
Sur les côtes tunisiennes, la période de maturation de *Sciaena umbra* s'étale du mois d'avril au mois de juin; elle est suivie par l'émission des gamètes qui a lieu essentiellement au courant des mois de juillet et d'août. Des variations sensibles du rapport hépatosomatique indiquent le stockage de réserves lipidiques et leur utilisation progressive pour les besoins de la reproduction. La croissance pondérale relative, invariable en fonction du temps, est la même pour les mâles et pour les femelles ce qui est corroboré par un embonpoint inaltéré quelque soit la période de l'année.

Mots clés: Reproduction, fishes, Western Mediterranean.

Bien que largement répandu en Méditerranée, *Sciaena umbra* (corb) est un poisson osseux nectobenthique côtier encore peu connu. Cette espèce est moins fréquente en Méditerranée nord-occidentale, où elle est pêchée occasionnellement, que dans le sud du bassin méditerranéen, où elle serait surexploitée en particulier sur les côtes d'Afrique du Nord. Ces dernières années [1, 2, 3], on a relevé que sur les côtes françaises de Méditerranée, les stocks de corbs sont beaucoup moins importants que ceux signalés par le passé et que leur densité est toujours relativement plus importante dans les aires protégées; ces auteurs passent en revue les facteurs de raréfaction du corb et indiquent que ce poisson a été sélectionné parmi les espèces marines à protéger.

A notre connaissance, les rares auteurs citant cette espèce se sont contentés de rapporter ou de situer succintement sa période de ponte; ainsi dans le but de fournir des éléments de base indispensables à une meilleure connaissance de la biologie de cette espèce menacée, les résultats préliminaires énoncés ci-dessous précisent le cycle reproducteur du corb sur les côtes tunisiennes et le complètent par une analyse des relations taille-poids.

Matériel et méthodes

Les poissons ont été recueillis auprès des mareyeurs lors des débarquements ou dans les marchés de la région de Tunis durant les années 1995 et 1996. Les corbs sont capturés aussi bien par la pêche côtière que chalutière à l'aide de filets maillants, palangres et chaluts; ils se répartissent en 339 femelles et 237 mâles de longueur standard (Lst) comprise respectivement entre 104 - 412 mm et 106,5 - 366 mm; le poids total (Pt) oscille entre 23 - 1958 gr pour les femelles et 27,5 - 1260,5 gr pour les mâles.

Pour les besoins de l'étude du cycle reproducteur, divers rapports ont été calculés pour les poissons matures de longueur standard supérieure à 205 mm :

- rapport gonadosomatique ou RGS = Pg x 100 / Pe (avec Pg : poids des gonades et Pe : poids éviscéré) ;
- rapport hépatosomatique ou RHS = Pf x 100 / Pe (avec Pf : poids du foie);
- facteurs de condition ou Kct = Pt x 100 / Lst^3 et Kce = Pe x 100 / Lst^3 .

Les valeurs moyennes de ces rapports ont été comparées deux à deux au moyen du test "t" de Student pour un risque de 5% [4]. Les relations taille-poids, calculées par la méthode des moindres carrés, sont exprimées par l'équation log P= b log Lst + log a; elles ont été établies annuellement et mensuellement pour chaque sexe. La comparaison des équations deux à deux s'est toujours faite en utilisant les tests sur les pentes (tpe) et sur les positions (tpo) pour un risque de 5% [5]. Pour déterminer la nature de l'allométrie, la pente observée "b" a été comparée à la valeur 3 à l'aide d'un test "t" pour un risque de 5%.

Résultats

L'évolution du RGS durant l'année, pour les poissons adultes mâles et femelles, est pratiquement synchrone (Fig 1.A; tabl. 1); deux périodes sont observées:

— repos sexuel en automne et en hiver (septembre à mars)

— à la maturation des gonades et à la période de frai. La ponte débute en juin pour les poissons les plus précoces et s'achève en août pour les plus tardifs.

Les variations du RHS en fonction du temps (Fig. 1.B; tabl. 1) indiquent que ce rapport commence à chuter au moment où le RGS est à

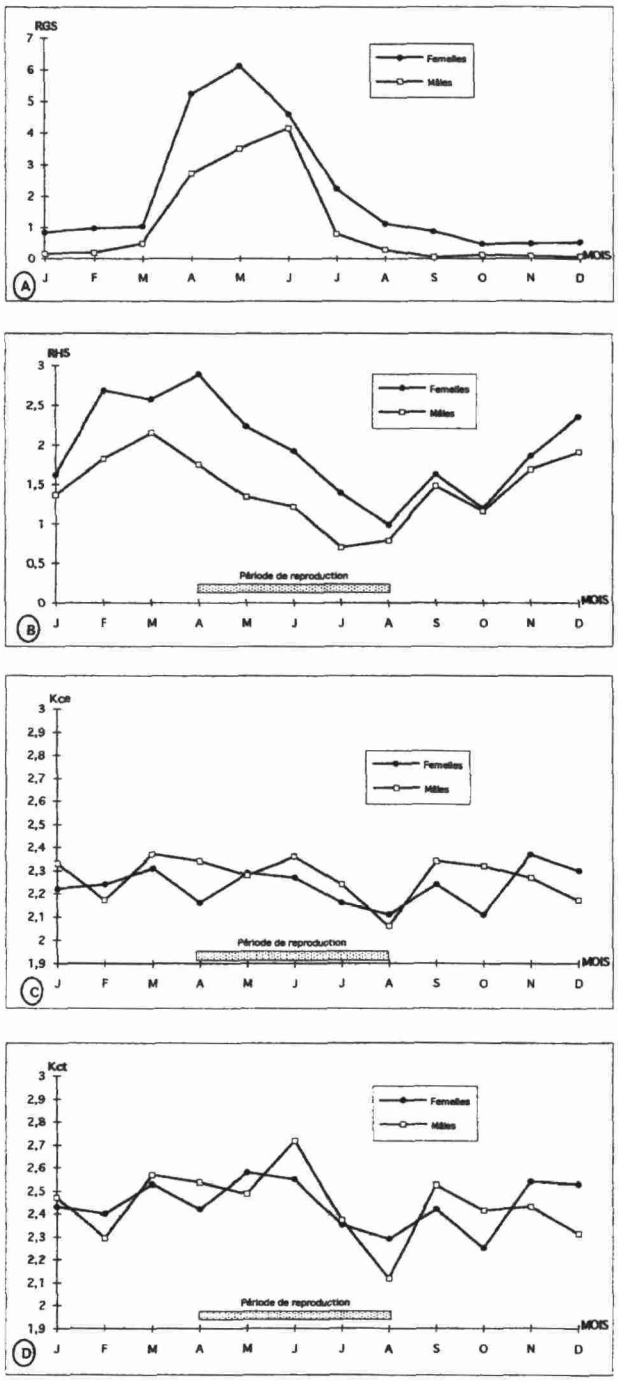

Fig. 1. Evolutionmensuelle des **A** : rapports gonadosomatiques (RGS); **B** : rapports hépatosomatiques (RHS); **C** : coefficients de condition (Kct) moyens pour les mâles et les femelles de *Sciaena umbre.*

ESSAI DE STANDARDISATION DE L'EFFORT DE PÊCHE À LA SENNE EN BAIE D'ALGER.

A. Chalabi [1]* et S. Akkacha [2]

[1] Institut des Sciences de la Nature ISN/USTHB, B.P. 32; El Alia, 16 111 Bab Ezzouar, Alger, Algérie
[2] Centre National du Développement pour la Pêche et l'Aquaculture, B.P. 67, 11 Bd Colonel Amirouche, 42 Bou Ismaïl, Algérie

Résumé

La baisse générale des captures s'est accompagnée d'une augmentation de l'effort de pêche sur les pêcheries pélagiques. Ainsi, divers paramètres spécifiques aux senneurs du port d'Alger ont été testés, auxquelles ont été corrélées les captures, sur la base du meilleur coefficient de corrélation. Le test indique que la chute de la senne, est classée avant la surface. Ce résultat s'explique par la particularité des métiers d'Alger qui pêchent à proximité, pour des raisons d'économie évidentes. La sardinelle Sardinella aurita, est la principale espèce capturée, en raison semble-t-il des conditions de dessalure caractéristique du littoral que l'espèce affectionne.

Mots clés: pelagic, fisheries, Algerian Basin

Introduction

La problématique de la pêche en Algérie, comme pour d'autres pays en particulier méditerranéens, se traduit par une baisse des captures, après plus d'un demi-siècle d'augmentation constante. Cette situation a conduit l'ensemble de la communauté halieutique, pêcheurs, scientifiques et administration, à plus de rigueur dans sa démarche. Parmi les recommandations formulées sur la base des études précédentes, l'effort de pêche (1, 2) s'oriente vers les maillons inférieurs de la chaîne trophique, constitués des petits pélagiques. La profession tente de compenser le manque à gagner dû au prix relativement bas de ces espèces, par des taux de capture plus élevés, en utilisant des engins plus performants, comme les chaluts pélagiques et/ou à cordes, armés en semi-pélagique. Cependant, en l'absence d'une réglementation précise et fine, combinant à la fois les mesures cœrcitives en matière de quotas, de périodes et de zones, et des mesures incitatives comme la garantie des prix, le risque de surpêche a été déplacé par une simple translation, accompagnée de nouvelles tensions intra-professionnelles, systématiques dès l'apparition de nouveaux métiers concurrentiels. Pour répondre à ces préoccupations, l'attention des scientifiques s'est portée sur la mise au point des outils de gestion simples et efficaces pour préserver la ressource en petits pélagiques tout en assurant un niveau de capture soutenu. Le port d'Alger regroupe une vingtaine de senneurs très différents en dimension et puissance. En conséquence, la première étape a consisté à caractériser l'activité, à identifier l'ensemble des rouages intervenant dans l'exploitation, puis à rechercher un indicateur spécifique au navire et proportionnel aux captures, à la fois facile à mesurer et suffisamment robuste pour décrire correctement l'exploitation. Ce paramètre, multiplié par le temps de pêche (à partir des jours, du nombre de sortie ou autre mesure), tente de corriger la disparité des navires pour aboutir à une unité d'effort soit mieux corrélée. Après une présentation succincte de la région algéroise, le protocole expérimental est rappelé et les résultats obtenus sont discutés. Quelques commentaires complètent la proposition d'unité d'effort préconisée et son éventuelle application dans un modèle d'exploitation.

Matériel et méthodes.

La baie d'Alger (fig. 1)

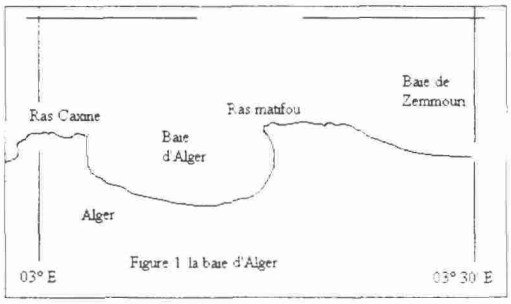

Figure 1: localisation de la baie d'Alger.

Les petits pélagiques débarqués par les pêcheurs algérois proviennent essentiellement de la baie d'Alger. De forme semi-circulaire, la baie comprise entre le Ras Caxine à l'ouest et le Ras Matifou à l'est, couvre une superficie de 23 km^2, avec une largeur d'environ 4 milles pour une longueur de 12. L'influence du courant atlantique sur les facteurs hydrologiques des côtes algériennes n'est plus à rappeler. Les travaux de Millot (3) et de Benzhora (4) ont permis d'identifier des tourbillons anticycloniques qui se forment après le front Almeria-Oran (entre 02 00 00 LW et 01 00 00 LE) en engendrant des upwellings côtiers épisodiques dont l'existence est fort probable en baie d'Alger (5). En effet la Méditerranée, considérée comme une mer oligotrophe enrichie par le courant atlantique, tend à s'appauvrir à mesure que les zones de pêche s'éloignent du détroit de Gibraltar (6).

La pêche en baie d'Alger est soumise à d'autres facteurs déterminants, comme la topographie du fond et l'action des vents. Ce dernier constitue un paramètre essentiel pour la pêche, à deux niveaux, tout d'abord en limitant le nombre de sorties en mer lorsqu'il souffle fort, et aussi en modifiant les structures hydrologiques qui affecteront à leur tour l'écologie et la biologie des organismes marins. Un vent violent peut agir localement sur la thermocline, importante pour la répartition des espèces pélagiques, sténothermes, en la déplaçant dans une zone plus profonde (7). La compilation des données météorologiques fournies par l'Office National de la Météorologie ONM (Alger), indiquent que deux secteurs de vents dominants s'imposent alternativement dans l'Algérois, les vents d'ouest soufflant généralement de novembre à mai, et ceux d'est entre juin et octobre. En définitive, la baie d'Alger, au plateau continental étroit, baigné par le courant atlantique, présente un caractère de province océanique plutôt que néritique, cas général des côtes algériennes dont le potentiel pélagique représente près de 70% des stocks halieutiques (6).

Le port de pêche représente une partie restreinte de la superficie du port d'Alger (184 ha). Sa capacité d'accueil (69 unités) se trouve actuellement réduite en raison du nombre croissant d'embarcation immobilisées. La pêche aux petits pélagiques y est pratiquée par les sardiniers ou "galéons" et par les chalutiers. La majorité de ces derniers est armée de septembre à juin de chaluts à grande ouverture verticale aux ailes à grandes mailles ou à cordes (généralement à quatre faces), conçus initialement pour la pêche pélagique; ils permettent notamment la capture des espèces pélagiques lorsqu'elles se trouvent en phase démersale (en hiver par exemple ou le jour) ainsi que diverses espèces indirectement inféodées au substrat (tab. 1). Les chalutiers sont armés à la crevette le reste de l'année. Le chalut typiquement pélagique, équipé de panneaux Süberkrub, est rarissime au port d'Alger, malgré quelques tentatives infructueuses.

Tableau 1. Espèces les plus fréquemment capturées par les senneurs du port d'Alger classées par ordre d'importance décroissant.

Famille	Espèce
Clupéidés	- *Sardinella aurita, Sardina pilchardus;*
Carangidés	- *Trachurus trachurus;*
Sparidés	- *Pagellus acarne; Boops boops; Sarpa salpa;*
Mugilidés	- *Liza sp;*
Engraulidés	- *Engraulis encrasicolus;*
Carangidés	- *Seriola dumereli; Lichia amia; Scomber scombrus*

Les senneurs travaillent toute l'année, quand les condition atmosphériques le permettent; c'est une pêche côtière caractérisée par la prédominance de la pêche sur petits fonds, sans utilisation de lumière pour attirer les bancs de poissons. Ces caractéristiques de la pêche à la senne se justifieraient selon certains professionnels par la pratique antérieure du lamparo (senne tournante non coulissante) qui n'est efficace qu'à petite profondeur. L'introduction de la senne coulissante, ou ring-net, en Algérie depuis plus d'un demi-siècle, n'a donc fait que remplacer un engin par un autre, toutefois plus efficace, sans pour autant faire évoluer radicalement la pêche dénommée autrefois "pêche au feu". Cette pêche à l'estime pratiquée de jour comme de nuit sans utilisation de la lumière, appelée communément par les pêcheurs Algérois "pêche à ouche", se base uniquement sur le sondeur pour détecter les bancs de poisson. Moins commune, la pêche à la lumière utilise une seule embarcation annexe, se pratique en été, lorsque le poisson est moins abondant, l'eau devenant moins trouble et l'état de la mer favorable. Elle a lieu au cours des nuits sans lune, les bancs de poisson détectés au sondeur, étant attirés vers la surface au moyen de lampes, alimentées par des générateurs depuis une quinzaine d'années. L'embarcation principale, en acier, en bois ou en polyester, mesure de 7 à 18 m. La puissance des moteurs varie de 45 à 430 cv. L'équipage comprend, en plus du patron de pêche et du mécanicien, 4 à 11 matelots selon les dimensions du navire. L'engin utilisé, le ring-net, mesure entre 180 et 550 m de long pour une chute variant le plus souvent entre 2000 et 7000 mailles de 18.4 mm étirée, dimension de maille préférée par les pêcheurs, car le petit poisson se maille peu et le relevage de la senne est facilité. La plupart des

CHAETOGNATHES DES CÔTES MAROCAINES. ANALYSE DESCRIPTIVE DU PEUPLEMENT

Larbi Cheggour [1]* et Mohamed Menioui [2]

[1] Unité de Reproduction et d'Environnement, Faculté des Sciences, BP. 1014, Rabat, Maroc
[2] Institut Scientifique B.P 703, Rabat-Agdal, Rabat, Maroc

Résumé

Les côtes marocaines aussi bien atlantiques que méditerranéennes comportent 29 espèces de chaetognathes ce qui correspond à, environ, 30% du total des espèces identifiées à l'échelle planétaire et dépasse de 45% celui des espèces connues de toute la Méditerranée. Dans cette étude, 13 espèces ont été identifiées tout au long de la côte atlantique du Maroc, depuis l'entrée de la Méditerranée jusqu'à la frontière avec la Mauritanie ce qui représente 44,83% du total des espèces recensées dans les eaux marocaines. Quantitativement, ce peuplement est essentiellement dominé par l'espèce *Sagitta fridirici*, suivie de *S. enflata* et *S. minima*. Elles sont également les mieux représentées dans les secteurs centre et nord alors que dans le secteur sud, c'est l'espèce *S. bipunctata* qui prédomine. Cette étude, la plus vaste dans une région (marocaine) où la Méditerranée puise l'essentiel de sa faune, montre que le peuplement est le plus riche (abondance) en été et le plus diversifié (nombre d'espèces) en hiver et qu'il est mieux représenté, quantitativement, dans le secteur nord à proximité de l'entrée de la Méditerranée.

Mots clés: Chaetognatha , biodiversity, Alboran Sea

Introduction

Les chaetognathes constituent un groupe d'une centaine espèces (102) dont quatre cinquièmes sont pélagiques (1). Les espèces des eaux marocaines n'ont fait l'objet que de peu d'études (2- 6). La présente étude s'intègre dans le cadre d'un vaste programme de recherche sur l'écosystème pélagique des côtes marocaines dirigé par l'Institut National des Recherches Halieutiques du Maroc et l'Institut ATLANTNIRO russe de Kaliningard; elle s'intègre aussi dans le cadre d'une expertise dirigée par le Programme de Nations Unies pour l'Environnement et le Ministère marocain de l'Environnement. Elle vise une meilleure connaissance de la diversité biologique marine du Maroc et sa typologie (8). L'intérêt de cette étude pour la Méditerranée réside dans le fait que:

- la faune méditerranéenne et celle de l'Atlantique constituent une seule et même entité qui serait la faune atlanto-méditerranéenne (9-11); l'élément méditerranéen serait constitué, dans sa plus grande partie, par l'élément atlantique, ce dernier constituant le réservoir où la Méditerranée puise l'essentiel de sa faune (12-15). L'affinité entre ces deux éléments serait de 84% (16);
- la circulation des espèces se fait plus facilement entre la région marocaine (sud du détroit) et la région méditerranéenne qu'entre cette dernière et la région ibéro-française (17);
- c'est la première fois que ce groupe a été étudié sur la zone étendue entre l'entrée de la Méditerranée et la frontière maroco-mauritanienne et aussi, la première fois qu'une étude fournit des données précises sur la structure de ce groupe dans cette région en étroite relation avec la Méditerranée.

Matériel et méthodes

Les prélèvements (Fig. 1), ont été effectués en hiver (janvier 1994) et en été (juillet, 1994). La première couverture concerne 85 stations entre 21°N et 34°30'N; la deuxième englobe 89 stations entre 21°N et 35°40'N. Cette zone, de près de 3000 km a été subdivisée, en fonction des conditions hydrologiques, en trois secteurs (18-20): - un secteur nord entre 35°40'N et 32°30'N caractérisé par des eaux côtières d'une température de 16°C et d'une salinité de 36,3‰, des eaux du larges d'une température de 20°C et d'une salinité de 36,7‰ et où le phénomène d'upwelling n'est pas très intense; - un secteur centre entre 32°30'N et 28°N; caractérisé par des eaux côtières d'une température de 17°C et d'une salinité de 36,2‰, 21°C et de 36,4‰ dans les eaux du large, et par un phénomène d'upwelling intense en périodes estivale et automnale;- un secteur sud qui s'étend entre Cap Juby et Cap Blanc (21°N); où la température et la salinité des eaux côtières sont respectivement de 15°C et 36,3‰, alors qu'elles sont de 18° et 36,7‰ dans les eaux du large et où le phénomène d'upwelling, quasi-permanent, est plus intense que dans le secteur centre. L'engin de pêche utilisé est le "Bongo" comportant 2 filets d'une ouverture de 25 cm de diamètre, dont l'un, spécifique du zooplancton, a un maillage de 168 μm. La récolte a été effectuée de façon oblique et en paliers, c'est-à-dire que le filet, une fois en profondeur, est traîné horizontalement pendant 3 min avec une vitesse de 2 à 3 noeuds; puis il est monté verticalement jusqu'au niveau immédiatement au-dessus et ainsi de suite jusqu'à atteindre la surface. Les niveaux d'échantillonnage sont 100 m., 50 m., 35 m., 20 m., 10 m. et 0 m. Après chaque trait, le prélèvement est intégralement recueilli dans un bocal, puis immédiatement fixé avec de l'eau de mer formolée à 5%. Afin de standardiser les effectifs des différentes stations, on a utilisé l'équation de d'Ahlstrom (21-23). Ainsi, le nombre d'individus des chaetognathes de chaque station correspond à l'effectif récolté dans une même unité de volume qui est de 100 m^3.

Résultats et discussion

Dans le cadre de ce travail, 13 espèces ont été identifiées qui appartiennent aux genres: Sagitta (*S. fridirici, S. enflata, S. minima S. bipunctata, S. serratodentata, S. hispida, S. hexaptera, S. lyra, S. decipiens* et *S. planctonis*); Pterosagitta (*P. draco*); Krohnitta (*K. subtilis*) et Eukrohnia (*E.hamata*). Ces 13 espèces représentent 44,83% du total des espèces connues sur l'ensemble des côtes marocaines (8), 65% de total des chaetognathes de toute la Méditerranée (29) et environ 13 % du nombre d'espèces de ce groupe à l'échelle planétaire. Les travaux réalisés sur ce groupe au Maroc et dans les régions voisines montrent que 9 espèces seulement ont été identifiées auparavant sur les côtes atlantiques marocaines de Tanger à Cap Juby (13), 19 espèces dans les eaux des Iles Canaries (24, 25). Dans la baie ibéro-marocaine, 12 espèces ont été déterminées (5). En Méditerranée occidentale, 5 espèces ont été identifiées en 1983 (26), 8 espèces en 1985 (26, 27). La Méditerranée, y comprie la mer Noire, abriterait 20 espèces de chaetognathes (29).

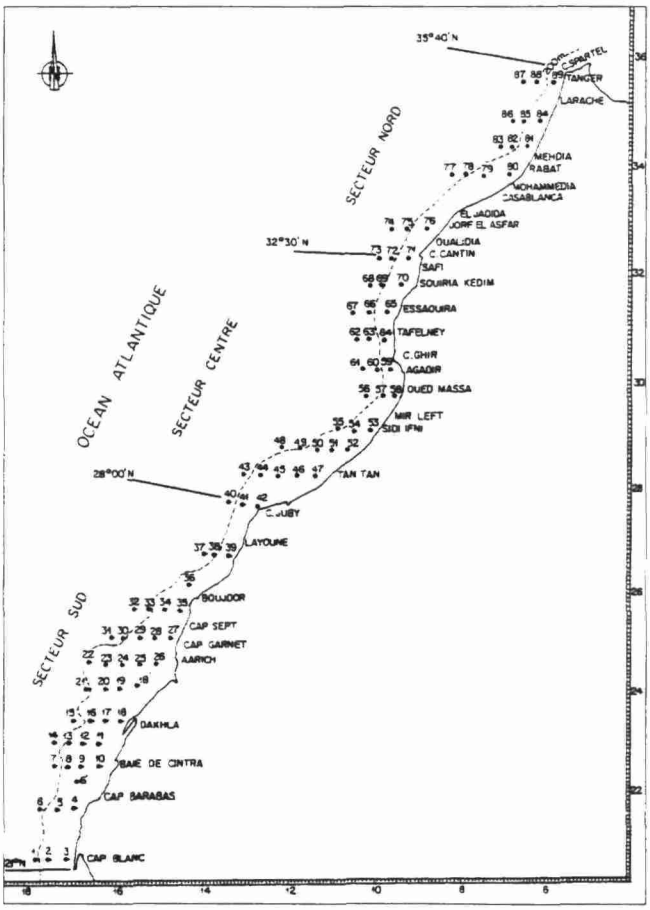

Figure 1. Carte d'échantillonage.

En fait, une synthèse de toutes les données relatives à ce groupe au Maroc montre que sur les deux façades maritimes du Maroc, 29 espèces de chaetognathes sont connues (8), soit 0,4% du total de la faune marine du Maroc. Ce groupe est constitué par 18 espèces du genre Sagitta (*S. abyssicola, S. bierii, S .bipunctata, S. decipiens, S. enflata, S. fridirici, S. furnestinae, S. hispida, S. lyra, S. macrocephala, S. maxima, S. minima,*

STRUCTURE BIOTYPOLOGIQUE DES CHAETOGNATHES DES CÔTES MAROCAINES

Larbi Cheggour [1]* et Mohamed Menioui [2]

[1] Unité de Reproduction et d'Environnement, Faculté des Sciences, BP. 1014, Rabat, Maroc
[2] Institut Scientifique B.P 703, Rabat-Agdal, Rabat, Maroc

Résumé

Le traitement par l'Analyse Factorielle des Correspondances, du peuplement des chaetognathes des côtes marocaines, a permis de montrer que la distribution des espèces paraît essentiellement régie par la composante horizontale du facteur hydrologique correspondant à une distribution côte-large. Elle a, en effet, favorisé la distinction, en premier lieu, entre des espèces néritiques (*Sagitta friderici, S. hispida*) et les espèces océaniques (*S. hexaptera, S. lyra, S. serratodentata, Pterosagitta draco* et *Krohnitta subtilis*), en passant par un groupe de transition constitué d'espèces semi-néritique (*Sagitta enflata, S. minima*). Le deuxième facteur agissant sur la distribution des espèces, en particulier côtières, est le phénomène d'upwelling.

Mots clés: Chaetognatha, hydrology, Alboran Sea

Introduction

Les chaetognathes, petit groupe marin, est constitué d'une centaine espèces (102) pour la plus part pélagiques (1). Dans les eaux marocaines, très peu d'études ont porté sur ce groupe (2-5) d'où le double intérêt de cette synthèse qui, d'une part, rend compte des résultats d'un vaste programme de recherche sur l'écosystème pélagique des côtes marocaines dirigé par l'Institut National des Recherches Halieutiques du Maroc et l'Institut ATLANTNIRO russe de Kaliningrad et, d'autre part, donne une idée sur les chaetognathes de la région étudiée (côte marocaine, en particulier atlantique) considérée comme la principale zone où la Méditerranée puise l'essentiel de sa faune (6.)

Matériel et méthodes

Les prélèvements ont été effectués en hiver (janvier 1994, 85 stations entre 21°N et 34°30'N) et en été (juillet, 1994, 89 stations entre 21°N et 35°40'N). Cette zone, de près de 3000 km a été subdivisée, en fonction des conditions hydrologiques, en trois secteurs (7, 8, 9) : un secteur nord entre 35°40'N et 32°30'N caractérisé par des eaux côtières d'une température de 16°C et d'une salinité de 36,3‰, des eaux du larges d'une température de 20°C et d'une salinité de 36,7‰ et où le phénomène d'upwelling n'est pas très intense; un secteur dit "centre" entre 32°30'N et 28°N caractérisé par des eaux côtières d'une température de 17°C et d'une salinité de 36,2‰, 21°C et de 36,4‰ dans les eaux du large, et par un phénomène d'upwelling intense en périodes estivale et automnale et un secteur sud qui s'étend entre 28°N et 21°N où la température et la salinité des eaux côtières sont respectivement de 15°C et 36,3‰, alors qu'elles sont de 18° et 36,7‰ dans les eaux du large et où le phénomène d'upwelling, quasi-permanent, est plus intense que dans le secteur centre.

L'engin de pêche utilisé est le "Bongo" comportant 2 filets d'une ouverture de 25 cm de diamètre, dont l'un a un maillage de 168 μm. La récolte a été effectuée de façon oblique et en paliers, c'est-à-dire que le filet, une fois en profondeur, est traîné horizontalement pendant 3 mn avec une vitesse de 2 à 3 noeuds, puis il est monté verticalement jusqu'au niveau immédiatement au-dessus et ainsi de suite jusqu'à atteindre la surface. Les niveaux d'échantillonnage sont 100 m., 50 m., 35 m., 20 m., 10 m. et 0 m. Après chaque trait, le prélèvement est intégralement recueilli dans un bocal et fixé avec de l'eau de mer formolée à 5%.

Afin de standardiser les effectifs des différentes stations, on a utilisé l'équation d'Ahlstrom (10, 11). Ainsi le nombre d'individus des chaetognathes de chaque station correspond à l'effectif récolté dans une même unité de volume qui est de 100 m^3.

L'étude typologique a été faite par l'Analyse Factorielle des Correspondances, avec un premier traitement hivernal, un second estival et un troisième global. C'est l'une des méthodes d'ordination, très utilisées dans la typologie des chaetognathes et du zooplancton en général (17-21). L'AFC suppose des données homogènes, ce qui est le cas de cette étude puisque seuls ont été pris en considération les effectifs des espèces. C'est une méthode simple où chaque donnée de la matrice est pondérée en divisant par la somme de la ligne et de la colonne correspondante, ce qui a pour effet de ne comparer que les profils des courbes de fréquences et de représenter sur un même graphique les point-espèces et les point-prélèvements.

Le premier tableau, hivernal, comporte les effectifs, sous forme de classes de 13 espèces dans 81 stations, le deuxième de 10 espèces dans 88 stations et le dernier représente la moyenne annuelle de 13 espèces dans 90 stations. Chaque espèce est représentée par son abondance (nombre d'individus /100 m^3) transformée en classe dont les limites forment une progression géométrique de raison 1,5; méthode ayant été utilisée pour la typologie de la faune marocaine (6).

Dans ces résultats préliminaires, nous nous sommes limités au seuls plans factoriels F1 x F2 qui expriment généralement plus de 50% de l'information disponible et, donc, les principaux facteurs régissant la distribution des chaetognathes le long des côtes marocaines.

Résultat et discussion

Typologie hivernale (fig.1). La projection des points-espèces sur le plan factoriel F1 x F2 (49,1% de l'inertie totale) montre que l'axe F1, avec 30% de cette inertie, est essentiellement expliqué par les deux espèces *Sagitta friderici* et *Sagitta hispida*, néritiques (2-5), situées du côté positif et qui, à elles seules comptent 77% de la contribution totale. Le côté négatif de cet axe regroupe un certain nombre d'espèces dont les plus importantes sont *S. hexaptera, S. lyra, S. serratodentata, Pterosagitta draco* et *Krohnitta subtilis* qui sont considérées comme des espèces océaniques (2, 3, 12).

Les espèces *Sagitta enflata* et *S.minima*, souvent qualifiées de semi-néritiques à tendance océanique (2, 3, 12 et 13) sont, graphiquement, positionnées entre les deux groupements des espèces néritiques et celles océaniques, bien que plus proches des espèces océaniques, ce qui paraît normal dans la mesure où elles sont à tendance océanique.

Dans le plan représentant la projection des points-stations, l'axe factoriel F1 est essentiellement caractérisé par l'isolement, de son côté négatif, de la quasi-totalité des stations du large (38 des 41 stations du large soit, 93%) alors que du côté positif sont positionnées la quasi-totalité des stations côtières, ou du moins toutes celles ayant une contribution relative significative, supérieure à la moyenne (1,23%). Les températures et les salinités des stations côtières et du large sont respectivement de 15, 83°C, 36, 29‰ et 16,46°C, 36, 39‰. Quant aux températures et salinités des différents secteurs, elles sont de : secteur nord 15.41°C, 36,25‰ sur la côte et 15.81°C, 36,34‰ au large; secteur centre 15.55°C, 36,24‰ sur la côte et 16.33°C, 36,33‰ au large; secteur sud 16.53°C, 36,37‰ sur la côte et 17.28°C, 36,42‰ au large

L'axe F1 représentent donc près du 1/3 de l'information totale paraît exprimer la zonation côte-large des espèces et la répartition de ces dernières paraît donc régie en premier lieu, par les variations horizontales du facteur hydrologique.

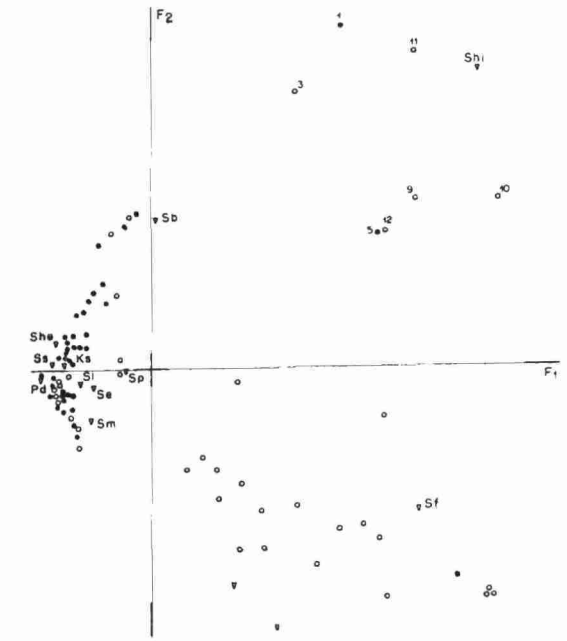

Figure 1: projection des point-stations (numéros) et des point-espèces (lettres) de la période hivernale dans le plan factoriel F1xF2
(cercles claires = stations côtières, cercles pleins = stations du larges, triangles = espèces).

STRUCTURE BIOGEOGRAPHIQUE DES COPEPODES DES CÔTES MAROCAINES

Brahim Chiahou [1*], Mohamed Menioui [2] et Mohamed Ramdani [2]

[1] Laboratoire d'Ecologie Appliquée, Département de Biologie, Faculté des sciences, Université Chouaib Doukkali, El Jadida, Maroc
[2] Département de Zoologie et Ecologie Animale, Institut scientifique, B.P. 703, Agdal, Rabat, Maroc

Résumé

La structure biogéographique de 223 espèces de copépodes des côtes marocaines a permis de montrer que la faune copépodologique marine du Maroc est essentiellement dominée par des formes cosmopolites à large répartition géographique. L'échange faunistique entre la Méditerranée et l'Atlantique se fait, apparemment, plus facilement avec la région marocaine qu'avec la région ibéro-française, avec possibilité d'existence d'une barrière biogéographique au niveau du détroit de Gibraltar.

Mots clés: Biodiversity, biogeography, copepoda, Alboran Sea

Introduction

Les affinités biogéographiques entre la faune marine des côtes atlanto-européennes et nord-ouest africaines ont, depuis longtemps, été remarquées par de nombreux auteurs (1-11). La faune copépodologique des côtes du Maroc est relativement mieux connue sur les plans systématique et faunistique que sur les plans écologique et biogéographique (10, 12-17).

Le Maroc, lieu de confrontation entre plusieurs types d'eaux d'origines et de densités différentes, appartient à la province atlanto-méditerranéenne (2, 6) et à la province lusitanienne (11).

Ce travail rentre dans le cadre de l'étude de la diversité biologique de la faune marine du Maroc, dont les copépodes constituent une composante essentielle de la fraction pélagique, qui vise une meilleure connaissance de la structure de cette faune, de son écologie et de sa dispersion géographique. Notre objectif est de mettre en évidence la structure biogéographique des copépodes marins du Maroc, des affinités biogéographiques de ces derniers avec celles des provinces voisines mais aussi, de comparer, au sein de la faune marine du Maroc la biogéographie de la faune pélagique représentée en grande partie par les copépodes et la faune benthique (11). Pour cela on adoptera les subdivisions et les définitions les plus récentes appliquées à la faune marine du Maroc (11).

Matériel et Méthode

La liste des espèces provient essentiellement de la bibliographie et des recherches sur le terrain (décembre1994-décembre1995). Les pêches planctoniques ont été effectuées, par des traits horizontaux et verticaux, à l'aide de divers types de filets, tels que le Juday-Bogorov (150 μm, 200 μm) ou le WP_2 (200 μm, 250 μm). La figure 1 montre la situation géographique des stations de prélèvements. Après détermination des espèces, nous avons établi une carte biogéographique pour chacune des espèces, en nous basant sur nos propres résultats ainsi que sur les travaux concernant la répartition des Copépodes dans diverses régions du monde (18-22).

Résultats

Des 301 espèces répertoriées (23), 223 cartes biogéographiques seulement ont pu être établies. Elles se répartissent en 10 groupes biogéographiques.

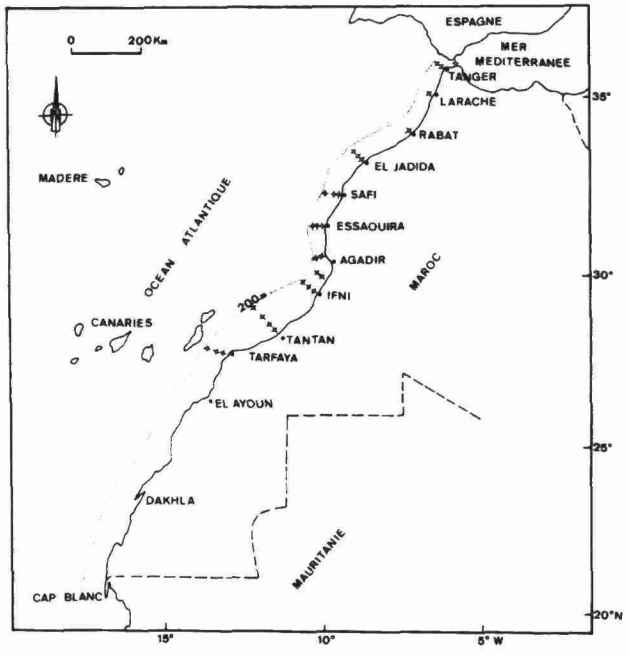

Figure 1. Situation géographique des stations des prélèvements. (◊ station).

Espèces à répartition Arctique à Lusitanienne. Trois espèces (1,3% du total des copépodes) appartiennent à ce groupe; il s'agit de *Paraeuchaeta norvegica* présente en Méditerranée alors que *Calanus finmarchicus* et *Halithalestris croni* y sont absentes.

Espèces à répartition Arctique à ouest-Africaine. Ce groupe monospécifique comporte l'espèce *Aetideopsis armata* (0,4% des Copépodes), absente de la Méditerranée.

Espèces à répartition Boréo-Lusitanienne. Treize espèces (5,8%) appartiennent à cette catégorie: *Acartia discaudata, Pseudocalanus elongatus, Diaixis pygmaea, Centropages hamatus, C. typicus, Labidocera wollastoni, Cymbasoma rigidum, Monstrilla helgolandica, Monstrillopsis dubia*; elles sont présentes en Méditerranée, contrairement à *Bradyetes inermis, Paroithona parvula, Aegisthus spinulosus, Cephalophanes refulgens.*

Espèces à répartition Boréale à ouest-Africaine. Cet ensemble est représenté par 8 espèces (3,6%) dont 4 connues de la Méditerranée (*Scolecithricella dentata, Pleuromamma borealis, Pontella lobiancoi, Hatschekia pagellibognravei*), et 4 absentes (*Scaphocalanus echinatus, Scolecithricella ovata, Corycaeus anglicus, Scolecithricella minor).*

Espèces à répartition Boréale à sud-ouest-Africaine. Ce groupe comporte 8 espèces (3,6%). Deux (*Candacia elongata, C. tenuimana*) sont connues de la Méditerranée, alors que les 6 autres espèces (*Euchirella bitumida, Pareuchaeta gracilis, P. sarsi, Diaixis hibernica, Pleuromamma robusta, Paraugaptilis buchani*) y sont absentes.

Espèces à répartition Lusitanienne. Vingt espèces (9%) appartiennent à cette catégorie. Dix ont une large dispersion dans la province lusitanienne (*Acartia latisetosa, Eucalanus monachus, Paracalanus nanus, P. pygmaeus, Pontella mediterranea, Labidocera brunescens, Oithona linearis, Corycaeus giesbrechti, C. limbatus, Lernanthropus brevis*), alors que les dix autres (*Onchocalanus steueri, Caligus ligusticus, C. pageti, C. apodus, C. pagelli, C. mugilis, Corycaeus brehmi, Clavellopsis strumosa, C. characis, Calocalanus tenuis*) s'étendent sur la Méditerranée et la région marocaine.

Espèces à répartition Lusitanienne à ouest-Africaine. Ce groupe compte 8 espèces (3,6%). Trois sont connues des régions ibéro-française et marocaine (*Paracalanus denudatus, Pseudocalanus minutus, Lucicutia gemina*); deux sont connues de la Méditerranée et de la région marocaine (*Acartia grani, Haloptilus fertilis*), et trois ne dépassent pas, vers le nord, la région marocaine (*Candacia paenelongimana, Labidocera scotti, Oncaea curta*).

Espèces à répartition Lusitanienne à sud-ouest-Africaine. Dix-sept espèces (7,6%) appartiennent à ce groupe; quatre ont une large dispersion dans la province lusitanienne (*Pseudochirella obtusa, Centropages chierchiae, Candacia varicans, Pontellina atlantica*); huit espèces, absentes de la Méditerranée, s'étendent vers le nord, sur les régions ibéro-française et marocaine (*Temora turbinata, Arietellus giesbrechti, Eucalanus pileatus, Euchirella amoena, Paraeuchaeta barbata, P. bisinuata, Valdiviella insignis, Candacia curta*) alors que les cinq autres (*Euchirella pulchra, E. splendens, Undinula vulgaris, Euaugaptilis longimanus, Arietellus aculeatus*) sont limitées, dans la province lusitanienne, à la région marocaine.

Espèces à large répartition géographique. Ce sont des espèces ayant une aire de dispersion qui s'étend sur au moins deux océans. Quatre-vingt quatre formes (37,6%) appartiennent à ce groupe biogéographique. Il s'agit de *Scolecithricella abyssalis, Calocalanus styliremis, Oithona brevicornis, Scottocalanus helenae, Alella macrotrachelus, Clavellopsis sargi, Cucullanus sp, Ergasilus lizae, Naobranchia cygniformis, Elytrophora brachyptera, Nogagus elongatus, Myticola intestinalis, Calanoides carinatus, Centropages kroyeri, C. bradyi, Ischnocalanus plumulosus, Rhincalanus cornitus, R. nasitus, Gaetanus miles, Euchirella curticaudata, E. brevis, E. messinensis, E. rostrata, Lophotrix frontalis, Scolecithrix bradyi, S. danae, Metridia princeps, M. venusta, M. brevicauda, Heterorhabdus papilliger, H. abyssalis, H. spinifrons, H. longicornis, Augaptilus longicaudatus, Arietellus setosus, Oncaea conifera, O. notopus, Sapphirina angusta, S. maculosa, S. auronitens, S. gemma, S. intestina, S. mettalina, S. opalina, S. ovatolanceolata, Paracalanus aculeatus, Euaetideus geisbrechti, Chirundina streetsi, Euchaeta acuta, E. media, E. pubera, Paraeuchaeta tonsa, Phaenna spinifera, Megacalanus princeps, Pleuromamma xiphias,*

DIVERSITÉ BIOLOGIQUE DES COPÉPODES DES CÔTES MAROCAINES

Brahim Chiahou [1*] et Mohamed Menioui [2]

[1] Laboratoire d'Ecologie Appliquée, Département de Biologie, Faculté des sciences, Université Chouaib Doukkali, El Jadida, Maroc
[2] Département de Zoologie et Ecologie Animale, Institut scientifique, B.P. 703, Agdal, Rabat, Maroc

Résumé

L'analyse systématique et faunistique des copépodes des côtes marocaines aussi bien méditerranéennes qu'atlantiques a révélé la présence de 301 espèces dominés par la famille des Augaptilidae qui compte 9 genres et 43 espèces. La structure quantitative est essentiellement caractérisée par la prédominance du peuplement des copépodes par un nombre restreint d'espèces dont principalement *Acartia discaudata.*, groupe qui serait le plus abondant en été et le moins prolifique en hiver.

Mots clés: Copepoda, Biodiversity, Alboran Sea

Introduction

Les copépodes constituent certainement les crustacés planctoniques les mieux représentés de la biomasse planctonique totale. Ceci est, entre autres, le cas en Atlantique nord oriental et plus particulièrement sur les côtes africaines (1-3). Les copépodes ont une grande importance écologique et économique dans les eaux marocaines puisqu'ils constituent un aliment de choix pour certains groupes pélagiques tels que les chaetognathes et, directement ou indirectement, pour de nombreux poissons d'intérêt économique (4, 1, 5) ayant un rôle stratégique dans l'économie marocaine. Les travaux ayant traité du zooplancton des côtes marocaines et plus particulièrement des copépodes sont très peu nombreux (3, 6-11) .

Ce travail entre dans le cadre d'une expertise initiée par le Programme des Nations Unies pour l'Environnement (PNUE) et le Ministère de l'Environnement marocain et vise une meilleure connaissance de la diversité biologique au Maroc, en particulier la structure et la distribution des différents groupes systématiques marins. Son intérêt pour la Méditerranée réside dans le fait que, la faune méditerranéenne est essentiellement alimentée par la faune atlantique (12) et plus particulièrement la région biogéographique marocaine pour les espèces superficielles (13,14).

Matériels et méthodes

Les pêches planctoniques ont été effectuées, par des traits horizontaux et verticaux, à l'aide de divers types de filets , tels que le Juday-Bogorov (150μm, 200μm) ou le WP2 (200μm, 250μm). L'étude quantitative est limitée aux copépodes pélagiques récoltés dans les côtes d'El Jadida durant la période décembre1994 décembre1995. Leur biomasse a été estimée à partir du poids sec des individus.

Résultats et discussion

Structure qualitative. L'inventaire systématique des copépodes des côtes marocaines (aussi bien atlantiques que méditerranéennes) a révélé la présence de 301 espèces réparties sur 40 familles et 96 genres différents (16).

L'analyse de la figure 1, illustrant la répartition, par familles, du groupe des copépodes du Maroc, montre que ce groupe est essentiellement dominé par les Augaptilidae, les Aetideidae, les Scolecithridae, les Sapphirinidae, les Euchaetidae, les Candaciidae, les Pontellidae, les Corycaeidae, les Metrididae et les Calanidae. Ces familles sont toutes représentées par au moins 10 espèces et représentent respectivement 14,3%, 7,3%, 6,9%, 5,9%, 5,3%, 4,3%, 4,3%, 3,9%, 3,6%, 3,3%; soit donc un total de plus de 59%, de l'ensemble des espèces identifiées au Maroc. Les familles des Paracalanidae, des Pseudocalanidae et des Eucalanidae sont représentées par 9 espèces chacune; celles des Lucicutidae, des Heterorhabdidae, des Caligidae et des Oncaeidae par 8 espèces chacune. Les familles des Acartiidae et des Oithonidae comptent 7 espèces chacune, les Centropagidae, les Phaennidae et les Areitellidae 6 espèces chacune, les Lernaeopodidae 4 espèces, les Temoridae, les Ectinosomidae, les Aegisthidae et les Monstrillidae, 3 espèces chacune, les Diaixidae et Clytemnestridae par deux espèces et une seule espèce pour les Mormonillidae, les Macrosetellidae, les Thalestridae, les Tachydiidae, les Lernaeoidae, les Ergasilidae, les Lernanthropidae, les Naobranchiidae, les Hatschekiidae, les Euryphoridae et les Pandaridae.

Structure quantitative. Devant l'impossibilité de fournir une idée précise sur la structure quantitative des copépodes tout au long des côtes marocaines, nous essayerons de donner une image de cette structure à travers un échantillon correspondant à une étude, durant un cycle annuel (décembre 1994 à décembre 1995) dans la région d'El Jadida (33°-33°16'09"N, 8°30'-8°45'W)

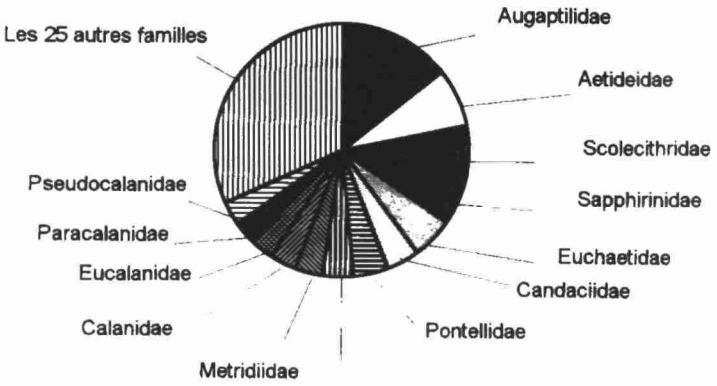

Figure 1. Répartition par famille des copépodes des côtes marocaines.

Dans cette étude, 949 539 individus au total ont été récoltés dans 30 prélèvements, correspondant chacun à 113 m d'eau de mer filtrée.

La densité moyenne annuelle est de 280 ind/ m^3; elle varie considérablement entre un minimum de 127 ind/ m^3 au mois de janvier et un maximum de 689 ind/ m^3 au mois de septembre. Les densités moyennes saisonnières sont de 181 ind/ m^3 en hiver, 348 ind/ m^3 au printemps, 423 ind/ m^3 en été et 206 ind/ m^3 en automne.

Quantitativement, le peuplement des copépodes de la région d'El Jadida est essentiellement dominé par un nombre restreint d'espèces (8 espèces, représentant chacune 10% de l'effectif total dans au moins un des 30 échantillons). L'ensemble de ces 8 espèces comptent 8,9% de la richesse spécifique totale et constituent, en moyenne annuelle, 74,6% de l'effectif total du peuplement. Il s'agit d'*Acartia discaudata* (21%), *A. clausi* (12,3%), *Paracalanus parvus* (10,1%), *Calanus helgolandicus* (9,1%), *Acartia grani* (8.,%) et *Centropages typicus* (6,6%), *Oithona nana* (3,7%) et *Clausocalananus arcuicornis* (2,9%). L'importance quantitative de ces espèces au sein du peuplement varie selon les saisons; c'est ainsi qu'en hiver, la communauté des copépodes est essentiellement dominée par *C. helgolandicus* (18,5%) suivi d'*A. clausi* (17,7%), *P. parvus* (13,5%) puis de *C. arcuicornis* (11,8%) et *C. typicus* (5,8%) représentant, ensemble, plus de 67% de l'effectif hivernal. Au printemps, ce peuplement est surtout dominé par les espèces *A. clausi* (17,4%), *A. discaudata* (16,6%), *P. parvus* (15,4%), *C. helgolandicus* (10,3%), *A. grani* (8,3%) et *C. typicus* (7,5%) qui constituent pendant cette saison 75,5% du total des copépodes. En été, ce groupe est essentiellement dominé par les 4 espèces: *A. discaudata* (44,5%) suivie d'*A. grani* (18,4%), puis *A. clausi* (7,5%) et *O. nana* (5%), représentant, à elles seules, près de 75,4% de l'effectif estival. Enfin, en automne, les copépodes montrent une nette dominance de *P. parvus* (14,6%), *C. typicus* (13,4%), *C.helgolandicus* (13,3%), *A. clausi* (11,7%) et *O. nana* (7,2%) qui comptent, pendant cette saison, plus de 60% du total de ce groupe.

La biomasse annuelle moyenne des copépodes sur la côte d'El Jadida est de 8,85 mg/m^3 avec un maximum de 18.4 mg/m^3 au mois de septembre et un minimum de 3,3 mg/m^3 au mois de décembre. Les moyennes saisonnières sont de 10.53 mg/m^3 en hiver, 9,09 mg/m^3 au printemps, 8,16 mg/m^3 en été et 8,11 mg/m^3 en automne.

Discussion

L'analyse systématique et faunistique des copépodes des côtes marocaines a révélé la présence de 301 espèces. Mais, nous pensons que cette valeur reste bien en deçà de ce qui existerait réellement dans

MESOZOOPLANKTON ABUNDANCE IN THE EASTERN MEDITERRANEAN DURING SPRING 1992

Epaminondas D. Christou [1], Ioanna Siokou-Frangou [1], Maria Grazia Mazzocchi [2], Laura Aguzzi [2]

1 National Centre for Marine Research, Ag. Kosmas, Hellinikon, 16604 Athens, Greece
2 Stazione Zoologica "A. Dohrn", Villa Comunale, 80121 Naples, Italy

Abstract

Within the framework of the international programme POEM-BC, mesozooplankton samples were collected at 20 stations in the Ionian Sea, Cretan Sea, Cretan Passage and Rhodes area (NW Levantine Sea), in March-April 1992. Vertical hauls were taken from 4 discrete depth layers in the upper 300 m water column. Depth-integrated abundances were decreased as follows: Ionian Sea, Rhodes area, Cretan Sea and Cretan Passage. Strong vertical gradients in zooplankton distribution were evident at almost all stations, especially in the Rhodos area where extremely high abundances at the 0-50 m layer were recorded. It seems that in spring 1992, the region affected by the Rhodes gyre acts as a strong upwelling area, as confirmed by the signal detected in the surface zooplankton abundance.

Key-words: Zooplankton, Eastern Mediterranean

Introduction

In the Mediterranean a west-east gradient in nutrients deficiency creates an oligotrophic environment (1) and even ultra-oligotrophic in its eastern-most part (2). The role of mesozooplankton in the pelagic ecosystem of the Eastern Mediterranean and the influence of hydrology upon it were included among the aims of the POEM-BC (Physical Oceanography of Eastern Mediterranean-Biology, Chemistry) project. In the frame of this project, coordinated international cruises were carried out throughout the EMED in October-November 1991 and March-April 1992. In the present study, we present the results on mesozooplankton abundances collected at 20 stations during spring (March-April) 1992.

Materials and methods

A multi-vessel quasi-synoptic survey (POEM BC-O92) was conducted in March-April 1992. Oceanographic data (physical, chemical and biological) were acquired on a grid of stations covering a major area of the Eastern Mediterranean. Mesozooplankton quantitative samples were collected at 20 stations in the Ionian Sea (Western part), Cretan Sea, Cretan Passage and Rhodos area (Fig. 1). The stations were located along transects chosen on the basis of the known circulation patterns, some of them in areas with permanent hydrological features (see 3). Zooplankton samples were collected in the upper 300 m of the water column. Vertical hauls were taken from 4 depth layers (0-50, 50-100, 100-200, 200-300 m) using a WP2 closing net (200 μm) in all studied areas.

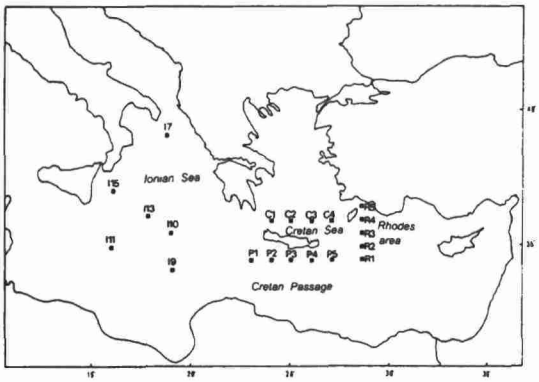

Fig. 1. Position of sampling stations.

Results

The highest depth-integrated (0-300 m) abundances were recorded in the Ionian stations I7 and I11 (341 and 337 ind.m^{-3}), neighboring to the Adriatic Sea and Sicily Channel (Table1, Fig. 1). High values were also reported in the Rhodos area, whereas the lowest value (74 ind.m^{-3}) was observed in the Cretan Passage (St. P2, Table1). The higher mean values were recorded for the Ionian Sea (250 ind.m^{-3}) and the Rhodos area (221 ind.m^{-3}), whereas the lower mean values were recorded for the Cretan Passage (119 ind.m^{-3}) and the Cretan Sea (149 ind.m^{-3}). One way ANOVA on depth-integrated values, revealed significant differences between areas (F= 4.87, P<0.05, 3 d.f.). The Tukey test indicated significant difference between the Cretan Passage and the Ionian Sea. Vertical profiles of zooplankton abundance displayed strong decreasing gradients from the surface to the deeper layers (Fig. 2). In all layers, but the surface (0-50 m), the highest mean abundances were reported in the Ionian Sea. In the surface layer, the highest mean value was recorded in the Rhodos area (988 ind. m^{-3}) being almost three times higher than those in the neighboring regions of Cretan Passage (311 ind. m^{-3}) and Cretan Sea (360 ind. m^{-3}). On the contrary, in the 50-100 and 100-200 m layers the lowest mean values (146 and 55 ind. m^{-3}, respectively) were obtained in the Rhodos area. In the 200-300 m layer, Cretan Sea, Cretan Passage and Rhodos area displayed similar mean abundances ranging from 34 to 43 ind. m^{-3}. The sharpest decreasing in the vertical profile was observed in the Rhodos area, with surface numbers representing 80% of the standing stock in the total water column, whereas the 200-300 m layer accounted only for 3% of the total. Although in the other regions this decrease was smoother, the deepest layer (200-300 m) accounted only for 5-7 % of the total water column.

Table 1. Depth-integrated values (0-300 m) of zooplankton abundance (ind. m^{-3}) at each station in the study area.

Ionian Sea						
Sts	I7	I9	I10	I11	I13	I15
ind m^{-3}	341	291	176	337	199	159
Cretan Sea						
Sts	C1	C2	C3	C4		
ind m^{-3}	236	119	138	104		
Cretan Passage						
Sts	P1	P2	P3	P4	P5	
ind m^{-3}	156	74	108	157	106	
Rhodos Area						
Sts	R1	R2	R3	R4	R5	
ind m^{-3}	309	183	246	207	162	

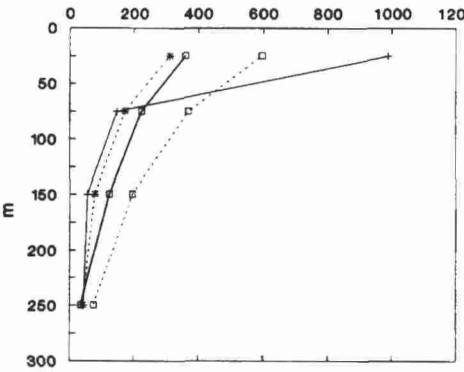

Fig. 2. Vertical profiles of total zooplankton abundances (ind. m^{-3}, mean values for each region).

Figure 3 shows the distribution of zooplankton abundance per station and layer. The highest surface (0-50 m) abundance was recorded in the central part of the Rhodos transect (1376 ind. m^{-3}, St. R3) representing the 95% of the total water column numbers, whereas the lowest was recorded in the Cretan Passage (239 ind. m^{-3}, St. P2). In Rhodos area, the lowest surface abundance was recorded at St. R5 (676 ind. m^{-3}). It is worth mentioning the high similarity among the surface abundances of the Cretan Sea stations, ranging from 341 to 375 ind. m^{-3}. One way ANOVA on surface abundances revealed significant differences between areas (F= 14.67, P<0.001, 3 d.f.). The Tukey test indicated significant difference between the Rhodos area and the other regions, while the Cretan Passage was significantly different from the Ionian Sea. In the deepest layer (200-300 m), the extreme low value of 3 ind. m^{-3} was recorded at St. R3 (Rhodos area, Fig. 3). In the same transect, St R1 differed from the other stations by displaying higher values in the layers below 50 m (Fig. 3). In the 50-100 m layer, the abundances recorded at Sts. R1 and R4 were from 1 to 5 times higher than those recorded at the other stations of this transect. The pattern of decreasing gradient with depth was not observed: (a) in the surface of St. C1 (Cretan Sea), (b) in the deeper layers of Sts R2 (Rhodos area), and (c) in the deeper layers of Sts. P1 and P2 (Cretan Passage). In order to check if the variability in the vertical distribution among stations could be attributed to zooplankton diel vertical migrations, one way ANOVA between day and night samples was performed. No significant differences (F= 0.74 P>0.05; 1 d.f.) between day/night data were detected.

DISTRIBUTION COMPARÉE DES PUFFINS (PROCELLARIIDÉS) DANS LE GOLFE DU LION EN JUILLET 1994

Conéjéro Sandrine * et Beaubrun Pierre

Laboratoire de Biogéographie et Ecologie des Vertébrés, École Pratique des Hautes Études, Univ. Montpellier 2 Case 94, 34095 Montpellier Cedex 5, France

Résumé

En juillet 1994, une prospection couvrant tout le golfe du Lion a permis d'étudier le peuplement estival de l'avifaune marine. La distribution des Procellariidés et leurs relations avec le milieu sont ici abordées. Le Puffin de Méditerranée se nourrit préférentiellement de petits poissons pélagiques sur les faibles profondeurs de la zone néritique alors que le Puffin cendré fréquente surtout le talus continental et les secteurs plus pélagiques.

Mots-clés : Biogeography, Birds, Diet, Trophic relations, Gulf og Lions

L'activité de l'avifaune en Méditerranée sur les sites de reproduction a fait l'objet de nombreux travaux, mais peu d'études traitent de la distribution des oiseaux marins au large des côtes françaises. En fait, seul Hemery [1] aborde la question pour l'ensemble du littoral, en se basant sur des observations faites en hélicoptère ou en bateau, et Zotier [2] examine plus spécialement la répartition du Puffin cendré (*Calonectris diomedea*) en mer. Pour combler ces lacunes, un programme de recherche a été mis en oeuvre dès 1991 par l'École Pratique des Hautes Études, et nous présentons ici les premiers éléments concernant la distribution estivale (juillet 1994) des Procellariidés dans le golfe du Lion.

Matériel et méthodes

Période et zone d'étude. L'ensemble du golfe du Lion a été prospecté de façon systématique, à bord du N/O *L'Europe*, entre le 11 et le 27 juillet 1994. Sur ce secteur de forme semi-circulaire qui s'étend du cap Creus à Marseille, le plateau continental est particulièrement large (40 milles nautiques au maximum), et se poursuit par un talus entaillé de profonds canyons. L'hydrologie particulière de cette zone est sous la triple influence du courant Liguro-provençal venant d'est, de l'extension vers le large du panache des eaux du Rhône et, par forts coups de Mistral ou de Tramontane, de phénomènes d'upwelling localisés. Il en résulte une forte productivité biologique qui fait du golfe du Lion un pôle traditionnel de pêche.

Méthodologie. Le plan d'échantillonnage, sous forme de radiales, a été défini par l'IFREMER dans le cadre des études entreprises sur l'estimation des stocks de petits poissons pélagiques (missions PELMED). Ces radiales, au nombre de 10, s'étendent de la côte jusqu'aux fonds de 500-1000 m, sont parallèles entre elles, espacées de 12 MN (voir figs 1, 2 et 4) et ont été parcourues à 8 noeuds. Les autres trajets ont été prospectés à 10 noeuds. Sur ces axes les oiseaux sont repérés à l'oeil nu en appliquant la méthode du "transect de ligne" [3], les jumelles ne servant qu'à résoudre une ambiguïté d'identification. L'unique observateur est situé à l'avant du bateau, et sa visibilité théorique est d'une portée de 5 MN. Ne sont retenues ici que les observations réalisées avec un état de la mer ≤ à 3 Beaufort. L'ensemble de la prospection a couvert 339 milles nautiques et nécessité 60 heures d'observation réalisées en 11 jours. La route suivie est enregistrée mille par mille (écho-intégrateur bifréquences OSSIAN-1500) et les oiseaux notés en continu. Le traitement des données au laboratoire est réalisé avec OEDIPE, logiciel de l'Ifremer sur la base unitaire de 1 mille.

Distribution des espèces

Place des Procellariidés dans le peuplement d'oiseaux marins. Durant la campagne, 2164 oiseaux appartenant à 9 espèces ont été observés, mais tous ne détiennent pas la même importance au sein du peuplement. Le Goéland leucophée (*Larus cachinnans*) domine largement avec 63% des effectifs recensés. Viennent ensuite les deux espèces de Procellariidés : le Puffin de Méditerranée (*Puffinus yelkouan*) et le Puffin cendré (*Calonectris diomedea*) qui totalisent ensemble 36% du peuplement. Les six autres espèces sont très faiblement représentées (1%); il s'agit de l'Océanite tempête (*Hydrobates pelagicus*), du Fou de Bassan (*Morus bassanus*), d'un Cormoran (*Phalacrocorax* indéterminé), des Mouettes rieuses (*Larus ridibundus*) et mélanocéphales (*L. melanocephalus*) et de la Sterne pierregarin (*Sterna hirundo*). Les Puffins constituent donc plus du tiers du peuplement estival fréquentant le golfe du Lion.

Le Puffin de Méditerranée (figure 1). L'espèce a été rencontrée dès 2.5 milles des côtes et sur l'ensemble du plateau continental jusqu'aux lignes de sonde de 200 voire 500 mètres. Elle semble plus fréquente dans le secteur sud-ouest du golfe, et au large de Sète et de la Camargue bien que, dans cette dernière zone, les oiseaux aient surtout été observés autour de bateaux de pêche en action et le biais existe peut-être d'une attirance par les activités humaines. L'examen de la distribution des individus selon des tranches bathymétriques croissantes (tableau 1) fait clairement apparaître une très nette préférence à fréquenter les faibles profondeurs : toutes mentions confondues, la médiane est axée sur les fonds inférieurs à 30 m, et elle se situe entre 50 et 100 m si on ne tient pas compte des observations faites autour des bateaux.

Fig. 1. Indices d'abondance du Puffin de Méditerranée notés tous les 5 milles dans le golfe du Lion, en juillet 1994.

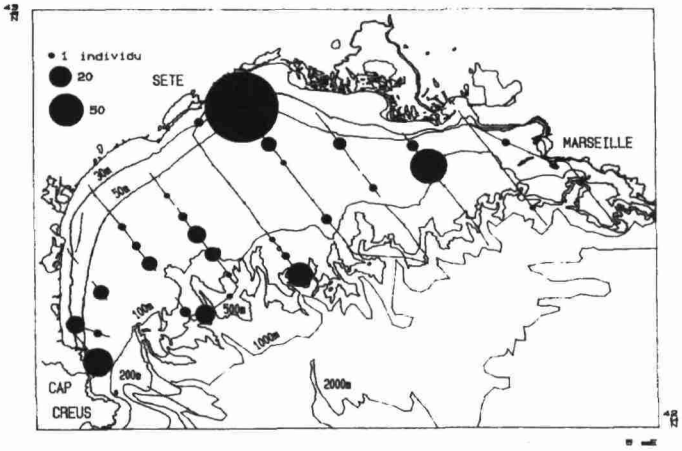

Le Puffin cendré (figure 2). Quelques Puffins cendrés peuvent être vus, en petit nombre, sur les profondeurs comprises entre 30 et 100 m, et parfois très près des côtes à proximité des caps. Cependant il apparaît être incontestablement l'hôte préférentiel du rebord du plateau continental et du large. La médiane de sa répartition est située sur les fonds de 200 à 500 mètres (tableau 1).

Fig. 2. Indices d'abondance du Puffin cendré notés tous les 5 milles dans le golfe du Lion, en juillet 1994.

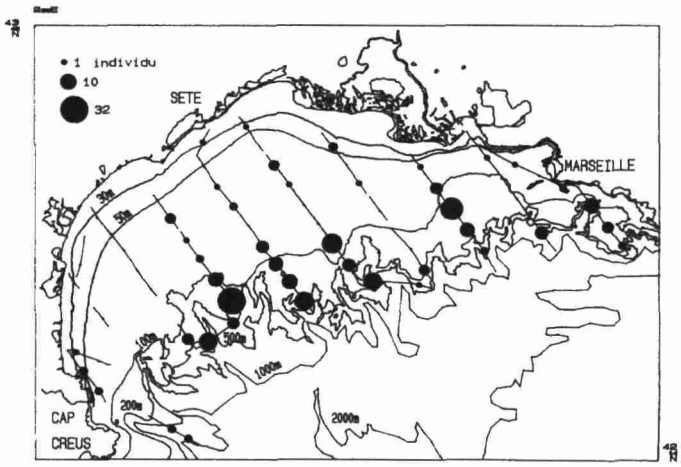

RELATIONSHIP BETWEEN RNA, DNA AND PROTEIN CONTENT AND LARVAL DAILY GROWTH IN ALBORAN SEA SARDINE (*SARDINA PILCHARDUS*)

D. Cortés, T. Ramirez and A. García*

Centro Oceanográfico de Fuengirola, Apdo. 285, 29640 Fuengirola, Málaga, Spain

Abstract

A population of 124 sardine (*Sardina pilchardus*) larvae from the Bay of Málaga (Alborán Sea) were sampled during the peak spawning period (January, 1995) and analized individually for daily growth, nucleic acid and protein content. The daily growth pattern fits well a potential relationship, as well as, the allometric relationship between SL and otolith radius. The estimated daily growth rate was 0.71 mm/day for a 10 mm larvae and 0.42 mm/day for a 17 mm larvae. Larval size expressed in terms of SL, DNA and protein content follow likewise good potential relationships with otolith radius, wet weight and age. RNA/DNA and protein/DNA ratios show an increasing trend with size/age of the larvae.

Key words: larvae, growth, analytical methods, fishes, Alboran Sea

Introduction

The Alborán Sea sardine (*Sardina pilchardus*) starts to spawn during early autumn (October), attains its peak spawning season in winter (December-January) and steadily declines its spawning activity till late spring (May). The spawning grounds are located off the coasts of Málaga, from the littoral waters attaining maximum densities at 100 m depth. The inshore waters of the Bay of Málaga (Fig. 1) is considered as their nursery grounds (1), and its coastal waters had been the most heavily exploited by an artisanal fleet targetting on the late larval stages of sardine (2).

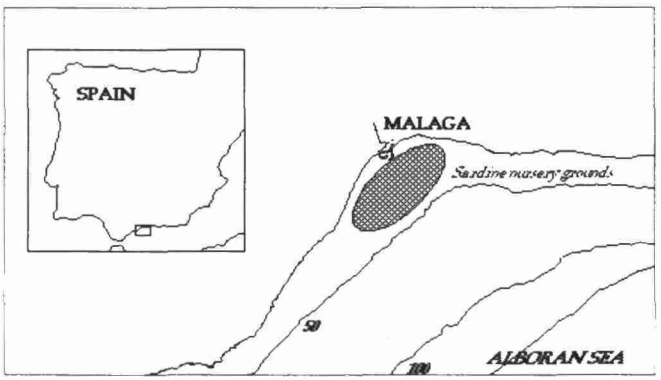

Fig. 1. Sardine larvae sampling area.

The fishing activity targetting on this resource normally works during nocturnal periods, particularly during the early morning hours before sunrise. Thus, most of the sampling was carried out at these times. Nevertheless, it was observed that sardine larvae abundance decreased as daylight hours progressed.

Sardine larvae were analized individually for daily growth analysis, RNA, DNA and protein content estimates. A total of 124 larvae were analized ranging from 8.4 to 28.3 mm (mean size at 17 mm).

Otolith microstructure analysis has proven in the past years a useful tool for recruitment studies. On the other hand, the analysis of larval condition through the estimation of nucleic acid content as a measurement of the nutritional status can aid in the assessment of the environmental impact on the biological variables of individuals. Well fed larvae and fast growing larvae show higher RNA/DNA ratios and wider daily increment deposition than starving larvae.

Material and methods

The plankton sampling was carried out by means of short duration superficial tows (≈ 5 min) with a WP-2 plankton net equipped with 1mm mesh. The depth range of the area of sampling varied from 10 m to 30 m off the litoral waters of the Bay of Málaga. During January 1995, sardine larvae were by means of a series of repetitive tows with a WP-2 plankton net (1 mm mesh) towed superficially. The depths covered ranged from 10 to 30 m depths, although generally most tows were in 15 m depth. The sampling was carried out during the early morning hours (sunrise) and late evening hours (dusk). The tows were in general around 5 minutes long. On board, the plankton sample was sorted for sardine larvae and conserved in liquid nitrogen.

The method followed for the joint analysis of otolith microstructure and nucleic acid and protein quantification was as follows. Larvae were defrosted, measured and ulteriorly, otoliths extracted and mounted with common nail lacquer on glass slides. The same larvae were used for determining the nucleic acid content and protein content. The analytical methods followed are described in (3) and (4).

Sagittal otoliths were used for daily increment counts. Otoliths were projected to a video monitor and the increments were counted in the screen by means of an specifically designed software for increment counts (5). Increments were counted after the visualization of the check ring which defines the first feeding stages of the larvae. The software package gives an output of the resulting increment counts and the increment widths.

The statistical analysis carried out for the different regressions were done with the statistical package KaleidaGraph Version 2.1.0 running on a MacIntosh computer.

Results and discussion

Daily growth fits a potential relationship (R= 0.96) (Fig. 2). The instantaneous growth rate calculated for larvae of 10 mm was 0.71 mm/day, while for larvae of 17 mm (mean size of analized larvae) was 0.42 mm/day. These values are higher than those observed for the Portuguese sardine (6). Nevertheless, the daily growth pattern of the Portuguese sardine was fit to a linear relationship because the size ranges sampled were limited to the early larval stages. However, this difference can also be due to the characteristics of the sampled area. The area has been traditionally considered as ideal for sardine and anchovy nursery grounds due to its particular hydrological conditions. It is characterized by well mixed waters. The wind regime enhances enrichment processes which eventually favours feeding availability.

The allometric relationship between size and otolith radius also followed a potential relationship (R=0.97).

DNA and total protein content are intimately associated with larval cellular mass, and thus, their quantity is related to their relative growth status. Consequently, these show high correlations with larval size, otolith radius, wet weight and age (Table 1). On the other hand, RNA, as an index of protein production, shows a higher variability since it is mainly dependent on the success of feeding during the early life stages (Table 1).

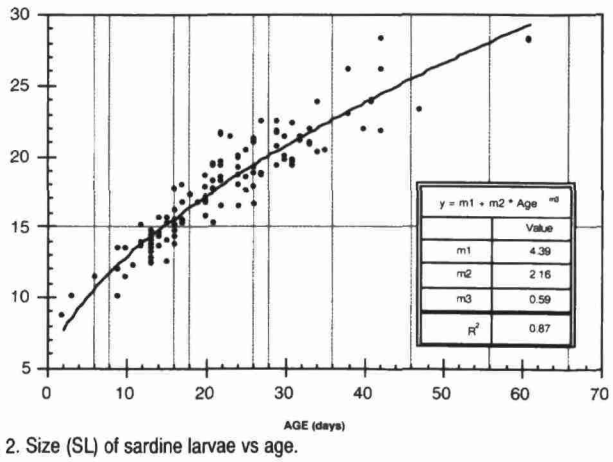

Fig. 2. Size (SL) of sardine larvae vs age.

FEEDING GUILDS OF POLYCHAETES ASSOCIATED WITH *MYTILUS GALLOPROVINCIALIS* (LAM.) ASSEMBLAGE IN THE NORTH AEGEAN SEA

P. Damianidis * and C. C. Chintiroglou

Aristotle University, School of Biology, Dept. of Zoology, P.O. Box 134. GR-540 06 Thessaloniki, Greece

Abstract

The present study has demonstrated 8 polychaete feeding guilds in the assemblage of *Mytilus galloprovincialis*. Among these feeding guilds, the most abundant are the microphagous, sedentary polychaetes. Regarding the macrophagous feeding guilds, the carnivorous are the most numerous. The distribution of the microphagous/sedentary polychaetes shows a significant fluctuation in time, which is related to the surface available to the polychaetes to settle on, which in turn depends directly on the abundance and the structure of the population of the bivalve (*M. galloprovincialis*). In contrast, the fluctuation in the distribution of the discretely motile polychaetes in time is the result of the process of reproduction of the species *Prionospio* sp., which is known for its multiannual reproductive efforts . The variety of the feeding guilds of the polychaetes in the assemblage agrees with its particular physiognomic aspect, as determined by the *M. galloprovincialis*.

Keywords : Infralittoral, Polychaeta, Trophic Relations, Aegean Sea

Introduction

As it is known, the assemblages of *Mytilus galloprovincialis* can develop in heavily polluted areas as well as in clean or semi-polluted areas (1, 2). This is a fact of great importance, since the frequent observation of the composition of these assemblages can provide us with very useful information about the impact of pollution on the assemblages of hard substrates. According to Wenner (3) the structure of the mussel community is regarded as a good biological indicator for monitoring marine pollution. On the other hand, the study of the benthic assemblages requires the knowledge of both their structure and their composition (4, 5). Information about the structure of the assemblages of *Mytilus galloprovincialis* in the Aegean Sea is available in the studies of Kocatas (6) and Topaloglou (7), while the studies of Bellan-Santini (2), Tursi (8), Desrosiers (5) and Matarrese (9) refer to the assemblages in the western Mediterranean and the Adriatic.

The study of the assemblages of *Mytilus galloprovincialis* which develop on the eastern shore of the Bay of Thessaloniki has been included in a research programme concerning the assemblages of the artificial hard substrates in Thermaikos Gulf. This paper presents preliminary results regarding the structure of the polychaete fauna of this assemblage and the organization of their populations in time.

Materials and methods

The sampling area is located on the eastern coast of Thessaloniki bay (Agia Triada), in the North Aegean Sea. Sampling was carried out by scuba diving. Samples were taken by means of the sampling methods described by Chintiroglou and Koukouras (10). The area covered by this sampler is 400 cm^2 (20 x 20 cm) which is the minimum necessary quadrat area for the investigation of the hard substrate (2, 11). During each sampling period 3-4 replicates were taken. The samples, 14 in total, were collected during winter and summer of 1994 and 1995. After sampling, the specimens were preserved in a 10% formalin solution and were transferred to the laboratory for further treatment. In the sampling area, the depth was 1.5 - 2 m; water temperature was 11°C ± 0.9 in winter and 24.5°C ± 3.8 in summer; salinity 38 ± 0.3‰ (winter) and 36.9 ± 0.3‰ (summer), dissolved O2 6.3-7.1ppm and pH 8-8.7. The annual fluctuation of the salinity agrees with the facts that were recently presented by Anagnostou (12).

Classification of Polychaetes' feeding guilds

The families of polychaetes, that have been identified in our samples, have been classified in eight feeding guilds, based on the models of Fauchald and Jumars (13), and then divided into three categories. The first one divides the polychaetes into macrophagous and microphagous, according to the size of the portions of the food they get. The second category divides them into carnivores and herbivores, according to the kind of food they consume and then the third category in motiles, discretely motiles and sessiles, according to the activity they show during the consuming of their food.

Hypotheses and analyses

The null hypotheses tested in this study were : 1. the various feeding guilds of the polychaetes in time were equally abundant, 2. the number of individuals (NI= abundance) in the different feeding guilds were equally distributed among the samples in time. Non-parametric methods, such as Kruskal-Wallis, Friedman two-way analysis of variance and Mann-Whitney Test were used (14).

Results and discussion

In order to quantify the contribution of the various feeding guilds mean abundance and partial mean dominance (Table 1) were calculated (15). The following eight feeding guilds were indentified among the 1743 individuals of polychaetes living in *M. galloprovincialis* assemblages. BMX: burrowers, motile, unarmed pharynx; CDJ: carnivores, discretely motile, jawed pharynx; CMJ: carnivores, motile, jawed pharynx; CMX: carnivores, motile, unarmed pharynx HMJ: herbivores, motile, jawed pharynx; FST: filter-feeders, sessile, tentaculated; SDT: surface deposit-feeders, discretely motile, tentaculated and SST: surface deposit-feeders, sessile, tentaculated (for definitions, see 13). The number of individuals (NI) of the polychaetes differed significantly between feeding guilds. From Figure 1, it can be seen that the abundance of feeding guilds SST, CMJ, CMX, HMJ and BMX was very low. FST was the most abundant type, followed by SDT. The results from the Kruskal-Wallis Test for the comparison of abun-

Table 1. Polychaetes with type of feeding guilds associated with *Mytilus galloprovincialis* . (Am) mean abundance, (Dmp) partial dominance, Number of Taxa and Number of individuals.

	Feeding	Winter 94		Summer 94		Winter 95		Summer 95	
Polychaetes species	Guilds	Am	Dmp	Am	Dmp	Am	Dmp	Am	Dmp
Amphitrite sp1	SST	-	-	1	0.4	-	-	-	-
Amphitrite sp2	SST	-	-	0.3	0.1	-	-	-	-
Capitella capitata	BMX	-	-	-	-	-	-	0.3	0.3
Capitellidae	BMX	-	-	2.5	1.1	-	-	2	2.2
Ceratonereis sp.	HMJ	-	-	-	-	-	-	0.3	0.3
Cirratulidae	SST	2.3	1.8	6	2.6	0.3	3.9	3.3	3.6
Dodecaceria concharum	SST	0.3	0.2	-	-	-	-	-	-
Eunice sp.	CDJ	-	-	0.3	0.1	-	-	-	-
Eunicidae	CDJ	-	-	-	-	-	-	-	-
Harmothoe impar	CMJ	2	1.6	-	-	-	-	-	-
Harmothoe sp.	CMJ	2	1.6	3.5	1.5	-	-	0.3	0.3
Heteromastus sp.	BMX	-	-	0.3	0.1	-	-	-	-
Hydroides pseudouncinata	FST	3.5	2.7	9	3.9	2.3	29.9	30	32.4
Kefersteinia cirrata	CMJ	1.8	1.4	4.3	1.9	-	-	13	14
Kefersteinia sp.	CMJ	-	-	0.3	0.1	-	-	-	-
Lepidasthenia sp.	CMJ	-	-	0.3	0.1	-	-	-	-
Lepidonotus clava	CMJ	-	-	-	-	-	-	1.3	1.4
Lysidice ninetta	CDJ	-	-	0.3	0.1	-	-	-	-
Lubrineris funchalensis	CDJ	-	-	2.3	1	0.3	3.9	0.3	0.3
Lubrineris sp.	CDJ	-	-	0.8	0.4	-	-	-	-
Magalia sp.	CMJ	3	2.3	-	-	0.3	3.9	-	-
Marphysa fallax	CDJ	-	-	0.3	0.1	-	-	-	-
Marphysa sanguinea	CDJ	-	-	0.3	0.1	-	-	-	-
Nereis caudata	HMJ	-	-	-	-	-	-	1	1.1
Nereis zonata	HMJ	-	-	0.5	0.2	-	-	1.7	1.8
Nereis irrorata	HMJ	-	-	-	-	-	-	0.3	0.3
Paleanotus sp.	CMX	0.3	0.2	0.8	0.4	-	-	-	-
Phyllodocidae	CMX	2	1.6	2.8	1.2	0.7	9.1	2	2.2
Platynereis dumerilii	HMJ	2.5	2	-	-	0.3	3.9	8.3	9
Polydora caeca	SDT	1.3	1	2	0.9	-	-	2	2.2
Polydora ciliata	SDT	-	-	0.5	0.2	-	-	-	-
Polydora sp.	SDT	0.5	0.4	0.5	0.2	-	-	1.7	1.8
Polymnia sp.	SST	0.3	0.2	-	-	-	-	-	-
Potamila reniformis	FST	-	-	-	-	-	-	0.7	0.8
Prionospio sp.	SDT	-	-	72.3	31.3	0.3	3.9	3	3.3
Pygospio sp.	SDT	-	-	18.8	8.1	-	-	-	-
Sabelaria spinulosa	FST	5	3.9	2	0.9	-	-	-	-
Sabellidae	FST	-	-	0.8	0.4	0.3	3.9	-	-
Serpula concharum	FST	-	-	13	5.6	-	-	-	-
Serpula vermicularis	FST	4	3.2	67.3	29.1	1.3	16.9	8	8.7
Serpula vermiliopsis	FST	1	0.8	-	-	-	-	-	-
Serpulidae	FST	28.5	22.5	-	-	-	-	-	-
Sphaerosyllis sp.	CMJ	-	-	-	-	0.3	3.9	-	-
Spio filicornis	SDT	-	-	-	-	-	-	0.3	0.3
Spionidae	SDT	1.5	1.2	1	0.5	-	-	-	-
Spirobranchus polytrema	FST	54.8	43.3	0.8	0.4	1	13	-	-
Spirocephalus polytrema	FST	6.3	5	-	-	-	-	-	-
Staurocephalus rudolphii	CDJ	-	-	2.3	1	-	-	-	-
Staurocephalus sp.	CDJ	-	-	7.8	3.4	0.3	3.9	5.7	6.2
Syllidae	CMJ	2.5	2	3	1.3	-	-	3.7	4
Terebella lapidaria	SST	1	0.8	2.3	1	-	-	3.3	3.6
Terebellidae	SST	-	-	1	0.5	-	-	-	-
Vermiliopsis sp.	FST	0.3	0.2	-	-	-	-	-	-
Number of Taxa	23	35	12	23					
Number of individuals	526	921	24	272					

OBSERVATIONS DE CÉTACÉS ET D'OISEAUX MARINS SUR DEUX TRAJETS TOULON (FRANCE) - PORT SAÏD (EGYPTE)

David Léa [1]*, Ruffay Xavier [2] et Beaubrun Pierre [1]

[1] Lab. de Biogéographie et Ecologie des Vertébrés, Ec. Pratique des Htes Etudes, 2, Place Eugène Bataillon, 34095 Montpellier, France
[2] G.R.I.V.E, Maison de l'Environnement, 16 rue F. Fabre, 34000 Montpellier, France.

Résumé

Deux traversées ont été effectuées entre Toulon (France) et Port-Saïd (Egypte) en novembre 96 et mars 1997. L'observation continue a été assurée pendant 121 heures (1220 MN), selon la méthode du transect de ligne. Deux espèces de cétacés et quatorze d'oiseaux marins ont été contactées. Les cétacés se sont avérés peu abondants. Dans l'ensemble les densités d'oiseaux marins ont été faibles, surtout en novembre, dans le bassin oriental. Elles sont plus importantes en mars, avec le retour des reproducteurs qui se concentrent près des colonies côtières et des endroits riches en nourriture : détroits et ports.

Mots-clés : cetacea, birds, open sea

Deux traversées de la Méditerranée ont été faites : Toulon-Malte-Port Saïd (8-14 novembre 96) et Port-Saïd-Athènes-Toulon (2-11 mars 97).

Matériel et méthode

Le principe du "transect de ligne" [1] a été appliqué par un à deux observateurs en veille continue sur des trajets à cap et vitesse (10 noeuds) constants, avec une visibilité théorique de 4,5 ou 5,5 milles nautiques. 121 heures ont permis de prospecter 1220 MN (649 à l'aller, 571 au retour), dont 862 MN (71%) par mer ≤ à 3 Beaufort et vent ≤ à 4 Beaufort.

Espèces rencontrées.

Sur l'ensemble des deux trajets, 2 espèces de cétacés et 14 espèces d'oiseaux marins ont été identifiées de façon certaine.

Cétacés (carte 1). Deux Rorquals (*Balaenoptera* sp., probablement *B. physalus*) ont été aperçus en mars en mer Tyrrhénienne, à l'est des Bouches de Bonifacio. L'endroit est connu pour être fréquenté par l'espèce à cette période [2]. Deux *Tursiops truncatus* ont été vus au nord-ouest de Malte où l'espèce est fréquente [3, 4].

Les autres petits Delphinidés totalisent 9 observations dont une seule (4 *Stenella coeruleoalba*) à l'est des côtes sardes. Les 8 autres (67 individus) ont eu lieu essentiellement dans l'est du bassin oriental parmi lesquelles 4 mentions certaines de *Stenella coeruleoalba* (57 individus). Quatre observations (17 individus) furtives ou lointaines n'ont pas permis de certifier l'espèce. La majorité des contacts concernait des groupes de faibles effectifs (2-10, taille moyenne de groupes de 5,5 ind.) vus avant 8 heures ou après 16 heures locales. La plus grande bande (40 *Stenella*) a été rencontrée en pleine journée.

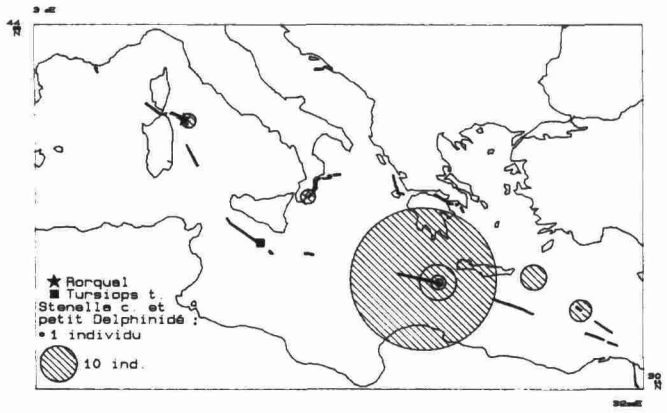

Carte 1. Trajets effectués par mer ≤ à 3 Beaufort et vent ≤ à 4 Beaufort, et cétacés observés (individu)

Oiseaux marins. Au total 4089 oiseaux marins appartenant à sept familles ont été contactés. Très peu de Procellaridés ont été vus en novembre (0.02 ind./MN) Ils étaient plus nombreux en mars (0.91 ind./MN) et pour l'essentiel en péninsule hellénique et dans les Bouches de Bonifacio (cartes 2 et 3).

En novembre les Puffins de Méditerranée (*Puffinus yelkouan yelkouan*) sont dispersés dans les deux bassins (13 individus vus) et les Puffins cendrés (*Calonectris diomedea*) ont migré vers l'Atlantique (3 notés). En mars, le Puffin de Méditerranée qui est un nicheur précoce est déjà sur ses colonies (0.79 ind./MN) : il a été contacté en Grèce,

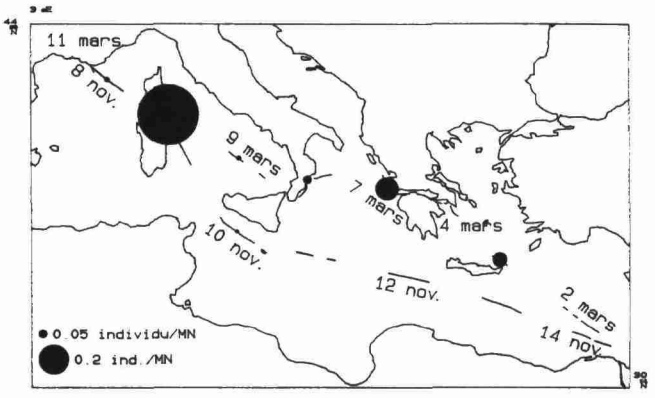

Carte 2. Dates des trajets et puffins cendrés observés (nombre moyen journalier d'individus par MN).

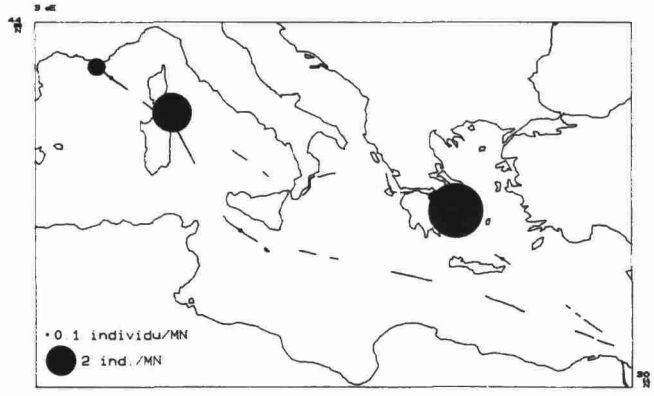

Carte 3. Puffins de Mediterranée observés sur les trajets (nombre moyen journalier d'individus par MN).

dans les Bouches de Bonifacio et près des îles d'Hyères. Par contre, le Puffin cendré commence juste à rejoindre les siennes (0.12 ind./MN) et a été vu près de la Crète, en mer Ionienne et dans les Bouches de Bonifacio.

L'Océanite tempête (*Hydrobates pelagicus*) est le seul Hydrobatidé méditerranéen. Un unique individu a été noté en novembre dans le détroit de Sicile, à proximité des plus importantes colonies de l'espèce [5]. Le Fou de Bassan (*Morus bassanus*), représentant des Sulidés, est connu pour hiverner régulièrement dans le nord du Bassin occidental : 7 ont été vus en novembre et 2 en mars au large des côtes françaises. L'espèce est bien plus rare dans le bassin oriental [6] : un individu noté en mars au sud de l'Italie. Un seul Cormoran huppé (*Phalacrocorax aristotelis*) a été rencontré en mars dans les Bouches de Bonifacio où il niche.Parmi les Stercorariidés, deux Labbes pomarins (*Stercorarius pomarinus*) et un Grand labbe (*Stercorarius skua*) ont été vus à quelques milles d'intervalle en novembre à proximité de Port-Saïd, ainsi que trois Labbes parasites (*Stercorarius parasiticus*) à l'entrée même du port, ce qui avait déjà été noté auparavant [7, 8]. Il s'agit très probablement de migrateurs de passage.

SPATIO-TEMPORAL DISTRIBUTION OF THE EUROPEAN HAKE *MERLUCCIUS MERLUCCIUS* OFF CATALAN COAST (NORTHWESTERN MEDITERRANEAN)

M. Demestre and P. Sánchez

Instituto de Ciencias del Mar (CSIC). P. Joan de Borbó, s/n. 08039 Barcelona, Spain

Abstract

The spatio-temporal distribution pattern of *Merluccius merluccius* off the Catalan coast during 1991 has been investigated, considering separately three size groups, trawl-recruits, juveniles, and adults. The species showed a wide bathymetric distribution throughout the shelf and the slope, mainly between 48 m - 300 m. Changes in the spatial distribution and abundance of the three groups were observed throughout the year. Spring showed the highest abundance, due to the massive incorporation of trawl-recruits to the demersal population at different depths, although they appeared in all seasons. Trawl-recruits were not concentrated in closed nursery areas. Movements of the species were associated with a certain segregation by size.

Key-words: coastal waters, recruitment, fishes, Balear Sea

Introduction

The European hake *Merluccius merluccius* (Linnaeus, 1758) is a demersal species which is abundant throughout its main distribution area. It is one of the most valuable fishing resources in both the northeastern Atlantic and Mediterranean waters and represents one of the main target species of the trawling fleet. Furthermore, two other gears, the long-line and gillnet catch hake, mainly large specimens, which are the most scarcely represented in trawling. The catches are carried out simultaneously with trawling in some fishing grounds in the northwestern Mediterranean (1). Information related to different aspects of the biology of this species, such as growth, feeding habits and reproduction, and fishery is relatively abundant (2-7). Considerable research has been devoted to distribution, abundance and size composition of *Merluccius merluccius*. However, detailed information on seasonal changes in the abundance and length distribution by depth is rather limited, and an explanation is required which relates the variability observed in abundance with size, depth and time of the year.

In this study the changes of the spatio-temporal distribution pattern of the hake has been investigated, and sources of these variations have been identified. Therefore, three different size groups of the population have been considered separately, given that it has been observed that these groups show differences in their distribution: 1) trawl-recruits, the firts immatur individuals 0-1 years old that exploit the trawl, 2) juveniles, the remainder immatures till to reach first size maturity, and 3) adults, all matur individuals. Smallest size fully recruited to the trawling gear corresponded to individuals of around 10-13 cm total length.

Material and methods

The Catalan coast extends for about 550 km (Fig. 1). The material was collected from 259 experimental hauls on board of commercial trawlers along the Catalan coast from March to November 1991 (Table 1). The sampling area covered a wide range of depths, from 12 m to 643 m. Hake was caught in 219 hauls from 25 m to 643 m. The bottom otter trawl is the main gear used in commercial fisheries in the Mediterranean. The mesh size of the cod-end was 38 mm streched. A covering bag was used (9 mm mesh size streched) for the cod-end in each sampling months in order to catch the smaller specimens. For each haul, the location, duration, the minimum and maximum depth (m), and the hake catch, in number of specimens and weight (kg), were recorded. Given that duration of hauls and proportion of hauls within each stratum for each season were variable, data were standardized to number of specimens per trawling hour (no. h^{-1}). The total number of specimens caught during the sampling was 87041. A representative sample of the specimens caught in each haul was measured (total length, TL, in cm). Size frequency distribution by depth stratum and season were obtained and expressed in number per hour (no.h-1). In addition, to show more precisely the changes in the spatio- temporal abundance of each size group separately, these data were organized according to three size categories within the population structure. These groups were referred to as trawl-recruits (<14 cm TL), juveniles (14 -34 cm TL), and adults (>34 cm TL) (considering 34 cm is the average of the length at first maturity of both sexes (7)).

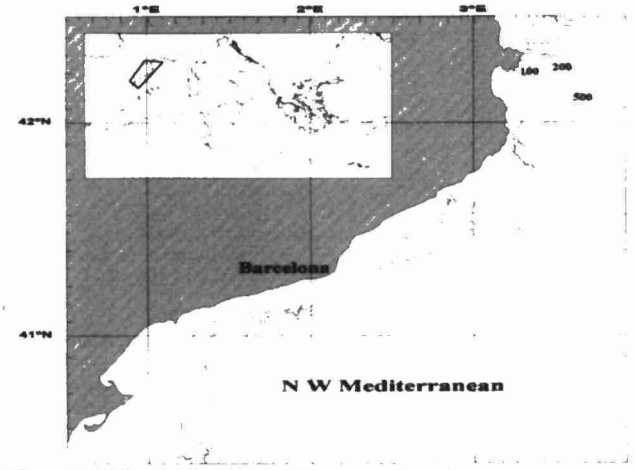

Figure 1. Catalan coast where sampling was performed.

Table 1. Summary of the sampling data. Monthly distribution of hauls. In parenthesis number of hauls with cover cod-end.

Season	total hauls	hauls with hake	total number of specimens	abundance (numer/hour)
Winter	48 (8)	45	11055	345
Spring	72 (18)	55	48715	1246
Summer	77 (20)	60	19999	297
Autunm	62 (12)	59	7275	168

Results

The results show the very wide bathymetric distribution (25-643m) of *Merluccius merluccius*, which appeared in the sampling. Hake was found widely distributed between 48 and 300 m throughout the year.

Specimens of a size <14 cm TL occurred in all four seasons. Spring showed a higher abundance, mainly in May and June, due to the massive caught of trawl-recruits, their abundance being lowest in autumn. The smallest fish (2 cm TL) (Table 2 and Fig. 2) was caught in May. The <14 cm TL individuals were found distributed throughout the shelf and the slope. The wide range of depths where trawl-recruits were found indicates that they were not concentrated in a defined nursery area. The adults (>34 cm TL) were much less abundant (Table 2 and Fig. 2). The largest fish (73 cm TL) appeared in August.

Table 2. Distribution of trawl-recruits, juveniles and adults, in percentage, per stratum and season.

	trawl-recruits (<14.0cmTL)				
	<75	75-150	150-300	>300	totaln/h
Winter	8.8	29.2	61.4	0.7	220
Spring	88.0	6.3	5.4	0.3	887
Summer	19.145.7	27.3	7.9	124	
Autunm	15.239.8	42.9	2.1	39	
	juveniles (14-34cmTL)				
	<75	75-150	150-300	>300	totaln/h
Winter	38.326.6	32.3	2.8	121	
Spring	42.4	15.0	41.5	1.1	347
Summer	19.7	28.4	44.5	7.3	167
Autunm	17.4	48.8	29.4	4.4	122
	adults (>34cmTL)				
	<75	75-150	150-300	>300	totaln/h
Winter	2.2	54.2	14.3	29.2	4
Spring	1.3	77.1	8.3	13.2	13
Summer	7.5	22.3	0.0	70.2	6
Autunm	9.9	38.8	21.7	29.6	6

LE SENS DU TRAJET AURAIT-IL UNE INFLUENCE SUR LA VARIATION CONSTATÉE DES INDICES D'ABONDANCE CHEZ LES CÉTACÉS DANS LE BASSIN LIGURO-PROVENÇAL ?

N. Di-Méglio

Lab. de Biogéographie et d'Écologie des Vertébrés, E.P.H.E., UM2, Place Eugène Bataillon, 34095 Montpellier cedex 05, France

Résumé

La réalisation régulière d'un trajet Cannes/Calvi à différentes périodes de la saison estivale 1995 a permis de mettre en évidence des variations mensuelles des indices d'abondances pour les diverses espèces de cétacés rencontrés, chez les Mysticètes comme chez les Odontocètes. Par contre, des variations d'abondance apparaissent au cours d'un même mois chez les Petits Delphinidés et pourraient-être en relation avec le sens dans lequel le parcours a été effectué (Cannes/Calvi ou Calvi/Cannes).

Mots-clés : Ligurian sea, density

Matériel et méthode

Durant la saison estivale 1995 un transect a été effectué régulièrement de début mai à fin août entre Cannes et Calvi à différentes dates (tableau 1). La plate-forme utilisée est un ex-chalutier de 25 m gréé à la voile sur le pont duquel la visibilité théorique est comprise entre 3,9 et 4,5 milles. Les observations de cétacés ont été faites en appliquant la méthode du "transect de ligne" [1] : vitesse constante (7 nds), état de la mer inférieur ou égal à 3 Beaufort, pression d'observation constante effectuée par 3 personnes.

Tableau 1 : Dates et sens des transects effectués entre Cannes et Calvi durant la période estivale 1995.

	Sens du transect	
Dates	Cannes/Calvi	Calvi/Cannes
4-5/5/95	X	
6/7/95	X	
7/6/95	X	
21/7/95		X
8/8/95		X
20/8/95	X	

Le peuplement rencontré sur les trajets Cannes/Calvi

L'allure générale de la variation des indices d'abondances (figure 1) indique que les animaux deviennent de plus en plus nombreux dans la zone de mai à juillet, puis se stabilisent à leur maximum jusqu'à fin août. Quels que soient les mois, ce peuplement est largement dominé par la présence des petits Delphinidés (entre 81,1% et 97,6% des individus rencontrés au cours de chaque transect) et très probablement par une seule espèce puisque tous les individus identifiés avec certitude étaient des *Stenella coeruleoalba*. *Balaenoptera physalus* est le Mysticète de loin le plus commun puisqu'un seul *Balaenoptera acutorostrata* a été rencontré pendant ces prospections estivales. Sur le trajet Cannes/Calvi, le Rorqual commun atteint son pic d'abondance début juillet et ses effectifs semblent plus réduits fin août.

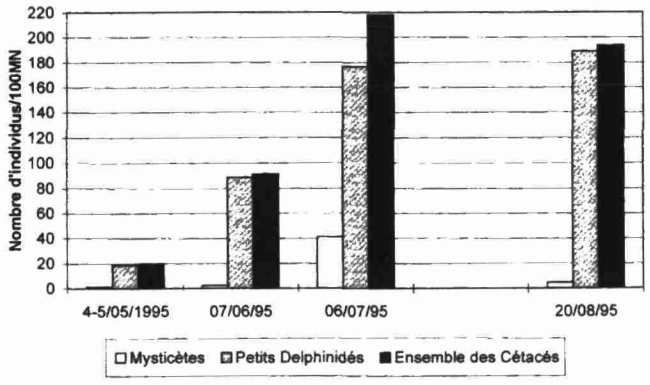

Figure 1. Evolution des indices d'abondance des cétacés rencontrés sur les transects Cannes/Calvi au cours de l'été 1995.

Influence du sens du transect sur la détection des animaux

Les trajets effectués en juillet et en août dans le sens Cannes/Calvi ont été réalisés, les mêmes mois, dans le sens inverse : Calvi/Cannes. Le nombre de transects faits dans ces conditions est insuffisant pour nous permettre de faire une analyse statistique. Toutefois, les résultats obtenus sur les parcours de retour font nettement apparaître des valeurs d'indices d'abondance toujours bien plus faibles (figure 2). Le sens dans lequel est effectué le transect semble donc avoir une influence sur la détection des Cétacés. L'examen approfondi des différentes catégories de cétacés observées de ces deux jeux de données "aller" et "retour" montre que l'abondance des Petits Delphinidés rencontrés sur les trajets Cannes/Calvi (X = 182,8 individus/100MN, n = 270) est toujours supérieure à celle notée dans le sens Calvi/Cannes (X = 28,2 individus/100MN, n = 52)(figure 3). L'influence du sens du transect semble donc importante sur le dénombrement des Petits Delphinidés sur ce trajet.

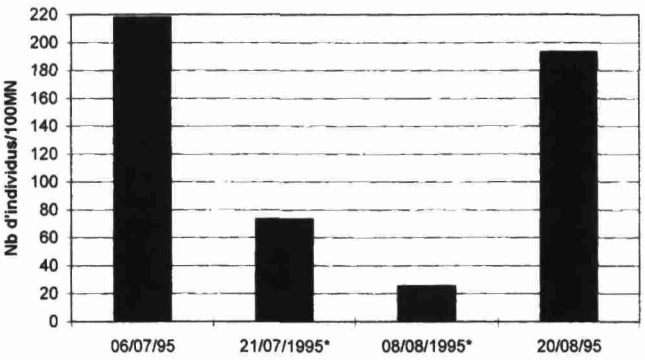

Figure 2. Fluctuation des indices d'abondance de l'ensemble des cétacés rencontrés sur les transects Cannes/Calvi et Calvi/Cannes * au cours de l'été 1995.

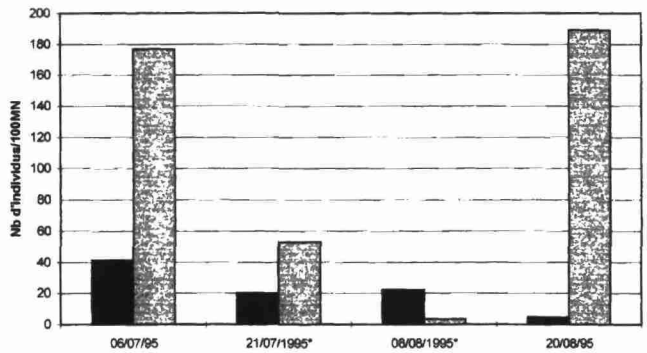

Figure 3. Fluctuation des indices d'abondance des petits delphinidés (gris) et des mysticètes (noir) rencontrés sur les transects Cannes/Calvi et Calvi/Cannes * au cours de l'été 1995.

Les indices d'abondance relevés pour les Mysticètes de début juillet à la fin août montrent par contre une tendance à une diminution constante et indépendante du sens du parcours (figure 3). Ceci est confirmé par l'évolution du nombre de contacts avec ces animaux : 18,1 contacts/100MN avec des Rorquals le 6 juillet et 7,6 contacts/100MN fin août. Les variations constatées sur l'abondance des Rorquals dans cette zone ne paraissent donc pas influencées par le sens dans lequel a été effectué le transect. Elles retracent plutôt un phénomène de saisonalité déjà mis en évidence par des travaux antérieurs [2, 3] : les effectifs de Rorquals dans le bassin Liguro-provençal régressent lentement de l'été à l'automne.

COMPOSITION OF JUVENILE FISH POPULATIONS IN THE DONJI MOLUNAT BAY, SOUTHERN ADRIATIC (SUMMER ASPECT)

J. Dulcic [1]*, M. Kraljevic [1], V. Kozul [2] and B. Skaramuca [2]

[1] Institute of Oceanography and Fisheries, P.O.B. 500, 21000 Split, Croatia

[2] Institute of Oceanography and Fisheries-Split, Biological Station Dubrovnik, P.O.B. 39, 20000 Dubrovnik, Croatia

Abstract

A total of 1172 fishes belonging to 27 species were caught in July (283) and August (883) 1996, in the Donji Molunat Bay in the southern Adriatic, using a 50 m long beach seine. *Chromis chromis* (48.29%), *Spicara smaris* (13.40%), *Oblada melanura* (8.11%) and *Mullus barbatus* (6.57%) comprised 76,37% of the total. *O. melanura* was dominant in July (83) and *Ch. chromis* in August (566). The remaining species comprised from 5.03% to 0.09% of the catch. The overall value of richness D was 3.68, ranging from 2.65 in July to 2.95 in August. Diversity H values were 1.71 in July and 1.33 in August, with an overall value of 1.94. The annual value of eveness J was 0.59, fluctuating from 0.44 in August to 0.62 in July. Preliminary results of the present study provide a basis for future studies to elucidate what additional aspects may influence the distribution and abundance of juveniles during different seasons in the Donji Molunat Bay.

Key-words: Biodiversity, fishes, coastal waters, Adriatic Sea

Introduction

Numerous studies have been published on fish populations in lagoons, estuaries and coastal regions (bays and coves) in many parts of the world (1) indicating that such concentrations are due to their higher productivity and that many species utilize these areas as nursery and feeding grounds. The composition of juvenile fish communities in inshore areas of the Eastern Adriatic is poorly known, although it is a very important biogeographical area that joins the Mediterranean fauna. There are only few papers on juvenile fish populations of the Eastern Adriatic. Some researchers dealt with the temporal distribution of young mugilids in the coastal area of the Eastern middle Adriatic (2, 3), some with feeding of striped seabream *Lithognathus mormyrus* (4), and annular bream *Diplodus annularis* (5). Composition and temporal fluctuations of inshore juvenile fish populations in the Kornati Archipelago were presented elsewhere (6).

The present study provides the preliminary data on juvenile fish composition in the Donji Molunat Bay in July and August 1996.

Material and methods

The Donji Molunat Bay is located in the southern part of the Eastern Adriatic coast between City of Dubrovnik and Boka Kotorska Bay (Fig. 1). It is a traditional area of fishing, especially of yellow-tail *Seriola dumerilli*. The maximum depth of the entrance of the bay is 29 m. The sampling area was characteristically sandy and sandy-mud overgrown by meadows of *Posidonia oceanica* and *Cymodocea nodosa*. Sampling was conducted in July and August of 1996 in Donji Molunat Bay in the Southern eastern Adriatic. Fish samples were collected using a 50 m long beach seine. Net depth was 30 cm and 250 cm at the central part together with the sac. The mesh size was 8 mm at the outer wing and 4 mm at the central sac. Collected specimens were sorted and preserved in 4% formalin (pH from 8.5 to 9.0). Fish species were identified using (7) and (8). The juveniles of the species were taken as specimens with already formed scales after metamorphosis, and were taken as such until the moment of first sexual maturity (9). Total lengths were measured to the nearest 0.1 cm. The weight of specimens was determined to the nearest 0.01 g. The community structure was specified by species richness (D), diversity (H) and evenness (J), using the equations proposed by Margalef (10), Shannon (11) and Pielou (12) respectively

Results

Twenty-seven species were caught in July and August 1996. (Table 1). Sixteen species were caught in July and twenty-one in August. A total of 1.172 fishes were collected, 289 in July and 883 in August. *Chromis chromis* (48.29%), *Spicara smaris* (13.40%), *Oblada melanura* (8.11%) and *Mullus barbatus* (6.57%) comprised 76.37% of the total. *O. melanura* was dominant in July (83) and *Ch. chromis* in August (566). The remaining species comprised from 5.03% to 0.09% of the total catch.

The overall D value was 3.68, ranging from 2.65 in July to 2.95 in August. The H value was 1.71 in July and 1.33 in August, with an overall value of 1.94. The annual value of J was 0.59, ranging from 0.44 in August to 0.62 in July.

Discussion

Adriatic Sea is an oligotrophic area (13). It is relatively rich in ichthyofauna and according to (8) has 407 fish species and subspecies. Occupied either permanently or temporarily by at least 27 species in summer period, the Bay of Donji Molunat is rich in terms of fish species. Juveniles of four species (*Chromis chromis*, *Spicara smaris*, *Oblada melanura* and *Mullus barbatus*) were dominant forming 76.37% of the total. Grubisic (14) and Jardas (8) indicated that the most common species of the eastern Adriatic spawn in spring and summer. We propose recruitment timing of four mentioned species could be the reason for a high abundance during July and August. Estuaries, coves and bays probably play an important role as nursery grounds for fish in inshore-offshore migration during their early life history. Such areas also provide suitable food, shelter and a reduction in predation. The nursery function of such areas has been well-documented in the world (15, 16, 17, 6). A number of parameters (*e.g.* temperature, salinity, substrate type, depth, pH) could influence the distribution of juveniles and relative importance their differs from species to species. Perhaps the only common denominator is the preference of juveniles for relatively shallow water. The values of diversity, richness and eveness could be comparable to values obtained for Kornati Archipelago (eastern middle Adriatic), and are lower in the same

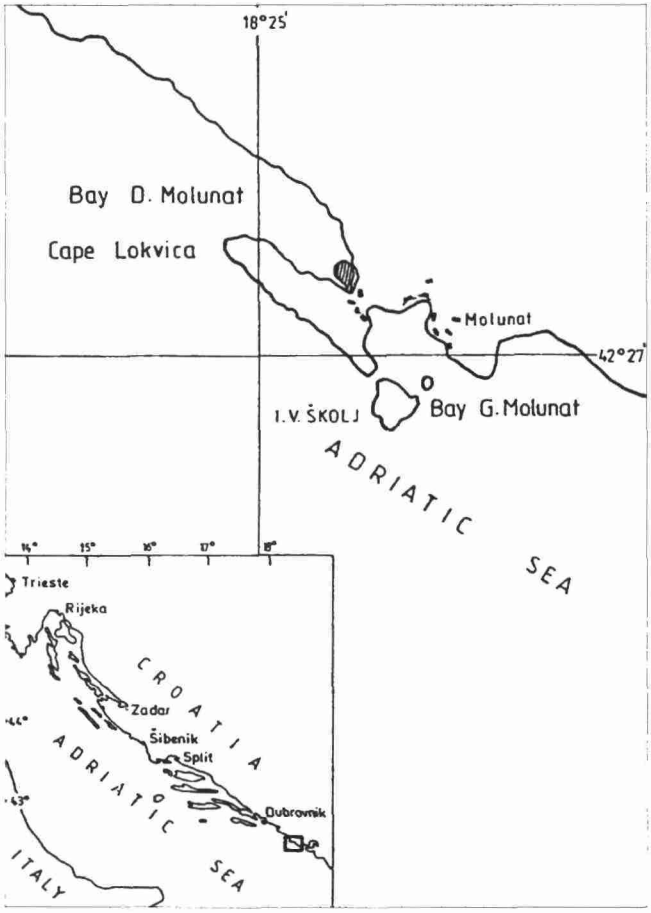

Fig. 1. Study area (The Donji Molunat Bay - southern Adriatic).

NOTE ON FEEDING OF *SCIAENA UMBRA* L. (OSTEICHTHYES: SCIAENIDAE) IN THE CENTRAL ADRIATIC SEA

Gianna Fabi *, Monica Panfili and Alessandra Spagnolo
Istituto di Ricerche sulla Pesca Marittima, CNR, Largo Fiera della Pesca, 60125 Ancona, Italy

Abstract
Feeding of *Sciaena umbra* collected around some man-made structures placed along the Italian coast of the central Adriatic sea was described through the analysis of the stomach contents. Benthic species dominated in the diet. Decapods, mainly represented by *Liocarcinus vernalis*, were the most important prey items followed by amphipods, polychaetes and benthic fish.

Key words: Fishes, diet, artificial reefs, Adriatic Sea

Sciaena umbra is a hard-substrate species living in shelters in rocky habitats. Along the Italian side of the central and northern Adriatic sea it can be only found around man-made substrates (artificial reefs, gas-oil platforms, wrecks, etc.) and in the few existing natural rocky habitats (*i.e.* Conero Promontory, Gabicce Promontory).

From January 1995 to February 1997, 174 specimens of *S. umbra* ranging from 15 to 38 cm of total length were collected during experimental fishing surveys carried out with trammel nets around two concrete artificial reefs and a gas-oil platform placed along the Adriatic coast between Ancona and Ravenna, on a sandy-muddy bottom, at depths ranging from 10 to 15 m. The stomach of each specimen was cut out and preserved in 7% formalin. The stomach fullness was noted employing the scale proposed by Vesey and Langford (1) and contents were identified to the lowest taxonomic level possible, counted and weighted. Percentage of frequency of occurrence F (2), percentage by number N (3) and percentage by weight W (4) were calculated for each prey species and/or group. The values obtained were used to calculate the "relative importance index" RI (5), which is based on the "absolute importance index" AI as follows:

$$AI = F + N + W \qquad RI = 100 * AI \,/\, \sum_{1}^{n} AI$$

where n is the number of the different prey categories.

This normalized index allowed to directly evaluate the contribution of the different prey items to the diet.

Because no differences were noticed in the diet of individuals caught at the three different places, in the final analysis all the data were pooled together. The results obtained were summarized in Fig. 1 and in Table 1.

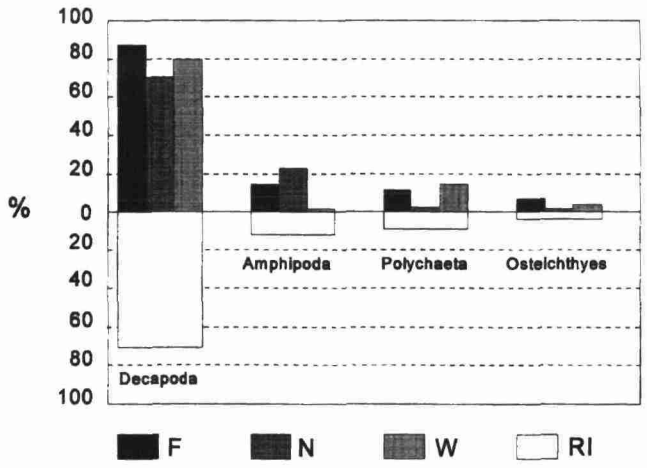

Figure 1. Values of F, N and W computed for the most important prey taxa. The corresponding RI values are also reported.

37% of the stomachs observed were full, 39% were partially full and the remaining 24% were completely empty.

Diet of *S. umbra* was characterized by benthic organisms and was dominated by crustaceans that occurred in 88% of stomachs and formed 94% by composition in number and 81% in weight. Decapods were the most representative group (RI = 70.53; Fig. 1); their percentage of occurrence was similar to their abundance, either by number and by weight, suggesting a homogeneous predatory behaviour of *S. umbra* towards these preys.The group of Decapoda was dominated by *Liocarcinus vernalis*, a very common species living in shallow waters and sandy-muddy bottoms. It showed the highest percentage by occurrence and by weight (Tab. 1) and mainly consisted of small-size individuals having an average weight of 0.5 ± 0.2 grams.

Other important decapods in the diet were: *Athanas nitescens, Brachynotus gemmellari, Processa edulis* and *Thoralus cranchii* (9.9 ≥ RI ≥ 5.7).

Amphipods (RI = 11.35) and polychaetes (RI = 8.48) came respectively second and third in order of importance. These two groups showed similar values of occurrence (Fig. 1), but the first ones were more important as number of specimens while the second ones were more representative as weight. *Elasmopus rapax* was the most abundant species among the amphipods and also showed the highest percentage by number in respect to all the other preys (Table. 1). Polychaetes were almost exclusively represented by *Marphysa sanguinea*, an ubiquist organism living in burrows in sandy-muddy bottom or in galleries formed in fissures of rocks. It is common in the benthic community settled either on the man-made structures and in the soft bottom just close to them (6, 7).

Finally, fish occurred in 6.8% of stomachs and were only found in specimens ranging from 24 to 31.5 cm of total length. The other animal groups showed a very low importance in the diet of *S. umbra*, as evidenced by the corresponding RI values ranging from 1.22 (Gasteropoda) to 0.17 (Foraminifera). Algae fragments were recorded only in one specimen.

These results clearly indicate that, in the size range considered, *S. umbra* feeds on a variety of animal organisms, but it shows a high preference for decapods. This agrees with what referred for the same species in the Gulf of Tunis by Chakroun and Ktari (8), even though these authors found also a high occurrence of plant food, probably ingested when the fish prey on the crustaceans living on either algae or phanerogames. The sporadic presence of plant food reported in the present study was likely because the vegetation cover is very poor in the investigated areas.

References

1- Vesey G., Langford T., 1985. The biology of black goby, *Globus niger* L, in an english south coast bay. *J. Fish Biol.*, 27: 417-429.
2- Kennedy M., Fitzmaurice P., 1972. Some aspects of the biology of gudgeon *Gobio gobio* (L.) in Irish waters. *J. Fish Biol.*, 4: 425-440.
3- Crisp D.T., Mann R.H.K., McCormack J.C., 1978. The effects of impoundment and regulation upon the stomach contents of fish Cow Green, Upper Teesdale. *J. Fish Biol.*, 12: 287-301.
4- Gibbons J.R.H., Gee J.H., 1972. Ecological segregation between longnose and blacknose dace *(Rhinichthys)* in the Mink river, Manitoba. *J. Fish Res. Bd. Ca,.*, 25: 1505-1507.
5- George E.L., Hadely W.H., 1979. Food and habitat partitioning between rock bass *(Ambloplites rupestris)* and smallmouth bass *(Micropterus dolomieui)* young of year.
Trans. Am. Fish Soc., 108: 253-261.
6- Bombace G., Castriota L., Spagnolo A., (in press). Benthic community on concrete and coal-ash blocks submerged in an artificial reef in the central Adriatic Sea. 30th Europ. Mar. Biol. Symposium, Southampton, U.K., 18-22 Sept. 1995.
7 Castriota L., Fabi G. Spagnolo A., 1996. Evoluzione del popolamento bentonico insediato su substrati in calcestruzzo immersi in Medio Adriatico. *Biol. Mar Medit.*, 3(1):120-127.
8- Chakhroun N., Ktari M.H., 1981. Régime alimentaire des Sciaenidae (poissons téléostéens) du golfe de Tunis. *Bull. inst. nat. scient. ocean. Salammbô*, 8:69-80.

EVOLUTION DE LA CONSOMMATION DES PROIES CHEZ LES LARVES DE SOLE (*SOLEA SENEGALENSIS* KAUP) EN FONCTION DU JEUNE ET DE L'AGE

R. Fehri-Bedoui [1], M. H. Dinis [2] et F. Maamouri [1]

[1] Laboratoire de Biologie marine, Faculté des Sciences, Campus universitaire, 1060 Tunis-Belvédère, Tunisie
[2] Unidade de Ciencias e Tecnologias dos Recursos Aquaticos Universidade do Algarve Campus de Gambalas 8000 Faro Portugal

Résumé

L'effet du jeûne sur la quantité des proies ingérées (nauplii d'Artemia) a été examiné chez les larves de sole, *Solea senegalensis*. Les larves, âgées de 10, 15 et 21 jours, sont soumises au jeûne de diverses durées. Le comptage du nombre de proies présentes dans le tube digestif des larves, 2 heures après la distribution des proies, nous a permis de constater que la quantité de proies ingérées augmente avec l'accroissement de l'âge des larves, les larves de sole supportent le jeûne prolongé (96 heures), et le jeûne influence la capacité d'ingestion.

Mots-clés : teleostei, aquaculture, larvae, behaviour, eastern Mediterranean

Introduction

En élevage de poissons téléostéens, le jeûne constitue un facteur susceptible d'affecter la survie à divers stades de leur développement. Les études relatives au jeûne ont concerné plus particulièrement les stades larvaires et juvéniles. Divers auteurs ont étudié, chez certains poissons marins et d'eau douce, l'effet du jeûne sur l'évolution de la morphologie et de l'histologie de leurs organes digestifs (1-5). Par ailleurs, le jeûne a été abordé d'un autre point de vue ; l'évolution de l'ingestion des proies en fonction de la durée du jeûne a été suivie chez les larves de loup (6). Au cours du présent travail, nous adoptons cette dernière approche pour les larves de sole (*Solea senegalensis*). Aussi, nous suivrons l'évolution de la consommation des proies en fonction de la durée du jeûne et de l'âge et nous établirons la durée convenable de jeûne pour chacun des âges étudiés.

Matériel et méthodes

Les larves examinées sont issues de pontes naturelles de géniteurs en captivité. Elevées dans un bac cylindroconique de 500 litres, elles sont nourries de nauplii d'Artemia dès l'ouverture de la bouche. Les expériences sont réalisées dans des seaux de 10 litres, ils sont équipés d'un diffuseur en grès poreux qui engendre une légère aération (débit d'air, 0.05l / mn). L'eau, stagnante, a une température de 19° C et une salinité de 35‰. L'éclairage est assuré à l'aide de tubes néon situés à 2 mètres au dessus des seaux. 11 lots de 200 larves ont été constitués à l'âge de 10, 15 et 21 jours. Les lots, prélevés par âge, ont été soumis à 3, 6, 9, 12, 18, 24, 36, 48, 60, 72 et 96 heures de jeûne.

Au terme du jeûne, des nauplii d'Artemia sont distribués à raison de 4 nauplii/ml. Deux heures après la distribution de la nourriture, 10 individus ont été prélevés, fixés dans une solution de formol à 4 %, puis disséqués sous la loupe pour compter le nombre de proies présentes dans le tube digestif. Les proies seront classées en proies digérées et proies non digérées. Pour comparer l'ingestion des proies en fonction de l'âge des larves, nous avons appliqué le test de Student (7) aux moyennes des proies totales ingérées par les larves âgées respectivement de 10, 15 et 21 jours. Ainsi, les lots de larves étaient considérés 2 à 2 (10-14/15-19, 15-19/21-25 et 10-14/21-25 jours) et les moyennes de proies étaient, aussi, comparées 2 à 2 et à des durées égales de jeûne.

Résultats

Les larves soumises au jeûne ont montré un comportement actif lors de la capture des proies (Tabl. 1 et Fig. 1). Aucun cas de mortalité n'a été observé au cours de l'expérimentation.

a-larves de 10-14 jours : pour le jeûne d'une durée de 3 à 12 heures, le nombre des proies ingérées est croissant. Le nombre des proies digérées est supérieur à celui des non digérées. De 18 à 96 heures de jeûne, le nombre total de proies est décroissant, cependant, le nombre de proies digérées reste toujours supérieur à celui des non digérées.

b-larves de 15-19 jours : le nombre de proies ingérées est croissant jusqu'à 24 heures de jeûne. A partir de 36 heures de jeûne, le nombre de proies ingérées diminue graduellement. Le nombre de proies digérées, nettement supérieur à celui des non digérées, est croissant jusqu'au jeûne d'une durée de 48 heures.

c-juvéniles de 21-25 jours : le nombre de proies est croissant jusqu'au jeûne d'une durée de 36 heures. Le nombre des proies digérées, nettement supérieur à celui des non digérées, est croissant jusqu'au jeûne d'une durée de 60 heures.

Ainsi la capacité d'ingestion des proies est en étroite relation avec la durée du jeûne, à laquelle la larve est soumise. Cette capacité est dépendante de l'âge. En effet, l'application du test de Student a montré que les différences des moyennes des proies étaient significatives au seuil de probabilité 95 et même 99% (ddl=18, $t_{0,05}$=2,1 et $t_{0,001}$=2,88) excepté, chez les couples de lots des larves 10/15 et 15/21 jours pour la durée de jeûne la plus faible (3 heures). Cependant, nous avons observé une diminution du nombre de proies ingérées à partir de 18 heures chez les individus les plus jeunes (10-14 jours) et à partir de 36 et 48 heures pour les larves et les juvéniles âgés respectivement de 15-19 et 21-25 jours. Il est probable que le jeûne affecte la vitalité des larves et des juvéniles et que ces derniers réagissent différemment en fonction de leur maturité digestive.

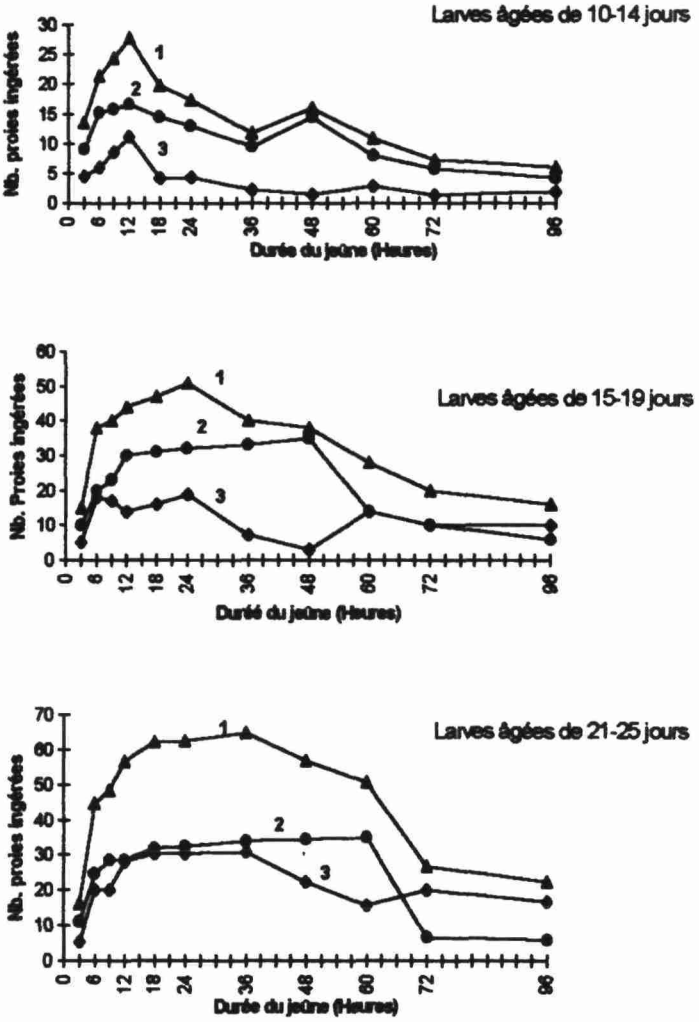

Figure 1. Effets du jeûne sur le nombre de proies ingérées chez les larves de soles (*S. senegalensis*). proies **1:** totales; **2** : digérées; **3** : non digérées.

Discussion-conclusion

Il a été observé, chez les alevins de plusieurs téléostéens, une augmentation de la quantité consommée jusqu'à une certaine durée de

SPATIAL AND SEASONAL VARIABILITY OF THE ZOOPLANKTON IN THE BALEARIC SEA (WESTERN MEDITERRANEAN)

Fernandez de Puelles M.L. *, Jansa J., Morillas A., Amengual B. and Vicente L.
Spanish Inst. of Oceanography. P.O. Box 291, 27015 Palma de Mallorca, Spain

Abstract

In order to know the temporal variability of the zooplankton community in the Balearic Sea, a sampling study of the water column was started in January 1994 during a period of two years. Three stations were monthly sampled in the waters off the Mallorca island at different depth. Besides the zooplankton, hydrographic and chlorophyll data were also collected and related. During the study the three stations presented close zooplanktonic fluctuations, however the coastal station was slightly different to the other two and more related to the chlorophyll pattern distribution, almost due to higher influence from deeper waters at the farther stations. According to the low biomass and the abundance organisms of the zooplankton, the area can be related to other transition areas in the Mediterranean Sea. The first year study, the zooplankton biomass was higher at the three stations, where two peaks were observed, in winter and spring. However during the second year, when the water was slightly warmer in winter and chlorophyll concentrations were lower, such clear oscillations of zooplankton were not observed. Considering the seasonal abundance of zooplankton (as n°ind/m^3) more fluctuations appeared and besides the winter and summer peaks the autumn one was also important due to groups other than copepods. So that, besides the seasonal variability observed higher interannual variability may be appreciated in the study area. No correlation was found between the copepods and the total mesozooplankton biomass in any of the stations indicating the high contribution from other zooplankton groups.

Key-words: zooplankton, biomass, Balearic Sea.

Introduction

Spatial zooplankton studies carried out in open areas of the Balearic Sea have given synoptic description for certain periods of the year (1-4) however temporal studies, describing the zooplankton pattern distributions are very few, specially in the Balearic Sea (5, 6). In other areas of the Western Mediterranean Sea, as the Liguro-Provenzal sea, the Iberian shelf and the Alboran sea, different temporal studies of the zooplankton have been described (7-10). The lack of this kind of studies in open areas and the strategic situation of the Balearic Islands in the central part of the Western Mediterranean where waters from different origins pass through motivated the present study as part of the Hercule project when the coastal station has been sampling weekly since April 1993. The time-scale of the different planktonic communities is also discussed in order to integrate the main events and interpretate the oscillations observed.

Studied area

The Balearic Sea is a transition area into the Western Mediterranean, that keeps two sub-basins apart with different waters masses. In the northern part, the Gulf of Lions, where the cool and saline water originates and in the southern part, the Algerian basin which is a receptor of warm, less saline Atlanctic water. The Balearic Islands form a geographical barrier between them, whose coast, depending on the time of the year, is influenced by these waters as well as by others from the eastern side (11, 12). The channels between the islands act as tranfer areas for dissolved and particulate material whose inflows/outflows strongly influence the distribution of the planktonic communities. The area chosen was located in the open sea where the platform down rapidly to the edge of the continental shelf (200 m depth) attempting to select a marine area, easily accesible, open to the main water circulation, thereby to study the seasonal fluctuations of the zooplankton in the Balearic Sea.

Material and methods

From January 1994 to December 1995 the three stations at 75, 100 and 200 m depth (St. 1, 2 and 3 respectively) were visited monthly at the same time each day. Zooplankton was sampled by a Bongo Plankton net, 250 μm mesh, by means of oblique hauls. To determinate hydrographic and phytoplanktonic parameters 3 l. Niskin bottles were used at depths of 0, 5, 15, 25, 50, 75, 100, 125 and 200 m. (whenever the depth was possible). CTD data were also recorded. The zooplankton samples, reserved for structural studies, were fixed in 4% neutralised formaldehyde buffered with borax. The samples for biomass studies were frozen at -20°C and 15 days later were analysized as (13) has recomended. The subsamples analysed were obtained using a Folsom Plankton splitter and the statistical treatment was recommended (14). Since the factors studied were not causative the analysis was mainly descriptive showing the pattern of the zooplankton in relation to some of the main oceanographic parameters.

Results and discussion

Seasonal changes of temperature, based on measurements made synchronously with the zooplankton, can be seen in Figure 1. The seasonality of fluctuations is clear and very similar for temperature at all three stations where the temperature ranged from 13.16°C in February to 27.1°C in July, both values observed in 1994. However, during 1995 the values varied from 13.5 in May and 26.5 in July, being warmer in winter. Besides that, a typical thermal regime of the Western Mediterranean was observed (15) with a seasonal thermocline, between 20 to 50 m depth from May to November, defining the stratification period and determining the seasonal biological production in the area. The mixed layer only appeared during

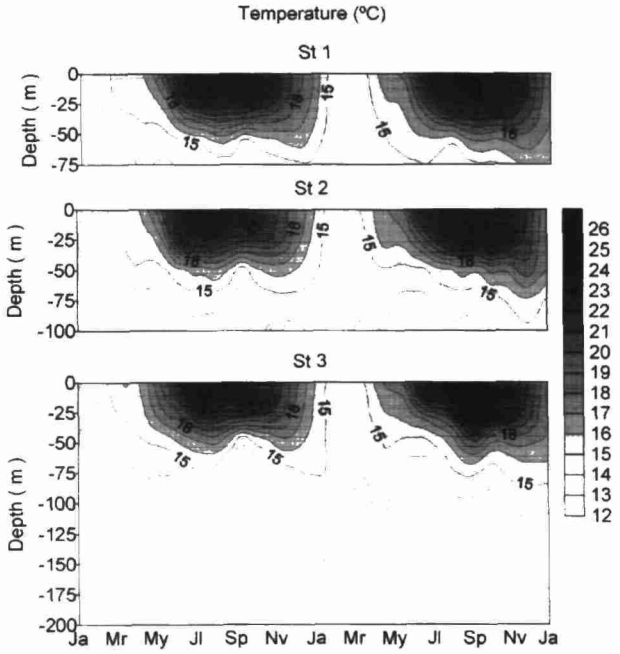

Figure 1. Temperature variation during the two-year study at the three stations of the Balearic Sea

the winter months when the water was cooler than 15°C. Considering the salinity, in 1994 the higher values were found during the winter and the lower in summer. However, in 1995 more irregular fluctuations appeared with lower salinity values, which ranged from 38.3 to 36.91, both at st. 3, indicating the influence of different water masses in the area.

It is important to point out that the euphotic layer was 70 m, on average. At this depth the light did not seem to be a limiting factor for phytoplankton in contrast to the low concentrations of nutrients. These are found throughout the year and are typically low, mostly undetectable during the stratification period on the surface, while higher nutrient levels were detected in deeper waters. In spring and autumn, when the thermocline starts and breaks down, the bottom nutrients come up to the euphotic zone, where they are consumed by the phytoplankton cells. The seasonal fluctuations of chlorophyll are observed in Figure 2 where the maximum concentration (1.3 μg/l) was located at the coastal station in January but was also important at the other stations. In 1994, a large phytoplankton bloom in the whole water column was observed, while in 1995 the winter bloom was seen only in the surface layer. Besides this, another important and regular phytoplankton concentration appears in May around 75 m with the highest value recorded (2 μg/l) however during the summer, below the thermocline, appeared high concentrations in contrast with the poor seasonal values (>0.4 mg/l).

During the first annual cycle the seasonal variability of the mesozooplankton biomass (Fig. 3) showed mainly two peaks: a) one at the begin-

AUGMENTATION DE LA MORTALITE DE *BALAENOPTERA PHYSALUS* EN 1995-96 DANS LE BASSIN LIGURO-PROVENÇAL-CORSE

Frodello J.P. [1]*, N. Terris [1] et D. Viale [2]

[1] Doctorants à l'Université de Corse, Faculté des Sciences et Techniques, Laboratoire d'Ecologie Méditerranéenne,
[2] Directrice du Laboratoire d'Ecologie Méditerranéenne, B.P. 52, 20250 Corte, France

Résumé

Une augmentation des échouages de *Balaenoptera physalus* dans le bassin Liguro-Provençal-Corse apparaît en 1995-96, significativement supérieure à celle des deux décennies précédentes ; en même temps, trois cas sont repérés d'une maladie contagieuse manifestée par un érythème cutané avec perte d'épiderme ; parallèlement des avortements sont constatés. Une forte mortalité infantile apparaît anormale.

Mots clés : Cetacea, metals, pollution, Western Mediterranean

Introduction

Quatre séries d'événements ont focalisé l'attention sur la mortalité des Baleinoptères (noté *Balaenoptera* p.) dans le bassin Liguro-Provençal-Corse en 1995-96, nous les envisagerons successivement. Les résultats de nos investigations sur les causes de mortalité de Baleinoptères seront discutés. De plus une comparaison avec les événements survenus chez *Stenella coeruleoalba* (noté *Stenella* c.) sera effectuée afin de tenter de fournir une explication aux événements décrits.

Matériel et méthodes

- missions en mer sur un navire océanographique du C.N.R.S./INSU,
- autopsies des cadavres de cétacés échoués sur les côtes de Corse, histologie des organes prélevés lors de l'autopsie, au Laboratoire d'Ecologie Méditerranéenne avec contrôle histopathologique par le centre d'anatomopathologie du CHU de Nice, (Pr. Loubière),
- analyse de métaux toxiques en spectrophotométrie d'absorption atomique sur les mêmes organes, au Laboratoire de l'INSERM de Nice, (Dr Roméo).

Résultats

Les observations de terrain

- Un jeune baleinoptère de 18 mètres s'échoue dans le golfe d'Ajaccio fin octobre 1995. Il présente un érythème cutané très fort avec exfoliation de l'épiderme par plaques. L'ablation de cet épiderme évoque le soulèvement de l'épiderme dans les cas de varicelle ; il met à nu un derme fortement congestionné (1, 2). Ce jeune baleinoptère appartenait à un troupeau de huit individus qui est resté dix jours dans la zone du golfe d'Ajaccio, pénétrant même dans le port au fond du golfe.
- Une mission océanographique (N/O *G. Petit* du CNRS-INSU du 27.10 au 3.11.95) nous permet d'observer plusieurs jours consécutifs un groupe de sept baleinoptères dont deux petits présentant les mêmes symptômes d'érythème cutané avec des taches dues à une ablation de l'épiderme; des photographies ont été publiées dans Guibourgé *et al.* (2). Parallèlement à notre mission, à l'ouest d'Ajaccio à 40 milles de notre zone, un énorme rassemblement de baleinoptères est observé pendant six heures ; on peut estimer l'effectif dans une fourchette de 350 à 700 individus (3). Ce troupeau est suivi pendant six heures dans son déplacement vers le sud-est. Cette preuve d'un déplacement migratoire saisonnier vers le sud ne semble pas concerner le troupeau des sept baleinoptères que nous observons et retrouvons sur place le lendemain. Ces derniers n'ont pas répondu aux signaux acoustiques émis par le grand troupeau en migration.
- D'autre part, le 1.11.95 une baleine est observée longeant la côte est du Cap Corse (Haute Corse) flanquée d'un baleineau probablement en difficulté puisque tous deux restent en surface. On s'attendrait à un échouage du baleineau dans les jours suivants mais nous n'en n'avons pas eu connaissance. En revanche un baleineau est trouvé échoué le 29.11.95 à Nonza (Haute Corse) et un autre le 11.12.95 à Venzolasca (Haute Corse). L'étude histologique de ces deux spécimens montre que tous les deux sont avortés.
- Au total ce sont quatre baleinoptères qui s'échouent en 1995 sur notre zone d'étude (Corse). Viennent s'ajouter cinq individus en 1996.

Comparaison du nombre d'échouages de Baleinoptères de 1974 à 1996

La moyenne annuelle des cadavres de baleinoptères retrouvés échoués au cours de la décennie 1984-94 est de 1,2 (écart type de 0,87) et pour la décennie 1974-83 celle-ci est de 0,6 (écart type de 0,66).

Tableau 1 : nombre de baleinoptère échoué chaque année.

1984	1985	1986	1987	1988	1989	1990	1991	1992	1993
3	1	1	2	1	0	1	2	0	1

Les effectifs de baleinoptères en Méditerranée ont-ils augmenté ces dernières années ?

Des évaluations d'effectifs ont été tentées par divers auteurs. En été 1992, Forcada *et al.*, (4) aboutissent à une estimation de 4200 Baleinoptères pour la Méditerranée occidentale dont la moitié dans le nord du bassin. L'évaluation de cette population (ou stock au sens de la Commission Baleinière Internationale) a été ensuite un peu modifiée par ces mêmes auteurs (5). L'Atlas préliminaire de distribution des Cétacés de Méditerranée (CIESM) propose également une estimation de 2000 Baleinoptères pour la partie nord du bassin occidental et plus spécialement 600 à 1700 Baleinoptères pour le Bassin Liguro-Provençal (6). La présence du Rorqual dans ce bassin pendant l'hiver est attestée par des observations beaucoup moins nombreuses que celles d'été, vus le petit nombre de navires à la mer et les difficultés météorologiques d'assurer des campagnes. Gannier (7) estime la densité de Baleinoptères à 0,012 individus au km^2 en été, et 0,0015 en hiver. De même, il donne un indice de 0,013 individu au km^2 en été. La densité calculée par Forcada (5) correspond à 0,024 en août dans le Bassin Liguro-Provençal et a été induite à tout le Bassin occidental. Notarbartolo di Sciara (9) donne un indice de 0,017 individu au km^2 en été pour la bassin Corso-Ligure en 1993. Ainsi avec une telle amplitude de variation il est difficile d'apprécier une éventuelle augmentation d'effectif, depuis 1992.

Discussion

L'hypothèse d'une augmentation du nombre d'échouages peut être reliée à différents facteurs :

1) soit une augmentation de l'effectif de *Balaenoptera physalus* en Méditerranée nord-occidentale,
2) soit une forte concentration des individus dans le bassin Liguro-Provençal,
3) soit une diminution des réponses immunitaires et une fragilisation des systèmes de défense face à diverses agressions du fait de leur contamination par des toxiques,
4) soit un affaiblissement de l'état général des individus du fait de leurs charges en cadmium et en plomb augmentant la morbidité,
5) soit une augmentation brutale de la mortalité par une épizootie nouvelle comme cela est survenu chez *Stenella coeruleoalba* en 1990-91.

Il est possible que ces différentes causes puissent agir ensemble de façon complexe.

Des tests immunologiques ont été réalisés sur des prélèvements de peau de la baleine porteuse d'érythème cutané et sur les deux baleineaux avortés. Ils ont été faits par le Dr. J. Kennedy (Irlande) avec des souches de "delphin distemper virus", identifié par lui au cours de l'épizootie de 1991 sur *Stenella c.* provenant de Méditerranée. D'autres tests ont été réalisés par le Dr. R. Chappuis (France) avec diverses souches identifiées de Morbillivirus ainsi que la souche de la rougeole humaine. Les résultats sont tous négatifs : cela ne permet pas d'écarter totalement l'hypothèse du Morbillivirus souche D.D.V ; car il aurait peut-être fallu réaliser des tests sur d'autres tissus des individus échoués, tels que le cerveau, par exemple.

D'autre part, il nous est apparu intéressant de prélever des biopsies de peau sur les deux baleinoptères vivants et malades observés en mer et identifiés par des taches rouges dues à l'exfoliation épidermique. Nous avons fait des tentatives de prise de biopsies mais l'approche des jeunes baleineaux s'est avérée impossible du fait du comportement de surprotection par les autres membres du troupeau.

Des analyses de métaux toxiques : cadmium, mercure, cuivre et zinc ont été faites sur les trois baleinoptères échoués (10). Comme le montre le tableau 2 de résultats des analyses des métaux les deux

BIOMETRIC RELATIONSHIPS AND GROWTH OF THE MEDITERRANEAN HAKE (*MERLUCCIUS MERLUCCIUS* L.) FROM THE SANTA POLA BAY (SPAIN)

M. García-Rodríguez* and A. Esteban

Instituto Español de Oceanografía, Centro Oceanográfico de Murcia, c/ Varadero 1, 30740-San Pedro del Pinatar, Murcia, Spain

Abstract

The Hake, *Merluccius merluccius* (Linnaeus, 1758), is a widely distributed groundfish species on the continental shelf and slope off Europe and in the Mediterranean Sea. Hake is a target species in the trawl fisheries. In this paper its biometric relationships and growth are described. From the different biometric-relations estimeted, we propose as length-weight relationship those founded for the total population Weight = 0.0048 * Length $^{3.12}$. The Von Bertalanffy Growth Function parameters were obtained using different packages, given high K values, proposing the following expression $L_t = 106 * (1 - e^{-0.2 (t - 0.4)})$ for the total population.

Key-words: Teleostei, Biometrics, Western Mediterranean

The hake *Merluccius merluccius* (Linnaeus, 1758) is a widely distributed groundfish species on the continental shelf and slope off Europe and in the Mediterranean Sea at depths between 30 and 1 000 m, though it is most abundant between 70 and 370 m. The species carries out daily vertical feeding migrations, staying close to the bottom in the daytime and rising off the bottom to adopt a midwater habit at night, and is a target species in trawl fisheries. In this paper are described some biometric relationships and growth, in order to contribute to the knowledge on the biology of the species.

The data base includes data obtained from sampling of commercial trawl fleet landings at the Santa Pola fish wharf (Figure 1). Sampling was carried out monthly, and 36 samples were collected from January 1991 to December 1993. A total of 20 806 individuals were measured (total length at the nearest lower cm). Each month more detailed observations were carried out : total length in cm, total weight in g,gutted weight in g, girth around the base of the pectoral fins in cm, and sex determination; they were obtained on a subsample over a total of 2 889 individuals.

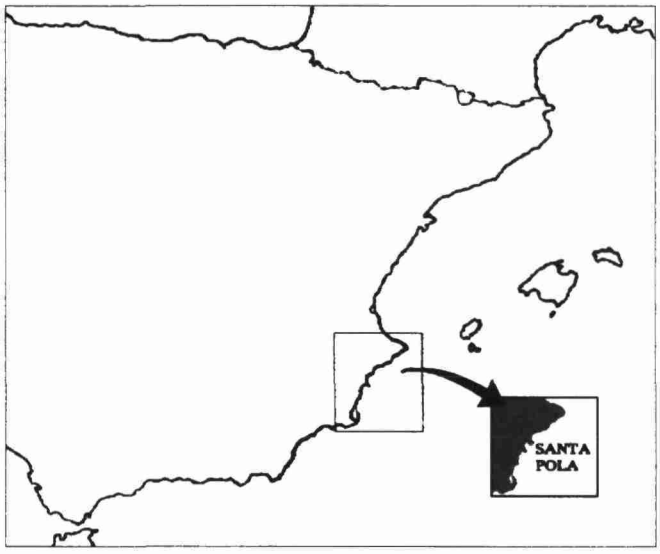

Figure 1. Situation of the area of study

The relationships between several parameters were determined. For total length/total weight and girth/total weight, the data was expressed by a power equation of the form $W = a*L^b$. For the other parameters total weight/gutted weight and total length/girth, the data were adjusted by linear regression: $Y = a + bX$. The relationships were established separately for males, females, individuals of undetermined sex (immature), and the population as a whole.

The age-length relationship was computed from size frequencies. Monthly data samples were extrapoled to the total number of individuals caught per month by the fleet. Then they were grouped by 2cm size class, separated by sexes using the sex ratio by size, and smoothed over three classes; the pool of individuals for which sex could not be determined was divided equally between males and females. The Von Bertalanffy growth function (VBGF) was used as growth expression, and the growth parameters ($L\infty$, K and t_0) estimated using the Elefan (1) and Fishparm (2) automatic computer programs. Estimations of the "best combination" of the VBGF parameters were done, giving a value of t_1= 12 cm to determine t_0. The method of Bhattacharia (MPA mode of the Elefan program) was applied to the quarterly histograms and the results were then applied to the Fishparm program.

Length distribution ranged between a minimun of 4 cm to a maximun of 68 cm and the length range between 4 to 20 cm represented the 86 % of the total number of individuals. The results for the relationships between the various biometric parameters of hake established in this study have been presented as follows :

The length-weight relationships are presented in Table I, the coefficient b significantly differs from 3 in all cases except in males.

Table I.- Parameters of relative growth (Length-Weight relationship: Weight = a * Length b) calculated for the different groups (undetermined, males, females and total) of *Merluccius merluccius*; significance levels = ***<0.001, NS<0.1 in a "t"Test.

Group	a	b	err.b	signif.	r2	n	range
males	0.006	3.05	0.02941	NS	0.96	502	13.5-52.5
females	0.0048	3.12	0.01259	***	0.99	955	11.5-68.0
undeterm.	0.0056	3.06	0.01681	***	0.96	1 369	4.0-32.5
total	0.0048	3.12	0.00477	***	0.99	2 826	4.0-68.0

The girth-weight relationships are presented in Table II, show a significant difference between b and 3 in all cases except in the undetermined (immature).

Table II.- Parameters of relative growth (Girth-Total Weight relationship: Weight = a * Girth b) calculated for the different groups (undetermined, males, females and total) of *Merluccius merluccius*; significance levels = ***<0.001,NS<0.1 in a "t"Test.

Group	a	b	err.b	signif.	r2	n	range
males	0.210	2.72	0.03390	***	0.93	437	13.5-52.5
females	0.214	2.71	0.01683	***	0.96	819	11.5-68.0
undeterm.	0.125	2.93	0.02464	NS	0.91	1 230	4.0-32.5
total	0.141	2.86	0.00675	***	0.99	2 486	4.0-68.0

The girth-length relationships are presented in Table III, resulting a relation between parameters in the form that the girth is nearly the half of the length.

Table III.- Parameters of relative growth (Length-Girth relationship: Girth = a + b Length) calculated for the different groups (undetermined, males, females and total) of *Merluccius merluccius*.

Group	a	b	r2	n	range
males	-0.289	0.42	0.86	437	13.5-52.5
females	-1.552	0.48	0.92	819	11.5-68.5
undeterm.	0.080	0.38	0.90	1 230	4.0-32.5
total	-0.995	0.46	0.97	2 486	4.0-68.5

The gutted weight-total weight relationships are shown in Table IV. The size-weight relationship values obtained, were similar to the values calculated by other researchers in the Western Mediterranean, (3). In general the values of b were higher than 3. Differences between group sizes were small and were mainly ascribable to the fact that the size ranges for the immature and for males were smaller than for

ABOUT A COUPLE OF *THYSANOTEUTHIS RHOMBUS* (CEPHALOPODA,THYSANOTEUTHIDAE) FOUND IN THE STRAIT OF MESSINA (SICILY)

Daniela Giordano*, Francesco Perdichizzi, Silvestro Greco

Istituto Sperimentale Talassografico - C.N.R., Spianata San Raineri 86, Messina, Italy

Abstract

The capture of two large specimens of *Thysanoteuthis rhombus* in the waters of the Straits of Messina (Sicily) is reported. Body measurements and data on reproductive biology are given. *T. rhombus* seems unique among squids by its monogamy, where pairs consisting of a male and female of the same size remain together from their juvenile stage until death (probably the main function of this paired lifestyle is reproductive).

Key-words: Cephalopods, reproduction, Strait of Messina

The diamond-shaped squid *Thysanoteuthis rhombus* Troschel, 1857 is the only species of the family Thysanoteuthidae. This squid is a non-abundant epipelagic inhabitant of warm tropical and partially subtropical waters (water temperature >20 to 21°C, usually 23 to 26°C) of the World Ocean including the Mediterranean. The squid penetrates into the higher latitudes of subtropical and temperate waters (Japan Sea, waters of South Africa and America) with warm currents (the Tsushima, Kuroshio, Agulhas and Brazil Currents, and the Gulf Stream) (1, 2, 3). *T. rhombus* were sometimes found dying in near-shore waters or stranded at the outer limits of the species range (4-9). The present note reports the recovery of two adult specimens of *Thysanoteuthis rhombus* that were found on the beach in June 1993 in the falcate zone of San Raineri (Straits of Messina). The first specimen of *T. rhombus* was described by Troschel in 1857 from the same waters. Following these findings of juveniles of this species were cited (10) (11); but from 1857 to 1993 captures of mature adults not reported from this area. More recently two mature specimens of *T. rhombus* in the waters of Mazara del Vallo (Sicily) were described (12).

Material and methods

The two adult specimens of *T. rhombus* described here were caught a few metres from the shore of the falcate zone of San Raineri. The specimens were brought to the laboratory where the morphometric characteristic and the sexual determination were recorded.

Discussion

Diamond-shaped squid have rhomboidal fins as long as the mantle and relatively short arms, with a very well developed protective membrane. It can reach 100 cm in dorsal mantel length and 20 kg in weight (2). The measurement of the two *T. rhombus* examined are given below:

	Female	Male
Total length	1450 mm	1300 mm
Dorsal mantle length	780 mm	710 mm
Width across fins	670 mm	605 mm
Total weight	18 kg	14.5 kg

In these specimens the arms appear not very robust with respect to the conspicous dimension of the animal. The apex of the tentacle club presents very small suckers, with four rows of greater stalked suckers having diameters up to 5 mm; other small suckers are situated close to the base of the club and a single row is in terminal position. Along the tentacular shaft, proximal to the club, a row of about 9-10 small suckers is present; distance between suckers varies from 10 mm to a maximum of about 28 mm close to the end. The gladius is horny with the typical "point of lance" shape, transparent and with longitudinal ribs.

The reproductive biology of *Thysanoteuthis rhombus* is poorly known. The structure of the sexual system has been analyzed mainly on the basis of immature specimens (13, 14, 4, 6, 15).

The reproductive biology of *T. rhombus* was reviewed and the morphology and anatomy of the sexual system of mature adults has been analyzed (16). It is characterized by rather primitive features with respect to gonad attachment and structure of the hectocotylus, and mostly secondary characters, including small oviducts and very large oviducal glands and ovary. Sex may be distinguished visually in animals greater than 100 to 120 mm in ML by the appearance of primordial nidamental glands in females, and a primordial spermatophoric gland in males.

In the ovary of mature females, oocytes were at various stages of ripening, thus exhibiting asynchrony in their development. It was possible to distinguish 6 size groups of oocytes that corresponded to the following stages of oocyte development (17). Size group I corresponded to the second phase of previtellogenesis ("primary follicle"), oocytes were polygonal in outline, and the centrally situated nucleus was oval and large. Group II corresponded to the third phase of previtellogenesis ("simple follicle"), oocytes were either oval or goblet-shaped, and the cytoplasmic volume was increased in comparison to the preceding size group. Group III obviously corresponded to an intermediary period of oocyte development ("complicated follicle"); oocytes were leaf-like in outline, of dark color, with numerous shallow longitudinal grooves together with follicle cells that protruded into the grooves. The nucleus was not visible. Group IV corresponded to the first and second phases of trophoplasmatic growth ("vacuolization and vitelline accumulation"). Oocytes were covered with reticulate grooves, and were dark in color. Group V corresponded to the third phase of trophoplasmatic growth ("expulsion of follicles"); oocytes were rounded and yellow, the reticulate grooves having almost disappeared. Group VI corresponded to the fourth phase of the trophoplasmatic growth ("ripe oocytes"). Oocytes had a smooth surface and were oval and crimson-violet.

According to the above authors (18, 19), the testis of males <150 mm is a narrow, long strip hanging from the mesentery of the sexual coelom. In immature males <400 mm ML, the length of the testis varies significantly from 3-4 to 18-20% ML. In larger males, the relative length of the testis stabilizes at 10 to 16% ML. In mature males, the testis becomes broader and more robust in shape, like an elongate oval. Formation of the spermatophores in different parts of the spermatophoric gland (SG) is similar to that in other squid and cuttlefish. Spermatozoa enter into the first section of the SG from the spermaduct and mix with its gelatinous secretions. The frequency of occurrence of developing spermatophores (% of the male squid samples that contain spermatophores in a given section of their SG) varies in different sections of the SG. The spermatophores of *Thysanoteuthis rhombus* are large, ranging from 60-70 mm in males of 420 mm ML to 95-100 mm in males of 850 mm ML. The number of spermatophores located in different parts of the SG does not depend on the length of males. Usually, in both the SG and the spermatophoric duct there are 3 developing spermatophores; in rare cases there were 2 or 4 spermatophores. The number of developing spermatophores also does not depend on the total number of ripe spermatophores in the Needham sac: in a male of 695 mm ML there were 15 spermatophores in the Needham sac and 3 developing spermatophores in the SG; in a male of 850 mm ML, 11 and 4, respectively; in a male of 770 mm ML, 6 and 3. The total number of spermatophores in the Needham sac varied from 5 to 10, commonly 8 or 9. Therefore, the total number of spermatophores located in both the SG and the Needham sac is low and does not exceed 15 to 17. Probably, males form 15 to 20 spermatophores between each mating. This assumption is supported by the total number of spermatangia found on the buccal membrane of females (no more than 20), which are the traces of the previous copulation.

Spawning grounds of *Thysanoteuthis rhombus* were identified as those areas in which egg masses, larvae and completely mature squid were found. All occurrences of *T. rhombus* egg masses, larvae and mature squid in peripheral regions corresponded with strong warm currents such as the Agulhas or Kuroshio (7, 15, 9). This squid does not reproduce in subtropical oligotrophic waters of the World Ocean, except in the Mediterranean Sea. *T. rhombus* spawns throughout the year in tropical waters. In peripheral regions such as in the Mediterranean (20) (21), near southern Japan (22) (23) and in the southeast Pacific (24), spawning takes place during the warm seasons (summer and early autumn).

THE IMPACT OF TEMPERATURE AND SALINITY ON THE VOLUME OF THE ROTIFER *BRACHIONUS PLICATILIS* O.F. MULLER UNDER LABORATORY CONDITIONS

Niksa Glavic *, Bosko Skaramuca and Valter Kozul

Institute for Oceanography and Fisheries, Laboratory for Ecology of Shellfish and Fish Rearing, Dubrovnik, Croatia

Abstract

We tried to rear rotifers of different size fractions, kept at controlled, sea water temperatures and salinities and fed with the unicellular algae *Nannochloropsis* sp., by combining three temperatures and three salinities in nine different ways. Observations on the growth and volume of the rotifers lasted ten days. Rotifers reared at 22° C and 20 ‰S averaged 758692 mm^3 (SD-+199504 μm^3), while those reared at 34° C and 35 ‰S averaged 425358 μm^3 (SD- +152530 μm^3). The ANOVA one way analysis of variance showed different results between the groups of rotifers (P<0.05), thus, we can conclude that higher temperatures and salinities influence rotifers by decreasing body volume.

Key-words : aquaculture, plankton, biometrics, larvae

Introduction

The rotifer *Brachionus plicatilis* O.F. Muller, since it was first used as fish larvae food in the 60-ties (1), is one of the most frequently used food organisms in the artificial rearing of larval fish and crustaceans. This organism was a favourite in live food production, due to its simple, mass rearing, fast reproduction, short generation time, and relatively high nutritional value. Also, the advantages of its euryhaline and eurytherm properties allow it to be reared under a variety of natural conditions, broadening its range of applications.

The food intake process is relatively complex in fish larvae. The conversion rate depends not only on available food quantities and their qualitative composition, but also on the size of the prey or food particle. Prey size is related to the mouth size of fish larvae (2, 3), and does not in average surpass 38% of mouth of the larvae (4, 5, 6) claim that prey size for fish larvae increases with the increase in larvae size. Thus, in artificial rearing, there is a need for rotifers of different size fractions, in order to successfully meet the nutritional needs of several larval fish. The aim of this experiment was to estimate the influence of temperature and salinity on the body structure of rotifers. Information on the possible effects of mentioned abiotic conditions is given by Fukusho (7, 8), who report that in populations of *Brachionus plicatilis* found in natural ecosystems, S (small)-type individuals predominate in the summer and L (large)-type individuals during the lower, winter temperatures.

This paper displays the preliminary results based on experiments concerning the synergistic effects of temperature and salinity on the body volume of rotifers under controlled, laboratory conditions. We tried to discover how different combinations of temperature and salinity influence the body volume of rotifers in rearing conditions.

Material and methods

We reared rotifers in 30 l plastic containers, filled with 15 l of sea water, with medium aeration. We fed them with unicellular planctonic algae *Nannochloropsis* sp., maintained at a constant concentration of 1,2-1,5 x 10-6 ml. The sea water used was taken from the aquarium system, located near our laboratory, from a depth of 8 m. The salinity of the sea water was 35 ‰S and the temperature 18° C. Prior to its use, the sea water was filtered through three mechanical filters (10,5 and 1 μm) and was sterilized by means of a flow through UV lamp. In the thermostatic chamber, in which the experiment was conducted, the temperature was maintained at a constant 22° C and the photoperiod was 12/12 (light/darkness).

The influence of different temperatures and salinities was examined in three separate experiments. In each experiment, rotifers were reared under different temperatures and salinities. The temperatures were constantly maintained by using aquarium, ceramic heaters with a thermostat (SICCE model RTR 25/300W) and the salinity was kept constant by mixing sea and tap water. The experiments were conducted from November 20 to December 23, 1995, each experiment lasting ten days.

During the first five days, rotifers were nurtured to achieve a satisfactory growth and to reach a constant phase of population. Between the fifth and the tenth day, measurements were taken of the length and width of the lorica. Rotifer samples were taken every day for measurement and were examined under the binocular microscope WILD HERRBRUG Typ 325400, and the results were automatically printed using WILD HERRBRUG MMS 325. 100 individuals were measured per container. We obtained rotifers for measurement by filtering 0.25 l of suspension through a plancton net of 53 um.

The volume was calculated according to Ruttner-Kollisko (9), simplified formula : V = 0.12 x a3

where body volume, a = length of lorica and 0.12 = coefficient.

The data on the body volume was statistically computed using the ANOVA one way analysis of variance in the Statgrapher *vs.* 2.6 programme, and SD was computed in the 2 D Graphing programme.

Results

Figures 1, 2 and 3 show changes in the average body volume of rotifers and Table 1 shows the numerical values. The average values, measured every day, did not change considerably throughout the experiment, but it is evident that there is a difference in the body volume of rotifers kept at the same salinities, but at different temperatures (Fig. 1, 2, 3). The differences between the groups are most obvious in the second experiment (Figure 2), with the following average values of body volume : 647 840 μm3 at 27 ‰S and 22° C ; 520 590 μm3 at 27 ‰S and 28° C ; and 421 410 μm3 at 27 ‰S and 34° C. The greatest difference in body volume can be found between the group at 35 S and 34° C, with V =758 692 μm3, and the group at 20‰ S and 22° C, with V = 425 358 μm3, which is only 56.65% of the first, greatest value. The ANOVA one way analysis of variance showed three, clearly divided size fractions of rotifers (P<0.05). The first consisted of four groups : 9, 8, 7 and 6, with smaller rotifers (Figure 2). The second

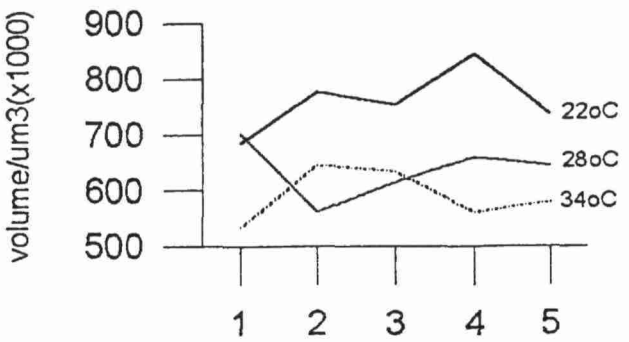

Figure 1. Body volume of rotifers during Experiment 1, at 20‰S.

Table 1. Average body volume of rotifers an SD given for each combination of temperature and salinity (V/μm^3 and SD x 1000).

Groups	S‰/t°C	V/μm^3	SD
1	20/22	758	±199
2	20/28	636	±159
3	20/34	590	±133
4	27/22	638	±177
5	27/28	549	±168
6	27/34	439	±140
7	35/22	446	±195
8	35/28	455	±169
9	35/34	425	±152

GEOGRAPHICAL AND HISTORICAL DISTRIBUTION OF THE CETACEANS IN CROATIAN PART OF THE ADRIATIC SEA

Hrvoje Gomercic [1]*, Duro Huber [1], Ana Gomercic [2], and Tomislav Gomercic [1]

[1] Faculty of Veterinary Medicine, University of Zagreb, Zagreb, Croatia

[2] Department of Animal Physiology, Faculty of Sciences, University of Zagreb, Zagreb, Croatia

Abstract

The following dolphin, porpoise, and beaked whale species have been found in the Croatian part of the Adriatic Sea: common dolphin, *Delphinus delphis* (Linnaeus, 1758), bottlenose dolphin, *Tursiops truncatus* (Montagu, 1821), striped dolphin, *Stenella coeruleoalba* (Meyen, 1833), Risso's dolphin, *Grampus griseus* (Cuvier, 1812), harbour porpoise, *Phocoena phocoena* (Linnaeus, 1758), northern bottlenose whale, *Hyperoodon ampullatus* (Forster, 1770), long-finned pilot whale, *Globicephala melas* (Traill, 1809), false killer whale, *Pseudorca crassidens* (Owen, 1846), sperm whale, and three species of the suborder Mysticeti. Among them the only true residents were the common and bottlenose dolphins. Before the Second World War the common dolphin was prevalent, but today only the bottlenose dolphin lives in the Adriatic Sea.

Key-words: Cetacea, coastal waters, Adriatic Sea

Introduction

Descriptions of marine mammals in the Croatian part of the Adriatic Sea date from as long ago as the 16th century. The first mention of the Mediterranean monk seal in the written Croatian language is to be found in the papers of Mavro Vetranovic Cavcic (1482-1576) (1), who described Mediterranean monk seal on the small island of Sveti Andrija, near Dubrovnik. The first formal mention of the dolphin can be found in the dictionary compiled by Faust Vrancic in 1595 (2) (Latin: Delphin; Italian: Dolfino; German: Meer-Svvein; Croatian: Duppin; Hungarian: Dizno Hal). However, the first scientific descriptions of cetaceans in Croatian Adriatic waters date from the end of the 19th century (3, 4). According to data in literature the following cetacean species in Croatian waters have been found and described: common dolphin, *Delphinus delphis* (Linnaeus, 1758), bottlenose dolphin, *Tursiops truncatus* (Montagu, 1821), Risso's dolphin, *Grampus griseus* (Cuvier, 1812), harbour porpoise, *Phocoena phocoena* (Linnaeus, 1758), northern bottlenose whale, *Hyperoodon ampullatus* (Forster, 1770), long-finned pilot whale, *Globicephala melas* (Traill, 1809), false killer whale, *Pseudorca crassidens* (Owen, 1846), sperm whale, *Physeter catodon* (Linnaeus, 1758), fin whale, *Balaenoptera physalus* (Linnaeus, 1758), minke whale, *Balaenoptera acutorostrata* (Lacépède, 1804), northern right whale, *Eubalaena glacialis* (Müller, 1776) (5-13), and, in October 1991, striped dolphin, *Stenella coeruleoalba* (Meyen, 1833) (14). Cuvier's beaked whale, *Ziphius cavirostris* (Cuvier 1823) (15) has also been found in Italian Adriatic waters. Apart from those species, descriptions of the Adriatic dolphin, *Tursiops parvimanus* (Reinhardt, 1888) (4,10) and the blue whale, *Balaenoptera musculus* (Linnaeus, 1758) (4,9) are to be found in literature, although they were misidentified. In addition to the foregoing published data, sightings of sperm whale, long-finned pilot whale, common dolphin, and bottlenose dolphin in Croatian waters, and striped dolphin on the outer limits of Croatian territorial waters were noted between 1972 and 1992 (16). The purpose of this work was to establish all the cetacean species which are to be found in the Croatian part of the Adriatic Sea, as well as their present status.

Materials and methods

We examined and identified the skeletons and corresponding documents housed in the Croatian Natural History Museum in Zagreb, where there are 25 skeletons, together with relevant documentation on dolphins found between 1873 and 1935 in various parts of the Croatian Adriatic Sea.

In the past decade we have determined species for 211 individual live cetaceans in different areas of Croatia's Adriatic Sea (between about N42°15' and N45°35' latitude) and divided in 30 by 30 minute (latitudinally and longitudinally) (16) squares. For this purpose we used a small motor boat with which we were able to approach the dolphins to within a distance of less than 50-60 meters. In the period June - August of each year we sailed through specific areas of Croatian waters, to a total of 100 hours and 1,000 km. We also manned an observation point on the shore of the central part of the Croatian Adriatic Sea (E15°15'25", N44°23'12"). It should be noted that it is probable that our observations did not always involve different animals, and that some individuals could have been registered more than once, at different locations and at different times.

Over the past seven years we have examined and determined species of 15 carcasses of dolphins that either died from natural causes or were accidentally caught in fishing nets. The dolphins were aged by growth-layer groups in the dentine (17), or else were adult specimens, determined by the complete ossification of vertebrae.

Results

Of 25 dolphins found in Croatian waters between 1873 and 1935 and whose skeletons and documents are housed in the Croatian Natural History Museum in Zagreb, 15 specimens were common dolphins, 9 were bottlenose dolphins and one was a Risso's dolphin. Therefore, of all the collected dolphins to have died in the Croatian part of the Adriatic Sea before the Second World War, 60% were common dolphins and 36% were bottlenose dolphins.

Of the 211 living individuals to have been identified in the last decade in Croatian Adriatic waters, one was a juvenile whale belonging to the family Balaenopteridae, 10-15 m long, seen on 8 September 1990, at N44°58'32", E14°55'. We probably observed the Risso's dolphin twice (11 August 1990 and 2 May 1992) from the coastal observation point. On the first occasion the Risso's dolphin was in the company of two bottlenose dolphins; on the second occasion it was solitary. The remaining 208 dolphin sightings were bottlenose dolphins, seen at different times of the year, in almost all 30 by 30 minute (latitudinally and longitudinally) (16) squares of Croatian Adriatic waters.

Of the 15 examined carcasses of the dolphins, 14 were bottlenose dolphins which had died from natural causes, or were accidentally caught in fishing nets along the whole Croatian coastline and islands (between N42°43'45" and N45°06'05"). They were of both sexes, from cub to adult, with body masses of between 52 and 279 kg, and a body length of between 163 and 290 cm. Only one was a striped dolphin (N42°55', E17°11'25"), stranded in October 1991 (Table 1). This was a physically mature animal and, according to interviews with witnesses, it had displayed some neurological symptoms before stranding; that is to say, the animal rolled and swam in small circles. In November 1990, an 11-metre-long carcass of a fin whale was found on the coast of Silba island (N44°21', E14°44').

Table 1. General data of examined dead dolphins in Croatian part of the Adriatic Sea (F = female; M = male).

Species	Found	Sex	Age	Location	Length	Mass
	month/year		year	north/east	cm	kg
Tursiops truncatus	10/90	F	4	45°03'N,13°35'E	250	204
Tursiops truncatus	11/90	F	<1	45°05'40"N,13°38'40"E	164	52
Stenella coeruleoalba	10/91	?	adult	42°55'N,17°11'25"E	?	?
Tursiops truncatus	6/92	M	7	45°04'N,13°34'E	263	240
Tursiops truncatus	summer/93	?	?	44°23'30"N,14°40'E	?	?
Tursiops truncatus	9/93	M	3-4?	44°33'40"N,14°23'E	242	?
Tursiops truncatus	3/94	F	6	45°04'25"N,13°38'20"E	219	120
Tursiops truncatus	5/94	F (pregnant)	6	44°52'05"N,14°E	265	?
Tursiops truncatus	9/94	M	<1	42°43'45"N,16°53'40"E	163	75
Tursiops truncatus	4/95	F	adult	45°18'N,14°33'E	?	?
Tursiops truncatus	12/95	M	9	43°43'40"N,15°53'30"E	278	237
Tursiops truncatus	4/96	F	5	44°49'30"N,13°51'05"E	240	?
Tursiops truncatus	8/96	?	young	43°12'30"N,16°33'20"E	210	?
Tursiops truncatus	10/96	M	12	45°06'05"N,13°37'50"E	290	279
Tursiops truncatus	4/97	F (pregnant)	7	44°46'20"N,14°19'15"E	?	?

APPLICATION OF GENERALIZED LINEAR MODELLING TO THE STUDY OF CATCH RATES OF WESTERN MEDITERRANEAN TRAWL FLEETS

Raquel Goñi and Federico Alvarez*

Centro Oceanográfico de Baleares, Inst. Español de Oceanografía, Muelle de Poniente s/n, Aptdo. 291, 07080 Palma de Mallorca, Spain

Abstract

Generalized Linear Modelling (GLM) techniques are used to develop a model for catch rates of European hake by the Spanish trawl fleet fishing off the coast of Castellón (E Iberian Peninsula) between 1991 and 1996. The model includes a factor for vessel category of GRT, as a means of adjusting for fishing power effects, as well as factors for year, month and fishing closure effects. Vessel capacity, season and year are shown to have a significant effect on hake catch rates of this fleet, with vessel capacity alone explaining about 54% of the total variation in the data. Significant first order interactions are found between all three effects with only the year by month interaction being highly significant and probably related to the varying timing of the bimonthly annual closure of the fishery. The model explains 63% of the variation in the CPUE data, an amount similar or above that obtained by other authors. Introduction of additional factors, such as location, skipper ability and knowledge, vessel specific improvements in fishing technology or any other determinants of fishing power, and effects of other species in the model, may be used to reduce the amount of unexplained variation and therefore to increase the reliability of the derived abundance indices.

Key-words: demersal, fishes, trawl surveys, stock assessment, Western Mediterranean

Introduction

Groundfish trawl fishing is widely spread all over the Mediterranean. At present, there are about 1234 trawlers operating off harbours along the Spanish Mediterranean littoral (1) with annual landings reaching 60 000 t. Although these are multispecies fisheries -up to 40 different species may appear in the landings- a small number of them account for a large proportion of the catch and of its economic value. The main target species are: European hake (*Merluccius merluccius*), red mullet (*Mullus barbatus*), sole (*Solea solea*), monkfish (*Lophius* spp.), octopus (*Octopus vulgaris*), squid (*Loligo vulgaris*), cuttlefish (*Sepia officinalis*) and red shrimp (*Aristeus antennatus*). Due to the multispecies nature of the fisheries and the large number of landing harbours involved, it has been traditionally difficult to gather long and reliable series of data of the activity and catches of the fleets which would allow to carry out stock assessments. Fisheries management tools applied in Spanish Mediterranean groundfish trawl fisheries are effort controls (12 hours fishing per day and a maximum power of 500 HP), permanent closure above 50m depth, minimum mesh size, minimum landing sizes, and since 1991 a two-month spring-summer closure in certain areas (*i.e.* off Castellón).

For fisheries where only series of catch and effort data are available, catch per unit effort (CPUE) information from commercial fishing vessels is frequently used as biomass indices for stock assessment purposes. For most stocks, indices are averaged across fishing gears, areas, months and then within years to produce indices of annual abundance (2). However, given the tendency of fleets to increase their efficiency with time, it is not easy to obtain reliable standardized measures of the effective effort through the years. A number of factors contribute to this. In addition to changes in fleet composition and changes in fishing power of individual vessels, factors such as fishermen behaviour and market prices may also contribute to increasing or reducing the effective effort exerted over any particular stock in a multispecies fishery. Seasonal fluctuations in abundance or availability due to changes of fish behaviour or oceanographic conditions, also influence catch rates of a given species.

A method based on a multiplicative model for CPUE developed by Robson (3) has proven useful for obtaining standardized catch rates when appropriate information is available (4, 2). The multiplicative model relates the catch rate of a certain vessel type (i) at a certain time (t) to the catch rate of a reference vessel (v1) at a reference time (t1), times a factor which is the abundance in time (t) relative to that of time (t1), times a factor which is the efficiency of vessel type (i) relative to that of vessel type (v1). The model can accommodate effects such as year, area, season, and fishing power. The coefficients of factors can be estimated by using Generalized Linear Modelling (GLM). This method has been widely applied for the standardization of CPUE indices in the tuna fisheries managed by the ICCAT(4,5) and to a lesser extent to groundfish fisheries for, *e.g.*, *Gadus morua* (6), *Sebastes alutus* (7), *Solea solea* (2).

Objectives

This study uses linear multiplicative models to describe and estimate the CPUE of European hake (*Merluccius merluccius*) from Spanish trawlers fishing off the coast of Castellón (E Iberian Peninsula). Catch rates, defined as average daily catch, have been modelled taking vessel characteristics (capacity), time (year), season (month) and fishing closure as factors. This analysis is intended to: a) improve our knowledge of factors affecting hake trawl catch-rates, and b) investigate methods to obtained annual standardized abundance indices. European hake (*Merluccius merluccius*) has been chosen for the study due to its importance in the trawl fleet landings (12% in weight of Castellón total in 1995) and its high economic value (21% of Castellon total first sale value in 1995). The trawl fleet which operates from the harbour of Castellón is singled out as a case study in the wider context of the Western Mediterranean groundfish trawl fleets.

Material and methods

The data set of the trawl fleet operating from the harbour of Castellón contains vessel monthly landings of 21 commercial species and groups of species together with the number of days fished and vessel characteristics (GRT, HP, and length) for the 36 vessels making up the fleet during the period of 1991 to 1996. These data have been gathered by the Instituto Español de Oceanografía sampling and information network.

Tonnage (GRT) is chosen as the most relevant vessel characteristic reflecting fishing power for this fleet instead of the more commonly used horse-power (HP). GRT and HP data available are nominal values and for HP they are known to depart significantly from the effective values. This is because since power is regulated and also taxes are paid accordingly, there is an incentive to conceal the real power of the vessel. To corroborate this, the relationship between nominal GRT and HP was examined. On this basis and pursuant to the examination of the GRT/HP plot, vessels were grouped into three categories of nominal GRT: <35, 35-55 and >55 GRT. For each combination of vessel, month and year, catch rates were calculated as the total recorded landings of hake (assumed equal to catches since discards of this species can be considered negligible (data from IEO/EU project 94/027) divided by the total number of days fished.

To investigate the effect of fishery vessel type together with annual and monthly variation on catch rates from the hake trawl fishery, generalized linear models (GLMs) (8) were applied using routines contained in the S-Plus programming environment (9). A gamma distribution was used in the analysis since the frequency distribution of the catch rates was skewed and the variance proportional to nearly the square of the mean weight (9). The gamma density function is expressed within generalized linear models in terms of the mean μ and the parameter ν which determines the shape of the distribution. The parameter ν, assumed constant for all observations, is σ^{-2}, where σ is the coefficient of variation. The gamma variance $V(\mu) = \mu^2/\nu$, and a logarithmic-link $\log(\mu)$ functions were used to relate the expected catch rates to the predictors. Independent variables vessel class, year, month and fishing closure were introduced as factors. The following generalized linear model was used

$$\ln(\mu_{ijkl}) = f + \beta_i^I + \beta_j^J + \beta_k^K + \beta_l^L$$

where μ_{cmyp} is the expected catch for vessel class c, month m, in year y and following or not a closure period p. Analysis of deviance to evaluate the significance of the factors in the model was performed by comparing models excluding one term at the time.

Summary of main effects

Main effect	Data
Vessel category (GRT) (c)	< 35, 35-55,> 55
Year (y)	1991,1992,1993,1994,1995, 1996
Month (m)	12 months of the year
Closure period (p)	Yes, No

Results and discussion

Table I shows the results from the analysis of deviance which indicates that differences in catch rates between vessel classes is significant and also the variation with month and year (probability of F <0.0001). Conversely, catch rates are not significantly affected by the fishing closure term (probability of F>0.2). Monthly variation differs between vessel classes and also between years (probability of interactions < 0.05). The model incorporating all independent variables and interactions reduces de null deviance

PRELIMINARY DATA ON THE BATHYMETRIC DISTRIBUTION OF CEPHALOPODS IN THE NORTHERN ALBORAN SEA

M. González, P. Torres and L. Gil-de-Sola*

Instituto Español de Oceanografía, Centro Oceanográfico de Málaga, Puerto Pesquero s/n, 29640 Fuengirola, Málaga, Spain

Abstract

The results of three trawl surveys carried out from 1994 to 1996 in the Alboran sea are analysed. A total of 26 cephalopod species were found between 30 and 790 m of depth. Cephalopods make up about 8 % of the catch. *Octopus vulgaris* and *Alloteuthis* spp. were the most abundant species in the area.

Key-words: Demersal, cephalopods, Biogeography, Trawl surveys, Alboran Sea

Introduction.

The Cephalopods are well known in the Mediterranean, as can be seen from general articles about this taxonomic group (1-3) and about its geographic and bathymetric distribution (4-10). However, there are certain areas, like the Alboran sea, where such studies are lacking. The aim of this article is to improve the knowledge of this important animal group in this particular area.

Material and methods.

The Cephalopods taken in this study were collected during three bottom trawl surveys in the Spanish Alboran sea in October 1994, 1995 and 1996 (Fig. 1), within the research programme "Demersal fishing of the Spanish Mediterranean" financed by the Ministerio de Agricultura y Pesca. A total of 98 bottom trawl hauls were carried out on the research vessel *Francisco de Paula Navarro*, between 36 and 790 m of depth. Each haul consisted of one half hour of effective trawling carried out during day-light hours.

For this study we have used 82 hauls made with the commercial bottom trawl gear named "baka". For the cephalopod study, the area was divided in five bathymetric strata: A=30-100 m (28 hauls), B=100-200 m (16 hauls), C=200-300 m (13 hauls), D=300-400 m (13 hauls) and E=400-800 m (12 hauls). The abundance and biomass index were standarised to one hour of trawling. Further details of the sampling procedure are given in Gil de Sola (11).

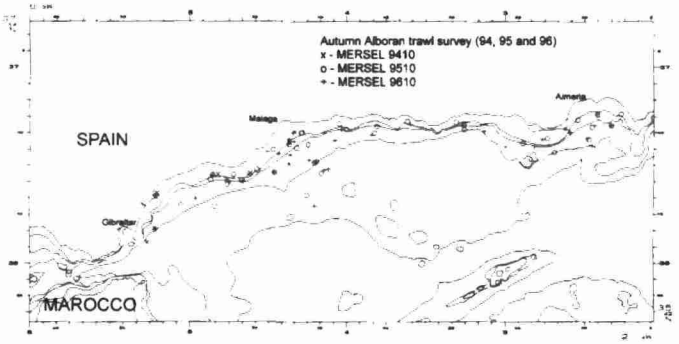

Figure 1. Location of the samples in the study area.

Results and discussion.

Cephalopods appear in 80 of the 82 hauls made. A total of 26 species were caught (Table I) corresponding to 452 kg and 69.868 specimens. The cephalopods were 8% of the total catch in weight (Fig. 2). This percentage is lower than in other Mediterranean zones: in the northern Tyrrhenian Sea cephalopods represented 9-17 % of the total commercial catches, in the lower Adriatic Sea cephalopods reach about 20 % of the catch and in the Ionian Sea they make up about 17 % of the commercial catch. *Rondeletiola minor, Sepietta oweniana, Alloteuthis media* and *Sepia elegans* were the most occurrence species, and *Sepia officinalis, Onychoteuthis banksii, Heteroteuthis dispar, Histioteuthis reversa* and *Ancistroteuthis lichtensteinii* have appeared only in one haul. This is not surprising since *S. officinalis* have a lower catch in the bottom trawl fishing than with other types of gear (12), and the others are oceanic species (6).

The more coastal cephalopods are represented by *Sepiola intermedia*, confined within the first stratum, *Loligo vulgaris*, caught at 97.4% in stratum A, *Scaeurgus unicirrhus* and *Octopus vulgaris. A. media, S. elegans, Alloteuthis subulata, Eledone moschata, Todaropsis eblanae, Illex coindetii, Eledone cirrhosa, Octopus salutii , Brachioteuthis riisei, Rossia macrosoma, S. oweniana* and *R. minor* are species with a wide distribution range, from continental shelf to middle slope. The first six species were more frequently captured between 30-200 m depth, *I. coindetii* between 100-200 m and *E. cirrhosa* was more abundant from 100 to 300 m of depth. T*odarodes sagittatus, Abralia veranyi, Bathypolypus sponsalis* and *Neorrossia caroli* are the most bathyal species.

Table 1. Cephalopod specimens of the bottom trawl survey MERSEL 94, 95 and 96. *D. min. : minimum depth; D. max. : manimum depth; Freq. : frequency of appearance for each species.*

	D. min (m)	D. max (m)	Freq. (%)
Sepiola intermedia	36	74	4.9
Octopus vulgaris	36	217	48.8
Sepia elegans	36	245	58.5
Alloteuthis subulata	36	250	47.6
Eledone moschata	36	304	43.9
Illex coindetii	36	314	31.7
Eledone cirrhosa	36	341	51.2
Alloteuthis media	36	341	61.0
Loligo vulgaris	42	146	14.6
Brachioteuthis riisei	59	475	4.9
Rossia macrosoma	60	423	13.4
Sepietta oweniana	62	477	61.0
Sepia officinalis	63	63	1.2
Rondeletiola minor	63	477	62.2
Sepia orbignyana	70	423	30.5
Todaropsis eblanae	75	351	15.9
Octopus salutii	85	341	14.6
Scaeurgus unicirrhus	94	138	2.4
Todarodes sagittatus	191	714	18.3
Abralia veranyi	239	341	6.1
Bathypolypus sponsalis	239	790	13.4
Onychoteuthis banksii	241	241	1.2
Neorrossia caroli	304	614	13.4
Heteroteuthis dispar	423	423	1.2
Histioteuthis reversa	447	447	1.2
Ancistroteuthis lichtensteinii	714	714	1.2

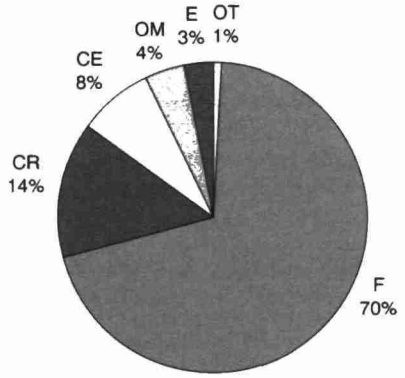

Figure 2. Mean value of the catch composition expressed in percentage. *F= fishes; CR = crustaceans; CE = cephalopods; OM = other molluscs; EC = echinoderms, OT = others.*

BENTHIC FLORA AND FAUNA IN A SUBMARINE CAVE IN THE CENTRAL ADRIATIC SEA

Grubelic Ivana, Antolic Boris*, Span Ante
Institute of Oceanography and Fisheries, 21000 Split, I.Mestrovica 63, Croatia

Abstract

Benthic flora and fauna and its structure and distribution in a submarine cave were studied as a part of biological and ecological studies of Rogoznica area (middle Adriatic). Samplings were performed around the entrance to the cave, at the entrance itself and inside the cave. SCUBA divers collected the samples from hard and mobile substrates between 2 and 28 m depth. A total of 185 benthic species (106 taxa of benthic flora and 79 taxa of benthic fauna) were identified.

Keywords: phytobenthos, zoobenthos, Adriatic Sea

Introduction

The eastern Adriatic coast is mainly built of jurassic limestones and is therefeore rich in karst relief such as submarine and above sea steeps, caves, holes and others due to abrasion by rainfall, waves and other atmospheric effects.

The level of the Adriatic Sea have changed on several occasions through its long geological history, which also has affected the geomorphology of its bottom and coast, as well as its ecological conditions and biota; the cave described in this paper, with its limestone forms such as stalactites, which could have been formed only in the land caves, supports this theory.

It is generally known, as shown by the studies and descriptions of different submarine cave types, that, as to the light conditions, they can be semi-dark or completely dark. Therefore the biocoenoses which develop in the caves are divided into the biocoenoses of semi-dark and biocoenoses of dark caves, where the animal component prevails over the plant component (1- 6).

Materials and methods

The study was carried out in July 1993 in the cave situated in the utmost, closed and shallow part of the Soline Cove (Rogoznica: 43°32' N, 15°57' E). The research covered the rocky and sediment bottom around the entrance to the cave (I; Fig. 1), the narrow eroded part of the cave entrance (II), the vertical parts of the siphonal entrance to the cave (III), the inner semi-dark part of the cave down to 15 m depth (IV), the inner completely dark part of the cave down to 28 m depth (V) and the sediment of the sea bottom in the cave between 18 and 28 m depth (VI).

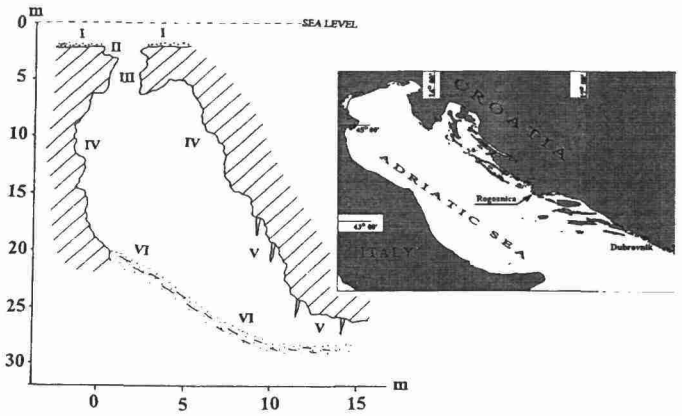

Fig. 1.Schematic representation of the cave complex.

The samples from hard and mobile bottoms were collected by SCUBA divers. Benthic flora and fauna (qualitative composition and distribution) was expressed by numerical and percentage relations between systematic compartments of benthic algae (Rhodophyta, Phaeophyta and Chlorophyta) and marine phanerogams (Angiospermae; 7, 8).

The review of qualitative composition and distribution of benthic fauna includes the species of the following systematic groups of macrobenthic invertebrates: Porifera, Cnidaria, Echinodermata, Mollusca, Annelida, Crustacea, Bryozoa, Brachiopoda, Echinodermata and Tunicata. Numerical and percentage relationship between species of systematic compartments of flora, fauna and between flora and fauna are also given for the study area.

Results and discussion

Phytobenthos

A total of 105 taxa of benthic algae (Rhodophyta 74 or 69.8%, Chlorophyta 17 or 16.0% and Phaeophyta 14 or 13,2%) and marine phanerogam *Cymodocea nodosa* were collected and determined from the mentioned parts of the cave complex.

The number of algal taxa steadily decreased from surface (I) across the entrance (II and III) to the cave interior (IV) where only 14 taxa were recorded (Fig. 2). This was to be expected since light intensity is suddenly reduced in this direction causing substantial decrease in the number of autotrophic organisms, that is in the benthic algae.

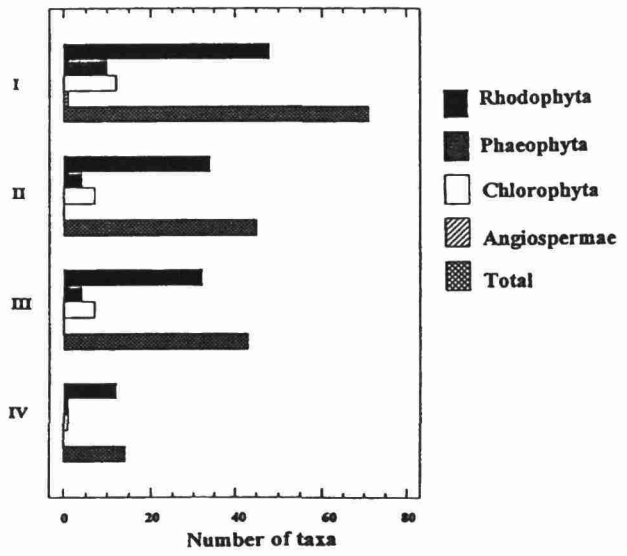

Fig. 2. Numerical presence of benthic algae and marine phanerogam in the cave complex.

Rhodophyta gradually decreased and the percentage increased from surface (I) to the cave interior (IV) where the lowest number (12) and highest percentages (85.7%) were recorded from this systematic compartment of the entire cave complex. In Chlorophyta and Phaeophyta a reduction in the number and percentages, also recorded from surface (I) towards the cave interior (IV), was more conspicuous as far as the numbers are concerned than the percentages (Fig. 2).

It should be mentioned that the benthic algae inside the cave (IV) were mainly epibiota of different sponge species.

In total 70 taxa of benthic algae were determined in the parts II, III and IV, or 66% of all determined taxa of benthic algae recorded from the cave complex. As to the composition and structure of benthic vegetation developed in the various parts of the cave complex, it should be emphasized that in the surface cave part (I) the photophil species *Cystoseira adriatica* with a large number of epilitic (*Cystoseira schiffneri, Padina pavonica, Halopteris scoparia, Anadyomene stellata, Acetabularia actebulum, Dasycladus vermicularis*) and epiphytic (*Ceramium tenuissimum, Spyridia filamentosa, Wrangelia penicillata, Chondria tenuissima, Laurencia obtusa, Sphacelaria cirrosa, Sphacelatia fusca*) species are well developed. The marine phanerogam *Cymodocea nodosa*, present in cystoseira setlement in places with somewhat thicker sand sediment belongs to the same ecological supergroup. Approaching the other cave parts inhabited by algae (II,

CONTRIBUTION À L'ÉCOLOGIE DE *DENTEX MAROCCANUS* (VALENCIENNES, 1830) DES CÔTES ALGÉRIENNES: RÉPARTITIONS GÉOGRAPHIQUE, BATHYMÈTRIQUE ET EN FONCTION DU SUBSTRAT

F. Hemida * et R. Ghazli

Laboratoire Halieutique, ISN- USTHB, BP.39 El-Alia, Bab-Ezzouar, Alger, Algérie

Résumé

Dentex maroccanus est absent des zones chalutables de l'ouest et du centre du pays. Par contre dans la région est, il est très fréquent et très abondant. Le denté du Maroc est capturé entre 40 et 200 m de profondeur, pour des températures allant de 13°C à 16°C. La tranche de profondeur 80-120 m, caractérisée par une température de 16°C, correspond à la zone de rendement maximal. La taille des individus varie de 9 à 25 cm. La gamme de taille 12-22 cm fréquente les profondeurs comprises entre 40 et 200 m. L'espèce vit sur les fonds meubles, préférentiellement les fonds à sable fin.

Mots-clés: Fishes, Distribution coefficient, Algerian basin

Introduction

Le denté du Maroc (ou encore coq rouge), plutôt rare dans la région d'Alger, est fréquent dans les pêcheries d'Annaba où il est appellé "cocotte". Ce poisson téléostéen appartenant à la famille des Sparidae est pêché communément sur tout le littoral est algérien, de Jijel à la frontière algéro-tunisienne. Il est inconnu au centre et à l'ouest du pays. Fischer *et al.* (1) signalent pourtant cette espèce dans tout le bassin sud de la Méditerranée, alors que selon Bauchot et Pras (2) sa présence dans cette mer est occasionnelle. L'étude des répartitions géographique, verticale et en fonction du sédiment a été réalisée à partir des données de la campagne de prospection de 1982, entreprise par le navire océanographique *Thalassa* (3) le long de la côte algérienne.

Méthodes d'étude

Le travail est basé d'une part, sur les données récoltées en septembre 1982 lors de la campagne du navire océanographique *Thalassa* (3), d'autre part, sur des observations régulières, depuis 1994, des apports exposés sur les carreaux de la pêcherie d'Alger.

La campagne océanographique s'est déroulée en deux phases. La première s'est intéressée au stock démersal des fonds chalutables. Au cours de cette première phase effectuée d'ouest en est, 182 stations de chalutage ont été réalisées entre 15 et 820 m de profondeur. Les stations ont été réparties par secteurs géographiques: Béni-Saf et Arzew (Ouest) ; Bou-Ismail et Zemmouri (Centre); Jijel, Skikda et Annaba (Est). Deux types d'engins ont été utilisés : le chalut de type Lofoten (ouverture verticale de 2.5 m) et le chalut à grande ouverture verticale (5 m). La durée des coups de chalut variant de 17 à 120 mn, le nombre d'individus a été rapporté pour chaque station à une heure de trait afin d'homogénéiser les données. Deux indices ont permis l'analyse des différentes répartitions : la fréquence relative ou Fr et le rendement R (ou abondance relative). Le rendement de l'espèce en fonction du secteur géographique, de la profondeur et de la nature du sédiment a été calculé. Pour ce faire, les limites supérieure et inférieure de profondeur de capture dans la gamme prospectée ont été déterminées (figure 1). Le nombre total de stations (ST) est relatif à cette gamme de capture (aire où l'espèce est supposée vivre) :

- les traits (ou cales) ayant ramené le denté sont notés S^+.
- les traits n'ayant pas ramené l'espèce sont notés S^-.

Le raisonnement tient compte de l'influence non négligeable des stations S^- dans l'analyse effectuée: ces dernières ont des températures identiques, présentent un même faciès et surtout se trouvent à la même profondeur que les stations S^+ mais n'ont pas ramené l'espèce.

Les fréquences relatives (Fr) ainsi que les rendements (R) seront ainsi définis:

$$Fr = \frac{\text{Nombre de stations ayant ramené l'espèce}}{\text{Nombre total de stations}} = \frac{S^+}{ST}$$

$$R = \frac{\text{Nombre d'individus capturés dans une région donnée (ou prof. donnée)}}{\text{Nombre total de stations}} = \frac{N}{ST}$$

De plus, les cales ont été regroupées par tranches de 40 m de profondeur. Pour chaque cale la profondeur moyenne est déduite de la demi-somme des profondeurs de virage et de filage. Les températures ont été mesurées sur le fond à l'aide d'une bouteille à renversement. Elles n'ont pas été relevées systématiquement, ce qui a nécessité une extrapolation à une même tranche de profondeur, tout le long de la côte. *Dentex maroccanus* a été capturé sur six types de fond: sable grossier, sable coquiller, sable fin, vase sableuse, vase compacte et vase liquide. On a calculé les indices Fr et R pour chacun de ces fonds. L'étude des répartitions géographique et bathymétrique est basée sur un effectif de 5880 individus, capturés au cours de la campagne. La distribution des fréquences de taille en fonction de la profondeur n'a pu être réalisée qu'à partir de 1561 individus. En effet, toutes les espèces capturées étant ciblées, seuls quelques sous-échantillons, considérés par l'équipe participant à la campagne, ont fait l'objet de mesures de la longueur totale. Le calcul des tailles moyennes dans les différentes tranches bathymétriques est suivi d'une comparaison de ces moyennes par le test de l'écart-réduit (ε).

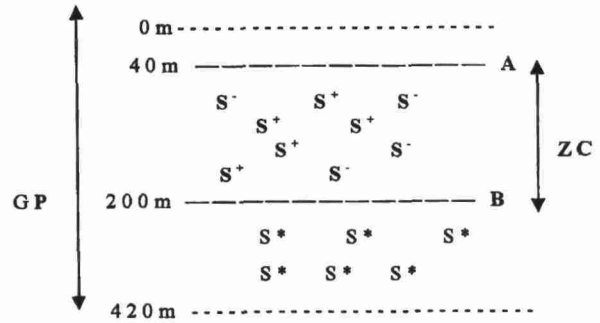

Figure 1. Limites extrêmes (A et B) de la zone de capture (ZC) et gamme de prospection (GP) dans une région donnée. (S*: cales en dehors des limites de capture).

Résultats et discussion

1. Répartition spatiale

Le tableau 1 montre que *D. maroccanus* est capturé dans la région est seulement. La fréquence et le rendement augmentent sensiblement d'ouest en est. Nos récentes observations (1994-1997) permettent de signaler la commercialisation quasi quotidienne, surtout pendant le printemps, de plusieurs casiers de *D. maroccanus* au niveau de la pêcherie d'Alger. Après investigations de notre part, il a été prouvé que ces apports proviennent encore exclusivement de l'est du pays, ce qui permet de confirmer les résultats de 1982.

Tableau 1: Limites de capture et valeurs des fréquences relatives et des rendements dans les secteurs du littoral algérien où *D. maroccanus* a été péché.

Secteur géographique	Gamme de prospection	NS	Limites de capture	S^+	S^-	ST	Fr	N	R
Béni-Saf	20-820m	44	/	/	/	/	/	/	/
Arzew	17-541m	28	/	/	/	/	/	/	/
Bou-Ismail	36-647m	25	/	/	/	/	/	/	/
Zemmouri	28-77m	7	/	/	/	/	/	/	/
Jijel	16-418m	23	74-115m	3	3	6	0 50	570	95
Skikda	24-522m	15	54-175m	7	1	8	0 88	858	107
Annaba	24-636m	40	42-187m	20	2	22	0 91	4452	202

NS: nombre de stations dans la gamme de prospection. S+: station présentant l'espèce. S-: station ne présentant pas l'espèce. ST: total des stations Fr : fréquences relatives N: nombre d'individus. R : rendement.

SPARIDAE IN CATCHES OF THE COASTAL FISHING GEARS IN THE EASTERN ADRIATIC SEA

I. Jardas *, P. Cetinic, A. Pallaoro, J. Dulcic, M. Kraljevic
Institute of Oceanography and Fisheries-Split, Croatia

Abstract

Catches of 6 coastal fishing gears were analysed regarding to presence of the Sparidae fishes in the catches. Among 18 Sparidae species and subspecies in the Adriatic Sea 16 were noted in the catches. Except "tramata" all other target fishing gears harvested Sparidae in small quantities; participation of Sparidae in the "tramata" catches usually amounts more than 96% in number and 98% in weight, and other fishing gears amount between 6.5% and 26.0% in number and between 2.6% and 26.5% in weight in total catches. The most common Sparidae fishes are: *Oblada melanura, Sarpa salpa* ("tramata"), *Diplodus* spp. (all fishing gears), *Pagellus erythrinus* (trammel bottom set, "tartana", coastal beach seine), *Boops boops* (coastal beach seine).

Key-words: Fishes, fisheries, coastal waters, Adriatic Sea

Introduction

The Adriatic ichthyofauna includes 18 Sparidae family species and subspecies (1-5) which is 75% of all Sparidae species and subspecies registrated in the Mediterranean, *i.e.*, on the other hand, 6 species less than in the other Mediterranean parts (6). All Sparidae species and subspecies inhabit shelf area mostly up to 100 m depth. They belong to benthopelagial, what determines the type of fishing gears and the way of their fishing.

Some east-Adriatic Sparida fishes are commercialy valuable. This especialy refers to species *Sarpa salpa, Obalda melanura, Boops boops, Sparus aurata, Pagellus erythrinus* and *Spondyliosoma cantharus*, catches of which, depending on species, amount, between 50 and 200 tons annually, and this is considerably more compared to the catches of the most other Sparidae species. Vertical distribution, seasonal migrations and time of reproduction are important factors which limit their commercial catches.

In this paper we discuss about the participation of Sparidae fishes in the catches of 6 coastal fishing gears: trammel bottom set, small coastal bottom beam trawl ("strasin"), small coastal bottom trawl with beam before wings ("kogol"), small coastal otter trawl type tartanas ("tartana"), coastal beach seine and fishing with gill nets using ropes (tramata fishing, "tramata"). The fishing of mentioned gears is of a seasonal character and is used mostly for harvesting of certain fish species.

Researched area, material and methods

Researches were performed along the whole east-Adriatic coast but with different width from gear to gear. Areas, where the analyses of catches by mentioned fishing gears took place, actually respond to areas of thier most frequent or exclusive usage (*e.g.* "strasin"). The catches were realised by usual fishing methods characteristic for commercial fishing. Seasons in which researchers took place mostly coincided with seasons of usage of particular fishing gears regulated by the Croatian law on sea fisheries, except the trammel bottom set which was used in our researchers all over the year. All other fishing circumstances (depth, type of bottom, fishing effort units) were equal as those in the commercial fishing (Table 1). Except of trammel bottom set, all other coastal gear catches were realised by professional fishing crews.

Table 1. Fishing areas, depth, sort of bottoms, fishing periodand number of analysed coastal fishing gear catches along the eastern Adriatic coast.

Fishing gear	Fishing area	Depth (m)	Bottom	No. of analysed catches	Period
Trammel bottom set	Middle and South Adriatic: from Vir Island to Konavli	to 30	vsriable	243	1987-1996: all year
"Stralin" (1)	Middle Adriatic: Trogir area	to 20	sandy-muddy Posidonia beds	6	1988: autumn
"Kogol" (2)	Middle Adriatic: Brač, Šolta, Korčula and Hvar Islands	to 20	sandy-muddy Posidonia beds	15	1991-1992: autumn
"Tartana" (3)	Middle Adriatic: Tribunj area, Pag, Murter and Vrgada Islands	to 40	sandy-muddy Posidonia beds	17	1991-1992: winter, spring
Coastal baech seine	Middle Adriatic: Šibenik and Primošten areas, Murter and Šolta Islands	to 30	sandy-muddy Posidonia beds	35	1991-1996: autumn, winter spring
"Tramata" (4)	North Adriatic: Istra peninsula, Krk, Cres and Lošinj Islands Middle Adriatic: Šibenik, Split and Makarska areas, Pag, Silba, Drvenik, Hvar, Lastovo, Korčula and Vis Islands	to 50	variable	47	1986 -1993: summer

(1) small coastal bottom beam trawl. (2) small coastal bottom trawl with beam before wings. (3) small coastal otter trawl type tartanas. (4) fishing with gillnets using ropes (tramata fishing).

Fishing gears characteristics and ways of usage

Trammel bottom set is the most widely distributed in Croatian coastal fisheries. It can be used from August 15th to April 30th. All benthic and benthopelagic fish species and other sea animals and even bigger pelagic species can be caught with it. It is used during the night and on all types of bottoms, usually up to 30 m depth.

"Strasin" and "kogol" are two types of small coastal bottom trawl which are used during the night primarily for the picarel fishing although other bottom species in the coastal fisheries can be caught with them. They can be used only on boats with the engine power of 18.5 KW (25 HP) in the period from October 1st to April 30th. They are used from 5 to 20 m depth. Bar of mesh in the cod end must not be less than 12 mm.

"Tartana" is small coastal otter trawl which can be used on the boats with the engine power of 18.5 KW (25HP). It is designed primarily for picarel fishing from 20 to 50 m depth, during the period from November 1st to March 1st, exclusively during the night. With the "tartana" fishing otter boards are used. Bar of mesh must not be less than 12 mm.

Coastal beach seine is designed primarily for daily picarel fishing, but some others benthic fish species and other sea bottom animals could be caught. It is used from October 1st to April 30th. Fishing with coastal beach seine is done on bottom up to 30 m depth. It is pulled on the coast or on the boat moored to the coast. Bar of mesh in the cod end of coastal bech seine must not be less than 12 mm.

"Tramata" is the way of fishing with gill nets using ropes for fish scaring. Ropes are used for enclosing a larger sea area and gathered fish is harvested by the gill nets. This kind of fishing is done only during the summer period and only Sparidae fishes are caught, primarily saddled bream (*Oblada melanura*) and salema (*Sarpa salpa*), but also all other Sparidae fishes. This kind of fishing is odne only in coastal areas up to 50 m depth.

Results and discussion

A great number of authors (7-18, 5) have already carried out some general data about mentioned fishing gears and their catches. On this matter authors have concentrated their attention to constuction features of gears, the way of their use, efficiency, common qualitative and quantitative structure of catches and the noxiousness. (19) have published results of analysis of presence of Centracanthidae fish family in catches of the coastal fishing gears in the eastern Adriatic during the winter period. They have analysed catches of three types of coastal bottom trawl designed mostly for the Centracanthidae catches, especially of picarel (*Spicara smaris*), and these are "strasin", "kogol" and "tartana" as well as coastal beach seine also designed for picarel catches.

Present Sparidae fish species and subspecies in the catches of targeted coastal fishing gears is done in the Table 2 and 3. From the total of 18 Sparidae species and subspecies living in the Adriatic Sea 16 were established in the catches. Two species are missing: *Pagrus coeruleostrictus* and *Dentex* (Dentex) *macrophthalmus*. Both fishes can be usually caught in the area deeper than 50 m, mostly in south and some parts of mid-Adriatic (20). Population density of these fishes is mainly small. Sparidae species and subspecies were presented in analyses trammel bottom set catches in small quantities: 19.33% in number and 14,43% in weight. The most common were shallow-water species *Diplodus annularis*, followed by *Pagellus erythrinus* with considerable lower share.

In one earlier fundamental study of trammel bottom set catches along the whole east-Adriatic coast in the period 1971-1984 (5) from the quantitative and qualitative point of view more than 110 fish,

CONTRIBUTION À LA CONNAISSANCE DE LA NOURRITURE DE *TRACHURUS MEDITERRANEUS* (STEIND.) ET DE SON INFLUENCE SUR LES CHAÎNES ALIMENTAIRES DE LA MER ÉGÉE CENTRALE

Nikolaos A. Kyrtatos

Centre de Recherches Marines et Côtières, Tinos, Grèce et Institut für Meereskunde an der Universität Kiel, Allemagne

Résumé

La nourriture de *Trachurus mediterraneus* se compose principalement de larves de poissons, de copépodes pélagiques et de mysidacés benthopélagiques. La population de *T. mediterraneus* de la mer Égée centrale appartient à une des principales espèces capturées, avec 47 158,9 kg de substance organique pêchés annuellement autour des Cyclades du nord-est, et joue un rôle prépondérant dans l'écosystème marin pélagique avec 137 525,4 kg (ou 5,1 x 1010 individus) de larves, surtout de postlarves, de poissons consommées par an.

Mots clés: Teleostei, plankton, predation, food webs, Aegean Sea

Introduction

La connaissance de la place des poissons dans les chaînes alimentaires est utile pour comprendre le fonctionnement des écosystèmes marins et combien ceux-ci sont influencés par les interventions naturelles et humaines. En ce qui concerne le régime alimentaire de *T. mediterraneus*, poisson très abondant en mer Égée, il existe relativement peu d'études quantitatives (1, 2, 3).

Matériel et méthodes

La provenance du matériel et la méthode employée pour l'évaluation des quantités et de la composition de la nourriture ont été décrites par Kyrtatos (4). Pour l'évaluation du degré de similitude de la composition de la nourriture de divers groupes, j'ai utilisé l'indice de similitude de Whittaker et Fairbanks (5). La sélection de certains organismes a été estimée par l'indice de sélectivité de Jacobs (6).

Résultats et discussion

Les proies prédominantes sont les larves et postlarves de poissons (39,14% de la biomasse ingérée), les copépodes pélagiques (19,74%) et les mysidacés benthopélagiques (11,43%) (Fig.1). Les autres proies sont par ordre décroissant, *Sagitta* spp., gastropodes, méduses, ostracodes, isopodes, décapodes, juvéniles de poissons, euphausiacés, tuniciers, larves de stomatopodes, oeufs de poissons, amphipodes et d'autres catégories de nourriture identifiés.

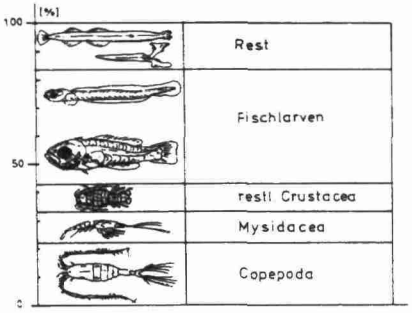

Figure 1. Composition de la nourriture de l'ensemble de la population de *Trachurus mediterraneus*.

La plupart des espèces importantes composant la nourriture de *T. mediterraneus* de la mer Égée centrale appartient au macrozooplancton, mais aussi au mesozooplancton, à l'hyperbenthos et au micronecton. Il s'agit de proies plus agiles, mais relativement plus grandes et plus riches en énergie que le reste des participants au plancton, qui sont, au moins en partie, activement attaquées par les chinchards et ainsi sélectionnées de la biomasse planctonique (Fig.2). La sélection dépend de l'abondance des divers organismes dans le plancton et de leur "accessibilité" aux prédateurs.

Pour les jeunes *T. mediterraneus*, les proies les plus importantes sont les copépodes calanoides, puis les larves de poissons (Fig. 3). Les chinchards d'une longueur moyenne se nourrissent de larves de poissons, de copépodes et mysidacés. Les grands individus consomment surtout des post-larves et des juvéniles de poissons. Pendant la nuit, surtout par nuit claire, la participation des représentants de groupes benthopélagiques (Mysidacea, Isopoda, Gammaridea) est plus forte que pendant le jour (Fig. 4).

Les larves de plusieurs espèces de poissons (*Pagellus acarne, Diplodus sargus* et divers autres Sparidae, *Spicara smaris*) caractérisent le spectre alimentaire des chinchards au printemps (Fig. 5), tandis qu'en été, après et pendant la période de ponte de *T. mediterraneus*, les estomacs des individus adultes sont pleins de larves et de juvéniles

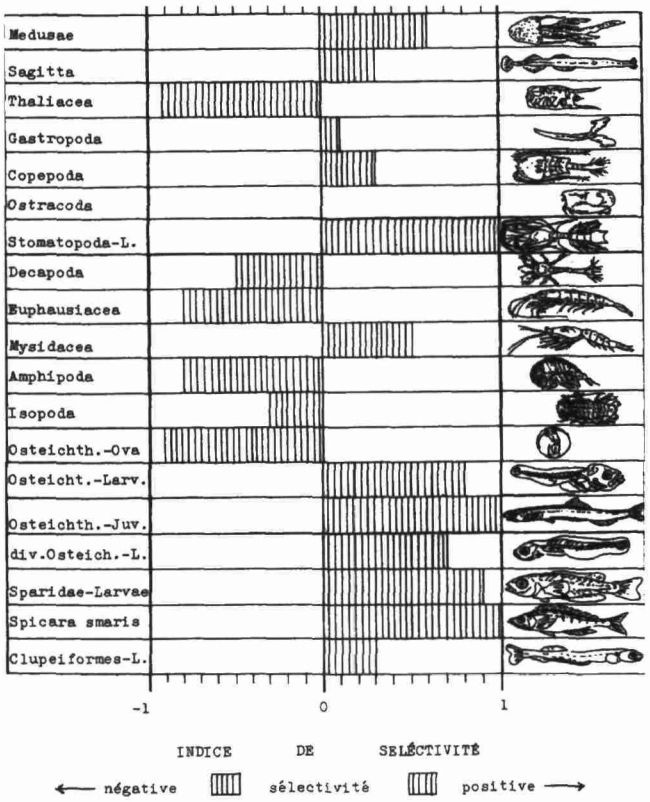

Figure 2. Indice de sélectivité du macroplancton par l'ensemble de la population de *T. mediterraneus* pour ses principales proies. (Les résultats ne sont pas très représentatifs à cause de l'efficacité réduite du filet à plancton pour les orgnismes agiles.)

d'*Engraulis encrasicolus*. Les jeunes chinchards se nourrissent en automne et en hiver de copépodes et d'autres relativement petits crustacés, mais aussi des abondants Appendicularia (dédaignés au printemps) et d'espèces qui effectuent des migrations considérables ou caractérisent les zones d'upwelling, comme toutes les espèces communes d'Euphausiacés méditerranéens et quelques copépodes (*Lucicutia flavicornis, Pleuromamma* spp., *Calanus* spp., *Euchaeta* spp.).

Les classes de tailles voisines (Fig. 6) montrent une relativement grande similitude concernant la composition de leur nourriture, contrairement aux classes éloignées et aux autres groupes de *T. mediterraneus* comparés.

Le spectre alimentaire de *T. mediterraneus* en mer Égée (qui contient surtout les stades juvéniles de poissons et des crustacés pélagiques et semi-pélagiques) ressemble à ceux des chinchards qui habitent d'autres endroits de la Méditerranée (1, 2, 3).

La sélection positive de larves de poissons par le chinchard fait de *T. mediterraneus* un prédateur de premier ordre pour ce stade de vie des poissons et un régulateur naturel de leur recrutement : 5,1 x 1010 larves correspondant à 137 525,4 kg de substance organique, 2,2 x 1010 oeufs ou 1783,8 kg et 2,5 x 107 juvéniles de poissons ou 3348,8 kg sont consommés par an par une population de 47 158,9 kg de substance organique de *T. mediterraneus* (269 479,6 kg de matière

EVALUATION DE QUELQUES PARAMÈTRES QUANTITATIFS RELATIFS À LA NUTRITION DE *TRACHURUS MEDITERRANEUS* (STEINDACHER 1868) EN MER ÉGÉE CENTRALE

Nikolaos A. Kyrtatos

Centre de Recherches Marines et Côtières, Tinos, Grèce et Institut für Meereskunde an der Universität Kiel, Allemagne

Résumé

Une population de 47 158,9 kg de substance organique de *Trachurus mediterraneus*, qui constitue les captures annuelles en mer Égée centrale, consomme 351 369,9 kg de substance organique de nourriture, une valeur qui correspond à 7,5 fois à son poids ou environ à 4,2 fois le total de la biomasse macrozooplanctonique. Le taux d'évacuation de l'estomac est de 0,0643% à 0,1354% du poids du corps par heure. Les individus adultes ingèrent par rapport à leur poids davantage de nourriture que les individus plus jeunes et transforment les aliments moins efficacement en matière corporelle.

Mots clés : Teleostei, predation, biomass, zooplankton, Aegean Sea

Introduction

La présente étude a pour objet l'évaluation de quelques paramètres relatifs à la nutrition de *T. mediterraneus*: la vitesse du transit stomacal, la taux de conversion alimentaire et l'efficacité de l'assimilation des aliments. Une première estimation des quantités de nourriture ingérée par l'importante population de *T. mediterraneus* de la Mer Égée centrale a été effectuée.

Matériel et méthodes

Des chinchards *Trachurus mediterraneus* ont été prélevés sur les captures de la pêche commerciale autour des îles Cyclades du nord-est (Tinos, Rinia, Dilos et Mykonos) en mer Égée centrale entre avril 1979 et mars 1980. Pour évaluer la ration consommée par les poissons et la composition de la nourriture, la méthode suivante a été choisie: 985 *T. mediterraneus* d'une longueur de 8-38 cm ont été groupés en 5 classes de taille. Une fois par mois un échantillon de poissons appartenant à chacune des trois principales classes de taille et provenant des prises de jour et de nuit, claire et noire a été étudié. Le poids sec a été évalué en desséchant des organismes planctoniques; la matière organique a été déterminée en soustrayant le poids des cendres du poisson sec, selon la bibliographie (par ex. 1). Le contenu stomacal moyen de chaque prélèvement a été calculé à partir de la somme des poids de tous les groupes d'espèces consommées. La quantité de chaque espèce-proie est le produit du poids et du nombre des individus de l'espèce-proie. La formule décrite par Jones (2) nous donne le taux d'évacuation de l'estomac r_{NG} (g poids frais par heure):

$$r_{NG} = 1^{00,035\,(T_o - T_c)} \cdot (L_o)^{1.4} \cdot x^{0.46} \cdot Q \cdot \frac{}{L_C}$$

x (g) = poids du contenu stomacal.
L_o (cm)= longueur du poisson prédateur.
T_o (°C) = température de l'eau.
Q (g/h) = coefficient de digestion ou taux d'évacuation de 1 g de nourriture.

Q dépend de la nature des aliments, de leurs dimensions et de la fréquence de l'alimentation. A l'aide des données de Fortunatova (in 3), j'ai calculé pour *T. mediterraneus* d'une longueur L_c = 15 et pour une température de l'eau T_c = 20°C des Q (entre 0,093 et 0,312) qui sont 1,4 fois plus hauts que ceux de Jones (2). Pour chaque prélèvement d'une classe de taille, on a additionné les taux des groupes d'espèces-proies selon les proportions de leurs poids dans l'estomac moyen (voir 4) pour recevoir son taux d'évacuation en g frais par heure qui est ensuite transformé en g substance organique (sans cendres) par heure.

Tous les taux d'évacuation pour les chinchards des prises de jour, des prises par nuit noire ou des prises par nuit claire, d'une classe de taille et d'un certain trimestre ont été regroupés en proportion des quantités des captures correspondantes et en raison inverse de l'efficacité relative des bateaux de pêche et des efforts de pêche. Ainsi nous avons évalué le taux d'évacuation pour chaque trimestre et ensuite le taux par journée et par an pour un poisson et pour la partie de la population correspondant aux captures. Le degré de similitude des quantités a été calculé par le Mann-Whitney-test (voir 5). La formule de Conover (6) a été employée pour estimer l'efficacité de l'assimilation A (%) de la nourriture:

$$A = (1-E)\,F \cdot 100 \quad \text{avec} \quad F = \frac{F - E}{}$$

F = quantité de nourriture ingérée en substance organique par rapport au poids sec de la nourriture

E = quantité d'élément nutritif excrétée en substance organique par rapport au poids sec dans les déjections.

Résultats et discussion

Le taux moyen d'évacuation par heure varie entre 0,0643% du poids du corps pour les *T. mediterraneus* de taille moyenne et 0,1354% pour les individus très grands (Fig. 1). La ration journalière correspond, selon la taille, à 1,51 - 2,12 (-3,25) % et la ration annuelle à 6-8 fois (12 fois au maximum) au poids du corps, en moyenne à 7,5 fois.

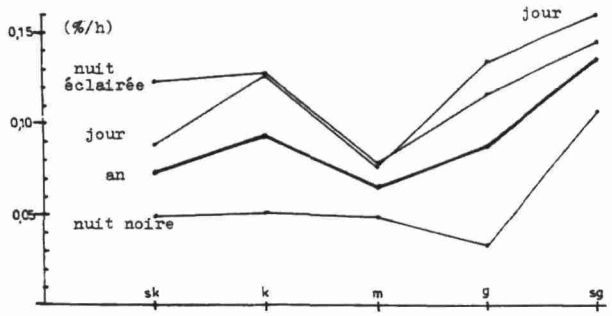

Fig. 1. Taux relatif moyen annuel d'évacuation de l'estomac de *T. mediterraneus*, taux de jour et de nuit.
sk : très petits individus ≤ 10,9 cm; k : petits ≤ 11-15,9 cm; m : moyens ≤ 16-20,9 cm; g : grands ≤ 21-25,9 cm; sg : très grands ≥ 26 cm;

En tenant compte des relations taille-poids $G = 4{,}88 \cdot 10^{-3} \cdot L^{3.16}$ (G = poids total, L = longueur totale, r = 0,99, n = 906) et taille-poids stomacal $N_{max} = 1{,}24 \cdot 10^{-5} \cdot L^{3.95}$ (N_{max} = poids stomacal, L = longueur totale, r = 0,96, n = 15), des observations personnelles sur le terrain et des données de la bibliographie sur la périodicité de l'activité trophique de *T. mediterraneus* (3, 7), on peut constater que *Trachurus mediterraneus* consomme une quantité de l'ordre de 3 (ou 4) fois au maximum le contenu stomacal par jour, ce qui correspond, selon la taille, à (4,74-) 6,38 – 8,95 (-10,40) % du poids du corps par jour ou environ à 2,7 - 5,1 fois à la ration journalière moyenne qui a été calculée indépendamment du taux d'évacuation.

La similitude est relativement grande entre les taux constatés pour des prises de jour et ceux par nuit claire et aussi entre les taux des classes de taille voisines. Une similitude modérée existe entre les taux de nuit noire et ceux de nuit claire, entre les taux de *T. mediterraneus* pendant les diverses époques de l'année et aussi entre les taux de *T. mediterraneus* et ceux de *Boops boops*, les deux espèces dominant l'ichtyofaune en 1979-80. Les taux d'évacuation de jour et de nuit noire (Fig. 2) ont une ressemblance minime.

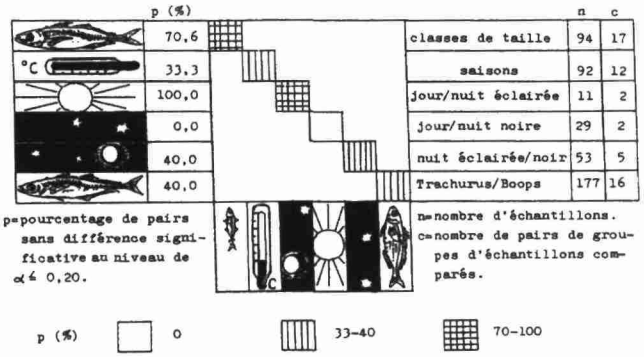

Figure 2. Degré de similitude des taux relatifs d'évacuation entre divers groupes de *T. mediterraneus* et entre *T. mediterraneus* et *Boops boops* calculé par le Mann-Whitney-test.

La ration de jour est supérieure à celle de la nuit (Fig. 1) Il n'y a pas une tendance unique saisonnière parmi les diverses classes de taille : le taux relatif moyen d'évacuation diminue avec la croissance de taille en automne, mais il augmente en été (Fig. 3). Les plus grandes valeurs se trouvent pour les petits et moyens individus en automne et au printemps; pour les grands chinchards en été et ensuite au printemps. C'est en hiver que sont consommées les plus petites rations.

T. mediterraneus constitue une exception parmi les poissons étudiés par le fait que les individus âgés consomment proportionnellement à leur poids

A LIVE COMPUTER SIMULATION OF SWARM DEVELOPMENT IN *SALPA FUSIFORMIS* (TUNICATA : THALIACEA) IN THE FRONTAL ZONE OF THE LIGURIAN SEA (MEDITERRANEAN)

Philippe Laval

CNRS URA 2077 / Université P. et M. Curie, Station zoologique F-06234 Villefranche-sur-Mer, France

Abstract

Self-reproducing artificial creatures are used to simulate the spreading of a salp swarm in space. Each individual is modeled as an autonomous software object, containing its own thread of control. These individuals "live" concurrently and asynchronously: they swim, eat food, metabolize, and reproduce like real salps. The 21 life-cycle and physiological parameters of the creatures were first calibrated with food regularly scattered in all directions (in what I call a virtual mesocosm). The space is then modified to include a process simulating the convergence current carrying organic matter, with food periodically added in the upper layers to simulate phytoplankton growth.

Key-words : models, zooplankton, blooms, particle flux, Ligurian Sea

Introduction

Salps are fragile macroplanktonic organisms, difficult to keep in the laboratory during several generations [1]. Their explosive asexual multiplication allows them to quickly form large swarms which have considerable impact on the pelagic ecosystem. However, their presence or absence is very difficult to predict, and costly investigations (for example with submersibles), which should be planned in advance, may well find only a few specimens [2]. Salp asexual multiplication may be described by analytical mathematical models [3]. However, how a salp swarm is triggered, and how it extends in space, are phenomenons too difficult to write down in mathematical terms.

A software simulation of salp swarms may help to answer the above questions, provided:

1) The software is complicated enough to take into account the existing biological and physiological knowledge about salps;

2) Real-time and concurrency techniques are used to simulate the complex interactions of individuals living simultaneously, but not synchronously;

3) The software has a strong, biologically meaningful, architecture. An ad-hoc design, like the ones often found in object-oriented programs, constitutes a too weak foundation.

Principles of software engineering should be followed from the beginning. These principles tell us: design the architecture first, and then flesh it with the peculiarities of the domain. This is rarely adhered, because biologists are not exposed to software engineering notions during their curriculum. Moreover, concurrent programming is much more difficult than the sequential programs they may have written to compute equations in mathematical models.

Having a biological background in gelatinous macroplankton, and a long experience with the Ada programming language, I have tried since several years to write a simulation software along these lines.

Methods

1) Software design

The software architecture is made along the lines of a software engineering methodology called HOOD (for Hierarchical Object-Oriented Design) [5]. This method considers the domain to be programmed as a hierarchical decomposition in more and more detailed abstract machines. The first level is the whole system itself. It is then split in a few abstract entities, which together provide the same functionalities. This first step is one of the more difficult, because it is necessary to devise logical abstractions which will remain consistent with the subsequent decomposition of their sub parts in the following levels. This usually require a number of iterations to arrive at a stable structure. The decomposition of the child objects stops when an object needs not be further decomposed (terminal object).

2) Artificial salps

Only one artificial oozooid is necessary to initiate a swarm development, because this individual gives birth to a chain of aggregates; each aggregate in the chain gives in turn a new oozooid, and so on. Oozooids and chains are variants of a software module containing several fields keeping local information (birth date, actual position and direction, amount of reserves, etc.). Another field contains a pointer to an Ada task [6]. This task executes all the events making up the life cycle of the individual. It is an asynchronous process running periodically, attached to the particular individual containing the pointer. The cycles of the task correspond to the individual biological clock, running on a "daily" basis. A "day" lasts in fact 1.5 second of computer time, but all actions have proportionally scaled durations relatively to this day length. This permits to observe several generations in less than 300 s.

To visualize the salp population, each individual is displayed with a little colored dot on the computer screen. The screen corresponds to a vertical bi-dimensional grid of 222 x 318 positions, which is the space where the individuals move (for short I call zooids both oozooids and chains when a distinction is not needed). Chains are represented by only one special "individual", because its composing aggregates are clones with the same behavior, about the same position, the same age, etc.

The actions executed by the task are programmed to correspond closely to the biology and physiology of *S. fusiformis*. These actions are parameterized with 21 coefficients or initial values, corresponding to life-cycle characteristics (number of chains emitted by an oozooid, minimum number of aggregates composing a chain, delay for the first chain emission, between-chains interval, oozooids and chains maximum longevity, etc.), or to metabolic parameters (initial and adult weight of oozooids and chains, growth coefficients, metabolic coefficients, etc.). More details are available in [4]. When possible, values were taken from the literature or from laboratory data. If no previous knowledge is available for a parameter, best guesses are made and the results controlled by "dissecting" some individuals:their weight, their amount of reserves may be accessed. Direct observation of the screen provides feedback on the duration of life stages, of the number of oozooids produced by a chain and other data. At the end of the simulation detailed data are recovered by recursively traversing the tree of pointers starting from the first created oozooid.

In fact, the whole system is a model, but more detailed and with a finer spatial resolution than a mathematical model.

3) Environment

In a first stage, the software was calibrated by providing regularly spaced food patches in the grid. I call this setting a "virtual mesocosm" [4]. This step was necessary to verify that the artificial organisms have acceptable physiology and life-cycle.

Once the artificial salps behave convincingly, their environment may be complicated to represent a known ecological situation. The problem of a suitable spatial scale should first be solved. If one dot on the computer screen corresponds to one individual, the resulting scale is too detailed: the software simulates only a small swarm in a reduced volume of water. To extrapolate to a larger water mass, some kind of compromise is unavoidable. It is possible to consider, without too much loss of information, that:

- The actions effected by an individual at a grid position during 1 "day" are average daily actions: feeding is the filtering of the volume at this location during 1 day, metabolism is a mean daily metabolism, and so on.

- In particular, a movement from one position to the next represents the mean distance traveled in a day. For S. fusiformis, this corresponds to about 1,000 m (in projection) in the horizontal direction. In the vertical direction, it is convenient to think that the grid displays only the upper 100 meters. To introduce volumes, the grid has a small depth (not seen in projection) of 0.5 m. Thus, the grid represents a thin vertical slice of 222 x 318 "cells" of 0.5 x 1,000 x 0.5 m = 250 m^3 each. The density of food is computed relatively to this volume.

To structure the physical environment according to the situation prevalent in a frontal zone like the one of the Ligurian Sea, in a preliminary setting I have added another concurrent process. This periodic

PRELIMINARY OBSERVATIONS ON AMPHIPOD ASSEMBLAGES ASSOCIATED WITH *MYTILUS GALLOPROVINCIALIS* LAMARCK BEDS FROM THERMAIKOS GULF (AEGEAN SEA)

Marina Lantzouni*, Eleni Voultsiadou and Chariton Chintiroglou
Department of Zoology, School of Biology, Aristotle University, Box 134, GR-54006 Thessaloniki, Greece

Abstract

Quantitave sampling on mussel beds attached on artificial substrates at three sites of Thermaikos Gulf, in summers and winters of two successive years, revealed the presence of 6600 amphipod individuals belonging to 17 species. The most dominant species were: *Elasmopus rapax, Maera inaequipes* and *Corophium acutum.* Significant differences in the abundances of amphipods and in diversity indices between the two seasons were found, the former increasing as the latter decreases in summer.

Key-words: Crustacea, Population dynamics, Rocky shores, Zoobenthos, Aegean Sea

Introduction

The assemblage of mussel beds as a facies of the photophilic algae biocoenosis (1) has been investigated in the Western Mediterranean and the European Atlantic coast (2, 3, 4, 5), while in the Eastern Mediterranean only two works include information on its structure; those by Topaloglou and Kihara (6) who studied the mussel community in Bosphorus Strait and Kocatas (7) who gave some qualitative and quantitave information on its structure in a broader study of hard substrate populations in the Gulf of Izmir. On the other hand, although amphipods play an important role in the benthic ecosystem, their ecology has not been sufficiently studied especially in the eastern part of the Mediterranean. All the relative literature has been reviewed by Stephanidou & Voultsiadou (8) in a faunistic study of amphipods of the North Aegean.

This study is a part of a broader research aiming to study the structure of *Mytilus galloprovincialis* beds in the Bay of Thessaloniki; as proved by Koukouras & Russo (9) and Nicolaidis (10), Thermaikos Gulf in general, and more specifically the area of the sampling stations, is subjected to the effects of pollution which is mainly organic. Under these circumstances, the structure of the populations associated with *M. galloprovincialis* beds in this areamay change in time due to pollution. In the present paper some preliminary results concerning the amphipod populations associated with mussel beds are presented.

Materials and methods

Sampling was carried out in three sites located on the east coast of the Bay of Thessaloniki (Fig. 1): Perea (site 1), Nei Epivates (site 2) and Agia Triada (site 3). On the artificial hard substrate of the piers built in the above sites, dense populations of *Mytilus galloprovincialis* exist. The sampling areas can be characterized as "polluted" although pollution is not as heavy as on the western coast of the Bay, where the industrial area is located (9). Scuba diving was employed for sampling with a special hard substrate sampler designed by Chintiroglou and Koukouras (11), in summer and winter of two successive years, 1994 and 1995. Samples were preserved in a 10 % formaline solution. Totally 36 samples were taken (3 samples per site, per season), each covering an area of 400 cm^2. In order to quantify the contribution of the various species, mean abundance and partial mean dominance were calculated (3). The Shannon-Wiener information function (H') was used as a diversity index (12). For the comparison of amphipod abundance between seasons and ammong different sites, Kruskal-Wallis test (13) was employed. Ward's method was used to construct hierarchical classification of amphipod faunal similarities between stations using Euclidean distances (14).

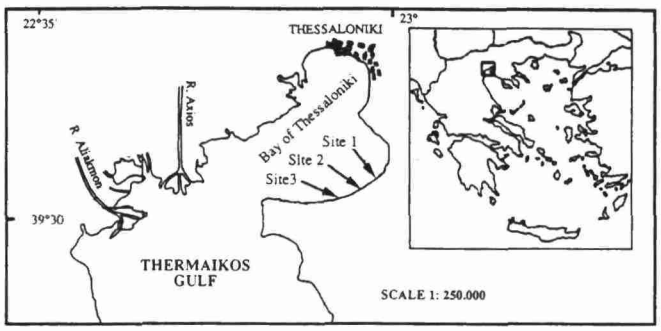

Fig. 1: Map of sampling sites. Site 1= Perea; Site 2= Nei Epivates; Site 3= Agia Triada.

Results

6600 amphipods, belonging to 14 genera and 17 species (16 Gammaridea and 1 Caprellidea) were found associated with *Mytilys galloprovincialis* beds in the three sampling sites (Table 1). Mean abundances and partial mean dominances for the aamphipod species found, as well as total numbers of species, individuals and Shannon-Wiener index are presented in Table 1. In Figure 2, the number of amphipod individuals per site and season is compared with the corresponding numbers of species and Shannon-Wiener indices, the former increasing as the other two decrease, in the summer season.

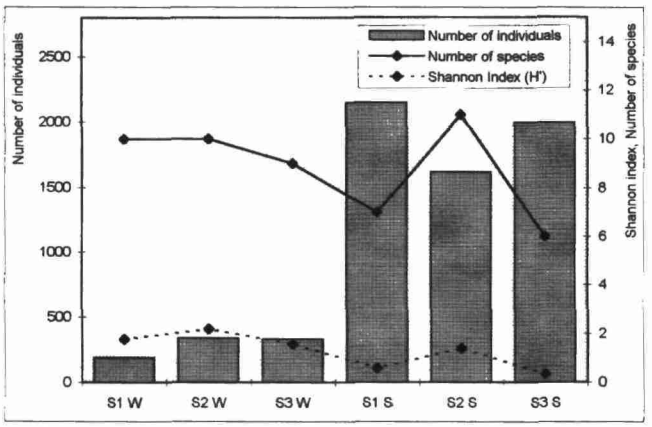

Fig. 2: Number of individuals and Shannon-Wiener Index for each season and site S1= site 1; S2= site 2; S3= site 3; W= winter; S= summer.

The most dominant amphipod species, by far, is *Elasmopus rapax* (mA=151.6, pmD=82.7); second is the species *Maera inaequipes* (mA=14.8, pmD=8.1) and third *Corophium acutum* (mA=7.8, pmD=4.2). Four more species, namely *Erichthonius brasiliensis, Jassa marmorata, C. sextonae* and *Microdeutopus stationis* had high abundances in some of the samples.

Shannon index calculated separately for each site had similar values in sites 1 and 3 (0.74 and 0.61 respectively), but higher in site 2 (1.63). Comparison of the three sites on the basis of their amphipod abundance by the Kruskal-Wallis test, showed no significant differences among them either in summer (H=1.064, p=0.5873) or in winter (H=4.999, p=0.082). Samples were grouped according to their similarity as in the dendrogram of Figure 3. As we can see, they are divided into two groups corresponding to the two seasons (summer and winter). In each season, the samples of the three sites had high affinities reaching 62% in the summer and 89% in the winter. Shannon index differed between seasons: winter values for the three sites were 1.76, 2.18 and 0.57 while summer values were 0.58, 1.39 and 0.33 respectively (Fig. 2). Significant differrences in the abundances of the three sites examined as a total between the two seasons were found by Kruskal-Wallis test (site 1: H=9.791, p=0.0204; site 2: H=9.513, p=0.0232; site 3: H=7.615, p=0.04). From Figure 2, it is also obvious that the number of individuals was greater in summer than in winter samples.

Discussion

Mussel beds form one of the facies of the photophilic soft algae biocoenosis, usually appearing on hard substrates of the harbours (1). Other facies of the same biocoenosis have been recently examined in the Aegean Sea, such as that of *Anemonia viridis* (11). The composition of the assemblages associated with sponges (15, 16) and the scle-

CEPHALOPOD REMAINS IN THE STOMACH-CONTENT OF BEAKED WHALES, *ZIPHIUS CAVIROSTRIS* (CUVIER, 1823), FROM THE IONIAN SEA

Eugenia Lefkaditou [1]* & Yannis Poulopoulos [2]

[1] National Centre for Marine Research, Ag. Kosmas Helliniko, 16604 Athens, Hellas
[2] Hellenic Cetacean Research and Conservation Society, Ymittou 2, 12132 Peristeri, Hellas

Abstract

Seventeen beaked whales, *Ziphius cavirostris* (Cuvier, 1823) were found stranded on the southwestern Greek Ionian coasts on 12-15 of May 1996. The stomach contents of 7 beaked whales were made up entirely of cephalopod remains which included detached heads and bodies, crown of arms, isolated buccal masses, loose beaks and eye lenses. Identified beaks attributed to two oceanic teuthoid cephalopods: *Histioteuthis bonnellii* and *Octopoteuthis sicula*. This suggests that, as shown by previous workers, *Ziphius cavirostris* is an exclusive predator of midwatwer squids and that both squid species, although are seldom caught by fishing gears, are quite abundant in the mesopelagic zone of the Ionian sea. In *Histioteuthis bonnellii* the size range of the beaks is wider than those of the same species found in the stomach content of blue sharks and swordfishes caught in the Adriatic sea

Key-words : Cetacea, food webs, cephalopods, Ionian Sea

Introduction

Cuvier's beaked whale, *Ziphius cavirostris*, is a pelagic species, cosmopolitan in temperate and tropical waters. In the Mediterranean important populations have been recorded along Spanish, French and Italian coasts where isolated individuals or couples are usually encountered and very rarely schools up to 25 individuals (1). Several strandings of beaked whales have been recorded in the last twenty years, on New Zealand (2), northeastern Atlantic and Mediterranean coasts (3, 4, 5, 6, 7), however this is the most numerous stranding of the species that has ever been recorded.

According to Clarke (8) Ziphiidae and Physeteridae are the most important odontocete squid eating cetaceans. There is only one detailed analysis of *Ziphius cavirostris* diet from one specimen stranded at New-Brigton, New Zealand (2). An animal stranded on Northwestern Spanish coasts was examined, but had empty stomach (6). This is the first study on the stomach-content of the species in the Mediterranean.

Materials and methods

From the 17 stranded beaked whales, on the western coasts of Peloponnesos, it was possible to examine only seven of them, 6 males and 1 female, whose sizes were between 5 and 6 m. The samples included detached heads and bodies, crown of arms, isolated buccal masses, loose beaks and eye lenses. The whole stomachs from three beaked whales were kept separately frozen, while the cephalopod beaks and lenses from the rest specimens were put together in a jar, in formalin solution. Beaks were counted and identified according to Clarke (9). The rostral, hood and crest lengths were measured with vernier calipers to an accuracy of 0.01 mm. Lower rostral length (LRL) distributions and the size at which the lower wings become dark are determined for each species. Darkening has been proved to coincide with the onset of maturity (10) and this is useful for comparisons with other collections.

Results

A total of 33 lower and 33 upper beaks (mandibles) were recorded. Only two species were represented by lower beaks. The number of lower and upper beaks of each taxon collected from beaked whales is given in the Table I.

Table I. Cephalopod beaks found in *Ziphius cavirostris* stomach content.

		Ziphius cavirostris specimens			
		1	2	3	Rest
CEPHALOPODA					
Octopoteuthis sicula	LB	3	6	1	8
(RUPPEL, 1848)	UB	2	1		11
Histioteuthis bonnellii	LB	-	2	2	11
(FERUSSAC, 1834)	UB	-	1	-	13
Unidentified	UB	-	1	4	-

LB: lower beaks, UB: upper beaks

Octopoteuthis sicula was the most abundant prey in the stomach of beaked whales accounting for 48.5 % of the total number of beaks. Flesh was present in one stomach, comprising one complete squid (ML: 16 cm, AL: 20 cm) and one crown (AL: 24 cm). Eight pairs of beaks were removed from buccal masses while isolated were found 10 lower and 6 upper beaks. The plot (Figure 1) of upper rostral length against lower rostral length, for 8 pairs of *Octopoteuthis sicula* beaks seems to follow a straight line, at least in the case of smaller beaks (LRL< 8.5 mm), which comprise the major part of the paired beaks. The estimated regression equation is:

$$URL = - 0.873 + 1.176\ LRL \qquad r^2 = 0.964$$

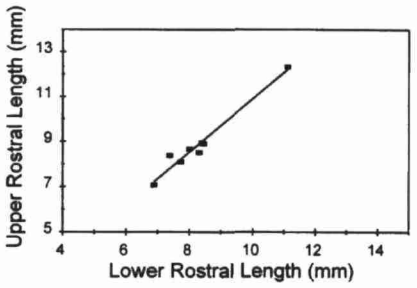

Figure 1. Relationship of upper rostral length against lower rostral length in *Octopoteuthis sicula*.

An histogram of the LRL (Figure 2) has two main peaks at 8 and 12 mm. Five lower beaks with a rostral length of 4.2, 6.9, 7.7, 7.8 and 8.4 mm had transparent wings while four other beaks with LRL of 5.9, 7.4, 8.0 and 8.4 mm presented club-shaped dark areas on the wings with transparent margins. The upper limit of the range is lower than the mode of LRL of beaks found in the stomach of striped dolphins stranded on the western Mediterranean coast (11).

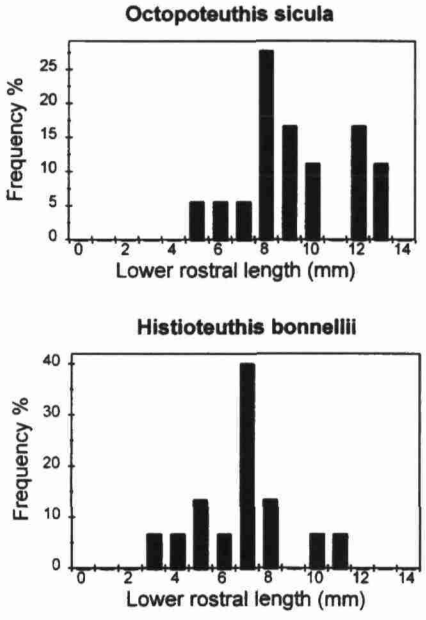

Figure 2. Percentage frequency histograms of the rostral lengths of lower beaks of *Octopoteuthis sicula* and *Histioteuthis bonnellii*

BIOMETRIC STUDY OF THE *ACTINAUGE RICHARDI* CNIDOME *(ACTINIARIA: ANTHOZOA)*

S. Loukmidou* and C. C. Chintiroglou

Aristotle University, School of Biology, Dept. Zoology P.O. Box. 134, 54006 Thessaloniki, Greece

Abstract :

The cnidome is characteristic of the Cnidaria phylum. The type and dimensions of nematocysts can be used as criteria for the identification of actinians at the species level. This is demonstrated here in the case of *Actinauge richardi.* Biometries of the cnidome and statistical analysis revealed that tentacle and acontia basitrichs possess constant characteristics.

Key-words: Aegean Sea, Bathyal, Cnidaria, Zoobenthos

Introduction

Nematocysts are found in all Cnidaria and are diagnostic of the phylum. They cannot be renewed and after discharge are extruded from the epithelium. In one species of actiniarian the cnidome of different functional regions (tentacles, pharynx, filaments, column, basal disc) may differ in composition and size and be used taxonomically (1-9). Satisfactory classification characteristics can also be provided by cnidome biometry (9). Even though the biometry of the cnidome can contribute significantly to the classification of Cnidaria, authors occasionally questioned the extent to which it can be used to distinguish among species. It has been reported that the size of cnidae can vary with age or size of the individual (10, 11). Variation was found in cnidom biometry for hydrozoan *(Campanulariidae)* populations from Mediterranean and Scandinavian shores (12). It was also noted that the biometry of some types of cnidae (*e.g.* length and width) was significantly associated with age in the genus *Telmatactis* (13). Experiments on cnidogenesis in anemone tentacles have revealed little evidence for migration. In *Calliactis tricolor* it was shown a decrease in nematocyst discharge with increase in the amount of food ingested (14, 15). It was also found that depleated tentacles of Anemonia viridis regained their normal complement of cnidae after 5-6 days (16).

Although these data seem to indicate that physical and biological parameters can influence the cnidae types present in the tissues (both qualitativly and quantitatively), few researchers have analysed the influence of these parameters on the biometry of the cnidae.

Recent works have shown that cnidome biometry can depend on body weight, resulting in a number of cases in an inability to use the cnidome as a diagnostic characteristic for classification (17, 18). This work presents a biometric study of the cnidome of *Actinauge richardi,* a bathyal species of the *Hormathiidae* family, occuring in the Eastern Aegean Sea (19). The aim is to investigate correlations between cnida biometry and either size or age of individuals and to find out whether the species can be characterized by these means.

Material and methods

Samples of *Actinauge richardi* (Marion, 1882) were collected with fishboats from the North Aegean Sea, from a depth of 260-450 m. The sampled stations were between Thasos and Samothrake and between Mount Athos and Limnos. They belong to the biocoenosis of the muddy detritic bottoms (23).Ten specimens of various sizes were preserved in 10% formalin /sea water solution. The following morphological variables were measured for each specimen, after preservation: column height (HC, mm), wet weight in crude units of biomass (wW), diameter of the column's base (DB, mm). These variables were considered to reflect, with satisfactory credibility the maturity state of the individuals, their metabolic level (energetic costs) and their relative age (17,18, 20). Cnidae measurements were taken on undischarged capsules of squash preparations. The terminology used was based mainly on England (1987) (9).

For squash preparations, (in a drop of 7.5% formalin) small portions of preserved tissue (approximately 2 mm^3), were taken from different functional regions. The types of cnidae used basitrichs from the tentacles and the acontia. Other types of cnidae were very rare or not found at all. Thirty undischarged capsules of each type were measured and their length (L) and width (W) were recorded. The ratio L/W is considered to be a significant parameter of cnidae biometry (17, 21). This procedure was carried out for each anemone and for each examined body part (tentacles, acontia).

All measurements were taken using an optical microscope (with 10 x 100 objectives) equiped with a camera lucida.

As the distribution of data was unknown, non parametric testing was required. Relationship between column height (HC, mm), column base diameter and wet weight with the means of the nematocyst length and L/ W ratio was investigated using the non- parametric test of Spearman's rank correlation coefficient, usually abbreviated as rs. This test has been frequently used, especially for small data sets (22).

Results and discussion

Tables 1 and 2 and figure 1 contain the results of the correlation tests between cnidae length and L/W ratio, and the morphological variables (wet weight, coloumn height, diameter of the pedal disc). They show that the basitrichs of the tentacles and of the acontia do not demonstrate a correlation with the morphological parameters of the body.

TABLE 1. Spearman's rank correlation coefficients based on the relation-ship between length of cnidae and the body variables. (HC = height of column, wW = wet weight, DB= base diameter of Actinauge richardi individuals)

Type of cnidae	HC (mm)		wW (g)		DB (mm)	
	Rho	p	Rho	p	Rho	p
Basitrichs of tentacles	0.6	0.1	0.3	0.34	-0.1	0.78
Basitrichs of acontia	0.1	0.69	-0.2	0.6	-0.4	0.18

TABLE 2. Spearman's rank correlation coefficients based on the relation-ship between the ratio length/ width (L/W) of cnidae and the body variables. (HC = height of column, wW = wet weight, DB= column base diameter of Actinauge richardi individuals)

Type of cnidae	HC (mm)		wW (g)		DB (mm)	
	Rho	p	Rho	p	Rho	p
Basitrichs of tentacles	0.04	0.9	-0.2	0.64	-0.1	0.8
Basitrichs of acontia	0.2	0.4	-0.2	0.65	-0.4	0.23

Actinians have different types of cnidae which are functional in food capture, defense and aggression. It has been reported that various biological factors can affect the categories of cnidae present in an individual actinian (15, 24, 25, 26). During everyday activity (*i.e.* feeding) nematocysts may greatly decrease in number or even disappear (17, 18).

The absence of certain types of nematocysts from the tissues may lead to classification problems. No correlations between physiological functions of the organism (reproductive period, food gathering ability, defense etc.) and nematocyst biometry have been found. Nevertheless, most taxonomists regard cnidae biometry as essential for classification. Some authors have suggested to use certain statistical tools for the study of cnida morphology (mean, standard deviation, and range) in order to overcome differences resulting from evaluation methods (6, 13, 19). Unfortunately, no concise comparative method has yet been put forward and parametric data cannot been used for classification and taxonomy.

In an identification key, stressing presence versus absence of certain types of nematocysts can induce into error (24, 25). This can be overcome by the combined use of biometrics and statistical analysis (17, 18, 27, 28).

It has been shown here that the basitrichs of the tentacles and the acontia can be considered as taxonomically reliable and constant and can be adequately used as diagnostic characteristics for the species *Actinauge richardi.*

ANNUAL VARIABILITY IN THE POPULATION DENSITY DISTRIBUTION OF APPENDICULARIANS IN COASTAL AREAS OF THE SOUTHERN ADRIATIC

Davor Lucic

Institute of Oceanography and Fisheries-Split, Laboratory of Plankton Ecology Dubrovnik,
Kneza Damjana Jude 12, HV-20001 Dubrovnik, Croatia

Abstract

Annual variability in the population density distribution of appendicularians was investigated in coastal areas of the southern Adriatic, Croatia. Appendicularians were registered in high abundances (>3000 ind.m^{-3}), especially for the juvenile specimens. In the moderately eutrophicated Gruz Bay, the total population densities in appendicularians significantly surpassed those registered in the oligotrophic Lokrum Channel (Student's *t*-test, $p<0.001$). Results indicated the existence of different density values for each 5-m depth interval.

Key-words: zooplankton, vertical profile, Adriatic Sea.

Appendicularians play important roles in transporting picoplankton production to higher trophic levels (1). Furthermore, the weight-specific filtering and growth rates are higher for appendicularians than for those of copepods (2, 3). During previous research on appendicularians in the Adriatic Sea, samples were collected using plankton nets of 250-300 (m mesh netting (4, 5, 6, 7). For these investigations, most of the appendicularian populations passed through the plankton nets, as proved by a sampling experiment (8). Consequently, accurate data on the quantitative composition of appendicularians could not be obtained from the samples.

This paper presents the results of a one-year study of appendicularian population density distributions at two stations (22-m depth) in the coastal waters of Dubrovnik (Fig. 1). The first station in the Lokrum Channel is located in an oligotrophic area that is directly influenced by offshore waters. The second station in the Gruz Bay is influenced by discharge from the karst River Ombla, offshore waters and slight anthropogenic eutrophication.

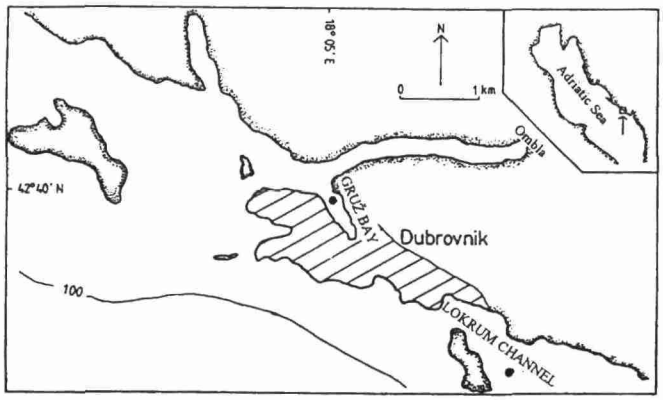

Figure 1. Location of the sampling station.

Thirteen daytime plankton samples were taken from March 1989 to May 1990. Appendicularians were sampled with a 250 l volume plankton sampler "Adriatic" (9), at 5-m intervals from the surface to the bottom using a gauze of 125 (m mesh netting. Temperature and salinity were determined by a Hydrobios LF 191 probe.

At both stations, an increase in surface temperatures in spring resulted in a thermal stratification of the water column as early as in May and a thermocline in summer, up to a 15 m depth. The vertical gradient weakened during autumn and a moderate temperature inversion occurred until springtime. The temperature range was from 12.3 to 25.4 °C in the Lokrum Channel and from 11.3 to 23.9 °C in the Gruz Bay. Salinity values recorded in the Lokrum Channel exceeded 37 psu below a 5 m depth and 38 psu below a 15 m depth. A minimum of 31.3 psu was recorded at the surface in August. The influx of waters from the River Ombla into the Gruz Bay resulted in low salinity values between 0 to 10 m depths, especially in spring, with a minimum of 26.7 psu at the surface in April. During the summer-autumn period, values >37 psu were found below 10 m depths.

In the Lokrum Channel, *Oikopleura longicauda* was the dominant species and contributed with 50.3% of the total abundance of appendicularians (Table 1). *Oikopleura dioica* dominated in the Gruz Bay and contributed with 45.9% of the total appendicularians. Both species were present in plankton throughout the year. *O. longicauda* was more abundant in the warmer season, and *O. dioica* during winter and spring. Among other appendicularian species, an increased number in *Oikopleura fusiformis* was recorded in fall, whereas *Fritillaria pellucida* was abundant in winter. *Fritillaria borealis* was present in all seasons, but never occurred in high numbers. In the Lokrum Channel, the species *Oikopleura cophocerca*, *Oikopleura graciloides*, *Oikopleura parva* and *Fritillaria haplostoma* occurred mostly in winter and *Kowalevskia tenuis* in summer. However, in spite of a relatively small sample volume (250 l), the previously established qualitative composition was confirmed (6).

Table 1. Appendicularian species found in Lokrum Channel and Gruz Bay, with their mean and Std abundance (Mean ± Std, ind.m^{-3}), maximum values of abudance (Max, ind.m^{-3}) and mean percentage of the total appendicularians abundance (%) during 1989/90.

	Lokrum Channel			Gruž Bay		
Species	Mean ± Std	Max.	%	Mean ± Std	Max.	%
Oikopleura cophocerca	1.1 ± 4.3	9	0.2			
Oikopleura dioica	41.9 ± 59.7	360	11.4	318.3 ± 416.8	1827	45.9
Oikopleura fusiformis	73.5 ± 164.2	750	18.9	98.4 ± 182.2	505	14.2
Oikopleura graciloides	1.5 ± 4.6	27	0.4			
Oikopleura longicauda	188.1 ± 272.6	1656	50.3	151.6 ± 227.3	1155	21.9
Oikopleura parva	0.3 ± 1.5	9	0.1			
Fritillaria borealis	12.5 ± 22.7	80	3.3	17.2 ± 35.7	72	3.0
Fritillaria haplostoma	2.5 ± 7.8	36	0.7			
Fritillaria pellucida	54.6 ± 191.4	1440	14.6	104.1 ± 336.1	1872	15.0
Kowalevskia tenuis	0.5 ± 2.7	9	0.1			

In addition, we have observed that in the shallow parts of the sampled area, daytime appendicularian density values were not uniformly distributed from the surface to the bottom. Therefore, the results obtained on the basis of the vertical hauls gave only average values per water column and did not reveal accurate total appendicularian numbers. In the Lokrum Channel, aggregations of juvenile specimens were recorded in increased numbers at all layers (Fig. 2). Their total number was 1.7 times more than that of adults. As many as 1590 ind.m^{-3} were noted at depths of 5 m in August, 1368 ind.m^{-3} at 20 m in December and 1836 ind.m^{-3} at 10 m in February. The majority of adults were found in layers below 15 m depths, except for February, due to the intrusion of *F. pellucida* (Fig. 2). Higher numbers were found in August, 1660 ind.m^{-3} and in late May, 1755 ind.m^{-3}.

In the Gruz Bay, total appendicularian population densities significantly surpassed those registered in the Lokrum Channel (Student's *t*-test, $p<0.001$). Most of the juvenile specimens were found at 5 and 10 m depths (Fig. 3), namely in the layers where surface brackish and offshore waters mingled. According to Vilicic *et al.*, (10) the highest concentrations of picoplankton can be found in these surface waters as many as 2828 ind.m^{-3} were recorded at depths of 5 m in August and 3200 ind.m^{-3} at 10 m in February. The total in juvenile specimens at this station was 1.9 times more than that of adults. As opposed to the Lokrum Channel, adult aggregations in the Gruz Bay were recorded throughout the water column. The highest values of 2181 ind.m^{-3} and 3890 ind.m^{-3} were noted at 15 m depths in August and in February, respectively (Fig. 3). In the Gruz Bay high average densities of bacterioplankton (2.6 x 10^9 cells l^{-1}) and nanophytoplankton (1.37 x 10^6 cells l^{-1}) tripled those recorded for open coastal waters (10, 11, 12). This is the reason why we consider the high appendicularian numbers in the Gruz Bay comparable only to the results presented by Uye and Ichino (13) for the eutrophic coastal area in the Seto Inland Sea, Japan. These authors have reported values of 10 to 50 ind.l^{-1} on the basis of samples collected during the night with vertical hauls using a plankton

ANALYSE MODALE ET ESSAI D'ESTIMATION DES PARAMÈTRES DE CROISSANCE ET DE L'ÂGE DE TROIS ESPÈCES D'HOLOTHURIES ASPIDOCHIROTES (HOLOTHUROIDEA : ECHINODERMATA) DE LA RÉGION DE SIDI-FREDJ (ALGÉRIE)

Karim Mezali* et Rachid. Semroud

Institut des Sciences de la Mer et de l'Aménagement du Littoral, BP. 54 Sidi Fredj. 42321 Tipasa, Algérie

Résumé

Les études portant sur la croissance des holothuries aspidochirotes méditerranéennes sont quasiment inexistantes. Afin d'évaluer l'âge de ces espèces, des analyses modales par décomposition en classes de tailles ont été établies par les méthodes indirectes sur l'ensemble des populations (tous sexes confondus) constituées de 494 *Holothuria tubulosa*, 281 *H. polii* et 192 *H. sanctori*. L'échantillonnage a été réalisé de juin 1994 à février 1996 à -3 m de fond dans la station de Sidi-Fredj, caractérisée par la présence d'un herbier à *Posidonia oceanica*. Les paramètres de croissance de l'équation de Von Bertalanffy ont été estimés pour les espèces étudiées par la méthode d'Abramson Tomlinson et comparés à d'autres méthodes. Le mois de recrutement a été déterminé pour chaque espèce et les courbes théoriques de croissance linéaire montrent que *Holothuria polii*, l'espèce caractéristique de l'herbier de Posidonie, a une longévité plus grande que *H. tubulosa* et *H. sanctori*. Les résultats obtenus ont été comparés à ceux d'autres espèces d'Holothuries méditerranéennes et tropicales.

Mots-clés : posidonia, growth, recruitment, Algerian Basin

Introduction

Les holothuries aspidochirotes, composant important du compartiment benthique de l'herbier à *Posidonia oceanica* [1, 2], participent activement au recyclage de la matière organique [3]. Elles sont impliquées dans le processus de "bioturbation" [4], organisent le retour des éléments nutritifs à la couche d'eau [5] et mettent en valeur la production des bactéries associées au sédiment [6] en stimulant l'activité de ces bactéries, lesquelles contribuent à la destruction de certain type de détritus ingérés par l'holothurie comme ceux dérivés des herbiers sous marins [7].

Les holothuries aspidochirotes fond l'objet d'une industrie florissante dans le Sud-Est asiatique. Elles sont d'une part utilisées dans les mets chinois, et rentrent dans la fabrication des produits médicamenteux, d'autre part [8]. Par ailleurs, elles sont utilisées comme appâts de pêche [9]. Quelque soit la profondeur à laquelle elles vivent, les holothuries hébergent sur leur peau et dans leurs corps, une faune impressionnante, transformant l'holothurie en un véritable habitat mobile [10].

Du point de vue écologique les holothuries se sont révélées être des indicateurs benthiques très sensibles à la pollution chimique d'origine industrielle [11]. Le biotope particulier et le comportement sciaphile de ces holothuries font que ces espèces sont particulièrement difficiles à échantillonner limitant ainsi les possibilités d'étude de la structure et de la croissance des individus constituant leur population. En ce qui concerne l'âge de ces espèces, peu d'études ont été réalisées par des méthodes indirectes [12, 13] et des méthodes directes [14, 15].

Matériel et méthodes

Des mesures de la longueur contractée d'individus de *Holothuria tubulosa*, *Holothuria polii* et de *Holothuria sanctori*, ont été effectuées *in situ* en scaphandre autonome durant une période de 19 mois avec une fréquence de mesure mensuelle de 26, 15, 10 individus respectivement pour *Holothuria tubulosa*, *H. polii* et *H. sanctori* ; dans une station superficielle (-3m) étirée sur une superficie de 500 m^2 (Fig. 1) et caractérisée par la présence de la phanérogame marine *Posidonia oceanica*.

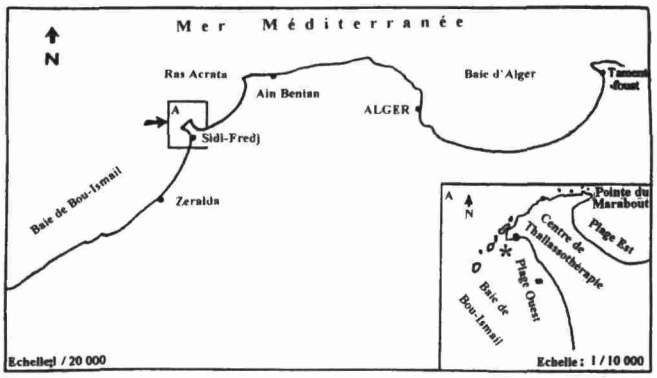

Fig. 1. Situation géographique de la presqu'île de Sidi-Fredj. A : Détails de la presqu'île. * Zone d'échantillonnage.

Le choix de cette méthode non destructive se justifie par le fait que les holothuries possèdent potentiellement la possibilité d'effectuer des déplacements à grande échelle dans une direction donnée en réponse à un stimuli (modification de ressources trophiques, hydrodynamisme par exemple) [16, 17].

La longueur est le critère de dimension le plus facile à mesurer *in situ*. Les holothuries étant capables de changer de taille, la seule manière d'obtenir des comparaisons raisonnables, est de standardiser la technique de mesure ([17]). La contraction maximale est supposée être le point pour lequel il n'y a pas de raccourcissement supplémentaire qui se reproduit après les avoir compressées [16, 17]. La longueur contractée de chaque individu (de la bouche à l'ouverture du cloaque) a été mesurée sous l'eau à l'aide d'une règle semi-cylindrique avec une précision de lecture de 0.5 cm.

Pour les trois espèces d'holothuries étudiées, nous avons essayé de dégager les différentes classes de tailles à partir des histogrammes établis sur toute la période d'échantillonnage; pour cela nous avons essayé les différentes méthodes de décomposition, en premier lieu la méthode de Bhattacharya [18], pour laquelle l'étude du taux d'accroissement a été révélé satisfaisant seulement pour *H. polii*, ce qui n'est pas le cas pour *H. tubulosa* et *H. sanctori*, Ceci nous a conduit à éliminer les classes de taille les plus grandes.

Pour éviter ces résultats erronés, nous avons utilisé une autre méthode de décomposition, celle de Gueno et Leguen [19]. Cette méthode des maximums successifs basée sur l'analyse de la progression modale consiste à décomposer la distribution de taille en groupe d'individus de certain âge et de suivre leurs devenir dans le temps ; elle donne des résultats satisfaisants. Les paramètres de croissance linéaire de l'équation de Von-Bertalanffy ($L\infty$, K, t_0) ont été estimés par le logiciel FISHPARM [20]. $L_t = L\infty(1-e^{-K(t-t_0)})$ avec : $L\infty$ = Taille asymptotique, t_0= Age correspondant à la taille zéro, K= Coefficient de croissance.

Les valeurs obtenues par le logiciel FISHPARM ont été comparées aux valeurs obtenus soit par calcul suivant la méthode de Ford Walford (in [21] soit par un autre logiciel (ELEFAN) [22]. L'utilisation du logiciel ELEFAN nous a permis de définir le mois de recrutement (Fig. 2, Tab. 1).

Résultats

1 - Progression modale pluriannuelle et estimation du mois de recrutement voir Fig. 2-A-B-C.

2- Courbes de croissance linéaire et estimation des paramètres de croissance (Fig. 3)

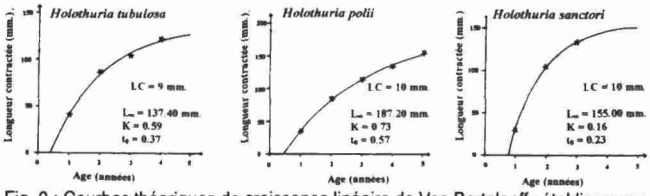

Fig. 3 : Courbes théoriques de croissance linéaire de Von Bertalanffy établies pour chaque espèce d'holothuries étudiées $L\infty$ = Longueur asymptotique, K = Coefficient de croissance, t_0 = Age correspondant à la taille zéro. I.C = Intervalle de classe (mm).

Discussion

Les résultats de la détermination des paramètres de croissance calculés pour l'espèce *H. tubulosa* sont en accord avec ceux obtenus par [20]. Comme il a été démontré par [20] à Port Cros (France), il est difficile d'attribuer ces tailles à des classes d'âges, compte tenu de la légère variabilité induite par la méthode de mesure. La croissance des jeunes individus est très rapide, et devient très lente chez les individus âgés [23]. Toutes les valeurs de $L\infty$ obtenues sont sous-estimées, ce qui semble être due à l'élimination des groupes d'âge avancé du fait de l'augmentation du taux d'accroissement.

PHYTOPLANKTON-ZOOPLANKTON TROPHIC INTERACTIONS ALONG THE SALINITY GRADIENT (GULF OF TRIESTE)

Patricija Mozetic* and Lovrenc Lipej
Marine Biological Station Piran, Fornace 41, 6330 Piran, Slovenia

Abstract

The response of phytoplankton to nutrient inputs of the Soca River and its interactions with zooplankton were studied monthly from 1993 to 1995 and during short-time field experiments in June 1995. The major influence of riverine discharges on phytoplankton biomass was observed after autumn freshets, especially in October 1993 and October-December 1994. In these periods, when diatoms dominated the phytoplankton community, the highest grazing rates of the copepod Acartia clausi were measured (5.31 and 2.49 ng Chla ind.$^{-1}$). An increase of phytoplankton biomass was observed after a freshwater discharge in June 1995. Despite the high phytoplankton standing stock in the Soca River plume, grazing rates of *A. clausi* were lower in comparison to less-diluted areas.

Key-words: plankton, trophic relations, river input, Adriatic Sea

Introduction

Direct inputs from land-based sources and atmospheric deposition are the main sources of plant nutrients in estuarine and coastal waters. In such areas increasing nutrient and organic matter inputs have been paralleled with marine eutrophication for some decades (1, 2). This is the case with the northern Adriatic (3) and its shallowest part, the Gulf of Trieste with the Soca River as the largest freshwater source. Development of phytoplankton blooms and changes in phytoplankton community usually follow seasonal and interannual fluctuations in freshwater discharges in the Gulf of Trieste (4, 5). Coastal waters and estuaries are also suitable sites for studying interactions between phytoplankton and zooplankton due to increased phytoplankton standing stock after external nutrient enrichment of the waters (6). The question that arises is what is the zooplankton response to phytoplankton fluctuations (in time and space)? This can consequently provide useful information about the fate of phytoplankton biomass.

The aim of this work was to assess the influence of freshwater inputs on the phytoplankton community, and subsequently the response of the zooplankton community to favorable nutritional conditions. Phytoplankton-zooplankton trophic interactions were followed on an annual basis and during short-term field experiments with Soca River discharges as the main nutrient inputs.

Material and methods

The Gulf of Trieste is a shallow, semi-enclosed gulf with a maximum depth of ca. 25 m in the central part. It is characterized by large temperature variations (6-26°C in the surface layer and 6-20°C above the bottom) and, following the seasonal freshets, surface salinity oscillations (<30 to 38.5). From mid-April through September typical thermal stratification develops, while in other seasons the water column is mixed. Most of freshwater enters the Gulf with the Soca River inflow on the northwestern side (annual average of 150 m^{3}s^{-1}; 7).

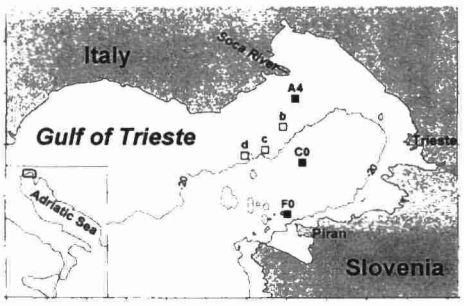

Fig. 1: Locations of sampling stations during the September 1993 - June 1995 period (station F0) and during short-term experiments in June 1995 in the Gulf of Trieste; (■) stations along the salinity gradient (June 13 and 19 1995), (□) stations along drifter trajectory (June 15, 16 and 21 1995).

Sampling was carried out from September 1993 to June 1995 on station F0 (21 m depth) in the southeastern part of the Gulf (Fig. 1). Samples for phytoplankton biomass and abundance were collected monthly at five depths (0, 5, 10, 15 and 21 m). Samples for grazing measurements in terms of gut pigment content were collected separately in approximately week intervals.

Additionally, five short-term experiments near the Soca River plume were conducted in June 1995 (8). Two 24-hours experiments (June 13 and 19) were performed at three stations along the salinity gradient (A4, C0 and F0). The station A4 is directly influenced by freshwater inputs, station F0 is under marine water influence and station C0 is influenced by water of both origins. The other three experiments (June 15, 16 and 21 1995) were set up as drifting experiments. A surface drifter was released at station A4 and tracked to station d within 12 hours. The trajectory A4-d represents the transport of the water mass of the Soca River plume during its movement to the mid-gulf area. Sampling protocol for gut pigment content and chlorophyll a biomass is described in detail in Lipej *et al.* (9).

Phytoplankton biomass, expressed as chlorophyll *a* concentration, was determined fluorometrically (10). Phytoplankton was identified in formaldehyde fixed samples (800 ml) and counted on the inverted microscope at 200x magnification (11). Chlorophyll a concentrations from discrete depths were integrated over the whole water column.

The live mesozooplankton samples were obtained by vertical net tows and transported to the laboratory within 15 minutes. During field experiments in June 1995, samples were immediately stored in liquid nitrogen after capture. Comparison of the effect of two handling procedures on the gut pigment content showed no statistical differences between them (ANOVA, P<0.31; 12). *Acartia clausi* was chosen as the most representative copepod, which often dominates the mesozooplankton community of the Gulf of Trieste (13). The gut fluorescence method was used to assess grazing (14, 15). Twenty to thirty freshly caught adults of *A. clausi* were picked out from the container using a stereomicroscope and placed in tubes with 90% acetone and stored in a dark refrigerator overnight. Chlorophylla and phaeopigment content were determined fluorometrically (10), and their concentrations were computed using the equation of Dagg & Wyman (16). Most gut content analyses were carried out in 3-6 replicates. Gut pigment content was expressed as ng Chl *a* • individual^{-1}. Data of daily river flows were provided by Hydrometeorological Survey of Slovenia.

Results and discussion

Seasonal variations (September 1993 - June 1995). Most of Soca River freshwater is generally density-driven out of the Gulf along the northern coastline. Only after autumn freshets does the low-salinity surface water of the Soca River plume reach the southeastern part of the Gulf after a few days' interval (8). This situation was observed also during our study.

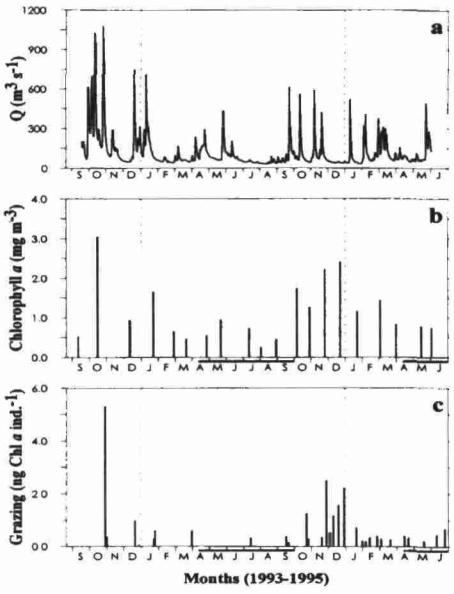

Fig. 2: (a) Daily flow of the Soca River, (b) depth integrated concentrations of chlorophyll *a*, and (c) gut pigment content of *A. clausi* at the station F0 in the period September 1993 - June 1995. Bold lines below the X axis denote the periods of stratified water column.

COMMERCIAL CATCH COMPOSITION IN NEPHROPS FISHING GROUNDS

Ch. Mytilineou*, C.-Y. Politou and A. Fourtouni
National Center for Marine Research, Ag. Kosmas 16604, Athens, Greece

Abstract

The composition of the commercial species in *Nephrops* fisheries is examined from experimental surveys in different fishing grounds of the North Evoikos Gulf (Greece). In the study area, the catches by weight of *N. norvegicus* represented 6% of the total catch and 10% of the commercial catches, whereas in the main *Nephrops* fishing ground they represented 16% and 24% respectively. This species ranged first among the commercial species by numbers and fourth by weight. The commercial by-catch included 49 species, representing 54% of the total catch by weight. The main species by weight were *M. merluccius, M. poutassou, I. coindetii, T. m .capelanus* and *L. budegassa.*

Key-words: fisheries, trawl surveys, decapoda, fishes, Aegean Sea

Introduction

Nephrops norvegicus (L.) (Norway lobster) is one of the most commercially important species among the sea products of the Greek waters, with a very high market price. In 1994, the total landings in the country reached 1087 metric tons (National Statistical Service of Greece, 1995). No specialized fishery for *Nephrops* exists in the Greek waters, however the fishermen know well the species grounds and so they may direct in a way their catches. Trawling is mainly used for *Nephrops* fishing, but in regions where this gear is prohibited, trammel nets are also used. This last method is exercised only in some restricted localities, and so it corresponds to a very low percentage of the total *Nephrops* catch. *Nephrops* trawl fishery is a multispecies fishery, and hence other commercial or not species of various sizes are also by-caught (1, 2, 3).

In the present study, the commercial species from *Nephrops* fisheries are examined from experimental surveys in the North Evoikos Gulf, a geographical area that consists a *Nephrops* fishing ground for the Greek waters (1994: 138 metric tons, National Statistical Service of Greece, 1995). The composition of these commercial species by numbers and weight are analysed by different locations of different depth and fishing conditions. The ratio by weight of all the commercial species to the total catch (C/T) was also calculated for each location.

Material and methods

Samples were collected during 17 experimental surveys, carried out between October 1993 and September 1995 in the North Evoikos Gulf (western part of the Aegean Sea). A commercial trawler was used equipped with a trawl of 16 mm cod-end mesh size (from knot to knot). Four different stations, characterised by different depth or fishing conditions, were selected for the sampling (A: 220-330 m depth, open to trawling; B: 100-137 m depth, open to trawling; C: 115-192 m depth, closed to trawling; D: 60-85 m depth, closed to trawling). The duration of each experimental haul lasted from half to two hours according to the depth and the bottom morphology, although during professional fishing each haul lasts 6 hours usually. For comparison purposes, all the catches were standardized to 1 fishing hour. The total number and the total weight of each commercial species as well as the weight of the total catch for each station were recorded on board.

The analysis was based on the mean number and the mean weight of each species per station for the overall of the 17 surveys. The coefficient of variation (CV) was also estimated. The Friedman's test and the Wilcoxon paired-sample test were applied for comparisons between stations.

Results

According to our results (Tables 1 and 2), in station D, where the highest number of commercial species was caught (46), *Trisopterus mimutus capelanus* was the most abundant species (Table 1). It was followed by *N. norvegicus, Merluccius merluccius* and *Pagellus acarne. Illex coindetii* and *Mullus barbatus* were fished in lower numbers. However, regarding the mean weight (Table 2), *M. merluccius* presented the highest value, followed by *T. m. capelanus,* whereas *Lophius budegassa. P. acarne, N. norvegicus* and *I. coindetii* followed with lower weight values. *Scorpaena scrofa* represented a considerable weight value (>10 Kg/h), although it was found in very low numbers. In station C, characterized by 23 commercial species accompanying *N. norvegicus, Micromesistius poutassou* was the main contributor to the catch with more than 1000 individuals per fishing hour (Table 1). *N. norvegicus, I. coindetii, Lepidorhombus boscii* and *T. m. capelanus* followed with quite lower values. *Eutrigla gurnardus, M. merluccius* and *Liocarcinus depurator* were caught in low numbers (<100 N/h). From the estimation of the mean weight (Table 2), *M. poutassou* showed again the highest value. It was followed by *I. coindetii* and *M. merluccius. N. norvegicus, L. boscii* and *L. budegassa* showed lower values. In station B, characterized by 26 commercial species apart from *N. norvegicus,* the latter showed the highest mean number

Table 1. Mean number of specimens per fishing hour (N/h) and Coefficient of variation (CV) for the commercial species caught per station (17 surveys) and total mean value (AVG) for all stations together in the N. Evoikos Gulf.

LOCATION	A		B		C		D		AVG	
SPECIES	N/h	CV	N/h	CV	N/h	CV	N/h	CV	N/h	CV
FISH										
Citharus linguatula			0.14	0.00			17.84	1.36	4.49	544.35
Conger conger	0.41	1.57	0.03	0.00			0.96	0.85	0.35	265.09
Dasyatis pastinaca							1.65	2.50	0.41	1001.33
Diplodus annularis							8.06	1.28	2.02	513.02
Engraulis encrasicholus			0.07	0.00			0.71	0.00	0.19	2781.82
Eutrigla gurnardus	1.25	0.00	10.49	1.21	88.92	1.20	7.17	1.63	26.96	306.95
Galeorhinus galeus							0.12	0.00	0.03	0.00
Galeus melastomus *	267.7	1.13	0.03	0.00	48.89	2.83	2.35	0.00	79.75	340.83
Lepidorhombus boscii	43.20	0.98	7.65	1.48	113.7	0.58	6.94	5.91	42.88	147.63
Lophius budegassa	2.86		2.19		8.53		14.24			
Lophius piscatorius	0.06	0.00	0.03	0.00	0.06	0.00	0.24	0.00	0.10	692.11
Merlangius merlangus							0.71	1.42	0.18	566.67
Merluccius merluccius	4.95		10.29		90.87		228.1			
Micromesistius poutassou	34.90		101.5		1144.		14.41			
Mullus barbatus			5.08	3.32	10.85	1.36	65.14	1.52	20.27	368.46
Mullus surmuletus							11.88	0.00	2.97	0.00
Myliobatis aquila							11.88	0.00	2.97	0.00
Pagellus acarne							204.4	1.00	51.12	401.16
Pagellus erythrinus							0.24	0.00	0.06	0.00
Phycis blennoides	8.36	1.07	2.83	3.26					2.80	322.11
Raja clavata *					0.58	7.02			0.14	2808.70
Raja montagui *					0.65	4.78			0.16	1910.93
Raja naevus *			0.07	0.00					0.02	0.00
Raja radula *					0.05	0.00			0.01	0.00
Scomber scombrus							18.51	0.99	4.63	394.11
Scorpaena notata			0.03	0.00			0.81	0.00	0.21	3160.80
Scorpaena porcus							0.35	0.00	0.09	0.00
Scorpaena scrofa	0.03	0.00					10.70	0.52	2.68	232.99
Serranus cabrilla							0.16	0.00	0.04	0.00
Solea vulgaris			0.06	0.00	0.14	1.57	25.05	0.87	6.31	348.57
Spicara flexuosa			0.24	0.00			6.16	0.63	1.60	369.60
Spicara smaris			1.11	3.13	0.35	2.83			0.37	822.25
Trachurus mediterraneus			0.06	0.00			2.36	1.69	0.60	839.73
Trachurus trachurus	0.06	0.00	6.79	2.95	6.82	3.15	4.87	2.19	4.63	398.78
Trigla lucerna							0.08	0.00	0.02	0.00
Trigla lyra							0.34	3.40	0.08	1360.00
Trigloporus lastoviza							0.94	0.00	0.24	0.00
Trisopterus minutus	0.25	4.52	64.28	1.17	105.4	1.07	684.8	0.80	213.7	199.18
Uranoscopus scaber							0.41	0.66	0.10	263.94
Zeus faber			0.15	1.70	1.52	1.96	7.32	0.99	2.25	287.15
DECAPODS										
Hommarus gammarus							0.08	0.00	0.02	0.00
Nephrops norvegicus	**140.0**	**0.49**	**610.3**	**0.50**	**408.7**	**0.28**	**369.7**	**0.53**	**382.2**	**55.77**
Scyllarus pygmaeus							1.06	2.83	0.26	1133.33
Squilla mantis *							3.01	3.13	0.75	1250.25
Liocarcinus depurator *	28.77	1.06	82.91	0.60	57.81	1.45	8.64	1.46	44.53	134.18
CEPHALOPODS										
Eledone cirrosa					0.05	0.00	9.36	3.80	2.35	2003.01
Illex coindetii	57.79	1.30	66.17	0.99	333.2	0.73	80.03	0.62	134.3	132.12
Loligo vulgaris							18.27	2.40	4.57	960.28
Octopus vulgaris			0.17	2.05	0.05	0.00	0.65	1.28	0.22	515.16
Sepia officinalis					0.40	0.00	2.55	3.25	0.74	1028.16
TOTAL	590.6		972.7		2422.		1853.		1045.	

*indicates the species of low commercial value, sometimes discarded

(Table 1). *M. poutassou* was found in quite lower abundance, followed by *L. depurator, I. coindetii* and *T. m. capelanus.* Regarding the mean weight values, these did not surpass generally 10 Kg/h (Table 2). *N. norvegicus* presented again the highest value by weight. It was followed by *I. coindetii, M. poutassou* and *M. merluccius.* In station A, where the lowest number of commercial species was caught (18), the most important species by number and weight was *Galeus melastomus* (Table 1 and 2). *N. norvegicus* followed in terms of numbers (Table 1), and *L. budegassa* and *I. coindetii* in terms of weight.

Regarding all the studied stations, the most abundant commercial species accompanying *Nephrops* were *M. poutassou, T. m. capelanus, I. coindetii, M. merluccius* and *G. melastomus* (Table 1). However, the most important in terms of weight were *M. merluccius* and *M. poutassou* (Table 2).

CHLOROPHYLL *A* AND PRIMARY PRODUCTION OF SIZE FRACTIONATED PHYTOPLANKTON IN THE MIDDLE ADRIATIC SEA

Zivana Nincevic and Ivona Marasovic

Institute of Oceanography and Fisheries, Setaliste I. Mestrovica 63, P.O. Box 500, Split, Croatia

Abstract

Phytoplankton biomass and primary production were measured monthly in the nearshore and offshore waters of the Adriatic Sea from January 1994 to January 1995. At the same time, various size fraction categories (> 10 μm, 2-10 μm, < 2 μm) were determined in respect to total biomass and primary production. In the nearshore water phytoplankton biomass the most abundant category was microplankton while nano and picoplankton were less numerous. In the open sea waters this relationship is reversed.

Key-words: phytoplankton, primary production, Adriatic Sea.

Introduction

Phytoplankton biomass is important factor in determining the trophic level of marine ecosystem. In recent years, the interest for size-fractionated biomass and production was increased and size of phytoplankton cells has become an ecological variable [1] linked with the food chain. The cognition that the size of primary producers influences the oceanic carbon cycle [2, 3] and discovery of picoplankton [4] are the reasons for it. There have been only a small number of studies of the eastern Adriatic picophytoplankton. The aim of this work is to compare the coastal and offshore waters in regard to the vertical and spatial distribution of various size-fraction phytoplankton biomass and their contribution to the primary production in the middle Adriatic.

Materials and methods

In 1994, samples were taken monthly at two stations in coastal waters (03 and 25) and at one station in offshore waters (09) of the middle Adriatic Sea (Fig. 1). Chlorophyll *a* was determined fluorometrically in 90% acetone extracts using a Turner 112 fluorometer [5]. Primary production within the euphotic zone was measured *in situ* by ^{14}C - method [6,5]. Measurement of chlorophyll *a* and primary production were carried out on three size fractions (micro- > 10 μm; nano- 2-10 μm; picoplankton < 2 μm). All samples were pre-filtered through a 330 μm mesh net to remove large zooplankton. Measurment of chl *a* . Picoplankton samples filtered through 2 mm polycarbonate membrane filters and retained on the glass microfibre filters (GF/F). Nanoplankton samples pre-screened through 10 μm mesh net and retained on the glass microfibre filters. Microplankton obtained after subtraction of the picoplankton and nanoplankton fraction from whole water samples filtered through the glass microfibre filters. Micro- and nanophytoplankton cells were counted by the Ultermöhl method (1958). Samples of 25 ml taken at coastal stations were analyzed microscopically after a sedimentation time of 24 hours, whereas 100 ml offshore samples after 72 hours. The phytoplankton cells with a maximum length between 2 and 10 μm were designated as nanoplankton, and cells longer than 10 μm as microplankton.

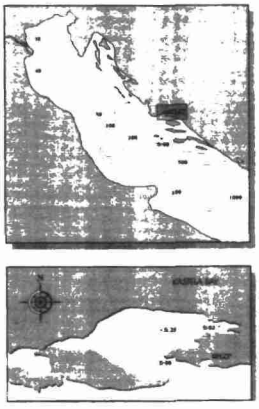

Figure 1. Location of sampling stations in middle Adriatic.

Results and discussion

During the investigation period, at station 09 chlorophyll *a* was ranged from 0.07 to 0.7 mg chl *a* m^{-3} except in September, when subsurface chlorophyll *a* maxima (SCM) (1. 18 mg chl *a*) were recorded around 30 meters depth. This SCM arised immediately after disappearance of the thermocline and microplankton contributed more than 90 % to total chlorophyll *a*. Chlorophyll *a* at station 25 ranged from 0.10 to 3.46 mg m^{-3}. Seasonal fluctuation in chlorophyll a at both station showed maximum value in winter while it was lower in the warmer period of year. This fact is in accordance with Ercegovic [7] who established the phytoplankton seasonal cycle for the Adriatic Sea. On the contrary, at station 03 the seasonal distribution of phytoplankton showed no regularity which is the characteristic of the eutrophicated area. Chlorophyll *a* ranged from 0.21 to 3.65 mg m^{-3} except in August during the bloom of the dinoflagellate *Gonyaulax polyedra* when it was 24.87 mg m^{-3} in the surface layer and 12.89 mg m^{-3} around 5 meter depth. Since 1980, when it was recorded for the first time, it has become regular occurrence in this part of Kastela bay and occasionally it has been accompanied by marine organisms mortality caused by the oxygen depletion in the bottom layer [8]. Chlorophyll *a* at these stations decreased with distance from the land. Size-fractionated biomass showed that the greatest part of the biomass at the offshore station 09 was consisted of the < 10 mm size fractions during the whole period except in September when the microplankton prevailed due to the SCM. Picoplankton size fractions were determined from July 1994 to January 1995. During the whole period it contributed more than 20 % of the total biomass and more than 50 % in July at the depths of 10, 30 and 50 meters. At station 25 the contribution of > 10 mm size fraction was greater than at station 09. Moreover, its greatest contribution was recorded at the surface layer (33-97%) while its importance was decreasing towards the bottom (Fig. 2). The greatest contribution of microplankton to the total biomass was at station 03 where it prevailed during the whole period of investigation. The relative contribution of the three size fractions to total chl a differed appreciably between nearshore and offshore stations (Fig. 3). In the rich nutrient area (station 03) microplankton prevailed [9], while in the low nutrient area (station 09) picoplankton had more important role because of its ability, due to larger cellular surface in respect to volume, to assimilate nutrients more efficiently than bigger phytoplanktonic organisms [10]. According to [11] the various size fractions reached different concentrations of chl *a*, but each of them had different limit. The comparison of our results which are also within these limits with their results is given in Table 1. Such results support the hypothesis that the picophytoplanktonic biomass is more stable, whereas temporal and spatial variations in total biomass are due to larger cells.

Table 1. Maximum concentrations of chl a in the various size fractions in the Western Mediterranean [11] and the middle Adriatic Sea (present study).

Raimbault et al. (1988)		Middle Adriatic	
size-fraction	mg chl a m^{-3}	size-fraction	mg chl a m^{-3}
< 1µm	0.5		
1-3 µm	1.3	< 2µm	0-0.47
3-10 µm	2	< 10 µm	0.03-1.64

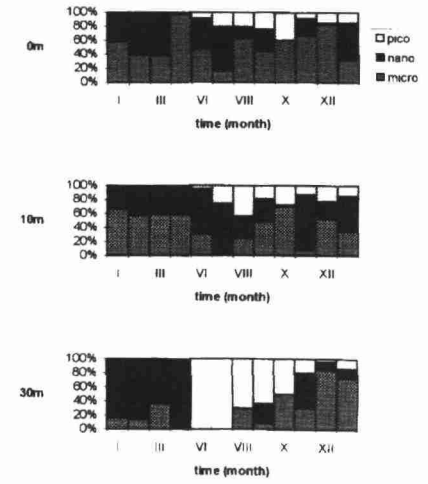

Figure 2. Various size fraction categories of phytoplankton in total biomass at different depths at station 25

MEGANYCTIPHANES NORVEGICA (CRUSTACEA, EUPHAUSIACEA) IN THE LIGURIAN-PROVENÇAL BASIN: NOTES ON POPULATION SIZE STRUCTURES AND GROWTH

L. Orsi Relini, G. Relini, G. Palandri, M. Relini, F. Garibaldi, C. Cima, G. Torchia, C. Costa

Istituto di Zoologia, Laboratori di Biologia Marina ed Ecologia Animale, Università di Genova, Via Balbi, 5, 16126 Genova, Italia

Abstract

In the period 1990 - 1994, by several R/V surveys, a large scale sampling of *Meganyctiphanes norvegica* was performed in the Ligurian-Provençal basin. Seasonal patterns of the size structure of the catches were described.. The distribution of age groups in the Ligurian-Provençal stock appears to be related to the general circulation of the basin. The growth resulted similar to those registered in the NE Atlantic.

Key-words: crustacea, population dynamics, circulation, Ligurian Sea

Introduction

The Euphausiid *Meganyctiphanes norvegica,* the North Atlantic and Mediterranean krill, is a key species in the food webs of the Ligurian-Provençal basin, both in pelagic and demersal environments (1, 2). Recent studies about morphology and reproduction of the species were conducted in the area (3, 4); however, at the best of our knowledge, the growth has never been investigated. Since 1990 we have planned a large scale collection of data in the Ligurian-Provençal basin to investigate the dynamics of the stock. In this study we report some preliminary results, obtained from the surveys 1990 - 1994.

Material and methods

Since 1990 we have established a sampling grid for IKMT hauls, covering an area of 8600 square nautical miles, between the Ligurian coast and the isle of Corsica. The sampling stations were located along four transects: A, Genoa-Calvi; B, Monaco-Calvi; C, Marseille-Gulf of Porto; D, perpendicular to B. The long term target was to repeat the sampling along the transects once or several times in the four seasons, but, given times and costs of work at sea, the sampling is still in progress. In this study we refer on a total of 70 hauls, in which spring and summer samples were abundant (respectively 26 and 35) and autumn and winter samples scarce (8 and 1).

In each station the main hydrological characteristics were measured by CTD profiles and the macroplancton-micronecton was sampled with an open IKMT (15 feet, 2x2 mm mesh size). Oblique tows, 750 m to the surface, were performed. Each haul lasted two hours at a ship speed of 3 knots. The catches were sorted in the following main subdivisions: Fish, Cephalopods, Crustacean Decapods, *Meganyctiphanes norvegica,* other Euphausiids, other Crustaceans, Pteropods, jelly macroplancton, which were measured in terms of volume. *M. norvegica* individuals in the total catch or subsamples were counted. A total of about 15.000 specimens was measured in terms of total length, from eye to telson. In subsamples, sex was determined in specimens >23 mm long.

Results

Some information about hydrological characteristics and total catches of *Meganyctiphanes norvegica* and other macroplankton in terms of volumes per haul have been previously reported (5, 6, 7).

Size structure of the IKMT catches during the year

The seasonal size composition of the catches gives clear indications of the growth of *M. norvegica* in the study area (fig. 1). Recruits appear in late spring (fig. 1a), in accordance with the times of maturation and spawning in the Ligurian Sea, *i.e.* from March to May (4). The frequency distribution of juvenile total length in June shows a bimodal pattern (fig. 1a). Considering stations along a single transect (fig. 2), juvenile sizes increase from the coast to the offshore waters. The smallest individuals were found in the stations close to the slope.

The summer samples give indication of the rapid growth of the young euphausiids (fig. 1b represents the sum of 20 stations sampled in August) and in the same time show a group of "old" individuals in the same length range of those observed in late spring. Considering frequency distribution of length recorded in August at single stations (fig. 3), it can be noted that the relative importance of the two age groups, juveniles and adults, changed from North to South: young euphausiids dominated at stations C4, C6, C8, B4, B5, B6, B7, A7 and A9.

In autumn young specimens were close to merge with the old group (fig. 1c). In winter the distribution appears unimodal (fig.1d). This last distribution, recorded in February at station A1 over the slope coincided, in terms of size range, with those of stranded shoals of the same month.

Stranded animals are mature adults, the majority of which, both males and females, are bearing spermatophores. Identical reproductive patterns have been observed in the winter IKMT hauls (fig. 1d).

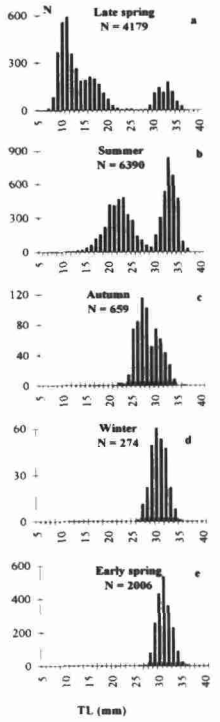

Fig. 1 Frequency distribution of total length (TL) of *Meganyctiphanes norvegica* in different seasons.

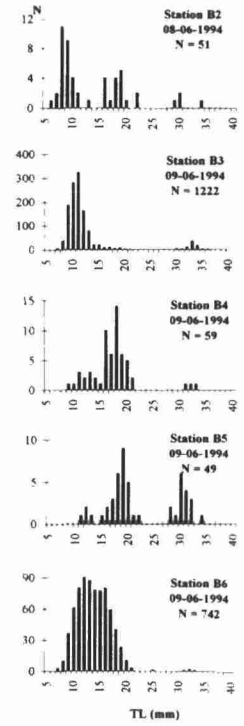

Fig. 2. Size gradients of juveniles in June along the transect B.

CETACEAN STRANDINGS IN THE AEGEAN AND MEDITERRANEAN COASTS OF TURKEY

B. Öztürk[1]* and A. A. Öztürk[2]

[1] Faculty of Fisheries, [2] Science and Technology Institute, Istanbul University, Ordu Cad. 200, Laleli-Istanbul, Turkey

Abstract

Cetacean fauna on the Turkish coast of the Aegean and Mediterranean seas has little been studied. To elucidate the cetacean fauna in the area, we compiled the cetacean stranding data during 1990-1997 on the Turkish coasts of the Aegean and Mediterranean seas. A total of 23 stranded cetacean was recorded. Those were (number of individuals): *Tursiops truncatus* (9), *Stenella coeruleoalba* (7), *Ziphius cavirostris* (3), *Delphinus delphis* (2), *Physeter catodon* (1), and *Pseudorca crassidens* (1).

Key-words: cetacean, Eastern Mediterranean

Turkey has a long coastline along the Aegean and Mediterranean Seas. However, not much effort has been made to understand the cetacean fauna there and little information is available so far (1, 2, 3). Cetacean fauna can be investigated by studying accidentally caught and stranded animals as well as by direct observation of live animals at sea and from land. The present study was made preliminarily to elucidate the cetacean fauna on the Turkish coast of the Aegean Sea and Mediterranean Sea by compiling the information on strandings.

The present study was made on the Turkish coasts of the Aegean and Mediterranean Seas, from the western end of the Çanakkale Strait in the north to the Syrian border in the east (Fig. 1) from January 1990 to April 1997. Stranded specimens were collected and identified. Fresh specimens were measured, the sex was identified and photos were taken. As a total, 23 strandings were recorded (Table 1). This number is small in spite of the seven years of study period and the long coastline of the Aegean and Mediterranean Seas. We assume that many of the strandings were not reported. Thus the result and conclusion presented here are considered to be only preliminary.

The most common stranding species was *Tursiops truncatus* (9 individuals), followed by *Stenella coeruleoalba* (7 individuals). *Ziphius cavirostris, Delphinus delphis, Pseudorca crassidens,* and *Physeter catodon* were rare. Marini *et al.* (4) reported that the most frequently encountered species was *T. truncatus* followed by *S. coeruleoalba* in the Aegean Sea. Assuming that the stranding data reflect the fauna partly, if not fully, the present result agrees with Marini *et al.* (4) as well as the strandings in the Hellenic Seas (5). Beside those reported here, as a member of the cetacean fauna in the Turkish waters, *Balaenoptera physalus* should also be included since one specimen stranded in Antalya in 1971 (3). Some other species, such as *Grampus griseus* and *Globicephala malaena*, which can be seen in the Turkish Mediterranean Sea (2,3), were not reported here.

No seasonal trend nor distributional trend was observed, probably due to the small sample size. The Aegean and Mediterranean coasts of Turkey are crowded with many tourists during summer, thus one can assume that the chance of finding strandings is higher compared to quiet winter months, if there is no seasonal trend. However, we did not see any peak of strandings in summer. It possibly means that there may be more strandings during off-touristic season. However, the sample size is too small to make conclusion here.

In 1990-1991, the epizootic affected *S. coeruleoalba* in the Mediterranean, which resulted in mass die-offs of this species (6), followed by the second outburst in 1991-1992 (7). Many strandings were reported in all Mediterranean countries, including Greece, which shares the Aegean Sea with Turkey (5). On the Turkish coast, we identified no stranding of *S. coeruleoalba* during that period, except one specimen in Karaburun and another one in Sifne in 1993, after the outbreak. However, some local source indicated that there were about 20 strandings of *S. coeruleoalba* in 1992 in Kusadasi in the Central Aegean Sea (unpublished data). We could not confirm this strandings by ourselves, as we learned this information in 1993, this could be the evidence of the effect of the epizootic, as mentioned by Aguilar and Borrell (7) and Visser *et al.* (8). Except this information, no other mass die-offs were reported. This may be due to the low survey effort or the effect was not so strong as in the other Mediterranean countries such as Spain, Italy and Greece.

The present study agreed to the fundamental composition of the cetacean fauna of the Aegean and Mediterranean seas, however it points out the necessity to establish a national cetacean stranding network along the coastline of Turkey and also to educate volunteers to cover wider areas on the Turkish coastline and to collect more systematic and reliable data on species identification as well as other biological parameters.

Table 1. List of strandings along the Turkish coasts of the Aegean and Mediterranean Seas in 1990-1997.

Species	B.L. (cm)	Sex	Place*	Year	Month
Stenella coeruleoalba	-	-	Davutlar(A)	1990	Jan
Physeter catodon	525	-	Seferihisar(A)	1990	Jan
Tursiops truncatus	230	M	Mordogan(A)	1990	Jan
Stenella coeruleoalba	-	-	Kusadasi(A)	1990	Mar
Delphinus delphis	224	-	Cesme(A)	1991	-
Tursiops truncatus	238	F	Foca(A)	1992	Sep
Stenella coeruleoalba	-	-	Cesme(A)	1993	Feb
Tursiops truncatus	286	-	Kemer(M)	1993	May
Stenella coeruleoalba	-	-	Karaburun(A)	1993	Jul
Tursiops truncatus	268	-	Karatas(M)	1993	Aug
Stenella coeruleoalba	180	M	Gokceada(A)	1994	Jul
Ziphius cavirostris	800	-	Serik(M)	1994	Jul
Pseudorca crassidens	390	F	Urla Port(A)	1995	Jan
Tursiops truncatus	-	-	Behramkale(A)	1995	Mar
Stenella coeruleoalba	-	-	Marmaris(A)	1995	Apr
Ziphius cavirostris	-	-	Oren(A)	1995	Jun
Delphinus delphis	-	-	Turgutreis(A)	1995	Jun
Stenella coeruleoalba	187	M	Karatas(M)	1996	May
Tursiops truncatus	245	F	Iskenderun(M)	1996	-
Tursiops truncatus	-	-	Alanya(M)	1996	-
Tursiops truncatus	-	-	Fethiye(A)	1996	-
Tursiops truncatus	219	-	Narlidere(A)	1997	Apr
Ziphius cavirostris	610	M	Dalyan(A)	1997	Apr

Place*: (A)-Aegean Sea coast, (M)-Mediterranean Sea coast

Acknowledgments

We thank to Nuri Basusta at Mustafa Kemal Univeristy, Ayhan Dede at Istanbul University, as well as local volunteers who have been helping our study, and Turkish Marine Research Foundation for the financial support.

References

1 - Marchessaux D., 1980. A review of the current knowledge of the cetaceans in the Eastern Mediterranean Sea. *Vie Marine,* 2: 59-66.

2 - Öztürk B., 1995. Marine mammals inventory of Turkey. In: European Research on Cetaceans - 9, Evans P.G.H., Nice, H., eds., Kiel, Germany: 96-98.

3 - Öztürk B., 1996. Whales and Dolphins. Anahtar Publ., Istanbul: 119p. (In Turkish.)

4 - Marini L., Carpentieri P., Consiglio C., 1995. Presence and distribution of the cetological fauna of the Aegean Sea: Preliminary results. In: European Research on Cetaceans - 9, Evans P.G.H., Nice, H., eds., Kiel, Germany: 99-101.

5 - Frantzis, A., 1997. Cetaceans and cetology in the Hellenic Seas. In: European Research on Cetaceans - 10, Evans P.G.H., ed., Kiel, Germany: 114-118.

6 - Aguilar A., Raga J. A., 1993. The striped dolphin epizootic in the Mediterranean Sea. *Ambio,* 22(8): 524-528.

7 - Aguilar A., Borrell A., 1994. Abnormally high polychlorinated biphenyl levels in the striped dolphins *(Stenella coeruleoalba)* affected by the 1990-1992 Mediterranean epizootic. *The Science of the Total Environment,* 154: 237-247.

8 - Visser I. K. G., van Bressem M. F., Barrett T., Osterhaus A. D. M. E., 1993. Morbillivirus infections in aquatic mammals. *Vet. Res.,* 24: 169-178.

ENVIRONMENTAL CHARACTERISATION AND MACROBENTHIC COMMUNITIES OF THE NORTHERN ADRIATIC "PAGURO" WRECK

Massimo Ponti *, Alessandro Capra, Giovanni Gabbianelli & Victor Ugo Ceccherelli
Corso di Laurea in Scienze Ambientali, University of Bologna, Via Tombesi Dall'Ova 55, 48100 Ravenna, Italy

Abstract
The "Paguro" drilling platform wreck has today come to constitute an artificial reef of particular interest. The aim of this study has been to characterise this habitat and to investigate the distribution of macrobenthic communities in relation to the main chemical and physical parameters of the water. For this purpose, a graphic three-dimensional reconstruction of the wreck has been made, direct samples of macrobenthos have been taken, and, finally, photographic transects have been performed. The data thus obtained have been subjected to statistical analysis.

Key-words : Artificial Reefs, Zoobenthos, Biodiversity, GIS, Adriatic Sea

Introduction

Artificial reefs, whether intentionally constructed (such as, for example, pyramids of concrete blocks and cages) or accidentally created by wrecks, not only substantially contribute to enhance biological coastal resources but also permit the exploitation of marine coastal eutrophication, as numerous studies carried out world-wide have shown (1, 2, 3, 4, 5, 6).

The area covered by the present research is that of the AGIP "Paguro" drilling platform wreck. The platform sank 12 miles offshore from Ravenna (Adriatic Sea) on September 29, 1965 owing to the eruption of underground methane gas. The wreck currently lies on a 24-m deep pelitic soft bottom.

Regarding the Northern Adriatic, several studies have been conducted on first fouling stages (7, 8) and on the mussel's communities (9). Unfortunately, however, know exhaustive studies as so far been made on the macrobenthic communities of the artificial substrata at the climax stage.

The wreck provides refuges and burrows which afford protection to the reproducing organisms, to the juvenile forms of many species, and to Crustacea during moulting. It also constitutes an ideal environment for the spawning of Cephalopoda and Gastropoda. These reefs represent an attraction centre for esteemed fish (tertiary consumer), thanks to the protection and abundant nourishment afforded by them, and moreover become an important tourist attraction.

Material and Methods

The study has entailed several phases beginning with initial area recognition followed by submerged structures surveying and by subsequent sampling. The area surveying was carried out both from the sea surface using a GPS receiver, a Side Scan Sonar and an Echosounder and underwater employing a tape measure and a depth gauge. Twenty-four direct samples and five photographic transects were taken for the purpose of identifying and defining the benthic communities colonising the area as well as their distribution as a function of the more salient environmental parameters. The samples were obtained by scraping off all organism from 20 x 20 cm quadrates. The photographic transects include 55 pictures for a total usable covering area of about 7.8 m^2.

Discussion

The survey permitted the graphical reconstruction both of the original platform and of the present wreck (Fig. 1). Gas eruption has created a crater about 10 metres in depth so that the metallic structures raise up to a height of 8 to 34 metres below the surface. The three-dimensional model of the wreck was then entered, according to its actual position, in a digital cartography obtained by the geographical information system (GIS), on the basis of which it was possible to highlight the interactions between communities and environment and to follow their development over time.

Amongst the more important environmental parameters taken into consideration are the meteomarine ones (wind, current, wave) and chemical and physical ones such as temperature, dissolved oxygen, salinity, pH, etc.. All these parameters were closely monitored over time.

Direct samples were taken on areas of standard size in order to study the benthic communities on the basis of preliminary visual and photographic evidence (10). Moreover, vertical photographic transepts were made according to the cartographic literature of benthic communities (11). These transects permitted to extend the information derived from the samples to a wider area and to identify the transitions from one community to another along the vertical gradients. Analysis of the samples yielded interesting information, revealing in fact an unusual situation, not wholly falling within the parameters of traditional bionomic classifications (12). In fact organisms typical of infralittoral and circalittoral hard bottoms were here found to be associated with other organisms which normally populate various types of soft substrata. A possible explanation is that these organisms on the wreck may be able to exploit the organic and inorganic debris of the microhabitat which accumulate in crevices of the wreck structure and among the shells of mussels, found between -8 and -12 m, and those of oysters, encountered between -12 m and the bottom (Fig. 1). Typical organisms found in the samples include the common brittle star *Ophiothrix fragilis*, the polychaetes which are characteristic of detrital environments *(Harmathöe spinifera, Marphysa sanguinea, Polydora ciliata, Nereis succinea,* etc.) and of hard bottoms *(Syllis hyalina, Serpula vermicularis, Pomatoceros triqueter,* etc.), the decapods *(Alpheus sp., Pisidia longimana, Pilumnus hirtellus,* etc.), the isopod *Janira* sp. and the anphipods *Corophium sextone* and *Microdeutopus similis.* As it was to be expected, numerous bivalve species, amongst which the prevalent ones included *Mytilus galloprovincialis* and *Crassostrea gigas,* barnacles *(Balanus trigonus),* sponges, anthozoa (in particular *Epizoanthus arenaceus)* and sipunculida, were also found.

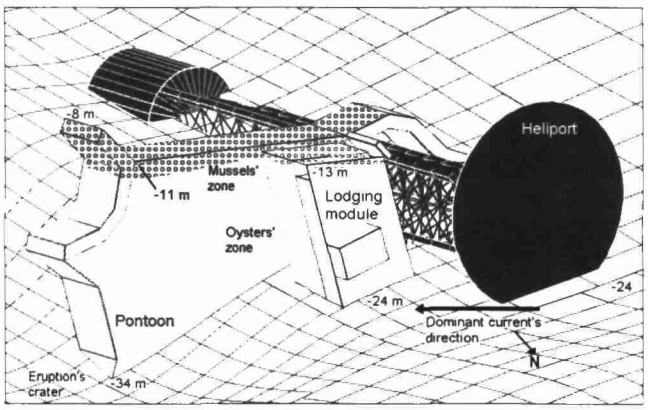

Fig. 1 - Graphic three-dimensional reconstruction of the wreck obtained with a computer using CAD software integrated in a Geographical Information System. The highest biodiversity is observed in more exposed walls to the current of the lodging module.

All data were processed by non-parametric multivariate analysis (13, 14). One of the most interesting aspects which emerged from statistical analyses is the interpretation of community distribution as a function of the different environmental variables considered. Amongst these variables, the most significant ones were found to be oxygen and salinity, which vary with depth, and exposure to dominant currents (Fig. 1). These findings agree with those of other authors (15). Amongst the hypotheses formulated, there is the possibility for the mobile organisms such as echinoderms and crustaceans to avoid the risk of anoxia which may occasionally occur near the bottom, even in this area which is so far from the coast, by migrating along the structures (Fig. 2).

The "Paguro" wreck can therefore be considered an interesting example of an artificial reef characterised by a high biodiversity and by a complex community distribution pattern. By furnishing a considerable surface area for the colonisation of sessile organisms, the wreck's structures permit an increase and diversification of algae and

BEHAVIOUR OF THE EXPLOITED DEMERSAL RESOURCES OF THE LIGURIAN SEA THROUGH TWELVE YEAR SERIES OF BIOMASS INDICES.

G. Relini*, A. Zamboni, D. Massi, F. Fiorentino

Università degli studi di Genova, Istituto di Zoologia, Laboratori di Biologia Marina ed Ecologia Animale, Via Balbi 5, 16126 Genova, Italia

Abstract:

Two short time series of independent biomass indices were used to describe behaviour of the main demersal resources of the Ligurian Sea (NW Mediterranean Sea). Data were obtained from seasonal stratified trawl surveys and the monitoring of landings of the commercial trawlers. Although there were differences between the two sets of data, the overall trends seem to be quite coherent. *Eledone cirrhosa* has shown a clear increase from 1987 onward, while *Aristeus antennatus* has been decreasing since 1988. Other species, such as *Merluccius merluccius* and *Mullus barbatus* show evident seasonal variation in both indexes, with no signs of an overall trend. *Nephrops norvegicus* fluctuates with lowest levels of abundance between 1989 and 1993; at the present it is in an increasing phase. *Micromesistius poutassou* shows no evident regularities in biomass fluctuation.

Key-words: demersal, trawl surveys, time series, Ligurian Sea.

Introduction

The variation of abundance of the exploited resources is one of the most exciting subjects in stock assessment. Although most of the models used assume the steady state, it is evident that only few species behave according to the equilibrium hypothesis. The aim of this study is to describe the abundance dynamics of the main demersal resources of the Ligurian Sea (NW Mediterranean Sea) by means of two short time series of independent biomass indices obtained from seasonal trawl surveys and the monitoring of commercial landings. Although there are often discrepances in results given by the two different methods, the comparison of abundance trends indicated by surveys and observations of landings is considered one of the most promising approaches in stock assessment (1).

Materials and methods

The indices of abundance have been assessed during programmes on the evaluation of demersal stocks, promoted by Italian Government and the European Union from the middle of the 80s onward.

Data concern the main demersal target species in the Ligurian area and in most of the seas surrounding Italy: *Mullus barbatus* Linneus, 1758, *Merluccius merluccius* (Linneus, 1758), *Micromesistius poutassou* (Risso, 1826), *Eledone cirrhosa* (Lamark, 1798), *Aristeus antennatus* (Risso, 1816) and *Nephrops norvegicus* (Linneus, 1758).

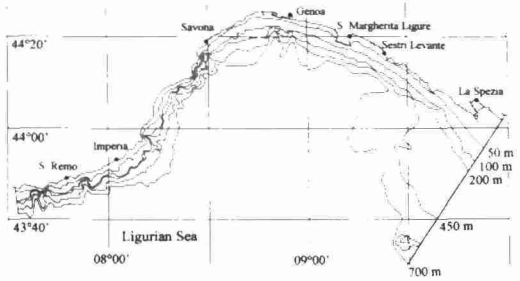

Fig. 1 - Ligurian bottoms sampled during the trawl survey programmes. The isobaths delimiting the bathymetric strata are shown. The main trawling sites of the Ligurian coast are also indicated.

The first set of data consists of standardized catch indices obtained during trawl surveys from 1985 to 1995, carried out in spring and in late summer/early autumn (2, 3). Hauls were effected during day light on bottoms at depths between 10 and 700 m off the Ligurian coast (Fig.1). Catches per hour of trawling were used to estimate two different average indexes of biomass in the sea for each survey. Since data do not present a normal distribution, the traditional arithmetic mean is given together with the median.

The second set of data derives from the monitoring of commercial landings made by trawlers from Santa Margherita Ligure (eastern Ligurian coast), which is the most representative fishing site on the Ligurian coast in terms of numbers of trawlers and variety of trawling types (4).

The fishing grounds trawled by the S.Margherita Ligure fleet are in the central/eastern part of the area explored by the trawl surveys from the canyons off Genoa eastward (Fig.1). Landings were monitored from July 1987 onward twice a month. Mean monthly landings per boat per day of fishing (CPUE) were calculated keeping trawlers fishing on bathyal bottoms separated from those operating on neritic grounds. Data shown were smoothed by means a three - point running average.

Results

The evolution of the biomass indices of the main resources shows different patterns. Hake seemingly fluctuates without a clear trend (Fig.2). However, it is possible to find regular signs of the late spring/early summer hake recruitment, which is the most important of two occurring every year in the Ligurian Sea (5, 6), observing the high biomass indexes in summer/autumn trawl surveys. These maxima, due mainly to recruits of 0+ groups, seem to become peaks in landings during the late winter and spring of the following year, when fish belong to 1+ group. Unfortunaly data are insufficient to test the lag between the two index maxima statistically.

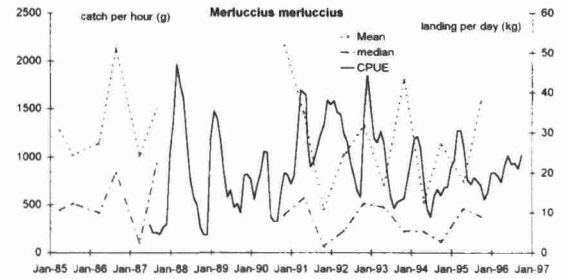

Fig. 2 - Evolution of abundance of hake as shown by trawl surveys and the monitoring of commercial trawler yields. Trawl survey biomass indices are given as mean and median of catches per hour of trawling; landings as average per trawler per fishing day (CPUE).

Differently, white horned octopus show a clear overall increase from 1987 onward, both on the basis of landings and trawl surveys (Fig.3).

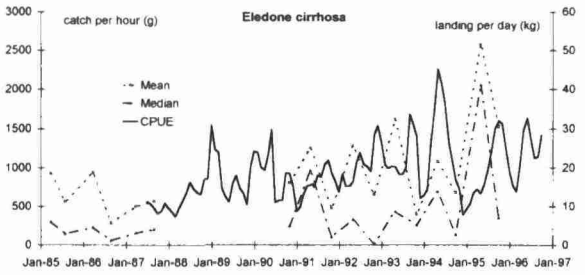

Fig.3 - Evolution of abundance of white lesser octopus as shown by trawl surveys and the monitoring of commercial trawler yields. Trawl survey biomass indices are given as mean and median of catches per hour of trawling; landings as average per trawler per fishing day (CPUE).

Red mullet show a regular seasonal variation in both biomass indices with maxima during the autumn (Fig.4). These high catches are due both to the growth of young fish recruited in August in infralittoral bottoms (7) and to autumn migration on deeper levels, which increase their vulnerability to trawling.

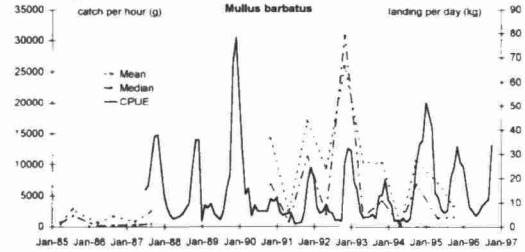

Fig.4 - Evolution of abundance of red mullet as shown by trawl surveys and the monitoring of commercial trawler yields. Trawl survey biomass indices are given as mean and median of catches per hour of trawling; landings as average per trawler per fishing day (CPUE).

NURSERY AREAS AND SOME BIOLOGICAL INFORMATION OF TUB GURNARD *(TRIGLA LUCERNA L.* 1758) OFF TUSCANY COASTS (ITALY)

F. Serena, A. Voliani,* R. Auteri

Agenzia Regionale per la Protezione Ambientale della Toscana (G.E.A.), Via dell'Ambrogiana 2 - 57127 Livorno, Italy

Abstract

Trigla lucerna is a demersal species that lives on the shelf up to 150 metres. Data proceed from several trawl surveys carried out in the North Tyrrhenian Sea; the major concentration zones and the nursery areas are defined. The length/weight relationship and the von Bertalanffy growth parameters are estimated: $W = 0.0139 * L^{2.8592}$; $K = 0.39$ $L\infty = 65.9$ $t_0 = 0$. The growth performance results similar to that estimated for Atlantic French coasts, but a clear time shift for the reproductive processes is observed.

Key-words: Fishes, recruitment, Tyrrhenian Sea, growth

Introduction

Trigla lucerna is a species that, in the northern part of Tuscany, has a certain commercial importance. It is often landed as a part of boxes composed by different species mixtures. Large sized fish are also landed but in this case, due to their greater commercial value, the boxes are composed exclusively by individuals of this species. In this note, the high density zones as well as the nursery areas, positioned on the northern portion of the studied area, are described. Moreover estimates of the parameters for both, von Bertalanffy growth equation and length/weight relationship are given.

Material and methods

From 1985 to 1996, several bottom trawl-surveys have been carried out in the northern portion of the Tuscan Archipelago (North Tyrrhenian Sea). Some of these surveys were done monthly and utilising an extremely small meshed cod end (mesh size = 3 mm). This allowed us to catch the fish immediately after they were recruited to the ground. For the estimation of the length/weight relationship, morphobiometric data of 538 individuals separated by sex and ranging from 2 to 70 cm of total length were utilised. The von Bertalanffy growth parameters were estimated by means of the analysis of the length distributions, utilising the program MULTIFAN (1).

Results and Discussion

a) The analysis of the trawl-surveys data carried out in the area defined by the Magra River towards the North and the Elba Island towards the South (GRUND Program) (2) allowed to define a major concentration of individuals of *T. lucerna* just off the Versilian coasts (3) (fig. 1). The species was found on a wide depth range from shallow waters to 150 meters, but the higher densities were observed near shore, between 10 and 70 m. Moreover the existence of a clear relationship between the abundance of certain size classes and the depth has been observed. In fact, the younger individuals have been more frequently found in shallow waters while the adults more dispersed towards off shore and a consistent nursery area was identified along the coastal area where several river mouths (Arno, Magra and Serchio rivers) are positioned (4) (fig. 1).

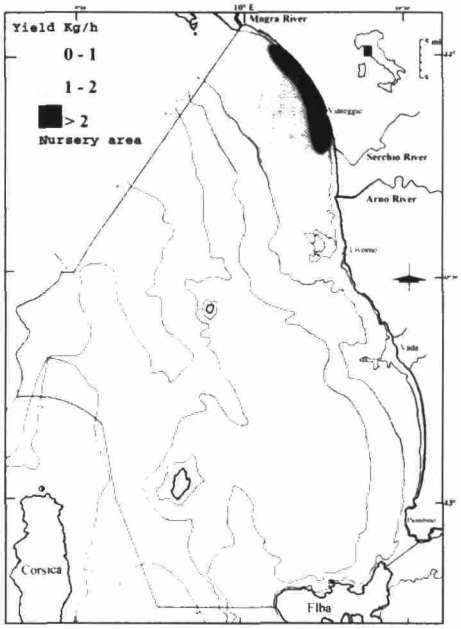

Fig. 1 Geographical distribution and nursery area of *T. lucerna*.

This is in agreement with what has been observed in other Mediterranean and Atlantic areas. In fact, in these areas, juveniles of *T. lucerna* are concentrated in shallow waters, mainly in estuarine waters where food is abundant (5, 6, 7, 8). The geomorphologic and biological characteristics of the bottom make the environment suitable for the juveniles needs. Along the Versilian coasts, the presence of the above mentioned river mouths produces a very high nutritional loading (9) and very specific bio-sedimentological characteristics. In shallow waters up to 10 m, the medium sandy bottoms prevail; towards higher depths, the muddy component increases, reaching practically the 100% level at depths higher than 50 m (10). Moreover marine phanerogams prairies are not locally present and the benthic assemblage is that characteristic of the circalittoral zone, mainly composed by shelf terrigenous mud (11). These facts should explain the massive presence of the species in this area.

b) 11025 individuals of tub gurnard were caught, with a strong dominance of individuals smaller than 15 cm TL. The following parameters of the length/weight equation were obtained:

$W = 0.0139 * L^{2.8592}$ ($r^2 = 0.994$),

where W = weight in grams and L = total length in cm.

There were not found statistically significant differences between sexes. This is in agreement with the Papaconstantinou (6) results.

The von Bertalanffy growth parameters, estimated with the MULTIFAN program utilising length distributions (fig. 2) are:

$K = 0.39$ $L\infty = 65.9$ $t_0 = 0$

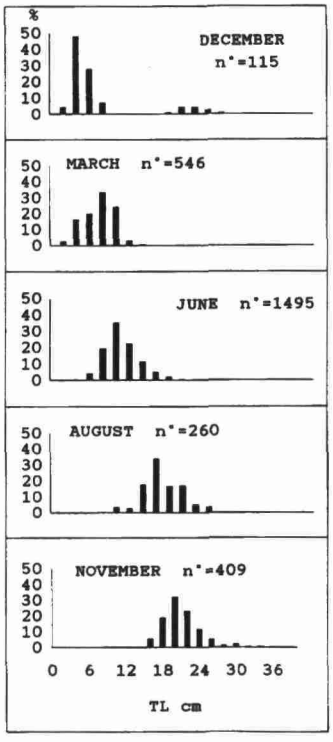

Fig. 2 Length distributions (T.L.) of *T. lucerna*.

A SYNTHESIS OF THE ECHINODERM FAUNA OF THE TYRRHENIAN SEA

Paola Rinelli

Istituto Sperimentale Talassografico, C.N.R., Spianata San Raineri 86, Messina, Italy

Abstract

The bathymetrical distribution of 100 species of echinoderms of the Tyrrhenian Sea is reported. The data mentioned in this paper are obtained both from literature and from quantitative samplings carried out during several oceanographic cruises and trawl surveys.

Key-words: Zoobenthos, biogeography, bathymetry, Tyrrhenian Sea

Existing data on echinoderms of the Italian coast are very scarce, specially in the southern Tyrrhenian sector. Besides this taxon, rarely considered on a bionomic level, has already shown to be an effective environmental describer in previous studies (1, 2).

This contribution deals with the results of a long-term (1988-1996) faunistic study on echinoderms. A list with the relative bathymetrical distribution of the Tyrrhenian Sea echinoderm fauna is reported (Tab. 1).

The described results refer to samples taken from several oceanographic cruises carried out, by our research group, in different areas of the Tyrrhenian Sea: Tuscan and Pontian Archipelago, Eolian Islands, Straits of Messina, south Tyrrhenian coast from Praia a Mare (Calabria) to Capo S. Vito (Sicily). Samplings were carried out, from mediolittoral to bathyal level, by dredge, grab or trawl net, according to the aim of the project. Moreover these data have been integrated with the scarce existing literature. At this regard the species, most of them very little known along italian coasts, signalized only by Tortonese in his work of 1965 (2) are distinguished in table 1 ("T") from the others reported in specific papers' faunistic lists published in the following years (4-10).

A total of 100 species of echinoderms (2 Crinoidea, 31 Holothurioidea, 22 Asteroidea, 23 Ophiuroidea, 22 Echinoidea) are known, till now, in the Tyrrhenian Sea. Therefore at the present state of the art, the tyrrhenian species are the 65 % of the whole mediterranean echinoderm fauna. Infact at the moment 153 species are known in the Mediterranean Sea; Tortonese in 1979 in a wide review of the mediterranean echinoderm fauna enumerated 144 species, after that at least nine more species were signalized in different area of this basin (11-17).

Generally, as regard the spatial distribution the fifty percent of the species is widespread in the whole Tyrrhenian Sea. Only few species were collected in one or two sampling area. Amongst the 100 Tyrrhenian species reported in this paper, 14 are mentioned only in Tortonese's (1965) work (nearly all findings are referred to the Gulf of Naples) and never mentioned in any more pubblications. Moreover 6 species *(Ocnus petiti, Leptosynapta inhaerens, Amphiura securigera, Ophiactis balli, Ophiocomina nigra, Echinocardium mediterraneum)*, considered rare in the whole mediterranean basin, are recorded for the first time in the Tyrrhenian Sea.

In particular amongst the brittle stars, three species are worth mentioning: *Ophioconis forbesi* collected only in the Tuscan and Pontian Archipelagoes, species characteristic for detritic bottoms; *Amphiura securigera* signalized up to now only three times in the Mediterranean Sea (18) and *Ophiactis balli,* an atlantic very rare species found in the Messina Straits so abundant to form a facies (19).

Besides, in the Straits of Messina, that however must be considered a very particular environment, two more "rare" species were collected: the echinoid *Arbaciella elegans* (20), signalized only four more times in italian waters (21, 22, 10, 23) and the little sea cucumber *Ocnus petiti,* found in the Mediterranean only along French coasts (22). Four specimens of this species (Rinelli, not yet published) were collected dredging over hard substrata characterized by populations of the Stylsteridae *Errina aspera* (19).

Moreover amongst the sea stars *Sclerasterias richardi,* rarely found in the Italian Mediterranean Sea, was collected only in the Tuscan Archipelago and along Sicilian coast, with only one specimen per each site. *Chaetaster longipes,* considered scarce in the Tyrrhenian Sea, was collected only along Sicilian coast by trawl net (two specimens). As regard the distribution in the Mediterranean Sea of this species, the recent literature reveals that it is not more so rare as thought in the past (24).

As regard Holothurioidea taxon, in addition to *O. petiti* mentioned above, other two little rare species were found: *Molpadia musculus* (Tuscan Archipelago and Calabrian coast) and *Leptosynapta minuta,* recorded for the second time in the Italian Mediterranean Sea (25 and Rinelli not yet published). However also this species is now more widespread in the Mediterranean (5, 17) than was stated in the older literature.

It is not easy to make a confront with the echinoderm fauna of other Italian sectors, because of the scarce literature. Besides the two synthesis works of Tortonese (3, 5) the few data available regard the central and south-western Adriatic Sea (26, 27), the Ligurian Sea (28, 29, 30, 31, 32) and the Sardinia seas (33). It is worth underlining the presence in the italian waters of 14 mediterranean species not yet found in the Tyrrhenian Sea, namely *Labidoplax buski, Sclerasterias neglecta, (Adriatic Sea), Thyone gadeana, Pseudothyone raphanus, Ceramaster grenadensis, Allopatiria ocellifera, Amphilepis norvegica, Ophiocten abyssicolum, Ophiura grubei, Ophiura carnea, Hemiaster expergitus, Echinocardium fenauxi, Plagiobrissus costai* (Ligurian Sea) and *Odontaster mediterraneus* (Sardinia).

References

1.- Giacobbe S., Rinelli P., Spanò N., 1996. Echinodermi e crostacei decapodi in fondi mobili litorali del versante calabro dello Stretto di Messina. *Biol Mar. Medit.* 3(1): 400-406.

2.- Rinelli P., Spanò N., 1996. Decapod crustaceans and echinoderms in insular detritic environments: Tuscan Archipelago and Pontian Islands. *Annales SHN,* vol 9 (3): 73-78.

3.- Tortonese E., 1965. Echinodermata - Fauna d'Italia, VI. Ed. Calderini, Bologna, XIII+422 pp., 186 figg.

4.- Gustato G., Villari A., 1979. About the question of the taxonomic status of *Holothuria stellati* Delle Chiaje. In: Proceedings of the Europ. Colloquium on echinoderms. 3-8 september 1979. Eds. Balkema, Amsterdam: 107-111.

5.- Tortonese E., 1979. Review of the present status of knowledge of the Mediterranean Echinoderms. In: Proceedings of the Europ. Colloquium on echinoderms. 3-8 september 1979. Eds. Balkema, Amsterdam: 141-149.

6.- Focardi S., Fresi E., Gambi M.C., 1982. Analisi della distribuzione degli echinodermi dei fondi mobili di due aree del tirreno: un'applicazione di tecniche multidimensionali. *Natur. Sicil., S.* IV, VI (suppl.), : 531-540.

7.- Colagnola R., Labanchi L., Fresi E., Chessa L.A., 1983-84. Distribuzione degli echinodermi nei fondi mobili del Golfo di Salerno: aspetto invernale. *Nova Thalassia,* suppl. 6: 637-644.

8.- Tortonese E., 1983. Gli Asteroidi viventi nei mari intorno alla Sicilia e Sardegna. *Natur. Sicil., S.* IV, VII (1-4): 19-33.

9.- Pellegrini D., 1990. Echinodermi del Mar Tirreno Settentrionale. *Oebalia,* suppl., vol. XVI-2: 721-724.

10. - Franceschini G., Chimenz Gusso C., 1994-95 – Echinodermi delle coste laziali. *Bull. Ist. Biol. Univ.* Genova, 60-61: 191-200.

11.- Lopez-Ibor Alino A. and Galan Novella C., 1982. Primera cita de *Aslia lefevrei* (Barrios, 1882) (Echinodermata; Holothuroidea) en el Mediterraneo. *Cah. de Biol. Mar.,* XXIII:269-273.

12.- Ocana A., De La Morena I., Moriana M., Alonso M. R., Ibanez M., 1982. Algunos Equinodermos de la costa de Malaga (Mar de Alboran). *Inv. Pesq.,* 46(3): 433-442.

13.- Alvarado R., Galan C., Lopez-Ibor A., 1986. Sobre la presencia de *Protoreaster nodosus* (Linneo, 1758) (Echinodermata, Asteroidea) en el Mediterraneo (Mallorca, Baleares). *Boll. Soc. Hist. Nat. Balears,* 30: 61-67.

14.- Perez-Ruzafa A., Lopez-Ibor A., 1986. Presencia de *Holothuria* (Vaneyothuria) *lentiginosa lentiginosa,* Marenzeller, 1893 (Echinodermata: Holothuroidea) en el mar de Alboran (Mediterraneo Occidental). *Bol. Int. Esp. Oceanogr.,* 3(4): 105-109.

15.- Alva V., 1987. Equinodermos batiales de la cubeta Catalano-Balear (Mediterraneo Nor-occidental). *Misc. Zool.,* 11: 211-219.

16. - Pancucci M. A., 1994a. Distribution and Zoogeography of the echinoderm fauna in Greek waters. *Biol. Gallo-hellen.,* 22: 355-361.

PRELIMINARY DATA ON AGE DETERMINATION OF THE BLUEFIN TUNAS *(THUNNUS THYNNUS L.)* CAUGHT IN THE ADRIATIC SEA

Vjekoslav Ticina* and Ivo Kacic

Institute of oceanography and fisheries, Set. I. Mestrovica 63, 21000 Split, Croatia

Abstract

Age determination of the bluefin tuna *(Thunnus thynnus L.)* was done using cross section of the first spin in the first dorsal fin. The age is determined in the 100 specimens with various fork lengths. The range of the fork lengths of the sampled specimens was between 50 and 127 centimeters. Six different age-classes are found in the sample.

Key-words: fishes, biometrics, Adriatic sea

Introduction

The age of bluefin tuna can be determined in different ways. Some different methods for this purpose can be used. Usually, rhythmic markings on caudal vertebrae and in the otoliths were used (1, 2 and 3). Scales are not very useful, due to the small differences between summer and winter rings. Since Compean-Jimenez and Bard (4, 5) and Cort (6, 7) found that well-defined growth marks were evident on the first dorsal spines of bluefin tuna, we chose the first dorsal spine as a source for age estimation. Also, we found this method the most appropriate for our sample because there was a little damage to the sampled fish. Thus, the commercial value of the sampled fish did not decrease.

Scaccini (8), Morovic (9), Vilicic (10), Alegria-Hernandez (11,12) and Ticina (13) reported that mainly small and juvenile specimens of bluefin tuna were caught in the Adriatic sea by purse-seiners. However, the age composition of these fish have not been determined. The objectives of our study were to estimate the age of bluefin tunas caught in the Adriatic, from growth bands on dorsal spine sections.

Material and methods

The random sampling of the bluefin tuna for age determination was done at sea from March to October of 1993 and 1994 year. Specimens used for the analyses were taken from different catches of the bluefin tuna obtained by purse-seine in the Adriatic sea. First spines of the first dorsal fins were cut near the spine base, using a fine saw (Fig. 1.). We collected 100 first dorsal spines from the specimens with various fork lengths.

Figure 1. Sampling of the first dorsal spine.

Cross sections of the dorsal spines were done using a slow rotation fine saw. After that, cross sections were ground until a thickness of 0.5 mm was reached and washed in the 95 % ethyl alcohol. Binocular microscope was used for age reading.

Typical growth patterns on bluefin tuna spines included a narrow translucent zone, which we assumed to be a winter slow-growth stage, and wider opaque zones which probably represents fast growth during summer (Fig. 2). On the basis of these differences in the skeletal structure of the spines, the age of different specimens was determined. In addition, the diameter of the spine was measured, with tolerance +/- 0.01 mm.

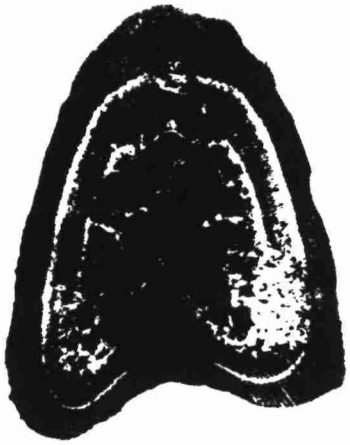

Figure 2. Cross section of the first dorsal spine of bluefin tuna (*Thunnus thynnus* L.)

Results

Fork lengths of the specimens of the sampled bluefin tunas were between 50 and 127 centimeters. Length structure of the sample, grouped in the 5 cm classes, is shown on the Figure 3. After age reading analysis, six different age-classes are found in the sample.

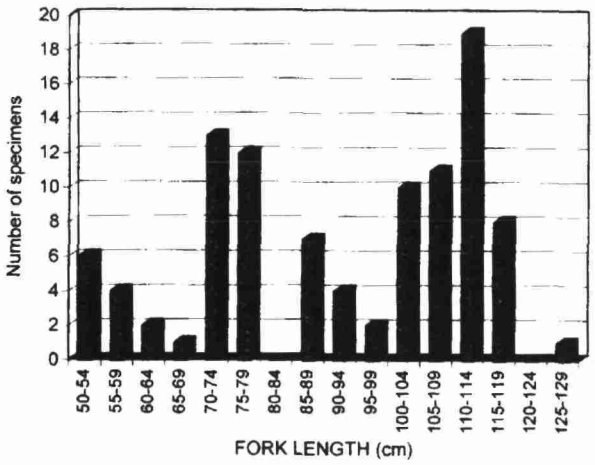

Figure 3. Length structure of the sample.

In the first class we found fish till one year old ($A=0^+$) with fork length less than 58 cm and weight till 3.5 kg. Diameter of the spine was less than 3.15 mm.

In the second class we found fish till two years old ($A=1^0$ and $A=1^+$) with fork length more than 60 and less than 75 cm. This specimens weighted from 4.5 to 8.5 kg. Diameter of the spine was 3.60 - 4.54 mm.

DECAPODA CRUSTACEA IN THE SOUTHERN TYRRHENIAN SEA - FIVE YEARS OF RESEARCH

Nunziacarla Spanò

Department of Animal Biology and Marine Ecology, University of Messina, Salita Sperone 31, S.Agata 98167 Messina, Italy

Abstract

We report data on Crustacea Decapoda in the Southern Tyrrhenian Sea, with their bathymetric distribution and biogeographic characteristics. A total of 297 stations were sampled; 95 species of Crustacea Decapoda were identified. The data reported provide a contribution to the knowledge of Crustacea Decapoda, on which there is very little documentation in the Southern Tyrrhenian Sea.

Key-words: decapoda, Tyrrhenian Sea, Bathymetry, Biogeography

Introduction

The current knowledge concerning the faunistic composition of benthic populations, in the Southern Tyrrhenian Sea, is still very scarce. In fact, although the sea-bed of this area has been studied since 1970 (1, 5), no specific research line has ever been carried out. The data reported in this paper concern a specific project carried out by our group on the biodiversity in this area. In particular the results reported here are the first concerning the Crustacea Decapoda, taxon on which there is still very little documentation.

Materials and methods

The results refer to several oceanographic cruises carried out in the Southern Tyrrhenian Sea between 1992 and 1996. The studied area extends from Capo S. Vito (Western Sicily) to Capo Suvero (Calabria). Samples of sediment were taken with a modified "Van Veen" grab with sampling capacity of 70 dm^3 and 0.25 m^2 surface area. Living macrofauna was obtained by sieving the sediment through a 1 mm mesh screen. Trawl-survey samplings were carried out by a trawl net with a mesh size of 40 mm. The Crustacea Decapoda were extracted and determined to specific level.

Results and discussion

Altogether the Crustacea Decapoda were found in 137 stations, from 0 to 140 meters depth, and in 160 hauls between 0 and 700 m. In table 1 the list of the species found is shown. In particular, the species collected along the Sicilian coast (75 species) resulted being more abundant than those found along the Calabrian coast (50 species).

With regard to the bathymetric distribution, 44 Decapoda were found between 0 and 60 meters deep in the infralittoral zone, 11 were found between 60 and 200 meters in the circalittoral zone and 10 in the bathyal zone below 200 meters. Finally, some species show a wide distribution (about 0-500 m).

The biogeography of Crustacea Decapoda shows the same characteristics of this all Mediterranean fauna (6, 7, 8). Taking the Mediterranean as a "province" of the wide Atlantic area, we notice that 65.4 % of this species shows an Atlantic-boreal distribution (8). Even if within the Mediterranean Sea there is a further division between the Western, Central and Eastern basins, our data faithfully reflect Fredj's distribution (1974). In fact the most of the species encountered by us must be considered as species with Atlantic affinities. Such a "western" characteristic is considered even more evident by the presence of *Pilumnus inermis*, A. Milne Edwards & Bouvier, 1894. This species considered in literature to be predominantly Atlantic (9), in spite of numerous findings in the Western Mediterranean (10, 11, 12).

Nevertheless, it is worth underlining the presence of *Albunea carabus* (L., 1758) that Pérès (1967) considers as an element of a "Senegalian relict fauna", with a continuous distribution throughout the Eutyrrhenian Era. This author has also suggested that at present climatic barriers prevent the expansion of the Ibero-Moroccan species in the Eastern basin (14).

Finally, another species, found in the Southern Tyrrhenian Sea deserves a particular mention: *Parthenope expansa* (Miers, 1879) sampled exclusively in the Western Ionian Sea, along the Sicilian coasts, North of the Gulf of Catania, and also found by us in the Straits of Messina (12).

The faunistic diversity found in the Southern Tyrrhenian Sea is due to the particular geographical position of the examined area, which is situated between the western and central basins, with their respective fauna. In fact, although Crustacea Decapoda are characterized by a low population density, they have a good descriptive role even as far as biogeography is concerned (15).

References

1 - Arena P., Bombace G., 1970. Bionomie benthique et faune ichtyologique des fonds de l'étage circalittoral et bathyal des golfes de Castellammare (Sicile nord- occidentale) et de Patti (Sicile nord-orientale). *Journ. ichthyol.*, 145-156. XXII CIESM, Roma.

2 - Arena P., Li Greci F., 1973. Indagine sulle condizioni faunistiche e sui rendimenti di fondali batiali della Sicilia occidentale e della bordura settentrionale dei banchi della soglia siculo-tunisina. *Quad. Lab. Tecnol. e Pesca*, 4: 157-201.

3 - Bombace G., 1970. Sulle biocenosi e sulla malacofauna vivente e fossile del margine continentale e della zona batiale di alcuni fondali tirrenici della Sicilia. *Boll. Pesca Piscic. Idrobiol.* XXV: 169-181.

4 - Rinelli P., Spanò N., Greco S., 1997. Distribuzione di Crostacei Decapodi ed Echinodermi dei fondi strascicabili del Mar Tirreno Meridionale. *Biol. Mar. Medit.* in press.

5 - Spanò N., Potoschi A., 1997. Crostacei Decapodi ed Echinodermi di fondi mobili strascicabili del Basso Tirreno. *Biol. Mar. Medit.* in press.

6 - Fredj G., 1974. Stockage et exploitation des données en écologie marine. C - Considérations biogéographiques sur les peuplements benthiques de la Méditerranée. *Mem. Inst. Oceanogr. Monaco*, vol. 7:1-88.

7 - Fredj G., Laubier L., 1985. The deep Mediterranean benthos. In M. Moraitou- Apostolopoulou e V. Kiortsis (eds.) Mediterranean Marine Ecosystem: 109-145.

8 - Di Geronimo S.I., 1990. Biogeografia dello zoobenthos del Mediterraneo: origine e problematiche. *Oebalia* Suppl., Vol. XVI-1: 31-49.

9 - Manning R.B., Holthuis L.B., 1981. West african brachyuran crabs (Crustacea: decapoda). *Smith. Cont. to Zool.*, 306: 1-379.

10 - Garcia Raso J.E., 1985. New records of Crustacea decapoda from Alboran Island (Spain). *Bol. Soc. Entomol.*, suppl. 1: 11-18.

11 - Di Geronimo S.I., Fredj G., 1987. Les fonds à *Errina aspera* et *Pachylasma giganteum*. *Doc et Trav. IGAL*, 11:243-247.

12 - Spanò N., 1996. Distribution of Crustacea decapoda in the Straits of Messina. Colloquium Crustacea Decapoda Mediterranea Florence 12-15 September 1996. *Journ Nat. Hist. London*, 32, 6.

13 - Pérès J.M., 1967. The Mediterranean benthos. *Oceanogr. Mar. Biol. Ann. Rev.*, 5: 449-533.

14 - Giacobbe S., Spanò N., 1996. New records of *Albunea carabus* (L.) (Decapoda, Anomura) in the Mediterranean Sea. *Crustaceana*, 69,6: 719-726.

15 - Almaca C., 1985. Evolutionary and zoogeographical remarks on the mediterranean fauna of brachyuran crabs. In M. Moraitou-Apostolopoulou e V. Kiortsis (eds.) Mediterranean Marine Ecosystem: 347-366.

ESTIMATES OF DISCARDS IN THE HELLENIC COMMERCIAL TRAWL FISHERY

K.I. Stergiou [1]*, A. Economou [2], C. Papaconstantinou [2], N. Tsimenides [3], S. Kavadas [2]

[1]Aristotle University of Thessaloniki, Department of Biology, P.O. Box 134, 54006 Thessaloniki, Hellas
[2]National Centre for Marine Research, Agios Kosmas, Hellenikon, Athens 16604, Hellas
[3]University of Crete, Department of Biology, P.O. Box 1470, 71110 Iraklion, Crete, Hellas

Abstract

In the present work a first attempt is made to assess discards for the commercial trawl fishery in Hellenic waters. Overall, on-board sampling was conducted on 16 commercial trawlers for a total of 128 fishing days on 16 trawlers, carried out in 32 trips in four fishing areas during two fishing seasons (autumn-winter 1993, spring 1994). Our results showed that discarding is important for the Hellenic commercial trawl fishery and could be as high as 45% of the total trawl catch. Discard rates varied between species, areas and seasons and were found to be positively related to tow duration.

Key-words: Fisheries, Eastern Mediterranean

Introduction

Discarding at sea, which is an important problem in fisheries and a major source of uncertainty in fisheries management, may result from economic constraints or from legal and administrative obligations imposed by the managerial scheme employed (1). Available studies have estimated the global discarded bycatch of fisheries at about 27 million t per year (2). The Mediterranean fisheries are highly diverse in terms of species and fishing gears used and are not managed based on TACs and quotas. Hence, discarding is perceived mainly as throwing away unmarketable species or species and size groups of low commercial value, because of legal obligations imposed by regulations on minimum landing sizes. Currently, there is not any information on numbers, weights and sizes of fish discarded by fishing vessels in the Eastern Mediterranean other than those derived from experimental surveys (*e.g.*, 3). However, because the term "non-commercial" is subjective it cannot be applied to research vessel catches. In the present work a first attempt is made to assess discards for the commercial trawl fishery in Hellenic waters through on-board estimates.

Materiel and methods

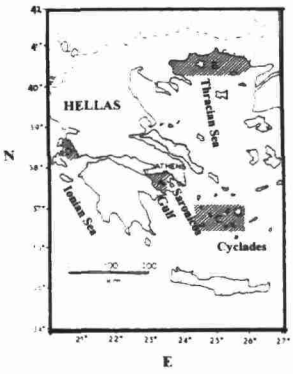

Fig. 1. The four study areas

In the present study, the term "discards" refers to the part of the total catch of fish, molluscs and crustaceans that is thrown back into the sea (1) but not to organisms such as echinoderms, sponges and algae, even if some of them have a potential market value. Sampling took place in autumn-winter 1993 and spring 1994 in four regions (Fig. 1). The selected vessels: (a) were representative of the studied areas in terms of size and construction characteristics, (b) used the same cod-end mesh size, 14 mm bar length, and (c) have been operating routinely in the studied areas for many years. The selected areas are among the most important Hellenic fishing grounds (4). In addition, these areas are representative of major geographical fishing divisions, established by the National Statistical Service of Hellas, and for which yearly total estimates of landings are available (4).

Overall, on-board sampling was conducted during a total of 128 fishing days on 16 trawlers that carried out 32 trips in four fishing areas during two seasons. The following information was recorded on-board: (a) number and weight of total and retained catches and (b) number and weight per major non-commercial species discarded, commercial-undersized species discarded, and commercial species discarded. For data analysis, haul data were grouped on a daily basis, and the daily catch was treated as a single "sample". In addition, the lengths of discarded specimens of selected species were also measured on board (either by measuring all individuals if their total number was <80 or by measuring a representative sample). Length frequencies were subsequently raised to the haul total and then to the season total.

Results

Overall, 49,960 kg were caught during 640 h of trawling (Table 1). Catches and discard and retained rates were all higher in the Thracian Sea and Saronikos Gulf than in the other two areas whereas the lowest values were recorded in the Ionian Sea.

The species composition by weight of the total catches differed greatly between areas and, to a lesser extent, between seasons. For Saronikos Gulf, the catches in autumn-winter 1993 were dominated by *Trachurus* spp. (12.1%), *Merluccius merluccius* (9.3%), cephalopods (6.2%), *Nephrops norvegicus* (6%), *Micromesistius poutassou* (5.8%), *Gadiculus argenteus argenteus* (4.9) and *Trisopterus minutus capelanus* (4.5%) whereas all remaining species each contributed less than 3%. In spring 1994, the catches were also dominated by *Trachurus* spp. (37.1%; mainly *T. mediterraneus*) and to a lesser degree by *M. merluccius* (9.3%), cephalopods (6.8%), *Mullus barbatus* (3.3%) and *M. poutassou* (3%) whereas all remaining species each contributed less than 3%.

TABLE 1. Trawl fishery, 1993-1994. Total catch in kg (TC), discard catch in kg (D), hours of trawling (H), total catch per hour (TC/H), discards per hour (D/H) and retained catch per hour (R/H) in the four study areas per season (AW = autumn-winter, SP = spring).

Area	Season	TC	D	H	TC/H	D/H	R/H
Saronikos	AW 1993	9442	5516	100.2	94.3	55.1	39.2
	SP 1994	8235	3448	93.4	88.2	36.9	51.2
Thracian	AW 1993	10272	3983	126.7	81.1	31.4	49.7
	SP 1994	7263	2974	68.0	106.8	43.7	63.0
Cyclades	AW 1993	3651	1270	50.3	72.5	25.2	47.3
	SP 1994	4320	1693	55.6	77.7	30.5	47.3
Ionian	AW 1993	2845	1219	68.8	41.3	17.7	23.6
	SP 1994	3932	1020	77.1	51.0	13.2	37.8

For the Thracian Sea, the autumn-winter 1993 catches were dominated by *M. barbatus* (22.9%), followed by cephalopods (10.5%) and *M. merluccius* (3%) whereas all remaining species each contributed less than 3%. The spring 1994 catches were also dominated by *M. barbatus* (21.5%), followed by cephalopods (9.7%) and *M. merluccius* (3%), with the remaining species each contributing less than 3%.

For Cyclades, the autumn-winter 1993 catches were dominated by Decapoda (15.3%), *M. merluccius* (14.9%) and *T. mediterraneus* (14.4%), followed by *M. poutassou* (7.8%), cephalopods (4.8%), *Squalus acanthias* (4.8%), *Raja* spp. (3.9%) and *Argentina sphyraena* (3.3%). The spring 1994 catches were composed mainly of *T. mediterraneus* (21.8%), *M. merluccius* (15.6%) and Decapoda (14.4%), followed by *M. poutassou* (7.2%), cephalopods (7.1%), *M. barbatus* (4.6%) and *M. surmuletus* (4.1%) whereas all remaining species each contributed less than 3%.

The catches from the Ionian Sea in autumn-winter 1993 were dominated by *M. merluccius* (32.5%), followed by cephalopods (7.5%), *Boops boops* (4.5%), *M. barbatus* (4.1%) and *T. m. capelanus* (3%). The spring 1994 catches were also dominated by *M. merluccius* (24.2%), followed by *T. mediterraneus* (13.7%), *M. poutassou* (7.9%), *G. a. argenteus* (6.7%), shrimps (4.2%), *Raja* spp. (3.9%) and *Lophius budegassa* (3.3%) whereas all remaining species each contributed less than 3%.

The discard rate (*i.e.*, discarded/total-catch) varied between areas and seasons, reflecting the differences in local market demand and species compositions (Fig. 2a). Hence, the discard rate in autumn-winter 1993 was highest in the Saronikos Gulf and lowest in Cyclades (Fig. 2a). In contrast, in spring 1994 the discard rate was similar for the Saronikos Gulf, Thracian Sea and Cyclades whereas it was lower in the Ionian Sea (Fig. 2a). The (commercial-discards)/(total-discards) ratio in both seasons was much lower in the Saronikos Gulf, Thracian and Ionian Seas (ranging from 0.02 to 0.42) than in Cyclades, where it was 0.70 (Fig. 2b). This indicates that in Cyclades most of the discarded specimens belonged to commercial species. Anomura (Munida and Gallathea) were the main invertebrates discarded. They made up an important component of the catches on an individual haul basis, ranging from about 5% in Cyclades to about 35% in the Saronikos Gulf. With respect to fishes, the main non-commercial species discarded were *Serranus hepatus*, which made up 1.3% in the Saronikos Gulf, 2.2% in the Thracian Sea and 0-0.1% in Cyclades and Ionian Sea; and G. a. argenteus, which made up 1.6-4.9% in the Saronikos Gulf, 1.9-2.2% in Cyclades and 0.2-6.7% in the Ionian Sea. The following non-com-

DONNÉES PRÉLIMINAIRES SUR LES ORGANISMES DE PROXIMITÉ DES SOURCES SOUS-MARINES SULFUREUSES DU LITTORAL ROUMAIN DE LA MER NOIRE

Victoria Tiganus, Florin Aonofriesei, Teodora Onciu*
Université "Ovidius" Constantza, Roumanie

Abstract

The composition of the macrobenthos from areas of submarine geothermal vents in the Romanian shallow waters of the Black Sea is analysed in the paper. Twelve macrobenthic species were observed which well resist to the levels of H_2S, four of them being more numerous in the waters with H_2S than in the normal ones *(Fabricia sabella, Capitella capitata, Middendorfia caprearum and Hydrobia pontieuxini)*. A rich sulfur-oxidizing chemoautotrophic microbiological community was identified near the vents both on living organisms and on inert substrata. The bacteria constitute an abundant primary food source for some opportunistic species with high ecological tolerances.

Key-words: zoobenthos, thermal vents, Black Sea

Introduction

Il est bien connu que l'hydrogène sulfuré est un composant toxique pour les organismes aérobies. Des recherches réalisées pendant les 20 dernières années ont mis en évidence que certains organismes ont des mécanismes de résistance à l'action toxique de l'hydrogène sulfuré, surtout quand la présence de celui-ci n'est pas associée à une longue période d'anoxie (1, 2, 3). En milieu marin, on trouve des habitats riches en hydrogène sulfuré, soit à l'intérieur de certains substrats sédimentaires anoxiques, soit autour des sources géothermales sous-marines. Ces types de source, bien que situées à de faibles profondeurs, influencent seulement des aires très réduites, mais permettent d'étudier la tolérance de différents organismes en présence de l'hydrogène sulfuré.

Le sud du littoral roumain comporte beaucoup de sources géothermales sulfureuses côtières (0-15 m), dont la température atteint 20°C, mais les organismes qui vivent autour de ces sources n'ont jusqu'à présent fait l'objet d'aucune étude. Nous avons commencé notre étude par les sources de la zone de Mangalia, qui sont les plus accessibles. On y trouve plusieurs sources (10-15), dans l'infralittoral rocheux supérieur (0,5-1 m de profondeur) (4, 5).

Matériel et méthode

Les sources sulfureuses sont d'origine souterraine. Au niveau des sources la concentration en hydrogène sulfuré est de 0,45 mg/l (déterminée par la méthode Fonselius) (6), la salinité de 0,5‰ (méthode Knudsen) et la concentration en oxygène 0 cc/l (méthode Winkler). À seulement 2 m de la source, l'hydrogène sulfuré atteint 0,05 mg/l, la salinité 8-9‰ et l'oxygène 5 cc/l. À plus de 10 m de la source, l'eau de mer a déjà des caractéristiques normales: H_2S - 0‰, salinité 17,5‰ et oxygène 7-8 cc/l.

Conformément à ces conditions, nous avons prélevé un nombre total de 60 échantillons de benthos pendant les mois de septembre et octobre dans les trois types de zones:

- zones A - situées à proximité immédiate d'une source située à 0,5 m (20 échantillons);
- zones B - intermédiaires, à deux mètres de la source (20 échantillons);
- zones C - considérées normales, sans H_2S et bien oxygénées (10-12 mètres de la source) (20 échantillons).

Les zones étudiées sont situées dans un golfe artificiel protégé par des digues, où il y a un hydrodynamisme réduit de l'eau de mer. Nous avons prélevé les échantillons par le grattage du substrat rocheux sur une aire de 20/20 cm, à l'aide d'un dispositif de prélèvement par une boîte métallique pourvue à un bout d'un bord tranchant, et à l'autre bout d'un sachet en toile.

Les échantillons ont été analysés en laboratoire conformément aux méthodes usuelles d'étude du benthos. Nous avons considéré comme organismes macrobenthiques ceux qui dépassaient la taille de 2 mm.

Parallèlement, des échantillons microbiologiques ont été prélevés et analysés et feront l'objet d'une publication séparée plus détaillée. Nous en évoquerons toutefois certains résultats dans le présent travail.

Résultats et discussions

Seules deux espèces de macrophytes ont été identifiées dans les zones du type A: *Ceramium rubrum* et *Enteromorpha intestinalis*. Leur thalle était couvert d'une couche blanchâtre de bactéries sulfoxydantes.

Les analyses microbiologiques préliminaires ont mis en évidence à proximité des sources une grande richesse qualitative et quantitative de microorganismes sulfoxydants, autant photoautotrophes que chimioautotrophes, qui forment une couche presque continue sur tous les substrats vivants et inertes de ces zones. Ces agglomérations fonctionnent comme interfaces très actives dans la métabolisation du H_2S, limitant sans doute sa diffusion et son effet toxique.

Les bactéries appartiennent à deux groupes majeurs: bactéries sulfoxydantes phototrophes incolores (les genres *Beggiatoa, Chlorobium* et *Pelodictyon*) et bactéries sulfoxydantes incolores (les genres *Beggiatoa, Thioploca* et *Thiothrix*), les dernières étant dominantes. La présence de ces denses peuplements bactériens assure une production primaire importante autour des sources.

En ce qui concerne le zoobenthos, nous avons observé 13 espèces macrobenthiques dans les zones A, 18 espèces dans les zones B et 31 dans les zones C (tableau 1). Sur les 13 espèces à proximité des sources, quatre sont des espèces sessiles; leur présence y est donc permanente. Parmi celles-ci, *Fabricia sabella* et *Mytilaster lineatus* sont le plus fréquemment présentes dans les échantillons (55 % et 66 % respectivement). Les colonies de *M. lineatus* sont recouvertes d'une pellicule blanche bactérienne.

Pour les espèces vagiles, les plus fréquemment présentes dans les échantillons sont les isopodes *Idotea baltica* et *Sphaeroma pulchellum* (90 %), le gastéropode *Hydrobia pontieuxini* (75 %) et le polyplacophore *Middendorfia caprearum* (60 %).

Quoique ces organismes soient vagiles, certains étant même très mobiles, comme *I. baltica* et *S. pulchellum*, ils sont quand même des éléments permanents dans ces zones, comme le prouve l'épaisse couche de bactéries sulfoxydantes les recouvrant. Cette couche est formée surtout par des bactéries du genre *Thiothrix* qui forment un réseau dense, dans les mailles duquel se développent de nombreuses populations de *Beggiatoa alba.*

Dans les zones intermédiaires apparaissent encore 5 espèces: un cirripède et quatre amphipodes, qui ne sont présents que dans 20 % des cas (tableau 1).

Dans les zones C, la macrofaune s'enrichit non seulement par la présence d'encore 13 espèces, mais aussi par des plus grands pourcentages de présence pour la plupart des espèces. On peut ainsi constater un gradient d'espèces selon leur tolérance. Le groupe le plus sensible à la présence de l'hydrogène sulfuré semble être celui des amphipodes, qui fait presque complètement défaut dans les zones A, à l'exception de quelques exemplaires de *Corophium bonelli*, arrivés là probablement accidentellement, comme semble l'indiquer l'absence de l'épibiose bactérienne.

Quantitativement, on constate que les valeurs générales de la densité du macrobenthos sont minimales dans les zones A et augmentent graduellement dans les zones B et C (tableau 1). L'augmentation de la densité vers la périphérie des sources se fait principalement au détriment des populations des 13 espèces des zones A. Ainsi ces espèces représentent 99,3 % de la densité générale du macrozoobenthos dans les zones B et 70,2 % dans les zones C.

Dans la zone A, les plus grandes densités concernent les espèces *Idotea baltica* (23 %), *Fabricia sabella* (16,3 %), *Hydrobia pontieuxini* (15 %), *Sphaeroma pulchellum* (12 %) et *Mytilaster lineatus* (10,1 %). Ces espèces maintiennent en général des densités relatives similaires en zone B, mais la plupart d'entre elles diminuent fortement en zone C, à l'exception des isopodes *S. pulchellum* et *I. baltica.* Ainsi, les 6 plus denses espèces de la zone A (82,5 %) ne représentent plus que 43,4 % de la densité en zone C.

Bien que les valeurs de densité totale soient inférieures à proximité des sources sulfureuses, elles restent toutefois relativement élevées et montrent qu'un certain nombre d'espèces sont capables de prospérer dans des eaux en permanence chargées en H_2S, dessalées et hypoxiques comme la couche épaisse des bactéries sulfoxydantes qui les recouvrent semble l'indiquer. Trois de ces espèces - *F.sabella, M.caprearum* et *H.pontieuxini* - présentent même des densités plus grandes dans les zones du type A et B que dans les eaux normales (C).

Il apparaît donc que dans les zones de proximité des sources, la présence du H_2S crée des conditions défavorables pour beaucoup d'organismes benthiques, mais permet l'établissement et le développement abondant d'espèces plus tolérantes. Les deux macrophytes identifiées dans les zones A - *Enteromorpha intestinalis* et *Ceramium rubrum* - sont connues comme éléments opportunistes (7).

ANALYSIS OF CATCH AND EFFORT DATA OF *LOLIGO VULGARIS* IN THE W. THRACIAN SEA (NE MEDITERRANEAN, GREECE) USING A DEPLETION MODEL

Tsangridis A. [1*], E. Lefkaditou [2] and A. Adamidou [3]

[1] National Agricultural Research Foundation, Fisheries Research Institute, N.Peramos, 640 07 Kavala, Greece
[2] National Centre for Marine Research, Institute of Marine Biological Resources, 166 04 Hellenikon, Athens, Greece
[3] Ministry of Agriculture, Fisheries Laboratory, 15 Karaoli-Demetriou Str., 185 31 Greece

Abstract

Loligo vulgaris is one of the most common squids in the Mediterranean. Despite the recent studies to the biology of *L.Vulgaris,* there is a great gap in the knowledge of its population size and behaviour. Catch and effort data for *L.Vulgaris* were collected daily for the fishing period October 1994 to May 1995 for trawlers and beach seiners fishing in the W.Thracian sea (NE Mediterranean, Greece). The data were analysed on a fortnightly basis using the no recruitment depletion model. Given the uncertainty of M (Natural mortality rate) values, the analysis was done at three (M) levels (0.01, 0.04, 0.08). It seems that there is no serious problem in the squid population studied but we have to note that their short life-cycle makes squid stocks very vulnerable to overfishing.

Key-words : Aegean Sea, cephalopods, fisheries, stock assessment

Introduction

European squid *(Loligo vulgaris)* is one of the most common squids along the north-eastern Atlantic and Mediterranean coasts. Within the Mediterranean, studies on *L. Vulgaris* are relatively few and these focused on biology, distribution and life history (1-7).

In the Mediterranean sea and especially along the coasts of Spain, Italy and Greece, *L. Vulgaris* is commercially important. Despite this, there is no systematic research directed on stock assessment and management. In Greece, fisheries for European squids are based on catches of beach seiners and by-catches of trawlers. Over the last decade the average annual catch of the European squid in Greek waters amounted to about 1080 tonnes, 38% of which was fished by bottom trawl, 30% by beach seine, 9% by purse seine and 23% by other gears of small scale fisheries. In the W.Thracian sea, *L. Vulgaris* is among the main target species of beach seiners. It is also fished by trawlers as a by-catch species. The average annual catch of *L. Vulgaris* in this sea over the last twenty years is 20.25 tonnes.

The aim of this presentation is to contribute to the assessment of squid fisheries in the Mediterranean using recently developed methods and help in the development of appropriate management measures.

Material and methods

Total catch for all species and effort data for *L. Vulgaris* were daily collected for the fishing period October 1994 to May 1995 for trawlers and beach seiners fishing in the W.Thracian sea (N.Aegean, Greece). The data from trawlers were collected at the fishing port of Kavala. For the beach seiners of Kavala and Thassos island, the data were collected at landing sites through personal interviews .

The catch per unit effort (CPUE) data were analysed separately, for trawlers and beach seiners on a fortnightly basis. The no recruitment depletion model was applied (8), *i.e :*

$N_{t+1} = e^{-M} . N_t - e^{-1/2.M} . C_t$,

where N_t : population numbers at start of fishing period *t* (fortnight); M: natural mortality rate (per fortnight); C_t : total catch during *t*.

Sensitivity analysis was applied using the three available error models (Least squares, Gamma, Log transform) to find the best fit (8). Given the uncertainty of (M) values, the analysis was done at three M levels (0.01, 0.04, 0.08).

Results

There is a clear decline in *L. Vulgaris* catches from the winter to the late spring with a peak on the second half of November which is more evident for beach seiners (Fig.1).The importance of the *L. Vulgaris* catch to the total catch of each gear differs (Fig.2).

The trends of the effort and CPUE seem to follow the catches trends in both gears, generally declining from winter to the summer time (Figs 3, 4). It is interesting to note that the CPUE values of *L. Vulgaris* for the beach seiners are clearly larger from those of trawlers in October, November and the second half of January (Fig.5).

The analysis of the trawl and beach seiner data indicates that the best fit is for M= 0.010 (4). For the sake of brevity we present only the best fits and the corresponding graphs (Figs 6, 7) out of the eighteen trials at the three (M) levels.

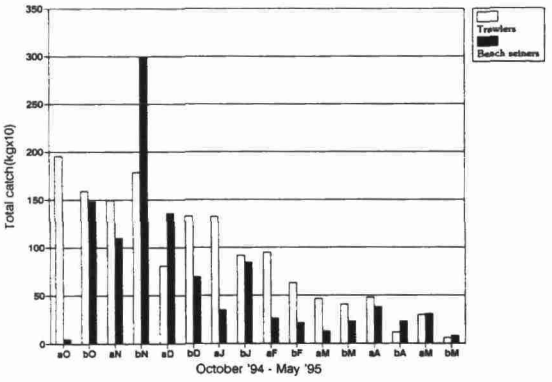

Figure 1. Total catch of *L. Vulgaris* for Trawlers and Beach seiners during the fishing period October '94 - May '95. Data presented on a fortnightly basis.

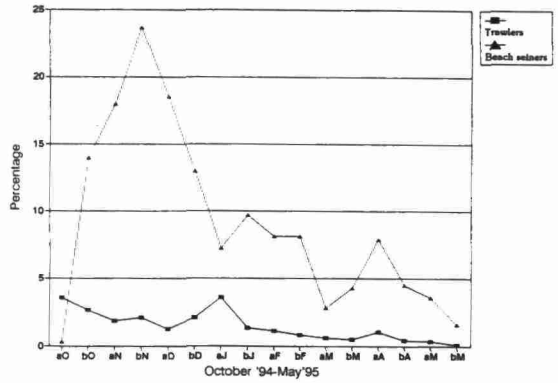

Figure 2. Percentage contribution of *L. Vulgaris* catch to the total catch of Trawlers and Beach seiners. Data presented on a fortnightly basis.

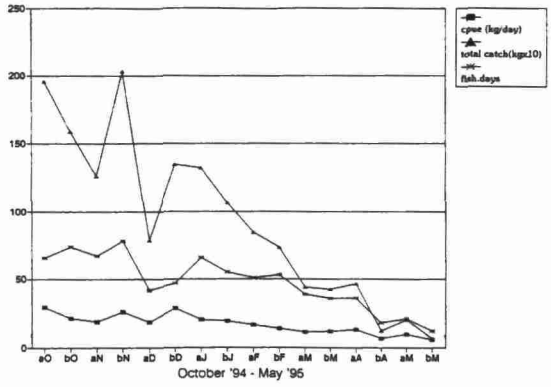

Figure 3. Total catch of *L.Vulgaris*, cpue and fishing effort for Trawlers during the fishing period October '94 - May '95. Data presented on a fortnightly basis.

MAPPING OF FOURSPOTTED MEGRIM, *LEPIDORHOMBUS BOSCII* (RISSO, 1810), RESOURCE ON SOUTH-WESTERN ADRIATIC SEA TRAWLABLE BOTTOMS.

N. Ungaro, G. Marano*, M. Martino

Laboratorio Provinciale di Biologia Marina, Molo Pizzoli (Porto), 70123, Bari, Italy

Abstract

The authors report data about fourspotted megrim resource distribution and abundance on south-western Adriatic trawlable bottoms, elaborated by means of geostatistical method. The species distribution shows the highest biomass indices between 150 m and 500 m depth (200 m and 400 m for the recruitment) and higher aggregation during late autunm in comparison with late spring seasons; this last result is probably related to the reproductive cycle of the species.

Key-words: teleostei, Adriatic Sea, GIS.

Since 1985 seasonal (late spring - late autumn) trawl-surveys were carried out on south-western Adriatic trawlable bottoms in order to evaluate the quali-quantitative distribution of demersal resources (1, 2, 3); the fourspotted megrim results one of the most valuable resources of investigated area (4, 5, 6).

Quantitative data (kg / trawl haul) came from n° 252 hauls (n° 126 "spring" hauls, '91, '92, '94, '95 surveys; n° 126 "autumn" hauls, '91, '92, '94, '95 surveys) carried out in south-western Adriatic Sea (Lat. 40°-42°N; Long. 16°-19°E); the sampling gear was an "italian" trawl net (cod-end stretched mesh = 36 mm) while the sampling design was random stratified.

The data were standardized to the "unit of area" (km^2) by using the net hydrodynamic parameters measurements (7). In order to map the biomass indices (kg/km^2) the geostatistical method was applied (8, 9, 10); the use of the above mentioned technique to fishery assessment purpose has risen lately in Mediterranean area (11, 12).

The semivariograms obtained by data analysis (cumulative samples distribution for "spring" surveys and "autumn" ones) show a low spatial correlation; this result (increase of point distance = strong decrease of correlation) suggested the use of spherical model to a best data fitting (Figure 1).

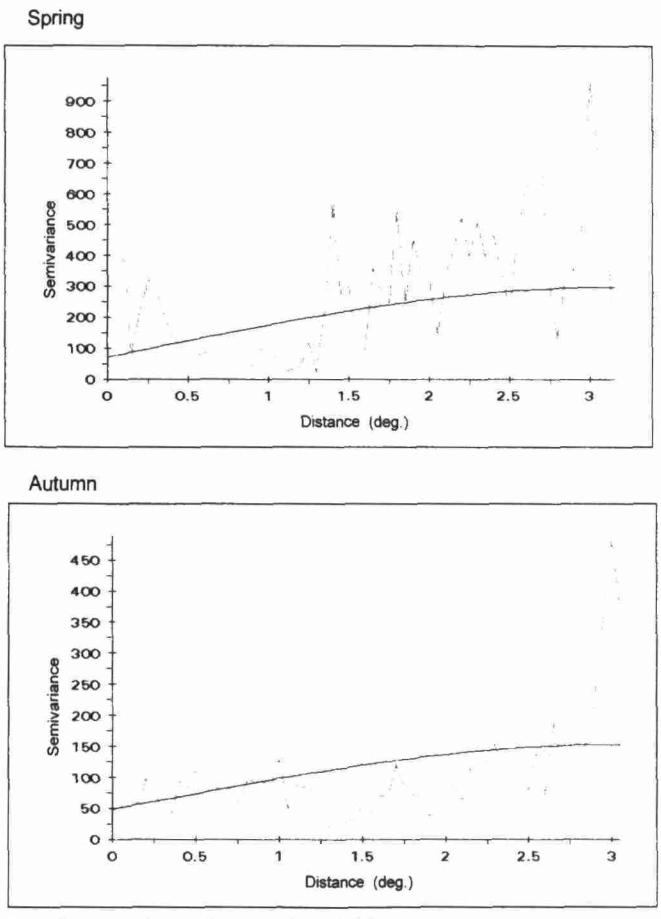

Fig. 1. Experimental semivariograms and spherical fit.

The fitted spherical model, referring to the pooled spring surveys and the pooled autumn ones, gave the results shown on figure 2. Generally the kriging variance appears to be rather large in both seasons; this result is probably due to the well known irregular space-distribution of fish populations together with the low sampling density. However the estimate reliability is higher in relation to spring season.

According to the depth, the highest values of the biomass indices can be found between 150 m and 500 m (for both seasons) while the recruitment to the fishery (here specimens with total length less than 12 cm) is mostly concentrated between 200 m and 400 m.

The different "aggregation intensity" showed in relation to the spring and autumn seasons could be explained by the knowledge of species biology; the fourspotted megrim spawning time in the investigated area is around late winter (6), therefore it is possible to suppose a specimens concentration (to a reproductive purpose) during late autumn-winter times and a more homogenous distribution during late spring times (inter-genetic stage).

The global results of the analysis confirm that geostatistical methods can be useful to describe and to compare the space-time distribution of fishery resources, also in relation to species biology and ecology.

Acknowledgments

The authors would like to thank "Planetek Italia s.r.l." for collaboration in data processing.

References

1 -AA.VV., 1988. Valutazione delle risorse demersali dell'Adriatico meridionale dal promontorio del Gargano al capo d'Otranto: relazione finale triennio '85-'87. Min: Mar. Mer., Roma.

2 -AA.VV., 1993. Valutazione delle risorse demersali dell'Adriatico meridionale dal promontorio del Gargano al capo d'Otranto: relazione finale triennio '90-'93. Min: Mar. Mer., Roma.

3 -AA.VV., 1996. Valutazione delle risorse demersali dell'Adriatico meridionale dal promontorio del Gargano al capo d'Otranto: relazione finale triennio '94-'96. M.R.A.A.F., Roma.

4 -Ungaro N. & Marano G., 1995. Analytical models for mediterranean species: an application on the *Lepidorhombus boscii* (Risso) resource in the lower Adriatic. *Rapp. Comm. Int. Mer. Médit.*, 34: 260.

5 -Ungaro N., Marano G., Marsan R., 1996. The use of the swept area method for the estimate of biomass: a first attempt relative to three demersal finfishes (hake, red mullet, fourspotted megrim) in south-western Adriatic sea. *Fao Fish. Rep.*, 533 (suppl.): 101-104.

6 -Ungaro N. & Martino M., in press. *Lepidorhombus boscii* (Risso, 1810): biologia dellla specie e demografia della popolazione sui fondi strascicabili dell'Adriatico pugliese. Convegno "Risorse Demersali dei Mari Italiani", Fano (Italy) 20-22/03/1996.

7 -Fiorentini L., Cosimi G., Sala A., Palumbo V., 1993. Misura dei parametri idrodinamici delle attrezzature a strascico, utilizzate dalle UU.OO. di valutazione delle risorse demersali, al fine di renderne confrontabili i risultati. Rapporto finale. Min: Mar. Mer., Roma.

8 -Royle A. G., Clausen F. L., Frederksen., 1981. Practical universal kriging and automatic contouring. *Geoprocessing*, 1: 377-394.

9 -Burrough P.A., 1986. Principles of geographical information system for land resources assessment. Oxford University Press, New York.

10 -Oliver M. A., 1990. Kriging: a method of interpolation for geographical information systems. *Int. Journ. of Geog. Inf.* Sys., 4 (4): 313-332.

11 -AA.VV., 1995. Mapping of italian demersal resources. Final Report. Contract CE - DG XIV - 1/MED/91/013.

12 -Maynou F. & Palomera I., 1995. Mapping and assessment of anchovy *(Engraulis encrasicolus)* egg production by geostatistics. *Rapp. Comm. int. Mer. Médit.*, 34: 249.

EXPLOITATION OF BEDS OF TRUNCATE DONAX *(DONAX TRUNCULUS L.)* ALONG ADRIATIC COASTS OF ALBANIA

R. Vaccarella [1]*, E. De giosa [2], B. Troplinj [2], P. Paparella [1]

[1] Laboratorio di Biologia Marina, Molo Pizzoli (Porto) 70123, Bari, Italia
[2] Albamar, Rruga, Porto Durresi, Durres, Albania

Abstract

In Albania *Donax trunculus* L. fishery began in 1989 and it has been always carried out by hand rake. In August 1994, with the help of a boat geared with "metal rake", dredgings have been carried out in Durres and Lales Gulf in order to obtain a first estimate of biomass index, and the possibility of fishing at depth never investigated until now.

Key-word : fisheries, bivalves, Adriatic Sea

Introduction

From the lake of Skoder, that represents the border between Albania and Jugoslavia, up to Vlore, the Adriatic Sea laps on a low and sandy coast with extended beaches separate by small capes. The Gulf of Drin, Lales Bay and the Gulf of Durres are bordered by the capes of Rodonit, Palles, Durres and Lagit. The infralittoral bottoms are incoherent, largely covered by the seagrass *Posidonia oceanica* Delile; the bottoms without vegetation, host beds of commercial bivalve molluscs, such as *Chamelea gallina* (L.), *Ensis siliqua* (L.), *Acanthocardia tuberculata* (L.), *Donax semistriatus* Poli and *D. trunculus* L.

The fishery of the latter two species, started in 1989, has represented, until October 1994 (episodes of cholera), the only economically profitable activity for the Albanian fishermen. But the harvest of truncate donax, if effected even by hand rake, due to the increasing number of fishermen and of the little littoral band on which it is practiced (0.5-1 m depth), could determine, to short term, a crisis in the availability of the resource. This has induced us to test the capability of developing this fishing activity, with tools fit to harvest *D. trunculus*, at greater depth than those allowed by the use of the hand rake.

Materials and methods

In August 1994, samples were collected by means of a "tellinara" boat 8.50 meters long with inboard 28 HP engine, geared with "metallic rake" (1, 2). The rake had an opening of 120 cm of width and 20 cm of height. The rake was 90 cm long and the grid had steel rods set at 7.5 mm from each other. The metallic basket ended with a nylon net with 19.5 mm mesh.

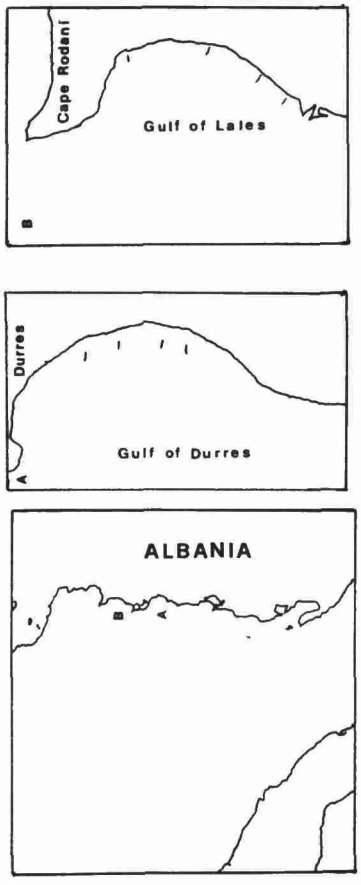

Fig. 1. Sampling transects.

In the Gulfs of Durres and Lales (Fig. 1), the position of 32 sampling stations has been defined by means of G.P.S, set for a precision of 9 meters. Samples consisted of 50 m long dredgings, parallel to the coast, at 0.5 meter steps, until where the truncate donax occurred (-2 m), along eight transects perpendicular to the coast. Transects were spaced about 4 km from each other. An overall 2,000 m^2 surface was surveyed.

The maximum sampling depth was established following preliminary observations by SCUBA diving, which showed that there was no truncate donax deeper than -2 m, in both examined areas. The density data refer to 50 m^2 sampling surfaces.

The composition of the species in the samples was determinated and the density and biomass index of the Donacidae were evaluated. The comparison among the data, mapped in both areas, was tested by the non-parametric test of Friedman. In addition, the morphometric parameters of truncate donax were evaluated.

Because of the lack of previous information on the mollusc density in the sampling sites, our sampling may be deemed random (3). The biomass index was calculed following the swept area formulas (4, 5), in which the coefficient of catchability = 1 was applied, since we are dealing with commercial size (length ≥ 20 mm) samples.

Results

The molluscs *D. trunculus, D. semistriatus, A. tuberculata* and *Mactra corallina* are the species most abundant, followed by the crustaceans, *Liocarcinus vernalis* (Risso) and *Portumnus latipes* (Pennant) and echinoderms (Tab. 1).

Table 1 - Mean density and biomass of the species collected in the four transects of the Gulf of Lales and Gulf of Durres.

Gulf of Lales weight :	g/ 50 m²				Individuals / 50 m²			
depth	0.5	1	1.5	2	0.5	1	1.5	2
Donax trunculus	1,382.795	675.483	100.895	167.445	652.500	290.000	38.250	69.500
Donax semistriatus	0.000	2.220	2.388	5.700	0.000	0.500	1.250	3.500
Nassarius mutabilis	1.384	13.768	17.008	23.448	1.250	11.250	12.500	19.500
Mactra corallina	0.000	29.970	69.618	46.065	0.000	3.750	8.250	8.250
Mactra glauca	0.000	3.743	54.380	16.828	0.000	2.000	12.750	4.500
Chamelea gallina	12.230	54.025	84.800	181.335	4.750	18.000	23.000	59.000
Acanthocardia tuberculata	0.000	1.358	2.558	12.510	0.000	0.750	1.000	3.500
Liocarcinus vernalis	26.298	50.213	78.995	51.228	7.000	15.250	25.750	20.000
Portumnus latipes	12.513	6.430	0.428	0.928	7.000	5.250	0.250	0.750
Hermit crabs	8.143	16.183	25.508	36.573	6.500	12.000	17.250	27.000
Astropecten jonstoni	0.000	0.000	0.000	5.240	0.000	0.000	0.000	0.750
Echinocardium cordatum	0.000	0.000	1.160	2.200	0.000	0.000	0.500	1.250
Gulf of Durres weight :	**g/ 50 m²**				**Individuals / 50 m²**			
depth	**0.5**	**1**	**1.5**	**2**	**0.5**	**1**	**1.5**	**2**
Donax trunculus	1,344.913	441.448	58.623	23.748	603.750	170.500	23.500	9.250
Donax semistriatus	0.000	2.755	4.405	0.000	0.000	2.250	4.500	0.000
Nassarius mutabilis	6.635	30.958	72.373	53.353	4.350	22.250	49.500	35.750
Mactra corallina	1.188	80.333	226.138	273.313	0.250	5.000	22.750	27.500
Mactra glauca	13.053	95.360	252.983	283.805	2.000	14.500	41.000	37.750
Chamelea gallina	0.673	9.005	28.358	105.840	0.500	3.750	10.750	33.500
Acanthocardia tuberculata	0.000	0.000	23.413	14.775	0.000	0.000	0.500	0.500
Liocarcinus vernalis	1.480	5.773	19.870	6.765	1.050	3.750	12.750	4.250
Portumnus latipes	4.488	0.838	1.610	0.000	4.250	0.750	1.250	0.000
Hermit crabs	12.970	20.978	72.313	55.968	9.650	15.750	55.000	42.000
Astropecten jonstoni	1.560	0.000	1.043	5.438	0.300	0.000	0.250	1.250
Echinocardium cordatum	0.000	7.463	13.255	2.090	0.000	0.500	0.750	0.500

In both Gulfs of Durres and Lales (overall examinated area = 200 m^2), we report the values of the index of abundance (number and weight) of the species collected, the diversity's index of Shannon - Weaver, and the evenness index, by sampling depth (Tab. 2). We could observe that the H' index increases with the reduction of the *D. trunculus* facies. H'≤0.33 linked to the most littoral band of fine sands, while at 1.5 m - 2 m of depth H' ≥ 2.33, the species *Chamelea gallina, Mactra glauca* and *M. corallina* become more abundant.

Table 2 - Overall bionomic indices per depth stratum in terms of number of individuals (n) in terms of weight(w); sampled area in each stratum = 200 m2. S = number of species; N = number of specimens; W = weight of specimens; H' = Shannon-Weaver's diversity index; e = eveness index.

Gulf of Durres							
Depth m	*S*	*N*	*W*	H'_n	e_n	H'_W	e_W
0.5	9	2,504	5,548.0	0.30	0.01	0.27	0.09
1	10	956	2,779.6	1.58	0.48	1.77	0.53
1.5	12	892	3,097.6	2.77	0.77	2.60	0.73
2	10	768	3,300.4	2.66	0.80	2.33	0.70
Gulf of Lales							
Depth m	*S*	*N*	*W*	H'_n	e_n	H'_W	e_W
0.5	6	2,716	5,773.6	0.32	0.13	0.33	0.13
1	10	1,436	3,413.6	1.21	0.36	1.26	0.38
1.5	11	564	1,750.8	2.78	0.80	2.73	0.79
2	12	872	2,198.0	2.62	0.73	2.58	0.72

The density of *D. trunculus* decreases rapidly as depth increases. In the Gulf of Durres, at 0.5 meters, it presents mean values of 603.75 ±544.65 (s.d.) specimens/ 50 m^2, while at 1 m it is reduced to 170.5 specimens/ 50 m^2. Table 3 shows that about 75 % of density was found at - 0.5 m, whe-

THE SMOOTH SCALLOP, *CHLAMYS GLABRA*, FISHERY IN THE GULF OF MANFREDONIA (SOUTH-WESTERN ADRIATIC SEA)

R. Vaccarella*, P. Paparella, G. Bello and G. Marano
Laboratorio di Biologia Marina, Molo Pizzoli, 70123 Bari, Italy

Abstract

The scallop fishery in the Gulf of Manfredonia (south-western Adriatic Sea) is targeted to the capture of smooth and proteus scallops, *Chlamys glabra* and *Chlamys proteus* (Mollusca: Bivalvia: Pectinidae). Presently ten boats are dredging for scallops in a 44.3 km^2 area, from 4 to 16 m of depth; each boat catches 70-80 kg/day of scallops. The analysis of the size frequency distribution of smooth scallops shows that all dredged individuals are older than 1 year and most of them are older than 2 years and have reproduced at least once. The biocoenotic composition of scallop beds was also examined to detect the degree of disturbance by scallop dredging.

Key-words: Bivalves, fisheries, biometrics, Adriatic Sea

Introduction

The smooth and proteus scallops, *Chlamys glabra* (Linnaeus, 1758) and *Chlamys proteus* (Dillwyn, 1817) (Mollusca: Bivalvia: Pectinidae), represent an important shellfish resource in the Gulf of Manfredonia (south-western Adriatic Sea). In this area, *Chlamys* spp. live on chalk weed beds, from 4 to 16 m of depth, and are fished by dredges. The smooth scallop fishery in the Gulf of Manfredonia started in the late '70s. In the years 1981/82 a death mass occurred that almost destroyed the scallop beds of the Gulf and strongly hindered the fishery (1): up to the early '90s only a couple of boats went on occasionally dredging for scallops. In the last four years the density of scallops increased and, consequently, the number of scallops dredgers increased as well.

A preliminary survey in 1994, by experimental hydraulic dredge (66 samples taken along 12 transverses) (Fig.1: area A + area B) showed that the overall *C. glabra* and *C. proteus* biomass was 22.46 ±11.80 metric tons/44.3 km^2 (2). Today, ten boats are fishing for smooth and proteus scallops on the overall area (A + B). Purpose of the present study is to survey the status of scallop beds in the Gulf of Manfredonia by the actual catches of commercial dredging, in order to provide management advise.

Material and methods

In January and February 1997 a preliminary approach to the study was conducted by interviewing the port authorities and scallop dredgers in order to get information on the number of boats actually dredging for scallops, fishing effort, and yields.

In March and April 1997 an experimental fishery campaign was carried out. In the fishing area B (Fig.1), a commercial boat with twin-dredges, 65 HP, was used. The dredge had a rectangular mouth 160 x 30 cm wide and carried a nylon net whose cod end mesh size was 50 mm stretched. The dredge was towed, at about 1.5 knots, from 10 to 30 minutes according to the ground conditions. Thirteen samples were collected; the sampling stations were chosen according to the fisherman knowledge of the best dredgeable zones, in agreement with the purpose of the present survey. The number and weight of scallops caught in each sample were taken. Three samples were used to establish the percentages of commercial shellfish (scallops and other molluscs) and discards.

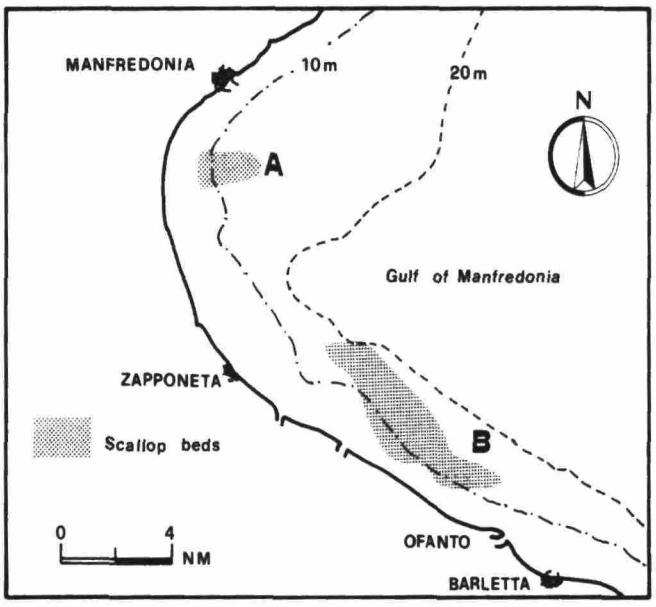

Fig. 1 - The scallop beds in the Gulf of Manfredonia.

A 16 kg subsample of discarded material, randomly chosen from discards of several samples, was fully examined to study the biocoenotic composition. In addition, 952 randomly chosen specimens of *C. glabra* were measured to analyze the frequency distribution of lengths (antero-posterior distance). Another stock of 344 randomly chosen smooth scallops were used for biometrical analysis. The following measures were taken: length, height, width, weight of empty shell, wet weight of autoclave boiled meat and weight of dried meat (oven dehydration at 60°C for 24 hours) (3). The correlation between wet weight of meat and shell length was studied by predictive regression analysis.

Results

The scallop fishery

In the Gulf of Manfredonia fishing for scallops is carried out on an area of about 44.3 km^2, from January to May. Later on in the year scallops become stressed because of their spawning and easily die when caught, hence their commercial value drops down. Presently ten boats, with 2-3 person crew, are involved in this fishery; boat gross tonnage = 4.5-9.4 metric tons; engine power = 36-120 HP. They trawl twin dredges, on bottoms from 12 to 16 m of depth, about 3 nautical miles off the coast. Each dredge, locally called "cassa", is made of an iron rectangular mouth devoid of teeth, weighing 15 kg, carrying a 2.5 m long net; the mesh size is 50 mm stretched. Usually each trawling lasts from 20 to 30 minute, at about 1.5 knots, with the engine running at 1,000 RPM. Scallop fishing is carried out in the morning, 5-6 hours per day.

The average daily catch per boat is 70-80 kg of scallops, mostly *C. glabra*. The wholesale value of scallops is about 5,000 Italian lire/kg (or 2.9 US$/kg). In addition, 160-200 kg of the muricid gastropods *Phyllonotus trunculus* (L., 1758) and *Bolinus brandaris* (L., 1758) are collected. Due to their low value (about 700 Italian lire/kg or 0.4 US$/kg), fishermen discard most of them and usually keep and market some 50 kg of them.

Experimental survey

During the experimental fishing, the average CPUE of scallops was 12.733 kg/h, standard deviation = 3.046. The weight percent composition of caught scallops was

Chlamys glabra	67.42%
Chlamys proteus	29.10%
Pecten jacobaeus	3.20%
Chlamys varia + *Aequipecten opercularis*	0.28%

As shown in the above list, the smooth and proteus scallops make up the bulk of the catch (96.52%). It has to be stressed that all the specimens of the third most important species, *P. jacobaeus* (L., 1758), are juveniles (length range = from 4.1 to 6.1 cm). According to Castagnolo & Aralla (4), *P. jacobaeus* become sexually mature at about 8 cm length. The remaining two scallops, *C. varia* (L., 1758) and *A. opercularis* (L., 1758), are not at all important in this fishery because of their very occasional capture.

The length frequency distribution of smooth scallops is given in Fig. 2. Their size ranges from 2.1 to 4.6 cm; only one specimen was 5.1 cm long. Saracino *et al.* (1) report that the smooth scallop becomes sexually mature and reproduce when 2 years old; the average length at age 1 is 21.85 ± 1.14 mm and the length at age 2 is 31.27 ± 1.63 mm. According to these data, it appears that all the sampled smooth scallops are older than 1 year (age classes 1+ and older). In addition, it can be assumed that virtually all specimens longer than 3.0 cm (as well as many others in the length range 2.3-3.0 cm) are older than 2 years and, hence, have reproduced at least once before being caught (Fig. 2).

Weight of meat is correlated to shell length by the power equation: $W = 0.0446\ L2.729$ (weight in g; length in cm); $r = 0.972$; $p < 0.001$ (Fig. 3). The expected weight at 3 cm length is 0.894 g, *i.e.* 3 times higher than that at 2 cm length, 0.296 g.

DISCARDING AT SEA BY COMMERCIAL TRAWLERS IN GREEK WATERS

V. Vassilopoulou* & C. Papaconstantinou
National Centre for Marine Research, Hellinikon, 16604, Athens, Greece

Abstract
Discarding at sea by commercial trawlers was studied in the Cyclades area plateau and in the Saronikos Gulf, both being important fishing grounds of Greek Waters. Higher catch values, as well as discarding rates, appeared to the Cyclades. Fish, both marketable and discarded, dominated the catches of both areas. In the Cyclades, the majority of the discarded part, in terms of hourly yield, was mainly Chondrichthyes species. In the Saronikos, the bulk of the discarded fraction was composed of certain low demand species, among which *T. trachurus* dominated.

Key-words: Trawl surveys, fishes, Aegean Sea

Introduction

Discarding at sea is a serious problem in fisheries and a major source of uncertainty in management of resources. Estimates of fishing mortality, based on landings rather than catches, which include discards, are likely to be biased downward. Inclusion of discards when these are significant, will reduce the inaccuracies, especially of recruitment and improve the potential quality of assessments.

There is no information on numbers, weight and sizes of fish discarded by fishing vessels, other than extremely rough estimates, mainly from experimental surveys conducted by research Institutions. Data on discarding at sea by commercial trawlers in Greek waters were presented for the first time by Tsimenides *et al.* (1). The Saronikos Gulf and the Cyclades plateau are two major fishing grounds of Greek waters. The former is a semi-enclosed basin, that receives sewage effluents from Athens and the latter is an open sea area, larger and deeper than the Saronikos. The objective of this study, which is part of an EU project dealing with the analysis of trawl's discard operation in the Mediterranean Sea, is to report on the species that mainly contribute to the discarded part of the trawl catch and to assess the proportion of this part in relation to the total yield in the two areas.

Material and Methods

The fishing operations of two commercial trawlers in each study area in autumn 1995 were analysed, in order to obtain first estimates of the species composition, as well as the proportion of discards from trawl fishery. The selected trawlers were representative of the fishing fleet operating there; all four vessels had a 500 HP engine and were equipped with a trawl net having a cod-end mesh size of 14 mm from knot to knot. Data were collected from six hauls in each depth stratum (A: 0-150 m, B: 150-300 m, C: >300 m). For the Cyclades Islands data from 18 hauls were recorded, while in the Saronikos Gulf, the number of the hauls did not exceed 11 because of the bathymetry of the area (the greatest depth of the Saronikos Gulf is about 250 m, except for a very restricted area where it reaches 350 m). The number of hauls worked up per day usually varied from 1 to 3, depending on the depth, duration of the hauls, size of the catch, distance between the successive hauling positions and the prevailing weather conditions. Information regarding the haul characteristics (*e.g.* location, duration, depth) and concerning the quantity and quality of the catch in each haul was recorded. Data were grouped per depth stratum in each area and the catch composition, defining whether the collected species were characterized as marketable or discarded, was analysed. The percentage of the marketable and discarded fraction in relation to the total yield was also estimated. For comparative reasons raw catch values were transformed to hourly yield ones (g/h).

Results and Discussion

In the Cyclades, in stratum A and B total catches appeared to be greater than those in stratum C, where discarding rates exhibited the lowest value (Table 1). The majority of the discarded part consisted mainly of chondrichthyes (Raja, Scyliorhinus, Squalus, Oxynotus) reaching 19000 g/h in terms of mean hourly yield. In the Saronikos, mean total yield value was higher in the 150-300m depth zone, where the marketable fraction of the catch appeared also to be increased in relation to shallower waters. The bulk of the discarded volume was again fish, mainly *T. trachurus* (2116 g/h) and Scyliorhinus species (923 g/h). Between the two study areas, higher mean total catch values existed in the Cyclades. In the Saronikos discarding rates (%) displayed lower values.

Table 1. Mean total yield and relative proportion of discarded fraction in each stratum of the two study areas in October 1995.

AREA	STRATUM	Discarded yield			Total yield	
		g/h	%	std	g/h	std
CYCLADES	A	61959.2	59.2	61478.5	104707.2	63068.8
SARONIKOS		36049.8	53.3	11960.2	65797.4	19015.1
CYCLADES	B	79190.4	63.2	29546.2	125310.0	16775.4
SARONIKOS		44957.4	40.9	7506.0	110018.6	11845.0
CYCLADES	C	20564.8	36.7	8118.4	56098.0	12395.7

The percentage composition of the catch in the two areas, distinguished into four major taxonomic groups (*i.e.* fish, crustaceans, cephalopods, other invertebrates) is presented in Figure 1. Fish, both marketable and discarded, were the most important in terms of percentage weight (g/h) in all three strata of the Cyclades. The discarded part of fish was increased in stratum A and B. Regarding Crustaceans, in strata A and B almost all specimens, belonging mainly to Portunidae and Galatheidae were discarded, while the significant marketable portion appearing in stratum C was influenced by the presence of *Parapenaeus longirostris* and *Nephrops norvegicus*. In Cephalopods, constituting a limited portion of the total catch, the marketable fraction *(Sepia officinalis, Illex coindeti, Octopus vulgaris, Loligo vulgaris)* was more important in terms of percentage weight (g/h) as compared to the discarded one in all depth strata. Almost the whole part of the other invertebrates that were collected, belonged mainly to Echinoderma and especially Olothuria species, that were all discarded. In the Saronikos, fish species also dominated the catches. Discarded fish contributed more than the marketable ones to the percentage of the hourly yield in stratum A, while in deeper waters the marketable fraction was more important. The vast majority of the Saronikos catches mainly comprised *Trachurus* specimens, which influenced both the marketable and discarded portion of the catch. This was due to the fact that the species was either retained in relatively larger quantities, in cases when the rest of the marketable fraction was low, or discarded, either when the volume of the marketable species with significant commercial value was relatively high, or when the specimens were undersized (< 20 cm Total Length). The increased proportion of marketable crustaceans in both strata of the Saronikos was influenced by the significant presence of *P. longirostris*. Discarded crustaceans were mainly specimens of Munida sp. In relation to Cephalopods the greatest part was marketable. *I. Coindetii* and *Eledone* sp. were the most important in terms of hourly yield (g/h). Other invertebrates in the latter area, mainly Olothurians, were all discarded.

In order to investigate the contribution of the primarily commercial species to the marketable/discarded fraction of the trawl catch, the five most important species, in terms of both commercial value and abundance *(Merluccius merluccius, Mullus barbatus, Mullus surmuletus, Pagellus erythrinus* and *P. longirostris)* were considered as target species for the trawl fishery and were distinguished from all the rest (not-target species). In strata A and B the majority of the catch (54%) coincided with discarded not-target species (mainly Chondrichthyes species and then certain low demand ones such as *T. trachurus, Boops boops*), while marketable not-target species (mainly *Centracanthus cirrus, Dentex macrophthalmus, Pagellus bogaraveo*) exhibited a

COMPARATIVE SAMPLING OF THE MESOZOOPLANKTON WITH 333 AND 125 MICROMETER MESH SIZE NETS IN THE KASTELA BAY

Olja Vidjak

Institute of oceanography and fisheries, Setaliste I. Mestrovica 63, 21000 Split, Croatia

Abstract

In order to test the adequacy of the 333 micrometer mesh size net used until now in mesozooplankton sampling in Kastela Bay, parallel sampling with the 125 micrometer mesh size net was performed in this area. The 125 micrometer net was equally efficient in sampling cladocerans, adult stages of larger copepods, chaetognaths, thaliaceans, ostracods and decapod larvae, but more efficient in sampling calanoid copepodites, small copepods (cyclopoids and *Oncaea* spp.), appendicularians, pteropods and larval stages of bivalves, polychaets, gastropods and echinoderms which constitute the major part of mesozooplankton in this shallow neritic area. Therefore, it should entirely substitute the 333 micrometer mesh size net in mesozooplankton sampling in Kastela Bay.

Key-words: zooplankton, sampling methods, Adriatic sea

Introduction

When sampling zooplankton with any type of plankton net, the loss of organisms whose dimensions lie close to the mesh size is inevitable. Even organisms larger than the mesh size can sometimes pass through it due to their morphology, elasticity of the net itself and the fact that the pores are seldom of exactly the same size (1).

This problem is especially evident in neritic and eutrophicated areas, where inadequate sampling gear can lead to great loss of organisms through the meshes, even complete omission of zooplankton groups or species from the catch regardless of their abundance, and underestimation of the total biomass.

Although there are long term and regular data on zooplankton of the Kastela Bay (2-9), so far sampling has been performed with the 333 micrometer mesh size Hensen net exclusively. In this investigation, the adequacy of this mesh size in sampling the neritic zooplankton has been tested by parallel sampling with the 125 micrometer mesh size net.

Material and methods

Sampling was performed by the R/V Bios of the Institute of oceanography and fisheries of Split, from January to November 1995 (except in August) at one station (43°31'N: 16°19'E) located in the middle part of the Kastela Bay, a shallow and enclosed neritic area (Fig. 1). Zooplankton was sampled both with a Hensen net (mesh size 333 micrometers and 0.418 m^2 mouth area), and a Nansen net, (125 micrometers mesh size and 0.255 m^2 mouth area), by successive vertical hauls from bottom (35 m) to the surface. The samples were preserved in 2.5 % formaldehyde-seawater solution buffered with $CaCO_3$. Analysis of the subsamples (1/32 or 1/64 of the total sample) was performed under a WILD stereomicroscope at a magnification of 80x. Abundance was expressed as No. ind. m^{-3}. The significance of the differences in abundance of the recorded mesozooplankton groups between 333 and 125 micrometer net catches were tested with the Student's t-test.

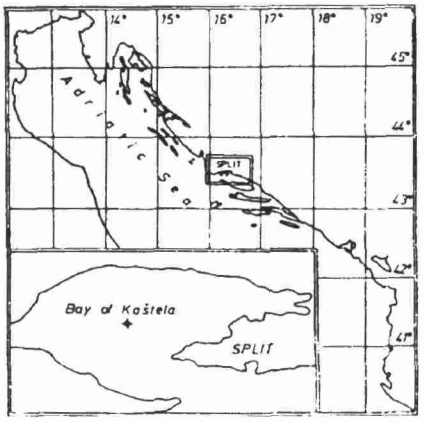

Figure 1. The study area.

Results and discussion

In 1995 at the investigated station the following zooplankton groups were recorded: Copepoda, Cladocera, Ostracoda, Appendicularia, Thaliacea, Pteropoda, Chaetognatha, Siphonophora, Medusae and larval stages of benthic organisms. In the 125 micrometer net samples ("Nansen" samples) mesozooplankton maxima were recorded in March, June and November with highest abundance in November (13966 ind. m^{-3}). In the 333 micrometer net ("Hensen" samples), mesozooplankton maximum was recorded in September with 3742 ind. m^{-3} (Fig. 2).

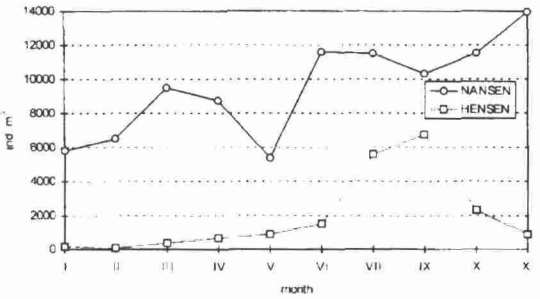

Figure 2. Annual variability of total mesozooplankton in "Nansen" and "Hensen" net catches in 1995.

Copepods Calanoids

According to Regner (5, 6, 7, 8) dominant species in this area which determine the copepod annual abundance are: *Acartia clausi, Centropages typicus, Centropages kroyeri* and *Temora stylifera.* Although no significant differences in abundance of those adult larger copepods were found between "Nansen" and "Hensen" net catches (Tab. 1), because of the incomplete data on the abundance of the smaller calanoids *(Paracalanus, Clausocalanus* and *Ctenocalanus)* we cannot state the adequacy of the 333 micrometer net in sampling all calanoids. Nichols and Thompson (10) found that the smallest copepod *Paracalanus parvus* is poorly sampled by the 270 micrometer mesh size, since even adult forms appear to pass through the meshes.

Calanoid copepodites

In "Nansen" samples, calanoid copepodites constituted 28.6 - 66.9% of the total copepod numbers, while in "Hensen" samples their contribution was 27.6 - 54.1 %. Statistically significant difference in calanoid copepodites abundance between "Nansen" and "Hensen" net catches was found (Tab. 1).

Table 1. Summarized data of Student's t-test for mesozooplankton groups.

	Significance between 125 and 330 micrometer samples
adult Calanoida	Ns
calanoid copepodites	P< 0.001
Cyclopoida	P< 0.001
Oncaea spp.	P< 0.001
Cladocera	Ns
Bivalvia larvae	P<0.05
Gastropoda larvae	P<0.001
Polychaeta larvae	P<0.05
Echinodermata larvae	P<0.001
Decapoda larvae	Ns
Appendicularia	P<0.001
Pteropoda	P< 0.05
Ostracoda	Ns
Thaliacea	Ns
Chaetognatha	Ns

Ns, Not significant

SEASONAL PHYTOPLANKTON DISTRIBUTION IN THE OFFSHORE SOUTHERN ADRIATIC WATERS

Damir Vilicic[1*], Nenad Leder[2], Zvonko Grzetic[2]

[1] University of Zagreb, Faculty of Science, Department of Botany, Rooseveltov trg 6, 10000 Zagreb, Croatia
[2] State Hydrographic Institute, P.O.Box 219, 21000 Split, Croatia

Abstract

Seasonal variations of phytoplankton, thermohaline conditions and nutrients in the oligotrophic, offshore southern Adriatic have not been published to date. Data were collected at five stations along the Bari-Dubrovnik transect (across the southern Adriatic Pit), in the 0-50 m layer, during irregularly performed case studies - from January to September, in the period from 1980 to 1990. Mixing and inflowing currents from the Ionian Sea predominate in the period from January to April, resulting in higher salinity and renewal of nutrients in the euphotic layer. The offshore southern Adriatic is characterised by microphytoplankton blooms, appearing usually in April. In May, average temperature reach 18°C, phytoplankton bloom exhaust nitrates to average concentration lower than 0.5 μmol l^{-1} and disappear. In May, phytoplankton blooms could be recorded in the eastern or western neritic waters. Following May, phytoplankton density remains low until next spring.

Key-words: Nutrients, temperature, salinity, open sea, Adriatic Sea

Introduction

The southern Adriatic is the deepest part of the Adriatic, an area with unknown dynamics of phytoplankton, because regular seasonal sampling during the same year has not been ever performed in this area. Present knowledge of natural characteristics in the southern Adriatic mainly refer to water circulation (1, 2, 3, 4), and thermohaline characteristics (5, 6). The current system in the southern Adriatic is characterised by the inflowing northerly oligotrophic current of more saline water from the Ionian Sea (predominant along the eastern coast in winter), and the outflowing southerly current of eutrophicated Adriatic water of lower salinity (predominant along the western coast in summer). The discharge of the river Po, and the exchange of water masses through the Otranto strait, influence plankton production (7), and phytoplankton distribution (8, 9). The cyclonic gyre in the southern Adriatic Pit area is a permanent physical factor (2), inducing winter/early spring upwelling and accumulation of phytoplankton in its interior, mostly in April (10, 11).

The scope of this paper is 1) to present seasonal changes of phytoplankton cell density, thermohaline conditions and nutrient concentrations along the Bari-Dubrovnik (SW-NE) transect across the Southern Adriatic Pit, and 2) to find out possible reasons of variability in phytoplankton cell density and distribution.

Materials and methods

Water samples for the analyses of phytoplankton were collected from five stations (15, 14, 13, 12, 11 in the SW-NE direction) located across the Southern Adriatic Pit, using 5-litter Niskin bottles, in the 0-50 m layer (at 0, 10, 20, 50 m), during five irregularly performed cruises of the R.V. *Andrija Mohorovicic* (January 1980, March 1990, April 1986, May 1990, July 1989, August 1986 and September 1988) (Fig. 1). Samples were preserved in a 2% (final concentration) neutralised formaldehyde solution. The cell counts were obtained by the inverted microscope method (12).

Salinity and temperature were determined using an Autolab-MK-IV inductive salinometer and Richter-Wiese reversing thermometers and CTD multisond (SEA Bird Electronics Inc., USA), respectively. The nutrient samples were taken with Niskin bottles and stored in polyethylene bottles. Phosphate and nitrate were determined by using standard methods (13). The absorbance readings were made on a Varian-Super Scan 3 spectrophotometer with 10-cm cells.

Results and discussion

Data from different cruises (from January to September in the period from 1980 to 1990) are pooled together in order to obtain an approximative seasonal variation of phytoplankton density, thermohaline conditions and nutrient concentrations in the offshore southern Adriatic.

Presented results indicated several ecological characteristics in the investigated area:

1) Thermic stratification of water column becomes evident in April, and culminate in August (Fig. 2). Temperature and salinity values are represented by single depth determinations. The thermic stratification at any one station (in figure 2) can be determined by measuring distance between upper point (warmer surface layer) and the lowermost point (colder, 50 m -layer). Mixing and inflowing current from the Ionian Sea predominate in the period from January to April, resulting in higher salinity (1, 6). On the other hand, the increased discharge of the river Po induce stronger outflowing current from the northern Adriatic. Such an transport of water of lower salinity (37.5‰ at station 15), along the Italian coast was recorded in the period from April to August. Relatively low salinity values (<38‰) were also recorded at the easternmost station 11, due to snow melting and discharge of Albanian rivers in May 1990. In August 1986, relatively low surface salinity was evident, probably due to intensive surface outflowing current, throughout the southern Adriatic.

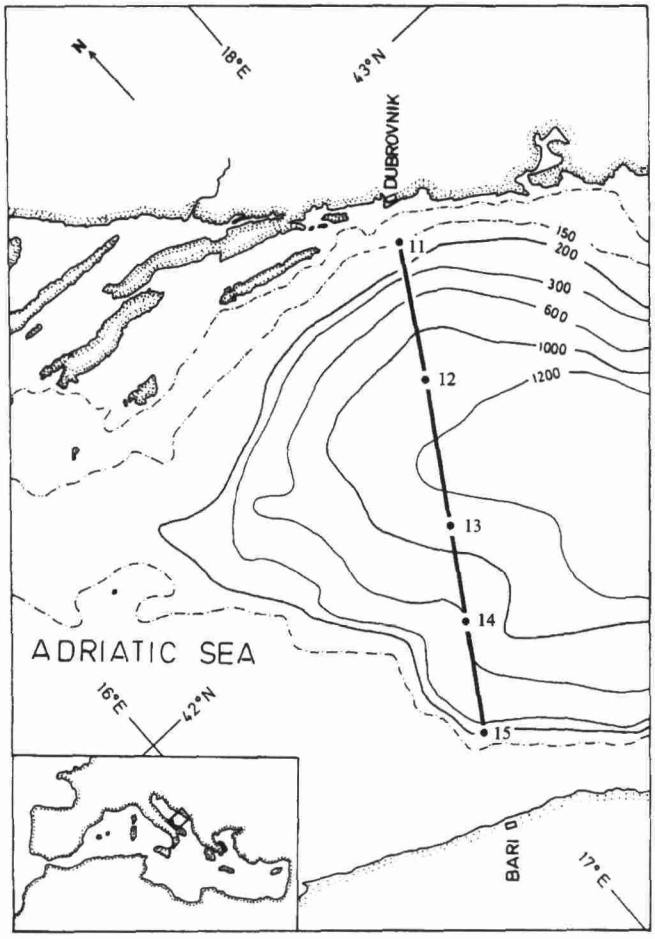

Fig. 1. Location of stations along the Bari-Dubrovnik transect.

2) Southern Adriatic contains extremely oligotrophic water, with <0.2 μmol l^{-1} PO_4 (most frequently about 0.1 μmol l^{-1}) and <3 μmol l^{-1} NO_3 (most frequently about 1 μmol l^{-1} NO_3)(Fig. 3). Winter mixing enrich upper euphotic layer with nitrate, providing short pulses of 2.5 μmol l^{-1}. In winter-spring period, concentration of orthophosphate is relatively low and constant, and progressively decrease to the minimum values (<0.03 μmol l^{-1}) in September.

IMPACT DES AMÉNAGEMENTS D'UNE ZONE HUMIDE MÉDITERRANÉENNE (LAC SMIR, MAROC) SUR *ORCHESTIA GAMMARELLUS* (CRUSTACEA, AMPHIPODA, TALITRIDAE)

M. Aksissou [1*], M. Errami [1] & M. Ménioui [2]

[1] Dépt. de Biologie, Faculté des Sciences, B.P. 2121, Tétouan, Maroc
[2] Dépt. de Zoologie et Ecologie Animale, Institut Scientifique, B.P. 703, Rabat, Maroc

Résumé

Les côtes méditerranéennes du Maroc ont connu ces dernières années des aménagements, la région du lac Smir a connu également la construction du barrage "Smir" et du port "Kabila", ce qui a entraîné des modifications de l'hydrologie du lac et de sa biodiversité. Après cet aménagement, le lac devient saumâtre et la plupart des marécages disparaissent, la reproduction d'*Orchestia gammarellus* devient continue, la fécondité et la longévité maximale se réduisent, le sex-ratio d'origine génétique reste très stable avec une population semi-annuelle et multivoltine. Cette population du lac Smir présente donc une grande plasticité de ses caractères reproductifs et démographiques lui permettant de survivre malgré la variation du milieu environnant sous l'action climatique ou anthropique.

Mots clés : crustacea, coastal management, Western Mediterranean

Introduction

Le lac Smir est une étendue d'eau se situant sur le littoral méditerranéen du Maroc à 35°43'N et 5°21'W, il a connu en 1990 un aménagement se résumant à la construction du barrage Smir et du port de plaisance "Kabila". Ceci a entraîné des conséquences sur l'hydrologie et la biodiversité de cet écosystème.

Orchestia gammarellus est un Amphipode Talitridae vivant sous les laisses des marées dans la zone supralittorale. Il joue un rôle écologique dans la dégradation de la matière organique et constitue un maillon important dans la chaîne alimentaire des oiseaux et des petits mammifères (1,2). Cette espèce montre une large répartition géographique depuis la Suède (3), l'Angleterre (4), la France en Atlantique (5) et en Méditerranée (6,7), le Maroc (8), les Açores, Madère et les Canaries (9) et sur le littoral atlantique argentin (10). Son cycle reproducteur, son cycle de mue et sa croissance ont été étudiés en Suède (3), en Angleterre (2,11,12), en France (5,1) et au Maroc (13).

Disposant d'une étude écologique antérieure à cet aménagement, il nous a paru intéressant d'évaluer les conséquences de cette action anthropique. La présente étude essaye également de tester l'impact des aménagements sur la dynamique des populations d'*O. gammarellus* afin d'évaluer l'effet anthropique sur cet écosystème humide du littoral méditerranéen du Maroc et proposer des solutions pour sa conservation.

Méthodologie

Dans le lac Smir, *O. gammarellus* se répartit sous les laisses et aussi sous des amas d'argile. Pour les individus vivant sous les laisses, la méthode d'échantillonnage est la suivante: les laisses déposées en bandes ou cordons d'une largeur d'environ 0,20 m sont prélevées sur une longueur de 2,5 m et remuées dans un bocal à large ouverture rempli d'eau formolée. Le nombre d'individus capturés reflète la densité par 0,5 m^2. Pour les individus existant sous les amas d'argiles, ils sont prélevés sur un carré de 625 cm^2 (25 cm x 25 cm) et cette opération est répétée huit fois. La densité finale est la somme des densités par 0,5 m^2 de laisses et 0,5 m^2 d'amas d'argile.

Au laboratoire, les échantillons sont triés, comptés et séparés en plusieurs groupes:

1- groupe des juvéniles, immatures sans sexe différencié dont la taille du corps est comprise entre 2 et 6 mm.

2- groupe des intermédiaires, immatures mais avec différenciation morphologique externe du sexe (développement du propodite de la deuxième paire des gnathopodes chez le mâle, oostégite de la femelle) et de taille comprise entre 6 et 9 mm.

3- groupe des adultes, individus reproducteurs avec différenciation nette des caractères sexuels secondaires (propodite hypertrophié de la deuxième paire des gnathopodes chez le mâle et chez la femelle présence d'oostégites développés et ciliés) dont la taille est supérieure à 9 mm. Ce groupe des adultes est subdivisé en mâles et femelles, ces dernières sont de trois types: femelles non reproductrices à oostégites petits non ciliés, femelles ovigères ou gestantes et femelles reproductrices vides à oostégites grands et ciliés. Le nombre et la taille des individus de chaque groupe sont mesurés. De même, le contenu du marsupium des femelles gestantes est compté et la taille des individus est notée.

Résultats et discussion

La population d'*Orchestia gammarellus* dans le lac Smir en milieu naturel (avant l'aménagement) montre une activité reproductrice marquée par un bref repos sexuel en hiver (février) et un long arrêt de la reproduction durant tout l'été, de juin à septembre. Cette activité devient continue après l'aménagement, cependant avec une réduction du taux d'activité reproductrice pendant l'été et l'hiver (fig. 1). Il apparaît ainsi que le changement du régime hydrique d'un système affecté essentiellement par les précipitations vers un système dépendant de la marée, agit sur la reproduction de cette population. En effet, le biotope de la population devient après l'aménagement en permanence humide et indépendant des précipitations, la marée semi-diurne apporte l'eau saline au lac le long de l'année et la population est toujours présente avec ses différentes stades. Les adultes présents toute l'année assurent une reproduction continue. La population du lac Smir a toujours une vie brève de 8 mois environ et se reproduit l'année même de sa naissance; mais avant l'aménagement, les individus nés au printemps se reproduisaient fin septembre-début octobre (4 mois après) et leur activité reproductrice se poursuivait de manière continue jusqu'en janvier, alors qu'après l'aménagement, les individus nés en une saison se reproduisent la (ou les) deux saisons suivantes. Cette différence est due à l'absence de la mortalité estivale des adultes après l'aménagement puisque l'eau est présente en permanence, alors qu'avant l'aménagement une mortalité massive d'adultes en été ne permettait la survie que d'un petit lot de femelles de 9 à 11 mm.

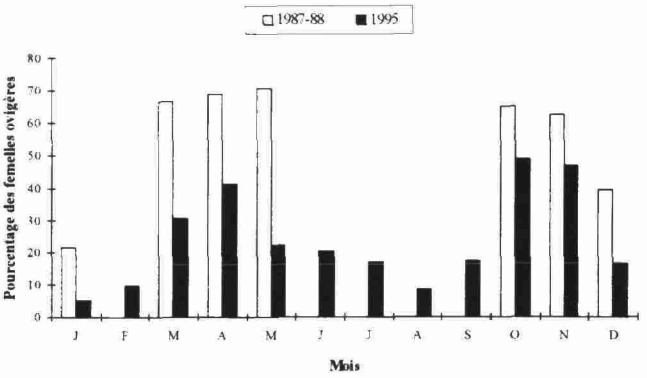

Figure 1 : Impact de l'aménagement du lac Smir sur le taux d'activité reproductrice chez *Orchestia gammarellus*.

Les phases de repos sexuel et de mortalité d'adultes ou d'atténuation de la reproduction reflètent une action des facteurs hydrologiques et climatiques. L'action du "froid hivernal" avant l'aménagement et après l'aménagement est de courte durée et s'exerce au travers de l'inhibition de la reproduction et de l'accouplement (1). Cette action climatique était surtout spectaculaire avant l'aménagement dès la mi-juin et durant l'été où on notait à côté des températures moyennes de 22°-25° C, des températures maximales de 35° à 37° entre 12 et 15 heures sur le site de cette population du lac Smir. De telles températures ne peuvent être tolérées plus d'une heure (14). Dans ces conditions environnementales, les adultes ne peuvent résister et la recherche de refuges, surtout entre les fentes de dessiccation des vases, est une nécessité absolue, ce qui avantage les individus de petite taille et pourrait expliquer la survie des juvéniles trouvant plus facilement un habitat adéquat. Alors qu'après l'aménagement, l'effet de la marée réchauffe l'eau en hiver et la rafraîchit en été, d'où la présence conti-

A MAP OF SEAGRASS MEADOWS IN PALAEOCHORI BAY (MILOS ISLAND, GREECE), A MARINE AREA WITH HYDROTHERMAL ACTIVITY

Stefano Aliani [1]*, C. Nike Bianchi [2], Silvia Cocito [2], Paul R. Dando [3], Roberto Meloni [1], Carla Morri [4], Adelbert NieMeyer [5], Andrea Peirano [2] and Wiebke Ziebis [6]

[1] Istituto per lo studio dell'Oceanografia Fisica, CNR, Forte Santa Teresa, 9036 Pozzuolo di Lerici (La Spezia), Italy
[2] Marine Environment Research Centre, ENEA Santa Teresa, P O Box 316, 9100 La Spezia, Italy
[3] School of Ocean Science, University of Wales-Bangor, Menai Bridge, Anglesey LL59 5EY, U.K.
[4] Istituto di Zoologia, Università, via Balbi 5, 6126 Genova, Italy
[5] Vincenz-Statz Str 16, Köln, Germany
[6] Max-Planck-Institute for Marine Microbiology, Celsiusstr. 1, 28359 Bremen, Germany

Abstract

Cymodocea nodosa (Ucria) Ascherson and *Posidonia oceanica* (L.) Delile form extensive meadows in Palaeochori Bay, but only the former lives in close proximity to actively venting sites and brine seepage areas.

Key-words : phanerogams, thermal vents, Aegean Sea

Introduction

Seagrass meadows are dominant and conspicuous communities, of prime importance to the ecology of marine coastal areas (1). Five seagrass species occur in the Mediterranean Sea, but only *Posidonia oceanica* (L.) Delile forms major meadows. *Cymodocea nodosa* (Ucria) Ascherson may also be abundant in certain areas. The importance of seagrass meadows, both from an ecological point of view and for the coastal equilibrium, induced many Mediterranean countries to map their extension (*e.g.*, 2, 3 and references therein).

In the Aegean Sea, seagrasses are known to occupy an important area (2) but only few sites have actually been mapped : Gulf of Geras, Lesvos Island (4), Saronikos Gulf (5), Gulf of Thermaikos (6).

In this paper, we present a first map of seagrass meadows in Palaeochori Bay, an area located to the SE of Milos Island, which is strongly influenced by hydrothermal activity (7, 8). First observations on the biological communities in this area showed that both *Posidonia oceanica* and *Cymodocea nodosa* were present (9, 10).

Methods

The coastline of Palaeochori Bay was surveyed in June 1996 by compass traverse, using aerial photography as a basis. The sea-floor of the bay was mapped from an inflatable rubber boat equipped with an echo-sounder and post-processing dGPS (~ 10 m accuracy) connected to a portable computer. While the boat was holding courses perpendicular to the coast, an observer gave the computer technician a "mark" every time the boat was exactly above an edge of the meadow. Thanks to the great water visibility (20 m and more), the canopy cover was estimated visually, as done in manta tow surveys (11). Position of most vent sites was located by snorkelling or SCUBA diving. Depth contours and the other data recorded were elaborated using ®Surfer and ®Autocad software packages.

Results and discussion

A qualitative map of the seagrass meadows in Palaeochori Bay was originally produced at a scale 1 :10,000 but is reproduced at a smaller scale in the present paper (Fig. 1). Mapping was restricted to a depth

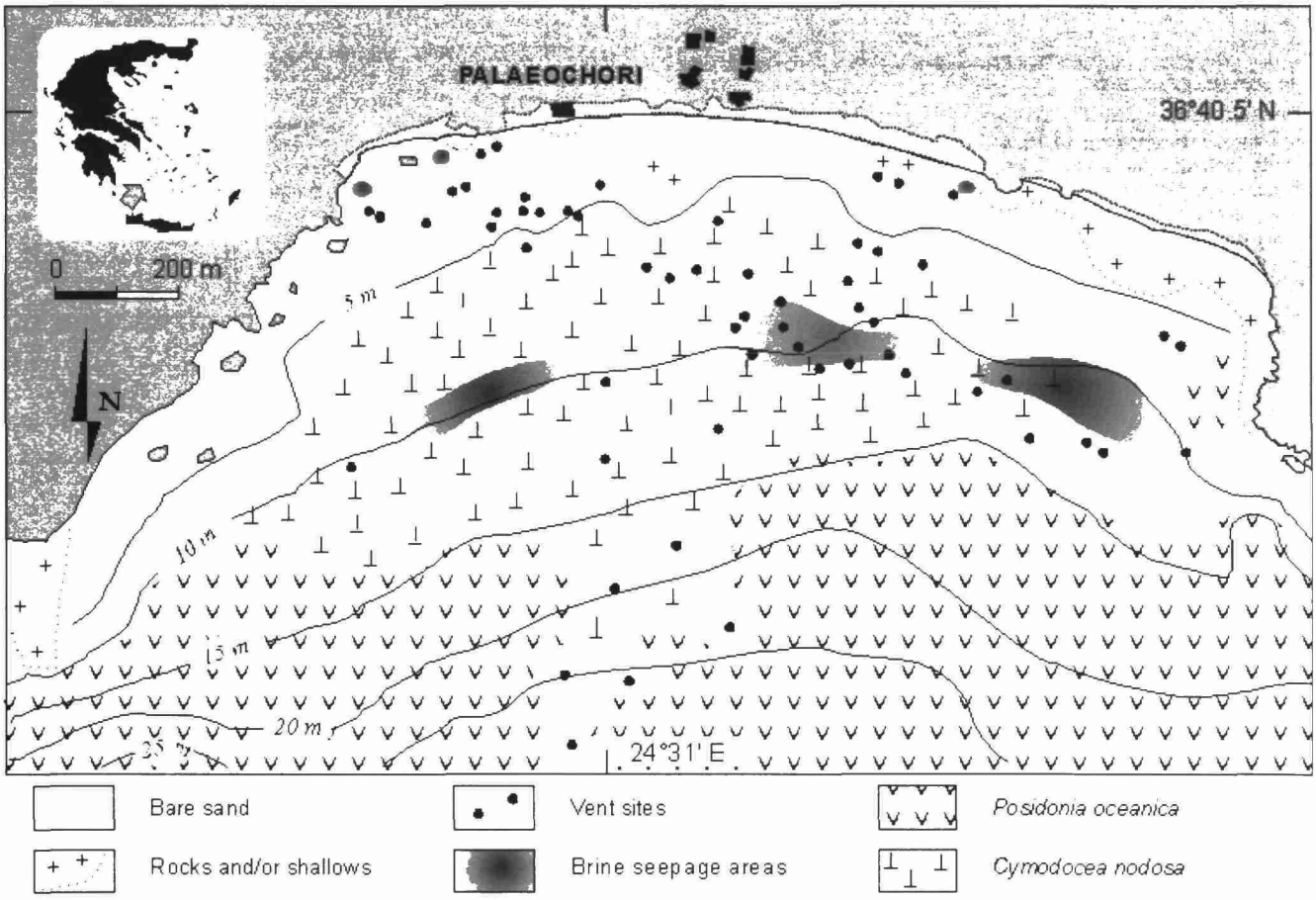

Figure 1 : Bathymetric map of Palaeochori Bay, Milos Island, with hydrothermal sites and seagrass meadows.

BOUGIE PLAGE : EVOLUTION DU TRAIT DE COTE. CAUSES ET CONSEQUENCES

A. Baazizi*, R. Belkessa, F. Bahloul, H. Mezidi
Ismal, B.P 54, Sidi - Fredj, 42321 Tipaza, Algérie

Résumé
A Bougie plage l'érosion marine s'exerce surtout aux dépens des rivages établis dans des formations meubles. L'exemple de Bougie plage concernant son recul est unique à l'échelle nationale. Une étude sur l'évolution du trait de côte nous a aidé à évaluer l'intensité du recul.

Mots-clés : erosion, shoreline evolution, Western Mediterranean

Introduction

Les franges côtières sont des milieux dynamiques, en constante évolution, riches en ressources naturelles et en écosystèmes à forte productivité (1). Le paysage littoral de la façade orientale de Bougie plage est actuellement très affecté par l'érosion qui a entraîné une dégradation rapide du milieu naturel. Cet état de fait nous a incité à entreprendre une étude de l'évolution du trait de côte au niveau de ladite région. La zone d'étude se situe à 236 Km à l'est d'Alger . Elle est limitée à l'ouest par le port et s'étend sur 2.5 Km de côte jusqu'à 150 m derrière la piste de l'aéroport. Elle est positionnée entre 36° 44' 15"N - 5° 04' 15"E 36° 44' 45"N - 5° 05' 18"E.

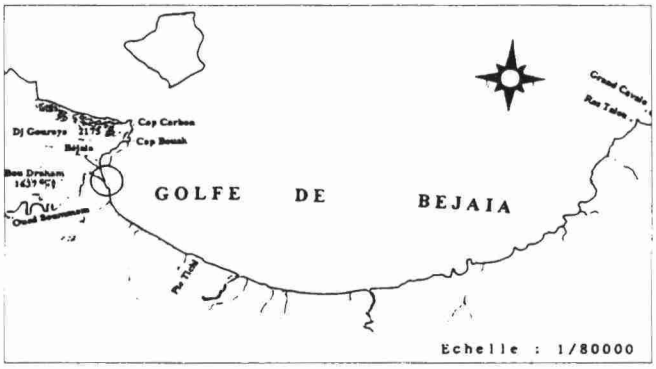

Figure 1 : Situation géographique.

Evolution du trait de côte

L'étude des variations des traits de côte constitue un élément important pour avoir une meilleur connaissance sur l'évolution des plages et sachant que le trait de côte est dynamique par nature, nous avons établis un linéaire récent (juillet 1996).

L'érosion marine affecte surtout les rivages établis dans les formations meubles. C'est le cas de Bougie plage qui est constituée de dépôts fluviatiles quaternaires. Des cartes marines, topographiques et de photos aériennes relatives à six missions (1922, 1953, 1976, 1991, 1992 et 1996) ont été utilisées pour l'étude de l'évolution du trait de côte (fig. 2).

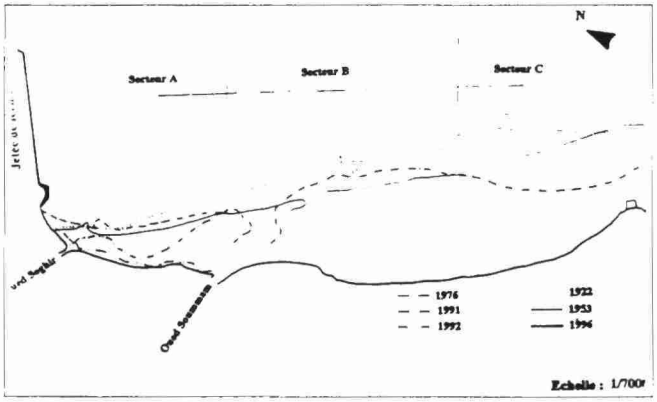

Figure 2 : Evolution du trait de côte de Bougie plage.

L'évolution du trait de côte est un paramètre très important qui permet de juger sa dynamique. L'érosion marine affecte surtout les rivages établis dans les formations meubles. Localement on enregistre des reculs rapides. A court terme, certains secteurs pourraient également se trouver menacés. Cette différence d'érosion qui affecte le littoral est liée surtout à l'impact de la houle, cette dernière étant liée aux changements bathymétriques.

La comparaison des différentes variations du trait de côte est basée sur l'estimation métrique, de son recul ou de son avancée, pour ce faire nous avons divisé la zone d'étude en trois secteurs : A, B et C (fig.3).

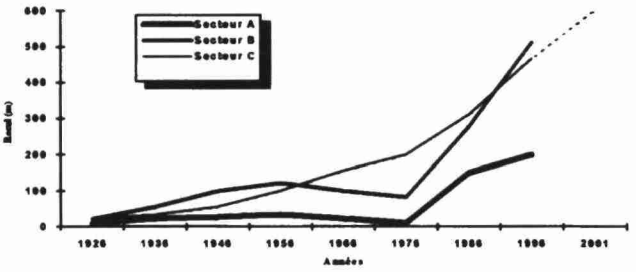

Figure 3 : Situation géographique.

Nous remarquons que l'érosion du secteur C est plus intense, elle est de 500 mètres en 74 ans. A première vue, nous penserons que ceci serait dû aux agents hydrodynamiques qui concentreraient leur énergie dans ce secteur, néanmoins, la diminution des apports fluviatiles a engendré un recul rapide (Table 1).

Table 1 : Estimation en mètres du recul du trait de côte pour les trois secteurs

	1922-1953	1953-1976	1976-1991	1991-1992	1992-1996	TOTAL
A	-34.40	+24	-70	-69	-16.5	-165.9
B	-122	+35.50	-409			-495.5
C	-79.50	-44	-289			-512.5

(-) : recul du trait de côte (érosion).
(+) : avancée du trait de côte (engraissement).

Toutefois, l'année 1976 a été marquée par un engraissement de la plage, ce dernier est visible dans les secteurs A et B. Ces derniers sont en contact direct respectivement avec les oueds Seghir et Soummam, ceci permet d'en déduire que cette année a été riche en apports solides. Ce fait s'explique par la longue période sèche qui a précédé la saison des crues. Les sols se trouvants ainsi secs sont facilement érodables d'où les apports importants durant la saison automnale.

La période allant de 1991 à 1992 a été marquée par une très forte érosion; celle-ci a été appréciée à l'échelle mensuelle, voire à l'échelle journalière. Le gros des matériaux rencontrés sur les plages est d'origine terrigène et, à cet égard, les apports des cours d'eau sont les plus substantiels (2) .

Causes de l'érosion

Longtemps peu fréquenté, le littoral est aujourd'hui le siège de nombreuses activités humaines (industries, stations d'épurations, développement touristique) qui font peser des menaces sur les milieux littoraux fragiles, pouvant aller jusqu'à leur disparition. Les activités humaines sont souvent la source de dégradation :

- lorsqu'elles perturbent les échanges entre les compartiments des accumulations en modifiant la dynamique marine (digues, épis, enrochements);
- lorsqu'elles entraînent la destruction de la végétation (piétinement, passage de véhicules), elles favorisent l'érosion éolienne (3).

TARGET SPECIES AND CPUE OF TRAMMEL, GILLNET AND COMBINED NET IN SANDY AND ROCKY BOTTOMS

Romano Baino, Paolo Righini* and Roberto Silvestri
Agenzia Regionale Protezione Ambientale Toscana
Consorzio Regionale di Idrobiologia e Pesca
Via dell'Ambrogiana 2, I-57127 Livorno, Italy

Abstract
Catch Per Unit Effort data have been used to evaluate the performance of the most common bottom-nets utilized by the tuscanian artisanal fisheries. Fishing experiments were carried out since 1976 with three different nets in four areas with various environmental characteristics. Total productivity and C.P.U.E. of target species are described in relation to both gear type and fishing grounds.

Key-words : fisheries, instruments and techniques, Tyrrhenian Sea

Introduction

Trammels, and gillnets are the most common gears in the artisanal fisheries along the Tuscany coast. This activity represents an important productive reality since it involves more than 1300 fishermen and 600 boats with annual catches over 4000 tons. The traditional boats are fairly small, between 4 and 10 m of length with an average of 1 gross tonnage and engine of 15 KW; the mean age of this fleet is 15 years, even if some of them are over 30. Nevertheless, in the last decades only a couple of scientific works (1,2) have been published on this topic. Also in the whole Italy only few papers point to the productivity of artisanal nets (3,4,5).

Materials and Methods

The collected data arise from 556 fishing experiments carried out during the last 20 years closely south of Livorno in 4 areas with different environmental characteristics: A zone with sandy bottom and depth lower than 15 m ; B zone with rocky bottom and depth lower than 15 m ; C zone with intermediary grounds to the precedings ; D zone with muddy bottom of the slope around 30 m depth. The fishing experiments have been performed from the sunset to the dawn using from 500 to 1000 m of net of three different types: Bottom trammels are 1.5 m high with internal mesh size of 21 mm and external mesh of 150 mm (223 experiments). Gillnets are 3 m high with 35 mm mesh size and 0.25 mm nylon filament diameter (used in 255 experiments). The combined trammel-gillnets are high 5 m, the upper gillnet of 3.5 m has 35 mm mesh size, the lower trammel has 31 mm and 200 mm mesh size (78 experiments).

The whole catch has been sorted to species level, weighted and counted. The data stored in a database have been standardized into Catch Per Unit Effort (CPUE) expressed in grams for 100 m of net.

Results

Globally, it has been fished 94 species of fishes, crustaceans and cephalopods, even if only 20 of these represent in weight more of the 90% of the catch (Fig.1).

The CPUE were analyzed in relation to the used gear:the combined trammel-gillnet is the more productive (1133 g/100m) with the trammel (1012 g/100m), while the productivity of gillnet is significantly lower (684 g/100m).

Error estimate of total catch was computed by means of standard deviation between years: in all cases it is close to 300 g/100 m (298, 269 and 273 g/100 m respectively). Statistical analyses show that catch data from trammel are normally distributed while those from gillnet are lognormal. This is related to the catch composition: trammel catches are mainly groundfishes close to the bottom (the net is 1.5 m high) with elements of territorial behavior and consequent random pattern. The catches of gillnet (3 m high) are dominated by semi-pelagic species clustered in shoals (7) which determine lognormal distribution.

The target species of gillnets are grey mullets (*Liza ramada* 75 g/100 m, *Mugil cephalus* 56 and *Chelon labrosus* 55) and salema (*Sarpa salpa* 101 g/100 m). These species are common also in the combined net (*Liza ramada* 100, *Chelon labrosus* 52, *Mugil cephalus* 39 and *Sarpa salpa* 116), but in this case the catch is dominated by cuttlefish (*Sepia officinalis* 298 g/100 m) and rays (*Raja clavata*, *R. asterias* and *R. undulata*, 218 g/100 m altogether). The trammel catches mainly scorpionfish (*Scorpaena porcus* 193, g/100 m), cuttlefish (*Sepia officinalis*, 176), *Octopus vulgaris* (169), mullet (*Mullus surmuletus*, 84) and wrasse (74 g/100 m).

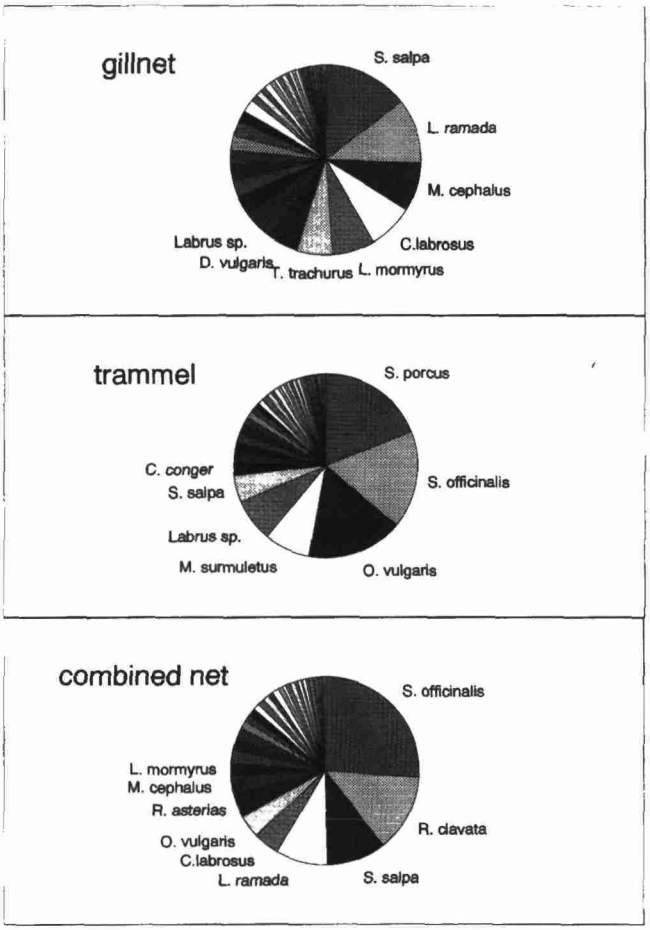

Figure 1 : Catch composition of the different nets.

In relation to the environmental typology of the bottom, the gillnet catches are similar in all the coastal areas (793 g/100 m in A zone, 569 in C zone, 617 in B zone) and lower offshore (217 g/100 m in D zone). On the other hand, the trammel productivity increases from the sandy grounds toward the rocky grounds (652 g/100 m in A zone, 888 in C zone and 1315 in B zone) and depth (1593 g/100 m in D zone).

Obviously, the species composition changes too: on sandy bottoms about 20 % of the yield is composed by cuttlefish alone, significant are also grey mullets and stripped bream (*Lithognathus mormyrus*). On intermediate grounds octopus, scorpionfish and red mullets increase while cuttlefish slightly decrease. Catches in rocky areas close to the reefs are dominated by scorpionfish, octopus and red mullets. In the D zone (30 m depth) the main species is the pandora (*Pagellus erythrinus*) which represents about a half of total catches.

The 20 years of available data have been analyzed looking for quantitative trends in the CPUE of some species and/or gears. The fluctua-

INFLUENCE OF ISOLATION AND PECULIAR ECOLOGICAL PROPERTIES ON BIODIVERSITY AN EXAMPLE OF MARINE LAKE ZMAJEVO OKO NEAR ROGOZNICA (ADRIATIC SEA)

Tatjana Bakran-Petricioli [1*], Donat Petricioli [2] and Antonieta Pozar-Domac [1]

[1] Department of Zoology, Faculty of Science, Zagreb University, Rooseveltov trg 6, 10000 Zagreb, Croatia

[2] DIIV Ltd., 23281 Sali, Croatia

Abstract

In a small marine lake Zmajevo Oko (Dragon's Eye) near Rogoznica (middle Dalmatia, Croatian coast of Adriatic Sea) upper water layer is in contact with surrounding coastal sea through fissures in karstic rocks, so tides are noticeable but reduced. Almost permanent water column stratification (temperature, salinity, oxygen concentration, presence of H_2S) is present in the lake. We investigated biological properties of the lake several times in period from 1993 to 1996. Benthic communities in the lake differ from communities that can be found in surrounding coastal sea. In Zmajevo Oko fewer species with denser populations were observed and some common species were not observed at all. We discuss possible reasons for such situation. Proper evaluation of scientific and natural values of this rare karstic phenomenon of our coast should be done.

Key-words : zoobenthos, stratification, Adriatic Sea

Introduction

A marine lake Zmajevo Oko (Dragon's Eye) is located on Gradina Peninsula near village of Rogoznica, about 30 km SE from Sibenik on the Croatian coast of Adriatic (Fig. 1). It is a small body of sea water, 150 x 70 m in size, maximum depth 15 m, surface of which is estimated to be 5300 m^2 (1). There is no visible contact with surrounding coastal sea but tides are present in the lake (although they are reduced). The lake is surrounded by vertical karstic rocks from up to 4 m high (on its northern side) to up to 24 m high (on its southern side) above the water level. Vertical rocks continue into the water, where on depths from 1 to 7,5 m sediment bottom begins. The bottom is then gradually sloping towards the deepest part of lake on 15 m.

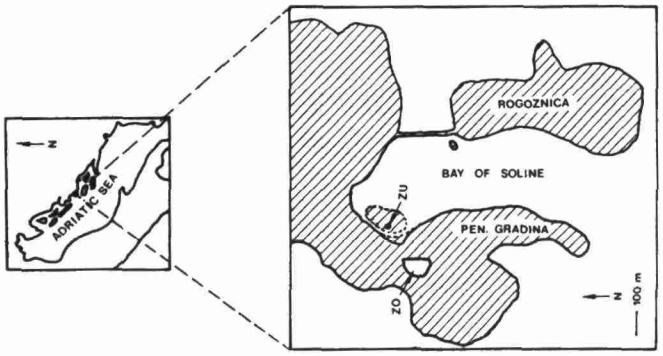

Figure 1 : Location of the marine lake Zmajevo Oko (ZO ; Dragon's Eye) on Gradina Peninsula near Rogoznica. Building of nearby nautical centre threatens to endanger this rare karstic phenomenon of Croatian Adriatic coast. Broken line shows approximately the position of already finished artificial island (which is a part of the mentioned nautical centre). Location of already endangered sunken marine cave Zmajevo Uho (ZU ; Dragon's Ear), which is now in the middle of the artificial island, is also shown.

A geological origin of the lake is thought to be connected with a collapse of the roof of primary underground cavity formed by palaeostreams. Due to postglacial sea level rise, it was filled with seawater through underground fissures (2).

Water column stratification in the lake with regard to temperature, salinity, density, oxygen concentration and presence of hydrogen sulfide is almost always present (3, 4, 5). A high primary production on the basis of chlorophyll a distribution was noted in the lake. Namely, 2-3 times higher chlorophyll a concentrations was present in the lake in comparison to surrounding coastal sea (6).

Sediment in the lake is characterised as an authigenic carbonate sediment of mainly biogenic origin belonging to the anoxic-sulfidic sedimentation environment. Sedimentation accumulation rate was estimated to be 0.093 gcm^2 per year (approx. 4.5 mm per year) which can be considered quite high in comparison to surrounding coastal area (2).

Recently, the building of a nautical centre in nearby Soline Bay stirred up a lot of public discussions about natural value of this rare karstic phenomenon. In spite of a wide public action aimed towards the protection of Zmajevo Oko it was not possible to achieve its classification in one of the natural protection categories regulated by law.

Methods

In period from 1993 to 1996 we have dived ten times in the lake, in irregular intervals, but mostly during winter because of better visibility. We used standard SCUBA equipment and strong underwater lights. We took photos with underwater camera (Nikonos V; objectives 28, 35 and 80 mm). Quantitative biological samples of benthos we collected from 50x50 cm squares and weighted them on simple household scale.

Results and discussion

Stratification of water column in the lake was so strong that it was possible to note it even without special instruments, not only visually and thermally but olfactory as well. Namely, smell of hydrogen sulfide is passing through a diving mask. During research period, only in November 1993 layer with hydrogen sulfide was not present in the lake. At all the other occasions when we have dived, layer was present from the bottom to up to 8 meters of depth (in January 1993).

A very narrow supralittoral zone is present in the lake. A dark green zone (from blue-green algae in/on the rocks) is wide only up to 20 cm. In that zone we noticed isopod Ligia italica Fabr.

In a shallow zone down to 2m on the northern side of lake (which is more exposed to sunlight) green algae *Codium tomentosum* Stackhouse and *Cladophora* sp. were more often present. A red alga *Antithamnion* sp. was also present there as well as on rocky walls along the southern side of the lake (which is in a shadow considering sunlight due to high rocks around the lake on that side). A very dense population of little mussel *Mytilaster* sp. (somewhere up to 4000 individuals per m^2) was also present in that shallow zone. On the rocks, all around in the lake, consequences of boring activity of sponge *Cliona celata* (Grant) and bivalve *Petricola lithophaga* (Retzius) could be seen. Rocks around fissures through which water in lake communicates with surrounding sea (7) and rocks along the southern (shaded) side of the lake (on depths from 2 to 4 m) were completely covered with ascidian *Pyura dura* Heller, another frequent organism in the lake. Settlements of these animals in such areas could reach population density of up to few hundreds of individuals per m^2 and an average wet biomass of up to 10 kg per m^2.

Different animal groups were noticed in the lake: jellyfish *Aurelia aurita* Lam., echiuran *Bonellia viridis* Rolando; gastropods: *Gibbula divaricata* (L.), *Trunculariopsis trunculus* (L.) (empty shells only), *Gourmya rupestris* (Risso), *Berthella aurantiaca* (Risso); bivalves: *Mytilus galloprovincialis* Lam., *Ostrea edulis* L.; crustaceans: *Palaemon* sp., *Homarus gammarus* (L.), *Palinurus elephas* (Fabr.), *Xantho poressa* (Olivi); fishes: *Conger conger* (L.), *Dicentrarchus labrax* (L.), *Chromis chromis* (L.), *Blennius pavo* Risso, *Oligopus ater* Risso, *Gobius bucchichii* Steind., *Gobius* sp., *Mugil* sp., *Tripterygion* sp. Their distribution in the lake as well as their relative abundance is shown on Table 1. A few collected species of sponges, polychetes and bryozoans are not determined yet.

On the sediment bottom, we did not notice any of common macrobenthic organisms. We noticed only a dense population of prawns *Palaemon* sp., which was present from the water surface all the way down to anoxic water layer.

In small caves (up to 8 m long) and crevices in the lake, we noticed a rich living community. Different species of sponges which overgrew each other dominated in the entrance part while deeper, in darker part of the caves, the ascidian *Pyura dura* prevail. Ascidians in the caves were regularly developed and without fouling, on the contrary to those

RECHERCHES SUR LA BIOTYPOLOGIE DES MOLLUSQUES DE LA LAGUNE DE MOULAY BOUSSELHAM, MAROC

H. Bazairi et A. Bayed*

Institut Scientifique
Département de Zoologie et Ecologie Animale
B.P. 703 - Agdal, 10106 Rabat, Maroc

Résumé

L'étude biotypologique de la lagune de Moulay Bousselham est approchée à l'aide de la malacofaune récoltée dans 285 relevés (15 stations intertidales et 15 stations dans le chenal) effectués entre février 94 et février 95. 33 espèces ont été récoltées dont 23 sont nouvelles pour la lagune. Les facteurs hydrodynamiques (marée, houle), climatiques (température) et hydrologiques (salinité) conditionnent la répartition de la macrofaune. Les facteurs hydrodynamiques et édaphiques paraissent plus prépondérants en zone intertidale que la salinité qui semble contrôler davantage la distribution de la malacofaune dans le chenal.

Mots-clés : Lagoons - Mollusca - Temperature - Salinity - Western Mediterranean

Matériel et méthodes

La lagune de Moulay Bousselham est située sur le littoral atlantique marocain à 150 km au nord de Rabat. De forme générale elliptique, elle occupe une surface de 30 km^2 avec une longueur maximale de 9 km et une largeur maximale de 5 km. Elle est divisée en deux merjas de dimensions inégales : La merja Kahla et la merja Zerga. Le climat qui y règne est de type méditerranéen sous influence océanique. L'alimentation en eau douce se fait par l'oued Drader, à l'est et par le canal du Nador, au sud. Par le biais de la marée, l'eau de mer pénètre régulièrement dans la lagune et son influence dépend de l'amplitude de la marée et de la morphologie du goulet.

L'échantillonnage de la faune a intéressé la zone intertidale et les chenaux (Fig. 1). En zone intertidale, 15 stations ont été échantillonnées mensuellement entre février 1994 et février 1995. Les récoltes sont réalisées à la bêche sur une surface de 0.25 m^2 pour une profondeur d'environ 20 cm. Au niveau des chenaux, 15 stations ont été choisies où des dragages ont été effectués une fois par trimestre entre avril 1994 et janvier 1995, à l'aide d'une drague Picard. Dans les deux types d'échantillonnage, le tamisage a été effectué sur place au moyen d'un tamis de 1 mm^2 de vide de maille. Les prélèvements biologiques ont été couplés avec les mesures de température et de salinité et par des prélèvements de sédiment. Celui-ci sera caractérisé par la médiane granulométrique, le taux de pélites et le taux de matière organique.

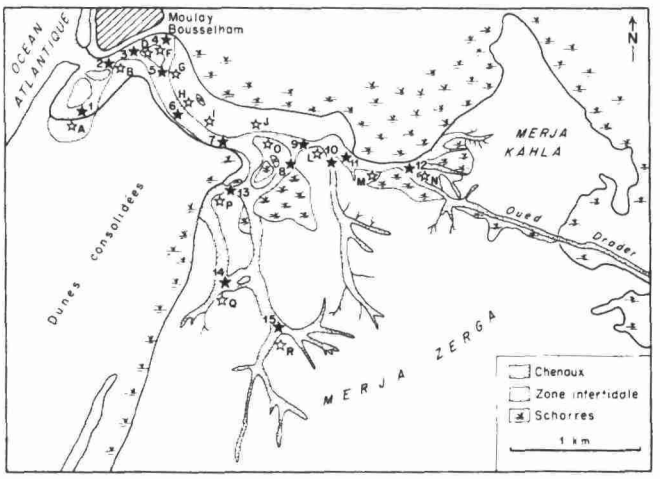

Figure1 : Présentation générale de la lagune de Moulay Bousselham et localisation des stations intertidales (étoiles claires) et des stations du chenal (étoiles sombres).

L'analyse biotypologique a été approchée en utilisant l'AFC. En zone intertidale, l'élément général de la matrice des données correspond à l'abondance moyenne de chaque espèce sur les 13 relevés mensuels. Pour les dragages nous avons utilisé comme élément général de la matrice la dominance partielle moyenne de chaque espèce sur les quatre relevés saisonniers. En raison de la forte variation des valeurs de dominance entre espèces, nous étions amenés à utiliser la transformation log(n+1), n'étant la dominance moyenne.

Résultats

L'ensemble des relevés permet de recenser 33 espèces de mollusques qui se répartissent entre bivalves (20 espèces), gastéropodes (12 espèces) et Polyplacophores (1 espèce). Parmi cette malacofaune, 23 espèces sont nouvelles pour la lagune (13 bivalves, 9 gastéropodes et 1 polyplacophore) soit 70% des espèces rencontrées.

Pour l'AFC appliquée aux prélèvements intertidaux, nous retiendrons le plan factoriel F1xF2 avec les axes F1 et F2 qui totalisent 79% de l'inertie totale (Fig. 2). Trois ensembles peuvent être distingués : E1 (stations A, B, D, F, H, I et O) avec l'espèce *Cerastoderma edule*, E2 (stations G, J, L, P, Q et R) avec *Scrobicularia plana* et E3 (stations M et N) avec *Haminaea* sp.

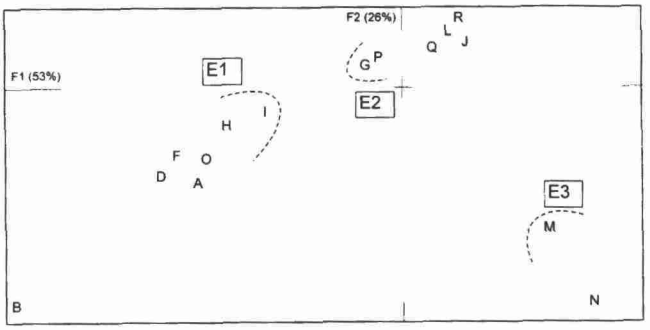

Figure 2 : Représentation graphique du nuage des points stations dans le plan factoriel F1xF2 de l'AFC appliquée à la zone intertidale.

Dans le but de donner une signification écologique aux axes factoriels, nous avons confronté, sous forme de représentation graphique en nuage de points, la position des stations selon un axe factoriel, d'une part, et chacune des variables du milieu, d'autre part. Cette représentation fonctionnelle des axes factoriels est testée par l'utilisation du coefficient de corrélation de rang de Spearman [1]. L'expression fonctionnelle de l'axe F1 se traduit par une corrélation significative avec la température interstitielle, le taux de sables grossiers et graviers, le taux de sables fins, le taux de pélites, la médiane granulométrique, et la salinité (Fig. 3). L'axe F2 exprime une corrélation significative avec les taux de sables fins et de pélites.

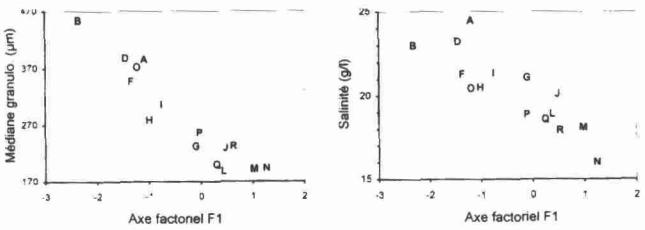

Figure 3 : Expression fonctionnelle de l'axe factoriel F1 en fonction de la médiane granulométrique et de la salinité.

Dans le cas des chenaux, le plan factoriel F1xF3 a été retenu, les deux axes cumulant 46% de l'inertie totale (Fig. 4). Le nuage des points stations se scinde en trois noyaux : Le premier (N1) comporte

IMPORTANCE DES NEMATODES LIBRES DANS LE SUIVI ECOLOGIQUE D'UN MILIEU LAGUNAIRE PERTURBE : L'ECOSYSTEME ICHKEUL (TUNISIE)

H. Beyrem * et P. Aissa

Laboratoire d'Ecobiologie Animale, Faculté des Sciences de Bizerte, 7021 Zarzouna, Tunisie

Résumé

Le "lac" Ichkeul est un écosystème particulièrement important pour l'avifaune. Dans ce milieu aux composantes physico-chimiques peu stables tant à l'échelle spatiale que temporelle, il est entrepris un suivi saisonnier des peuplements de nématodes libres à partir de six stations de prélèvement couvrant l'ensemble du plan d'eau. Le cycle des communautés révèle à la fois leur homogénéité structurale et leur pauvreté quantitative et surtout qualitative. Les densités, les biomasses totales et la diversité spécifique qui ne montrent pas de grandes fluctuations saisonnières suivent un gradient spatial décroissant du canal Tinja le plus marinisé vers l'intérieur du lac. Cette gradation semble surtout dépendante de la teneur en fraction fine des sédiments.

Abstract

"Lake" Ichkeul is a seasonally highly variable ecosystem which is particularly important for the avifauna. A seasonal survey of free-living nematodes from six sampling stations covering the whole lake showed structurally homogeneous nematode communities with low density and diversity. Densities, total biomass and species diversity do not show large seasonal fluctuations and decrease spatially from Tinja's channel under marine influence towards the interior of the lake. This gradation seems to be particularly dependent to the fine fraction of sediments.

Mots-clés : Nematoda - density - biomass - biodiversity - bio-indicators

Introduction

L'écosystème Ichkeul, situé au nord de la Tunisie, est une zone humide protégée servant d'aire d'hivernage à de nombreux oiseaux d'eau migrateurs [1]. Sa principale composante, le "lac" Ichkeul (8900 ha en moyenne), est une lagune secondaire qui débouche par l'intermédiaire d'un étroit canal, l'oued Tinja, dans la lagune de Bizerte directement reliée à la Méditerranée (Fig. 1). Durant la période hivernale, plusieurs oueds alimentent substantiellement le lac Ichkeul en eaux douces à l'origine d'une élévation du niveau d'eau et d'un courant sortant en direction de la lagune de Bizerte. Par contre, durant l'été, la sécheresse et la baisse de l'étiage provoquent une inversion du courant d'eau, devenu entrant dans le lac, et donc une augmentation de la salinité.

La construction de plusieurs barrages sur les principaux cours d'eau se déversant dans le lac a entrainé une réduction des apports en eaux douces [2] et une importante augmentation de la salinité pouvant atteindre, en période d'évaporation intense, la valeur excessive de 70 ‰ (août et septembre 1995. Mesure effectuée par l'Agence Nationale de Protection de l'Environnement en dehors des périodes de prélèvements du matériel biologique). Les caractéristiques hydrologiques et sédimentologiques du lac Ichkeul qui montrent de grandes fluctuations saisonnières, mensuelles et même journalières, expliquent la complexité de ce milieu menacé par des perturbations d'origines diverses (hypersalinité non contrôlée, apports de polluants par le canal Tinja), lesquelles risquent de se répercuter sur sa biodiversité et de remettre en question son statut unique en Méditerranée de réserve de la biosphère et de zone humide d'intérêt international. Diverses études pluridisciplinaires ont été entreprises pour comprendre le fonctionnement actuel du lac Ichkeul et définir une stratégie pour sa sauvegarde [3, 4, 5].

La présente étude se propose d'apporter sa contribution à une meilleure définition de ce milieu original en fournissant les premières données sur les communautés de nématodes libres. Ces métazoaires, les plus abondants dans les sédiments aquatiques [6], représentent l'un des premiers maillons trophiques en milieu marin ou lagunaire [7]. Ils constituent un matériel biologique de choix pour l'étude des perturbations d'un plan d'eau, en raison de la brièveté de leurs cycles vitaux, de leur grande diversité spécifique et de leur résistance relative aux agressions environnementales [8].

Matériel et méthodes

Des échantillons saisonniers d'eaux et de sédiments ont été prélevés de l'été 95 à l'été 96 à partir de six stations réparties le long de deux radiales Est-ouest et Nord-sud (Fig. 1). Trois carottes de sédiment de 10 cm^2 de section [9] et de 16 cm de hauteur ont été extraites en vue d'étudier la faune. Les nématodes, séparés par la méthode de lévigation-tamisage [10] ou de centrifugations successives [11], sont comptés sous la loupe binoculaire. La détermination de la structure spécifique des peuplements de nématodes et de leur biomasse totale sont estimés, après observation microscopique, à partir d'un sous-échantillon représentatif de 100 individus préalablement fixés. La biomasse est calculée selon la méthode volumétrique d'Andrassy [12].

Le test t de Student [13], ainsi que le calcul des indices de diversité, de richesse spécifique et d'affinité faunistique sont utilisés pour suivre l'évolution spatiale et saisonnière des communautés. L'analyse statistique est réalisée après transformation des densités moyennes X du type Y = log X en raison de la distribution contagieuse des nématodes [14]. La diversité spécifique est estimée par l'indice $H' = \Sigma \frac{ni}{N} \cdot Log_2 \frac{ni}{N}$ [15] où ni et N sont

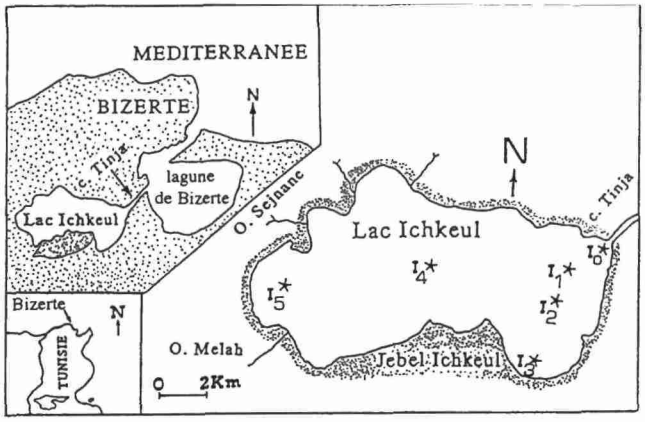

Fig. 1 : Localisation des stations de prélèvements dans le lac Ichkeul.

respectivement la fréquence relative de l'espèce de rang i et l'effectif total de nématodes. La richesse spécifique est évaluée par le rapport $R.S = \frac{S-1}{Log\ N}$ [16], S étant le nombre d'espèces et N le nombre total d'individus. L'indice d'affinité faunistique [17 et 18] entre deux prélèvements est la somme des plus faibles dominances des espèces communes aux deux stations considérées. Plusieurs paramètres abiotiques ont été mesurés en parallèle (température, salinité, oxygène dissous, teneur du sédiment en fraction fine de taille inférieure à 40 µm).

Résultats et discussion

Les paramètres physico-chimiques du lac montrent, pour la plupart, de grandes fluctuations spatiales et saisonnières (Tab. 1). La comparaison de la qualité des eaux entre les saisons estivales de 95 et 96 fait apparaître aussi d'importantes variations d'une année à l'autre.

Cette instabilité des paramètres abiotiques, susceptible de toucher l'équilibre biologique du plan d'eau, affecte sa faune endogée. Si les den-

Table 1 : Paramètres abiotiques du lac Ichkeul au moment des prélèvements. En **gras** : valeurs moyennes toutes stations confonfues. En *italique* : valeurs minimale et maximale.

Saison / Paramètre	Eté 95	Automne 95	Hiver 96	Printemps 96	Eté 96
Salinité (g/l)	**51,5** *40 - 56*	**56** *42 - 66*	**20,15** *19,5 - 21*	**20** *19,6 - 20,3*	**31,25** *29,6 - 35*
Température (°c)	**27,6** *27,1 - 28,2*	**15,03** *14 - 16*	**16,72** *14,8 - 18,2*	**23,73** *22,6 - 24*	**24,15** *22,8 - 24,6*
Teneur en O2 dissous (mg/l)	**8,35** *7,1 - 9,3*	**8,71** *8,1 - 9,1*	**10,03** *9,1 - 11,2*	**10,95** *10,2 - 12,1*	**8,93** *8,1 - 10,1*
Profondeur (cm)	**79,5** *40 - 110*	**100,83** *50 - 145*	**175,83** *120 - 235*	**152,5** *90 - 205*	**108,33** *85 - 140*
Transparence (cm)	**36,16** *25 - 55*	**74,5** *45 - 110*	**85** *70 - 105*	**62,5** *40 - 100*	**73,3** *40 - 95*
Teneur séd. en fraction. fine (%)	**86,6** *78 - 92*	**87,75** *84 - 94*	**87,7** *78 - 95,5*	**88,9** *79 - 96*	**89,4** *81,5 - 94*

PREMIÈRES DONNÉES SUR LA PRODUCTION PRIMAIRE D'UN HERBIER À *POSIDONIA OCEANICA* (L.) DELILE EN ALGÉRIE (ANSE DE KOUÂLI, TIPAZA)

Boumaza Salima*, Semroud Rachid

Laboratoire de Biologie et d'Ecologie du Phytobenthos Institut des Sciences de la Mer et de l'Aménagement du Littoral
B.P. 54 Sidi-Fredj, 42321 (Gouvernorat d'Alger), Algérie

Résumé

La production primaire de l'herbier à *Posidonia oceanica* dans l'anse de Kouâli est évaluée, dans quatre stations situées à 0.3, 0.7 m, 2 m et 10 m de profondeur, en utilisant une technique récente qui s'appuie sur la phénologie des faisceaux foliaires et sur la lépidochronologie. La production foliaire (limbe et pétiole) varie entre 772.6 à 1445.9 g Ps/m^2/an en fonction de la profondeur. La production des rhizomes est comprise entre 26.5 et 50.0 g Ps/m^2/an. La production primaire passée, estimée sur une période de 4 ans, montre des variations inter-annuelles.

Mots- clés : posidonia, primary production, phytobenthos, Algerian Basin

Introduction

Posidonia oceanica (Linnaeus) Delile et ses épiphytes jouent un rôle important dans la production primaire benthique en Méditerranée (1, 2). Une technique récente qui s'apparente à la dendrochronologie terrestre (lépidochronologie), associée à la phénologie (biométrie foliaire) permet d'estimer cette production. Cette méthode présente l'avantage d'être à la fois rapide et sûre; de plus, elle permet d'évaluer les productions primaires actuelles et passées dans les différentes parties de la plante (limbe, pétiole et rhizome) (2). Dans cette étude, les productions primaires actuelles et passées ont été mesurées par la méthode lépidochronologique dans quatre stations à différentes profondeurs, afin d'évaluer les fluctuations en fonction de la profondeur et au cours du temps.

Matériel et méthodes

Vingt rhizomes orthotropes sont prélevés tous les mois, de juin 1992 à juin 1993, pour l'étude phénologique et tous les trois mois, de juillet 1992 à avril 1993, pour l'étude lépidochronologique dans quatre stations de l'anse de Kouâli, située dans la partie occidentale de la baie de Bou-Ismaïl à 80 km à l'ouest d'Alger. Ces stations sont choisies selon un gradient de profondeur (Figure 1).

- Station SFI : sur le front interne du récif-barrière (-0.3 m).
- Station SFE : sur le front externe du récif-barrière (-0.7 m).
- Station S02 : au niveau du prérécif (-2 m).
- Station S10 : à la sortie de l'anse (-10 m).

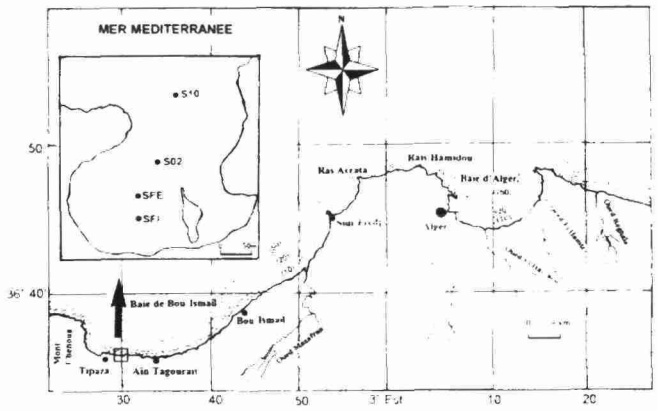

Figure 1 : Localisation des stations étudiées.

La densité (nombre de faisceaux par m^2) est estimée à l'aide d'un quadrat de 40 cm de côté ; 10 répliquats sont réalisés dans chaque station (3).

Les écailles sont très soigneusement détachées du rhizome en respectant l'ordre distique de leur insertion en partant des plus anciennes vers les plus récentes (Figure 2) (4).

Le rang des minima et des maxima d'épaisseur est noté. Les tronçons de rhizomes délimités par deux minima d'épaisseur des écailles sont mesurés, séchés (72 heures à 70 °C) puis pesés. La phénologie des faisceaux (nombre de feuilles, biométrie foliaire) est également étudiée selon la méthode de Giraud (5). Le poids sec de la feuille de rang 1 de chaque rhizome est calculé. La production primaire (limbes et pétioles) est estimée à partir de trois paramètres :

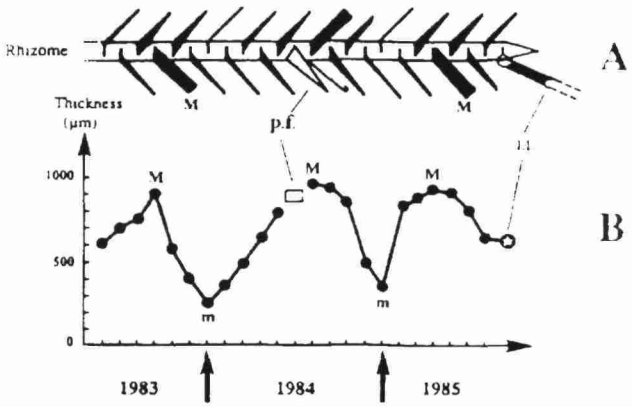

Figure 2 : Mode d'insertion des écailles le long d'un rhizome orthotrope (A) et la correspondance en cycles des variations d'épaisseur des écailles (B). La signification chronologique des cycles (années lépidochronologiques) est également indiquée. M = écailles avec un maximum d'épaisseur ; m = écailles avec un maximum d'épaisseur ; p.f. = pédoncule floral ; 1.1. = première feuille vivante (2).

(i) le nombre moyen de feuilles produites annuellement : ce paramètre est déterminé à partir du cycle de renouvellement des feuilles (2) ;

(iii) la longueur moyenne de la feuille de rang 1 qui possède encore son apex déterminée grâce aux données phénologiques ;

(iii) la densité de la feuille de rang 1 (poids par unité de longueur (6)), est mesurée sur un cycle annuel. Elle dépend de la largeur et de l'épaisseur des feuilles mais également de leur âge et de leur date d'apparition dans le faisceau (7).

Sur la base de ces trois paramètres, la production primaire PIf (limbes et pétioles) est mesurée (8).

PIf = N x L x D

avec N : nombre de feuilles formées annuellement ; L : longueur moyenne des feuilles adultes de rang 1 en cm ; D : densité moyenne de la feuille ou de l'écaille en mg Ps/cm.

Connaissant la densité (d) de l'herbier, la production primaire nette par m^2 (PI) est estimée à partir de la relation :

PI =PIf x d

L'existence d'une relation hautement significative entre la longueur du pétiole et la longueur totale de la feuille possédant encore son apex mise en évidence par Pergent (4) permet d'estimer la production primaire passée très rapidement à l'aide des paramètres suivants :

(i) le nombre d'écailles par cycle pour chaque année antérieure ;

(ii) la longueur théorique des feuilles tombées durant une année calculée à partir de la longueur moyenne des écailles qui persistent le long du rhizome grâce à la relation morphométrique entre la longueur du pétiole et la longueur totale de la feuille ;

(iii) la densité des limbes et des écailles correspondant à celle calculée au cours de l'année étudiée en admettant que sa valeur varie peu d'une année à l'autre (2).

Résultats et discussion

Estimation de la production primaire foliaire nette

La production primaire par faisceau (limbes et pétioles) augmente en fonction de la profondeur, alors que la production estimée par m^2

RELATION ENTRE LES NIVEAUX EN NUTRIMENTS ET LA BIOMASSE DES ÉPIPHYTES DANS UN HERBIER À *POSIDONIA OCEANICA*

Cancemi G. [1] , Villedieu S. [2] & C. Pergent-Martini [2]

[1] International Marine Center, Coastal Ecosystems Group, Oristano, Sardinia

[2] Equipe Ecosystemes Littoraux, Université de Corse, France

Résumé

Les concentrations en nutriments et la biomasse des épiphytes foliaires ont été mesurés dans un herbier à *Posidonia oceanica*, soumis à l'impact d'une ferme acquacole. Ces paramètres, ainsi que le coefficient A (% de feuilles brisées), sont plus élevés à proximité des installations acquacoles, et confirment donc l'hypothèse de l'impact de la ferme sur cet herbier. L'épiphytisme important observé surtout à proximité des installations aquacoles, pourrait être une des causes de la régression de l'herbier.

Mots clés : coastal processes, pollution, phanerogams, western Mediterranean.

Introduction

Signalée depuis plusieurs décenies, la régression généralisée des herbiers de phanérogames marines (1) doit être mise en rapport avec la dégradation de l'environnement littoral résultant de l'augmentation des pressions anthropiques (2).

La croissance et la morphologie des plantes marines sont, souvent, étroitement liées au teneurs en nutriments présents dans le milieu (3). Des études récentes ont également montré que, dans plusieurs cas, l'augmentation de la concentration en nutriments pouvait être responsable de la disparition de grandes surfaces d'herbier (4). Ces régressions peuvent, à leur tour, entraîner une modification des bilans sédimentaires, un appauvrissement qualitatif et quantitatif des espèces végétales et animales, y compris pour les espèces exploitées et, donc, un dommage au niveau écologique et économique (5).

La phanérogame marine *Posidonia oceanica*, espèce endémique de Méditerranée, couvre de vastes étendues entre 0 et 40 m de profondeur, et maintient la stabilité des équilibres littoraux. Ces herbiers sont de plus en plus soumis aux pressions anthropiques, et ce malgré les mesures de protection légales dont ils font l'objet (6). Parmi ces pressions, le développement de l'aquaculture en milieu côtier semble à l'origine de phénomènes de régressions localisées (7). En effet, les rejets en matière organique de ces installations et l'augmentation des nutriments qui en résulte, semblent à l'origine des régressions observées (8).

Aussi, dans le cadre de cette étude, nous avons mesuré la teneur en nutriments du sédiment et le développement de la couverture épiphytique dans un herbier à *Posidonia oceanica* soumis à l'impact d'une ferme aquacole (9).

Matériel et méthode

Les deux stations prises en compte sont situées dans la baie de Figari (Corse du Sud) où, depuis 1985, une ferme marine est installée sur un herbier à *Posidonia oceanica*. Les deux stations d'échantillonnage, situées à 10 m de profondeur, sont déterminées en fonction de la distance par rapport aux installations et des différentes caractéristiques de l'herbier (densité des faisceaux, couverture foliaire) (9) : station 1 à 20 m des cages, station 2 à 100 mètres des cages.

Des prélèvements d'eau sont réalisés à deux saisons, en janvier 1995 et en juillet 1996, dans le sédiment (eau interstitielle) à l'intérieur de l'herbier à *Posidonia oceanica*. Le prélèvement est réalisé à l'aide de seringues de 60 ml, munies d'une aiguille vétérinaire, introduites entre 8 et 10 cm dans le sédiment (sept réplicats). Ces échantillons sont ensuite filtrés (filtre Whatmann GF/C de 47 mm de diamètre) et conservés au frais (4°C) pour analyse au laboratoire.

Les concentrations en phosphate, nitrate et ion ammonium sont, ensuite, mesurées à l'aide d'un spectrophotomètre HACH DR/2000 (10). Pour chaque station, 15 à 20 faisceaux de *Posidonia oceanica* sont prélevés afin d'évaluer la biomasse en épiphytes des feuilles et le coefficient A (pourcentage de feuilles ayant perdu leur apex) (11).

Résultats et discussion

Les concentrations en nutriments mesurées dans l'eau interstitielle apparaissent relativement élevées, en particulier pour les phosphates, avec 3.7 µM et 2.3 µM, respectivement dans la station 1 et la station 2, en période hivernale (Figure 1.C). Pour les nitrates et les ions ammonium, au contraire, les concentrations les plus élevées sont enregistrées en été : 3.5 µM, pour les premiers et 12.2 µM, pour les seconds (Figure 1.A et B). Ces valeurs élevées sont enregistrées surtout dans la station 1, la plus proche des cages acquacoles.

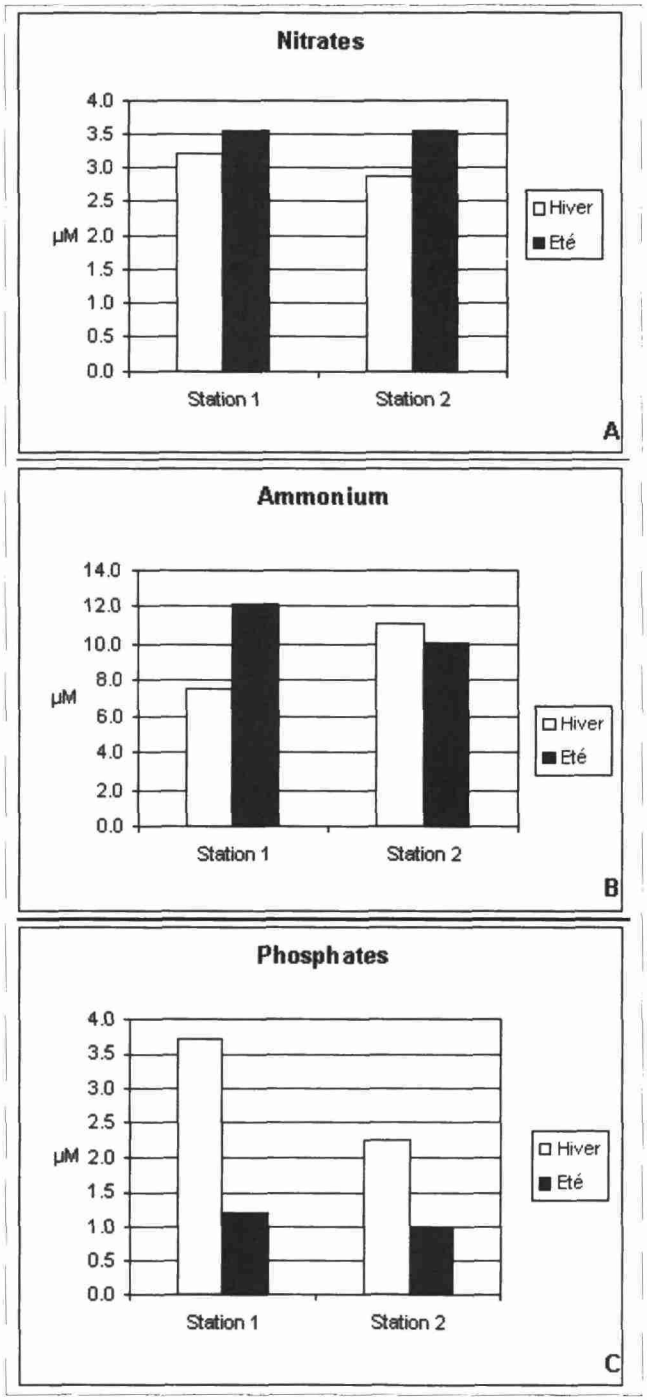

Figure 1 : Evolution de la concentration en nutriments (en µM), dans le sédiment de l'herbier à *Posidonia oceanica* de Figari. A : $[NO_3^-]$; B : $[NH_4^+]$; C : $[PO_4^{3-}]$

STRUCTURAL ASPECTS OF *ANEMONIA VIRIDIS* (FÖRSKAL, 1775) (CNIDARIA, ANTHOZOA) POPULATIONS IN THE NORTH AEGEAN SEA

Chariton C. Chintiroglou

Aristotle University, Department of Zoology, Box 134, 54006 Thessaloniki, Greece

Abstract

This paper is concerned with the structural aspects of the *Anemonia viridis* populations found in the North Aegean Sea. It was found that the mean wet weight of anemone individuals and the density of the populations increases with depth and distance from the shore. The differences in the structure exhibited by *Anemonia viridis* populations, were attributed both to the specific hydrodynamic characteristics of the biotope and to several biotic interactions.

Key-words : Infralittoral, Population dynamics, Aegean sea, Cnidaria, Zoobenthos

Introduction

For a long time *Anemonia viridis* has been regarded as one of the most common representatives of the sea anemone populations of the Mediterranean and NE European shores (1,2,3,4). Chintiroglou & Koukouras (5) have described the seasonal structural (size classes) variations of the populations, while Schlichter (6), Janssen & Möller (7) and Chintiroglou & Koukouras Chintiroglou *et al.* (8) have reported on its feeding habits. The aim goal of the present study-work is to determine whether there is any structural (size classes) variation in the population which may be related to vertical distribution.

Material and methods

Sampling was carried out in Nea Plagia in Chalkidiki peninsula, along a straight, gently shelving transect line (off shore -150 m) on a shore fully exposed to Southern winds. Three distinct biotopes (zones A, B and C) were observed and discribed by Chintiroglou *et al.* (8). The number of samples collected from each zones was arbitrary with a minimum of 5 samples, and was influenced by the homogeneity of the biotope. 42 samples were collected using 50x50 cm quadrats. Among these, 24 samples were collected from zone A, 13 from zone B and 5 from zone C. All samples were preserved in 7% formalin solution. Size classes of anemones were defined according to wet weight according to Chintiroglou *et al.* (5).

All data were tested for normality (chi-square test) and when normal distribution was observed, examination of the distribution of the frequencies was also carried out. One-way analysis of variance (ANOVA) and Fischer LSD testing were used to test the differences between the means of wet weight and number of individuals of *A. viridis* populations. Multiple regression analysis was used to determine any correlation between the parameters of the sampling locations (depth and distance from shore) and the anemones' wet weights (9). To compare the densities of the populations in the three zones, non-parametric Kruskal-Wallis ANOVA and Mann-Whitney test was used. All statistics tests were carried out by using the Statistica and Stat View software.

Results

The size classes frequency distribution of wet weight of *A. viridis* exhibited a normal distribution in zones A (X^2=0.13, p=0.029) and B (X^2=0.09, p=0.033). However, in zone C the size classes were not normally distributed (X^2=0.09, p=0.18), although their distribution was were very close to a normal one (68.27% of individuals followed normal distribution; see Fig.1a-c). Differences also existed between mean wet biomass from zone to zone (F=46.131, df=4, p=0.0001). Individual mean biomass was at its lowest in zone A and in its highest in zone C. Differences existed between all populations (A-B, A-C and B-C; Fisher LSD values, 0.096, 0.144 and 0.133 respectively).

Results on density of populations also differed from zone to zone (Kruskal-Wallis anova, z=24.45, p=0.0001). Although differences existed for the mean number of individuals between zones A / B, and zones A / C (Mann-Witney, z=4.45 p=0.0001, and z= 3.19, p=0.0014, respectively), no significant difference appeared between individuals of zones B / C (z =1.43, p=0.154).

Results of multiple regression analysis between mean wet weight, depth and distance from the shore indicated that the weight of the individuals was positively correlated with depth as well as with distance (r = 0.80, df=2/27, p.=0.0001; r=0.90, df=2/27, p.=0.0001).

It is thus obvious from all the above results, that size class composition of *A. viridis* populations in the three infralittoral zones, differed with respect to mean individual biomass and in density of populations. More specifically, as we moved from zone A to zone C, we observed

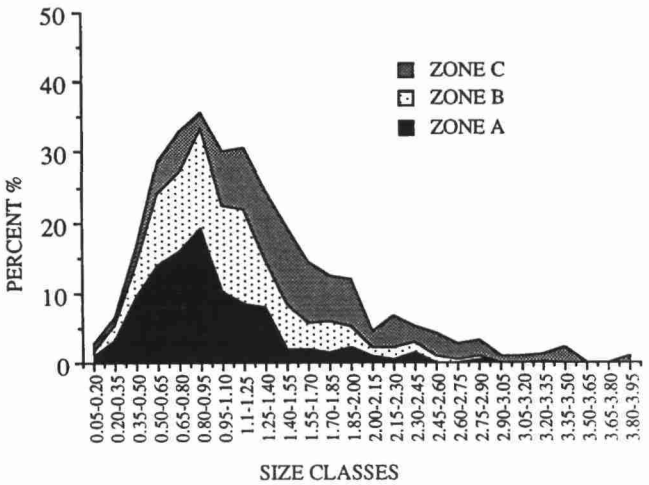

Figure 1 : Frequency distribution of size classes (based on wet weights).

a right shift in the distribution of size classes, towards larger individuals. This tendency was evident by the increase in the frequency of larger size classes, as we moved deeper. In zone A larger size classes (10 and over) made up 10.72% of the population. In zone B this percent increased to 24.65%, reaching a final value of 56.54% in zone C.

Discussion

Since several years it is well known that larger *A. viridis* specimens are more commonly found than smaller ones with increasing depth (2,3). The present study provides for the first time clear statistical results to support this point. Similar observations have been made by Gosse (10) for the genus *Metridium senile*, and for *Anthopleura elegantissima* and *A. xanthogrammica* by various authors (11, 12, 13, 14, 15). Besides this more or less general remark about the distribution of *A. viridis*, nothing is known precisely about its bathymetric distribution and its size classes range. Some information on the seasonal variations of the structure of the *A. viridis* populations was given by Chintiroglou *et al.* (5), who found significant differences in both populations density and mean wet biomass of the individuals.

The limited participation of the large size classes in shallow waters could be a result of increased hydrodynamism in zone A and B, as their biotope is frequently exposed to strong winds from various directions (S, SW, N, and NW), whose frequency (year round) ranges from 20 to 34% (16). This observation is further indicated by the positive correlation of biomass with both depth and distance from shore. This observation is also supported by the fact that, while the population density in the two zones (B and C) did not differ significantly, mean wet biomass in the two zones was significantly different. This difference could be attributed to a number of biotic factors, such as intraspecific competition between smaller and larger members of the colony, predation, feeding abilities and changes in migratory behaviour by larger individuals. Examples of such behaviour are given for *Anthopleura elegantissima* (11, 12) and for *A. xanthogrammica* (13, 14, 15). Recently, Williams (17) noted two separate forms of behaviour in response to mutual tentacular contact between individuals of the sea anemone *A. viridis*: acrorhagial aggression and pedal disk detachment. During previous laboratory and field observations by our team, it has been noted that when two individuals of *Anemonia viridis* are compe-

ETUDE DU PHYTOBENTHOS DES COTES SUD-EST D'ATTIQUE, EN VUE DE L'INSTALLATION DU RÉSEAU D'ASSAINISSEMENT DES EAUX USÉES, DE LA BANLIEUE EST D'ATHÈNES (RÉSULTATS PRÉLIMINAIRES)

F. Chryssovergis et P. Panayotidis*

Centre National des Recherches Marines (C.N.R.M.)
Agios Kosmas, Hellinikon, 16604, Grèce

Résumé

Une étude des phytocénoses benthiques, de l'infralittoral supérieur, des côtes SE d'Attique, a été effectuée, au moyen des rélevés phytosociologiques, en vue de l'installation du réseau d'assainissement des eaux usées, de la banlieue SE d'Athènes. Les premiers résultats montrent la dominance des espèces du genre *Cystoseira* et la présence d'une flore algale assez riche en espèces mais présentant des Indices de Diversité très fluctuants, de 0,973 a 3,375, dépendant de la densité de la strate arborescente à *Cystoseira* sp.

Mots clés : Phytobenthos, Pollution, Aegean Sea

Le présent travail fait partie du programme "Investigation de l'écosystème marin des cotes Sud-Est d'Attique" du C.N.R.M., financé par la Compagnie des Eaux. De nombreux travaux ont été consacrés à l'impact des eaux urbaines sur le phytobenthos (1, 2, 3)

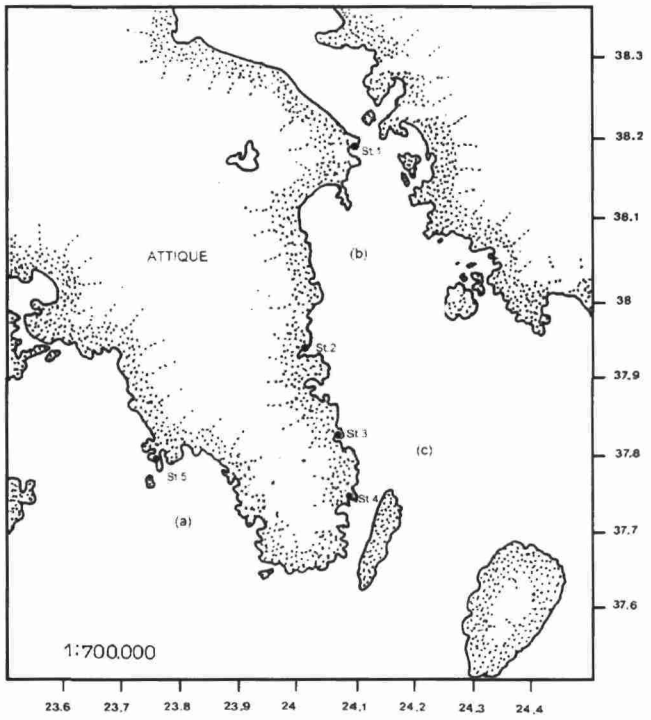

Figure 1 : Carte de la région étudiée.

Des études similaires concernant les mers grecques ont été effectuées dans le golfe Thermaikos (4), et dans le golfe Saronikos (5), deux secteurs affectés par la pollution urbaine.

Présentation du site

La région étudiée constitue la partie sud d'Attique (golfe Saronikos et golfe Sud Euvoikos). Du point de vue hydrologique elle peut se subdiviser en trois secteurs (Fig. 1), où l'hydrodynamisme augmente progressivement du secteur a au secteur c (6, 7).

Des mesures des paramètres physicochimiques, à la proximité de la côte, au golfe Sud Euvoikos, ont montré qu'il s'agit d'une région oligotrophe. Plus specialement, l'oxygène dissous varie de 4,7 à 5,7 ml/l, les nitrates et les phosphates ne surpassent pas les 0,5 µgr-at/l et les 0,2 µgr-at/l respectivement. La concentration de la chl-a varie de 0,15 à 0,45 µgr/l (6, 7).

Pendant toute l'année les vents dominants sont les vents du Nord, ceux ci sont plus fréquents pendant l'été. La région étudiée présente une marée faible d'une amplitude de 20 cm.

Les stations sont d'hydrodynamisme calme, d'orientation S-SE et de profondeur 0,3 à 0,5 m, sous le niveau de la marée basse.

Matériel et Méthodes

Le peuplement algal, de substrat dur, de quatre stations situées dans le golfe Sud Euvoikos (St.1, St.2, St.3, St.4) et d'une (St.5) dans le golfe Saronikos, a été étudié, au moyen de relevés phytosociologiques. Des rélevés de 20 x 20cm, deux répliques par station, ont été effectués pendant deux saisons, (automne et hiver). Ils ont été analysés en laboratoire suivant les techniques décrites par Boudouresque (8).

Les phytocénoses

Les phytocénoses photophiles, de l'infralittoral supérieur, dominées par les algues dressées arborescentes du genre *Cystoseira*, (qui, en Méditerranée, correspondent aux phytocénoses "climax"), font l'objet de notre étude.

Dans toutes les stations, les espèces du genre *Cystoseira* représentent l'élément végétal predominant. Huit espèces du genre *Cystoseira* ont été identifiées ; *C. crinita* est la plus fréquente. Les peuplements denses formés par *C. crinita* entre 0,3 et 0,5 m sont accompagnés par ceux à *C. Compressa*, qui constituent une ceinture étroite au niveau de l'eau. Ces observations s'accordent avec celles de Huve (9) qui a decrit les biotopes des Cystoseires de la Mer Egée.

La frondaison de *Cystoseira* sert de support à plusieurs épiphytes comme *Sphacelaria cirrosa*, plusieurs espèces de Ceramium, *Chondria coerelescens*, *Dipterosiphonia ringens*, *Corallina granifera*, *Jania rubens*, *Dasya corymbifera*, *Spermothamnion repens*.

La sous-strate sciaphile est peu développée avec :

- une strate arbustive constituée de *Halimeda tuna*, *Dilophus fasciola*, *Padina pavonica*, *Rytiphlaea tinctoria*,
- une strate gazonnante avec très peu d'espèces comme *Anadyomene stellata*, *Valonia utricularis* et
- une strate encroûtante presque inexistante (*Lithophyllum* sp, Corallinaceae).

Du point de vue phytosociologique ce peuplement se rapproche de *Cystoseiretum crinitae*, phytocénose photophile de mode calme (10). Dans deux stations *C. crinita* est remplacée par *C. crinitophylla* accompagné soit de *C. compressa* soit de *C. mediterranea*. Une station est caractérisée par la présence de *C. barbata* associée de *C. compressa* et *C. crinitophylla*.

Résultats quantitatifs

Le nombre d'espèces (N) par station varie de 21 à 43. Ces valeurs sont comparables à celles des autres golfes grecs, comme le golfe de Kalloni, de 31 à 56 (11), le golfe Maliakos, de 36 à 106 (12) et aussi le golfe Sud Euvoikos, de 42 à 52 (13).

Le recouvrement (R) varie de 69% à 209% (Tableau 1).

L'étude de la dominance quantitative (DR) des grands groupes systématiques permet de constater que dans toutes les stations les Phaeophyceae sont largement dominants, de 58% à 90%, les Rhodophyceae étant en deuxième, de 8,4% à 34,5%. Les Chlorophyceae présentent une valeur très faible, de 1,2% à 6,9%. A la station St.5 du golfe Saronikos, la DR des Chlorophyceae est de 13,7%, due à la présence de l'espèce *Caulerpa racemosa*, qui a fait son apparition récemment dans les mers grecques (14) et qui envahit même le substrat dur, riche en matière organique.

Les Indices de Diversité (H, Shannon) et d'Equitabilité (E) sont généralement faibles (Tableau 2). Elles sont dues au développement des *Cystoseira* qui empêchent l'installation d'autres espèces.

ETUDE ENVIRONNEMENTALE EN VUE DE L'INSTALLATION D'UN ÉLEVAGE ICHTYOLOGIQUE OFF-SHORE EN SARDAIGNE

Andrea Cossu [1*] e Vittorio Gazale [2]

[1] Dipartimento di Botanica ed Ecologia Vegetale dell'Università di Sassari, Italia
[2] Battelle-Softec, Centro ricerche di Tramariglio, Sassari, Italia

Résumé

Afin de contribuer au développement de l'aquaculture en Sardaigne, nous nous occupons depuis plusieurs années de caractériser les sites aptes à l'élevage en aquaculture. Dans le Golfe d'Orosei a été repérée une zone présentant une rhéophylie et une oligotrophie particulières des eaux et pouvant être retenue intéressante pour l'élevage en cages flottantes. Ce travail présente en particulier une analyse de la distribution des herbiers à *Cymodocea nodosa* et à *Posidonia oceanica*.

Mots-clés : aquaculture, Posidonia, coastal management, conservation, Tyrrhenian Sea

Introduction

Notre travail a consisté à déterminer quels pouvaient être les éléments essentiels permettant d'évaluer la compatibilité entre une zone protégée et la probable installation, dans une zone toute proche, d'une activité avec un fort impact sur l'environnement telle que l'élevage ichtyologique intensif en cages flottantes. Il a donc été nécessaire de définir avant tout les principaux peuplements benthiques (1) et, plus particulièrement, les phanérogames marines; il est en effet bien connu que les activités concernant l'aquaculture intéressent les peuplements benthiques, et surtout les herbiers à posidonie (*Posidonia oceanica*), sensibles aux dépôts de particules organiques et à la diminution de la transparence des eaux (6; 8; 9).

Le Golfe d'Orosei a une grande importance du point de vue du paysage et de l'environnement. Pour certaines zones ont donc été établis des projets régionaux, nationaux et communautaires visant la connaissance, la sauvegarde et la valorisation des ressources naturelles côtières et marines (L.N. 979/82; L.N. 394/91; L.R.31/89).

Le territoire, plutôt boisé dans son ensemble, est riche en calcaires mésozoiques et en petites effusions basaltiques; le paysage est de type karstique et présente des falaises et des dolines. L'orographie est extrêmement tourmentée, représentée par d'étroites vallées, situées au cœur d'un paysage très primitif et dominé par de hauts reliefs irréguliers et sauvages. Les zones côtières présentent des maquis thermoxérophiles. Vers l'intérieur, fait son apparition une forêt mixte de sclérophilles avec de nombreuses espèces endémiques.

Il y a encore quelques années, la zone marine recensait parmi ses espèces le phoque moine (*Monachus monachus*), avec une colonie comptant une dizaine d'individus à l'intérieur de la grotte de Fico (4). De plus, dans le golfe d'Orosei on a signalé la découverte de plusieurs tardigrades (2; 3; 5).

La zone la plus septentrionale, et plus particulièrement la zone choisie pour l'installation de l'élevage, qui est caractérisée par des affleurements de lave (Punta Nera), est moins riche en espèces importantes pour le patrimoine naturel et elle possède un intérêt naturel moins fort, dû en partie à l'impact négatif du fleuve Cedrino. Pour toutes ces raisons, la zone n'est pas protégée par les lois dont il est question plus haut.

Eté comme hiver, la zone est parcourue par de faibles courants superficiels allant du sud vers le nord; la zone choisie en vue de l'installation des cages flottantes est surtout influencée par des courants qui résultent des vents dominants. En ce qui concerne les données de Capo Bellavista, les vents dominants proviennent du nord-ouest et ils influencent modestement les masses d'eau étant donné la morphologie tout à fait particulière des côtes. Il faut également souligner l'importance des vents quadrants I et II (NE et SE) qui ne montrent une certaine intensité qu'en de rares occasions. Les principaux éléments géomorphologiques sont représentés par deux canyons, celui de Orosei et celui de Gonone. Ce dernier qui est en activité coupe profondément la plate-forme, sa partie supérieure, en retrait, remontant jusqu'à -50 m; ajoutons qu'il se trouve à une distance de 0,4 mille de la ligne de côte. De façon générale, la plate-forme continentale peut être partagée en deux zones ayant des caractères morphologiques bien différents.

Le secteur méridional présente un bord net avec une extension contenue, d'une profondeur inférieure à 120 mètres. Les principales morphologies sont représentées par des palé-ofalaises se logeant dans des calcaires mésozoiques. On trouve également des plate-formes d'abrasion s'installant sur des formations de calcaires ainsi que sur des bases cristallines.

Le secteur septentrional est remarquablement plus étendu que le précédent et il a enregistré des oscillations eustatiques tout en conservant des alvéoles et des deltas d'origine paléolithiques, des cordons littoraux, "beach rocks" avec des dépressions de paléo-lagunes qui leur sont associées.

Méthode

En ce qui concerne la méthode d'étude, ce travail date de 1995 et se base sur l'analyse des photos aériennes (7) qui nous a permis de tracer les principales typologies côtières, les formations végétales sous-marines des étages superficiels ainsi que les morphologies produites par le cône de déjection de l'embouchure du fleuve Cedrino. Une vérification *in situ* a été effectuée grâce à l'utilisation d'un bathyscope, des plongées et des sorties au cours desquelles a été utilisée une caméra guidée allant jusqu'à une profondeur de 80 mètres.

Le long de certaines radiales, considérées comme significatives, ont été réalisés des transects côte-large, et des échantillons de matériel biologique ont été prélevés sur 30 stations (fig. 1), matériel qui nous a permis de caractériser au mieux l'importance et la structure des peuplements pris en considération.

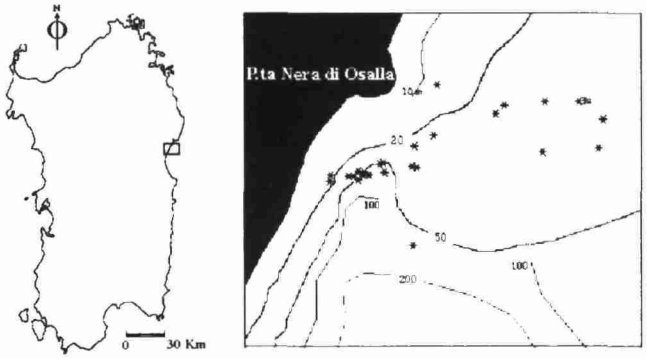

Figure 1 : Carte bathymétrique et des stations d'échantillonnage

Résultats

Les résultats concernant les travaux sur les caractéristiques physiques et chimiques de la colonne d'eau montrent une situation d'oligotrophie pour toutes les stations examinées, due à la trasparence des eaux (disque Secchi, >35 m) au contenu minimum de phosphore ($P\text{-}PO_4$ 1-2 mg m^{-3}; P-Ptot 5-7 mg m^{-3}) et d'azote ($N\text{-}NH_3$ 0 mg m^{-3}, $N\text{-}NO_2$ 0-5 mg m^{-3}, $N\text{-}NO_3$ 1-5 mg m^{-3}) que l'on considère comme se trouvant à la limite de la sensibilité de la méthode, et au contenu minimum de chlorophylle "a" phytoplanctonique (0-1 mg m^{-3}).

Les espèces dominantes font partie des rhizophytes jusqu'à une profondeur d'environ 30 mètres; à une plus grande profondeur se développe la biocénose du détritique côtier ayant divers faciès. Dans le voisinage de l'embouchure du fleuve Cedrino, la zone est intéressée par un continuel apport de particules qui rendent le substrat fortement instable et les caractéristiques chimico-physiques de l'eau plutôt variables; cette condition produit un appauvrissement de la composante de la flore et de la faune.

Les peuplements végétaux sont répartis selon des bandes bathymétriques bien définies: de 10 à 20 mètres de profondeur se trouvent des peuplements de *Cymodocea nodosa*; à partir de 20 m de profondeur s'affirme *Posidonia oceanica*. Cette phanérogame est présente sur toute la côte sur 1,5 km environ, exception faite pour la zone située en face de l'embouchure du fleuve, se trouvant sur des fonds sableux

INVESTIGATION ON THE MEDITERRANEAN MONK SEAL *MONACHUS MONACHUS* (HERMANN, 1779) IN GÖKÇEADA ISLAND (NORTHERN AEGEAN SEA)

Ayhan Dede

University of Ystanbul, Faculty of Fisheries, Turkey

Abstract

The distribution of Mediterranean monk seal *Monachus monachus* (Hermann, 1779) in the Northern Aegean Sea is very important because this species is facing a danger of becoming extinct from Turkey and the world. The monk seal prefers quiet and isolated islands, islets and beaches. However, due to overurbanization and degradation of coastal ecosystem, this species is losing its habitat. This study was carried out between 1993-1996 in Gökçeada, one of the Turkish islands in the Northern Aegean Sea, during which two seals were observed. As a result of the field surveys on the north shore of the island, 5 caves suitable for seals were found. Public awareness activities about the protection of Mediterranean monk seals were held with the fishermen to give them the information about the species protection around the island.

Key-words : cetacea, conservation, Aegean Sea

Introduction

The distribution of the seals around Gökçeada Island is in the overlapping zone with that around the nearby Greek islands. Around these islands, namely Limnos and Samotraki Islands, the occurrence of the monk seal is known (1). Therefore the distribution and identification of the seal individuals in this overlap zone are important for the appropriate protection measures and strategies.

The studies on the distribution of the Mediterranean monk seals around Gökçeada are rather few. Marchessaux (2), as a result of the short period studies he made in Turkey, estimated that there were about 10 individuals living in the shore between Çanakkale Strait and Baba Cape including Gökçeada and Bozcaada in the Northern Aegean Sea. Mursaloglu (3) reported that monk seals in Turkish coastlines may be seen rarely around Gökçeada, Bozcaada Island to Baba Cape. Öztürk, (4) stated that there were two individuals, one young and the other old, observed in Gökçeada. On the other hand, in Lesvos Island (Greece) a minimum population of six seals was identified during the period of 1989-90 and presence of seals in Ag. Efstratios, Limnos and Samotraki Islands were indicated (1). In addition, 4-5 seals were reported in Samotraki Island (5). The present study was aimed to collect more detailed information regarding the distribution and protection of Mediterranean monk seal around Gökçeada, in the Northern Aegean Sea.

Materials and methods

The study was carried out between 23-29 September 1993, 17-30 July 1994, 17-29 July 1995, 21-27 March 1996 and 15-29 August 1996 in Gökçeada. During the study period, observations were made directly at the sea and from the land. In the sea observations, 9 m wide and 28 HP boat named *Yunus* was used. During these observations, caves suitable for seals were examined by skin diving and photographs were taken. Field studies and observations were made on the north shore of the island between Kuzu Port and Kömür Cape (Figure 1). Damages to the fishing net and death or stranded animals were also examined.

Results and discussion

During the study period, two individuals were observed. One was generally seen swimming between Katkaval Cape and Kaleköy on 25.9.1993, 27-29 July 1994 and 21.7.1995, while the other was observed resting on the beach of the cave near Kömür Cape, between coordinates 400 10'12"N- 250 42'24"E on 27.9.1993 and 27.7.1994 (Figure 1). The latter individual also observed around Kömür Cape on 24.7.1995.

The swimming seal was observed 150 m off shore. This individual was about 2 m in length, dark grey to black in color and spotted with whitish marks on its dorsal and ventral sides. The individual seen on the cave beach (and around the cave) was about 3 m in length, grey in color and spotted with white marks all over the body.

It is supposed that these animals are not the same individual due to their different size and coloration. There is also a possibility that these seals are the same individuals as those indicated in Öztürk (4).

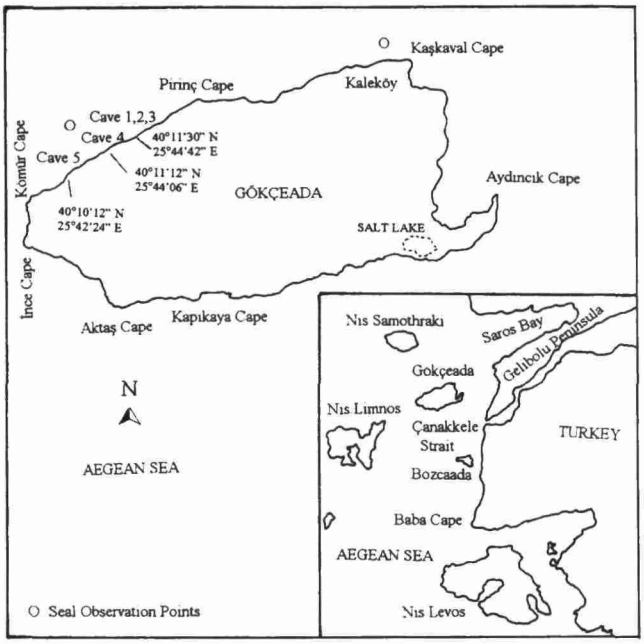

Figure 1 : The location of caves and seal encounter points in Gökçeada Island and nearby Greek Islands, in the Northern Aegean Sea.

In this area, any research on seal caves had not been reported. We found five caves on the north coast of Gökçeada. All these caves were considered suitable for seals due to aerial space, long entrance and large stony or rocky substrata. Among these caves, especially the 4th and 5th caves, can be quiet seal habitat. The 5th cave can also be used as a breeding ground since it has larger and more isolated space than the others. The caves are marked in Figure 1 with the coordinates and features of the caves are shown in Table 1.

Monk seals are known to damage fishing nets. This is the reason why some fishermen show antagonistic attitude towards them (6). However, during this study, 70 gill nets were examined and we did not find any damages in these fishing nets. This may be explained by the abundance of fish or low fishing effort in the island. In addition, no dead seal nor seal pup had been recorded in the area recently.

As a conclusion, most of the north shore of Gökçeada is quite clean and very suitable for the Mediterranean monk seals since it has potential habitats and low human population, and this species has not yet diminished from the Northern Aegean Sea. However, more detailed studies should be made in this seal overlap zone between Turkey and Greece to implement effective protection measures.

POLYCHAETES FROM THE MANAVGAT RIVER DELTA (TURKISH MEDITERRANEAN COAST)

Zeki Ergen [1], Melih Ertan Çinar [1] and Mustafa Ünsal [2]

[1] Ege University, Faculty of Fisheries, Dept. of Hydrobiology, Bornova, Izmir, Turkey
[2] ODTU, Institute of Marine Sciences, Erdemli, Yçel, Turkey

Abstract

This study deals with the polychaete fauna from the Manavgat River Delta situated in the southern coast of Turkey. The samples were collected at 14 stations in July 1995, from the depths 10 to 165m. A total of 378 individuals belonging to 68 species was recorded. The collection included two species, *Lysidice collaris* and *Rhodine loveni* with Red Sea affinities. The most widely distributed worms in the area were *Lumbrineris gracilis* and *Cirratulus chrysoderma*. The stations having relatively low salinity, situated at the mouth of Manavgat River, were characterized by low and fluctuating diversity index values, whereas in the deeper stations, far from the influence of the river, these values were higher and fairly constant. The similarity between the stations was compared and discussed.

Key-words : Polychaeta, biodiversity, Eastern Mediterranean

Introduction

The Manavgat River Delta, situated in the north-western part of the Levantine Basin along the southern coast of Turkey, has become a fashionable resort site (Fig 1). In spite of its importance, no study regarding Polychaeta, which is known as a key taxon for monitoring the marine water quality (1), has been published in the area. Concerning inshore of the Turkish Mediterranean coast, limited number of papers are available on Polychaeta fauna (2,3,4). Within the framework of the polychaete studies being continued since 1972 along the Turkish coasts, some benthic samples were collected in this area in July 1995.

Material and methods

Samples (one replicate in each station) was taken using a Van-Veen Grab, sampling ca. 10 dm3 volume of sediment, in 14 stations from 10 to 169 m depths (Table 1). Salinity of the stations varied from 37.75‰ (Stations 3 and 4) to 39 ‰. The samples were washed through sieve with 1 mm mesh size, fixed with 5 % formalin and preserved in 70% ethanol. Polychaetes were identified and counted. Diversity Index (H'), Evenness Index (J'), Frequency Index and Similarity Index were calculated according to Shannon-Weaver (5), Pielou (6), Soyer (7) and Bray and Curtis (8), respectively.

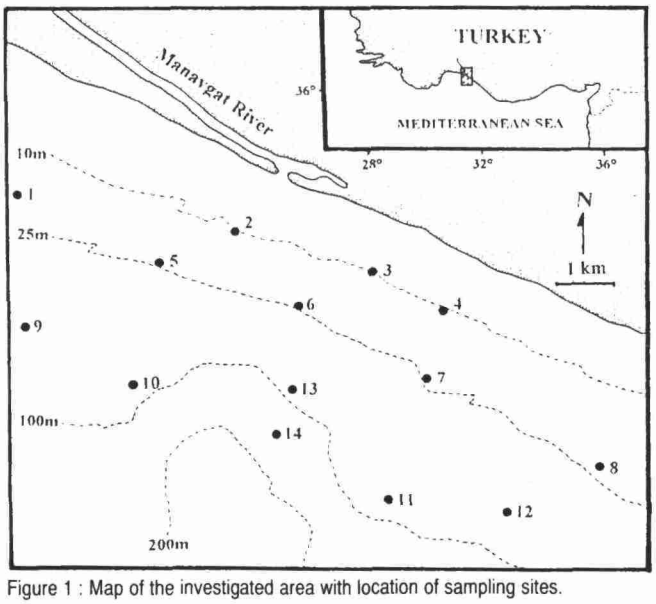

Figure 1 : Map of the investigated area with location of sampling sites.

Table 1. Depths, biotop structures, total number of species (S) and individuals (N), and dominant species of the stations.

Station	Depth	Sediment	S	N	Dominant Species
1	18 m	muddy sand	6	9	*Lumbrineris gracilis* (22.2%)
2	10 m	muddy sand	3	3	*L. gracilis* (33.3%)
3	10 m	muddy sand	1	1	*L. gracilis* (100%)
4	10 m	muddy sand	2	2	*L. gracilis* (50%)
5	23 m	muddy sand	14	25	*Cirratulus chrysoderma* (20%)
6	23 m	muddy sand	21	77	*Scoloplos armiger* (24.7%)
7	23 m	muddy sand	14	19	*Melinna palmata* (15.8 %)
8	23 m	muddy sand	10	12	*Glycera rouxii* (16.7%)
9	65 m	sandy mud	8	17	*Prionospio* sp. (35.3%)
10	85 m	sandy mud	10	31	*Prionospio* sp. (45.2%)
11	85 m	sandy mud	9	22	*Prionospio* sp. (45.5%)
12	65 m	sandy mud	13	27	*Prionospio* sp. (33.3%)
13	85 m	sandy mud	12	55	*Prionospio* sp. (43.6%)
14	165 m	sandy mud	14	78	*Monticellina heterochaeta* (38.5%)

Results and discussion

A total of 68 taxa belonging to 28 families, represented by 378 specimens, was determined. The following species, *Eteone lactea*, *Ancistrosyllis hamata*, *Aricidea* cf. *longobranchiata*, *Therochaeta flabellata*, *Monticellina heterochaeta* and *Ampharete grubei*, were new to the Turkish fauna. Thirty-four species are newly reported from the Turkish Levant coast (Table 2).

Table 2. List of species found and their abundance at the stations

SPECIES	STATIONS 1	2	3	4	5	6	7	8	9	10	11	12	13	14
Harmothoe impar	-	-	-	-	-	-	-	-	-	-	-	1	-	-
**Harmothoe lunulata*	-	-	-	-	-	-	-	-	-	1	-	-	-	-
Harmothoe sp.	-	-	-	1	-	-	-	-	-	-	-	-	-	-
**Pholoe synophthalmica*	-	-	-	-	-	-	-	1	-	-	-	-	-	-
Sigalion mathildae	-	-	-	-	-	-	2	-	-	-	-	-	-	-
Pelogenia arenosa	-	-	-	-	-	-	1	-	-	-	-	-	-	-
Aphroditidae gen. sp.	-	-	-	-	-	-	-	-	-	-	-	1	-	-
Euphrosyne sp.	-	-	-	-	-	-	-	1	-	-	-	-	-	-
***Eteone lactea*	-	-	-	-	-	1	-	-	-	-	-	-	-	-
***Ancistrosyllis hamata*	-	-	-	-	-	-	-	-	-	-	-	-	1	-
Syllis armillaris	-	-	-	-	-	-	-	1	-	-	-	-	-	-
Syllis cornuta	-	-	-	-	-	-	-	1	-	-	-	-	-	-
Nereis sp.	-	-	-	-	-	1	-	-	-	-	-	-	-	-
**Glycera convoluta*	-	-	-	-	-	-	1	-	-	-	-	-	-	-
**Glycera capitata*	-	-	-	-	-	-	-	-	-	-	-	-	1	-
**Glycera rouxi*	1	-	-	-	-	-	-	2	-	1	1	-	-	-
**Nephthys caeca*	-	-	-	-	-	-	-	-	1	-	-	-	-	-
**Nephthys incisa*	-	-	-	-	3	-	1	-	-	-	-	-	-	-
**Goniada emerita*	-	-	-	-	-	1	1	-	-	-	-	-	-	-
Lysidice collaris	-	-	-	-	-	-	-	1	-	-	-	-	-	-
Lumbrineris gracilis	2	1	1	-	-	2	1	-	1	-	-	1	2	1
Lumbrineris latreilleii	-	-	-	-	-	1	-	-	-	-	-	-	-	-
Lumbrineris coccinea	-	-	-	-	-	1	-	-	-	-	-	-	-	-
Scoletoma impatiens	-	-	-	-	1	5	-	-	-	-	-	1	-	-
Scoletoma fragilis	-	-	-	-	-	7	-	-	2	2	-	1	-	-
Scoletoma funchalensis	-	-	-	-	1	-	-	-	-	-	-	-	-	-
Aponuphis fauveli	-	-	-	-	-	1	-	-	-	-	-	-	-	-
**Scoloplos armiger*	-	-	-	-	3	19	2	-	-	-	-	-	-	-
**Spio filicornis*	-	-	-	-	1	-	-	-	-	-	-	-	-	-
**Nerine foliosa*	-	-	-	-	1	1	-	-	-	1	-	-	-	-
**Spiophanes bombyx*	-	-	-	-	2	-	1	-	1	-	-	-	-	-
**Laonice cirrata*	-	-	-	-	-	1	-	-	4	-	-	-	-	-
**Prionospio cirrifera*	-	-	-	-	-	5	-	-	-	7	4	1	3	5
**Prionospio steenstrupi*	-	-	-	-	-	-	-	-	-	-	-	-	1	4
Prionospio sp.	-	-	-	-	-	3	-	-	6	14	10	9	24	9
***Aricidea* cf. *longobranchiata*	-	-	-	-	-	-	-	-	-	-	-	1	1	5
**Paradoneis lyra*	-	-	-	-	-	-	-	-	-	1	-	-	-	-
**Magelona papillicornis*	-	-	-	-	-	-	-	-	-	-	1	-	-	-
**Poecilochaetus serpens*	-	-	-	-	-	-	-	-	-	-	1	-	-	-
***Therochaeta flabellata*	-	-	-	-	-	-	-	-	-	1	-	-	1	1
Cirriformia sp.	-	-	-	-	1	-	-	-	-	-	-	-	-	-
**Cirratulus chrysoderma*	-	-	-	-	5	5	2	-	1	2	-	4	1	11
**Chaetozone setosa*	-	-	-	-	-	-	-	-	-	-	2	-	-	1
***Monticellina heterochaeta*	-	-	-	-	-	7	-	-	-	-	-	-	14	30
Cirratulidae gen. sp.1	2	-	-	-	-	-	-	1	-	-	-	-	-	-
Cirratulidae gen. sp.2	-	1	-	-	-	-	-	-	-	-	-	-	-	-
Notomastus latericeus	-	-	-	-	-	2	-	-	1	-	-	-	-	-
***Notomastus* cf. *lineatus*	-	-	-	-	-	-	-	-	-	-	-	1	-	-
Pseudoleiocapitella fauveli	-	-	-	-	-	2	-	1	-	-	1	-	-	-
Capitellidae gen. sp.	2	-	-	-	-	-	-	-	-	-	-	-	-	-
**Euclymene gracilis*	-	-	-	-	-	-	-	-	-	-	-	-	2	2
Euclymene sp.	-	-	-	-	-	-	1	-	-	-	1	-	-	-
**Rhodine loveni*	-	-	-	-	1	-	-	-	-	-	-	-	-	-
**Petaloproctus terricola*	-	-	-	-	-	2	-	-	-	-	-	-	-	-
Cossura sp.	-	-	-	-	-	6	-	-	-	-	-	-	-	1
**Sternaspis scutata*	-	-	-	-	-	4	-	1	-	1	-	4	4	4
**Terebellides stroemi*	-	-	-	-	-	-	-	-	-	-	-	-	-	2
***Ampharete grubei*	-	-	-	-	-	-	-	-	-	-	-	-	-	2
Melinna palmata	1	1	-	-	3	-	3	2	-	-	-	-	-	-
Amphitrite sp.	-	-	-	1	-	-	-	-	-	-	-	-	-	-
**Pista cristata*	-	-	-	-	1	-	-	-	-	-	1	-	-	-
Pista unibranchiata	-	-	-	-	-	-	1	-	-	-	-	-	-	-
Polycirrus sp.	-	-	-	-	1	-	-	-	-	-	-	-	-	-
Chone collaris	1	-	-	-	-	-	-	-	-	-	-	1	-	-
**Chone* cf. *acustica*	-	-	-	-	-	-	-	-	-	-	-	1	-	-
Chone sp.1	-	-	-	-	1	-	1	-	-	-	-	-	-	-
Chone sp. 2	-	-	-	-	-	-	1	-	-	-	-	-	-	-

* species new to Turkish Levant fauna ** species new to the Turkish fauna

COMPORTEMENT ALIMENTAIRE DE PARACENTROTUS LIVIDUS (*ECHINODERMATA: ECHINOIDEA*) EN MILIEU LAGUNAIRE

Catherine Fernandez [1*] et Angela Caltagirone [2]

[1] Equipe Ecosystèmes Littoraux, Université de Corse BP 52, 20250 Corté, France
[2] UMR-DIMAR3 COM, Parc Scientifique et Technologique de Luminy, Université de la Méditerranée, Case 901, 13288 Marseille, France

Résumé

Le régime alimentaire de *Paracentrotus lividus* est analysé dans trois biotopes d'une lagune méditerranéenne (Urbinu, Corse). Les résultats montrent que, dans l'herbier de Cymodocées, cet oursin se comporte comme un brouteur et exerce un choix en consommant essentiellement des feuilles de Cymodocées. Par contre, lorsque les ressources végétales sont rares (sur des fonds de sable ou de galets) *P. lividus* se comporte comme un racleur ou un détritivore utilisant toutes les sources de nourriture disponibles. Ceci montre la faculté d'adaptation de cette espèce, l'importance du comportement de couverture et du caractère omnivore de *P. lividus* pour sa survie dans les milieux lagunaires.

Key-words : Echinodermata, Diet, Lagoons

Introduction

Les oursins jouent un rôle primordial dans l'évolution des peuplements phytobenthiques (1). En Méditerranée, *Paracentrotus lividus* (Lamarck) est une espèce déterminante dans la dynamique du phytobenthos et a souvent fait l'objet d'études de régime alimentaire (2). Ces études ont été effectuées principalement sur des populations de *P. lividus* vivant en mer ouverte, sur des fonds rocheux ou dans les herbiers à *Posidonia oceanica* Linneaus Delile. En Méditerranée, *P. lividus* est également présent dans des milieux lagunaires (3, 4) où il est confronté à des conditions de vie très difficiles. Dans cette étude, nous avons analysé le régime alimentaire chez des populations de *P. lividus* qui vivent dans différents biotopes d'une lagune méditerranéenne présentant des ressources trophiques très contrastées. Ceci permettra de mieux comprendre le comportement alimentaire de cet oursin dans ce type de milieu.

Matériel et méthodes

Les oursins ont été prélevés au printemps (Avril) dans l'étang d'Urbinu, (Méditerranée, France, côte Est de Corse), dans 3 des 4 principaux biotopes ou types de fond de cet étang (5) : (i) les fonds de sable nu (sans ressources végétales fixées), (ii) les fonds de galets (ressources végétales très limitées) et (iii) les herbiers à Cymodocea nodosa (Ucria) Ascherson (ressources végétales abondantes). Pour chaque biotope, dix oursins, d'un diamètre de 30 à 45 mm, ont été prélevés puis disséqués. Le contenu digestif a été analysé par la méthode des "contacts" (6) adaptée à *P. lividus* (7). Pour chaque oursin, 100 "contacts" sont effectués, ce chiffre suffisant pour avoir des résultats représentatifs (2). La contribution d'un aliment due à ces contacts (CSPi) s'évalue par le rapport entre le nombre de contacts obtenu pour cet aliment i (ci) et le nombre total de contacts réalisés (C), exprimé en pourcentage : CSPi=100xci/C

L'homogénéité des contenus digestifs des oursins dans un même biotope a été analysée grâce au coefficient de similarité de Steinhaus (8).

Résultats et Discussion

Les caractéristiques générales du régime alimentaire de *P. lividus* vivant dans les herbiers à *C. nodosa* (Figure 1), à la saison considérée (printemps), montrent que la fraction végétale, qui est prépondérante (95.4%), n'est représentée que par *C. nodosa* avec une nette préférence pour les feuilles vivantes. La forte proportion de gaines ainsi que la consommation de rhizomes seraient dues à la localisation des oursins dans l'herbier, du moins dans la journée, (fixés à la base des touffes de *C. nodosa*). Dans cet herbier, la flore algale est totalement absente du régime alimentaire de *P. lividus*. Ceci est dû au fait que ce biotope est relativement pauvre en algues, que les Cymodocées sont peu épiphytées et que cette espèce est appréciée par *P. lividus* (9).

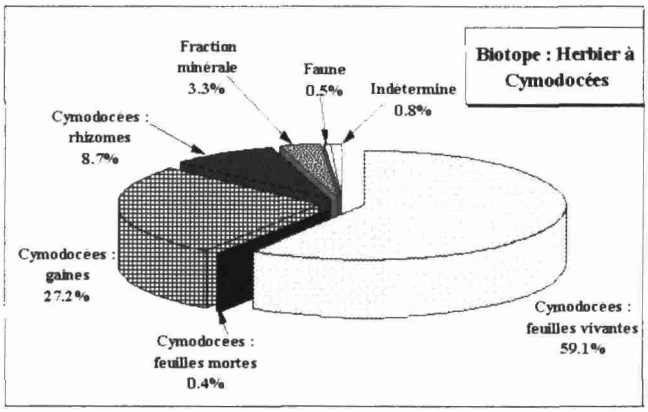

Figure 1 : Principaux aliments consommés par *Paracentrotus lividus* vivant dans les herbiers à *Cymodocea nodosa* de l'étang d'Urbinu (contributions moyennes données en pourcentage).

La fraction animale, peu abondante, est essentiellement composée de très jeunes gastéropodes vivant sur les feuilles de *C. nodosa*. Leur consommation est sans doute fortuite et liée à la présence de ces organismes sur les feuilles ingérées. L'indice de similarité de Steinhaus, très élevé (0.91) traduit une grande homogénéité du régime alimentaire dans ce site.

Lorsque les individus vivent sur les fonds de sable, le régime alimentaire présente une forte dominance végétale (Figure 2) (la contribution de la flore totale varie de 52% à 97% selon les individus). Elle est composée essentiellement d'Ulvophycées vivant à l'état libre (Enteromorpha, Chaetomorpha, Cladophora) ainsi que de *C. nodosa* et autres phanérogames, terrestres ou marines, en épave. La fraction minérale est assez importante (14.7% en moyenne et jusqu'à 36% chez certains individus). L'ingestion du sable entraîne la présence dans les contenus digestifs de ces oursins d'éléments comme des grains de pollen, des fèces de gastéropodes (sans doute de Murex), ainsi que des diatomées et des foraminifères.

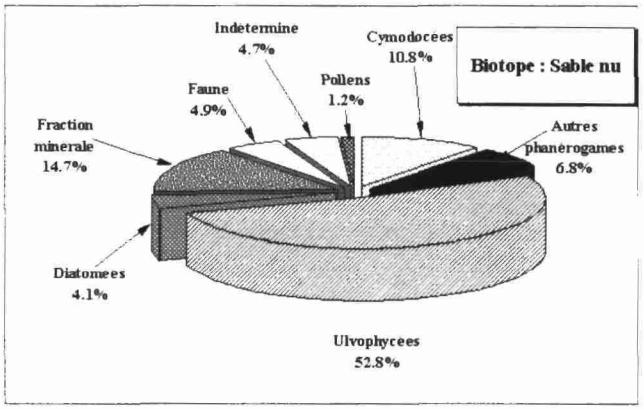

Figure 2 : Principaux aliments consommés par *Paracentrotus lividus* vivant sur des fonds de sable nu dans l'étang d'Urbinu (contributions moyennes données en pourcentage).

La faune, également présente, est variée. Les gastéropodes et les bivalves de petite taille sont sans doute ingérés avec les Ulvophycées libres; les foraminifères le sont avec le sable; les éponges et les crustacés (mues) le sont comme des végétaux quand aucune autre nourriture n'est disponible. Le régime alimentaire de *P. lividus* très varié dans cette station fait appel au phénomène du comportement de couverture ("covering reaction") (10). Les oursins situés loin de toute source de nourriture se recouvrent de débris végétaux ou animaux,

THE PALEOGEOGRAPHIC ENIGMA OF A SHIPWRECK FOUND OFF MA'AGAN MICHAEL, CENTRAL ISRAEL

Daniela Friedmann [1*] and Yossi Mart [2]

[1] Israel Oceanographic and Limnological Research, Haifa 31080, Israel
[2] Leon Recanati Center for Marine Studies, Haifa University, Haifa 31905, Israel

Abstract
A 2,400 years old shipwreck, discovered in the shallow continental shelf off central Israel, shed light on the recent paleogeography of that region. Analyses of the sand near the wreck-site suggest stable sealevel and wave climate since that time.

Key-words : ocean history, sediment transport, eastern Mediterranean

A 2,400 years old shipwreck was discovered buried in the sand in the shallow sea off Ma'agan Michael in central Israel (Figure 1). The pine and oak built vessel was 13 m long, 4 m wide, and it was remarkably well preserved. The ship was discovered at water depth of 1.5 m, with its bow facing southeastwards, toward the beach (1). This archaeological discovery instigated a multidisciplinary research, the sedimentological part of it used the wreck as a temporal bench-mark in the reconstruction of the coastal paleogeography. The Ma'agan Michael coast is sandy, and is protected from the erosional effect of the winter storms by a ridge of late Pleistocene calcareous sandstone. Most of the ridge is submerged, but for several small islands which protrude above sealevel, the largest being HaYonim Island. The water depth between the sandstone ridge and the coast is less than 2 m in most places. It was of paleogeographic and archaeological interest to reconstruct the sailing conditions of the ship during its wreckage. Ma'agan Michael is located 2 km north of the present mouth of Crocodile River. Aerial photographs show that the river mouth shifted nearly 1 km southwards due to sediment transport along the coast (see also 2). We presume that the river mouth was located close to the wreck-site some 2,400 years ago. Rivers were known to be preferred site for harbors in antiquity, because they were better protected from the wrath of nature and ferocity of man (3). It is presumed that the ship beached while trying to enter the river mouth to find safe haven.

The coastal sand in the proximity of the wreck was sampled in 12 shore-normal profiles and analyzed for its size and mineralogy. Two 5 m deep boreholes were drilled on the coast, 220 m apart, in the lee of HaYonim Island, and a series of probes was carried along the coast and in the shallow offshore zone. Qualitatively, the sand at Ma'agan Michael comprises mainly quartz grains of Nilotic origin, which is the major constituent of all the size fractions. Minor components, which were found in all the fractions as well, are opaque mineral grains, shell fragments, and microfauna such as foraminifers and ostracods. The sampling of the coastal sand in Ma'agan Michael shows that the principal fraction of the sand is fine grained (0.25-0.125 mm), and the second most abundant fraction is medium grained (0.5-0.25 mm). While most fractions were found to be nearly uniform in all the profiles, the spatial analyses of the medium-grained fraction presented some geographically meaningful variations. The quantity of medium-grained sand increases towards the breaker zone and in the segment of the beach, which is not protected by the submerged ridge (4). It seems that the increased amount of coarser sand reflects higher level of wave energy along the coast. A detrital fraction of a different provenance is a very coarse sand and grit, comprising mainly shells and shell fragments of *Glycymeris* sp. Considerable increase in this fraction was encountered in the boreholes at depth of approximately 2 m, where a 0.5 m layer was encountered. The jet probes of the coastal and offshore sand also encountered that layer, and observations during the excavation of the wreck indicated that the hull was embedded in that anomalous layer, enriched with large shells of *Glycymeris* sp. as well. These coarse fragments suggest either a depositional environment of higher hydraulic energy than the present one, or anthropogenic interference.

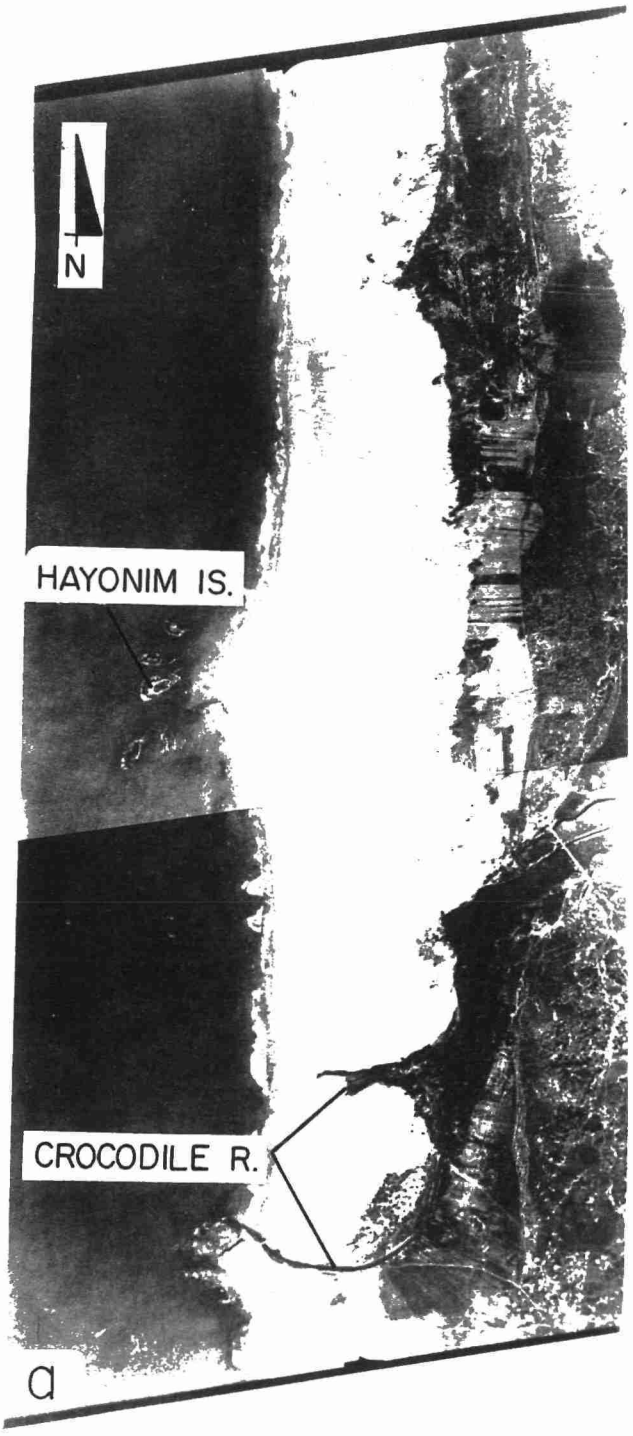

Figure 1. a. The coast of Ma'agan Michael, and the site of the shipwreck.

LA POLLUTION EN MILIEU PORTUAIRE: APPROCHE DE LA POLLUTION INDUSTRIELLE ET DOMESTIQUE À TRAVERS LA DISTRIBUTION DU MACROZOOBENTHOS DU PORT D'ORAN (ALGÉRIE)

S. Grimes

Laboratoire des Ecosystèmes Benthiques
ISMAL-BP 54 Plage Ouest, Sidi-Fredj, Gouvernorat d'Alger, Algérie

Résumé

L'aboutissement "naturel" des eaux usées et industrielles dans les ports est incontestablement un facteur des plus menaçants d'altération de l'écosystème côtier. Le port d'Oran, deuxième ville d'Algérie n'échappe pas à cette "logique". La description des peuplements benthiques de cette enceinte a permis d'individualiser cinq zones d'inégale perturbation; une zone azoïque, une zone très polluée, une zone de transition I, une zone polluée et une zone subnormale. Celles-ci s'organisent selon un gradient de pollution décroissant à partir du "panache" de rejet du grand collecteur d'Oran. La prépondérance numérique de *Capitella capitata, Corbula gibba, Chaetozone setosa* et *Scolelepis fuliginosa* corroborent ce constat.

Mots clés: bio-indicators, pollution, zoobenthos, western Mediterranean

Introduction

Les modalités de distribution topographique des peuplements atteints par la pollution ont fait l'objet de nombreux travaux en écologie benthique notamment (1-7). L'essentiel de ces travaux montre des modifications substantielles de la structure des communautés benthiques en relation avec le degré de perturbation du milieu. La description de ces modifications devient alors impérative afin d'estimer quantitativement le dommage écologique global que subit le milieu récepteur.

La présente étude se propose d'évaluer les dommages occasionnés au compartiment benthique d'un port à vocation industrielle et commerciale: le port d'Oran. Cette évaluation repose sur la notion d'indicateurs écologiques développée par Bellan (8).

Méthodologie

Pour une large couverture des fonds prospectés (fig. 1), 20 stations (profondeur 7-18 m) sont échantillonnées à l'intérieur du port, quatre stations dans la zone avant-port (18-24 m) et une station est prospectée à l'extérieur du port (32 m). Les prélèvements portant sur une surface de sédiment de 1/4 m^2 ont été réalisés en Juin 1995, à bord du N.O. algérien *M.S. Benyahia* avec une benne de type "Van Veen". Les paramètres physico-chimiques (température, salinité et oxygène dissous) ont été mesurés pour les eaux de fond. Pour la caractérisation et mise en évidence des peuplements macrobenthiques il est fait appel aux descripteurs numériques classiques (l'abondance, la densité, la dominance, la fréquence, l'indice biologique). Par ailleurs, pour l'évaluation des stades de déséquilibre des peuplements prospectés, les indices de diversité de Shannon et Weaver (9) et d'Equitabilité Pielou (10) sont calculés.

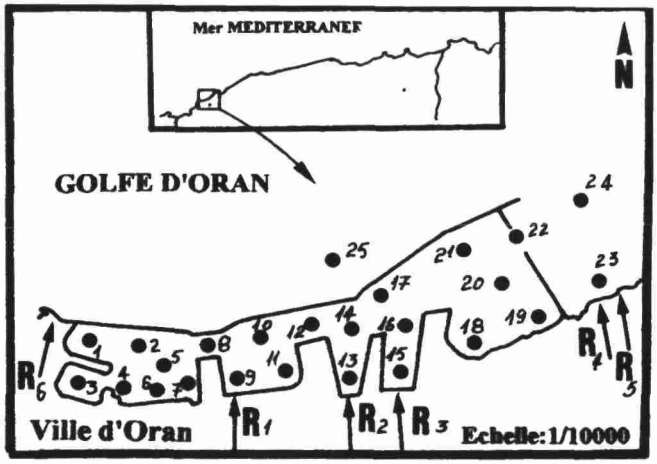

Fig. 1: Localisation des stations prospectées au port d'Oran

Résultats

Paramètres physico-chimiques

La température des eaux du fond oscille entre 18 et 22°C. La valeur minimale est mesurée à l'entrée du port (O24) et dans les bassins de Skikda et de Mostaganem (O10, O12 et O21). Les maxima sont essentiellement le fait de la zone très confinée (O1, O3 et O4). Du point de vue hyalin, les plus faibles valeurs sont enregistrées aux stations O5, O20, O23 et O24 (35.2-35.45 p.s.u.). La plus forte salinité est obtenue à la station O18 (36.9 p.s.u.).

Les teneurs en oxygène dissous fluctuent entre 4.7 et 7.3 mg/l. Le seuil minimal est le fait de la station O12 alors que les concentrations maximales sont enregistrées aux stations O19 et O9 avec respectivement 7 et 7.3 mg/l. Le peu de variations des paramètres température et salinité d'une part et la sous oxygénation d'autre part traduisent parfaitement le caractère semi-fermé et confiné du port d'Oran.

Peuplements macrozoobenthiques

Deux espèces déséquilibrent considérablement les peuplements prospectés; l'indicatrice de matière organique le bivalve *Corbula gibba* dans le secteur de confinement où cette espèce atteint la dominance extrême de près de 99 % (bassin de Ghazaouet). L'indicatrice de pollution d'ordre I, le polychète *Capitella capitata* type I et II est majoritaire dans le bassin de Skikda et la zone avant-port où cette espèce atteint la valeur significative de 94% au niveau de la passe. L'organisation trophique des peuplements révèle une prépondérance quantitative des suspensivores (S) au fond du port et des détritivores de surface (DS) au niveau de la passe et dans le secteur avant port (tableau 1).

Zonation en fonction du degrés de perturbation

La cartographie des peuplements macrobenthiques du port d'Oran permet de dégager un schéma d'organisation des espèces en cinq zones. Cette organisation rappelle celle décrite par Bellan (8) au port de Marseille et Hily (11) dans la rade de Brest sous forme d'auréoles, disposées selon un gradient décroissant à partir d'une source principale de pollution. (fig.2):

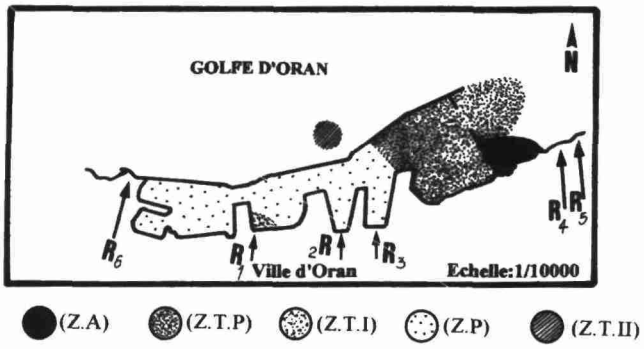

Fig. 2: Etat d'équilibre des peuplements du port d'Oran.

1- La zone azoïque (Z.A) ou zone de pollution maximale: caractérisée par une absence totale de toute vie macrobenthique, très probablement du fait de sa proximité de la zone qui reçoit les effluents drainés par le grand collecteur de la ville d'Oran (zone avant-port Sud).

2- La zone très polluée (Z.T.P): Cantonnée dans le bassin de Skikda et au niveau de la passe, les peuplements de ce secteur sont dominés par les espèces indicatrices de pollution (IP), soit des stocks supérieurs à 70 %. Les espèces leaders de ce secteur sont *Scololepis fuliginosa, Polydora antennata*, mais surtout *Capitella capitata* qui représente jusqu'à 80.75%, 72.57 % et 75 % respectivement des peuplements des stations O19, O20 et O21.

3- La zone de transition I (Z.T.I): Représentée par la station O9, localisée en face du rejet qui se déverse dans le bassin de Ghazaouet, le stock des indicatrices de matières organiques (IMO) avec 43.04 % est aussi important que celui des indicatrices de pollution (IP), soit 51.51%. L'espèce leader du peuplement de cette station est le bivalve *Corbula gibba*.

4- La zone polluée (Z.P) ou zone de déséquilibre: C'est la plus grande zone en terme de surface. Les peuplements de cette zone sont nettement dominés par *Corbula gibba* qui représente plus de 90 % de l'effectif total des peuplements des stations (O1, O2, O3, 6 et O7). Néanmoins les peuplements de cette zone sont enrichis d'espèces communes aux milieux perturbés (*Ruditapes decussatus, Abra alba, Chaetozone setosa, Parvicardium exiguum et Prionospio malmgeni...*)

5- La zone subnormale ou zone de transition II (Z.T.II): Cette zone est représentée par la seule station O25 située à l'extérieur du port où est noté

IMPACT DE LA POLLUTION INDUSTRIELLE ET DOMESTIQUE SUR LES PEUPLEMENTS MACROZOOBENTHIQUES DE LA RÉGION DE SKIKDA

Grimes S.* et Arkam M.

ISMAL, BP. 54 Plage Ouest, Sidi Fredj, Gouvernorat d'Alger, Algérie

Résumé

L'étude de l'organisation des peuplements macrozoobenthiques de la région de Skikda révèle l'incontestable impact de l'activité du complexe urbano-portuaire sur le milieu. La mise en évidence d'une zone de déséquilibre dans le nouveau port est annonciatrice du début de déstructuration des peuplements de cette enceinte. La structure des peuplements de l'ancien port révèle une stabilisation depuis 1990 due principalement à la persistance de "l'hégémonie" numérique des espèces indicatrices de pollution. De même que la prépondérance d'*Abra alba*, *Corbula gibba* et *Audouinia tentaculata* est significative. L'organisation en mosaique des peuplements du golfe traduit l'absence d'un axe d'écoulement privilégié de la pollution.

Mots clés: bio-indicators, pollution, zoobenthos, western Mediterranean

Introduction

Très peu d'attention a été accordée à l'évaluation des dommages occasionnés à l'écosystème benthique de la région de Skikda du fait de l'industrie pétrochimique et de l'urbanisation intense. Cette étude se propose donc d'en mesurer les repercussions à travers le degré de "destructuration" des peuplements macrozoobenthiques, bio-indicateurs par excellence (1-5).

Méthodologie

La prospection des peuplements macrozoobentiques réalisée le 23/06/1995 à bords du N.O. *M.S. Benyahia* porte sur les fonds meubles de la région de Skikda (fig. 1). La récolte des échantillons est effectuée avec une benne piocheuse de type VAN VEEN portant sur une surface de substrat de 1/4m^2. Cette étude vise l'évaluation des caractéristiques de ces peuplements, leur structuration, le degré de dépendance de leur organisation avec un éventuel gradient de perturabation du milieu. L'étude de la diversité spécifique est réalisée par l'indice de Shannon (6) donné par la formule: Is=-Σ ni/Nlog$_2$ ni/N où S représente le nombre d'espèces, N l'effectif total et ni le nombre d'individus de l'espèce. L'équitablité «Eveness» est calculée à partir de la formule de Pielou (7): E=Is/ln N où Is est l'indice de Shannon et N l'effectif total. L'évaluation des stades de "degradation" repose sur la notion d'espèces caractéristiques developpée par Picard (8). La cartographie des zones prospectées s'inspire des modèles proposés par Bellan (9), Reish (10), Hily (11) et celui de Lizarraga-Partida (12).

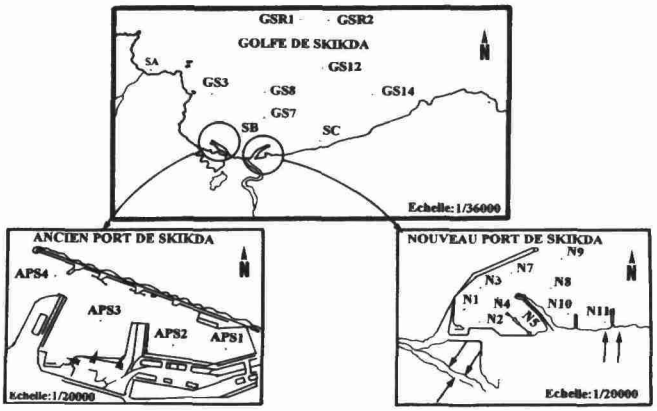

Fig.1: Localisation des stations prospectées dans la région de Skikda

Résultats

L'analyse des groupes systématiques révèle l'importance numérique (100-1768 ind./m^2) et pondérale (1.2 g de PSLC/m^2) des mollusques dans les peuplements des deux ports. Les bivalves *Corbula gibba*, *Abra alba* et à un degré moindre *Tellina pulchella* sont responsables de cette situation. Les polychètes dominent dans les peuplements des stations APS2 (172 ind./m^2), N7 et N8 (1076 et 632 ind./m^2). Dans le golfe les proportions des différents groupes ne montrent pas de tendance particulière. L'étude des groupes écologiques permet une approche plus précise de l'organisation des espèces car elle tient compte de leurs affinités. Les onze groupes individualisés traduisent une prépondérance numérique indicatrices de matière organique (IMO), des indicatrices d'instabilité (II) et des indicatrice de pollution (IP). La structure trophique révèle la dominance des suspensivores aux stations de l'extérieur de l'ancien port APS3 et APS4 (67 et 45 %) et des detritivores de surface (DS) aux stations les plus confinées APS1 et APS2 avec 62.5 et 56.1 %. Les suspensivores (S) dominent dans l'essentiel des stations du nouveau port (33.4-60 %).

Diversité spécifique et équilibre numérique

Les valeurs de l'indice de Shannon aux stations du golfe SC (1.17), GSR1 (1.54) et aux stations APS3 (1.83) et APS1 (1.93) de l'ancien port montrent un déséquilibre numérique des peuplements de ces stations. Par ailleurs, dans les secteurs Nord-Est et Nord-Ouest du golfe (4.13 et 4.7) et aux stations N7 et N8 (4.58 et 3.98) du nouveau port, les peuplements semblent très peu déséquilibrés. Les valeurs de l'indice d'équitabilité (0.29 à 0.92) permettent d'aboutir au même constat. En effet, les plus faibles valeurs de cet indice sont observées aux stations APS1, APS3 de l'ancien port et aux stations du golfe (SC, GS3 et GSR1). L'allure concave, la pente marquée et très peu étendue des courbes des diagrammes rang/fréquence des stations N1, N3 et N8 du nouveau port et des stations du golfe (SC, GS3, GS8 et GSR1) rappellent les déformations decrites par Frontier au stade I. Cette allure de la courbe suppose une prépondérance numérique d'un petit groupe d'espèces. Contrairement aux DRF obtenues aux stations N2, N4, N5 et N7 qui traduisent des peuplements matures et numériquement plus ou moins équilibrés. Dans l'ancien port, les courbes sont à pente raide avec une tendance à la concavité aux stations APS2 et APS3 due à une structure peu évoluée du peuplement car profondément affectée par les perturbations. Alors que la convexité de la courbe à la station APS4 signifierait un équilibre relatif de son peuplement. Les stations SA, GSR2 et GS 12 du golfe de Skikda montrent des courbes nettement convexes sur toute leur longueur. Cet ensemble serait celui des peuplements les plus équilibrés.

Zonation et degré de perturbation

L'organisation des peuplements du nouveau port (fig. 3) permet de dégager trois zones d'inégale perturbation; une zone de déséquilibre (N1, N2, N5, N7 et N11) où dominent les indicatrices de pollution (IP>15 %), principalement du fait d'*Audouinia tentaculata* et *Heteromastus filiformis* signalées par Bellan dans la zone polluée externe du port de Marseille et d'espèces caractéristiques de milieux hypertrophiés (*Corbula gibba*, *Abra alba*, *Chaetozone setosa*), la zone de transition I (N9 et N10) est moins riche en espèces. Alors que la zone de transition II (N3, N4 et N8) est caractérisée par une faible présence de l'indicateur de pollution *Audouinia tentaculata* et l'absence total de l'indicateur de pollution d'ordre *I Capitella capitata* aux stations N3 et N4. Le peuplement de cette zone est co-dominé par les espèces indicatrices d'instabilité (II) et de matière organique (IMO). Les stations prospectées dans l'ancien port révèlent la stabilisation de la structure de leur peuplement depuis 1990 (13). En effet, ce sont toujours les indicatrices de pollution qui dominent largement ces peuplements, particulièrement au niveau des stations les plus confinées avec un stock des IP>60 % (APS1, APS2 et APS3). De même que la prépondérance numérique d'*Abra alba*, *Corbula gibba* et *Audouinia tentaculata* se maintient. Le peuplement de la zone avant-port (APS4) ne semble pas non plus avoir subi des modifications sensibles depuis 1990. En effet une meilleure répartition quantitative des espèces les caractérise; les sabulicoles dominent avec 25 % des stocks des indicatrices d'instabilité (17.5%), des vasicoles et des indicatrices de pollution, avec 10 % pour chacune d'elles. Dans le golfe, trois zones s'individualisent (fig. 3). La zone polluée, située dans le secteur Nord-Est de l'ancien port (SB et GS8) qui correspond à la partie du golfe la plus affectée (IP>20.57%). Les rejets drainés par oued Safsaf sont en partie responsables de la degradation des peuplements de ce secteur. La zone subnormale traverse le golfe d'Ouest en Est et regroupe les stations SC, GS7, GS14, GS7, GS3 et SA caractérisées par des peuplements de transition. Les stations GSR1, GSR2 et GS12 situées plus au large délimitent une zone normale apparement épargnée par l'influence accrue de la pollution. Il en ressort un modèle de distribution en mosaïque des peuplements du golfe, traduit par l'absence d'un réel gradient de perturbation à partir des sources principales de pollution de ce secteur de la côte.

Discussion

L'étude de la répartition spatiale des peuplements propectés fait ressortir l'étroite relation qui existe entre leur organisation et le stade de dégradation du milieu. La destructuration des peuplements de l'ancien port semble persister et confirme la tendance observée par Grimes et Bakalem (13). Les peuplements du port industriel semblent plus stables. Cependant, la mise en évidence d'une zone de déséquilibre et d'une zone de transition, même si elle reflète un caractère peu dégradé des peuplements de cette enceinte portuaire de construction assez récente, présage de leur destructuration à long terme si il y a persistance des sources d'altération. La zone d'évolution entre les deux ports semble plus affectée du fait de l'influence des rejets qui se

FISH FAUNA OF THE GENOA-QUINTO *POSIDONIA OCEANICA* BED (LIGURIAN SEA, NORTH-WESTERN MEDITERRANEAN)

Guidetti P., Bussotti S., Conti M.*

Istituto di Anatomia Comparata, Università di Genova, Viale Benedetto XV 5, 16132 Genoa, Italy

Abstract

The fish assemblage associated with the *Posidonia oceanica* bed of Genoa-Quinto (Ligurian Sea) was censused by SCUBA diving from October 1995 to May 1996 using the visual census method. It comprised 28 species (9 families) and was numerically dominated by planktivorous species (*Chromis chromis, Spicara smaris, Spicara maena* and *Boops boops*), while Labridae and Sparidae were the most speciose families. Among Labridae, *Coris julis* and *Symphodus ocellatus* were the most abundant species, while Sparidae (*Boops boops* excepted) were quite scarce. The possible influence of several factors in governing fish community structure is discussed.

Key-words: fishes, Posidonia, coastal systems, Ligurian Sea

Introduction

Posidonia oceanica beds represent one of the most complex and productive systems in the littoral zone of the Mediterranean Sea (1) supporting a very diversified invertebrate fauna (2) and a rich fish community (3). Seagrass meadows are reported to provide shelter and food to juvenile fishes of commercial interest (4; 5; 6). In the last decades, a number of studies was devoted to the fish fauna of P. oceanica in the Mediterranean; these investigations were carried out both in marine reserves (7; 8; 9; 10) and in other coastal areas (11; 12; 13).

The present study is aimed to provide information about the structure and species composition of the fish community inhabiting a *P. oceanica* bed from an urbanized coast: Genoa-Quinto, next to Genoa city.

Materials and methods

The study area was localized off Genoa city (Genoa-Quinto, Ligurian Sea: 44° 23.1', 9° 0.7'E; Fig. 1) in a *P. oceanica* bed settled on coarse sand and rocky substrate and showing a shoot density of 342 shoots/m^2 at about 10 m depth, where the transects were placed. The studied meadow, extending from about 6 m to 28-30 m depth (14), was represented by large patches of *P. oceanica* interspersed with sand and rocky formations rich in crevices and colonized by photophilic arborescent algae.

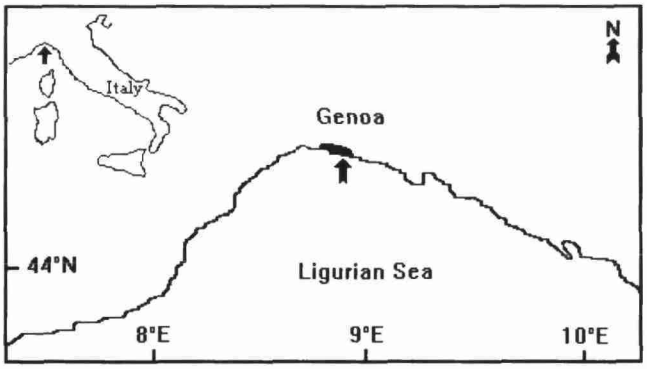

Figure 1 : Location of the sampling area.

Data on abundance and size of recorded fishes were collected using the SCUBA visual census methodology according to Harmelin-Vivien *et al.* (15). A total of 11 censuses (replicated 2-4 times by different observers) were carried out, between 10 a.m. and 3 p.m., along transects 25 m long and 6 m width (150 m^2) from October 1995 to May 1996. Each censused individual was classified as small, medium and large according to the maximum recorded total length (16). Counts were made according to abundance classes following a geometrical progression with a base 2 (1, 2-5, 6-10, 11-30, 31-50, 51-100, 101-200, 201-500, >500). Density was expressed as number of individuals/150 m^2; frequency of occurrence (number of census in which a given species was recorded/number of total censuses performed in percent) was reported for each species. The assignment of feeding-guilds to each species was made according to the classification of Bell and Harmelin-Vivien (17): 1) Herbivores; 2) Microcarnivores; 3) Mesocarnivores (Type 1: all Labridae); 4) Mesocarnivores (Type 2); 5) Macrocarnivores.

Results

The whole recorded fish community comprised 28 species belonging to 9 families (Tab. 1) and was dominated by Labridae (11 species, 39.3 % of the total censused species) and Sparidae (8 species, 28.6 %), which together accounted for up to 65 % of the total censused species. The number of species per census was variable without any particular trend and ranged between 11 and 21 with an average of 16.5 ± 3.1 species.

Table 1 : List of species censused at Genoa-Quinto site. Freq. (%): frequency of occurrence; Abundance: mean (standard deviation); Feeding guilds: see "Materials and Methods".

Families	Species	Freq. (%)	Abundance m (s.d.)	Feeding guilds
Centracanthidae	*Spicara maena*	100.0	62.2 (88.2)	2
	Spicara smaris	45.5	92.8 (143.2)	2
Gobidae	*Gobius bucchichii*	9.1	0.1 (0.3)	4
Labridae	*Coris julis*	100.0	54.0 (22.3)	3
	Labrus merula	36.4	0.3 (0.6)	5
	Labrus viridis	36.4	0.3 (0.6)	5
	Symphodus cinereus	36.4	0.7 (1.0)	3
	Symphodus doderleini	63.6	0.8 (0.9)	3
	Symphodus mediterraneus	54.5	0.9 (0.7)	3
	Symphodus melanocercus	90.9	1.5 (1.2)	3
	Symphodus ocellatus	100.0	14.2 (18.9)	3
	Symphodus roissali	90.9	1.2 (1.0)	3
	Symphodus rostratus	90.9	2.3 (1.7)	3
	Symphodus tinca	72.7	2.2 (1.7)	3
Mullidae	*Mullus surmuletus*	63.6	0.7 (0.8)	4
Muraenidae	*Muraena helena*	9.1	0.1 (0.3)	5
Pomacentridae	*Chromis chromis*	100.0	326.2 (153.1)	2
Scorpaenidae	*Scorpaena porcus*	9.1	0.1 (0.3)	5
Serranidae	*Serranus cabrilla*	100.0	5.8 (3.5)	5
	Serranus scriba	63.6	1.5 (1.7)	5
Sparidae	*Boops boops*	9.1	22.7 (75.4)	2
	Dentex dentex	18.2	0.1 (0.2)	5
	Diplodus annularis	100.0	2.4 (1.9)	4
	Diplodus sargus	36.4	0.3 (0.5)	4
	Diplodus vulgaris	100.0	5.3 (3.1)	4
	Oblada melanura	18.2	0.1 (0.3)	2
	Pagrus pagrus	27.3	0.4 (0.7)	5
	Spondyliosoma cantharus	18.2	2.2 (5.2)	4
Total abundance: m (s.d.)		**601.4 (244.6)**		
Species richness (n)		**28**		

The most frequent species were *Spicara maena, Chromis chromis, Coris julis, Symphodus ocellatus, Serranus cabrilla, Diplodus annularis* and *D. vulgaris*, which were observed in all samplings, while *Gobius bucchichi, Muraena helena, Scorpaena porcus* and *Boops boops* were the least frequent species.

The abundance of the whole fish population exhibited strong fluctuations, from 174.5 to 1007.0 ind./150 m^2 (mean value = 601.4 ± 244.6) due to the presence of more or less numerous groups of planktivorous and gregarious species. The most abundant species (Tab. 1) were *Chromis chromis, Boops boops, Spicara smaris* and *S. maena*; their pooled abundance data accounted for 83.9 % of the whole censused stock. The most abundant Labrids, *Coris julis* and *Symphodus ocellatus*, accounted for 13.0 % of censused specimens. The least abundant species were *Oblada melanura, Gobius bucchichi, Muraena*

NIVEAU DE PRODUCTION ET RENDEMENT D'UNE LAGUNE MÉDITERRANÉENNE: LE LAC MELLAH (ALGÉRIE)

Par M. Hichem Kara* et Lamya Chaoui
Université d'Annaba
Département de Biologie Marine
BP 230 Oued kouba, Annaba 23003, Algérie

Résumé
Nous analysons ici la production et le rendement d'une lagune du sud de la Méditerranée (le lac Mellah) durant huit années consécutives (1987 à 1994). Pour cela, nous nous sommes basés sur les données statistiques disponibles sur place et jugées fiables. Avec 85 kg/ha/an, ce milieu est classé en cinquième position par rapport aux 14 lagunes nord-africaines, dont le rendement moyen est de 145 kg/ha/an.

Mots clés: fisheries - biomass - brackish water - Algerian basin

Les lagunes sont connues pour leur richesse en sels nutritifs qui favorisent une importante production planctonique. Leur rôle de nurseries pour les juvéniles de poissons marins est reconnu. Issus de pontes marines, ces derniers effectuent des migrations, le plus souvent limitées dans le temps et dans l'espace, et se retrouvent dans un milieu hautement productif. Ils présentent alors des taux de croissance bien supérieurs à ceux de leurs congénères du milieu marin.

Unique du genre en Algérie, la lagune du Mellah occupe une superficie d'environ 865 ha. Située à l'extrême est du pays (8°20'E et 36°54'N), elle est reliée à la mer par un chenal long d'environ 900 m et d'une dizaine de mètres de large. Profonde de 3,5 m en moyenne, ses caractéristiques physico-chimiques, hydrologiques et biologiques, ainsi que les principaux aménagements qu'elle a connus ont fait l'objet d'une récente compilation (1).

La pêche au lac Mellah intéresse principalement 5 familles de poissons: anguillidés, mugilidés, serranidés, sparidés et soléidés. Elle est assurée essentiellement par une bordigue, mais des filets trémail et monomaille sont également employés du fait qu'une partie du peuplement demeure dans le lac. Des nasses de 1 à 2,5 m de long et 0,5 m de diamètre sont aussi utilisées pour la capture des anguilles. Les structures conchylicoles consistent en une soixantaine de tables de mytiliculture (type étang de Thau), dont seul le tiers est en service, couvrant une superficie de 1500 m^2 environ.

Le tableau 1 montre la production du lac entre 1987 et 1994 selon les statistiques locales. Malheureusement, ces dernières ne font pas de distinction entre les différentes espèces d'un même genre (*Mugil* sp, *Diplodus* sp). Malgré cette limite et d'autres lacunes lors du recueil des informations, les chiffres disponibles restent utiles et permettent des références générales correctes. Il apparaît que la contribution des différents groupes et espèces au produit global est différente. Les poissons dominent avec 56 tonnes/an, suivis des mollusques avec 17 tonnes/an. Les premiers sont représentés essentiellement par l'anguille *A. anguilla* (58%) et les différentes espèces de mugilidés (31%); les seconds par la moule *M. galloprovincialis* (61%).

L'évolution du rendement annuel de la lagune entre 1987 et 1994 (fig. 1) montre une nette tendance à la baisse. Cette situation s'explique d'une part par la réduction du nombre de tables conchylicoles fonctionnelles, et, d'autre part, par la mise hors de service d'une partie de la bordigue suite à l'élargissement du chenal. Le rendement annuel moyen pendant cette période est de 85 kg/ha. Ce chiffre est inférieur à la moyenne calculée pour les 14 lagunes nord-africaines et qui atteint 145 kg/ha/an (tab. 2).

Tableau 1 : Production (en kg) de la lagune du Mellah entre 1987 et 1994.

Genres et espèces	1987	1988	1989	1990	1991	1992	1993	1994	P.A.M.E
Crustacés									
P. kerathurus	-	-	206,5	83,5	51,5	4	-	-	43
Poissons									
Solea sp	251,5	158	-	656	1107	70,5	-	191	304
D. labrax	5553	7163	1091	2629	4472	663,5	3194	8779	4193
S. aurata	-	-	-	1838	918	116	4544	2761	1272
Diplodus sp	40	-	65	637	100	-	39	-	110
Mugil sp	30612	24000	8321	11916	18081	4532	27459	15168	17511
A. anguilla	66928	72265	52622	46700	21603	1143	-	-	32657
Mollusques									
M. galloprovincialis	3171	3541	15954	27034	22350	6263	6263	-	10572
V. decussatus	-	-	-	364	120	206	32519	12524	5716
C. gigas	3309	132	105	-	-	-	-	-	443
C. glaucum	-	-	-	-	-	252	240	-	61
Divers	-	-	-	1249	581	3109	3145	2633	1339
Production annuelle	109864	107259	78364	93106	69383	16359	77662	42056	Moyenne: 74256

P.A.M.E: Production annuelle moyenne par espèce

CROISSANCE DU LOUP DICENTRARCHUS LABRAX (L.) DANS LA LAGUNE DU MELLAH (ALGÉRIE)

Par M. Hichem Kara* et Lamya Chaoui
Université d'Annaba Département de Biologie Marine
BP 230 Oued kouba, Annaba 23003, Algérie

Résumé
Cette étude s'intéresse à la croissance linéaire absolue et à la croissance relative du loup *Dicentrarchus labrax* dans la lagune du Mellah. Les femelles grandissent plus vite que les mâles et présentent une allométrie majorante. La comparaison avec la population voisine du Golfe d'Annaba indique une meilleure croissance des individus lagunaires durant la première année uniquement. Ces derniers présentent à taille égale des poids nettement inférieurs.

Mots clés: fishes, population dynamics, brackish water, Algerian basin

Situé à l'extrême Nord-Est de l'Algérie (8°20'E et 36°54'N), le Mellah est une lagune de 865 ha, reliée à la mer par un chenal long d'environ 900m et d'une dizaine de mètres de large. Elle est caractérisée par la présence d'une bordigue qui permet de piéger les espèces euryhalines dans leur phase migratoire. La bordigue n'est pas seulement une structure de capture, mais aussi un instrument qui empêche les poissons de retourner à la mer. La lagune devient alors un milieu pour l'aquaculture extensive.

Espèce migratrice, utilisant les lagunes comme nurseries, *Dicentrarchus labrax* réside en permanence dans la lagune du Mellah du fait de l'existence de la bordigue et s'y reproduit (1). Les répercussions de cet "isolement"sur les modifications morphologiques de l'espèce (2), nous incite à examiner son effet sur sa croissance, par rapport à la population marine voisine du golfe d'Annaba (3).

Pêchés dans la lagune à l'aide de filets fixes (trémail et monomaille), les loups sont examinés frais. La longueur totale et la masse totale de 214 individus (96 mâles et 118 femelles) sont notés. Sur chaque individu, des écailles sont prélevées sous la nageoire pectorale gauche, nettoyées et observées au microscope à faible grossissement (x 35). La longueur totale correspondant à chaque âge est rétrocalculée par la méthode de Lee (4), et, les croissances linéaire et pondérale sont ajustées au modèle de Von Bertalanffy (5). Les paramètres $L\infty$, K et to de ce modèle sont déterminés par la méthode de Ford-Walford (6).

La croissance relative est établie entre la longueur totale (Lt en cm) et la masse totale (Pt en g) selon la relation de Teissier (7) : $Pt = aLt^b$. Le coefficient d'allométrie b est comparé à la valeur 3 au seuil $\alpha = 0,05$. La relation taille-masse porte sur 106 individus (81 mâles et 25 femelles).

Le tableau 1 présente les longueurs totales rétrocalculées jusqu'à l'âge de 7 ans. Les paramètres de croissance obtenus sont donnés dans le tableau 2. La figure 1 montre que la croissance linéaire est très rapide durant la première année. Son taux annuel diminue ensuite progressivement, surtout à partir de la troisième année, en raison probablement de l'acquisition de la première maturité sexuelle. Cependant, à âge égal, les femelles ont toujours une longueur légèrement supérieure à celle des mâles.

Tableau 1 : Longueurs totales rétrocalculées chez *D. labrax* de la lagune du Mellah.

Age	1	2	3	4	5	6	7
Mâles	21,05	30,26	37,91	42,89	48,17	53,39	55,66
Femelles	21,12	30,73	38,45	44,95	50,44	55,08	60,08
Sexes confondus	21,08	30,47	37,96	43,91	49,30	54,23	56,19

La croissance relative est allométrique chez les deux sexes (tab. 2), minorante chez les mâles et majorante chez les femelles, ce qui indique une meilleure croissance pondérale chez ces dernières.

Tableau 2 : Paramètres du modèle de croissance de Von Bertalanffy et corfficients d'allométrie chez *D. labrax* de la lagune du Mellah.

Paramètres	$L\infty$	K	to	Coefficient d'allométrie
Mâles	65,85	0,22	- 0,55	2,64*
Femelles	76,70	0,16	- 0,97	3,37*
Sexes confondus	68,35	0,20	- 0,83	3,15

*différence significative

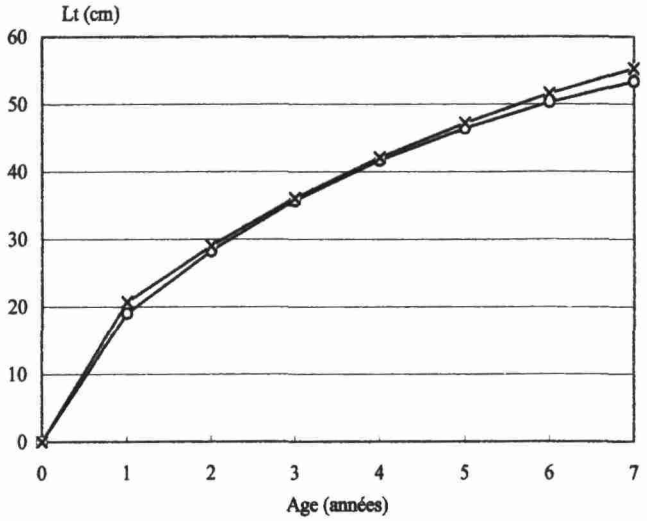

Figure 1 : Croissance linéaire absolue de *Dicentrarchus labrax* (o : mâles, x : femelles) dans la lagune du Mellah.

La figure 2 compare la croissance linéaire absolue de *D. labrax* dans la lagune du Mellah et dans d'autres localités méditerranéennes. Durant la première année, les loups de la lagune présentent la meilleure croissance, ce qui s'explique par une plus grande disponibilité alimentaire dans ce milieu réputé riche en plancton, alimentation de base des jeunes stades. Au-delà, les individus du golfe d'Annaba reprennent l'avantage jusqu'à l'âge de 3 ans. A 4 ans, la population du golfe du Lion bénéficie d'une taille supérieure. Cependant, *D. labrax* des côtes égyptiennes montre un développement nettement plus lent.

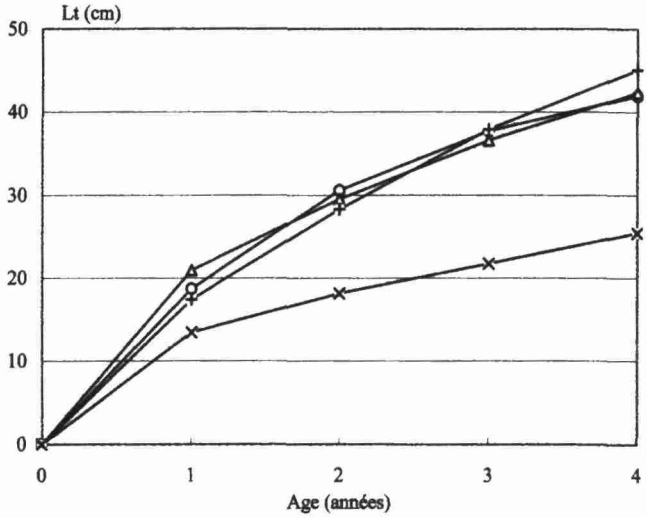

Figure 2 : Croissance linéaire absolue de *Dicentrarchus labrax* (sexes confondus) dans différentes localités méditerranéennes (x : Alexandrie (8); + : golfe du Lion (9); o : golfe d'Annaba (3); Δ : lagune du Mellah).

A MULTIVARIATE PROCEDURE FOR THE DISCRIMINATION OF EUTROPHIC LEVELS IN COASTAL MARINE ECOSYSTEMS

D. Kitsiou & M. Karydis*

Aquatic Ecosystems Laboratory

Dept. of Environmental Studies - University of the Aegean 81100 Mytilene - Greece

Abstract

A methodological procedure for eutrophication assessment at a spatial scale is proposed using numerical classification. The values of five ecological indices (number of species, Menhinick's, Odum's, Margalef's, Evenness) describing the phytoplankton community structure in Saronicos Gulf, Greece were calculated and their horizontal distributions were developed. The simulated data produced were used for the classification of the trophic state of the subareas of the Gulf. A stepwise description of the methodology is given and the advantages of the procedure in coastal studies are discussed.

Key-words: eutrophication, GIS, phytoplankton, bio-indicators, Aegean Sea

Introduction

A number of studies has already been carried out to quantify eutrophication using parameters describing the eutrophic conditions such as nutrient, chlorophyll-*a* concentrations and phytoplankton cell number [1, 2]; in addition the use of ecological indices has been proposed [3, 4] for assessing water quality. However, most of these studies don't consider the spatial distribution of the parameters examined and as a consequence the trophic conditions in coastal areas cannot be clearly discriminated. The parameters that describe eutrophication show different horizontal distributions and therefore, all the information they incorporate has to be taken into account if a general assessment of the eutrophic level of the coastal water body is required.

In the present work, a methodological procedure is proposed for eutrophication assessment at a spatial scale based on the horizontal distributions of five ecological indices (number of species, Menhinick's, Odum's, Margalef's, Evenness) describing phytoplankton community structure. Methods of digital cartography were applied for the development of five thematic maps and the simulated data from these maps were used for classifying the trophic levels by cluster analysis. A case study was performed in Saronicos Gulf, Greece and the different areas of the Gulf were assessed as far as their trophic levels are concerned using the proposed methodological procedure.

Material and methods

Study area and source of data. The present work is concerned with the inner Saronicos Gulf, Greece a relatively shallow basin (maximum depth 100m) which receives sewage effluents from the metropolitan area of Athens. The sources of data have been described in previous publications [5] as well as the study area and the location of the sampling sites [6]. The mean values for each ecological index during the stratification period (April-September) were calculated and are shown in Table 1. The indices used were [7] the number of species (S), the Menhinick's index [$D_{Mn}=S/\sqrt{N}$], the Odum's index [$D_{Od}=(Sx1000)/N$], the Margalef's index [$D_{Mg}=(S-1)/\ln N$] and the Evenness index [$E=H'/H$], where N stands for the phytoplankton cell number (cells/l), H'for the sample diversity and H'_{max} for the maximum sample diversity.

Table 1 : Mean values for the phytoplankton cell number (N) and the ecological indices (S : number of species, D_{Mn}: Menhinick's index, D_{Od}: Odum's index, D_{Mg}: Margalef's index, E:Evenness index) during the stratification period (April-September) in the sampling station.

Samp. Stations	S	N	D_{Mg}	D_{Mn}	D_{Od}	E
1	25	1484919	1.680	0.025	0.02	0.28
2	24	1635705	1.680	0.030	0.06	0.36
3	14	197644	1.095	0.057	0.40	0.46
4	16	302134	1.230	0.045	0.22	0.43
5	20	444945	1.520	0.042	0.13	0.35
6	14	197968	1.130	0.038	0.10	0.36
7	18	347708	1.380	0.043	0.18	0.34
8	18	449577	1.320	0.037	0.11	0.32
9	15	502245	1.140	0.043	0.27	0.29
10	40	$1.4x10^9$	1.900	0.001	0.01	0.28
11	40	$1.15x10^9$	1.900	0.001	0.01	0.28
12	16	117405	1.300	0.060	0.40	0.47
13	15	84490	1.310	0.080	0.66	0.61
14	14	74087	1.150	0.070	0.37	0.59
15	-	-	-	-	-	-
16	-	-	-	-	-	-
17	-	-	-	-	-	-
18	17	1708041	1.340	0.050	0.31	0.49
19	20	214015	1.710	0.080	0.46	0.65
20	14	106238	1.420	0.100	1.05	0.69

Data analysis. The generation of the spatial distributions of the five ecological indices was based on the application of the Inverse Distance Weighted interpolation method [8, 9]. This method was applied on the data of Table 1 with a spatial resolution of 100x100m using the program Arc/Info, version 7.0.2 (ARC/INFO-Environmental Systems Research Institute, Inc). Therefore, the study area was represented by a grid / surface for each one ecological index.

The next step of the methodology developed was the division of the study area into 22 sub-areas, approximately 5x5Km each (Figure 1). For each one of these areas, the median of the simulated values within its boundaries was calculated for each ecological index. Consequently, each area was thereafter characterized by five values representative of the five ecological indices under examination.

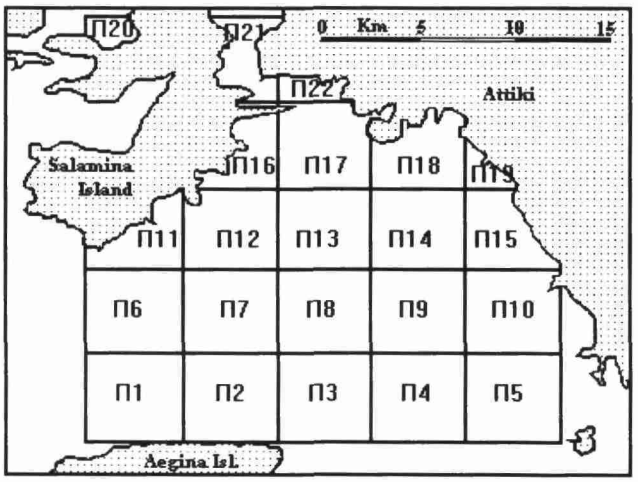

Figure 1 : the 22 areas of Saronicos Gulf

Cluster analysis [10] was applied for the 22 areas and clusters of areas were formed according to the values of the ecological indices. It is noticed here that the Euclidean Distance was used as the dissimilarity index of the analysis [10] and that before the application of the method, standardization of the data was performed [11] due to the different scales that the variables are measured. Subsequently, the non-parametric randomization test (Analysis of Similarities - ANOSIM) was applied for determining whether areas which appear to be in the same clusters, form distinct, significantly different groups [12].

The clusters derived from the ANOSIM method were representative of the existing different eutrophic states in the marine environment and were characterized accordingly as follows. For the areas belonged to each distinct group, the median of their representative values for the phytoplankton cell number (median of the simulated values within their boundaries), was calculated and the obtained values were compared to a eutrophication scale [6] which is given in Table 2. In that way, each distinct group was characterized precisely according to its eutrophic level (eutrophic, upper-mesotrophic, lower-mesotrophic, oligotrophic).

Table 2 : Eutrophication scale based on the phytoplankton cell number (N).

Eutrophication Scale for the phytoplankton cell number (cells/l)			
oligotrophic	lower-mesotrophic	upper-mesotrophic	eutrophic
0	$6x10^3$	$1.5x10^5$	$9.6x10^5$

ANNUAL PRODUCTION OF *ARTEMIA PARTHENOGENETICA* IN A SOLAR SALTWORKS

Tufan Koray

Faculty of Fisheries, Department of Hydrobiology, Bornova, 35100, Izmir, Türkiye

Abstract

Production of *A. parthenogenetica* was estimated using Hynes size-frequency method in a solar saltworks. Annual production of *Artemia* was 13.98 g dw m^{-2} yr^{-1}. Mean annual standing stock biomass was 0.066 g dw m^{-2} . The population was unevenly distributed among instar and adult stages. Linear predictive models such as multiple regression and principal component analyses were evaluated for the practical aim of estimating annual *Artemia* production. The results obtained from the Hynes method were used to highlight the contribution of each instar stage to total production. Production for each size group was estimated by an empirical technique which incorporated ln instar number and total length ($\ln P_j = 1.193(\pm 0.063) \ln n_j + 0.295(\pm 0.123)L_j$). The predictive ability of the model was highly significant ($R^2 = 0.991$, $p<0.05$).

Key-words: crustacea, secondary production, growth, aquaculture

Introduction

The brine shrimp *Artemia* spp. (Crustacea, Anostraca) are found in temporary and permanent hypersaline environments (1). Beside natural saline lakes, salt ponds in which seawater evaporates to produce sodium chloride are also suited to the development of natural populations of brine shrimp (2, 3). The high salinity (80 - 180) of salt ponds often makes this filter-feeding brachiopods the top consumer in ponds lacking vertebrates in a saltern. Yet the role of brine shrimp in the trophic structure of these hypersaline ecosystems has been largely unexplored.

No studies have examined secondary production for *Artemia* in solar saltworks even though they are valuable food supply in for aquaculture species, as well as for flamingos, shelducks, gulls, eared grebes and phalaropes (4, 5, 6). The brine shrimp is a small (total length of adults 1.0-1.3 mm.), euroxybiont and eurysaline filter-feeding herbivorous crustacean that feeds on bacteria and algae in hypersaline environments. The formation of encysted, ametabolic embryos or cysts assures the survival of the species in winter and drought conditions (1).

Artemia parthenogenetica is abundant in the Izmir Çamalti Saltern, Türkiye (7). High rates of production have been reported in previous years (approx. 300 kg dry cysts and/or 500 kg wet-weight ha^{-1}) and this harvest has been used for local aquaculture of sole, red sea bream and sea bass. However, the density of the cysts and adults have decreased dramatically during recent years probably due to overharvesting and bad weather conditions. The objective of the present study is to determine annual biomass production of *A. parthenogenetica* through the use of data on natural populations and laboratory reared *Artemia*. This study is the first to measure annual production of brine shrimp for all instars with size-frequency (Hynes) method in a salt pan.

Methods

The salt pans of Izmir Çamalti saltern are located in the north-eastern part of the bay of Izmir (38° 32'N-26° 57'E). The saltern has a mean depth of 0.5 m. The salt pan in which the experiments were conducted covers an area of 0.2 ha with a mean depth of 0.6 m. Annual temperature range was 2°-32°C in January and July respectively with a mean annual temperature of 16.63±3.05. The salinity in the experimental salt pan ranged from 90-160 in January-September but 170-320 in October-November. No fish lived in the pan because of high salinity. Planktonic rotifers and cladocerans were also absent. Dissolved oxygen in the sub-surface water (0.25 m) ranged from 2.1 mg l^{-1} in March to 6.6 mg l^{-1} in January and varied between 3.1-5.4 mg l^{-1} in other months. The annual mean of dissolved oxygen was 4.27±1.14 mg l^{-1}.

The samples were collected monthly with a plexiglass nansen bottle at ten points located at 50 m intervals between the years 1990-1991. The bottle was lowered to the mud surface. Water with *A. parthenogenetica* individuals was transfered to a 1.5 liter galon with a Masterflex peristaltic pump. For determination of instar density of the brine shrimp a one liter water sample was fixed with 40 % formalin (final concentration 2-4 %) and allowed to settle for 48 hr. The superficial water was decanted with the aid of a siphon and the settled *Artemia* individuals were totally counted and total lengths were measured using a standard microscope.

Brine shrimp eggs from Çamalti Saltern were hatched in the laboratory and newly hatched first instars were reared in two ten liter plexiglass tank to determine instar development time. Instars were maintained at 23±1.0°C on a 16:8 h L/D photoperiod and fed with non-filtered natural experimental salt pan water with yeast solution (1.25 µg l^{-1} dry weight). Every two or three days 25 nauplii were collected and total lengths were measured. *Artemia* were dried at 40°C and weighed with a decimal micro balance to obtain mean individual dry weight and determine biomass. The exponential equation was used to relate the weight to length.

$$M_j = \exp^{a.Lj} \cdot b \,. \qquad \text{(eq.1)}$$

with M_j as weight in µg, L_j as lenght in mm, a and b as the constants. For time-dependent growth, lenght was calculated as sigmoid logistic growth curve

$$L_j = \frac{a}{(1+b \cdot \exp(c \cdot D_j))} \,. \qquad \text{(eq.2)}$$

where a, b and c are contants; L_j, lenght in mm; D_j, duration (8).

The size-frequency method (9, 10) was used to estimate annual production of *A. parthenogenetica* following the calculation of Menzie (11), Krueger and Martin (12) and Runck and Blinn (13).

$$P = (N_j - N_{j+1})(M_j \cdot M_{j+1})^{0.5}. \qquad \text{(eq.3)}$$

P is the annual production, Mj the mean dry weight of size class j, c the number of size classes (j = 1-8), and N_j the number of individuals that developed into size class j during the year. The fifteen instars of *A. parthenogenetica* were morphologically distinct based on total lenght and were used as eight size classes in the production calculation: instar 1 to 3, below 1000 mm.; instar 4, 1000-1500 mm.; instar 5, 1500-2000 mm.; instar 6, 2000-2500 mm., instar 7, 2500-3500 mm., instar 8, 3500-5000 mm., instar 9 to 11, 5000-7000 mm., instar 12 and up 7000< mm. (14). Because the duration of each instar was unequal, P_e/P_a correction was used, where P_e is the estimated proportion of the life cycle spent in each size class (e.g. 1/c), and P_a is the actual proportion of the life cycle spent in a particular size class (9, 11, 13). The duration of the instars were estimated from rearrangement of eq. 2, D_j was derived:

$$D_j = (1/c) \{\ln [(a-Lj)/(L_j.b)]\} \cdot \qquad \text{(eq.4)}$$

D_j were used to estimate P_a for each instar.

The annual cohort production interval (CPI) which is the time from hatching to the attainment of the largest aquatic size class was estimated from laboratory rearing data as 30 days. Nj was estimated by

$$N_j = n_j (P_e/P_a)(GP/CPI)(c) \cdot \qquad \text{(eq.5)}$$

Growth period (GP) is the number of days during the year over which production estimated and except the period between 1 January - 15 April in which *A. partenogenetica* diapouse has been occurred, GP is 260 days.

The empirical approach that was used to determine the rate of changes between total annual production and production of each instar stages was a principal component analysis with standardized data as the independent variables. Standardizations of the original dependent and independent variables were required to stabilize the variance (8, 14). For predictive purposes, yearly productivity of each instar stage was calculated from the length and instar numbers:

$$\ln P_j = a L_j + b \ln n_j \cdot \qquad \text{(eq.6)}$$

with P_j, L_j and n_j as above, a and b as constants. The total annual production was then predicted as:

$$\sum \ln P_j = \sum (a L_j + b \ln n_j) \cdot \qquad \text{(eq.7)}$$

Results

Annual production for *A. parthenogenetica* calculated by the size frequency method was 13.98 (±1.27) g dw m^{-2} yr^{-1} ($p<0.05$). Mean annual standing stock biomass of *A. parthenogenetica* was 0.066 g dw m^{-2} and was unevenly distributed among all instar and adult stages. On the basis of the area of the salt pan (2500 m^2), the total annual production by *A. parthenogenetica* was 34.95 kg dw yr^{-1}. The average density was 4552 animals m^{-2} (SE=525, n=140) during the whole sampling period. The brine shrimp was multivoltine (cohort=20.35) in the Çamalti saltern.The density of *A. parthenogenetica* was lowest (zero) between January and early April due to diapause, peaked in early May (13783 animals m^{-2}), declined through July, peaked again in September (6457 animals m^{-2}) and declined gradually through the remainder of the year. First instars (ins. 1-3) made up an average of 57.34 % of the *A. parthenogenetica* population during 1990-91. Fourth instars made up 23.09 %, fifth instars 9.05 %, sixth instars 7.09 %, seventh instars 1.90 %, eighth instars 0.44 %, nineth-eleventh instars 0.67 % and adults 0.42 % of the population. First six instars were the most commonly encountered stages and were abundantly collected on each sample dates. Adults were uncommon but were collected on all sampling periods except early May in which the first increase in the abundance of first instars began.

APPLICATION DE LA TELEDETECTION ET DES SYSTEMES D'INFORMATION GEOGRAPHIQUE A LA DETERMINATION DES SITES AQUACOLES

A. Lamrini* et A. Moustatir

Institut Agronomique et Vétérinaire Hassan II
Département HIDAOA. B.P 6202. Rabat- Instituts, Maroc

Résumé

Le principal objectif de cette étude est de justifier que l'utilisation de la télédétection spaciale et des systèmes d'information géographique (SIG) permet de déterminer les zones à potentiel aquacole sur la côte marocaine. La lagune de Nador, connue par son potentiel aquacole confirmé, a été utilisée comme site pilote d'application. L'imagerie satellitaire SPOT s'est avérée d'une grande utilité pour caractériser la répartition des matières en suspension et cartographier la bathymétrie de la lagune. Par ailleurs, les critères retenus pour le choix du site et ayant fait l'objet des couches d'informations dans un SIG sont la profondeur, la turbidité, la salinité, l'oxygène dissous, les phospates et les nitrates. A l'issue des croisements des couches d'informations, on constate qu'effectivement, la surface exploitée actuellement en aquaculture se trouve bien au sein de l'étendu reconnue comme zone à potentiel aquacole.

Mots clés : remote sensing, GIS, aquaculture, Western Mediterranean

Introduction

Le Maroc dispose d'une longue façade maritime sur laquelle les sites aquacoles potentiels sont plus ou moins bien connus. L'identification de tels sites par les méthodes classiques nécessitera des travaux très importants et honéreux. L'utilisation de la télédétection et des systèmes d'information géographique (SIG) permet d'arriver au même résultat très rapidement et à moindre coût ; la première application a démarré en 1987 (1). Cependant, bien que l'application conjointe de l'imagerie satellitaire et des SIG ait été raffinée dans plusieurs régions du globe, une mise en garde a été portée sur les méthodes d'analyse parce qu'elles ne sont pas intégralement exploitables et doivent être adaptées aux conditions locales. La lagune de Nador, domaine aquacole bien confirmé, a été choisie en tant que site pilote d'application.

Caracteristiques du site aquacole

Pour choisir judicieusement un site, il est nécessaire de présenter les limites optimales des différents paramètres permettant de juger de sa convenance. Par la suite, il faut examiner les conditions réelles du site d'étude. La lagune de Nador est située sur le littoral méditerranéen au Nord- Est du Maroc. D'une superficie de 11500 hectares, elle communique avec la mer par une seule passe et possède une forme allongée Nord-Ouest, Sud-Est.

A l'intérieur de la lagune, les courants circulent essentiellement le long des rives délimitant une masse d'eau centrale dont les caractéristiques et les mouvements sont stables (2,3). La profondeur ne dépasse pas 8 m, elle augmente vers la direction du centre.

La bordure continentale est formée d'une bande de sable terrigène. Les rives internes sont constituées de sable fin, et l'ensemble de la partie centrale est tapissé d'un sable vaseux. En outre, les produits d'érosion de la rive sud et les apports terrigènes provoquent une turbidité accentuée le long de cette rive.

S'agissant des paramètres physico-chimiques, l'analyse de leur évolution dans le temps et dans l'espace révèle des variations très significatives. Les fonds sont recouverts d'herbiers thalassiques mixtes (4).

Application de la télédétection

Les satellites offrent une vue globale et répetitive de la mer et des lagunes. Cependant, l'information apportée est d'interprétation délicate. D'une part, les capteurs ne mesurent pas directement les paramètres océaniques mais seulement des luminances de surface qui doivent être corrigées et transformées et d'autre part, le rayonnement électromagnétique ne peut pas fournir d'information directe sur l'état interne de l'eau.

L'étude de la lagune de Nador devrait donc combiner des données spatiales, des données de terrain et une modélisation des phénomènes. Le choix de l'image satellitaire spot s'est basé sur le fait qu'elle permet une étude spatiale plus fine avec son capteur HRV. les canaux XS1 et XS2, opérant dans le visible, ont permis d'extraire quelques informations sur les matières en suspension et la bathymétrie de la lagune.

Matières en suspension

La détermination de ce paramètre a été réalisée à l'aide d'un modèle linéaire qui suppose la correlation entre les valeurs radiomètriques des canaux XS1 et XS2 et les concentrations des MES.

En présence de matières minerales en suspension (indice s), de phytoplancton et derivés (c)et de matières organiques (y) dans l'eau (w), et en notant bx et ax les coefficients de rétrodiffusion et d'absorption spécifiques de l'élement x, cx sa concentration, la réflectance marine sous la surface s'écrit (5) :

$R = \alpha\ (bw + bs.cs + bc.\ cc + by.cy) / (aw + as.\ cs + ac.\ cc + ay\ cy)$

α = constante

Avec l'hypothèse que les matières en suspension sont non absorbantes et plus rétrodiffusantes que le phytoplancton et les matières organiques, la réflectance devient :

$R = \alpha\ (bw + bs.\ cx) / (aw + ac\ .\ cc + ay.\ cy)$

Si l'on considère que la composition en phytoplanction et matières organiques varie très peu dans la zone considérée, en un point x :

$R\ (\mu, x) = A\ (\mu) + Bs\ (\mu).\ Cs\ (\mu)$ μ = longueur d'onde.

Cette bande s'intègre sur chaque bande spectrale et devient :

$R\ (X\ si, X) = Ai + Bi.\ Cs\ (X)$ i = 1,2

Dans chaque canal X Si, cette équation linéaire se cale en deux points [R (X Si), Cs]. On suppose qu'au large R = O et Cs = Omg/l. Les mesures insitu de concentrations de matières en suspension ont permis d'attribuer à un point Xo, de réflectance RXo (Xsi), la valeur C (Xo) en mg/l. De ce calage on déduit :

$C\ X\ si = [R\ (X\ si).\ C\ (Xo)] / R\ Xo\ (X\ si)$

En faisant l'hypothèse que les R (X si) et les radiométries sont très correlées, on peut substituer les valeurs de réflectance par les valeurs radiométriques.

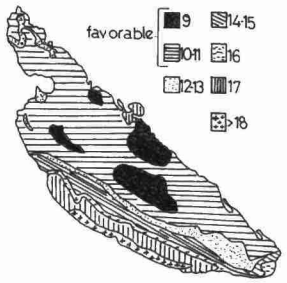

Figure 1 : Résultat du modèle des matières en suspension (mg/l).

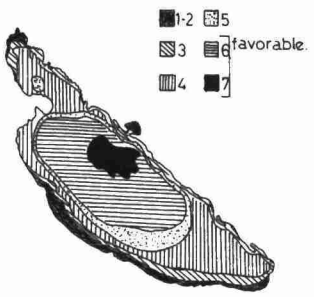

Figure 2 : Résultat du modèle bathymétrique en mètres.

En faisant la moyenne des valeurs trouvées dans les deux canaux, les images traitées ont des pixels qui ne sont plus représentés par radiométrie mais plutôt par une charge de matières en suspension ce qui a permis de caractériser les différentes zones de la lagune et de mettre en évidence des situations différentes au niveau de l'image traitée (Fig 2). Ce résultat a été confirmé par les mesures de terrains réalisées pendant la même période.

Bathymetrie

Le modèle adopté (logarithmique) suppose une correspondance des valeurs radiomètriques des canaux X S1 et X S2 avec la profondeur réelle.

Ainsi plusieurs points de calage ont été relevés. Les couples « radiométrie mesurée - bathymétrie réelle » servent au calcul des coefficients A, B et C de l'équation de modélisation (6).

$Z = A\ .\ \ln (R_1 - R_1\ inf) + B \ln (R_2 - R_2\ inf) + C$

Z = profondeur 1,2 = indices des canaux X S1 et X S2

R = radiométrie Rinf = radiométrie infinie sur les grands fonds.

L'application de cette équation sur l'image a donné des résultats à très grande marge d'erreurs, ce qui amène à effectuer une compensation (méthode des moindres carrés), l'équation obtenue s'écrit :

ÉTUDE PRÉLIMINAIRE DE LA STRUCTURE DE TROIS POPULATIONS DE MOULES *MYTILUS GALLOPROVINCIALIS* LMK. SUR LA CÔTE EST DE LA BAIE DE THESSALONIKI

S. Le Breton , C.C. Chintiroglou*

Aristotle University of Thessaloniki, School of Biology, Dept Zoology, Box 134
54006 Thessalonoki (Macedonia) Greece

Résumé

Mytilus galloprovincialis est depuis longtemps une espèce de bivalve cultivée en Méditerranée, de grand intérêt économique et scientifique. Ce document montre les résultats préliminaires sur les structures de population de 3 moulières naturelles sur substrat artificiel sur la côte Est de la baie de Thessaloniki. De facon générale, les résultats montrent l'existence d'une cohorte de moules de taille moyenne en hiver et de deux cohortes au mois d'août : une de moules de petite taille et une très peu représentée de moules de grande taille. Au mois de septembre, la cohorte des grands individus a disparu. Les comparaisons de la longueur moyenne des moules entre les sites montrent des différences significatives dans le temps et dans l'espace. Les trois sites étudiés de la baie de Thessaloniki supportent néanmoins d'importantes populations de moules *Mytilus galloprovincialis* et présentent certaines ressemblances avec d'autres populations du bassin méditerranéen.

Abstract

Mytilus galloprovincialis *has been for a long time an intensively cultivated bivalve species in Mediterranean Sea of considerable economic and scientific interest. The present paper provides preliminary results on the structure of three natural mussel beds on the eastern coast of Thessaloniki bay. Generally, it has been shown the existence of one cohort of middle-size individuals in winter and two cohorts in August one of small-size mussels, and one, present in very low proportion, of big individuals. In September, the cohort of big individuals has disappeared. A statistical comparison of the mean mussel length shows significant differences both in time and space. Nevertheless, the eastern areas of Thessaloniki bay sustain well established mussel populations of* Mytilus galloprovincialis *which are relatively similar to those of other regions in the Mediterranean Sea.*

Mots clés : Bivalves, Aegean sea, Population dynamics, Rocky shores, Zoobenthos

Introduction

De nombreuses études ont été réalisées dans l'ouest de la Méditerranée et en Adriatique concernant *Mytilus galloprovincialis* (1,2,3,4). Cependant, les connaissances de l'écologie de cette espèce en mer Egée sont assez restreintes et limitées à quelques travaux (5, 6, 7). Pourtant, *Mytilus galloprovincialis* a été cultivée de facon intensive depuis longtemps en Grèce et surtout dans le nord-ouest du golfe de Thermaikos où la production annuelle est d'environ 14.000 tonnes (6, 7). Le but de notre étude, l'analyse des structures des populations naturelles de moules sur substrat artificiel, devrait permettre d'apprécier la dynamique de cette espèce dans les sites sélectionnés.

Matériels et méthodes

La zone d'étude se situe à l'est de la baie de Théssalonique, et est divisée en trois sites : Perea Skala, Neoi Epivates Skala et Agia Triada Skala (Fig 1). Ceux-ci ont été choisis pour deux raisons : Tout d'abord, ce sont les seuls substrats artificiels (digues en béton) où se trouvent des populations importantes de *Mytilus galloprovincialis*. Ensuite, ces localités sont les moins polluées de la baie (8, 9, 10).

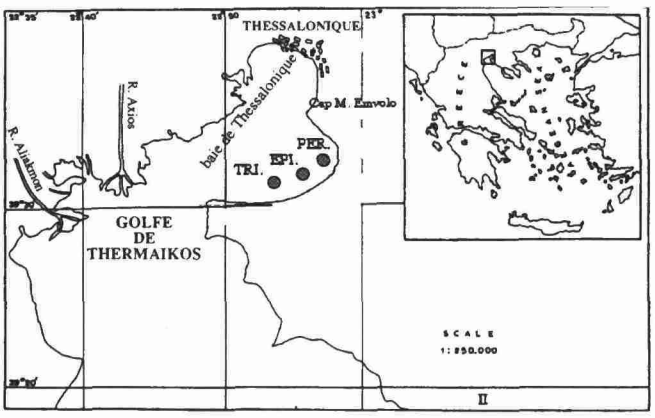

Figure 1 : Localisation des sites de prélèvements dans la baie de Théssaloniki (PER = Perea Skala, EPI = Neoi Epivates Skala et TRI = Agia Triada Skala).

Les prélèvements, réalisés en plongée, ont été effectués en utilisant des quadrats de 20 x 20 cm, soit 400 cm^2, ce qui représente la surface minimale nécessaire pour une étude dynamique en substrat dur (10). L'échantillonnage a été réalisé sur une base bi-saisonnière (hiver, été) en 1994 et 1995, et pour chaque site, 5 réplicats étaient collectés (surface totale de 2000 cm^2 par saison et par site) . Les individus récoltés ont été conservés dans une solution de formol à 10%.

Des mesures des paramètres physico-chimiques (température, salinité, conductivité et PH) ont également été effectuées chaque mois en 1994 et lors des prélèvements en 1995.

Pour chaque individu récolté, La longueur (L), (en millimètres ± 1mm près), a été mesurée. Seules les moules de longueur supérieure à 5 mm ont été utilisées lors des analyses. La répartition des moules suivant la longueur a été analysée dans chaque site et à chaque saison à l'aide de logiciels informatiques et par la méthode de (11) et des comparaisons entre les sites effectuées par des ANOVA à un et deux facteurs suivis de tests de Fisher PLSD.

Résultats

A. Facteurs abiotiques

Aucune variation n'a été observée entre les sites pour la plupart des paramètres physico-chimiques mesurés. La température en hiver a une valeur moyenne de 11± 0,9°C et en été 24,5 ± 3,8°C. La conductivité varie de 52,5 ± 0,4 mS/cm en hiver à 49,9 ± 0,1 mS/cm en été et la salinité de 38,0 ± 0,3 ‰ à 36,9 ± 0,3 ‰. Les valeurs de PH se situent entre 8 et 8,7. Ces valeurs ne diffèrent pas de celles notées par Zarkanellas *et al.* (8) et Koukouras *et al.* (9).

B. Distribution suivant la longueur

L'analyse des histogrammes de taille (Fig 2 et 3) par la méthode de Harding (11) a permis d'identifier les différentes cohortes.

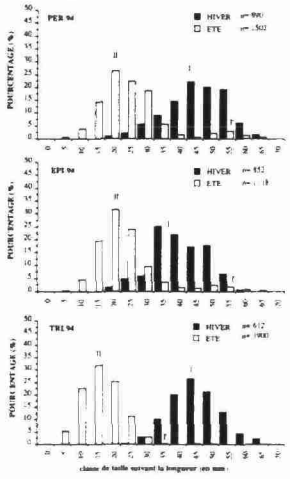

Figure 2 : Distribution (en %) des populations de moules *Mytilus galloprovincialis* par classe de taille (en mm) dans les trois stations de la baie de Thessalonique. Année 1994.

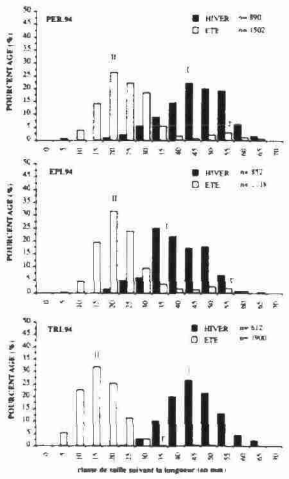

Figure 3 : Distribution (en %) des populations de moules *Mytilus galloprovincialis* par classe de taille (en mm) dans les trois stations de la baie de Thessalonique. Année 1995.

En hiver 94 et 95, une seule cohorte a été mise en évidence dans chaque site, composée de moules de grande taille dont le mode est compris entre 35 et 55 mm, excepté à Neoi Epivates en 94, où deux cohortes ont été identifiées, l'une ayant un mode entre 35 et 40 mm, l'autre ayant un mode entre 50 et 55 mm. De plus, des milliers d'individus (non dénombrés), de taille

ACCIDENT DU *FENES* : ASPECTS BACTERIOLOGIQUES ET CHIMIQUES DE LA FERMENTATION DU BLE EN MILIEU MARIN

M. Marchand [1] *, P. Le Guerroue [1], E. Jacq [2] & B. Fily [2]

[1] Cedre. Technopôle Brest-Iroise, BP 72, 29280 Plouzane, France

[2] MICROMER. Technopôle Brest-Iroise, Site du Vernis, rue Charles Cadiou, 29200 Brest, France

Résumé

Le 25 septembre 1996, le céréalier "Fenes", transportant 2 650 tonnes de blé s'échouait au sud des îles Lavezzi dans les Bouches de Bonifacio (Corse). La semaine qui suivit l'accident, une forte tempête détériorait les cales et occasionnait le déversement de la totalité de la cargaison de blé par des fonds de 10 à 20 mètres sur une surface d'environ un hectare. Les effets immédiats du blé sur les herbiers de posidonies se traduisirent par des mortalités par étouffement. Un autre problème, minimisé au départ, fut celui de la fermentation du blé et de ses effets indésirables. L'apport de matière organique, représentée par la masse de blé, a favorisé très rapidement le développement d'une microflore anaérobie sulfato-réductrice qui fut à l'origine d'une forte production d'hydrogène sulfuré à partir de la réduction des sulfates de l'eau de mer. L'hydrogène sulfuré est un gaz chimiquement réactif et fortement toxique pour les plantes, les animaux et les hommes. Cette étude permet de suivre les aspects bactériologiques de cette pollution et ses conséquences chimiques pouvant avoir un impact non négligeable autour de la zone d'échouage.

Mots-clés : pollution, Strait of Bonifacio

Accident du Fenes

Le 25 septembre 1996, le cargo panaméen *Fenes*, transportant 2 650 tonnes de blé à destination de l'Albanie, s'échouait sur des rochers dans les Bouches de Bonifacio, au Sud de la Corse. Le lieu de l'échouement, l'île Lavezzi, est un milieu écologique sensible, classé réserve naturelle des Lavezzi (Figure 1). Le site se caractérise par l'existence d'herbiers de posidonies (*Posidonia Oceanica*), espèce protégée en France et de

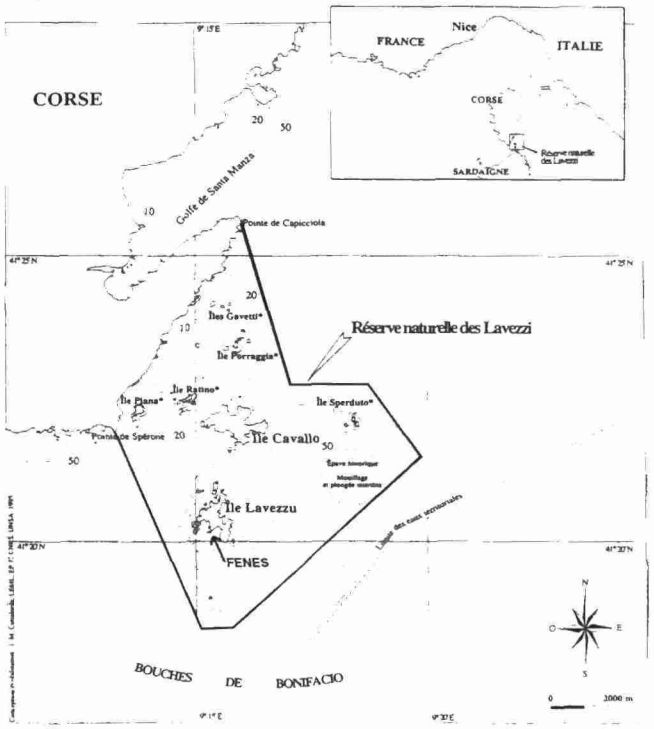

Figure 1 - Zone d'échouage du céréalier Fenes dans les Bouches de Bonifacio.

manière plus générale par les pays signataires de la Convention de Barcelone.

Immédiatement après l'accident, les autorités françaises mettent en demeure le commandant du navire de faire cesser le danger de pollution représenté par le navire et sa cargaison [1]. Le 20 octobre, suite à la dislocation progressive du navire, la totalité de la cargaison repose sur les fonds marins, couvrant une surface estimée à plus d'un hectare autour de l'épave. L'épaisseur de la couche de blé est comprise entre 50 cm et 2 m. Les tempêtes d'automne amplifient l'impact du blé sur de plus grandes surfaces (5 à 6 hectares) et trois zones de concentration de blé sont identifiées autour de l'épave. Les travaux de pompage du blé débutent le 4 décembre à l'aide d'une pompe (1 200 m^3/h). Le blé est égoutté et stocké sur une barge, puis immergé à nouveau en mer par des fonds supérieurs à 300 m.

Très rapidement, les plongeurs évoluant sur le site observent une attaque superficielle de leurs ceintures de plongée et le personnel travaillant sur la barge est sujet à des nausées, vomissements et irritations, provenant de fortes émanations d'hydrogène sulfuré (H_2S) liées à la fermentation du blé. Les teneurs d'hydrogène sulfuré mesurées dans l'air ambiant sont suffisamment fortes (jusqu'à 20 ppm) pour décider les autorités à suspendre provisoirement les travaux de récupération du blé qui reprendront fin décembre et se termineront définitivement le 13 janvier 1997. Les épaisseurs résiduelles de blé sont inférieures à 40 cm et il est admis que le pourcentage de blé évacué est supérieur aux deux tiers de la cargaison du Fénes.

L'impact écologique immédiat d'un tel déversement s'est traduit par un recouvrement des peuplements d'algues (*Cystoseria balearica*) et de phanérogames (*Posidonia oceanica*) localisés sur un à deux hectares [2]. Le second point concerne les aspects liés à la dégradation bactérienne du blé en milieu marin. Nous présentons les résultats des deux premières campagnes de prélèvements bactériologiques et chimiques réalisées sur le site du naufrage du *Fenes*.

Matériel et méthodes

Au cours de la première mission (décembre 1996), les échantillons étaient prélevés sur la barge de récupération et sur deux points (A et B) d'une zone d'accumulation de blé : quatre échantillons de blé, quatre eaux interstitielles prélevés à -10 et -20 cm dans la masse de blé, deux échantillons d'eau prélevés à l'interface avec la masse de blé et deux échantillons d'eau d'égouttage du blé récupéré sur la barge. L'échantillonnage de la seconde mission (mai 1996) était réalisé sur deux stations A et B, localisées sur la même zone d'accumulation du blé : échantillons de blé, de sédiment et d'eaux (eaux interstitielles, eaux d'interface mer/blé, eaux à + 0,2 et + 1,0 m au-dessus de la masse de blé) (Figure 2).

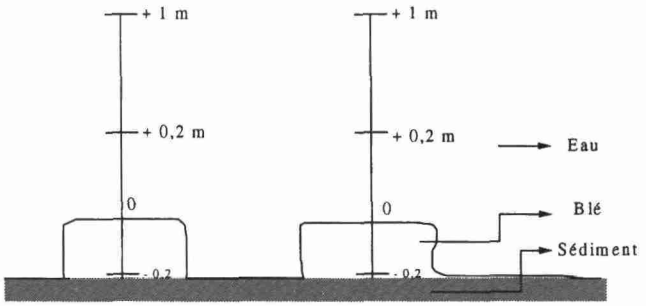

Figure 2 - Schéma des prélèvements sur la zone I d'accumulation du blé.

Les analyses chimiques, réalisées sur les échantillons d'eaux, ont porté sur les paramètres suivants : pH, oxygène dissous (O_2) et hydrogène sulfuré (H_2S). L'oxygène dissous est dosé selon la méthode de Winkler [3]. Le dosage de l'hydrogène sulfuré est réalisé par méthode colorimétrique après complexation des sulfures avec le diméthyl-phénylenediamine [4]. Les mesures de pH sont effectuées à l'aide d'un pHmètre équipé d'une électrode de verre et d'une électrode de référence au Calomel (Ag/AgCl).

Pour les analyses bactériologiques, les échantillons sont récoltés dans des flacons à plasma hermétiques, stérilisés et dégazés sous N_2/CO_2 (80:20) pour ceux destinés aux dénombrements des bactéries anaérobies. Les milieux Marine Agar et PCA sont utilisés respectivement pour le dénombrement des bactéries hétérotrophes capables de se développer sous différentes conditions de salinité. Les dénombrements des bactéries sulfato-réductrices (BSR) sont réalisés sur deux milieux de culture : les milieux LAYE [5] et Widdel [6] qui ont pour donneurs d'électrons l'acétate et/ou le lactate et comme accepteur d'électrons le sulfate. L'analyse de la répartition des différents groupes de BSR a été abordée par des dénombrements

BIOMASS PARTITIONING IN ADRIATIC SEAGRASS ECOSYSTEMS (*POSIDONIA OCEANICA, CYMODOCEA NODOSA, ZOSTERA MARINA*)

Mazzella L.[1], P. Guidetti[1*], M. Lorenti[1], M.C. Buia[1], V. Zupo[1], M.B. Scipione[1], A. Rismondo[2], D. Curiel[2]

[1] Laboratorio di Ecologia del Benthos, Stazione Zoologica "A. Dohrn" di Napoli, P.ta S. Pietro I-80077, Ischia Porto, Napoli, Italy

[2] Dipartimento di Biologia, Università di Padova, Via Trieste 75, 35121 Padova, Italy

Abstract

Biomass measurements of different plant compartments and associated flora and fauna (epiphytic and vagile invertebrates) were conducted on *Posidonia oceanica*, *Cymodocea nodosa* and *Zostera marina*. Samples were collected in February 1997 in two different areas (Otranto and Grado) located in Southern and Northern Adriatic, respectively. *P. oceanica* shows the highest total biomass, due in particular to scales, leaves and living rhizomes, while in *C. nodosa*, living rhizomes and roots dominate other components. In *Z. marina* dead rhizomes and roots account for up to 50 % of overall biomass. Highest values of total biomass of epiphytes have been observed in *C. nodosa*, while *Z. marina* shows highest biomass and numerical abundance of associated vagile invertebrates.

Key-words: biomass, phanerogams, coastal systems, Adriatic Sea

Introduction

The paramount importance of seagrass ecosystems for the coastal waters dynamic and functioning has been largely described for several seas (1). For the Mediterranean Sea, and in particular for the Adriatic Sea, early studies testify their importance for the coastal environments (2; 3). Interestingly, in the Adriatic Sea all five species recorded for the Mediterranean are present. These species colonize different coastlines and type of substrata or habitats, according to their life requirements and adaptation to the marine and/or lagoon environment (4; 5). In particular, *Posidonia oceanica* (L.) Delile is mainly present along the open coasts in Southern and North-Eastern Adriatic (6; 7), while *Cymodocea nodosa* (Ucria) Ascherson and *Zostera noltii* Hornem. are more evenly distributed and *Z. marina* (L.) is confined to the North (5). In the frame of the general decay of environmental quality in the Adriatic Sea, recent investigations demonstrate a massive regression of seagrass meadows in northern Adriatic (8; 9; 10).

In a framework of a large national Italian programme (PRISMA) aimed at understanding the dynamical processes at various scales and the evolution of biotic communities in the Adriatic Sea, a project finalized to investigate biomass partitioning and nutrient stocks and fluxes in some seagrass species and their ecosystems took start. In the present paper, first results are reported pertaining to biomass partitioning in three species, *Posidonia oceanica*, *Cymodocea nodosa* and *Zostera marina*, which have different architecture and differently influence the local environment by amplifying the substrate through their leaf canopy development and affecting the biodiversity of associated communities.

Materials and methods

Marine phanerogams were sampled in February 1997 by SCUBA diving or snorkelling, dependent on depth, in two different areas located in the South and North of the Adriatic Sea, namely Otranto (Lecce) for *P. oceanica* and Grado (Gorizia) for *C. nodosa* and *Z. marina*.

The *P. oceanica* meadow at Otranto was located at 6.5 m depth on a coarse sand bottom. Water temperature, during the sampling campaign, was about 11.8 °C and salinity was recorded as 38 ‰. Both *C. nodosa* and *Z. marina* were settled outside the eastern portion of the Lagoon of Grado, on a pelitic sand bottom at 1.2 and 0.5 m depth, respectively; water temperature was 8.9 °C and salinity 34% near the *C. nodosa* meadow, while *Z. marina* sampling site was characterized by a temperature of 8.8 °C and a salinity of 30 ‰.

Shoot density was measured in situ within 30 x 30 cm quadrats for *P. oceanica* (2 replicates) and *Z. marina* (10 replicates), and 20 x 20 cm quadrats (10 replicates) for *C. nodosa*. For each species, a total of 20 shoots were collected and examined for the phenological analysis, taking into account the number of leaves per shoot, leaf length, leaf width, brown tissue and the percentage of broken apex. Leaf Area Index (LAI) was determined by multiplying the mean leaf surface per shoot by the meadow shoot density.

Biomass was sampled by removing a clod within a quadrat 30 x 30 cm for *P. oceanica* (2 replicates) and by means of corers of 23.6 cm diameter (5 replicates) for the other above mentioned seagrasses. In order to determine dry weight, expressed as g x m^{-2} (mean ± s.d.), plant material was rinsed after sieving to remove sediment. The aboveground portion was subdivided into leaf blades, living sheaths, scales persisting on the rhizomes (only for *P. oceanica*), brown tissue, and separated from living roots, dead roots, living rhizomes, dead rhizomes and detritus. Biomass of algal epiphytes and sessile invertebrates, epiphytic on the leaves, was also estimated. For this purpose, the leaf surface was gently scraped with a razor blade following a treatment in 2% acetic acid for 1 hour. Subsequently, the various components were dried at 60 C° for 48 hours. At each sampling site, vagile fauna was collected by means of a "suction sampler" operated over a surface of 1 m^2, according to Russo *et al.* (11), sorted into the main taxa and lyophilized.

Results

The three meadows show different structure, with *C. nodosa* accounting for the highest values of density and *Z. marina* for the lowest; on the other hand, *P. oceanica* is responsible for the highest LAI (Tab. 1). Leaf length in the sampling period is highest in *Z. marina*, followed by *P. oceanica*, this latter showing a leaf width rarely exceeding 0.8 cm and the highest percentage of eroded apices (Tab.1).

Table 1 : Shoot density and phenological characteristics of the three investigated species.

Parameter	*P. oceanica*	*C. nodosa*	*Z. marina*
n° shoot / m^2	483.5 ± 7.8	977.5 ± 158.3	277.8 ± 44.6
leaf area index (m^2 / m^2)	2.72	0.43	1.26
n° leaves per shoot	7.2 ± 1.2	3.3 ± 0.7	5.6 ± 1.0
mean leaf lenght (cm)	12.4 ± 10.5	7.4 ± 7.3	21.3 ± 19.7
mean leaf width (cm)	0.63 ± 0.23	0.18 ± 0.05	0.38 ± 0.12
broken apex (%)	40.6	29.8	23.2

Three different figures are obtained when biomass partitioning in the three species is considered. *P. oceanica* accounts for the highest total biomass, with a striking difference in comparison to the other species (Fig. 1). Leaf scales, persisting on the rhizomes, and living rhizomes are responsible for the 73.1% of the total biomass, followed by leaves which represent the 19.0%, while living roots give a lower contribution (5.7%) to the total biomass (Fig. 1). In *C. nodosa* living rhizomes and roots account for the 85.7%, while, in *Z. marina*, dead rhizomes and roots account for 57.8% and leaves for 27.4% of the total plant biomass (Fig. 1).

Different results among the three species are also obtained when comparing the biomass of associated communities (Fig. 2). In this case, *C. nodosa* accounts for the highest biomass, imputable to algal epiphytes, which however, are represented by microalgae (Diatoms) in mucilage tubes and by entrapped sediment and in a lesser extent by some macroalgae. In *P. oceanica* equal importance of algal epiphytes (encrusting algae) and sessile invertebrates (Hydroida, Bryozoa and

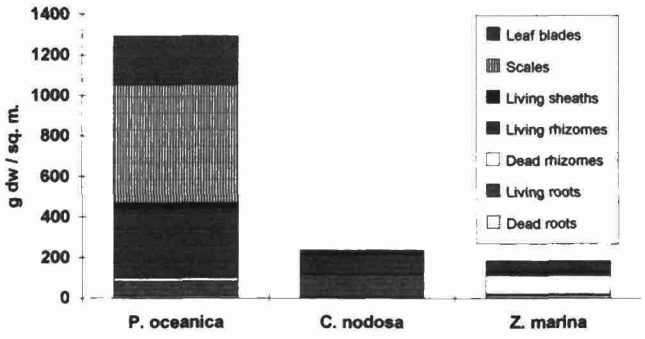

Fig. 1 - Biomass of different plant compartments of the three seagrass species.

EUTROPHICATION AND MACROPHYTES IN THE GULF OF THESSALONIKI, GREECE THE BIOTOPE OF AGIA TRIADA

Orfanidis S.[1], Lazaridou E.[2], Seferlis M.[3] & Haritonidis S.[3]*

[1] Fisheries Research Institute, 64007 N. Peramos, Kavala, Greece
[2] Greek Biotope-Wetland Centre, 57001 Thermi, Thessaloniki, Greece
[3] Botanical Institute, Aristotle University of Thessaloniki, 54006 Thessaloniki, Greece

Abstract

Seasonal variation of key eutrophication and benthic community features have been studied on a shallow area at Agia Triada, Gulf of Thessaloniki, Greece, between April 1994 and April 1995. By using cluster and multidimensional scaling analysis (MDA), two main communities, one dominated by *Ulva rigida* and the other by *Enteromorpha intestinalis* have been identified in the biotope. Seasonal trends of nitrogen and phosphorus concentrations in the water suggest the dependence of nitrogen upon biomass density. The N/P atomic ratios in the water and in algal tissue have been used to estimate the nutritional state of the studied biotope.

Key-words: Aegean Sea, coastal waters, phytobenthos, nutrients

Introduction

Efflux of municipal sewage, industrial waste water and run off from agriculture development into shallow and closed marine baseness lead to an increase of primary production as a consequence of an extended increase of macrophytic communities dominated by green algae of the genera *Ulva* and *Enteromorpha*. Field (1) and laboratory experiments (2) indicate that the increase of biomass of these genera is directly related to nutrients concentrations, mainly nitrogen and phosphorus. However, as these nutrients are often supplied in pulses, N/P ratio is constantly altered depending on both pulse and uptake rate. The discussion concerning the role of N/P ratio as a control factor of the community structure and thus as limiting factor of primary production is still open and controversial (2,3).

The present study was realized within the framework of the joint research programme "Eutrophication and Macrophytes" (EUMAC). The results presented concern the effects of eutrophication on the benthic macrophytic communities in the Ag. Triada biotope, Gulf of Thessaloniki.

Study area

The Gulf of Thessaloniki is situated in the northeast of the Aegean Sea (Fig. 1) comprising a shallow (maximum depth 28m) and confined basin of 165km^2 surface area. The study area of Ag. Triada extends for 3 km along the south east coast of the gulf. The seabed is mainly sandy with scattered stones and rock where upon benthic vegetation develops.

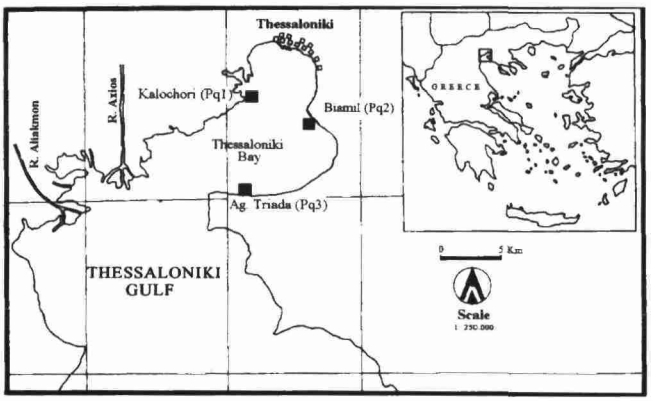

Figure 1. Map of the studied area.

Materials - Methods

Algae segments were collected from approximately 1m depth on a monthly basis along with the monitoring of physicochemical parameters during the period from April 94 to April 95.

Biological parameters: Biomass (wet and dry weight), coverage (%). The applied methodology is according to Littler (4) and has been described in details by Lazaridou *et al.* (5).

Physicochemical parameters: Temperature, salinity, pH, dissolved oxygen, irradiance, water transparency, suspended solid mater and inorganic nutrients. The methodology used is described in details by Haritonidis *et al.* (6).

Results and Discussion

Structure of macrophytic communities

Diversity and dominance indicate a tendency to degradation of the marine environment of the Gulf of Thessaloniki as a consequence of the efflux of municipal sewage and industrial and agricultural effluents (see also 7, 8, 9). The low species diversity as documented for the biotope (5) is a well known effect of long term pollution in the coastal marine environment (10, 11, 12).

Based on coverage data, the dominant species were: *Ulva rigida*, *U. curvata*, *Enteromorpha linza*, *E. intestinalis*, *Ectocarpaceae spp.*, *Petalonia fascia*, *Scytosiphon lomentaria* and *Hypnea musciformis*. Cluster (not shown) and MDA analysis (Fig. 2) have shown two main communities. The first (I) is dominated by the species *E. intestinalis* and the second (II) by the species *U. rigida*. The *E. intestinalis* community dominates the biotope in winter and spring, where the *U. rigida* community dominates during summer and autumn. In October'94 the biotope was dominated by *U. rigida* and *H. musciformis* and is shown at the scatter diagram as a separate point. With the exception of *H. musciformis*, the rest of dominant species belong to short-lived opportunists which are characteristic of eutrophicated temperate coastal areas (10, 11, 12). Based on the coverage and MDA analysis data a simple scheme of the macrophytic succession in the biotope was produced (Fig. 3).

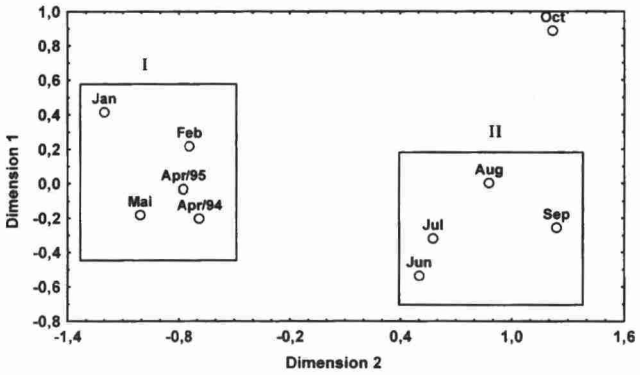

Figure 2. Multidimensional scaling analysis (MDA) based on coverage data.

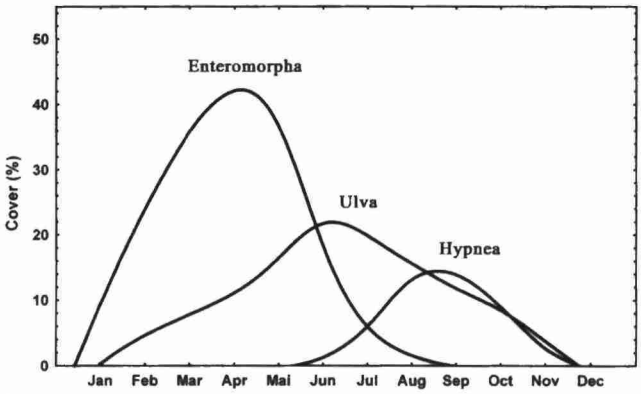

Figure 3. Simple sheme of macrophytic succession based on coverage data and the results of MDA.

Physicochemical parameters and macrophytic abundance

The exact determination of the factors which are responsible for the increase of the macrophytic biomass in the marine environment, especially in shallow and enclosed areas, is a difficult task (1). Figure 4 shows the seasonal variation of the macrophytic biomass (dry weight) in the study area. Correlation analysis between physicochemical parameters and biomass showed a statistically significant correlation ($p<0,05$) only within total dry biomass (TDB) and irradiance. However, TDB and inorganic nutrients, mainly nitrates, are correlated as follows: Total inorganic nitro-

NOTE SUR LA PRÉDOMINANCE D'UNE CHLOROPHYTE CAULERPALE *CAULERPA PROLIFERA* (FORSSKAL) LAMOUROUX AU VOISINAGE D'UNE CENTRALE À PRODUCTION D'ÉLECTRICITÉ (804 M.W.) DE MERS- EL HADJADJ (GOLFE D'ARZEW; OUEST ALGÉRIEN)

Ould-Ahmed Nora [1] et Meinesz Alexandre [2]

[1] Laboratoire de Biologie et d'Ecologie du Phytobenthos. Institut des Sciences de la Mer et de l'Aménagement du Littoral B.P. 54 Sidi-Fredj 42321,W. Tipaza, Algérie

[2] Laboratoire Environnement Marin Littoral. Université de Nice Sophia Antipolis Faculté des Sciences 06108 Nice Cedex 2

Résumé

Des relevés saisonniers de phytobenthos sont réalisés au voisinage de la centrale thermique de Mers- El- Hadjadj (de l'été 1989 au printemps 1990). Parallèlement à l'étude effectuée à des niveaux superficiels (de 0 à -0.50m) qui marque un gradient décroissant du phytobenthos en s'éloignant de la tache thermique, une exploration en profondeur (de -2 à -10 m) montre la présence presque exclusive d'une algue verte : *Caulerpa prolifera*; espèce thermophile à affinités subtropicales. Au total seulement 48 espèces (essentiellement des Ceramiales) accompagnent cette algue dans 55 relevés (de 25 cmx25 cm chacun). Les résultats obtenus au niveau d'une station à -5m de profondeur (taille et nombre des frondes, longueur des stolons et valeur de biomasse) sont comparés à ceux trouvés dans un site naturel des côtes continentales françaises.

Mots clés : phytobenthos, thermal pollution, Algerian Basin

La centrale thermique de Mers-El- Hadjadj, inaugurée en 1984, constitue le complexe thermoélectrique principal du pays. Sa puissance est de 804 M.W., elle fonctionne en mer ouverte sur le littoral ouest algérien (Fig. 1).

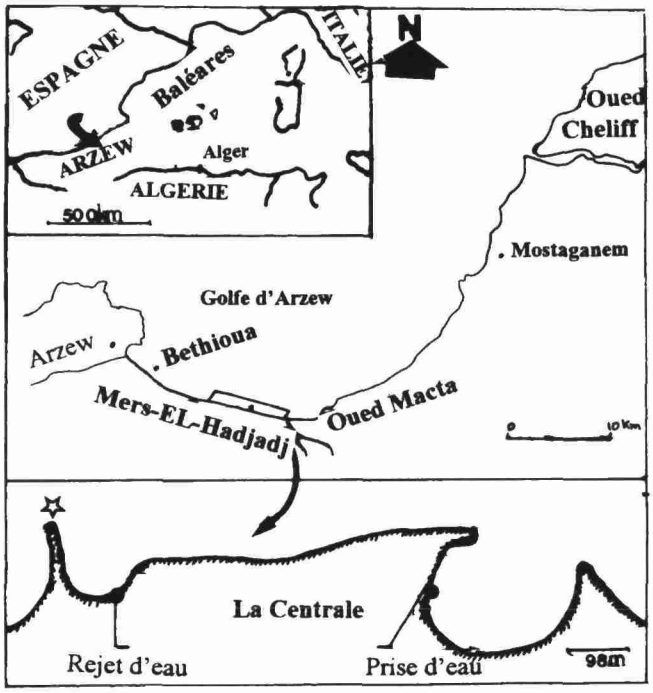

Figure 1 : Localisation ( )de la zone d'étude * station de prélèvement.

Les organismes qui s'y trouvent sont exposés à une élévation de la température de 7 à 8°C au-dessus de la normale (T° moy. 18.3 °C) et à une concentration en chlore de 0.5 ppm.

Une exploration en profondeur (de -2 à -10m) montre la présence d'une couverture végétale dense et homogène constituée d'une Chlorophyte Caulerpale: *Caulerpa prolifera*; espèce photophile thermophile à affinités subtropicales (Fig.2).

C. prolifera a déjà été signalée (1) dans l'ouest (Arzew), le centre (Alger et Béjaia) et l'est (Annaba) de l'Algérie. Cependant, selon nos prospections et les inventaires récents (2), (3) et (4) *C. prolifera* semble avoir régressé sur les côtes algériennes à l'exception du golfe d'Arzew. Dans le site étudié, très peu d'espèces existent en présence de *C. prolifera*. La plupart d'entre elles sont des Ceramiales à affinités chaudes qui lui sont épiphytes. Dans l'ensemble du site et dans la totalité de nos relevés l'herbier de *Posidonia oceanica* (L.) Delile est très dégradé. Il n'existe que sous forme de matte morte et de quelques faisceaux de feuilles en mauvais état. La dominance de *C. prolifera* dans ce site nous a amenés à évaluer sa biomasse, à mesurer la longueur de ses frondes et de ses stolons, à dénombrer ses frondes primaires et secondaires puis à comparer ces caractéristiques à celles trouvées dans un site naturel des côtes continentales françaises (5).

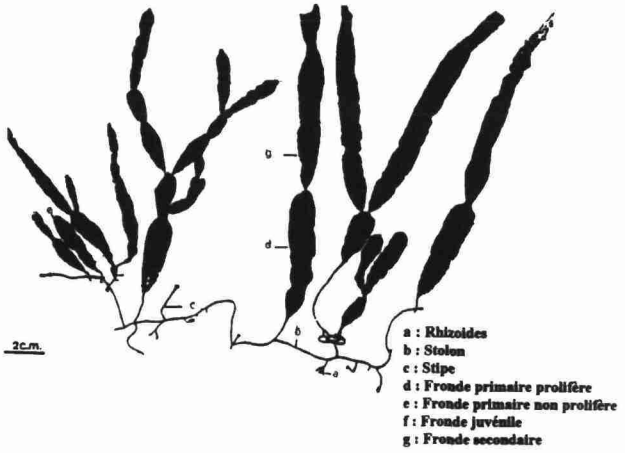

Figure 2 : *Caulerpa prolifera.*

Matériel et méthodes

Les prélèvements sont réalisés en scaphandre autonome sur un cycle saisonnier de l'été 1989 au printemps 1990 . La méthode de récolte consiste à effectuer un grattage complet de la surface à échantillonner; soit un carré de 25 cm sur 25 cm. La station se situe à 140 m du rejet, à 40 m du rivage par 5 m de profondeur.

Résultats et discussion

Les résultats obtenus dans le tableau ci-après montrent que *Caulerpa prolifera* du golfe d'Arzew présente des stolons dont la longueur totale maximale atteint 380.48 m/m², ce qui dépasse largement le maximum observé sur le littoral des Alpes-Maritimes (235 m/m²). Il en est de même pour le nombre de frondes primaires et pour le nombre de frondes par mètre de stolon. Quant à la longueur moyenne des frondes primaires non prolifères (>2 cm), la longueur maximale notée dans les Alpes-Maritimes est de 5.32 cm, alors que la valeur minimale obtenue dans le golfe d'Arzew est de 5.5 cm et la maximale de 10.5 cm. Il a été démontré (5) que la période d'absence de tout développement de l'algue est observée lorsque la température est la plus faible. Nos résultats confirment ces observations.

Les valeurs minimales des stolons et de la biomasse ont été enregistrées à Arzew en hiver. Dans les deux stations (Alpes-Maritimes et Arzew) c'est à l'automne que l'on trouve les longueurs maximales des frondes.

Conclusion

Les résultats obtenus permettent de montrer que les conditions d'un rejet thermique peuvent être favorables à l'établissement d'une population pérenne et dense de *Caulerpa prolifera* dans une région où l'algue est rare. Ces observations confirment le succès d'une trans-

GROTTES ARTIFICIELLES POUR L'ÉTUDE DE LA CROISSANCE DU CORAIL ROUGE DE MÉDITERRANÉE

Ounais-Thèvenin N., Allemand D., Thèvenin T., Gilles P., Théron D.,
Debernardi E., Ferrier-Pagès C.*

Association Monégasque pour la Protection de la Nature
7 Rue de la colle, MC-98000 MONACO

Résumé

Afin de reconstituer les populations de corail rouge de Méditerranée dans les zones sur-exploitées, l'AMPN a conduit deux expériences de coralliculture dans des grottes artificielles. Les premières grottes, réalisées en béton ont permis de démontrer la faisabilité de la transplantation de corail sur un substrat artificiel. Un prototype de grotte en fibre de verre et résine de polyester a ensuite été construit. Les colonies ont parfaitement survécu à la transplantation et se sont reproduites. Les résultats obtenus montrent que les grottes artifielles, en captant les jeunes larves, pourraient être utilisées dans des expériences de restauration de biotopes dégradés.

Abstract

The high economic value of the red coral has generated over-exploitation. The AMPN has therefore built artificial reefs to conduct an in situ study of transplantation. The first experiment with concrete caves demonstrated the feasability of coral transplantation. Coral colonies reproduced and exhibited a high growth rate. The second experiment was performed with a glass fiber cave prototype which can be easily transported and immerged. First results show that transplanted colonies survived and were able to produce larvae. This gives us hope for future use of caves as "diffusers" of larvae for experimental reintroduction of red coral.

Mots-clés : cnidaria, conservation, growth, Ligurian Sea, marine parks.

La disparition du corail rouge (*Corallium rubrum*) des zones côtières de faibles profondeurs a posé le problème de la gestion de cette ressource et a stimulé la recherche sur la biologie de cette espèce, encore fort méconnue [1; 2]. Dans le but d'étudier la faisabilité de la culture du corail rouge *in situ* afin de reconstituer les populations des zones sur-expoitées, l'Association Monégasque pour la Protection de la Nature (AMPN) a mis en place un programme de construction de grottes artificielles susceptibles de reproduire l'habitat original du corail. Les objectifs de ces expériences étaient :

- l'étude de l'adaptation et du développement de colonies de corail transplantées de leur substrat naturel sur un substrat artificiel et replacées dans un milieu naturel identique,
- l'étude de la multiplication par voie asexuée ("bouturage") des colonies mères de corail,
- le suivi de la croissance de ces colonies déplacées à l'intérieur de grottes artificielles,
- la reproduction éventuelle du corail dans ces nouvelles conditions d'implantation.

A ce jour, deux types de grottes ont été expérimentés. La première expérience a été réalisée avec quatre grottes en béton (Fig. 1, 3 x 2 x 2.2 m ; 8 tonnes chacune) qui ont été immergées dans la réserve sous-marine de Monaco et dans la réserve à corail rouge en décembre 1988 à une profondeur d'environ 30 m. Les colonies de corail ont été transplantées dans ces grottes et fixées grace à une résine époxy sous-marine (Devcon), sur des supports de porphyre eux-mêmes fixés sur des plaques horizontales de polypropiléne.

Grâce à cette méthode, il apparait que la survie des colonies, quatre ans après l'implantation, approche 100%. Deux ans après le début de l'expérience, 10 à 15 colonies par m^2, nées par reproduction sexuée des colonies bouturées, recouvrent le plafond de la grotte. La plupart de ces colonies ont une forme trapue, avec deux ou trois petites ramifications. Leur taux de croissance est élevé (12 à 16 mm d'accroissement linéaire par an). Ce taux de croissance est plus important que celui observé dans des expériences similaires conduites en laboratoire, où six mois après la fixation de la larve née du corail recueilli à faible profondeur, de jeunes colonies avec seulement deux polypes ont été observées [3]. D'autres jeunes colonies se sont également fixées sur la résine Devcon et sur les plaques de polypropylène. Ces observations démontrent que les colonies de corail transplantées sont parfaitement capables de survivre et de se développer sur un substrat artificiel. Leur capacité de reproduction est entière. Les bons résultats obtenus, tant en ce qui concerne la "manipulation" des colonies, que la fixation rapide, permet d'être optimiste pour une future utilisation de ces grottes comme "capteurs", "diffuseurs" de larves et producteurs de jeunes colonies dans des programmes de recolonisation.

Les résultats très encourageants de cette première expérience nous ont amenés à essayer d'affiner et d'optimiser la conception de ces grottes. L'objectif de la seconde phase a donc été d'améliorer le concept des grottes en réalisant une structure beaucoup plus légère, qui puisse être facilement transportée sur le site, immergée et éventuellement déplacée et qui puisse assurer également un suivi facile. Un prototype de grotte artificielle en fibre de verre et résine polyester a été réalisé (Fig.2). Cette grotte est en partie démontable, légère (150 à 250 kg) et munie de 6 barres également en résine polyester, destinées à recevoir les colonies de corail. L'accès des plongeurs a été facilité par la présence de panneaux amovibles permettant ainsi le travail à l'intérieur de la grotte comme à l'extérieur. Le 23 juillet 1993, la grotte a été immergée à 39 m de profondeur, au pied du tombant du Loews. Les barres ont été immergées plus tard, le 28 juillet 1993, après y avoir fixé les colonies de corail : 18 colonies ont été fixées entières alors que

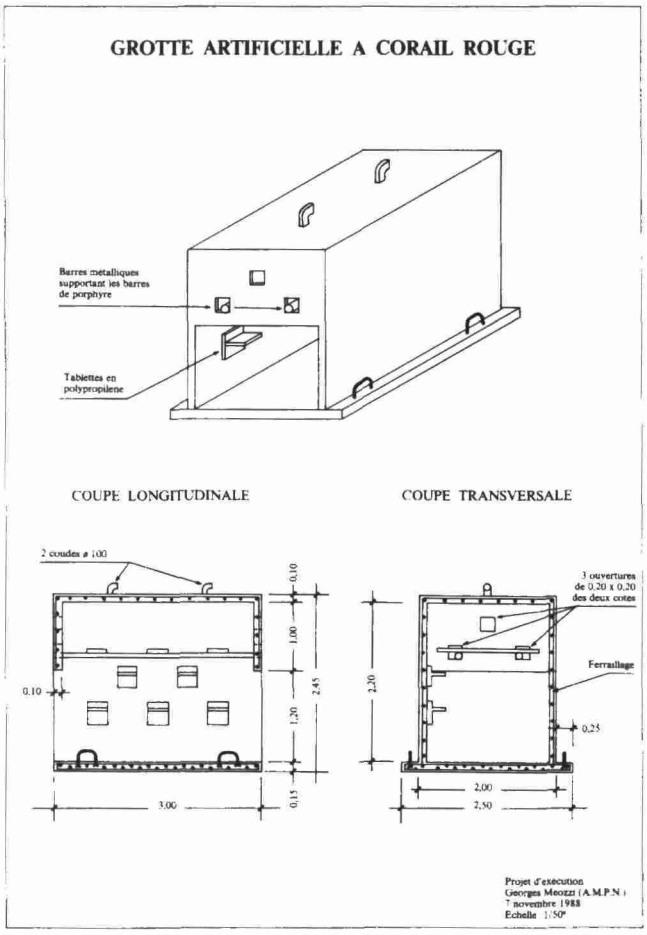

Figure 1.

MONITORING OF THE MEDITERRANEAN MONK SEALS IN THE TURKISH COAST OF THE AEGEAN SEA

B. Öztürk

Istanbul University, Faculty of Fisheries, Laleli-Istanbul, Turkey

Abstract

The status of the Mediterranean monk seals in the Turkish coasts of the Aegean Sea was studied from 1986 to 1996 for 10 years. During the study period, 41 individuals were identified in the Aegean Sea, among them 28 individuals survive, while 13 were dead. Only four pups were determined to survive. Except for two individuals in the Bodrum Peninsula, all monk seals were single individuals. Therefore, the population of the Mediterranean monk seals is not stable in the Aegean Sea. Main causes of the decline of the monk seal population were deliberate killings, loss of habitats and overfishing.

Key-words: cetacea, conservation, Aegean Sea

The Mediterranean monk seal, *Monachus monachus* (Hermann, 1779) is a mammal facing the danger of extinction and it is listed as one of the world's six most threatened mammals (1). Caltagirone (2) pointed out that there are 200 to 300 individuals worldwide, including only 100 to 150 remaining in the Mediterranean Sea. In the Aegean Sea, there are small quiet islets, isolated islands, calm beaches and underwater caves, which are most important habitats for the survival of the monk seals. Recent studies showed that in the Aegean Sea the number of seals ranged greatly from 50 to 90 individuals (3-11). However, most of the information is either old or controversial, thus more accurate data are needed for implementing appropriate protection measures. Therefore the aim of this study is to monitor the monk seals in the Aegean coast of Turkey.

This study was conducted from October 1986 to October 1996 in the Turkish part of the Aegean Sea, between Çanakkale Strait to Finike (Fig. 1). Direct observations were made from the fishing, research and private boats, as well as from the land. Besides, seal sighting information and reports of dead animals were collected from the fishermen and local authorities. This information was then carefully reviewed for avoiding double sightings, locations and dates. The population size reported below for each area represents the minimum number of individual seals identified by the author. For the individuals identification, size, color and other peculiarities were concerned. Photos and videos were taken for this purpose. The animals less the 120 cm were considered as juveniles, between 120-200 cm as subadults and larger than 200 cm as adults, according to Öztürk (11).

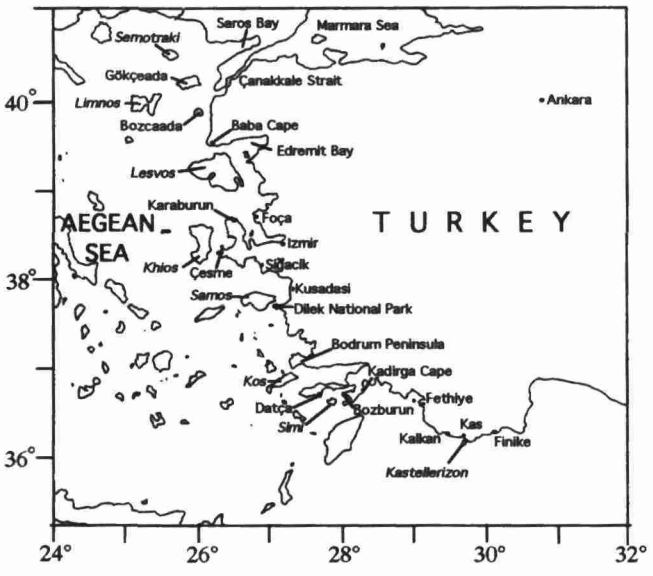

Figure 1 : Map of the Turkish coast of the Aegean Sea. Greek islands are indicated in italics.

During 10 years of the study, a total of 41 seals were identified in the Aegean coast of Turkey, of which 28 individuals survived at the end of the study period in 1996.

There are three seals in the Northern Aegean Sea, including Saros Bay, Gokceada, Bozcaada and Baba Cape. Two of them were adult and the other was subadult. On the western side of this area, there are two Greek islands, Limnos and Semotraki, which are also known as seal habitats (13). This area is one of the overlap zones in the Aegean Sea, where monk seals are encountered on both the Turkish and Greek sides.

In the Central Aegean Sea, including Foca Monk Seal Protection Area, five seals were determined. Four of them were adult, one was subadult. Three of them were sighted in Foca Region and two of them in Karaburun Region. Marchessaux (7) estimated three to five seals in the same region. This area is considered to be one of the core zones for the survival of the monk seal in the central Aegean Sea, due to effective *in situ* protection measures implemented by the local people. In other parts of the Central Aegean Sea between Karaburun to Kusadasi, seven individuals were determined. These were three adults, one subadult and three pups. These individuals were isolated from one another, except for two of them sighted together off Cavus Island, west of the Bodrum Peninsula. Marchessaux (7) estimated 10 animals in this zone in 1987. Between Kusadasi to the Bodrum Peninsula, eight individuals were determined. Those were four adults, two subadults, one juvenile and one pup. Marchasseux (13) estimated 20 individuals in Dilek National Park and five seals in the Bodrum Peninsula. Öztürk (8) reported six individuals in the Bodrum Peninsula and small islands around it.

In the southern Aegean Sea, between Bodrum to Finike, five individuals were identified. Three of these seals were adult and the others were juvenile. Bozburun, Uzunada, Kizilburun, Kadirga Cape, the Delikadalar (off Fethiye), the Catalada (off Kalkan) and the Ic Islands (off Kas) were habitats for monk seals. Berkes (14) estimated 50-100 individuals in this area, including those in Antalya Bay, east of Finike.

Total mortality reported was 13 individuals in the Aegean Sea. Five of them died from deliberate killing, five were drowned in the fishing nets and three died for unknown reason. Among them two individuals were pups. On the other hand, only four pups were determined survive; three in 1992 and one in 1995 in the Central Aegean Sea.

For the protection of the monk seals, the main problems in the Turkish Aegean coasts is deliberate killing. To realize the survival of monk seals it is necessary to continue mass public awareness campaign, especially for fishermen. At the same time, to compensate the net damage done by seals, fishermen should be able to find some supports such as supply of cheap oil, subvention, cold storage facilities and reduction of their port tax. In addition, Dilek National Park must be facilitated with better equipment for in situ protection.

In the Aegean Sea, there are "overlap" zone between Turkey and Greece for the monk seals as several islands and islets are very close to both countries and seals possibly move freely cross the border for feeding and breeding. Berkes (15) also reported possible migration of the monk seals in the Aegean Sea between Turkey and Greece and listed the following four areas where such migration is likely to occur: Lesvos - Babakale - Edremit Bay, Samos - Kusadasi, Kastellorizon - Kas, and Simi - the Datça Peninsula. An international survey with the participation of both countries is indispensable for the census of the exact number of monk seals in the the Aegean Sea. Moreover, continuous and regular monitoring studies should be carried out in all the Turkish Aegean coasts.

Acknowledgments

The author thanks to Dr.Ayaka Amaha Öztürk for reviewing this manuscript, and Turkish Ministry of Environment and Turkish Marine Research Foundation for the financial support.

IMPACT DES ANCIENNES EXPLOITATIONS MINIÈRES SUR LA CONTAMINATION EN MÉTAUX-TRACES DU LITTORAL CORSE

Pergent-Martini C.*, Camuglio V., Pergent G.

Equipe Ecosystèmes Littoraux, Faculté des Sciences, Université de Corse, BP 52, 20250 Corte, France

Résumé

La Corse est généralement considérée comme un secteur peu anthropisé, dont les teneurs en métaux-traces sont relativement faibles (« bruit de fond »). Toutefois, la présence d'anciennes exploitations minières est de nature à générer des contaminations localisées. Aussi, une étude a été entreprise afin d'estimer l'importance de ces apports sur la contamination du littoral insulaire, en utilisant la phanérogame marine *Posidonia oceanica* comme bioindicateur de la teneur en métaux-traces (cuivre, zinc, plomb, mercure et arsenic). Les résultats obtenus ne constituent pas, à l'exception de l'arsenic, des teneurs de base. En outre, dans la quasi totalité des sites, il y a correspondance entre les composés métalliques qui ont été exploités au niveau du bassin versant et les métaux-traces retrouvés majoritairement dans les faisceaux de *Posidonia oceanica*, prélevés à proximité de l'embouchure des fleuves côtiers. Ce travail confirme les potentialités de *Posidonia oceanica*, en tant qu'indicateur de la pollution métallique du milieu littoral.

Mots-clés : Bio-indicators, Bio-accumulation, Metals, Posidonia, Western Mediterranean

Introduction

Dans les biotopes photophiles de l'étage infralittoral méditerranéen, la phanérogame marine *Posidonia oceanica* constitue de véritables prairies sous-marines appelées "herbiers". Outre leur rôle écologique, sédimentologique et économique majeur, ces herbiers sont de véritables intégrateurs de la qualité des eaux littorales (1). En effet, *Posidonia oceanica*, à l'égal de nombreuses macrophytes, accumule les métaux-traces présents dans l'environnement. De plus, elle semble capable de mémoriser ces éléments dans ses tissus sur de longues périodes de temps (2, 3).

Du fait du faible degré d'industrialisation de la Corse, les principales sources de métaux-traces dans l'environnement correspondent soit à des apports atmosphériques exogènes, en provenance de régions plus industrialisées (Ligurie, Provence, Rhône-Alpes), soit de l'altération naturelle du socle ou d'apports liés aux exploitations minières (lessivage, ruissellement). Si de nombreuses études ont été réalisées pour estimer l'importance des apports atmosphériques sur la contamination du milieu littoral méditerranéen (4, 5), en revanche, on connaît peu de choses sur la contamination liée aux anciennes exploitations minières.

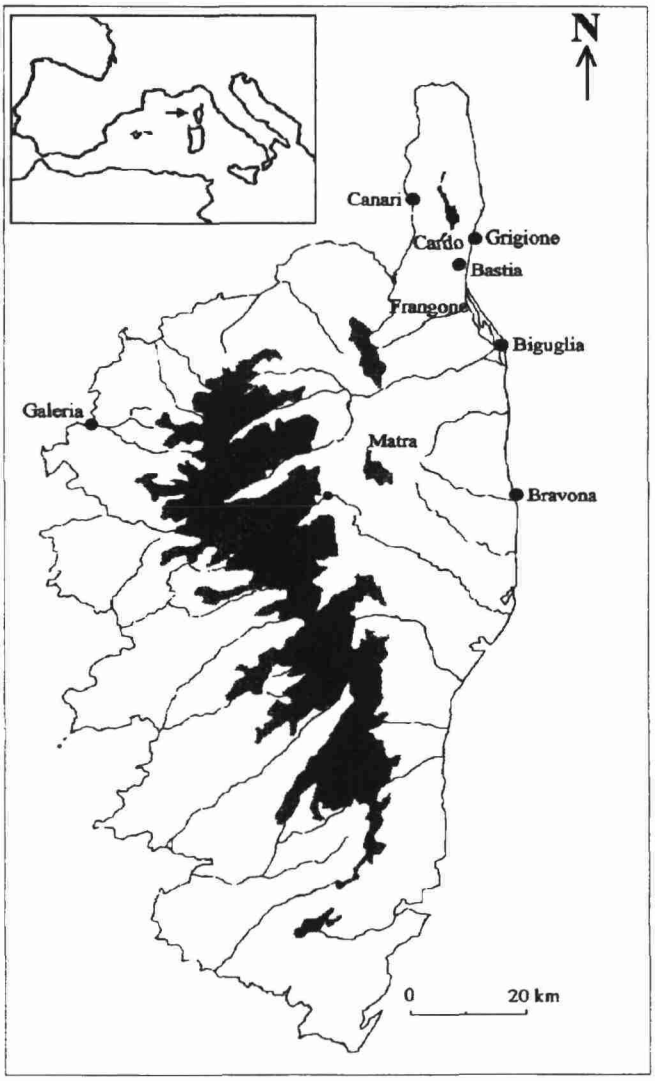

Figure 1 : Localisation des sites étudiés.

Cette étude s'intègre dans un programme de recherches pluridisciplinaires intitulé « Systèmes anthropisés en environnement méditerranéen insulaire » qui vise à suivre le devenir de différents métaux-traces depuis la source (secteur minier) jusqu'à la mer. Nous nous sommes plus particulièrement intéressés aux teneurs de cinq métaux (mercure, arsenic, plomb, cuivre et zinc) présents chez *Posidonia oceanica*, au droit de bassins versants abritant d'anciennes exploitations minières.

Matériel et méthodes

Les prélèvements de *Posidonia oceanica* (trois réplicats de 10 faisceaux par station) sont réalisés, en scaphandre autonome, dans cinq sites (Galéria, Canari, Grigione, Biguglia et Bravona) de Haute Corse, au niveau ou à proximité de l'embouchure de fleuves côtiers (Figure 1).

Les prélèvements sont effectués entre 5 et 6 m de profondeur. Les faisceaux foliaires sont séparés du rhizome, puis décortiqués en respectant l'ordre distique d'insertion des feuilles. Les tissus foliaires sont subdivisés en trois fractions : pétiole des feuilles adultes, limbe des feuilles adultes et limbe des feuilles intermédiaires. Les anciens pétioles persistants (=écailles) qui sont fixés sur le rhizome sont détachés et analysés séparément du tronçon de rhizome nu.

Tableau 1 : Teneurs moyenne en métaux-traces des tissus de *Posidonia oceanica*, dans les différents sites étudiés. Les teneurs sont exprimées en μg.g-1 de poids sec.

	Cu	Zn	As	Hg	Pb	Cu	Zn	As	Hg	Pb
Pétioles	18.7 ±2.6	13.4 ±13.9	0.20 ±0.04	0.07 ±0.01	0.48 ±0.44	20.8 ±5.5	13.3 ±22.6	0.19 ±0.06	0.12 ±0.03	0.00
Limbes adultes	39.9 ±14.3	346.5 ±372.4	0.37 ±0.12	0.04 ±0.01	3.29 ±0.48	13.4 ±6.5	143.8 ±111.5	0.33 ±0.09	0.04 ±0.01	4.23 ±2.82
Limbes Intermédiaires	38.3 ±16.2	264.6 ±80.1	0.40 ±0.03	0.05 ± 0.01	2.30 ±0.37	28.3 ±8.9	171.2 ±85.5	0.41 ±0.16	0.06 ±0.01	3.13 ±1.03
Ecailles	14.1 ±1.5	9.1 ±16.5	0.99 ±0.12	0.11 ±0.02	1.85 ±1.38	10.9 ±3.0	4.5 ±6.9	1.04 ±0.09	0.12 ±0.02	0.75 ±0.39
Rhizomes	39.9 ±4.6	166.8 ±168.6	0.25 ±0.03	0.25 ±0.03	1.47 ±0.57	27.7 ±1.5	65.2 ±70.4	0.21 ±0.05	0.16 ±0.04	2.29 ±1.16

	Grigione					Biguglia				
	Cu	Zn	As	Hg	Pb	Cu	Zn	As	Hg	Pb
Pétioles	21.6 ±3.3	11.1 ±10.6	0.22 ±0.05	0.08 ±0.03	0.03 ±0.07	24.0 ±4.3	21.7 ±17.7	0.22 ±0.04	0.05 ±0.01	0.03 ±0.07
Limbes adultes	38.3 ±20.5	324.4 ±265.0	0.86 ±0.72	0.06 ±0.03	2.20 ±0.86	12.3 ±5.6	160.1 ±208.2	0.57 ±0.32	0.03 ±0.01	3.01 ±0.29
Limbes Intermédiaires	35.6 ±14.5	145.6 ±29.8	0.44 ±0.08	0.05 ±0.01	0.91 ±0.39	19.7 ±8.3	133.1 ±10.7	0.41 ±0.08	0.05 ±0.01	2.60 ±1.02
Ecailles	27.1 ±13.4	2.4 ±1.4	1.20 ±0.42	0.12 ±0.01	2.08 ±1.17	15.7 ±6.1	2.03 ±5.30	1.74 ±0.51	0.11 ±0.03	3.59 ±1.38
Rhizomes	44.8 ±2.4	66.6 ±74.2	0.23 ±0.03	0.13 ±0.01	1.64 ±1.61	27.4 ±2.0	50.6 ±61.6	0.24 ±0.05	0.12 ±0.02	1.23 ±0.31

	Bravona				
	Cu	Zn	As	Hg	Pb
Pétioles	21.2 ±2.2	12.6 ±11.9	0.51 ±0.02	0.07 ±0.02	0.14 ±0.18
Limbes adultes	36.6 ±11.8	154.4 ±143.1	0.38 ±0.01	0.03 ±0.01	4.68 ±1.51
Limbes Intermédiaires	50.3 ±16.5	130.7 ±23.3	0.44 ±0.09	0.05 ±0.01	4.69 ±0.78
Ecailles	10.2 ±3.6	3.88 ±4.13	1.84 ±0.36	0.11 ±0.05	1.74 ±2.16
Rhizomes	19.7 ±8.0	44.7 ±61.9	0.34 ±0.11	0.13 ±0.05	1.26 ±0.24

DIATOMS FROM THE SALTERN OF STON (CROATIA)

Andjelka Petrovic

CEP - Center for urban development planning, SAI MAR - Council for integrated mariculture,
Zahumska 34, 11000 Beograd, Yugoslavia

Abstract

The published information on algal microflora of the Croatian salterns is extremely rare. This paper is a part of phytoplankton investigation at the salterns along the eastern Adriatic coast. The principal aim of this research was to present the list of diatoms in a different salinity gradients in the natural temporary salt ponds in Ston salina. From 106 samples, 96 diatoms were identified in Ston lagoon and 73 in salt ponds at salinity range from 23.2 to 210 ppt. Diatoms prevailed in the phytoplankton community of the lagoon and Ia series of evaporators, where salinity ranged from 23.21 to 50.00 ppt and temperature from 17.0 to 29.0oC. The most euryhaline and eurythermal diatoms were *Amphora coffeaeformis*, *A. cymbifera* and *Nitzschia sigma*.

Key-words: diatoms, lagoons, Adriatic Sea

Introduction

Reports on the presence of diatoms in a salinity gradient of the salt works are relatively few in comparision of diatom investigation in the world coastal waters. This paper reports an extensive analytical and identification study of diatoms in salt ponds due to their importance for integrated mariculture development in the eastern coastal Adriatic area. In the Croatian salterns there is no development of fish farming activities and the *Artemia* population, which is of considerable importance in fish and shellfish larviculture (1) is not present (2). Many parts of the salterns and sea shores around them, along the eastern Adriatic coast, can be transformed for aquaculture activities. For that economic reason, phytoplankton investigation and ecological data collection have been taken in nonmodified saltponds of ancient solar salina in Ston.

Location and the properties of the ponds

The temporary salt ponds in Ston (42°50'N; 17°41'S) are situated at 0.40-0.67 m below the zero sea level at the north-west part of the Ston lagoon. The phenomenon of tides has always been used to flood the saltern with seawater necessary for salt production. The total area of the saltern is 429840 m^2 and it consists of I (245800 m^2), II (47400 m^2+ 50400 m^2) and III series of evaporators (25690 m^2), adjusting ponds (20570 m^2) and crystallizers (39980 m^2). The concentration of salty water, salt precipitation, salt collecting and storing last for around 4-5 months (15 April to 15 September). In spring, the whole saltern is drained dry for a month or two (March, April) and lagoon waters of usuall aboat 35-38 ppt are poured in (April or May), to obtain a sequence of sea water salinities (end of July, August) by distribution of the waters, in accordance with the usual requirements of salt production process. During autumn, winter and a part of spring, the saltern is sometimes flooded by runoff rainwater. There are no brine storage ponds at the saltern and all remaining brine goes back to the sea in the lagoon after the production is finished (November). In winter, during low tides, a part of the lagoon in front of the saltern can be dry that brackish or fresh water flows out of the saltern. Sometimes, during cold winters, ice forms in some parts of the saltern.

Material and methods

Phytoplankton samples were collected in all seasons, in nonregular intervals, always at the same stations in the salt ponds during the period from 1987 to 1991. Intensification of samples collecting, every two week was done from the beginning of June to the end of August, when a sequence of sea water salinities was obtained in evaporators' series. Except to the first salt pond of Ia series of evaporators, where the maximum sea water depth for a short period can reach up to 150 cm, in other ponds water depth vary, depending of the salt processing aproximatelly, from 2.5 up to 20 cm. Phytoplankton samples were collected by bucket and preserved in polyethylene bottles in 2% neutralized formaldehyde solution. Phytoplankton cells were enumerated on an inverted Uterm–hl microscope after sedimentation period of 24 hr and global diversity index after Margalef (3) was used. For qualitative analysis samples were prepared according to Hustedt (4). Benthic samples were collected directly from the bottom mats in the shallow salt ponds and used for qualitative analyses. Parallel with fixed samples, samples with live material have also been taken for identification study, for species isolation and their rearing in limiting volumes as well as for mass production in indoor and outdoor cultures for zooplankton production. Salinity was measured by refractometer or Bauméter and temperature by termometer. Oxygen was determined by the method of Winkler, pH by pH meter and nutrient concentrations (nitrates, nitrites, ammonia, phosphates and silicates) according to the standard methods (5).

Results and discussion

Diatoms dominated in qualitative-quantitative composition of the phytoplankton in seawater of Ston lagoon and their abundance vary in total phytoplankton in salt ponds along the saltern. For example, in IIa series there was a density of 13175 cells ml^{-1} which was 11.1% of the total phytoplankton. The most abundant species (73,62 %) in IIa series was *Dunaliella salina* which dominated also in adjusting ponds with relative abundance 88.1%, where mean cell diatom density was 2100 cells ml^{-1}. From the saltponds where natural mass production of phytoplankton has been observed, the natural food have been taken for mass rearing brine shrimp *Artemia* and ciliate *Fabrea salina* for mariculture purpose.

The highest number of species (96), diversity index (5.61) and relative abundance of diatoms in total phytoplankton were observed in lagoonal waters (23.20-40.60 ppt) with which the saltern is filled for operation. The high fluctuation of nitrates and phosphates were recorded in the lagoon as well as in the saltern. This may be due to the both, land fresh water influence and submarine fresh water springs of the lagoon. These influences are strong especially in the spring, when lagoon water is poured in dry saltern for operation. Some bottom springs of the fresh water were also recorded in the I, II and III series of evaporators. The maximum ratio between nitrates and phosphates indicates a hypernutritification of the lagoon temporary (6). Concentration of the ammonia was about seven times higher in comparison to typical ammonia concentration in temperate coastal zones (7). There is evidence of high nitrates values (> 150 µmol dm^{-3}) also in the Ib and IIa series of evaporators. Organic and inorganic nutrients may cause hypernutrification, possibly phytoplankton blooms, oxygen depletion and formation of anoxic situation (22) which was observed once in one pond of Ib series when phytoplankton bloom was observed.

A total of 115 diatom taxa representing 18 genera were identified in saltponds in salinity range from 23 to 210 ppt and temperature from 5 to 39°C (Table 1). *Cocconeis placentula* var *lineata* was present in salt ponds in a salinity range from 33.67 to 120 ppt and was the most abundant species in the lagoon and Ia series of evaporators in a salinity range from 23.21 to 51.00 ppt and temperature from 17.0 to 29.0°C. This species is abundant in a salinity range from 20.00 to 78.00 ppt in first three section of Tarquinia saltworks. The diatom number and diversity index started to be inversely proportional to salinity (8) in the saltponds of series Ib.

In series of Ib evaporators (51.00-90.00 ppt) *Nitzschia delicatissima* dominated. Maximum diatom density was observed in IIa series of evaporators, in a salinity range from 98.6 to 110.0 ppt, where *Nitzschia seriata* complex together with *Cocconeis placentula* var. *lineata* and *Amphora delicatissima* dominated among diatoms. In IIb series of evaporators *Amphora coffeaeformis* and *A. cymbifera* dominated in the diatom community and in the saltponds of III series of evaporators *Amphora coffeaeformis* was the most abundant species. In adjusting ponds (salinity: 207 to 250 ppt) among the mentioned 3 diatoms which were presented in 210 ppt, Amhora coffeaeformis was the dominant species. In crystallizers (salinity: 255 to 290 ppt), diatoms were not observed. Different temperature and salinity gradients for diatoms have been recorded (9). The most euryhaline and eurythermal diatom in this salina genera were Amphora, and Nitzschia. *Amphora coffeaeformis*, *A. cymbifera* and *Nitzschia sigma* were presented at salinity of 210 ppt, where maximum temperature of 39.0°C was measured.

References

1. Bengston D., LÖger P., Sorgeloos P., 1991. Use of *Artemia* as food source. In: Artemia biology, Browne R., Sorgeloos P., C.N.A. Trotman, ed., CRC, Boca Raton: 255-285.
2. Majic A.,Vukadin I., 1987. Preliminary report on the brine shrimp (*Artemia*) from Yugoslavian saltworks: 145-149. In: Artemia Research and its Aplications. Vol. 3. Ecology, Culturing, Use in Aquaculture. P. Sorgeloos, D. A. Bengtson, W. Decleir i E. Jaspers (Eds). Universa Press, Wetteren, Belgium, 556 pp.
3. Margalef R., 1951. Diversidad de especies en las comunidades naturales. *Publ. Inst. Biol. apl. Barcelona*, 9: 5-27.
4. Hustedt P., 1956. Kieselalgen (Diatomeen). Kosmos. Stuttgart.
5. Strickland J.D., Parsons T.R., 1972. A practical handbook of seawater analysis. *Fish. Res. Bd. Can. Bull.*, 167: 310 pp.
6. Olivotti R., Faganeli J., Malej A., 1986. Eutrophication of coastal waters - Gulf of Trieste. *Wat. Sci. Tech.*, 18: 303-316.
7. Ilirn J., 1988. Eutrophication in the Mediterranean sea. In: Receiving capacity and monitoring of long term effects. MAP Technical Reports Series No 21, UNEP Athens: 161-187. .
8. Barg U.C., 1992. Guidelines for the promotion of environmental management of coastal aquaculture development (based on a review of selected experiences and concepts). FAO Fisheries Technical Paper. No. 328. 122 pp.
9. Dor I., Ehrlich. A., 1987. The Effect of Salinity and Temperature Gradients on the Distribution of Littoral Microalgae in Experimental Solar Ponds, Dead Sea, Israel., P.S.Z.N.I: *Marine Ecology*, 8 (3): 193-205.

WASTE DISPOSAL AND RIVERS DISCHARGE EFFECTS ON THE EUTROPHICATION CONDITIONS OF THERMAIKOS GULF (N.W. AEGEAN)

R. Psyllidou-Giouranovits*, A. Pavlidou, E. Georgakopoulou-Gregoriadou
National Centre for Marine Research, Agios Kosmas 16604, Hellinikon, Hellas

Abstract

Dissolved oxygen and nutrient concentrations, were studied seasonally from May 1995 until March 1996, in order to estimate the impact of the disposal of the urban wastes and the discharge of the rivers on the eutrophication conditions of the Thermaikos Gulf. The results reveal that the waste disposal causes an accumulation of nutrients in the Bay of Thessaloniki (especially in the deeper layer of the upper part), with a decrease of the DO concentrations. In the northwestern part of the Thermaikos Gulf, due to the discharge of fresh water from the rivers, high surface nutrient concentrations were measured mainly during winter and spring.

Key-words: eutrophication, oxygen, river input, Aegean Sea

Introduction

Thermaikos Gulf is a semi- enclosed shallow (maximum depth 42 m) water body located at the northwestern part of the north Aegean Sea. It receives approximately 150.000 m^3/d of urban wastes as well as about 60.000 m^3/d of industrial effluents untreated or partially treated. Moreover fresh waters from three main rivers Axios (20-170 m^3/d depending on the season), Loudias (10-30 m^3/d) and Aliakmon (10-80 m^3/d) are influencing the hydrological regime of the western part of the Gulf (1) Oceanographic studies concerning eutrophication conditions of the Gulf were carried out in the past during the years 1975-76 (2, 3, 4, 5) and 1985-86 (6, 7). Recently Thermaikos was studied during 1992 (8, 9) and 1995-96. The present work deals with the results of the years 1995-96, aiming to access the impact of the above mentioned sources of pollution on the eutrophication conditions of the Gulf.

Materials and methods

Water samples were collected seasonally from standard depths over 19 sampling stations (Figure 1), using 8 L NISKIN bottles attached to a Rosette Multi-Bottle Array System. Determination of DO was carried out on board according to Carritt *et al.* (10). Nutrients were measured according to methods described by Psyllidou *et al.* (11).

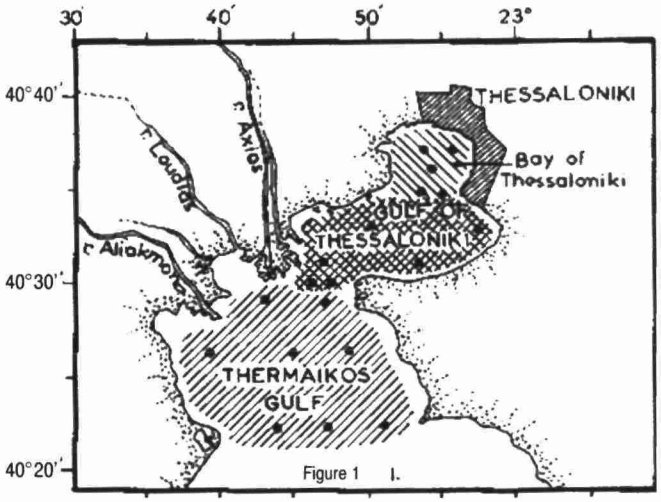

Figure 1

Results and discussion

For better estimation of the results the study area was divided into three water masses (subareas): the Thessaloniki Bay (5 sampling stations), the Thessaloniki Gulf (6 sampling stations) and the Thermaikos Gulf (8 sampling stations)

Dissolved oxygen

During May, high concentrations of DO were measured at the surface layer. The vertical distribution shows decreasing concentrations with increasing depth. Within the bottom layer of the upper part of the Bay the DO concentration reached 0.98 ml/l corresponding to a saturation of 17.16%. These low concentrations were related to high concentrations of nutrients, revealing the impact of the urban wastes on the deep waters of the area. Figure 2 shows the horizontal distribution of DO concentrations at a depth of 20 m (or the maximum depth of stations with depths slightly lower than 20 m) during May 1995.

During August, the vertical distribution of the DO concentrations at the southern part of Thermaikos, shew maximum concentrations at depths between 20 and 40 m, due to better conditions for photosynthesis at these depths, during the summer period. Within the bottom layer of the Bay of Thessaloniki, saturation did not exceed 69.6% (23.15-69.6%).

During winter and early spring (December 1995 and March 1996), due to the vertical mixing of the water masses, the vertical distribution of the DO concentrations was nearly homogeneous and the saturation ranged between 73.7 and 98.9% in December and between 78.7 and 109.3 in March, depending on the station. The discharge of fresh waters at the northwestern part of Thermaikos, near the estuaries, during March, was obvious from the high surface DO concentrations. Figure 3 shows the horizontal surface distribution of DO during March.

Nutrients

In spring (May 1995), nutrient concentrations in the southeastern part of Thermaikos were low and were characteristic of the oligotrophic Aegean Sea waters. In the surface layer (<5 m) of the area near the estuaries of the river Axios, an inflow of fresh waters of higher temperature, lower salinity and high nutrient concentrations was observed (PO_4 0.28, SiO_4 5.97, NH_4 0.68, NO_3 1.64 μg-at/l). This inflow caused a stratification of the upper layer, preventing the vertical mixing of this water with the Aegean waters of the deeper layer. Water masses from the Thermaikos move towards the Gulf of Thessaloniki along the eastern coast, while the water exchange between the Gulf and the Bay of Thessaloniki is not significant. The discharge of urban wastes, mainly from the northeastern coast of the Bay, in combination with the very low water renewal, resulted in an enrichment of nutrients within the deep layer (PO_4 1.27,SiO_4 6.45, NH_4 1.29, NO_3 0.23 μg-at/l). The horizontal distribution of silicates at the surface and of phosphates at the depth of 20 m are shown in Figures 4 and 5.

In summer (August 1995), the influence of fresh water on the concentration of nutrients in the northwestern Thermaikos, was lower than during spring (PO_4 0.14, SiO_4 2.10, NH_4 1.87, NO_3 0.82 μg-at/l), due to the low inflow and the predominant cyclonic surface circulation. The surface water masses from the eastern and central upper Thermaikos, after mixing with the masses of the eastern Thessaloniki Gulf, moved southwest to the Aegean Sea together with the fresh waters of the rivers. The high surface temperatures in the Bay of Thessaloniki, resulted in an intense stratification causing accumulation of nutrients within the deeper layer (PO_4 3.53, SiO_4 19.85, NH_4 13.58, NO_3 0.14 μg-at/l). Figure 7 shows the horizontal distribution of ammonium at a depth of 20 m.

In early winter (December 1995), the vertical distribution showed that the water column was nearly homogeneous in the Bay and the Gulf of Thessaloniki. The vertical mixing of the masses of the Bay resulted in a decrease of the concentration of nutrients (PO_4 0.61, SiO_4 2.36, NH_4 2.31, NO_3 0.89 μg-at/l) in the deeper layer. The water exchange between the masses of the Gulf of Thessaloniki and Thermaikos Gulf was significantly lower as compared to the previous sampling. The increased concentration of nutrients in the northwestern part of Thermaikos, indicated an increase of fresh water discharge (PO_4 0.60, SiO_4 5.42, NH_4 1.72, NO_3 2.55 μg-at/l).

In late winter- early spring (March 1996), the Bay and the Gulf of Thessaloniki were characterized by the lower temperatures and the greater water column homogeneity of the whole sampling period. Nutrient concentrations were low as compared to those measured in December. High surface concentrations near the estuaries of Axios river (PO_4 0.23, SiO_4 25.02, NH_4 1.28, NO_3 13.86 μg-at/l), in combi-

STRUCTURE ET ORGANISATION DE LA MACROFAUNE BENTHIQUE DES SUBSTRATS MEUBLES DU PORT DE BENI-SAF (ALGERIE)

W. Refes*, K. Benzada, K. Dali

Institut des Sciences de la Mer et de l'Aménagement du Littoral (ISMAL) B.P.54 Sidi Fredj 42321 Tipaza, Algérie

Résumé

Il ressort de cette première investigation sur les peuplements benthiques du port de Béni-Saf: une richesse spécifique observée de 80 espèces, qui est importante par rapport à la superficie du bassin portuaire en comparaison avec les données de la littérature consultée la présence d'espèces indicatrices d'une surcharge en matière organique (*Capitella capitata*; *Corbula gibba*) l'absence (*Scolelepis fulginosa; Nereis caudata; Audouinia tentaculata; Staurocephalus rudolphii*) ou la limitation démographique (*Capitella capitata*) d'espèces opportunistes; une zonation biologique réduite par la présence uniquement d'une zone subnormale, indicatrice d'une faible pollution du bassin portuaire de Béni-Saf.

Mots clés: Zoobenthos, Bio-Indicators, Biodiversity, Pollution

Introduction

Le port de Béni-Saf (35°18'26"N, 1°23'16"W) est situé à l'ouest de la côte algérienne. Cette étude servira à la définition d'un état de référence sur la répartition spatiale des peuplements benthiques du port de Béni-Saf et permettra d'apprécier les modifications à long terme de la structure de la macrofaune benthique de l'enceinte portuaire à la suite des travaux de draguage et d'aménagement qui s'effectuent au niveau du port de Béni-Saf.

Matériel et méthodes

L'échantillonnage des 16 stations (figure 1) a été réalisé en juillet 1995 à l'aide d'une benne "Van Veen". A chaque station, deux coups de benne sont réalisés pour l'échantillonnage de la macrofaune benthique, soit une surface de prélèvement de 0,2 m^2. Le sédiment est tamisé et lavé sur un tamis à maille carrée de 1 mm de côté.On a relevé la richesse spécifique, la densité (le nombre d'individus par m^2), la biomasse (en mg de poids sec libre de cendres par m^2), l'indice de diversité de Shannon-Weaver H', l'indice de régularité de Pielou J' et l'indice de constance de Dajoz C.

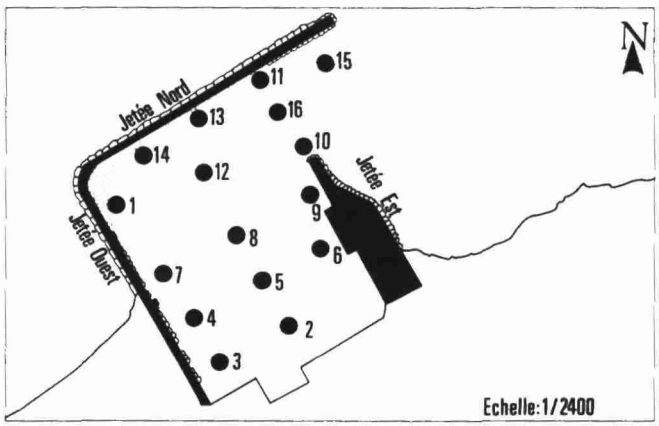

Figure 1 : Localisation des stations de prélèvement au niveau du port de Béni-Saf.

Résultats

80 espèces ont été récoltées sur l'ensemble des prélèvements effectués, qui se répartissent inéquitablement entre trois groupes zoologiques: les mollusques (57 espèces), les polychètes (19 espèces) et les crustacés (4 espèces); parmi les mollusques, les bivalves représentent 42,5% de la totalité des espèces recensées et les gastéropodes représentent 70,31% de la totalité des individus dénombrés. L'indice de constance permet de classer les différentes espèces récoltées en 60 espèces rares (présentes dans au moins 3 stations), 14 espèces communes (présentes dans 4 à 8 stations) et 6 espèces constantes (présentes dans au moins 9 stations). Les plus faibles richesses spécifiques (1 à 6 espèces) ont été observées (tableau 1) au niveau de la bande sableuse (stations 1, 13 et 14) et au fond du bassin portuaire (stations 2 et 4) alors que dans le reste du port, la richesse spécifique est comprise entre 11 et 33 espèces dont les valeurs maximales sont localisées à l'extrémité de la jetée est (stations 9: 33 espèces; station 10: 24 espèces) et en face du principal égout du port (station 3: 20 espèces). La distribution spatiale des densités est similaire à la richesse spécifique au niveau des différentes stations; les plus faibles densités sont localisées au niveau de la bande sableuse (15 à 20 ind/m2) et au fond du bassin portuaire (20 à 30 ind/m2); les densités les plus élevées ont été observées à l'extrémité de la jetée est (1200 à 3670 ind/m2) et en face du principal égout du port (2085 ind/m2).

L'analyse des données de la biomasse a permis de mettre en évidence un gradient spatial croissant de l'intérieur vers l'extérieur du port; les faibles valeurs sont localisées au fond du port et au niveau de la bande sableuse (1 à 25 mg/m2); les biomasses élevées sont observées au centre du bassin portuaire et au niveau de la passe (119 à 4763,5 mg.m-2). Les valeurs de l'indice de diversité de Shannon-Weaver (H') et de l'indice de régularité de Pielou (J') calculés à partir des effectifs sont faibles au niveau de l'ensemble des stations prospectées; elles varient de 0 (station 1) à 2,626 (station 11) pour H' et 0 (station 1) à 0,693 (stations 4 et 14) pour J'; la faiblesse des valeurs enregistrées tient à la très grande disparité numérique entre les espèces recensées.

Discussion et conclusion

Sur le plan qualitatif, la macrofaune benthique du port de Béni-Saf est comparable par sa composition spécifique aux peuplements benthiques recensés dans d'autres milieux portuaires (tableaux 1 et 2). La richesse spécifique recensée dans le port de Béni-Saf est aussi importante que celle citée dans la littérature consultée; malgré la faible

Tableau 1: Principales caractéristiques démographiques des stations étudiées dans le port de Béni-Saf. N: richesse spécifique; d: densité(ind.m^{-2}); PSLC : poids sec libre de cendres(mg.m^{-2}); H' : indice de diversité de Shannon-Weaver; J' : indice de régularité de Pielou.

Stations	N	d(ind.m^{-2})	PSLC(mg.m^{-2})	H'	J'
1	1	40	7	0	0
2	6	30	15,5	1,792	0,693
3	20	2085	25	0,646	0,149
4	4	20	16	1,387	0,693
5	18	235	405	2,496	0,598
6	12	120	119	2,246	0,626
7	13	365	127,5	1,987	0,537
8	14	200	588,5	2,097	0,551
9	33	3670	591	1,826	0,362
10	24	1200	1034,5	2,151	0,469
11	16	110	285,5	2,626	0,656
12	18	175	232	2,541	0,609
13	6	35	15,5	1,748	0,676
14	3	15	<1	1,099	0,693
15	15	145	4763,5	2,536	0,649
16	11	995	1123,5	1,235	0,357

Tableau 2 : Comparaison du nombre d'espèces (N) et des densités (d) de la macrofaune benthique de différents milieux portuaires.

Auteurs	Port	N	d(ind.m^{-2})
Bellan (1967)	Marseille	212	0 à 10320
Bakalem & Romano (1985)	Alger	165	-
Bakalem & Romano (1989)	Béjaïa	85	1420 à 4390
Rebzani-Zahaf (1990)	Alger	270	0 à 30224
Grimes & Bakalem (1993)	Skikda	91	635 à 12620
Menioui & Benabdallah (1995)	M'Diq	88	-
Présente étude	Béni-Saf	80	15 à 3670

BENTHIC BIODIVERSITY IN FIVE COASTAL BRACKISH WATER LAGOONS OF AMVRAKIKOS GULF, HELLAS

Reizopoulou S., Kormas K.* and Nicolaidou A.
Department of Zoology- Marine Biology, School of Biology,
University of Athens, Panepistimiopoli, 157 84 Athens, Hellas.

Abstract
Species abundance and community diversity were studied in five coastal brackish-water lagoons in Amvrakikos Gulf, Hellas. Both parameters showed statistically significant negative correlation with confinement, while diversity was positively correlated with % coarse material in the sediment.

Key-words : lagoons, biodiversity, Ionian Sea

Introduction

Amvrakikos Gulf holds one of the most important lagoonal systems in Greece, yet very little is published concerning their ecology (1,2,3). Most papers deal with populations of individuals species (4,5). The present paper attempts to relate species abundance and community diversity in five lagoons of Amvrakikos Gulf to a number of environmental parameters.

Materials and methods

The lagoons studied, Logarou, Tsoukalio/Rodia, Tsopeli, Mazoma and Pogonitsa, are formed on the North coast of Amvrakikos Gulf under the influence of the rivers Louros and Arahthos (Fig.1). Their depth ranges from 0.2 to 2.5m. Environmental parameters were measured monthly, except in Pogonitsa where a one time survey took place in November. Sediment and benthic samples were collected seasonally or bimonthly, using a Ponnar 0.05m^2 grab. The samples were sieved through a 1 mm mesh sieve. The total area sampled in each lagoon is given in Table 1. Diversity was calculated by the index of Shannon-Wienner. To obtain a quantitative estimation of confinement for use in statistical analyses, each station was assigned to a zone according to Guelorget & Perthuisot (6) , with mixed stations being ordered between the respective zones. Then a number was given to each rank (Zone I=1, Zone I-II=2, Zone II=3, ...Zone V=9).

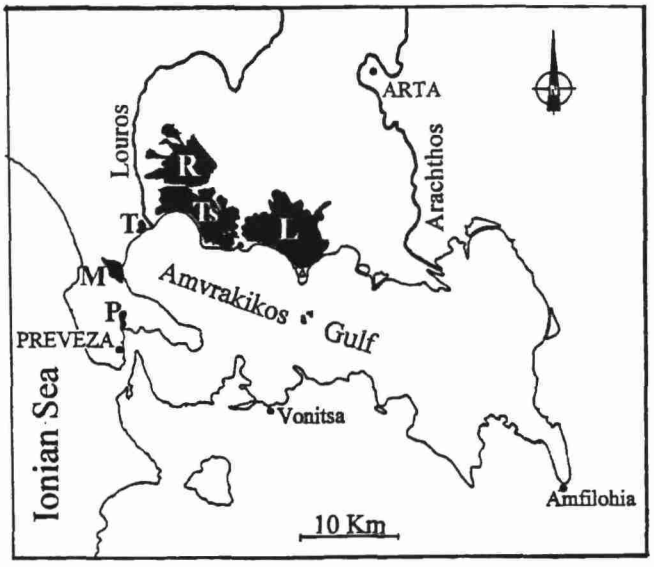

Figure 1 : Map of study area

Results

The range of temperature and salinity measured in the water, as well as the % of coarse material and the organic carbon content of the sediment in each lagoon are shown in Table 1. Tsoukalio/Rodia and Mazoma showed the wider range of both temperature and salinity. The higher values of organic matter in the sediment were approximately the same in all the lagoons except for Logarou, where it was considerably lower.

Abra ovata was one of the dominant species in all the lagoons except in Pogonitsa where it was substituted by the other bivalve, *Loripes lacteus*. The presence of the polychaete *Nephtys hombergi* was also important in almost all the lagoons. Apart from those two, different species dominated in each lagoon. *Cerastoderma glaucum* and *Iphinoe serrata* were numerically important in Logarou and *Loripes lacteus*, *Mytilaster minimus* and *Cyclope neritea* in Tsoukalio/Rodia. In Tsopeli there was dominance of *Gammarus insensibilis*, *Idotea baltica* and *Chironomidae* larvae and in Mazoma of *Mytilaster minimus, Nainereis laevigata, Tanais cavolini* and *Idotea baltica*. Finally, the dominant species in Pogonitsa were *Heteromastus filiformis, Microdeutopus gryllotalpa, Tanais cavolini* and *Cymodoce truncata*.

Confinement based on the species composition (Table 1) was highest (Zones IV-V) in Tsopeli which, at the time of sampling had only one channel of communication with Amvrakikos and where water circulation was further obstructed by a number of radiating dykes. Pogonitsa, on the contrary, had the lowest confinement (Zones II and III) being small and close to the opening of Amvrakikos to the Ionian Sea (Fig.I).

Table 1 : Environmental parameters, confinement, number of species (S) and diversity (H) in the five lagoons studies.

Lagoons	Total sample area (m^2)	depth (m)	S psu	T (°C)	coarse %	org.C %	confinement zone	S	H'
Logarou	2	0.7-1.0	16-29	22-25	6.4-32.0	2.2-3.5	III-IV	49	0.3-2.3
Tsoukalio/Rodia	5.75	0.5-3.0	11-31	18-30	6.3-79.0	1.2-5.1	III-V	49	0.8-3.5
Tsopeli	1.2	0.2-1.5	21-38	8-29	6.7-66.3	1.1-5.3	IV-V	82	0.9-2.5
Mazoma	2.5	1.0-1.4	14-37	9-13		2.7-5.9	II-IV	45	1.4-2.7
Pogonitsa	0.75	1.3-3.0	27-30	13-14	6.8-81.5	0.8-17	II-III	58	1.7-2.6

The number of species was highest [82] in Tsopeli followed by that of Pogonitsa (58). In the latter, however, the total area of samples collected was much smaller. Highest diversity, H'= 3.5, occurred in Tsoukalio/Rodia and did not coinside with the highest number of species, obviously affected by the Eveness of distribution of individuals among species. The number of species and the diversity were regressed against depth, salinity, temperature, % organic carbon and % coarse material in the sediment at all stations and lagoons together. They were also correlated with plant biomass in Tsopeli, Mazoma and Pogonitsa, for which data were available. Statistically significant correlations were obtained for diversity versus confinement and % coarse material in the sediment (Fig. 2a,b). Diversity decreased with increasing confinement and increased with increasing coarse material in the substratum. In addition, the number of species showed statistically significant negative correlation with confinement (R=-0.5285, n=49 and P=0.0038).

Discussion

Diversity in the lagoons examined was much lower than that of the shallow water areas of Amvrakikos Gulf itself (7). It was comparable, however, to the diversity of other Mediterranean lagoons (8,9,10). Low diversity is a result of the very changeable environmental conditions in lagoons, which result from their shallowness and their restricted communication with the open sea. In this sense lagoons could be considered as stressed environments. This explains the observed decrease of the number of species and diversity with increasing confinement. It is maintained (6,11) that with decreasing communication with the sea (increasing confinement) in a lagoon there is a decreasing variety of species and an increase in density. The results of the present investigation indicate that the theory could also be extended to community diversity which is a function of both species diversity and population density of individual species.

Sediment particle size was also important in controling diversity in the lagoons studied as it is known for other benthic communities (12).

CHANGES IN THE BENTHIC COMMUNITIES OF HARD AND SOFT BOTTOMS AT THE HYDROGRAPHIC BOUNDARIES IN THE VENICE LAGOON

Sacchi C.F. [1], Sconfietti R. [1], Occhipinti Ambrogi A. [2*]

[1] Dip. Genetica e Microbiologia, Sez. Ecologia, piazza Botta 10, 27100 Pavia, Italy
[2] Dip. Scienze dell'Ambiente e del Territorio, Università degli Studi di Milano, via Emanueli 15, 20126 Milano, Italy

Abstract

In the central sub-basin of the lagoon of Venice hard and soft bottom communities have been investigated in four stations, from March 1994 to March 1995. A surprising concordance of the ecological picture has been pointed out. The Sette Morti station at the southern boundary of the central sub-basin showed its own peculiarities, sustained by both a favourable hydrodinamism and the high lagoon trophism. At the opposite extreme the station near the Poveglia island is similar from the hydrodynamic point of view, but differs for its ecological features, being negatively influenced by the proximity of Venice and Marghera industrial pole.

Key-words:zoobenthos, brackish water, Adriatic Sea

Introduction

From an hydrological point of view, the lagoon of Venice is divided into three sub-basins, each corresponding to a lagoon mouth. Our ecological investigations in the middle basin of the Venetian lagoon are part of a national research programme of the former "Ministero della Marina Mercantile", which includes analogous investigations in other five brackish water basins spread on the Italian territory: the Valli of Comacchio (Emilia-Romagna), the lagoon of Orbetello (Toscana), the Lago of Sabaudia (Campania), the Lago of Marsala (Sicilia) and the Stagno of Casaraccio (Sardegna). The research programme was co-ordinated by Prof. Cognetti of the University of Pisa [1].

Here soft and hard bottom communities are compared as environmental indicators of boundary conditions existing at the limits of tidal influence of the waters entering through the central mouth.

Methods and material

Samples were collected at nearly 90 days interval from March 1994 to March 1995 in four sites (fig. 1). The Malamocco Port (MA), the Valgrande Channel (VG) and the Valle dei Sette Morti (SM) are distributed along a vivification gradient induced by tidal influence, from the sea to the inner part of the basin towards the southern limit of the central sub-basin. This area is largely used for sea food production exploiting its natural conditions, as far as possible. On the contrary, the Poveglia Island (PO) is located at the opposite extreme of the central sub-basin closed to its northern boundary, towards the urban centre of Venice and the industrial area of Marghera.

Hard bottom biological associations were scraped from the wooden piles, marking the navigable canals, with a handled metal-framed net (0.5 mm mesh size) just below the intertidal zone, on a surface of about 25x50 cm. Soft bottom communities were sampled with an Ekman-Birge grab of 225 cm2 area; three replicates were collected at each site. All samples were fixed with formalin 4%.

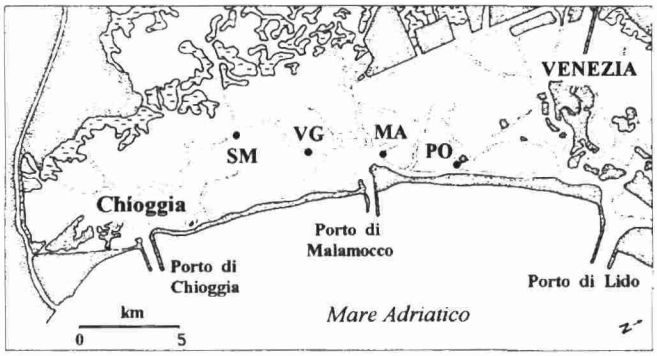

Fig. 1 - The collecting sites in the central sub-basin of the lagoon of Venice. **SM** = Valle dei Sette Morti; **VG** = Valgrande Channel; **MA** = Malamocco Port; **PO** = Poveglia Island

In our laboratory the specimens were sorted, identified at a specific level and counted. The structure of the communities were investigated by means of biotic indexes: the species richness, Shannon diversity and Simpson dominance. The cluster analysis was also applied on similarity indexes by Sörensen and Kulczynski [2].

Results and discussion

On hard substrata 37 species of Peracarid Crustaceans (27 Amphipods, 8 Isopods, 2 Tanaids) and other 54 species of sessile macrobenthos (13 Bryozoans, 8 Hydrozoans, 6 Sponges, 6 Bivalves, 6 Serpulids, 6 Ascidians and 1 Entoprocts) were collected. For soft bottoms 62 Polychets, 26 Molluscs (22 Bivalves and 4 Gastropods) and 21 Peracarids (16 Amphipods, 3 Isopods, 1 Tanaid) were found.

Two species are new for the Mediterranean Sea: the Amphipod *Caprella scaura* Templeton, well diversified from the other caprellids of the Venetian lagoon for its macroscopic differences at a morphological level, and the Bryozoan *Celleporella carolinensis* Ryland [3].

The stations are not different in terms of diversity and dominance; seasonality also is not remarkable, except for a few species.

On the contrary, clustering of the stations is very similar irrespective of the three investigated communities [4], despite the different methods to estimate the abundances of the species. Quantitative data are available only for soft bottom communities; qualitative methods were used for hard substrata, for the difficulty to obtain a really quantitative sample. Although data were heterogeneous, a coherent environmental picture emerges, indicating that Sette Morti area (SM) is clearly separated from the other three (fig. 2).

This finding is strongly indicative of a remarkable ecological originality of this area, located near the southern watershed boundary. Sette Morti is remote from direct anthropic influence and enjoys a relatively good exchange with the Adriatic Sea. In fact, as a consequence of the gredging of the deep Malamocco-Marghera Channel the central basin became enlarged at the expense of the other sub-basins; the watershed boundaries among them were shifted towards Venice on one side and towards Chioggia on the other.

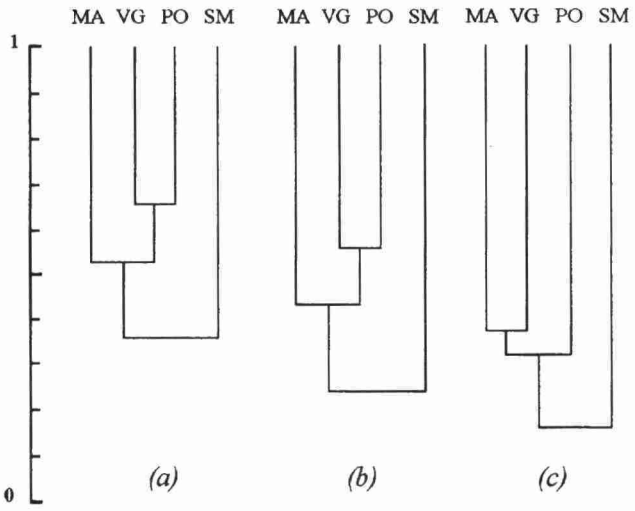

Fig. 2 - Cluster analysis by Kulczynski's index of similarity: sessile (a) and peracarid (b) communities on hard bottoms; soft bottom communities (c).

Conclusions

The uniqueness of the Sette Morti station (SM) corresponds to a clear-cut ecological situation, encompassing the advantages of the high lagoon trophic state and of the still active vivification from the sea.

The Malamocco station (MA) shows a high hydrodinamism, that can become a limitant factor for the biotic community, having largely marine features. For istance, as regards Peracarids, Malamocco and Sette Morti show a similar temporal pattern, although based on different values of density, the inner populations being more abundant [5].

At the opposite extreme of the centra sub-basin, the Poveglia Island (PO) has hydrodynamic conditions similar to the Sette Morti area. But here the biotic community is very different; the proximity of the urban centre of Venice and the industrial area of Marghera operate a severe selection, resulting in a poor and trivial community.

THE GENUS *CAULERPA* (CAULERPALES, CHLOROPHYTA) IN ADRIATIC SEA

Ante Span, Boris Antolic [1]* and Ante Zuljevic [2]
Institute of Oceanography and Fisheries
Set. I. Mestrovica 63, 21000 Split, Croatia

Abstract

In this paper geographical locations of *Caulerpa* genus in Adriatic Sea are described. So far, the alga *C. prolifera* has been found on three locations: Gargano peninsula (Italy), islands Tremiti (Italy) and around town Rovinj (Croatia). In our recent research, the alga was found on three new grounds: Rijeka Dubrovacka bay near Dubrovnik, Skrivena Luka bay (island Lastovo) and Starigrad bay (island Hvar). The first records for *C. taxifolia* in Adriatic Sea are also presented. The alga was found on three locations: Starigrad bay (island Hvar), Malinska (island Krk) and island Dolin. Characteristics of substratum, bathymetric amplitude and predominate species on the new locations of *C. prolifera* and *C. taxifolia* colonies are described.

Key-words: algae, Adriatic Sea

Introduction

The genus *Caulerpa* comprises about 72 (1) species living in temperate and especially tropical seas. There are eight taxa, six species and two varietas, of the genus living in the Mediterranean (2). Two species of *Caulerpa* are indigenous to the Mediterranean: *C. prolifera* and *C. ollivieri*. Three *Caulerpa* species are probabely lessepsian immigrants: *C. scalpelliformis*, *C. mexicana* and *C. racemosa*. According with this hypothesis they have entered the Mediterranean from Red Sea through the Suez Canal (3, 4).

The alga *C. scalpelliformis* was observed for the first time in the Mediterranean offshore Beirut (Lebanon) in 1930. It was found in Palestine and in Syria where it forms dense populations (5).

The first record for Red Sea species *C. mexicana* was in Palestine, 1941. It was also spotted on several locations in Syria (3, 5).

Most common tropical species *C. racemosa* was recorded for the first time in the Mediterranean in 1926 offshore Tunis. After that date it was spotted on many locations (Turkey, Syria, Lebanon, Israel, Egypt, Tunis) (3, 5). Rayss (6), Rayss *et al.* (7) and Di Martino and Giaccone. (8) propose that *C. racemosa* and *C.mexicana* might be a relic of the Tethys. If that was the case the both species would not be a lessepsian immigrant.

Tropical species *C. taxifolia* has colonised Mediterranean since 1984. The alga was found offshore Monaco. From that time on, it was spotted on many locations on the French, Spanish, Italian and Croatian coast (4, 9). It seams that the transport of the thallus cuttings in the anchor casings of pleasure craft or fishing nets is the dispersal mechanism along great distances through the Mediterranean (10). Sexual reproduction has not been observed so far. It colonises all types of substrate: rock, sand, mud or seagrass meadows. *C. taxifolia* forms continuous meadows to 20 - 30 meters depth, having a patchy distribution at deeper areas. It can survive up to a depth of 90 m in the clearer waters (4, 11).

The alga *C. ollivieri* was found mixed with *C. prolifera* at Balearic island, French and Levant coast. Taxonomy of this species is dubious. It is possible that *C. ollivieri* is a subspecies or form of *C. prolifera* (5).

Indigenous Mediterranean species *C. prolifera* is widely distributed offshore Mediterranean (12, 13). The alga *C. prolifera* in Adriatic Sea has been found on three locations: Gargano peninsula (Italy), islands Tremiti (Italy) and around town Rovinj (Croatia) (16).

This paper presents data on three new localities of genus *caulerpa* (*C. prolifera* and *C. taxifolia*) on the Croatian east Adriatic coast.

Materials and methods

The investigations were performed by SCUBA diving at 5 stations between 1977 and 1996: in the Dubrovnik area - Rijeka dubrovacka bay (42°40'20"N, 18°5'54"), in the Lastovo island area - Skrivena luka bay (42°44'3"N, 16°53'22"E), in the Hvar island area - Starigrad bay (43°10'54"N, 16°35'E), in the Dolin island area (44°44'16"N, 16°53'32"E) and in the Krk island area - port of Malinska (45°7'30"N, 14°31'56"E).

Material was collected along depth transects and conserved in 4% formaldehyd solution.

Results and discussion

The alga *C. prolifera* was found at three new locations on Croatian coast of Adriatic sea: Rijeka Dubrovacka bay near Dubrovnik, Skrivena Luka bay (island Lastovo), Starigrad bay (island Hvar) (Fig. 1).

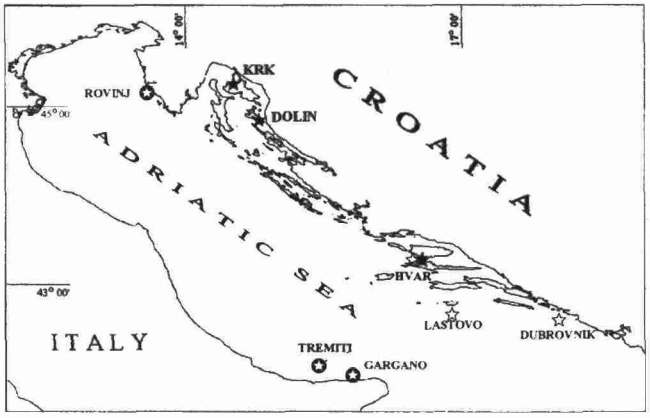

Figure 1 : Distribution of genus *Caulerpa* in Adriatic Sea. *C. taxifolia* ★; *C. prolifera* ☆ our records; *C. prolifera* ✪ previous records (Giaccone, 1978).

The first record was in Rijeka Dubrovacka bay in 1977 (Fig. 1). According to the citizens of Rijeka Dubrovacka, the alga was brought by an Austrian aquarist about 1930. Today, the alga individually grows on sandy-muddy substrate between 8 and 10 metres depth. The algae species (*Rytiphloea tinctoria, Gracilaria verrucosa* and *Cladophora prolifera*) common for that type of substrate are presented (Table 1).

The second record of *C. prolifera* on east side of Adriatic Sea was in 1981 in Skrivena Luka bay, island Lastovo (Fig. 1). It grows in a quiet bay forming a small patches on sandy and sandy-muddy substrate between 0.5 and 5 metres depth. The predominate plant species living with algae are *Padina pavonica* and *Rytiphloea tinctoria* and seagrass *Cymodocea nodosa* (Table 1).

The last record was in Starigrad bay (island Hvar) in 1995 (Fig. 1). *C. prolifera* forms a small, 4 m in diameter, meadow inside a large *C. taxifolia* colony. The community is formed by *Cymodocea nodosa*, *Cystoseira adriatica* and *C. schiffnerii* (Table 1).

Table 1 : Characheristics of new *caulerpa prolifera* population in the Adriatic Sea.

Location	First observation	Depth (m)	Substratum	Predominante species
Luka Dubrovačka bay	1977	8-10	sandy-mudy	*Rytiphloea tinctoria* (Clem.) C.Ag *Gracilaria verrucosa* (Huds.) Papen *Cladophora prolifera* (Roth) Kutzing
Skrivena Luka bay	1981	0.5-5	sandy, sandy-mudy	*Cymodocea nodosa* (Ucr.) Ascher *Rytiphloea tinctoria* (Clem.) C.Ag *Padina pavonica* (L.) Thivy
Starigrad bay	1995	1.5-3	rocky sandy	*Caulerpa taxifolia* (Vahl) C.Ag *Cymodocea nodosa* (Ucr.) Ascher *Cystoseira adriatica* Sauv. *Cystoseira schiffneri* Hamel

Opposite to Adriatic sea, *C. prolifera* is a very common species in other parts of the Mediterranean, specially on its eastern part covering mostly sandy-muddy and sandy bottom to 100 meters depth (14, 15). It grows with seagrasses *Cymodocea nodosa, Zostera noltii* and *Posidonia oceanica* (17, 18, 19). It can be concluded that *C. prolifera* in east Adriatic Sea settles on same type of bottoms as in other parts of Mediterranean. It occupies sandy or sandy-muddy bays up to 10 meters depth. On the contrary, in east Adriatic it forms small and sparse patches.

INFLUENCE OF ENVIRONMENTAL CONDITIONS ON EXTENSIVE AQUACULTURE IN TWO COASTAL LAGOONS OF THE NESTOS RIVER DELTA, NORTHERN GREECE

V. S. Theocharis [1], G. Sylaios [2], N. Stamatis [2*] & V. Ragias [3]

[1] N.AG.RE.F., Bureau of Applied Hydroecology, P.O. Box 1103, 451 10 Ioannina, Greece
[2] N.AG.RE.F., Fisheries Research Institute, 640 07 Nea Peramos, Kavala, Greece
[3] Lagoon Fish Farmers Co-operative of Kavala, Kavala, Greece

Abstract

The alteration of environmental conditions, under the influence of drainage canals and the intensification of agriculture the latest years, seems to be responsible for the qualitative change of fisheries at the lagoons Vassova and Eratino, Northern Greece. We have used a number of water quality parameters (temperature, salinity, nutrients) at selected stations as well as random samples of Dicentrarchus labrax (sea bass) population in order to study the influence of environmental conditions on the extensive aquaculture of the coastal lagoons of Nestos River. Results show that the reduction of water temperature during the winter period appears to be responsible for fish deaths reported at the winter enclosures. Condition factor analysis shows that peak nitrite and ammonium concentrations did not influence fish growth at winter enclosures. On the contrary, condition factor appears related to fish sex in the lagoonal samples and to food availability in the environment of the lagoon and the hatchery. The stabilization and reclamation of the lagoonal ecosystem demands the improvement of the biotope in nitrites and ammonium, the elimination of water discharged into the laggons from drainage canals, the better oxygenation of the water column during the summer and the application of selected fertilizers during autumn.

Key-words: Eutrophication, monitoring, mortality, growth, Aegean Sea

Introduction

Coastal lagoons are key fishery ecosystems. Mediterranean in particular, offers a number of advantages and potentialities for lagoon aquaculture with high productivity. However, due to gaps in knowledge and technology, the majority of Mediterranean coastal lagoons are underexploited, with an annual production of 50-100 kg/ha/yr.

The lagoons Vassova and Eratino, shallow and small in size, having an area of 270 and 340 ha, respectively, and a depth that rarely exceeds 2 m., consist part of a coastal lagoonal system, with total area of 1700 ha, located at the western bank of Nestos River delta, Northern Greece (figure 1). Nestos River has a discharge, excluding the lower and upper five percentiles, which ranges from 8 to 106 m^3/sec with an annual mean of 57 m^3/sec [1].

Water circulation and mixing inside the lagoons depends strongly on the prevailed tidal conditions, wind effects and precipitation. Tidal range has a maximum value of 0.96 m. during spring tides and a minimum of 0.20 m. during neap tides [2]. Meteorological conditions show moderate NNE winds prevailing during autumn and winter periods, and stronger SW winds dominating during summer [3]. Annual rainfall at the area is on average less than 400 mm [4], while evaporation varies between 150-155 mm [5].

The eutrophic lagoons of Northern Greece are being exploited by the local fishermen cooperative using fish weirs, fish traps and facilities for size sorting and separation into special basins for fish wintering. Fishery production during the decade 1970-1980 was of the order of 17 kg/ha/year [6], while nowadays production dropped to 9 kg/ha/year, which is also accompanied by a negative qualitative change of production. This production level is near the minimum limit of the fishery production range (0.2-80 kg/ha/year) at a global scale [7].

The alteration of environmental conditions, under the influence of drainage canals and the intensification of agriculture during the last years, seems to be responsible for the qualitative change of fisheries. Especially for species like sea bass Dicentrarchus labrax and sea bream Sparus aurata, production during the same period dropped from 10 to 3 kg/ha/year, according to data from the local Aquaculture Cooperative. The main problems of local fishermen concern the massive winter deaths of fish that take place at the winter enclosures of the lagoons and the poor entry of fry in the basins.

The aim of this work is to report the seasonal evaluation of current meteorological and hydrological patterns at the basins of the lagoons Vassova and Eratino, to describe their eutrophic character and to study the results of the experimental enrichment of these lagoons by sea bass fry.

Materials and Methods

Sampling of surface waters at six selected stations (B1, B2, B3 & B4 for Vassova, E1 & E2 for Eratino) took place with a monthly rate, during the period July 1994 - January 1996, at the aquatic ecosystem of the lagoons Vassova and Eratino. Stations B1, B2, and E1 are located at the main basins of these two lagoons, stations B3 and E2 at the adjacent drainage canals and station B4 at the coastal area out of the lagoons (figure 1).

The collection and preservation of water samples in plastic bottles of 100 ml for the determination of nutrients followed the methodology of [8]. Nutrients concentration was determined by photometric methods as : nitrates [9], nitrites [10], ammonium [11] and phosphates [12].

Data sampling was always taking place at the above stations on the day of maximum tidal range (spring tide), during the entrance of saline water into the lagoons. This sampling strategy eliminates the effect of tidal circulation on the temporal variability of the physical and chemical parameters of the system [13].

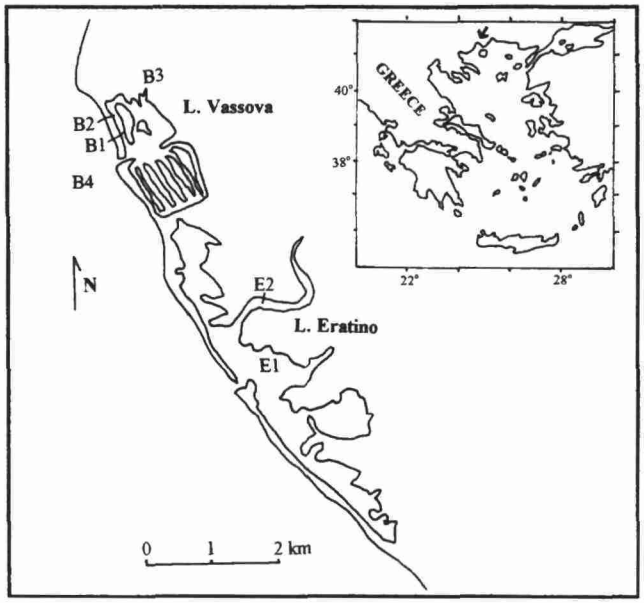

Figure 1 : Map of Vassova - Eratino lagoons and sampling stations.

Random sample (N=224) of *Dicentrarchus labrax* population was examined on a weekly basis for the whole fishing period (November - February 1993-94), for the determination of their main biometric characteristics, such as total length, fork length, net body weight and gross body weight, for both sexes. Comparative fish sample (N=76) was taken once (October 1994) from a nearby hatchery (Fanari) in order to examine the growth of the same population under culture conditions. A calculated index, named condition factor "Clark" [14] was considered as appropriate to compare the growth of populations under different feed and environmental conditions, between the lagoons and the hatchery.

Results and Discussion

The seasonal patterns of the physicochemical parameters and nutrients concentrations at three stations representative of fresh, brackish and saline water at Vassova lagoon, are presented at figure 2. The reduction of water temperature during the winter period at the lagoons Vassova and Eratino appear to be responsible for the fish deaths reported at the winter enclosures. Low winter water temperature inhibits fish growth, a mechanism not well recorded as summer anoxia, while the influence of strong winds flowing over these shallow lagoons increases turbidity causing fish deaths [15]. The summer phosphate peak occurring at the lagoons Vassova and Eratino follows closely the amount of fresh water discharged in the system. This fact indicates the long-term influence of fresh water into the lagoon and the sinking of phosphates which reappear in the water column during summer remineralization [16, 17].

Reduced precipitation and fertilizers are the most important factors determining nitrate concentration. The concentration of nitrates, in comparison to nitrogen fertilization loading of the broader area (100

REVIEW OF TURKISH SPONGE FISHERIES

Bülent Topaloglu
Faculty of Fisheries, University of Istanbul. Türkiye

Abstract

In this study, sponge fisheries in the Turkish seas were reviewed. Turkey had an important place in the world sponge market due to its high quality sponges. Its annual production of 15 tons was mostly exported to Greece. Sponge populations of the Mediterranean Sea including the ones on the Turkish coasts dramatically decreased because of epidemic sponge disease. The sponge production of Turkey decreased to 7 tons per year since 1986 because of this disease. Prior to the epidemy there were 40 boats and 120 fishermen engaged in sponge fisheries in Bodrum in central Aegean Sea. There are 47 boats with 140 fishermen engaged in sponge fisheries in the Çanakkale Strait and in the Marmara Sea which have not been effected by the disease. Sponge fisheries was performed in Anamur, Antalya, Finike, Kas, Fethiye, Marmaris, Gökova Bay, Bodrum, Güllük Bay, Çesme, Edremit Bay, Ayvalyk, Gökçeada, Bozcaada, Saros Bay, Çanakkale Strait in the Aegean-Mediterranean region and Imraly Island, Marmara Island and Gelibolu in the Marmara Sea. Sponges have been harvested in a number of ways: skin diving, surface air supply system and special designed beam-trawl.

Key-words: Porifera, Fisheries, Eastern Mediterranean

Introduction:

Due to their skeletons that consist of spongin networks, their soft building and high water containing capacity, sponges have been used since antiquity. Studies of past decades have engendered their use in the fields of pharmacy, medicine and cosmetics .

Turkish sponge is highly seeked in the world markets because of its high quality. Turkey possesses a number of sponge centers led by Bodrum in Central Aegean sea. Despite these, Turkey does not dominate in world markets due to its unregulated sponge fisheries and processing. The sponge disease which first appeared in 1986 caused serious damage on stocks and caused sharp reductions in production (1). Aquaculture of sponges has gained impetuous following this period. The first sponge study in Turkish waters was published by Forbes in 1844 (2). Devejian (3) mentioned bathing sponge (*Euspongia equina*) and toilet sponge (*Euspongia mollisima*). Places of concentration of these species were given as well. Besides, Kalimnos, Symi and Castellorizo Islands, Bodrum and Kas, were also mentioned as main locations of sponge fisheries. He also paid attention to the fact that sponge diving methods and sponge divers changed after 1867 because of the diving suit. Four different fishing methods were mentioned. These were fishing with a diver suit, skin diving, spear sponge fishing and trawling. Teams that were equipped with diver suits were differentiated to three. The least equipped of these referred to as third class diving teams were mentioned as fishing sponges on the Anatolian coast.

Sponge studies in Turkish seas were mostly focused on possibilities of aquaculture (4-6). Canyigit (7a) gave statistical information on Turkey's sponge production and exports for 1961. The article mentioned that sponge production had continued for a long time due to favorable weather conditions. Bodrum led the production with 15 tones follow by Marmaris 7-7,5 tones and Gökçeada and Bozcaada with 5 tones each. Canyigit (7b) also pointed out four different ways for sponge fisheries: spear fishing, beam-trawlz, skin diving and diving suit with surface air supply system.

Arysoy (8) examined Turkish sponge industry based on the conditions of the day, distribution according to different locations and the sponge export of the country between 1951-1962. Attention was drawn to the correlation between sponge and sponge fishing boats registered in Bodrum port and sponge production and sponge export. The author concluded that the most important buyer of Turkish sponges was Greece.

In the magazine of the Ministry of Aquaculture Forestry and rural affairs (9) an article repeated that eventhough Turkish sponge were seeked in all world market Turkey's sponge export plunged from 100 tons in 1910 to 13 tons in 1980. The reasons for this were given as technical insufficiency, negative trends in ecological conditions and unhealthy and unsuitable working conditions of divers. The article pointed out decrease in the number of divers has been observed due to the insufficiency of the diving infrastructure and due to decompression disease.

Atahan *et al.* (10) discussed Turkish sponge fishing, its place in the world market and variations in annual production and related the decrease in sponge production to overfishing. Besides, the author put the sponge disease forward as an important reason, too. He concluded that sponge disease that appeared in Turkish waters in 1986 had effected the economically important species negatively, and added that the Çanakkale (Dardanelles) Strait and the Marmara Sea were not hit by the same disease. With respect to sponge fishing methods he wrote that surface air supply diving method was getting prevalent displacing trawl which had caused overfishing and the depletion of sponge stocks. Same author also reported that Bodrum was the center of sponge fisheries until 1986 when the sponge disease was first seen. There were 40 sponge fishing boats with 120 personal in Bodrum. There were 7 sponge fishing boats and 21 personnel in the Çanakkale Strait and Marmara Sea in the same period. It can be conducted from these data Bodrum was hit worst by the disease. Sponge fishing boats increased to 43 with 144 personnel in the Çanakkale Strait and the Marmara Sea following the appearance of the disease. Other factors that have led to this increase can be started as the prevalence of sponges between depths of 2-15 meters and fisherman substituting sponge fishing instead of fishing in summer. Sponge fishing boats decreased to 8 with 21 personnel in the Aegean and the Mediterranean Number of sponge fishing boats shown in Table 1. The disease was more destrictive where salinity and water temperature were higher according to the author.

Table 1 : Sponge fishing boat registered in Bodrum (Aegean Sea) after Arysoy, (8).

Boat type	number
Trawl boat for sponge fishing	26
Diving equipment sponge boat	12
Surface air supply sponge boat	5
Total	43

Katagan *et al.* (1) evaluated by comparing with the world sponge production accompanied by same figures. It's concluded that even though Turkish sponges were highly seeked due to its qualities in the world market, insufficiencies in processing caused Turkey not to exert any influence on the same market. Great losses in sponge stocks engendered by the sponge disease which has led to overstrain on non-diseased stocks and poor working and living conditions of sponge divers which have caused sponge fishing boats to be used in tourism have been pointed out as factors for the decrease of sponge production.

Results and Discussion

Sponge fisheries is prevalent mainly in Bodrum, Anamur, Antalya, Finike, Kas, Fethiye, Marmaris, Gökova Bay, Güllük Bay, Çesme, Edremit Bay, Ayvalyk Bay, Gökçeada, Bozcaada, Saros Bay in Aegean Sea and Çanakkale Strait; also in Imraly Island and Marmara Island in the Marmara Sea which was not affected by the disease (Fig 1).

A significant decrease in sponge export is detected from 1960's to present. Between 1960-1993 the highest amount of export was recorded in 1965 (40.3 tons), followed by 1972 (24.8 tons), 1978 18.9 tons), 1986 (15 tons), 1988-1989 (13.5-13.6 tons). Amount of sponge export is shown in Fig. 2. The sponge disease which was first observed in 1986 effected the export in 1990. The reason for this is the fact that sponge can be stored raw or semi processed products for 3-4 years until good buyer comes. After finishing such stored sponges, in 1990 the annual sponge export of Turkey decreased to 1-5 tons a year.

Heavy working conditions of sponge divers are other factors in the decrease in sponge production. The decompression disease which effects to sponge divers has claimed many lives and injured many

COASTAL EUTROPHICATION ASSESSMENT: DEVELOPMENT OF A WATER QUALITY CLASSIFICATION SYSTEM USING PHYTOPLANKTON ECOLOGICAL INDICES

G. Tsirtsis* and M. Karydis

Aquatic Ecosystems Laboratory, Dept. of Environmental Studies, Univ. of the Aegean,17 Karantoni str., 81100 Mytilini, Greece

Abstract.

A classification system was developed for water quality assessment in coastal regions. Phytoplankton enumeration/classification data from areas known as eutrophic, mesotrophic and oligotrophic were used for the calculation of five ecological indices. These indices were further processed with descriptive discriminant analysis to optimize the separation of the trophic states. Margalef's, Menhinick's indices and cell number were selected as the most efficient for the separation of the trophic levels, whereas Hill's N0 and Gleason's indices did not show any sensitivity in assessing eutrophication. The discriminant functions obtained from the analysis were used to plot a territorial map, divided into three clearly defined regions, a eutrophic, a mesotrophic and an oligotrophic. The classification scheme was evaluated in a case study from 23 stations spaced out along coastal areas in the Aegean sea, Eastern Mediterranean. Each station was represented with a point in the map and its water quality could be assessed. The classification system developed can be proposed as a methodological tool for coastal water quality assessment in a wide spatial scale.

Key-words: Coastal management, eutrophication, Aegean Sea

Introduction

Many attempts have been reported for the quantitative assessment of coastal eutrophication. The information related to nutrients and chl. á concentrations has been analyzed extensively [1, 2, 3], whereas both univariate and multivariate statistical methods have been applied on phytoplankton ecological indices [4], which seem to be nowadays standard practice in monitoring environmental changes [5] and also in water quality assessments [6].

The evaluation of water quality reported so far assumes the empirical selection of some impacted and unimpacted sites in the area under investigation, that have been used for the development of a local eutrophication scale. This approach in water quality studies shows certain shortcomings: (a) it is strongly affected by the expertise of the researcher about known trends in the investigated area and (b) the effectiveness of the developed eutrophication scale for water quality assessment is limited to the investigated area since it is based on data representing the local conditions.

In the present work a classification system for coastal eutrophication assessment was developed using the multivariate statistical method of discriminant analysis on phytoplankton ecological indices. This classification method was based on a large number of data selected from different regions in the Aegean Sea and its effectiveness was tested in a case study, so it can be proposed as a classification method for water quality assessment in a wide spatial scale.

Methodology

Source of data. Three datasets on phytoplankton enumeration / classification characteristic of the Eastern Mediterranean [2] formed the basis for the development of the classification procedure. The first dataset (22 observations) from two sampling sites S1 and S2 (Fig. 1) came from an area known as eutrophic [2], located in the vicinity of the sewage outfall of the Metropolitan area of Athens, Greece. The data of the second set (80 observations), characterizing mesotrophic conditions [2], were collected from seven stations S3-S9 (Fig. 1) located in the remaining area of the inner Saronicos Gulf. The data of the third set (78 observations) were collected from 5 stations along the N.W. side of the Island of Rhodes (Fig. 1) from an area known as oligotrophic [7].

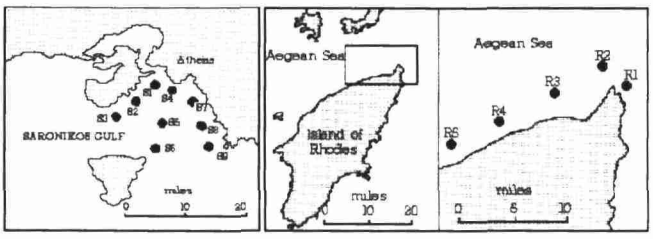

Figure 1. Location of sampling sites in Saronikos Gulf and along the Island of Rhodes (Greece): stations S1 & S2 characterize eutrophic marine environment, stations S3-S9 show mesotrophic character and stations R1-R5 are characteristic of oligotrophy.

Ecological indices. Four ecological indices expressing phytoplankton community diversity were selected for further consideration on the basis of their efficiency to detect eutrophic trends in previous work [4]:

(a) Gleason's index $D = \frac{S}{\ln N}$ [8]

(b) Margalef's index $D = \frac{S - 1}{\ln N}$ [8]

(c) Menhinick's index $D = \frac{S}{\sqrt{N}}$ [8]

(d) Hill's NO = S [8], where S is the number of species and N is the number of individuals in a sample. The cell number has been also used in the analysis as an index of biomass.

Statistical analysis. The multivariate method of discriminant analysis has been used in a descriptive way [9], that is to exhibit optimal separation of the eutrophic, mesotrophic and oligotrophic group, based on certain linear transforms of the measured ecological indices. Prior to the analysis, data were tested for normality and equality of variances (homoscedasticity), since these two assumptions are required for the application of the discriminant analysis [10]. The Kolmogorov-Smirnov test was used to test the goodness-of-fit to the normal distribution and the variance ratio test for the equality of variances [11]. A stepwise variable selection algorithm has been used in order to arrive in a good model; the five diversity indices were included in the dataset, among which a limited number was selected for better group separation. The variable selection criterion applied in the present work was the minimization of Wilk's lambda [12]. Thus at each step, the index that results in the smallest Wilk's lambda for the discriminant function is selected for entry.

After the selection of the indices resulting to the better group separation, the coefficients were estimated for the two discriminant functions so that their values to differ as much as possible between the eutrophic, mesotrophic and oligotrophic groups. Furthermore, a two dimensional territorial map can be drawn, having in its axes the two discriminant functions. The map is divided into three clearly separated regions, a eutrophic, a mesotrophic and an oligotrophic. Based on the discriminant functions, it is possible to calculate the two discriminant scores for each case under consideration, which can be plotted as a point in the territorial map.

Results

Summary statistics of the ecological indices used in the present analysis can be shown in Table 1. A gradual increase in cell number, species number (Hill's N0), Margalef's and Gleason's indices can be observed from oligotrophy to eutrophication, whereas the opposite trend was observed for Menhinick's index. All the datasets have shown homoscedasticity and nor-

Table 1. Summary statistics of the ecological indices used in the discriminant analysis.

Parameter	Indices				
	A Eutrophic waters				
	Gleasons	Margalefs	Menhinicks	Hills N0	Cell number
Range	0 84-2.96	0 76-2 87	0 02-0 11	10-34	53400-519581
Median	1 94	1 86	0 05	24	188334
	B Mesotrophic waters				
	Gleasons	Margalefs	Menhinicks	Hills N0	Cell number
Range	0 51-2 99	0 42-2 90	0 02-0 18	6-33	13600-137272
Median	1 61	1 52	0 09	18	31400
	C Oligotrophic waters				
	Gleasons	Margalefs	Menhinicks	Hills N0	Cell number
Range	0 85-2 59	0 73-2 47	0 10-0 27	7-23	2320-7440
Median	1 40	1 29	0 19	12	4240

PHENOLOGY OF *POSIDONIA OCEANICA* (L.) DELILE IN THE GULF OF KOPER (GULF OF TRIESTE), NORTH ADRIATIC

Robert Turk [1*] and Aleksander Vukovic [2]

[1] Intermuniciple Institute for Protection of Natural and Cultural Heritage Piran, 6330 Piran, Slovenija
[2] National Institute of Biology, Marine Biological Station, 6330 Piran, Slovenija

Abstract

Investigations were carried out in the only remaining *Posidonia oceanica* meadow in the Gulf of Trieste, the northernmost part of the Adriatic. The sampling site is located on the Slovenian part of the gulf, between the towns of Koper and Izola. The meadow is approximately 1 km long, it starts close to the coastline and it extends 50 meters off shore. A one-year investigation of the basic phenological parameters of the meadow started in April 1997. Together with the number of shoots per square meter the following parameters were studied: the number, length and width of leaves, the length of leaf sheaths, the Coefficient "A" and the Leaf Area Index. The results were compared with data from Banyuls-sur-mer and Port-Cros.

Key-words: Adriatic Sea, Posidonia, density, growth

Introduction

Posidonia oceanica (L.) Delile is together with *Cymodocea nodosa* (U.) Ascherson the most common seagras in the Mediterranean. It is widespread in the whole basin except for the area close to the strait of Gibraltar, the North Adriatic, the coast of Israel, the Bosphorus, the sea of Marmara and the Black Sea (1). According to an previous work of Benacchio (2) it was quite common also on the silty bottom of the Gulf of Trieste in the North Adriatic. Further investigations (3; 4) however showed a drastic change in its distribution in this northernmost part of the Adriatic. It is very likely that at present there is only one very restricted meadow of *Posidonia oceanica* in the Gulf of Trieste. The area is on the Slovenian coast between the towns of Koper and Izola. The mapping of the area that was carried out in 1993 (5) showed that the meadow is approximately 1 km long, starts close to the coastline (water depth 0.5 m) and extends 50 m off shore (water depth 4 m). The meadow is formed of islands of *Posidonia oceanica* of different sizes and shapes and does not fit into normal meadow types (6).

In order to establish the state of the meadow, its general features and its possible progression or decline in the future a one-year study of phenology and lepidocronology was started in 1997. The aim of the study is to obtain the basic information on the characteristics of the meadow and on the phenology of *Posidonia oceanica* in the Gulf of Koper. The final results will allow us to make an estimate of the dynamics of the meadow. The data from April 1997 presented in this preliminary report allow a tentative comparison with data from other sites in the Mediterranean basin.

Material and Methods

The sampling site is located on the Slovenian part of the Gulf of Trieste in the North Adriatic between the towns of Koper and Izola (Fig. 1).

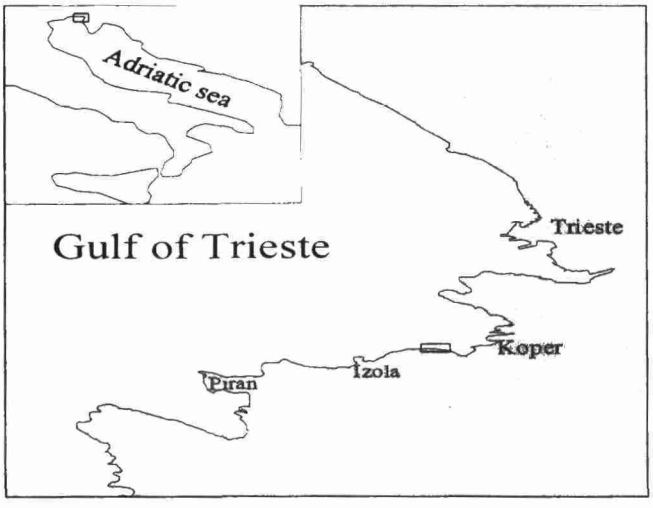

Figure 1 : The Gulf of Trieste (North Adriatic) with the investigated site.

The Gulf of Trieste is a shallow marine ecosystem where characteristics of the coastal and open waters of the Northern Adriatic are combined. With few exceptions the depth does not exceed 25 m. Because of its shallowness and the freshwater inputs as well, the waters of the gulf experience considerable temperature (8 - 26°C) and salinity (33 - 38‰) variations. Also remarkable is the tidal amplitude, which can be as much as 1.5 m. The transparency of the water is often quite low. The Secchi values for the Gulf of Koper can be as low as 3 - 4 m and hardly exceed 8 m (7). The transparency of the investigated area can be even lower due to the shallowness of the water , its proximity to the coastline, its exposure to the NE winds and as a consequence to the resuspension of the sediments.

The investigation was carried out in the central part of the area, on a more or less homogeneous part of the meadow. The site was 15 to 25 meters from the coastline, at a depth between 2 and 3 m, with the surface of approximately 1200 m^2. The number of shoots was counted *in situ* by SCUBA diving on a square of 0.14 m^2 at 8 different locations. Due to the fact that the investigation was carried out on the only remaining *Posidonia oceanica* meadow in the northernmost part of the Adriatic a limited number of only 15 shoots was taken for further phenological and lepidochronological analysis. Together with the number of shoots per square meter the following phenological parameters were studied: the number, length and width for the different categories of leaves - juvenile, intermediate, and adult (8) per shoot, the length of leaf sheaths, the L.A.I. (Leaf Area Index) and the Coefficient "A" (8). Mean values of the studied parameters for the whole sampling site were calculated. The results were compared with the data from other parts of the Mediterranean basin (9).

Results and Discussion

Meadow density

The density of the investigated meadow in the Gulf of Koper varies from 360 to 588 shoots per m^2 with the mean value being 460. The comparison with some of the data from the work of Pergent & Pergent-Martini (9) (Table 1) shows that the density of the meadow in Koper is relatively low considering the shallowness of the site and that it can be compared with the densities of meadows at much greater depths.

Table 1 : Mean density of *Posidonia oceanica* shoots per m^2 in the Gulf of Koper (North Adriatic) compared with the values from different stations (different depths) at Banyuls-sur-mer and Port-Cros (9).

	Koper	Banyuls-sur-mer				Port-Cros				
St.		B1	B2	B12	B19	P1	P2	P11	P23	P32
Depth	-2,5	<-1m	-2m	-12m	-19m	-0,7m	-2m	-11m	-23m	-32m
Density	460	1278	1163	535	367	942	645	317	283	205

Shoot and leaf structure

The mean values for some of the studied phenological parameters of the shoots and leaves of the *Posidonia oceanica* from the Gulf of Koper are shown in Table 2. The number of leaves (adult and intermediate) in the investigated shoots varies between 5 and 7 with the mean value of 5.9. Nine shoots out of 15 presented juvenile leaves.

The mean length of the adult leaves shows considerable variation (271 mm - 730 mm). It has to be considered, though, that the number of the adult leaves with damaged apexes is very high. The mean value of the Coefficient "A" for the adult leaves was calculated to be 90.5%. The high number of adult leaves with damaged apexes is comprehensible in view of the microlocation of the investigated site (high tidal amplitude, strong north winds and wave motion). A much lesser

AMPLITUDE D'HABITAT ET DIVERSITE FAUNISTIQUE DU PEUPLEMENT MALACOLOGIQUE D'UNE LAGUNE MEDITERRANEENNE (LAGUNE DE NADOR, MAROC)

Nasser Eddine Zine [1*] et Mohamed Menioui [2]

[1] Faculté des Sciences, B.P. 4010 Beni M'hmmed, Meknès, Maroc
[2] Institut Scientifique, B.P. 703, Rabat-Agdal, Rabat, Maroc

Résumé

L'utilisation des paramètres de l'Analyse Factorielle des Correspondance (amplitude d'habitat et diversité faunistique) appliquée aux mollusques de la lagune de Nador et à 11 stations réparties dans l'ensemble de cette enceinte lagunaire, a permis de mettre en évidence un double gradient qui, du centre de la lagune vers le bordure continentale et vers les deux extrémités NW et SE, s'exprime par un accroissement de la diversité faunistique, traduisant une augmentation des potentialités écologiques des stations, et par une augmentation du nombre d'espèces exclusives exprimant une réduction de l'amplitude d'habitats des espèces.

Mots clés: mollusca, biodiversity, Western Mediterranean.

Introduction

La lagune de Nador, située sur la côte méditerranéenne entre les parallèles 35° 7'N, 35° 16'N et les méridiens 2°44' W 2° 80'W., est la plus grande lagune du Maroc (115 km²). Elle a fait l'objet de nombreuses études hydrologiques, sédimentologiques, écologiques et biotypologiques (1- 9). Ce milieu communique avec la Méditerranée par un chenal (Bokana), dont l'emplacement sur le cordon dunaire a varié plusieurs fois au cours de la période comprise entre 1545 et 1981. Cette passe s'obstrue périodiquement, et s'ouvre régulièrement par les tempêtes. La dernière réouverture date de 1981, actuellement, elle est presque fermée ce qui a réduit considérablement les échanges avec la mer.

D'après un travail de synthèse (7) est essentiellement constituée par des espèces euryèces (5) dominée par les mollusques (180 espèces, 60% du total de la faune), les crustacés (51 espèces, 17,2%), et les annélides polychètes (41 espèces, 13,8%). Les autres groupes, peu représentés, sont les foraminifères (16 espèces), les échinodermes (4 espèces), les pycnogonides, les acariens et les spongiaires (2 espèces chacun). Les cnidaires et les insectes sont représentés chacun par une seule espèce.

Des 180 espèces de mollusques, 141 espèces ont été trouvé à l'etat vivant, et 39 rencontrées uniquement à l'état de coquilles vides. Ces espèces sont constituées de gastéropodes (99 espèces, 55% du total des mollusques), de lamellibranches (75 espèces, 41%). Les polyplacophores, les scaphopodes et les céphalopodes n'excèdent, dans leur ensemble, 4% du total de ce groupe. Quantitativement, les mollusques sont nettement dominés par *Corbula gibba, Loripes lacteus,* et *Lucina fragilis* dans les stations où prédominent les substrats meubles, surtout vaseux. On y rencontre deux gisements naturels: de palourde, *Venerupis decussata*, (à proximité de la bordure continentale) et de nacres *Pinna nobilis* (non loin de la passe). Les espèces *Bittium reticulatum* et *Cerithium rupestre* y sont relativement abondantes, alors que dans les stations des substrats durs, il y a une nette dominance des Mytilidés *(Mytilus* et *Modiolus*).

L'objectif de ce travail est de contribuer à une meilleure connaissance de l'autoécologie des espèces (espèces exclusives, espèces intermédiaires) du peuplement malacologique et de la qualité écologique des stations à l'intérieur de cette lagune et ce, à travers l'étude des amplitudes d'habitats des espèces, et la diversité faunistique des stations déterminées par l'analyse factorielle des correspondances. C'est un travail qui, en fait, complète l'étude sur la typologie des mollusques dans cette lagune (9).

Méthodologie

L'échantillonnage des mollusques a été effectué dans 11 stations, dispersées sur l'ensemble de la lagune. Il a été réalisé sur substrat meuble à l'aide d'une benne; la surface prélevée est de 900 cm² correspondant à l'aire minimale au niveau des substrats meubles.

En ce qui concerne l'exploitation des données, celle-ci a été faite par l'analyse Factorielle des correspondances (AFC). Cette méthode appliquée aux peuplements infralittoraux superficiels des côtes marocaines s'est montrée particulièrement efficace pour la compréhension de la distribution des espèces. Pour cela, nous avons dressé deux tableaux à double entrée de n espèces [34] et p stations [11]; pour la valeur du couple (n,p) nous avons utilisé l'abondance annuelle de chaque espèce, transformée en classe suivant une progression géométrique de raison 2. Les stations, H et K pauvres en espèces ou complètement azoïques ont été traitées en éléments supplémentaires. Pour l'amplitude d'habitat des espèces et la qualité écologique (diversité) des stations, la formule de Chessel *et al.* in (12), qui se base sur les propriétés de l'analyse factorielle des correspondances où les espèces sont représentées par leurs abondances annuelles (12).

$$Vi(q) = \sum_{j=1}^{P} \frac{ni\,nj.}{ni.} C^2j(q) - \lambda(q)\, C^2i(q) \qquad Vi(q) = \sum_{j=1}^{p} \frac{ni\,nj.}{ni.j} C^2i(q) - \lambda(q)\, C^2j(q)$$

Vi(q)= Variance de la position de l'espèce i sur l'axe q: amplitude d'habitat Vj(q)= variance de la position de la station j sur l'axe q: diversité faunistique. (q= numéro du facteur ou de l'axe considéré ; i= espèce; J= station; Nij= effectif de l'espèce i dans la station j; ni.= effectif total de l'espèce i dans toutes les stations; n.j= effectif total des espèces dans la station j; Ci(q)= coordonnées de l'espèce i sur l'axe q; Cj(q)= Coordonnées de la station j.; λ(q)= valeur propre de la station j).

Résultats et discussions

Du travail sur la typologie de la malacofaune de la lagune de Nador (9), il découle que ce milieu est constitué de quatre zones:

Zone I: non schématisée sur les figure 1a et 1b, formée par les stations K et H pratiquement azoiques, (amplitudes d'habitats des espèces et valences écologiques des stations trop faibles, donc mises en éléments supplémentaires), et caractérisées par un substrat instable et un taux de pélites extrêmement faible.

Zone II: C'est la partie de la bordure continentale (station C) qui reçoit des rejets industriel et des eaux usées drainés par l'Oued Selwane. Elle est qualitativement pauvre en espèces mais dominée par *Corbula gibba* (91,1% du total des mollusques) préférentielle des milieux riches en matières organiques (13).

Zone III: Correspond aux deux extrémités NW et SE de la lagune et à une partie de la bordure continentale (Stations B, I, et F), de faibles profondeurs et qui sont riches en espèces (entre 16 et 21); mais quantitativement pauvres en individus. Elles se singularisent par des apports en matière organique en provenance de la ville de Nador (Station B) et par le phénomène d'eutrophisation dû au confinement (stations I et F). Les mollusques y sont essentiellement dominés par des espèces euryèces parfois indicatrices d'instabilité du milieu et, souvent, caractéristiques de la biocénose des milieux lagunaires. Il s'agit, entre autres, de *Venerupis aurea, Tricolia speciosa, Abra, alba Jujubinus striatus, Modiolus phaseolinus* et *Gastraena fragilis*.

Zone IV : Elle englobe le reste des stations, situées au milieu de la lagune et caractérisé par une importante profondeur, une oxygénation satisfaisante, et le taux de pélites relativement élevé (9,56% en moyenne). Avec des fonds tapissés par l'algue *Caulerpa prolifera*. Elle est caractérisée par des espèces euryèces, plus ou moins vasicoles telles que *Loripes lacteus, Corbula gibba, Lucina fragilis* et *Nucula sulcata*. Ces espèces représentent respectivement 36,4%, 26,8%,14,5%,et 5,5% du total de la malacofaune ce qui constitue un total de 83,2% de l'ensemble de ce groupe. En ce qui concerne l'amplitude de l'habitat, on distingue trois groupements de stations (A, B et C) correspondant à trois groupements d'espèces (Fig 1a). Ces derniers sont constitués de sous groupements comportant chacun des espèces qui sont exclusives, communes ou préférentielles de ces stations.

**** le groupement A***, correspondant à la zone typologique III qui englobe les trois stations B, F et I et qui comporte:- un premier sous groupement Aa relatif à la station B qui contient, comme espèces exclusives, les formes *Venerupis pullastra, V. decussata, Gibbula tingitana, Rissoa membranacea* et *R. guerini*. Ce sous groupement, bien individualisé, est caractéristique de la station B dont toutes les espèces montrent de faibles amplitudes d'habitat ne dépassant pas 0.01.

- un deuxième sous groupement Ab formé des deux stations des extrémités NW et SE (F et I) avec *Cerithium rupestre* (0.02) exclusive de la station F et *Jujubinus striatus* (0.07) ayant une amplitude relativement plus importante puisqu'elle est présente dans les deux stations F et I, bien que très abondante dans la stations F.
- un troisième sous groupement Ac englobant les trois stations (B. F et I) et leurs espèces communes: *Acanthocardia echinata* (0.64), *Modiolus phaseolinus* (0.35) et *Hinia costulata* (0.6) préférentielles de la station B.